CONF-840806--Vol.1

DE85 012484

PROCEEDINGS of the 18th DOE NUCLEAR AIRBORNE WASTE MANAGEMENT AND AIR CLEANING CONFERENCE

Held in Baltimore, Maryland
12-16 August, 1984

Sponsors: U.S. Department of Energy
The Harvard Air Cleaning Laboratory

Editor
Melvin W. First

Published
March, 1985

with an INDEX to the 17th and 18th CONFERENCES

PROGRAM COMMITTEE

W.L. Anderson

C.B. Bastin

R.R. Bellamy

A.G. Croff

H.L. Ettinger

A.G. Evans

W.P. Gammill

H. Gilbert

R.T. Jubin

M.J. Kabat

J.L. Kovach

W.H. Miller, Jr.

D.W. Moeller

K.S. Murthy

A.C. Richardson

T.R. Thomas

A.K. Williams

CONFERENCE CHAIRMAN

Melvin W. First
Harvard Air Cleaning Laboratory

FOREWORD

The Eighteenth DOE Nuclear Airborne Waste Management and Air Cleaning Conference was held in Baltimore, MD, August 12-16, 1984, under sponsorship of the U.S. Department of Energy (DOE) and the Harvard Air Cleaning Laboratory. Attending the Conference were 267 air cleaning specialists from the United States, Belgium, Canada, the Federal Republic of Germany, France, Italy, Japan, the Netherlands, People's Republic of China, Portugal, Spain, Sweden, the United Kingdom, and Yugoslavia.

Those familiar with prior Air Cleaning Conferences, will be aware that the Conference title has been expanded to DOE Nuclear Airborne Waste Management and Air Cleaning Conference. This title does not trip off the tip of the tongue as smoothly as Nuclear Air Cleaning Conference, but perhaps it only needs another 30 years to sound natural. Indeed, for those of us who have been coming to the Nuclear Air Cleaning Conferences for many years, the change seemed at first to be a serious usurpation of a long-established and successful enterprise. But on further reflection, I hope it will come to be recognized that the commitment of the U.S. Government to the support of the nuclear air and gas cleaning research and development has declined seriously in recent years. The government budget people see a mature nuclear power industry able to support its own technology. They see a halt in the construction of new nuclear power plants. They also hear that the engineered safeguards at TMI II, including the air cleaning components, did their job by preventing significant emission of radioactive products of concern to the environment. The conclusion they have reached is not one that we air and gas cleaning specialists can applaud because we are aware of important gaps and uncertainties in our knowledge and in our practices. Nevertheless, the situation I have described exists, and government support for air cleaning conferences has waned.

On the other hand, interest and concern for nuclear wastes have increased enormously in recent years. Inasmuch as nuclear airborne waste management incorporates a very large component of air and gas cleaning technology, the combination is a natural one and it is logical to conclude that combining the two, as we have done at the 18th Conference, will enrich our knowledge of both, and benefit both. Therefore, we look ahead to a continuation of these Conferences that will maintain their central position in the field of air and gas cleaning, and, in addition, assume a new importance in the field of airborne waste management. I hope you join me in looking ahead to an exciting future in our chosen professional fields.

A meeting of the Government-Industry Committee on Filters, Media, and Media Testing was held immediately prior to the opening of the Conference to provide a forum for the exchange of viewpoints between suppliers and users of air cleaning equipment and the presentation of reports by various task groups addressing specific issues and developing air cleaning standards.

A conference of this size and complexity requires the dedicated service and wise counsel of many. The Chairman of the 18th DOE Conference wishes to record his appreciation of the firm support and willing assistance provided by the Program Committee throughout the lengthy planning process and during the Conference, itself. Administrative support for the Conference and preparation of the Proceedings was ably provided by Mrs. Joan Sullivan at the Harvard School of Public Health.

Melvin W. First
Conference Chairman

DEDICATION

The Proceedings of the 18th DOE Nuclear Airborne Waste Management and Air Cleaning Conference are dedicated to the memory of Clifford A. Burchsted in recognition of his long identification with the planning of these Conferences and his many valuable technical contributions

CLIFFORD A. BURCHSTED
1921 - 1983

PRESENTATION OF AN AWARD TO CLIFFORD A. BURCHSTED

by

Dr. Ronald Bellamy

on behalf of the

American Society of Testing and Materials

On behalf of the American Society of Testing and Materials (ASTM), it is my special honor to perform the task before me today. I have an award to present and, like everything we seem to do these days, there are good points and there are bad points associated with it. The award is not really a posthumous award, awarded after the fact to Clifford Burchsted, but an award that the ASTM approved prior to April 1983. As a matter of fact, the award was approved on March 4, 1983. Unfortunately, the ASTM sometimes works with the same haste as some of our governmental bodies and there was no opportunity to present the award to Cliff. We are all aware of Cliff's technical contributions and accomplishments in the field of nuclear air cleaning, as well as his efforts, indeed, his pleasure, in doing the jobs on standard committees that we all dislike so much, such as serving as chairman and as secretary. In recognition of his long and meritorious service in the development of concensus standards, ASTM has prepared this plaque. It reads as follows:

> "Clifford A. Burchsted is granted an AWARD OF MERIT and the honorary title of FELLOW for an active and constructive role in ASTM standards, especially in Committee D-28 on Activated Carbon Work, serving as chairman, secretary, and as secretary to Subcommittee D28.04 since 1967. By action of the Board of Directors, March 1983. Signed by the President and the Chairman of the Board."

This plaque is now presented to Mrs. Clifford (Betty) Burchsted.

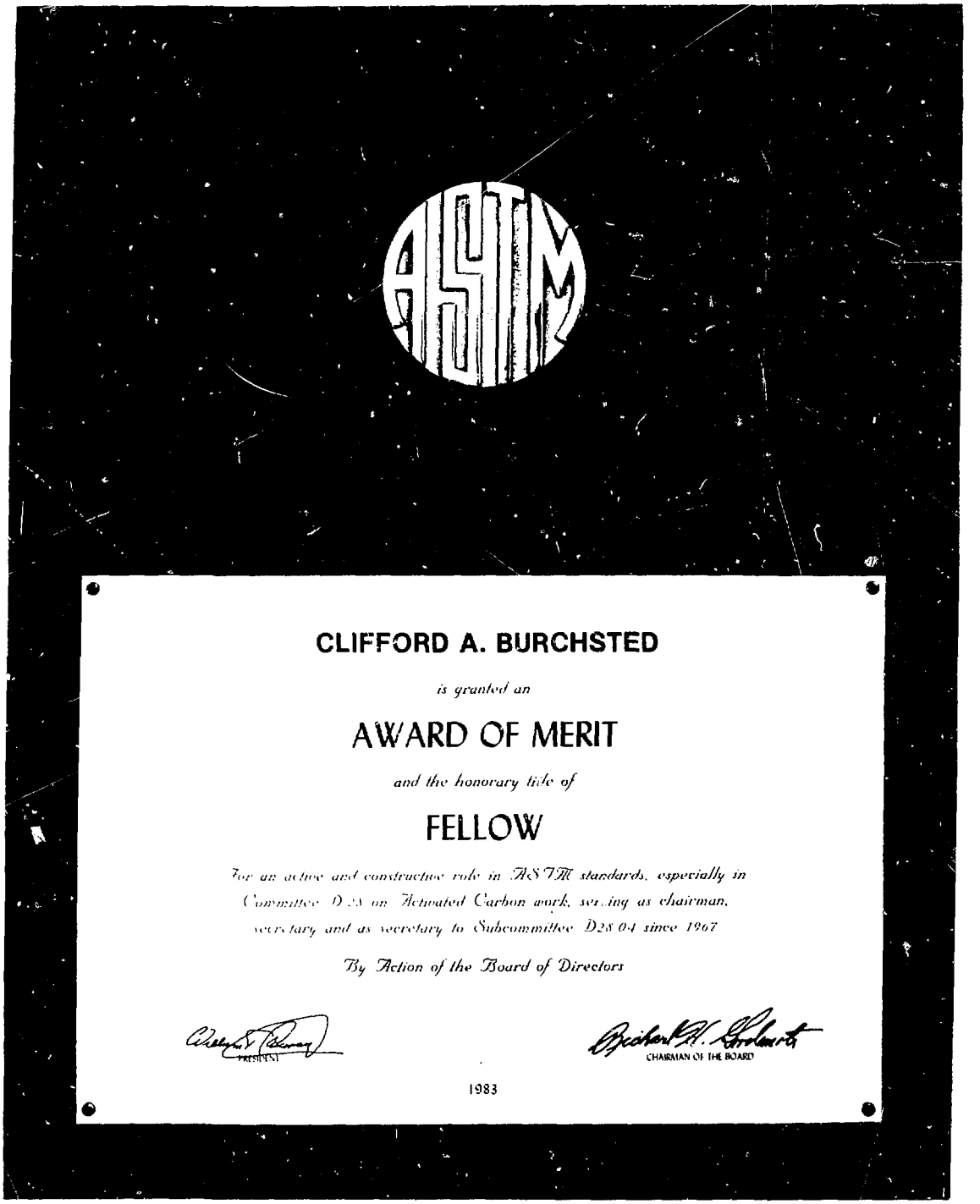

CLIFFORD A. BURCHSTED

is granted an

AWARD OF MERIT

and the honorary title of

FELLOW

For an active and constructive role in ASTM standards, especially in Committee D-28 on Activated Carbon work, serving as chairman, secretary and as secretary to Subcommittee D28.04 since 1967

By Action of the Board of Directors

PRESIDENT

CHAIRMAN OF THE BOARD

1983

TABLE OF CONTENTS

VOLUME I

Session 2

IODINE ADSORPTION AND ADSORBENTS

MONDAY: August 13, 1984
CHAIRMEN: M.J. Kabat
Onatrio Hydro
J.W. Jacox
Jacox Associates

Session 3

PERFORMANCE OF HVAC AND AIR CLEANING SYSTEMS IN NUCLEAR POWER PLANTS

MONDAY: August 13, 1984
CHAIRMEN: A.G. Evans
E.I. duPont de Nemours
J.P. Pearson
Nuclear Consulting Services

Session 4

SOURCE TERMS AND ENVIRONMENTAL IMPACTS

MONDAY: August 13, 1984
CHAIRMEN: A.G. Evans
E.I. duPont de Nemours
J.P. Pearson
Nuclear Consulting Services

Session 5

FILTERS, FILTRATION, AND FILTER TESTING

TUESDAY: August 14, 1984
CHAIRMEN: W.L. Anderson
Consultant
Commission
R.G. Dorman
Consultant

Session 6

RECOVERY AND RETENTION OF AIRBORNE WASTES: PROTOTYPE AND OPERATIONAL SYSTEMS

TUESDAY: August 14, 1984
CHAIRMEN: A.G. Croff
W. S. Groenier
Oak Ridge National Laboratory

Session 7

WORKING LUNCHEON

TUESDAY: August 14, 1984
CHAIRMAN: D.W. Moeller
Harvard School of Public Health

Session 8

FIRE, EXPLOSION, EARTHQUAKE, TORNADO

TUESDAY: August 14, 1984
CHAIRMEN: H.J. Ettinger
S.C. Soderholm
Los Alamos National Laboratory

Panel 9

SOURCE TERM IN RELATION TO AIR CLEANING

TUESDAY: August 14, 1984
MODERATOR: J.L. Kovach
Nuclear Consulting Services

PANEL MEMBERS:
A.P. Malinauskas
Oak Ridge National Laboratory
J.A. Gieseke
Battelle Columbus Laboratory
P.S. Littlefield
Yankee Atomic Electric Company
R.M. Bernero
U.S. Nuclear Regulatory Commission

Session 10

RECOVERY AND RETENTION OF AIRBORNE WASTES: PREPARATION FOR DISPOSAL

TUESDAY: August 14, 1984
CHAIRMEN: C.B. Bastin
R. Philippone
U.S. Department of Energy

Panel 11

BEST AVAILABLE AND MOST READILY AVAILABLE TECHNOLOGY FOR OFF-GAS TREATMENT AND GASEOUS WASTE RETENTION

TUESDAY: August 14, 1984
ARRANGED BY: R.T. Jubin
Oak Ridge National Laboratory
MODERATOR: A.G. Croff
Oak Ridge National Laboratory
PANEL MEMBERS: W.S. Groenier
Oak Ridge National Laboratory
K. Naruki
Tokai Works
W. Hebel
Commission of the European Communities

E. Henrich
Kernforschungszentrum
Karlsruhe

VOLUME II

Session 12

AIR AND GAS CLEANING METHODS

WEDNESDAY: August 15, 1984
CHAIRMEN: W.P. Gammill
J. Hayes
U.S. Nuclear Regulatory Commission

Panel 13

NUCLEAR AIR CLEANING FIELD EXPERIENCES

WEDNESDAY: August 15, 1984
MODERATOR: W.H. Miller, Jr.
Sargent & Lundy

PANEL MEMBERS:
R.R. Bellamy
U.S. Nuclear Regulatory Commission
D.M. Hubbard
Duke Power Company
J.W. Jacox
Jacox Associates
W.R. Lightfoot
Florida Power & Light

Session 14

RECOVERY AND RETENTION OF AIRBORNE WASTES: NOBLE GASES

WEDNESDAY: August 15, 1984
CHAIRMEN: R.R. Bellamy
U.S. Nuclear Regulatory Commission
V. Deitz
Naval Research Laboratory

PANEL 15

PROS AND CONS OF STORAGE AND COLLECTION OF RADIO-KRYPTON, -IODINE, -CARBON AND -HYDROGEN

WEDNESDAY: August 15, 1984
MODERATOR: K.S. Murthy
Pacific Northwest Laboratory

PANEL MEMBERS:
T.R. Thomas
Westinghouse Idaho Nuclear
K. Ebert
Kernforschungszentrum Karlsruhe
P. Mellinger
Pacific Northwest Laboratory
D.M. Wuschke
Atomic Energy of Canada Research

Session 16

HEPA FILTER PERFORMANCE UNDER HIGH HEAT AND HUMIDITY CONDITIONS

WEDNESDAY: August 15, 1984
CHAIRMEN: H. Gilbert
Consultant
J. D'Ambrosia
U.S. Department of Energy

Session 17

SAFETY SYSTEMS PERFORMANCE

WEDNESDAY: August 15, 1984
CHAIRMEN: H. Gilbert
Consultant
J. D'Ambrosia
U.S. Department of Energy

Session 18

RECOVERY AND RETENTION OF AIRBORNE WASTES: RESEARCH

WEDNESDAY: August 15, 1984
CHAIRMEN: T.R. Thomas
S.J. Fernandez
Westinghouse Idaho Nuclear Company

Session 19

OPEN END

THURSDAY: August 16, 1984
CHAIRMEN: M.W. First
Harvard School of Public Health
S. Steinberg
Air Techniques, Inc.

Session I

OPENING OF THE CONFERENCE

MONDAY: August 13, 1984
CHAIRMAN: M.W. First
Harvard School of Public Health

WELCOME AND OBJECTIVES OF THE CONFERENCE
Melvin W. First

KEYNOTE ADDRESSES:

ADVANCEMENT IN REPROCESSING TECHNOLOGY
Clinton B. Bastin

NEW SOURCE TERMS: WHAT DO THEY TELL US ABOUT ENGINEERED SAFETY FEATURE PERFORMANCE
Robert M. Bernero

IN MEMORY OF CLIFFORD BURCHSTED:

INTRODUCTION OF MR. HUMPHREY GILBERT
Melvin W. First

A RECOLLECTION OF MR. CLIFFORD BURCHSTED
Humphrey Gilbert

INTRODUCTION OF MR. JOHN W. LANDIS
Melvin W. First

NUCLEAR STANDARDS: CURRENT ISSUES AND FUTURE TRENDS
John W. Landis

WELCOME AND OBJECTIVES OF THE CONFERENCE

Melvin W. First
Harvard School of Public Health
Department of Environmental Science and Physiology
665 Huntington Avenue
Boston, Massachusetts 02115

It is my pleasant duty as Chairman to welcome you to the first session of the 18th DOE Nuclear Airborne Waste Management and Air Cleaning Conference on behalf of Harvard University and the U.S. Department of Energy (DOE), the two sponsors of this Conference.

For those of you for whom the 18th is the first Conference of this series that you have attended, you will be interested to learn that the Conferences were started in 1950 under the joint sponsorship of Harvard University and the then U.S. Atomic Energy Commission. They continued unchanged during the brief period of the U.S. Energy Research and Development Administration and then to 1982 under the U.S. DOE. The Conferences were originally intended only to assist the U.S. effort in the development of nuclear energy and, indeed, some of the very early Conferences had presentations that were classified. Most presentations in this category were not published and those that were, are now declassified. When it was decided to accept only non-classified papers and to hold the Conference in locations that did not require security clearance for entry, they began to attract non-U.S. scientists and engineers interested in nuclear air and gas cleaning technology who first came as spectators but were soon invited to present papers on their own country's activities in these areas. Although still sponsored by a Department of the U.S. Government, these Conferences have become truly international in scope. On behalf of both sponsors, I wish to make it very clear that we welcome this participation at the meetings and the contributions by those from outside the U.S. to the air and gas cleaning literature that appear in the Conference Proceedings. Indeed, it is only by such world-wide participation in the contents of the Proceedings that the Proceedings have come to be regarded as the most important and most complete respository of information on nuclear air and gas cleaning, and it is available to all.

So, once again, a warm welcome to all newcomers to these Conferences, and a very special welcome to those who came from other countries to expand our knowledge and enrich our fellowship.

Although we have been downhearted by the recent state of the civilian nuclear power industry in the US, there are many encouraging signs that the essential safety of nuclear power is being increasingly accepted by regulatory agencies and more fairly reported in the popular news media. The progress of nulcear power in countries outside the US shows no abatement and there is hope that a new confidence in the safety of civilian nuclear power will be generated in the US.

I am firmly of the opinion that the work of those who have contributed to nuclear air and gas cleaning technology has had an important part in assuring that safety assessment and I look forward to airborne waste management technology generating a similar confidence in the essential safety of current waste disposal plans.

We hope you enjoy this Conference and that you leave Baltimore with important new information plus a renewed confidence in our ability to manage the nation's nuclear enterprises in a thoroughly safe manner.

I would like to take this occasion to thank my Program Committee. The names are listed in the program. They have not only been supportive of the Chairman, but they have taken a leading role in developing the program and will continue to lead by chairing sessions and panels throughout the week. I also wish to thank the Samuel Steinbergs for their assistance with local arrangements.

ADVANCEMENTS IN REPROCESSING TECHNOLOGY
KEYNOTE ADDRESS FOR THE 18TH DOE AIRBORNE WASTE MANAGEMENT AND AIR CLEANING CONFERENCE

Clinton Bastin
Manager, Reprocessing Development
Office of Nuclear Energy
United States Department of Energy
Washington, D.C. 20545

The United States Department of Energy has developed significantly improved concepts for reprocessing nuclear power reactor fuels. These concepts, which build on successful operating experience in DOE reprocessing plants at Hanford, Washington, Idaho National Engineering Laboratory, and the Savannah River Plant, give promise for satisfactory resolution of many of the institutional, technical, and regulatory problems which have hindered reprocessing plant deployment in the U.S. Moreover, the reprocessing concepts allow for plant configurations that are more compatible with likely advanced nuclear power plant deployment plans.

Good reprocessing systems are needed for the U.S. and other nations to obtain full benefit of the potential promise of nuclear power. Reprocessing is needed to isolate and convert highly radioactive fission product wastes to forms most suitable for disposal - and of course reprocessing is essential for deployment of breeder reactor systems.

Many political leaders in the U.S. are in favor of reprocessing. Others have objected - on the grounds that it leads to proliferation of nuclear weapons. This Administration correctly perceives that effective use of nuclear materials is essential for other nations - breeders will be deployed, and fuel will be reprocessed. Table 1 - a synopsis of power fuel reprocessing programs abroad - dramatizes the lack of any impact of the past self-denial of reprocessing by the United States. Other nations are reprocessing, and additional reprocessing is planned.

The U.S. must be a participant if we are to have any voice in what is done to control spread of sensitive technology - and if we are to have a voice in proper safeguards of nuclear materials. The reprocessing technology under development by the Department of Energy provides an excellent base for this participation as well as an excellent base for reestablishing viable reprocessing in the United States.

Advancements in reprocessing technology have been made through concerted effort of Argonne National Laboratory, Allied General Nuclear Services, Battelle Pacific Northwest Laboratory, DuPont Savannah River Laboratory, Exxon Nuclear Company, GA Technologies, Hanford Engineering Development Laboratory, Los Alamos National Laboratory, and the Oak Ridge National Laboratory. Through technology exchange programs, Power Reactor and Nuclear Fuel Development Corporation (PNC) of Japan, and the United Kingdom Atomic Energy Authority have contributed to these advancements.

Since 1978, the U.S. Government's power reactor fuel reprocessing R&D efforts have been combined under the Consolidated Fuel Reprocessing Program. This program is directed by our office; and field management is by the Oak Ridge Operations Office (ORO) and Oak Ridge National Laboratory (ORNL), with the bulk of the R&D being done by ORNL and its subcontractors.

Primary emphasis of the Program has been research and development directed toward reprocessing liquid metal fast breeder reactor uranium-plutonium fuels. A limited effort is focused on reprocessing thorium based fuels, carried out at GA Technologies in San Diego. Most of the Development is generic and applicable to light water and other reactor fuels.

I was pleased to note that the Germans plan to use several advanced concepts similar to ours in their proposed WA-350 reprocessing plant - but a little envious that they appear to be moving ahead with reprocessing so much faster than the U.S. I was in Japan week before last, and learned that PNC has incorporated many advanced concepts similar to ours in their proposed Fast Breeder Reactor Fuel Recycle Pilot Plant.

A major advancement is a new remote operating, sampling, and maintenance concept which is more versatile, provides for remote repair of more complex equipment, and allows repairs or replacements of equipment to be made in a much shorter time. The new remote concept provides greater radiation protection to the workforce, enhances safeguard protection of fissile materials, and minimizes cell penetrations and openings. Many features of the remote systems can be applied to other activities which must be carried out in hostile environments.

The new remote system has six major features: (1) reprocessing equipment installed on "frames" or "modules" with remote connectors on more complex and failure-prone equipment to permit easy disassembly; (2) modules placed along the walls of the cells, with the center aisle open; (3) overhead cranes with lifting devices and a suspended transporter which holds servomanipulators and television cameras; (4) servomanipulators which incorporate several unique features which I will discuss later; (5) television viewing instead of shielded windows and periscopes; (6) and a remotely operated sampling vehicle which operates within the cell or canyon space.

The sampling vehicle travels on a track, stops at designated processing or accountability locations, obtains a sample and replaces an empty sample vial, then delivers the sample tray to a central station where filled sample vials are sent to an analytical laboratory. This eliminates expensive sample galleries, and reduces personnel exposure to radiation.

The new servomanipulator systems for future reprocessing plants have three unique features which will permit significantly improved maintenance. They have force feed back, so that an operator will have feel of the tasks he or she is performing. Variable forces from 1 to 50 pounds can be handled, with forces proportioned down to prevent tiring of the operators. The new servomanipulators have an "elbows down" configuration like a human being, which allows the manipulator to reach into modules. Through the wall master slave manipulators presently used in hot cells have the elbows up configuration which were designed for table top operation and are not versatile for large-cell usage. The new manipulators use gears and torque tubes instead of tape and cable drives used in the present manipulators. Tape and cable drives are prone to failure and must be decontaminated before they can be repaired using contact maintenance. However, the use of gears and torque tubes permits the advanced servomanipulators to be modularized so that one arm can repair the other, in place, by simply replacing the faulty module such as a wrist or arm.

Those developments have been made possible in many cases because of the many advancements in electronic technology which has miniaturized very reliable components. Most of the equipment described uses digital controls. During my visit in Japan, I saw the new high resolution television system developed for use by PNC. This system, which has 25 times the resolution (number of lines) of conventional television, will greatly facilitate viewing of operations and maintenance tasks. A radiation-hardened version of this system is under development.

Major advancements have also been made in reprocessing equipment. A very important one is development of advanced centrifugal solvent extraction contactors. These were originally developed at the Savannah River Plant and have been used successfully in a reprocessing plant there for several years. Argonne National Laboratory and Savannah River Laboratory designed and fabricated smaller units for 0.5 tons heavy metal per day and 0.1 tons heavy metal per day capacity visualized for breeder fuel reprocessing. Experimental work has shown these units can be used in all three cycles of Purex reprocessing thus replacing tall pulse columns and saving plant construction costs. Most importantly, centrifugal contactors have rapid response, coming to steady state operation in a matter of minutes compared to several hours for mixer settlers and several days for pulse columns. The short contact time also minimizes radiation damage to solvent and permits processing of higher radiation level fuels. The new centrifugal contactor design incorporates remote maintenance features to permit rapid replacement of failed parts.

Breeder fuels differ from LWR fuels in that the fuel pins are encased in a stainless steel shroud. A system has been developed which uses a laser to cut the end fittings and slit the shroud so this metal can be removed and permit the shearing of the fuel pins directly.

A remotely operable and maintainable shear has been developed. This shear is hydraulically powered with the main hydraulic system outside the cell. The in-cell portion of the shear is in modules which can be easily replaced if parts fail. It can handle both LWR and breeder reactor fuels.

Another significant development is a continuous dissolver. Its primary advantage is the large capacity achievable through continuous operation. It also minimizes the surges of off-gas when the acid first hits the spent fuel and its washing action dissolves the fuel from the cladding more rapidly. The dissolver is a cylinder which is divided into compartments; the fuel is moved by baffles which transfer the fuel from one compartment to the next when the direction of rotation is reversed. The cylinder is mounted on rollers in a sealed steam chest. Acid is introduced in a countercurrent direction. The hulls are monitored as they are discharged. The rotary dissolver is also designed for remote maintenance.

Developments in off-gas processes are largely completed and have been the subject of several papers through the years at this conference. Our work on this process is largely completed but we are continuing to perform work on krypton ion implantation at Battelle Pacific Northwest Laboratory in Richland. This process, which has also been described at previous conferences, promises a more permanent and stable way of storing krypton than in cylinders.

The advancements in reprocessing technology that I have discussed - maintenance features on the equipment components and systems, electromechanical servomanipulators, in-cell automatic sampler - minimize cell penetrations and openings and are compatible with a sealed-cell, low-ventillation-flow concept. Although there are uncertainties in how contamination will build up, we believe the low-ventilation-flow concept should be pursued since it may provide a more positive control of plant effluents. It allows use of an inert atmosphere and helps in cell atmosphere temperature control. There should be particular interest in this conference in a facility concept which has ventilation requirements of a few thousand cubic feet per minute compared with the normal few hundred thousand cubic feet per minute.

Prototypical reprocessing equipment incorporating the advanced concepts has been fabricated and testing has recently started in the Integrated Equipment Test Facility at ORNL. The testing program is in two parts, one for remote operation, sampling, and maintenance, and the other for integrated process tests. Our test facilities incorporate state-of-the-art instrumentation and computerization, and will serve as a basis for major improvements in reprocessing plant safeguards.

Final steps in the Department of Energy's reprocessing development program will be a "hot" test with irradiated breeder reactor fuel. Conceptual design on such a test capability - which we call "Breeder Reprocessing Engineering Test", or BRET - has been ongoing over the past year.

BRET and the incorporated advanced reprocessing technology can provide a technical framework for U.S. participation in international cooperation in reprocessing technology, including the important goal of formulating adequate safeguards on an international basis. The advanced reprocessing technology provides an excellent base for reestablishing viable reprocessing in the United States.

TABLE 1

SYNOPSIS OF POWER REACTOR FUEL REPROCESSING*

OUTSIDE THE U.S.

Country	Facility	Present Capacity MgHM/yr.	Planned Capacity MgHM/yr.	Comment
Argentina	Ezeiza	0	1	HWR fuel pilot plant under construction; scheduled startup 1986.
Belgium	HERMES	0.5	0.5	Hot chemistry LWR and FBR fuel plant
	Eurochemic	0	0	12.5 MgHM/yr. LWR fuel facility closed in 1974. Future startup with expansion to 30 MgHM/yr. being considered.
Brazil	Rio de Janerio Area	0	0.5	Hot chemistry LWR fuel plant under construction.
Canada	Whiteshell	0.01	0.01	Hot chemistry CANDU/thorium fuel pilot plant.
China				China has nuclear explosive materials reprocessing capability which may be adaptible for power fuels.
Federal Republic of Germany	Milli	0.01	0.01	Hot chemistry LWR & FBR
	Jupiter	0	0.1	HTGR fuel pilot plant awaiting license for startup
	WAK	10	10	LWR fuel pilot plant
	WA-350, sites in Baveria and Lower Saxony under consideration	-	350 LWR	Proposed construction start 1985, hot operation 1992.
France	UP1-Marcoule	0	400-450	Presently used for nuclear explosives materials reprocessing, but being modified for Magnox type fuel.
	UP2-LaHague	250-400 LWR or 800 Magnox	800 LWR	Expansion program scheduled for completion in 1988.
	UP3-LaHague	-	800 LWR	Under construction; completion scheduled for 1990.
	AT-1 (LaHague	0.1	0.1	Hot chemistry FBR fuel pilot plant.
	SAP/TOR (Marcoule)	1	5	LWR and FBR fuel pilot plant-TOR head-end provides higher thruput.
	PURR (Marcoule	-	50-100	FBR fuel plant has been under consideration, but construction deferred

Table 1 - continued

Country	Facility	Present Capacity MgHM/yr.	Planned Capacity MgHM/yr.	Comment
India	PREFRE (Tarapur)	25	25	LWR, HWR and "research" reactor fuels plant
	Kalpakkam	-	25	Under construction; scheduled for startup mid 1980's. Includes small FBR fuel capacity.
Italy	EUREX	5	5	LWR fuel pilot plant
	ITREC	1	1	FBR and thorium fuel pilot plant
Japan	Tokai-LWR	35	35	
	JNFS-No site	-	800	Planned early 1990's
	Chemical Processing Facility (Tokai)	0.01	0.01	Hot chemistry FBR fuel pilot plant
	FBR Fuel Recycling Pilot Plant	-	6	For MONJU FBR fuel
Pakistan	Rawalpindi	0.5	0.5	Hot chemistry HWR fuel pilot plant reported to be under construction
	Chasma	-	15	
USSR	Khlopin Radium Institute, Leningrad	0.1	0.1	LWR fuel pilot plant
	?	?	?	LMFBR fuel pilot plant
	?	?	?	East European nation and other purchaser of USSR LWR reactors will return spent fuel to USSR, but no information available on facilities or facility plans.
United Kingdom	Sellafield (Windscale) - Magnox	2000	2000	
	Sellafield - LWR	-	Small	25 ton/yr. Facility closed in 1973; may be operated for R&D.
	Sellafield - THORP (LWR/AGR)	-	1200	Parts under construction. Completion scheduled 1989 or later.
	Sellafield Pilot Plant	0.1	0.1	Hot chemistry to support THORP
	Dounreay	1	1	FBR fuel pilot plant

NEW SOURCE TERMS: WHAT DO THEY TELL US ABOUT ENGINEERED SAFETY FEATURE PERFORMANCE

Robert M. Bernero
Director, Division of Systems Integration
U.S. Nuclear Regulatory Commission

Abstract

The accident behavior models which are the basis of engineered safety feature design are generally simple, non-mechanistic and concentrated on volatile radioiodine. Now data from source term studies show that models should be more mechanistic and look at other species than volatile iodine. A complete reevaluation of engineered safety features is needed.

There are more than 100 nuclear power reactors operating or close to operating in the United States today. These reactors are a single generation with respect to the general basis for their design of engineered safety features. The models of accident behavior used for these reactors can be traced back 20 years. These models were used to describe accident behavior and thereby controlled the design of engineered safety features. Not only did these models control the design but through that control they influenced the development of the data base for the designs. One example of that influence is the current work on a round robin test program for nuclear carbon filters, which I believe was reported in a paper yesterday afternoon.

What then were these original models of accident behavior which still affect so much today? The principal one is described in TID-14844,[1] which has served as the technical basis for many U.S. regulatory decisions. This document was published in early 1962, to be used as a technical basis for regulatory decisions regarding the siting of nuclear reactors, and thereby became a very important basis for the design of containment and related engineered safety features. These early models, in TID-14844 and related work, were developed in an era when few power reactor designs were available to analyze, and the reactor accident experience was dominated by the Windscale reactor accident of 1957. Thus, it is not surprising that early models were rather general, not very mechanistic, and focussed on the transport and release of radioiodine as the principal interest. The use of these models was most significant in the 10CFR Part 100 dose calculation. This calculation, which has been made for every power reactor in the U.S., simultaneously challenges the reactor containment with the pressure and temperature loads of the largest loss-of-coolant accident and the fission product release of a core melt as derived from TID-14844. The source term or accident release of interest here is the release from the fuel and reactor coolant system into containment. Later one is interested in the release or source term for the environment.

Given these combined loads, and assuming the tested leak tightness of the containment, the analyst must show that people offsite will not suffer unacceptable radiation doses to the whole body or the thyroid, even in bad meteorological conditions. From this postulated set of conditions we get some expected sensitivities. From the loss-of-coolant accident conditions we get very high humidity, especially important if we use charcoal filters as engineered safety features. From the TID-14844 we get a lot of volatile iodine. It is not surprising that in all the years of these calculations it was the thyroid dose, the radioiodine contribution, that controlled. Our attention, and our engineered safety features, concentrated on controlling radioiodine. We have installed charcoal filters and used chemical additives to containment spray to enhance iodine capture. We have imposed very tight leakage requirements on very large containment buildings and built a system of emergency response which concentrates on radioiodine release. We have even considered the distribution of potassium iodide tablets to the general public to block the intake of radioiodine.

And then on March 28, 1979 the worst light water reactor accident in the U.S. power industry occurred. Many of you probably participated as I did in the response to and the study of that accident. You may recall that in the response to that accident we kept projecting the release of radioiodine and looking for it, but did not find it. We learned quite a few lessons from that TMI accident, and are still learning some today. We say that, in spite of the many safety design features, a minor mishap could escalate into a serious core damage event. We saw the importance of operator error in the cause of accident, and of operator prudence in the recovery from accident. We saw 50% cladding reaction produce so much hydrogen that its ignition produced a vigorous pressure pulse in containment, while our rules of calculation[2] showed less than 5%. We saw the humidity of loss-of-coolant accident, but no direct containment leakage. We saw much radioiodine apparently release from the fuel but after the hydrogen combustion and containment spray of the first day we saw no iodine in the containment atmosphere, and essentially none released.

Many wanted to conclude from the TMI-2 accident and other accident experience that there would be no significant release from a light water reactor in a severe accident. The NRC and others chose to take a hard scientific look at the matter, to revise our models accordingly, to reexamine our regulatory analysis and to follow to conclusions which could be supported by the scientific evidence.

The first step in this effort was completed with the publication of NUREG-0772[3] in 1981, the NRC's first evaluation of LWR severe accident behavior since the Reactor Safety Study[4] of 1975. The Reactor Safety Study had begun the work of reassessing core melt behavior in a much more mechanistic way than TID-14844 but lacked the time or the resources to pursue detailed questions of fission product form and transport. In 1981 NUREG-0772 did not provide a new source term or source terms for reactor accidents but it did provide a solid technical basis for the direction of NRC's source term reevaluation.

By the end of 1982 there was so much source term related work going on under NRC sponsorship and by others, that the NRC formed a special Accident Source Term Program Office (ASTPO) to coordinate the work. I have had the privilege of directing that office. To bring the source term work to a useful conclusion we set up a program of four elements. The first two of these elements are essentially complete now, the third is nearing completion, and the fourth element, the reassessment of source terms, will be published for comment early next year. This four-element program is based on recognition of the complexity of source terms. If we define severe accidents as those in which severe core damage or core melt takes place, we must recognize that severe accident behavior and attendant fission product transport will be unique to each different accident scenario in each different type of reactor used in this country. This complicates the process of evaluation by requiring the consideration of a broad range of physical conditions in accident scenarios such as core melt taking place at different reactor coolant system pressure levels, with different amounts of water at different places in the reactor system and the containment, etc. This complexity is compounded then when you move to the different reactor and containment system designs we use in this country. We have pressurized water reactors (PWR) and boiling water reactors (BWR). We have three PWR vendors, each with some variation in the product line offered. Containments for PWRs include large dry, subatmospheric, and ice condenser designs. The large BWRs, although sold by a single vendor have many variations, including three basically different containment system designs. All of this complexity means that for each design and each scenario there is a unique source term, almost too many to number. The challenge for the analyst is to explore the range to determine just how different one is from another. The problem becomes much more tractable if many such source terms are adequately represented by a single description, for example, one of the release categories of the Reactor Safety Study. In the face of this complexity the NRC has pursued a source term reevaluation program which considers the range of designs and scenarios.

The first element of the four-element program was to gather together the many sources of data and analysis upon which one can base estimates of fission product behavior in the course of a severe accident. This data base is relatively large, diverse, and is still growing. Earlier this month Test 1-3 was run in the Power Burst Facility reactor at the Idaho National Engineering Laboratory. This test subjected a bundle of high burnup reactor fuel to actual core melt conditions, up to about 2500°K, with extensive monitoring of its behavior and its releases. This test is one example of the continuing growth of the data base which is the foundation of our models for reevaluation and later the confirmation of that work. A compendium report of the data base has been prepared by Oak Ridge National Laboratory and will be released shortly as ORNL/TM-8842.

The second element of the NRC source term program is the calculation of radionuclide release under specific LWR accident conditions. The principal part of this work has been performed by Battelle Columbus Laboratories under NRC contract. The results of this work are just now being published as draft volumes of BMI-2104.[5] The Battelle work analyzes accident sequences in six reference plants which cover the spectrum of U.S. designs. They include three PWRs; Surry (subatmospheric containment), Zion (large dry containment), and Sequoyah (ice condenser containment), and three BWRs; Peach Bottom (Mark I

containment), Grand Gulf (Mark III containment), and Limerick (Mark II containment). The Limerick plant was added to the list quite recently and its report will be published a little later this year. These Battelle analyses are not intended to be comprehensive accident sequence and risk assessments of these plants. Rather they are analyses of specific accident conditions, chosen to cover the range of interest for all plants so that others could develop groups of sequences, related to these, to characterize the risk of any plant. The Battelle reports being published now have already undergone extensive peer review, but are being released as drafts to encourage even wider comment.

And that brings me to the third element of the NRC source term program, peer review. As I said before source terms are important to regulatory decisions. The experience of TMI and the analysis in NUREG-0772 both suggest that substantial reductions in regulatory source terms may be in order. The NRC is not willing to make any leap of faith to adopt lower source terms. The technical basis for such revision must be painstakingly developed - and thoroughly reviewed to ensure that no unfounded regulatory positions are taken. In addition, a thorough, public review process by its very nature makes the work and the use that can be made of it open to the general public. The peer review of the NRC source term work comes from many sources. First, there is independent work of a similar nature being performed by peers in the field. Examples are the studies on four of the same plants being conducted by the Industry Degraded Core Group (IDCOR) and the technical studies of a special committee of the American Nuclear Society under Dr. William Stratton. NRC and its contractors are following these activities very closely and comparing their models and their results to those we have sponsored. There is a substantial amount of severe accident research going on in foreign countries too; we are taking great care to follow this work as well.

In addition to regular comparison with similar work by others, the NRC source term work has been undergoing structured peer review. All through 1983 and into 1984, the BMI-2104 work was presented and reviewed step by step with a selected panel of experts in public meetings. And then in mid 1983 the American Physical Society, under a grant from the NRC, formed a Source Term Study Group to review the scientific basis for source term estimation. That Study Group is chaired by Professor Richard Wilson of Harvard University. They have been reviewing this work since last year and are now preparing their evaluation. We expect to see the American Physical Society report at the end of 1984. With it we feel that the scientific basis of the source term work will have received an acceptable level of peer review.

The first three elements of the source term work then are; one, the gathering and identification of the data base for source term estimation, two, the use of that data base to calculate releases under specific accident conditions, and three, the thorough peer review of the work. What then is the fourth element? Element 4 of the source term work is the use of the new fission product behavior information to reevaluate the spectrum of severe accident releases from a plant or, in other words, to reevaluate the risk of that plant. To assess the risk of a plant a synthesis of fission product transport estimates and other factors is needed. The first thing needed is a list of the important accident sequences for the plant along with their

frequencies of occurrence. Then for each accident sequence one must estimate the likelihood of different modes of containment failure. The containment failure path has very great significance for the release estimate. Then, with a tabulation of accident sequences and containment failure outcomes, one can add the fission product transport appropriate to the scenario and generate a listing of accident releases and their frequencies. Such a listing is the input to a risk code such as CRAC, and defines the public risk from the plant. For the six reference plants being studied in the NRC source term studies, there already exists a probabilistic risk assessment (PRA). In addition, the NRC-sponsored Accident Sequence Evaluation Program (ASEP) is reviewing the accident frequencies for these plants and correcting them to reflect later knowledge and things like the post-TMI changes. In the containment area important new work is taking place. For years PRAs have modelled overpressure failure of reactor containments an ultimate strength bursting, somewhat like the bursting of a balloon. Only in the past year or so have analysts begun to construct and obtain data for leak-before-break models. These models are much more suitable for treating the complexities of overpressure and overtemperature behavior. The NRC has formed two working groups to obtain the best estimates of containment behavior. The Containment Loads Working Group is developing the estimates of the pressure and temperature challenges to the containment. The Containment Performance Working Group is developing the estimates of the mechanical response of the containment to these challenges.

As the results of this work are becoming available the product of Element 4 is taking shape. It is a sequel to NUREG-0772 and will be called NUREG-0956, a Reassessment of the Technical Bases for Estimating Fission Product Behavior During LWR Accidents. NUREG-0956 will pull together all of this work with its uncertainties and assess the risk and regulatory significance of it all; it will be published in draft form for public comment shortly after the release of the American Physical Society report. That should be very early in 1985.

If the results of all this work won't be complete until early next year, what can we say now about their effect on engineered safety feature performance? Right now I think the volumes of BMI-2104 are a very useful source of information. If we look there now we can see that many of the old models are substantially incorrect. In many sequences the relative humidity is not so close to saturation. In all of the sequences most of the radioiodine moves as the salt, cesium iodide, and not as one of the more volatile forms. Aerosols, inert aerosols, appear in abundance in many sequences. Although the total quantities available for release appear to be substantially lower, different elements compete with iodine for importance. Our old practice of using radioiodine as the controlling form of radioactive release is no longer valid. I urge your attention to these reports now. When this work is completed next year a substantial reevaluation of engineered safety features is warranted.

References

(1) DiNunno, J. J., et al., "Calculation of distance factors for power and test reactor sites," TID-14844, March 23, 1962.

(2) Title 10, Code of Federal Regulations, Part 50.44.

(3) NUREG-0772, "Technical bases for estimating fission product behavior during LWR accidents," June 1981.

(4) WASH-1400, NUREG-75/014, "Reactor safety study -- an assessment of accident risks in U.S. commercial nuclear power plants," October 1975.

(5) Gieseke, J. A., et al., "Radionuclide release under specific LWR accident conditions," BMI-2104, Vols. 1-7, Battelle Columbus Laboratories, July 1984.

DISCUSSION

HULL: As a minor correction, I should indicate that Windscale was an air-cooled not a gas-cooled reactor. My question is; Can you estimate when the current source term study might lead to some modification of the emergency planning zone?

BERNERO: Yes, quite true about Windscale. I was trying to contrast gas (air)-cooled vs. water-cooled for effect on soluble species such as iodine. The current source term studies will culminate with the publication, in early 1985, of NUREG-0956 which will recommend prompt reconsideration of emergency planning requirements. How long it will take to get it into the regulatory and political process is difficult to say. For interesting new insights on emergency planning see NUREG-1062 and NUREG-1082 (to be published in about 60 days) which are based on WASH-1400 source term. Prompt attention is being given to this work and the conclusions reached just as fast as they are published. There have been public meetings and public peer review. They enable all, whether against or in favor of nuclear power, or neutral, to see what's going on, to hear what's going on, and to have very prompt access to it. If I were to guess at all, I would say next year, with the availability of formal positions being taken by the NRC, formal positions possible by others as well, that you could expect to see a prompt address of this information.

KAISERUDDIN: What do you see as the major impact(s) of the new studies on the U.S. reactors which are operating, or are in advanced stages of construction?

BERNERO: The principal impacts on operating reactors and near term operating licenses will be in changed perceptions on emergency planning and on possible relaxation of requirements for engineered safety features, such as containment leak rate testing, iodine filtration, etc. If nothing else, our emergency planning regulation says, "a planning radius of ten miles", but most people have interpreted it to be an evacuation radius. I have been trying to argue people out of that for a number of years. It is supposed to be "planning", not necessarily evacuation. I think the new information, even if it doesn't change the radius at all, will give people the appropriate perspective, that the focus of attention is at the fence, not 10 miles away from the fence. If you look at the new data, the new analyses, you will find that even in the first half mile or mile, noble gases and things like that make you want to pay attention. If you ever get in extremis, and have releases, those are the people you need to worry about with a sense of promptness. The people out at 10 miles have a great deal of time, even with the old analyses, to deal with a matter of very low probability. So what I see is at least a very substantial tempering of our safety understanding. Reactors just aren't as risky as they have been portrayed in the reactor safety study.

INTRODUCTION OF MR. HUMPHREY GILBERT

by

Melvin W. First

Our program has been didicated to the memory of Clifford Burchsted whom, I'm sure, most of you knew not only personally but through his writings as well. We have invited Mrs. Burchsted to come and be with us this morning during this program and I am delighted that she is here in the audience. She wrote me a letter recently and asked if I would read it. She said:

> "My sincere thanks for your invitation to attend the air cleaning conference as a guest. I look forward to hearing Humphrey Gilbert's memory of Clifford Burchsted and the memorial lecture that follows. Among Cliff's greatest satisfactions was his work with the various technical society committees, the air cleaning conferences, and the Harvard air cleaning workshop. He certainly treasured his friendship with all his associates in these various activities. Thank you for your kindness. Sincerely yours, Betty Burchsted (Mrs. Clifford A. Burchsted)."

Our first speaker in this section of the program is Mr. Humphrey Gilbert who is a consultant in the field of nuclear air and gas cleaning technology. Prior to his becoming a consultant, he was an empolyee of the Division of Safety of the original Atomic Energy Commission, starting at the time of the Manhattan Project, and he continued in this activity until his retirement a few years ago from the successor agency. His retirement was not in any sense a withdrawal from his technical work but merely a transfer to another sphere. Humphrey Gilbert was a leader in the development of nuclear safety through air and gas cleaning developments, starting from the very beginning of this activity. Certainly, he had a enormous influence on, and hand in, the development of the high-efficiency particulate air filter that we know today as the HEPA filter, and he has had an important role in the development of nuclear carbon for the adsorption of volatile iodine. Not only did he help in the development of the technology, but he constantly urged all of the installations that were under the control of the Atomic Energy Commission to improve their facilities and bring them up to a satisfactory standard. If we were to choose one important thing, out of many that he has accomplished, in my opinion, it would be his continual emphasis of the role of safety and the influence he has had in making all the sites much more safety-conscious, as well as safe.

A RECOLLECTION OF MR. CLIFFORD BURCHSTED

(A Memorial)

Humphrey Gilbert
Consultant
McLean, Virginia

Clifford A. Burchsted, "Cliff" to his friends and associates, was engaged in the air cleaning field for 16 years. In that period of time he established a record of performance and achievement rarely accomplished in several decades of endeavor.

Upon his entry into air cleaning in 1967, there were only two manuals available in the high-efficiency area, a small elementary booklet on filter installation and maintenance[1] and a treatment of British systems by White and Smith[2] of the United Kingdom Atomic Weapons Research Establishment at Aldermaston. A more detailed manual on high-efficiency air cleaning was considered necessary for the use of the national nuclear energy program. The Atomic Energy Commission (AEC) referred the need to their Oak Ridge Operations Office. It was delegated, in turn, to the Oak Ridge National Laboratory (ORNL) where Cliff Burchsted and A. B. Fuller were enlisted to compile and edit the publication. They completed their assignment and the original edition of the manual was issued in 1970.[3] Cliff likewise was senior editor for a revised edition of the manual published in 1976.[4]

Clifford Arnold Burchsted was born August 19, 1921, in Braintree, Massachusetts, received his B.S. degree cum laude in industrial and mechanical engineering from Northeastern University, Boston, Massachusetts, and in 1959 he earned an M.S. degree summa cum laude from the University of Tennessee. Cliff served with the U. S. Army Air Corps from 1942 to 1946 during World War II and then was an engineer in 1948 with Tuttle and Bailey of New Britain, Connecticut. Later in 1948 he became a plant engineer with Sample Durick Company, Chicopee, Massachusetts. In 1952 he joined Oak Ridge National Laboratory.

During his tenure at ORNL, Cliff served on a significant number of committees of national standardizing bodies, the American Society for Testing and Materials (ASTM), American National Standards Institute (ANSI), and American Society of Mechanical Engineers (ASME), for example. This stood him well. It provided him with ideal experience for his subsequent association with the air cleaning field. In fact, Clifford was particularly well qualified for the technology. He became very interested in air cleaning and his association with the pursuit was a highly compatible relationship from the beginning. He had a sharp and retentive mind and often was able to supply from memory the specific details of certain codes and standards needed at the moment. He was a readily available compendium of codes and standards.

Cliff's affiliation with air cleaning seemingly was brief. During that short period, however, his interest and effort were unabated. He was most energetic, never refusing a committee assignment and often volunteering, usually to be secretary of the committee, a tedious position rarely sought. Yet, he performed in a timely and effective manner.

In his association with air cleaning, Cliff charted an enviable record of performance and achievement. He was a fellow of the American Society of Mechanical Engineers. In 1974 he received the Monroe Seligman award of the Institute of Environmental Sciences for his contributions to air cleaning. He was named a fellow of the Royal Society for Health, United Kingdom. He produced the first standard on nuclear-use activated carbon for the Atomic Energy Commission. He lectured at the industrial ventilating conference of the University of North Carolina and annually at air cleaning workshops conducted by Harvard University School of Public Health. He served on committees of the American Society of Mechanical Engineers, American Society for Testing and Materials, the American National Standards Institute, and the American Association for Contamination Control. In addition, he was able to present eleven papers to various nuclear air cleaning conferences and one to a symposium held at the United Nations in New York City by the International Atomic Energy Authority. He still found time to serve as advisor to the Boy Scouts Explorers of Clinton, Tennessee, and he chaired the local Citizens Advisory Committee. His last task was secretary of the committee to formulate policy for filter test facilities of the Department of Energy.

In retrospect, he did well. His service and accomplishment have accorded the air cleaning field a lasting endowment.

References

1. Gilbert, H., and Palmer, J.H., High Efficiency Particulate Air Filter Units, Inspection, Storage, Handling, and Installation, TID-7023, August 1961, National Technical Information Service (NTIS), Springfield, VA 22161.

2. White, P.A.F., and Smith, S.E., High-Efficiency Air Filtration, 1964, Butterworths, London, England.

3. Burchsted, C.A., and Fuller, A.B., Design, Construction, and Testing of Air Filtration Systems for Nuclear Application, NSIC-65, 1970, NTIS.

4. Burchsted, C.A., Fuller, A.B., and Kahn, J.E., Nuclear Air Cleaning Handbook, ERDA 76-21, 1976, NTIS.

INTRODUCTION OF MR. JOHN W. LANDIS

by

Melvin W. First

John W. Landis is senior vice president and a director of Stone & Webster Engineering Corporation of Boston, Massachusetts. His responsibilities include worldwide business development, governmental relations, advance technology, liaison with professional societies and trade associations, and public information. He is a licensed professional engineer and a member of the National Academy of Engineering.

Before joining Stone & Webster early in 1975, Mr. Landis held various executive positions with two power-system suppliers, Gulf General Atomic Company (a division of Gulf Oil Corporation) and The Babcock & Wilcox Company. As group vice president and then president of Gulf General Atomic from 1968 to 1975, he was in charge of the development and commercialization of three types of advanced nuclear power systems, including basic components and services. From 1965 to 1968 he was general manager of B&W's Washington (D.C.) operations. In twelve previous years with B&W he had risen from director of customer relations in the Atomic Energy Division to manager of that Division. His major accomplishments included obtaining B&W's initial nuclear-power contracts, establishment and management of the Lynchburg nuclear complex, and overall supervision of several pioneering nuclear-power projects, including the Consolidated Edison Thorium Reactor (Indian Point 1), the N.S. Savannah, and the Advanced Test Reactor.

Prior to 1953 he was a reactor and project engineer for the Atomic Energy Commission, and independent consultant in guided missiles and nuclear energy, head of science and engineering test development for the Educational Testing Service, a Navy ordnance officer during World War II, and a research engineer with Eastman Kodak Company.

For many years Mr. Landis has been active in the effort to establish uniform standards in the energy industry. He was a director of the American National Standards Institute from 1968 to 1980 and president of the Institute from 1975 to 1978. From 1966 to 1971 he was vice chairman and then chairman of the Institute's Nuclear Technical Advisory Board and from 1969 to 1974 chairman of its Nuclear Standards Policy Committee. He is now a trustee of the Institute's International Fund.

In his capacity as chairman of the Environmental Protection Committee of the United States National Committee of the World Energy Conference, Mr. Landis is a leader of the nation's anti-pollution movement. He is also a director of the USNC.

Mr. Landis was one of the founders of the American Nuclear Society and has served the Society in many capacities, including treasurer, vice president and president. He was elected a fellow in 1966 and currently is chairman of the Public Education Program Advisory

Committee, finance chairman of the NEED Committee, and a member of the Standards Steering and Standards Policy Committees.

He is also a fellow of the American Society of Mechanical Engineers.

Chairman of the Board of Trustees of Randolph-Macon Woman's College, a trustee of Lafayette College, and a member of several university advisory committees, Mr. Landis continues to devote a substantial amount of time to improving the nation's educational system. He is a charter member of the Republican Senatorial Inner Circle and of the Republican Presidential Task Force. He has been a director of Central Fidelity Banks, Inc. since it was organized in 1970.

Mr. Landis was graduated from Lafayette College summa cum laude in 1939 and received an honorary Doctor of Science degree from the College in 1960 for his contributions to the development of nuclear power. The George Washington Kidd award, which memorializes the College's first graduate, was presented to Mr. Landis in 1972 in recognition of his "distinguished accomplishments in nuclear engineering". He is a member of Phi Beta Kappa, Tau Beta Pi, Sigma Xi, Omicron Delta Kappa and Pi Delta Epsilon.

He has been awarded eleven prizes and fellowships and has written over 120 papers and given over 300 addresses on technical subjects. He has served on the boards of numerous educational, charitable, trade and civic organizations, and as a member of ten federal and state government advisory committees. He is currently a member of the Department of Energy's Energy Research Board.

NUCLEAR STANDARDS: CURRENT ISSUES AND FUTURE TRENDS

John W. Landis
Senior Vice President
Stone & Webster Engineering Corporation

Clifford Burchsted Memorial Lecture

I am indeed grateful for the opportunity you and your Conference Committee have given me to add another voice to the many raised today to honor the memory of a departed colleague whose life and works are an inspiration not only to all who knew him personally but also to many who knew of him and took the time to review his distinguished technical publications and standards activities.

It is particularly pleasing to note that the audience for my brief remarks is such a large group of eminent and influential scientists and engineers. This observation encourages me to try to initiate a dialogue today rather than just state my own beliefs and opinions -- which are largely derived from the beliefs and opinions of the people with whom I have been associated in the standards movement during the past three decades. I therefore invite those of you who have comments to make on my discourse to relay them to me either right after this morning session ends or during breaks in the afternoon program. I would sincerely appreciate your input.

My presentation will be, first, a summary of the important issues that currently face us in the nuclear-standards field, and, second, a concise discussion of how each of these issues is being -- or can be -- resolved.

To clarify my thoughts as much as possible, I shall put the issues in question form, listing them not in the order of their importance but in an order that hopefully knits them into a coherent whole. Listening to the gamut of issues prior to hearing a digest of the proposed solutions and implementing actions should help you cross the many bridges that interconnect them.

Although I realize that a number of you are well-versed -- indeed expert -- in the development and use of standards, and that you probably have at least as deep an appreciation of the vital role that standards play in our lives as I have, I cannot resist the temptation to spend two or three minutes, prior to getting into the main body of my presentation, outlining some personal views on standards.

Standards are one of the main foundations of modern civilization in that they condense in documentary form the vast technological experience that man has accumulated. This experience

has been obtained primarily from commercial operations, not experimentation in laboratories. Thus, standards to a great extent spring from what scientists, engineers, craftsmen and allied workers have learned in the past, and in turn standards determine the nature and quality of most of the materials, equipment and facilities we use today -- not to mention how we use them.

Properly developed standards produce great economic benefits by:

- Establishing, and gradually raising, acceptable levels of performance, reliability and safety.
- Increasing productivity and reducing overall costs.
- Simplifying and routinizing many commercial and technical operations so that maximum effort can be devoted to improvement and innovation.
- Minimizing environmental effects.
- Expediting licensing.
- Providing a rational basis for contracts.
- Reducing misunderstanding between suppliers and users.
- Expanding both international and intranational trade.
- Fostering new applications of existing technology.

Standards should not be used, except in very unusual circumstances, to introduce new ideas, methods, materials, equipment or facilities. This would be a clear case of "putting the cart before the horse". Since the quality of modern life, not to mention modern life itself, depends in large measure on the validity of the standards we adopt, we must be extremely careful to base them on germane experience, sensible interpretation and logical generalization and to insure their acceptance by all interested parties. This is especially true in view of the fact that standards developed by the voluntary consensus standards system utilized in the United States and many other countries are often incorporated into codes used by local, state or national-government agencies to regulate various business activities.

In other words, standards are normally derived or developed from commercial experience well after commercial feasibility has been demonstrated; they underpin the economic viability of industrialized nations; and because they have such a profound effect on our lives they must be drafted prudently and judiciously by a cross-section of all the parties involved.

I like to conclude this mini-essay with a simple but perhaps provocative statement: One can, in my opinion, evaluate the technological maturity and capability of a nation more readily by

examining the body of engineering standards it has developed than by any other means. If that body is incomplete, capriciously organized, burdened with unnecessary requirements, based in significant measure on fragmentary or unsubstantiated data, generally vague and confusing, and/or institutionally oriented, the technological foundation of the nation is bound to be weak.

One more bit of preliminary information may be useful before I hit you with my list of issues. This concerns the role of the American National Standards Institute (ANSI) in leading the voluntary consensus standards movement in the United States.

ANSI does not write (develop) standards. Its main functions are to crystallize national standards policy, to help identify national and international standards needs and priorities, to arrange for competent and willing organizations to undertake the necessary development, to provide effective procedures for this development and the subsequent consensus approval process, to monitor compliance with these procedures, and finally to certify compliance and publish the results.

ANSI gives coherence to a massive program involving more than 200 professional and trade organizations and 900 companies -- reducing duplication and conflict and providing many other managerial services. It is therefore often described as the "national clearinghouse for standards".

The issues I have assembled for you are these:

1. Does the extant library of nuclear standards satisfy the current needs of the nuclear industry?

2. What actions on standards must be taken -- and by whom -- to meet the future needs of the nuclear industry?

3. Should nuclear standards generally be developed prior to the promulgation of regulations, in concert with the promulgation of regulations, or after the promulgation of regulations?

4. Are there any rules-of-thumb that can be utilized to determine when the applicable technology has matured enough to warrant the development of specific nuclear standards -- particularly those concerned with design, construction and/or operation?

5. How can we insure better communication and coordination between nuclear-standards developers and nuclear regulators?

6. What additional procedures should be established to resolve differences between approved nuclear standards and published nuclear regulations?

7. In what ways do or should standards help to improve quality in the nuclear industry?

8. What must be done to insure more effective and more uniform use of nuclear standards?

9. Is the existing voluntary standards system adequate for the development, approval, distribution and use of nuclear standards?

10. Should a major thrust of the nuclear-standards program now be toward revision of standards to reflect experience gained from past plant design, construction, operation and maintenance?

11. Are new standards or modifications of existing standards needed in the following key areas?

    * Storage of spent nuclear fuel
    * Reprocessing of spent nuclear fuel
    * Nuclear waste management
    * Nuclear spare-parts management
    * Human-factors engineering for nuclear facilities
    * Probabilistic risk assessment for nuclear facilities
    * Decommissioning of nuclear facilities
    * Performance analysis of nuclear facilities

12. In what other nuclear areas are new standards or modifications of existing standards needed?

Now the answers to these questions -- which I am confident will contain clear signals regarding future directions of nuclear-standards activities.

1. Does the extant library of nuclear standards satisfy the current needs of the nuclear industry?

   In large measure -- yes. Several areas of deficiency have been identified, however. They include electrical systems, control systems, instrumentation, valves, and emergency procedures.

2. What actions on standards must be taken -- and by whom -- to meet the future needs of the nuclear industry?

   Standards-development organizations must take aggressive action to upgrade the membership of certain nuclear-standards committees. Too often companies contributing personnel to these committees offer only individuals who happen to be available, not those who are best qualified to undertake the difficult and complex work of the committees. Corporate top managements must be convinced of the importance of the nuclear-standards program. They

must be made to realize that unless talented, straight-thinking, experienced people are assigned to standards committees and stimulated by adequate compensation and recognition, the nuclear industry will be in even greater jeopardy in the future than it is today.

A bona fide, lasting commitment must be obtained from a sufficient number of corporate leaders to guarantee that the nuclear-standards program is properly funded and staffed. If it is not properly funded and staffed, the standards which form the foundation for acceptable levels of public safety and high-quality performance and reliability will be flawed and misleading. Correcting the massive errors that would result would be prohibitively expensive.

While it is recognized that members of nuclear-standards committees will present their personal and/or company viewpoints, clear instructions must be given to them, when appointed, that in the final analysis they are working for the industry as a whole, not their parochial interests.

Many existing nuclear standards need substantial overhauling, simplifying, and updating. If this job is put off much longer it may be impossible to perform on anything but a crash basis -- which would be both inefficient and disrupting. All nuclear standards must be treated as living documents -- that is, continuously adapted to current conditions.

Safety considerations must not be permitted to overwhelm other aspects of quality in the nuclear industry. Standards must be written with not only safety in mind, but also performance, reliability, cost, and production feasibility. Safety standards are useless if they only apply to facilities and equipment that cannot be built or will not run.

Additional planning for and coordination of the nuclear-standards program must be provided by the American National Standards Institute. A possible means of accomplishing this would be to increase industry involvement in the Nuclear Standards Management Board. Public review of proposed nuclear standards -- and institutional response to such review -- must be expedited.

In all nuclear-standards development the main objective should be to achieve high quality the <u>first time</u> a task is performed.

3. Should nuclear standards generally be developed prior to the promulgation of regulations, in concert with the promulgation of regulations, or after the promulgation of regulations?

Prior to the promulgation of regulations whenever possible. The nuclear industry is not an orderly operation, however, and occasionally it will be necessary to develop standards after the promulgation of regulations. It is not feasible under present conditions -- or under conditions envisaged for the near future -- to develop standards in concert with the promulgation of regulations.

4. Are there any rules-of-thumb that can be utilized to determine when the applicable technology has matured enough to warrant the development of specific nuclear standards -- particularly those concerned with design, construction and operation?

   The only rule-of-thumb that appears to apply across the board in the nuclear-standards program is: Whenever, in the collective judgment of the cognizant committee, there are sufficient hard data from a verified calculation, an experiment, a series of experiments, operation of a prototype plant, or operation of a demonstration plant to support a crystallization of design and performance criteria, the process of preparing a nuclear standard may commence.

5. How can we insure better communication and coordination between nuclear-standards developers and nuclear regulators?

   By implementing the provisions of the National Policy on Standards that call for establishment of a Private Sector Standards Coordinating Center and a counterpart Government Sector Standards Coordinating Center. When formed, one of the chief duties of these two centers will be to improve communication and therefore coordination between nuclear-standards developers and nuclear regulators. Also by encouraging nuclear-standards committees to deal directly with the Nuclear Regulatory Commission (NRC) whenever practicable and appropriate. In this connection, the NRC should be asked to give more authority to its unit that deals with nuclear-standards bodies and to publish periodically for use by these bodies a concise summary of NRC needs and proposed actions.

6. What additional procedures should be established to resolve differences between approved nuclear standards and published nuclear regulations?

   The Nuclear Regulatory Commission's appeal process should be streamlined.

7. In what ways do or should standards help to improve quality in the nuclear industry?

By defining and/or establishing acceptable solutions of recurring problems; by enhancing engineering, manufacturing and construction efficiencies through establishment of performance criteria, characteristics of products, procedures, methods, materials and systems -- and through interchangeability; and by serving as a basis for improved communication and promotion of mutual understanding.

8. What must be done to insure more effective and more uniform use of nuclear standards?

   The Institute of Nuclear Power Operations (INPO) should take steps to feed the voluminous information it is collecting to appropriate nuclear-standards committees. The American National Standards Institute should assist in this distribution by keeping INPO informed of the activities and mailing addresses of all active committees.

   Nuclear-standards committees should be on the distribution lists for pertinent publications of the Nuclear Regulatory Commission and the Electric Power Research Institute.

   Internal committee procedures should be modified to permit effective digestion and utilization of these data and reports.

9. Is the existing voluntary standards system adequate for the development, approval, distribution and use of nuclear standards?

   Yes, if the provisions of the National Policy on Standards are implemented.

10. Should a major thrust of the nuclear-standards program now be toward revision of standards to reflect experience gained from past plant design, construction, operation and maintenance?

    Yes. This trend is already well under way. Several technical societies represented at this Conference have launched formal programs to weed out obsolete, superfluous or misleading standards, upgrade marginal standards, resolve differences in interpretation of certain standards that have confused their users, and halt the production of all proposed standards that are not absolutely essential. This trend will gain strength, in my opinion, throughout the next decade.

11. Are new standards or modifications of existing standards needed in the following key areas?

    * Storage of spent nuclear fuel

* Reprocessing of spent nuclear fuel
* Nuclear waste management
* Nuclear spare-parts management
* Human-factors engineering for nuclear facilities
* Probabilistic risk assessment for nuclear facilities
* Decommissioning of nuclear facilities
* Performance analysis of nuclear facilities

Yes -- primarily in the areas of nuclear waste management, nuclear spare-parts management, human-factors engineering for nuclear facilities, and performance analysis of nuclear facilities.

12. In what other nuclear areas are new standards or modifications of existing standards needed?

Additional action should be taken in the area of certification and qualification of QA personnel to prevent the Federal Government from requiring that inspection and auditing be done by its designated agents.

There you have the thoughts that I have been able to pull together on the current issues and future trends of the national nuclear-standards effort. I close with a comment dedicated to the memory of Cliff Burchsted.

Much has been written in the last decade about the importance of voluntarism in the United States. We've heard a great deal about people who serve without pay on government commissions and committees and indeed occasionally in full-time government jobs. We've seen articles in Reader's Digest and other national magazines extolling the virtues of garden clubs who beautify communities and countrysides at their own expense, of senior citizens who donate their time to helping children and young adults in various ways, of boy and girl scouts who take on civic-improvement projects, of women who work sans salary as hospital aides, of men's clubs who organize and underwrite various charitable operations, of volunteers in the Peace Corps, of people who serve without compensation of any sort in all manner of neighborhood and eleemosynary enterprises. I acknowledge the worth of these activities. I contend, in fact, that without them the quality of life in America would be disagreeably low. But let's not forget that voluntary standards action falls in this same category and that it too is vital to an acceptable quality of life.

Every individual that I know of who serves on a voluntary standards committee contributes a significant portion of his own free time to the committee's work. This is akin to the contributions made by physicians serving on hospital boards or the contributions of businessmen serving on the boards of civic institutions. In many cases the work is vocation-related -- but it is well beyond the call of duty and untainted by personal gain.

This is the type of service that Cliff Burchsted rendered to society for over 30 years.

DISCUSSION

FIRST: I was struck by your comment near the end of your address about the vital need for certification for quality assurance personnel. I noticed it particularly because of a fairly bitter experience our Committee on Nuclear Air and Gas Treatment has had over the past few years. We have prepared a personnel certification standard for those who test air and gas cleaning equipment in nuclear power plants, usually referred to as in-place testing. This document has been uniformily rejected by the utilities and by the nuclear standards board of ASTM on the basis that NQA-1 has all the information that is necessary for this type of qualification. We think that NQA-1 is far less specific than it should be, and we think there needs to be specific qualification criteria. I wonder if you would care to comment on what I think is a very difficult and leading question.

LANDIS: You stated the case very well and, in part, answered the question. I would just add that I agree with Dr. First that we do need to establish more specific guidelines, maybe not standards at first, but guidelines, at least with respect to accreditation of certain people in the QA field; particularly inspectors and auditors. I would say that it is much more desirable, and this is my main point, for us as an industry to develop a standard to do that rather than have someone outside the industry, some agency or some group, dictate to us what we should do in the way of accreditation. I believe that that type of thinking is more straight-forward, more cogent for the body of people working in the QA field than for the people in the government, or in management, or in some regulatory operation.

Session 2

IODINE ADSORPTION AND ADSORBENTS

MONDAY: August 13, 1984
CHAIRMEN: M.J. Kabat
Ontario Hydro
J.W. Jacox
Jacox Associates

REGENERATION OF THE IODINE ISOTOPE-EXCHANGE EFFICIENCY FOR NUCLEAR-GRADE ACTIVATED CARBONS
V.R. Deitz

INFLUENCE OF AGING ON THE RETENTION OF ELEMENTAL RADIOIODINE BY DEEP BED CARBON FILTERS UNDER ACCIDENT CONDITIONS
H. Deuber

LONG-TERM DESORPTION OF ^{131}I FROM KI-IMPREGNATED CHARCOALS LOADED WITH CH_3I, UNDER SIMULATED POST-LOCA CONDITIONS
A.C. Vikis, J.C. Wren, C.J. Moore, R.J. Fluke

A STUDY OF ADSORPTION PROPERTIES OF IMPREGNATED CHARCOAL FOR AIRBORNE IODINE AND METHYL IODIDE
L. Qi-dong, H. Sui-yuang

EVALUATION OF QUATERNARY AMMONIUM HALIDES FOR REMOVAL OF METHYL IODIDE FROM FLOWING AIR STREAMS
W.P. Freeman, T.G. Mohacsi, J.L. Kovach

INVESTIGATIONS ON THE EXTREMELY LOW RETENTION OF ^{131}I BY AN IODINE FILTER OF A BOILING WATER REACTOR
H. Deuber, K. Gerlach, J.G. Wilhelm

TRANSMISSION OF RADIOIODINE THROUGH SAMPLING LINES
P.J. Unrein, C.A. Pelletier, J.E. Cline, P.G. Voilleque

ANALYSES OF CHARCOAL FILTERS USED IN MONITORING RADIOACTIVE IODINES
S.M. Langhorst

OPENING REMARKS OF SESSION CHAIRMAN KABAT:

Welcome to the second session of the 18th DOE Nuclear Airborne Waste Management and Air Cleaning Conference. Traditionally, the radioiodine sessions significantly contributed to the high technical standard of previous Air Cleaning Conferences. It is evident that at this session we shall also hear valuable data and information on recent developments in this challenging area - carbon aging and regeneration, the identification and removal of airborne species of radioiodine, its long term desorption from KI-impregnated charcoal, new impregnation methods and materials, radioiodine retention in sampling lines, and the analysis of radioiodine sample collectors.

REGENERATION OF THE IODINE ISOTOPE-EXCHANGE EFFICIENCY FOR NUCLEAR-GRADE ACTIVATED CARBONS

Victor R. Deitz
Naval Research Laboratory
Washington, D.C. 20375

Abstract

The removal of radioactive iodine from air flows passing through impregnated activated carbons depends on a minimum of three distinguishable reactions: (1) adsorption on the carbon networks of the activated carbons, (2) iodine isotope exchange with impregnated iodine-127, and (3) chemical combination with impregnated tertiary amines when present. When a carbon is new, all three mechanisms are at peak performance and it is not possible to distinguish among the three reactions by a single measurement; the retention of methyl iodide-127 is usually equal to the retention of methyl iodide-131. After the carbon is placed in service, the three mechanisms of iodine removal are degraded by the contaminants of the air at different rates; the adsorption process degrades faster than the other two. This behavior will be shown by comparisons of methyl iodide-127 and methyl iodide-131 penetraton tests. It was found possible to regenerate the iodine isotope-exchange efficiency by reaction with airborne chemical reducing agents with little or no improvement in methyl iodine-127 retention.. Examples will be given of the chemical regeneration of carbons after exhaustion with known contaminants as well as for many carbons removed from nuclear power operations. The depth profile of methyl iodide-131 penetration was determined in 2-inch deep layers before and after chemical treatments.

I. Introduction

The research activities at the Naval Research Laboratory in the field of nuclear-grade carbons may be divided into three categories. First, new carbons from several sources were systematically degraded by exposure to unfiltered outdoor air flow in three geographical locations for time periods up to two years. All carbons were found to degrade with respect to the radioactive iodine trapping efficiency[1]. The penetration for three types of impregnation are shown (Figure 1); those containing only KI_x did not do as well as those containing both KI and TEDA (triethylenediamine).

Secondly, the question was then raised as to the behavior of an activated carbon after service (thus exposed to weathering) under a postulated DBA (design basis accident). The Regulatory Guide 1.52 (Revision 2, March 1978)[2] stipulates that the carbon in Atmosphere Cleanup Systems must operate in an average radiation level of 10^9 rads for iodine buildup on the adsorber. It was reported in 1982(3) that service carbons exposed to radiation levels of 10^7 to 10^9 rads actually improved on the iodine isotope exchange capacity as measured by methyl iodide-131 exchange (Figure 2). Moreover, the same samples showed little or no improvement in the adsorption of methyl iodide-127. This observation established the existence of completely independent reactions that can take place within the domain of impregnated activated carbons.

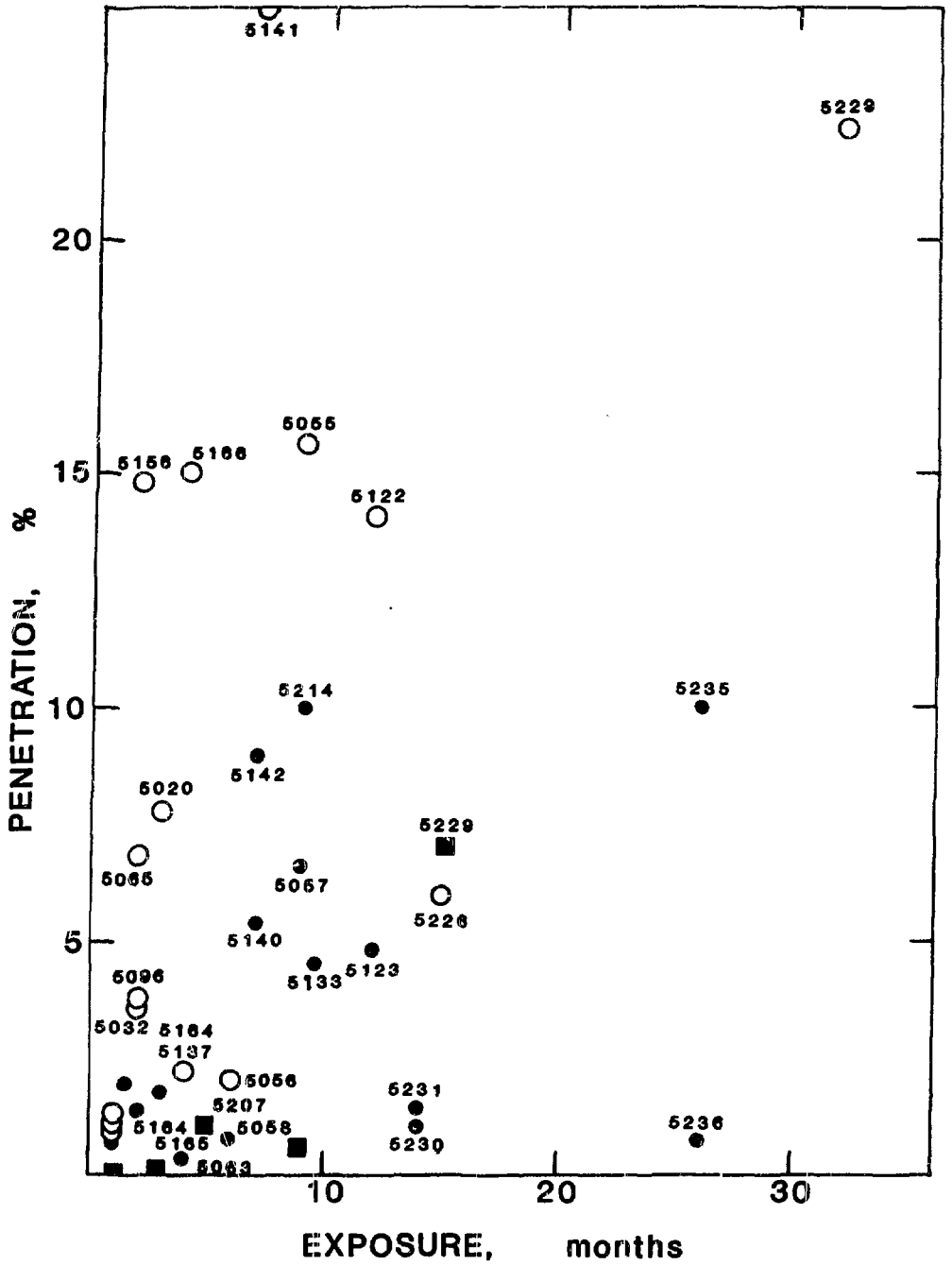

Figure 1: The dependence of the penetration of methyl iodide-131 with duration of outdoor air flow:
○ KI_X, ■ TEDA alone, ● TEDA + KI

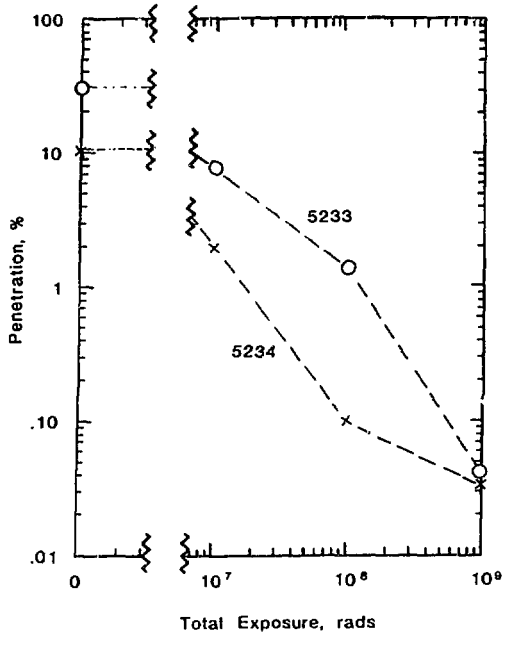

Figure 2: Decrease in penetration of methyl iodide-131 with increase of total exposure on the NRL LINAC.

Third, it has now been found possible to regenerate the iodine isotope exchange efficiency of a used carbon by reaction with air-borne chemical reducing agents at ambient temperature. Examples are given for carbons degraded with known contaminants and for carbons removed from nuclear power operations.

II. Experimental Results

Chemical changes upon Degradation and Regeneration

The atmospheric contaminants that chemically degrade nuclear carbons include ozone, sulfur dioxide and the nitric oxides. Special attention has been directed to ozone. The reaction of ozone with potassium iodide in a weak alkali solution is known to be as follows:

$$3O_3 + I^- \rightarrow 3O_2 + IO_3^-$$

If the same reaction takes place on a KI-impregnated carbon, one would expect to find KIO_3 in a weathered carbon. In order to test this hypothesis a coconut shell carbon (GX-212) was impregnated with aqueous KIO_3 (2 wt%). The penetrations of methyl iodide-127 and of methyl iodide-131 with methyl iodide-127 as carrier were determined before and after irradiation to 10^8 rads on the NRL LINAC. If the radiolytic reactions reduce the iodate, a significant decrease in methyl iodide-131 penetration would be observed. The results (Table 1) demonstrate that this indeed took place. There was little change in the methyl iodide-127 penetration, determined under similar conditions (using an electron capture detector [4]), indicating no change in the adsorptive properties, only changes in the iodine isotope exchange process.

Table 1: Penetration of Methyl Iodide Through a New Coconut Carbon Impregnated with KIO_3 (2 wt. %) (Preparation 1)

Exposure	Test Gas	Penetration, %
Original	MeI-131	6.0
Original	MeI-127	5.0
LINAC at 10^8 rads	MeI-131	0.89
LINAC at 10^8 rads	MeI-127	6.9

The results (Table 1) are consistent with earlier observations[3]. Since the original carbon was new, i.e., not weathered, the methyl iodide-131 penetraton agreed with that for methyl iodide-127. After irradiation, there was a 100-fold decrease in methyl iodide-131 penetration, but that for methyl iodide-127 was about the same. It can be concluded that the KIO_3 of the impregnation was converted by radiolysis into a chemical species that exchanged more readily with methyl iodine-131.

Several organic compounds are available that chemically reduce KIO_3 in solution and one of these, hydrazine, reacts as follows (5):

$$2\ KIO_3 + 3\ N_2H_4 \rightarrow 3\ N_2 + 2\ KI + 6\ H_2O$$

A second quantity of the impregnated activated carbon (2.1% KIO_3 dry basis on NACAR G-212) was prepared and the methyl iodide-131 penetrations were determined for the following: (1) original impregnation, (2) after irradiation to 10^8 rads on the NRL LINAC, and (3) after chemical treatment with a dilute hydrazine solution. The solution was sprayed into a slowly rotating cylinder containing the carbon and the product air dried in a glass tray. The results (Table 2) indicate a close correlation between the chemical reactions in radiolysis and the chemical reduction of KIO_3 by hydrazine to form KI.

Table 2: Comparison of Radiolysis and Chemical Treatments of KIO_3 Impregnated Carbon (2 wt. %) (Preparation 2)

Exposure	Test Gas	%Penetration
Original KIO_3 Impregnation	MeI-131	4.4
LINAC at 10^8 Rads	MeI-131	0.13
Chemical Treatment	MeI-131	0.3

The depth profiles of methyl iodide-131 retained in the test beds (Figure 3) were exponential and indicate the uniformity of the impregnated and the treated materials.

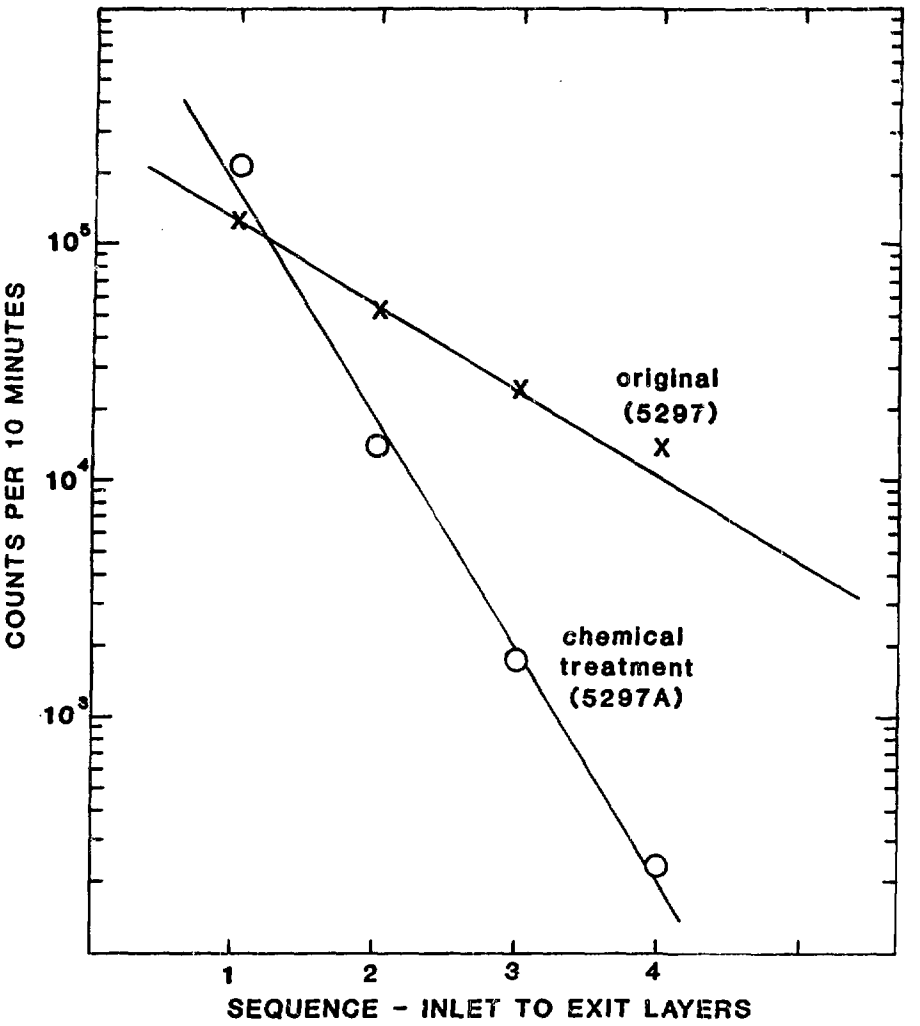

Figure 3: Gradient of CH_3I-131 retained in the test bed before and after chemical treatment (NRL 5297) (2nd preparation of KIO_3 impregnated carbon).

The oxidized iodine species need not necessarily be an iodate ion. In order to demonstrate this possibility, a stream of ozone in oxygen (0.10%) was directed through a new KI-impregnated activated carbon (MSA 463563) for 10 hours. No odor of ozone was detected at any time in the effluent. Aliquots of the ozone-treated carbon were then treated with hydrazine in one case and methyl-hydrazine in the second. The results (Table 3) indicate improvement with hydrazine after the ozone treatment of a new carbon. In other examples, the ozone pretreatments were made in the presence of water vapor and lead to extensive degradations having 10-20% penetration of methyl iodide-131 for similar new carbons [1].

Table 3: Chemical Treatments of Ozone-Treated Carbons With KI Impregnation.

Treatment	Methyliodide-131 Penetration
None	0.05
Ozone	1.0
Chemical reduction	0.52

It may be concluded that the two independent operations -irradiation and chemical reduction - lead to the formation of iodide ion (I^-) and thus convert the original iodate, or other oxidized iodine species,into one that readily exchanges with I-131.

Chemical Treatment of Carbons Removed from Service

The carbons removed from service in commercial adsorbers had been exposed to a large variety of contaminants, some of which are oxidants like ozone; the presence of other contaminants can also interfere with rates of chemical reduction. Samples of service carbon that had been removed from service (NRL 5291) were treated with different amounts of hydrazine. The initial material had a penetration of methyliodide-131 of 38.5% when not prehumidified and 42.2% when prehumidified (16 hours at 95% RH). The carbon was rotated slowly in a horizontal cylinder with lifting vanes while the small volume of solution containing the hydrazine was slowly introduced by spraying. The carbon retained a dry appearance after the addition.

Each sample was then tested for methyliodide-131 penetration and the results (Figure 4) showed improvement in direct proportion to the amount of hydrazine introduced. Good reproducibility is shown by the two points at "C" in Figure 4, namely 8.0 and 7.8% respectively. The carbon before removal had been in service for about four years and, as mentioned above, the initial penetration of methyliodide-131 was considerable. Had the carbon been treated periodically, for example, after about 6 months service, the recovery would have been more complete.

The reducing agent to be used in this application is not intended by itself to remove radioiodine that might be released from nuclear reactors. Such a scheme was proposed in 1966 (6,7) and entailed the formation of a stable aerosol by the gas phase reaction of hydrazine (or its unsymmetrical dimethyl derivative) with released radioiodine, followed by the aerosol filtration. The present objective is to reform the isotope-exchange properties of the impregnated activated carbon which will then continue to function after the reducing agent has reacted.

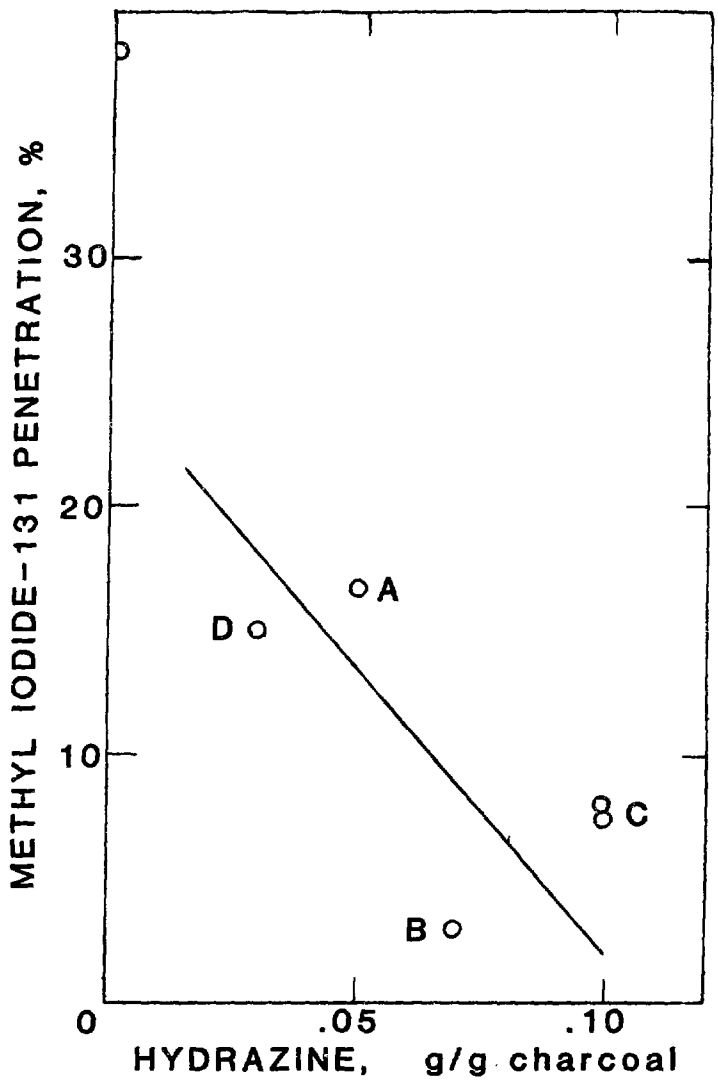

Figure 4: Improvement in methyl iodide-131 retention after hydrazine treatments. (Initial penetration was 38.5%).

A second carbon sample removed from service at another site (NRL 5143) improved from 31.0% to 3.0% after hydrazine treatment. The sample was also treated in a different experimental arrangement and improved from 31.0% to 2.2% with respect to the penetration of methyl iodide-131. The test bed had been prepared in four equal layers and each was counted before and after the test. The depth profiles (Figure 5) of the methyl iodide-131 retained by the test sample after the treatments were not quite linear as they are for a uniform packing.

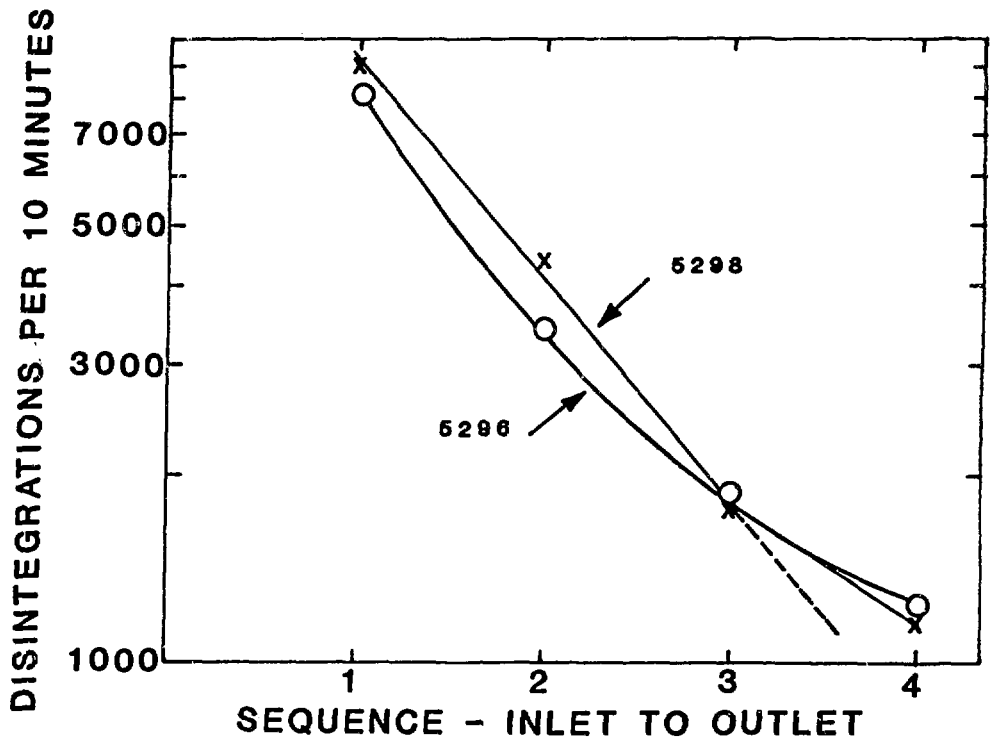

Figure 5: Depth profile after chemical treatment.

Three additional samples of GX-176 removed from service (Savannah River Laboratory) were treated with hydrazine and the results (Table 4) are compared with the starting material [8] and with LINAC irradiation samples.

Table 4: Methyl Iodide-131 penetration with GX-176 samples removed from service (Savannah River Laboratory)[8]

	Methyl Iodide-131 Penetration, %		
	Original	10^8 Rads	Hydrazine
C-3 compartment, 30 months	69	41	7.4
K-3 compartment, 18 months	41	0.16	1.9
P-2 compartment, 14 months	28	0.21	9.0

III. Concluding Remarks

Important requirements of airborne reducing agents for the regeneration of the iodine-isotope exchange capacity of nuclear-grade carbons include the following:

1. Wetting of the carbon surface
2. Mobility on the carbon surface
3. Rapid desorption of possible products
4. Reaction at ambient temperatures

In general, chemical reactions in solution (*in vitro*) are subjected to different constraints than between the same reactants adsorbed on carbon (*in carbono*). The radiolysis in vapor and liquids can be different than with the same reactants adsorbed on carbon. Some basic reasons for this behavior are given below:

I. The activation energy may be different in each of the modes, i.e. bond-breaking in the gas phase is less probable than in a liquid at the same concentration and temperature.

II. The entropy changes may be different in each mode because of the adsorption of products *in carbono*; the molecular orientation in the adsorbed phase relative to that in solution.

III. The concentration gradients may influence the attainment of steady states from mass action point of view to different extents.

IV. Solvation effects in liquids may not be present in gas or vapor.

V. Dimensional changes in carbon-adsorbed mode are different than volume changes in vitro.

References

(1) Deitz, V.R. "Effects of Weathering on Impregnated Charcoal Performance", NUREG/CR-2112, NRL Memorandum Report 4516 (September, 1981).

(2) "U.S. NRC Regulatory Guide 1-52, Revision 2, March 1978" U.S. Nuclear Regulatory Commission, Attn.: Director of Document Control, Washington, D.C. 20555.

(3) Deitz, V.R., "Charcoal Performance under Simulated Accident Conditions" Proc. 17th DOE Nuclear Air Cleaning Conference, 641-651 (1982).

(4) Deitz, V.R., and Romans, J.B., "Testing Iodized Activated Carbon Filters with Non-Radioactive Methyl Iodide" NRL Memorandum Report 4240, (May 30, 1980).

(5) Bray, W.C., Cuy, E.J., J. Am. Chem. Soc., 46, pp. 858-875, (1924).

(6) Viles, F.J., Jr., Silverman, L. Proc. 9th AEC Air Cleaning Conf., 1 pp. 273-297, (1966).

(7) J. Mischim, L.C. Schwendiman, L.L. Burger, and R.A. Hasty, Proc. 9th AEC Air Cleaning Conf., 1, pp. 298-318, (1966).

(8) Evans, A. Gary "Confinement of Airborne Radioactivity" Progress Report January - December, 1977. DP-1497 E.I. du Pont de Nemours and Co., Savannah River laboratory, Arken, S.C. 29801 Published January, 1979.

DISCUSSION

DEUBER: In many cases the aging of activated carbons is primarily due to adsorption of organic compounds, we found this in our nuclear power stations in Germany. In these cases there would be little improvement by application of hydrazine. Do you agree?

DEITZ: Although a large number of volatile organic vapors are not retained by activated carbon in continuous air flows, there are some vapors from paint formulations and degreasing solvents that are retained. Eventually, the surface can attain a sufficiently high coverage to block the access of all airborne vapors. That will decrease the contact of the hydrazine with whatever you are trying to reduce. For the most part, we find that you can't regenerate.

VIKIS: Does hydrazine accumulate on charcoals? Are there any risks of an explosion?

DEITZ: Hydrazine does not accumulate on charcoals in the flows used in our laboratory work. Instruments are being developed and tested at the Naval Research Laboratory to detect concentrations in the parts per billion range and the effluent from the charcoal appears to be below these low levels.

KOVACH, J.L.: What were the temperature, humidity, and pre-equilibration time and other test conditions for the tests which you

presented?

DEITZ: The methyl iodine-131 tests for samples withdrawn from service were made at 30°C, 95% RH and no prehumidification. The flow parameters were those given in D-3803, ASTM.

KOVACH, J.L.: You got only 6% penetration on standard test conditions with KIO_3 impregnation?

DEITZ: Yes, for that particular one. We started with a new base carbon, and impregnated it with about 2% potassium iodate. Remember it was new carbon. You can load these carbons with ozones from a swimming pool generator that emits concentrations up to 1%. It will reduce efficiency down to about 30 to 40% penetration but, in this case, you can regenerate.

WATSON: Have you data on the rate of aging after hydrazine regeneration?

DEITZ: Insufficient data are in hand at present to answer this query. In one set of experiments, we regenerated it after exposure to outdoor air, then exposed it to ozone and regenerated with hydrazine, making tests as we went along. So far, three cycles is about as far as the money has gone.

INFLUENCE OF AGING ON THE RETENTION OF ELEMENTAL RADIOIODINE BY DEEP BED CARBON FILTERS UNDER ACCIDENT CONDITIONS

H. Deuber
Laboratorium für Aerosolphysik und Filtertechnik
Kernforschungszentrum Karlsruhe GmbH
Postfach 3640, D-7500 Karlsruhe 1
Federal Republic of Germany

Abstract

No significant difference was found in the retention of I-131 loaded as I_2, by various impregnated activated carbons that had been aged in the containment exhaust air of a pressurized water reactor over a period of 12 months. In all the cases, the I-131 passing through deep beds of carbon was in a nonelemental form. It is concluded that a minimum retention of 99.99 %, as required by new guidelines for certain accident filters, can be equally well achieved with various carbons in deep beds.

I. Introduction

German pressurized water reactors are equipped with iodine filters for cleanup of the annulus exhaust air in an accident.[1] These filters are deep bed carbon filters (see below). According to new guidelines, the minimum retention to be achieved with these filters in a design basis accident (LOCA) is 99.99 % for elemental radioiodine.[2] (The corresponding value for organic radioiodine is 99 %.)

In order to ascertain by which carbons the minimum retention of 99.99 % can best be achieved, investigations were performed on the retention of elemental I-131 by various impregnated activated carbons in deep beds under simulated accident conditions.

In this paper investigations with four impregnated activated carbons are covered. In order to determine the influence of pollutants, the carbons were aged in the containment exhaust air of a pressurized water reactor over a period of 12 months. The results obtained with these carbons without aging have already been presented.[3] More data, pertaining in particular to additional carbons, have been published elsewhere.[4]

Previous studies on the retention of elemental I-131 by impregnated activated carbons, mostly in shallow beds, have been reviewed in the paper on new carbons.[3]

II. Data of PWR Annulus Exhaust Air Filters (LOCA)

Data on design and operation of annulus exhaust air filters in German pressurized water reactors (PWRs) during a LOCA have already been presented in the paper indicated.[3] The data are summarized in Table I. It is in particular obvious that a high temperature (definitely below 150 °C) has to be expected for a short period only (clearly shorter than one day).

From data pertaining to serious accidents[5] it can be concluded that in this event, if the integrity of the inner containment shell were maintained, the challenge of the annulus exhaust air filters would not be much more serious than in a LOCA.

III. Experimental

Data of the four impregnated activated carbons covered here have already been indicated in the paper on new carbons.[3] They are given again in Table II. The carbon 207B (KI) is mostly used in the iodine filters of German nuclear power plants.

The carbons were challenged with the containment exhaust air of a PWR over a period of 12 months during power operation of the reactor. In this exhaust air the main pollutants are usually toluene, xylene, nonane, decane and dodecane.[6,7,8,9] The face velocity of the air in the carbons was the same as that in the annulus exhaust air filters and in the subsequent laboratory tests (50 cm/s).

The parameters of the laboratory tests are given in Table III. As with new carbons, two combinations of temperature and relative humidity were used: (a) 30 °C and 98 to 100 % R.H. and (b) 130 °C and 2 % R.H.. The second combination may be regarded as conservatively representing the conditions in the annulus of a PWR during the first phase of a LOCA and the first combination the conditions thereafter (see Table I).

Total test bed depth and residence time (25 cm and 0.5 s, respectively) were shorter than those used in the annulus exhaust air filters (50 cm and 1.0 s, respectively).

The purging time (elution period) was one week (168 h). This time is much longer than the anticipated operating time of an annulus exhaust air filter at a high temperature (< 24 h).

As with new carbons, the test beds were sectioned to establish the penetration as a function of the bed depth or residence time. In the laboratory tests the original arrangement of the carbon was maintained, i.e. the sequence of the beds (sections) was the same as that during the exposure to the containment exhaust air.

As previously, also the backup beds were sectioned to allow differentiation of the iodine species penetrating the test beds.

The backup beds, preceded by a particulate filter, were (in the direction of flow):

(a) 2 beds of sorbent DSM11 for retention of I_2;

(b) 2 beds of sorbent AC6120 for retention of easy-to-trap organic iodine species, such as CH_3I;

(c) 7 beds of carbon 207B (KI) for retention of more penetrating iodine species.

Data of the sorbents DSM11 and AC6120 are to be found in the literature.[10,11] The carbon 207B (KI) was the same as that indicated in Table II.

The backup beds were operated at the favorable retention temperature of 80 °C.

As previously, the elemental iodine was tagged with I-131. The minimum detectable penetration was again 10^{-5} %.

IV. Results

In this chapter the results are presented of the investigations on the retention of I-131 loaded as I_2, by the four carbons contained in Table II under the conditions indicated in Table III. First the I-131 penetration will be dealt with, then the chemical form of the penetrating I-131.

I-131 Penetration

The Figs. 1 to 8 display the penetration of the carbons by I-131 loaded I_2, as a function of the bed depth at different aging times (no aging or aging over 12 months) and different temperatures. The effect of aging is clearly visible: with the aged carbons, the penetration was up to about three orders of magnitude higher.

The penetration curves are generally steep up to a bed depth of 5 cm and then flatten out. It is only at 130 °C with the aged carbons that these two parts of the penetration curves cannot be clearly distinguished. The steep part of the penetration curves can be ascribed to elemental iodine and the flat part to more penetrating iodine species present as impurities or formed in the test bed.

Table IV and the Figs. 9 and 10 give an overview of the penetration of the carbons by I-131 at different bed depths, aging times and temperatures. The main results are as follows:

(a) Temperature of 30 °C (Fig. 9):
The penetrations found with different carbons differed to a small extent only. At an aging time of 12 months, the penetrations were higher by one to three orders of magnitude, compared with no aging. At a bed depth of 25 cm (residence time: 0.5 s) the penetrations of the aged carbons were about 10^{-2} %.

(b) Temperature of 130 °C (Fig. 10):
The penetrations obtained with different carbons differed more than at 30 °C. However, with the aged carbons the difference was relatively small. At an aging time of 12 months, the penetrations were again higher by one to three orders of magnitude, compared with no aging. At a bed depth of 25 cm the penetrations of the aged carbons were between about 10^{-2} and 10^{-1} %.

From these results it is obvious that the permitted maximum penetration of 10^{-2} % for elemental I-131, as required by the new guidelines, may be exceeded if the chemical form of the penetrating I-131 is not taken into account.

Chemical Form of Penetrating I-131

As already mentioned, the backup beds consisted of different components to determine the percentage of particulates (particulate filter), of I_2 (sorbent DSM11), of easy-to-trap organic iodine species, such as CH_3I (sorbent AC 6120) and of more penetrating iodine species (carbon 207B (KI)).

The distribution of I-131 among test and backup beds at different aging times and temperatures of the test beds is displayed in the Figs. 11 to 18. The particulate filters are not indicated because in no case was any significant amount of I-131 detected on these components.

The effect of aging is again clearly visible: with the aged carbons, much higher fractions of I-131 were found on the test beds 2 to 10 and on the backup beds.

The results shown in the Figs. 11 to 18 may be summarized as follows:

(a) Temperature of 30 °C (Figs. 11 - 14):
The I-131 was completely trapped by the backup beds. With the new carbons, the I-131 was found on AC6120 only. With the aged carbons, most of the I-131 was again observed on AC6120. No or comparatively little I-131 was detected on DSM11.

(b) Temperature of 130 °C (Figs. 15 - 18):
Mostly, in particular with the aged carbons, the I-131 was not completely captured by the backup beds. With the new carbons, the I-131 was strongly retained by AC6120, apart from the case in which the test beds were made up of 207B (TEDA). With the aged carbons, the I-131 was rather evenly distributed among AC6120 and the subsequent 207B (KI). Again, no or comparatively little I-131 was detected on DSM11.

From the distribution of the I-131 on DSM11 it has to be concluded that practically no I-131 in the elemental form passed

through the test beds. Any elemental I-131 would have been largely trapped by the first DSM11 bed, i.e. an uneven distribution of the I-131 on the DSM11 would have resulted. (The small amounts of the I-131 found on DSM11 are due to the retention of organic I-131.) The conclusion that practically no elemental I-131 passed through the test beds, is in agreement with the penetration curves shown in the Figs. 1 to 8.

From this conclusion it follows that the permitted maximum penetration of 10^{-2} % for elemental I-131 is clearly not exceeded if the chemical form of the penetrating I-131 is taken into account.

The distribution of the I-131 on AC6120 and the subsequent 207B (KI) shows that at 30 °C the I-131 was mostly in the form of CH_3I or in similar easy-to-trap forms. At 130 °C the I-131 was in more penetrating forms. The nature of these forms is not known.

V. Summary and Conclusion

Investigations were performed on the retention of elemental I-131 by various impregnated activated carbons in deep beds under simulated accident conditions to ascertain by which carbons a minimum retention of 99.99 % can best be achieved. According to new guidelines this retention is required for the annulus exhaust air filters of German pressurized water reactors in a design basis accident (LOCA).

No significant difference was found in the retention of I-131 loaded as I_2, by various impregnated activated carbons that had been aged in the containment exhaust air of a pressurized water reactor over a period of 12 months. In all the cases, the I-131 passing through deep beds of carbon (25 cm equivalent to a residence time of 0.5 s) was in a nonelemental form. It is concluded that the minimum retention of 99.99 % can be equally well achieved with various carbons in deep beds.

Acknowledgments

The work was supported by the Federal Minister of the Interior of the Federal Republic of Germany.

K. Bleier, W. Sellien, S. Winkler, H. Fischer and A. Ladanyi participated in the performance and evaluation of the tests.

References

(1) Wilhelm, J.G.,
Iodine Filters in Nuclear Installations,
Commission of the European Communities,
V/2110/83 (1982)

(2) Reaktorsicherheitskommission,
RSK-Leitlinien für Druckwasserreaktoren,
Gesellschaft für Reaktorsicherheit (1981)

(3) Deuber, H., Wilhelm, J.G.,
Retention of Elemental Radioiodine by Deep Bed Carbon Filters Under Accident Conditions,
17th DOE Nuclear Air Cleaning Conference,
Denver,2. - 5.8.1982,
CONF-820833 (1983) 248

(4) Deuber, H.,
Abscheidung von elementarem ^{131}I an Aktivkohlen unter Störfallbedingungen,
KfK 3776 (1984)

(5) Dillmann, H.-G., Pasler, H.,
Theroretical and Experimental Investigations Into the Filtration of the Atmosphere Within the Containments of Pressurized Water Reactors After Serious Reactor Accidents,
16th DOE Nuclear Air Cleaning Conference,
San Diego, 20. - 23.10.1980,
CONF-801038 (1981) 373

(6) Furrer, J. et al.,
Alterung und Vergiftung von Iod-Sorptionsmaterialien in Kernkraftwerken/Aging and Poisoning of Iodine Filters in Nuclear Power Plants,
Kerntechnik 18 (1976) 313

(7) Wilhelm, J.G. et al.,
Behavior of Gasketless Deep Bed Charcoal Filters for Radioiodine Removal in LWR Power Plants,
16th DOE Nuclear Air Cleaning Conference,
San Diego, 20. - 23.10.1980,
CONF-801038 (1981) 465

(8) Deuber, H., Gerlach, K.,
Untersuchungen zur Abscheidung von ^{131}I durch ein Iodfilter eines Druckwasserreaktors,
KfK 3594 (1983)

(9) Deuber, H., Gerlach, K.,
Untersuchungen zur Alterung von Aktivkohlen in der Abluft eines Druckwasserreaktors (DWR4),
KfK 3711 (1984)

(10) Deuber, H., Wilhelm, J.G.,
Determination of the Physico-Chemical ^{131}I Species in the Exhausts and Stack Effluent of a PWR Power Plant,
15th DOE Nuclear Air Cleaning Conference,
Boston, 7. - 10.8.1978,
CONF-780819 (1979) 446

(11) Deuber, H., Wilhelm, J.G.,
Occurrence of Penetrating Iodine Species in the Exhaust Air of PWR Power Plants,
16th DOE Nuclear Air Cleaning Conference,
San Diego, 20. - 23.10.1980,
CONF-801038 (1981) 1354

(12) British Standard Institution,
Specification for Test Sieves,
BS 410 (1976)

(13) American Society for Testing and Materials,
Standard Test Method for Particle Size Distribution of Granular Activated Carbon,
ASTM D2862 (1970)

Table I Data of PWR annulus exhaust air filters (LOCA)

Parameter	Unit	Value
Bed depth	cm	~ 50
Face velocity	cm/s	~ 50
Residence time	s	~ 1
Temperature [a]	°C	< 150; ≥ 30
Relative humidity [a]	%	< 10; ≤ 100
Length of filter operation [a]	d	< 1; < 60
I concentration	mg/m^3	< 1
I loading	mg/g [b]	< 1

a) First value: early phase of LOCA;
second value: late phase of LOCA

b) mg I/g carbon

Table II Activated carbons investigated [a]

Designation	Base material	Particle size [b] (mesh)	Impregnant	Supplier
207B (KI)	coal	8 - 12	KI	Sutcliffe Speakman, U.K.
207B (TEDA)	coal	8 - 12	TEDA	Sutcliffe Speakman, U.K.
Kiteg II	coconut shell	8 - 16	KI, tertiary amine	Nuclear Consulting Services, U.S.A.
Radshield 25	coconut shell	8 - 16	tertiary amine	Charcoal Engineering, U.S.A.

a) New or aged in the containment exhaust air of a PWR over a period of 12 months

b) 8 - 12 mesh: BS410 [12]; 8 - 16 mesh: ASTM D2862 [13]

Table III Values of test parameters

Parameter	Unit	Value
Carrier concentration	mg/m^3	1
Temperature	^oC	30 or 130
Relative humidity [a]	%	98 - 100 or 2
Face velocity	cm/s	50
Pressure (absolute)	bar	1
Bed depth [b]	cm	2.5
Residence time per bed	s	0.05
Preconditioning time [c]	h	$\geq$ 16 or 1
Injection time	h	1
Purging time	h	168

a) 98 - 100 % at 30 ^oC; 2 % at 130 ^oC (dew point : 30 ^oC)

b) Ten successive test beds of depth 2.5 cm were used. The first two test beds consisted of sections of depth 1.25 cm. (Bed diameter : 2.5 cm)

c) $\geq$ 16 h at 30 ^oC; 1 h at 130 ^oC

Table IV Penetration of various impregnated activated carbons by ^{131}I loaded as I_2 (compare Figs. 9 and 10)

Carbon	Bed depth (cm)	Residence time (s)	Penetration (%)			
			30 °C, 98 - 100 % R.H. a)		130 °C, 2 % R.H. a)	
			0 month b)	12 months b)	0 month b)	12 months b)
207B (KI)	5	0.1	$2.7 \cdot 10^{-3}$	$7.0 \cdot 10^{-2}$	$3.0 \cdot 10^{-3}$	$1.0 \cdot 10^{1}$
	25	0.5	$1.2 \cdot 10^{-4}$	$1.4 \cdot 10^{-2}$	$1.9 \cdot 10^{-4}$	$7.8 \cdot 10^{-3}$
207B (TEDA)	5	0.1	$1.5 \cdot 10^{-3}$	$3.2 \cdot 10^{-1}$	$3.8 \cdot 10^{-1}$	$1.2 \cdot 10^{1}$
	25	0.5	$1.2 \cdot 10^{-4}$	$1.2 \cdot 10^{-2}$	$3.7 \cdot 10^{-3}$	$4.3 \cdot 10^{-2}$
Kiteg II	5	0.1	$2.4 \cdot 10^{-3}$	$9.2 \cdot 10^{-2}$	$4.3 \cdot 10^{-2}$	- c)
	25	0.5	$1.9 \cdot 10^{-4}$	$1.1 \cdot 10^{-2}$	$4.4 \cdot 10^{-4}$	- c)
Radshield 25	5	0.1	$1.1 \cdot 10^{-3}$	$2.6 \cdot 10^{-1}$	$5.2 \cdot 10^{-3}$	$6.0 \cdot 10^{0}$
	25	0.5	$3.0 \cdot 10^{-5}$	$2.8 \cdot 10^{-2}$	$3.5 \cdot 10^{-4}$	$1.2 \cdot 10^{-1}$

a) Values of additional parameters: see Table III;

b) Aging time (in the containment exhaust air of a PWR);

c) No reliable results obtained (mechanical defect)

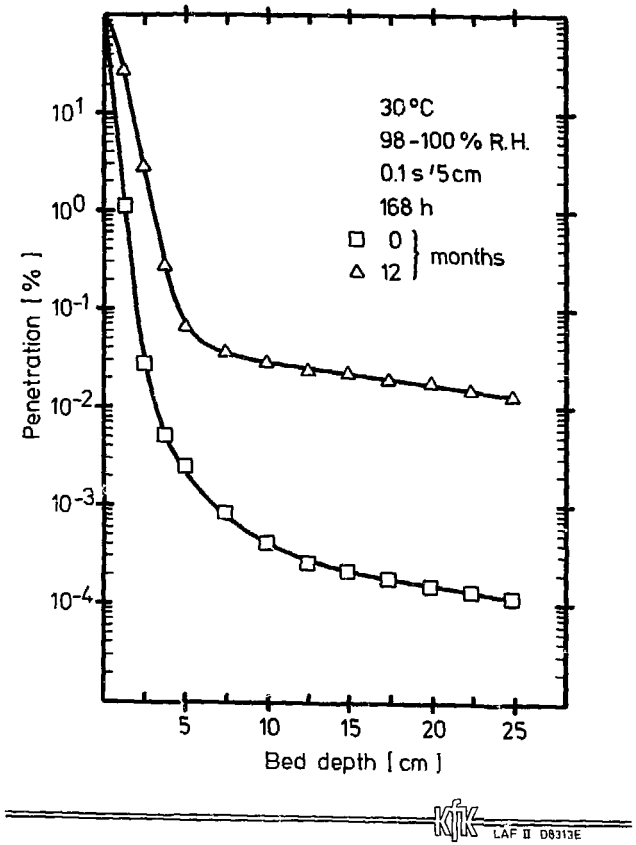

Penetration of 207B (KI) by ^{131}I loaded as I_2, at different aging times

Fig. 1

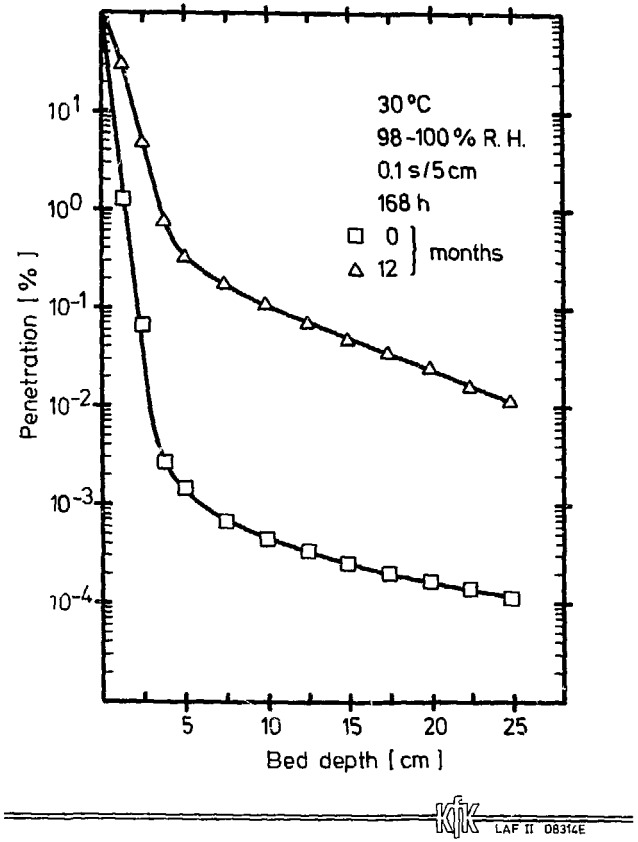

Penetration of 207B (TEDA) by ^{131}I loaded as I_2, at different aging times

Fig. 2

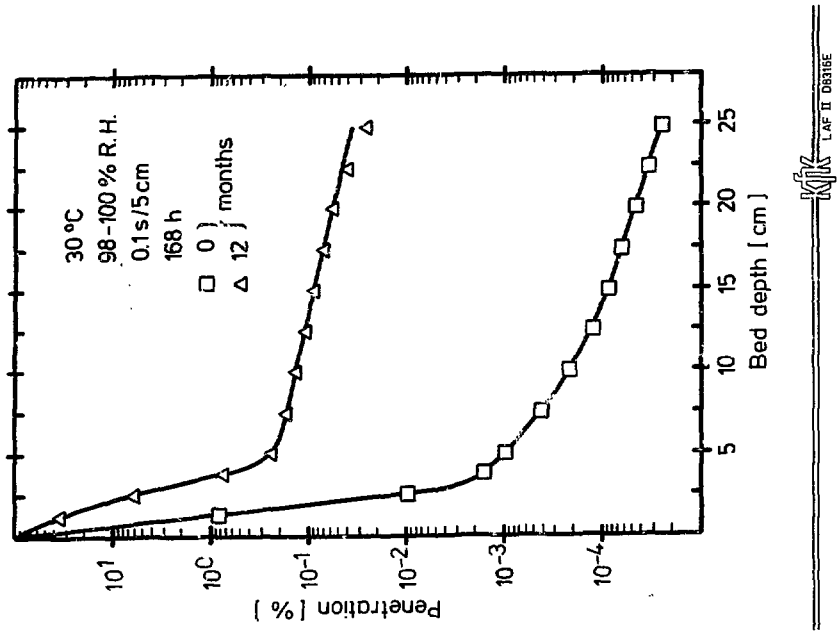

Penetration of Radshield 25 by ^{131}I loaded as I_2, at different aging times

Fig. 4

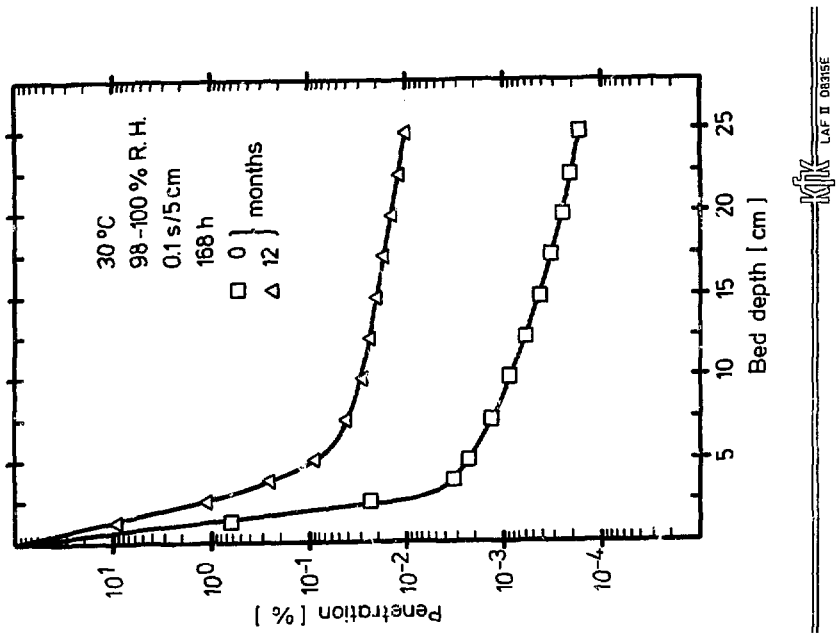

Penetration of Kileg II by ^{131}I loaded as I_2, at different aging times

Fig. 3

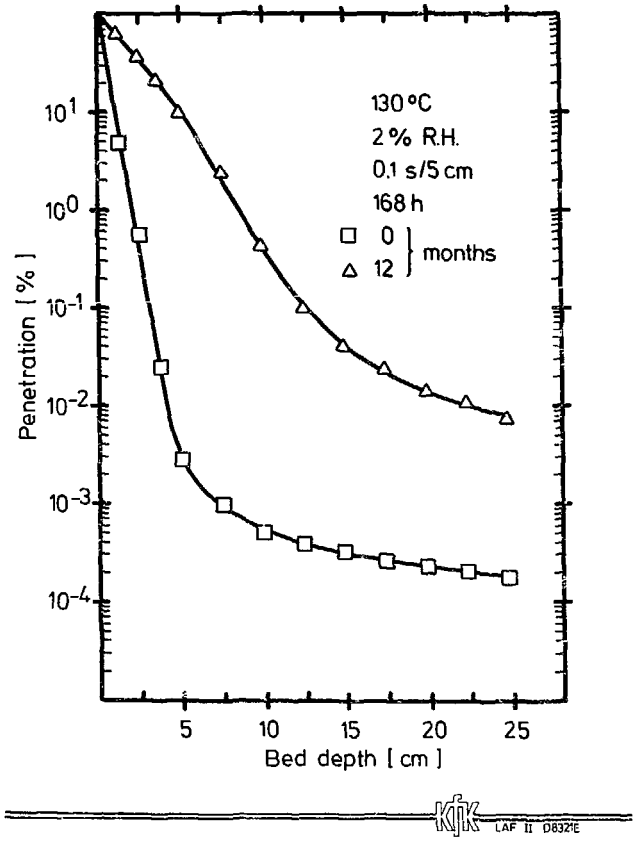

Penetration of 207B (KI) by ^{131}I loaded as I_2, at different aging times

Fig. 5

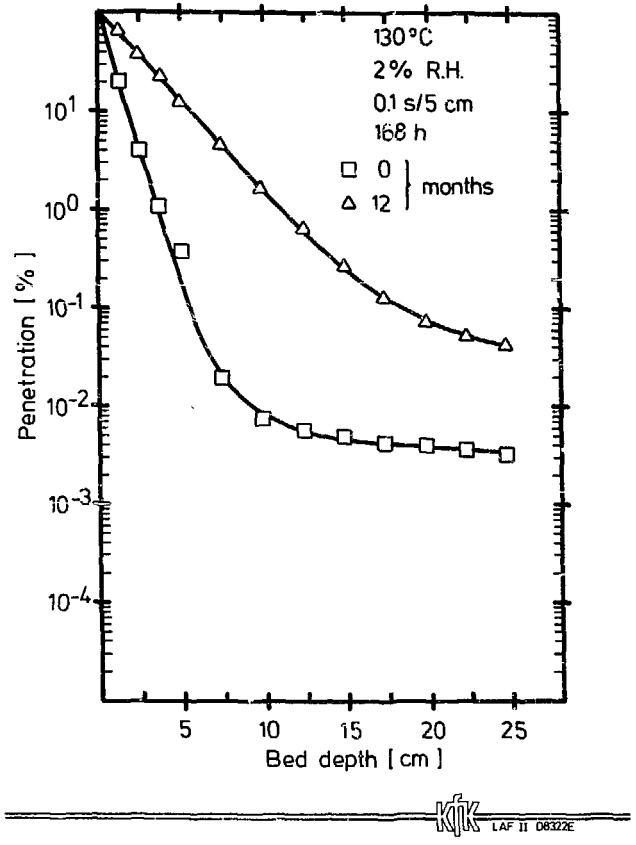

Penetration of 207B (TEDA) by ^{131}I loaded as I_2, at different aging times

Fig. 6

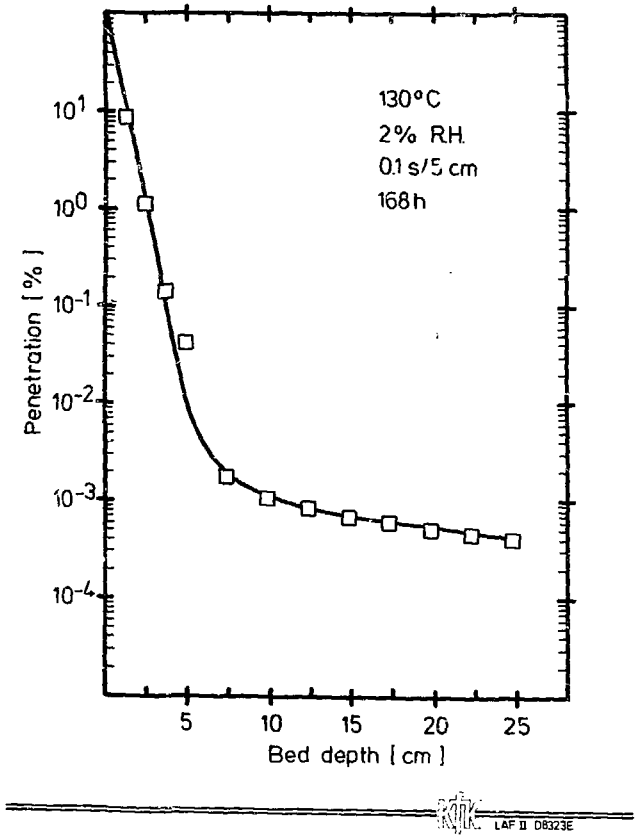

Penetration of Kiteg II by ^{131}I loaded as I_2 (no aging)

Fig. 7

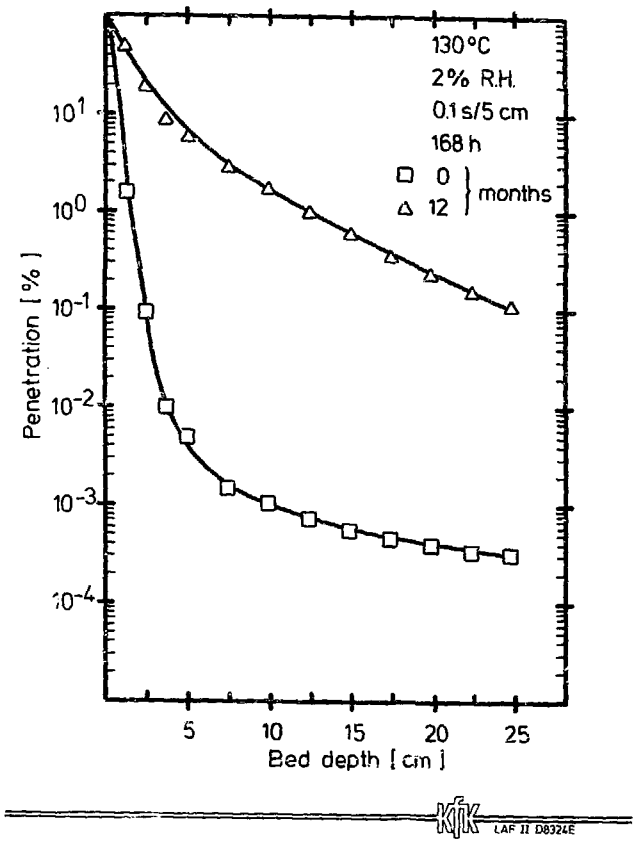

Penetration of Radshield 25 by ^{131}I loaded as I_2 at different aging times

Fig. 8

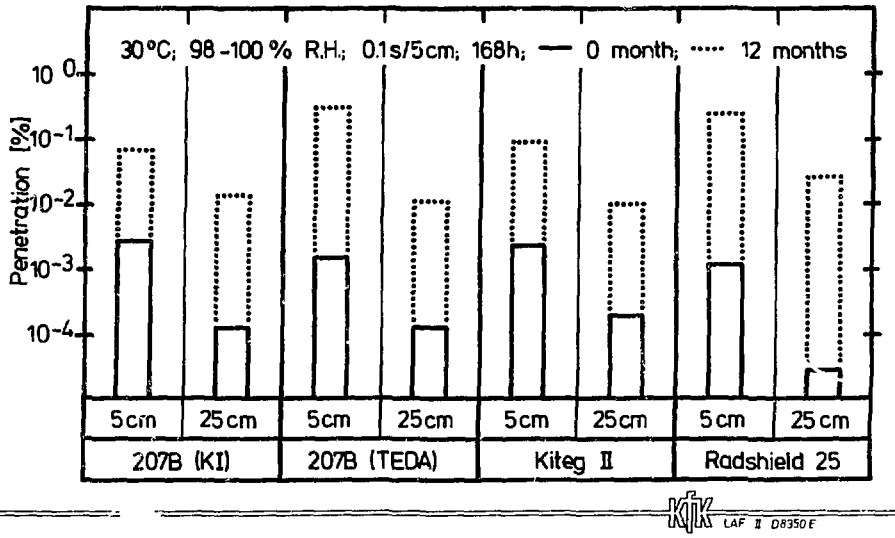

Penetration of various impregnated activated carbons by ^{131}I loaded as I_2, at different bed depths and aging times

Fig. 9

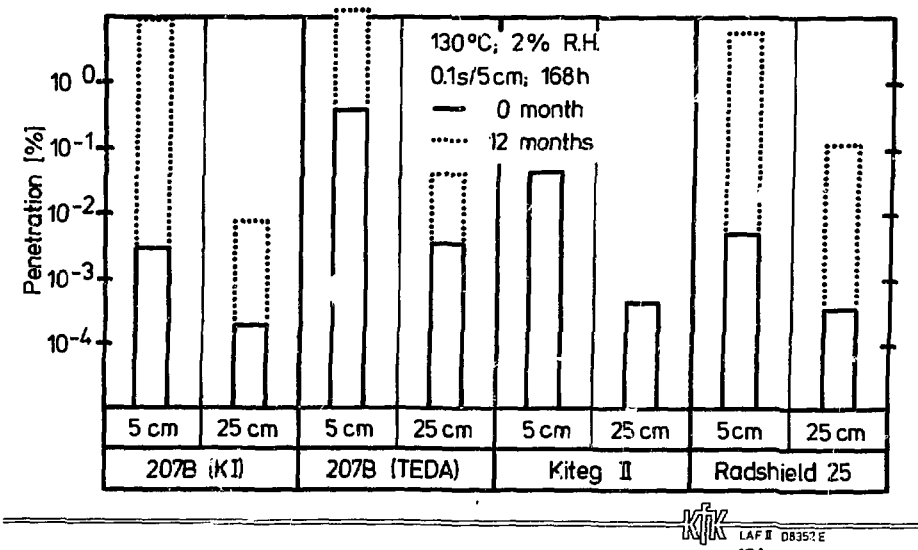

Penetration of various impregnated activated carbons by ^{131}I loaded as I_2, at different bed depths and aging times

Fig. 10 a)

a) No reliable results obtained for aged Kiteg II (mechanical defect)

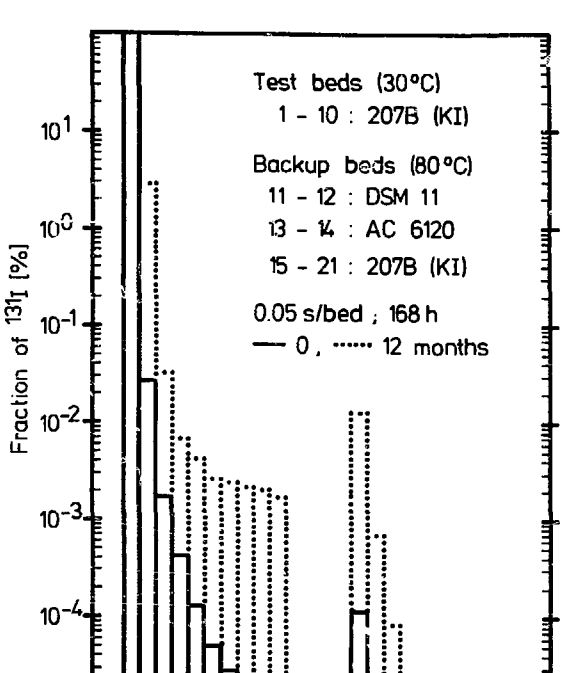

Distribution of ^{131}I among test and backup beds at different aging times (^{131}I as I_2)

Fig. 11

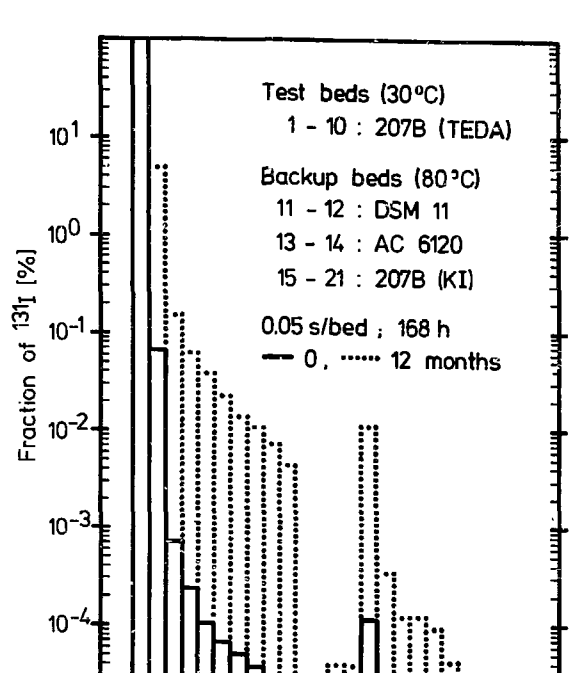

Distribution of ^{131}I among test and backup beds at different aging times (^{131}I as I_2)

Fig. 12

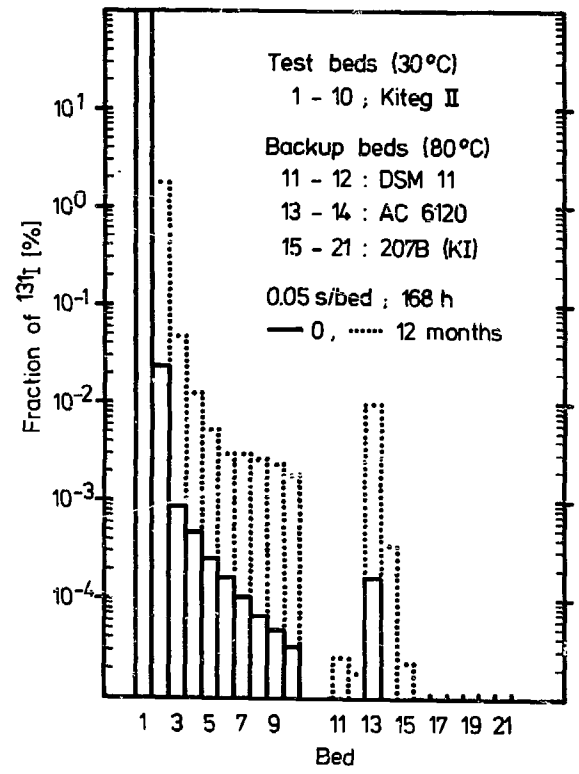

Distribution of ^{131}I among test and backup beds at different aging times (^{131}I as I_2)

Fig. 13

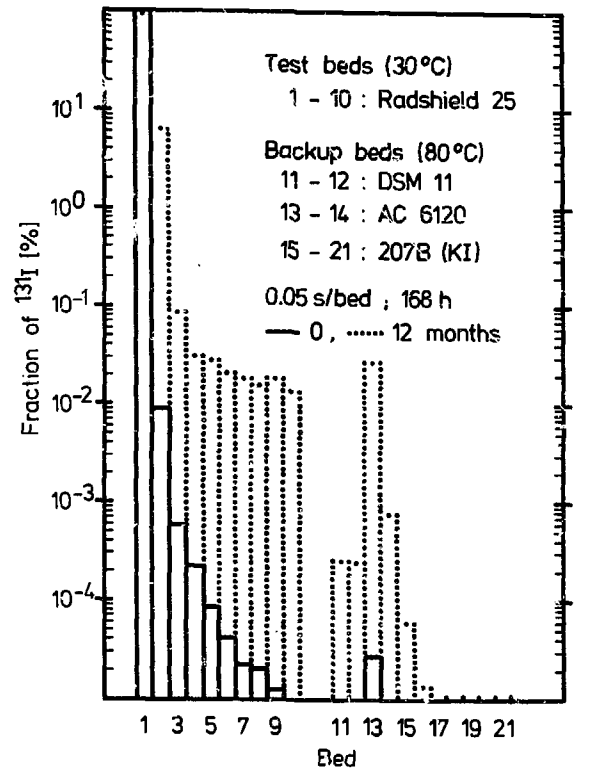

Distribution of ^{131}I among test and backup beds at different aging times (^{131}I as I_2)

Fig. 14

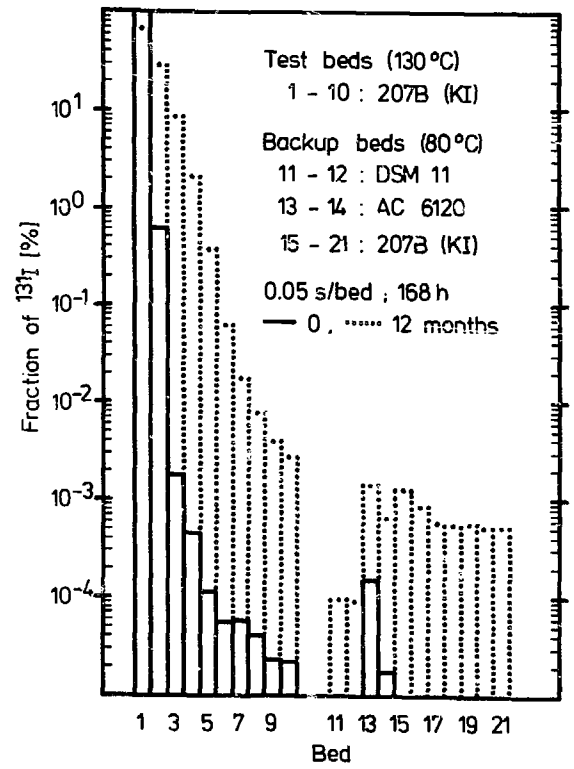

Distribution of ^{131}I among test and backup beds at different aging times (^{131}I as I_2)

Fig. 15

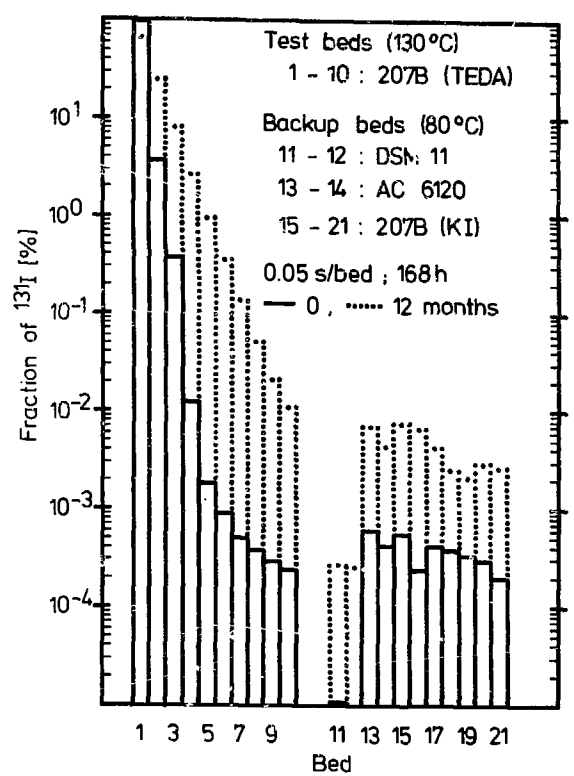

Distribution of ^{131}I among test and backup beds at different aging times (^{131}I as I_2)

Fig. 16

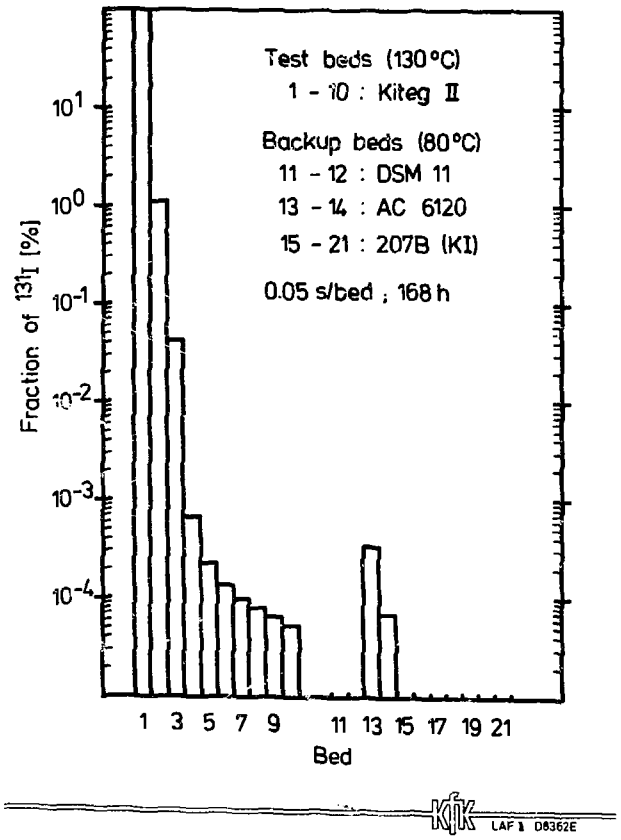

Distribution of ^{131}I among test and backup beds (no aging; ^{131}I as I_2)

Fig. 17

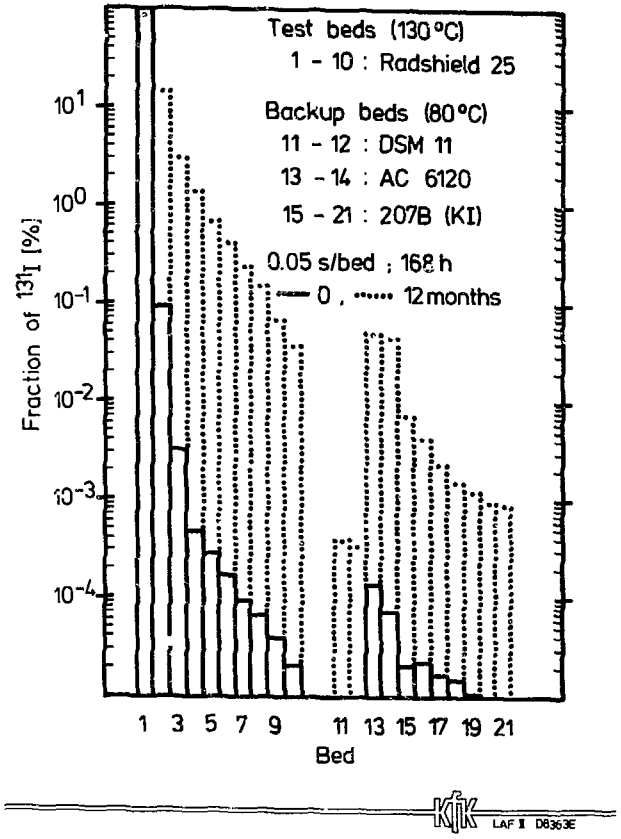

Distribution of ^{131}I among test and backup beds at different aging times (^{131}I as I_2)

Fig. 18

DISCUSSION

VIKIS: You mentioned an iodine form more penetrating than methyl iodide; would you care to comment what that form may be.

DEUBER: This is, of course, a very important question and the same question always arises, but I cannot give you a positive answer. I can only give you some comments. There will be a second paper this afternoon where penetrating iodine will also be dealt with and maybe we can speak about it again. But, as far as these investigations are concerned, the penetrating iodine species cannot be particulate iodine since the backup beds were preceded by a particulate filter. Apart from that, I cannot give a definite answer.

LONG-TERM DESORPTION OF ^{131}I FROM KI-IMPREGNATED CHARCOALS LOADED WITH CH_3I, UNDER SIMULATED POST-LOCA CONDITIONS

A.C. Vikis, J.C. Wren and C.J. Moore
Research Chemistry Branch
Atomic Energy of Canada Research Company
Whiteshell Nuclear Research Establishment
Pinawa, Manitoba, Canada R0E 1L0

and

R.J. Fluke
Nuclear Studies and Safety Department
Ontario Hydro
700 University Avenue
Toronto, Ontario, Canada M5G 1X6

ABSTRACT

The long-term (1100 h) desorption of ^{131}I from KI-impregnated charcoal filters, loaded with CH_3I, has been studied under simulated post-LOCA conditions. A charcoal filter bed (20 cm long, 5.0 cm in diameter), which was pre-equilibrated with air at 353 K and a relative humidity of 72%, was exposed to 1.7 g of CH_3I (containing 320 MBq of ^{131}I) over a period of one hour. The ^{131}I released was monitored continuously during loading and during the 1100-h purging period. The activity distribution along the length of the charcoal filter was also monitored during purging, using an external γ-ray detector. Iodine-131 release rates ($Bq \cdot h^{-1}$) as a function of purging time (in hours) were: $2.3 \times 10^6\ t^{-6.26 \pm 0.32}$ (for t = 1-5 h) and $2.0 \times 10^3\ t^{-0.64 \pm 0.08}$ (for t = 5-1100 h). The ^{131}I activity distribution along the length of the charcoal bed decreased exponentially from inlet to outlet. Also, a small broadening and displacement (towards the outlet) of the initial ^{131}I distribution were observed during purging. These data show that in post-accident environments deep-bed charcoal filters impregnated with KI are effective barriers to both the short-term and long-term release of $CH_3{}^{131}I$.

INTRODUCTION

Charcoal filters are used in nuclear reactor ventilation systems to safeguard against the release of radioiodines during routine reactor operation and under accident conditions[1,2]. The charcoals are normally impregnated with potassium iodide (KI) and/or triethylene diamine (TEDA). The KI impregnant is used to dilute potential releases of radioiodine, via isotopic exchange with non-radioactive iodine. TEDA is used to enhance the efficiency of charcoals in retaining organic iodides, through formation of quaternary ammonium salts. According to risk analyses of various postulated loss-of-coolant-accident (LOCA) scenarios, the active iodines dominate the radiological impact term. It is therefore important to demonstrate that charcoal filters would perform satisfactorily under LOCA conditions.

The performance characteristics of impregnated charcoals have been studied thoroughly under the ambient conditions associated with

routine reactor operation[2-6]. However, there is insufficient data on the long-term performance of these charcoals, particularly for post-accident conditions, where high temperature, humidity, radioiodine challenge and radiation fields may exist[7]. We have therefore initiated a study to determine the performance characteristics of KI- and TEDA-impregnated charcoals, for CANDU* post-LOCA conditions. This study is being done at the Whiteshell Nuclear Research Establishment of Atomic Energy of Canada Limited, in collaboration with Ontario Hydro.

In analyzing the performance of CANDU multi-unit containment systems under accident conditions, the long-term desorption of radioiodines from charcoal filters is an important parameter. For a certain time period after a LOCA, the vacuum building will maintain the containment envelope sub-atmospheric, thus preventing any releases. Once the vacuum is lost, the Emergency Filtered Air Discharge (EFAD) system may be used to vent portions of the containment atmosphere through a filtered pathway, thereby preventing the uncontrolled leakage of radioactivity. The EFAD system could be used after a LOCA until the cleanup operation is completed. Thus, long-term desorption of radioiodines from the charcoal filters in the EFAD system is a major parameter in determining the radiological consequences of an accident.

In this publication, we present results on the long-term (1100 h) performance of KI-impregnated charcoal, which has been exposed to a large challenge of CH_3I. The desorption of ^{131}I, which was used as a tracer, was monitored continuously for 1100 h, while the charcoal filter was purged with air at a temperature of 353 K and a relative humidity of 72%. The ^{131}I activity distribution along the length of the charcoal bed was also monitored during the experiment.

EXPERIMENTAL

The flow system used in this study is shown schematically in Figure 1. It was constructed using Pyrex glass to minimize radioiodine adsorption on the walls of the system, particularly for anticipated experiments with I_2. Greaseless O-ring joints and teflon stopcocks were used where necessary. In this study the CH_3I storage vessel was constructed of stainless steel.

The methyl iodide, labelled with ^{131}I (190 MBq/g CH_3I), was purchased from ICN, Chemical and Radioisotope Division, California. It was introduced into the main flow by vapour saturation of a stream of N_2 carrier gas, at a temperature of 273 K. The main carrier gas was dry air.

The required steam was generated using distilled water. To achieve the desired relative humidity, at the charcoal filter temperature, excess steam was introduced into the main flow, prior to condenser #1 in Figure 1. Final humidity adjustment was accomplished by controlling the column temperature of condenser #1. The

*CANada Deuterium Uranium - Canada's heavy-water moderated, natural-uranium fuelled reactor.

condenser was made of Pyrex glass and had a column packed with 4-mm glass beads, for efficient liquid-vapour equilibration. The column was thermostatted to within ±1 K by means of water flowing through an annular jacket surrounding the condenser column. Excess vapour condensed and flowed to the bottom of the condenser into a 1-L flask maintained at room temperature.

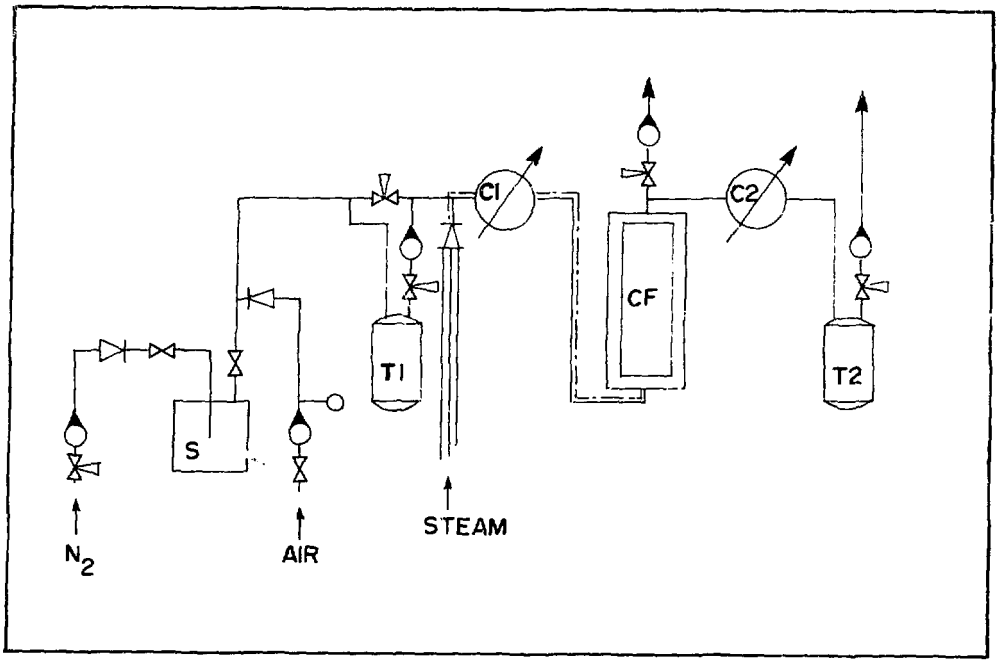

Figure 1. Diagram of charcoal filter test facility. (S is the CH_3I storage vessel; T1, T2 are ^{131}I counting stations; CF is the charcoal filter; C1, C2 are condensers.)

From condenser #1, the air, CH_3I, and steam flowed to the charcoal filter through a connecting tube that was heated to avoid water condensation. The charcoal filter canister was also made of Pyrex glass. It was 30 cm long and 5 cm I.D., and was thermostatted to within ±1 K with water circulated through an annular jacket surrounding the canister. The KI-impregnated charcoal was supported on a 7.5-cm thick layer of 4-mm glass beads. The glass beads distributed the flow uniformly through the cross-section of the charcoal bed.

After the charcoal filter, a known fraction of the flow was diverted through condenser #2, which was identical to condenser #1, to dry the stream prior to reaching counting station #2. The rest of the flow was passed through a silver mordenite trap, to remove the CH_3I, and then was routed to the active ventilation system of the building.

The $CH_3{}^{131}I$ was monitored before and after the charcoal filter, by diverting known fractions of the flow through the two counting stations shown in Figure 1. At each counting station the CH_3I was sorbed in a sampler containing a column (5.0 cm long and 2.2 cm in diameter) of 13.5 g of silver mordenite (Zeolon 900, 15-20 weight % Ag). The capability of each sampler to retain 100% of the CH_3I was verified experimentally. Each sampler was precision-fitted into the well (2.54 cm in diameter and 5.2 cm deep) of a NaI scintillator crystal/photomultiplier assembly.

Tennelec single-channel analyzers, set to monitor the 0.365 MeV γ-ray, were used to count the ^{131}I deposited in each sampler. The count rate from each station was monitored independently, and recorded automatically at predetermined intervals, using a Tennelec counter-timer-printer system. The dead-time of this counting system was $\sim 1 \times 10^{-7}$ s. The counting efficiency, determined by calibration with $CH_3{}^{131}I$, was 25%.

The activity distribution along the length of the charcoal filter was measured by translating a shielded γ-ray detector along a vertical slit (8.5 mm wide and 200 mm long) cut in the lead shield of the charcoal filter. The horizontal viewing angle (5.5°) of the detector was defined by a cylindrical slit (5 mm in diameter and 52 mm long) in the detector lead shield and by the width of the vertical slit on the filter lead shield. The vertical viewing angle (11.0°) was defined by the detector slit. A charcoal-filter volume element of 17.1 cm^3 was thus viewed in each measurement, except for the first and second volume elements, from the inlet, which were 8.5 cm^3 and 14.8 cm^3, respectively.

Prior to introduction of the CH_3I challenge, the system was equilibrated for a period of 20 h. Then 1.7 g of CH_3I was introduced at a uniform rate for a period of 60 min. The released activity was monitored for 1100 h. Fresh silver mordenite traps were installed periodically to minimize a possible deterioration in efficiency of the sorbent, and to discard accumulated ^{131}I, in order to detect low ^{131}I release rates more easily. A summary of the experimental conditions is given in Table 1.

Table 1. Conditions for long-term CH_3I desorption test.

Charcoal - type:	Sutcliffe-Speakman, Type 208C, cocoanut shell charcoal, 5 weight % KI
- bed length:	20 cm
- bed diameter:	5 cm
Temperature:	353 K
Relative humidity (353 K):	72%
Linear flow rate:	23 $cm \cdot s^{-1}$
Pre-equilibration period:	20 h
CH_3I challenge - total:	1.7 g (320 MBq)
- loading rate:	46 $mg \cdot s^{-1}$ (90 $kBq \cdot s^{-1}$)

RESULTS AND DISCUSSION

The variation of the total ^{131}I activity deposited on the charcoal filter and released from it, during CH_3I loading and for an hour afterwards, is shown in Figure 2. Noticeable activity breakthrough was observed about 20 min into the test, and the activity rose exponentially thereafter until a few minutes after termination of the CH_3I loading. The trends in the released activity, during loading and afterwards, are discussed below.

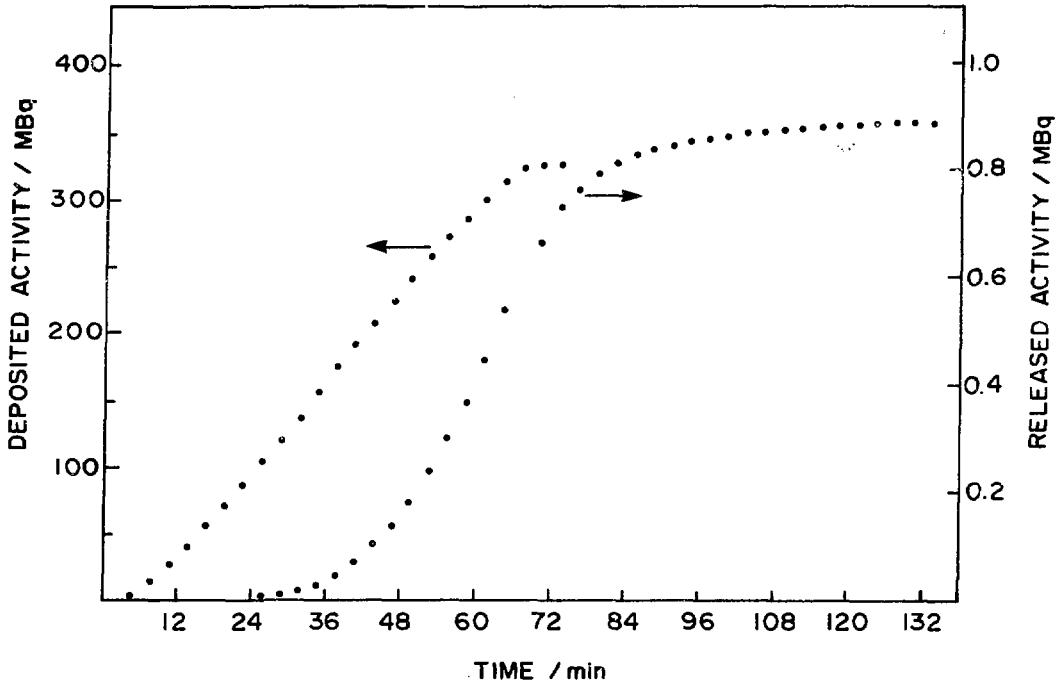

Figure 2. Deposited and released ^{131}I activity for the period 0-2 h.

Samples of the same charcoal were also tested for $CH_3{}^{131}I$ decontamination under a range of conditions: humidity (0% to 95%), temperature (313 K to 383 K), CH_3I challenge concentration ($0.5\ ng \cdot cm^{-3}$ to $10\ ng \cdot cm^{-3}$), and charcoal bed length (10 cm and 20 cm). The decontamination factors (DFs) obtained in these experiments were in the 10^4 to 10^5 range. The DF immediately prior to termination of the high CH_3I challenge fell to a value of $\sim 2 \times 10^2$. This large drop in the DF was expected as the charcoal bed approached saturation.

We have analyzed the variation of the DF during CH_3I loading, using the Wheeler and Robell[8] equation. This equation was originally derived for fixed-bed catalytic flow reactors and later adapted to gas penetration through a charcoal bed[5,9]. The data near the onset of the activity release obeyed this equation well and a value of 1.2×10^{-2} g CH_3I/g charcoal was determined for the loading capacity of the charcoal. Also, from the same equation the pseudo first-order rate constant for adsorption of CH_3I on charcoal was

determined. The latter was 14 s^{-1}, which is approximately the correct magnitude to account for the high DFs determined with low CH_3I concentrations ($\ell nDF = kt$, where k is the pseudo first-order rate constant, and t is the residence time of CH_3I on the charcoal filter).

The activity released following termination of the CH_3I loading is shown in Figure 3 as a function of purging time. Each curve represents the activity accumulated on a new batch of sorbent.

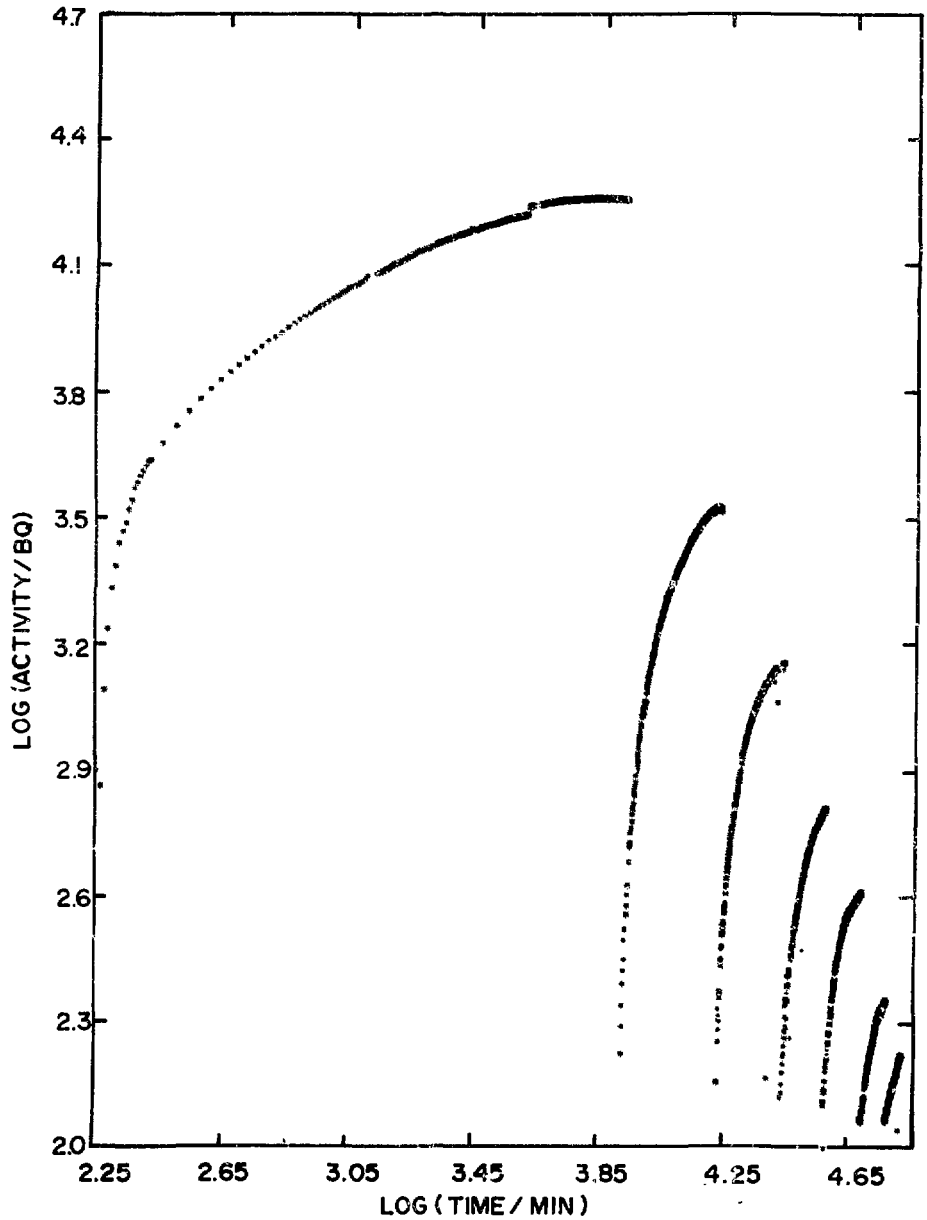

Figure 3. Released ^{131}I activity for the period 3-1100 h.

Each point represents a measurement of the activity during the time interval Δt, between $t-\Delta t/2$ and $t+\Delta t/2$. The counting interval was gradually increased from 5 min at the beginning of the test, when the ^{131}I release rate was high and changing rapidly, to 60 min towards the end of the test, when the ^{131}I release rate was low and changing slowly. The data were corrected for ^{131}I decay during the test, and then differentiated to derive the corrected release rates shown in Figure 4. The observed release rates can be obtained by multiplying each corrected release rate by the ^{131}I decay term, $\exp(-t\ln 2/t_{1/2})$, where $t_{1/2}$ is the decay half-life of ^{131}I and t is the time from the beginning of the test.

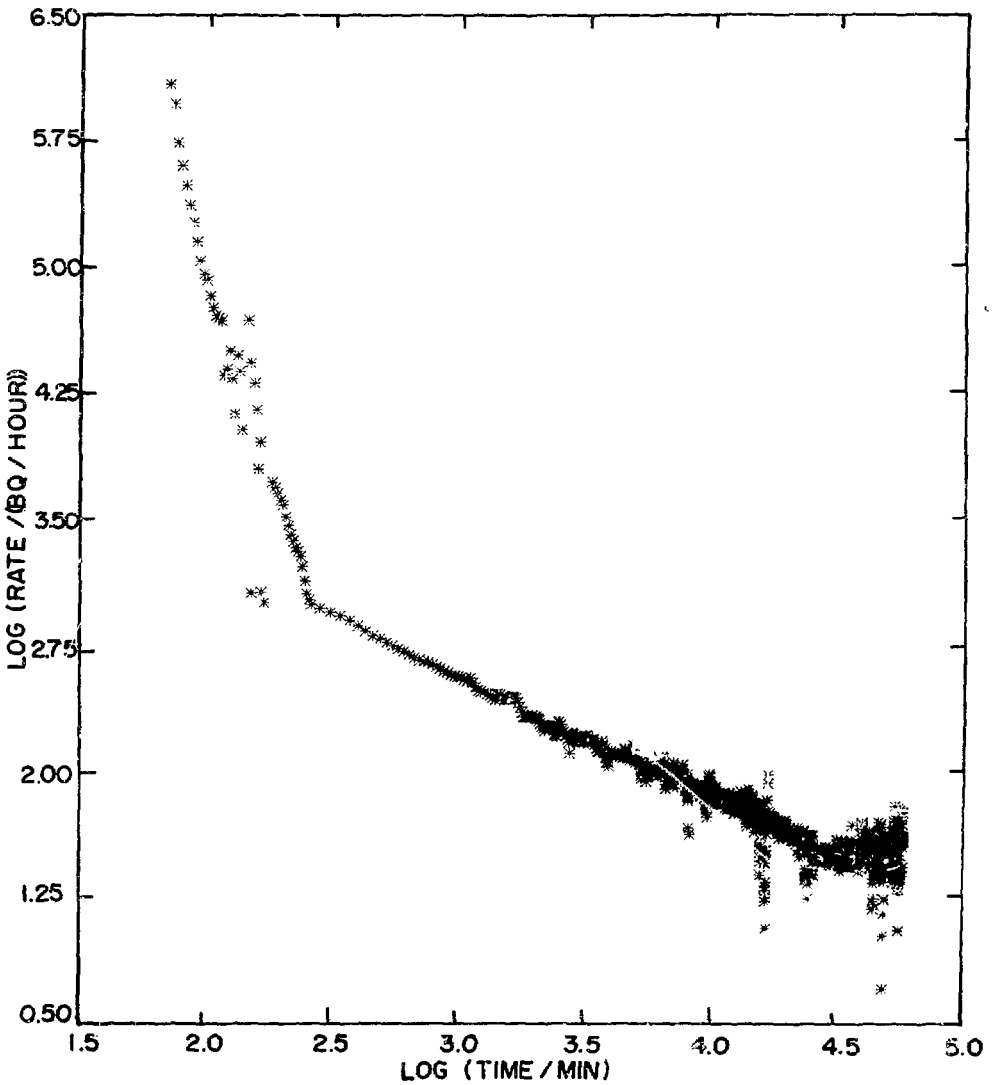

Figure 4. Iodine-131 release rate for the period 2-1100 h.

Two distinct trends in the corrected release rate (R) vs time (t) relationship were observed:

(a) For the period 1-5 h, the release rate fitted eq. (1):

$$R/(Bq \cdot h^{-1}) = 2.3 \times 10^{6} \, (t/h)^{-6.26 \pm 0.32} \quad . \qquad (1)$$

(b) For the period 5-1100 h, the release rate fitted eq. (2):

$$R/(Bq \cdot h^{-1}) = 2.0 \times 10^{3} \, (t/h)^{-0.64 \pm 0.08} \quad . \qquad (2)$$

The observed release rates can be obtained by multiplying the right-hand side of eq. (1) and (2) by $\exp(-t\ell n2/t_{1/2})$, as explained above. Table 2 lists the observed and corrected releases as a percentage of the deposited activity for various time intervals.

Table 2. Percent of deposited ^{131}I released during various time intervals.

Time Interval (h)	Observed	Corrected for ^{131}I Decay
0 - 1[a]	1.9×10^{-1}	1.9×10^{-1}
1 - 5[a]	8.4×10^{-2}	8.4×10^{-2}
5 - 50[b]	3.5×10^{-3}	3.9×10^{-3}
50 - 300[b]	3.7×10^{-3}	6.3×10^{-3}
300 - 1100[b]	1.0×10^{-3}	7.9×10^{-3}
0 - 1100	2.8×10^{-1}	2.9×10^{-1}

(a) Values for these intervals were obtained from actual measurements.

(b) Values for these intervals are mean values calculated from eq. (2).

The normalized activity distribution along the length of the charcoal bed at various times is shown in Figure 5. This distribution was corrected for end effects, which affected the first (0 cm) and second (1 cm) measurements near the inlet, and for background, which affected the lower count-rate values of Figure 5. The distribution decreased approximately exponentially from inlet to outlet and indicates that the bulk of the ^{131}I was adsorbed on the first few centimeters of the charcoal bed. A slight broadening and shift (towards the outlet) of the distribution were also observed during purging. Table 3 lists the percentage of the adsorbed activity in the various segments of the charcoal bed as a function of purging time. The observations regarding the activity distribution on the charcoal bed complement the release-rate data, by showing very slow activity migration towards the outlet.

The adsorption, desorption and isotopic exchange of CH_3I, using KI-impregnated charcoals, has been the subject of several previous studies[3,10-12]. The key reactions involved are as follows:

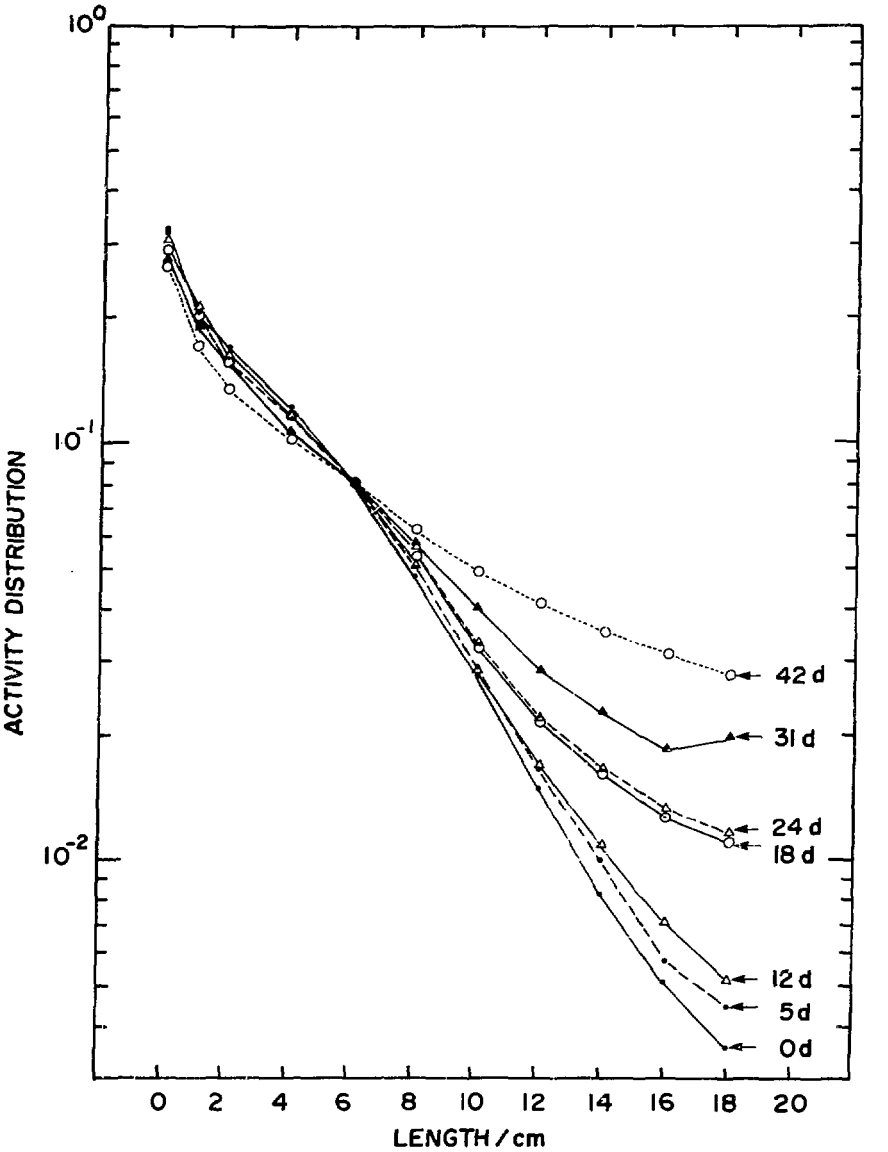

Figure 5. Normalized ^{131}I activity distribution on charcoal filter as a function of purging time.

$$CH_3I(g) \rightleftharpoons CH_3I(a) \quad (3)$$

$$CH_3I^*(g) \rightleftharpoons CH_3I^*(a) \quad (4)$$

$$CH_3I^*(a) + KI(s) \rightleftharpoons CH_3I(a) + KI^*(s) \quad (5)$$

$$CH_3I(g) \rightarrow \text{release} \quad (6)$$

$$CH_3I^*(g) \rightarrow \text{release} \quad (7)$$

Table 3. Percent of total activity deposited in various segments of the charcoal bed.

Time (d)	First 5 cm	First 10 cm	First 15 cm
0	68	92	98
5	66	91	98
12	66	91	98
18	62	87	95
24	62	87	95
31	57	82	93
42	50	75	89

In the above equations, ^{131}I is denoted by I*, and (g), (a) and (s) denote the gaseous, adsorbed and solid phases, respectively. The release of CH_3I and CH_3I* occurs following a number of adsorption/desorption steps along the length of the charcoal bed.

Pertinent data (rate constants, isotherms) are not available for a quantitative understanding of the observed release rates. However, a qualitative understanding can be developed using the above reactions. For instance, the early (1-5 h) fast release and subsequent (5-1100 h) slow release trends can be explained in terms of the relative rates of the above reactions. The rates of reactions (3) and (4) are expected to be comparable to the collision rates of a gas with a surface, and hence are relatively fast. On the other hand, the rate of reaction (5) would be slow due to the limited mobility of the adsorbed and solid phases. Thus, we propose that the early (1-5 h) fast release was CH_3I, which had not yet equilibrated isotopically with the KI on the charcoal. The subsequent (5-1100 h) slow release was CH_3I that was in isotopic equilibrium with the KI on the charcoal.

The functional form of the observed release rates ($R \propto t^{-n}$) is attributed to the nature of the CH_3I-charcoal isotherm and the number of elementary adsorption/release cycles along the length of the charcoal bed. Desorption along a type I isotherm, under conditions of continuous purging, is known from the theory of gas chromatography to result in tailing distributions[13], as observed here.

We are presently modelling this system, using the concepts discussed above, to increase our understanding of the underlying processes so as to be able to predict the behaviour of these filters under various conditions.

CONCLUSIONS

A practical conclusion of this study is that in post-accident environments simulated by this test, deep-bed charcoal filters (impregnated with KI) are an effective barrier for both short-term and long-term release of the most penetrating radioiodine species (CH_3I). In this study, a CH_3I challenge of 9×10^{-3} g CH_3I/g charcoal was used which is about one hundred times larger than the total iodine (^{131}I, ^{129}I and ^{127}I) challenge expected in a worst-case accident in a CANDU reactor. Even so, very low release rates were

observed, which fell from about 0.3% per day for the first day, to less than about 1.5×10^{-3}% per day thereafter. These values are below the rate of 1% per day used in past CANDU licensing analyses.

In addition to the above, this study has provided detailed data that will allow us to increase our understanding of the underlying processes, particularly, the role of isotopic exchange. Understanding the underlying processes is important for predicting the behaviour of these systems under a variety of post-accident conditions.

REFERENCES

1. "Radioiodine removal in nuclear facilities, methods and techniques for normal and emergency situations", IAEA Tech. Rep. Ser. No. 201, Vienna, 1980.

2. Kovach, J.L., "The evolution and current state of radio-iodine control", Proc. 16th DOE Nuclear Air Cleaning Conference, Vol. 1, 417 (1981).

3. Wood, G.O. and Valtez, F.O., "Nonradiometric and radiometric testing of radioiodine sorbents using methyl iodide", Proc. 16th DOE Nuclear Air Cleaning Conference, Vol. 1, 448 (1981).

4. Deitz, V.R. and Jonas, L.A., "Catalytic trapping of methyl iodide by beds of impregnated charcoal", Nucl. Technol., 37, 59 (1978).

5. Jonas, L.A., Deitz, V.R. and Romans, J.B., "Desorption kinetics of methyl iodide from impregnated charcoal", Nucl. Technol., 48, 77 (1980).

6. Shiomi, H., Yuusa, Y., Tani, A., Ohki, M. and Nakagawa, T., "A parametric study of removal efficiency of impregnated activated charcoal and silver zeolite for radioactive methyl iodide", Proc. 17th DOE Nuclear Air Cleaning Conference, Vol. 1, 199 (1983).

7. Jefford, J.D. and Fluke, R.J., "Experimental data required for the design and analysis of emergency filtered air discharge systems", Proc. 16th DOE Nuclear Air Cleaning Conference, Vol. 1, 225 (1981).

8. Wheeler, A. and Robell, A.J., "Performance of fixed-bed catalytic reactors with poison in the feed", J. Catal., 13, 299 (1969).

9. Jonas, L.A. and Rehrmann, J.A., "The kinetics of adsorption of organo-phosphorus vapors from air mixtures by activated carbons", Carbon, 10, 657 (1972).

10. Romans, J.B. and Deitz, V.R., "A non-radioactive determination of the penetration of methyl iodide through impregnated charcoals during dosing and purging", Proc. 15th DOE Nuclear Air Cleaning Conference, Vol. 1, 313 (1979).

11. Kovach, J.L., "Adsorbents; review and projection", Proc. 10th Air Cleaning Conference, Vol. 1, 149 (1968).

12. Davis, W. Jr., "Models for calculating the effects of isotopic exchange, radioactive decay and recycle in removing iodine from gas and liquid streams", Nucl. Sci. Eng., 61, 11 (1976).

13. Keulemans, A.I.M., Gas Chromatography, 2nd ed., Reinhold, New York, 1959.

DISCUSSION

OSLINGER: During a LOCA scenario, radioiodine loading rate is weighted to the beginning of the scenario. Why was linear loading (constant rate) chosen? This is optimistic.

VIKIS: We used a linear loading rate as a matter of choice to simplify experimental interpretation by reducing the number of variable parameters.

OSLINGER: What I am thinking about is, you are saying that the release of radioiodine is more significant at the beginning. But that happens for a relatively short time period. This is when you are loading the charcoal bed at the maximum rate. After 5 hours, there may not be much radioiodine getting to the charcoal bed because most of the iodine that was going to get to the charcoal bed would have already gotten there. I have the preception that when you look at the two curves you may say that most of the time we are not releasing at a very high rate. In reality, the first five hours is when you would have released most of it anyway. That is why I thought when you loaded it, in a case where 90% of the loading occurred in the first hour or two hours, you might find that the second part of your experimental curve wouldn't be very significant when applied to a real load case. I can see that when you did the experiment, you wouldn't want to vary too many parameters at once, but I am thinking that, maybe the next step would be non-linear loading just to simulate reality a little bit closer.

VIKIS: Yes, perhaps what you are proposing may be more realistic. Yes, but as you said, in deciding to try an experiment you want to minimize variables and that is what we did.

KABAT: Your test bed, which contained approximately 200g of charcoal, was loaded with 1.7g of CH_3I. What would be the total activity of radioiodine, at this loading, in a full scale adsorber unit?

VIKIS: The loading in this experiment on a g I/g charcoal basis is about 100 times higher than that predicted in a "worse-case" accident. I do not recall the activity loading for this kind of accident, but I would expect it to be higher than the activity loading (1.6 MBq/g charcoal) used in the present test, which was used solely for the purpose of monitoring rather than simulating radiation effects.

DEUBER: Do you have corresponding data for carbon without an impregnant? These data could help to understand the processes involved.

VIKIS: No, we do not yet have other data. I also agree with you that data with non-impregnated charcoals (or with plain $CH_3{}^{127}I$) would be valuable in assessing the relative importance of the isotope effect vs. physical adsorption. The effect was much higher than we expected because we wanted to cover any situation and to show the worse kind of release that we can have.

DEUBER: I understand why you have this high loading, but on the other hand, I doubt whether isotopic exchange is very important with this very high loading.

VIKIS: We are talking about 1.7 g of methyl iodide versus 10 g of potassium iodide for that particular charcoal. So there is still lots of iodide to achieve isotopic exchange. Of course, any isotopic exchange would have a limited rate and certainly at the beginning, as you saw it, it looks like the system was still equilibrating.

A STUDY OF ADSORPTION PROPERTIES OF IMPREGNATED CHARCOAL FOR AIRBORNE IODINE AND METHYL IODIDE

Li Qi-dong, He Sui-yuang

Fudan University

Shanghai, China

Abstract

The adsorption characteristics of airborne radioiodine and methyl iodide on impregnated charcoal were investigated.

The activated charcoal tested was made from home-made oil-palm shells, and KI and TEDA were used as impregnants. A new technique was used to plot the dynamic partial adsorption isotherm at challenge concentrations (concentration range of iodine: 1-20 ppm v/v).

Some adsorption properties of the impregnated charcoal were estimated with the dynamic partial adsorption isotherm.

The dependences of the adsorption capacity and penetration behavior for airborne iodine and methyl iodide on the ambient conditions (temperature, relative humidity, and superficial velocity) were studied.

I. Introduction

The gaseous effluent is of primary importance during the operation of nuclear power plants under normal and accident conditions. If some radioactive wastes are released to the environment, radioactive iodine and methyl iodide are conspicuous in the gaseous effluent.

For many years, therefore, on generation of iodine, the release mechanism, the properties, the forms, the trapping and retention behavior and health effects have been the subject of numerous studies.[1]

The impregnated charcoal we have developed was made from oil-palm shells impregnated with TEDA, KI, and its optimum operation parameters were determined.

In this study, we have carried out screening tests and a series of experiments for adsorption characteristics of the impregnated charcoal.

We have used 23 types of charcoal in our screening test, as described in Table 1, and we chose oil-palm shell base carbon with 2% TEDA-2% KI impregnation for further experiments. The adsorption of elemental iodine and methyl iodide has been experimentally evaluated to observe the effect of varying certain operating parameters, such as inlet concentration, temperature, relative humidity, superficial velocity, and bed depth. The parameters presented may be useful in designing charcoal adsorber systems for radioiodine retention in nuclear power plants.

Table 1 Kinds of Activated Carbon used in Screen Tests

Sample No.	Base Carbon	Impregnation	Benzene Adsorption %
3	Oil-palm shells	15 % Hypo	30.0
8	Oil-palm shells	Washing with water	38.0
11	Oil-palm shells	10 % Piperazine	38.0
13	Oil-palm shells	None	37-38
14	Oil-palm shells	10 % KI	37-38
15	Oil-palm shells	10 % HMTA	37-38
16	Oil-palm shells	10 % TEDA	37-38
17	Oil-palm shells	2 % TEDA-2 % KI	37-38
18	Wood (Sawdust)	None	-
20	Oil-palm shells	5 % TEDA-2 % KI	-
21	Oil-palm shells	2 % TEDA-2 % KI	-
22	Phenolic resin fibre	None	-

II. Preparation of Activated Carbon and Screening

Preparation of Impregnated Charcoal

We have prepared 23 different kinds of charcoal. The procedure for producing impregnated charcoal is as follows:

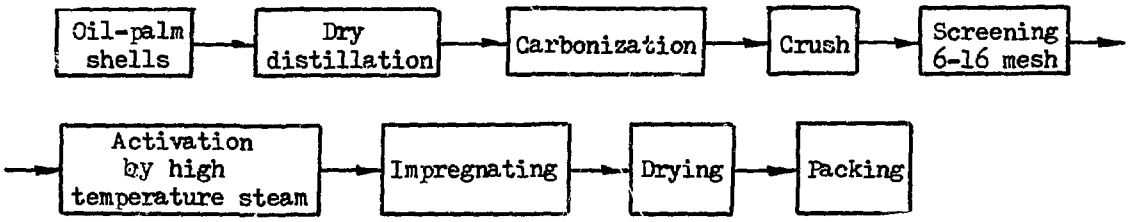

Fundamental properties of oil-palm shell base carbon before impregnating are listed below (Table 2).

Procedure for Screening

Test equipment. By the above process, we obtained 23 different impregnated charcoals and then screening tests were carried out sequentially under the same conditions.

Table 2. Fundamental properties of oil-palm shell base carbon.

		Pore size distribution	
Benzene adsorption	-	Pore size r (Å)	Pore volume (%)
Particle size	6-16 mesh	0 - 20	33.44
Moisture content	-	20 - 40	25.67
Specific surface	1013.4 m^2/g	40 - 80	14.48
Wear strength	98 %	80 - 120	12.72
Spontaneous ignition temperature	490 °C	120 - 160	8.13
Mode pore size	10 Å	> 160	5.56
Mean pore size	11 Å		

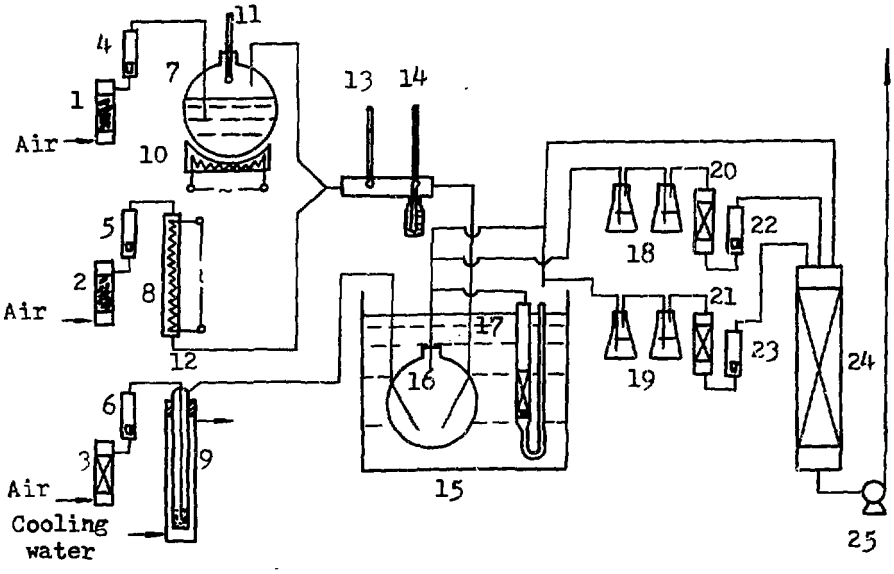

FIGURE 1. FLOWSHEET OF TEST EQUIPMENT FOR ADSORPTION OF ELEMENTAL IODINE

1,2 glass wool prefilter. 3,20,21 gas dryer. 4,5,6,22,23 rotameter. 11 controlling thermometer. 13 dry-bulb thermometer(controllable). 14 wet-bulb thermometer. 10 automatic contral heater(furnace). 7 steam generator. 8 automatic control heater (piped). 12 radioiodine generator. 9 cooling jacket for iodine generator. 15 constant temperature bath. 16 gas mixer. 17 adsorption tube(I.D. 18 mm). 18,19 gas absorption bottles. 24 safeguard. 25 vacuum pump.

Figure 1 presents a schematic diagram of the experimental system employed to carry out screening and to acquire experimental information on the adsorption properties of radioiodine on charcoal beds.

The experimental system was placed in a ventilation chamber and kept at constant temperature.

Air entered the experimental system from three different inlets:

(1) Wet air: Air was permitted to flow through glass wool prefilter 1, and rotameter 4. It then entered steam generator 7, by controlling thermometer 11, to acquire the air moisture required.

(2) Heated air: Air was permitted to flow through glass wool prefilter 2 and rotameter 5, then enter automatic control heater 8 to acquire required temperature.

(3) Iodine air: Air was permitted to flow through gas dryer 3 and rotameter 6, then enter radioiodine generator 12, where crystals of elemental iodine labeled with I-131 were allowed to sublime. The effluent from the iodine generator is iodine in air.

First, wet air and heated air were mixed. By dry-bulb and wet-bulb thermometer, relative humidity was determined and the temperature and relative humidity regulated. Then, the mixed air and iodine air were combined in gas mixer 16. The effluent from the gas mixer was test gas.

The test gas was permitted to flow through 1% KI solution in gas absorber 18, gas dryer 20, and rotameter 22. Total iodine concentration (normal iodine and radioactive iodine) in the flow was determined by iodimetry analysis and calculation. The test gas from the gas mixer was introduced into the charcoal bed and adsorption tests were carried out at constant temperature. The exhaust air flowed through safeguard 24 into a discharge vent.

This test system operated at negative pressure to assure security of operational personnel.

For the sorption test with methyl iodide, the equipment in Figure 2 was used.

This test equipment is almost the same as that shown in Figure 1. The only differences are in the radioiodine generator, sampling, and analysis.

Figure 3 is the methyl iodide generator. It is almost the same one as presented in reference (2).

In the experiment, the generator was placed in the ice water bath. Challenge methyl iodide concentration was regulated by changing the temperature of the ice water bath and the diameter of the diffusion tube. A temperature of -5 to -10°C and a diameter of 0.25 mm were used for the low concentration test. The detector for total methyl iodide was a gas chromatograph (Type 104) with a linearized electron capture detector. Gas was sampled directly from the system. This test system operated at positive pressure.

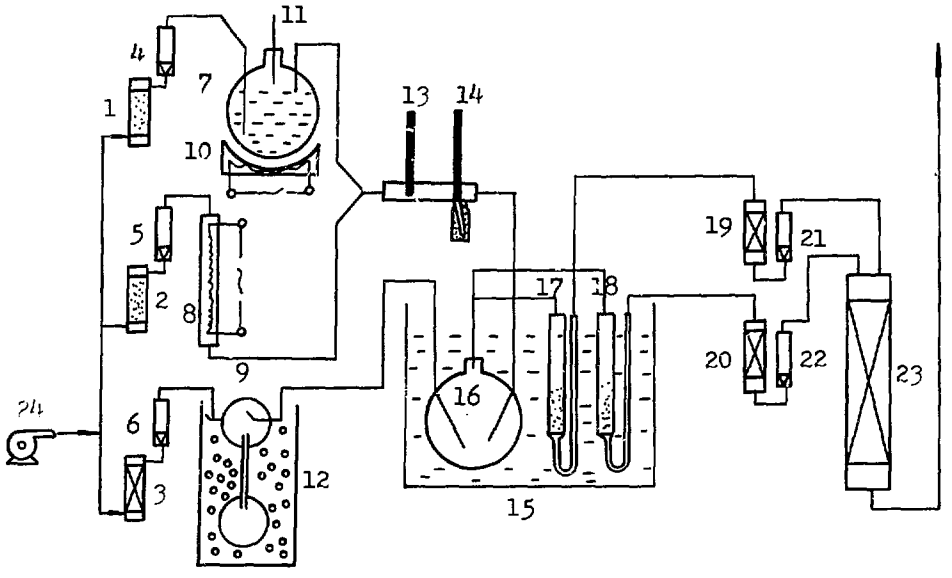

FIG. 2 FLOWSHEET OF TEST EQUIPMENT FOR SORPTION OF METHYL IODIDE

1,2 glass wool prefilter. 3,19,20 gas dryer. 4,5,6,21,22 rotameter. 7 steam generator. 8 automatic control heater(piped). 9 methyl iodide generator. 10 automatic control heater(furnace). 11 controlling thermometer. 12 vacuum flash. 13 dry-bulb thermometer(controllable). 14 wet-bulb thermometer. 15 constant temperature bath. 16 gas mixer. 17 adsorption tube(I.D. 18mm). 18 adsorption tube for preadjestment. 23 safeguard. 24 compressor.

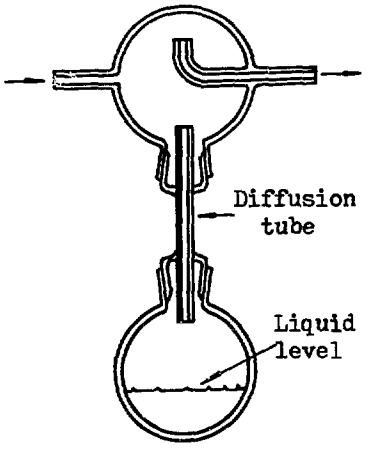

FIGURE 3

METHYL IODIDE GENERATOR

Principle of screening. The principle of screening is to compare the decontamination factors of various impregnated charcoal at the same experimental conditions, Table 3.

Table 3. Screening test conditions for various impregnated charcoals for adsorption of iodine and methyl iodide

Conditions of adsorption	Iodine	Methyl iodide
Particle size (mesh)	8-16	8-16
Adsorption temperature (^{o}C)	40 ^{o}C	40 ^{o}C
Relative humidity (%)	95 %	95 %
Superficial velocity (Cm/sec)	28.4	28.4
Inlet concentration (µg/L)	150	146
Specific radioactivity (ci/L)	10^{-7}	$5X10^{-8}$
Duration of run (hr)	1	1/6

Results of screening.

(1) The oil-palm shell base carbon was better than wood base carbons, phenolic resin fiber base carbons and oil-palm base carbons, because it adsorbs iodine as well as methyl iodide. The fiber base carbon had excellent characteristics for adsorption of elemental iodine so the fiber base carbon may be used in nuclear air cleaning if it can be impregnated successfully.

(2) The oil-palm shell base carbon was treated by different impregnants including $Na_2S_2O_3.5H_2O$, piperazine, KI, HMTA, TEDA and washed with water. TEDA is the best impregnant among them because it has the biggest decontamination factor and KI was used as a secondary impregnant.

(3) Selected 2% TEDA-2%KI impregnated charcoal was used as adsorption material for iodine filters (summary of properties in Table 4). Because all TEDA to KI ratio impregnated charcoals have a high decontamination factor, spontaneous ignition temperature and cost are considered.

Table 4. Fundamental properties of 2 % TEDA-2 % KI impregnated charcoal

		Pore size distribution	
Benzene adsorption	38 %	Pore size r (Å)	Pore volume (%)
Particle size	8-16 mesh	0-20	72.13
Ash content	3 %	20-40	6.58
Moisture content	5 %	40 - 80	9.86
Specific Surface	1000 m^2/g	80 - 120	6.70
Wear strenth	92 %	120 - 160	3.10
Spontaneous ignition temperature	425^{o}C	> 160	1.62
Mode pore size	14 Å		
Mean pore size	11 Å		

III. Adsorption properties of impregnated charcoal for airborne elemental iodine

In this section, adsorption characteristics of elemental iodine are given. The dynamic saturation capacity of impregnated charcoal was determined over a challenge concentration range. Partial adsorption isotherms were obtained. Also, the effect of temperature, superficial velocity, and relative humidity on decontamination by impregnated charcoal was examined.

Experimental procedure

The experimental system used is presented in Figure 1. The mesh size of 2% TEDA - 2% KI impregnated charcoal was 8-16 mesh and it had been exposed to static air for one year (as would be the case in a standby system). The adsorption pipe had an inside diameter of 13mm and a bed depth of 5cm was used.

In the test of iodine removal, the charcoal bed was divided by filter paper into 10 segments, and each segment contained about 0.7 g of charcoal. Inlet iodine concentration, 8 ppm v/v. Test duration time, 1 hr. The radioactivity of each segment was determined and the decontamination factor of each segment obtained by the following equation:

$$DF_n = \frac{\sum A_i}{\sum A_i - \sum_{1}^{n} A_i} \qquad (1)$$

where DF_n: the overall decontamination factor of 1st to n th segments of the charcoal bed

$\sum A_i$: Sum of the radiocounts of all segments of the charcoal bed

$\sum_{1}^{n} A_i$: Sum of the radiocounts of n segments of the charcoal bed

In the test to determine isotherms, the charcoal bed was also divided into 10 (5 cm long) segments, but each segment contained different quantities of charcoal: 0.3, 0.3, 0.3, 0.5, 0.5, 2.0, 1.0, 0.4, 0.4, 0.3 g. The test duration of every run depended on the concentration of the gas. The following conditions were satisfied: (1) The 1st and 2nd segments should give approximately equal counts. (2) The counts of the last segment should be as low as the background. A few hours to dozens of hours were used, and then each segment was removed from the adsorption pipe and their activity counted.

Radioactivity on the impregnated charcoal was determined by a well-type NaI scintillation spectrometer.

The dynamic saturated adsorption capacity of impregnated charcoal (S) was obtained by Equation 2.

$$S = \frac{A_i}{\Sigma A_i} \times \frac{C\,Q\,t}{W} \times 10^{-6} \qquad (2)$$

where A_i : Radiocounts of the 1 st segment

ΣA_i: Sum of the radiocounts of all segments

C : Inlet concentration of iodine, ($\mu g\ I_2/L$)

Q : Airflow rate through sorbent bed, (L/hr)

W : Weight of charcoal of the first segment (g)

t : Duration of adsorption (hr)

S versus C_o was plotted, and it gave the dynamic adsorption isotherm.

Results and discussion

Dynamic adsorption isotherm of iodine

The adsorption isotherm of iodine was obtained at low concentration and dynamic conditions. The conditions were: iodine concentration 1 - 20 ppm v/v size 8 - 16 mesh, bed depth of 5 cm, relative humidity of 100%, superficial velocity of 28 cm/sec. temperature of 40°C. A plot of S gI/gC versus C ppm v/v is presented in Figure 4.

From Figure 4, we can see that the curve looks like the 4th type of Brunauer's isotherm.

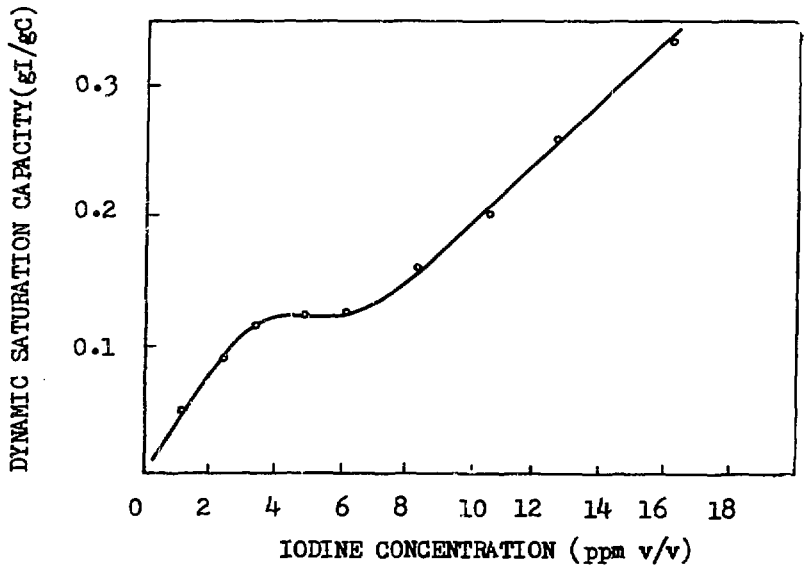

FIGURE 4 DYNAMIC PARTIAL ADSORPTION ISOTHERM OF IODINE ON IMPREGNATED CHARCOAL

This isotherm shows that adsorption of elemental iodine on impregnated charcoal is a kind of physical adsorption, and with increasing concentration of iodine, multimolecular adsorption occurs. Further it shows that elemental iodine is largely adsorbed physically on charcoal surfaces, irrespective of any impregnant.

In addition, we can obtain dynamic saturation adsorption capacity of the impregnated charcoal at different concentrations from this isotherm by interpolation or extrapolation.

Effect of temperature. In order to test the effect of temperature on the DF, four temperatures were tested: 40°C, 50°C, 60°C, and 70°C. Other conditions were: size of 8-16 mesh bed depth of 5 cm, concentration of iodine of 8 ppm v/v, R.H. of 95%, superficial velocity of 28 cm/sec, duration of 1 hr.

Figure 5 shows that the decontamination factor tends to decrease with increasing temperature.

Effect of relative humidity. In order to test the effect of relative humidity of DF, four relative humidities (40%, 50%, 60% and 100%) were tested. Other conditions were: size of 8-12 mesh, temperature of 40°C, bed depth of 5 cm, concentration of iodine of 8.7 ppm. superficial velocity of 28 cm/sec. duration of 1 hr.

Figure 6 shows that the DF of iodine decreases as the relative humidity is increased while the other variables are kept constant.

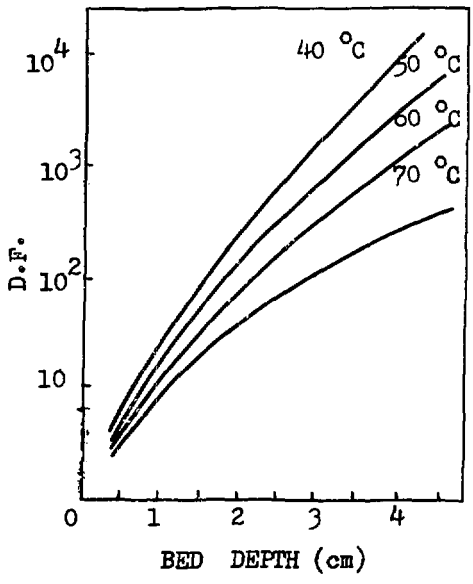

FIGURE 5 I_2 DECONTAMINATION FACTOR AS A FUNCTION OF BED DEPTH AND TEMPERATURE

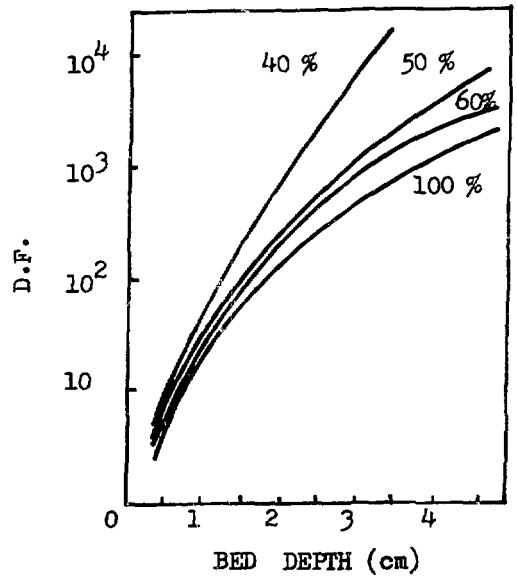

FIGURE 6 I_2 DECONTAMINATION FACTOR AS A FUNCTION OF BED DEPTH AND RELATIVE HUMIDITY

Effect of superficial velocity

Three superficial velocities: 28 cm/sec, 40 cm/sec, 50 cm/sec, were tested. The other variable conditions were: size of 8--16 mesh, temperature of 40°C, bed depth of 5 cm, inlet concentration of 8.5 ppm, R.H. of 100%, duration of 1/2 hr.

A plot of efficiency versus bed depth was made for superficial velocities of 28, 40, and 50 cm/sec. Figure 7 shows that adsorption efficiency tends to decrease with increase in superficial velocity at lower bed depth. But the adsorption efficiency tends to keep constant at a bed depth above 3 cm.

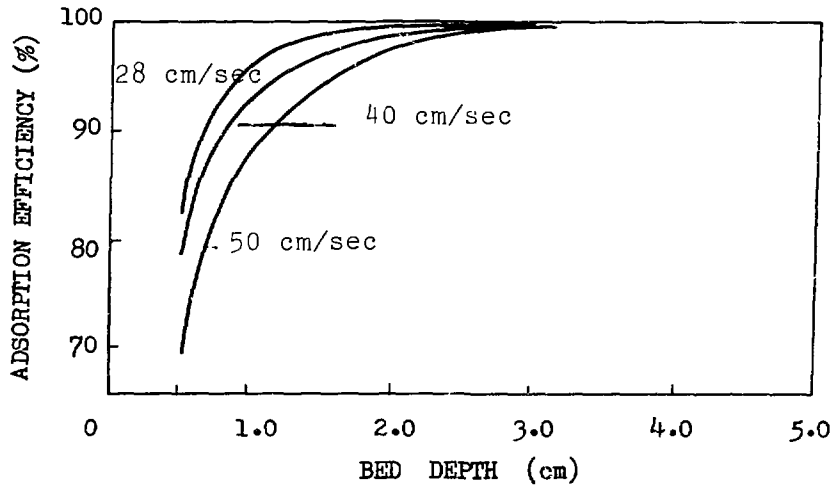

FIGURE 7 I_2 DECONTAMINATION FACTOR AS A FUNCTION OF BED DEPTH AND SUPERFICIAL VELOCITY

IV. Penetration properties of the impregnated charcoal for methyl iodide

It seems that methyl iodide predominated, followd by elemental iodine and products identified as HCI, from the TMI-II accident. In addition, the adsorption capacity of general activated carbon was greater for elemental iodine than for methyl iodide. Therefore, the adsorption characteristics of impregnated charcoal for methyl iodide was the crucial matter in the study of adsorbents for iodine removal.

The apparatus and the flow sheet used in the test are given in Figure 2.

Results and Discussion

Effect of inlet concentration of methyl iodide on penetration

Penetrability is defined as the point when the exit gas concentration equals 1% of the inlet concentration.

Many studies have been carried out on the relation between the breakthrough time and inlet concentration, and many equations have

been established(3).

In this experiment, the inlet concentration was varied from 1 to 100 ppm v/v. The results of experiments are presented as a plot of log t_b versus log C_o, which shows a good linear relationship in the range of concentrations of the test (Figure 8).

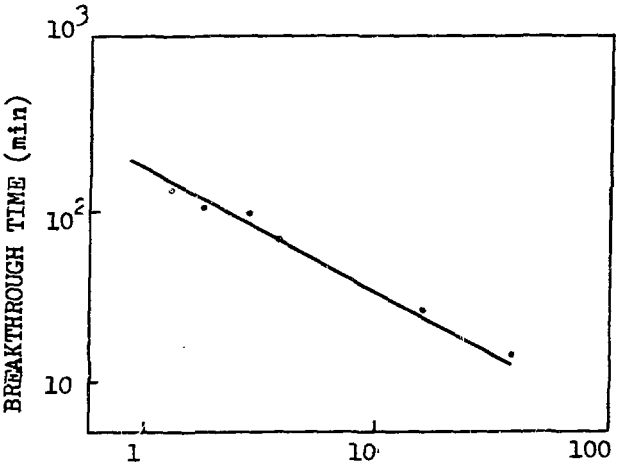

Conditions of the test :

Mesh size: 12 - 16

Bed depth: 5 cm

Face velocity: 28 cm/sec

R.H.: 95 %

Temperature: 40°C

DF: 100

FIGURE 8 BREAKTHROUGH CURVES FOR METHYL IODIDE

From Figure 8, the breakthrough time t_b can be approximated by the following equation:

$$t_b = 570 \times C_o^{-0.545} \qquad (3)$$

From Equation 3 we can obtain the breakthrough time - concentration relation in limited concentration range by extrapolation.

Effect of temperature of carbon column

The effect of carbon temperature was studied in the adsorption test of elemental iodine, but opposite results were obtained in the methyl iodide tests. That is, the breakthrough time tended to increase exponentially with increase in temperature. This result is presented in Figure 9.

The conditions of test: inlet concentration of 15 ppm v/v, size of 12-11 mesh, bed depth of 5 cm, face velocity of 28 cm/sec, R.H. 95% penetrability of 1%.

From Figure 9, the breakthrough time is approximatedy by the following equation:

$$t_b = 4.65 \times e^{0.0846\,T}$$

where,

t_b: Breakthrough time (min)

T: Temperature of column (°C)

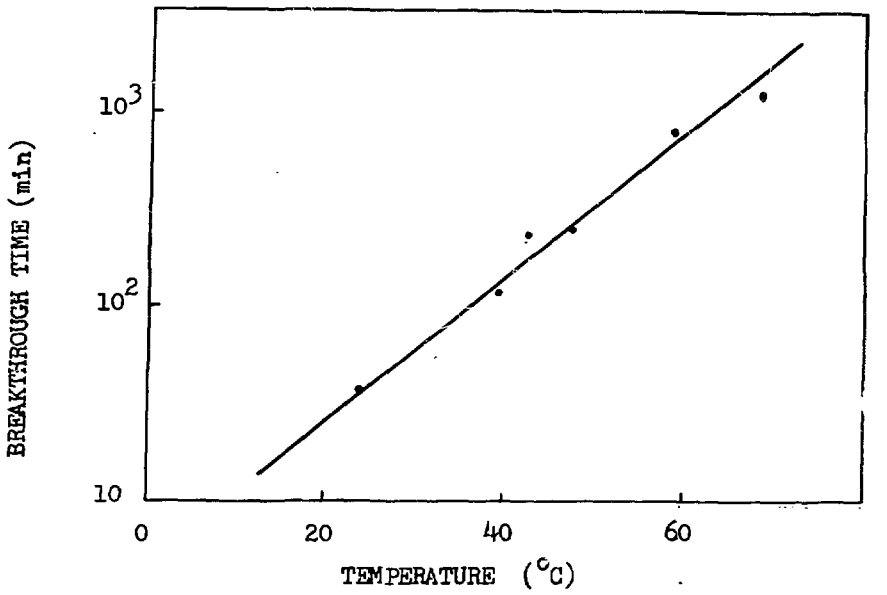

FIGURE 9 BREAKTHROUGH TIME AS A FUNCTION OF TEMPERATURE

Effect of depth of carbon bed

The deep bed filter has recently drawn attention from experts all over the world. Therefore, we think it is necessary to test the effect of bed depth.[1][4]

The variation of methyl iodide breakthrough time with carbon bed depth is presented in Figure 10

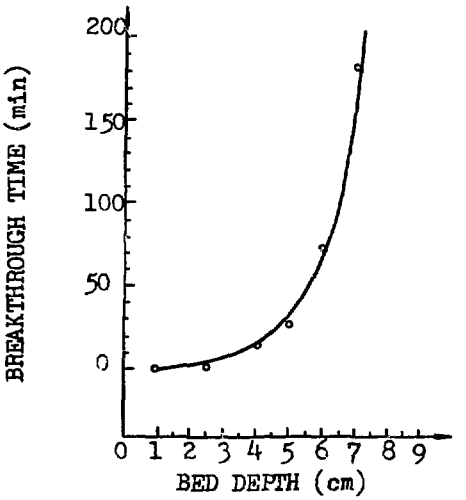

The conditions of test:

Concentration: 24 ppm v/v

R.H. : 95 %

DF: 100

Mesh size: 16 - 20

Face velocity: 28 cm/sec

Temperature: 40°C

FIGURE 10 BREAKTHROUGH TIME AS A FUNCTION OF DEPTH OF CARBON BED

Figure 10 shows that the breakthrough time increases rapidly with increases of bed depth.

Effect of superficial velocity

By varying the superficial velocity from 16 to 35 cm/sec, Figure 11 shows that the $CH_3{}^{131}I$ breakthrough time decreased as the flow velocity increased with the other variables kept constant.

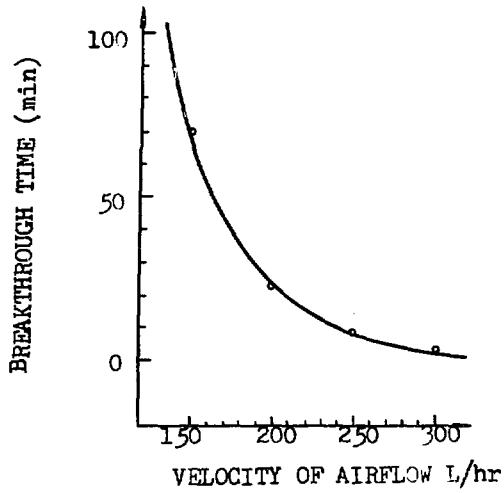

Test conditions :

Inlet concentration: 45 ppm v/v

Mesh size: 12 - 20

bed depth: 5 cm

R.H. : 95 %

DF : 100

Temperature: 40 °C

FIGURE 11 BREAKTHROUGH TIME AS A FUNCTION OF AIR-FLOW

VI. Properties of used impregnated charcoal for iodine removal

Fundamental properties of used impregnated charcoal for iodine removal are listed in Table 5. The data in Table 5 show

(1) A slight decrease in specific surface;

(2) A slight decrease in spontaneous ignition temperature;

(3) A great decrease in the number of micropores (i.e. for pore volume of pore size 0 - 20 Å)

The probable reason is that capillary walls collapsed after iodine removal.

Table 5. Properties of used impregnated charcoal for iodine removal

Specific surface 753.66 m^2/g	Pore size distribution	
	Pore size r (Å)	Pore volume (%)
Spontaneous ignition temperature 415 °C	0 - 20	40.20
	20 - 40	37.02
	40 - 80	19.35
	80 - 120	1.91
	120 - 160	0.91
	> 160	0.61
	Mode pore size	11 Å
	Mean pore size	11 Å

V. Concluding remarks

This is a study of the properties of an iodine removal filter for the first nuclear power plant in China. Additional 1:1 rig testing is being conducted in the pilot plant.

The experiments provided an effective impregnated charcoal for iodine removal filter and a series of parameters for operation and design.

The removal mechanism will be studied further.

References

(1) J. Louis Kovach, "The Evolution and Current State of Radioiodine control" CONF-801038 Vol. 1, P. 417, 1980.

(2) James M. McKelvey and H. E. Hoelscher, "Apparatus for Preparation of Very Dilute Gas Mixtures" Anal. Chem. Vol. 29, No. 1, P. 123, 1957.

(3) G. O. Wood, G. J. Vogt, and C.A.Kasunic, "Methyl Iodide Retention on Charcoal Sorbents at Parts-Per-Million Concentration" DOE Report CONF-780819 Vol. 1 P. 352-367, 1978.

(4) J. G. Wilhelm, H. Deuber, J. Furrer, K. Gerlach, "Behavior of gasketless Deep Bed Charcoal Filters for Radiodine Removal in LWR Power Plants" DOE Report CONF-801038, Vol. 1, P. 465, 1980.

EVALUATION OF QUATERNARY AMMONIUM HALIDES FOR REMOVAL OF METHYL IODIDE FROM FLOWING AIR STREAMS

W. P. Freeman, T. G. Mohacsi, J. L. Kovach
Nuclear Consulting Services, Inc.
Columbus, Ohio

ABSTRACT

The quaternary ammonium halides of several tertiary amines were used as impregnants on activated carbon and were tested for methyl iodide penetration in accordance with test Method A, ASTM D3803, 1979, "Standard Test Methods For Radioiodine Testing Of Nuclear Grade Gas Phase Adsorbents". The results suggest that the primary removal mechanism for methyl iodide-131 is isotopic exchange with the quaternary ammonium halide. For example, a 5 Wt % impregnation of each of the tetramethyl, tetraethyl, tetrapropyl and tetrabutyl ammonium iodides on activated carbon yielded percent penetrations of 0.47, 0.53, 0.78, and 0.08 respectively when tested according to Method A of ASTM D3803. A sample impregnated with 5% tetramethyl ammonium hydroxide gave a methyl iodide penetration of 64.87%, thus supporting the isotopic exchange mechanism for removal.

It has been a generally held belief that the success of tertiary amines as impregnants for radioiodine removal is a result of their ability to complex with the methyl iodide. The results of our present work indicates that the superiority of the tertiary amines similar to triethylene diamine and quinuclidine, when compared to their straight chain analogs, is a result of their ease in reacting with methyl iodide-127 to form the quarternary ammonium iodide followed by isotopic exchange.

INTRODUCTION

Tertiary amine impregnated carbon had originally been developed for the control of various halide type war gases by the formation of stable quaternary salts on the surface of activated carbon (1)(2)(3). Their use for the control of organic radioactive halides was introduced by British researchers (4)(5). The original optimium halide complexing amines were reported to be piperidine, morpholene, piperazine, 4-amino pyridine and triethylenediamine (TEDA). In the last few years other amines were reported to be as effective or superior to TEDA (7)(8). The use of these tertiary amine impregnated carbons is currently very extensive in the U.S. for air sampling and nuclear facility air cleaning application (9).

It has been generally assumed that the superiority of tertiary amines impregnated carbons vs. that of stable iodine impregnated carbons for removing $CH_3\,^{131}I$ was due to the ease with which the tertiary amines form a complex with the alkyl halide. Results of tests using $CH_3\,^{127}I$ alone (10) or detection of $CH_3\,^{127}I$ tagged with $CH_3\,^{131}I$ (11) supported the following removal mechanism for tertiary amine impregnated carbons:

$$CH_3I + N(CH_2 - CH_2)_3N = N(CH_2 - CH_2)_3\,\overset{+}{N}CH_3\;\overset{-}{I} \qquad (1)$$

More recent results (12) on a tertiary amine impregnated carbon saturated with $CH_3{}^{127}I$ and yet still showing excellent removal efficiency for $CH_3{}^{131}I$ support an additional removal mechanism:

$$N(CH_2\text{-}CH_2)_3\,NCH_3 + {}^{127}I^- + CH_3{}^{131}I = N(CH_2\text{-}CH_2)_3\,NCH_3 + {}^{131}I^- + CH_3{}^{127}I \quad (2)$$

i.e., isotopic exchange.

The extreme differences in reactivity (as evidenced by $CH_3{}^{131}I$ removal) between one tertiary amine and another (e.g., quinuclidine vs. triethyl amine (13) has been explained as follows:

> "Of two amines of equal base strengths but different steric requirements, the base with the lower steric requirements will react more rapidly with a given halide".

A recent paper (7) correlated earlier work (5) on amine impregnated carbons according to base strength but ignored steric considerations.

The cage like structure of quinuclidine and TEDA obviously favor their reaction with alkyl halide in general and methyl iodide in particular. Once the quaternary ammonium halide has been produced, the halide ion is available for isotopic exchange. Its rate of exchange should be a function of the stability of the positively charged nitrogen atom and the type of halide.

In an effort to further elucidate the removal mechanism of amine impregnated carbons for $CH_3{}^{131}I$, activated carbon impregnated with various quaternary ammonium halides were evaluated according to ASTM D3803 Method A and compared with results obtained for their tertiary alkyl amine analogs.

EXPERIMENTAL METHOD AND PROCEDURE

Radioiodine penetration tests were performed using Method A of ASTM D3803. Counting of radioiodine was performed at the 0.364 MeV gamma level using a 4 inch thallium activated sodium iodide well crystal. The substrate carbon for all tests was NUSORB G-60 8X16 coconut shell activated carbon.

RESULTS

TABLE 1 $CH_3{}^{131}I$ PENETRATION (%)

IMPREGNANT (WT %)	$CH_3{}^{131}I$ PENETRATION (%)
Trimethylamine (5%)	53.58
Triethylamine (5%)	47.16
Tributylamine (5%)	44.95

TABLE 2 $CH_3{}^{131}I$ PENETRATION

IMPREGNANT (WT %)	$CH_3{}^{131}I$ PENETRATION (%)
Tetramethyl Ammonium Iodide (5%)	0.47
Tetraethyl Ammonium Iodide (5%)	0.53
Tetrapropyl Ammonium Iodide (5%)	0.78
Tetrabutyl Ammonium Iodide (5%)	0.08

TABLE 3 $CH_3{}^{131}I$ PENETRATION

IMPREGNANT (WT %)	$CH_3{}^{131}I$ PENETRATION (%)
Tetramethyl Ammonium Bromide (5%)	29.18
Tetramethyl Ammonium Chloride (5%)	73.27
Tetraethyl Ammonium Bromide (5%)	24.77
Tetraethyl Ammonium Chloride (5%)	64.62
Tetramethyl Ammonium Hydroxide (5%)	64.87

DISCUSSION

Results in Table 1 indicate that the tri-alkyl amines are not effective for removing $CH_3{}^{131}I$ under the conditions of the test. The improvement in performance from the trimethyl amine to the tributhyl amine does not fit a simple mechanism. Due to less steric hindrance the trimethylamine would be expected to react faster even though both the triethyl and tributyl amines are stronger bases. Indeed in aqueous solution trimethyl amine was found to react 61 times faster with propyl iodide than triethyl amine (14). However, additional reactions between the tertiary amine and the alkyl halide can take place (e.g., elimination, rearrangment) that could explain the better performance of the relatively more hindered amine on the carbon surface.

The penetration results in Table 2 for the tetra alkyl ammonium iodides show marked improvement and support the isotopic exchange mechanism as a significant contributor for removing $CH_3{}^{131}I$ using tertiary amines. The low penetration value for the tetra butyl analog indicates again that other reactions may be taking place on the carbon or that the tetra butyl ammonium iodide promotes a higher exchange rate for the isotopes.

If isotopic exchange is the primary removal mechanism for the tetra alkyl ammonium halide then the rate of isotopic exchange for different halide should be $I > Br > CL$ and the corresponding $CH_3{}^{131}I$ removal should follow the same order (15). As seen in Table 3, the $CH_3{}^{131}I$ penetration increases markedly for both the bromide and the chloride derivatives, again supporting the isotopic exchange mechanism. The last impregnant in Table 3, tetra methyl ammonium hydroxide, while not promoting isotopic exchange, is a strong reagent for elimination and rearrangement type reactions and performs as well as the chloride derivatives, but indicates that reactions other than isotopic exchange are a minor factor for removing $CH_3{}^{131}I$.

CONCLUSION

The results of the present work support on isotope exchange mechanism for the removal of $CH_3\,^{131}I$ by activated carbons impregnated with tetra alkyl ammonium iodides. Recent work (16) using carbon -13 NMR spectroscopy confirmed the presence of the quaternary salt resulting from the reaction of TEDA and CH_3I. Thus the sucess of the tertiary amines like TEDA and quinuclidine for removing $CH_3\,^{131}I$ lies in their ability to rapidly form the stable quaternary salt and subsequent isotopic exchange.

Further work in this laboratory will entail looking at the removal of less reactive alkyl iodides than methyl iodide to further delineate the removal mechanism. Hopefully, this effort will enable more effective and less costly impregnants to be developed for removing $CH_3\,^{131}I$ based on essentially fundamental principles.

REFERENCES

1. Dolian, F. E. & Hormats, S., "Impregnated Charcoal", U.S. Report TDMR 767, Nov. 12, 1943.
2. Latimer, W.M. et. al., "Amine Impregnated Charcoals", U.S. Report WDRC CXLIX June 15, 1942 DV10-202, 152M5.
3. Goshorn, J.C. and Rockwell, P.O., "Improved Impregnated Charcoal Preparation and Test of Whetlerites Containing Sodium Hydroxide and Amines", U. S. Report EATR 153, May 29, 1934.
4. Collins, et. al., UKAEA Report 789 (w), 1964.
5. Collins, et. al., UKAEA Report 1300 (w), 1966.
6. Taylor, R., U.S. Patent 3,453,807, 1969.
7. Underhill, D. W. and Laskie, J. R., "Modified TEDA Impregnants for Methyl Iodide Removal", 16th DOE Nuclear Air Cleaning Conference.
8. Kovach, J. L., U.S. Patent 4,293,317, 1980.
9. Kovach, J. L., "The Evolution and Current State of Radioiodine Control", 16th DOE Nuclear Air Cleaning Conference, 1980.
10. Dietz, V. R. and Romans, J. B., "Testing Iodized Activated Carbon Filters with Non-Radioactive Methyl Iodide", NRL Memorandum Report 4240, May 30, 1980.
11. Wood, G. O. and Valdez, F. O., "Nonradiometric and Radiometric Testing of Radioiodine Using Methyl Iodide", 16th DOE Nuclear Air Cleaning Conference, 1980.
12. Kovach, J. L., Grimm, J. J. and Freeman, W. P., "TEDA vs Quinuclidine: Evaluation And Comparison Of Two Tertiary Amine Impregnants For Methyl Iodide Removal From Flow Air Stream, 17th DOE Nuclear Air Cleaning Conference, 1982.
13. Brown, H. C. and Eldred, N. R. "Studies in Stereochemistry XIV Reaction of Triethylamine and Quinuclidine with Alkyl Halides; Steric Effects In Displacement Reactions", J. Am. Chem. Soc. Vol 71 P445, Feb 1949.

14. Perrin and Williams, Proc. Roy Soc. (London), A159, 162 (1937).

15. Roginsky, S. Z., Theoretical Principles of Isotope Methods for Investigating Chemical Reactions, USAEC Report AEC - tr - 2873, 1956.

16. Resing, H. A., Dietz, V. P., and Murday, J. S., "Carbon-13 NMR Analysis of Charcoal Adsorbents: Reaction of CH_3I with the Impregnant Tri-Ethylene-Diamine", 16th Carbon Conference, July 1983.

DISCUSSION

WATSON: As you kindly referenced in your paper, work was done some twenty years ago at Windscale. It was, indeed, found that these halides, iodides in particular, were quite effective. It wasn't pursued at the time, I believe, because the compounds weren't readily available. They are more available now and a little more work has been done. They have been found to have excellent temperature properties, quite stable at 250°. The problem that was found was that these compounds did not perform very well on aging. In fact, under accelerated aging, which was the usual Windscale test of pure oxygen saturated with water vapor, triethylenediamine hydriodide-treated carbon soon performed less well than potassium iodide impregnated charcoals. As we know, accelerated aging doesn't always represent what really happens. I was wondering if you have done any work on more realistic aging.

FREEMAN: First, there seems to be some confusion about the type of compounds tested. We looked at quaternary ammonium salts, not the tertiary amine salts. Thus, the aging characteristics may be quite different than those found by the UKAEA. Secondly, we are in the process of determining static and dynamic aging of the quaternary ammonium halides, but have no data at this time. Finally, NUCON undertook this test program primarily to further the understanding of the removal mechanism for $CH_3{}^{131}I$.

DEITZ: I can add a little bit to his question, if I may. We have prepared crystalline addition compounds of methyl iodide and a large number of tertiary amines. Many of these were impregnated (2 wt %) on base charcoals and the penetration of methyl iodide I^{-131} was determined. The trapping was very good. However, like the previous speaker's comment, these materials were found to degrade rapidly upon weathering in flows of outdoor air.

INVESTIGATIONS ON THE EXTREMELY LOW RETENTION OF ^{131}I BY AN IODINE FILTER OF A BOILING WATER REACTOR

H. Deuber, K. Gerlach, J. G. Wilhelm
Laboratorium für Aerosolphysik und Filtertechnik
Kernforschungszentrum Karlsruhe GmbH
Postfach 3640, D-7500 Karlsruhe 1
Federal Republic of Germany

Abstract

An extremely low retention was observed of the I-131 contained in the exhaust air, by an iodine filter of a boiling water reactor. After filling the filter with fresh KI impregnated activated carbon (8 - 12 mesh), the decontamination factor dropped to about 1 within a few days. The extremely low retention of the I-131 was due to the occurrence of unidentified I-131 species in high proportions. By increasing the residence time to about 1 s and using a KI impregnated activated carbon of a smaller size, a somewhat higher retention can be achieved.

I. Introduction

After a large release of radioiodine to the reactor water of a boiling water reactor (BWR5) due to fuel element damages, unusually high concentrations of radioiodine occurred in the purge air (see below) and other exhaust air streams.(1) Concurrently an extremely low retention was observed of the I-131 contained in the exhaust air by the purge air iodine filter, although the latter was filled with an impregnated activated carbon of high quality widely used in the iodine filters of nuclear power stations (207B (KI)). The decontamination factor for I-131 contained in the purge air dropped from values of 10^2 and 10^3 to a value of about 1 within a few days. (Values of less than 1 were also found.) After filling the filter with fresh carbon, the same phenomenon was observed. By operation of a prefilter with unimpregnated carbon no improvement could be achieved.

In this paper investigations are described which in particular aimed at determining the reasons for the extremely low retention of I-131 by the purge air iodine filter of BWR5. Moreover, first findings were to be obtained on possibilities for improving the retention. Additional I-131 measurements in the exhaust air streams of BWR5 are dealt with elsewhere.(1)

II. Data of the Iodine Filter

The purge air filter of BWR5 is essentially used in normal operation to clean, possibly with an additional filter operated in parallel, the exhaust air from areas of the reactor building with potentially high radioiodine concentrations (e.g. containment and rooms with ducts containing reactor water).[1,2] Usually the purge air filter is almost only operated during the refueling outage. During the time of the investigations covered in this paper (refueling outage), only the purge air filter investigated was used. It was continuously operated with design flow (see below). Start of filter operation was two weeks prior to the beginning of the investigations.

The purge air filter contains the usual components: Upstream of the carbon filter a droplet separator, heater and particulate filter are installed, downstream another particulate filter. The bed depth of the activated carbon is 25 cm. Accordingly, the residence time is 0.5 s at the design face velocity of 50 cm/s (design flow: 12 000 m^3/h). During the investigations, temperature and relative humidity of the inlet were about 30 °C and 40 % R.H., respectively. These are favorable filter conditions.[3]

The purge air filter was filled with the activated carbon 207B (impregnant: KI; grain size: 8 - 12 mesh). The performance index (K) of the carbon for methyl iodide (CH_3I-131) was about 9 s^{-1} (30 °C, 98 - 100 % R.H., 50 cm/s). Thus, K was much higher than the required minimum value of 5 s^{-1}.[4] The carbon was filled into the purge air filter four weeks prior to the beginning of the investigations and two weeks prior to the start of filter operation.

III. Experimental

First, tests with I-131 are described which aimed at determining the retention of I-131 by different methods. Then additional investigations on the loading of activated carbons with organic compounds are dealt with.

Tests with I-131

An overview of the tests performed is given by Table I. Both tests on the iodine filter and on activated carbons were conducted. The test agents were either I-131 from the plant (contained in the exhaust air) or methyl iodide (CH_3I-131) prepared in the laboratory. (CH_3I-131 is generally used as model compound for organic iodine species in retention tests.) The performance of the tests is described only briefly in the following paragraphs. Details are to be found in the literature.[5]

Tests on the Iodine Filter

The tests on the iodine filter with I-131 from the plant were performed in the usual way by operating standard radioiodine species samplers in the inlet and outlet of the purge air filter

over periods of one week. (With the standard radioiodine species samplers particulate, elemental and organic radioiodine can be distinguished.)[6,7] After terminating the operation in the purge air, some samplers were purged with laboratory air under essentially the same conditions (purging time: one week). The tests with I-131 from the plant were carried out over four weeks (sampling periods 13 to 16).

With the tests indicated, the decontamination factors of the purge air filter for the I-131 species mentioned was to be determined. In addition, by the distribution of the I-131 on the carbon beds of the samplers, knowledge on the occurrence of penetrating I-131 species was to be gained. The purging of the samplers with laboratory air had the same aim.

The test on the iodine filter with CH_3I-131 prepared in the laboratory was also performed in the usual way by injection of CH_3I-131 into the inlet and simultaneous short-term sampling in the inlet and outlet. The test was carried out three weeks after the start of filter operation. In this test, by the retention of CH_3I-131 the leak tightness of the purge air filter was to be examined in the usual way.

Tests on Activated Carbons

In the tests on activated carbons with I-131 from the plant, bypasses were operated with different carbons (contained in 10 successive beds of 2.5 cm depth) under the conditions of the purge air filter over a period of two weeks. The following carbons were employed:

(a) 207B (impregnant: KI, grain size: 8 - 12 mesh);

(b) 207B (impregnant: TEDA, grain size: 8 - 12 mesh);

(c) RKJ1 (impregnant: KI, pellet size: 1 mm)
(207B is made from coal, RKJ1 from peat.)

With these tests, by the distribution of the I-131 on the carbon beds, it was to be examined by which type of impregnated activated carbon the I-131 from the plant can best be captured.

In the tests on activated carbons with CH_3I-131 prepared in the laboratory, the retention was determined of CH_3I-131 by different carbons prior to and after aging in the exhaust air over two weeks. The carbons of the above mentioned bypasses were used. (After the measurement of the I-131 from the plant, the beds were mounted in the laboratory test rig in the original sequence.) The test conditions were the same as the operating conditions in the exhaust air (30 °C, 40 % R.H., 50 cm/s). With these tests , the aging of the different activated carbons with respect to the retention of CH_3I-131 was to be investigated according to the standard procedure.

Other Investigations

As already mentioned, the loading of activated carbons with organic compounds was also measured. To this end the CS_2 extracts of the carbon from the purge air filter (207B (KI)) and from one of the bypasses (RKJ1) were analyzed by mass spectrometry.[8] With these investigations the reason for the aging of the carbon was to be clarified. Moreover, penetrating iodine species were to be identified.

IV. Presentation of the Results

In this chapter the results of the investigations are essentially presented only. The discussion of the results is reserved for the next chapter.

Tests with I-131

First the results obtained in the tests on the iodine filter will be presented, then those from the tests on activated carbons.

Tests on the Iodine Filter

As for the tests with I-131 from the plant, Table II contains the I-131 concentrations and fractions of the I-131 species in the inlet and outlet of the purge air filter in the sampling periods 13 to 16. The fraction of the organic I-131 was generally predominant. The fraction of the particulate I-131 was usually insignificant.

The decontamination factors calculated from the concentrations of the elemental and organic I-131 are given in Table III. The decontamination factor for elemental I-131 was mostly higher than 10^3. That for organic I-131 was higher than 1 in the sampling periods 13 and 14 and lower than 1 in the sampling periods 15 and 16. Thus, in the last two sampling periods the desorption of I-131 was greater than the adsorption.

The distribution of the I-131 in the radioiodine species samplers operated in the sampling periods 13 to 16 is illustrated in Figs. 1 to 4. In the section for organic I-131 (RKJ1 beds), mostly a decrease of the I-131 loading in the direction of flow was found. However, in the inlet the I-131 loading of the second RKJ1 bed was higher than that of the first RKJ1 bed in sampling period 14. The same applies to the outlet in sampling period 15. This means that in these cases large proportions of penetrating I-131 occurred. From the distribution of the I-131 on the RKJ1 beds it is obvious that in the inlet the proportions of the penetrating I-131 were generally smaller than in the outlet.

The distribution of the I-131 in the radioiodine species samplers operated in the inlet in the sampling periods 14 and 15, both prior to and after purging, is given in Figs. 5 and 6.

In sampling period 14 a large migration of the I-131 in the RKJ1 beds was observed, in sampling period 15 a small migration only.

As for the tests with CH_3I-131, the decontamination factor of the purge air filter, measured between the sampling periods 13 and 14, was $2.4 \cdot 10^3$. Thus, it was as high as the decontamination factor for elemental I-131 measured in sampling period 13 ($2.6 \cdot 10^3$; see Table III).

Tests on Activated Carbons

First the tests with I-131 from the plant will be dealt with. The distribution of the I-131 on the beds of different activated carbons is displayed in Figs. 7 to 9. Both with 207B (KI) and 207B (TEDA), I-131 was detected on all the beds. By far the most I-131 was found on the first bed. A nearly continuous rise of the I-131 loading was observed from bed 3 till the last bed. This means that even at a residence time of 1 s the I-131 was not completely trapped. With RKJ1, I-131 was detected on the first ten beds only. Most of the I-131 was again found on the first bed. An additional maximum occurred at the beds 5 and 6.

The results of the tests with CH_3I-131 are presented in Figs. 10 to 12. These figures show the penetration as a function of the bed depth at different aging times. The penetration curves for the fresh and aged carbons differed slightly only. The aged carbons exhibited a somewhat flat course of the penetration curve at low bed depths. This means that a very small aging occurred, but at small bed depths only.

Additional Investigations

The mass spectrometric determination of the loading of activated carbons yielded the following results. On the carbon 207B (KI) employed in the purge air filter during the time of the investigations, essentially toluene and xylene were detected. These are compounds that cause aging to a small extent only.[9,10,11,12] With the carbon RKJ1 from one of the bypasses (beds 5, 10 and 15; compare Fig. 9), no loading was detected, compared with the fresh carbon. In no case were iodine compounds identified.

V. Discussion of the Results

On principle the following reasons have to be considered for the extremely low retention of I-131 from the plant by the purge air filter:

(a) leakage;

(b) aging;

(c) occurrence of penetrating I-131 compounds.

According to the decontamination factors for I_2-131 and CH_3I-131 of higher than 10^3 (Table III), the leakage was lower than 0.1 %. Hence, leakage has to be excluded. The same applies to aging.

This is obvious from the mentioned decontamination factor of the purge air filter for CH_3I-131. It is also evident from the low penetration of the carbon 207B (KI) by CH_3I-131 after exposure to the purge air (Fig. 10). An additional evidence is the loading of the carbon from the purge air filter with compounds that contribute to aging to a small extent only (toluene, xylene).

Hence, only the occurrence of penetrating I-131 species has to be considered for the extremely low retention of I-131 from the plant. Indeed, as mentioned in the preceding chapter, from the distribution of the I-131 on the RKJ1 beds of the radioiodine species samplers (Figs. 1 to 4), the occurrence of penetrating I-131 species is obvious. The fraction of the I-131 that was retained by the RKJ1 beds 2 to 4 (sampler components 6 - 8) can be regarded as the approximate percentage of the penetrating I-131 species. Thus, in the inlet fractions of these species of up to about 50 % result (sampling period 14). Consequently, by delayed penetration (desorption) only very low decontamination factors can be measured. Additional evidences for the occurrence of penetrating I-131 species are the migration of the I-131 in the RKJ1 beds of the radioiodine species samplers during the one week purging (Figs. 5 and 6) and the penetration of the I-131 into deep layers of fresh activated carbons (Figs. 7 to 9).

The nature of the penetrating I-131 species is not known. However, from the distribution of the I-131 on the carbon beds it can be concluded that I-131 species which can be volatilized from alkaline aqueous solutions (often referred to as "HOI") play no significant part.[7,13,14,15]

With the carbon 207B, over two weeks some of the I-131 passes, independently of the impregnant, through layers of 50 cm equivalent to a residence time of 1 s (Figs. 7 and 8). Hence, by change of the impregnant no improvement in the retention of the penetrating I-131 can be achieved. With these carbons the same applies to the increase of the design data of the filter by e.g. a factor of 2. In the small-size carbon RKJ1 the migration velocity of the penetrating I-131 is comparatively low (Fig. 9). Hence, with this carbon a somewhat lower penetration can be achieved.

From the findings indicated it follows that the sources of the penetrating I-131 should be determined with the aim of eliminating the penetrating I-131 in the exhaust air. Corresponding investigations are being performed.

VI. Summary

Investigations were performed on the retention of I-131 by a purge air iodine filter, filled with the activated carbon 207B (KI), of a boiling water reactor (BWR5) in order to determine the reasons for the extremely low retention of I-131 from the plant (contained in the exhaust air). Moreover, first findings were to be obtained on possibilities for improving the retention.

The main results are as follows:

(a) The extremely low retention of I-131 from the plant was due to the occurrence of unidentified penetrating I-131 species in high proportions (up to about 50 %).

(b) By increase of the design data of the iodine filter by e.g. a factor of 2 (increase of the bed depth to 50 cm and the residence time to 1 s) nearly no improvement of the retention of the penetrating I-131 can be achieved with large-size carbons, such as 207B (KI) and 207B (TEDA) (grain size: 8 - 12 mesh). With a small-size carbon, such as RKJ1 (pellet diameter: 1 mm), a somewhat lower penetration can be achieved.

Acknowledgments

The tests were performed and evaluated by: R. Butz, K. Görtz, A. Hengst, R. Kauffeld, A. Ladanyi, E. Sebök, R. Sommerlatt and S. Winkler (LAF II).

The mass spectrometric investigations were carried out by W. Roth and L. Stieglitz (IRCh).

References

(1) Deuber, H.,
Die physikalisch-chemischen ^{131}I-Komponenten in der Abluft eines Siedewasserreaktors (SWR5),
KfK 3666 (1984)

(2) Deuber, H.,
Die physikalisch-chemischen ^{131}I-Komponenten in der Abluft eines Siedewasserreaktors (SWR4),
KfK 3424 (1982)

(3) Deuber, H., Gerlach, K.,
Parametrische Untersuchungen zur Abscheidung von Methyliodid an einer KI-imprägnierten Aktivkohle,
KfK 3746 (1984)

(4) Normenausschuß Kerntechnik im DIN,
Lüftungstechnische Anlagen in Kernkraftwerken,
DIN 25414 (1983)

(5) Wilhelm, J. G.,
Iodine Filters in Nuclear Installations,
Commission of the European Communities,
V/2110/83 (1982)

(6) Deuber, H., Wilhelm, J. G.,
Determination of the Physico-Chemical ^{131}I Species in the Exhausts and Stack Effluent of a PWR Power Plant,
15th DOE Nuclear Air Cleaning Conference,
Boston, 7.- 10.8.1978,
CONF-780819 (1979) 446

(7) Deuber, H., Wilhelm, J. G.,
Occurrence of Penetrating Iodine Species in the Exhaust Air of PWR Power Plants,
16th DOE Nuclear Air Cleaning Conference,
San Diego, 20.- 23.10.1980,
CONF-801038 (1981) 1354

(8) Stieglitz, L. et al.,
Das Verhalten von Organohalogenverbindungen bei der Trinkwasseraufbereitung,
Vom Wasser 47 (1976) 347

(9) Furrer, J. et al.,
Alterung und Vergiftung von Iod-Sorptionsmaterialien in Kernkraftwerken/Ageing and Poisoning of Iodine Filters in Nuclear Power Plants,
Kerntechnik 18 (1976) 313

(10) Wilhelm, J. G. et al.,
Behavior of Gasketless Deep Bed Charcoal Filters for Radioiodine Removal in LWR Power Plants,
16th DOE Nuclear Air Cleaning Conference,
San Diego, 20.-23.10.1980,
CONF-801038 (1981) 465

(11) Deuber, H., Gerlach, K.,
Untersuchungen zur Abscheidung von ^{131}I durch einen Iodfilter eines Druckwasserreaktors,
KfK 3594 (1983)

(12) Deuber, H., Gerlach, K.,
Untersuchungen zur Alterung von Aktivkohlen in der Abluft eines Druckwasserreaktors (DWR4),
KfK 3711 (1984)

(13) Emel, W. A. et al.,
An Airborne Radioiodine Species Sampler and Its Application for Measuring Removal Efficiencies of Large Charcoal Adsorbers for Ventilation Exhaust Air,
14th ERDA Air Cleaning Conference,
San Valley, 2.-4.8.1976,
CONF-760822 (1977) 389

(14) Kabat, M. J.,
Selective Sampling of Hypoiodous Acid,
14th ERDA Air Cleaning Conference,
San Valley, 2.-4.8.1976,
CONF- 760822 (1977) 490

(15) Deuber, H.,
Retention of ^{131}I Volatilized from Aqueous Solutions, by Sorbents,
KfK 3778 (to be published)

Table I Tests performed with ^{131}I (purge air) a)

Type	Agent	Time b)
Test on the iodine filter	I-131 from plant c)	weekly during continuous operation of the filter over 4 weeks (SP 13 to 16)
	CH_3I-131	after continuous operation of the filter over 3 weeks (between SP 13 and 14)
Test on activated carbons	I-131 from plant c)	prior to and after aging of 3 activated carbons in bypasses of the filter over 2 weeks (SP 14 and 15)
	CH_3I-131	

a) conditions: (ca.) 30 °C, 40 % R.H.

b) start of filter operation: at the beginning of SP 11
(SP: sampling period of 7 days)

c) contained in the purge air

Table II ^{131}I concentration and fraction of the ^{131}I species in the inlet and outlet of the purge air filter

Sampling period	I-131 concentration a) (Ci/m^3)	Fraction of the I-131 species b) (%)		
		Particulate	Elemental	Organic
Inlet				
13	1.3 (-10)	< 1	16	84
14	1.4 (-10)	< 1	26	74
15	1.9 (-10)	11	63	26
16	3.3 (-12)	2	38	60
Outlet				
13	3.2 (-11)	< 1	< 1	100
14	6.1 (-11)	-	-	100
15	3.0 (-11)	-	-	100
16	4.4 (-12)	-	-	100

a) 1.3 (-10) = $1.3 \cdot 10^{-10}$ etc.

b) I-131 species (compare Figs. 1 to 4):

particulate : I-131 retained on GF/A
elemental : I-131 retained on DSM11
organic : I-131 retained on RKJ1

- : detection limit of 2 (-15) Ci I-131/m^3 not exceeded

Table III Decontamination factor of the purge air filter for ^{131}I from the plant [a)]

Sampling period	Decontamination factor		
	Elemental I-131	Organic I-131	Total I-131 [b)]
13	2.6 (3)	3.4	4.1
14	> 1.8 (4)	1.7	2.2
15	> 5.9 (3)	1.6 (-1)	5.5 (-1)
16	> 6.3 (2)	4.4 (-1)	7.3 (-1)

a) according to the values of Table II

b) elemental and organic I-131

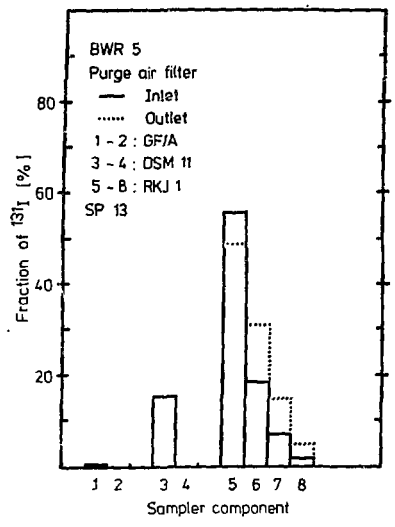

Distribution of ^{131}I in the radioiodine species sampler

Fig. 1 a)

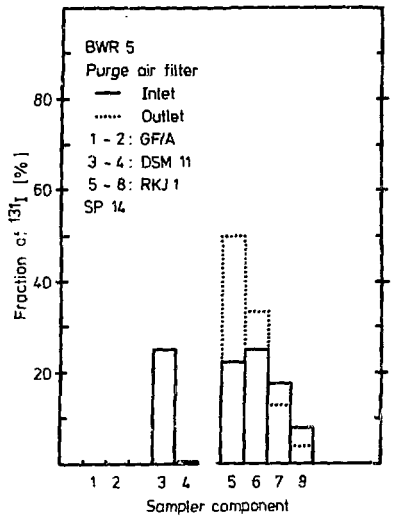

Distribution of ^{131}I in the radioiodine species sampler

Fig. 2 a)

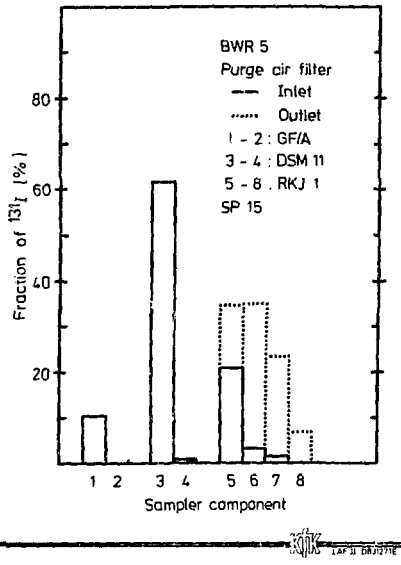

Distribution of ^{131}I in the radioiodine species sampler

Fig. 3 a)

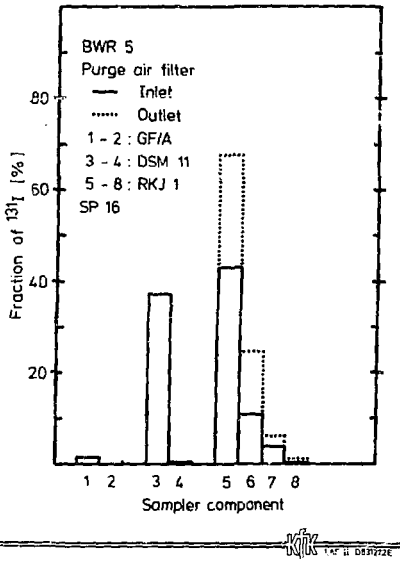

Distribution of ^{131}I in the radioiodine species sampler

Fig. 4 a), b)

a) I-131 from the plant (also in Figs. 5-9); residence time: 0.075 s/bed; sampling time: 7 days (also in Figs. 5 and 6); sampler components: see footnote b) of Table II

b) Sampling time in the outlet 4 days only (mechanical defect)

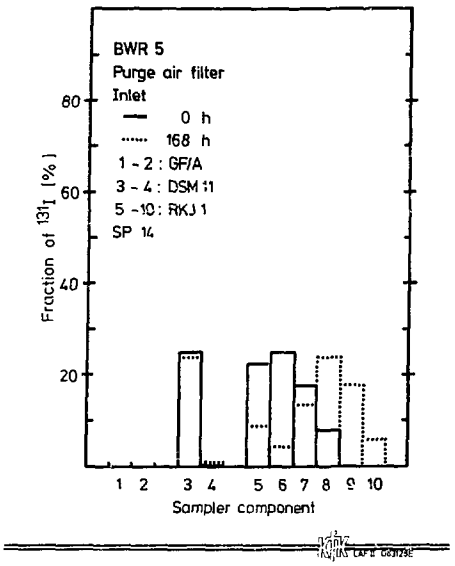

Distribution of ^{131}I in the radioiodine species sampler at different purging times

Fig. 5 a)

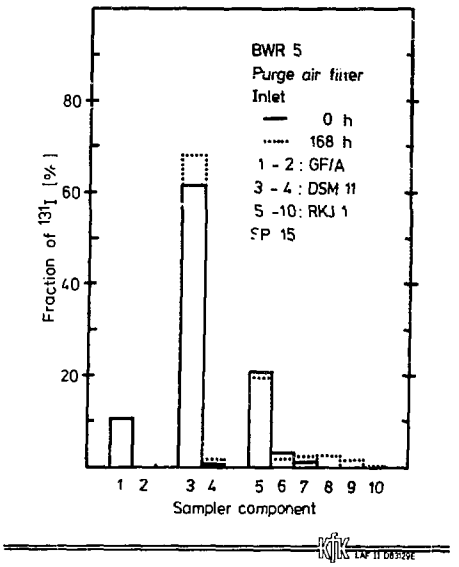

Distribution of ^{131}I in the radioiodine species sampler at different purging times

Fig. 6 a)

a) Sampler components 1 and 2 not used during purging with laboratory air; sampler components 9 and 10 only used during purging with laboratory air

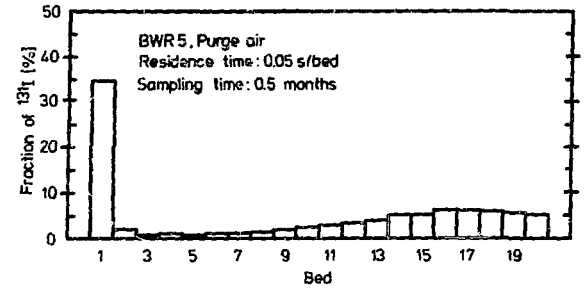

Distribution of ^{131}I on activated carbon beds: 207B(KI)

Fig. 7

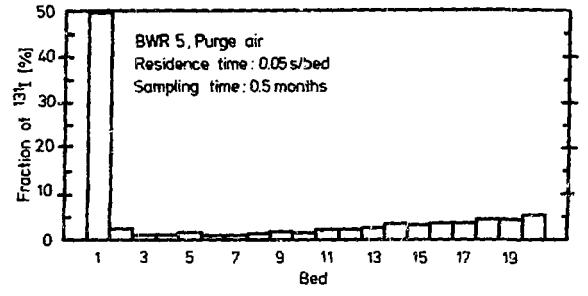

Distribution of ^{131}I on activated carbon beds: 207B(TEDA)

Fig. 8

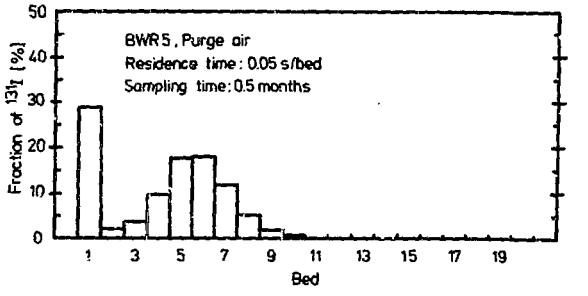

Distribution of ^{131}I on activated carbon beds: RKJ 1

Fig. 9

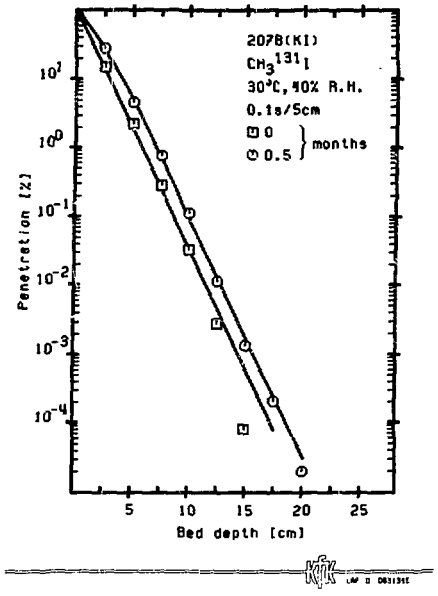

Penetration as function of bed depth at different aging times (Purge air)

Fig. 10 a)

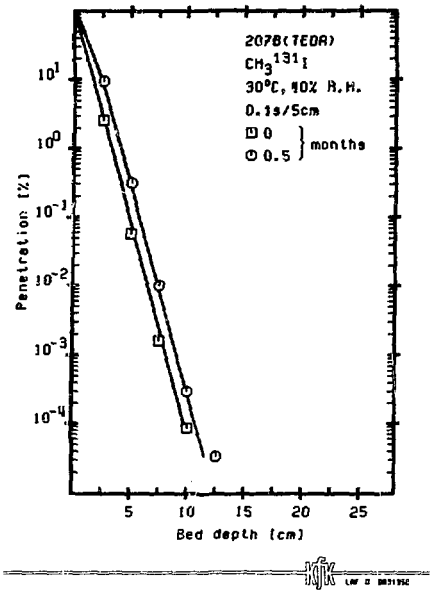

Penetration as function of bed depth at different aging times (Purge air)

Fig. 11 a)

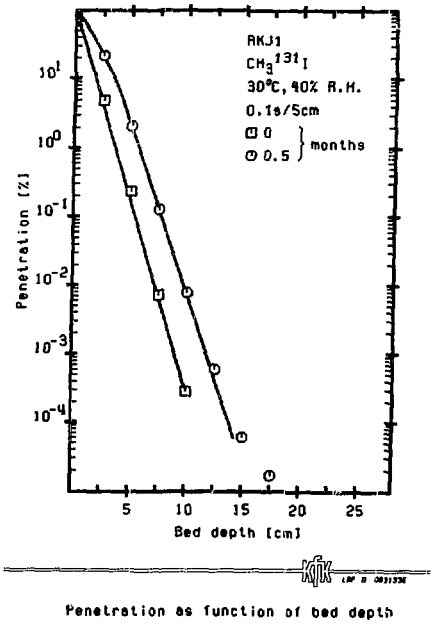

Penetration as function of bed depth at different aging times (Purge air)

Fig. 12 a)

a) CH_3I-131 prepared in the laboratory

DISCUSSION

KOVACH, J.L.: Have you analysed the KI (impregnant) content of the SS207B carbon which was in place during the high penetration episode to see if it was in fact impregnated to the normal level?

DEUBER: We did not analyze the KI content. But tests with $CH_3{}^{131}I$ show that the carbon was of high quality with respect to retention of $CH_3{}^{131}I$.

WILHELM: I would like to add that when people at the power station found that they had had an iodine release from the stack, they got nervous and changed the carbon. And they changed it three or four times in a relatively short time. All the carbons that were changed were tested in the laboratory and found to be all right when tested with methyl iodide, but we have penetrating iodine. We didn't release the information before because we had tested the exhaust air from boiling water reactor stations and from pressurized water reactor stations for years and only found penetrating forms of iodine in the region of less than 1%. But, in this case, we had certain conditions we hadn't had before: one was that we had a relatively high content of iodine-^{131} and the coolant was higher than we had seen before. Let's say it was a kind of little incident, or a thing like that. Under those condition, the filter definitely didn't work. Because we have experience in this field since 1968, we just didn't believe that you could have so large an amount of penetrating iodine. So we tested everything, such as filter leakage and in-place tests with methyl iodine. The filter worked excellently. We tested the carbon in the laboratory with methyl iodine and it worked excellently. Finally, we produced long samplers, 50 cm. deep, and loaded them with exhaust air for only a short time and you could see the peak of the penetrating iodine in the front of the column. Now, if you ran laboratory air through it, you could move the iodine. We have a lot of data on this. There is absolutely no doubt that there was penetrating iodine and it amounted to, as Dr. Deuber said, up to 50%. In certain sidestreams which added to the total exhaust from the stack, it was 100%. I think it is a very serious question. How good are iodine filters which work under normal operation conditions, but don't work under accident conditions? It is, finally, the question that is behind all this work. I feel its a very serious question.

SKAFI: Measurements in another BWR-plant were repeated under similar conditions as in the mentioned one, immediately after fuel inspection shutdown Within the measurement limits, no penetrating iodine was observed. You mentioned 50%, 50% of what? What is the absolute value?

DEUBER: I mean 50%. Our measurements performed in both BWRs and PWRs over years always gave low percentages of penetrating iodine. (order of magnitude, 1%) This is the only case where we found much higher percentage. We had never found anything like it and we came to the conclusion that the percentage of penetrating iodine species which you can very often find is a very low order of magnitude, about

1%. Therefore, we did not believe these measurements at first, and this is the reason we made all these different kinds of measurements, to look at the problem from all sides. Finally, we had no other explanation than what I have given. That means that during those weeks when we made these measurements, as far as the purge air was concerned, an important stream in these German PWRs which contributes a lot of I^{131} to the stack zone, there was a very high percentage of penetrating iodine species, much more than usual. Whether it was 40, 50, 60, or 90%, that is something that is less important. What is important, I think, is that it was very high. As I mentioned,we only found it in this case, never before or later. All these measurements referred to a refueling outage last year. When we repeated the measurements in the fueling outage of this year, we found normal behaviour, meaning very low or non-measurable amounts of penetrating iodine.

SKAFI: It seems we are dealing with a special case here. At the time of the measurement, perhaps, the air stream was contributing 100% of the ultimate 1 or 5% of these penetrations.

DEUBER: What are the reasons? We don't know. What are the species? We don't know. We used mass spectrometry and we couldn't identify the reasons. We can continue the discussion, but this would only be speculation.

TRANSMISSION OF RADIOIODINE THROUGH SAMPLING LINES

Philip J. Unrein, Charles A. Pelletier,
James E. Cline, and Paul G. Voillequé
Science Applications, Inc.
Rockville, Maryland 20850

Abstract

An experimental program to measure radioiodine transmission through sampling lines is described. The transmission depends upon both deposition on and resuspension from the walls of the line. The deposition and resuspension processes are themselves controlled by the length, diameter, and material of the line and the conditions under which it is operated. The operating conditions under study are sampling flow rate, temperature and relative humidity. Measurement results have been interpreted in terms of a four-compartment model of radioiodine deposition and resuspension. The model is applied to each of twenty or more segments of the line. Experimental measurements of short-term transmission fractions and the deposition velocities derived from them are presented for six lines. Data on resuspension rates for the same lines were obtained and are also discussed.

I. Introduction

Transmission of radioiodine through a sampling line depends upon the characteristics of the line and on the radioiodine species present. Early measurements in operating power plants[1] showed that deposition and subsequent resuspension of radioiodine were important processes and that changes in chemical form probably occurred while the material resided on the surface. Previous measurements of deposition of iodine species onto test coupon surfaces in the laboratory[2,3] and onto vegetation[4] have shown that elemental iodine (I_2) is the most reactive of the gaseous species. The deposition velocity of hypoiodous acid (HOI) is $\leq$ 5% of that for I_2. Deposition velocities of organic iodides, such as methyl iodide (CH_3I), are even smaller, ~0.1% of the deposition velocity of I_2. Thus the gaseous species of greatest interest is I_2.

To measure the deposition and resuspension rates for sampling lines, Science Applications, Inc. (SAI) constructed the Radioiodine Line Loss Measurement Facility. This facility, shown schematically in Figure 1, is designed to permit measurements of inlet and outlet concentrations of radioiodine in replicas of actual sampling lines. The length, diameter, and material of the test lines are the same as those of the installed sampling lines. The operating parameters--sampling flow rate, heat-trace temperature, and relative humidity--are also duplicated during the experiments.

This paper describes experimental work in progress in the Radioiodine Line Loss Measurement Facility. Section II describes the experimental methods used to test sampling lines in our facility. Section III describes the model of radioiodine transport through sampling lines. The experimental measurements, presented in Section IV, are interpreted in the context of the transport

Figure 1

IODINE LINE LOSS MEASUREMENT FACILITY

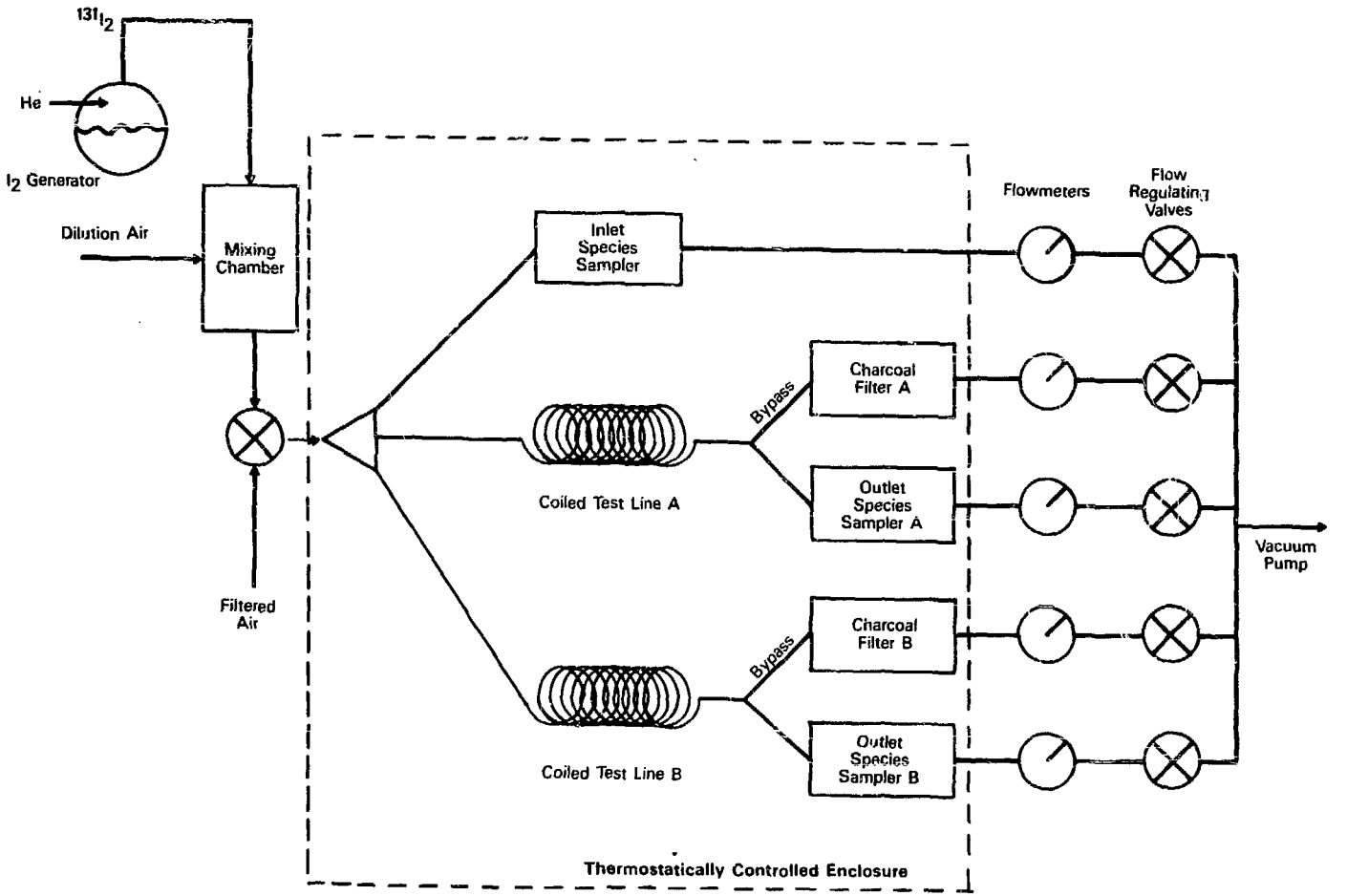

model. In Section V, tentative conclusions about the problem are presented.

II. Experimental Methods

Figure 1 shows the sampling line replicas coiled in an isothermal enclosure. The diameter of the coils was ~2.4 m. Radioiodine (^{131}I) can be injected into two lines simultaneously. During the injection period, radioiodine concentrations and species distributions were measured using the SAI radioiodine species samplers.[1,5,6] Following the injection period, the mixing chamber was isolated and the sampling lines were purged with filtered laboratory air to measure resuspension of radioiodine deposited on the interior surface of the line. The chemical forms of resuspended radioiodine were determined when the activity levels were adequate. To assure positive detection, only total airborne radioiodine was measured when the total activity was low.

All sampling cartridges were counted for ^{131}I using a Ge(Li) spectrometer whose calibration is traceable to the National Bureau of Standards. Counting results were corrected for decay from the end of the sampling period to the time of analysis. Some sampling periods were long with respect to the half-life of ^{131}I (8.04 days). Radioactive decay during sampling was taken into account. This decay correction assumes that the concentration of ^{131}I in the air stream was constant during the sampling period.

Most of the tests conducted have employed the most reactive gaseous species, elemental iodine (I_2). It was generated using the Dushman reaction.

$$IO_3^- + 5I^- + 6H^+ = 3I_2 + 3H_2O \qquad (1)$$

A reaction vessel (2-neck boiling flask) containing 20% sulfuric acid and potassium iodate was heated, stirred, and simultaneously purged with a flow of helium. The production rate of labeled elemental iodine was controlled by using a peristaltic pump to inject the sodium iodide solution containing radioactive ^{131}I tracer into the reaction mixture. This method allows an almost constant production rate over long periods of time.

III. Radioiodine Transmission Model

Prior to discussing the measurement results, it is useful to describe the conceptual model of radioiodine transmission through sampling lines and to define the parameters being measured. Previous studies of the behavior of airborne radioiodine in building ventilation exhaust and in discharge lines[1] have shown that

- o decay of the short-lived isotopes exceeds that expected based on air transit times
- o chemical species changes occur that shift the activity balance from reactive (depositing) to nonreactive forms.

A simple two-compartment model was developed[1] that incorporated the most probable mechanisms that account for the observed species

changes and aging of the radioiodine. The mechanisms are deposition of reactive species on surfaces, species transformations on the surfaces, and resuspension of deposited radioiodine. The deposition and resuspension phenomena have been observed in many studies of radioiodine behavior. Although they have been observed frequently, the species transformation processes are not well understood.

An improved, four-compartment model, shown in Figure 2, includes three compartments for airborne radioiodine species: depositing forms (iodine associated with particulates and elemental iodine), HOI, and organic iodides. The original model[1] assumed that the total air volume and surface of the line could be treated as single compartments. For long sampling lines, that assumption is frequently not valid. The line is now treated as a sequence of segments in which the assumption is valid. The model, for simplicity, assumes a single form of iodine on the surface that has different reaction rates to form each of the airborne species. This simplification may limit the ability of the model to fit the data. As more data become available, we will improve the model as needed. The new four-compartment model is applied to each segment of the sampling line. Two segments of a line are shown in Figure 2, but a typical application may involve 20 or more line segments. As is shown, the outlet activity from one segment is the input for the next line segment.

A single compartment is used for the I_2 and iodine associated with particulates because, operationally, the two forms are not readily separated. It is known that some I_2 is sorbed by particulate filters, but the amount is variable. Also, desorption of I_2 from particulates has been observed. Treating the two forms together will tend to overestimate the deposition in a sampling line. The degree of conservatism will depend upon the size of the particles present.

The species transformations are believed to take place on the surfaces, but the transformation chemistry is not considered in detail in this model. Deposition velocities for HOI and organic iodides are much smaller than for I_2.

The four simultaneous differential equations that describe the model in a particular line segment in Figure 2 are:

$$\frac{dq_{12}}{dt} = I_{12} + r_{12}q_s - (\lambda + \lambda_v + \delta_{12})\, q_{12} \qquad (2)$$

$$\frac{dq_3}{dt} = I_3 + r_3 q_s - (\lambda + \lambda_v + \delta_3)\, q_3 \qquad (3)$$

$$\frac{dq_4}{dt} = I_4 + r_4 q_s - (\lambda + \lambda_v + \delta_4)\, q_4 \qquad (4)$$

$$\frac{dq_s}{dt} = \delta_{12}q_{12} + \delta_3 q_3 + \delta_4 q_4 - (\lambda + r)\, q_s \qquad (5)$$

Figure 2

IODINE LINE LOSS FOUR-COMPARTMENT MODEL

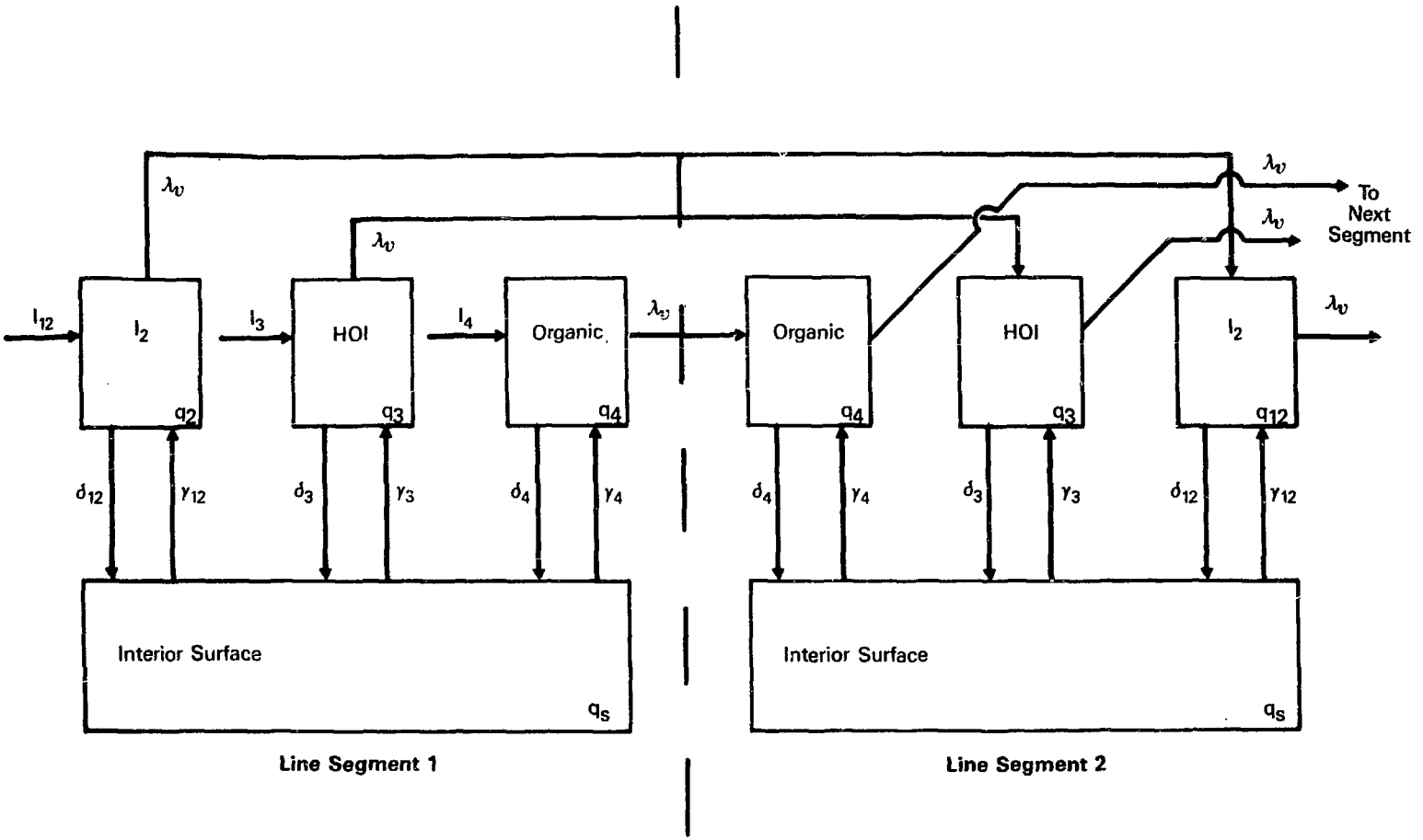

in which q_{12} is the airborne radioiodine activity (μCi) in elemental form or associated with particulates
q_3 is the airborne activity (μCi) of HOI
q_4 is the airborne activity (μCi)residing on the surface of the line
I_{12} is the mean rate of injection of particulate and elemental forms into the sampling line (μCi/sec)
I_3 is the mean rate of injection of HOI into the sampling line (μCi/s)
I_4 is the mean rate of injection of organic iodides into the sampling line (μCi/s)
r_{12} is the average resuspension rate constant (s^{-1}) for particulate and elemental forms
r_3 is the average resuspension rate constant (s^{-1}) for HOI
r_4 is the average resuspension rate constant (s^{-1}) for organic iodides
r is the total resuspension rate constant (s^{-1}) ($r_{12} + r_3 + r_4$)
λ is the radioactive decay rate constant (s^{-1})
λ_V is the rate constant (s^{-1}) for removal of airborne radioiodine in the air exiting the sample line
δ_{12} is the deposition rate constant (s^{-1}) for elemental iodine and that associated with particulates
δ_3 is the deposition rate constant (s^{-1}) for HOI
δ_4 is the deposition rate constant (s^{-1}) for organic iodides.

The last four rate constants in the list, λ_V and the δ_i, can be expressed in terms of other parameters. The rate constant λ_V is equal to Q/V, where Q is the sampling flow rate (cm^3/s) and V is the line segment volume (cm^3). The deposition rate constants for the different species, δ_i, are the products V_{di} (A/V), where the V_{di} are the deposition velocities (cm/s), and (A/V) is the surface-to-volume ratio (cm^{-1}) for the line segment.

IV. Experimental Results

Sampling Line Characteristics

Six different sampling line replicates have been studied. All of the lines were stainless steel and normally operate at ambient temperature and relative humidity. Test conditions were comparable, with temperatures between 25° and 30°C and relative humidities in the range 25 to 70%. None of the lines was chemically cleaned prior to testing. The characteristics of the lines thought important to radioiodine deposition and resuspension are given in Table 1. Lines 1, 2, 5, and 6 have similar diameters and surface-to-volume ratios (A/V), with lengths ranging from 15 to nearly 80 m. Line 3 is also rather similar to these four lines. The most unusual line in the group is Line 4, with a surface-to-volume ratio that is three times greater than that of the other lines and the lowest sampling flow rate.

Table 1. Characteristics of Sampling Lines Tested[a]

Characteristic	Line 1	Line 2	Line 3	Line 4	Line 5	Line 6
Inside Diameter (cm)	2.22	2.22	1.91	0.64	2.21	2.12
Length (cm)	3048	1524	4293	4267	7803	7498
Flow Rate, Q (cm^3/s)	1416	1416	944	28.3	944	1321
Ratio A/V (cm^{-1})	1.80	1.80	2.10	6.30	1.81	1.89

a. All lines tested were made of Type 316 or 304 stainless steel.

Deposition Velocities

The radioiodine species of greatest interest for these studies is I_2, and it was used in most of the experiments. One test was performed in which CH_3I was injected into Lines 3 and 4; no evidence of deposition was found although evidence exists[3,7] for the deposition of organic iodine. Table 2 shows the radioiodine injection periods, measured transmission fractions, and the average deposition velocities for I_2 estimated for in these sampling lines.

Table 2. Injection Periods, Measured Transmission Fractions, and Average Deposition Velocities for I_2 in Sampling Lines

	Experimental Results for Elemental Iodine (I_2)		
Line	I_2 Injection Period (hr)	Measured Transmission Fraction	Average Deposition Velocity (cm/s)
1	1.2	0.75	0.020
2	1.2	0.78	0.032
3	0.5	0.23	0.054
3	2.1	0.62	0.018
4	0.5	0.0013	0.027
4	2.1	0.0045	0.021
5	4.3	0.58	0.0095
6	4.3	0.72	0.0088

The observed deposition velocities are similar to the value of 0.018 cm/s reported by Kabat[3] for untreated stainless steel coupons under low humidity conditions. However it should be noted that the measured transmission fractions (Table 2) are much larger than would be predicted using the model proposed in the same paper. That method[3] does not consider resuspension and greatly overestimates deposition losses in sampling lines.

Resuspension Rates

Following the period of radioiodine injection, filtered laboratory air containing no ^{131}I was drawn through the test line at the normal sampling flow rate. The line outlet concentrations were monitored to determine the ^{131}I activity resuspended from the interior surface of the line. Table 3 shows the number of resuspension rate measurements made and the total duration of the sampling. Following testing of Lines 1 and 2, the resuspension sampling periods were shorter and more frequent. It was necessary to increase the sampling period as the measurements progressed to assure that the ^{131}I activity collected would be adequate for analysis. Estimated average total resuspension rates are given in the last column of the table.

Table 3. Measured Resuspension Rates

Line	Number of Measurements	Total Duration (hr)	Average Resuspension Rate[a] (r, s^{-1})
1	4	455	6×10^{-6}
2	4	455	5×10^{-6}
3	9	742	7×10^{-6}
3	15	904	1×10^{-5}
4	9	742	1×10^{-6}
4	15	904	1×10^{-6}
5	9	282	7×10^{-6}
6	9	282	1×10^{-5}

a. Resuspension rate decreased with time; multiple component parameter would be more representative.

The measured distributions of the species of radioiodine resuspended from the sampling lines are shown in Table 4. Elemental iodine was nearly always the dominant form. The fractions of HOI and organic iodides were generally larger during later sampling periods, but the increase was not monotonic.

The average resuspension rates lie between 10^{-6} and 10^{-5} s^{-1}. However, as noted in the table, the results suggest that there is more than a single resuspension rate present. This gives the effect of a resuspension rate that changes with time. This would be the case if there were more than the single surface reaction box assumed by the model. We may have to modify the model either to include more surface compartments or to describe resuspension by a more complicated expression that accounts for the same phenomenon.

Table 4. Measured Distributions of Resuspended Radioiodine Species (%)

Line	Part.[a]	I_2	Organic HOI	Organic Iodides
1[b]	15.1	81.5	1.0	2.4
2[b]	10.4	85.8	1.3	2.6
3	9.2	79.3	7.0	4.5
3	2.5	85.5	8.0	4.0
4	~12[c]	~53	~23	~12
4	<0.4[d]	38	36	25
	6.8	83.9	5.6	3.7
	4.9	85.9	5.5	3.8

a. Radioiodine associated with particulates.
b. Laboratory air drawn through the line was not filtered.
c. Species concentrations variable; one or more components were below detectable levels during some sampling periods.
d. Radioiodine species measurements made during first resuspension period; total ^{131}I activity measured during the other 14 periods.

V. Conclusions

Both (a) deposition and (b) resuspension of deposited activity affect the transmission of radioiodine through sampling lines. Measurements of transmission factors, deposition velocities, and resuspension rate constants using replicas of sampling lines have been performed in SAI's Radioiodine Line Loss Measurement Facility. Transmission of radioiodine has been found to be strongly dependent upon iodine species and upon the characteristics and operating conditions of the sampling line. Measured short-term transmission factors have ranged from less than 0.5% to nearly 80%. The experimental data have been interpreted in terms of a four-compartment radioiodine deposition and resuspension model. Deposition velocities for elemental iodine derived from the measurements have varied by about a factor of six, 0.01 to 0.06 cm/s, with no clear correlation with operating parameters. Deposition of methyl iodide was not detectable. Resuspension rates estimated from the measurements lie between 10^{-6} and 10^{-5} s^{-1}. There is evidence that the simplified model employed may be inadequate to describe the observed resuspension.

VI. References

1. C. A. Pelletier, E. D. Barefoot, J. E. Cline, R. T. Hemphill, W. A. Emel, and P. G. Voillequé, Sources of Radioiodine at Boiling Water Reactors, EPRI Report NP-495 (February 1978).

2. R. T. Hemphill and C. A. Pelletier, Surface Effects in the Transport of Airborne Radioiodine at Light Water Nuclear Power Plants, EPRI Report NP-876 (September 1978).

3. M. J. Kabat, Deposition of Airborne Radioiodine Species on Surfaces of Metals and Plastics, in Proceedings of the 17th DOE Air Cleaning Conference (1982).

4. P. G. Voillequé and J. H. Keller, Air-to-Vegetation, Transport of ^{131}I as Hypoiodous Acid (HOI), Health Phys., 40, 91 (1981).

5. J. H. Keller, F. A. Duce, and W. J. Maeck, A Selective Adsorbent Sampling System for Differentiating Airborne Iodine Species, in Proceedings of the 11th AEC Air Cleaning Conference, CONF-700815 (1971).

6. W. A. Emel, D. C. Hetzer, C. A. Pelletier, E. D. Barefoot, and J. E. Cline, An Airborne Radioiodine Species Sampler and Its Application for Measuring Removal Efficiencies of Large Char- coal Adsorbers for Ventilation Exhaust Air, in Proceedings of the 14th ERDA Air Cleaning Conference, CONF-760822 (1977).

7. J. E. Cline, E. D. Barefoot, D. S. Cameron, J. A. Daniel, J. W. Hollcroft, D. G. Keefer, T. L. McVey, E. A. Schlomer and C. D. Thomas, Jr., Measurements of Airborne ^{129}I and ^{137}Cs Concentrations In TMI-2 Containment During Decontamination Studies, Science Applications, Inc., August 6, 1982.

DISCUSSION

KOVACH, J.L.: What experimental data do you have for the identification of the compound called HOI in your experiment?

VOILLEQUE: The radioiodine species sampling system used in our experiments is described in References 5 and 6 of the paper. The original identification of HOI and the basis for the arrangement of beds in the sampling system were discussed in "Hypoidous Acid: An Airborne Inorganic Iodide Species in Steam-Air Mixtures", presented at the Eleventh Air Cleaning Conference, by J.H. Keller et al.

KOVACH, J.L.: With numerous laboratories reporting an inability to get HOI into the vapor phase, how do you justify results showing deposition and redeposition with a compound many people claim does not exist in the vapor phase.

VOILLEQUE: As I said at the outset, my discussion of species is an operational one. And that is, what is called HOI is that which is trapped on the four alumina beds, loaded with iodophenol.

KOVACH, J.L.: Isn't it analogous to saying that "I'm not responsible for the crime because somebody else made the gun."

VOILLEQUE: I am not in a position to debate whether or not HOI exists.

KOVACH, J.L.: You are reporting a deposition and a resuspension of that compound, so you have to be responsible for it.

VOILLEQUE: We define HOI to be that fraction of the iodine-131 that is trapped on iodophenol after passing through cadmium iodide.

GUEST: Recent tests at Bruce A Nuclear Station have shown that similar stainless steel sample lines, 1 inch in diameter and 56 ft. long, transmit 100% of injected methyl iodide and molecular iodine. We have found that there is absolutely no deposition in the line. This is at very low concentrations - less than micrograms per meter cubed. The analysis was performed by neutron activation of samples collected on charcoal. We sampled from two to four hours with these lines and found absolutely no loss whatsoever. I am quite surprised to see your results.

VOILLEQUE: What species?

GUEST: We injected methyl iodide and molecular iodine.

VOILLEQUE: I would certainly not expect to find any loss with methyl iodide.

GUEST: We were surprised, but we found no loss with molecular iodine either.

VOILLEQUE: What was the flow rate through this line?

GUEST: 72 Lpm, similar to your flow.

VOILLEQUE: In a one inch diameter line?

GUEST: Yes.

VOILLEQUE: Well, that is not terribly different from what we have seen. For comparable lines, we saw, over a two hour period, transmission of 75-80%.

GUEST: We saw 100%.

ANALYSES OF CHARCOAL FILTERS USED IN MONITORING RADIOACTIVE IODINES

S. M. Langhorst
University of Missouri
Research Reactor Facility
and
Nuclear Engineering Program
Columbia Missouri

Abstract

Monitoring gaseous effluents for radioactive iodine is often performed using small filters containing activated charcoal impregnated with TEDA. In sampling effluents, these filters experience an aging or weathering effect, much like that observed in large charcoal filter beds. Evaluation of the radioiodine monitoring procedure used at the University of Missouri Research Reactor has led to the development of several analysis techniques designed to estimate the filter collection efficiency, to measure amounts of stable halogens captured on the filter, and to investigate water collection and TEDA loss during the sampling period.

I. Introduction

Due to the low concentrations of radioiodines typically found in the gaseous effluent of a nuclear facility, large volumes of the air stream must be processed in order to monitor for the radioiodine release. Concentration of the radioiodines is usually performed using small filters containing activated charcoal impregnated with TEDA. Activated charcoal provides an excellent adsorption medium for many elements, especially the halogens. An impregnant, such as TEDA, is added to the charcoal to increase the filter's ability to capture organic forms of the radioiodines.

Investigation of the radioiodine monitoring procedure at the University of Missouri Research Reactor was undertaken to determine the capture efficiency of the charcoal filters used in the stack effluent monitor. An efficiency was to be measured and incorporated into the effluent release calculations and monitor calibration procedures. From filters used in sampling the stack effluent, the capture efficiency was found to decrease with increased sampling time. As has been observed in large charcoal filter beds[1,2,3], the sampling filters were experiencing an aging or weathering effect, which caused a decrease in capture efficiency with increase in use.

What was the cause of this aging effect? Could the decrease in capture effiency be prevented? How could the capture efficiency be easily measured? Investigation of these questions led to the development of several analysis techniques for the charcoal filters. A more intensive gamma-ray analysis was developed to observe how the

radioiodines were captured on the filters. Neutron activation analysis (NAA) was employed to measure the quantity of stable elements captured, in order to look for an "aging agent". Also, prompt gamma neutron activation analysis (PGNAA) was used to measure hydrogen and nitrogen content of the charcoal, in order to assess possible water vapor collection and loss of TEDA during sampling. The procedures and results are summarized in this paper.

II. Iodine Monitoring at the MURR

The University of Missouri Research Reactor (MURR) is a 10 MW, light water moderated, pool-type research reactor. The core is fueled with eight plate-type elements containing 6.2 kg of fully enriched uranium, and has a maximum flux of 6×10^{14} neutrons$\cdot$cm$^{-2}\cdot$sec^{-1}. The reactor is typically operated at full power, 24 hours a day, 7 days a week; with two to three shutdowns per week for refueling and sample changeouts; and one shutdown day every two weeks for routine maintenance. The stack emissions released from the MURR include air and gases exhausted from the core, pool, and various experiments, all of which can contribute to radioiodine release. Air flow in the stack is estimated to be 5×10^5 ℓ/min, with temperature ranging between 24-31°C and relative humidity ranging between 22-57%.

A continuous sample of stack air is monitored using a Nuclear Measurements Corporation Air Monitor, Model AM-22IF[4], which combines particulate, iodine, and gas monitoring. Air is sampled, using an isokinetic probe, at a flow rate of ~ 220 ℓ/min. The iodine monitor consists of a shielded chamber containing a NaI(Tl) detector and the charcoal filter housing. The buildup of activity on the front face (air inlet) of the charcoal filter is continuously monitored by the NaI(Tl) detector, which provides a signal to a logarithmic ratemeter circuit and graphic recorder located in the reactor control room. The part of the gamma spectrum which is real-time monitored is a 200 keV energy window around the 364 keV gamma-ray emission of I-131. The counts from this energy window provide conservative, on-line estimate of possible I-131 release.

The charcoal filters[5] used in the MURR iodine monitor contain ~ 25g of activated charcoal impregnated with 5% TEDA. Dimensions of the filters are 5.7 cm diameter and 2.5 cm thickness. Normally, a filter is used, or loaded with activity, in the iodine monitor for one week with the flow rate of 220 ℓ/min. When removed, the filter is quantitatively analyzed for gamma-ray activity using high resolution gamma-ray spectroscopy. This consists of a 1000 sec live-time count with the front face of the charcoal filter set on the face of a Ge(Li) detector. The radioiodines usually observed from this weekly gamma analysis include I-131, I-132, I-133, I-134, and I-135.

The activity measured on the loaded charcoal filters each week is related to the concentrations of radioiodines released in the stack effluent by the sample air flow rate, sampling time, and half-lives of the isotopes. A factor which had not been determined was

the efficiency of the charcoal filter to capture the radioiodines. These filters are designed to sample for radioiodines rather than to completely trap them, and thus a collection efficiency of < 100% would be considered acceptable, if this efficiency were known. Attempts to measure this capture efficiency for the charcoal filters loaded in the MURR stack monitor led to the discovery that as the filters sampled more of the stack air, the capture efficiency decreased, or aging occurred.

Humidity and trace gaseous pollutants have been identified as causes of aging in activated charcoals[2,3,6,7,8]. The cause of the change in capture efficiency observed in the charcoal filters used at the MURR was not readily apparent. In an effort to measure how activity was loaded onto the charcoal filter, a second gamma-ray analysis was added to count the back face (air outlet) of the filter. A "front-to-back" ratio (F/B) for I-131 activity was calculated for each loaded filter. A high F/B (~ 2) would indicate more activity was captured on the front portion of the filter, while a low F/B (~ 1) would indicate activity was captured more evenly throughout the filter. Filters exhibiting a lower F/B would be suspected of having a lower capture efficiency. An average I-131 F/B for the stack loaded filters was found to be 1.3 ± 13%, with values ranging from 0.980 to 1.71. The I-131 F/B for 58 filters loaded at different times over one year was not found to be highly correlated with either air temperature or humidity (correlation coefficients < 0.4).

III. Layered Filter Analysis

A more extensive gamma-ray analysis was developed to observe in greater detail how the radioiodines were captured on the charcoal filter. This analysis involved separately determining iodine concentrations on sequential layers of the charcoal filter, thus providing a loading profile of the filter. Differences in the radioactive loading profile on the charcoal filter were also known to affect the counting geometry, as was evident from the F/B data. The analysis of individual layers of charcoal not only provided data on the loading profile, but also provided a more consistent counting geometry by which to determine the quantity of radioiodines captured on the charcoal, and hence a more accurate analysis.

To prepare a charcoal filter for this layered filter analysis, the charcoal was removed from its polypropylene holder and then replaced into eight approximately equal layers, with thin tissue paper between each layer. The filter was placed in an iodine monitoring system, which sampled stack air parallel to the normal stack monitor. Because of the layering and tissue paper, a greater pressure drop occurred across these filters, but the flow rate was adjusted to maintain the same flow rate as in the stack monitor. Sampling times used for this parallel monitor ranged from one to fourteen days. Immediately following the completion of sampling, the filter was analyzed intact (front and back faces) for gamma-ray activity. Front-to-back ratios were calculated for the radioiodines. Next, the filter was disassembled and each charcoal layer analyzed, as well as the

filter case, for gamma-ray activity. The mass of each layer of charcoal was then measured.

Listed in Table 1 are data from two filters analyzed in this manner. Filter 30 was used to sample stack air for ~ 1 day and Filter 37 for ~ 1 week. Some differences can be seen between the two filters in the F/Bs and the total activity captured. Filter 30 captured a lower amount of I-131, but appeared to have a greater capture efficiency (higher F/B). The radioiodines with shorter half-lives, I-132 and I-134, were captured at the same activity levels on both filters, but the F/Bs on Filter 37 were lower. These two iodine isotopes reached an equilibrium, apparently within one day, where the rate of activity captured equaled the rate of decay. However, the aging of the charcoal filter still changed the capture profile for these isotopes. Equilibria may have also been established within the week long sampling period for I-133 and I-135.

The layered filter data were used to estimate the capture efficiency by relating the cumulative activity captured as a function of charcoal mass. Using a least-squares fit program[9], the data were fit to the following equation:

$$C = C_o\ (1 - e^{-ax}) \qquad (1)$$

where:

C = Cumulative activity captured at x (μCi)

C_o = Maximum cumulative activity captured (μCi)

x = Measure of charcoal depth given in mass (g)

a = Capture profile coefficient (g^{-1})

An equation of the same form was used by Shiomi, et.al.[10], in a study of removal efficiencies for methyl iodide. Given data points (x,C), the coefficients, C_o and a, were determined from the curve fitting program. If an infinite amount of charcoal were used in a filter, then the capture efficiency could always be considered to be 100%.

The data and fitted curves for Filters 30 and 37 are shown in Figures 1 and 2. To compare the relative capture profiles, the graphs are given in % captured vs. charcoal mass. While the F/Bs between isotopes cannot strictly be compared, due to the different gamma-ray energies used for identification, the ranking of capture efficiencies was in fairly good agreement with the corresponding ranking of F/Bs. Differences in the ranking of I-132 and I-134 were observed and attributed to the poorer counting statistics as these isotopes decayed during the analysis. Typical analysis time was 3.5 hours for one layered filter. For many of the layered filters analyzed, activity for I-134 was less than the detection limits.

The total activity and capture efficiencies for the radioiodines detected in each layered filter analysis are listed in Table 2. The

Table 1. Radioiodines captured on layered filters

	Layer	Mass (g)	Activity* (μCi) I-131	I-132	I-133	I-134	I-135
Filter 30							
Total Vol. Air	1	3.13	7.2E-4	1.1E-3	4.1E-3	3.2E-3	4.7E-3
3.7E8 mℓ	2	2.85	4.4E-4	8.5E-4	2.7E-3	1.6E-3	3.0E-3
	3	2.88	2.8E-4	8.8E-4	1.9E-3	7.3E-4	2.5E-3
Ave Flow Rate	4	2.97	1.9E-4	5.0E-4	1.4E-3	7.1E-3	2.1E-4
220 ℓ/min							
	5	2.61	8.8E-5	4.5E-4	7.5E-4	1.2E-3	1.5E-3
	6	3.18	5.8E-5	1.5E-4	6.6E-4	9.6E-4	1.1E-3
	7	3.45	1.2E-4	3.1E-4	6.0E-4	5.8E-4	7.3E-4
	8	3.89	5.2E-5	1.7E-4	3.6E-4	5.3E-4	6.6E-4
	Ave Counting Error		±25%	±20%	± 5%	± 40%	± 20%
	F/B		2.13	1.72	1.73	1.62	1.90
	Total	24.96	1.9E-3	4.4E-3	1.2E-2	1.6E-2	1.4E-2
Filter 37							
Total Vol Air	1	3.54	5.8E-3	8.8E-4	5.0E-3	1.5E-3	3.2E-3
2.2E9 mℓ	2	3.46	5.3E-3	5.7E-4	4.5E-3	1.3E-3	2.6E-3
	3	3.12	4.6E-3	6.9E-4	4.0E-3	1.9E-3	3.3E-3
Ave Flow Rate	4	2.57	2.9E-3	4.5E-4	2.5E-3	1.1E-3	2.1E-3
220 ℓ/min							
	5	3.12	2.6E-3	6.4E-4	2.7E-3	9.1E-4	1.9E-3
	6	3.17	1.8E-3	4.8E-4	1.9E-3	6.6E-4	1.6E-3
	7	2.78	1.2E-3	2.5E-4	1.3E-3	9.5E-4	7.5E-4
	8	2.98	1.1E-3	2.6E-4	1.1E-3	4.3E-4	1.1E-3
	Ave Counting Error		± 5%	± 20%	± 5%	± 40%	± 20%
	F/B		1.49	1.36	1.42	1.33	1.19
	Total	24.74	2.5E-2	4.2E-3	2.3E-2	8.8E-3	1.7E-2

* All activities decayed to end of sampling period.

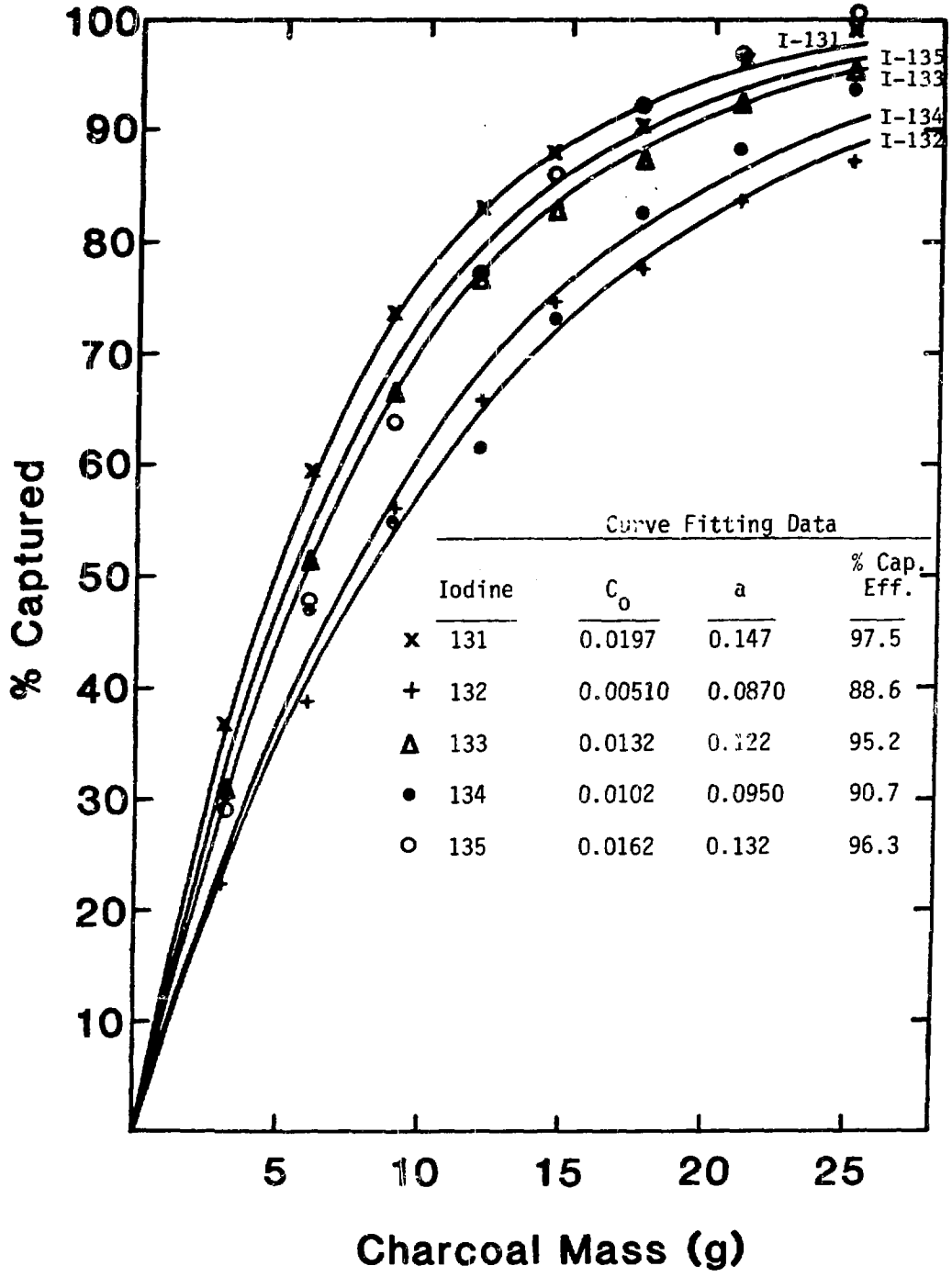

Figure 1. Capture profiles for Filter 30.

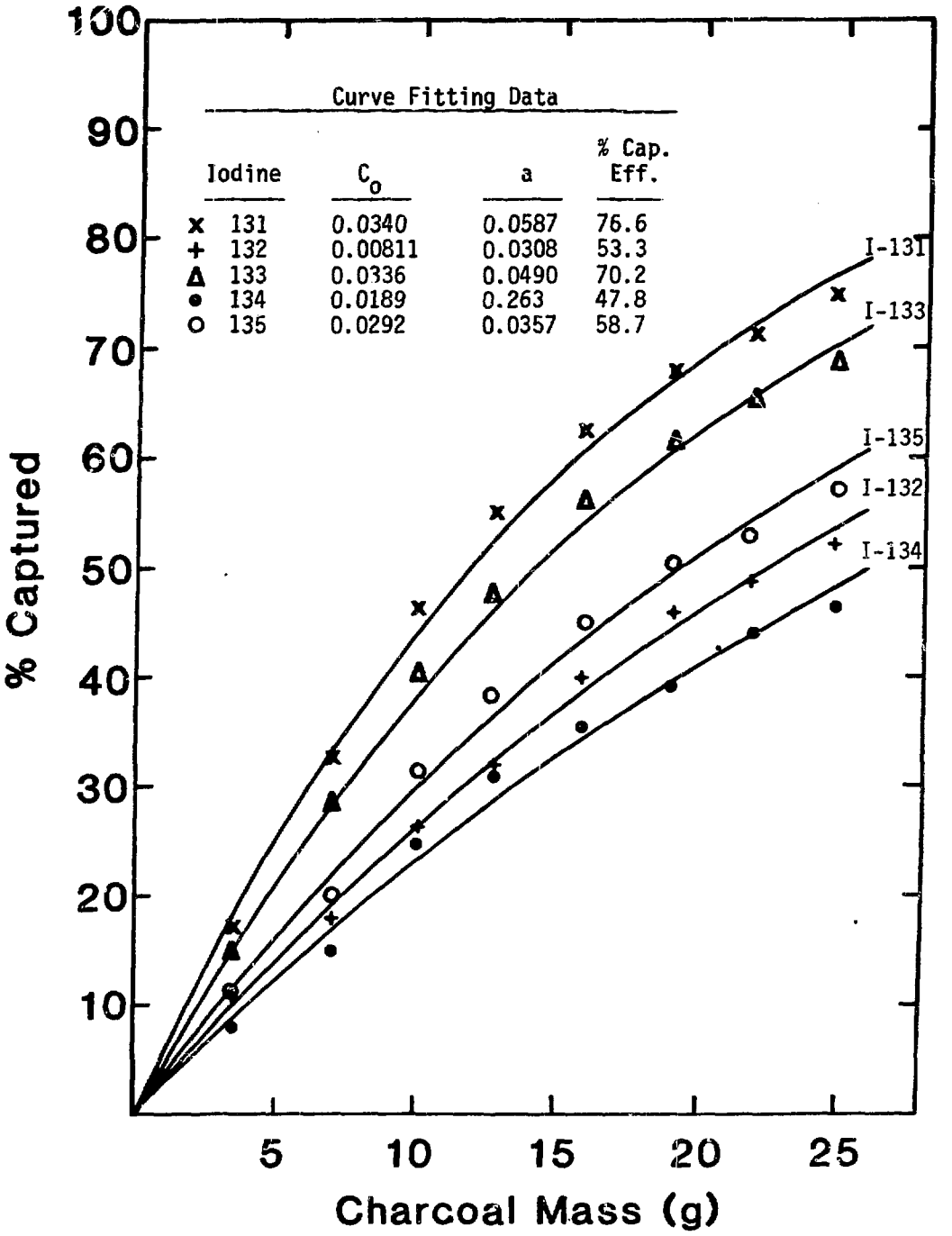

Figure 2. Capture profiles for Filter 37.

Table 2. Activity and capture efficiencies of radioiodines in layered filter analysis

Filter# (Days of Sampling)	I-131		I-132		I-133		I-134		I-135	
	Act[a] (μCi)	Eff[b] (%)	Act[a] (μCi)	Eff[b] (%)	Act[a] (μCi)	Eff[b] (%)	Act[a] (μCi)	Eff[b] (%)	Act[a] (μCi)	Eff[b] (%)
17(7)	1.2E-2	87	3.9E-3	82	1.7E-2	81	8.5E-3	63	1.4E-2	86
22(7)	9.8E-3	95	2.6E-3	95	1.2E-2	91	9.0E-3	85	9.9E-3	87
23(7)	6.4E-3	93	3.4E-3	86	1.0E-2	91	1.0E-2	86	1.0E-2	82
29(7)	7.1E-3	89	2.9E-3	87	1.4E-2	87	7.7E-3	79	1.1E-2	81
30(1)	2.0E-3	97	4.4E-3	89	1.3E-2	95	9.5E-3	91	1.6E-2	96
31(1)	2.0E-3	93	2.8E-3	82	7.9E-3	95	---[c]	--	6.8E-3	90
32(5)	6.3E-3	74	3.0E-3	69	1.5E-2	68	8.4E-3	69	1.4E-2	58
35(7)	9.1E-3	78	2.4E-3	73	2.0E-2	65	---[c]	--	1.5E-2	53
36(7)	1.2E-2	77	3.2E-3	80	1.7E-2	62	9.4E-3	47	1.6E-2	61
37(7)	2.5E-2	77	4.2E-3	53	2.3E-2	70	8.8E-3	48	1.7E-2	59
38(14)	1.2E-2	69	4.7E-3	48	1.2E-2	51	9.5E-3	47	1.2E-2	65
39(14)	1.0E-2	48	1.9E-3	11	1.2E-2	23	---[c]	--	1.2E-2	37
40(14)	1.2E-2	66	3.4E-3	55	1.4E-2	53	9.9E-3	86	9.6E-3	58
41(14)	1.6E-2	38	2.7E-3	10	2.3E-2	4	---[c]	--	1.5E-2	12
42(14)	2.3E-2	48	2.4E-3	13	1.9E-2	10	---[c]	--	1.4E-2	23
43(14)	3.6E-2	65	6.7E-3	32	5.2E-2	31	9.4E-3	60	4.3E-2	31
44(7)	2.0E-2	47	3.8E-3	64	2.5E-2	45	1.1E-2	81	1.7E-2	42
45(7)	1.4E-2	70	1.9E-3	36	1.8E-2	65	---[c]	--	1.1E-2	58

[a] Sum of activity detected in all layers.
[b] Capture efficiency.
[c] I-134 activity at minimum detectable for several layers.

layered filter analysis of these filters was considered too extensive for routine analysis of the stack filters. Instead, use of the F/B to estimate the capture efficiency was studied. This relationship for I-131 is given in Table 3.

Table 3. Relationship of F/B to capture efficiency for I-131

Range of I-131 F/B	No. of Data Points	Average Capture Eff. (%)	Sample Error (%)
> 2.2	0	100	---
2.0 - 2.2	1	97	---
1.8 - 2.0	3	93	3
1.6 - 1.8	7	90	4
1.4 - 1.6	6	80	5
1.2 - 1.4	6	61	20
1.0 - 1.2	2	42	20

The relation appeared to be non-linear, with significant decrease occurring with F/B < 1.4.

IV. Neutron Activation Analysis of Charcoal Filters

The capture efficiency of the charcoal filters used in the MURR iodine monitor was observed to decrease as the filters sampled stack air. However, the capture efficiency measured at the end of sampling was not constant for each week-long sampling period. Neutron activation analysis (NAA) was used to measure some of the stable elements that were also captured on the charcoal and which may have affected the capture of radioiodines.

An initial qualitative analysis of unused and stack loaded charcoals revealed the additional capture of stable isotopes of iodine, chlorine, and bromine from the stack air. Iodine and chlorine were captured in significant quantities on the filters and, thus, were considered to be possible causes of aging. Quantitative NAA for stable iodine and chlorine content was then performed on the layered charcoal filters.

Three replicate samples of charcoal were prepared for NAA from each layer of the layered charcoal filter. Each sample was irradiated for 5 sec in a thermal flux of $\sim 10^{14}$ neutrons$\cdot$cm$^{-2}\cdot$sec^{-1} and analyzed, using high resolution gamm-ray spectroscopy to measure the I-128 and Cl-38 induced activities. Data reduction was done via standard comparison.

Data from the NAA and the layered filter analyses for Filter 45 are shown in Figure 3. The curve fitting program was also used to fit the stable iodine and chlorine data, where C and C_o were cumulative masses and given in units of milligrams. The stable iodine was captured with the greatest efficiency, while the stable chlorine

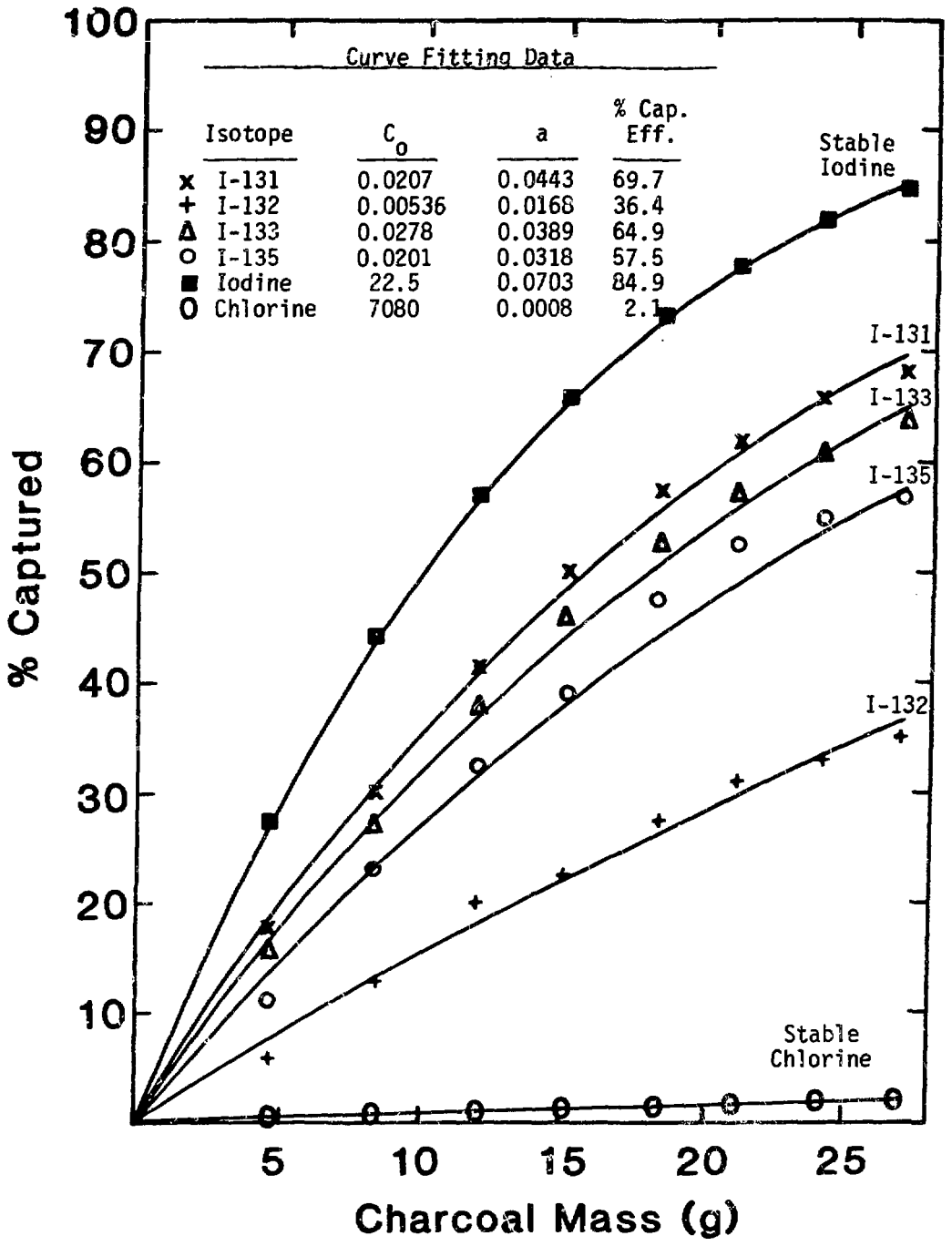

Figure 3. Capture profiles for Filter 45.

appeared to have reached saturation. Comparisons of stable iodine and I-131 capture efficiencies to the total cumulative amounts of iodine and chlorine in several layered filters are listed in Table 4. Due to the apparent saturation, curve fitting of the chlorine content did not readily converge, and therefore was not calculated for the other filters.

Table 4. Comparison of capture efficiencies to iodine and chlorine captured

Filter	Capture Efficiency (%)		Total Cumulative Capture (mg)	
	I-131	I	I	Cl
22	95	99	16	130
23	93	94	10	150
29	89	90	12	230
30	97	72	7	310
31	93	84	2	430
35	78	92	7	170
39	48	20	23	150
40	66	71	14	83
41	38	27	20	83
44	47	64	23	130
45	70	85	19	160

The values of capture efficiency for I-131 showed a low correlation to the quantity of stable iodine ($r = 0.79$) and chlorine ($r = 0.59$) captured on the charcoal filter. In laboratory tests, large amounts of stable iodine and chlorine (10 to 50 times greater than normal stack loading) were loaded onto a charcoal filter and did not significantly reduce the capture efficiency of I-131. For sampling periods greater than one day, correlation ($r = 0.89$) was observed between the capture efficiencies determined for I-131 and stable iodine, indicating both were affected by the aging process. Although iodine and chlorine were found to also be captured on the stack loaded charcoal filters, they did not readily appear to be the cause of aging.

V. Prompt Gamma Neutron Activation Analysis of Charcoal Filters

Even though no high degree of correlation between capture efficiency and humidity of stack air was obvious, the possibility existed that water vapor might be captured on the charcoal filter. Masses of the layered filters were measured before and after loading to determine any change in mass, possibly from the collection of water vapor. The changes in mass for a week of sampling ranged from a loss of 0.3973 g to a gain of 1.3832 g. Decrease in the filter mass suggested the possibility that a filter may have undergone volatilization of TEDA impregnant during sampling.

Prompt gamma neutron activation analysis (PGNAA) was used to analyze for hydrogen and nitrogen content in samples of unused charcoal and in charcoal from Filter 41. PGNAA employs the technique of identifying elements by detecting the prompt gamma emissions from neutron capture reactions. The MURR has a PGNAA facility[11] which provides a thermal flux of ~ 5 x 10^8 neutrons$\cdot cm^{-2} \cdot sec^{-1}$. Hydrogen content was identified using the prompt gamma peak at 2.22 MeV and the nitrogen content from the prompt gamma peak at 1.88 MeV.

The charcoal samples were prepared for analysis by weighing and encapsulating the sample in 1 mil thick Teflon bags. Teflon was used to keep the background hydrogen content as low as possible. The charcoal samples were loaded in the PGNAA facility and placed under vacuum to reduce background nitrogen content from air. Typically, the samples were analyzed for a 14 to 16 hour data collection period. The detection limits for hydrogen and nitrogen were both estimated to be ~ 1 mg/g charcoal.

Results of the PGNAA on the charcoal samples are listed in Table 5. The unused charcoal samples were obtained from filters which had not been exposed to any air flow and samples were obtained from each layer of Filter 41. Filter 41 had been loaded with stack air for a two week period, over which time the filter increased 0.336 g in mass. The capture efficiency for I-131 on the filter was determined, through curve fitting, to be 37.8%.

Table 5. Hydrogen and nitrogen content of charcoal

Sample ID	Sample Mass (g)	Concentration (%)	
		H	N
Unused Charcoal			
1	0.578	0.80[a]	0.75[b]
2	0.534	0.87	1.1
3	0.577	0.78	1.1
4	0.630	0.83	0.80
Layers of Filter 41			
1	0.570	1.3	< 0.1[c]
2	0.595	1.4	1.1
3	0.558	1.5	1.0
4	0.679	1.4	0.91
5	0.413	1.3	0.55
6	0.465	1.5	1.1
7	0.411	1.3	0.75
8	0.464	1.3	1.6

[a] Average counting error for hydrogen < 0.1%.
[b] Average counting error for nitrogen ~ 25%.
[c] Less than detection limit.

Charcoal impregnated with 5% TEDA was expected to contain 0.54% hydrogen. The hydrogen content of the unused charcoal was higher than expected, possibly due to hydrogen naturally found in charcoal. Samples of activated charcoal containing no TEDA were analyzed for hydrogen content. The content of hydrogen was 0.53% in untreated charcoal samples and 0.48% in samples dried at 95°C for 24-48 hours. The activated charcoal was shown to contain hydrogen which was not in the form of adsorbed water vapor that could be removed through evaporation. Charcoal samples from layered Filter 41 appeared to contain more hydrogen than the unused charcoal samples. Assuming that the unused TEDA impregnated charcoal contains an average of 0.82% hydrogen, the increase in hydrogen content was calculated for each layer mass and the sum was 0.15 g. If this hydrogen was assumed to be in the form of adsorbed water vapor, an increase in filter mass of 1.3 g would be expected. This large increase in mass was not observed for Filter 41.

Charcoal impregnated with 5% TEDA was expected to contain 1.25% nitrogen. The nitrogen content measured in the unused and Filter 41 samples averaged lower than the expected value, and no significant difference in nitrogen content was observed for the two groups. The long data collection periods were required for the PGNAA of charcoal samples to obtain better counting statistics for the nitrogen peak. The typical count rate at the 1.88 MeV peak was 0.03 counts/sec. The Compton contribution from the 2.22 MeV hydrogen peak resulted in high background counts at the 1.88 MeV nitrogen peak, which increased the counting error. The possibility of using a higher energy capture gamma for nitrogen, such as the 10.8 MeV peak[12], is being investigated.

VI. Discussion of Results

The development of the analysis procedures described in this paper to study the charcoal filters used in the stack effluent iodine monitor at the MURR led to several interesting observations. Foremost was the realization that the charcoal filters undergo an aging effect while in use which decreases the efficiency of capturing radioiodines. While a capture efficiency of < 100% can still be useful for sampling purposes, that efficiency must be known so that its effect can be incorporated into the measurement calculation. Filters were found to differ in their measured capture efficiencies even when loaded under similar conditions. An average capture efficiency could therefore not be determined for all filters sampling stack air for a week, but instead some means was needed to measure the capture efficiency for each filter.

The layered analysis of filters provided a means of estimating the capture efficiency by curve fitting the data to Equation (1). The capture efficiencies measured on a filter differed between the radioiodines. Neglecting I-132 and I-134, the ranking of capture efficiencies from highest to lowest was usually I-131, I-133, and I-135. Was this ranking due to the half-lives of these isotopes or could the isotopes be in different chemical forms? This question is

still under investigation. The values determined for I-132 and I-134 capture efficiencies were not consistantly ranked in the same order. Was this perhaps due to their shorter half-lives allowing for poorer counting statististics and enabling a relatively short time to reach capture equilibrium on the filters?

Measurement of the radioiodine concentrations released from the MURR stack effluent is based on integrated values for the week of sampling. Concentrations of the radioiodines do vary over the week due to operation of some experiments and due to normal shutdown of the reactor. The concentration of stable iodine is also known to vary, reaching lowest levels during weekend hours when work in the laboratories is at a minimum. So, the capture efficiency of a particular radioiodine may very much be dependent on when during the week the isotope is captured on the filter. Changes in the effluent concentrations can lead to change in the capture equilibrium already established on the filter.

Use of the analyses described in this paper did not result in any definite identification of a cause for aging in the filters. The capture of stable iodine and chlorine could not be shown to affect the capture efficiency for I-131. However, the capture efficiency of stable iodine was also found to be affected by the aging process, indicating that the stable iodine was behaving in the same manner as the radioiodines. An increase in hydrogen was observed in charcoal from a stack loaded filter showing very low capture efficiencies, but the capture profile for hydrogen did not readily fit to Equation (1). Whether the capture of hydrogen affected the radioiodine capture has not been established. Loss of TEDA was not evident from the PGNAA of Filter 41. Variation in the amount of nitrogen measured in different charcoal samples raised the questions as to whether the charcoal was impregnated with exactly 5% TEDA, how uniform was its concentration, and was the analysis technique sensitive to these possible changes.

While the cause of aging in these filters has not been identified, the technique of determining the F/B for I-131 did provide a quick method of estimating the I-131 capture efficiency. More data is being gathered to better define that correlation. Use of the capture efficiency to establish the counting geometry of the charcoal filter is also possible. A correlation of F/B and capture efficiency may also be useful for the other radioiodines.

VII. References

(1) Pelletier C.A., Barefoot E.D., Hemphill R.N., and Frederickson J.P., Long Term Performance of Charcoal Absorbers Removing Radioiodine in Ventilation Exhaust Air, EPRI-NP-534 (1977).

(2) Bellamy R. and Deitz V., "Confirmatory research program - effects of atmospheric contaminants on commercial charcoals", Proc. 15th DOE Nuclear Air Cleaning Conf., CONF-780819, Vol II, p. 299 (1978).

(3) Kovach J.L. and Rankovic L., "Evaluation and control of poisoning of impregnated carbons used for organic iodine removal", Proc. 15th DOE Nuclear Air Cleaning Conf., CONF-780819, Vol II, p. 368 (1978).

(4) Air Monitor Model AM-22IF. Nuclear Measurements Corporation, Indianapolis, Indiana (1971).

(5) Charcoal Filter Specifications for TC-12 Cartridges, Hi-Q Environmental Products Company, La Jolla, California.

(6) Ackerman F.J. and Grens J.Z., "Mechanisms that affect the adsorption of methyl iodide on charcoal under humid conditions", Proc. 9th AEC Air Cleaning Conf., CONF-660904, Vol I, p. 230 (1966).

(7) Collins D.A., Taylor L.R., and Taylor R., "Development of impregnated charcoals for trapping methyl iodide at high humidity", Proc. 9th AEC Air Cleaning Conf., CONF-660904, Vol I, p.159 (1966).

(8) Ackley R.D. and Adams R.E., "Aging and weathering of impregnated charcoals used for trapping radioiodine", Proc. 10th AEC Air Cleaning Conf., CONF-680821, p. 170 (1968).

(9) Bevington P.R., Data Reduction and Error Analysis for the Physical Sciences, McGraw-Hill Book Company, New York, p. 232 - 246, 1969.

(10) Shiomi H., Yuasa Y., Tani A., Ohki M., and Nakagawa T., "A parametric study on removal efficiency of impregnated activated charcoal and silver zeolite for radioactive methyl iodide", Proc. 17th DOE Nuclear Air Cleaning Conference, CONF-82-0833, Vol I, p. 199 (1982).

(11) Hanna A.G., Brugger R.M., and Glascock M.D., "The prompt gamma neutron activation analysis facility at MURR", Nucl. Inst. Meth., 188 p.619 - 627 (1981).

(12) Failey M.P. and Zoller W.H., Neutron-Capture Prompt Gamma-ray Activation Analysis: A Versitile Nondestructive Technique for Multi-element Analysis of Complex Matrices, Tech Report ORO-5173-008, p. 182 , 1979.

DISCUSSION

PAPAVRAMIDIS: What source did you use for the Ge(Li) detector?

LANGHORST: A standard europium-antimony cartridge from NBS Analytical Services.

PAPAVRAMIDIS: Was that a phase loaded cartridge with most of the activity deposited on 5 mm of the cartridge?

LANGHORST: No, it was dissembled and put into a uniform distribution within the sample.

DEITZ: We have made many elemental analyses of activated carbons and the hydrogen content is usually less than 0.1%. Hence, the high values reported by the speaker are most probably due to the presence of water. On the other hand, the N-contents of base carbons are in the range 0.3 to 0.6%. This has made it difficult to determine the presence of N from a TEDA impregnation of activated carbon.

LANGHORST: We were not able to observe nitrogen in some analyses that we have done with unimpregnated coconut charcoals. It may indicate we need to develop our technique a little further.

DEITZ: Charcoal is an agricultural product so it can vary from source to source.

DEUBER: We have found few differences in the retention of radioisotopes with different halflives, but there was a tendency for better retention of the isotopes with short halflives, contrary to your results.

CLOSING REMARKS OF SESSION CHAIRMAN JACOX:

This session was very interesting as it was one of the first iodine sessions to include specific applied research that provided data to solve specific engineering problems, such as sample line plateout. There is continuing research to understand the exact details of how $I-^{131}$ is removed by various types of carbon impregnants. This indicates the industry is becoming more mature.

Session 3

PERFORMANCE OF HVAC AND AIR CLEANING SYSTEMS IN NUCLEAR POWER PLANTS

MONDAY: August 13, 1984
CHAIRMEN: A.G. Evans
E.I. duPont de Nemours
J.P. Pearson
Nuclear Consulting Services

COMMENTARY ON NUCLEAR POWER PLANT CONTROL ROOM HABITABILITY - INCLUDING A REVIEW OF RELATED LERs (1981-1983)

Dade W. Moeller, Ph.D., Member
and
Janet P. Kotra, Ph.D., Fellow

Advisory Committee on Reactor Safeguards,
U.S. Nuclear Regulatory Commission
Washington, DC 20555

Abstract

A review of Licensee Event Reports filed by the operators of commercial nuclear power plants from 1981 through 1983 has revealed that approximately three percent pertain to systems that maintain or monitor control room habitability. Dominant contributors were deficiencies in normal and emergency trains of heating, ventilation, air conditioning and air cleaning systems (45%), deficiencies in atmospheric monitors for toxic and radioactive substances (27%) and deficiencies in fire protection systems (13%). To correct the situation revealed by these analyses and by information provided from other sources, we recommend that the NRC incorporate into its program plan the development of information that anticipates the conditions within a control room during emergencies, and that criteria for habitability within the control room be better defined. In addition, we suggest than an improved protocol for testing control room air-related systems be developed, that the required thickness and number of layers of charcoal adsorption beds for control room air cleaning systems be re-evaluated, and that steps be taken to improve the quality of heating, ventilating, air conditioning and air cleaning components. We also recommend that greater emphasis be placed on maintaining nuclear power plant control rooms in a habitable condition during emergencies so that the operators can remain there and safely shut down the plant, in contrast to placing reliance on the use of remote shutdown panels or auxiliary control facilities.

I. Introduction

The function of control room heating, ventilating, air conditioning and air cleaning systems in a nuclear power plant is to assure a safe and habitable environment for plant operators and equipment during normal operation and during postulated design basis accident conditions. These systems are designed to maintain an appropriate temperature and to provide a continuous and adequate flow of clean air to the control room. To accomplish these objectives, such systems must be capable of detecting life-threatening contaminants, subsequently isolating the control room, and then providing it with contaminant-free air following either an accident within the plant or an inadvertent on- or off-site airborne release of toxic materials. The control room ventilation and air purification systems must, themselves, also be protected from damage occurring

as a result of external natural phenomena such as earthquakes, floods and tornadoes.

The objective of this study was to review commercial light-water reactor operating experience contained in Licensee Event Reports (LERs) in order to identify and evaluate sources of failures and inadequacies in those systems responsible for the maintenance of an acceptable control room environment. The study included a detailed review of the LERs submitted by the utility plant operators to the U.S. Nuclear Regulatory Commission (NRC) during the years 1981 through 1983. Abstracts of LERs were searched using the keyword file maintained by the Nuclear Operation Analysis Center (formerly the Nuclear Safety Information Center (NSIC)) located at the Oak Ridge National Laboratory. This file is accessible through the Department of Energy (DOE) REmote CONsole (RECON) System. Compendia of abstracted LERs for 1982 and 1983 were published by the NSIC [1,2]. Further searching of these data was carried out using the Sequence Coding and Search System software developed by the NRC Office for Analysis and Evaluation of Operational Data (AEOD). Additional information was obtained from the "Information Notices," issued by the NRC Office of Inspection and Enforcement and the bimonthly "Power Reactor Events"[3] issued by AEOD.

Supplementing these reviews was a series of discussions held over the past several years during meetings of the NRC Advisory Committee on Reactor Safeguards Subcommittees on Reactor Radiological Effects and Air Systems. The information made available at these meetings has been utilized, particularly in Section III. Commentary and Recommendations.

II. Findings

Of approximately 12,600 LERs filed for commercial light-water nuclear power plants during the years 1981 through 1983, 368 or about 3%, pertain to the maintenance of control room habitability. Of these reports, 195, or 53% document violations of plant technical specifications for control rooms or control room systems which serve two or more operating units. Presented in Table 1 are data on control room habitability LERs for boiling water reactor (BWR) and pressurized water reactor (PWR) units, as well as for all light-water-reactor (LWR) units.

As may be noted, well over 60% of the LERs for BWR units were reported during pre-commercial operation. While this might appear to suggest that many inadequacies within control room habitability systems are corrected in the early stages of plant operation and do not recur, the data in this case are biased inasmuch the majority of these events (43 out of 68) were reported by a single licensee. In the case of PWR units, the fraction of total events reported by plant operators during the pre-commercial stage of operation is far less (about 26%). It is interesting to note that overall, the number of LERs per reactor-year for BWR and PWR installations is about the same (1.5 vs. 1.8).

The major categories of air-related control room system events reported for BWRs, PWRs and all LWRs are presented in Table 2, along with the percentage contribution of each event category to the respective totals.

Deficiencies of heating, ventilating, air conditioning and air cleaning systems, shown as the first item in Table 2 are further subdivided in Table 3.

Table 1. Control Room Habitability Related LERs 1981-1983

	Stage of Operation		
	Pre Commercial Operation*	Commercial Operation	Total
BWR Installations			
Number of LERs	68 (62%)	41 (38%)	109
Number of LERs per reactor-year	23	0.6	1.5
PWR Installations			
Number of LERs	67 (26%)	192 (74%)	259
Number of LERs per reactor-year	9.7	1.4	1.8
All Units			
Number of LERs	135 (37%)	233 (63%)	368
Number of LERs per reactor-year	13.6	1.1	1.7

* Licensed only for fuel loading and low power testing at time of LER

Table 2. Summary of Control Room Habitability Events 1981 - 1983

System Deficiency	BWRs Number	BWRs %	PWRs Number	PWRs %	All LWRs Number	All LWRs %
Heating, Ventilating Air Conditioning, and Air Cleaning	57	52	107	41	164	45
Atmospheric Monitors	26	24	74	29	100	27
Fire Protection Systems	15	14	31	12	46	13
Electrical Systems	3	3	12	5	15	4
Bottled Air Systems	-	-	9	3	9	2
Miscellaneous Failures	-	-	3	1	3	1
Procedural Violations	8	7	23	9	31	8
Totals	109	100	259	100	368	100

Table 3. Heating, Ventilating, Air Conditioning, and Air Cleaning System Events, 1981-1983

Subsystem Deficiency	BWRs Number	BWRs %	PWRs Number	PWRs %	All LWRs Number	All LWRs %
Ventilating/Air Flow	37	65	49	46	86	52
Air Conditioning/Chillers	9	16	41	38	50	31
Impaired Filter or Adsorber Efficiency	11	19	17	16	28	17
Totals	57	100	107	100	164	100

For both BWRs and PWRs, failures of such systems to conform to technical specifications accounted for almost half of the reported events. For BWR units, however, ventilation/air flow system deficiencies accounted for the predominant percentage, whereas for PWR units, problems in air conditioning/chiller systems were also a major contributor. For each type of unit, failures of atmospheric monitors accounted for 24% to 29% of the total, deficiencies in fire protection systems for 12% to 14%, failures in electrical systems for 3% to 5%, and procedural violations for 7% to 9%. The last group is of interest since these are reportable occurrences that have resulted from either a discrepancy between the as-built systems and the specifications listed in the Final Safety Analysis Report, or from a failure of the plant staff to perform tests of components within the requisite time limit designated in the plant technical specifications. The affected systems are defined as inoperable and may require plant shutdown, until the required modification and/or evaluation is performed.

An itemization of the major causes of reportable occurrences as attributed by the licensees, as well as the percentage contribution of each cause category, is shown in Table 4.

As may be noted, mechanical component failures were the predominant contributor, accounting for 37% of the reported events in BWR installations and 56% in PWR installations. These include failures of components directly responsible for control room habitability as well as failures of components in related systems, the loss of which would result in the unavailability of a system necessary for the maintenance or monitoring of the control room environment. The next major contributor was human error which accounted for 31% of the reported events for BWRs and 22% for PWRs. Such errors either caused the event directly or served as a factor that compounded an initial mechanical failure. These errors included faulty or improper maintenance or installation of a piece of equipment, or the utilization of improper procedures.

Control Room Heating, Ventilating, Air Conditioning and Air Cleaning Events

As was reported in Table 2, deficiencies of heating, ventilating, air conditioning and air cleaning systems represented the largest subcategory (45%) of control room habitability-related LERs. Thirty-two percent of the reported events resulted in the unavailability of at least one train of the emergency air cleanup system for the affected control room and 12 percent resulted in the unavailability of all redundant trains of emergency air cleanup available to a given control room. These conditions represent limiting conditions of operation such that availability of both trains must be restored within a specified period of time or the plant must be shut down. Reported events in these systems and their causes are listed in Table 5. Reported separately are those events involving air conditioners/chillers, those involving ventilation/air flow systems (blowers and dampers), and those involving inadequate filter or adsorber efficiency.

Examples of specific events that may be of generic interest are discussed below.

Table 4. Reported Causes of Control Room Habitability Events, 1981-1983

Reported Cause	BWRs		PWRs		All LWRs	
	Number	%	Number	%	Number	%
Mechanical Component Failure	40	37	145	56	185	50
Human Error	34	31	56	22	90	25
Design Error or Flaw	10	9	25	10	35	10
Mechanical Failure Compounded by Human Error	6	6	12	5	18	5
Component Unavailable due to Corrective Maintenance	10	9	3	1	13	3
Instrument Drift	6	6	7	3	13	3
Unknown	3	3	11	4	14	4
Totals	109	100	259	100	368	100

Table 5. Events Involving Control Room Heating, Ventilating, Air Conditioning and Air Cleaning Systems, 1981-1983

Reported Cause	Air Conditioners/ Chillers	Ventilation/Air Flow (Blowers and Dampers)	Impaired Filter or Adsorber Efficiency
Mechanical Component Failure	36	40	12
Human Error	5	24	10
Design Error or Flaw	3	15	1
Component Unavailable due to Corrective Maintenance	2	1	0
Mechanical Failure Compounded by Human Error	2	4	2
Unknown	2	2	3
Totals	50	86	28

Failures in control room air chillers and humidifiers at three different plants resulted from the fouling of service water due to mineral salts and biological debris. This, in turn, led to plate out on heat exchange surfaces or the clogging of screens.

On numerous occasions throughout the three year period, improper design of control room chillers led to failures of additional plant systems. For example, as a result of increased demand for service water by the control room chillers at one plant during the summer months, suction was lost to pumps which provide component cooling water to the charging pumps. Until this design problem could be corrected, it was necessary to throttle off the chiller line to restore adequate flow to the charging pumps. At another plant a control room toilet, clogged by a crowbar, overflowed. The water, seeping through fire barriers into the cable spreading room below, shorted various electrical components.

Failures in ventilation dampers and blowers, that occurred at five different plants, were the direct result of vibration which caused wing nuts, set screws or attachment pins to become loose. The replacement of these hardware components with locknuts, or other secure attachments, restored the availability of the emergency air flow system and easily rectified the problem.

At another plant, a path for the flow of outside, unfiltered air directly into the control room through an uncapped ventilation duct escaped detection (and correction) for 17 months. The duct was inadvertently left uncapped during modifications to the ventilation system. At another unit, the exhaust from the emergency diesel generator was located too close to the ventilation intake of the control building and had to be relocated to prevent the intrusion of exhaust fumes into the control room. Lack of sufficient familiarity with control room emergency ventilation design, and its proper function, was a major contributing cause to these problems.

Several events were reported that involved the potential loss of the pressurization barrier to the control room. These included one event in which the control room design was such that floor and equipment drains presented a leak path to outside areas. In a second case, analyses showed that a seismic event could cause leakage around pipes that penetrated the control room walls.

The majority of LERs related to HEPA filters and charcoal adsorbers reflect that the performance of such units degrades with time and that routine tests reveal that their efficiencies do not meet technical specifications. The normal licensee response is to replace the units. More serious occurrences, however, include the fouling of charcoal adsorbers by welding and/or paint fumes and the occasional wetting of filters or adsorbers by drainage water or the inadvertent actuation of their associated fire protection deluge systems. At one plant, paint fumes so contaminated the control room emergency charcoal filters that their measured removal efficiencies were significantly degraded. Apparently, the control room emergency ventilation system was in a recirculation mode during the painting of an adjacent room. Backflow through component drain lines into filter packages necessitated their replacement at one plant when the level control tank drain line was inadequate to carry the leakage of the loop-seal level control. Unintentional actuation of fire suppression systems was reported at three nuclear power plants during the three year period of this study. This rendered the filters and adsorbers inoperable and they had to be replaced.

Atmospheric Monitor Events

As was shown in Table 2, 27% of the reportable occurrences affecting the control room environment involved deficiencies of atmospheric monitoring equipment. This includes the equipment that monitors the ambient temperature as well as that which monitors airborne toxic or radioactive particles and gases. Shown in Table 6 are further details on atmospheric monitor events and their reported causes.

The most frequent problem (accounting for over half of all events in this category) was the mechanical failure of chlorine monitors. Most such monitors (as well as those for monitoring ammonia) at nuclear power plants use a dripping electrolyte which is particularly prone to failure. Clogging of the electrolyte orifice or wick can result from precipitate buildup or excessive dust in the sampling line. Since redundant monitors generally sample air from the same intake, they are subject to a common mode failure. Excessive consumption or evaporation of the electrolyte fluid is also a significant source of failure for these monitors. At one plant, heat tracing at a common intake, intended to prevent freezing in the sample line during cold weather, malfunctioned and caused the electrolyte to dry out and the monitors to fail.

Because of the number of events being reported that involved the degradation and subsequent common-cause failure of toxic gas detectors, the NRC Office of Inspection and Enforcement (IE) issued in September, 1983, an IE Information Notice related to this problem[4]. The importance of operable gas detectors was highlighted by a review of a chlorine gas release that occurred at one nuclear power plant in 1983, and previous releases that had occurred at other plants in 1978 and 1979. To correct the problem of the deficiencies in chlorine gas detectors, the NRC Staff recommended that consideration be given either to increased surveillance of these detectors or that they be replaced with a type less subject to recurrent failure.

Fire Protection/Detection Deficiencies

The frequency of fire protection/detection related LERs and their causes are listed in Table 7.

Such events comprised approximately 13% of all control room habitability occurrences reported during the three-year period of this study (Table 2). The bulk of these LERs concern the inadequate maintenance of proper fire barriers in the control building. This generally occurs when, in the absence of proper procedures and/or in ignorance of the fire barrier requirements, operators penetrate existing barriers in order to gain access to other systems. The negative impact of the inadvertent actuation of fire protection, especially deluge, systems on other safety functions has been discussed above and elsewhere[5].

Impact of Electrical System Failures

Although they represent only 4% of the total number of events tabulated in Table 2, the number of LERs involving control room habitability that were due to failures in plant electrical systems appears to be increasing. Examples include actuation of control room emergency ventilation systems due to false alarms of

Table 6. Events Involving Control Room Atmospheric Monitors, 1981-1983

Reported Cause	Monitor Type					All Monitors	
	Chlorine	Radiation	Ammonia	Butane	Temperature	Total	%
Mechanical Component Failure	54	6	4	2	1	67	67
Human Error	4	1	1	2	2	10	10
Design Error or Flaw	2	2	0	2	0	6	6
Instrument Drift	0	5	5	0	0	10	10
Component Unavailable due to Corrective Maintenance	0	1	0	0	0	1	1
Mechanical Failure Compounded by Human Error	1	0	0	0	1	2	2
Unknown	1	3	0	0	0	4	4
All Causes	62	18	10	6	4	100	100

Table 7. Events Involving Control Room Fire Protection Systems, 1981-1983

Reported Cause	Type of System: Fire Barriers	Halon Systems	Fire Alarms	Smoke Detectors	Total No.	%
Mechanical Component Failure	10	0	4	1	15	33
Human Error	13	0	1	0	14	31
Unavailable due to Corrective Maintenance	6	0	0	1	7	15
Design Error or Flaw	5	0	0	1	6	13
Mechanical Failure and Human Error	2	0	0	0	2	4
Unknown	0	1	1	0	2	4
Totals	36	1	6	3	46	100
%	78	2	13	7	100	

process and atmospheric monitors caused by spurious electrical signals, as well as similar alarms resulting from repairs and/or tests of control room electrical equipment.

III. Commentary and Recommendations

Dominant among the events reported above were deficiencies in normal and emergency trains of control room heating, ventilating, air conditioning and air cleaning systems (making up 45% of the reported events), deficiencies of atmospheric monitors of airborne toxic and radioactive substances (representing 27% of the events), and deficiencies in fire protection systems (representing 13% of the events). A variety of similar events has been reported by private consulting organizations and other groups at meetings of the ACRS Subcommittees on Reactor Radiological Effects and Air Systems[6,7].

As a result of these meetings, and in response to recommendations from the ACRS, the U.S. Nuclear Regulatory Commission has launched an aggressive and responsive program to address these problems. This includes improved organization within the NRC Staff to review and evaluate the needs in this subject area; the development of an associated program plan; initiation of a series of workshops in which other groups (including the U.S. Army Research Institute of Environmental Medicine and the U.S. Navy Nuclear Submarine Program) are encouraged to share their knowledge and expertise with the NRC Staff; and site visits to evaluate control room habitability problems at operating nuclear power plants and those nearing operation. These site visits include surveys of control room designs against the present habitability criteria of the NRC, and also against newly proposed criteria developed as part of the program plan. These surveys are also designed to determine the manner in which conformance of the as-built control rooms to the system design is achieved and to gather information on how licensees utilize the preoperational and operational testing of systems and/or components to show they meet their design specifications, their technical specification requirements and their functional requirements. Details of these surveys and the findings of the NRC Working Group on Control Room Habitability are the subject of the next paper in the Proceedings[8] and a forthcoming report[9].

Other examples of action by the NRC Staff on problems related to control room habitability include the IE Information Notice, previously cited, that alerted licensees to the potential degradation and subsequent common-cause failure of toxic gas detectors at nuclear power plants. In a similar manner, the NRC issued in 1982 an IE Information Notice[10] which cited the failure of personnel at several plants to correct for pressure differentials between the air streams in the line being sampled and the associated offline sampling system. This could lead to serious errors in measurements of airborne toxic chemical and radioactive material concentrations.

In 1983 the NRC Staff issued a generic letter to all nuclear power plant licensees clarifying the surveillance requirements for HEPA filters and charcoal adsorber units in emergency safety feature air cleaning systems[11]. Several inaccuracies have been identified in this letter since its release. They include errors in the technical specifications of allowable filter bypass leakage in the requirements for in-place filter and adsorber testing, and in the requirements for laboratory charcoal testing. We support the recommendation[9] that this letter be rescinded to correct those sections which are in

error. More recently, the NRC issued an IE Information Notice [12] citing discrepancies in record keeping and material defects in heating, ventilating and air conditioning (HVAC) units manufactured by an industrial organization. These problems were revealed by NRC inspectors who found that liquid penetrant inspections conducted at the factory were not completed during the actual manufacture of the charcoal adsorption units. Inspection reports, instead, were based on the personal notes and memories of the inspectors. Installed units at one nuclear power plant had low-strength carbon steel fasteners substituted for the required ASTM-A449 fan motor anchor bolts and self-tapping stainless steel screws were substituted for ASTM-A193-GR B9 bolts used for mounting the cooling coils. In addition, the weld filler material heat lot number was not recorded for eight of the units. Units at another plant had welds with cracks, lack of fusion, and undercut or material reduction which exceeded 1/64 inch. There were also missing welds and welds not made in accordance with the design drawings. When some of the welds were reinspected with dye penetrant, unacceptable indications were found.

As may be noted by these actions on the part of the NRC Staff, problems associated with control room habitability go far beyond the failures revealed in the LERs submitted by the Licensees. As part of the government-industry effort in this field, we believe that it is important that certain key problems be addressed. In support of this work, we offer the following recommendations:

1. That information be developed to serve as a guide in determining the envelope of conditions to be anticipated, and the functions to be maintained, within a control room under emergency situations. In short, what are realistic conditions relative to temperature, smoke concentrations, radiation dose rates, humidity, air exchange and leakage rates, etc., with which the control room must be designed to cope? The current efforts of the NRC to better define the source term for nuclear power plant accidents [13] should be helpful in answering this question. Estimates of toxic vapor concentrations in the control room resulting from postulated external releases have been made [14].

Concurrently, the criteria for habitability within a control room need to be more clearly specified. Without relevant criteria, the performance requirements for the control room engineered safety features cannot be defined. There is also a need to specify under emergency situations what environmental conditions the operators are expected to endure, what error rates can be tolerated, and for how long operator performance at some specified level must be sustained.

Maximum temperature limits for control rooms are currently designated at approximately 120°F (primarily based upon operational requirements of equipment). As humidity increases at this temperature with a low air exchange rate, the situation could rapidly become uninhabitable for plant operators. We recommend that separate temperature criteria be established for equipment and for personnel and that temperature be monitored in the control room appropriate to each criterion.

2. The NRC Staff needs to expedite its efforts to develop a protocol for testing control room heating, ventilating, air conditioning and air cleaning systems. Such tests should be conducted under realistic operating conditions.

They should include testing of complete systems as well as individual components, and should include consideration of the adequacy and accessability of remote shutdown panels and emergency operations facilities. The accessability of these facilities is of particular importance due to recent reports of deficiencies in respiratory protective equipment for emergency use [15].

Criteria for acceptance should be based on conditions that permit the continued function of equipment and some reasonable level of human comfort during prolonged emergency situations. All parts of the systems, including dampers, ducts, etc., should be tested simultaneously as an integral unit under both positive and negative pressures. Particular attention should be given to assure that sections of such systems that are under negative pressure will not bring in contaminants, which later can be transferred to the control room. Possible damage to vital equipment due to pressure surges and the accompanying disruption of heating, ventilating, air conditioning and air cleaning systems should also be evaluated.

Efforts should be made to incorporate into such procedures recently developed improved field testing methods. Included in such tests should be measurements in control rooms and other vital areas of the rates of temperature increases and the maximum temperatures that would be reached in cases of reduced air flow.

3. There is also a need to conduct laboratory or field tests to obtain the data necessary for defining the optimum locations of control room air intakes and for evaluating under emergency conditions the location and performance of existing control room air intakes for operating nuclear power plants. A downwash analysis applicable to emergency intake and exhaust openings would be appropriate for this kind of assessment. Such data would appear to be mandatory in the case of standard plant applications and could be approached on a generic basis.

4. Because of potential problems associated with the release of hazardous chemicals near nuclear power plants, studies should be conducted to assess the possible benefits of increasing the minimum thickness and number of layers required in charcoal adsorption beds used in the protective air cleaning systems for control rooms. In this regard, it should be noted that deeper beds are just as effective for high acute exposures as they are for chronic low exposures (up to the capacity of the charcoal to retain the contaminants). As a result, deeper beds are better able to handle high acute contaminant concentrations. In addition, it should be recognized that the U.S. philosophy that control rooms be sealed rather than designed to cope with high air intake concentrations will be fully effective only for those plants having auxiliary compressed air tanks for pressurizing the room; other plants must take in outside air to maintain pressurization.

Requirements pertaining to charcoal beds should be closely tied to the precise nature of the anticipated hazards and the characteristics of specific nuclear power plant sites. The importance of such protection is shown by the fact that, as was pointed out in this review, accidental releases of chlorine have occurred near three commercial nuclear power plants in the U.S. since 1978.

5. Fire dampers currently installed in nuclear power plants are intended to prevent the spread of a fire but are not designed or certified to hold back the accompanying smoke or potentially toxic gases. If leak rates are as high as has been reported, there may be situations and/or systems in which auxiliary dampers should be installed to provide supporting seals. This review of LERs (Table 7) has indicated that failures in fire barriers were the most common type of failure in control room fire protection systems. Due to the special situations surrounding control rooms, it may well be that dampers that are acceptable for normal industrial use are not acceptable for nuclear power plant usage. In this regard we are pleased to note that proposed standards, being prepared by the Committee on Nuclear Air and Gas Treatment of the American Society of Mechanical Engineers (ASME) contain recommendations for maximum permissible leak rates for dampers and movable louvers.

6. There is also a need to direct some effort to conducting failure modes and effects analyses for all systems related to control room habitability. The results of such analyses would prove useful in assigning priorities to the correction of the types of problems cited above as well as those revealed through this study of LERs.

7. Data presented to the ACRS Subcommittees on Reactor Radiological Effects and Air Systems during the course of this study indicated a wide range in the quality of heating, ventilating, air conditioning and air cleaning components. This was particularly true with respect to HEPA filters. We are pleased to note that NRC Staff is currently reconsidering its policy not to have the certification of such filters confirmed by one of the filter test stations of the U.S. Department of Energy. In addition, it was not clear whether Quality Product Listing (QPL) certification is an essential part of the military specifications. The NRC should contact appropriate groups, such as the Edgewood Arsenal and the ASME Committee on Nuclear Air and Gas Treatment, for clarification on this matter. Relevant information and decisions, as appropriate, should be included in the upcoming revision of Regulatory Guide 1.52 [16].

8. Additional potential problems that appear to need evaluation in terms of control room habitability include:

a. The impact of the loss of all AC power, of auxiliary services to chiller systems, of service air, and of component cooling water;

b. More careful evaluation of all potential sources of heat input in assessing possible temperature increases in degraded operating modes;

c. The potential need for monitoring oxygen concentrations and steam intrusion into the control room; and

d. Whether the current detection limits for contaminants in the control room air intake are sufficiently sensitive to protect operating personnel.

As a final comment, we might note that too often the regulatory assumption is made that, if the control room becomes uninhabitable, the plant operators can retreat to the remote shutdown panel and manage the situation from there. Since the shutdown of a nuclear power plant on an emergency basis is a serious matter,

we believe the preferred option is to assure the habitability of the main control room to permit the operators to remain at their normal posts. The analyses of Licensee Event Reports, and the recommendations presented in this paper, are offered with that concept in mind.

References

1. "License Event Report (LER) Compilation," NRC Report NUREG/CR-2000 ORNL/NSIC-200 1 (1-12) Nuclear Safety Information Center, Oak Ridge National Laboratory (1982).

2. "Licensee Event Report (LER) Compilation," Report NUREG/CR-2000, ORNL/NSIC-200, 2 (1-12), Nuclear Safety Information Center, Oak Ridge National Laboratory (1983).

3. "Power Reactor Events," U.S. Nuclear Regulatory Commission, Washington, D.C. 20555 (1981-1983).

4. "Failure of Redundant Toxic Gas Detectors Positioned at Control Room Ventilation Air Intakes," IE Information Notice No. 83-62, U.S. Nuclear Regulatory Commission, Washington, D.C. 20555 (September 26, 1983).

5. "Actuation of Fire Suppression System Causing Inoperability of Safety-Related Equipment," IE Information Notice No. 83-41, U.S. Nuclear Regulatory Commission, Washington, D.C. 20555 (June 22, 1983).

6. "Control Room Habitability," Report of the Advisory Committee on Reactor Safeguards, U.S. Nuclear Regulatory Commission, Washington, D.C. 20555 (August 18, 1982).

7. "ACRS Subcommittee Report on Control Room Habitability," Advisory Committee on Reactor Safeguards, U.S. Nuclear Regulatory Commission, Washington, D.C. 20555 (May 17, 1983).

8. Hayes, J.J., D.R. Muller and W.P. Gammill, "NRC Study of Control Room Habitability," paper presented at the 18th DOE Nuclear Airborne Waste Management and Air Cleaning Conference, Baltimore, MD (August 12-16, 1984).

9. "Control Room Habitability", Report of the Control Room Habitability Group to the Executive Director for Operations, U.S. Nuclear Regulatory Commission, Washington, D.C. 20555 (June 1984).

10. "Correction for Sample Conditions for Air and Gas Monitoring," IE Information Notice No. 82-49, U.S. Nuclear Regulatory Commission, Washington, D.C. 20555 (December 16, 1982).

11. Eisenhut, D.G., "Clarification of Surveillance Requirements for HEPA filters and Charcoal Adsorbers Units in Standard Technical Specifications on ESF Cleanup Systems," NRC Generic Letter 83-13, U.S. Nuclear Regulatory Commission, Washington, D.C. 20555 (March 2, 1983).

12. "Discrepancies in Record Keeping and Material Defects in Bahnson Heating, Ventilation, and Air Conditioning Units," IE Information Notice No. 84-30, U.S. Nuclear Regulatory Commission, Washington, D.C. 20555 (April 18, 1984).

13. "Technical Bases for Estimating Fission Product Behavior During LWR Accidents," Report NUREG-0772, Office of Nuclear Regulatory Research, U.S. Nuclear Regulatory Commission, Washington, D.C. 20555 (June 1981).

14. Wing, James, "Toxic Vapor Concentrations in the Control Room Following a Postulated Accidental Release," Report NUREG-0570, U.S. Nuclear Regulatory Commission, Washington, D.C. 20555 (June 1979).

15. "Defective Emergency Use Respirator," IE Information Notice No. 83-21, U.S. Nuclear Regulatory Commission, Washington, D.C. 20555 (April 15, 1983).

16. Regulatory Guide 1.52, "Design, Testing, and Maintenance Criteria for Post Accident Engineered-Safety-Feature Atmosphere Cleanup System Air Filtration and Adsorption Units of Light-Water-Cooled Nuclear Power Plants," Office of Standards Development, U.S. Nuclear Regulatory Commission, Washington, D.C. 20555 (1978).

DISCUSSION

MacAULAY: You mentioned that the main fault of fire protection systems was false activation of the deluge sprinkler systems. I wonder if you can tell us what really caused this?

MOELLER: I am not sure I can answer this. My comment was that frequently the water deluge systems will activate and spray the charcoal when there is no reason to do so. Dr. Kotra recalls two incidents: spurious electrical signals and a false alarm by smoke detectors that indicated there was a temperature rise or a fire in the charcoal when there was not.

KOTRA: I just want to add that we brought that particular item out because it was of significance to the engineered safety features in the control room. The major source of fire protection LERs were, as mentioned in the talk, deviations of the as-built systems from the FSAR. These dealt primarily with fire barrier penetrations that were inadvertent on the part of control room operators or maintenance personnel.

NRC STUDY OF CONTROL ROOM HABITABILITY

J. J. Hayes, Jr., D. R. Muller, W. P. Gammill
U.S. Nuclear Regulatory Commission
Washington, D.C.

Abstract

Since 1980, The Advisory Committee on Reactor Safeguards (ACRS) has held several meetings with the NRC staff (staff) to discuss the subject of control room habitability. Several meetings between the ACRS and the staff have resulted in ACRS letters that express specific concerns, and the staff has provided responses in reports and meetings.

In June of 1983, the NRC Executive Director for Operations directed the Offices of Nuclear Reactor Regulation and Inspection and Enforcement to develop a plan to handle the issues raised by the ACRS and to report to him specific proposed courses of action to respond to the ACRS's concerns.

The NRC control room habitability working group has reviewed the subject in such areas as NRR review process, transformation of control room habitability designs to as-built systems, and determination of testing protocol. The group has determined that many of the ACRS concerns and recommendations are well founded, and has recommended actions to be taken to address these as well as other concerns which were raised independent of the ACRS. The review has revealed significant areas where the approach presently utilized in reviews should be altered.

I. Background

Introduction

Since 1980, the Advisory Committee on Reactor Safeguards (ACRS) has held several meetings with the NRC staff to discuss the subject of control room habitability. During this period, the ACRS has also discussed this topic with numerous applicants for a near-term operating license and with various nuclear steam supply system vendors. In addition, the ACRS has solicited information from consultants and architect-engineers. Table 1 summarizes the ACRS's general and specific comments as described in its most recent letter dated May 17, 1983.

In addition to the comments and recommendations presented in Table 1, the ACRS requested in that same letter that the staff:

(1) Determine the impact on control room habitability with the loss of
   (a) AC power;
   (b) auxiliary services to chillers;
   (c) service air; and
   (d) component cooling water.

(2) Evaluate all potential sources of heat input in the control room necessary for determining temperature increases while the heating, ventilating and air conditioning (HVAC) system is in degraded operating modes.

(3) Determine the potential need for monitoring O_2 concentrations and steam intrusion in the control room.

Table 1 Summary of ACRS Concerns and Recommendations on Control Room Habitability

ACRS Concern	ACRS Recommendation
General Comments	
1. NRC review is fragmented.	1. One NRC group should be designated for coordinating the review and evaluating the control room.
2. NRC does not perform an independent evaluation of the control room.	2. NRC should perform critical and independent reviews of the control room. Consequently, the NRC does not know whether the control room envelope will perform as intended.
3. NRC has not utilized various sources of data on equipment or system failure to determine the impact of these failures on the habitability of the control room.	3. NRC should utilize regional offices and INPO to obtain data on equipment and system failure.
Specific Comments	
1. Assistance could be provided in the determination of the optimum locations of alternate air intakes for control rooms through the use of a generic diffusion study.	1. NRC should reevaluate its response on the use of a generic diffusion study for determining the optimum location of control room intakes.
2. Temperature limit of 120°F for the control room is unacceptable. Additional conditions such as low air exchange rate, perspiration, ESF filter system heaters, etc. could affect habitability.	2. Temperature limits should be revised taking into account low air exchange rate, operation of ESF filter system heaters, and perspiration.
3. NRC does not have a protocol for testing control room HVAC systems.	3. NRC should develop a protocol for testing control room HVAC. Protocol should include determination of functionability of equipment, human comfort, complete filter system testing under positive and negative pressures, and impact of pressure surges.
4. NRC is not giving an appropriate amount of attention to the quality assurance aspects of HEPA filter manufacturing, installation and testing.	4. NRC regional offices should investigate whether NRC licensees are purchasing HEPA filters which do not meet RG 1.52, and take corrective action if needed. NRC should determine whether Qualified Products List (U.S. Army) testing is required from the Committee on Nuclear Air and Gas Treatment (ASME) RG 1.52 should be revised accordingly.
5. Fire dampers are not designed to prevent the spread of smoke or toxic gases through the control room.	5. NRC should determine the allowable leak rates for fire dampers, whether such leak rates can be achieved in practice, and whether auxiliary dampers should be installed to limit leakage.
6. NRC has dismissed the use of deep bed charcoal for treatment of toxic gases.	6. NRC should consider deep beds as a means of treating contaminants.

(4) Evaluate whether the present detection limits of toxic-gas monitors are sufficient to protect personnel.

The NRC Executive Director for Operations (EDO) determined that a substantial amount of staff time and effort was being expended in responding to the ACRS concerns, but little was being accomplished in the way of resolving the issue of control room habitability. Therefore he instructed the Offices of Nuclear Reactor Regulation (NRR) and Inspection and Enforcement (IE) to develop a plan to handle the issues raised by the ACRS, and to report to him specific proposed courses of action in response to ACRS concerns.

The Program Plan

A program plan was developed and approved for implementation on August 15, 1983. The EDO directed NRR to coordinate the program with IE and the NRC regional offices, as appropriate. The report of the Control Room Habitability Working Group was submitted to the EDO in June 1984.

The intent of the program plan was to assess the integrated response of the NRC in the area of control room habitability. The plan was designed to establish whether, and in what areas, problems exist and, if they exist, to implement recommended changes. To administer the program plan a working group was formed which was comprised of five individuals drawn from the technical branches most intimately involved in the control room habitability issue. These were the Meteorology and Effluent Treatment Branch (METB), the Auxiliary Systems Branch (ASB), the Chemical Engineering Branch (CMEB), the Accident Evaluation Branch (AEB), and the Human Factors Engineering Branch (HFEB).

A lead project manager familiar with the issues related to control room habitability directed activities of the working group. The group was responsible for the detailed analysis and evaluation needed to scope the problem and for developing and implementing recommendations.

The program plan consisted of five main areas. The first involved the review of the present criteria for control room habitability. These criteria were to be evaluated, modifications to the criteria were to be considered where inadequacies exist, and new criteria were to be developed where none existed.

The second part of the program plan involved the performance of several reviews. Review areas were to be identified for each NRR branch. IE and regional inspection activities were to be identified along with present programs in the Office of Research (RES). Information on system/equipment failure modes and rates was to be gathered. Three to five near-term operating license (NTOL) FSAR/SERs and three to five operating plants, being reviewed under TMI Action Plan Item III.D.3.4 (multi-plant action item F-70), were to be reviewed for consistency between perceived responsibilities and actual staff practice. The adequacy of review areas, criteria, documentation, interfaces, and staff practice was to be assessed and the issues raised by the ACRS were to be covered.

The third part of the program plan involved the survey of the as-built control rooms of three to five NTOL plants and the three to five F-70 plants for (1) consistency between requirements and practice and (2) actual practice in component and integrated testing. The working group was to confer with selected architect-engineering firms to discuss their control room design practices.

After these three parts of the program plan were completed, a report was to be written (the fourth part) which would provide recommendations and would specify the manner in which each of the recommendations would be handled in the regulatory process.

The fifth part of the program plan would involve maintaining an overview and management responsibility for implementing the recommended changes, evaluating the adequacy of implementation, and developing the overall strategy for moving the recommended changes through the regulatory process. The working group and steering group would be maintained during this period, but the detailed implementation of recommendations would likely be delegated to the appropriate branches. If the efforts resulted in new requirements which necessitated inspection to verify implementation, then IE would incorporate revisions into the inspection program.

II. Description of NRR Review Process

The NRR review of control rooms involves seven branches which have input to the staff's safety evaluation report (SER). Two additional branches that have no direct input to the SER interact with four of the "input" branches and provide significant material to them. Eleven other branches may interact with one of the seven "input" branches providing material upon request.

Figure 1 is a block diagram showing the seven branches which have input to those sections of the SER in which the function of the control room is described. The figure also shows routine interactions that occur as a normal part of the review process, and non-routine interactions that occur as required. The figure also details where those interactions involve significant input requirements. The figure illustrates the broad scope of the control room habitability review and how successful handling of the subject matter is dependent upon informal interaction between various branches.

III. Approach

The control room habitability study was performed in three phases. Phase 1 consisted of the determination of parameters that must be considered important to habitability. In addition, time was spent familiarizing the working group with the review performed by each of the branches having major review responsibilities in the area of control room habitability. Members of the working group described their branches' review procedure and their acceptance criteria. Phase 1 was also a period of information gathering. Sources outside the NRC were asked to address particular areas that they were familiar with and to provide comments on those areas of control room habitability that they may employ during their normal work assignments. This phase culminated in the Control Room Habitability Workshop which was held on November 28 and 29, 1983 in Harpers Ferry, West Virginia.

Phase 2 involved the final determination of the control room habitability parameters, the selection of a near-term operating licensee (NTOL) plant to which the working group would apply the present NRC review criteria, identification of those areas in which the present NRC review criteria are inadequate, and assessment of how the system design, as presented in the FSAR, is transformed to the as-built system. The latter assessment involved a site visit on January 24-25, 1984 to review the control room design of the NTOL plant selected for review.

Phase 3 involved the review of as-built control room designs at an NTOL plant and at two operating plants. These reviews are being performed under a technical assistance contract and are not scheduled to be completed until October 1984.

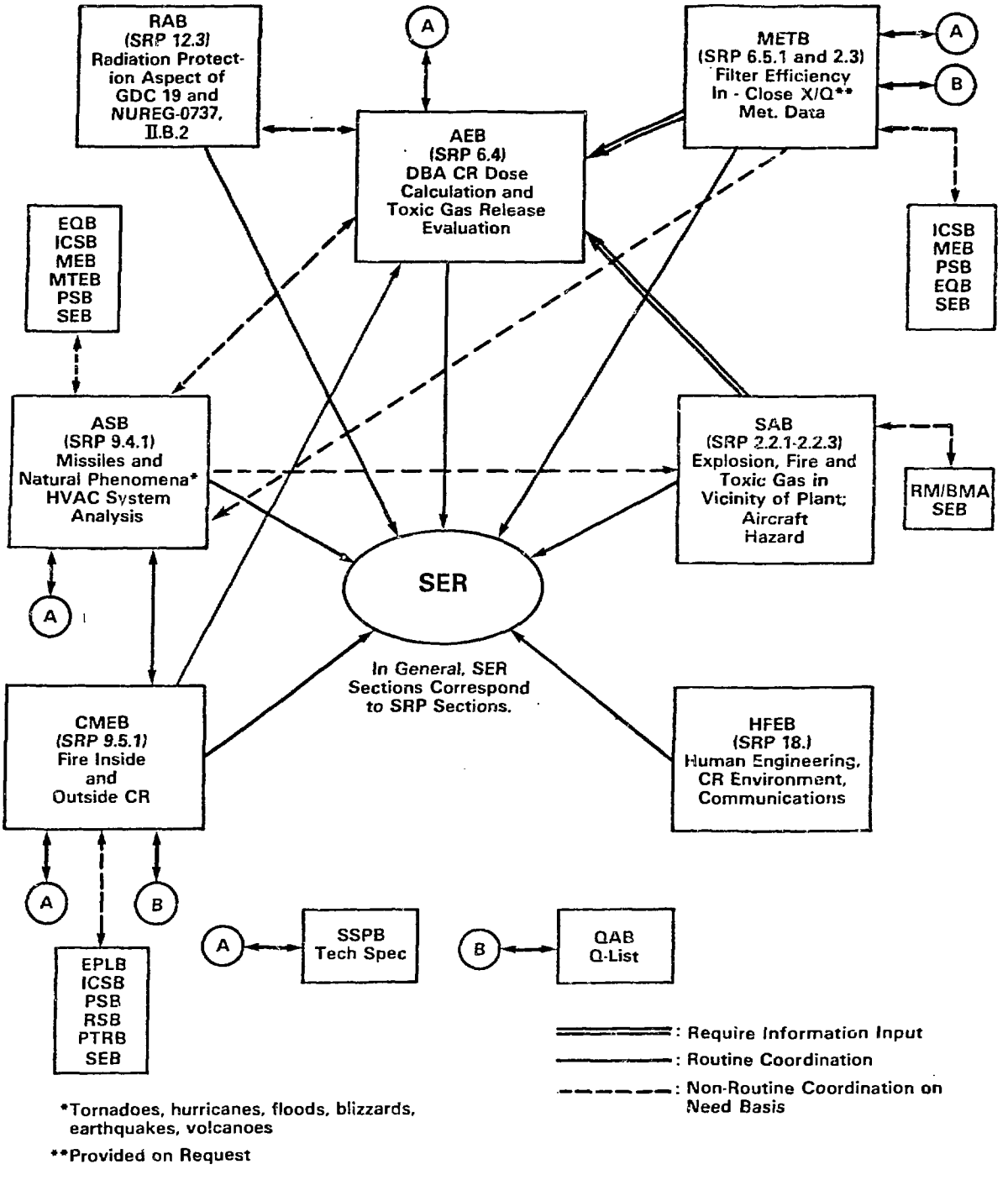

Figure 1 Control Room Habitability Block Diagram Showing Branches, Major Review Areas, and Interfaces

Phase 1

Phase 1 was spent:

(1) securing background information on habitability criteria of other organizations,

(2) providing a critique of present NRR staff review practices of control rooms,

(3) obtaining a perspective of how other organizations view the ACRS's concerns and recommendations, and

(4) determining which parameters are important to control room habitability and should be included in the design criteria.

Phase 1 was also a period during which the working group attempted to refine the program plan so that it would serve the study rather than direct it. The most striking refinement was that the working group established very early in its deliberations that the purpose of the group was not just to address the comments and recommendations of the ACRS. Rather, the group would focus on the subject of control room habitability as if it were a new safety area. The effort was made to place past practices in the background and to approach the situation as if it and its practices were being initiated today.

Determination of Habitability Criteria. One of the first orders of business for the working group was to develop a definition of a habitable control room and to identify the various parameters that must be maintained in order that the control room remain habitable.

Initially, it was established that the habitability goal was:

> To maintain the physical and environmental state of the control room such that it will allow the inhabitants to perform their intended functions unimpaired under both accident and normal operating conditions.

The working group agreed that the function of the control room operator is to maintain adequate control of the nuclear chain reaction so that the reactor is operated safely under normal conditions and is maintained in a safe condition in abnormal situations. Therefore, it is imperative that everything within reason be done to ensure that the control room operator is in a situation where such control may be maintained.

The conditions that affect the manner in which a control room operator performs his duties are similar to those that affect any worker. A worker functions best when he is safe, comfortable, stimulated, and confident. Thus, if a control room operator is free from large fluctuations in environmental parameters (temperature, relative humidity, lighting, noise, odors, and such), he is more likely to perform his tasks in a correct and safe manner. The operator can respond in a stimulated and confident manner if he knows that the tools or facilities necessary to perform the job are available. Such requirements would include adequate work space, access to communication equipment and other equipment and tools necessary to perform the job, and the capability to interact with the appropriate individuals necessary for the job.

Keeping all of these requirements in mind, the working group determined that the following items were important in establishing habitability criteria for the control room:

(1) radiological exposure (dose),
(2) communications,
(3) visibility,
(4) noise,
(5) illumination,
(6) ventilation,
(7) temperature,
(8) relative humidity, and
(9) contaminant levels (toxic gases).

Workshop. The working group sought to enlist the expertise of various industries and organizations that had habitability concerns for individuals in the course of their daily business and to learn how these organizations approach the problem of habitability. The working group received input from consultants, architect engineers, nuclear steam supply system (NSSS) vendors, academia, and government agencies and departments. These people were asked to address the ACRS comments and recommendations. Their views were presented at the Control Room Habitability Workshop held in Harpers Ferry, West Virginia, on November 28 and 29, 1983.

Familiarization With Habitability Review Areas. Phase 1 was also a period when each of the working group members broadened his knowledge in the review area of control room habitability. During this period each member of the working group prepared a presentation describing how his branch reviews those aspects of the control room design related to habitability. The intent of this presentation was to allow a critique of the review procedures as described by the working group members.

On several occasions the question was raised about whether the topic fell within the purview of this study, i.e., dealt with control room habitability or control rooms as a whole. The remote shutdown panel was one such topic. It was determined to include the remote shutdown panel in the review on a limited basis.

Phase 2

Final Determination of Habitability Parameters. Initially the working group believed that separate habitability criteria covering the environmental parameters defined above should be defined for both normal operation and accident conditions. This would have been inconsistent with the present NRC practice which has established most of the control room habitability criteria for normal operating conditions. The exception is the radiological accident. The present habitability criteria allow this environmental parameter to degrade in the event of an accident. After hearing a discussion at the workshop on performance under stressful conditions by an ergonomist and by other individuals involved in human factors, it was the consensus of the working group that the conditions under which a control room operator must function should be as good, if not better, during an accident as they are during normal operation.

In an attempt to implement this philosophy, the working group first determined the present requirements for normal operation associated with the various habitability parameters and second, assessed whether these requirements allowed the operator to maintain performance during normal operation. Then, the working group assumed these requirements were applied to an accident situation. The group

assessed whether these requirements still provided an environment in which the operator would continue to function in the intended manner. The working group found that some requirements were not defined for normal operation, but only for accident conditions. The allowable toxic gas concentration given in Table C-1 of RG 1.78 is such an example. The radiological dose parameters presented a different problem. Normal operation is governed by the criteria of 10 CFR Part 20. However, for accident conditions, the doses are allowed to increase to the levels given in General Design Criterion (GDC) 19 and Standard Review Plan (SRP) Section 6.4.

Application of NRC Review Process to NTOL Plant. During this phase the working group performed an in-depth review of a control room facility. Since this was an attempt by the working group to apply the guidance contained in the SRPs, it was believed that such a review could provide information and guidance for Phase 3 of this study and would reveal potential weaknesses and oversights in the review process.

The plant selected was an NTOL applicant scheduled for fuel loading in 1984. It was chosen because of its close proximity to a significant number of offsite toxic-gas sources which had been considered in the design of its control room.

The working group spent two days in early January 1984 discussing this plant's control room design and, in doing so, identified a number of questions about how the various branches perform their reviews. These questions were added to the concerns previously identified in Phase 1.

Following the two-day meeting, a list of questions, raised in the course of the review of the plant by the working group, was drafted and submitted to the applicant for the NTOL plant. The questions covered such areas as smoke detection, design temperature and relative humidity of the control room, testing of the isolation dampers, impact of failure of both HVAC systems, handling of toxic-gas challenges, utilization of the remote shutdown panel, fire-fighting strategy, and habitability parameters important to reactor operation. These questions dealt with plant-specific design application and were to be discussed during the plant visit.

Subsequently, the plant was visited, systems were inspected, and the questions were discussed with the plant staff.

Phase 3

The initial intent of the control room habitability program plan was to review three to five NTOL plants and three to five F-70 plants. This review was to determine the consistency between the staff's review responsibilities as perceived by the working group and actual staff practice. However, it was soon determined that this task presented some formidable problems. Most of the plants, including the NTOLs, had control room designs which were not based on the present regulatory guidance. Many plants had been reviewed during a time when criteria and standards were being revised and documentation that described the basis for the staff's review was not available. In addition, many of the reviewers who had performed the evaluation were no longer available for consultation, having been reassigned within NRC or no longer with the Commission. Because of such limitations, it was concluded that it was only practical to address present staff review practices.

The second task associated with the NTOL plants and the F-70 plants was to survey the as-built control rooms to determine how NRC design requirements were implemented and to determine which component and system tests are performed.

Selection of Plants To Be Surveyed. Although the original program plan called for surveying three to five NTOL plants and three to five F-70 plants, it was determined that this approach, which was originally broad in nature, should be modified to include fewer plants and to be conducted in a more comprehensive manner. Therefore, three plants were selected. Two of the plants had operating reactors, the third was an NTOL applicant. All three plants were PWRs. The NSSS for one plant was designed by Combustion Engineering and the other two by Westinghouse. The control rooms were designed by Ebasco Services, Inc., Sargent and Lundy Engineers, and the utility owner of the reactor. The three plants selected were chosen in the hope that their designs for habitability would reflect the types of control rooms one would find in the industry for that particular vintage of plant, although there are no means to confirm this readily.

The NTOL plant was chosen because its design was representative of several NTOLs under review. The plant is scheduled to receive its operating license in 1985.

Scope of Work of Control Room Survey. Argonne National Laboratories (ANL) was the contractor selected to survey the as-built control rooms. The objective of ANL's work is to review the control room habitability design to determine:

(1) the relationship between as-built control room and the system design as described in the FSAR or updated FSAR, and

(2) what routine operational tests and preoperational tests are performed on various control room systems and/or components to ensure that design specifications and/or surveillance requirements technical specification requirements are met, or that the system and/or components are functional.

The results of the survey will be reported in December 1984, in a supplement to the working group report.

IV. Recommendations of the Working Group

The recommendations of the working group were developed throughout the course of the review. A number of the recommendations address concerns originally expressed by the Advisory Committee on Reactor Safeguards (ACRS). Others came out of the workshop, the working group's critique of the review process, and plant visits.

Recommendation 1

The NRR process for conducting the design review of all systems related to control room habitability should be revised. The following changes are proposed:

(1) centralization of description of control room systems into one section of the Safety Analysis Report (SAR) through a revision to Regulatory Guide (RG) 1.70 and the designation of a lead branch with the responsibility for assuring an integrated review,

(2) utilization of a systems approach in the review rather than the present method, which is dispersed among engineering or scientific disciplines that independently perform their review,

(3) utilization of independent verification techniques by branches responsible for assessing the adequacy of control room designs.

Discussion. The primary responsibility for the review of systems and planned operations directly related to control room habitability is presently divided among seven branches within the Office of Nuclear Reactor Regulation. Thirteen other branches are frequently to occasionally involved in the review of specific areas whenever such a need is identified by a branch having primary responsibility. It is obvious from Figure 1 that control room reviews are diffuse. Such diffusion can lead to inadequate reviews because of omissions, oversights, and imposition of conflicting requirements.

During the working group's review of staff practices, criteria, and assigned responsibilities related to control room habitability, the members were alert to evidence of omission or inadequate review of systems, components or planned operations which could be attributed to the diffuse nature of the review. Considering the large number of branches involved in these reviews, surprisingly few examples of omission or breakdown, resulting from oversight, were discovered. However, the working group did not survey operating reactors to determine whether significant review flaws have been committed which have resulted in inadequate control room designs. Such a survey would be useful. Nevertheless, the working group believes that the present way in which these evaluations are organized and conducted unnecessarily increases the likelihood of such review flaws.

The fragmentation of the NRC review is evident in the safety analysis reports (SARs) which are submitted. NUREG-0800, "Standard Review Plan for the Review of Safety Analysis Reports for Nuclear Power Plants," was prepared for the guidance of staff reviewers in performing safety reviews of applications to construct or operate nuclear power plants. The principal purpose of the Standard Review Plan (SRP) is to assure the quality and uniformity of staff reviews and to present a well-defined base from which to evaluate proposed changes in the scope and requirements of reviews. It is also a purpose of the SRP to make information about regulatory matters widely available and to improve communication with interested members of the public and the nuclear power industry and to provide them an understanding of the staff review process.

The safety review is primarily based on the information provided by an applicant in an SAR. Section 50.34 of 10 CFR 50 of the Commission's regulations specifies, in general terms, the information to be supplied in an SAR. The specific information required by the staff for an evaluation of an application is identified in RG 1.70, "Standard Format and Content of Safety Analysis Reports for Nuclear Power Plants - LWR Edition." The SRP sections are keyed to the standard format, and are numbered according to the numbering scheme in the standard format. Putting together a detailed description of a control room system typically requires utilization of 13 volumes of an SAR. The working group believes that a separate section in RG 1.70 devoted to control room habitability, where descriptions of control room systems and their interfaces are centralized, would help assure that all significant material related to this subject is considered during the staff review. Such an organizational change would also allow the reader to focus on the subject in one section rather than continue the current approach in which the descriptions are divided among a minimum of seven sections.

The lead responsibility for these reviews should be assigned to one branch, either the Accident Evaluation Branch, the Meteorology and Effluent Treatment Branch, or the Auxiliary Systems Branch. It is important to recognize that this assignment will require the reviewers in the designated branch to develop a clear understanding of the control room habitability review and the interdependence of the various branch reviews involved. Additional personnel and fiscal resources will be required for that branch.

Merely assigning one branch overall responsibility for coordinating control room habitability reviews does not solve the problem of fragmentation. It makes the reviewers in one branch cognizant of the total review of control rooms but allows reviewers in the other branches to continue to perform their reviews in their usual fashion, i.e., focusing only on their specific area of responsibility. The working group found ample evidence that reviewers need a broader understanding of the systems being evaluated in order to avoid (1) imposing incompatible or conflicting requirements, or (2) allowing design modifications without knowledge of the impact upon other review areas.

The use of a lead branch will facilitate a more systems-oriented approach to the control room habitability review. The lead branch would coordinate the review conducted by the assigned reviewers from each of the branches having a primary responsibility for the subject review. Periodic meetings of this group of reviewers would allow any problems identified with the systems to be aired, anything unique about the design of the systems to be described, etc. This collegial approach initiates the systems interaction approach more effectively than the present method and expands the breadth of knowledge of the other reviewers. This approach was utilized by the working group for this study and an obvious broadening of members' knowledge in the various habitability areas was evident.

The ACRS expressed concern about the need for a more critical review and independent assessment by NRC staff members. The working group concludes that the ACRS concerns appear to be well founded for control room habitability. The working group noted a wide variation among branches in the extent to which reviewers attempt to independently verify design adequacy. These reviews may include repeating an applicant's calculations, comparing system designs with previously accepted designs, or accepting the applicant's commitment to use appropriate guides, standards, or codes. The working group recommends a uniform level of review that includes an independent verification of design adequacy.

Recommendation 2

The working group recommends that the staff increase its efforts in obtaining industry feedback on control room air cleaning systems through increased participation in professional societies such as ASME and ASTM.

Discussion. Recommendation 6 focuses on increasing the interaction between regional inspection and headquarters staff for the purpose of improving the quality of reviews and informing headquarters reviewers of problems identified by regional inspectors during construction and preoperational inspections. Another way to increase the quality of reviews and to become more familar with problems of as-built systems is to obtain industry feedback. One of the best ways is through participation in various professional societies such as ASME and ASTM.

NRC has historically co-sponsored, with DOE, the biannual Air Cleaning Conference. In the past arrangements have been financed by DOE. We understand that

DOE does not plan to finance this program beyond FY 1984. This conference has been of great value to both government and industry for more than 30 years. The NRC should consider sponsoring future conferences.

Recommendation 3

Control room habitability environmental criteria during the course of an accident should be equivalent to those during normal operation. These environmental criteria, as shown in Table 2 should include temperature, relative humidity, ventilation, illumination, visibility, and noise.

Discussion. Human performance is adversely affected by high levels of stress. Stress can be induced by many factors within the physical, physiological, and psychological environment of the control room operator and its severity is cumulative across these factors. Some amount of psychological stress is induced by the presence of an accident condition. The objective of the above recommendation is to minimize the overall stress load potential during the course of an accident by ensuring that the physical and physiological environment of the control room does not add to the operator's overall stress and thus increase the probability of human error. It will also ensure that, during a period of high stress, i.e., an accident, the physical environment experienced by the operator will be unchanged, familiar, and near optimum for performance and safe operation.

Recommendation 4

Limiting environmental conditions for operation in the control room should be established and should consider human performance as well as equipment operation as the basis for selecting of appropriate limits.

Discussion. The current technical specification limit for temperature in the control room is based on equipment qualification temperatures. If the human operator is considered to be an integral subsystem required for safe plant operation, then the limiting conditions for operation in the control room should be based on the more limiting performer whether it be equipment or human. Some of the environmental factors which should be included for consideration are temperature, noise, and illumination.

Effective temperature (ET) takes into account dry bulb temperature, relative humidity, and air velocity. Air velocity has a minimal effect in the low ranges expected in a control room (under 100 feet/minute) and can be safely ignored as a contributor to ET differences. An effective temperature of 85°F has been determined to be the maximum limit for reliable human performance. The 85°F (ET) ranges from 85°F dry bulb temperature at 100% relative humidity to 104°F dry bulb temperature at 20% relative humidity. The working group recommends that a maximum temperature limitation of 85°F (ET) be established for the control room as the limiting condition for operation. If relative humidity is not measured or monitored in a control room, a dry bulb temperature of 85°F should be used as the limiting condition. This limit should not be exceeded for longer than one hour.

The limiting condition for illumination incident upon the task area should be that which is considered to be minimum for safe manual operation under conditions which have resulted in some degree of normal illumination loss (e.g., loss of AC power). Ten foot-candles, as recommended by the Illuminating Engineering Society of North America and as presently adopted by the NRC staff, is recommended by the working group. This level of illumination is acceptable for periods up to one hour.

Table 2 Proposed Control Room Habitability Criteria

Parameter	Proposed Criteria	Source
A. TEMPERATURE AND RELATIVE HUMIDITY		
Floor Level to Head Level ΔT (F°)	10	NUREG-0700, 6.1.5.1
T (°F)	$73 \leq T \leq 78$	NUREG-0700,
RH (%)	$20 \leq RH \leq 60$	Exhibit 6.1-21
Maximum Allowable Temperature for 1 hour (°F)	85(*)	MIL-STD-1472 C; MIL-HDBK-759 A
B. VENTILATION		
I. Makeup Air (Outside)		
Per Occupant (cfm)	15	NUREG-0700, 6.1.5.2
II. Air Velocity (fpm)	<45	NUREG-0700, 6.1.5.2
C. RADIOLOGICAL DOSE (REM)		
I. Direct Exposure		
a. Normal Operation	(Per quarter)	
Whole Body(**)	1.25	10 CFR 20.101
Forearms, Hands	18.75	10 CFR 20.101
Skin	7.5	10 CFR 20.101
b. Accident		
Whole body (γ)	5	GDC 19 of Appendix A to 10 CFR Part 50
Skin (β)	75 (with protective clothing); 30 (without protective clothing)	GDC 19 of Appendix A to 10 CFR Part 50
II. Inhalation		
a. Normal Operation	Table I, Column 1, 10 CFR 20.103 Appendix B to 10 CFR Part 20	10 CFR 20.103
b. Accident (rem thyroid)	30	Application of GDC 19

See footnotes at end of table.

Table 2 (Continued)

Parameter	Proposed Criteria	Source
D. COMMUNICATIONS	Voice	NUREG-0700, pg 6.1.4
E. VISIBILITY	Unlimited plus purge fan capability of 10 volume changes per hour.(*)	
F. *ILLUMINATION*		
Panels, Auxiliary(†) Panels, Scale Indicator Reading, Printed or Typed Reading Maintenance and Wiring Areas (foot-candles)	$20 \leq I \leq 50$	NUREG-0700, Exhibit 6.1.22
Seated Operator Stations(†) Handwritten Reading Writing and Recording (foot-candles)	$50 \leq I \leq 100$	NUREG-0700, Exhibit 6.1.22
Reflectance		NUREG-0700, Exhibit 6.1.24
Ceiling	$60\% \leq R \leq 95\%$	
Upper Wall	$40\% \leq R \leq 60\%$	
Lower Wall	$15\% \leq R \leq 20\%$	
Instruments/Displays	$80\% \leq R \leq 100\%$	
Cabinet/Consoles	$20\% \leq R \leq 40\%$	
Floor	$15\% \leq R \leq 30\%$	
Furniture	$25\% \leq R \leq 45\%$	
G. NOISE		
Background [dB(A)]	≤ 65	NUREG-0700, Curve 6.1-26

See footnotes at end of table.

Table 2 (Continued)

Parameter	Proposed Criteria	Source
H. CHEMICAL CONTAMINANTS		RG 1.78, Table C-1
	(2 minute)(††)	
CO_2	1.0%	
CO	0.1%	
O_2	-	
Cl_2	15	
Acetaldehyde	200	
Acetone	2000	
Acrylonitrile	40	
Anhydrous NH_3	100	
Aniline	10	
Benzene	50	
Butadiene	0.1%	
Butenes	Asphyxiant	
Ethyl chloride	10,000	
Ethyl ether	800	
Ethylene dichloride	100	
Ethylene oxide	200	
Fluoride	2	
Formaldehyde	10	
He	Asphyxiant	
Hydrogen cyanide	20	
H_2S	500	
Methanol	400	
N_2	Asphyxiant	
Na_2O	2(#)	
SO_2	5	
H_2SO_4	2(#)	
Vinyl chloride	1000	
Xylene	400	

*Criteria are not presently implemented by NRC reviews.

**Limited to 3 rem maximum per quarter, provided 3 rem whole-body plus past accumulated whole-body dose not exceed 5 (N-18) rem where N = age of individual.

†Illumination levels are allowed to decrease to 10 foot-candles for event initiating a loss of illumination such as a loss of AC power event (5 foot-candles for an evacuation path).

††Parts of vapor or gas per 10^6 parts air by volume at 25°C and 760 mm Hg.

#Milligrams of particulate per m^3 of air at 25°C and 760 mm Hg.

Excessive noise not only induces stress but impairs verbal communications, critical to safe control room operations. The noise limits recommended by the American Conference of Government and Industrial Hygienists are 100 dB(A) for no longer than one hour and 85 dB(A) for no longer than eight hours.

Table 2 contains the habitability criteria proposed by the working group for inclusion into the plant technical specifications.

In developing and proposing limiting conditions for operationin the technical specifications, on the basis of human performance limitations, careful consideration must be given to the action statement if these limiting conditions are not met. A question that must be answered is whether the preferable action is to maintain the reactor operating or is it to begin the shutdown process with the control room operator functioning in a degraded control room environment.

Recommendation 5

The working group recommends that the following nine generic studies related to control room habitability be conducted:

(1) Evaluation of the adequacy of chlorine and other toxic-gas detectors presently in use at nuclear power plants.

Discussion. On the basis of a review of licensing event reports (LERs) conducted in 1982, the reliability of chlorine gas monitors was placed in doubt. This poor performance resulted in the release of IE Information Notice No. 83-62. These monitors continue to perform poorly. For this reason, the working group recommends that the reliability of the chlorine and other toxic-gas detectors be enhanced through identification of improvements in those detectors that are "failure prone" or replacement with more reliable monitors that are currently available.

(2) Evaluation of the potential for loss of both trains of the ventilation system and its effect on habitability and equipment operability. Consideration should be given to the need for providing guidance to control room operators on appropriate actions in such an event.

Discussion. The ACRS has expressed concern about temperature rise in the event of loss of all air cooling in the control room. The survey of LERs disclosed two events in which cooling capability of both trains of the ventilation system was lost. In one event, cooling was restored in minutes. For the other, the system was down for 30 minutes, during which time the control room temperature rose to 94°F. The LER included no information on whether or not the ventilation system remained in service bringing in outside air, whether temporary ventilation methods were used, or whether consideration was given to shutting the plant down in the event the cooling system could not be returned to service within a relatively short period of time. The working group recommended that this event be studied in more detail.

Input from architect engineers indicated that, if both ventilation systems were lost, the control room would heat up rapidly with estimates in the range of 1-3F° per minute for the first hour or so. At these heatup rates the control room would rapidly become uninhabitable.

The proposed study should also consider appropriate actions to be required by technical specifications in response to loss of one or more trains of the ventilation system and possible guidance which could be given to control room operators to decrease heat loads in the control room. By shedding heat loads, by

opening doors, and by taking other temporary actions, the operators may be able to extend their occupancy time long enough so that the ventilation system can be restored before the control room becomes uninhabitable.

(3) Determination if sufficient new information is available to justify revision of the Murphy-Campe methodology.

Discussion. This methodology is used to estimate atmospheric dispersion in the vicinity of structures through consideration of the locations of effluent release points and air intakes and characteristic building dimensions and meteorological conditions. A study to evaluate the feasibility of revising the Murphy-Campe methodology is proposed.

(4) Assessment of the optimum location or locations for toxic-gas monitors designated for the protection of the control room personnel.

Discussion. Toxic-gas monitors are frequently mounted on the exterior of the building adjacent to the normal control room air intake. This is not necessarily the best location for such a monitor, and could be of very little value whenever the emergency air intake is in use. There is a great variation in the design and proposed manner of operation of control room ventilation systems. For this reason, a special study is warranted to determine the optimum location for monitors.

(5) Determination of a minimum purge rate criterion for smoke removal from the control rooms.

Discussion. Although SRP Section 9.5.1 calls for the capability to purge smoke from the control room, no design criterion has been developed. Purge rates varying from 4,000 to 45,000 cfm have been found in the systems reviewed during this study. It is clear, for example, that a purge rate of only 4,000 cfm would be of little use in clearing smoke from a 200,000 ft^3 control room envelope; therefore, some criterion should be established. The working group has assumed a minimum of 10 volume changes per hour in Table 2, but a determination should be made as to whether this value is sufficient to purge the control room.

(6) Development of a method for conducting leakage tests on ventilation system isolation dampers.

Discussion. The working group discovered that there is no straightforward method of measuring leakage through the large dampers in the normal ventilation system used to isolate the control room. Although a leakage rate may be inferred from measurements taken during control room pressurization tests, these measurements are of limited value since systems, when operated in a recirculation mode, subject the dampers to a much higher pressure differential than they experience during the isolation test. Thus, the leakage rate could be much higher under these conditions.

In view of the number of problems with dampers, as reported in the LERs, the working group believes this matter warrants additional attention.

(7) Determination of the vulnerability of control rooms to steam intrusion.

Discussion. The ACRS raised the question of steam intrusion. The working group concluded that it had insufficient information on control room designs and the location of high pressure steam lines to assess the potential for steam intrusion.

Although no problems were identified for the systems that members of the working group have recently reviewed, designs vary markedly and the possiblity cannot be ruled out. Hence, further study of the matter is recommended.

(8) Assessment of whether the benefits of carpeting in control rooms outweigh its potential hazard which can be to emit toxic gases in the event of a fire.

Discussion. Carpeting is used in control rooms to help suppress noise and minimize fatigue. Many synthetic materials used in the padding and carpeting are known to generate large quantities of toxic gases when exposed to fire.

The working group found conflicting policies existed within two branches implementing control room habitability requirements. One branch's policy was that carpeting should not be installed in the control room; the other branch's position, however, was that carpeting should be installed.

The toxicity, resulting from fire, of many materials utilized in the control room has been studied. Such toxicity insofar as carpeting and its associated padding has not been studied.

Thus, a determination should be made as to whether carpet constitutes a hazard in existing control rooms or whether its benefit for improving the operator's environment exceeds this hazard.

(9) Effectiveness of fire dampers in limiting the spread of smoke or toxic gases in the event of a fire within the control room envelope.

Discussion. The ACRS expressed concern about the effectiveness of fire dampers in limiting the spread of smoke and toxic gases. This concern should be limited to a fire within the control room envelope. Fire dampers in the boundary penetrations should always be backed up by one or more isolation dampers.

The working group was unable to assess the need for better smoke control generated by fires within the control room envelope. A thorough study of this problem will involve defining temperatures, pressures, smoke, and toxic gases, conducting a realistic testing program for dampers typical of those presently used in control rooms.

Recommendation 6

There should be more interaction between headquarters and regional personnel during the OL reviews, especially during preoperational testing. Headquarters staff should be encouraged to participate in the preoperational inspection of systems related to control room habitability.

Discussion. The opportunity to inspect plant systems should substantially increase the competency of the headquarters staff, increase the quality of the reviews, and probably minimize conflicts between applicants and staff An integrated review process between headquarters and the regional offices is more likely to identify differences or inconsistencies between the design reviewed and the as-built system. Also, it will encourage more dialogue between regional personnel and headquarters staff, thereby increasing the likelihood that problems identified in the field will be brought to the attention of the proper reviewer.

Recommendation 7

The technical specifications involving control room systems should be expanded to include:

(1) habitability criteria such as temperature, illumination, noise, etc.;
(2) acceptable leak rates for isolation dampers;
(3) maximum flow rate for pressurization of the control room;
(4) HVAC system (safety grade); and
(5) corrections to existing technical specifications.

Discussion. The present technical specifications on control rooms are very limited. They only address toxic-gas monitors and engineered safety feature (ESF) filtration units. Habitability concerns for humans are not addressed, even though they may be more limiting than the equipment. Inclusion of the above recommended parameters in the technical specifications will provide assurance that the control rooms will be habitable during off-normal conditions. The technical specifications should assure that bottled air supplies are periodically surveyed to ensure that air is available and usable and that offsite replenishment capability is available; that appropriate limiting conditions for operation be specified for Modes 5 and 6 with both control room ESF filter systems inoperable; that Generic Letter 83-13 be rescinded to correct errors in the technical specifications covering bypass leakage of filtration units, in-place testing of HEPA filters and charcoal adsorbers, and laboratory tests of charcoal; that surveillance requirements include an acceptable leakage rate test for isolation dampers at design pressure; and that the surveillance requirements include a pressurization test stipulating maximum ventilation flow rate. Technical specifications should also be added covering safety-grade HVAC systems in the control room.

Recommendation 8

Regulatory Guides, standard review plans, and other documents such as NUREGs associated with control room habitability should be revised to bring them up to date with the latest information and review procedures, as well as with the recommendations of this study.

Discussion. RG 1.52, "Design, Testing and Maintenance Criteria for Post-accident Engineered-Safety-Feature Atmospheric Cleanup System Air Filtration and Adsorption Units of Light-Water-Cooled Nuclear Power Plants," has been under revision for about two years. A number of substantial changes are being proposed. A large number of additional changes were recommended at the Control Room Habitability Workshop in November 1983. The revision has not been finalized primarily because of a shortage of personnel resources within NRR. It is recommended that RES hire a contractor to complete this task.

Clarification of RG 1.78, "Assumptions for Evaluating the Habitability of a Nuclear Power Plant Control Room During a Postulated Hazardous Chemical Release," is needed as to the manner in which the staff determines allowable leakage rate for isolation dampers. In addition, inconsistencies between this regulatory guide and RG 1.94 should be eliminated.

The present specifications and acceptance criteria for the control room pressurization test are inadequate. New ones are needed.

SRP Sections 6.5.1, 9.4.1, and 18.0 should be revised. GDC 60 is not appropriate for SRP Section 9.4.1 and the definition of control room envelope in SRP Section 9.4.1 is inconsistent with the definition in SRP Section 6.4. Definitive subsections to SRP Section 18.0 have not been written, but should be. SRP Section 6.5.1 should be more explicit.

V. Conclusion

As directed by the EDO, the Control Room Habitability Working Group has reviewed the subject of control room habitability in such areas as NRR review process, transformation of control room habitability designs to as-built systems, and determination of testing protocol. In addition, the working group has investigated the ACRS concerns and recommendations. The working group has determined in its review that many of the ACRS concerns and recommendations are well founded, and the group has recommended actions to be taken to address these as well as other concerns which were raised independent of the ACRS.

The working group has not completed its assignment since the survey of as-built control rooms and their testing protocol is incomplete. The results of this survey will be supplied to the EDO in a supplement to the initial report. Nevertheless, the review of control room habitability has revealed significant areas where the approach presently utilized in reviews should be altered. These include:

(1) designation of the maintenance of human performance in the control room as important as the maintenance of equipment which serves the control room,

(2) centralization of the review of control room habitability so that interaction between branches becomes commonplace through integrated reviews and the control room is reviewed as a system and not in a diffuse manner,

(3) assurance that the branches responsible for control room habitability reviews independently verify the adequacy of control room designs,

(4) modification to existing technical specifications to increase areas covered and to correct present errors in the specifications,

(5) emphasis on increased interactions between headquarters reviewers and regional inspectors, and,

(6) increased staff participation in professional societies to provide input on regulatory policy and to obtain industry feedback.

DISCUSSION

SGALAMBRO: Could you please comment on the technical feasibility of implementing the recommendation to protect personnel against chemical releases? What is the policy of NRC about toxic and chemical releases? And what is the technical design for the protection systems? For example, should there be another filtration train for chemical release or improvement of operators' respiratory equipment? Have you any experience in power plants of such situations?

HAYES: The present NRC criteria require protection against toxic gases. The control room working group did not recommend any new requirements to handle toxic gas challenges that are different than those contained in Regulatory Guides 1.78 and 1.95. There are two different types of designs that can be considered. One is the isolation of the control room prior to the entrance of toxic gases, the other, the treatment of the toxic gases once they have entered the control room. The policy of most plants in the U.S. is to isolate. If you look at the Regulatory Guide, there is also an opportunity to clean up the toxic gas challenges with deep bed materials such as charcoal. But for the most part, the philosophy is that it is better to prevent the entrance of the toxic gas into the control room than to attempt to clean it up once it enters.

ORNBERG: What is the NRC's schedule for implementing the proposed recommendations and will the public have a further opportunity to comment? When will NRC officially rescind NRC Letter 83-13?

HAYES: Starting in September 1984 the NRC will put together a program for implementing the working group's recommendations. The implementation will be subject to CRGR approval within the NRC. The public will have an opportunity to comment on these recommendations. Before they can be implemented, there is a possibility of a year or two years. That is, provided they get acceptance by CRGR. In addition to what was discussed here, there is also a recommendation that some generic studies be performed. The input from these is not available yet. No date can be given when the NRC will rescind Generic Letter 83-13.

VOGAN: In terms of implementation of the recommendations you talked about, are you looking for a full backfit of existing control rooms for such things as additional isolation fire dampers, or is the regulation strictly directed towards new, future plants?

HAYES: The recommendations are not restricted to future plants. Before the NRC can require backfitting, the NRC staff must submit their recommendations to the NRC CRGR for approval. CRGR evaluates the safety implications of the recommendations and the costs associated with their implementation. Therefore, safety significance of these implementations must be demonstrated prior to the requirements for backfitting control rooms. The work with respect to fire dampers in leak rate capability will be dependent upon the results of a study which is, I think, done. You will see that an evaluation must be

done on existing control rooms to meet this criterion. Probably something similar to 3D34.

VOGAN: As you know from some of your reviews, some of the backfitting will be quite costly, and I haven't seen a report of the cost beneficiality yet.

HAYES: That is correct.

VENTILATION OF NUCLEAR ROOMS AND OPERATORS' PROTECTION

C. Vavasseur
Commissariat à l'Energie Atomique
Institut de Protection et de Sûreté Nucléaire, Département de Protection Technique
Service de Protection des Installations Nucléaires
91191 GIF SUR YVETTE CEDEX, France

I. INTRODUCTION

Ventilation systems are designed to guarantee air replacement in rooms so as to evacuate gases, odours and aerosols liable to be produced therein. This air is conditioned, filtered, heated, and the relative humidity checked. At the outlet, a filtration system adapted to the type of effluent prevents the external dispersion of toxic sustances.

Let us consider what happens in the room. Ventilation is defined by the air change time. A comfort rule recommends reducing the velocities reaching the person present in less than 0.2 m/sec. This reduction is achieved by adjusting the natural property of the jets, induction, by means of diffusers placed at the vents.

II. INDUCTION, HOMOGENIZATION AND TRANSFERS

The jets leaving the blower vents have specific properties that make them responsible for air movements in the rooms. These properties are the following :

- the velocity gradient between blown air and ambient air draws the latter, causing an increase in the flow rate procured by the jet : this is induction.
- the conservation of momentum distributed over the blown air and induced air gives the blowers a far greater range than the extractors. Induction normally ranges from 10 to 20.

$$I = \frac{Q(x)}{Q_o}$$

I : induction

Q_o : blow air flowrate

Q_x : flowrate of jet at distance x

Each blower vent creates a convective cell causing homogenization. Air change is defined by a characteristic time :

$$\tau_r = \frac{V}{Q_o}$$

V : volume of the room

Q_o : ventilation flowrate

Similarly, a characteristic homogenization time can be defined within a convective cell :

$$\tau_h = \frac{V_c}{IQ_o}$$

V_c : volume of convective cell

Q_o : blown flowrate at inlet opening

The velocities involved in this cell concerning pollutant emissions are the transfer velocities and homogenization takes place by multiple passage in the jet. Obstacles and small-scale turbulances also contribute to the diffusion of the substances emitted.

If two or more inlet exist, the associated convective cells interchange part of their mass. A homogenization rate is established between the cells, that can be characterized by a coupling coefficient :

$$\alpha = \frac{Q_H}{IQ_o}$$

Q_H : exchange rate between cells

and a characteristic homogenization time extended to the entire room :

$$\tau_H = \frac{V}{Q_H}$$

V : volume of room

Air change characteristic time and induction can be adjusted to optimize general ventilation systems from the protection standpoint. This action indirectly affects the transfer velocities and homogenization times. The transfer velocity and its direction conditions the number and distribution of the detection and alarm devices.

Homogenization reduces the amplitude of individual contaminations and simplifies the measurement of ambiant contamination.

III. PRACTICAL SITUATION

Unfortunately, the ventilation concept is never optimized for these objectives, and we shall show that it would be difficult to do this. The rooms are not empty and the furniture significantly alters the distribution. A strategy to coordinate the inlet opening and furniture distribution does not exist. Paradoxically, it is the distribution of the outlet opening that is analyzed, implicitly and in advance, allowing the existence of dead zones where the effects of induction are no longer felt, outlet opening at the lower part for heavy substances, and at the upper part for light products. The result yields a poor containment, and any atmospheric contamination occurs throughout, as well as slow homogenization that lengthens the interval between product emission and the alarm. In thin context, the operators must reduce the probability of individual and collective contamination, while minimizing the investment costs in measuring, detection and alarm devices. They must also shorten the decontamination times.

IV. FREQUENT CHARACTERISTICS OF CONTAMINATION ACCIDENTS

We shall consider the example of workshops equipped with many glove boxes. In this case, the potential sources are known and the emission points localized, including gloves and transfer locks.

The following is generally observed :

1) Predominance of surfade contaminations and settling below the emission points.
2) Atmospheric contaminations display wide contrasts near the emission points.
3) High sensitivity to local emission conditions in the division between what settles and what is diffused into the atmosphere.
4) Very narrowly contrasted atmospheric ocntamination throughout the room, apart from the immediate vicinity of the source.

This situation conforms closely to the one described in the previous chapter. Low velocities favor settling and preserve contrasted concentration zones in the space attended by the operators. The distribution of a blast is random, it exposes the personnel to major contamination risks, and it maybe undetected by the detection instrument. Outside the emission zone, the product is picked up by the convective movements and distributed throughout the room with low constrasts.

V. PROPOSED SOLUTION

The optimization of protection demands thorough control of tranfers and of homogenization. This function can only rarely be required of a general ventilation system. Settling is often a lesser evil. The question is how to avoid entraining settled materials while rapidly homogenizing the diffused air, if not by locally adjusting the velocities and the homogenization within limited volumes. The general ventilation system could then be devoted exclusively to the confort and replacement function with minimum investment outlay.

Systems of "Blow on exhaust" type can meet these objectives with low flowrates (10 to 20 m^3/h). In fact, they offer four major advantages :

- Directivity simplifying the installation of detection instruments.
- Homogenization reducing the risks of major contamination.
- Entrainment by induction in the jet direction.
- Local extraction which, even if imperfect, restricts the diffusion of contamination throughout the room.

This concept means treating the work zone directly as a dead zone, which is done implicitly, to avoid entraining settled materials. Since turbulences due to the general ventilation system become the disturbing factors in this case, the system must be reduced to the strict minimum. The investment outlay for a Pu laboratory is around 100 dollars for 1 m^3/h. A reduction form 5,000 to 2000 m^3/h means savings of 300,000 dollars, while preserving 3 to 4 replacements per hour.

From this point of view, local purification units not using the general ventilation system may also offer applications in case of incident, by preventing the contamination or clogging of the general ventilation filters, and would also help to cut airconditioning investments.

Finally, homogenization on the scale of the room is necessary for the fraction escaping local settling, which decreases the collective contamination. Hence it would be interesting to favor couplings between convective cells induced by the blowers, and this would accelerate the homogenization time without increasing the air velocities and hence the entrainments of settled materials.

VI. CONCLUSION

We should adopt a more directive attitude in optimizing protection, discard random effects, and try to control transfers and homogenization. This project, which should be conducted in close cooperation with the operators and the personnel, could culminate in relations optimizing as well as installation cost.

PERFORMANCE EVALUATION OF CONTROL ROOM HVAC AND AIR CLEANING SYSTEMS UNDER ACCIDENT CONDITIONS

F. Almerico*
Nuclear Engineering Program
University of Illinois
Urbana, Illinois

A. J. Machiels**
Electric Power Research Institute
Palo Alto, California

S.C. Ornberg and G. P. Lahti
Sargent & Lundy Engineers
Chicago, Illinois

Abstract

In light water reactors, control rooms and technical support centers must be designed to provide habitable environments in accordance with the requirements specified in General Design Criterion 19 of Appendix A, 10 CFR Part 50. Therefore, the effectiveness of HVAC and air cleaning system designs with respect to plant operator protection has to be evaluated by the system designer. Guidance for performing the analysis has been previously given in ANSI/ASME N509-1980 as well as in presentations at past Air Cleaning Conferences. This paper extends the previous work and presents the methodology used in a generic, interactive computer program that performs Main Control Room and Technical Support Center (TSC) habitability analyses for LWR nuclear power plants. For given accident concentrations of radionuclides or hazardous gases in the outdoor air intakes and plant spaces surrounding the Main Control Room (or TSC), the program models the performance of the HVAC and air cleaning system designs, and determines control room (or TSC) contaminant concentrations and plant operator protection factors. Calculated or actual duct leakage, air cleaning efficiency, and airborne contamination are taken into account. Flexibility of the model allows for the representation of most control rooms (or TSC) and associated HVAC and air cleaning system conceptual designs that have been used by the U.S. architect/engineers.

The program replaces tedious calculations to determine the effects of HVAC ductwork and equipment leakage and permits 1) parametric analyses of various HVAC system design options early in the conceptual phase of a project, and 2) analysis of the effects of leakage test results on contaminant room concentrations, and therefore operator doses.

I. Introduction

For nuclear power plants, control room habitability analyses can be broken down into a number of separate analyses. These include the following:

(1) initial accident source term;
(2) release to the environment, including performance of post accident fission product removal systems such as containment sprays and filtration systems;

*Present work affiliation: SADELMI-COGEPI, Milan, Italy.
**Also, adjunct associate professor of Nuclear Engineering, University of Illinois, Urbana, Illinois.

(3) atmospheric transport to the control room air intakes;
(4) performance of the control room HVAC system;
(5) conversion of control room airborne concentrations to radiological doses, and comparison with applicable regulatory limits.

The present research work has emphasized items (1), (2), and (4). However, only item (4), the performance of the control room HVAC system, is discussed in this paper. A detailed account of items (1) and (2) can be found in Refs. (1) and (2).

Control room or Technical Support Center (TSC) habitability systems are designed to ensure that operating personnel can remain inside the spaces comprised in the control room envelope with safety and comfort during all normal and abnormal station conditions, in compliance with 10 CFR 50, Appendix A, General Design Criterion 19.[3] In particular, much attention has been given by the U.S. Nuclear Regulatory Commission and architect/engineers to the control room Heating, Ventilation and Air Conditioning (HVAC) systems in an attempt to standardize their design and construction, while meeting all regulatory safety standards and requirements.[4-7]

At the present time, results of analyses of control room habitability and performance evaluations of control room HVAC and air cleaning systems are included in Safety Analysis Reports (SARs). Specifically, Sect. 6.4 deals with all the habitability systems and considers their related safety and protection features under a broad spectrum of possible events (fires, chemical accidents, nuclear accidents, etc...); Sect. 9.4 considers all the HVAC systems and describes their operation, and functional and power generation requirements; Chap. 15 deals with the evaluation of consequences of postulated nuclear accidents, and shows the calculational models adopted to estimate the radiation doses to population and personnel.

The calculational models shown in SARs for the evaluation of control room HVAC and air cleaning system performance for the most part are not easily adaptable to conceptual design variations; some models[5] have a greater potential for representing a number of conceptual designs. However, none of the published models include features that allow an evaluation of the effect of components layout and leakage characteristics on the radiation doses to control room personnel. These factors have been shown[7] to have an important bearing on control room Iodine Protection Factors (IPFs) and need to be considered in order to more realistically describe the behavior of a control room under accident conditions, improve system design criteria and methodology, and better specify and achieve a standardization of the quality requirements of manufacturing.

This paper is part of the results of a research effort specifically devoted to developing a methodology for the systematic analysis of nuclear power plants' control room or technical support center HVAC systems. The approach to air cleaning system duct design, described in the work presented by W. H. Miller, S. C. Ornberg, and K. L. Rooney[7] at the 16th DOE Nuclear Air Cleaning Conference, has been of special importance to the development of the model.

II. Mathematical Modeling of Control Room HVAC and Air Cleaning Systems

Several mathematical models have been investigated during the present study in an attempt to obtain a general, flexible, and computationally-fast computer code that would allow the designer to perform a detailed leakage analysis and calculate personnel protection factors. The model presented in the following sections is based on a network representation of the system, and leads to a matrix

formulation. This approach allows the inclusion of all aspects of design that are of interest from the point of view of control room protection performance. The model relies upon a system of consistent equations, and presents much flexibility with regard to variations of system parameters and conceptual design.

Representation of Ductwork Network

In order to evaluate the effect of ductwork leakages on the protection performance of a control room ventilation system design, it is necessary to evaluate (i) the flow rates in the ductwork that result from leakages in all duct segments, and (ii) the influence of the airborne radioactivity at the outside air intakes on the control room concentration of radioactive material.

The flow rates corrected for ductwork leakages and control room contaminant concentrations can be evaluated with the methodology illustrated hereafter. To facilitate the presentation of the method, Figs. 1 and 2 are referred to. Figure 1 shows a diagramatic representation of a typical nuclear power plant control room ventilation system. The ductwork system can be visualized as a network consisting of nodes and segments; each node corresponds to the junction of two or more segments, or to the ends of a segment. Nodal points are located where changes in network layout, or duct leakage characteristics, or both occur. The system schematized in Fig. 1 is graphically represented in Fig. 2.

The total number of nodes, N, is linked to the number of segments, S, by the following relationship:

$$N = S + 1 - N_R, \tag{1}$$

where N_R denotes the number of "rings" in the network; a "ring" is defined as a continuous connection of segments originating from and eventually terminating at the same nodal point.

Since the number of terminal nodes, N_T, is related to the number of internal nodes, N_I, by:

$$N_T = N - N_I, \tag{2}$$

substituting Eq. (1) into Eq. (2) yields:

$$N_T = S + 1 - N_R - N_I. \tag{3}$$

Conservation Equations

Conservation equations can be written for the air flow and for the airborne radioactive species; in the latter case, radioactive decay is neglected.

Air Flow

A conservation equation for the air flow can be written for each individual duct segment in accordance with the convention shown in Fig. 3:

$$F_{in,i} - F_{out,i} = L_i, \tag{4}$$

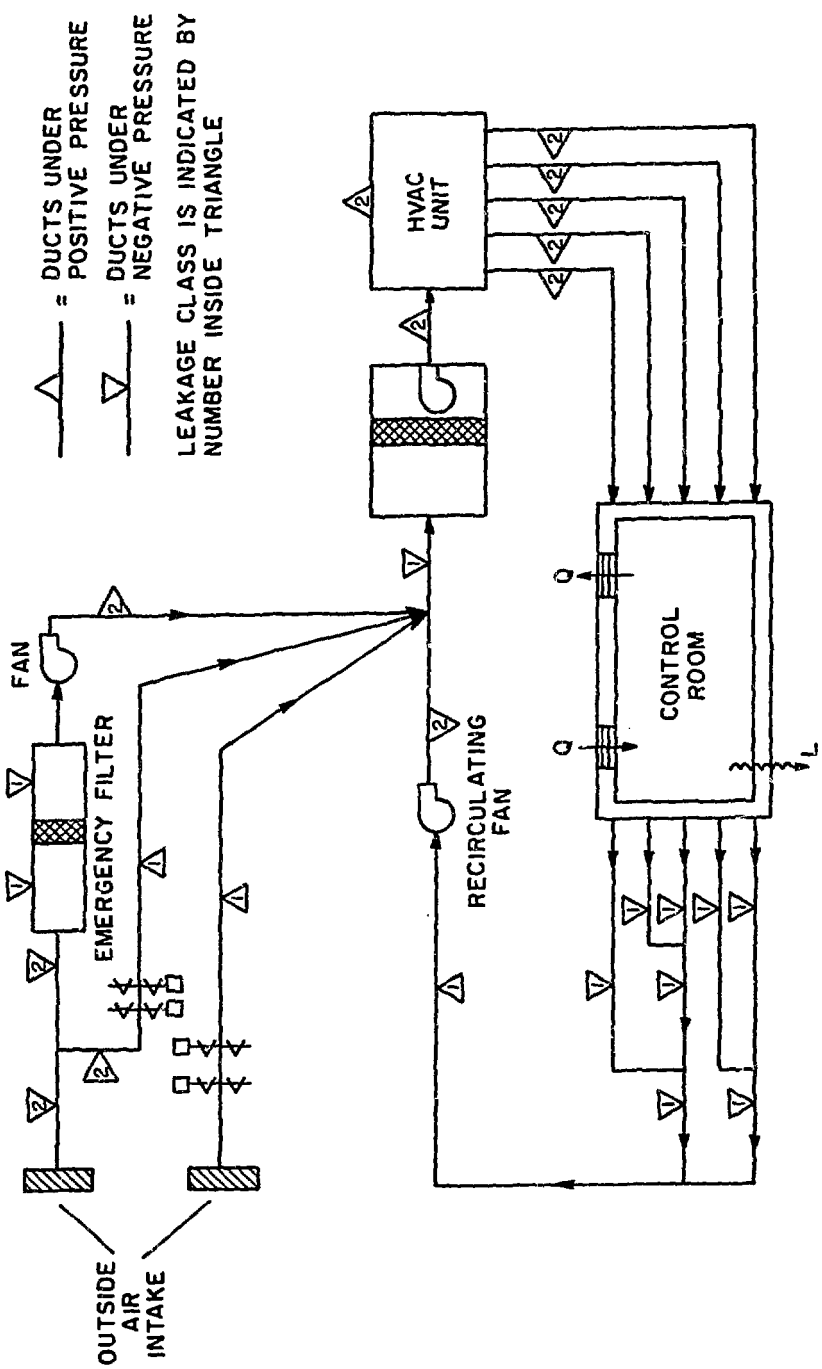

FIGURE 1
DIAGRAM OF A TYPICAL CONTROL ROOM VENTILATION SYSTEM

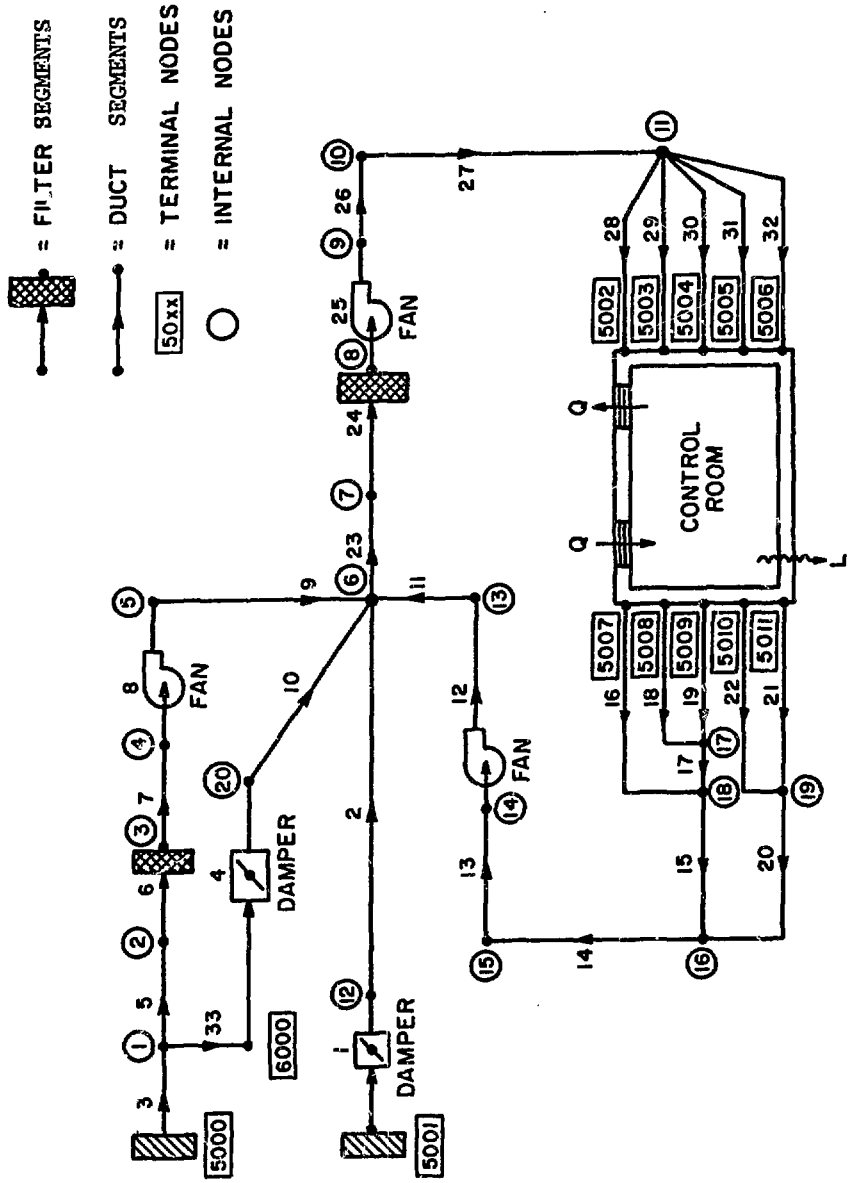

FIGURE 2
NETWORK REPRESENTATION OF THE CONTROL ROOM VENTILATION SYSTEM

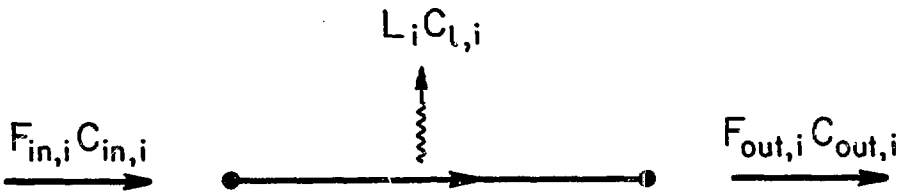

FIGURE 3
SEGMENT REPRESENTATION

where $F_{in,i}$ is the input air flow rate for segment "i"; $F_{out,i}$ is the output air flow rate for segment "i"; L_i is the leakage associated with duct segment "i" ($L_i > 0$ is defined as outleakage; $L_i < 0$ is defined as inleakage).

Similarly, a conservation equation can be written at each nodal point in accordance with the convention shown in Fig. 4:

$$\sum_j F_{in,j} - \sum_k F_{out,k} = 0, \tag{5}$$

where the two summations are performed over the "j" input and "k" output air flows that are respectively terminating or originating at the nodal point under consideration.

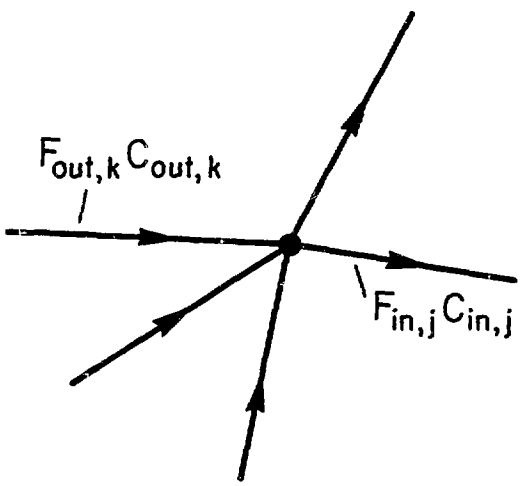

FIGURE 4
NODE REPRESENTATION

The leakage rates to be used are the (i) allowable leak rates, or (ii) assumed leak rates, or (iii) actual measured leak rates for an existing control room ventilation system. ANSI/ASME N509-1980[8] prescribes that the minimum of the values as determined by three different criteria be used as allowable leakage for design and testing. The three criteria are: (i) air cleaning effectiveness; (ii) duct/housing quality; and (iii) health physics requirements. In this model, the first two criteria only have been retained since the application of the third one cannot be performed a priori.

The number of equations of the type represented by Eq. (4) is equal to the number of segments, S, and the number of equations of the type represented by Eq. (5) is equal to the number of internal nodes, N_I. For each segment there are two unknowns, $F_{in,i}$ and $F_{out,i}$. Therefore, the number of degrees of freedom of the network, D_l, is given by:

$$D_l = 2S - (S + N_I) = N_R + N_T - 1, \tag{6}$$

after using Eq. (3).

This equation expresses the fact that in order to uniquely determine the flow rates in all ductwork segments, it is necessary to assign specific values to the number of flow rates given by Eq. (6). Once the required flow rates have been chosen, the system of Eqs. (4) and (5) can be solved for the unknowns $F_{in,i}$ and $F_{out,i}$.

Airborne Radioactivity

Conservation of radioactive species is expressed by equations similar to Eqs. (4) and (5):

$$F_{in,i}C_{in,i} - F_{out,i}C_{out,i} = L_iC_{l,i}, \tag{7}$$

and

$$\sum_j F_{in,j}C_{in,j} - \sum_k F_{out,k}C_{out,k} = 0. \tag{8}$$

where $C_{in,i}$ is the input concentration of radioactive material in segment "i"; $C_{out,i}$ is the output concentration of radioactive material in segment "i"; $C_{l,i}$ is the average concentration of radioactive material leaking out or into duct segment "i." For all outleakages, it is assumed that:

$$C_{l,i} = C_{in,i}, \qquad L_i > 0, \tag{9}$$

i.e., radioactive decay is neglected. The number of equations of this type is S_{OL}, representing the number of segments with outleakages. For each of the ductwork segments subjected to inleakages, it is assumed that:

$$C_{l,i} = K_iC_{OAI}, \qquad L_i < 0, \tag{10}$$

where K_iC_{OAI}, is the concentration of radioactive material outside the ductwork segment expressed as a fraction, given by K_i, of the concentration at the outside air intakes of the control room ventilation system. The values of C_{OAI} are known. The values of K_i give the distribution of the radioactive material in the control room building area. These fractions K_i may be derived from site meteorological data and wake and terrain effect data. The number of equations of this type is S_{IL}, representing the number of segments with inleakages.

A special case is that of a housing encompassing a filter unit. For these segments, the conservation equation is written as:

$$F_{in,i}C_{in,i} - F_{out,i}C_{out,i} - \varepsilon_i^s F_{in,i}C_{in,i} = L_i C_{1,i} \tag{11}$$

where ε_i^s is the filtration efficiency for radioactive species "s." The equation is based on the convention appearing in Fig. 5. The upstream housing section has been associated with the filter; the downstream portion of the filter housing can be treated as any other nonfiltrating segment.

For each segment, there are three unknowns: $C_{in,i}$, $C_{out,i}$ and $C_{1,i}$. Therefore, D_2', the number of degrees of freedom of the network is given by:

$$D_2' = 3S - S - S_{OL} - S_{IL} - N_I = N_R + N_T - 1, \tag{12}$$

after using Eq. (3), and

$$S = S_{OL} + S_{IL}. \tag{13}$$

The number of degrees of freedom is actually further reduced by assuming perfect mixing of air flow at internal nodes where several segments converge. This results in the equality of the concentrations at the input side of the ductwork segments that originate at the same internal node. Thus for the example shown in Fig. 6, these considerations translate into:

$$\begin{aligned} C_{in,4} &= C_{in,5}; \\ C_{in,6} &= C_{in,7}; \\ C_{in,8} &= C_{in,9}. \end{aligned} \tag{14}$$

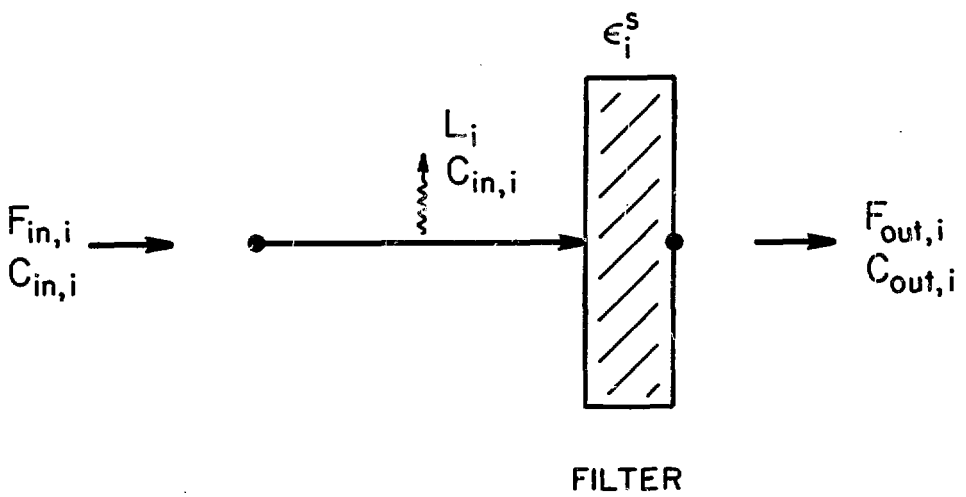

FIGURE 5
FILTER REPRESENTATION

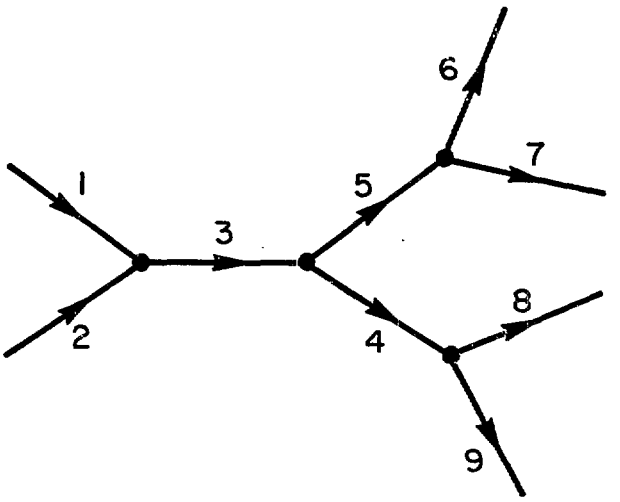

FIGURE 6
EXAMPLE OF NETWORK

It can be shown that the number of additional equations of the type represented by Eq. (14) is given by: $N_{T,OUT} - 1 + N_R$, where $N_{T,OUT}$ denotes the number of terminal nodes with output flow. Therefore, Eq. (12) becomes:

$$D_2 = N_{T,IN}, \tag{15}$$

where $N_{T,IN}$ denotes the number of terminal nodes with input flow, and

$$N_T = N_{T,IN} + N_{T,OUT}. \tag{16}$$

Thus, in order to determine the unknowns $C_{in,i}$, $C_{out,i}$, and $C_{1,i}$, it is sufficient to fix the values of the radioactive concentrations at all the terminal nodes where an input of air occurs.

Both flow rate and radioactivity conservation equations are linear with respect to flow rates and radioactivity concentrations. This leads to the result that the instantaneous value of the radioactivity concentration at any point of the ductwork network is a linear combination of the concentration at the outside air intake, C_{OAI}, which is known, and the concentration in the control room, C_{CR}, which is unknown and the main object of the evaluation. This condition is expressed by the equation:

$$C_{h,i} = a_{h,i}C_{CR} + b_{h,i}C_{OAI} \tag{17}$$

where the subscript "h" stands for "in," "out," or "1."

Network Configuration

The equations presented in the preceding section are segment or node equations and do not contain any information on how the system is configured. In order to account for the actual layout of components and for ductwork routing and branching, a matrix representation is adopted. For example, with reference to Fig. 7, the following matrix is defined:

$$[\alpha] = \begin{array}{c|c|cccccccc} & & \text{Segments} \longrightarrow & & & & & & & \\ & & 1 & 2 & 3 & 4 & 5 & 6 & 7 & 8 \\ \text{Nodes} \downarrow & 1 & -1 & 0 & 0 & 0 & 0 & 0 & 0 & 0 \\ & 2 & +1 & -1 & 0 & 0 & 0 & 0 & +1 & 0 \\ & 3 & 0 & +1 & -1 & 0 & +1 & 0 & 0 & 0 \\ & 4 & 0 & 0 & +1 & 0 & 0 & 0 & 0 & 0 \\ & 5 & 0 & 0 & 0 & -1 & 0 & 0 & 0 & 0 \\ & 6 & 0 & 0 & 0 & 0 & 0 & 0 & 0 & -1 \\ & 7 & 0 & 0 & 0 & 0 & 0 & +1 & -1 & +1 \\ & 8 & 0 & 0 & 0 & +1 & -1 & -1 & 0 & 0 \end{array} \qquad (18)$$

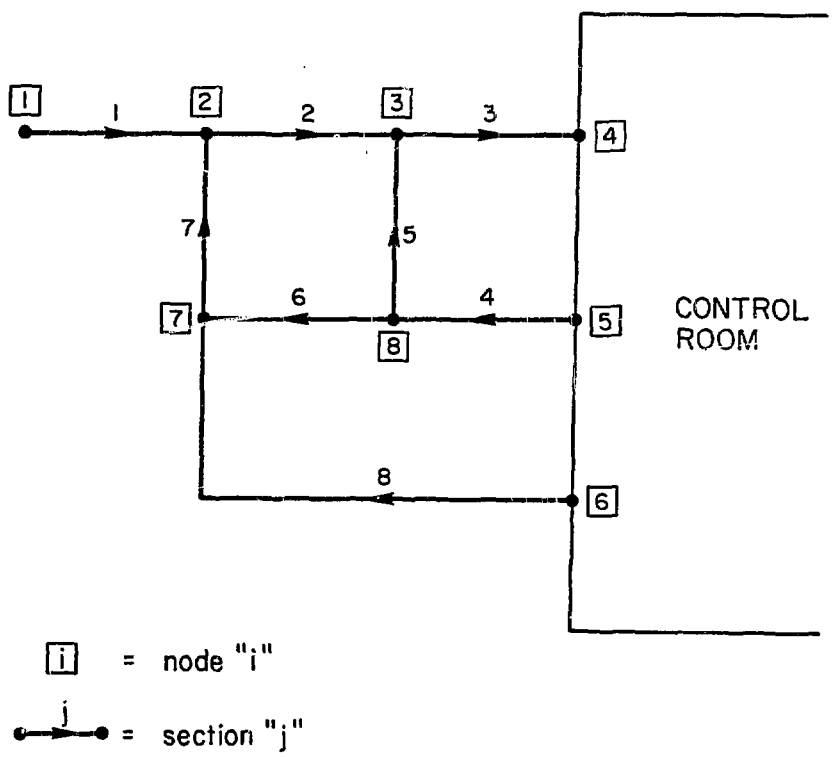

[i] = node "i"

j = section "j"

FIGURE 7
EXAMPLE OF NETWORK

where a matrix element α_{nm} has the following property:

α_{nm} = -1 if segment "m" originates from node "n";
α_{nm} = +1 if segment "m" terminates at node "n";
α_{nm} = 0 if segment "m" has no connection with node "n".

Any subnetwork of the general network is representable by a submatrix of $[\alpha]$. It is only necessary to eliminate the columns corresponding to the segment not present in the subnetwork and the rows corresponding to the nodes not present in the subnetwork.

Control Room Radioactive Contamination Concentrations

With reference to Fig. 8, the equation governing the time-dependent concentration of a radioactive species "s" in the control room is given by:

$$\frac{dC^s_{CR}}{dt} = -\lambda_s C^s_{CR} - \frac{LC^s_{CR} + QC^s_{CR} + \sum_p F_{in,p} C^s_{in,p}}{V_{CR}} + \sum_r b_{r\to s}\lambda_r C^r_{CR}$$

$$+ \frac{QC^s_{OAI} + \sum_q F_{out,q} C^s_{out,q}}{V_{CR}} \qquad (19)$$

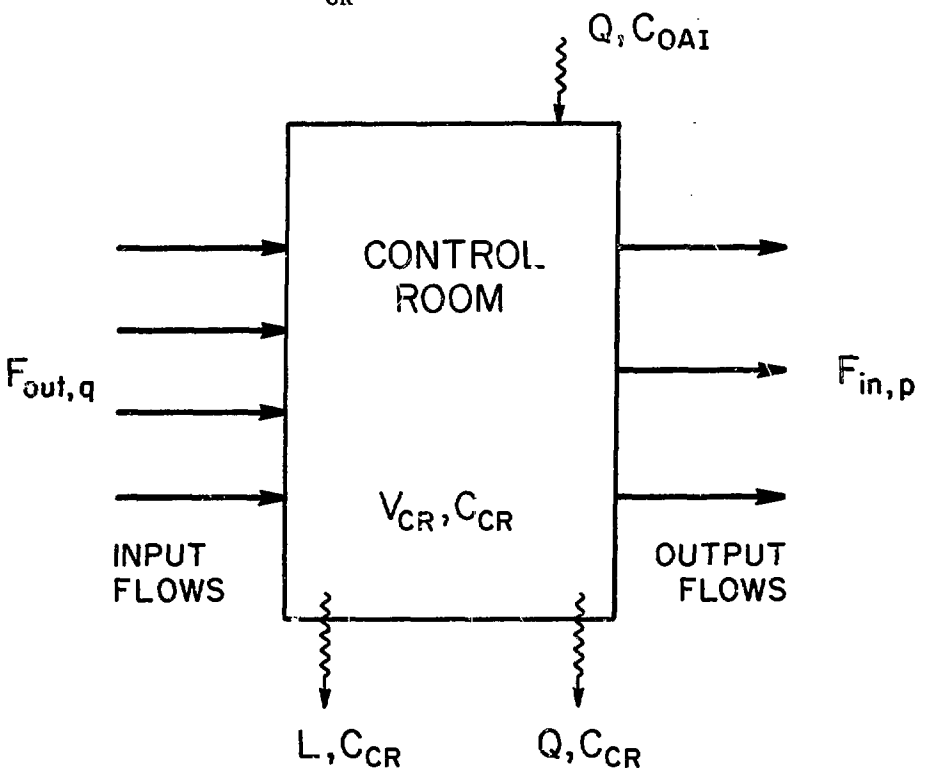

FIGURE 8
DIAGRAM OF A CONTROL ROOM

where:

V_{CR} = control room volume;
L = control room leak rate due to pressurization;
Q = infiltration due to personnel doors;
λ_s = decay constant of radionuclide "s";
λ_r = decay constant of radionuclide "r";
$b_{r\to s}$ = fraction of nuclide "s" produced by decay of nuclide "r".

Noting that:

$$C^s_{in,p} = C^s_{CR}, \tag{20}$$

$$L + \sum_p F_{in,p} = \sum_q F_{out,q}, \tag{21}$$

and using Eq. (17) to express $C^s_{out,q}$, Eq. (19) becomes:

$$\frac{dC^s_{CR}}{dt} = \left[-\lambda_s - \frac{Q + \sum_q F_{out,q}(1 - a^s_{out,q})}{V_{CR}} \right] C^s_{CR} + \sum_r b_{r\to s}\,\lambda_r C^r_{CR}$$

$$+ \frac{Q + \sum_q F_{out,q} b^s_{out,q}}{V_{CR}} C^s_{OAI} \tag{22}$$

Having previously determined all air flow rate values, one can solve for $C^s_{CR}(t)$, to which the dose rate is proportional, and for the Iodine Protection Factors. The time-dependent concentration integral in the control room, to which the dose is proportional, obeys the equation:

$$I^s_{CR}(t) = \int_0^t C^s_{CR}(t')dt', \tag{23}$$

with the initial condition:

$$I^s_{CR}(0) = 0. \tag{24}$$

The time-dependent concentration integral at the outside air intakes is given by:

$$I^s_{OAI}(t) = \int_0^t C^s_{OAI}(t')dt', \tag{25}$$

with the initial condition:

$$I^s_{OAI}(0) = 0. \tag{26}$$

Iodine Protection Factors: Simplified Approach

A simple solution for Eq. (22) can be obtained when the decay terms are neglected and C^s_{OAI} remains constant. This approach leads to the IPF obtained by Murphy and Campe.[4] For this case, the solution is given by:

$$C^s_{CR} = \frac{V^s C^s_{OAI}}{U^s} \left(1 - e^{-U^s t}\right) \tag{27}$$

where

$$U^s = \frac{Q + \sum_q F_{out,q}(1 - a^s_{out,q})}{V_{CR}} \tag{28}$$

and

$$V^s = \frac{Q + \sum_q F_{out,q} b^s_{out\ q}}{V_{CR}} \tag{29}$$

Specifying that the radionuclide "s" is an iodine isotope, the Protection Factor for this particular radioiodine can be obtained from Eq. (27):

$$IPF^s(t) = \frac{C^s_{OAI}}{C^s_{CR}} = \frac{U^s}{V^s(1 - e^{-U^s t})} \tag{30}$$

For a period of time long enough, Eq. (30) reduces to:

$$IPF^s = \frac{U^s}{V^s} = \frac{Q + \sum_q F_{out,q}(1 - a^s_{out,q})}{Q + \sum_q F_{out,q} b^s_{out,q}}, \tag{31}$$

which is equivalent to the approach adopted by Murphy and Campe.[4] When all radioiodine species are considered, Eq. (30) becomes:

$$IPF(t) = \sum_s \omega_s\ IPF^s(t), \tag{32}$$

with

$$\omega_s = \frac{C^s_{CR}}{\sum_s C^s_{CR}}, \tag{33}$$

where the summations are carried over the radioiodine species only. For a period of time long enough, Eq. (32) becomes:

$$IPF = \sum_s \omega_s \, IPF^s.$$

Iodine Protection Factors: General Approach

In the more general approach, the overall IPF, defined as the ratio of the total doses without and with protection, is given by:

$$IPF(t) = \frac{\sum_s I^s_{OAI}}{\sum_s I^s_{CR}}, \tag{34}$$

where I^s_{CR} and I^s_{OAI} are defined by Eqs. (23) and (25), respectively. The most general computation calls for the solution of the system of equations represented by Eq. (22).

The use of this more accurate definition of IPF leads to better estimates than those made from the simplified approach presented in the preceding section.

Mathematical Implementation

The mathematical model of control room ventilation systems under accident conditions discussed in the preceding sections has been incorporated in a computer code. The mathematical methods, flow diagrams, listings, and sample outputs are documented in Ref. (9).

Special Case: Multiple Filtration

The mathematical model described so far is formally exact but does not yield realistic results when the ventilation system presents two filtrating units in series. In fact, the model would result in a greater reduction of radioactivity due to the fact that the radioactivity not filtered by the first unit would be refiltered by the second unit with a filtration efficiency given by the efficiency of the second filter itself.

This can be more easily understood by looking at Fig. (9a), where

A_0 = activity at the inlet of the filter chain;
A_1 = activity at the outlet of the first filter;
A_2 = activity at the outlet of the filter chain;
ε_1, ε_2 = filtration efficiency of the first and second filter, respectively.

For this situation the following relationship holds:

$$A_2 = A_1(1 - \varepsilon_2) = A_0(1 - \varepsilon_1)(1 - \varepsilon_2). \tag{35}$$

The total filtration efficiency of the chain, ε_{tot}, is given by:

$$A_2 = A_0(1 - \varepsilon_{tot}), \tag{36}$$

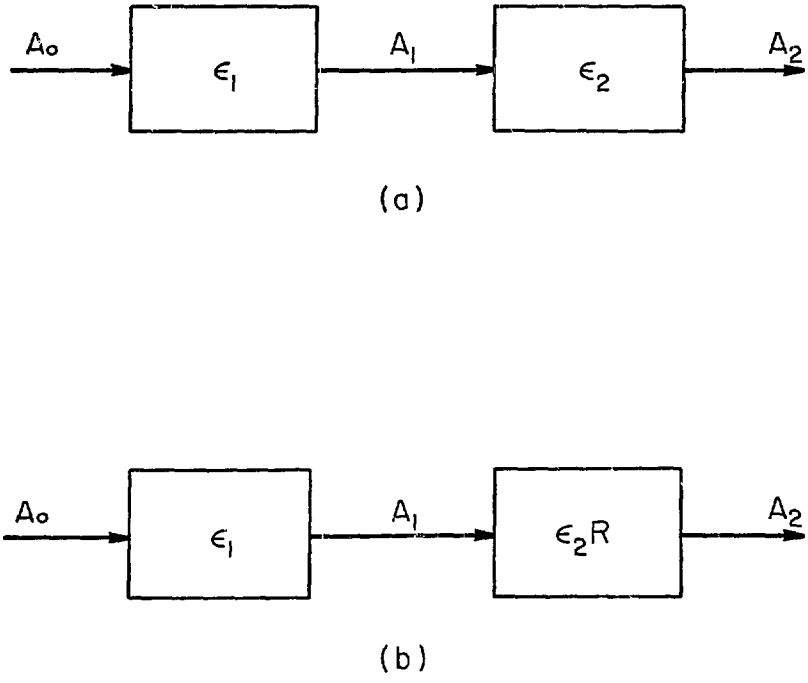

FIGURE 9
FILTRATING UNITS IN SERIES

from which:

$$(1 - \varepsilon_1)(1 - \varepsilon_2) = (1 - \varepsilon_{tot}), \tag{37}$$

or

$$\varepsilon_{tot} = \varepsilon_1 + \varepsilon_2 - \varepsilon_1\varepsilon_2. \tag{38}$$

However, Eqs. (35) and (38) are not exact because, as pointed out by Murphy and Campe,[4] the filtration efficiency of the second filter is not the same on a filtered stream as on an unfiltered stream. In fact, the filtration efficiency depends on the size distribution of particulates and on the concentration of the material to be removed from the stream. Therefore, as these conditions at the inlet of the second filter are different from those at the inlet of the first filter, the efficiency of the second filter is reduced, even when it has the same nominal efficiency as the first one.

On the basis of these considerations, the situation shown in Fig. 9a should be modified as shown in Fig. 9b, where R is the second filter filtration efficiency reduction factor, which accounts for the described effects and satisfies Eq. (37) modified as follows:

$$(1 - \varepsilon_1)(1 - \varepsilon_2 R) = (1 - \varepsilon_{tot}), \tag{39}$$

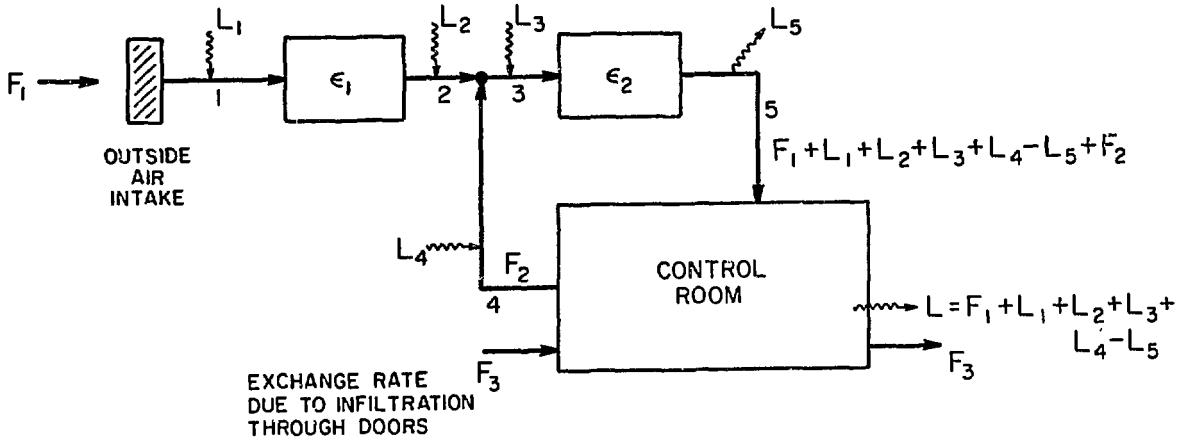

FIGURE 10
EXAMPLE OF NETWORK WITH MULTIPLE FILTRATING UNITS

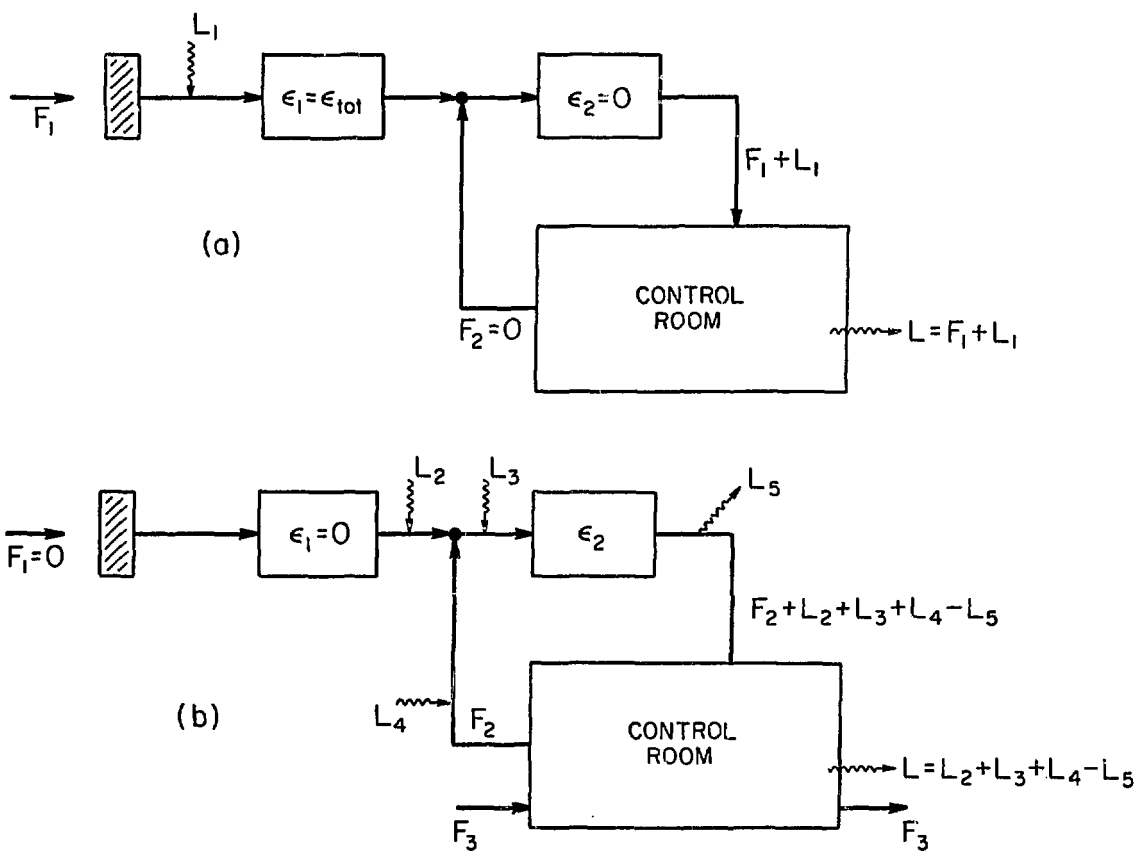

FIGURE 11
SUBNETWORKS REPRESENTATION

or

$$\varepsilon_{tot} = \varepsilon_1 + \varepsilon_2 R - \varepsilon_1 \varepsilon_2 R. \quad (40)$$

When the ductwork network presents a situation corresponding to multiple filtration in series, a special treatment of the model equations is therefore warranted. To tackle this problem, two overlapping system situations have to be considered. The performance of the simple control room ventilation system illustrated in Fig. 10 can be studied by applying the principle of superposition of effects to the two situations represented in Figs. 11a and 11b. In Fig. 11a, only the flow rates and the leakages that are filtered twice are taken into account; ε_{tot} is the filtration efficiency of the doubly filtered streams given by Eq. (40). In Fig. 11b, only the flow rates and the leakages that are filtered once are taken into account.

The final results, which take into account both situations, are obtained by superposition of the two effects by averaging the $a_{in/out,i}$ and $b_{in/out,i}$ weighted by the values of the fraction of the flow rates in each situation with respect to the total flow rates.

III. Example

The model has been tested on a sample problem, that is typical of nuclear power plant control room systems. The control room ventilation system is shown in Figs. 1 and 2. The main characteristics of the system are presented in Table 1. The input data are contained in Tables 2 and 3.

Ductwork leakages for each HVAC and Air Cleaning (AC) segment as resulting from the air cleaning effectiveness and the duct/housing quality criteria of ANSI/ASME N509-1980 are presented in Table 4. If a segment encompasses a damper, the latter is treated as a known air flow rate if the damper is closed in the operation mode under consideration. The input or output flow rate of the damper segment is then set equal to the leakage of the damper under the design or

Table 1. Main characteristics of the control room ventilation system

Control Room Volume:	100,000 ft**3
Air Cleaning System Rated Flow:	4,000 CFM
HVAC Rated Flow:	26,340 CFM
Control Room Exfiltration Rate at Design Pressure:	1,500 CFM
Control Room Infiltration Rate Through Access Doors:	10 CFM
Particulate and Elemental Iodine Filter Efficiency:	95%
Organic Iodine Filter Efficiency:	90%
Noble Gas Filter Efficiency:	0%
Second Filter Efficiency Reduction Factor:	0.842

Table 2. Description of the nodes.

Number of Network Nodes	= 33
Number of Internal Nodes of the Network	= 21
Number of Terminal Nodes of the Network	= 12
Number of Exhaust Terminal Nodes	= 0
Number of Control Room Terminal Nodes	= 10
Node Numbers	
5002 5003 5004 5005 5006	
5007 5008 5009 5010 5011	
Number of Outside Air Intakes Terminal Nodes	= 2
Node Numbers	
5001 5000	

operating pressure differential. Damper leakage values can be obtained from the damper manufacturer, actual test data, or ANSI/ASME N509-1980. The leakage characteristics of the two dampers found in the system are specified in Table 5.

As can be seen from Table 4, the quality criterion leads, in general, to more conservative results. Both the air cleaning effectiveness and the quality criteria lead to high values of leakages for the ductwork segments of the HVAC system in the Class II leakage. These leakages, however, do not compromise control room protection performance because they are outleakages. It can also be seen that most of the inleakages are filtered; moreover, the small unfiltered inleakage only affects the air cleaning system portion of the ventilation system. From a first look, this is a well-designed ductwork system and this will eventually be confirmed by the values of the IPF.

Three modes of operation have been considered: (i) filtered pressurization and unfiltered recirculation (Fig. 12); (ii) unfiltered pressurization and filtered recirculation (Fig. 13); and (iii) filtered pressurization and filtered recirculation (Fig. 14).

As an example, the flow rates obtained with the filtered pressurization and filtered recirculation operation mode are shown in Table 6 for the two following cases: (i) leakages are not taken into account; (ii) ductwork leakages according to the air cleaning effectiveness criteria and damper leakages are included.

When duct and equipment leakages are neglected, Table 7 presents the IPFs obtained from Eq. (31) for elemental and particulate iodines, and for organic iodine, for two different situations: (i) infiltration through the personnel doors is neglected ($Q = 0$); (ii) infiltration through the personnel doors is taken into account ($Q = 10$ CFM). For the latter situation, it is assumed that contaminant concentrations in the air finding its way into the control room through the doors are equal to the contaminant concentrations at the outside air intakes. The IPFs for those simplified situations reduce to simple formulae that can be found in Ref. (4); with reference to Fig. 8, they are:

Table 3. Description of the segments
(Number of segments of the network = 33)

Segment Description & No.	Segment No.	Input Node	Output Node	Leakage Class	Type (ESF or Non-ESF)	Width or Diameter (in)	Height (ft)	Length (ft)	Operating Pressure Differential (in. W.G.)	Design or Testing Press. Diff. (in. W.G.)	Nominal Flow Rate (CFM)
NO. OF DUCT SEGMENTS = 26											
No. of Round Segments = 2	26	9	10	2	ESF	48.0		2.0	+5.00	+7.5	26340
	8	4	5	2	ESF	20.0		2.0	+0.47	+4.0	4000
No. of Rectangular Segments = 24	23	6	7	1	ESF	38.0	38.0	12.0	-2.33	+4.0	26340
	21	5011	19	1	ESF	18.0	8.0	110.0	-4.00	+6.0	1220
	18	5008	17	1	ESF	26.0	20.0	42.0	-3.33	+5.0	10650
	16	5007	18	1	ESF	18.0	8.0	90.0	-3.33	+5.0	1100
	22	5010	19	1	ESF	26.0	20.0	37.0	-3.33	+5.0	10650
	19	5009	17	1	ESF	18.0	8.0	86.0	-3.33	+5.0	1220
	17	17	18	1	ESF	30.0	20.0	10.0	-3.33	+5.0	11870
	15	18	16	1	ESF	34.0	20.0	5.0	-3.33	+5.0	12970
	20	19	16	1	ESF	30.0	20.0	50.0	-4.00	+6.0	11870
	14	16	15	1	ESF	54.0	24.0	2.0	-4.00	+6.0	24840
	13	15	14	1	ESF	54.0	24.0	58.0	-4.00	+6.0	24840
	12	14	13	2	ESF	44.0	34.0	8.0	+0.30	+4.0	24840
	11	13	6	2	ESF	44.0	34.0	2.0	+0.30	+4.0	24840
	28	11	5002	2	ESF	40.0	14.0	60.0	+3.6	+5.0	11400
	29	11	5003	2	ESF	40.0	14.0	65.0	+3.6	+5.0	11400
	30	11	5004	2	ESF	18.0	8.0	160.0	+3.6	+5.0	1100
	31	11	5005	2	ESF	18.0	8.0	80.0	+3.6	+5.0	1220
	32	11	5006	2	ESF	18.0	8.0	162.0	+3.6	+5.0	1220
	3	5000	1	2	ESF	20.0	12.0	86.0	-1.5	+4.0	4000
	5	1	2	2	ESF	20.0	12.0	11.0	-3.0	+4.5	4000
	9	5	6	2	ESF	14.0	12.0	87.0	+0.47	+4.0	1500
	2	12	6	1	ESF	30.0	38.0	100.0	-2.33	+4.0	4000
	10	20	6	1	ESF	14.0	12.0	30.0	-2.33	+4.0	1500
	33	1	6000	2	ESF	20.0	12.0	9.0	-1.50	+4.0	1500
NO. OF HOUSING SEGMENTS = 5											
No. of Segments Upstream Filters = 2	6	2	3	1	ESF	5.33	6.75	27.0	-9.71	+13.5	4000
	24	7	8	1	ESF	9.66	9.75	7.0	-3.60	+6.0	26340
No. of Segments Downstream Filters = 3	7	3	4	1	ESF	5.33	6.75	7.0	-9.71	+13.5	4000
	25	8	9	1	ESF	9.66	9.75	14.8	-3.60	+6.0	26340
	27	10	11	2	ESF	10.0	8.50	8.0	+5.00	+7.5	26340
NUMBER OF SPECIAL SEGMENTS = 2	4	6000	20	1		20.0	12.0	0.0	0.0	10.	
	1	5001	12	1		36.0	0.0	0.0	0.0	10.	

Table 4. Results of leakage analysis.

Segment Number	Input Node	Output Node	Segment Surface Area (ft**2)	System	Leakage Class	Segment Type	Leak Rate For ACEF Criteria (CFM)	Leak Rate for Qual. Criteria at Oper. Pressure (CFM)
2	12	6	1133.333	AC	1	RECT. DUCT	-3.588	-2.735
3	5000	1	458.667	AC	2	RECT. DUCT	-23.107	-17.764
5	1	2	58.667	AC	2	RECT. DUCT	-2.955	-3.213
6	2	3	652.320	AC	1	HOUS. UPST.	-1.867	-3.214
7	3	4	169.120	AC	1	HOUS. DWST.	-.484	-.833
8	4	5	10.472	AC	2	ROUND DUCT	.528	.227
9	5	6	377.000	AC	2	RECT. DUCT	18.992	8.173
10	20	6	130.000	AC	1	RECT. DUCT	-.412	-.314
11	13	6	26.000	HVAC	2	RECT. DUCT	2.477	.450
12	14	13	104.000	HVAC	2	RECT. DUCT	9.907	1.801
13	15	14	754.000	HVAC	1	RECT. DUCT	-5.978	-2.384
14	16	15	26.000	HVAC	1	RECT. DUCT	-.206	-.082
15	18	16	45.000	HVAC	1	RECT. DUCT	-.357	-.130
16	5007	18	390.000	HVAC	1	RECT. DUCT	-3.092	-1.125
17	17	18	83.333	HVAC	1	RECT. DUCT	-.661	-.240
18	5008	17	322.000	HVAC	1	RECT. DUCT	-2.553	-.929
19	5009	17	372.667	HVAC	1	RECT. DUCT	-2.955	-1.075
20	19	16	416.667	HVAC	1	RECT. DUCT	-3.304	-1.318
21	5011	19	476.667	HVAC	1	RECT. DUCT	-3.779	-1.507
22	5010	19	283.667	HVAC	1	RECT. DUCT	-2.249	-.818
23	6	7	152.000	HVAC	1	RECT. DUCT	-1.205	-.367
24	7	8	270.964	HVAC	1	HOUS. UPST.	-26.340	-.813
25	8	9	576.477	AC	1	HOUS. DWST.	-1.650	-1.729
26	9	10	25.133	HVAC	2	ROUND DUCT	2.394	1.777
27	10	11	296.000	HVAC	2	HOUS. DWST.	28.196	20.930
28	11	5002	540.000	HVAC	2	RECT. DUCT	51.440	32.400
29	11	5003	585.000	HVAC	2	RECT. DUCT	55.726	35.100
30	11	5004	693.333	HVAC	2	RECT. DUCT	66.046	41.600
31	11	5005	346.667	HVAC	2	RECT. DUCT	33.023	20.800
32	11	5006	702.000	HVAC	2	RECT. DUCT	66.871	42.120
33	1	6000	48.000	AC	2	RECT. DUCT	-2.418	-1.859

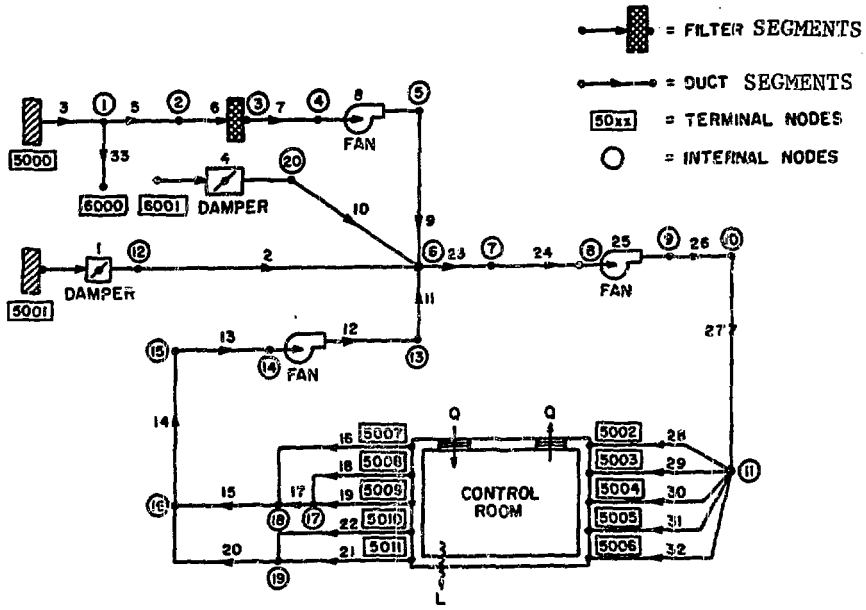

FIGURE 12
OPERATION MODE NO. 1: FILTERED PRESSURIZATION AND UNFILTERED RECIRCULATION

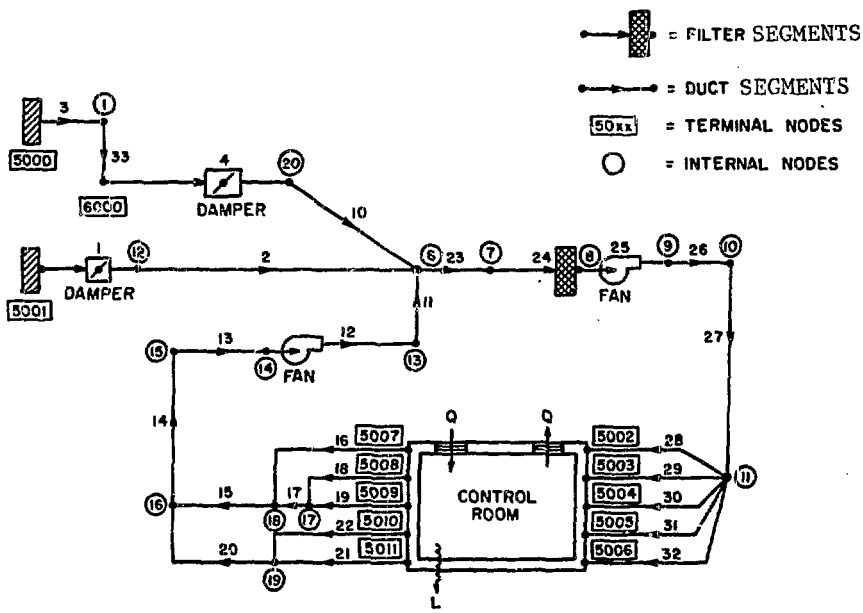

FIGURE 13
OPERATION MODE NO. 2: UNFILTERED PRESSURIZATION AND FILTERED RECIRCULATION

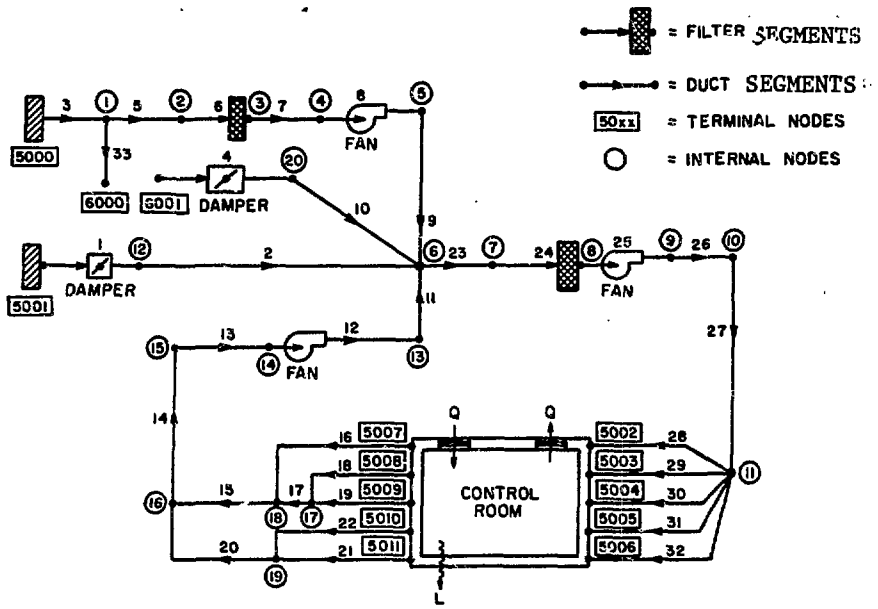

FIGURE 14
OPERATION MODE NO. 3: FILTERED PRESSURIZATION AND FILTERED RECIRCULATION

operation mode no. 1:

$$IPF = \frac{L + Q}{(1 - \varepsilon_1)L + Q}; \tag{41}$$

operation mode no. 2:

$$IPF = \frac{L + \varepsilon_2 \sum_p F_{in,p} + Q}{(1 - \varepsilon_2)L + Q}; \tag{42}$$

operation mode no. 3:

$$IPF = \frac{L + \varepsilon_2 \sum_p F_{in,p} + Q}{(1 - \varepsilon_{tot})L + Q}, \tag{43}$$

where ε_{tot} is given by Eq. (40).

These expressions have provided a simple means to check the accuracy of the code.

Table 5. Damper leakage characteristics

Segment Number	Input Node	Output Node	Cross Sectional Surface Area (ft**2)	Segment Type	Design or Test. Pressure Difference (in. W.G.)	Max. Allow. Leak Rate at Design or Test Pressure Diff. (CFM)
4	6000	20	1.667	Isol. Valve	10.000	.062
1	5001	12	7.069	Isol. Valve	10.000	39.500

Table 6. Operation mode no. 3: system flow rates without and with leakages. The leakage values are obtained from the air cleaning effectiveness criteria of ANSI/ASME N509-1980

	WITHOUT LEAKAGE	WITH LEAKAGE	
SEGMENTS	Input or Output Flow (CFM)	Input Flow (CFM)	Output Flow (CFM)
1	0	39.5	39.5
2	0	39.5	43.0
3	1500	1706.9	1730.0
4	0	-.06	-.06
5	1500	1732.5	1735.4
6	1500	1735.4	1737.3
7	1500	1737.3	1737.8
8	1500	1737.8	1737.3
9	1500	1737.3	1718.3
10	0	-.06	.35
11	24840	24855.2	24852.7
12	24840	24865.1	24855.2
13	24840	24859.1	24865.1
14	24840	24858.9	24859.1
15	12970	12979.2	12979.6
16	1100	1100.0	1103.0
17	11870	11875.5	11876.1
18	10650	10650.0	10652.5
19	1220	1220.0	1222.9
20	11870	11876.0	11879.3
21	1220	1220.0	1223.7
22	10650	10650.0	10652.2
23	26340	26614.5	26615.7
24	26340	26615.7	26642.0
25	26340	26642.0	26643.6
26	26340	26643.6	26641.3
27	26340	26641.3	26613.1
28	11400	11451.4	11400.0
29	11400	11455.7	11400.0
30	1100	1166.0	1100.0
31	1220	1253.0	1220.0
32	1220	1286.8	1220.0
33	0	-2.48	-.06

Table 7. Iodine Protection Factors calculated when duct and equipment leakages are neglected

Operation Mode No.	Q = 0		Q = 10 CFM	
	I_{el}/I_p	I_{org}	I_{el}/I_p	I_{org}
1	20	10	17.8	9.4
2	335	159	295	149
3	1673	656	1004	515

Note:

Q denotes the personnel door infiltration rate.

Table 8 presents the IPFs for operation mode no. 1, filtered pressurization and unfiltered recirculation, and mode no. 3, filtered pressurization and filtered recirculation, for various combinations of duct, door, and damper leakage. It is again assumed that all inleakages occur with air contaminated at concentrations equal to those existing at the outside air intakes. The results show that the IPF for mode no. 1 is reduced almost 50% when duct, door, and damper leakages are accounted for. With the interactive computer model, the IPF for mode no. 3 is easily determined. The impact of adding filtration into the recirculation air raises the IPF from 11.5 (mode no. 1 with duct, damper, and door leakage) to 818. Also, the effect of adjusting the leakage rates for duct, door and dampers can readily be seen on the IPF. As can be expected, the relative impact of a particular leakage or infiltration depends upon the location at which it occurs relative to the location of the control room and filters. For example, in operation mode no. 1, the high leak rate of the damper in segment 1 represents the most important factor in the reduction of the IPF, while in the operation mode no. 3, the most deleterious effect results from the personnel door infiltration. In all cases, duct leakages drive the IPF values down by another 10 to 25%. This example illustrates the usefulness of this program in rapidly evaluating the sensitivity of control room design concepts with respect to control room operators dose.

Figure 15 shows the time-dependence of several species in the decay chain of mass 131, as resulting from Eq. (22). The time dependence of the concentrations at the outside air intakes is also shown; they have been derived from an assumed Loss-of-Coolant Accident (LOCA) scenario more fully documented in Refs. (1) and (2). As can be seen, when the source term remains constant, the IPFs approach their asymptotic value with a time-dependence indicated by Eq. (30).

The time-dependent control room concentrations for all airborne radioactive species could be used as input to a standard control room dose calculation model, thus completing the control room habitability analysis. It should also be noted that the program can also be used to determine time-dependent, hazardous chemicals concentrations for various system configurations.

Table 8. Iodine Protection Factors for various scenarios.

CASE NO.	NO LEAKAGE	DOOR LEAK.	DUCT LEAK. NOTE (1)	DUCT LEAK. NOTE (2)	DAMPER LEAK.	IPF			
						I_{el} & I_p		I_{org}	
						Mode 1 (3)	Mode 3 (3)	Mode 1 (3)	Mode 3 (3)
1	X					20	1673	10	656
2		X				17.8	1004	9.4	515
3			X			--	1309	--	547
4			X		X	12.3	1213	7.7	513
5		X	X			--	861	--	446
6		X	X		X	11.5	818	7.4	423
7		X		X	X	--	752	--	384

NOTES:
(1) Leakages are obtained from the duct/housing criteria of ANSI/ASME N509-1980 at operating pressure.
(2) Leakages are obtained from the air cleaning effectiveness criteria of ANSI/ASME N509-1980.
(3) Mode 1: Filtered pressurization, unfiltered recirculation
Mode 3: Filtered Pressurization, filtered recirculation

IV. Conclusions

The methodology presented in this work allows the user to easily model and modify the system configuration, and therefore permits a systematic analysis of nuclear power plants' control rooms or technical support center HVAC systems. It has the capability of representing most conceptual designs adopted by the U.S. architect/engineers. The program replaces tedious calculations to determine the effects of HVAC ductwork and equipment leakage on control room operator doses, and permits 1) parametric analyses of various HVAC system design options early in the conceptual phase of a project, and 2) analysis of the effects of in-place leakage test results on contaminant room concentrations, and therefore operator doses.

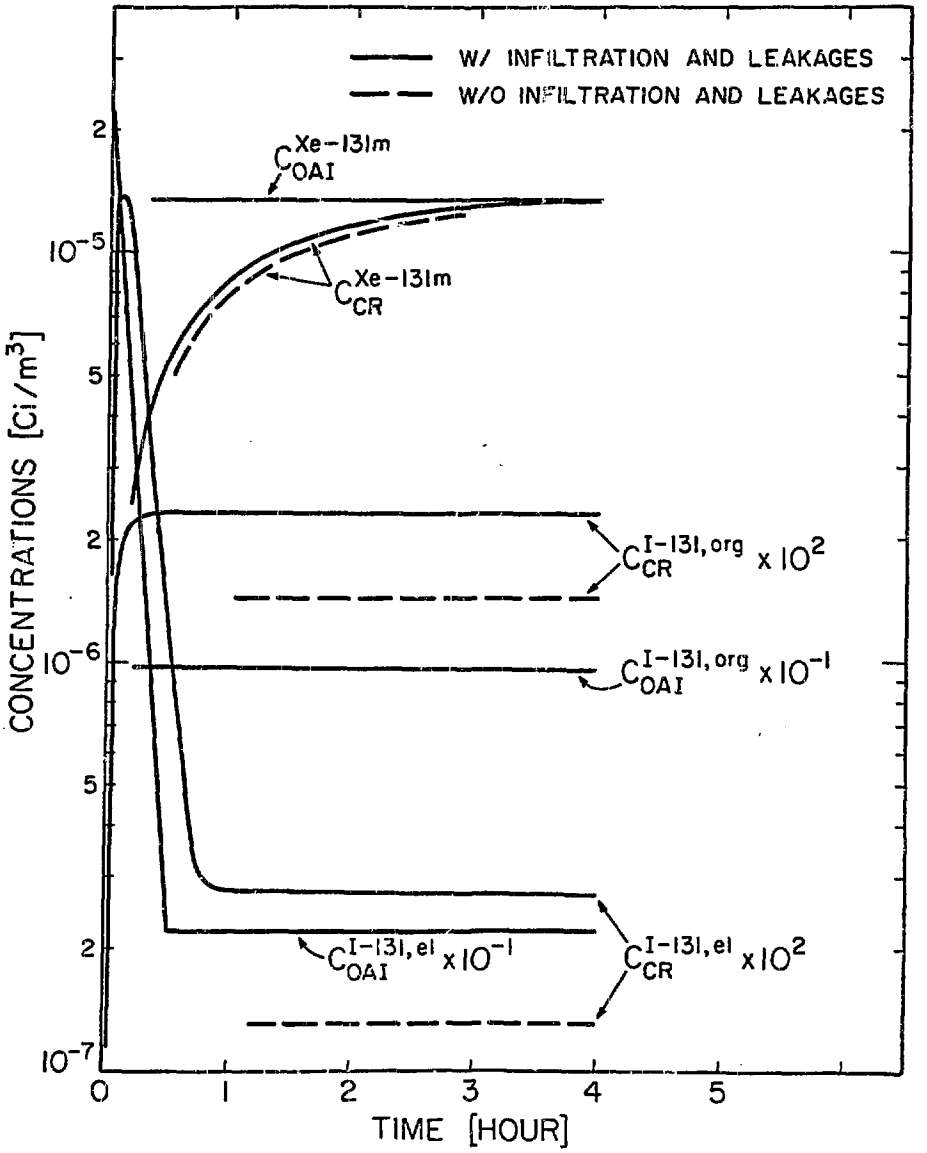

FIGURE 15
TIME-DEPENDENCE ANALYSIS FOR THE RADIONUCLIDES
IN THE DECAY CHAIN OF I - 131

Acknowledgments

The sponsorship of Sargent & Lundy Engineers is gratefully acknowledged.

References

1. F. Almerico and A. J. Machiels, "Performance Evaluation of Control Room HVAC Systems Under Accident Conditions - Part I: Modeling of Iodine and Noble Gas Release from the Core of a Light Water Reactor Following a Loss-Of-Coolant Accident," UILU-ENG-82-5362, University of Illinois, Urbana (May 1982).

2. F. Almerico and A. J. Machiels, "Performance Evaluation of Control Room HVAC System Under Accident Conditions - Part II: Modeling of In-Plant Contamination Transport," UILU-ENG-82-5363, University of Illinois, Urbana (July 1982).

3. Appendix A to Title 10 of the Code of Federal Regulations, Part 50, "General design criteria for nuclear power plants," Criterion 19 - Control Room.

4. K. G. Murphy, K. M. Campe, "Nuclear power plant control room ventilation system design for meeting general criterion 19," Proceedings of the 13th AEC Air Cleaning Conference (August 1974).

5. T. Y. Byoun, J. N. Conway, "Evaluation of control room radiation exposure," Proceedings of the 14th ERDA Air Cleaning Conference (August 1976).

6. G. Martin, Jr., D. Michlewicz, J. Thomas, "Fission 2120: A program for assessing the need for engineered safety feature grade air cleaning systems in post accident environments," Proceedings of the 15th ERDA Air Cleaning Conference (August 1978).

7. W. H. Miller, S. C. Ornberg, and K. L. Rooney, "A Consistent Approach to Air-Cleaning System Duct Design," Proceedings of the 16th DOE Nuclear Air Cleaning Conference (August 1980).

8. American National Standard "Nuclear power plant air cleaning units and components," ANSI/ASME N509-1980, The American Society of Mechanical Engineers (1980).

9. F. Almerico and A. J. Machiels, "Performance Evaluation of Control Room HVAC Systems Under Accident Conditions - Part III: Modeling of Control Room HVAC Systems and Calculations of Personnel Protection Factors," UILU-ENG-84-5303, University of Illinois, Urbana (August 1984).

CLOSING REMARKS OF SESSION CHAIRMAN PEARSON:

We wish to thank our authors for their excellent papers presented during this session. We also appreciate your participation during the question period. The papers presented today, together with contributions from researchers in the past, offer a firm foundation for future accomplishments in the area of control room habitability. The degree of concern evidenced by what we have heard today holds promise for the development of suitable tests methods and system design evaluations, the results of which will undoubtedly be the subject of our next session at the 19th Air Cleaning Conference.

Session 4

SOURCE TERMS AND ENVIRONMENTAL IMPACTS

MONDAY: August 13, 1984
CHAIRMEN: A.G. Evans
E.I. duPont de Nemours
J.P. Pearson
Nuclear Consulting Services

MONITORING OF NOBLE GAS RADIOISOTOPES IN NUCLEAR POWER PLANT EFFLUENTS
M.J. Kabat

NOBLE GAS CONFINEMENT FOR REACTOR FUEL MELTING ACCIDENT
P.R. Monson

TECHNICAL FEASIBILITY AND COSTS OF THE RETENTION OF RADIONUCLIDES DURING ACCIDENTS IN NUCLEAR POWER PLANTS DEMONSTRATED BY THE EXAMPLE OF A PRESSURIZED WATER REACTOR
H. Braun, R. Grigull, K. Lahner, H. Gutowski, J. Weber

DESIGN EXPERIMENTS FOR A VENTED CONTAINMENT
R. Hesbol

OPENING REMARKS OF SESSION CHAIRMAN EVANS:

This session is entitled Source Term and Environmental Impacts. Before the break we heard papers on reactor control room ventilation and in this particular session we will deal with a somewhat more hostile environment, the air from within the reactor room. The first paper will address monitoring noble gas radioisotopes in ventilation air, and the remaining papers will examine the feasibility costs and so on for trying to clean up various air streams. It is interesting to note that a couple of the papers represent different design concepts and also that this is truly an international conference. We have four papers and we have four different countries represented - Canada, U.S., West Germany, and Sweden. It is an interesting commentary on engineering design that we will hear how the operator of an older production reactor is trying to deal with the lack of containment, while new design concepts from Sweden are for power reactors that are proposing the use of deliberate ventilation bypass to deal with potential problems caused by containment.

MONITORING OF NOBLE GAS RADIOISOTOPES IN NUCLEAR POWER PLANT EFFLUENTS

M.J. Kabat
Ontario Hydro
Safety Services Department
757 McKay Road
Pickering, Ontario, L1W 3C8

ABSTRACT

Monitoring of gaseous radionuclides in the effluents of nuclear facilities is an essential requirement in effluent management programs. Since there is no practical way of removing noble gas radioisotopes from air at release pathways, their accurate monitoring is essential for providing appropriate environmental protection. Emitted gamma dose-rate is the limiting factor for concentration-time integral of noble gas in gaseous effluents of reactor facilities. The external exposure to the public from a semi-infinite cloud is directly proportional to both the noble gas isotope concentration and the integrated gamma energy per disintegration. Both can be directly measured in gaseous effluent pathways with a suitable detector.
The capability of NaI(Tl), CaF_2(Eu) and plastic scintillation detectors to measure the gamma-Ci.MeV content of noble gas releases was experimentally evaluated. The combination of CaF_2(Eu) detector in a pressurized through-flow chamber, with a charge integrating scaler well complied with both gamma energy response and detection sensitivity requirements. Noble gas source terms and effluent monitoring criteria are discussed, theoretical and experimental results are presented and a practical, on-line noble gas monitoring system is described in this paper.

I. INTRODUCTION

It has been generally accepted that radioactive effluents from nuclear facilities are to be maintained ALARA, recommended by the International Commission on Radiation Protection. The approval of site specific release limits (DRL) by national regulatory authorities has been a regular part of reactor licensing process. It is also generally required that radioactive effluents be monitored at the release pathways in order to provide data for the assessment of public doses, resulting from the operation of nuclear facilities, and to demonstrate the compliance with regulatory limits.

A complete system, used in Ontario Hydro nuclear generating stations for the monitoring of particulate radionuclides, radioiodines, noble gas and Tritium effluents, has been described in publication (1). The results of recent developments in the on-line, real time monitoring of variable mixtures of noble gas radioisotopes in nuclear power plant effluents, are presented and discussed in this paper.

II. PUBLIC EXPOSURE TO NOBLE GAS RADIOISOTOPES, RELEASED FROM NUCLEAR POWER PLANTS.

1. Gamma Ci.MeV Concept.

It was demonstrated in publication (2), that gamma dose rate from semi-infinite cloud of noble gas radioisotopes is the limiting factor for concentration-time integral of noble gas effluent from nuclear power plants.
Generally, the external dose rate from a semi-infinite cloud is directly proportional to both the noble gas isotopes concentration and their integrated gamma energy per disintegration ($\bar{E}\gamma$):

$$R = 0.25 \cdot \bar{E}\gamma \cdot C \qquad (rad.s^{-1}) \qquad \text{eq. [1]}$$

where:

$$\bar{E}\gamma = \sum (n_p \cdot E_p) \qquad (MeV.dis^{-1}) \qquad \text{eq. [2]}$$

C = atmospheric concentration of noble gas ($Ci.m^{-3}$)
n_p = number of gamma photons of energy E_p emitted per disintegration.

The gamma $MeV.dis^{-1}$ values for the most significant noble gas radioisotopes, calculated from decay data in reference (3), are listed in Table 1.

Radionuclide	Decay half-life	$\bar{E}\gamma$ ($MeV.dis^{-1}$)
^{85}Kr m	4.48 h	0.157
^{87}Kr	76.3 m	0.782
^{88}Kr	2.84 h	1.935
(^{88}Rb)	17.8 m	0.626
^{133}Xe	5.24 d	0.030
^{133}Xe m	2.19 d	0.024
^{135}Xe	9.11 h	0.245
^{135}Xe m	15.4 m	0.427
^{138}Xe	14.1 m	1.095
(^{138}Cs)	32.2 m	2.3

Table 1. Gamma-$MeV.dis^{-1}$ values of noble gas radioisotopes and their decay products in gaseous effluents of nuclear reactors.

2.2 Effective Tissue Dose

A number of theoretical models have been published (4,5,6,7,8) in which the ratio of exposure to dose, absorbed in critical organs (bone marrow, testes) of an anthropomorphic MIRD phantom were computed by the Monte Carlo technique, with considerations to the distribution of absorbed dose within a human body, relative risk of harm to different tissues of the body (weighting factors), non-uniformity of the radioactive cloud and its size, air-ground interface corrections and other factors.
Detailed discussion of this complex problem would not serve the purpose of this

paper. The required energy dependence of the noble gas effluent monitor has been approximated in this project to the 'environmental gamma monitors calibration curve', which was proposed in publication (9) from experimental data. In this publication A. Jones reported results of his experimental evaluation of weighted average whole body gamma dose, which was performed by measuring dose from photons (0.03 to 1.5 MeV energy range), absorbed at different points in a realistic phantom. From the measured energy dependence of the absorbed dose he derived calibration factors as a function of photon energy. The proposed energy dependence of calibration factors for environmental gamma-monitors is illustrated in Figure 1.

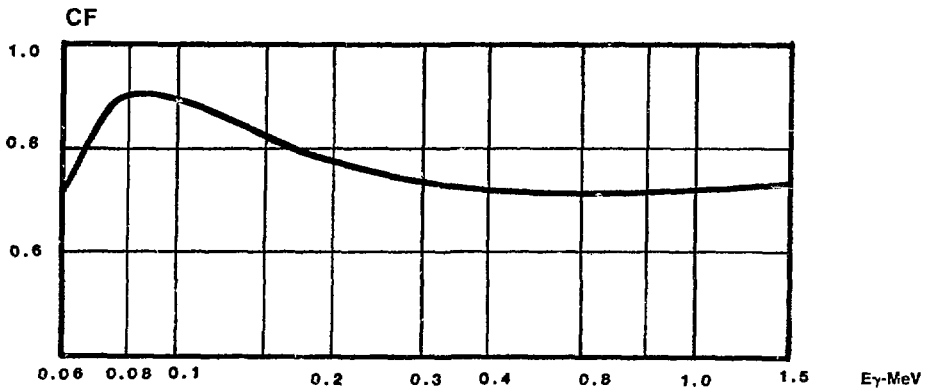

Figure 1. Energy dependence of calibration factors for environmental gamma monitors.

III. CHARACTERIZATION OF NOBLE GAS EFFLUENTS FROM CANDU NUCLEAR POWER PLANTS

On-line, real time gamma spectrum analysis of noble gas effluents was performed, under normal operating conditions, at Bruce NGS. with a multichannel gamma spectrum analyzer and a Ge(Li) detector in both, a pressurized-shielded and atmospheric pressure-nonshielded, through flow detection chambers. Several results were selected from the measurements at atmospheric pressure, to demonstrate the variability of noble gas composition in gaseous releases of this type of CANDU power plant.

Ventil. Stack	Date	Activity Concentration (8 hrs average) $\mu Ci.MeV.m^{-3}$ ^{133}Xe	^{135}Xe	^{88}Kr	^{41}Ar
0	80/10/28	0.37	0.22	0.26	ND
0	11/09	0.23	0.11	ND	0.71
0	12/01	0.83	0.34	0.23	ND
0	12/03	1.42	0.26	ND	ND
3C	09/06	0.22	0.11	ND	0.06
3C	09/17	0.03	0.05	0.24	8.98
3C	10/19	0.03	0.01	ND	1.61
4C	06/19	0.14	0.04	0.49	0.57
4C	07/09	0.34	0.23	0.12	2.56
4C	07/15	0.06	0.06	0.17	7.15
4C	07/21	11.24	0.15	ND	0.08

Table 2. Concentration range of major components in BNGS noble gas effluents.

It is evident from the above results that the composition of the major noble gas radioisotopes in stack effluents significantly changes, even under normal operating conditions. Gamma energies, emitted by the above radionuclides covers the range of 0.08 to 3.5 MeV.

IV. REVIEW OF METHODS AND SYSTEMS FOR THE MEASUREMENT OF NOBLE GAS EFFLUENTS.

A number of different methods and monitoring systems have been used for the monitoring of noble gas effluents from nuclear facilities. The most common ones are briefly reviewed:

- Direct detection of noble gas in air with beta detectors (GM or scintillation detectors) is relatively simple and sensitive, because external gamma background can be efficiently eliminated. However, it is suitable only in applications where a single radionuclide, or constant mixture of noble gas radionuclides is to be monitored in gaseous effluents.

- 'Gross counting' with non-corrected gamma detectors is also applicable for the monitoring of single noble gas isotopes and their mixtures with constant ratio.

- 'Gross gamma detection' of noble gas effluents with energy corrected GM tube was described in publication (1). While the energy response of this detector was found quite adequate for this purpose, its detection efficiency was not sufficient for the monitoring of chronic, low level noble gas releases from the Bruce and Darlington nuclear power plants.

- Real time, multichannel gamma spectrum analysis of noble gas effluent will generally provide required sensitivity and accuracy for non-routine analytical work. However such a system is not practical for routine, continuous monitoring of gaseous effluents because it is expensive, its operation is complex and requires much maintenance.

V. EVALUATION OF SCINTILLATION DETECTORS

The suitability of scintillation detectors for continuous, real time monitoring of gaseous effluents with variable composition of noble gas radioisotopes, was evaluated in this project. Preliminary theoretical considerations and the experimental program and results are further discussed.

1. Theoretical Considerations.

The portion of gamma ray energy, absorbed in some scintillators is proportional to its incident energy. The information on gamma dose rate can be obtained by the integration of electric charge from the photomultiplier. Since scintillation detectors have high efficiency and wide dynamic range for the detection of gamma radiation, they have good potential to satisfy most requirements on the real time monitoring of noble gas radioisotopes in nuclear power plant effluents.

Three types of scintillation detectors were considered for this purpose:
- Plastic scintillator type NE 105,
- NaI (Tl) crystal,
- CaF_2 (Eu) crystal,

The gamma energy dependence of their Mass Absorption Coefficients is illustrated in Figure 2.

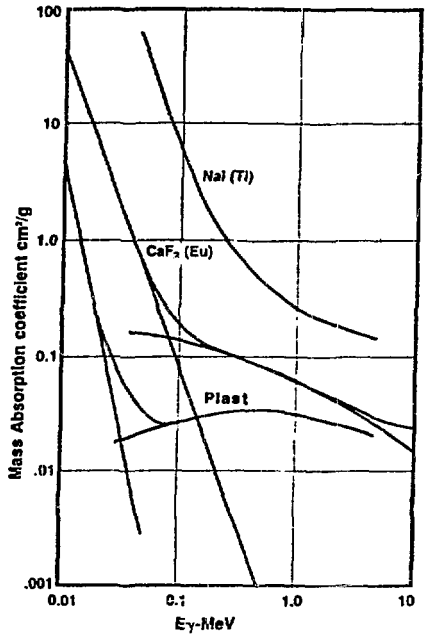

Figure 2. Energy dependence of mass absorption coefficients of NaI, CaF_2, and plastic scintillators.

The gamma energy loss in a plastic scintillator (from reference (10)), occurs mainly due to the Compton absorption component. The energy dependence of its Mass absorption coefficient is similar with water and muscle.

Cross section values of NaI and CaF_2 for gamma absorption, reproduced from reference (11), indicate large differences in their energy dependence. The graph shows that prevailing gamma absorption in NaI(Tl) occurs at low energies, up to 300 KeV, due to the photoelectric effect. This scintillator is very efficient for gamma detection, however, it also has strong energy dependence.

Compton absorption is the major mechanism of gamma absorption in CaF_2 scintillators over the required range of gamma energies. Slight contribution of photoelectric absorption at energies lower than 100 KeV is convenient for this purpose, to compensate for low energy gamma absorption in steel walls of a through-flow noble gas detection chamber. From the above data, CaF_2(Eu) detector was found to have the most suitable energy response for the purpose of the monitoring of 'gamma dose equivalent' from noble gas radioisotopes, released in gaseous effluents of nuclear reactors.

2. Optimization of Energy Response of Scintillation Detectors.

It was demonstrated above that the gamma energy dependence of the above three scintillation detectors increases in the order: Plastic scintillator < CaF_2(Eu) < NaI(Tl). With the use of 'photomultiplier charge integration' method, the energy response of plastic scintillator (type NE 105) would be similar to the tissue response. It was also apparent that the strong energy dependence of NaI(Tl) crystals would cause

significant error in the monitoring of the 'gamma dose equivalent' in gaseous effluents of nuclear reactors with variable ratio of noble gas radioisotopes.
While the portion of gamma energy, absorbed in plastic scintillators, is proportional to incident energy of the photons, practically every other scintillation detector needs to have its gamma energy response modified, to match the 'tissue response'. This can be performed in three ways:

- By dividing the measured range of gamma energy into several channels and multiplying detector counts from each channel by experimentally established calibration factors and integrating the product values to obtain the Ci.MeV values. This method would give the optimal approximation of the tissue (testes) response. However, it is not very convenient for field applications because it requires relatively complex instrumentation, calibration and maintenance procedure.

- By the integration of charge from Photomultiplier/Linear Amplifier and transferring it to digital signal. The rate of digital pulses from the 'Wilkinson Peak Amplitude to Digital Converter' is proportional to the portion of gamma energy, absorbed in the scintillation detector. However, the energy dependence of 'Total' Mass Absorption Coefficients of most scintillation gamma detectors still has to be compensated for, by additional electronic circuits or composite shielding of the crystal, in order to obtain a 'tissue equivalent response'.

- By Gamma filtration and direct counting of detector pulses.
Typical gamma detection crystals are more sensitive within a low to medium energy region (due to prevailing photoelectric absorption). This can be partially compensated for by the installation of an appropriate gamma absorber, which functions as a filter between the crystal and measured gas. This simple method has been frequently used for the energy compensation of GM gamma detection tubes in field dose survey instruments, however, for the monitoring of noble gas in reactor effluents it does not provide adequate approximation of dose to testes from the direct pulse rate of scintillation detectors.

- Combination of the above energy compensation methods.
Good approximation of the tissue response can be achieved from some combinations of a suitable scintillation detector with optimized gamma filters and charge digitizer/scaler pulse processing.
The combination of composite shielding with the first method above can also eliminate the need for individual calibration factors for each channel of the pulse processing system. This method of 'Ci.MeV monitoring', which was used in our experimental evaluation of selected scintillation detectors, is described in the next chapter.

VI. EXPERIMENTAL EVALUATION OF ENERGY RESPONSES.

1. Method Description.

The method used in this study is based on the integration of values, obtained from the multiplication of net pulses from each channel by its average gamma energy, which is expressed by following equation:

$$CME = DRV \cdot F \qquad \text{eq. [3]}$$

$$DRV = \sum_{1}^{15} (cpm_n \cdot \bar{E}_{\gamma_n}) \qquad \text{eq. [4]}$$

where:

CME	=	Ci.MeV equivalent	(Ci.MeV)
DRV	=	Detector Response Value	(cpm.MeV)
F	=	Calibration Factor	($Ci.cpm^{-1}$)
n	=	Energy channel number	
cpm_n	=	net count rate in channel 'n'	
$\bar{E}_{\gamma_n}$	=	mean gamma energy in channel 'n'	

The energy response of tested detectors was evaluated within the gamma energies range of 50 KeV to 3.3 MeV, which was divided into fifteen counting channels. Net counts from each channel were multiplied by the mean energy value of each channel and the resulting products integrated, to obtain 'Detector Response Values'. This process was repeated with each of 10 used radiation standards, covering the gamma energies range of 60 KeV to 3.3 MeV. The DRVs for the averaged energy of each radionuclide were plotted into the energy response graph for each tested scintillator-filter combination. The degree of approximation of the energy response of each measured detector-filter combination to the tissue response was then graphically evaluated.

2. Experimental Set-up.

Functional diagram of the testing system is illustrated in Figure 3.

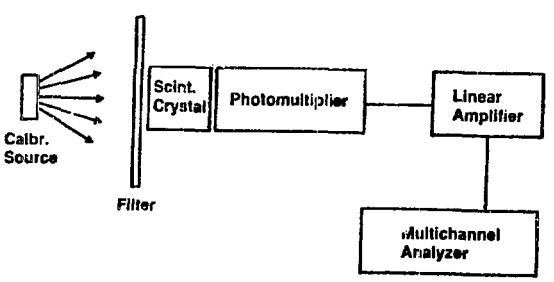

Figure 3. Experimental set-up for the evaluation of energy dependence of scintillation detectors.

Description of individual functional components and their technical specifications follow:

Radiation Sources:

Ten NBS and Amersham standard radiation sources were used for the evaluation of energy response of selected detector/filter combinations. The range of their major gamma energies and gamma activity values are listed in Table 3.

Radionuclide	Gamma energy range Eγ - MeV	Gamma activity μCi.MeV
^{241}Am	0.06	0.022
^{170}Tm	0.05-0.084	0.008
^{57}Co	0.12-0.137	0.258
^{75}Se	0.07-0.4	1.487
^{133}Ba	0.08-0.38	2.707
^{137}Cs	0.66	5.220
^{54}Mn	0.835	6.008
^{60}Co	1.17-1.33	11.80
^{88}Y	0.9 -1.8	0.352
^{56}Co	0.8-3.3	6.107

Table 3. Standard sources, used in the evaluation of energy dependence of scintillation detectors

Gamma Filters:

Several combinations of detection crystal with a filter, made of individual metals or their composite at different thicknesses, were tested. The suitability of following metals was evaluated: Stainless steel, Carbon steel, Aluminum and Lead. Their thickness and combination was calculated from their Mass Attenuation Coefficients, in relation to the energy response of NaI and CaF_2, to obtain the optimal approximation of the required 'tissue response'. Specific attention was given in the the calculations to proper utilization of the 'K edge' of lead, at 88 KeV, to flatten the energy response in the low energy region.

Detector Probes:

Three types of scintillation detectors were evaluated:

- Plastic scintillator, NE 105, sizes 10 x 50 and 50 x 50 mm,
- NaI (Tl) crystal, 50 x 50 mm,
- CaF_2 (Eu) crystals, 10 x 50 and 25 x 50 mm.

The above scintillators were optically coupled with a Harshaw assembly of a photomultiplier with a preamplifier. The detection probes were shielded with 100 mm of purified lead for the evaluation of the effect of external gamma background in operational field.

Energy Channels Analyzer:

A Canberra 8180 Multichannel Analyzer was used, in 15 channels mode, covering the gamma energy range of 0.05 to 3.3 MeV. Gamma background pulses were measured in each channel and subtracted from counts, measured in individual channels with the used standard radiation sources. Resulting 'net counts' were processed in the way, described in # VI. 1.

3. Discussion of Results.

The measured energy responses of the tested scintillation detectors were generally in agreement with calculated values.

From the experimental results the plastic scintillators were not found very suitable for this purpose, because, at discriminator bias setting identical with other tested scintillators, its detection efficiency was rapidly decreasing at gamma energies below 150 KeV. This was apparently caused by the combination of relatively low light transfer efficiency of plastic scintillators, with 50 KeV discrimination (to reduce PM noise and external background pulses). It would become still more significant with additional shielding, caused by metal walls of a through-flow sample chamber. Also the ratio of counts from activity/background was found to be much lower from plastic scintillators than from NaI(T1) and CaF_2(Eu) crystals.

Experimentally determined energy response curves of NaI(T1), 50 x 50 mm scintillator with several filter combinations, and CaF_2(Eu), 25 x 50 mm, with the optimal filter configuration are illustrated in Figure 4.

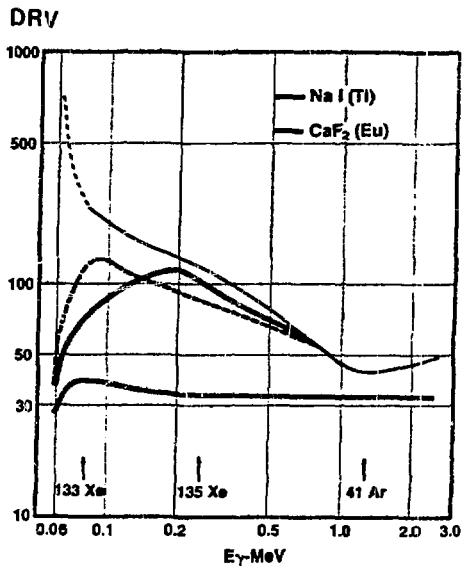

Gamma filters composition:

- with NaI (T1):

1. 1 mm stainless steel
2. 3 mm stainless steel + .24 mm lead
3. 1.5 mm stainless steel + 2 mm copper

- with CaF_2 (Eu)

4. 3 mm stainless steel + .24 mm lead

Figure 4. Measured energy response of scintillation detectors/gamma-filters.

The relative energy response of NaI and CaF_2 scintillators for four major components, (^{133}Xe, ^{135}Xe and ^{41}Ar and ^{85}Kr) in gaseous effluents of *CANDU* reactors, is further summarized:

The measured Detector Response Values of NaI(T1) detector were strongly dependent on gamma energy, within the range of 0.05 to 1 MeV, in all tested combinations with metal filters. The relative response of the above detector/filter combinations to three main components in noble gas effluents is summarized in Table 4.

Detector	Filter	Relative response of the detector to: ^{133}Xe	^{135}Xe	^{41}Ar
NaI(Tl)	1 mm stainless steel	5	3	1
	3 mm st.steel + 0.24 mm lead	3	2	1
	1.5 mm st.steel + 2 mm copper	1.8	2.5	1
CaF_2(Eu)	3 mm st.steel + 0.24 mm lead	1.2	1	1

Table 4. Relative response of detector/filter combinations (from Figure 4) to three major components in noble gas effluents.

The graph in Figure 4 also shows that the energy dependence of CaF_2(Eu) detector can be made very suitable for the monitoring of noble gas effluents by incorporating a filter, composed of 3 mm of stainless steel and 0.24 mm lead.

VII. EVALUATION OF A NOBLE GAS MONITOR PROTOTYPE WITH CaF_2(Eu) DETECTOR

Figure 5 shows that the energy response of CaF_2(Eu) detector, with the gamma filter of 3 mm stainless steel + 0.24 mm lead, was sufficiently similar with the proposed calibration curve. The stainless steel filter is also practical to form sufficiently strong walls, to satisfy structural requirements for a pressurized through-flow detection chamber, which is needed for achieving required detection sensitivity for the monitoring of noble gas effluents under the conditions of variable external gamma background. Therefore a gas detection system prototype was built and calibrated with radioactive gas, to experimentally asses its detection sensitivity under operational conditions.

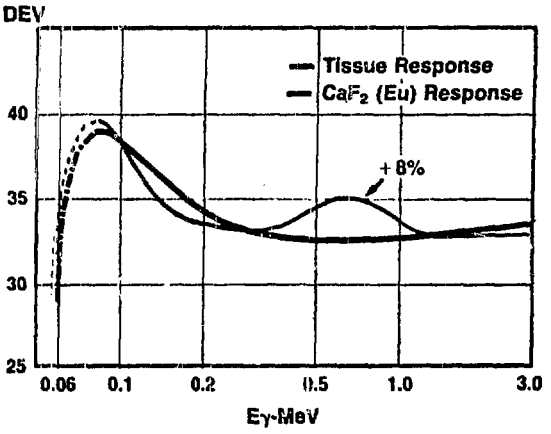

Figure 5. Comparison of the proposed calibration factors for environmental gamma monitors with the measured response of CaF_2 (from Figure 4).

1. Description of the Gas Detection System:

A Marinelli Beaker type detection chamber was made of 12 Gauge stainless steel, with internal volume of 5 l, shielded with 100 mm of lead pellets and a Harshaw 25 x 50 mm $CaF_2(Eu)$ scintillation detector (with a supplementary gamma filter) was inserted in its detection well. The detection efficiency of this system was calibrated with a secondary standard, ^{131}I in the form of CH_3I gas. The calibration measurements were repeated with different concentrations of the calibration gas (ranging from 0.3 to 48 $\mu Ci.MeV.m^{-3}$.
The signal processing method was the same as the method, used in the energy response evaluation (described in # 6.1)

2. Calibration Results:

At normal atmospheric pressure and average concentration of 20 $\mu Ci.MeV.m^{-3}$ of ^{131}I calibration gas within the detection chamber, following 'net DRV' and F value (see equation 3) were obtained:

$$\text{net DRV} = 4.67 \times 10^{3} \text{ cpm.MeV per } \mu Ci.MeV.m^{-3}$$
$$F = 2.14 \times 10^{-4} \ \mu Ci \text{ per cpm}$$

Exposing the detector to 25 $\mu R.hr^{-1}$ external gamma background, a value of 32.9 $\mu Ci.MeV.m^{-3}$ equivalent per $\mu R.hr^{-1}$ γ field was measured.

8. FIELD MONITORING OF NOBLE GAS EFFLUENTS

1. Field monitoring requirements are site specific. They are derived from:

- regulatory release limits (Ci or Ci.MeV per time period)
- total volume of air, discharged per time period (dilution factors)
- required dynamic monitoring range for noble gas concentrations in the effluents (MDA/maximum range)

The actual detection limits are then derived from following theoretical and operational factors:

- statistical counting error,
- external gamma background levels and its variability,
- internal contamination of detection chamber
- accuracy of effluent flow determination and its operational variability,
- internal pressure of the detection chamber and its variability,

2. Detection Limits of the Basic System.

Detection limits were derived for the Darlington NGS , which has the highest dilution of noble gas in gaseous effluents. The DEL value of 2.2×10^{5} $Ci.MeV.wk^{-1}$, at total effluent flow of 8.5×10^{4} $m^3.min^{-1}$, results in the 'gamma activity concentration' of 25.5 $\mu Ci.MeV.m^{-3}$.

Under constant background conditions and integrating period of 1 or 24 hrs following 'Detector Response Values' would be obtained from the above described prototype of noble gas monitor:

0.1 % DRLconc. – 'integrated DRV' = 7140 / hr, or 171360 / 24 hrs
ext.bkgr. 25 $\mu R.hr^{-1}$ – 'bkg DRV' = 49320 / hr, or 1183680 / 24 hrs
ext.bkgr. 500 $\mu R.hr^{-1}$ – 'bkg DRV' = 986400 / hr, or 23673600 / 24 hrs

Lower Detection Limit:

0.1 % of DRL could be measured, at 95 % confidence level, with the accuracy of:

7 % at 25 $\mu R.hr^{-1}$, or
28 % at 500 $\mu R.hr^{-1}$ and integrating period of 1 hr,

1.4 % at 25 $\mu R.hr^{-1}$, or
5.7 % at 500 $\mu R.hr^{-1}$ and integrating period of 24 hrs.

Upper Limits of Detection:

Noble gas concentrations of 10 x DRL can be measured with the dead time loss of < 4 % and concentrations of 40 x DRL (1 $mCi.MeV.m^{-3}$) with < 10 % loss.

Under variable background conditions, an increase of external gamma background by 25 $\mu R.hr^{-1}$ (averaged through the applied integration period) above the actually subtracted background level, would cause an overestimate of:

the noble gas activity concentration by 0.176 $\mu Ci.MeV.m^{-3}$,

or the release portion, reported for the integration period from an individual release pathway to be overestimated by 0.7 % of DRL.

The overestimation of effluent monitoring results, due to internal contamination of the detection chamber, would be negligible in complete monitoring systems in which a particulate and iodine sample collectors are installed upstream of the noble gas detection chamber.

Changes of internal pressure due to atmospheric pressure variations would have negligible effect on the detection efficiency. In pressurized chambers, constant positive pressure can be easily maintained within ± 10 % of the set-point.

3. Detection Errors in Operational Field.

The Design Target, established for the Ontario Hydro nuclear power stations, requires that radioactive releases to the environment be maintained below 1 % of DRL. The noble gas effluent monitor should be capable to measure a fraction of this target level with a reasonable accuracy.
Results of the above assessment show that 0.1 % DRLconc. can be accurately measured with the tested system under the condition that external background level remains absolutely constant. However, background variations of only 35 $\mu R.hr^{-1}$ would cause an

experimental error of 1 % DRL. Under the realistic assumption that typical levels of external background in the effluent monitor location are 0.1 ± 0.05 $mR.hr^{-1}$, the detection of ± 1.5 % of DRL in the effluent would be masked with these, relatively low, external background variations. Therefore, a significant improvement in the 'activity/background' signal ratio was needed to comply with the detection sensitivity requirements under actual field conditions. Three methods were considered for this purpose:

- the use of larger detected volume of the sample, at atmospheric pressure, does not sufficiently increase the sensitivity. At sample volumes exceeding 10 l the detection geometry factor is rapidly decreasing. Also, it is difficult and expensive to provide appropriate shielding for large volume detection chambers.

- sample collection by its physical adsorption with adsorbents is not practical for this purpose. Significant experimental errors would result from different adsorption coefficients for each element (Ar, Kr, Xe), and from strong dependence of the adsorption equilibrium on temperature and relative humidity of the gas sample (moisture content in the adsorbent).

- Maintaining gas sample at moderate pressures in the detection chamber was found to be the optimal method for this purpose. While the detection geometry and shielding requirements remain at their optimal values, the detected amount of sample can be easily increased up to tenfold with a regular air compressor and pressure control valve. Stainless steel walls, 3 mm thick, provide for sufficiently high safety factor even at operating pressure of 10 atm in the detection chamber. A schematic diagram of a pressurized detection chamber, which was used for the analysis of noble gas effluents at BNGS, is given in Figure 6.

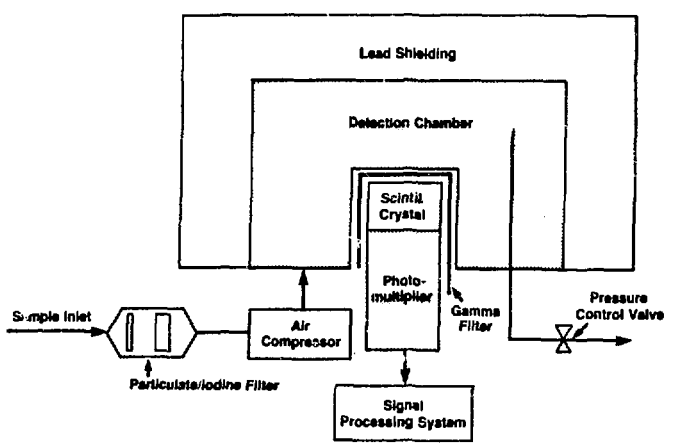

Figure 6. Schematic diagram of a pressurized, through-flow, noble gas detection chamber.

Detection errors, calculated from the above calibration data and detector's response to the external gamma background are summarized in Table 4.

Sample pressure in the detection chamber	Const.exter.backgr.	Variable external background			
	Stat.error in the measurement of 1 DRL at 95 % confid.level ($\pm$ 2 σ)	Detection error due to variability of external γ background $\pm$ 25 $\mu R.hr^{-1}$		$\pm$ 100 $\mu R.hr^{-1}$	
		% DRL	$\mu Ci.MeV.m^{-3}$	% DRL	$\mu Ci.MeV.m^{-3}$
1 atm	26×10^{-3}	0.7	0.179	2.76	0.704
5 atm	5×10^{-3}	0.14	0.036	0.56	0.143
10 atm	2×10^{-3}	0.07	0.018	0.28	0.071

Table 4. Summary of detection errors, occuring in the application of 25 x 50 mm $CaF_2(Eu)$ scintillator in 5 l detection chamber for continuous monitoring of noble gas effluents.

IX. CONCLUSIONS

A system was developed which is suitable for continuous monitoring of 'Gamma Ci.MeV Equivalent' of noble gas radioisotopes in nuclear power plant effluents. The system is based on a $CaF_2(Eu)$ scintillation detector with a charge integrating signal processor (e.g. Wilkinson peak amplitude to digital converter).
Its performance was experimentally evaluated under simulated, field monitoring conditions. Following conclusions were drawn from the results:

1. The measured energy response of this detector was within $\pm$ 5 % of the tissue response, from which calibration requirements for environmental gamma monitors were specified. This will efficiently eliminate energy dependence errors (from the variability of the noble gas composition), presently occuring in the monitoring of reactor effluents.

2. With a positive pressure (5 - 10 atm), through-flow detection chamber of 5 l volume, this noble gas monitor has sufficient sensitivity to measure a fraction of the 'Hydro Design Target' noble gas concentrations (0.255 $\mu Ci.MeV.m^{-3}$) in power plant effluents, even in variable ambient gamma background.

3. This detector also provides sufficiently wide dynamic range for the monitoring of noble gas effluents under emergency release conditions. It can detect activity concentrations of > 1 $mCi.MeV.m^{-3}$ with 'dead time counting loss' of < 10 %.

4. The operation, maintenance and calibration of this monitor would be relatively simple.

5. The optical and physical properties of $CaF_2(Eu)$ crystal are suitable for this purpose. It has high light collection efficiency, no 'afterglow' and high resistance to mechanical and thermal shocks. The temperature dependence of its light output is similar with other scintillation crystals.

Performance evaluation of a complete prototype of this noble gas monitor, assembled of commercially available modular components, is scheduled for the near future.

Acknowledgement

The author wishes to acknowledge the cooperation of J.L. Hartwell on the experimental part of this project.

X. REFERENCES

1. Kabat M.J.,
Recent Developments in Gaseous Effluent Monitoring in Ontario Hydro.
IAEA Seminar 'Monitoring of Radioactive Effluents from Nuclear Facilities'
Portoroz, 1978

2. Slade D.H., Meteorology and Atomic Energy, USAEC Rep. TID-24190/1968

3. Kocher D., Radioactive Decay Data Tables, DOE/TIC - 11026

4. Jones T.D., Auxier J.A., Snyder W.S.
Dose to Standard Reference Man from External Sources of Monoenergetic Photons.
Health Physics 24, 241-255, 1973

5. Poston J.W., Snyder W,S.
A Model for Exposure to a Semi-Infinite Cloud of a Photon Emitter.
Health Physics 26, 287-293, 1974

6. Dillman L.T.
Absorbed Gamma Dose Rate for Immersion in a Semi-Infinite Radioactive Cloud.
Health Physics 27, 571-580, 1974

7. O'Brien K., Sanna R.
The Distribution of Absorbed Dose-Rates in Humans from Exposure to Environmental Gamma Rays. Health Physics 30, 71-78, 1976

8. Ryman J.C., Faw R.E., Shultis K.
Air-Ground Interface Effect on γ-Ray Submersion Dose.
Health Physics 41, 759-768, 1981

9. Jones A.R., Proposed Calibration Factors for Various Dosimeters at Different Energies, Health Physics 12, 663-671, 1966

10. Radiological Health Handbook, US Dept. of Health, 1970

11. Harshaw Scintillation Phosphors, The Harshaw Chemical Company, 1978

DISCUSSION

KAISERUDDIN: What is the lower limit of detectability of the calcium fluoride detector?

KABAT: The table on the last page shows the sensitivity in microcuries per hour. For $\pm$ µR. hr^{-1}, external background, we can measure 0.02 µCi.MeV.m^{-3}. If the background is 100 µR. hr^{-1}, which is practically the maximum field change we would expect in operations, we can still measure 0.07 µCi.MeV.m^{-3} as the minimum detectable activity. Even thousandths of µCi.MeV.m^{-3} are measurable with good accuracy when the background is steady. That's the limiting factor and then there is only the statistical error.

KOVACH, B.: Did you consider using a software correction, rather than metal filters, for energy equalization in your dose rate calculations?

KABAT: Yes, that was one of the methods we considered and it is described in our preprint. However, it requires a different calibration factor for each channel. Software corrections would be applicable only in the "channel counting method," used in our experimental investigation. We used a TI59 for this simple task. However, this channel counting method is less suitable for field applications than the recommended "charge digitizing method," which does not need any correction of the detector's output.

KOVACH,B.: There already exists a software solution for that problem and I know it corrects all the energy curves.

KABAT: But, as I said, the input has to be divided into at least 5 or 7 channels, and that is the difficulty in the field.

NOBLE GAS CONFINEMENT FOR REACTOR FUEL MELTING ACCIDENTS*

Dup

Paul R. Monson
E. I. du Pont de Nemours & Co.
Savannah River Laboratory
Aiken, South Carolina 29808

Abstract

In the unlikely event of a fuel melting accident radioactive material would be released into the reactor room. This radioactive material would consist of particulate matter, iodine, tritium, and the noble gases krypton and xenon. In the case of reactors with containment domes the gases would be contained for subsequent cleanup. For reactors without containment the particulates and the iodine can be effectively removed with HEPA and carbon filters of current technology; however, noble gases cannot be easily removed and would be released to the atmosphere. In either case, it would be highly desirable to have a system that could be brought online to treat this contaminated air to minimize the population dose.

A low temperature adsorption system has been developed at the Savannah River Laboratory to remove the airborne radioactive material from such a fuel melting accident. Over two dozen materials have been tested in extensive laboratory studies, and hydrogen mordenite and silver mordenite were found to be the most promising adsorbents. A full-scale conceptual design has also been developed. Results of the laboratory studies and the conceptual design will be discussed along with plans for further development of this concept.

Introduction

Most commercial power reactors use a "leaktight" containment dome over the reactor vessel to contain the gases and aerosols released in a core melting accident. These radioactive gases are contained under the dome or in an auxiliary building until the highly radioactive species have decayed, at which time, the less hazardous krypton-85 can be safely released to the atmosphere. This is the scenario that occurred at TMI. However, the Savannah River Plant (SRP) production reactors were built without containment domes but with a very large buffer zone between the reactors and the public. A partial confinement system was added in the early 1960's which can effectively contain radioactive particulates and iodine, but cannot prevent the release of noble gases. Various improved confinement alternatives have been considered for these reactors, and one of the most promising techniques is adsorption of the noble gases on a solid. This technique is applicable not only to SRP reactors but also to power reactors with containment domes and auxiliary containment buildings which could leak, thus releasing the trapped radioactive gases to the environment before sufficient decay has taken place.

* The information contained in this article was developed during the course of work under Contract No. DE-AC09-76SR00001 with the U.S. Department of Energy.

This work is the application of earlier work by the Savannah River Laboratory[1,2] and others[3,4] on using adsorption for treating reprocessing off-gas. The purpose of the present work is to apply this technique to the much more difficult reactor accident case, including the development of a conceptual design for such a system. Table 1 is a comparison of the design basis for a full core melt accident versus reprocessing off-gas treatment.

Table 1. Comparison of reactor accident versus fuel reprocessing off-gas.

	Reactor	Reprocessing
Process	Accident response	Continuous
Air flow, cfm	8000	400
Radioactive isotopes	Kr-88, Xe-133	Kr-85
Concentrations, ppm	200 (Kr), 1700 (Xe)	15 (Kr), 80 (Kr)
Decay heat, watts	10^6	10^2
Curies	$>10^8$	10^6/year
Dose, rads/hr	10^9-10^{10}	10^2-10^3

Methods of Noble Gas Retention

Work has been carried out for many years on removing the radioactive noble gas krypton-85 from the off-gas of fuel reprocessing plants. Several competing and promising methods have been identified including: cryogenic distillation, fluorocarbon absorption, and solid adsorption. However, there are substantial differences in flow rates, decay heat, and dose between the reactor accident and the dissolver off-gas (DOG) cases (Table 1). These differences make the reactor accident case much more difficult. The potential application of these and other methods, based on both the physical and chemical properties of the noble gases, to confine the noble gases from a reactor accident are discussed below.

Cryogenic Distillation

Cryogenic distillation uses the difference in boiling points of the noble gases and nitrogen to effect a separation at low temperatures. While this method is well established as a means of routine air separation, and could be used in a nuclear fuel reprocessing plant, there are major problems with its use in the reactor case. Such a system would be very expensive to operate since it would need to be in a standby condition at cryogenic temperatures indefinitely in order to have the response time to handle an accident situation. Cryogenic distillation is also

carried out under relatively high pressure, thus decreasing reliability, and presenting a safety problem by having concentrated highly radioactive materials under high pressure. A severe hazard would exist with concentrated oxygen and the subsequent radiolysis of oxygen to produce ozone. These problems and expected high costs rejected cryogenic distillation from further consideration.

Fluorocarbon Absorption

Fluorocarbon absorption takes advantage of the solubility difference between the noble gases and nitrogen in fluorocarbon solvents such as fluorocarbon-12. This method has been extensively developed at ORGDP (Oak Ridge Gaseous Diffusion Plant), and a pilot plant has been operated there for several years.[5] The method was developed for removing Kr-85 from reprocessing off-gas and is expected to work well for that application. However, fluorocarbon absorption is impractical for the reactor accident situation because of scale-up problems, and would be prohibitively expensive. While the radiation damage to the fluorocarbon from Kr-85 is acceptable, the degradation in the much higher radiation fields in the reactor case would be prohibitive. Fluorocarbon absorption would be a viable method to treat the noble gases once they were contained and the highly radioactive isotopes decayed, but for the reactor accident case it would be unacceptable.

Selective Permeation

Selective permeation depends on the permeability difference of the noble gases and air through a membrane to effect a separation. Only small-scale laboratory studies have proved practical due to the difficulty of producing large homogeneous membranes. These membranes are usually organic materials and very susceptible to radiation damage.[6] Permeation also depends on a large pressure difference and would require having radioactive gases concentrated under high pressure. These problems preclude the further consideration of selective permeation.

Selective Ionization

Selective ionization would require the preferential ionization of one or more of the species Kr, Xe, N_2, and O_2 over the others. The ionization source could be a laser, conventional light source, electrical discharge, etc. The separation of the ionized species could be by a charged collector or through enhanced chemical reactivity which produces a chemical compound more easily separated from the others by conventional separation techniques. Unfortunately these techniques require concentrated levels (%, instead of ppm) of the species to be removed, and would require some means of preconcentrating the noble gases prior to selective ionization. (If we could easily preconcentrate we would have what we need already.) Other excitation techniques, such as photolytically producing fluorine atoms to react with Kr and Xe which are then separated as solids, have been carried out on a laboratory scale using concentrated noble gases, but this technique is not practical for large

scale, dilute systems. The many problems related to any selective ionization technique preclude the further consideration of this method at this time.

Gas Centrifugation

Due to the very large differences in atomic weights and gas densities one could conceive of a separation by gas centrifugation. However, present gas centrifugation techniques obtain a fraction of the throughput necessary while being enormous in size and expense. In addition they work at low pressure requiring high vacuum pumps. It is impractical to consider a large-scale centrifugation system to handle a core melting accident.

Inclusion Compounds

Inclusion compounds or cage type structures formed with the noble gases trapped within the cages have been made. Most of these cage compounds or clathrates are made with large organic molecules such as phenol (C_6H_5OH) and hydroquinone ($C_6H_4(OH)_2$); however, these organic structures cannot withstand the high radiation field. In addition high pressures and high noble gas concentrations are required. The same problems of high pressure and high concentrations limit the usefulness of the non-organic or ice clathrates formed with water.

Chemical Compounds

For many years the noble gases were truly inert gases in that no chemical compounds had been made with them. However, in 1962 the first noble gas chemical compounds were made with xenon, fluorine, and platinum. Since that time noble gas chemistry has continued to be a research laboratory curiosity with only tens of compounds made with xenon and fluorine (the most electronegative element). Harsh laboratory conditions of concentrated noble gas, and highly reactive fluorine, high pressure, and low temperature are required to make these compounds. The separation of the noble gases from air in a reactor accident situation using noble gas chemistry is far from being practical at this time.

Solid Adsorption

The last and most promising method to be discussed is the removal of the noble gases from air using solid adsorbents. Solid adsorption has been suggested by Monson,[1,2] Pence,[3] and Ruthven[4] as a method of removing krypton-85 from reprocessing off-gas. The chemical process industry uses similar techniques to clean process gases on a scale as large as 100,000 cfm, so scale-up should be no problem. The solids under consideration are all inorganic aluminosilicates which are highly resistant to radiation damage. The only potential problem, which can be handled by engineering design, is the effective removal of the decay heat. Since solid adsorption appears to be the most promising method for removing the noble

gases from a reactor accident, we chose to further develop this method. In this research we are seeking new materials with the best combination of noble gas capacity, krypton/nitrogen separation factor, and availability at a reasonable cost.

Experimental

The experimental technique and apparatus used is the same as that previously described.[1] Figure 1 is a photograph of this apparatus.

The candidate materials were sieved to 20 to 40 mesh, washed to remove fines and dried overnight in air at 100°C in an oven. The dried materials were then loaded into preweighed 10 foot by 1/8 inch stainless steel columns; the columns were then reweighed to give the net weight of material in each column. The columns were then placed in the oven of a Varian 1720 Trace Gas Analyzer equipped with helium ionization detectors, and conditioned overnight at 300°C with pure helium flow. All noble gas dynamic adsorption capacity measurements were made by injecting pure krypton and xenon onto the column using helium as the carrier gas. Comparisons were made with other work using the same material and conditions, but with nitrogen as a carrier (more like air than helium) and were found to be within 20% of the helium data.

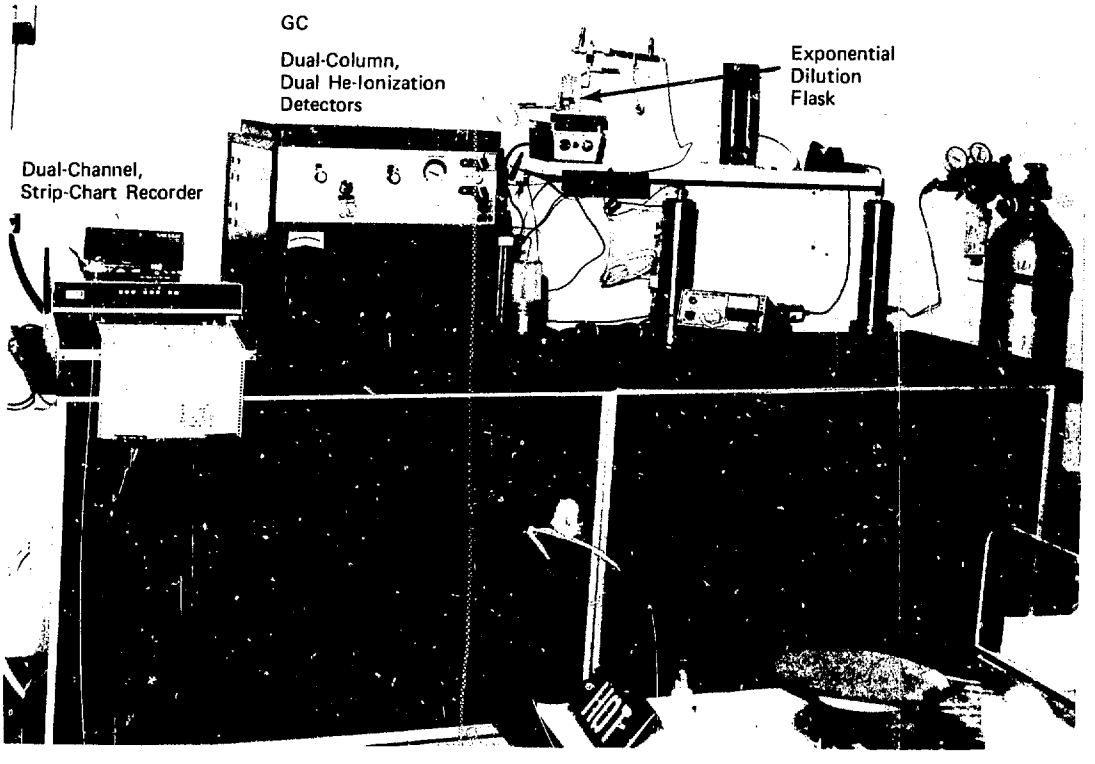

Figure 1. Experimental apparatus

Results

Over a dozen materials were investigated as part of the reprocessing off-gas work, and results on these materials have been published.[2]

Over a dozen additional materials were investigated during the present study. These materials can be grouped into three categories: (1) the synthetic zeolite molecular sieves (dealuminated and acid-washed hydrogen mordenite), (2) natural zeolites (Z-400®, Z-500®, Z-700®, and the Zeosorbs®), and (3) amorphous materials (charcoal and carbon molecular sieve). Table 2 summarizes the dynamic adsorption capacities for krypton, nitrogen, and xenon, as well as the krypton/nitrogen separation factor for each of these materials. The adsorption capacity indicates how effectively the material retains a certain gas, which relates to how much material

Table 2. Dynamic adsorption capacity in cc adsorbate/g adsorbent, expressed as one atmosphere partial pressure of adsorbate at 24°C.

Material	Krypton	Xenon	Nitrogen	Kr/N_2 Separation Facts
Hydrogen mordenite	60	560	15	4.0
Silver mordenite	160	10,000	85	1.9
Dealuminated hydrogen mordenite	50	390	15	3.3
Acid-washed hydrogen mordenite	50	380	15	3.3
[1]Zeolon-400®	5	15	-	-
[1]Zeolon-500®	60	1,650	120	0.5
[1]Zeolon-700®	60	-	90	0.7
[2]Zeosorb®	60	480	70	0.8
Zeosorb®-Ag	160	18,000	50	3.2
Zeosorb®-K	20	970	15	1.3
Zeosorb®-Ce	80	2050	130	0.6
SK-4 Charcoal	70	1,860	20	3.5
Carbosieve-S	360	10,900	55	6.5

1 - Norton Company (USA).

2 - Laporte Industries (England).

would be necessary to confine a given volume of that gas. The separation factor is equally important in that it indicates the efficiency of the separation between krypton and air (mainly nitrogen).

The table shows that the carbon molecular sieve Carbosieve-S has the greatest capacity for krypton, a very high capacity for xenon, and also the highest Kr/N_2 separation factor; however, it is not commercially available in large quantities and is thus prohibitively expensive. The other carbon material SK-4 Charcoal, also looks promising; however, the danger of combustion is present with any of the carbon materials while all of the other materials are noncombustible.

Silver exchanged Zeosorb® has a greater capacity for krypton, xenon, and a higher Kr/N_2 separation than silver mordenite; however, it is more expensive to produce (it contains a higher percentage of silver). Outside of the carbons, hydrogen mordenite still has the best separation factor as well as good capacity at a reasonable cost for this commercially available material. The Zeolon-500® and Zeosorb®-Ce have high affinities for xenon at low costs; however, both materials retain nitrogen more strongly than krypton.

A production separation system might use a mixture of these materials to obtain the desired capacity and separation while optimizing the size of equipment at a reasonable cost.

The data listed in Table 2 are for the adsorption of the gases at STP, but it is well known that the adsorption capacity is an inverse function of temperature, with increasing capacity at lower temperature. The capacity increases about a factor of 3 for a 30°C decrease in temperature. This means that there is an optimization of cost of cooling to lower temperatures versus advantages of increased capacity in terms of column size and reduced material costs.

Conceptual Design

Once the survey of possible methods of noble gas retention was completed and solid adsorption chosen as a promising candidate technique based on the small-scale laboratory studies, a conceptual design of such a system for SRP reactors was developed. Figure 2 is a schematic of such a system.

In the unlikely event of a fuel melting accident at SRP, the reactor room exhaust would be separated from the other process areas and the exhaust flow reduced to a minimum while maintaining negative pressure inside the reactor room (approximately 8000 cfm) at the same time water sprays would be turned on to reduce the airborne halogens. The diverted flow initially passes through a compressor provided to overcome the resistances in the downstream molecular sieve beds. The air stream next passes through a multi-purpose pretreatment unit that operates at elevated temperatures (>150°C). This unit consists of two beds. The first is a hydrogen recombiner (noble metal catalyst on zeolite) that converts the

gaseous hydrogen isotopes (H_2,T_2, and HT) to their oxide form for subsequent removal. The second bed uses silver mordenite to remove both elemental and organic forms of iodine. The size of the adsorbent (catalyst) particles in both beds in the pretreatment unit would be sized to remove particulates from the air stream.

The air stream exiting this pretreatment unit would contain radioactive noble gas and moisture. Next the air passes through a chiller to remove bulk moisture. The stream is further dried by a molecular sieve dryer. At this point, the stream contains dry noble gas laden air which enters the low temperature (-40°C) adsorption beds for noble gas removal. These beds are designed as standard heat exchangers containing the adsorbent on the tube side, and boiling CO_2 (-55°C) coolant on the shell side. This design provides the efficient removal of the decay heat. The tube side of the first double unit contains hydrogen mordenite (HZ) to hold up the xenon isotopes. The tube side of the second double unit (in series) contains silver mordenite (AgZ) to retain the krypton isotopes. The two units in parallel are used to provide enough surface area to reduce the face velocity while the units in series provide the needed holdup time. The purpose of HZ in the upper bed

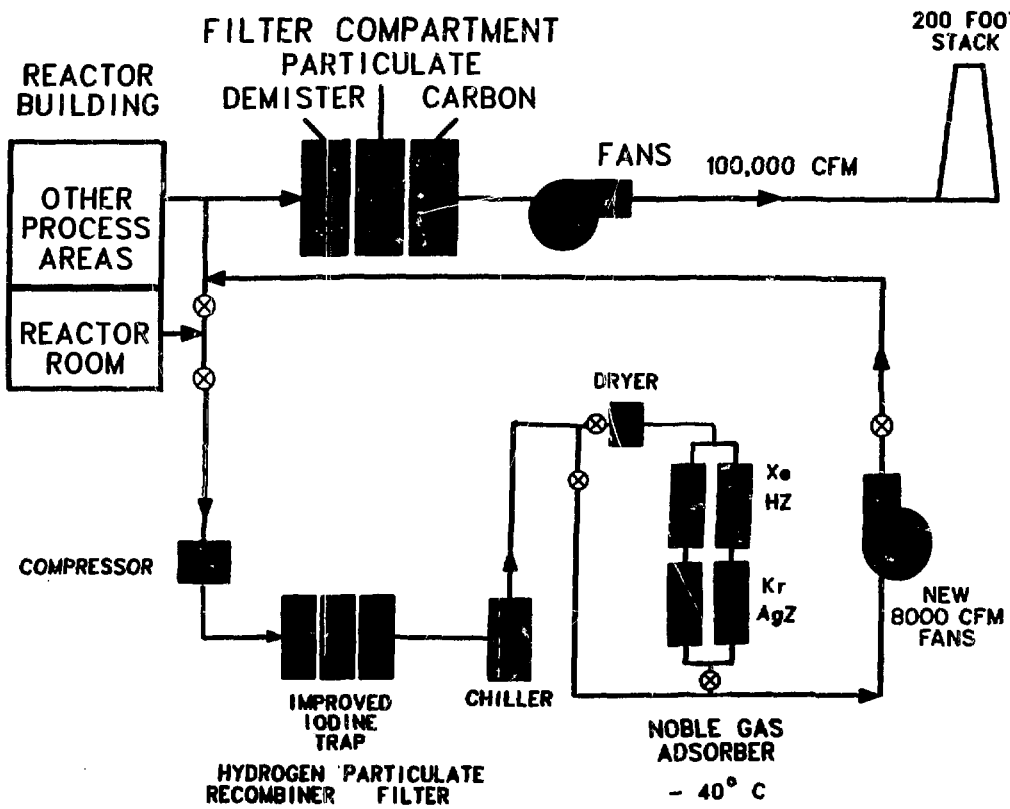

Figure 2. Low-temperature adsorption

is to help spread the heat producing noble gases more evenly throughout the beds, i.e., the xenon is held more strongly than krypton and would form a concentrated "hot spot" if both beds (series) were silver mordenite. The CO_2 coolant serves two functions in removing the noble gas decay heat, and increasing the adsorption capacity of the HZ and AgZ by allowing subambient operation. The low temperature adsorption system would have the capacity to remove >95% of the airborne releases from a prompt meltdown. The air exiting the noble gas system passes through the existing confinement filters to complete the loop. Once trapped and shut off before krypton breaks through the lower column, the noble gases would be kept in the cooled columns and allowed to decay up to fifty days, at which time the only remaining radioactive noble gas would be krypton-85. This krypton-85 could be either bottled and stored or released to the atmosphere in a controlled manner. The chiller and adsorbent beds would be kept at temperature with a dry purge in a stand-by condition at all times during normal reactor operation.

A similar but smaller (lower flowrate) skid-mounted system could be used for power reactor accident cleanup of contained noble gases to prevent subsequent leakage to the environment while awaiting decay to krypton-85.

Future

Work is continuing on the laboratory scale to seek better adsorbents, and a larger scale prototype of the conceptual design is being fabricated to provide improved engineering data for more realistic cost estimates.

References

1. Monson, Jr., P.R., "Krypton retention on solid adsorbents." Proceedings of the 16th DOE Nuclear Air Cleaning Conference, CONF 801038, Vol. 2, p 1387 (1980).

2. Monson, Jr., P. R. Krypton Retention on Solid Adsorbents. DP-1615, E. I. du Pont de Nemours & Co., Savannah River Laboratory, Aiken, SC (1982).

3. Pence, D. T. and Paplawsky, W. J. "Noble gas separation from nuclear reactor effluents using selective adsorption with inorganic adsorbents." Proceedings of the 16th DOE Nuclear Air Cleaning Conference, CONF 801038, Vol. 1, p 161 (1980).

4. Ruthven, D. M., et al. "Removal of Kr from N_2 by selective adsorption." IBID, Vol. 1, p 177 (1980).

5. Stephenson, M. J., et al. "Experimental demonstration of the selective adsorption process for krypton-xenon removal." Proceedings of the 12th AEC Air Cleaning Conference, CONF-720823, Vol. 1, p 11 (1972).

6. Stern, S. A. and Wang, S. C. "Permeation cascades for the separation of krypton and xenon from nuclear reactor atmospheres," AICHE Journal, 26(6), 891 (1980).

DISCUSSION

LAMBERGER: 1-The reactor room leak rate of 8,000 cfm is at what pressure differential? 2-What is the annual consumption, or cost, for the CO_2 required to keep the system in cold standby? 3-What is the capital cost of this system?

MONSON: 1-The 8,000 cfm would maintain the reactor room at less than 12 inches of water, which is equal to the water seal on the reactor room. 2-Estimated cost of CO_2 is less than $100,000 per year. I don't know what amount of CO_2 that represents. 3-We are in the process of generating more detailed engineering data to make a reasonable capital cost estimate. This information is not yet available.

MOELLER: What is the source of your CO_2 supply and how do you assure it is adequate for an emergency?

MONSON: Local suppliers of large quantities of CO_2 are available. Maximum cooling is only required for a short period of time (hours). The highly radioactive species are rapidly decaying, thus requiring much less coolant to maintain the operating temperature. In addition to CO_2, we are considering spraying liquid nitrogen on the top of the column initially so to cool the gases down when they first hit.

EVANS, A.G.: I might add just one more comment. We have a fairly extensive agricultural fertilizer industry in the area which generates CO_2 as part of their conversion of natural gas to nitrate so we have a readly supply of CO_2 in the area.

HULL: If you have to keep the medium cool, why wouldn't cooling the charcoal do as well, since cooling it should alleviate the fire hazard.

MONSON: Two points: (1) If we lost the coolant, the carbon could heat up and ignite, whereas the zeolites would not burn. (2) There is little or no capacity advantage of carbon over silver mordenite at the temperatures used in this system.

HULL: Somehow, it strikes me that that's really an awfully big hedge for an awfully small possibility.

MONSON: We are very safety conscious.

WIKTORSSON: Have you made any calculations of the radiation levels from and around this type of retaining system?

MONSON: This would be a non-personnel building that would be radiation resistant. The building itself and the columns would be shielded.

WIKTORSSON: What do you do in case you need any maintenance or service on the system?

MONSON: This is for an accident response and normally it is not

online at all. We are talking about a major accident. What we are trying to do is trap the noble gases from the initial part of the accident. Perhaps you are thinking that it is going to be regenerated or that we would want to maintain it. This is pretty much a one shot deal.

TECHNICAL FEASIBILITY AND COSTS OF THE RETENTION OF RADIONUCLIDES DURING ACCIDENTS IN NUCLEAR POWER PLANTS DEMONSTRATED BY THE EXAMPLE OF A PRESSURIZED WATER REACTOR

H. Braun*, R. Grigull**, K. Lahner+ , H. Gutowski++, J. Weber++

* Federal Ministery of the Interior, Bonn, FRG
\+ Brown Boveri Reaktor GmbH, Mannheim, FRG
** Brown, Boveri & Cie AG, Mannheim, FRG
\++ Linde G, Höllriegelskreuth, FRG

Abstract

The maximum allowable radiation doses during accidents in nuclear power plants, i. e. 5 rem whole-body dose and 15 rem thyroid dose, have been laid down in the German Radiation Protection Act. In order to ensure that these limits are not exceeded for all exposure paths including the ingestion path or, if possible, to remain far below them, the Federal Ministry of the Interior has initiated a study on the effectiveness and cost of additional safety features for reducing the release of activity and the dose exposure during accidents in nuclear power plants. Detailed investigations were carried out for the following three radiologically representative types of accidents:

- Break of a reactor coolant line
- Break of an instrument line in one of the outer ring rooms
- Break of a main steam line outside the containment

The technical basis of the study was a BBR-type nuclear power plant with pressurized water reactor and once-through steam generator. I 131 was chosen for determining the activity release as this is the critical nuclide for the ingestion path. Altogether 33 feasible technical measures were investigated and their potential improvement was assessed.

I. Introduction

The regulations of Article 28, Paragraph 3 of the German Radiation Protection Act (Strahlenschutzverordnung) stipulate that

- "Structural and other technical protection measures against accidents inside or at a nuclear power plant shall be planned in such a way that in the event of the maximum credible accident persons in the vicinity of the plant may not receive a radiation dose of more than 5 rem for the whole body and 15 rem for the thyroid gland."

This stipulation may be considered as fulfilled if the below cited safety criteria and guidelines for nuclear power plants are taken into account in the design of a plant.

The guidelines /1/, /2/ define the accidents, the methods, and conditions for radiation dose calculations on which the design has to be based. The draft guidelines which were in force on September 1, 1979 showed that due to highly conservative assumptions, e. g., the exclusion of any administrative measures regarding the consumption of contaminated food, difficulties arose with respect to meeting the limits /3/. The German Federal Ministry of the Interior thereupon ordered a study to be performed in order to show which technical possibilities exist for reducing the activity release into the environment by approx. 1 or 2 orders of magnitude.

The technical feasibility of corresponding new concepts and their costs of implementation were to be examined within the scope of this study /4/. The basis for the study was a BBR nuclear power plant with pressurized water reactor and once-through steam generator.

Based on radiological studies I-131 was identified as the critical isotope for the radiation exposure on the ingestion path. The measures described in the following are therefore restricted to a reduction of the release of this isotope to the surrounding atmosphere.

II. Work Performed to Date

II.1 General

The guideline (1) defines accidents whose radiological effects on the environment shall be examined. Three types of accidents were selected to be investigated in detail:

A Break of the primary loop (reactor coolant line)
B Break of a line containing reactor coolant outside the containment
C Break of a main steam line outside the containment.

Fig. 1 illustrates the systems examined in this context.

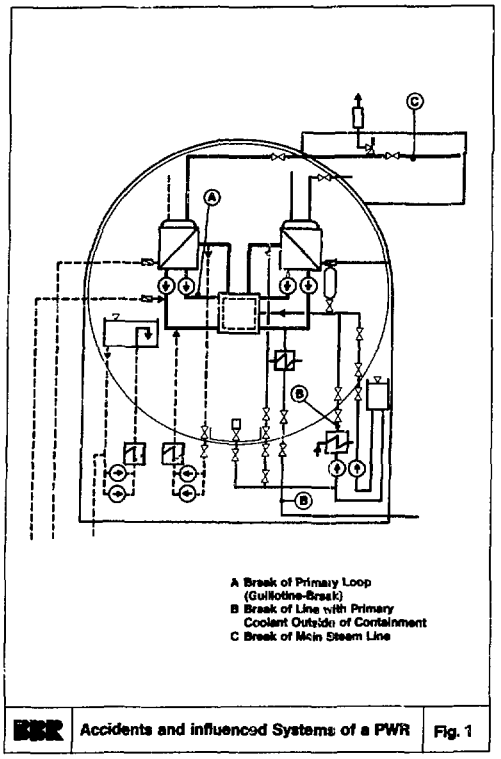

The coolant activity and the examination of I-131 in the various chemical and/or physical forms it is found were also dealt with according to the calculation regulations.

The following boundary conditions were used in calculating I-131 release:

I-131 release rate	2 μCiMW^{-1}S^{-1}
Release through cladding rupture	10 %
Proportion of this quantity entering	
the containment atmosphere	25 %
the containment sump	75 %
I-131 in the annulus air	
organic iodine	50 %
elemental iodine	50 %
Effectivity of filters:	
organic iodine	99 %
elemental iodine	99.99 %
aerosols	99.9 %

II.2 Description of the Accidents and Measures Taken

II.2.1 Break of a Reactor Coolant Line

In the event of a complete double-ended break (guillotine break) of the reactor coolant line the I-131 activity is released, depending on the evolution of the accident, via any of the following paths:

- Until the fast-closing dampers are closed (approx. 4 secs) activity is released through the air inlets directly into the atmosphere and/or via the subatmospheric pressure system to the vent stack.

- During the overpressure phase in the containment through leakage to the outer annulus and from there via the gap ventilation system and the vent stack or through leakage via connecting rooms and/or through the concrete to the atmosphere.

The release paths can be seen on the ventilation system schematic of Fig. 2.

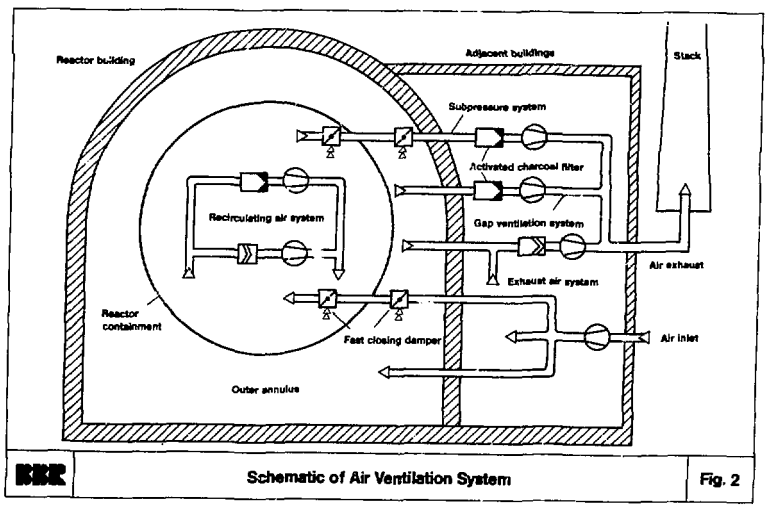

The I-131 concentrations released via the various paths were calculated on the basis of an activity flow chart. With the results of these calculations the following potential measures were examined:

- Reduction of the iodine concentration in the reactor coolant

  a) Increased purification rate

- Reduction of the exhaust air flow prior to the isolation of the containment ventilation system

  a) Shorter response time of the fast-closing dampers
  b) Reduced cross section of the ventilation ducts

- Reduction of the iodine concentration in the containment atmosphere

  a) By spraying water into the containment
  b) By spraying water plus chemical additives (*)
  c) Through purging by chemisorption of the recirculated air in the containment
  d) Through filtration of the recirculated air in the containment (*)

- Reduction of the leakage from the containment through more rapid lowering of the containment pressure

  a) Internal spray system in the containment
  b) Cooling of the containment shell with water
  c) Passing the recirculated air in the containment through ice
  d) Ice channel with containment partitions (pressure suppression system)

- Reduction of the activity concentration in the outer annulus atmosphere

  a) Recirculated air filter system in the outer annulus (*)
  b) Purging of the recirculated air in the outer annulus through chemisorption

- Reduction of the leakage from the outer annulus through faster lowering of the pressure in the outer annulus
  a) Increased flow rate of the gap ventilation system (*)

- Reduction of the activity release via the gap ventilation chain

  a) Purging of the exhaust air through chemisorption (*)

Only the five specially marked (*) measures were examined in detail. The increased purification rate has been investigated in more detail for the typ C accident. The flow diagramm for a purification system with increased capacity is shown in Fig. 3

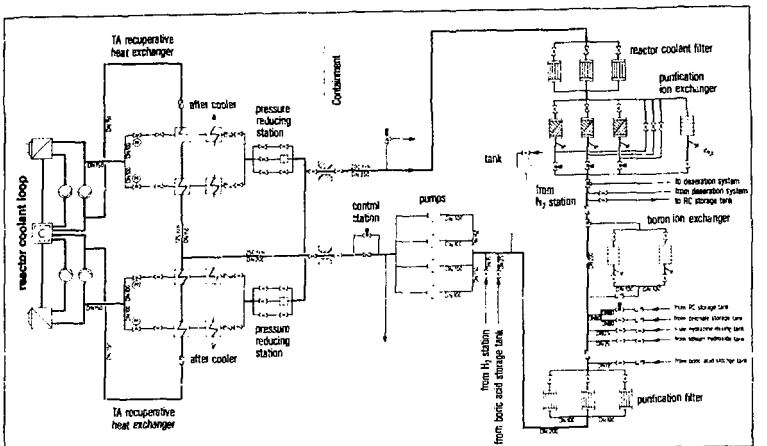

Flow Diagram for a Reactor Coolant Purification System (TA) of Increased Capacity — Fig. 3

The typical results of a reduction of the I-131 concentration for filtration of the recirculated air in the containment, according to the schematic of Fig. 4, is depicted in Fig. 5. For increased filtration of the outer annulus (gap) atmosphere as shown in Fig. 6 and for increased air flow the I-131 concentration is given in Fig. 7.

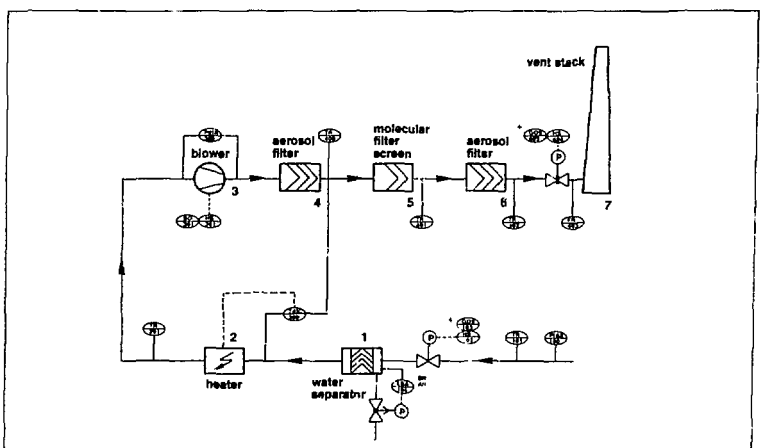

Schematic of a Recirculated Air Filter Train in the Containment — Fig. 4

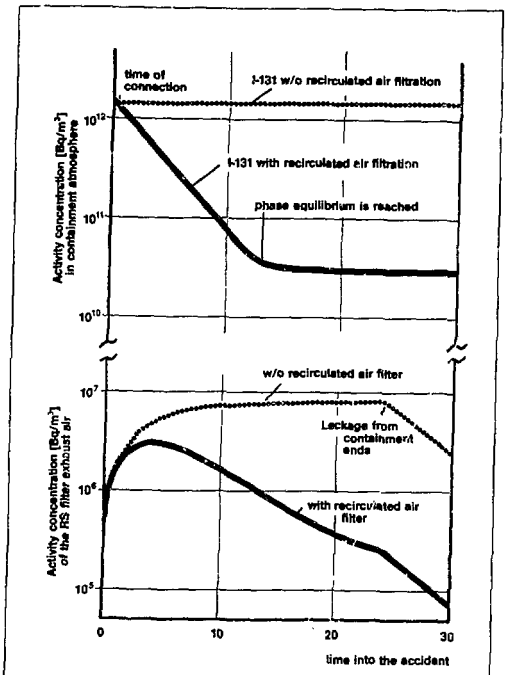

Activity Concentrations with Recirculated Air Filtration — Fig. 5

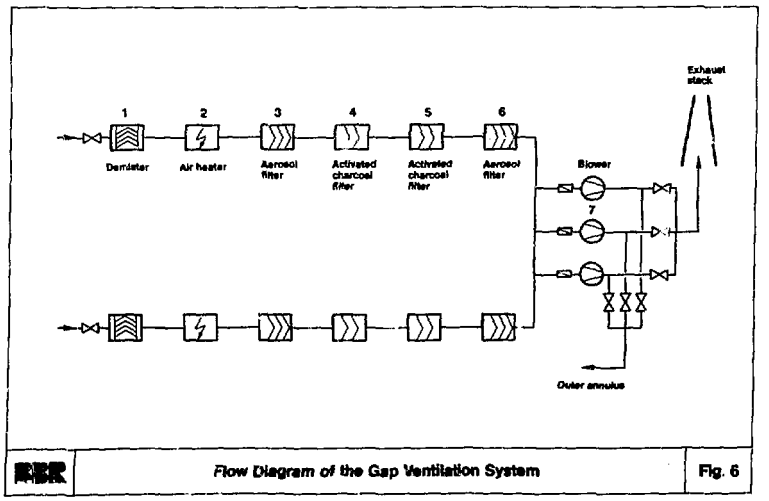

Flow Diagram of the Gap Ventilation System — Fig. 6

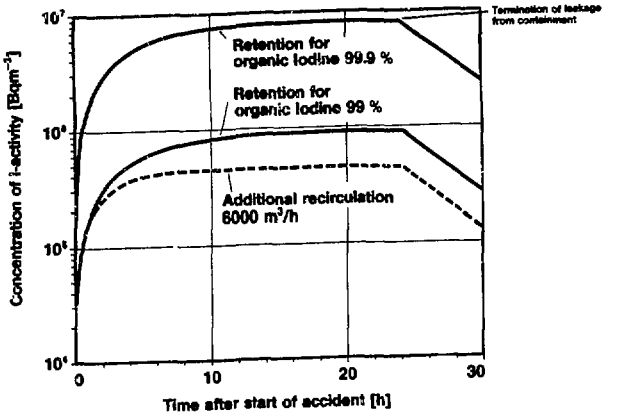

Concentration of Iodine after Accident with operation of Recirculating Air and Gap Ventilation Systems — Fig. 7

Tab. 1 sums up the results of all the examined concepts.

	Containment spray system	Containment filtration of recirculated air	Outer annulus: filtration of exhaust air	Outer annulus: + filtration of recirculated air	Outer annulus purging of exhaust air
Principle of operation	– Dissolving of gaseous I-131 – Reduction of I-131 leakage	– Adsorption & reaction of I-131 with a silver molecular sieve – Reduction of I-131 leakage	– Increased retention of organically fixed I-131	– Additional purification of the outer annulus atmosphere – Reduction of I-131 in filter supply air	– High retention rate of I-131 in organic compounds bonded by HNO_3
Calculated reduction factor	3.5	8.4	9.2	15.5	50.5
Probable biological effect	6.1	6.4	1.8	3.0	2.0
Technical implementation	Flow: 2 x 100 m³/h Additive: 50 % NaOH	Flow: 4 x 5000 m³/h Sorption filter: Molecular sieve	Sorption filter: Activated charcoal	– Filter as in exhaust air string – Recirc. air flow: 5000 m³/h	– HNO_3 counterflow Flow rate: 2 m³/h – Air flow 6000 m³/h
Problems	– Corrosiveness – Generation of H_2	– Size of structure – Clogged filters – Compressive strength	– Extra civil engineering costs – increased inspection & maintenance costs		– Not proven – Corrosiveness – Environmental problems – Waste disposal
Cost estimate: – Installation – Planning – Operation/ Maintenance	1300 TDM 100 TDM 5 TDM/yr	6100 TDM 500 TDM 25 TDM/yr	2000 TDM 200 TDM 8 TDM/yr		6100 TDM 500 TDM 30 TDM/yr

Summary of Results: Break of a Reactor Coolant Line — Tab. 1

II.2.2 Break of a Line Containing Reactor Coolant Outside the Containment

For the postulated rupture outside the containment of an isolatable connecting line containing reactor coolant two possibilities were examined:

A) A break of a low pressure injection and decay heat removal system line

B) A break of an instrument line

The break position for case A is illustrated in a section of the flow diagram of Fig. 8. In this case the I-131 is released with the reactor coolant directly into the outer annulus and will then be spread via the gap ventilation system and the vent stack or via leaks to the atmosphere.

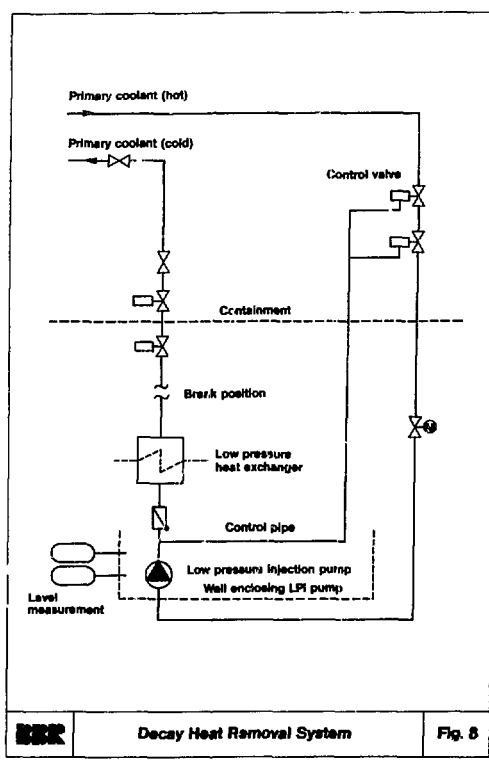

Because of the availability of isolation devices and resultant low quantity of released iodine case A is less interesting than case B and has therefore not been further examined.

The following potential measures were examined:

- Reduction of the iodine concentration in the reactor coolant
  a) Increased purification rate prior to the start of the shutdown procedure
  b) Increased purification rate after the start of the shutdown procedure
  c) Introduction of a waiting period during the shutdown process for purifying the reactor coolant

- Reduction of the leakage through the break opening
  a) A more rapid isolation of the line by means of a locating procedure, flow restricting devices, and automatic break detection devices

- Reduction of the activity release
  a) Additional retention devices

The filtration equipment of some more recent constructed nuclear power plants has been upgraded by adding an optional filtration system which is available on demand. Such a filter system as depicted in the schematic diagram of Fig. 9 is installed to filter the exhaust air when increased activity is present in the outer annulus or in the reactor auxiliary building.

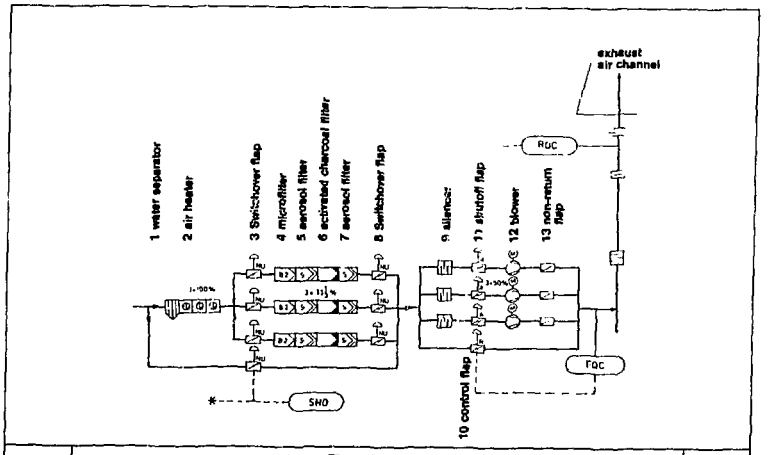

Flow Diagram for an Optional Filter System — Fig. 9

The investigations referred to in this section are based on the assumption that such a system has been put into practise.

With regard to the break of an instrument line outside of the containment a rupture of a boric-acid-analysis system line was established to be the critical break for the power plant system being examined. Fig. 10 depicts the flow diagram examined for this case. Fig. 11 shows the results of the activity release rate determination.

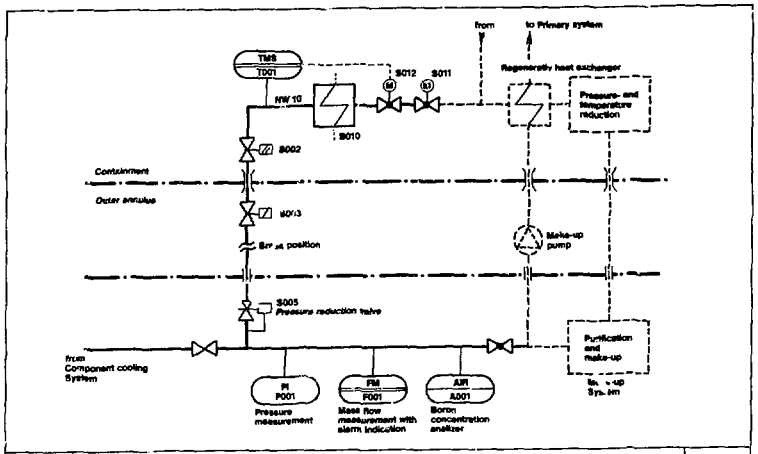

Flow Diagram for Boron Concentration Analysis — Fig. 10

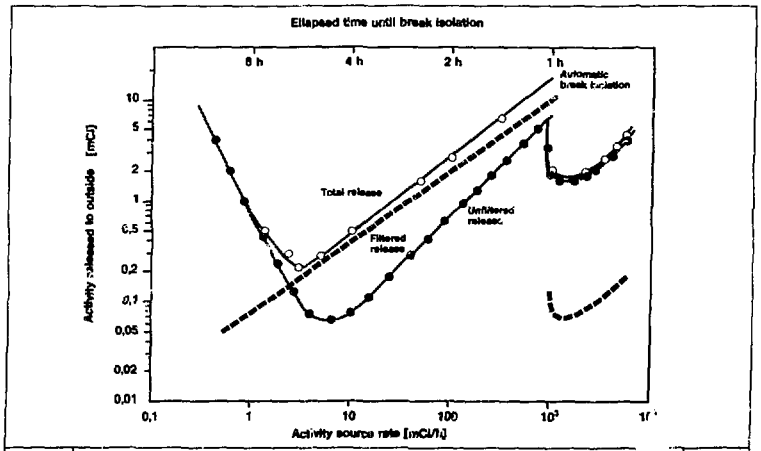

I 131 – Activity Release for Break of Instrument Line — Fig. 11

On this figure three regions can be distinguished. On the left there is a region of relatively small activity release rate (< 2 mCi/h). The activity is, therefore, not detected fast enough. Since isolation occurs rather late an accumulated, fairly large amount of activity can be released. In the second region ($<10^3$ mCi/h and >2 mCi/h) a break is quickly detected and the activity release is restricted through isolation. In the third region ($>10^3$ mCi/h), after the break the flow in the line becomes so large that the available break detection system (through monitoring of the temperature) will reduce the activity release considerably.

The measures which have been investigated concern an improvement of the filter systems as well as of the detection of a break through monitoring of the room activity or sensing of flow rates, temperatures, and humidity. Table 2 lists the reduction factors achieved thereby and the costs and potential problems to be encountered in putting the concept into practise.

	Optional filter system	Recirc. air filter systems	Location procedure for ambient air activity	Monitoring networks for ambient air activity	Flow restrictors	Temperature monitoring	Humidity detectors
Principle of operation	Filtration of iodine from RAB+annulus	Filtration of iodine from annulus atmosphere	Optimization of time for locating the activity source	Sensing of gas activity for a rapid localization of the activity source	Flow dependent isolation of lines	Temperature change through fast flowing medium	Change of electrical properties by humidity
Calculated reduction factor	5 to 100 (leaksize-dependent)	1	1 to 2	1 to 5	1 to ∞	1 to 10	1 to 5
Technical implementation	- 3 x 50 % ventilators - 3 x 33 % filters - Connection controlled by activity signal	- Upgrading of exist. recirc. air coolers - Connection controlled by activity signal	- requires a mathematical/statistical procedure - possible hardware: dedicated computer	- 10 inert gas monitors - Monitoring of ambient air - Multiplex operation	- Check valve controlled by differential pressure	- Standard thermocouple with bistable	- Electrical capacitor - Additional temp. sensing - Direct installation for insulated pipes
Problems	- Space requirements - Control concept - High control & maintenance expenditure	- Ineffective with postul. ventil. concept - Restrictions for locating the activ. source	- hardware design not known	- Effective only with release of inert gas - Increased insp. effort - Depends very much on ventilation concept	- Effective only in case of major leaks - Increased monitoring & inspection effort	- Limited utilization potential for examined NPP-design	- Signal/ background ratio - Expensive pipe claddings - Expensive processing electronics - Calibration and inspection
Cost estimate: - Installation - Planning - Operation Maintenance	10 000 TDM 2 000 TDM 240 TDM/yr	not evaluated	not evaluated	1 500 TDM 500 TDM 20 TDM/yr	3.5 TDM 30 TDM 1 TDM/yr	20 TDM 30 TDM 1 TDM/yr	1 000 TDM 200 TDM 20 TDM/yr

Summary of Results:
Break of Connection/Instrument Line

Tab. 2

II.2.3 Break of a Main Steam Line Outside the Containment

Regarding the release rates to be expected in case of a break of the main steam line the existance of a closed emergency condenser system (which is an unique feature of the BBR type of nuclear power plant) is important. Fig. 12 is a schematic representation of the major systems of the secondary loop.

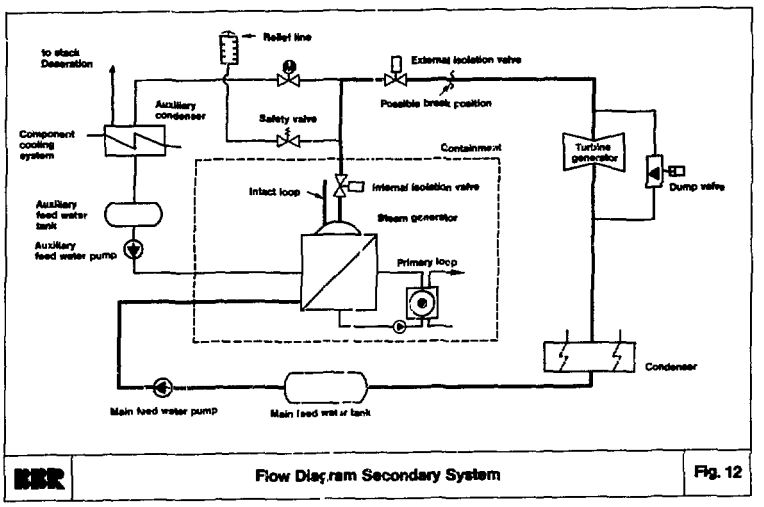

The main paths for an activity release are:

- Discharge through the break prior to the closing of the main steam isolation valve (approx. 5 secs)
- Discharge to the atmosphere through the main steam safety valves before the emergency condenser system becomes operational (approx. 50 secs)
- Release via the venting of the emergency condensers.

In all these cases additional a complete guillotine break of a steam generator tube is postulated. The activity of the main steam is then a function of the reactor coolant entering the secondary system through this tube break.

The measures taken for reducing the release from the main steam line break have to start at these paths. The following possibilities were investigated:

- Reduction of the iodine concentration of the reactor coolant
  a) Increased purification rate during normal operation (*)

- Reduction of the discharge through the break opening
  a) Preclusion of breaks upstream of the outer main steam isolation valve
  b) Reducing the closing time of the outer isolation valve
  c) Arranging a Venturi nozzle in the main steam line as a flow restriction

- Influencing the location of resultant radiation release by channeling the discharged medium
  a) from the break location to the vent stack or cooling tower
  b) from the main steam safety valves to the stack or cooling tower

- Additional retention devices
  a) Channeling the medium into a condensation system
  b) Conveying the steam released through the main steam safety valves to a condensation system (*)
  c) Flushing out or filtering of the activity released from the emergency condensers (*)

- Prevention of any discharge through the main steam safety valves
  a) Leakage-controlled closing of the main steam safety valves and
     Changing the design of the secondary side so that it can withstand the primary side pressure (*)
  b) Condensing the discharged steam in a closed system (*)

Only the five specially marked (*) measures were examined in detail.

Table 3 lists the reduction procedures thus obtained plus the main design data, possible problems, and costs.

	RC purification system of increased rate	Increased design pressure of safety valves and secondary side	Condensation of steam released via the safety valves	Increased capacity of emergency condenser	Exhaust gas filter for emergency condenser
Principle of operation	Coolant with reduced activity leaks from primary to secondary side	Retention of activity in the main steam and/or emergency feedwater system	Safety valves do not discharge to atmosphere	No ventilation of emergency condensers	Filtration of activities released from the emergency condensers
Calculated reduction factor [1] Biological effect [2]	5 – 20 4 – 12	∞ 2.2	∞ 2.2	∞ 1.05	> 10000 1.05
Technical implementation	– Double-string system – Flow 250 t/h – Purification in bypass operation	– Strengthened system components	– Water storage reservoir 177 m³ to condense 15 t of steam	– No change of existing concept	– Iodine absorpt. filter chain – Air flow approx. 10 m³/h
Problems	– Increased power requirements – Cooling load f. comp. cool. syst. – Heat loss in primary system – Response to transients	– Concept change – Handlg. & install. – Manufacture – Thermal & mech. transients	– Space required – Activated water – Restrictive effect on operation	– Suppression of ventilation may be unacceptable	– Increased civil engineering effort – Increased inspection & maintenance effort
Cost estimate: – Installation – Planning – Operation/ Maintenance	24000 TDM 15000 TDM 1700 TDM/yr	not evaluated	2100 TDM 200 TDM 20 TDM/yr	not evaluated	1950 TDM 250 TDM 10 TDM/yr

1) related to the release path 2) related to total release and release height

BBR

Summary of Results: Break of a Main Steam Line

Tab. 3

III. Summary

During the work performed under this contract 3 main accidents have been evaluated including a calculation of the possible activity releases. A total of 33 possible measures for a reduction of the activity releases have been examined. Out of these, 15 possibilities have been worked out in technical detail with estimates for their efficiency, technical realization, and cost. The main results have been discussed in this paper.

On the basis of the latest results of reactor safety research and radiation protection, e. g. , in the U.S.A. and in the Federal Republic of Germany, new guidelines were issued in August 1983 by the German Federal Government. In these guidelines much more realistic calculation parameters and calculation models were used for determining the radiation dose after a reactor accident. The statements about the effectiveness of the technical improvements described in this study by BBR/Linde remain valid but the new guideline made this implementations not neccessary and, therefore, they have not been taken into consideration in more recent NPP s in Germany. From all the results of the present study only the installation of an optional filter system available on demand would be used in German nuclear power plants for this reason.

The work of Mr. Hennings, BBR, during the earlier days of this project is greatfully acknowledged.

IV. Selection of References (all in German)

/1/ Guidelines for assessing the design of nuclear power plants with pressurized water reactor for its ability to withstand accidents, as defined in Art. 28, Para 3 of the Radiation Protection Act (Str.Sch.V.)
Published by the Federal Minister of the Interior (BMI)
RS II 4-511434/2 8/1/79

/2/ Basis for the calculation of accidents with respect to the BMI Guidelines on the assessment of the design of NPP's with PWR acc. to Art. 28, Para. 3 of the Str.Sch.V.

/3/ Activity release during accidents in nuclear power plants with PWR via the exhaust air path within the scope of a guideline on Art. 28, Para. 3 Str.Sch.V. (Status of Dec. 14, 1979)
Technischer Überwachungsverein (TÜV) Baden e.V., Mannheim

/4/ Technical possibilities for and costs of retaining radionuclides during accidents in nuclear power plants, demonstrated at the example of a pressurized water reactor
BROWN BOVERI REAKTOR GMBH, Mannheim
LINDE AG. Werksgruppe TVT, Munich
December 1983

DISCUSSION

MOELLER: What were the principal factors that led you to select the optional filter system as the one to install? Looking at Table 2 I gather that cost was not the dominant factor.

BRAUN: The optional filter system is now state of the art for NPP design in the FRG because of other reasons. This study demonstrated that this type of measure is quite effective for the examined accidents.

DESIGN EXPERIMENTS FOR A VENTED CONTAINMENT

Rolf Hesböl, MSc
Studsvik Energiteknik AB
S-611 82 Nyköping, Sweden

Abstract

A filtered containment venting system, operable late in 1985, is currently under installation at the Barsebäck twin nuclear power station in Sweden. The filter unit, which communicates with the containments of both reactor units, but is separated from them by rupture discs, consists of a concrete bed, 40 m high and 20 m in diameter, filled with gravel of grain size 25-35 mm.

The performance of the gravel bed under such accident conditions which might lead to an activation of this safe-guard system has been the subject for investigation within the FILTRA project. These investigations have shown that the gravel bed acts as

- an expansion volume for decreasing gas pressure and increasing gas residence time
- a heat sink for condensing steam
- an excellent filter medium for removing aerosols and elemental iodine
- a sump volume for collecting radioactive condensate.

In this report the results from iodine retention studies in gravel beds are mainly considered.

1. Background

Following the study and conclusions of the Swedish post-TMI Commission on Reactor Safety, the government, in 1981, proposed to parliament that the risks of radioactive releases from nuclear power plants to the environment in the event of a severe accident should be further reduced, even though the current risks were low. The release of radioactivity causing land contamination , in particular, should be reduced.

The government expected that every means leading to risk reduction would be exploited by the utilities and that, if necessary, additional safe-guard systems would be introduced even though they might entail appreciable costs in relation to the risk reduction achieved.

In practice the regulations suggested by the government required that

- the release of radioactivity to the environment, except for noble gases, should not exceed 0.1 % of the core inventory

- the measures adopted to limit the release of activity should be put in service by the end of 1985 for the Barsebäck site, and no later than 1989 for the other sites

- the twin 580 MWe BWRs at Barsebäck, which are located relatively close to large population centres (approximately 20 km from Malmö and Copenhagen), should be equipped with a system for filtered atmospheric venting of their pressure suppression containments.

In order to provide technical information two projects, the FILTRA project and the RAMA project, were initiated in co-operation with the utilities and the authorities.

The FILTRA project (abb. of FILtrerad TRyckAvlastning - Filtered Pressure Release) should only consider the application of filtered containment venting at the Barsbäck site. The FILTRA project has been completed and reported [1, 2].

The RAMA project (abb. of Reactor Accident Mitigation Analysis) is still in progress. The main tasks of the project are research and development work of a generic nature with regard to core accidents. These generic studies will support the specific assessments required for the individual nuclear units other than those at the Barsebäck site [3]. The final result will not necessary imply containment venting.

II. Objectives of the FILTRA project

The main objectives of the FILTRA project were two-fold:

- to gain a further understanding of the phenomena and effects caused by molten fuel in severe accidents, and

- to obtain the information required to design a functioning filter plant and evaluate its effectiveness.

Included in the first objective are detailed studies on core meltdown sequences, break-through characteristics of molten core material through the reactor vessel, interractions between core melt and concrete and other structures, and how the final cooling of the core melt proceeds. The purpose of these studies was to indentify events which challange the integrity of the pressure suppression containment, such as pressure build-up, hydrogen combustion, thermal impact, and missile generation. Such studies will supply data necessary for selecting a suitable design and defining the required capacity and limitations of a filtration device.

The second main objective includes examination and analysis of the performance of the containment vent filter with regard to particle and iodine retention, steam condensation, ageing effects, hydrogen ingnition, and post leakage effects within the design criteria.

The design criteria of the filter system issued by the Swedish Nuclear Power Inspectorate can be summarized as follows:

- The activation of the venting system due to over pressuration of the containment should be ensured and passive. In this context a rupture disc is regarded as a passive component.

- The venting system should operate passively for the first 24 hours. Beyond that time limit credit can be taken for such active measures as have been prepared.

- The filter system should limit the release of individual radioactive nuclides, noble gases excepted, to less than 0.1 % of the core inventory.

- The filter system should not interfere with the safety levels already assessed for the individual units.

- The filter system should withstand an earthquake of 0.15 g intensity.

III. Experimental and verification programme

In the past the use of sand or gravel bed filters has been discussed and proposed in dicussions on nuclear safety on several occasions in Sweden. Hence it was natural that the filter system decided upon should be a gravel bed. In the first instance a gravel bed with a volume of 10 000 m^3 filled with gravel which has a size fraction of 25-35 mm was selected. For this concept a comprehensive verification programme has been carried out. The experimental programme has included thermal and flow rate tests [4], retention tests on iodine and particulates, and studies of combustion sequences in mixtures of air and hydrogen in the gravel beds [5].

In this report only the iodine retention studies are discussed. The particle retention studies have been reported elsewhere [6].

IV. Iodine retention studies

Iodine might be released from the fuel in different chemical forms and might also be converted to other forms by secondary reactions inside the reactor vessel or the PS containment. One of the most penetrating iodine forms is methyl iodide. Studies of the TMI-2 accident showed, and it is also generally expected, that the yield of methyl iodide is quite low, less than 1 % of the total iodine. In addition methyl iodide does not represent any hazard with regard to land contamination.

The next volatile iodine compound to be considered was elemental iodine. In our approach it was assumed that the retention of other volatile inorganic iodine compounds in the gravel bed would exceed that of elemental iodine.

Conservatively it was thus assumed that iodine will be released completely as elemental iodine. Consequently the objective of the iodine retention studies was to prove that the filter concept decided upon would have the capacity to remove all the iodine released from the core as elemental iodine. Credit for any iodine retention in the reactor and containment vessels was not to be taken. The iodine retention studies comprised laboratory scale examinations with sand and large scale tests with gravel under steam conditions.

Laboratory scale experiments

The objective of the laboratory study was mainly a parametric study for the specific stone material, AB Sydsten, selected for the FILTRA bed. Tests were performed at different iodine loading rates, temperatures, flow rates, bed depths and relative humidities at ambient temperatures.

Gaseous elemental iodine tabelled with I-131 was introduced at a constant rate into a column filled with sand, grain size normally 1.4-2 mm. The test apparatus is shown in Figure 1.

Some typical results are shown in Figure 2 in which the ratio between the exit concentration, C, and inlet concentration Co of iodine is given as a function of time for different loading rates of iodine.

The results show that the iodine break through time depends strongly on the iodine loading rate. It is also recognized that break through iodine level within the experimental period never reached the inlet iodine concentration level, but a fairly constant lower level, which in the following is referred to as the break through level. A fraction of iodine thus seems to be retained completely in the bed. This retention is ascribed either to chemical interaction between iodine and the stone material, or to a long time diffusion of iodine into the stone matrix. In fact the retention is a combined effect of both. This has been demonstrated in tests with small beds. The iodine build-up is controlled by several mechanisms characterized by different rate constants. An iodine build up curve as a function of time is presented in Figure 3. In a prolonged test saturation was not obtained within 300 hours. Desorption studies have also shown that the desorption rate corresponds fairly well with the iodine build-up rate. However, an undesorbable residue is left in the bed. This residue is attributed to chemisorbed iodine. The effect of chemisorption is dominant at low iodine concentrations.

Within the parametric range studied the break through level increases with increasing flow rate, temperature, relative humidity and grain size. Some of these effects are illustrated in the Figures 4-7.

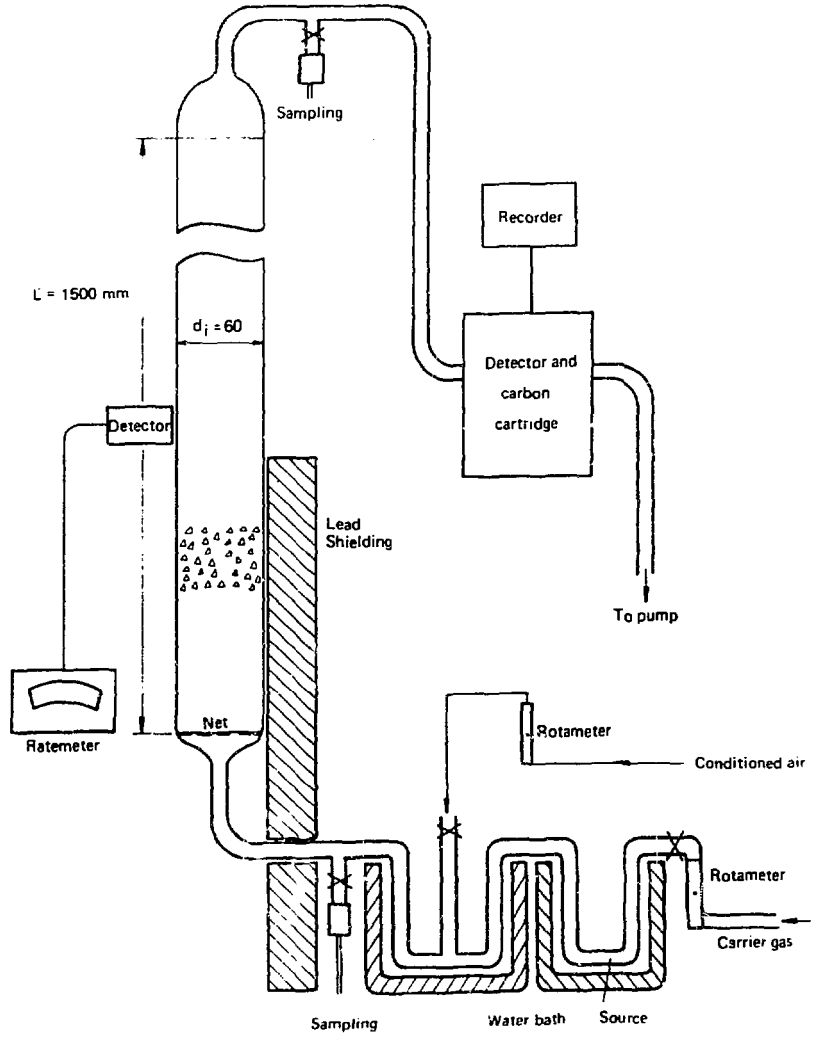

FIGURE 1
LABORATORY TEST APPARATUS FOR IODINE RETENTION STUDIES IN SAND

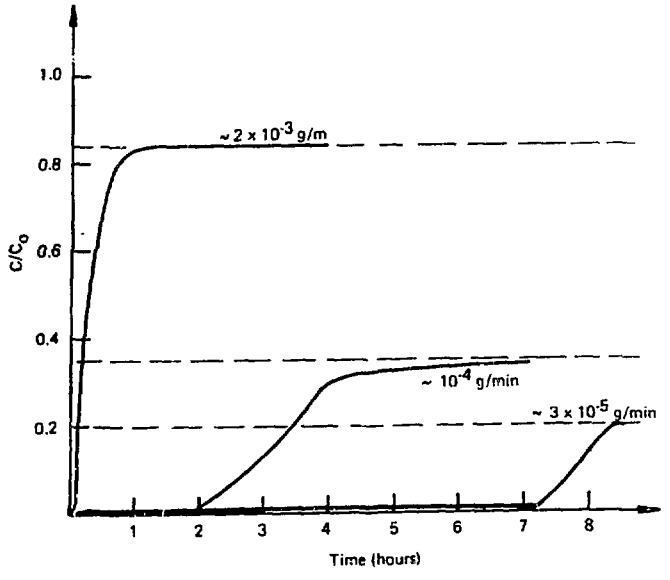

FIGURE 2
THE BREAK THROUGH OF IODINE FOR DIFFERENT IODINE LOADING REATES. THE FLOW RATE AND BED LENGTH WERE 4 l/min AND 1.5 m RESPECTIVELY. RELATIVE HUMIDITY WAS 98-100 %.

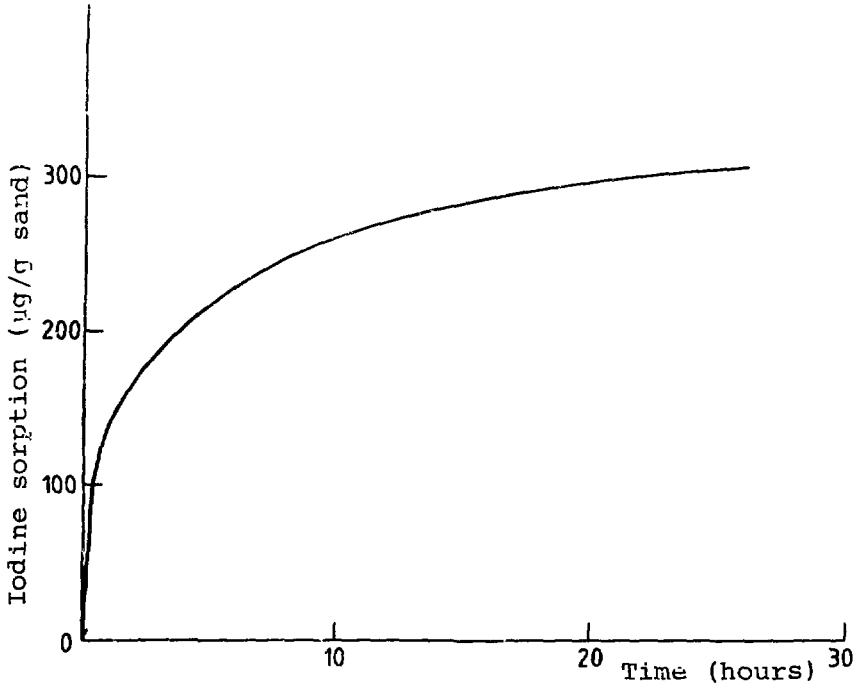

FIGURE 3
IODINE SORPTION AS A FUNCTION OF TIME FOR AMBIENT CONDITIONS AND A LOADING RATE OF 1.4×10^{-3} g/min.

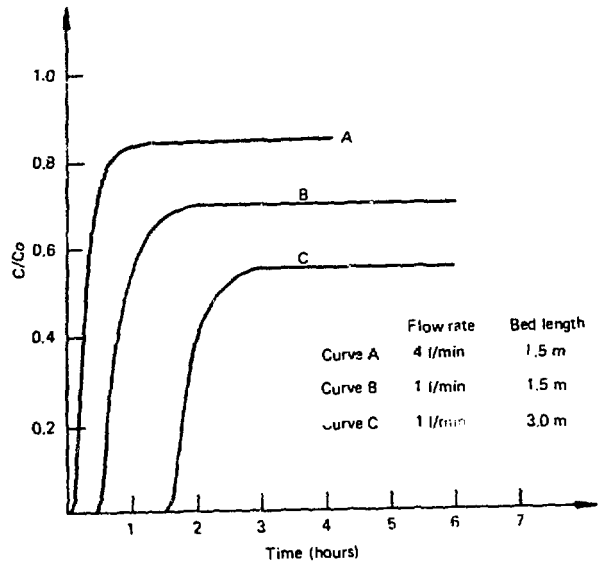

FIGURE 4
EFFECT OF FLOW RATE AND BED LENGTH ON IODINE RETENTION

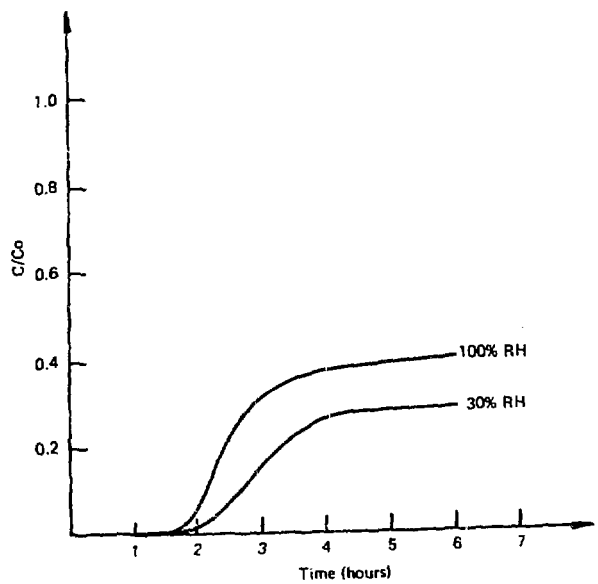

FIGURE 5
EFFECT OF RELATIVE HUMIDITY ON IODINE RETENTION IN SAND AT AMBIENT TEMPERATURES

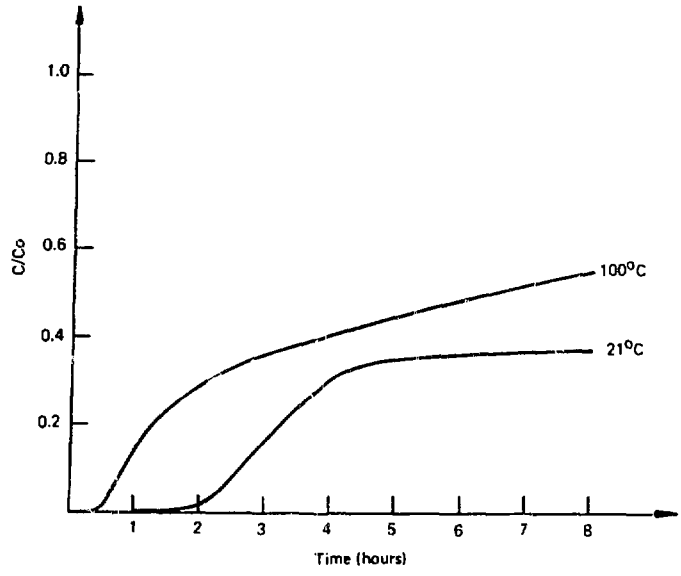

FIGURE 6
EFFECT OF TEMPERATURE ON IODINE RETENTION

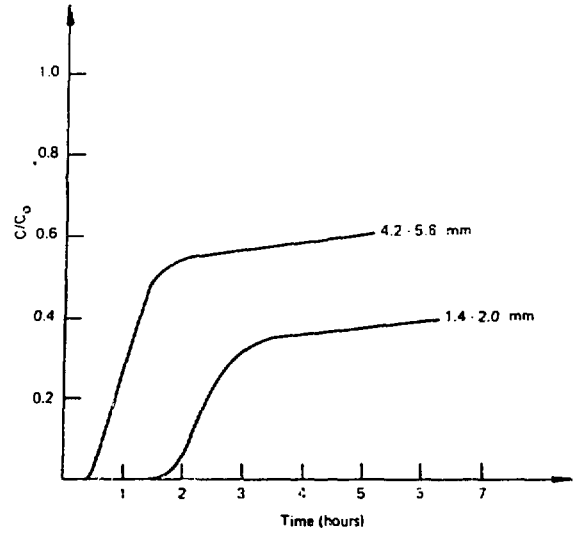

FIGURE 7
EFFECT OF GRAIN SIZE ON IODINE RETENTION

The sorption mechanisms are manifold and complex and the sorption of iodine on stone cannot be described by simple sorbtion models. Nevertheless a physical-mathematical model SAD (Surface Adsorption Desorption) describing the retention of iodine in gravel columns has been developed [7]. Theoretical and experimental values are compared in Figure 8.

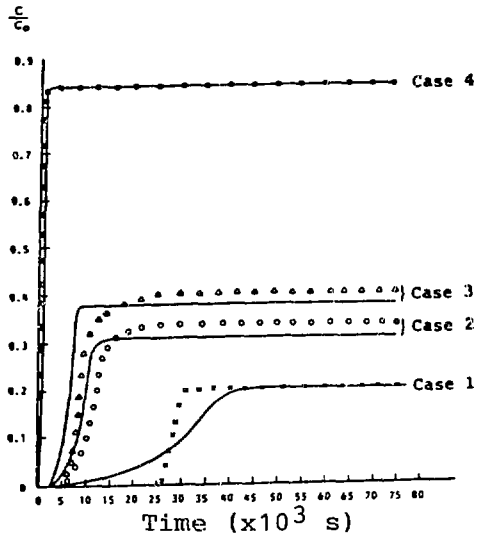

FIGURE 8
COMPARISONS BETWEEN CALCULATED AND OBSERVED VALUES. EXPERIMENTAL RESULTS ARE GIVEN AS DISCRETE POINTS (7).

Large scale experiments

The main objective of the large scale test was to demonstrate whether or not the laboratory test results could be transformed to large scale systems. Secondly the effect of steam and steam condensation was examined. A schematic diagram of the gravel bed filter test facility is shown in Figure 9. It consists of a sectional column, 7.5 m high and diameter 0.5 m, filled with gravel, grain size 25-35 mm. Gaseous elemental iodine labelled with I-131 was fed into the column at a constant rate for 5-10 hours. Gas samples were drawn through carbon cartridges just in front of the column and at column depths of 3 and 7.5 m. At the 7.5 m level (column exit) gas samples were also drawn through a May pack. Test results obtained under ambient conditions, a flow rate of 74 m^3/l and iodine loading rate of $7x10^{-3}$ g/min, are presented in Figure 10. The calculated break through level based upon the laboratory test results is also shown. As can be seen the correspondance between the predicted and experimental values is quite good.

The following runs were performed with steam mixed with some air to simulate uncondensable gases. The steam/air ratio was approximately 5. Prior to iodine injection the entire column was heated up by passing steam through it. During the heating up period it was recognized that condensation took place within a narrow zone, 5-10 cm thick, which moved slowly downwards through the column. The temperature fall across the condensation zone was pronounced from steam temperature to ambient. The condensate was self drained and collected in the bottom of the column. Any flow resistance due to accumulated condensate on the gravel is thus non-existent. These observations were later confirmed in thermal hydralic tests performed with columns 30 m high and 1 m in diameter (4).

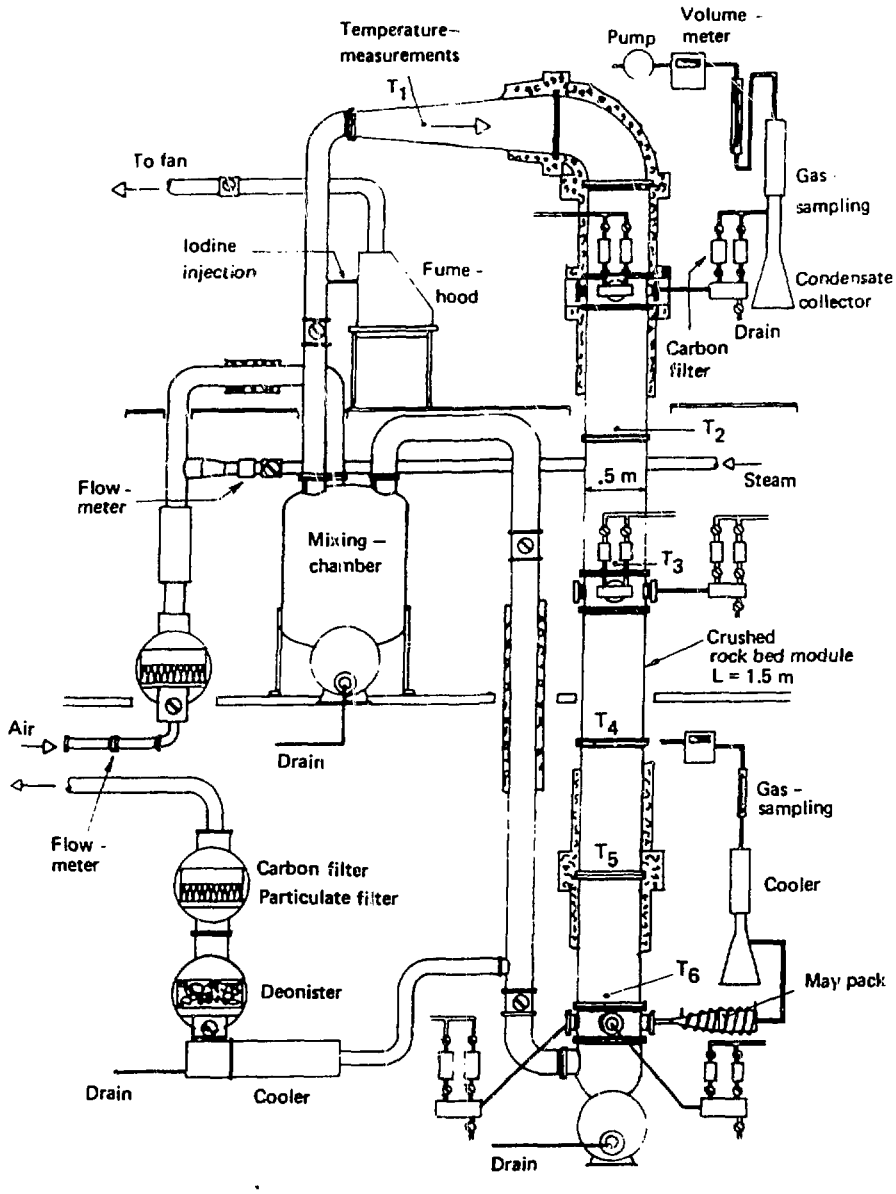

FIGURE 9
GRAVEL BED FILTER TEST FACILITY WITH IODINE INJECTION AND SAMPLING EQUIPMENT FOR LARGE SCALE EXPERIMENTS

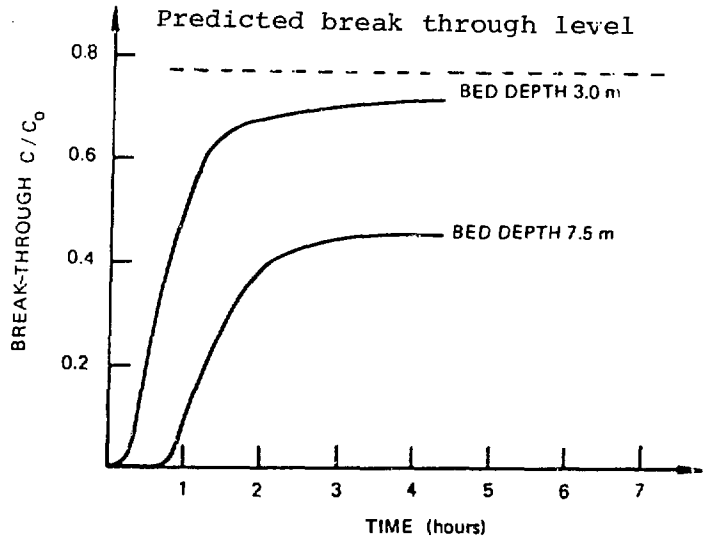

FIGURE 10
THE BREAK THROUGH C/Co FOR I_2 UNDER AMBIENT CONDITIONS. FLOW RATE AND IODINE LOADING RATE WERE 74 m^3/l AND $7x10^{-3}$ g/m RESPECTIVELY. PREDICTED BREAK THROUGH LEVEL FOR BED DEPTH 3 m

Following the heat up period iodine was introduced into the column. A typical result is shown in Figure 11.

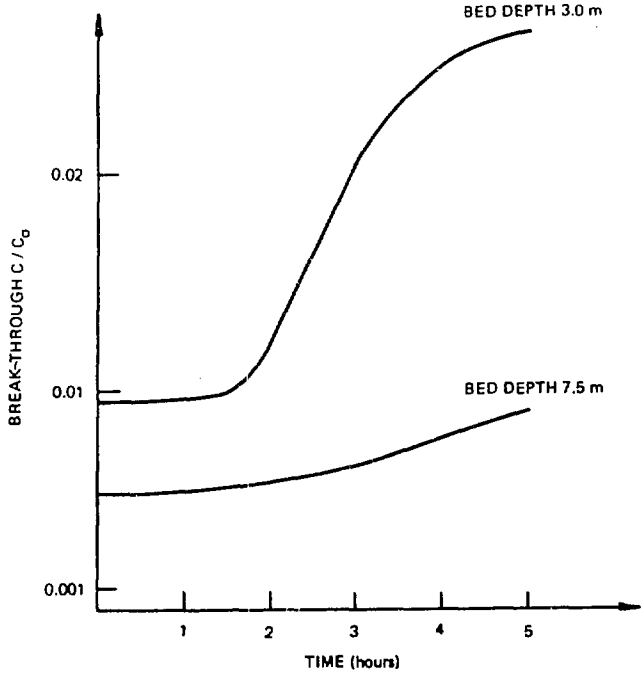

FIGURE 11
EFFECT OF STEAM CONDENSATION ON IODINE RETENTION IN A GRAVEL BED. THE IODINE LOADING RATE WAS $5.6x10^{-3}$ g/min.

In the run referred to the bed temperature was kept at 95 °C, which was the saturation temperature of the steam/air mixture. Hence the gravel was wet during the run.

By comparison of results in Figures 9 and 10 it can be seen that wet conditions and high temperatures strongly enhance iodine retention in gravel beds. Calculations have shown that hydrolysis effects are negligible and the enhancement is assumed to be due to chemical interaction.

The various forms of iodine present in the exit stream have been characterized by sampling through May packs. The May pack consists of silver plated screens, particle filters and a TEDA impregnated carbon back-up filter. Some results are shown in Table 1.

Table 1. The partition of iodine in % in May pack

		Dry conditions Ambient temp	Wet conditions High temp
Ag screen	1	79	55
	2	17	20
	3	3	6.7
	4	0.2	4.8
	5	0.1	3.7
Mp filter	1	0.1	1.2
Ag screen	6	0.06	1.4
	7	0.05	0.4
	8		0.1
Mp filter	2	-	-
Carbon bed		0.5	6.4

The results in Table 1 indicate that elemental iodine is dominant in the exit gas stream. The distribution of iodine between the silver screens is somewhat different for the different conditions, thus indicating an additional iodine species was present in the hot run. The iodine trapped in the carbon bed is assumed to be methyl iodide. By relating the iodine content in the carbon bed to the amount of iodine injected during the test the penetration of methyl iodide was found to be 0.15 % in the cold run and 0.07 % in the hot run. The lower number might indicate effects of methyl iodide hydrolysis.

It is concluded for the test conditions examined that the generation of penetrating iodine species in the gravel bed is negligble.

Iodine Retention in The Sand-Water System

The steam tests showed that wet conditions strongly enhanced the retention of iodine in a gravel bed. Some complementary laboratory tests have been performed to study this effect. In these tests elemental iodine dissolved in water passed a bed, 200 mm high and 23 mm in diameter, filled with sand of the same type as the gravel in the previous experiments.

The concentrations of I_2 and I_3^- were measured spectrophotometrically. The concentration of I^- was calculated using the equation.

$$\frac{\left[I_3^-\right]}{\left[I_2\right]\left[I^-\right]} = 768$$

The concentration of hypoiodic acid in the mother solution was assumed equal to

$$\left[HIO\right] = \left[I^-\right] + \left[I_3^-\right]$$

A typical test result is shown in Table 2, in which the iodine species concentrations are given in the inlet and exit streams at the termination of the test. The hypoidic acid concentration is assumed to be the same in the inlet and exit streams.

Table 2. Concentration changes of iodine species in water after passing a sand bed

Iodine species	Concentration mg/l	
	Inlet stream	Exit stream
I_2	100	46
I_3^-	3	17
I^-	4	42
HIO	5	5
Total	112	110

The results show that under wet conditions elemental iodine is reduced to nonvolatile iodides by the sand. The effect is pronounced. The reaction yield is far above 0.1 mg iodine/g stone.

V. Conclusions

Iodine retention

The conditions inside the gravel bed in the real case are very complex. After a while an upper hot region, a narrow condensation zone and a lower cold region will be established. To model the iodine retention for these combined conditions is very tedious and difficult. A retention model based upon the laboratory and large scale test results under dry conditions has been developed and applied for calculations on the iodine retention in the final FILTRA bed shown in Figure 12. This is a conservative approach, as no credit has been taken for the enhanced retention under wet conditions. For these less favourable conditions the retention of elemental iodine in the FILTRA bed is better than 99.99 %. It is expected that the results obtained are gravel material specific.

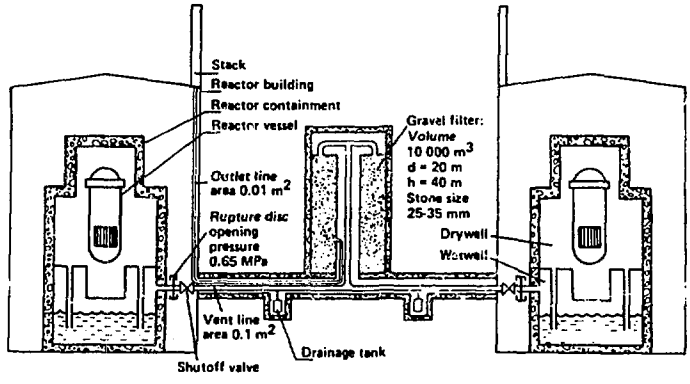

FIGURE 12
SCHEMATIC DRAWING OF FILTRA FILTERED VENTED CONTAINMENT SYSTEM

Conclusions of the FILTRA project

On the basis of the design experiments reported here and elsewhere the following conclusions can be drawn for the gravel bed, volume of 10 000 m^3, chosen for the Barsebäck site.

- Complete condensation of all steam produced within 24 hours of an accident will be obtained. Obviously by the extensive condensation itself a good filtration effect will be obtained.

- Radioactive aerosols and iodine that could cause long term land contamination will be efficiently removed in the gravel bed.

- The condensation of steam in a gravel bed is an continuous process. There is no risk that the condensate formed will plug the bed, thus impeding further condensation.

- Many of the phenomena studied are very plant specific. As regards reactors of the Barsebäck type, the following additional conclusions can be drawn.

- Filtered venting does not affect other safety functions to any appreciable extent.

- Venting prevents pressure failure of the reactor containment for such event sequences as might lead to over pressurization failure in the absence of venting.

- Analysis has shown that very rapid pressure transients caused by steam explosions, hydrogen combustion, or rapid steam formation, do not constitute a threat to the type of containment at the Barsebäck site.

- For the purpose of the FILTRA project only those events which might lead to containment overpressure have been examined. This means that the risk for radioactive releases has not been eliminated completely. Certain event sequences with very low probability are not affected by containment filtered venting of the type discussed in this context.

Acknowledgements

A large number of people have been involved in the FILTRA project of which the iodine retention studies was only a small part. The author addresses his thanks to all those he has colaborated with, and in particular to civ ing K Johansson for many valuable discussions.

References

1) FILTRA Final Report November 1982
Studsvik Library, S-611 82 Nyköping, Sweden.

2) FILTRA-Safety Assessment, Nov 1982
Studsvik Report NE-83/222.

3) Johansson, K et al
Severe Accident Mitigation Measures in Swedish Nuclear Power Plants ANS ENS International meeting on "LWR Severe Accident Evaluation". Aug 28 - Sept 1, 1983. Cambridge, Mass., USA.

4) Fredell, J
Steam and Flow Tests in a Stone Condenser.
ASEA ATOM, KUB 82-154, Mars 1982.

5) Almström, H and Berglund, S
Influence of Gravel Fill on the Course of Explosion of an Air-Hydrogen Mixture in a closed Space.
Swedish Defense Research Institute Report, C 20408-1, May 1981 (In Swedish).

6) Ström, L, Chyssler, J and Gebert, G
Experimental investigation of the retention of airborne particles in a bed of crushed rock, under conditions of condensing steam.
J. Aerosol Sci., 14, 225-228 (1983).

7) Häggblom, H
Iodine Retention in a Crushed-Rock Bed for some BWR core Meltdown Accident Scenarios.
ANS ENS International meeting on "LWR Severe Accident Evaluation", Aug 28-Sept 1, 1983, Cambridge, Mass., USA.

CLOSING REMARKS OF SESSION CHAIRMAN:

Today, we have heard a number of interesting research papers. Primarily on what to do with noble gas and iodine in accident situations, although the first paper was concerned with routine releases from the CANDU reactor. I think there are areas where further research in most of these areas would be quite fruitful and can be presented at the next Air Cleaning Conference. Particularly if some of the noble gas recovery concepts can be put into pilot scale demonstrations.

Session 5

FILTERS, FILTRATION, AND FILTER TESTING

TUESDAY: August 14, 1984
CHAIRMEN: W.L. Anderson
Consultant
R.G. Dorman
Consultant

IN-SITU CONTINUOUS SCANNING HIGH EFFICIENCY PARTICULATE AIR (HEPA) FILTER MONITORING SYSTEM
K.N. Kirchner, C.M. Johnson, J.J. Lucerna, R.L. Barnett

IN-PLACE TESTING OF MULTIPLE STAGE FILTER SYSTEMS WITHOUT DISRUPTION OF PLANT OPERATIONS IN THE PLUTONIUM FACILITY AT LOS ALAMOS
J.P. Ortiz

PROJECTS ON FILTER TESTING IN SWEDEN
B. Normann, C. Wiktorsson

EFFECT OF DOP HETERODISPERSION ON HEPA-FILTER-PENETRATION MEASUREMENTS
W. Bergman, A. Biermann

A NEW PROCEDURE FOR TESTING HEPA FILTERS
L. Hui, X. Song Niam, G. Liang Tian

THE DESIGN OF GRADED FILTRATION MEDIA IN THE DIFFUSION-SEDIMENTATION REGIME
K.S. Robinson

A DISPERSION MODEL FOR AIRBORNE PARTICULATES INSIDE A BUILDING
W.C. Perkins, D.H. Stoddard

OPENING REMARKS OF SESSION CHAIRMAN ANDERSON:

We welcome you to Session 5 of the 18th Air Cleaning Conference. This session will be divided into two segments; 5-A will contain those papers presented before the morning break, and 5-B chaired by Dick Dorman, will contain those following the break.

Our program for 5-A is dedicated to filter testing. Two of the papers are related to in-place testing, one to techniques of filter testing, and the fourth a comprehensive review of the testing programs, procedures, requirements in Sweden. Each of the papers is considered to be a significant contribution to their specific area of interest and should provide an interesting and informative session.

IN-SITU CONTINUOUS SCANNING HIGH EFFICIENCY PARTICULATE AIR (HEPA) FILTER MONITORING SYSTEM

Karl N. Kirchner, Charles M. Johnson,
Joseph J. Lucerna, and Randy L. Barnett
North American Space Operations
Rockwell International
Golden, Colorado

Abstract

The testing and replacement of HEPA filters, which are widely used in the nuclear industry to purify process air before it is ventilated to the atmosphere, is a costly and labor-intensive undertaking. Current methods of testing filter performance, such as differential pressure measurement and scanning air monitoring, allow for determination of overall filter performance but preclude detection of symptoms of incipient filter failure, such as small holes in the filters themselves. Using current technology, a continual in-situ monitoring system has been designed which provides three major improvements over current methods of filter testing and replacement. This system (1) realizes a cost savings by reducing the number of intact filters which are currently being replaced unnecessarily, (2) provides a more accurate and quantitative measurement of filter performance than is currently achieved with existing testing methods, and (3) reduces personnel exposure to a radioactive environment by automatically performing most testing operations.

An XYZ sample system was designed and constructed to transport a sample probe to any location on a given filter bank. Three stepping motors, one for motion in each direction, are used to move the probe along the twin-rail and rack and pinion axes. A serial interface card distributes movement commands to the proper axis indexer cards and driver cards which in turn supply power to the stepping motors. Laser single-particle analysis was chosen as the most sensititive detection method for this monitoring system. A microprocessor is used as the CPU for the target computer system. The target computer controls placement of the sample probe. It also acquires and analyzes the data obtained from the spectrometer. This sample system uses either ambient air or a generated aerosol to challenge the HEPA filters. It scans the downstream face of the filters to detect leaks. The target computer then calculates the filter efficiency.

I. Introduction

High Efficiency Particulate Air (HEPA) filters are used throughout the nuclear industry to filter building and process ventilation air prior to recirculation or exhaust to the

atmosphere. These filters capture radioactive particles and prevent their release into the biosphere. Many of the process cells ventilated through HEPA filters release acid vapors and substantial levels of particulates which degrade the filters and restrict airflow. The primary objective of this task is to apply currently available technology to provide continual in-situ monitoring of HEPA filter performance.

Advantages of a real-time monitoring system include: instant detection of filter failure, possible detection of incipient filter failure, a defineable and quantitative basis for initiating filter change-out, improved assurance of radioactive particle containment, and possible cost savings. In-situ monitoring of filter performance as currently practiced at Rocky Flats occurs only at installation and when abnormal conditions are detected by alpha monitoring. The system designed in this task provides a more accurate and thorough measurement of filter performance than is acheived with existing differential pressure and scanning air monitoring equipment. In-situ monitoring is needed to ensure that the performance of a filter installation is within specification, and to assure the plant operators (and the public) that degradation has not caused the system to fail.

Several techniques were evaluated for monitoring of HEPA filter performance. These included optical scattering particle measurement, laser single-particle analysis, radiometric measurement, sonic and vibrational technology, and enhanced differential pressure measurement. A concept considered important to the program was a method to challenge the filters without loading or decreasing their performance. The ideal challenge would be air entering the filter plenums to be filtered. This appears to be viable on the first stage and possibly the second. The third and fourth stages may require a small amount of challenge aerosol introduced into the plenum. Because of the low sensitivities the laser single particle analysis was the method chosen for this investigation.

II. Discussion

The HEPA Filter Monitoring Program is broken into three major subtasks: (1) Identification and selection of measurement techniques, (2) technology evaluation and feasibility testing, and (3) demonstration in a radioactive plenum.

Identification and Selection of Measurement Techniques

A literature search was conducted to identify available technologies for particulate and airflow measurement. Several weapons complex sites were visited to view and discuss their methods of monitoring HEPA filters. Rocky Flats Plant (RFP) utilities, filter installation and monitoring, and DOE Central Division HEPA Test Facility at RFP were contacted for input on

RFP methods of installation, monitoring, and testing of HEPA filters. With the information gathered from these contacts and the suggestions from Instrumentation and Control Systems Engineering (I&CSE) group at RFP, the following methods were considered: single-particle analysis, radiometric measurement, sonic and vibrational technology, and enhanced differential pressure measurement.

The following facts give some idea of the magnitude of the HEPA filter air cleaning system at RFP. RFP has approximately 9500 2 ft x 2 ftx 1 ft HEPA filters in use at any one time. These filters are distributed in about 80 plenums with each plenum containing 1 to 4 banks or stages. A typical stage of filtration contains 24 to 48 filters, although the number of filters in one stage can vary as high as 720 filters. Generally the stages are 4 filters high by 6 or 12 filters wide. HEPA filters are also subjected to a wide range of conditions from normal office air to corrosive plutonium recovery and waste treatment atmospheres. Filters are changed about every 3 years, with some areas as often as 6 weeks. About 1,000 to 5,000 filters are changed per year. Filter change out requires 9 to 11 people, half of these work in supplied air suits because of contamination.

There are three methods of monitoring in place HEPA filters at RFP and they all have problems. First differential pressure is insensitive to leaks and it is used mainly as a guide for the amount of filter plugging. Second are the radiometric monitors. They detect how much alpha activity is lost, but the alarm sounds after the leak occurs and if there is no radioactive material present, there is no way of knowing if there is a leak. Also, they are insensitive to incipient filter failure. The third method uses challenge aerosol. This labor intensive technique requires 2 to 4 people in supplied air suits and 1 person outside to read the instrument. This method is used only when filters are installed or when indicated by the presence of radioactive particles detected by the radiometric methods.

The following list of conditions were established for a proposed HEPA Filter Monitoring System to meet:

1. Improve the current methods of monitoring HEPA filters.

2. Develop a continuous real-time in-situ monitoring system.

3. Use current technology. This was not to be a basic research program.

4. No or very little challenge aerosol should be used in the plenums. This would imply a fairly sensitive technique with an attempt to use the ambient particles entering the plenum as a challenge.

5. Automate the system so there is little or no operator interaction with the equipment in order to decrease personnel exposure.

6. The system should be inexpensive when compared to the labor required for a manual check for filter performance.

7. Develop a reliable system. Reliability is very important in systems to be installed in a "hot" (radioactive) environment.

8. Design and construct scanning and data acquisition system such that a change in measurement technology would not necessitate a major system re-engineering.

After thorough consideration of the suggestions, laser single-particle analysis was chosen as the method that best met the above criteria. Laser single-particle analysis has good sensitivity and its use for HEPA filter monitoring has been demonstrated.[1-5] Optical scattering particle measurement was not used due to the small number of particles expected to be present and its low senitivity.[6] Radiometric instrumentation would require a constant source of radioactivity to verify filter integrity. Several areas have little or no radioactivity reaching the filters and challenging the filters would present problems. Sonic and vibrational technology have been excluded because of the amount of time and capital expense required to characterize frequencies present in the plenum environment. Differential pressure measurement was eliminated because of insensitivity to very small changes. Enhanced differential pressure, however, appears to be a viable technique for historical measurements of abnormal conditions occuring in HEPA filters.

Technology Evaluation and Feasibility Testing

Two computer systems were used in the development of the monitoring system. The target system is placed at the plenum and controls the sample system, monitors, and records the data. The second, the development system, remained in the laboratory for software and hardware development, and for data reduction.

A Digital Equipment Corporation (DEC) LSI 11/02 microprocessor was selected as the CPU for the target system. The CPU, DEC DRV11 parallel line unit, DEC DLV11-J four port serial line card, DEC MXV11-A memory and synchronous serial line unit, MSC 4604 memory card, DEC H9281-BB backplane, Burr Brown TM 71-IO microterminal, dual DEC TU58 cartridge tape drives, assorted power supplies to power the computer equipment, Power/Mate SW-24-K high power switching power supply to power the stepping motors, and inhouse designed relay and interface cards used in conjunction with the DRV11 parallel line unit make up the target system (Figures 1 and 2). The target system acquires data and controls the single-particle laser spectrometer in addition to controlling the movement of the sample system.

Figure 1. Front view of the target system.

Two XYZ sample systems were designed and constructed by the RFP Remote Engineering Department. The positioner was required to transport a sample probe to any location on the filter bank. The filter bank measures 114 in. wide and 93 in. high; however, the filters do not cover the entire bank. The probe had to be positioned automatically, not only along the filter bank but at varying distances from the filters. This required a 3-dimensional X, Y, and Z axis positioner. Two separate XYZ sample systems were built. Reliability of the two

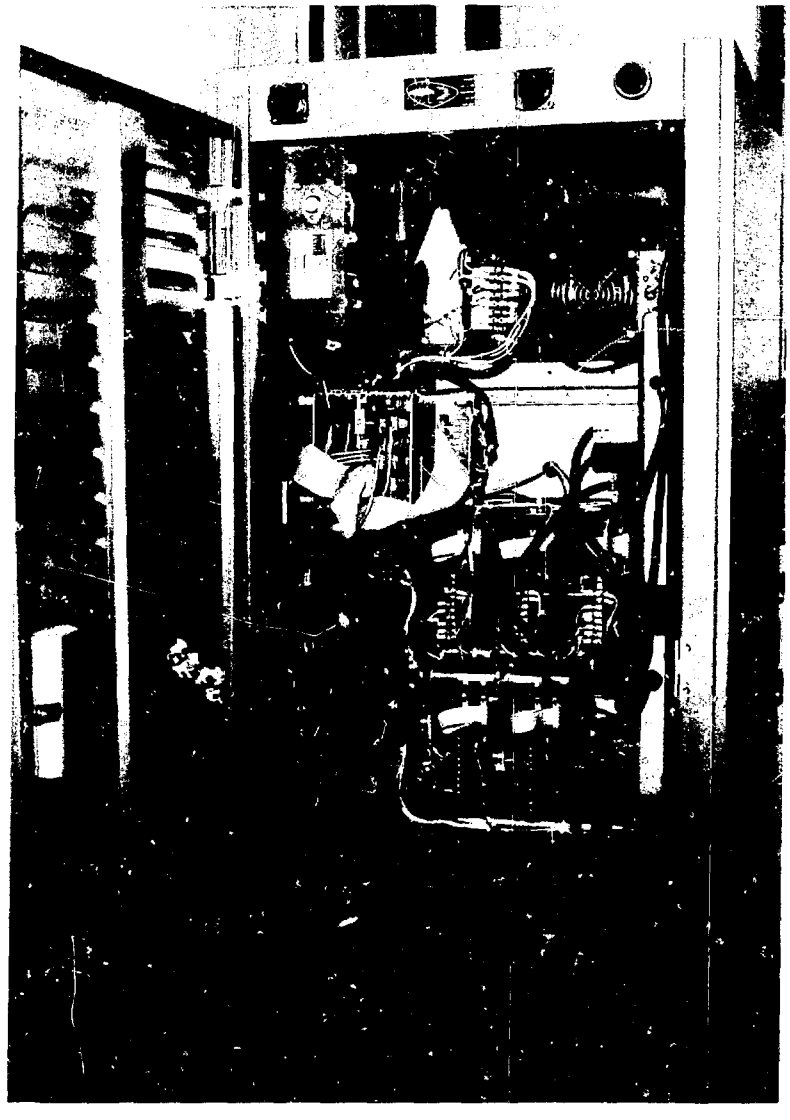

Figure 2. Back view of target system.

systems in operation will be documented. The best components of the two systems will be selected for the "hot" (radioactive) environments.

The first positioner was designed with a Lintech twin-rail shaft assembly for movement along the width of the plenum (Figure 3). A Saginaw Gear Company ball screw was used to propel a carriage holding a 7-ft tall mast. The horizontal ball screw is stationary. The carriage is positioned by a Slo-Syn stepping motor mounted on the carriage. Stepping motors were used for

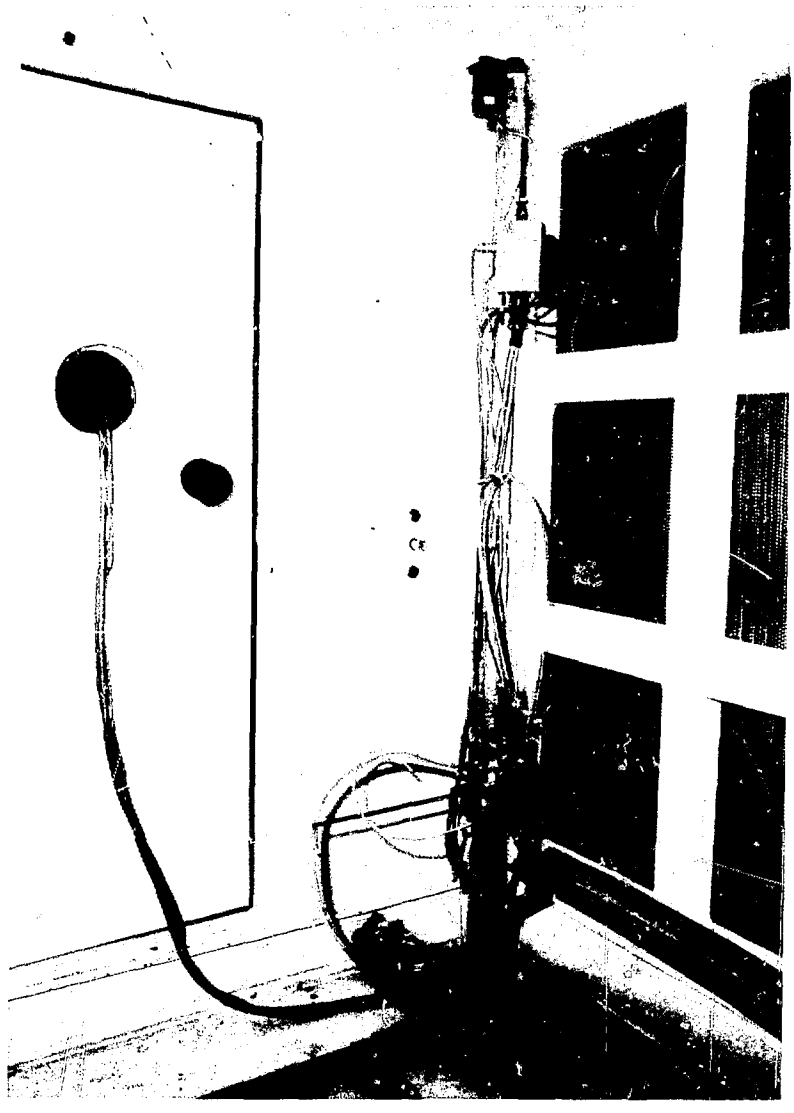

Figure 3. First XYZ positioner.

ease of programming and positional accuracy. The mast contains two teflon tracks that guide a small bracket up and down its length. Another ball screw within the mast is rotated by a Slo-Syn stepping motor and positions the bracket. The third axis, toward and away from the filters, is moved by a third Slo-Syn stepping motor. This motor rides up and down with the bracket. An 18-in. long 0.375-in. diameter gear rack is held by a rack mounting block so that it can slide lengthwise. A pinion on the motor shaft positions the gear rack. The sampling probe is attached to the gear rack (Figure 4).

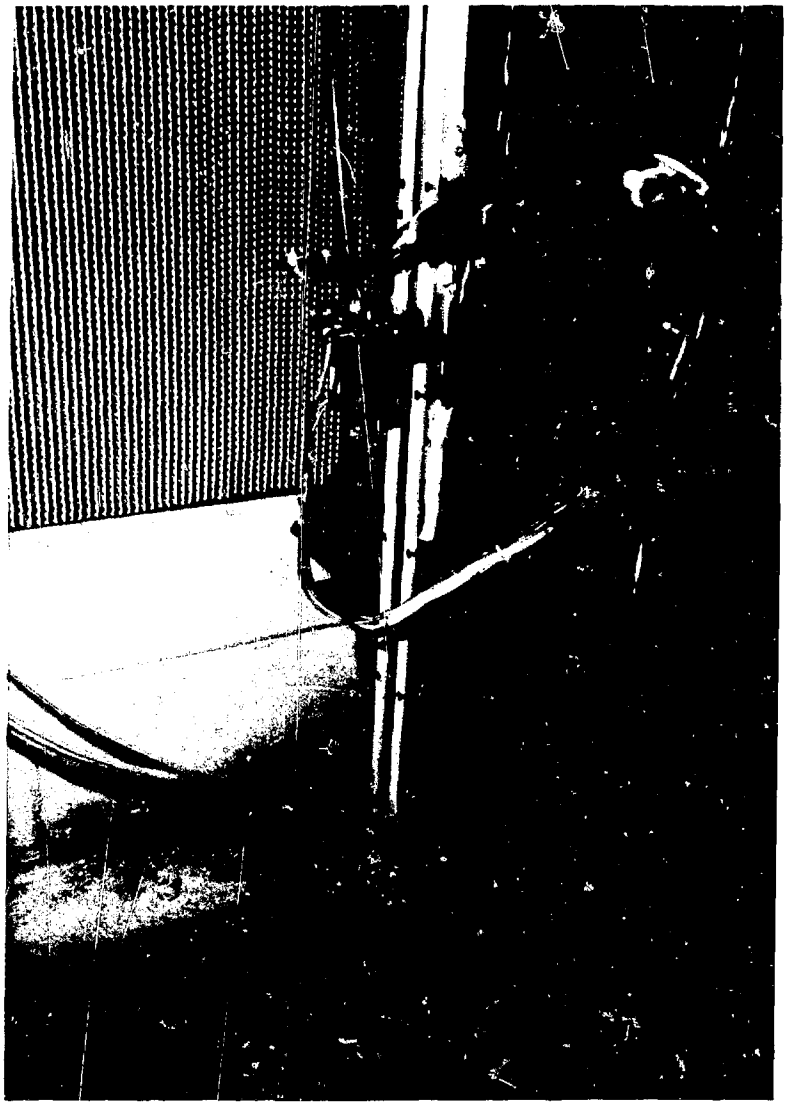

Figure 4. Sampling Probe.

The advantages to the first positioner are its light weight, low cost, simplicity of programming, highly accurate positioning, and finally, the probe position is held even when the power is turned off. The disadvantages are the instability of the mast, the great tension that must be exerted on the horizontal ball screw to minimize its sag, and the extra starting torque required of a stepping motor to turn the long vertical ball screw.

The second positioner was designed with the same basic structure as the first positioner (Figure 5). The ball screws were eliminated in favor of stationary gear racks with pinions. The Slo-Syn stepping motors were retained with one being used for motion in each of the three axes. The mast was made substantially larger for greater stability. Lintech shaft assemblies were used in pairs in all three axes. The axis which takes the probe closer to or farther from the filter was moved down so that it would not have to be raised by the stepping motor for the

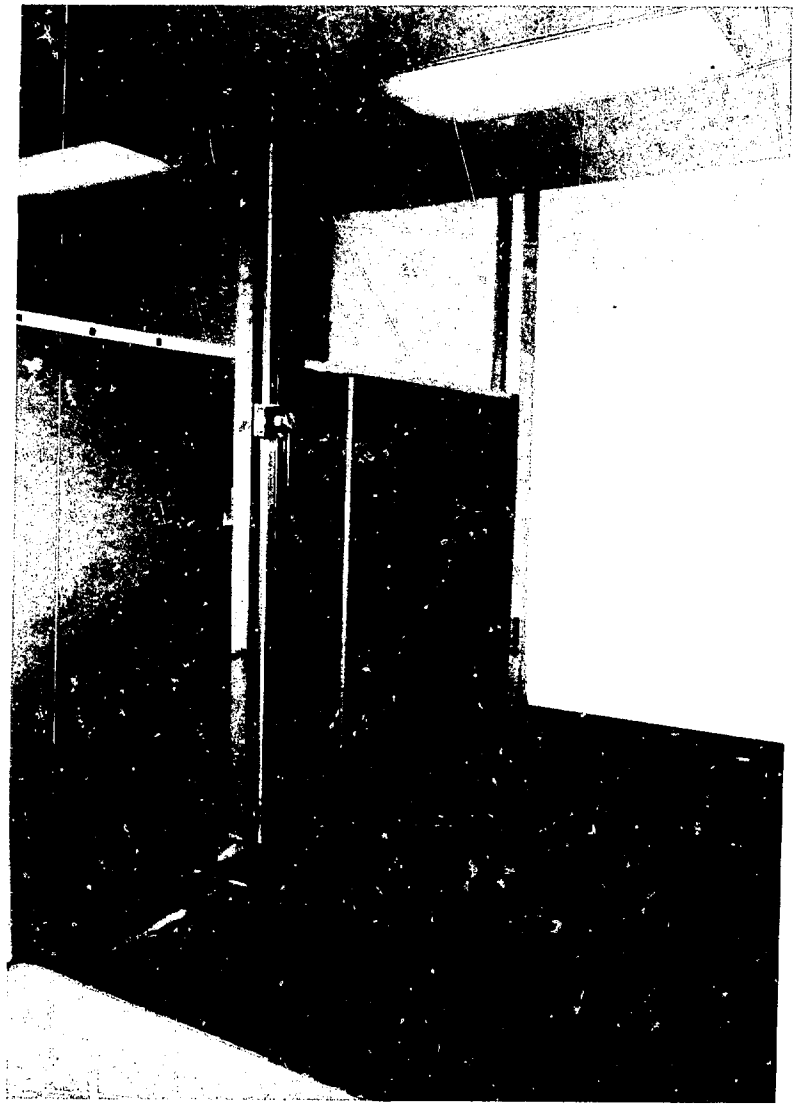

Figure 5. Second sample positioner.

vertical axis. The vertical axis required a method to keep the probes position even when the power was off. A counter balance was added which operates much like an elevator. The counter balance also greatly reduces the load on the vertical axis stepping motor.

The first sample system was equipped with micro-switches, or limit switches, for indexing and to sense when the motors are driving against a stop. These limit switches are wired to the target computer through the RFP designed interface and DRV11 parallel line unit. When one or more of the microswitches are depressed the computer stops all motor movement and determines the next action.

The XYZ sample system is controlled by the computer through a RS-232 serial-interface line, to Superior Electric Modulynx cards. The Modulynx cards used are an IOD004 interface card, IDD008 indexer cards, and DRD001 driver cards. The serial interface card distributes the movement commands to the proper axis indexers and driver cards. The stepping motors are powered by the switching power supply through the driver cards.

The single-particle laser spectrometers chosen were two Particle Measuring System, Inc. (PMS) LAS-X units. It was felt that they would give the information needed in the size range 0.09-3.0 microns. Final choice of the instrument for a four-stage working system will probably be able to use much simpler instruments. Control of the spectrometer by the target computer was accomplished by installing a relay in parallel with the spectrometer's reset switch. By sending a command to the interface via the DRV11, the relay is closed which causes the spectrometer to reset and send the acquired data to the target computer. Both spectrometers are operated in the manual mode so all sample count times can be controlled by the computer with the reset relay.

In addition to monitioring the limit switches and controlling the reset relay, the RFP designed interface card will control which sample area is routed to which spectrometer with the use of solenoid valves and a manifold. This will gain importance when the system is installed in a multi-stage plenum with the monitored stage selected and routed to the selected spectrometer.

With the exception of the XYZ sample system, all boards and electronics are housed in a 19-in. x 60-in. x 30-in. cabinet equipped with wheels for portability.

The development system was designed to develop software for the target system and to reduce the data acquired by the target system. The system consists of a DEC VT100 video terminal, DEC LA120 printer, Adac 1000 card cage and power supply, DEC LSI 11/23 processor with memory management and

floating point options, Trendata Pincomm 23S MM-148 memory module with 256 Kbyte capacity, DEC DLV11-J four-port serial line card, DSD 880x/30 data storage system with 30 Mbyte winchester, and 0.5 Mbyte single-sided double-density floppy disk, Hewlett-Packard 7470A Graphics Plotter with RS-232 interface option, dual DEC TU-58 cartridge tape drives, and ISOREG computer power supply. All of the development system components, with the exception of the printer, are housed in a 19-in. x 60-in. x 30-in. cabinet (Figure 6).

Figure 6. Development system.

Both the target and development systems are run with the DEC RT-11 operating system. All programming was done with DEC Fortran IV language.

The target system was designed for installation in plenum FU-6, an unused plenum in the 771 Chemicl Reprocessing Building. The plenum was modified for use of testing only. Instead of the usual intake from a process area and exhaust to the environment, it will recirculate the exhaust of the plenum to its intake (Figure 7). In addition, the modifications offer the option of opening the closed loop with 2 tees to take room air, filter it,

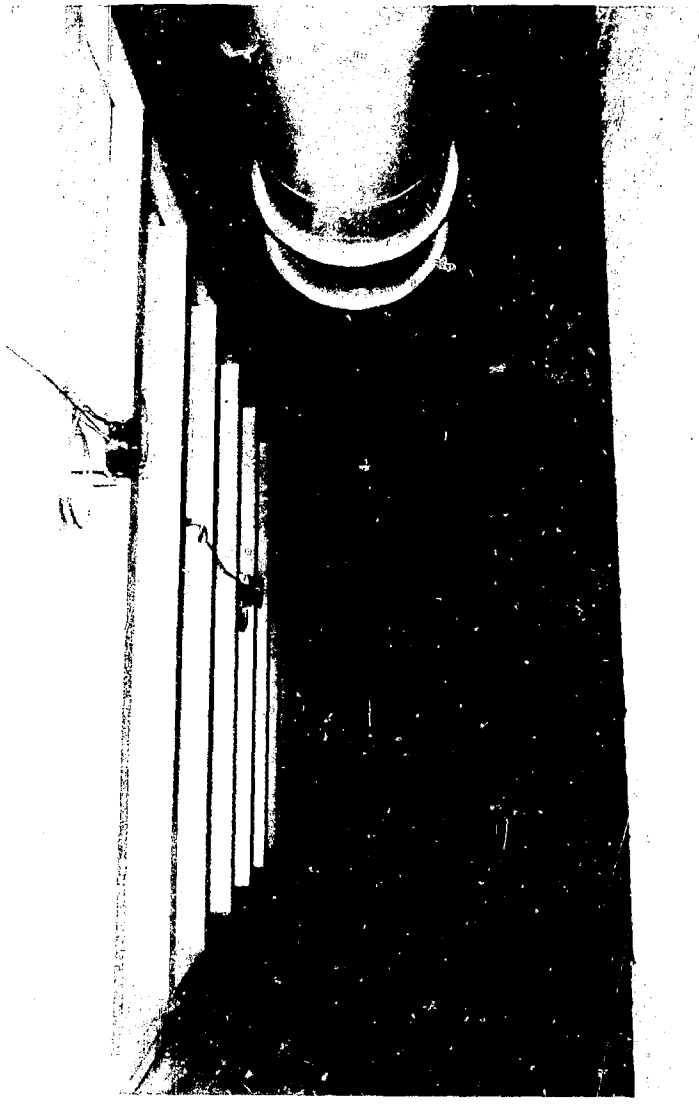

Figure 7. Recirculation of plenum FU-6.

and exhaust it to another portion of the area for ambient air challenge experiments. The plenum has four stages of HEPA filtration. Each stage or bank is 3 filters high by 4 filters wide. The XYZ scanning systems will be installed downstream of the last two stages (stages three and four). This will allow testing the system as if it were installed in stages one and two by removal of the first two stages of filters or testing of stages three and four with installation of stage one and two filters.

Upon completion of tests in the demonstration plenum (FU-6), the program will progress to the final phase which is a demonstration in a radioactive plenum.

III. Experimental

Several experiments were completed before the demonstration plenum was completed. Studies were made on ambient air to determine the size distribution of particles in air in an HEPA filtered building and sample line loss experiments using various lengths of sample lines and different line materials. A small four-stage test plenum was constructed using Plexiglas and four No. 2 HEPA filters. Additional experiments were completed on the small test plenum and are discussed later in this report.

A study of the room air determined the number and distribution of particles in the 0.09-3.0 microns range. The building air was HEPA filtered, and as it was primarily office areas and some machining operations, it was not expected to be one of the buildings with high particulate counts. A building with HEPA filtering was chosen to provide an indication of the particulate distribution and if the quantities were in the range that HEPA filters are least efficient. The building studied had 93 percent of the particles counted within the 0.09-0.21 micron range. These particles are in or close to the ranges HEPA filters are least efficient.[7,8]

Sample line losses would be an important factor in using the proposed LAS-X system. In the test plenum, the sample probe would be a maximum of 25 ft from the spectrometer. Significant line losses were particularly a concern using low particulate concentrations. Several tests were made to determine particulate losses in 0.125-in. outside diameter (OD) polyurethane ester base sample lines. Overall, the average was 0.85 percent loss per foot. This was too great a loss for the long runs in our applications. In addition, the purge time would be too long between samples. Instead, a 1-ft^3/min. sample delivery system was constructed to bring the downstream sample to the laser aerosol spectrometers.

A small test plenum for experiments in the laboratory was constructed. This plenum has four No. 2 (8 in. x 8 in. x 6 in.) HEPA filters in series (Figures 8 and 9). Each filter is separated by approximately 1 ft. The top of the small test plenum is

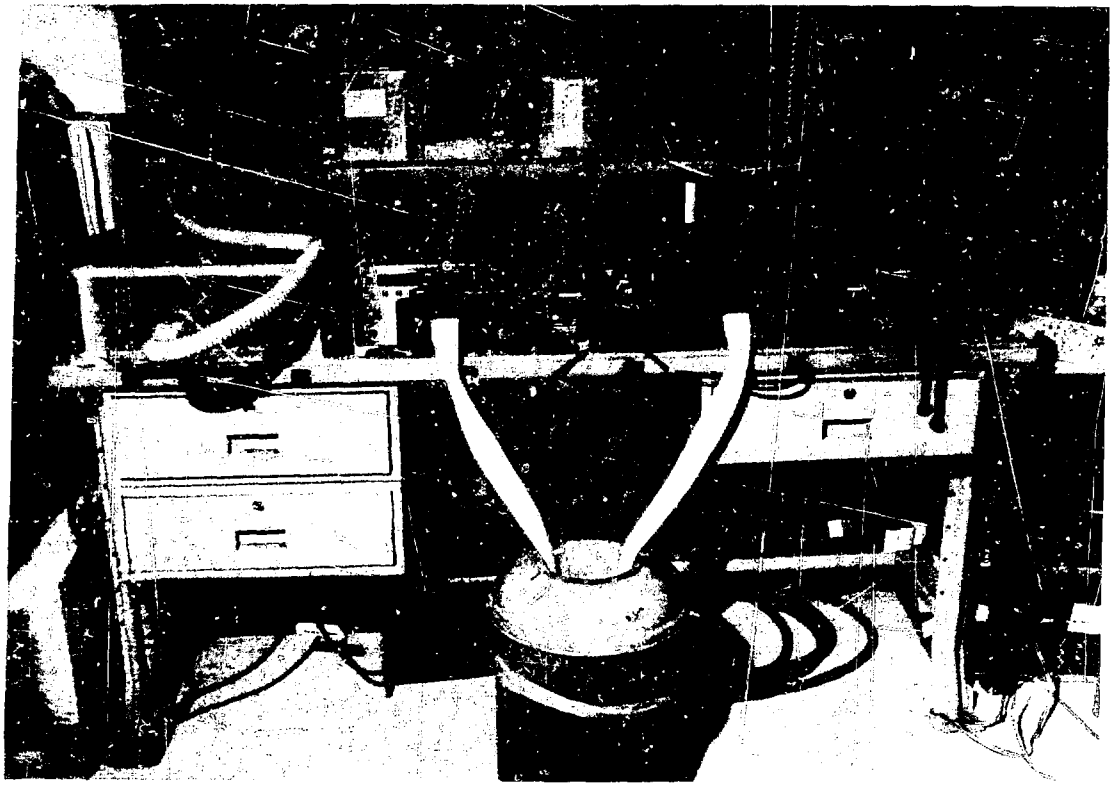

Figure 8. Small test plenum system.

removable to facilitate changing filters. There are holes in the top behind each filter to allow insertion of a sample probe. Air was drawn through the filters to simulate actual plenum operation. The filters were challenged with room air to test the feasibility of ambient air challenge. The results were both encouraging and disappointing. Unfortunately, the number of particles passed by stages three and four were nearly zero at 0.25 in. from the filter media. After a 30-minute sample time, few or no particles were counted in the 0.15-0.30 micron size range. However, the encouraging results came while moving the probe away from the media several inches. At that point, there were particles in the plenum between stages. These particles were due to in-leakage from outside and from around the filter mountings. This leakage will have to be quantified for each stage in the plenum when the system is installed. If enough particles are present, it may be possible to use them as a challenge aerosol.

Another test performed using the small test plenum mapped the dispersion cone of a hole in a HEPA filter. Determining the dispersion cone of a detrimental leak will enable the number of sample points and distance from the filter of the probe to be

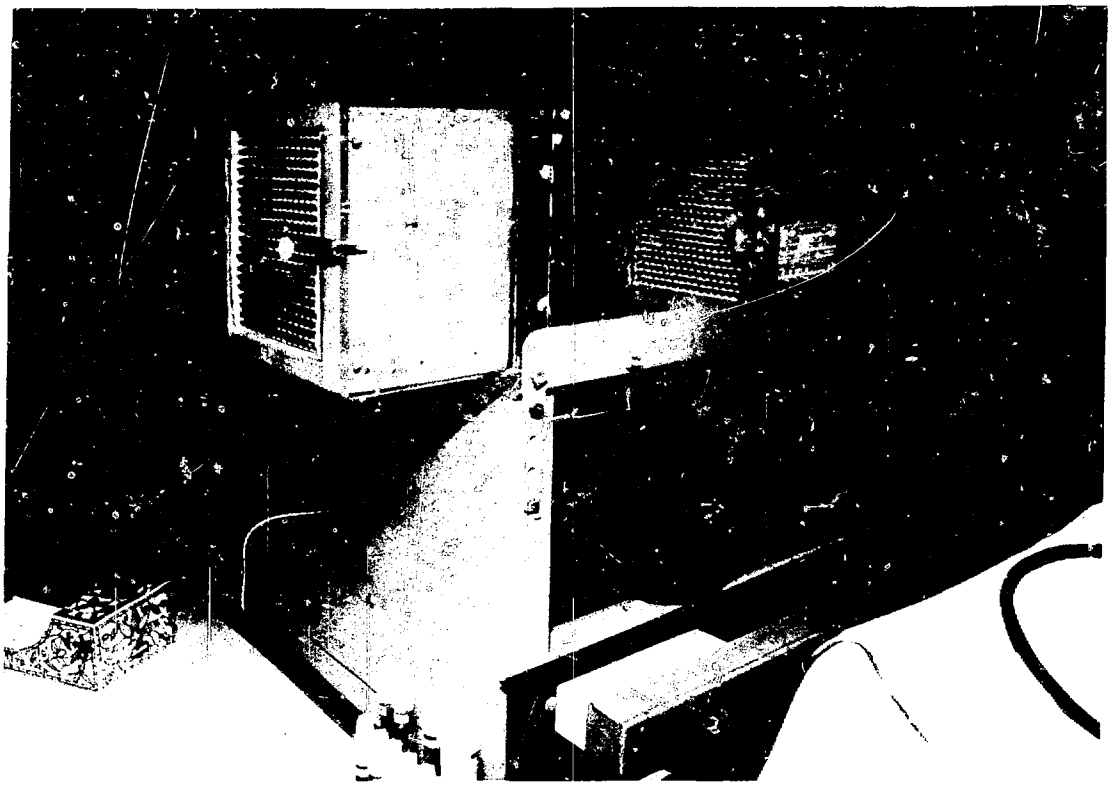

Figure 9. Close-up small test plenum.

calculated. The experimental plan called for several sizes of holes to be mapped. The ability to accurately measure probe position in the small plenum proved very difficult; therefore, only one hole was mapped and the remainder will be completed in the full scale test plenum. A 0.125-inch hole was made in the first stage filter. To map the dispersion of leaking particles, readings were taken every 0.25 inch in the X and Y directions with the input of the probe approximately 3.5 in. from the filter media. The particles from the 0.125-in. hole dispersed to form a cone approximately 2 in. in diameter (Figure 10). One-thousandth of a percent of the challenge particles passed was considered the minimum detectable amount with challenge concentrations of approximately one million particles counted per 3 minutes in the 0.09-0.195 micron size range.

Since completion of the test plenum, the first XYZ sample system has been installed and experiments have begun. These experiments have been structured to include traceability to the currently used standard, ANSI N510-1980. In order to provide traceability, the filter banks are challenged with a gas-thermal DOP generator. The upstream challenge aerosol is measured

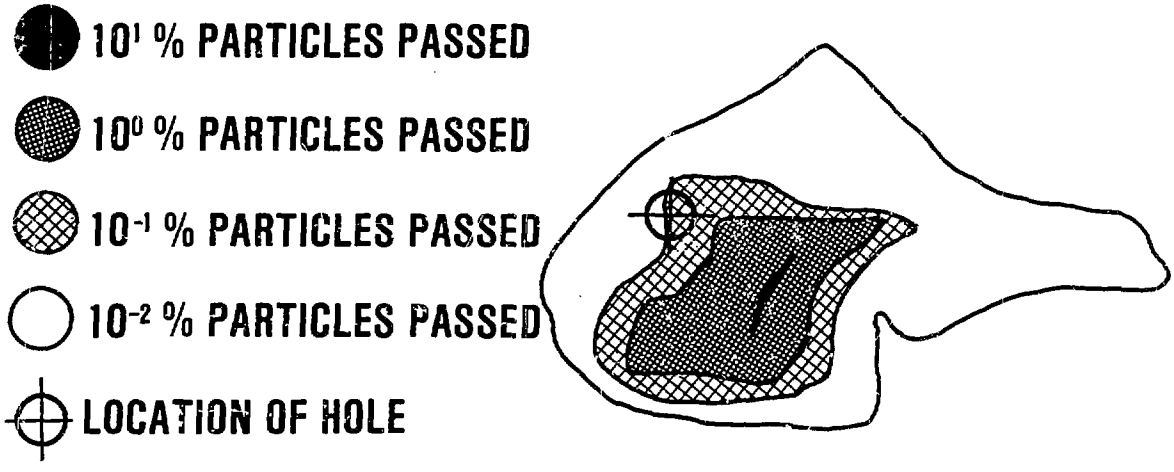

Figure 10. Percent particles passed 3.5 inches from hole.

directly with an aerosol photometer and a laser aerosol spectrometer through a dilution board (Figures 11 and 12). The downstream particulate concentrations are again measured with a photometer and a laser aerosol spectrometer, but without the dilution board.

First, the overall bank efficiency was checked using both the photometer and the laser aerosol spectrometers. Aerosol samples were taken downstream of the bank at the input of the fan and upstream approximately in the center of the bank of filters (Figure 13). The photometer produced a bank efficiency of 99.959 ± 0.002 percent and the laser aerosol photometers result was 99.967 ± 0.002 percent. These efficiencies were obtained as a baseline to compare all other bank tests.

Next, efficiency measurements were taken at the centers of each filter 9 in. downstream of the filter face. The laser aerosol spectrometer indicated an efficiency of 99.998 ± 0.002 percent, and the photometer's was 99.975 ± 0.009 percent. Additional measurements will be taken at various distances from the filters, and the single point on each filter measurement will be expanded to multiple points on each filter in an effort to best

Figure 11. Photometer and laser aerosol spectrometers.

represent the true bank efficiency. These efficiencies are better than the overall bank efficiencies obtained above due to in-leakage after the filters.

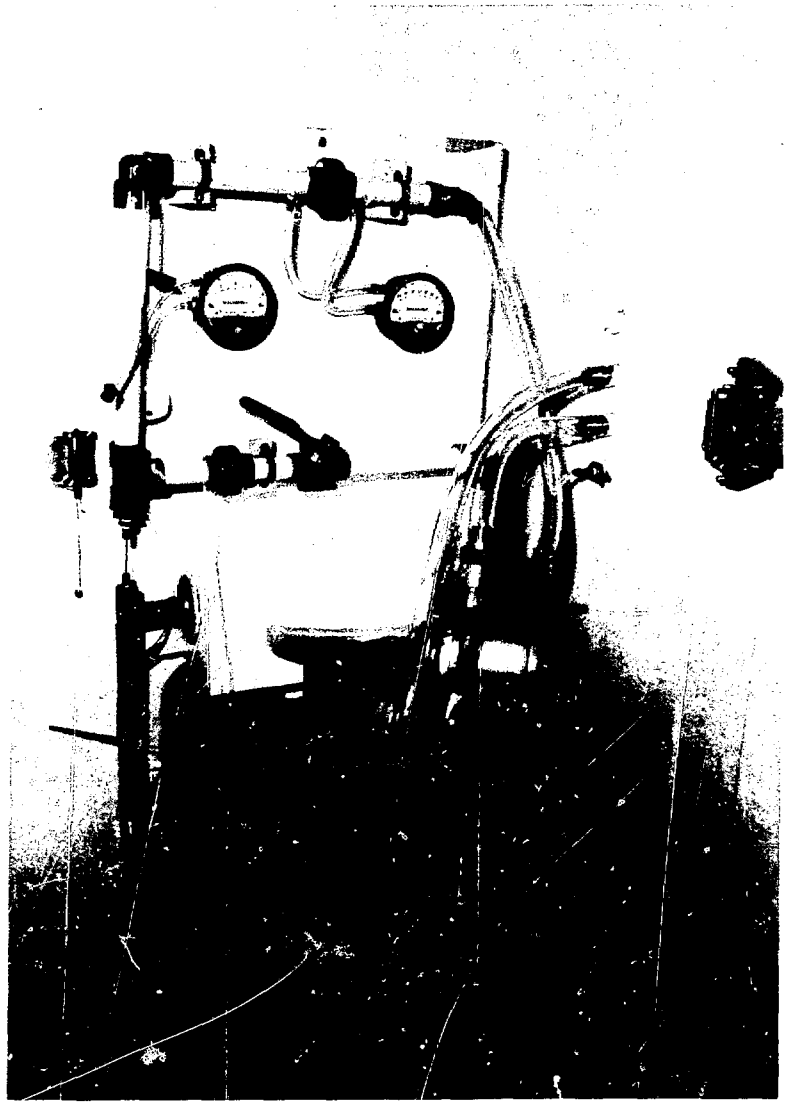

Figure 12. Dilution board.

IV. Conclusions

For this application, single particle laser spectrometry was the best application. The target computer system has been demonstrated to control the LAS-X's and the XYZ sample system in a viable manner. Laboratory tests indicate that the LAS-X will work on the first two stages of a filter plenum and possibly on the others.

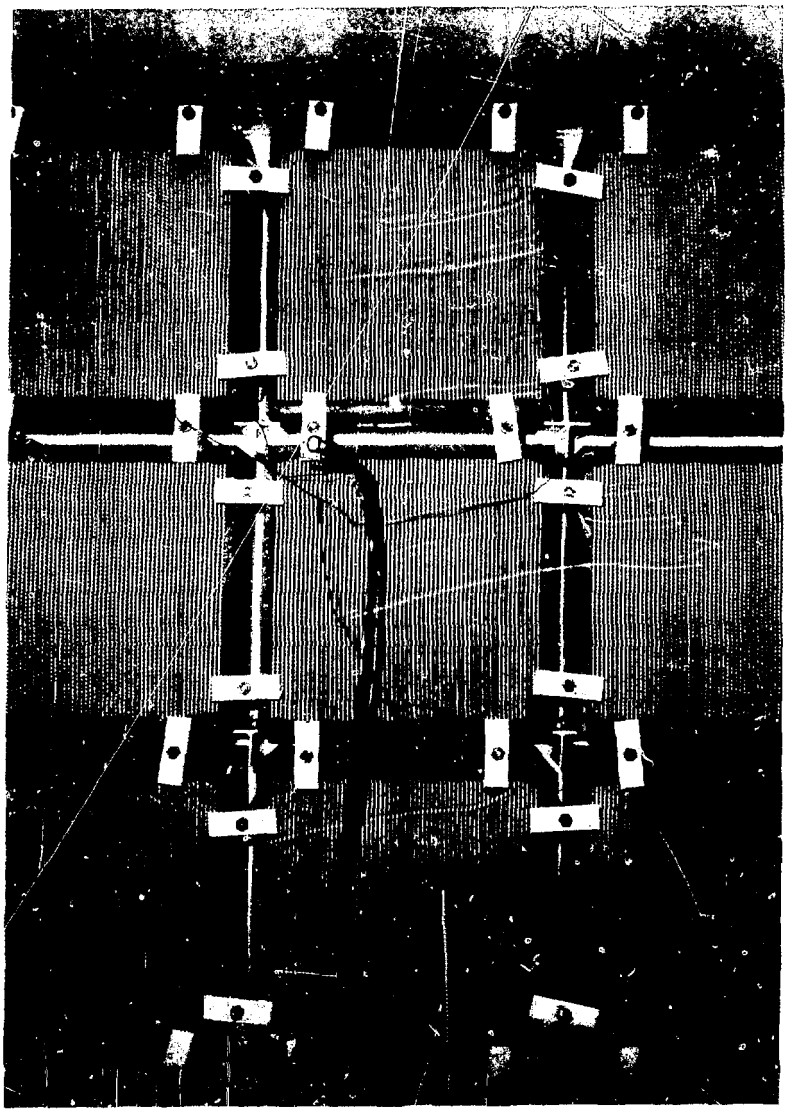

Figure 13. Upstream sampling point.

Acknowledgement

We wish to thank the following people and organizations: Airborne Waste Management Office, Idaho, for providing the funding for the program; R. E. Luehr, F. J. Smith, A. J. Dascher, R. G. Knollenberg, Particle Measuring Systems, Inc., M. I. Tillery, Los Alamos Scientific Laboratory, R.G. Pinnick, US Army Atmospheric Sciences Laboratory, S. J. Fernandez, Exxon Nuclear

Idaho Company, Inc., DOE Central Division HEPA Test Facility personnel, A. G. Garcia, Plenum Test and Certification, Rocky Flats Plant (RFP), for their invaluable information used for this program; C. A. Gonzales, Instrumentation and Control Systems Engineering (I&CSE), RFP, for her long hours plotting data; K. E. Kirchner and T. W. Coressel, I&CSE, RFP, for their hardware design on the program; and M. L. Meals and A. L. Tindal, I&CSE, RFP, for their software assistance.

References

1. Salzman, G. C., Ettinger, H. J., Tillery, M. I., Wheat, L. D., and W. K. Grace, "Potential Application of a Single Particle Aerosol Spectrometer for Monitoring Aerosol Size at the DOE Filter Test Facilities," Proceedings of the 17th DOE Nuclear Air Cleaning Conference, CONF-820833.

2. Schuster, B. G. and Osetek, D. J., "Tandem HEPA Filter Tests," American Industrial Hygiene Association Journal, 39, pp. 144-150 (Feb. 1978).

3. Schuster, B. G. and Osetek, D. J., "The Use of a Single Particle Intra-Cavity Laser Particle Spectrometer for Measurements of HEPA Filters and Filter Systems," Proceedings of the 14th ERDA Air Cleaning Conference, CONF-760822.

4. Schuster, B. G. and Osetek, D. J., "In-Situ Testing of Tandem HEPA Filter Installations with a Laser Single Particle Spectrometer System," Proceedings of the 15th DOE Air Cleaning Conference, CONF-780819.

5. Schuster, B. G. and Osetek, D. J., "A New Method for In-Place Testing of Tandem HEPA Filter Installations," American Industrial Hygiene Association Journal, 40, pp. 979-985, 11/79.

6. Murphy, L. P., Fernandez, S. J., Motes, B. G., "Comparison of HEPA Filter Test Methods in Corrosive Environments," Exxon Nuclear Idaho Company, Inc., Report ENICO-1037, July 1980.

7. Tillery, M. I., "Determination of Protection Factors for Tandem HEPA Filters," Los Alamos Scientific Laboratory, Report LA-UR-81-729, 1981.

8. Tillery, M. I., Salzman, G. C., and Ettinger, H. J., "The Effect of Particle Size Variation on Filtration Efficiency Measured by the HEPA Filter Quality Assurance Test," Proceedings of the 17th DOE Nuclear Air Cleaning Conference, 1982.

DISCUSSION

DYMENT: This is a very interesting paper. To the uneducated eye and ear, it seems that a lot of development work has been going on over the years on the improvement of test systems. And we are seeing an increase in the complexity of the hardware and software used in filter system evaluation. Traditionally, I think many of us have reservations about the use of highly sophisticated test gear for validating filtration systems. Do you think we are getting to a state now where in order to assure ourselves that the equipment is functioning correctly we have to have a test procedure for testing the testing equipment?

KIRCHNER: Yes, to a point, but I don't know if I am qualified to answer that. I think we might be. Some of other equipment is getting quite sophisticated but we are finding out a lot more about filters than we previously knew. I don't know if we need to have test equipment to test the test equipment as the system operates. However, you need checks to assure the equipment is operating properly For example, the use of limit switches on the XYZ sample system is a check to see that the motors don't drive against a stop. Software checks will be incorporated into the operating system to check the instruments and computer and to alert someone to a possible problem.

JENKINS: It seems like a lot of hardware in the housing of your plant assembly. What did you find as far as maintenance of the hardware and its ability to keep functioning without having people going and making adjustments or additional work that may have to be done to keep that sampling system functioning for, say, six months to a year? Did it see that kind of use, did it ever run continually for any prolonged period of time?

KIRCHNER: We haven't had extended operating use yet, and we are just getting to that point. We haven't had any problems with the portion inside the plant. As far as hardware inside, all you have is stepping motors to gear the ballscrew drivers.

JENKINS: You mentioned motors and gear drives, etc. From the little experience I have had, if that is intergral, which it is, as it is keeping your scanner moving and so forth, does it not require people to go in and make adjustments?

KIRCHNER: We have not required any adjustments up to now.

JENKINS: I guess my final question will be, what applications in commercial power plants do you see? Are you looking toward it being a viable means of scanning commercial nuclear power plants, or are you looking more toward refining plants, or someplace where you have higher doses in the ventilation ducting?

KIRCHNER: We were mainly designing to help ourselves at Rocky Flats, and any other nuclear complex, if they were interested. I am not familiar with the set-up in a nuclear plant, so I cannot comment on that.

GOULET: Could you give us an idea of the time required, using the spectrometer, to locate a leak in a standard 2' x 2' ft. filter?

KIRCHNER: It would depend upon the size of the leak, method of challenge (i.e., ambient air, DOP), and number of points sampled. With a DOP challenge and a single point sample, and a leak within the range of measurement of the instrument, probably within 4 minutes. With an ambient challenge and a multipoint sample scheme, it may take several hours. But, with no need for operator interaction time, it isn't that important.

Dup

IN-PLACE TESTING OF MULTIPLE STAGE FILTER SYSTEMS WITHOUT DISRUPTION OF PLANT OPERATIONS IN THE PLUTONIUM FACILITY AT LOS ALAMOS

John P. Ortiz
Industrial Hygiene Group
Health, Safety, and Environment Division
University of California
Los Alamos National Laboratory
Los Alamos, New Mexico 87545

Abstract

The Los Alamos National Laboratory Plutonium Facility has a number of multiple-stage air-cleaning systems. These systems operate on a continuous basis and economic considerations require that shutting down of the ventilation systems due to in-place testing be kept to a minimum.

Earlier methods of testing multiple-stage filter systems required scheduled shut down of the filter system. Methods such as injecting the test aerosol between the stages have proven costly because of the need to install temporary injection ducts and completely close off the ventilation from the process area. Also, additional personnel were needed to install and move injection and bypass ducts from one system to another. After considering these costly methods, we improved our current methods of testing to prevent interruption of plant operations.

The modified procedure uses a laser particle size spectrometer that has the capability of counting single particles downstream of two filter stages where decontamination factors of the first stage and overall system effectiveness is established. This procedure is similar to that of Nuclear Standard NEF 3-4IT, "In-Place Testing of HEPA filter systems by the Single-Particle, Particle-Size Spectrometer Method."

Decontamination factors of 10^9 are measured downstream of two stages. Particle size analyses of the challenge and the aerosol penetrating the first and second stages have been established. A cost estimation comparing two test methods show considerable savings in operational costs.

I. Introduction

Nuclear Standard NEF3-4IT[1] has been implemented as guidelines for in-place testing of HEPA filter systems at the Los Alamos National Laboratory. Improved techniques in aerosol detection and aerosol generation have contributed to the success of testing multiple-stage systems. By utilization of these methods, testing of filter systems can be accomplished without major interruption of programmatic operations at the Plutonium Facility. Testing by this method is considered to have an advantage over the stage-by-stage method using less sensitive instrumentation such as the light-scattering photometer.

The procedure for testing each stage individually required closing dampers to the process area in order to perform the

testing. The tests were completed in approximately 1 hour. Advanced notification of the impending tests was required so that processes could be suspended for the duration of the test. Needless to say, this practice had a serious economic impact in operational costs during the 1 hour it took to complete the testing.

A typical process area that is serviced by one of these systems may have up to 25 employees recovering or processing plutonium. It has been estimated that recovery revenues and the cost/hour/25 employees could be as much as $23,000.00 for the 1 hour interruption of process ventilation.

The additional sensitivity of the single-particle, particle-size spectrometer (SPPSS) permitted measurements of low aerosol concentrations, even those that penetrate two stages of filtration. Air-cleaning credit is established for the first and second stages by assigning decontamination factors (DF). The usefulness of this method is that the DF values for the system could be determined by real-time measurements rather than multiplying the DFs together, resulting in overestimation of overall system DF.

II. Description of Laser Spectrometer

The Laser Spectrometer, PMS model LAS-X[2] (Particle Measuring Systems Inc., Boulder CO), shown in Figure 1 as built into a sampling cart, is designed to identify and count single particles over a size range of 0.09 to 3.0 μm diameter. Four selective size ranges are used to cover this total dynamic range, with each range having fifteen linear size intervals.

The system has the capability of providing an interface signal where data acquisition is transferred directly to an HP-85 micro computer. Retrieval information includes, the number concentration (particles/cm^3), geometric mean diameter (μm), geometric standard deviation (σ_g), and the mass concentration (mg/m^3).

III. Aerosol Dilution

Since the SPPSS is a single-particle detector, the presence of more than one particle in the scattering volume will result in particle counting uncertainties. To overcome this problem when measuring the challenge aerosol, it is necessary to dilute the challenge aerosol to a sample dilution of at least 700:1. A diluter, shown schematically in Figure 2, was constructed with two dilution stages. The first stage provides dilutions of 250:1, while the econd dilution is 1000:1. The nominal dilution flow rate through the system is 3×10^{-4} m^3/s (18 L/min). Airflow in the system is maintained to approximate isokinetic conditions at the SPPSS sampling probe. Constant flow is maintained through the diluter and SPPSS during the testing.

Dilution ratios are determined by withdrawing a sample of the undiluted aerosol with a forward light-scattering photometer, then taking a portion of the diluted aerosol and establish a dilution

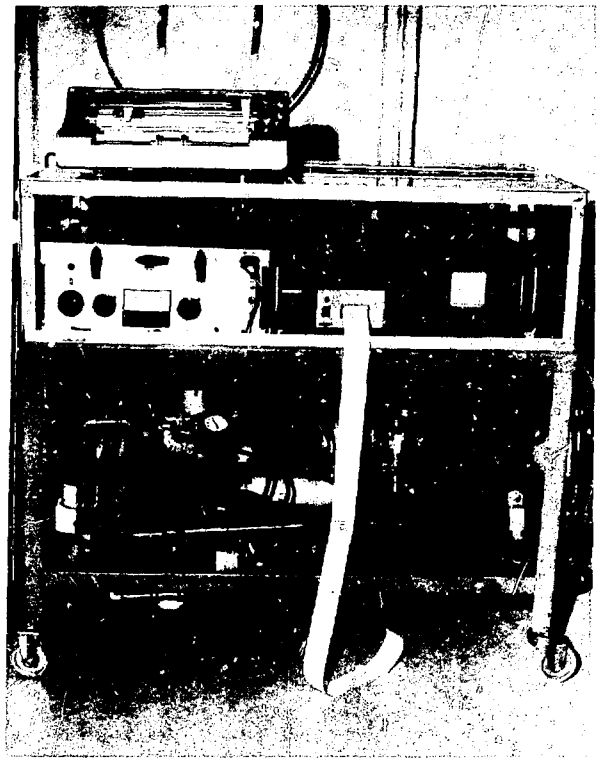

FIGURE 1
PHOTOGRAPH OF LASER SPECTROMETER

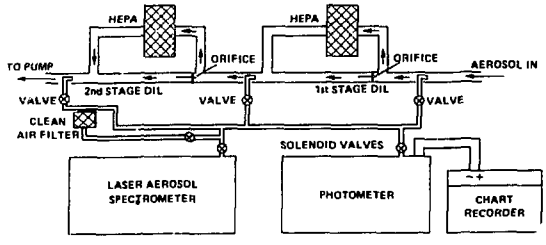

FIGURE 2
SCHEMATIC DIAGRAM SHOWING AEROSOL DETECTION INSTRUMENTATION INCLUDING AEROSOL DILUTION

factor from the ratio of the two values. It is not necessary to check the dilution each time a system is tested as long as constant flow is maintained in the system. However, periodic checks are advisable.

IV. Aerosol Generation

Figure 3 shows a schematic of a gas thermal generator that is capable of producing variable output concentrations of di-(2-ethylhexyl)phthalate (DEHP) aerosol. The generator includes a 37 liter reservoir containing liquid DEHP. Reservoir pressure and gas liquid mixture is maintained with carbon dioxide gas. Liquid DEHP is metered to the desired flow then is combined with CO_2 prior to entering the vapor core.

The core consists of a 76-mm (3.0-in.) di meter steel rod with 20 equally spaced channels machined on the core surface. The core is press-fit inside a heating chamber and a 300-watt heater is installed in the center of the core. Symmetrically surrounding the core assembly is a 1100-watt heater, controlled by a 38-350°C temperature controller. The preset core temperature is 315°C.

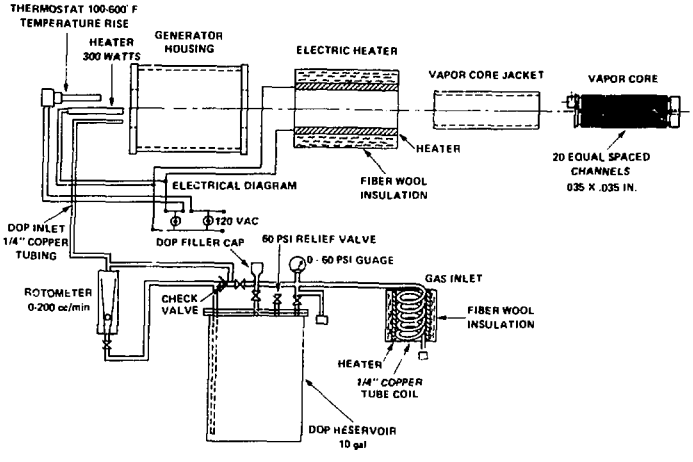

FIGURE 3
SCHEMATIC DIAGRAM SHOWING THE AEROSOL GENERATOR

Figure 4 shows one of the generators injecting test aerosol into a filter system which is being tested.

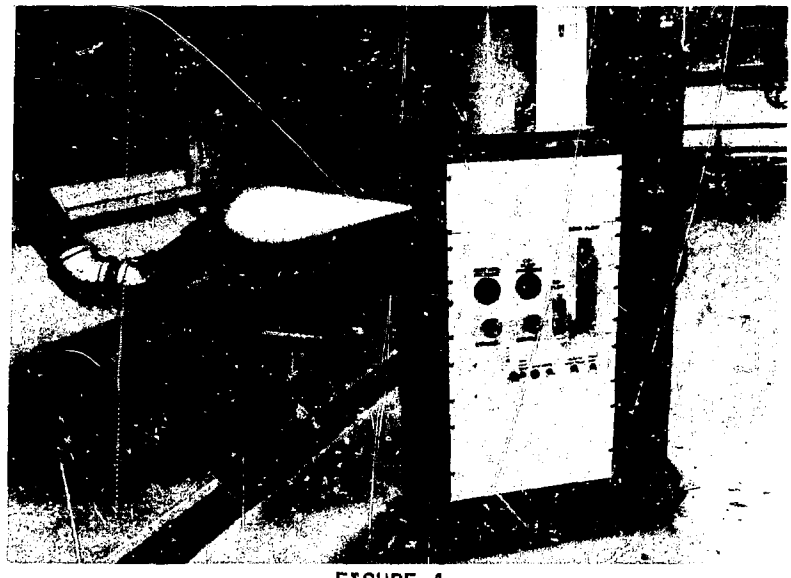

FIGURE 4
GENERATOR INJECTING TEST AEROSOL INTO HEPA FILTER SYSTEM

Figure 5 shows aerosol size distribution measured by the SPPSS at various liquid feed rates. Output concentrations of 2.8 x 10^5 particles/cm^3 at 30 cc/min and upwards of 5 x 10^8 particles/cm^3 at 150 cc/min were obtained. The mass concentration remained below 100 µg/liter as long as the feed rate did not exceed 70 cc/min. The output concentrations at 70 cc/min was 10^6 particles/cm^3, which is the recommended concentration outlined in NEF3-4IT for testing two-stage filter systems. The size distribution of the particles had geometric mean diameters of 0.24 µm at 30 cc/min, 0.33 µm at 70 cc/min and 0.47 µm at 150 cc/min. Average σ_g of the size distribution was 1.5.

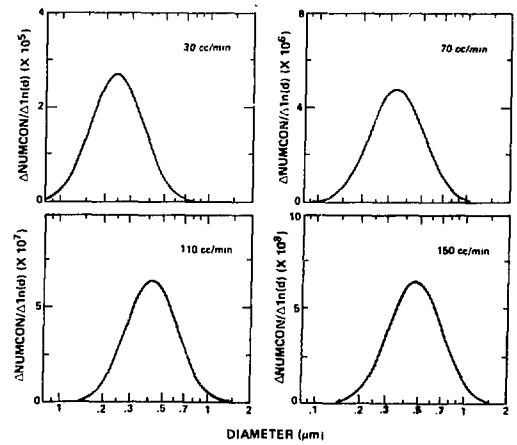

FIGURE 5
AEROSOL GENERATOR OUTPUT AS A FUNCTION OF NUMBER CONCENTRATION AND PARTICLE SIZE DISTRIBUTION

The size distribution at 10^6 particles/cm^3 is slightly larger than that recommended in NEF3-4IT. The standard recommends that the size distribution of the test aerosol have a geometric mean diameter of 0.25 μm and a σ_g of 1.4 maximum. Our testing of two-stage systems shows that the larger size characteristics of the test aerosol does not present any problems in yielding significant number concentrations downstream of two filter stages.

V. Previous Methods of Testing Individual Stages

Figures 6a and 6b show the arrangement previously used for testing each stage separately.[3] Testing the first stage required installation of a temporary aerosol injection duct (608-mm diameter, 6.2-m long) upstream of the first filter stage. A second duct was installed between and around the second filter bank. The dampers on the inlet side of the plenum and fan were closed and a temporary blank-off plate was installed at the fan inlet. Challenge and penetration concentrations were measured 10 duct diameters upstream

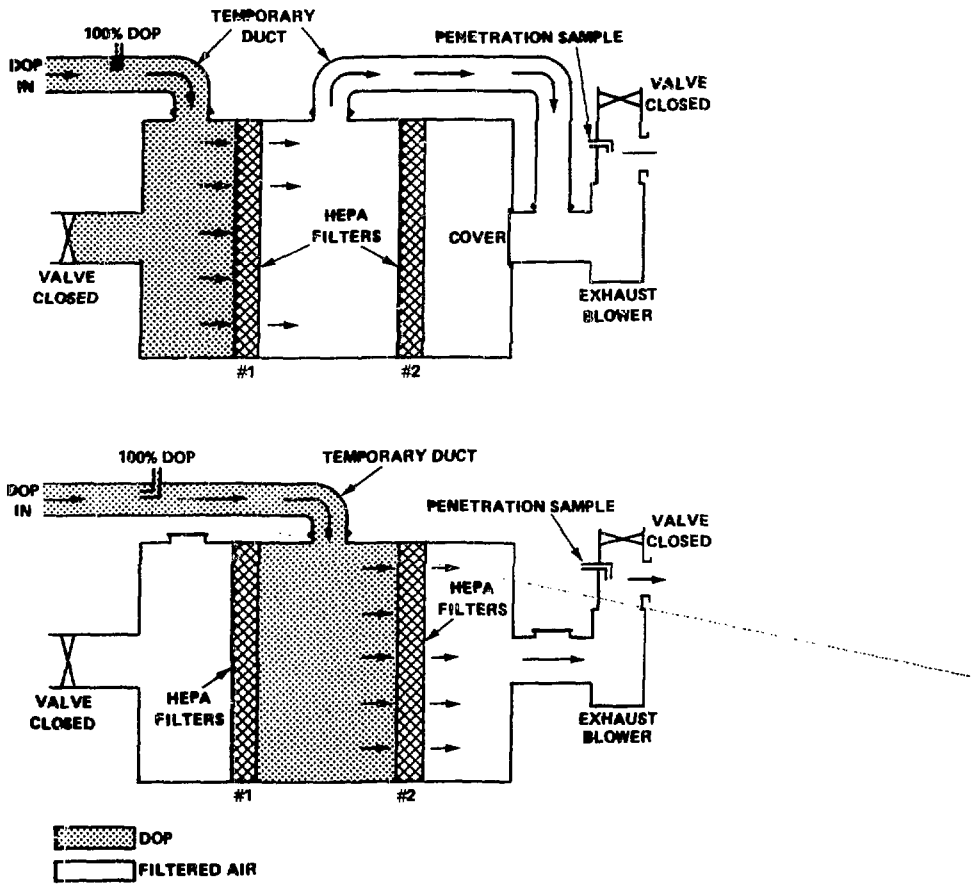

FIGURE 6a AND 6b

IN-PLACE TESTING OF MULTISTAGE HEPA FILTER SYSTEM PERMITTING INDIVIDUAL TESTS OF EACH STAGE

and at the fan discharge using a light-scattering photometer. The second stage is tested by injecting the aerosol between the stages and the photometer measured the upstream and downstream concentration as indicated. The temporary bypass duct and fan inlet blank-off were removed for this test. Testing a system by this method took approximately 1 hour to complete.

VI. Current Method--Testing of Multiple Stages

Shown in Figure 7 is the system arrangement for testing a multiple-stage filter system as one single unit using the SPPSS method.[4] A permanent aerosol injection duct 100-mm diameter (4-in. diameter) was installed at the inlet side of the plenum. Baffles were installed a short distance from the plenum inlet in order to redirect the turbulent flow conditions and accomplish complete mixing of the test aerosol. Three sampling manifolds were permanently installed: upstream of the first stage, upstream of the second stage, and at the exhaust fan inlet. The sampling manifolds provide 21 sampling orfices to sample the air stream uniformly inside the plenum. Figure 8 shows the SPPSS setup for testing. The procedure for counting by the SPPSS is very simple and no adjustments to the system air flows are necessary.

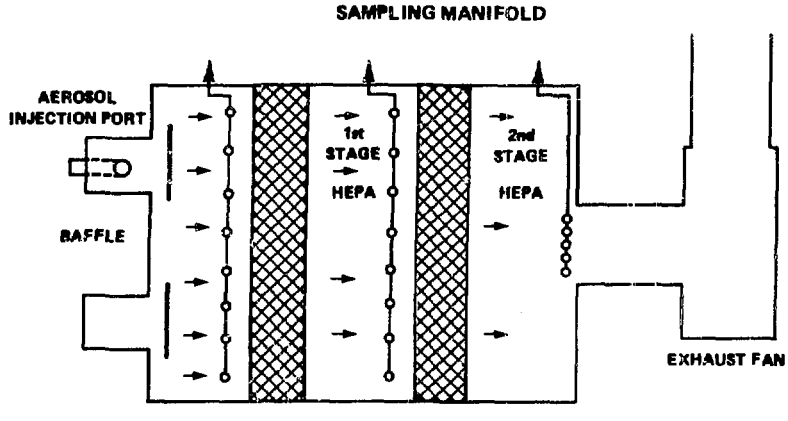

FIGURE 7
IN-PLACE TESTING OF MULTISTAGE HEPA FILTER SYSTEM
AS ONE SINGLE UNIT RATHER THAN INDIVIDUAL
TESTING OF EACH STAGE

The following outlines the procedure taken to conduct the tests:

1. Calibration. The SPPSS was calibrated in terms of particle size using polystyrene latex microspheres (PSL). Two nominal diameters were selected: 0.220 and 0.312 μm. The geometric mean diameter measured by the SPPSS produced 0.214 and 0.291 μm. The index of refraction for the PSL is calculated to be 1.59 and for DEHP is 1.48.[5]

FIGURE 8
LASER SPECTROMETER SETUP FOR TESTING

2. Background Particles. Because of the expected small concentrations of particles that penetrate two stages of HEPA filtration, it is necessary to make an evaluation of nontest particles (background) that are known to occur naturally in filter plenums. The procedure calls for setting up the SPPSS to count particles downstream of the second stage for a period of at least 10 minutes to allow statistical comparison with downstream concentrations collected in the test.

3. Aerosol Generation. Turn generator on and set the aerosol output to desired level and wait 5 minutes for the generator to achieve stable output.

4. Downstream Measurements of Second Stage. Without changing sampling locations, sample the airstream by collecting three 1-minute counts in each of the four size ranges. The sampling times can be adjusted to accumulate a minimum of 100 particles.

5. Downstream Measurements of First Stage. Move the SPPSS to the next sampling location without changing any of the test conditions. Sample the airstream by collecting three 1-minute, or three 10-second counts, depending on concentration in each of the four size ranges.

6. Upstream Measurements of First Stage. Because of the expected high particle concentrations, it may be necessary to dilute the sample. This is accomplished by withdrawing a sample from the plenum through the diluter and establishing a dilution factor as the ratio of undiluted to the diluted portion of the aerosol with a forward light-scattering photometer. Sample the aerosol at the diluter output with the SPPSS by collecting three 10-second counts of each of the four size ranges.

7. Scan Test. If penetration exceeds the specified acceptable DF of 2×10^3 for the first stage or 4×10^6 overall, it will be necessary to probe the entire downstream side of the affected stage. The scan test is conducted in accordance with section 10.5 of ANSI/ASME N510,[6] using a photometer. A source leak of at least 0.5 per cent measured with a photometer is considered to be significant for replacement of filters or sealing adjustments.

VII. Results and Discussion

A. System Evaluation

Evaluation of system protection has been established for a series of 20 tests of 2-stage, 10 m^3/s HEPA filter systems. The DF values shown in Table 1 were based on total particle counts in fifteen channels of each of four size ranges. DF values for the first stage show consistent levels above 10^3. Second stage or overall system protection DFs are consistently above 10^6 and up to 10^9. A comparison of the photometer results to those of the SPPSS indicate that some of the DF values of the first stage to agree reasonably well. The other DFs of Systems 1210, 20, 40, 1310, and 1320 show significant variation of the results when you compare the two methods. There was no clear cut evidence as to why the differences could be found. The only change was that the photometer and the SPPSS tests were conducted on different days. The other thing to remember is that the tests are conducted out in the field and sometimes the test conditions are less than ideal. The DFs across both stages measured by the SPPSS show different values in some of the tests compared to the photometer. Tests 1210, 70, and 80 show DFs below 10^6 as compared to DFs above 10^6 measured by the photometer for the same systems. Systems 1210, 70 and 80 were found to have leaks of the second stage and scanning substantiated those findings. As expected, by taking the products of the DFs of the first and second stages will result in an overestimation of system protection as expressed by the photometer method.

Table 1. Decontamination factors of first and second filter stages comparing two methods of testing.

DECONTAMINATION FACTORS (LASER SPECTROMETER)			DECONTAMINATION FACTORS (PHOTOMETER)			
SYSTEM	FIRST STAGE	OVERALL	SYSTEM	FIRST STAGE	SECOND STAGE	OVERALL (ESTIMATION)
1210	2.4×10^3	5.1×10^6	1210	6.0×10^3	5.0×10^3	3.0×10^7
1220	2.7×10^3	2.5×10^6	1220	3.6×10^3	3.3×10^3	1.2×10^7
1230	2.2×10^4	8.5×10^7	1230	2.4×10^3	1.4×10^4	3.4×10^7
1240	6.6×10^3	2.7×10^6	1240	8.0×10^3	1.0×10^4	8.0×10^7
1250	5.6×10^3	6.3×10^7	1250	5.8×10^3	1.2×10^4	8.1×10^7
1260	1.6×10^4	2.5×10^7	1260	1.2×10^4	2.8×10^3	3.3×10^7
1270	2.5×10^3	4.3×10^4	1270	2.4×10^3	2.3×10^3	5.5×10^6
1280	1.9×10^4	1.5×10^6	1280	1.3×10^4	5.3×10^3	6.9×10^7
1310	4.8×10^4	1.1×10^9	1310	1.0×10^4	2.5×10^3	2.5×10^7
1320	3.7×10^4	1.8×10^8	1320	1.0×10^4	1.0×10^4	1.0×10^8

B. Particle Size Distribution

Particle size analysis comparing the challenge to the first and second stages, shown in Figure 9, indicate very little change due to one stage of filtration. The second stage provided the greatest change reducing the particle size by approximately 38 per cent. A summary of the analysis shown in Table 2 indicates average particle size downstream of the first stage to be 0.34 μm, while the average particle size downstream of the second stage is 0.21 μm. The average geometric standard deviation of the distribution is 1.57 downstream of one stage and 1.45 downstream of the second stage.

VIII. Cost Comparison of Two Testing Methods

Items	Methods	
	Stage by Stage	SPPS
1. Instrumentation and miscellaneous equipment(initial cost)	$10-15K	$25 - 30K
2. Operations cost, (one hour interruption of process air)	$23K	None
3. Maintenance cost	<$ 1K/yr	$1-2K/yr

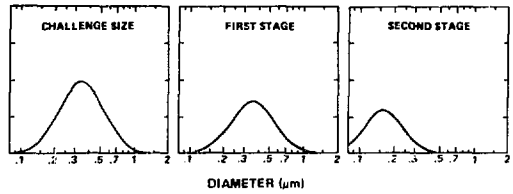

FIGURE 9
TYPICAL SIZE DISTRIBUTION COMPARING THE CHALLENGE DISTRIBUTION TO THE SUBSEQUENT FILTER STAGES

Table 2. Particle size distribution of the challenge aerosol and first and second HEPA stages of filtration.

PARTICLE SIZE DISTRIBUTION OF FILTER SYSTEMS 1210 – 60

MEASUREMENT LOCATION	GEOMETRIC MEAN DIAMETER (μm)	GEOMETRIC STANDARD DEVIATION (σg)
UPSTREAM OF STAGE 1	0.38	1.54
	0.39	1.51
	0.43	1.53
	0.35	1.54
	0.36	1.54
	0.36	1.54
DOWNSTREAM OF STAGE 1	0.34	1.58
	0.27	1.55
	0.37	1.60
	0.35	1.57
	0.34	1.59
	0.37	1.58
DOWNSTREAM OF STAGE 2	0.16	1.44
	0.25	1.38
	0.22	1.34
	0.26	1.48
	0.17	1.45
	0.20	1.35

IX. Summary

A laser particle spectrometer has been used to measure DFs of multi-stage filter systems. Measurements of DFs as high as 10^9 were obtained, which indicate a high level of sensitivity provided by the SPPS to adequately test two filter stages as one unit. The SPPS can also be used on single stages; however, the photometer is still the instrument of choice as a substitute. The SPPSS and associated equipment are more sophisticated, less rugged, and the initial costs are high. The advantage of the SPPSS method provides information on system performance without interruption of process ventilation, resulting in savings in operational costs and making the SPPSS test method very beneficial.

Acknowledgment

The author gratefully acknowledges the assistance provided by E.D. Garcia, S. Soderholm, V. Longmire and T.C. Short in performance of the field tests and in data acquisition and compilation.

References

1. Nuclear Standard, NEF3-4IT, "In-Place Testing of HEPA Filter Systems by the Single-Particle, Particle-Size Spectrometer Method," Department of Energy Nuclear Energy Programs, 1981.

2. Schuster, B.G. and Knollenberg, R., "Detection and Sizing of Small Particles in an Open Cavity Gas Laser," Appl. Opt., 2, 1515, 1972.

3. Mitchell, R. N., DeField, J., Stafford, R., McNeese, W., Eberhardt, W., and Laushkin, N., "Design of Ventilation and Air Cleaning Systems for the new Plutonium Facility," 13th AEC Air Cleaning Conference, 1972

4. Schuster,.B.G. and Osetek, D. J., "Tandem HEPA Filter Tests," Am. Ind. Hyg. Assoc. J, 39, 144, (1978).

5. Salzman, G. C., Ettinger, H. J., Tillery, M. I., Wheat L. D., and Grace, W. K., "Potential Application of a Single Particle Aerosol Spectrometer for Monitoring Aerosol Size at the DOE Filter Test Facilities," 17th DOE Nuclear Air Cleaning Conference, 1982.

6. American National Standards Institute/American Society of Mechanical Engineers, "Testing of Nuclear Air-Cleaning Systems," ANSI/ASME N-510, 1980.

DISCUSSION

DYMENT: There may be a very easy explanation but on the Table, system 1280 showed a decontainment factor of 1.9×10^4 in the first stage and only 1.5×10^4 overall for two stages. Can you explain the reason for this apparent paradox?

ORTIZ: You are referring to the results by the spectrometer, I believe. They stand out as probably being wrong. I don't have an explanation. Along with good data there is usually not so good data and I did not want to leave it out. I have no reasonable explanation for the distortion of the PF values.

SIGLI: Did you experience any problems with background counts after the first and second stages of filtration? If you have leaks in the duct, with negative air pressure in the duct holding the downstream filter, you can get some counts only from the background leakage.

ORTIZ: We don't do background checks downstream on the first stage, primarily because most of the time there are many, many particles, even approaching 10^3. The background particles wouldn't influence the overall determination of the decontamination factor.

SIGLI: Do you intend to use a fluorescent laser in connection with a suitable aerosol in order to avoid the problem of leakage in the duct?

ORTIZ: Yes, as a matter of fact, we have twin systems. One is the fluorescent spectrometer that we use in other systems. And we do generate fluorescent particles, even when we use latex. We have measured non-test particles that fluoresce using an ASASXF fluorescent spectrometer. Background particles are usually fewer than test aerosol particles. It hasn't been a difficulty, so we don't see the need of generating or measuring fluorescent particles.

ANON: What was the correlation between the results of testing with an artificial aerosol and the real radioactive aerosol you have in the plant?

ORTIZ: We have no figures to substantiate the comparison.

PROJECTS ON FILTER TESTING IN SWEDEN

Bård Normann
Studsvik Energiteknik AB
S-611 82 Nyköping, Sweden

Christer Wiktorsson
National Institute of Radiation Protection
S-104 01 Stockholm, Sweden

Abstract

The Swedish nuclear power program comprises twelve light water reactors. Nine are boiling water reactors of ASEA-ATOM design and three are pressurized water reactors of WESTINGHOUSE design. Of these, ten are in operation and two are under construction and planned to go into operation during late 1984 and early 1985 respectively.

The responsible authority for questions concerning filters in nuclear power plants is the National Institute of Radiation Protection. New regulations in the field of stand-by gas treatment filter systems are at present under discussion. The intention is to publish these regulations during 1984.

Frequent tests on the penetration of particles through HEPA filters, regular tests on the adsorption of methyl iodide in the stand-by carbon filter units by laboratory testing are being discussed.

The proposed new regulations are based on many years of experience of filter system operation and of tests in-situ and in the laboratory.

Moisture and water are factors that affect the functioning of filters. In addition, high loading of dust can give rise to increased penetration through HEPA filters, however pinholes could have less influence on the total penetration.

Laboratory tests show that DOP particles retain 30-40 percent in 90 mm carbon filters (8-12 mesh). However no effect on the ability of carbon to adsorb methyl iodide after DOP contamination in combined carbon/HEPA filters has been observed.

Leakage from ventilation ducts can cause radioactive contamination problems during filter testing with radioiodine. In-situ testing of control-room filters has been performed using inactive methyl iodide.

A type of carbon bed not previously used in Sweden has been introduced. Testing of this filter type will be discussed.

I. Introduction

In Sweden, as in other countries with nuclear power, the tendency has been towards larger units.

The first BWR, designed by ASEA-ATOM, is rated at 440 MW el whilst the two latest units, numbers 11 and 12 in the Swedish programme, are rated at approximately 1100 MW el each.

The increased ratings, experience from the earliest stations and increased safety requirements have lead to larger and more complicated air cleaning systems.

Some types of filter and other components in the radioactive air cleaning systems have been developed and are manufactured in Sweden, others are imported.

The methods used for controlling the filters and filter systems are also based on a combination of Swedish and foreign techniques.

For the units already in operation control of the filter material, for example carbon, full-scale carbon filters, and particle filters, has been obligatory before start up, and the carbon filter systems have then been tested regularly on-site.

II. Emission of Radioactivity

An investigation of digested slam and surface air around the units in Barsebäck on the South coast and in Ringhals on the West coast has given indications of considerably larger discharges of, for example, Co-60 than had previously been assumed[1].

The explanation for this could be that the emission to the surroundings occurs either through the stack or via personnel during the annual revision periods.

It has been suggested that it could be large particles which cause this, despite the fact that the gases are filtered through HEPA filters.

In order to determine the cause short and long term measurements of the stack contents in Ringhals BWR are being planned.

Specimens of the dust will be sampled using an impactor.

The particle filter currently in use will also be examined in particular with regard to its resistance to high humidity and dust contents. This examination is the first step towards a planned more extensive review of the functioning and response of the HEPA-filters in accident conditions.

In addition, improved contamination control has been introduced for persons leaving controlled areas in Swedish nuclear power plants.

III. Filters in Nuclear Power Plants

The so-called triple filter, consisting of a pre-filter (particle), carbon filter and a HEPA filter is one of the filters which has been designed in Sweden, see Figure 1.

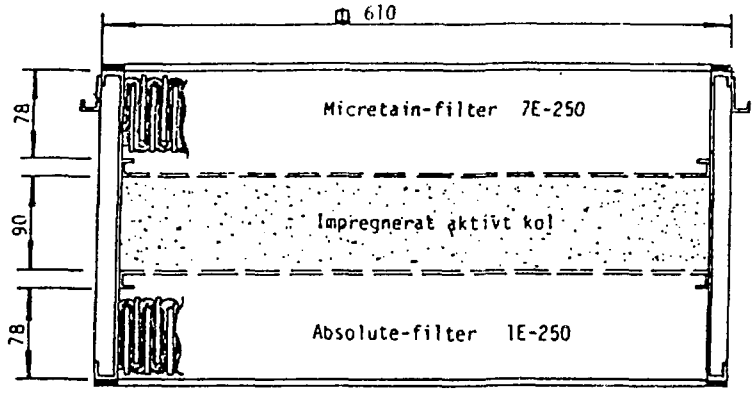

FIGURE 1
TRIPLE FILTER MANUFACTURED BY CAMFIL

Other carbon filters which are installed are the "shallow filter" type, see Figure 2, and filters in which the carbon can be replaced.

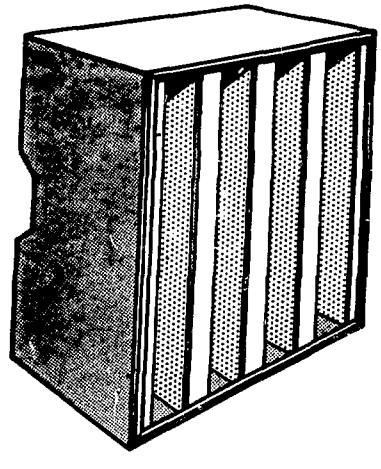

FIGURE 2
SHALLOW FILTER, OR FOLDED CARBON FILTER MANUFACTURED BY SOFILTRA

The specific design of the filter unit can vary with regard to choice of material and the filters are classified according to fire resistance, the filter house, amongst other things.

IV. Experiences from testing and operation

The Operational Environment

It has been found that there is a risk that humidity, in the form of partially or completely condensed steam from the leakage condensor can reach the filter via the off-gas system. In more recent BWR units this is prevented by a demister[2].

Incidents can also occur with water overflowing into the spent fule pit drainage system during fuel changes.

The particle filters used by the plants are stated to be humidity resistant, amongst other things, by their manufacturers. This often means that the fibre material and bonding agent are not readily soluble or are insoluble in water or under damp conditions.

In those cases, in which there is no demister, it is however necessary for the filters to tolerate damp conditions during operation, which means that they must be stronger since the condensate/water increases the pressure drop more than would otherwise be the case.

The separation requirements for a filter system can, on good grounds, often be set relatively low, 99.0 or 99.9 %.

In order to obtain a good safety margin HEPA filters are often installed in these systems.

Since these often give 99.997 % separation the use of HEPA filters is not always to be recommended. Without it being noticed a filter can have been damaged by damp and then be taken into operation and subsequently fail, see Figures 3 and 4.

These filters can, despite damage, be dried and then have a sufficiently low prenetration for the plant, for example 0.1 %[2].

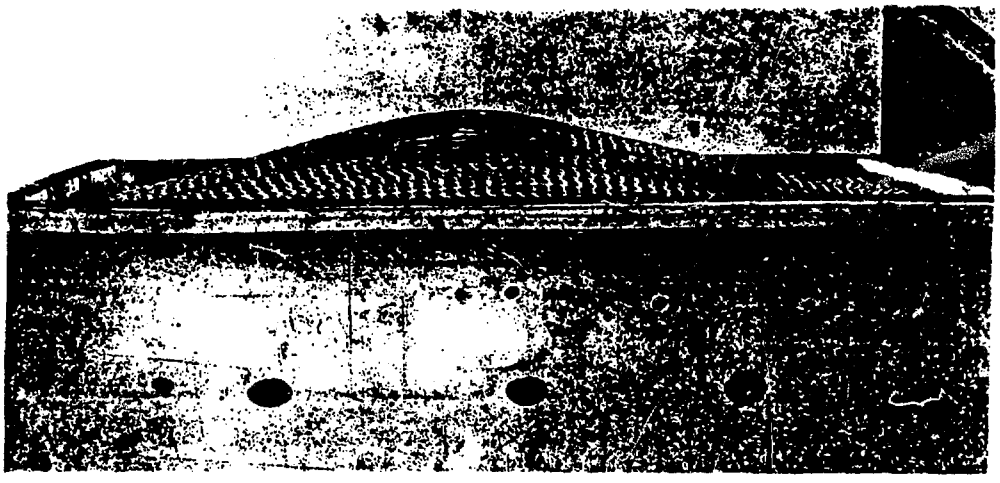

FIGURE 3
HEPA-FILTER, THE BULGE ON THE CLEAN AIR SIDE IS CAUSED BY WATER DAMAGE

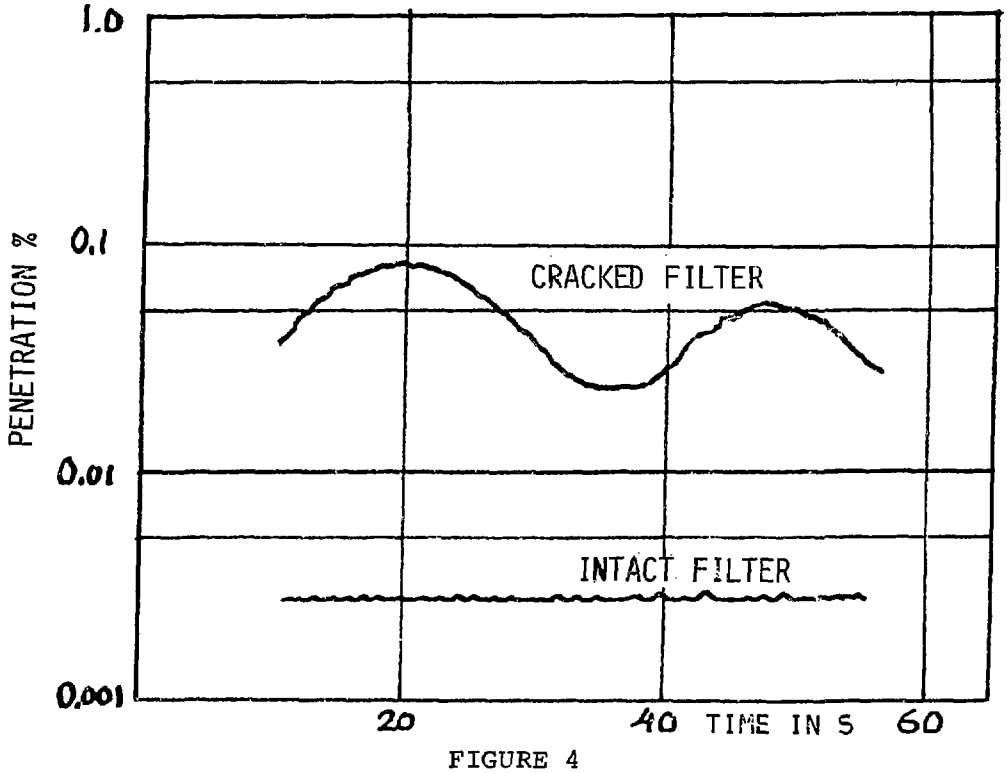

FIGURE 4
FLUTTER IN A CRACKED FILTER

Dust take up

During operation a particle filter becomes loaded with larger or smaller amounts of dust particles, and even carbon dust if carbon filters are positioned up-stream. When particle filters are used separately, when their life is not determined by the life of associated carbon filters, the effective filter area will be the determining factor for their life, strength and capacity.

The nominal capacity can vary between different manufacturers, according to their catalogues, and despite approximately the same initial pressure drop, from about 1700 to 3400 m^3/h for a 24" x 24" HEPA filter.

Information concerning the pressure drop as a function of dust load varies for the various makes of HEPA filter.

This means that it is not possible to calculate the life of a filter.

The accumulation capability can, according to the different manufacturers, vary between about 0.5 and 3 kg. A study of 4 different HEPA filters[3] indicates that the differences quoted are exaggerated in that instance.

The study was aimed at measuring the dust adsorption by the filters under equivalent conditions and for the length of time necessary to increase the total pressure drop to 50 mm wg. The results are shown in Figure 5.

The flow rate was 1700 m^3/h for all the filters.

It is commonly thought that in a HEPA filter the penetration decreases with increased dust load. That conclusion is however not supported by this study. Vibrations, the continual flow of air and the wear from the collected dust appear to have damaged the filter.

According to the results the penetration through two of the four particle filters tested increased from about 0.03 to about 2 %, whilst the penetration decreased for the other two filters tested.

The Length of Life for a HEPA Filter

The factors which are determining for the length of the life of a HEPA filter, apart from damage and increased penetration, are

- pressure drop
- changes in the flow rate
- amount of (radioactive) dust collected.

These factors are interrelated since the collection of dust increases the pressure drop and can decrease the flow rate.

The capacity of the fan can thus be determining for the life of the filter in some plants, whilst the strength of the filter can be the criterion in other plants.

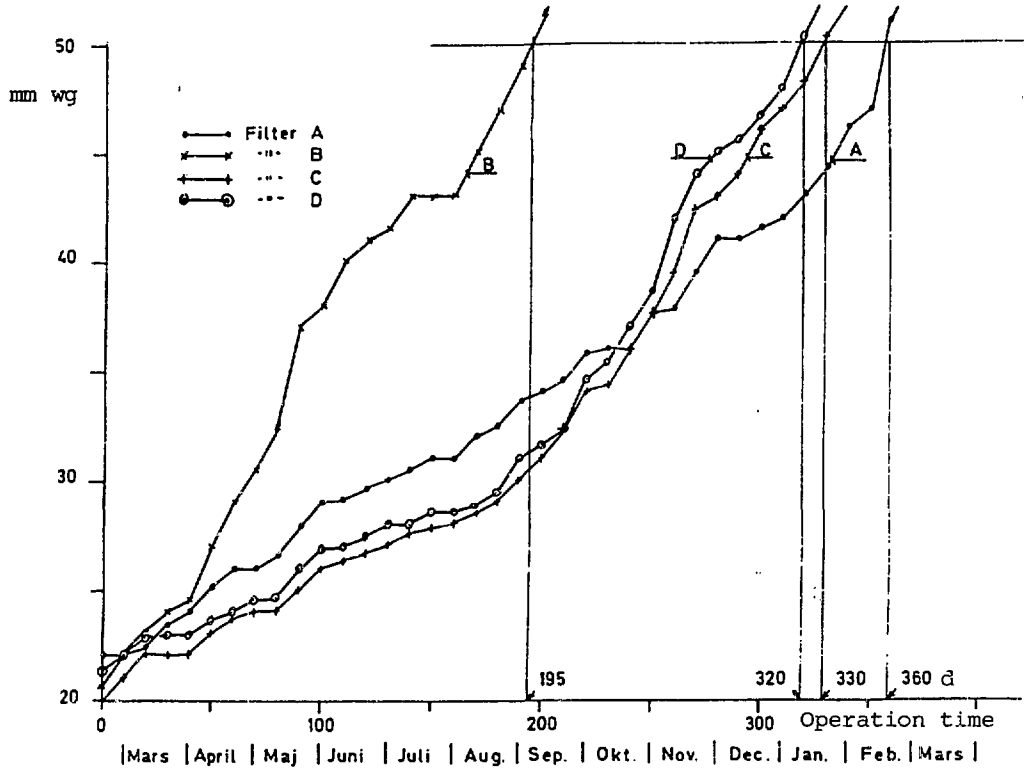

FIGURE 5
INCREASE IN RESISTANCE IN A HEPA-FILTER AS A FUNCTION OF OPERATIONAL TIME. THE DUST LOAD AT 50 mm wg: FILTER A: 0.7 kg, B: 0.45 kg, C: 0.72 kg and D: 0.70 kg

Under normal conditions a 24" HEPA filter can collect 0.5 - 0.75 kg dust if the maximum pressure drop permitted is 50 mm wg. For most brands this corresponds approximately to a factor of two on the initial pressure drop. The amount of dust collected in the filter, and the increased pressure drop, decrease the flow rate in the system, and increase the risk for filter failure, and the spread of fission products if the filter is subjected to high water contents or other sorts of shocks

The HEPA filters in continuous operation, for example in the off-gas system are normally monitored by measuring the pressure drop, and are usually changed when the pressure drop has increased by 100 %.

Pinholes

One possible way for large particles to pass through a particle filter is via pinholes: small holes in the particle filter which can be detected easily by an oil cloud and illumination of the particle stream which penetrates the hole, see Figure 7.

It is, however, difficult to detect pinholes during on-site testing. It can be shown by calculation, that the proportion of the test aerosol which penetrates the pinholes, is very small compared to what is permitted through the entire filter (Figure 6).

Turbulent flow and aerodynamic contraction are contributory factors.

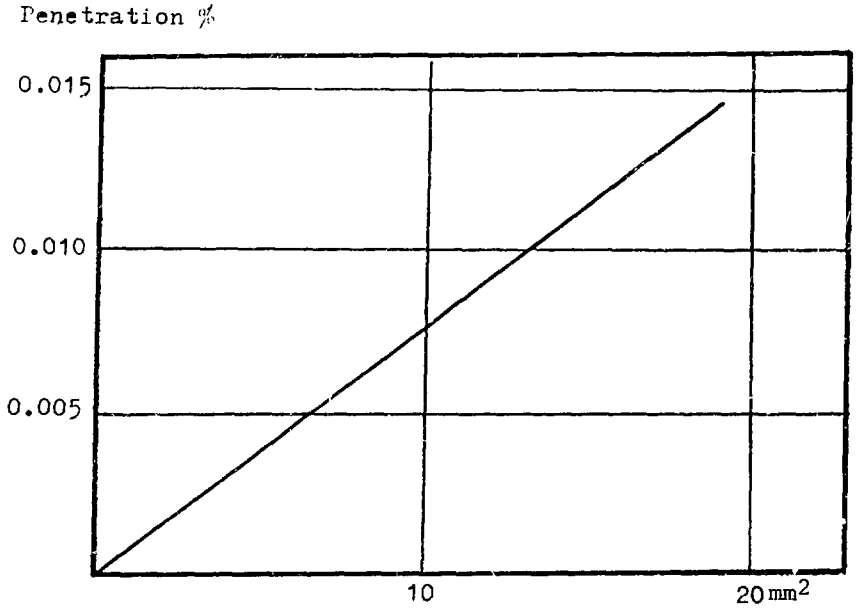

FIGURE 6
PROPORTION OF 0.3 µm PARTICLES WHICH PENETRATE THROUGH A PINHOLE FOR A 24" HEPA FILTER AT ABOUT 1700 m^2/h

FIGURE 7
DIFFUSE LEAKAGE AND PINHOLE LEKAGE IN A FILTER AFTER PROLONGED OPERATION, REVEALED BY A PARAFIN AEROSOL AND ILLUMINATION. THE FILTER IS AT THE BOTTOM OF THE PHOTOGRAPH AND THE ILLUMINATION FROM THE TOP

If a filter has an initial penetration of less than 0.015 %, which is not unusual, a 5 mm diameter hole will not increase the penetration to more than 0.03 %.

The filter can still be classified as a HEPA filter.

It should, however, be noted that much larger particles, which are normally trapped by the filter material, can pass through pinholes.

Transportation Damage

The design of the HEPA filter often results in direct contact with the filter material. Since this is brittle it must be handled with care.

Despite the fact that the filter is packed in corregated paper boxes, with extra corregated paper sheets to protect the front and back of the filter, damage can occur when loading/unloading, stacking or unpacking the filter.

The final danger is during the installation of the filter into the filter bank.

Sharp edges or fingers can damage the filter during installation.

V. Carbon Filters and DOP

The testing of combined iodine and particle filters is carried out in two steps, with separate tests: one for the iodine filter part and one for the particle filter.

Iodine filters are mainly tested with methyl iodide, often with traces of I-131.

DOP (Dioctyl phtalate), could be used as a test aerosol for particle filters.

A natural question which arises is whether the test aerosol based on DOP is adsorbed by the carbon and whether it poisons it.

In order to detect any effects of a poisoning mechanism for the active carbon during tests with DOP, a series or measurements has been performed in which DOP and methyl iodide are dosed alternately[4].

An 85 mm deep 24" carbon filter with a micretain filter upstream was used for the measurements. This corresponds to the configurations pertaining in the plants.

The micretain filter has a penetration of 5 % for 0.3 µm particles.

Before the series of dosing with DOP was started, a carbon sample was taken and tested with methyl iodide at 80 % RH. The method used is described in[5].

After this a DOP was dosed a number of times. Each dose, apart from the last one in the series, corresponded to a normal test: about 500 mg DOP per filter. The last dose was 2 g.

Between each dose the filter was tested with methyl iodide at ambient conditions.

Finally another carbon sample was taken for a laboratory test at 80 % relative humidity (RH).

Adsorption of DOP in carbons

The penetration of metyl iodide (CH_3I) measured for these tests was very low and showed no tendency to an increase because of the DOP load.

The penetration varied in the range 0.15×10^{-3} % to 0.8×10^{-3} %, chich can be considered to be normal values for new carbon and low humidity. The retention time was about 0.2 s.

The laboratory tests of carbon samples at 80 % RH were relatied to the performance index, K, which was determined from the equation

$$K = \frac{\log Df}{t}$$

where

Df = the decontamination factor and
t = the air retention time in seconds.

Results:

Sample 1: before DOP dosing: K = 15.02
Sample 2: after DOP dosing: K = 14.99.

Comments

The total amount of DOP dosed corresponds to 8-10 normal tests of a particle filter.

According to the results from the methyl iodide tests no deterioration of the carbon could be measured, either in dry or damp atmospheres.

VI. Tests of Control Room Filters

A common factor for the filter systems which are tested with I-131 is that the air cleaning systems are lead to the stack. This method is unsuitable for other systems which supply for example the control room, shelter and such like with filtered air, because of the inherent risk for leakage and the resultant dose for persons exposed to the release.

Non-Radioactive Methyl Iodide

According to[6] non-radioactive methyl iodide can be used for testing amine impregnated carbon (which has not been contaminated

with iodine impurities)
- unimpregnated carbon

- iodine impregnated carbon, if the instaneous penetration can be calculated by extrapolation.

Non-radioactive methyl iodide is toxic in high concentrations; modern instruments are however very sensitive.

Concentrations upstream can therefore be kept at levels within the permitted limits as specified in[8].

In order to test the carbon filters in the control room supply system safely, equipment has been developed and tested for on-site testing using non-radioactive methyl iodide. Experience from tests using non-radioactive methyl iodide has been obtained from[9], amongst other sources.

Methyl iodide is dosed upstream from the filters to be tested. The distance between the point of dosing and the filter should be so large that the concentration of the methyl iodide is uniform across the cross-section. Before and after filter perforated glass probes are mounted. These are connected via the sampling valve of a gas chromatograph to a pump. The gas sample from above the filter flows through a small sampling volume and that from below the filter through a large volume.

The concentration of the methyl iodide is determined upstream and downstream alternately[7]. In principle three concentration measurements are necessary to show that the concentration has probably been constant during the penetration measurements.

Dosing Methyl Iodide

Methyl iodide boils at 42.4 ^{o}C and the vapour pressure increases rapidly between 20 and 40 ^{o}C. This gives rise to difficulties in obtaining an even dose by evaporation in this temperature range.

After considering a number of different methods it was decided to boil methyl iodide using a controlled source of heat. For a filter bank with a flow rate of about 3000 m^{3}/h a dosing rate of about 0.1 to 1 g/min is necessary.

Sampling

A gas chromotaograph, AID model 611, with an internal sample volume of 2 µl is used to analyse the air samples; the external sampling volume of the instrument is exchangeable.

Results

The results of measurements from a typical filter system for a control room are shown in Figure 8. The carbon filters in the system were unused. As expected the results show that the penetration has been low.

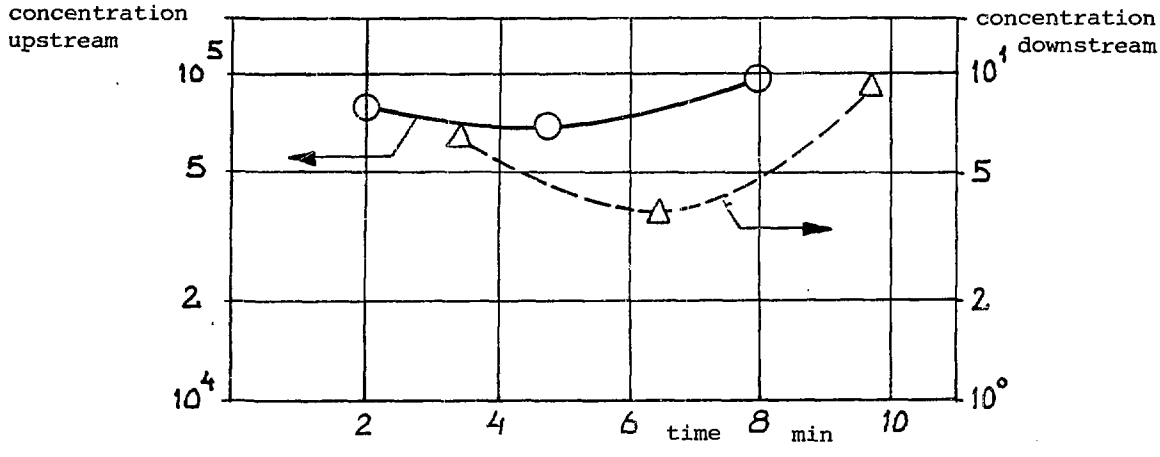

FIGURE 8
THE RELATIVE VARIATION IN METHYL IODIDE CONCENTRATION WITH TIME BEFORE AND AFTER THE CARBON FILTER

Limitations of the Method

As mentioned earlier, non-radioactive methyl iodide as a testing substance is limited to certain carbon filters. This is because of the isotope exchange which occurs in iodide impregnated carbon, which results in the formation and release of non-radioactive methyl iodide. This can also occur with amine impregnated carbon if it contains iodine impurities.

Non-radioactive methyl iodide can be used with advantage for fresh amine impregnated carbon, for example TEDA-carbon. This is also true for stand-by systems in which iodine contamination is unlikely, such as the control room filters of a nuclear power station.

VII. Regulations

The responsible authority for questions concerning filters in nuclear power plants is the National Institute of Radiation Protection. A draft for comments on new regulations on stand-by gas treatment filter systems has recently been published. Recommendations from two projects by Studsvik Energiteknik AB sponsored by the Institute of Radiation Protection have been used in the work [2, 7]:

The basis for the regulatory work has been:

1. The releases of radioactive substances in an accident shall be limited to an extent which is reasonably achievable.

2. A long service life is desirable for the filter units to minimize the amount of disposable waste from filter handling.

Only filters in emergency ventilation system are concerned by the regulations. Regulations for releases of radioactive materials during normal operation were published in 1977 [10].

Filter types

The filters used in Sweden are, as mentioned briefly in chapter III, basicly box filters with external dimensions 610 x 610 x 290 mm. The same casing can contain both particle and carbon filters.

The two reactors not taken into operation are equipped, amongst other filters, with a filter type not previously used in Sweden. In these filters the carbon is filled and purged out with special equipment. The carbon bed thickness is 100 mm. The amount of carbon in the filter is about 600 kg.

The carbon used in both types of filters is TEDA-impregnated.

This latter type of filter is equipped with prefilters (particle) upstream and HEAP-filters downstream from the carbon bed. Heaters and demisters are also included.

QA-progamme

A quality assurance programme for filter control has to be approved by the authorities. This programme should contain the following, at least:

- the education/competence of the personnel at the utilities responsible for filter testing
- instructions for calibration of equipment used
- a programme for calibrating equipment used on site against an independent laboratory and
- documentation system.

Experience has shown that impregnated carbon differs in quality. In order to ensure the correct performance, quality assurance tests must be performed according to the regulations.

These tests have to be performed with radioactive labelled methyl iodide (CH_3I - 131) under the following conditions:

Temperature	20-30 °C
Relative humidity	80 %
Face gas velocity	0.4 m/s
Bed depth	50×10^{-3} m
Bed diameter	25×10^{-3} m
Preconditioning time	16 hours
Loading time	0.5 hour
Desorption time	2 hours

These conditions are about the same as those recommended by NEA [11].

For TEDA impregnated carbon a K-factor (defined at page 10) of about 14 is required, i e carbon filters used should have an adsorption for methyl iodide of about 99.9 % at least.

HEPA-filters have to be controlled by a DOP-aerosol and have a retention of at least 99.97 % for 0.3 um particles.

In addition the HEPA-filter should meet the requirements in the US MIL standard or other comparable standards approved by the authority.

Periodic control

Carbon filters have to be tested both in the laboratory and in-situ.

The laboratory tests have to be performed regularly. The absorption of methyl iodide has to be checked at humid (80 % RH) conditions. The in-situ tests are considered as leakage tests and have to be performed.

- initially, and
- following filter change, maintenance work affecting the filters and following chemical release and/or fire in a ventilation zone communicating with the system.

The leakage measured in-situ with methyl iodide should be less than one percent at rated flow.

HEPA-filter systems have to be leakage tested regularly in-situ with DOP-particles to confirm a penetration of less than 0.03 % at the rated flow. A polydispers DOP aerosol is used.

In addition leakage and/or inspection tests should be performed

- initially
- following filter change or maintenance work in the bank, or following fire or suspected contact with water.

Documentation

The tests performed on site and/or at independent laboratories have to be documented and reported to the Institute of Radiation Protection.

Test methods and practice

Normally the test methods used in Sweden are the DOP-method for HEPA-filters and the CH_3 I-131-method for carbon and carbon filters (2, 12).

For control-room ventilation systems equipped with TEDA-impregnated carbon a method using inactive methyl iodide has been tested (7). The method has been used for in-situ testing of unused TEDA-impregnated carbon in Sweden. Laboratory testing of carbon in box filters is supposed to be carried out by testing one or more units choosen randomly from the filter bank.

For filters with refillable carbon the problem of sample representativity exists.

A method discussed in Sweden is to equip the unit with control filters parallel to the main filter. These control filters can than be tested in the laboratory. This method has to be licenced by the authorities before such filters are mounted onto the units. Laboratory experiments are planned to start this year to study the details of the design.

VIII. Plans for the Future

A high standard of the air filtering systems for emergency conditions is supposed to be achieved by

1 continuing research in two main areas

- Factors influencing degredation of filter efficiency, and
- The response of ventilation system to anticipated emergency conditions. Filters and other components in the systems are considered.

2 participation in international groups working with filter technology, and

3 analysing operating and test experience gained from nuclear power plant operation in Sweden and abroad.

References

1) Erlandsson, B et al
Co-60 measured in Surface Air around A Nuclear Power station - A comparison between estimated and reported releases.
Presented at the IAEA Symposium on the Environmental Loading from Radionuclides released from Nuclear Power Plants, Brussels, 17-21 October 1983.

2) Normann, B
Iodine and Particle Filter Systems in Nuclear Power Station - Functional Requirements and tests.
Studsvik Report NW-83/431 (1983). (In Swedish)

3) Skogulf, H
Study of the Accumulation Capacity of an Absolute Filter
AB Atomenergi TPM-SFS-68-1 (1968). (In Swedish)

4) Normann, B
Effect of Dioctyl Phtalate (DOP) on Carbon Filters
Studsvik Internal Report NW-83/586 (1983). (In Swedish)

5) Hesböl, R
Testing and Control of Iodine Filters
Studsvik Internal Report NW-82/376 (1982). (In Swedish)

6) Wood, G O and Valdez F O
Non-radiometric and radiometric testing of radioiodine sorbents using methyl iodide.
LA-UR-80-2864.

7) Pettersson, S O and Normann B
Tests of Carbon Filters Using Non-Radioactive Methyl Iodide II
Studsvik Internal Report NW-83/507 (1983). (In Swedish)

8) The Swedish Board of Occupational Safety and Health
Code AFS 1981:8.

9) Kabat, M J
Private communication.
Ontario Hydro, Canada.

10) The Swedish National Institute of Radiation Protection,
Limitation of Releases of Radioactive Substances from Nuclear Power Stations.
SSI FS 1977:2, Stockholm (1977).

11) Nuclear Energy Agency,
SINDOC (83) 268, 1984, Draft.

12) Dorman, R G
A Comparison of the Methods used in the Nuclear Industry to Test High Efficiency Filters.
Luxembourg (1981).

DISCUSSION

PAPAVRAMIDIS: What's your concentration of CH_3I^{-131} during the loading time of the carbon sampler? Is it in the order of micrograms?

NORMANN: Approximate loadings of the charcoal during in situ tests are about 0.1 µg CH_3I^{-131} per g charcoal, and during tests of samples, about 5 µg/g.

CADWELL: You mentioned that a filter with an initial penetration of less than 0.015% will have a penetration of less than 0.03 with a 5mm hole. Is not the penetration caused by the hole also functionally dependent on aerosol concentration and air flow volume?

NORMANN: The relations between the leakage through the pinhole and the penetration through the filter medium may depend a little bit on airflow. Airflow, in this canse, was normal, which means about 1700 m^3/h. Concerning the influence of the aerosol concentration, I think the results are independent of this.

EFFECT OF DOP HETERODISPERSION ON HEPA-FILTER-PENETRATION MEASUREMENTS*

Dup

by

W. Bergman and A. Biermann
Lawrence Livermore National Laboratory
P.O. Box 5505, Livermore, CA 94550

Abstract

The accuracy of the standard U.S. test method for certifying High-Efficiency Particulate Air (HEPA) filters has been in question since the finding by Hinds, et al. that the dioctyl phthalate (DOP) aerosol used in the test is not monodisperse as had been assumed and that particle-size analyzers, or owls, could not distinguish between different particle-size distributions with the same owl reading. We have studied theoretically and experimentally the filter efficiency for different DOP size distributions with the same owl reading. Our studies show that the effect of varying DOP size distributions on the measured HEPA-filter penetration depends on the light-scattering-photometer response and on the HEPA-filter penetration curve, both measured as a function of particle size. HEPA-filter penetration for a heterodisperse DOP aerosol may be increased, decreased, or remain the same when compared to the filter penetration for monodisperse aerosols. Using experimental HEPA-filter penetration and photometer response curves, we show that heterodisperse DOP aerosols (D_{cmd} 0.19 and σg = 1.4) yield 24% lower penetrations than that for monodisperse DOP aerosols (D_{cmd} = 0.3 and σg = 1.0). This surprisingly small effect of the DOP heterodispersion on HEPA-filter penetration is due to the response function of the owl that is similar to the response of the photometer. Changes in the particle-size distribution are therefore seen in a similar fashion by both the photometer and the owl. We also show that replacing the owl with modern particle-size spectrometers may lead to large errors in filter penetration because the particle-size spectrometers do not provide measurements that correspond to the photometer measurements.

I. Introduction

All of the standard filter-test methods used by the U. S. and other countries are based, more or less, on a heterodisperse test aerosol which challenges the filter and on integrated measurements of the sample aerosol concentration before and after the filter. Table 1 compares the four most widely used filter-test methods.

A large number of studies have been reported in the literature describing the major filter test methods listed in Table 1.[1-5] Correlations among the various test methods have also been reported.[6,8] One manufacturer of HEPA filters even reports filter penetration for each of the filter-test methods in their commercial literature.[9]

It is important to note that the same filter tested with each of the four methods described in Table 1 has different penetration results, with the British NaCl test yielding the lowest penetration and the French uranin test the highest. In general, for these four test methods, the smaller the particle size, the higher the penetration. This trend is illustrated in Fig. 1 where we have

*This work was performed under the auspices of the U.S. Department of Energy by Lawrence Livermore National Laboratory under contract NO. W-7405-ENG-48.

Table 1. Comparison of the four major filter-test methods used world-wide today.

Method (ref)	Test aerosol	Volume average diameter of aerosol	Aerosol measurement
German Paraffin (5)	nebulizing hot paraffin oil, liquid aerosol	0.35)m	light-scattering photometer measures aerosols directly
British NaCl(3)	nebulizing NaCl water solution, solid aerosol	0.65)m	flame photometer measures aerosols directly
U. S. DOP(3,4)	thermal-generated DOP, liquid aerosol	0.30)m	light-scattering photometer measures aerosols directly
French uranin(2)	nebulizing uranin water solution, solid aerosol	0.15)m	aerosols first collected on filter sample; uranin dissolved from filter and measured by fluorimetry

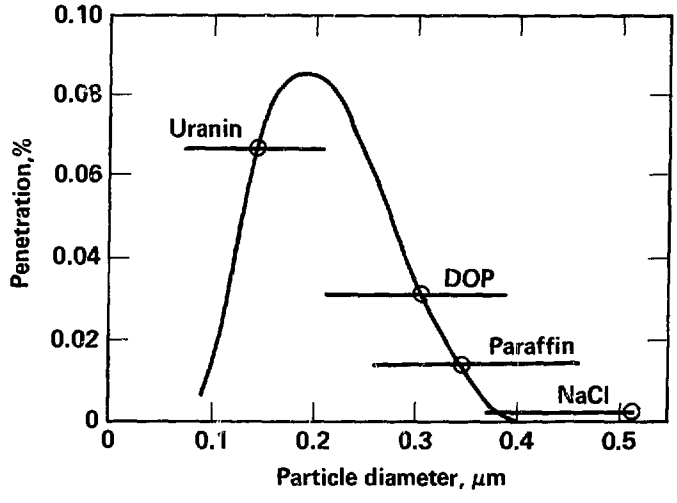

Fig. 1. Comparison of four major filter-test methods showing the portion of the filter-penetration curve measured by each technique.

plotted the HEPA-filter penetration as a function of particle diameter against the various filter-test methods. Note that the difference in the average particle-size results in considerable variation in measured penetrations. Since the aerosols listed in Table 1 also have a broad range of particle sizes, filter-penetration tests thus represent, at best, an average penetration integrated over the particle-size range.

Although experts have recognized the disparity in the results obtained from the different test methods for many years, no one seemed to question the accuracy of these methods. In reviewing the four test methods, Dorman[5] points out that each of the tests only "give a figure of merit toward the particular test aerosol and may bear little relation to that achieved in practice." The test methods using NaCl, DOP, paraffin, and uranin aerosols have been independently developed by Great Britain, United States, West Germany, and France, respectively, and these tests have evolved into national standards for certifying HEPA filters. Each filter method has been successfully used for many years to ensure that HEPA filters meet certain minimum standards. The fact that the same filter had different penetration values for different test methods did not matter, since each test method was at least repeatable and was able to distinguish between good and bad HEPA filters. Of course, this self-consistency argument fails when filter-test results are used in complying with absolute environmental and safety standards.

In 1978, Hinds, et al. questioned the ability of the U.S. DOP test method to even provide a reliable, if not absolute, measurement of HEPA penetration.[10] They found that the DOP aerosols are not monodisperse and the owl could not distinguish between different particle-size distributions having the same owl reading. The concern was that these different particle-size distributions would yield different filter penetrations as measured by the light-scattering photometer. We shall show that the effect of DOP heterodispersion has only a small effect on the HEPA penetration measurements.

II. Theory of Present Filter Test Methods

The basic problem with present filter-test methods is that the measured filter penetration, P_M, varies with the number of particles in a given size range, r, designated as N(r) [or the particle-size distribution], and the instrument response function, R(r).

In general, the way in which the instruments in Table 1 respond varies approximately with the volume of particles. The measurement of aerosols sampled before the filter, M_B, therefore, is an integrated measurement of the product of N(r) and R(r):

$$M_B = \int_0^\infty N(r)\, R(r)\, dr \quad , \tag{1}$$

where r is the particle size. This measurement of aerosols sampled before the filter is illustrated in Fig. 2, where we have plotted relative values of N(r), R(r), and the product N(r)R(r) as a function of r. Note that the instrument-response function gives primary weight to the larger particles in the tail of the particle distribution.

The measurement of aerosols sampled after the filter requires an additional factor to take into account that the filter has removed particles and thus has an altered particle-size distribution. The particle-size distribution of aerosols

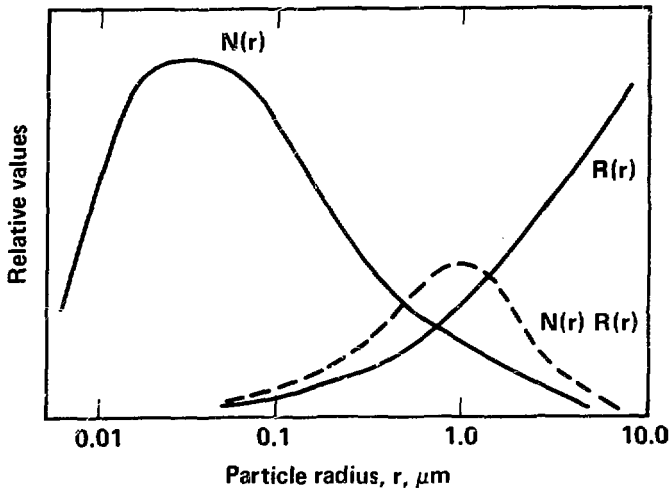

Fig. 2. The measurement of a typical heterodisperse aerosol with a single-valued detector (e.g., a photometer) equals the number of particles, N(r), multiplied by the instrument response, R(r), at each particle size, r, summed over all particle sizes.

sampled after the filter is the product of filter penetration, $P_F(r)$, defined by the fraction of particles passing through the filter, and the initial particle-size distribution of aerosols before the filter, N(r). Figure 3 illustrates this type of particle-size distribution. The measurement of aerosols sampled after the filter, M_A, is

$$M_A = \int_0^\infty N(r)\, P_F(r)\, R(r)\, dr \quad , \tag{2}$$

and is illustrated in Fig. 4 where we have plotted the curves for the particle-size distribution of aerosols after the filter, $N(r)P_F(r)$, R(r), the product of all three terms.

The complete filter-penetration measurement, P_M, is

$$P_M = \frac{M_A}{M_B} = \frac{\int_0^\infty N(r)\, P_F(r)\, R(r)\, dr}{\int_0^\infty N(r)\, R(r)\, dr} \quad . \tag{3}$$

The primary effect of a widely ranging particle-size distribution is an underestimation of the actual filter penetration, P_F, by the measured penetration, P_M, (or conversely, an overestimation of the filter efficiency). We would like to be able to measure the filter penetration directly, and that is only possible if we have monodisperse particles. In that case, the size distribution function becomes a delta function, $\delta(r-r_0)$, where r_0 is the monodisperse size. and Eq. 3 reduces to

$$P_M = P_M(r_0) = \frac{N_A}{N_B} \tag{4}$$

where N_A is the number of particles after the filter, and N_B is the number of particles before the filter. The filter penetration at particle size r_0 can, therefore, be determined by measuring the ratio of particles before and after the filter.

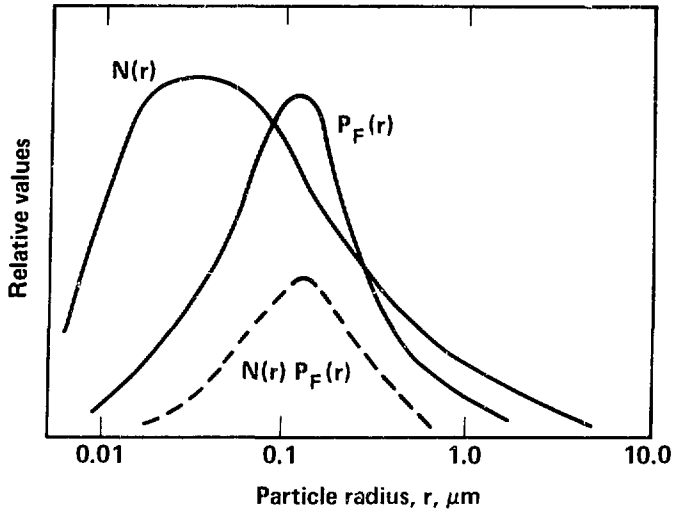

Fig. 3. The particle-size distribution of aerosols sampled after the filter equals the particle-size distributions before the filter, N(r), multiplied by the filter penetration, $P_F(r)$.

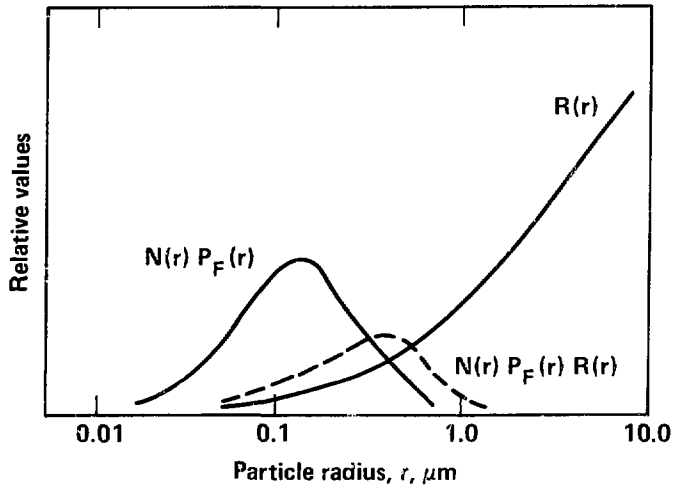

Fig. 4. The measurement of aerosols sampled after the filter with a single-valued detector (e.g., a photometer) equals the number of particles after the filter, $N(r)P_F(r)$, multiplied by the instrument response, R(r), at each particle size, summed over all particle sizes.

In order to avoid the overestimation of filter efficiency due to heterodisperse DOP aerosols, a large and complex vaporizer/condenser is used to generate monodisperse aerosols. Recent findings, however, have shown that DOP is not a monodisperse aerosol.

III. Accuracy of DOP Filter-Certification Test and Filter Penetration is Questioned

Several investigators have found that DOP aerosols in the HEPA-filter-certification tests are not monodisperse 0.3-μm-diameter particles as had been assumed, but rather, are heterodisperse aerosols with a count median diameter of 0.18 μm and a geometric standard deviation of 1.4.[7-12] There was serious concern that, because of the heterodispersion of this aerosol, the measured values of filter penetration were underestimations of the true filter penetration [$P_F(0.3)$]. This concern was compounded when researchers also discovered that the owl gave the same reading for a large number of different particle-size distributions.

The owl is an instrument that measures the size of monodisperse aerosols by measuring the ratio of scattered light at two polarizations. Parameters that control the DOP-aerosol generator are adjusted until the proper owl reading is obtained corresponding to 0.3-μm-diameter particles. A filter-penetration measurement can then be made by measuring an aerosol sample with a light-scattering photometer before and after the filter as shown in Fig. 5.

The owl's problem with the discovery that DOP aerosols are not monodisperse is its inability to uniquely define the particle-size distribution and the possible underestimation of the filter penetration. This is illustrated in Fig. 6 where three particle-size distributions yield the same owl reading. The broadest distribution in Fig. 6 is representative of the DOP aerosols used in HEPA-certification tests. Hinds et al.[10] determined that the owl sees an average particle size weighted to the power 8.1:

$$R_{owl}(r) = K_1 r^{8.1} \qquad (5)$$

where $R_{owl}(r)$ = the owl response to a particle of radius r and K_1 is a proportionality factor.

Any number of particle-size distributions, like the ones in Fig. 6 that have the same weighted average size given by Eq. 5, will yield the same owl reading. Thus, the validity of current DOP tests has been placed in question by the inability of the owl to uniquely measure the particle-size distribution.

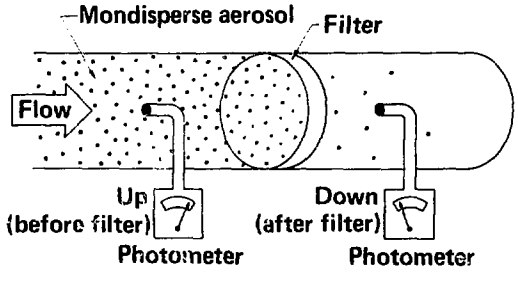

Fig. 5. Schematic showing the key components of a filter-test method using monodisperse aerosols and a single valued detector.

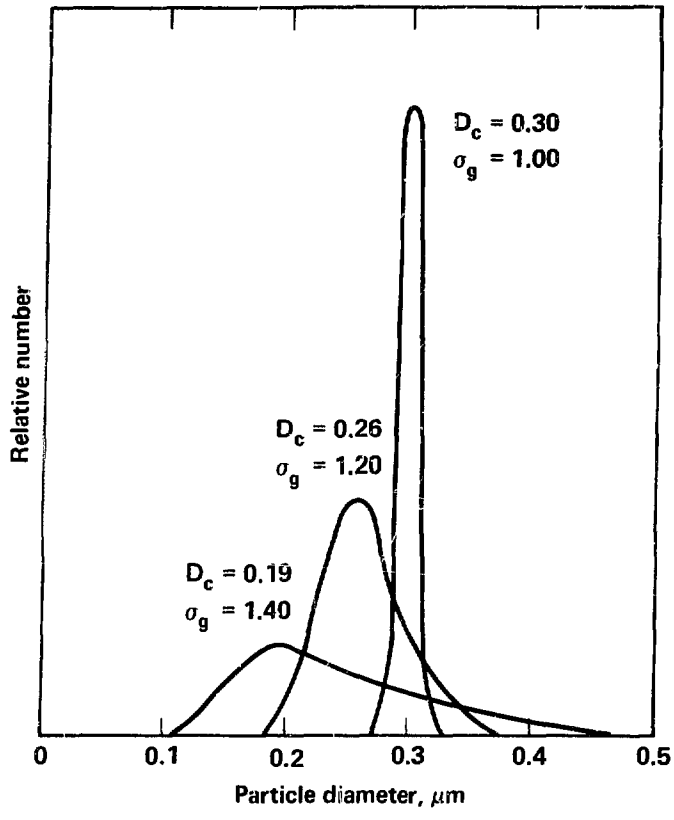

Fig. 6. Three different particle-size distributions that produced identical measurements of average size by the "owl."

IV. The Owl Performs Much Better than the Laser Spectrometer in the DOP Filter Certification Test

There is an effort by some researchers to replace the owl in the present DOP test with an instrument like the PMS-laser spectrometer (Particle Measuring System, Inc., Boulder, CO). This is an effort that we feel is unwarranted if filter penetrations are still measured with a light-scattering photometer. This effort is motivated by the fact that the owl cannot measure particle-size distributions while the PMS-laser can.[13] Independent tests with a PMS-laser spectrometer have shown that DOP aerosols have a broad range of particle-size distributions with a significant number of particles exceeding 0.3 μm in diameter. The concern is that these larger particles create deceivingly low HEPA-filter penetrations since a small increase in the size of DOP aerosols will result in a large decrease in filter penetration (Fig. 1). We feel that replacing the owl with a laser spectrometer may create serious problems with filter-efficiency tests.

Our analysis of the DOP filter tests has shown that the owl performs a complicated and necessary function in the filter test. The owl is used in adjusting the particle-size distribution so that the light-scattering photometer sees the heterodisperse DOP aerosol as monodisperse 0.3-μm-diameter particles. Figure 7 shows that the owl and the photometer have a similar instrument response as a function of particle diameter. Thus, as a first approximation, the

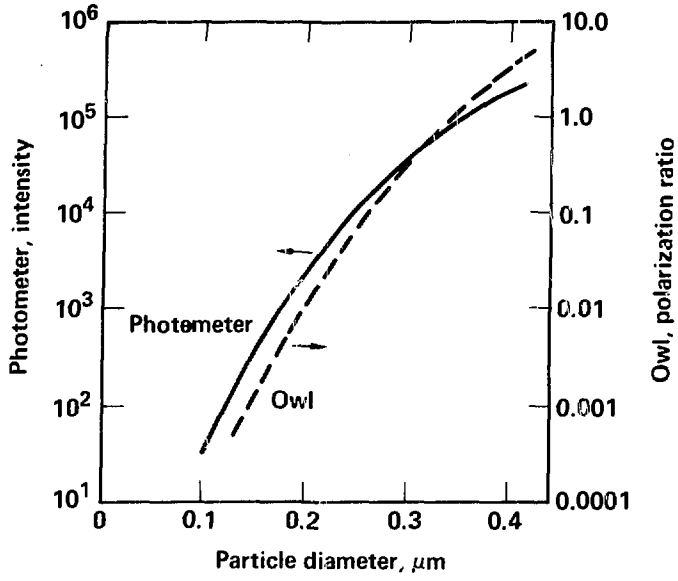

Fig. 7. Response of light-scattering photometer and owl to different particle sizes.

photometer also sees the various particle-size distributions shown in Fig. 6 as monodisperse 0.3-μm-diameter particles. This is only an approximation, and, as Fig. 7 shows, the two curves do not overlap exactly. The comparable equation for the photometer response was taken from data by Tillary, et al.[14] and is

$$R_{phot}(r) = K_2 \overline{r^{6.2}} \quad , \tag{6}$$

where K_2 is a proportionality constant. This equation is valid from diameters of 0.1 to 0.4 μm. If the particles have a log-normal distribution, then it is possible to calculate an equivalent monodisperse diameter that will give the same readings on either the photometer or the owl. The equivalent monodisperse diameters for the owl and the photometer are given by Eqs. 7 and 8, respectively:

$$\ln D_{owl} = \ln D_{cmd} + 4.05 \ln^2 \sigma_g \quad \text{and} \tag{7}$$

$$\ln D_{phot} = \ln D_{cmd} + 3.1 \ln^2 \sigma_g \quad , \tag{8}$$

where D_{cmd} is the count median diameter and σ_g is the geometric standard deviation of the particle-size distribution.

Equation 8 can be used to calculate equivalent monodisperse-particle diameters for heterodisperse aerosols as measured by the photometer. Figure 8 shows the equivalent diameter plotted as a function of increasing hetero-

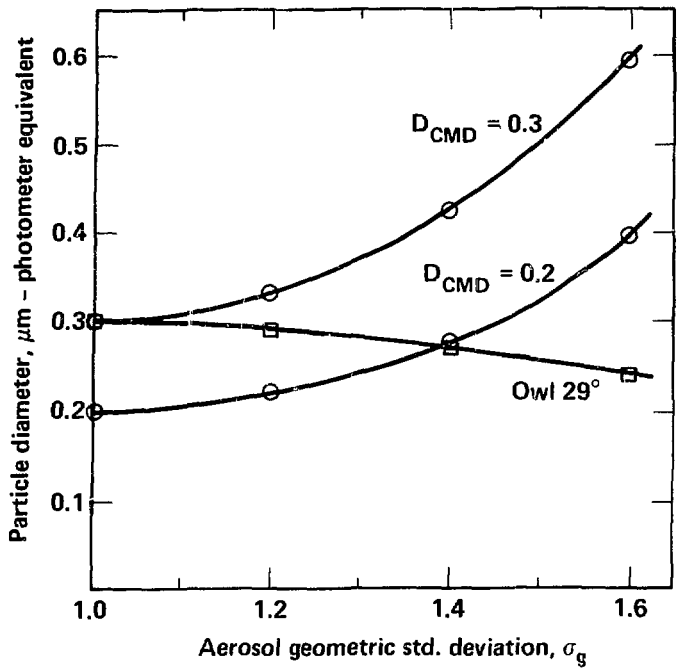

Fig. 8. The equivalent photometer diameter calculated from Eq. 9 for three different particle-size distributions as a function of increasing aerosol heterodispersion. The particle-size distributions for two of the curves have a constant count median diameter, D_{cmd}, as the heterodispersion, σ_g, increases. The particle-size distribution for the owl with a 29° reading is determined from Eq. 8 and shown in Fig. 6.

dispersion for three cases. The two identified as D_{cmd} = 0.3 and D_{cmd} = 0.2 represent particle-size distributions in which the count median diameters are kept constant and the heterodispersion is allowed to increase. Note that the equivalent photometer diameter increases significantly with increasing heterodispersion. The curve labeled owl 29° represents a series of increasingly heterodisperse aerosols, as shown in Fig. 6, in which the owl sees an equivalent 0.3-μm-diameter aerosol, as given by Eq. 7. Note that the equivalent photometer diameter for a constant owl value decreases only slightly as the heterodispersion of the aerosols increases. Thus, we see that the owl provides an approximate measure of 0.3-μm aerosol as seen by the photometer even for heterodisperse aerosols. We would therefore expect that the filter-penetration measurement using heterodisperse aerosols having a photometer equivalent diameter of 0.3 μm would yield similar results to penetration measurements using monodisperse 0.3-μm aerosols.

To test this hypothesis, we computed the penetration of a HEPA filter using Eq. 3 for various particle-size distributions, N(r), all having the same owl reading. Particle-size distributions with various D_{cmd} and σ_g were selected that had D_{owl} = 0.3 μm in Eq. 7. The filter-penetration function, $P_F(r)$, used in these calculations is the solid curve shown in Fig. 9 that represents a least-squares best fit of a log-normal distribution to the experimental measurements shown as triangles. The best fitting log-normal curve is characterized by D_{cmd} = 0.143 μm and σ_g = 1.47. Details of the experimental technique used to generate the HEPA-filter penetration curve are given in Appendix A. The photometer

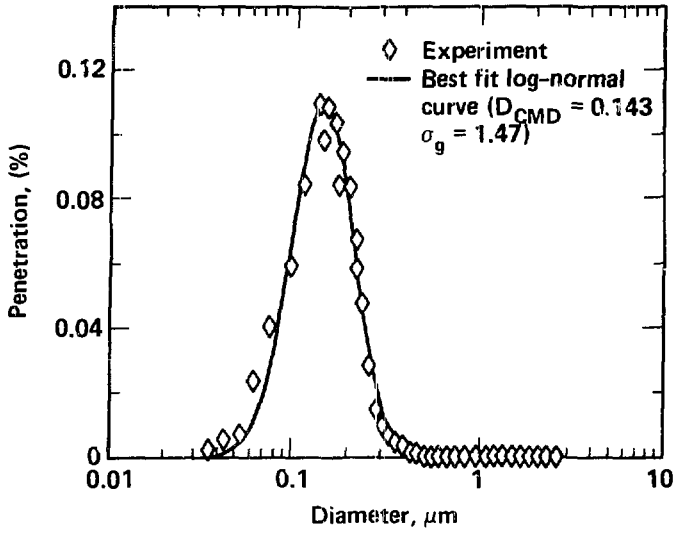

Fig. 9. Experimental penetration of a HEPA filter as a function of DOS particle diameter.

response function R(r) used in these calculations is given by Eq. 6 which is derived from data presented by Tillary, et al.[14] Figure 10 shows that increasing the heterodispersion of particle-size distributions that have the same owl reading of 29° (Fig. 6 shows three of these distributions) causes only a 24% reduction in filter penetration. In contrast, increasing the heterodispersion while maintaining a constant count medium diameter of 0.2 μm causes an 87% reduction in the filter penetration. The purpose of measuring the particle size in DOP filter certification tests is to ensure that filter-penetration measurements are made with DOP aerosols having an effective diameter of 0.3 μm. It is clear from Fig. 10 that the owl is better suited for measuring the effective particle size in the current filter test than a laser particle-size spectrometer.

Although these aerosol-size spectrometers are able to uniquely define the particle-size distributions, they are unable to perform the function that the owl so simply and so elegantly performs. Figure 10 also shows that potentially serious errors in filter penetration can arise with the replacement of the owl by an optical spectrometer. Only when the σ_g is within a narrow range of about 1.4 will the filter efficiencies obtained with an aerosol size spectrometer have results comparable to that of using an owl.

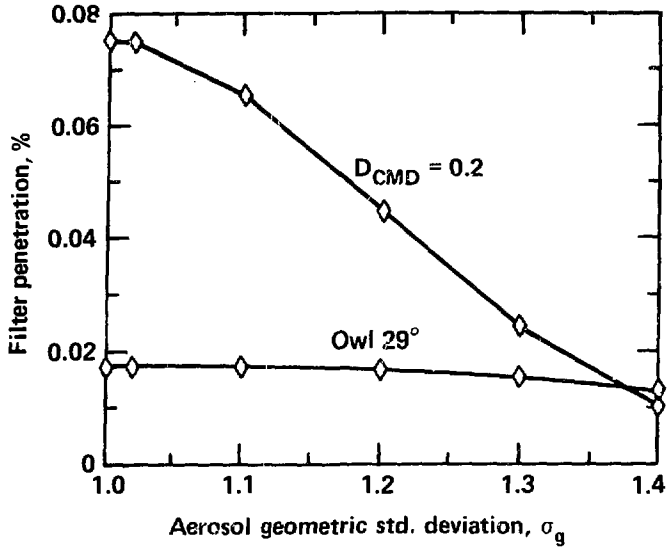

Fig. 10. Calculated filter penetration using Eq. 3 as a function of increasing aerosol heterodispersion. The curve for Owl 29° was calculated for particle size distributions satisfying Eq. 6 with D_{Owl} = 0.3 μm. The curve for D_{cmd} = 0.2 was calculated for particle size distributions having a constant D_{cmd}.

V. Sensitivity of DOP Filter Test to Heterodisperse Aerosols, HEPA Penetration Curve and Photometer Response Function

The filter penetration measurement is a function of the particle-size distribution, the filter penetration curve, and the photometer response as shown by Eq. 3. Our analysis of the effect of DOP heterodispersion on HEPA penetration was based on using experimental HEPA penetration and photometer response curves. However, in order to determine the sensitivity of our penetration calculations to variations in the HEPA penetration and photometer response curves, we repeated the calculations in the previous section.

The HEPA penetration curve used in generating Fig. 10 is characterized by a log-normal curve having D_{cmd} = 0.143 μm and σ_g = 1.47. We repeated the calculation of the filter penetration measurement using Eq. 3 for other values of D_{cmd} and σ_g. The previous photometer response curve given by Eq. 5 was also used in these calculations. As before, the parameters for the particle-size distributions having a constant owl reading of 29° are given by Eq. 7.

Figure 11 shows the calculated HEPA penetration using Eq. 3 as a function of increasing DOP heterodispersion for HEPA-filter penetration curves characterized by a constant D_{cmd} = 0.143 μm and σ_g values of 1.3, 1.4, 1.47 and 1.6. The solid curves represent filter-penetration calculations for DOP aerosols having a constant 29° owl reading. The parameters for these aerosol distributions are given by Eq. 7. The dashed lines represent DOP aerosols having a constant D_{cmd} = 0.2 μm and the σ_g values indicated on the abscissa. Figure 11 shows that the relative HEPA penetration for aerosol distributions having a constant owl reading

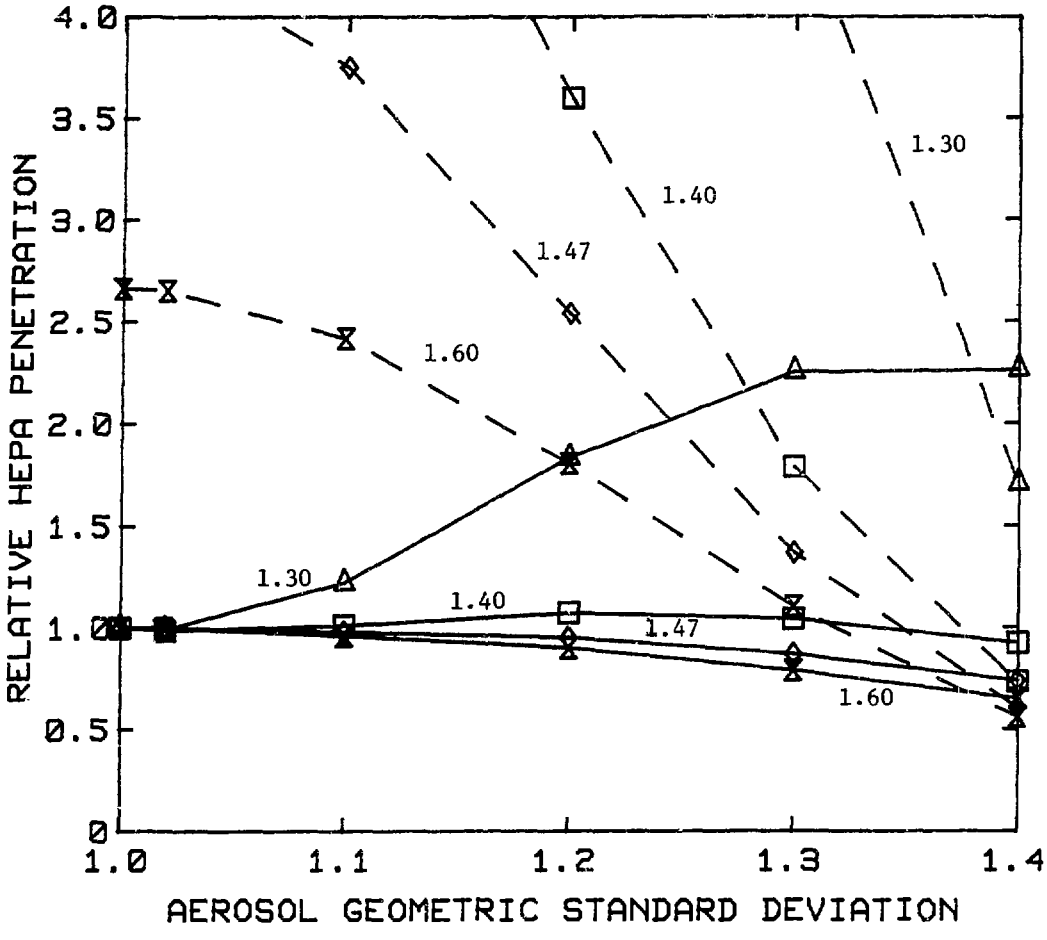

Fig. 11. Calculated filter penetration using Eq. 3 as a function of increasing aerosol heterodispersion for HEPA filter penetration curves characterized by a constant D_{cmd} = 0.143 µm and σ_g values of 1.3, 1.40, 1.47, and 1.6. The solid lines represent penetration calculations for DOP aerosols having a constant 29° reading (Eq. 7) while the dashed lines represent aerosols with a constant D_{cmd} = 0.2 µm.

deviates much less with increasing DOP heterodispersion than does the penetration for aerosol distributions having a constant D_{cmd}. It is noteworthy that the calculated filter penetration for aerosols having a constant owl reading is relatively insensitive to a broadening of the penetration curve as the σ_g increased from 1.47 to 1.6. However, a narrowing of the penetration curve from σ = 1.47 to 1.30 shows a significant deviation in calculated filter penetrations between monodisperse and heterodisperse DOP aerosols. In contrast, all of the curves in Fig. 11 for aerosols having a constant D_{cmd} = 0.2 µm show major charges in calculated filter penetration between monodisperse and heterodisperse DOP aerosols.

A similar series of calculated filter penetrations were made for HEPA-filter penetration curves having a constant σ_g = 1.47 and D_{cmd} values of 0.1, 0.143, 0.12, and 0.2. These calculations are shown in Fig. 12 for DOP aerosols having a constant 29° reading (solid lines) and for DOP aerosols having a constant D_{cmd} =

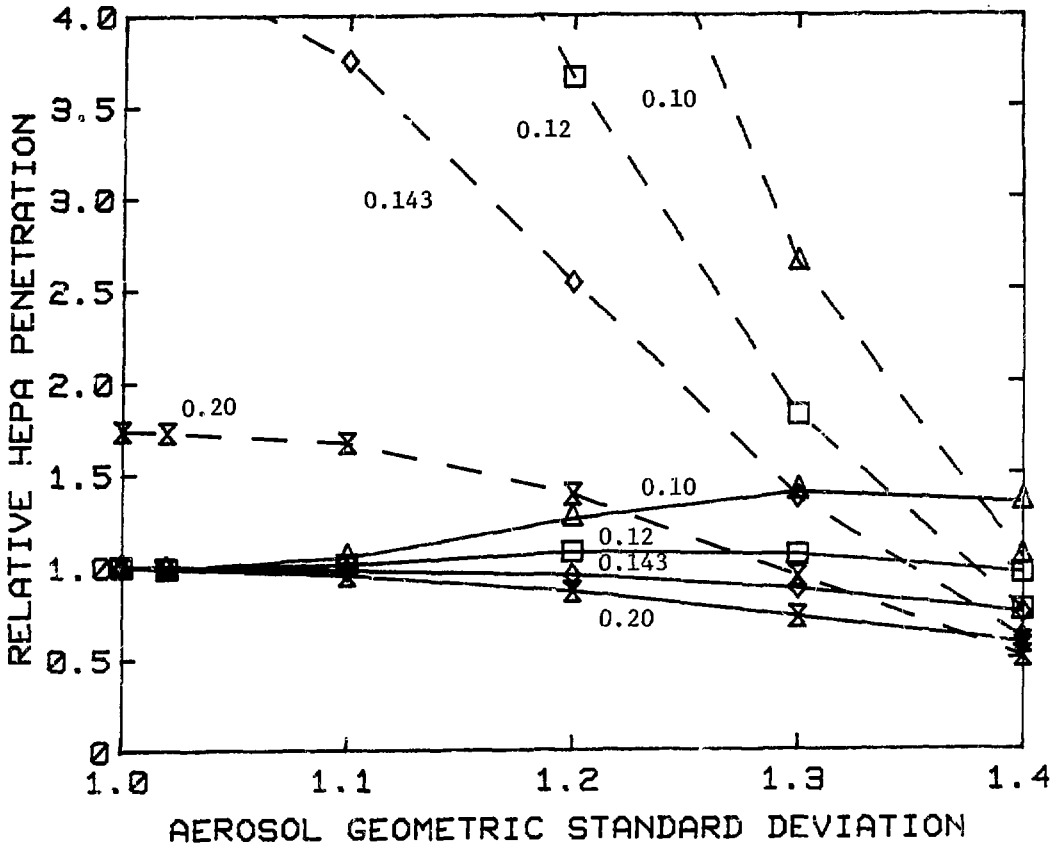

Fig. 12. Calculated filter penetration using Eq. 3 as a function of increasing aerosol heterodispersion for HEPA filter penetration curves characterized by a constant σ_g = 1.47 and D_{cmd} values of 0.10, 0.12, 0.143, and 0.20. The solid lines represent penetration calculations for DOP aerosols having a constant 29° reading (Eq. 7) while the dashed lines represent aerosols with a constant D_{cmd} = 0.2 μm.

0.2 μm (dashed lined). Again, it is apparent that the owl is preferred over particle-size spectrometers to maintain the desired DOP size distribution for use in HEPA-penetration measurements.

The sensitivity of the photometer response curve on the calculated HEPA penetrations was then examined. We used Eq. 6 in our previous calculations since this equation was derived from both theoretical[14] and experimental[15] data. To determine the sensitivity of changes in the photometer response curve on the calculated HEPA penetration, we have repeated the calculations using the following response functions.

$$R_{phot}(r) = K_3\, r^5 \qquad (9)$$

$$R_{phot}(r) = K_4\, r^7 \qquad (10)$$

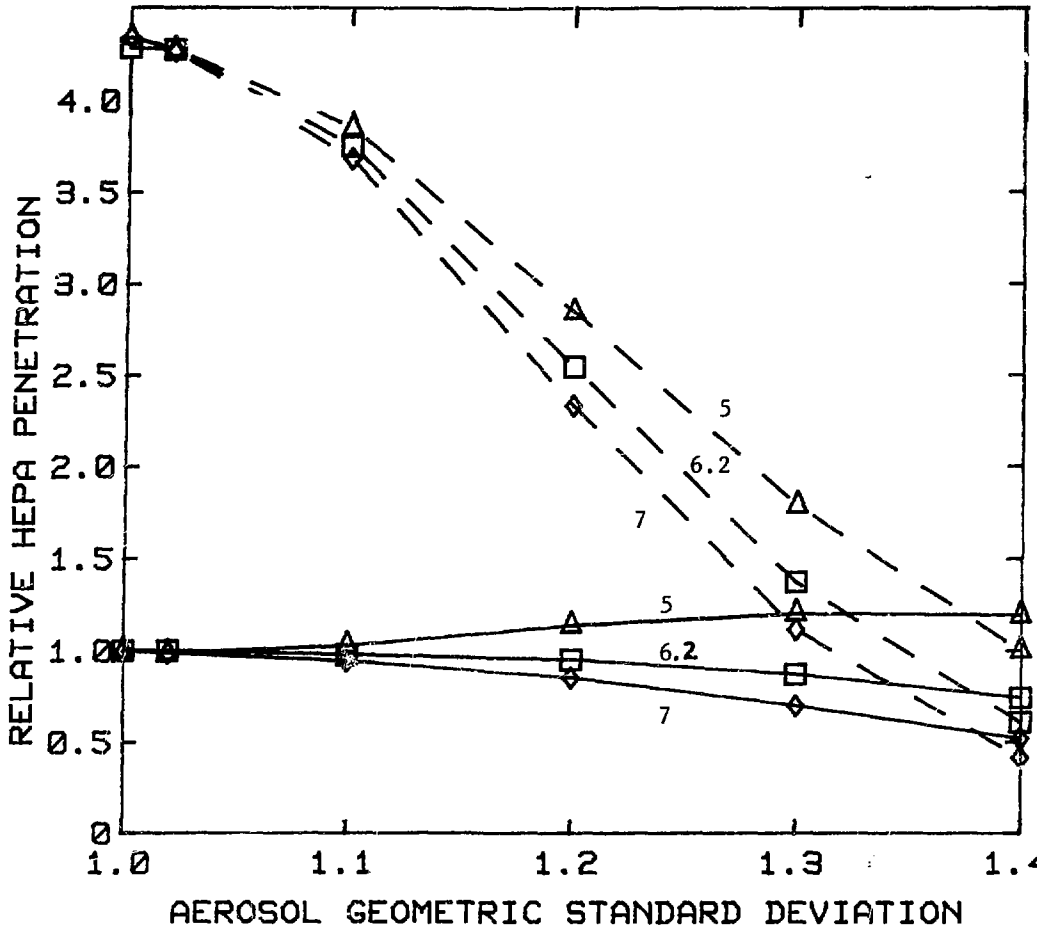

Fig. 13. Calculated filter penetration using Eq. 3 as a function of increasing aerosol heterodispersion for different photometer response functions characterized by r^5, $r^{6.2}$, and r^7. The solid lines represent penetration calculations for DOP aerosols having a constant 29° reading (Eq. 7) while the dashed lines represent aerosols with a constant D_{cmd} = 0.2 μm.

Figure 13 shows that the penetration curves for DOP aerosols having a constant 29° reading are relatively insensitive to changes from monodisperse to heterodisperse aerosols, while the calculated penetration for DOP aerosols having a constant D_{cmd} = 0.2 μm shows major changes in HEPA penetration as the DOP aerosol changes from monodisperse to heterodisperse.

A comparison of Figs. 11-13 shows that the DOP filter test is only moderately sensitive to the degree of aerosol heterodispersion, HEPA penetration, and the photometer response when the aerosol size distribution maintains a constant owl value of 29°. However, if the DOP aerosols are maintained at a constant D_{cmd} = 0.2 μm, then the DOP filter test becomes very sensitive to these three parameters. Although the owl cannot measure the size distribution of heterodisperse aerosols, the owl is superior to the spectrometers for measuring aerosol size in the current DOP-filter test. Figures 11-13 show that the DOP

filter test is far less sensitive to test variables when the owl is used than when a particle-size spectrometer is used for controlling the particle size. The primary reason for the owl's superior performance is that a constant owl reading yields a nearly constant photometer equivalent particle size as the degree of heterodispersion is increased.

This behavior is shown in Fig. 8. In contrast, maintaining a constant D_{cmd} with the aid of a particle-size spectrometer as the degree of heterodispersion increases will significantly shift the equivalent photometer diameter.

VI. Conclusion

We investigated the effect of DOP heterodispersion on HEPA-filter penetration measurements and determined that a typical heterodisperse DOP aerosol (D_{cmd} = 0.19 μm and σ_g = 1.4) results in a 24% lower penetration than that obtained for monodisperse DOP aerosols (D_{cmd} = 0.3 and σ_g = 1.0). The surprisingly small effect of the DOP heterodispersion on the HEPA-filter penetration is due to the response function of the owl that is similar to the response of the photometer. Changes in the particle-size distribution are therefore seen in a similar fashion by both the photometer and the owl. We have also shown that replacing the owl with particle-size spectrometers may lead to large errors in filter penetration. These errors are produced because the particle-size spectrometers do not provide measurements that correspond to the photometer measurements.

VII. Appendix A

Experimental Technique for Measuring HEPA-Filter Penetration as a Function of Particle Size

The essential experimental apparatus used to generate the HEPA-filter penetration as a function of DOS particle size is shown in Fig. A-1. An aerosol spectrometer is used to measure the concentration of aerosols as a function of particle size before and after the HEPA filter. The ratio of the aerosol concentration before and after the HEPA filter for each particle size increment yields the HEPA penetration as a function of particle size. The aerosol spectrometer used in these tests consists of two instruments: (1) a differential mobility analyzer (DMA) coupled to a condensation nuclei counter (CNC) (Thermal Systems, Incorporated, Minneapolis, Minnesota) for measuring particle-size distributions from 0.01 to 0.5 μm diameter, and (2) a LAS-X laser particle counter (Particle Measuring Systems, Bolder, Colorado) to measure particle-size distributions from 0.1 to 3.0 μm. Both of these instruments are interfaced to a LSI-11 computer that gathers data and reduces it to graphical output.

A dilution system is required to reduce the high aerosol concentration before the HEPA filter to a level acceptable to the aerosol spectrometer. The dilution system is primarily required for the LAS-X laser particle counter to prevent counting more than one particle at the same time. Figure A-2 is a schematic of the diluter we used. In order to reach the desired dilution rate of 1500:1, we had to use two diluters in series.

An important factor to know when using a diluter is the particle losses in the dilution system that results in a variable dilution as a function of particle size. Figure A-3 shows the dilution ratio as a function of particle size for the dilution system used in our tests. We have taken this variable dilution into account in computing the HEPA-filter penetration as a function of particle size that is shown in Fig. 9.

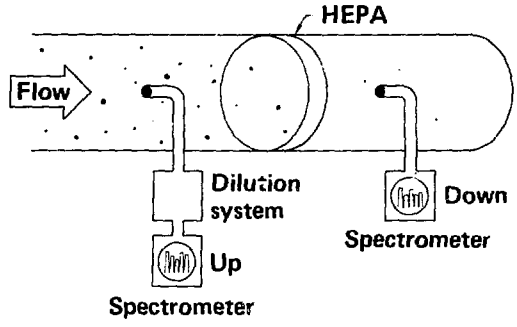

Fig. A-1. Schematic of filter test method for measuring filter penetration of HEPA filters as a function of particle size by using a dilution system to reduce the upstream concentration of aerosols.

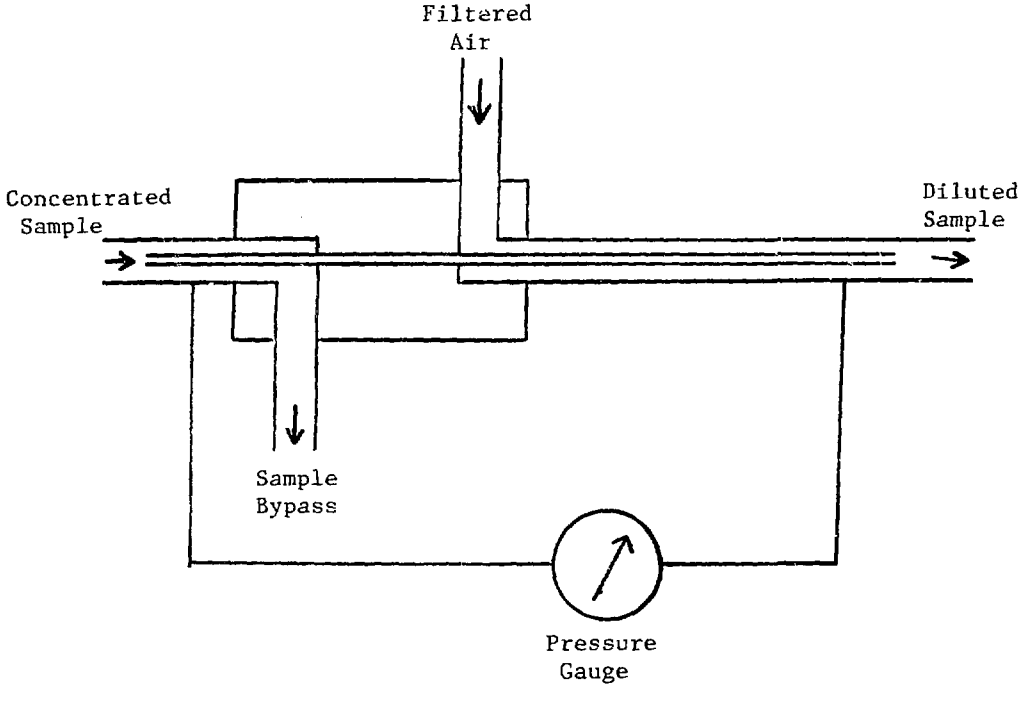

Fig. A-2. Schematic of diluter based on the principle of transferring a small volume of concentrated aerosols through a needle to a large volume of filtered air. The pressure differential across the needle determines the flow through the transfer needle.

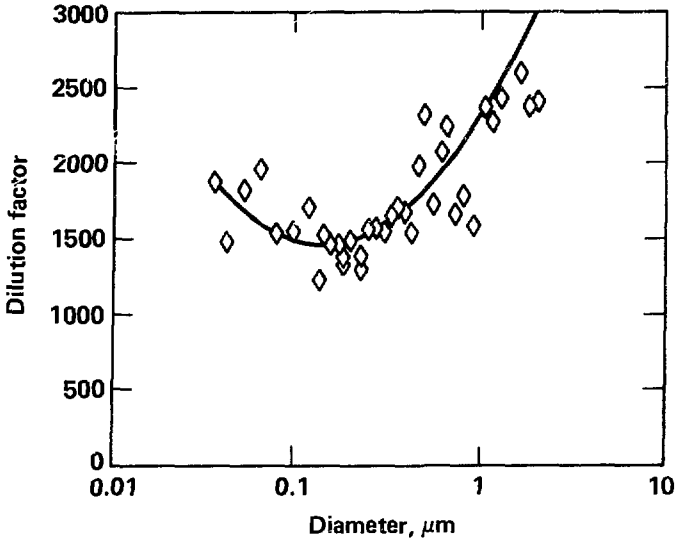

Fig. A-3. Dilution ratio as a function of particle size for two diluters in series. Solid curve represents least-squares fit.

Bibliography

(1) Dupoux, J. and Briand, A., "Air filter efficiency as a function of particle size and velocity," Water, Air, and Soil Pollution, 3, pp. 537-549, (1974).

(2) Dorman, R. G, Dust control and air cleaning, Pergamon Press, New York, (1974).

(3) Burchstead, C., Fuller, A., and Kahn, J., Nuclear air cleaning handbook, ERDA 76-21, National Technical Information Service, Springfield, VA, (1976).

(4) Riediger, G., "The testing of high efficiency particulate air filters according to the German Standard DIN 24 184," in Seminar on High Efficiency Aerosol Filtration, Aix-en-Provenc, France, Commission of the European Communities, November 22-25, (1976).

(5) Dorman, R. G. and Ward, A. J., "Filter evaluation and testing," in Filtration Principles and Practices, Part II," Clyde Orr, editor, Marcel Dekker, Inc., New York, (1979).

(6) Marshall, M. and Stevens, D. C., "A comparative study of in-situ filter test methods," CONF-801038, pp. 35-55, Proceedings of the 16th DOE Nuclear Air Cleaning Conference, San Diego, CA (1980).

(7) Dorman, R. G., "A comparison of methods for particulate testing of HEPA filters," CONF-801038, pp. 56-66, Proceedings of the 16th DOE Nuclear Air Cleaning Conference, San Diego, CA (1980).

(8) Murphey, L. P., Fernandez, S. J. and Mates, B. G., "Comparison of HEPA filter test methods in corrosive environments," CONF-801038, pp. 67-85, Proceedings of the 16th DOE Nuclear Air Cleaning Conference, San Diego, CA (1980).

(9) Sofiltra-Poelman, Societe industriele de filtration, 71BD National, 92250 La Garenne-Colombes, France.

(10) Hinds, W., First, M., Gibson, D., and Leith, D., "Size distributions of "HOT DOP" aerosol produced by ATI-O-127 aerosol generator," CONF-780819, pp. 1130-1144, Proceedings of the 15th Nuclear Air Cleaning Conference, Boston, MA, 1978.

(11) Skaats, C. D., "A study of dioctyl phthalate particles (DOP) generated in penetrometers and the devices used currently to measure their size," CONF-780819, pp.1127-1129, Proceedings of the 15th Nuclear Air Cleaning Conference, Boston, MA (1978).

(12) Gerber, B. V., "Selected polyethylene glycols as DOP substitutes," CONF_ 801038 pp. 109-124, Proceedings of the 16th DOE Nuclear Air Cleaning Conference, San Diego, CA (1980).

(13) Salzman, G. C., Ettinger, H. J., and Tillary, M. I., "Potential application of a single particle aerosol spectrometer for monitoring aerosol size at the DOE Filter Test Facilities," CONF-820833, pp. 801-820, Proceedings of the 17th DOE Nuclear Air Cleaning Conference, Denver, CO (1982).

(14) Tillary, M., Salzman, G., and Ettinger, H., "The effect of particle size variation on filtration efficiency measured by the HEPA filter quality assurance test," Proceedings of the 17th DOE Nuclear Air Cleaning Conference, Denver, Colorado, August 1982, National Technical Information Service, CONF-820833, pp. 895-908, 1982.

(15) Sinclair, D., "A new photometer for aerosol particle size analysis," Air Pollution Control Association Journal, 17, pp. 105-108, 1967.

DISCUSSION

SODERHOLM: A technical point in your paper, Equations 5 and 7 and Figure 7 reflect the response of the OWL being a radius to the 8.1 power. If you go back to the paper by Hinds et al., you will see that it is correct only over a limited size range, and is even an approximation over that size range. It is not a bad approximation the way you have used it, but I think, for the record, we should mention that it is limited and we don't want people using it all the way up to a micron or over, where it really becomes a bad approximation. Also, I would like to point out that partly based on your input to the DOE nuclear standards writing group, the geometric standard deviation that is allowed for a new aerosol has been set in the range of 1.3 to 1.5. Most of your curves, however, show what happens with a geometric standard deviation going from 1.0 to 1.4, a range that shows much more dramatic effects. There is actually a confluence of the two systems at a geometric mean diameter of 0.2 μm and a geometric standard deviation of 1.4. That is why we picked that point. We are allowing some variation around that one point. The very large, as you

call them, errors, or difference in measurements, which would occur with a monodisperse aerosol of 0.2 μm are not allowed under the new standards. Based on your input, we have tried to minimize the problem and we certainly agree that it is worthwhile evaluating new systems to gain more information on how the filter measurements we have been making correspond to reality. Therefore, we challenge the filters with a large range of aerosols. Finally, to give credit where it is due, Ron Scripsick obtained and presented many of the experimental results to which you referred in your talk as being presented by me.

BERGMAN: I agree with everything you have said and I apologize for not recognizing Ron Scripsick's excellent work on HEPA filter penetration as a function of size.

STEINBERG: Were all the numbers in your graphs derived from actual tests or as computer model work?

BERGMAN: They were computations of experimental data. The computations were an integration of the response curve, the HEPA penetration curve, and the size distribution curve; the products of all three. They were real numbers, measurements made in the laboratory.

STEINBERG: You kept going back and forth between the terms, photometer and OWL; when you said OWL, were you talking about the Tyndall-beam effect type of instrument that looks at the particle size, or were you talking about a scattering chamber?

BERGMAN: I will have to rely on you, since it is your instrument. I'll admit I didn't tear it apart, although I am familiar with LeMer's work.

STEINBERG: The OWL is used together with a particle size indicator to measure particle size. Is the polarization OWL what you were talking about or were you talking about forward light scatterming?

BERGMAN: The one that comes with your Q107 instrument.

STEINBERG: It contains both.

BERGMAN: I believe it is the polarization device, what else would 29° represent?

STEINBERG: That's why I asked you if they were real results or a computer model.

ANDERSON: They are real results.

SCRIPSICK: What was the percent deviation in your computations relative to the actual penetration (independent of the photometer response) as opposed to the penetration of strictly monodisperse 0.3 μm particles that is the reference condition in your presentation? I think this is an important comparison.

BERGMAN: The percent deviation will depend on what instrument is used to measure filter penetration. The deviations in the paper refer to those obtained with a light scattering photometer and represent an interpretation over the size distribution N(r), the filter penetration P(r), and the photometer response R(r) as shown by Equation 3. I want to emphasize that the penetrations calculated according to Equation 3 are actual penetrations. If one does not like to measure penetration with a photometer, one can also use a total particle counter, like a condensation nuclei counter, to measure the number of particles before and after the filter. In that case R(r)=1 in Equation 3. We did not do those calculations, although I can assure you the resulting penetration will differ significantly from that obtained when using a photometer. However, as strongly pointed out in my presentation, the only unambiguous penetration measurement is that obtained by directly comparing particle size distributions before and after the filter to yield the penetration curve shown in Figure 9.

DYMENT: (1) As a measure of the extent to which ideas on filter QA testing have changed recently - 10 years ago no one would have anticipated a speaker acclaiming the heterodispersity of DOP as a challenge aerosol. (2) Referring to Table 1 and Figure 1, the geometric standard deviation of the sodium chloride aerosol used in the British Standard Sodium Flame Test has been measured at 2.5, a much greater degree of heterodispersity than is considered for DOP Consequently, it has a significant proportion of particles in the range 0.1-0.2 μm, which covers the region of maximum penetration. (3) The ratio of DOP to NaCl penetration through a typical filter medium has been measured as 2-2.5:1, not 12:1 as Figure 1 suggests. (4) Earlier work with sodium chloride aerosols (quoted in Air Filtration by C.N. Davies) shows that average measured penetration (by mass) is a factor of 2-3 less than the maximum penetration obtained with particles 0.1-0.15 μm. (5) The sodium flame method of detection responds to all sizes of particles used in the challenge cloud. It measures mass (volume) concentration irrespective of any change in particle size distribution.

BERGMAN: I agree that there is a wide size distribution of the sodium chloride aerosol. The central point, 0.65 μm, represents the mass medium diameter and is what was plotted. The position of the various international test methods was put on the curve based on one number, which represents a volume average or a mass average. Sodium chloride appears to be unusually low on the curve based on actual penetration measurements. The reason it is in that position is because of your own references, and those of Mr Dorman. I agree, they overaccentuate the differences, but it does not change the basic trend, namely, because sodium chloride has a larger particle size, it gives a lower penetration than DOP or uranine.

DYMENT: I wish to emphasize that the trend has been greatly exaggerated in your figure.

BERGMAN: I find no fault with that. Comparing peak to average penetrations by any of the current methods using heterodisperse test aerosols is really comparing averages of averages. We know that averages knock off the peaks. Therefore, if you make dif-

ferential measurements over very small increments, instead of a 2 to 3 difference, you will get ten times, an order of magnitude, between the peak penetration and what the current U.S. DOP test shows. We have shown the same result with our laboratory sodium chloride aerosols, although they may not be the same in our laboratory as those used in England.

A NEW PROCEDURE FOR TESTING HEPA FILTERS

A method omitting testing at 20% rated flow

Liu Hui, Xin Song Nian, Guo Liang Tian

Radiation & Protection Branch
of Chinese Nuclear Society

Abstract

This article gives a theoretical analysis of HEPA penetration vs. pinholes in filter media. A calculation formula which shows the tendency of such changes was derived and has been demonstrated experimentally. By this formula "equivalent penetration" was calculated. Nomograms were used to facilitate the work. As a result, testing needs to be performed only at rated flow.

1. Theoretical Calculations of the Penetration of HEPA Filters Against Pinholes

It is well known for a given filter construction, filter media, and aerosol property, that penetration of a HEPA filter varies mainly with air flow rate and attention to sealing.

If pinholes occur in filter media and sealing compounds, the aerosol balance up- and downstream is shown in Fig. 1.

The balance is:

$$C_2(q + Q) = C_1Q + C_oq$$

Where:

C_o = aerosol concentration upstream

C_1 = aerosol concentration of the filtered air

C_2 = mean aerosol concentration of mixture of the filtered air and the air leaked through orifice

Q = volumetric flow rate of the filtered air

q = volumetric flow rate of the leaked air

from Equation (1),

$$\frac{C_2}{C_o} = \frac{C_1}{C_o} \cdot \frac{Q}{Q+q} + \frac{q}{Q + q}$$

$$\frac{C_2}{C_o} = \frac{Q}{Q+q}\left(\frac{C_1}{C_o} - 1\right) + 1$$

Since

$$\frac{C_2}{Co} = K_2 \quad , \qquad \frac{C_1}{C_o} = K_1$$

Where:

K_2 = average penetration of filter with holes.

K_1 = penetration of filter media at rated flow

Substituting and arranging,

$$K_2 = (\%) = 100 - \frac{Q}{Q+q}\left(100 - K_1\right) \qquad (2)$$

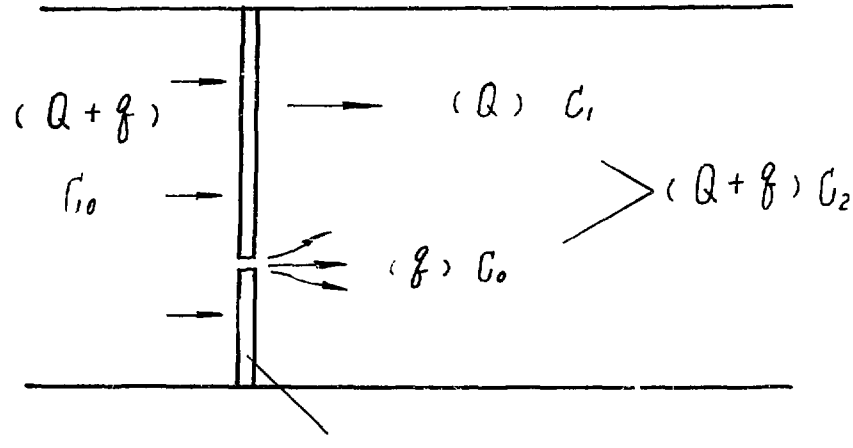

FIGURE 1 AEROSOL BALANCE

K_1, Q and q are closely related with filtration velocity V, and therefore are discussed separately below.

1. Penetration K_1 of Filter Paper

According to I. Langmuiry and C.N. Davies "logarithm penetration theory," K_1 can be expressed as:

$$K_1 = 10^{-\alpha H_s V^{-0.5}} \quad (3)$$

Where:

α = experimental coefficient of filter medium

H_s = resistance of medium, mm w.g., filtration velocity 1 cm/s

V = filtration velocity through medium, cm/s

2. Volumetric Flow Rate of the Filtered Air. Q, M^3/h

$$Q = 36\,VF \quad (4)$$

Where:

F = area of filterpaper, M^2

3. Volumetric Flow Rate of the Leaked Air

The volumetric flow rate of leaked gas depends on the flow pattern in the orifice. In general, when the differential pressure across the orifice is somewhat over a mm H_2O, turbulent flow occurs. The flow rate in M^3/h may be expressed as:

$$q = 0.978 f \sqrt{H}$$

Where:

f = the cross - section of the orifice, cm^2

H = the differential pressure across the orifice

0.978 = effluent coefficient of the orifice

Since the differential pressure across the orifice is the same as that across two sides of the filter,

$$H = RV$$

Where:

R = resistance coefficient of the medium

thus $q = 0.978\, f \sqrt{RV}$ (5)

substituting Equations (3), (4), (5) into Equation (2) and arranging,

$$K_2(\%) = 100 - \frac{36(F-f')v\left(100-10^{-\alpha H_s v^{-0.5}}\right)}{36\,(F-f')v + 0.978 f \sqrt{RV}}$$

Where f' = the cross - section of the orifice in M^2 which is much less than the surface area of filter paper and can be neglected. The equation thus becomes:

$$K_2(\%) = 100 - \frac{3600F - 36F\ 10^{-\alpha H_s v^{-0.5}}}{36F + 0.978\ f\ R^{0.5}\ v^{-0.5}} \qquad (6)$$

This equation indicates theoretically the penetration of filters with pinholes.

For a given filter, F, α, H_s and R are fixed, and K_2 is a function of cross-section of the holes and filtration velocity. Equation (6) also describes how penetration varies, which is consistent with the experimental results observed at home and abroad.

II. Determining Penetration at Low Flow Rate

At low flow rate the orifice effect grows significant. Penetration measurement at 20% of rated flow is used to examine whether the penetration is within the criterion set by the manufacturer i.e. even at this low flow rate the penetration should not excess the limit at rated flow. In other words,

$$K_2' \leq K_H$$

Where:

K_2' = filter penetration at 20% of rated flow

K_H = filter penetration at rated flow set by manufacturer as standard

If V_H is the filtration velocity at rated flow, at 20% of rated flow it should be 0.2 V_H and Equation (6) becomes:

$$K_2'(\%) = K_H = 100 - \frac{3600F - 36F10^{-\alpha H_s (0.2\ V_H)^{-0.5}}}{36F + 0.978 f_m R^{0.5} (0.2 V_H)^{-0.5}}$$

Where fm is the allowable cross-section of the holes at 0.2 V_H when keeping $K'_2 = K_H$. Hence

$$f_m = \frac{\dfrac{3600F - 36F \cdot 10^{-\dfrac{0.447}{100 - K_H}}}{-\alpha H_s V_H^{-0.5}} - 36F}{2.187 . R^{0.5}\ V_H^{-0.5}}$$

For a given filter, fm is fixed. Substituting fm for f in Equation (6), penetration at rated flow, K_m, can be calculated:

$$K_m\,(\%)=100-\frac{100-10^{-\alpha H_s V_H^{-0.5}}}{0.553+0.447\left(\frac{100-10^{-\alpha H_s V_H^{-0.5}}}{100-K_H}\right)^{0.447}} \quad (7)$$

Since $K_1 = 10^{-\alpha H_s V^{-0.5}}$, we obtain:

$$K_m(\%)=100-\frac{100-K_1}{0.553+0.447\left(\frac{100-K_1}{100-K_H}\right)^{0.447}} \quad (8)$$

K_m is the "equivalent penetration" we need.

From quation (8), it is found that K_m is only associated with K_1 and K_H. Physical analysis shows that the following relation should be observed $K_1 \leq K_H$ and $K_1 \leq K_m \leq K_H$

K_H is already a stipulated value. For example: 0.03%(DOP method), in United States; 0.01% (sodium flame method), in China.

K_1 can be determined through different ways:

(1) Calculate the filtration velocity from the filter's rated flow and the effective filter area. Then measure K_1 experimentally under this filtration velocity.

(2) Select a leak proof HEPA filter which has been checked by stringent scanning . Measure the penetration at rated flow, the result will represent K_1.

We calculated K_m from K_1 and K_H by Equation (8) and plotted the nomogram shown in Fig. 2. The use of the nomogram is illustrated with an example.

Given: $K_1 = 0.0013\%$ $K_H = 0.01\%$

To solve: $K_m = ?$

Solving:

K_1 (0.0013%) was found on the vertical (ordinate) axis, K_H (0.01%) on the horizontal axis, and K_m was found to be 0.0057%.

The nomogram has been demonstrated in lab. The experimental

conditions were: filter overall size 484 x 484 x 180 mm, rated flow 1000 M^3/h, filtration area 10 M^2, rated filtration velocity 2.8 cm/s, testing method sodium flame.

The Table 1 summarizes related data and test results from which the following can be found:

(1) For filter No. 28, checked by scanning, with no holes, the penetration at 20% of rated flow is much less than at rated flow.

(2) For filter No. 44, with holes, penetration at 20% of rated flow may reach the manufacturer's criterion (0.01%). The test of this filter shows that the penetration (0.0055%) measured at rated flow is approximately equal to K_m (0.0057%) obtained from Fig. 2.

(3) For filter No. 51, with holes, penetration at rated flow is near manufacture's criterion, but excessive penetration was measured at 20% of rated flow.

(4) For filter No. 1-3, testing indicates that the measured Km (0.033%) is near the K_m (0.035%) found from Fig. 2.

In general, the calculation represented by Fig. 2 is consistent with practice.

III. Summary

1. A theoretical expression (6) for penetration of filters with holes was derived from the theories governing filtration, aerosol behavior, and fluid dynamics.

2. The maximum cross-section of holes (fm) was calculated for which the penetration of the filter at rated flow should not exceed K_H.

3. Substituting the calculated fm into Equation (6) we obtained K_m, which representes the penetration of the filter at rated flow (and filtration velocity). K_m is called "equivalent penetration."

4. If $K_{100} \leq K_H$, it means that at 20% of the rated flow the penetration of this filter will not exceed K_H.

5. The new testing procedure makes it unnecessary to test each filter at low flow rate, though requiring a measurement of the penetration of the filter paper for each batch. Therefore, the filter test needs simpler equipment and takes less time.

6. The nomograms recommended have been demonstrated in the lab. Further experiments, especially in connection with filtration velocity and penetration of filter media, have been planned.

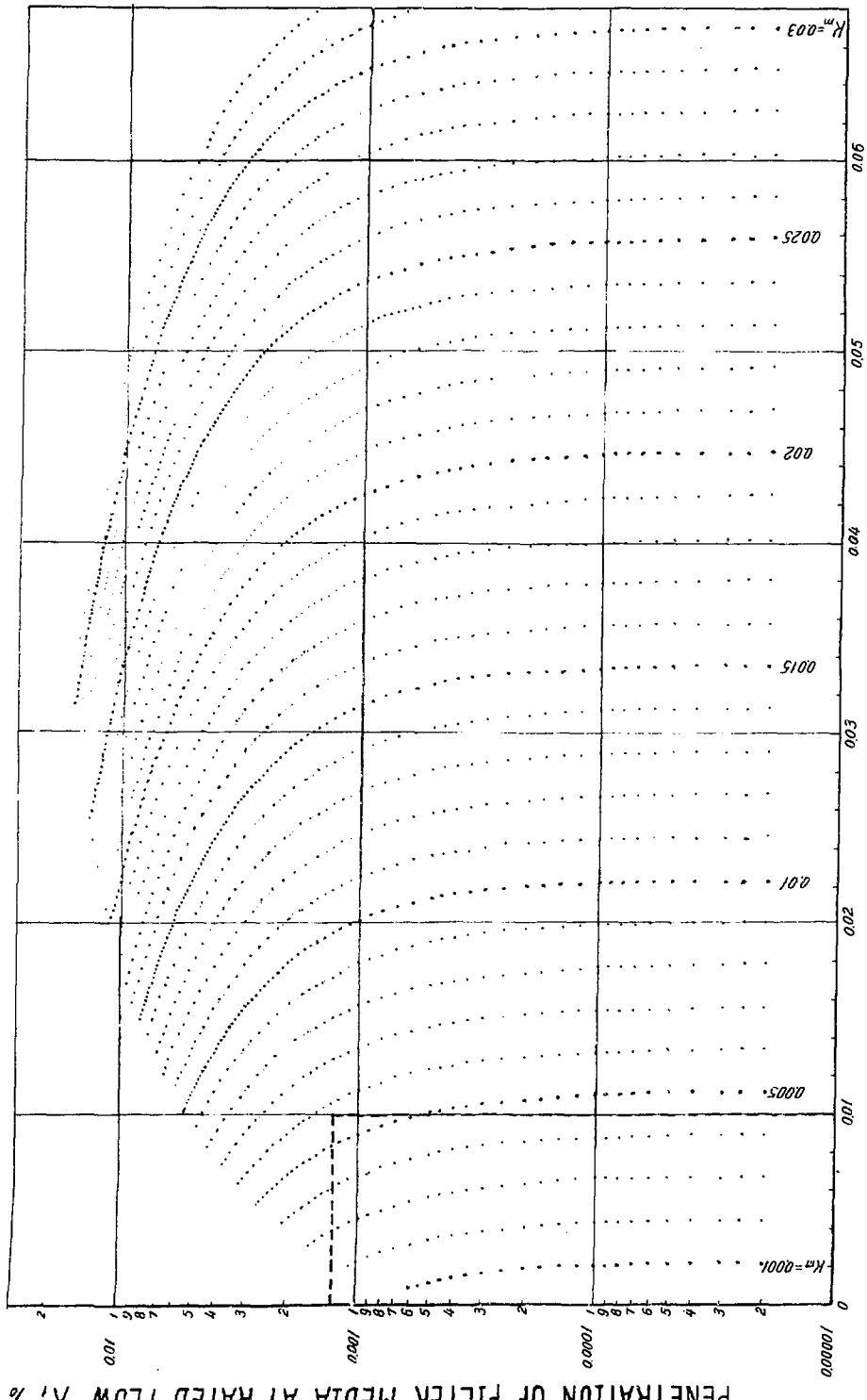

FIGURE 2 EQUIVALENT PENETRATION NOMOGRAM

Table 1 Results of filter testing

Filter Number	Penetration of Filter at Rated Flow K_1, %	Manufacturer's Criterion for Filter Penetration K_H %	Equivalent Penetration Found from Fig. 2 K_m %	Measured Penetration at 1000 M^3/h K_{100}, %	Measured Penetration at 200 M^3/h K_{20}, %
No. 28(1)	0.0013	0.01		0.0013	0.0005
No. 44(2)	0.0013	0.01	0.0057	0.0055	0.01
No. 51(2)	0.0013	0.01		0.011	0.026
No. 1 (1)	0.013	0.05	0.035	0.013	0.0008
No. 3 (2)	0.013	0.05	0.035	0.047	0.084
No. 2 (2)	0.013	0.05	0.035	0.033	0.05

Note: (1) No holes

(2) Holes

References

1. Linck F.J., Geer J.A., "In-place Testing of Multiple Stage HEPA Filter Plenum," 13th AEC Air Cleaning Conference, San Francisco, Califoria. (1974)

2. Xin Song Nian,"The Effect of Orifices on the penetration and Testing procedure for HEPA Filter," 1980, unpublished.

3. Adley F.E., Anderson D.E., "The Effect of Holes on the Performace Characteristics of High-efficiency Filters," 8th AEC Air Cleaning Conference, Oak Ridge National Laboratory (1963)

THE DESIGN OF GRADED FILTRATION MEDIA IN THE DIFFUSION-SEDIMENTATION REGIME

K.S. Robinson
Chemical Techology Division
AERE Harwell, Oxon UK

Abstract

The collection of a graphite aerosol on silica gel particles has been studied experimentally. These data, and data from Gebhart et al[1] have been used to obtain an empirical correlation for penetration in terms of diffusion and sedimentation mechanisms and an interaction term. In addition, a rapid graphical procedure for the design of graded packed beds is presented based on the assumption that a linear axial deposition profile will maximise bed operating lifetime.

I. Introduction

Modelling of Packed Bed Aerosol Collection

Over the past 25 years the collection of aerosols in packed beds of granular media has received considerable attention. Work has been carried out to determine the mechanisms involved in collection and the conditions under which each mechanism is either dominant or plays a significant role. The most extensively investigated collection mechanisms are diffusion[1,2,3], sedimentation[4,5] and inertial deposition[6,7]. Other collection mechanisms such as direct interception, thermophoresis, diffusiophoresis and electrostatic charge can also affect bed collection efficiency.

Models have been derived for the collection of aerosols in packed beds under conditions where one mechanism is effectively responsible for deposition. Generally the fractional penetration, P, of a packed bed aerosol collector can be expressed as:[7]

$$P = \frac{C_O}{C_I} = \text{Exp}\ (-K\,L) \qquad (1)$$

where C_O is the bed outlet aerosol number concentration, C_I is the bed inlet aerosol number concentration, K is the bed penetration coefficient and L is the bed length.

For collection by diffusion only the bed penetration, coefficient K_D, is given by:[3]

$$K_D = 6.54 \cdot \frac{1-e}{e} \cdot \left(\frac{D}{u}\right)^{0.66} \cdot \left(\frac{1}{d_c}\right)^{1.66} \qquad (2)$$

where e is the bed voidage, D is the aerosol diffusivity, U is the superficial gas velocity and d_c is the collector diameter.

For collection by sedimentation in downflow, the penetration coefficient, K_S, can be expressed as:[4]

$$K_s = \frac{1-e}{d_c} \left[0.056 \left(\frac{u_t}{u}\right)^{0.5} + 0.31 \left(\frac{u_t}{u}\right)^{0.78}\right] \quad (3)$$

where u_t is the particle terminal velocity in still air.

In circumstances where more than one mechanism is significant it has been assumed that the bed penetration coefficients are additive[8,9]. However, Fuchs[10] suggests that the bed penetration coefficients are additive only at low efficiency and Gebhart et al.[1] postulate that the additive principle should be modified at higher collection efficiencies with an interaction term $K_D.K_s$, although no experimental evidence or quantitative correlation is presented.

The work reported in this paper has been carried out in a regime where diffusion and sedimentation combine to affect aerosol deposition in a packed bed. An empirically derived equation is presented that successfully describes aerosol collection in this regime using in-house data and data abstracted from the work of Gebhart et al.[1].

The Design of Graded Packed Bed Collectors

The concept of graded beds, comprising layers of progressively smaller collector particles towards the bed outlet, has been employed to prevent filter cake, and hence pressure drop, build-up at the bed inlet. Graded packed bed aerosol collectors have been used industrially for the final polishing of ventilation off-gases from nuclear processing facilities in the USA[11,12] and are at present under investigation for similar applications in the UK. Work has also been carried out in the Federal Republic of Germany to design a graded bed to collect sodium oxide aerosol[9].

The large sand bed filters at Batelle PNL[11] and DuPont Savannah River[12] have given efficient service over many years and minor problems have been due to mechanical faults. However, Bohm and Jordan[9], in their work on sodium oxide aerosols, encountered filter cake build-up at the upstream end of their smallest grade collector which limited the operating life of their equipment. In order to facilitate the design of this type of equipment a rapid, graphical procedure has been developed which predicts the depth of each layer of collector particles required to give a near-linear deposition profile within the bed.

II. Experimental

The experimental equipment used in this work is shown in Figure 1. Filtered air was supplied to the bed by means of an unlubricated rotary vane compressor via a rotameter and bipolar ion source (polonium 210) which was used to bring to equilibrium any surface charge on the aerosol particles. Air samples were taken before, after and within the bed at a constant flowrate, diluted with filtered air and analysed using a Royco Particle Analyser. The results quoted are the mean of at least ten replicate one minute counts. The scatter was typically ±5% about the mean. Isokinetic sampling was compared with the above method over the range of

flowrates used for the aerosol size range of major importance (0.3 - 0.6 μm). The results obtained using isokinetic sampling were similar to those obtained using the simpler technique.

During preliminary experimental work, using what was thought to be laboratory air and ambient aerosol, it was found that the graphite vanes of the rotary compressor were producing an aerosol of constant size range (70% 0.3 - 0.6 μm) at a near constant mass concentration over the range of flowrates used. It was therefore decided to utilise this method of aerosol production throughout the experimental work. A scanning electron micrograph of the aerosol particles showed them to be approximately spherical, however, it was impossible to distinguish the degree of surface roughness. Therefore in the calculation of aerosol settling velocity and diffusivity the appropriate coefficient was used at a mean value between that for smooth and rough spheres. This assumption could lead to an error in the value of the calculated penetration coefficient, K_c, typically in the range ±2.5%, which is of similar order to the error band for the experimentally determined penetration coefficient.

The bed was filled with silica gel particles or pellets, dried at 120°C, and compacted by heavy tapping to obtain the maximum bulk density without the application of external forces. Physical properties of the collectors are given in Table 1. Particle envelope density, using gel dried to constant weight at 120°C, was measured using starch as a pseudo-liquid. Bed voidage, e, was calculated as:

$$e = 1.0 - \frac{\rho_e}{\rho_b} \qquad (4)$$

where ρ_e and ρ_b are the particle envelope density and packed bed bulk density respectively.

After filling the bed, any surface charge on the collector particles was brought to equilibrium using a Zerostat pistol. Before taking measurements the silica gel was allowed to come to equilibrium with the air supply.

III. Collection in Beds of Single Size Collector Particles

Results

A series of experiments was carried out at ambient temperature (18°C) to determine the fractional penetration of the silica gel particles in a 0.3m long, 0.045 m i.d. bed for mean aerosol diameters of 0.45 μm (0.3 - 0.6 μm) and 0.9 μm (0.6 - 1.2 μm). For all experimental conditions studied, the penetration measured with the equipment packed with collector particles, P_{EX}, was corrected for anomalous filtration in pipework, at the bed inlet and exit. The penetration through the bed of collector particles alone, P, is given by:

$$P = P_{EX}/P_{EM} \qquad (5)$$

where P_{EM} is the penetration measured with the empty equipment.

Experimental values for the penetration coefficient K_E were obtained from the slope of a plot of $\log_e$ penetration vs. bed length and are given in Tables 2 and 3. The values of K_D and K_S are also given. These were calculated using equations (2) and (3) respectively with D and u_t calculated according to Fuchs[11]. The density of the graphite aerosol was taken as $\rho_a = 2.25 \times 10^{-3}$ kg m^{-3}. The collector diameter, d_c, for the narrow size ranges of silica gel particles was taken as the mass median diameter of the distribution obtained by sieving. The volume surface mean diameter of the gel pellets was calculated from ten random length and diameter measurements. Penetration coefficients were also calculated for direct interception and inertial collection, for the most advantageous of the experimental conditions employed. The calculated penetration coefficient for inertial collection was several orders of magnitude less than those observed experimentally and direct interception contributed less than 2%. It was therefore assumed that collection was due to diffusion and sedimentation only.

Discussion

As would be expected, the experimental values K_E decrease with increasing velocity and collector diameter for a given aerosol mean diameter. It is also evident from Tables 2 and 3 that $K_E > K_D$ or K_S, and $K_E < (K_S + K_D)$ in agreement with observations of Fuchs[11]. Calculated values, K_D and K_S, suggest that as the aerosol mean diameter increases so collection by sedimentation becomes the dominant mechanism. Similarly, as the collector diameter increases so does the relative effect of sedimentation.

Further experimental data in this mixed regime were obtained from the work of Gebhart et al.[1] and are listed in Tables 4, 5 and 6. These results were obtained using latex aerosols ($\rho_a = 1.05 \times 10^3$ kg m^{-3}) and single sized glass ballotini collectors. They demonstrate trends similar to those found using the graphite aerosol.

Using both sets of data an empirical correlation for K_E in terms of K_D and K_S was found using an interaction parameter $K_D.K_S$ in the form: $K_E - (K_S+K_D) = f(K_S.K_D)$. In order that $K_C=0$, when K_D and $K_S=0$, the equation fitted to the data was constrained to pass through the origin. The best least squares fit to all the data was:

$$K_C = K_D + K_S - 4.4 \times 10^{-2} \cdot K_D.K_S + 7.72 \times 10^{-5} (K_D.K_S)^2 \quad (6)$$

Tables 2 to 6 inclusive show the good agreement obtained between K_E and K_C calculated using equation (6). For $K_E < 10$, equation (6) gives values for K_C that generally lie between K_E and $K_D + K_S$. For $K_E > 10$ the agreement with K_C is excellent.

IV. Collection in Graded Beds

Design Procedure

The design technique presented here is based on the premise that an axial penetration profile, as near linear as practicable,

will prevent filter cake build-up and maximise the use of available bed voidage and therefore bed operating lifetime, especially with narrow size range aerosols. For a linear axial profile;

$$P = \frac{C_o}{C_I} = 1 - \frac{L}{L_T} \qquad (7)$$

where L is any axial position in the bed and L_T is the total bed length. Figure 2 shows equation (7) and equation (1) for a graded packed bed, on linear coordinates, where K changes as a result of changes in collector diameter d_c and bed voidage e only. Although the implicit solution of equations (1) and (7) eliminating L_T, will lead to a solution for L with the appropriate value of K for each packing, it was thought desirable to obtain a rapid graphical solution, especially as the accuracy afforded by the mathematical solution could not be reproduced in practice, owing to variations in bed voidage e for replicate packings.

A rapid graphical method for obtaining the lengths of each packing grade is available when Figure 2 is replotted on log-linear coordinates, as in Figure 3, where the linear deposition profile, equation 7, becomes a curve.

The axial penetration profile for each packing is represented by a straight line with gradient -K passing through (0,1). The length of the least efficient packing, l_1, is found directly from the intersection of its penetration line with the linear profile at (L_1,P_1). The length of subsequent packings are then found by transposition of the appropriate penetration line through (L_{n-1},P_{n-1}) to meet the linear profile at (L_n,P_n) where the packing length required, l_n, is given by $L_n - L_{n-1}$. This procedure can be used to specify the lengths of available packings or to define the packing grades required to meet a given duty in as many grade steps as necessary to give a good approximation to the linear profile. Values of K can be obtained from existing correlations[1-7] or determined experimentally.

Experimental Validation of the Graded Bed Design Procedure

In order to test the design procedure for a graded bed collector a series of experiments was carried out at 0.01 and 0.035 ms^{-1} using a 1.2 m long x 0.045 m i.d. bed, with sample points at the interfaces between collector grades as well as at the bed inlet and outlet. It was decided to divide the bed into three sections and to aim at a penetration of 10^{-2} for 0.45 μm diameter aerosol. Three straight lines were therefore fitted, by eye, to the linear penetration profile, as shown in Figures 4 and 5. The slope of each line gave K_c and the intercepts on the x axis determined the depth of each packing. The diameter of packing required for each section was found, by trial and error, by substituting values for d_c in equations (2) and (3) and calculating K_c from equation (6) until the calculated value of K_c was within ±5% of that determined by the slope of each straight line fit to the linear profile. Where possible the grades of silica gel shown in Table 1 were used. In circumstances where this was not possible larger and smaller sizes

of gel were obtained by sieving or by crushing and sieving the existing material.

Results

The graded beds and the results obtained from them are shown in Figures 4 and 5. As can be seen the experimental values for penetration at the grade interfaces and bed outlet are in good agreement with the required design values at both 0.01 and 0.035 ms^{-1}.
These results clearly validate the design procedure for graphite aerosols in the diffusion-sedimentation regime.

Discussion

The work presented here on graded bed design assumes a narrow size range of aerosol that can be characterised by a single diameter. In cases where the distribution is more polydisperse a range of bed designs will be needed, as a function of aerosol diameter, and a compromise solution reached.

V. Conclusions

1. The empirically derived equation, incorporating an interaction term, used to predict penetration in the diffusion-sedimentation regime gives very good agreement with experimental results for aerosols of different densities over a range of collector diameter and gas velocity when $K_E > 10$.

2. When $K_E < 10$ agreement is less good, although better than that obtained with existing models.

3. The procedure for designing a graded packed bed aerosol collector with a penetration profile as near linear as practicable has been validated for graphite aerosols over a range of operating conditions.

Further work is being carried out at Harwell to examine the use of the design procedure in demisting and it is envisaged that further application may be found in other separation/filtration processes.

Acknowledgement

This work has been commissioned by the United Kingdom Department of the Environment, as part of its radioactive waste management programme. The results will be used in the formulation of Government policy, but at this stage they do not necessarily represent Government policy.

Nomenclature

C_o	aerosol number conc. at bed outlet	m^{-3}
C_I	aerosol number conc. at bed inlet	m^{-3}
D	diffusivity of aerosol	m^2s^{-1}
d_a	aerosol diameter	m
d_c	collector diameter	m
e	bed voidage	
K_D	penetration coefficient for diffusion	m^{-1}
K_E	experimental overall penetration coefficient	m^{-1}
K_S	penetration coefficient for sedimentation	m^{-1}
K_C	calculated overall penetration coefficient	m^{-1}
l	length of packing	m
L	axial location along bed	m
L_T	total bed length	m
P	penetration	
u	superficial linear velocity	ms^{-1}
u_t	aerosol terminal velocity in still air	ms^{-1}
ρ_a	aerosol density	Kg m^{-3}
ρ_e	media envelope density	Kg m^{-3}
ρ_b	media bulk density	Kg m^{-3}

Subscripts

1	course grade collector
2	intermediate grade collector
3	fine grade collector
EX	experimental value with packing
EM	experimental empty bed value

References

1. Gebhart, J., Roth, C. and Stahlofen, A. J. Aerosol Sci. 4, 355, 1973.

2. Balasubramanian, M. and Meisen, A. J. Aerosol Sci. 6, 461, 1975.

3. Wilson, E.J. and Geankopolis, C.J. Ind. Eng. Chem. Fund., 5, 9, 1966.

4. Thomas, J.W. and Yoder, R.E. AMA Arch Ind. Health 13, 545 and 550, 1956.

5. Pretsky, L.C. Ph.D. Thesis, The City University of New York, 1972.

6. Meisen, A. and Mathur, K.B. "The spouted bed aerosol collector: a novel device for separation small particles from gases", Symposium on Multi-Phase Flow Systems (Instn. Chem. Engrs. Symp. Ser. No.38), 1974.

7. Thambimuthu, K.V., Doganoglu, Y., Farrokhalee, T. and Clift, R. "Aerosol filtration in fixed granular beds" (SCI Symposium in Deposition of Particles from Gases and Liquids), 1978.

8. Dorman, R.G. in "Aerodynamic Capture of Particles" ed. E.G. Richardson (Pergamon Press, London) 1960.

9. Bohm, L. and Jordan, S.J. J. Aerosol. Sci. 7, 311, 1976.

10. Fuchs, N.A. in "The Mechanics of Aerosols" (Pergamon Press) 1964.

11. Work J.B. Hanford Atomic Products Operations, Report No.HW-11529, 1948.

12. Orth, D.A., Sykes, G.H. and Schurr, G.A. "The SRL sand filter: more than a pile of sand", (14th ERDA Air Cleaning Conference) 1976.

13. Whang, S.T. Ph.D. Thesis, London University, 1971.

Table 1. Properties of Silica Gel Collector Media

Nominal size range m	$0.5\text{-}1.0\times10^{-3}$	$0.7\text{-}1.5\times10^{-3}$	1×10^{-2}
Mass median diameter dc (sieve analysis), m	0.78×10^{-3}	0.96×10^{-3}	1×10^{-2}*
Envelope density, ρ_e Kg m^{-3}	1.18×10^{3}	1.22×10^{3}	1.23×10^{3}
Bulk density, ρ_b Kg m^{-3} (heavily settled)	0.75×10^{3}	0.71×10^{3}	0.68×10^{3}
Bed porosity, e	0.36	0.40	0.44

* Volume surface mean

Table 2. Calculated and Experimental Penetration Coefficients for d_a = 0.45 μm, ρ_a = 2.25 kgm.m^{-3} at 18°C

	u $ms^{-1}\times10^{2}$	K_{D_1} m	K_{S_1} m	$K_{D_1}+K_S$ m	K_{E_1} m	K_{C_1} m
$d_c=7.8\times10^{-4}$m	0.16	26	12	38	32	31.86
	0.65	10	5.0	15	13	13
	1.0	8.0	4.0	12	8.3	10.6
	2.9	4.0	2.4	6.4	5.0	6.0
$d_c=9.6\times10^{-4}$m	0.16	15	10	25	22	21
	0.65	6.0	3.6	9.6	8.0	8.7
	1.0	4.5	2.8	7.3	6.0	6.3
	2.9	2.2	1.8	4.0	3.5	3.8
$d_c=1.1\times10^{-2}$m	0.16	0.20	0.70	0.90	0.90	0.89
	0.65	0.08	0.30	0.38	0.40	0.38
	1.0	0.06	0.20	0.26	0.27	0.26
	2.9	0.03	0.14	0.17	-	

Table 3. Calculated and Experimental Penetration Coefficients for d_a = 0.9 μm, ρ_a = 2.25 kgm.m^{-3} at 18°C

	u $ms^{-1}x10^2$	K_{D_1} m	K_{S_1} m	$K_{D_1}+K_S$ m	K_{E_1} m	K_{C_1} m
	0.16	14	30	44	-	
	0.65	5.0	16.0	21	18	18
d_c=7.8x10^{-4}m	1.0	4.0	8.0	12.0	11	10.7
	2.9	2.0	4.2	6.2		
	0.16	8.0	20	28	23	23
	0.65	3.0	11	14	11	12.6
d_c=9.6x10^{-4}m	1.0	2.4	6.0	8.4	6.6	7.8
	2.9	1.0	3.2	4.2	4.0	4.1
	0.16	0.10	1.6	1.7	1.6	1.69
	0.65	4x10^{-4}	1.0	1.0	1.1	1.0
d_c=1.1x10^{-2}m	1.0	1.6x10^{-4}	0.40	0.40	0.40	0.40
	2.9	8x10^{-5}	0.20	0.20	-	-

Table 4. Calculated and Experimental Penetration Coefficients for d_a = 0.45 μm, ρ_a = 1.05 x 10^3 kgm.m^{-3} at 20°C

	u $ms^{-1}x10^2$	K_{D_1} m	K_{S_1} m	$K_{D_1}+K_S$ m	K_{E_1} m	K_{C_1} m
d_c = 5x10^{-4}m	0.30	32	8.0	40	33	33.8
	0.55	20	5.0	25	23	21.4
	2.2	8.2	2.6	11.0	10.3	9.9
d_c=1.6x10^{-4}m	0.30	4.6	2.6	7.2	4.9	6.68
	0.55	2.9	0.9	3.8	3.2	3.68
	2.2	1.1	0.5	1.6	1.4	1.57
d_c = 4x10^{-2}m	0.30	1.0	1.0	2.0	1.2	1.96
	0.55	0.65	0.65	1.3	0.90	1.28
	2.2	0.26	0.35	0.61	0.50	.60

Table 5. Calculated and Experimental Penetration Coefficients for d_a = 0.725 μm, ρ_a = 1.05 x 10^3 kgm.m^{-3} at 20°C

	u $ms^{-1}x10^2$	K_{D_1} m	K_{S_1} m	$K_{D_1}+K_S$ m	K_{E_1} m	K_{C_1} m
d_c = $5x10^{-4}$m	0.30	21	14	35	29	28.8
	0.55	13	9.0	22	18	17.9
	2.2	5.4	3.7	9.1	8.0	8.25
d_c=$1.6x10^{-4}$m	0.30	3.0	4.0	7	5.6	6.4
	0.55	1.9	2.7	4.6	3.5	4.3
	2.2	0.80	1.1	1.9	1.3	1.36
d_c = $4x10^{-2}$m	0.30	0.66	1.7	2.4	1.9	2.3
	0.55	0.42	1.1	1.5	1.2	1.5
	2.2	0.17	0.37	.54	0.50	.54

Table 6. Calculated and Experimental Penetration Coefficients for d_a = 1 μm, ρ_a = 1.05 x 10^3 kgm.m^{-3} at 20°C

	u $ms^{-1}x10^2$	K_{D_1} m	K_{S_1} m	$K_{D_1}+K_S$ m	K_{E_1} m	K_{C_1} m
d_c = $5x10^{-4}$m	0.30	15	24	39	33	33.2
	0.55	9.5	15	25	20	19.8
	2.2	3.8	6.2	10	8.3	9.0
d_c=$1.6x10^{-4}$m	0.30	2.1	7.5	9.6	7.3	9.2
	0.55	1.3	4.8	6.1	4.3	5.8
	2.2	0.56	1.9	2.5	1.7	2.4
d_c = $4x10^{-2}$m	0.30	0.43	3.0	3.4	3.0	3.4
	0.55	0.30	1.9	2.2	1.7	2.1
	2.2	$2x10^{-6}$	0.40	0.40	0.60	0.4

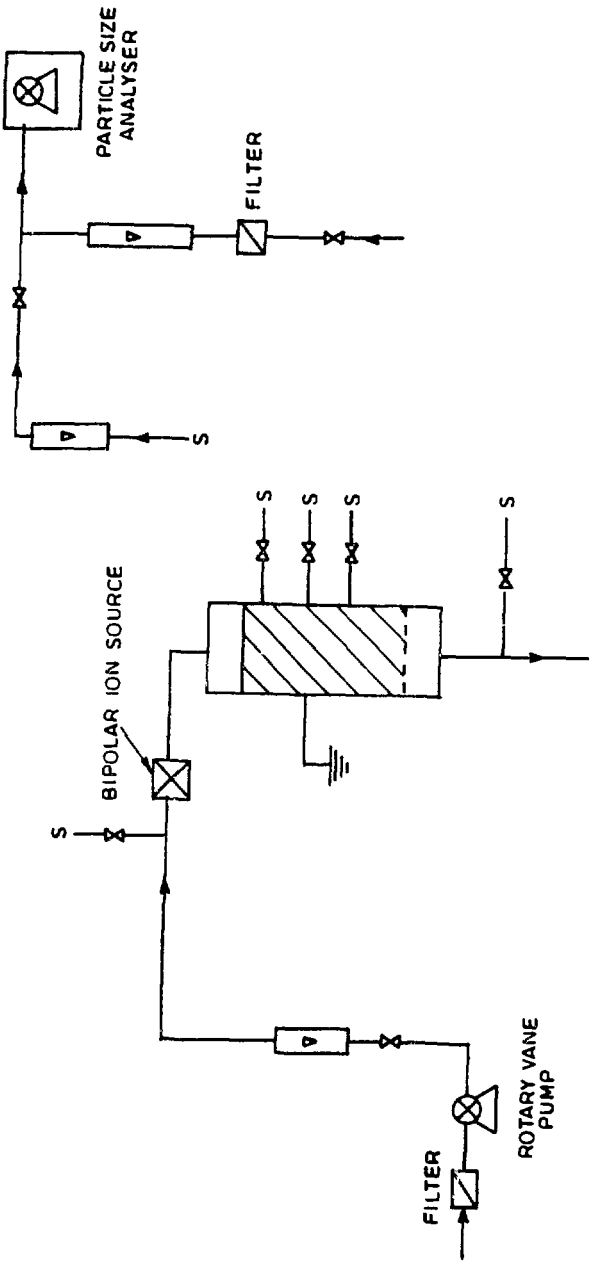

Fig. 1 Experimental equipment

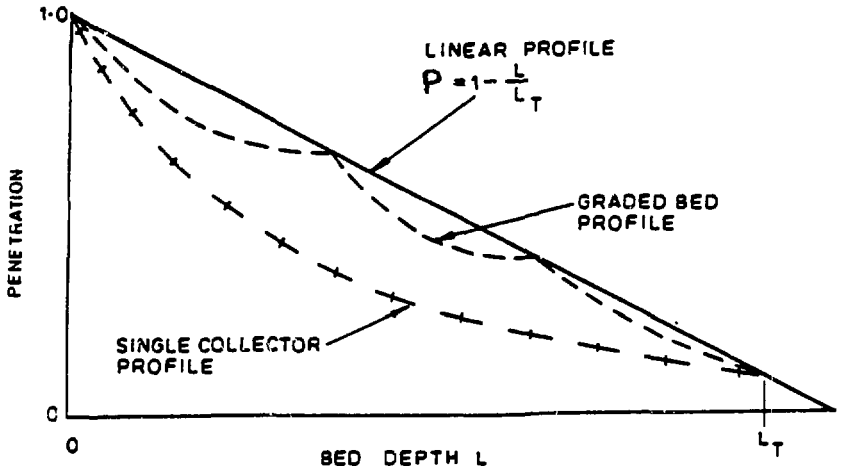

Fig. 2 Penetration profiles in a packed bed collector

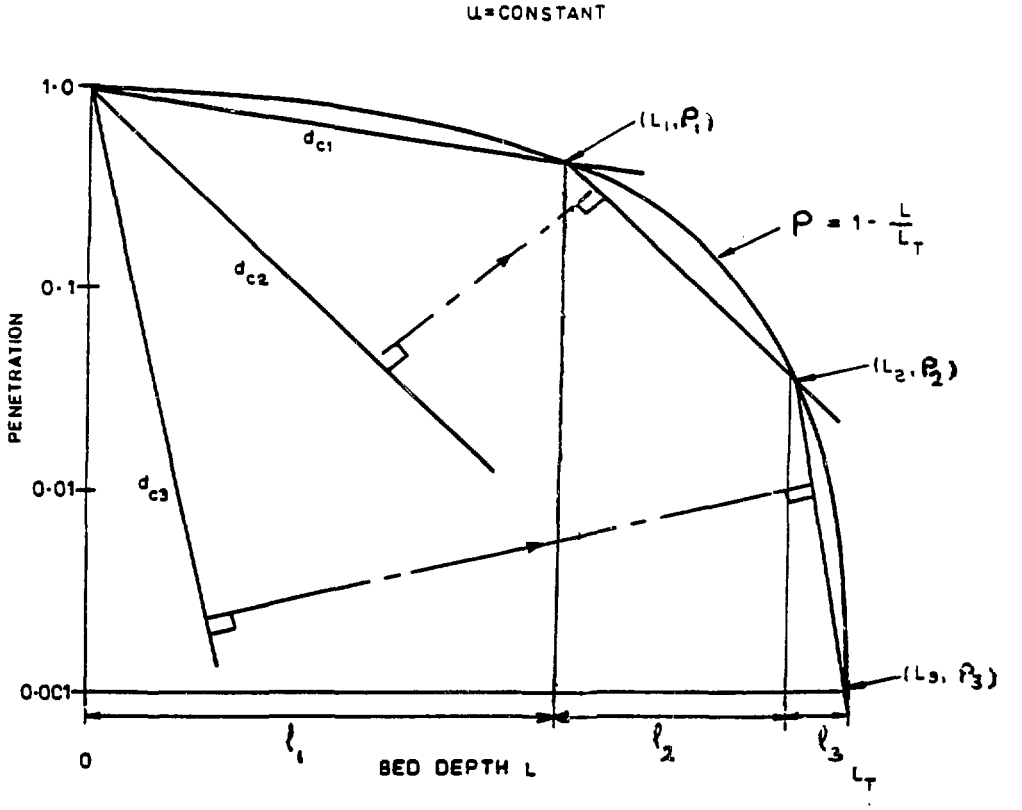

Fig. 3 Graded bed design procedure

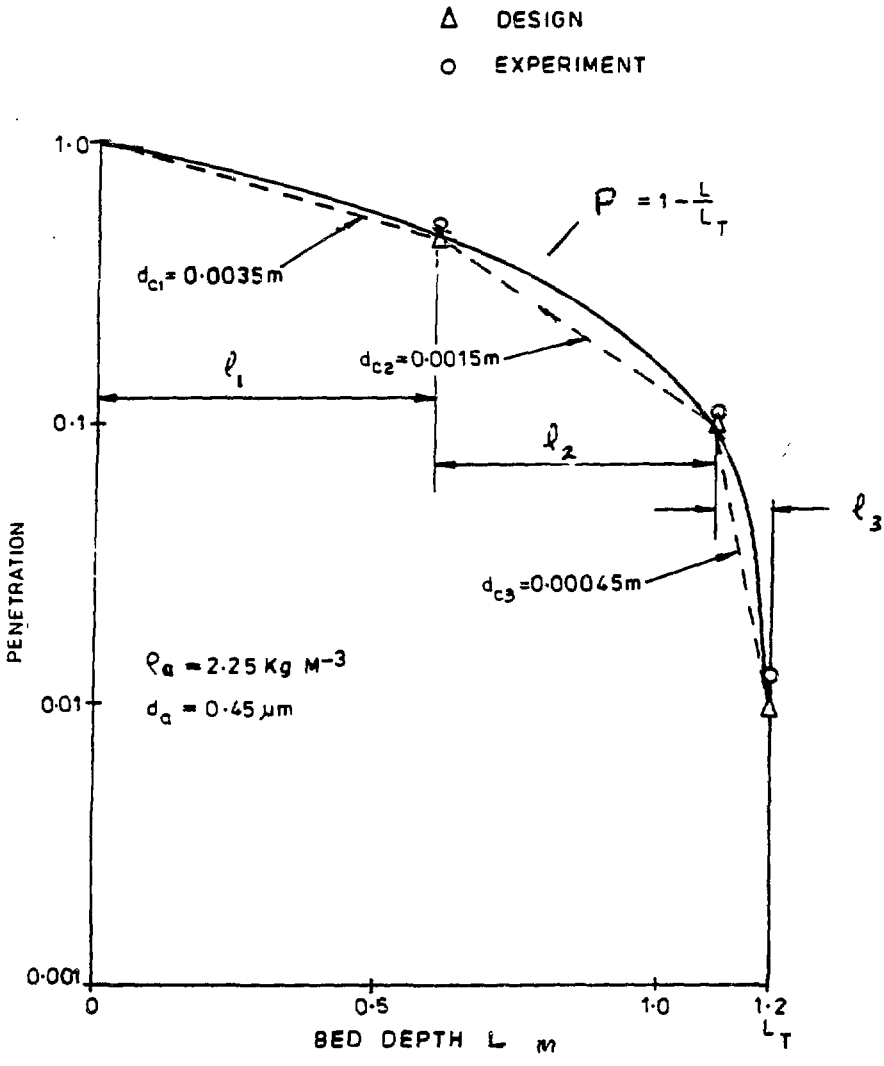

Fig. 4 Graded bed design and performance for $u = 0.01$ ms^{-1}, 18°C

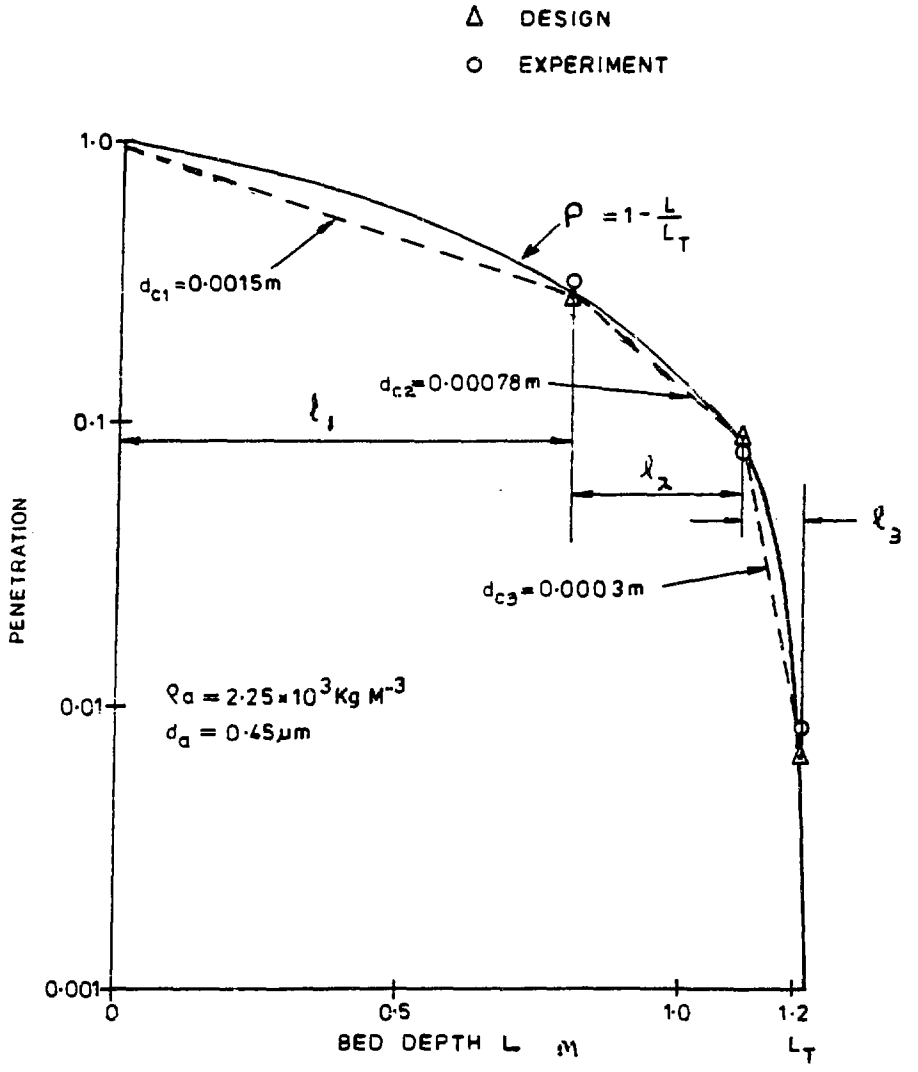

Fig. 5 Graded bed design and performance for u = 0.035 ms^{-1}, 18°C

DISCUSSION

DORMAN: It is gratifying to see one's name in the references when it is favorable. In your paper, it is perhaps a left-handed compliment. I plead that adding bed penetration coefficients is at least some sort of approximation and, although I believe that some modifications may be necessary at high efficiencies, I don't know how important they would be. In self defense, I don't think anyone else knows.

A DISPERSION MODEL FOR AIRBORNE PARTICULATES INSIDE A BUILDING*

Dup

William C. Perkins and Dean H. Stoddard
Savannah River Laboratory
E. I. du Pont de Nemours & Co.
Aiken, South Carolina 29808-0001

Abstract

An empirical model has been developed for the spread of airborne radioactive particles after they are released inside a building. The model has been useful in performing safety analyses of actinide materials facilities at the Savannah River Plant (SRP), operated for the U.S. Department of Energy by the Du Pont Company. These facilities employ the multiple-air-zone concept; that is, ventilation air flows from rooms or areas of least radioactive material hazard, through zones of increasing hazard, to a treatment system.

A composite of the data for dispersion of airborne activity during 12 actual case incidents at SRP forms the basis for this model. These incidents occurred during approximately 90 plant-years of experience at SRP with the chemical and metallurgical processing of purified neptunium and plutonium after their recovery from irradiated uranium.

The model gives ratios of the airborne activity concentrations in rooms and corridors near the site of the release. All data are normalized to the data from the air sampler nearest the release point. The model can be applied in predicting airborne activity concentrations from particulate releases elsewhere, if the facility in question has similar features of floor plan, air velocity, and air flow direction.

The multiple-air-zone concept has been applied to many designs of nuclear facilities as a safety feature to limit the spread of airborne activity from a release. The model illustrates the limitations of this concept: it predicts an apparently anomalous behavior of airborne particulates; namely, a small migration against the flow of the ventilation air. The following phenomena are suggested as possible mechanisms for this migration:

- eddy currents in the air flow
- leaks of ventilation air between zones
- open doors
- movement of personnel during an incident
- inadequate flow of ventilation air
- thermal gradients

---

* The information contained in this article was developed during the course of work under Contract DE-AC09-76SR00001 with the U.S. Department of Energy.

I. Introduction

This report documents the results of an effort at the Savannah River Laboratory (SRL) to construct a model to predict, in accident situations, the potential range and magnitude of the spread of airborne activity inside a processing building. The model is restricted to glovebox and cabinet facilities in which actinides, including plutonium and neptunium, are handled. In some Savannah River Plant (SRP) facilities, purified plutonium and neptunium are converted to final form, such as compacted oxides. In others, scrap materials are prepared for recovery. In all cases, the multiple-air-zone concept* was used in the design of the ventilation system.

The decision was made early not to attempt a theoretical calculation of the model from first principles. The difficulty in accounting for the many perturbing influences was deemed too large. Rather, an empirical model was planned, to be based on experience at SRP.[1,2] These decisions prompted an extensive research of SRP history that identified a limited, but sufficient, number of case incidents to supply data for a model. The details of each case were obtained from a variety of informal sources, such as personal recollections, air sampler logsheets, and heating/ventilation blueprints. None of these incidents resulted in injury or significant radiation dose to any personnel or in a release to the environment. Since these case incidents occurred in actinide materials handling facilities, the resulting model applies only to airborne particulate actinides, as opposed to gases and fission products.

II. The Dispersion Model

Only data from incidents in actinide materials facilities at SRP operating under the multiple-air-zone concept are used in the model. The data are taken from reliable measurements of airborne activity concentrations recorded soon after these incidents. However, the model should be regarded as an order-of-magnitude method for estimating the consequences of an accidental release of particulate activity, since its precision has not been evaluated.

Discussion

In each of the incidents used to develop the model, the airborne particles tended to migrate upstream against the prevailing flow of ventilation air. It is this apparently anomalous behavior that makes theoretical calculation of this phenomenon difficult and potentially ineffective. Consequently, an empirical model based on actual incidents was considered the more practical approach. The following are suggested mechanisms for the observed upstream migration:

---

* In the multiple-air-zone concept, ventilation air flows from clean areas through areas of increasing potential for radioactive contamination.

- eddy currents
- leaks of ventilation air through barriers
- movement of personnel during the incident
- low ventilation air flow
- temperature gradients

Some of the incidents used in the model illustrate situations where one or more of these mechanisms have been identified as a principal factor in a given release.

The model does not depend on the mechanism of a release or on the energy involved in causing the release. Although the input incidents involve only low-energy events, the model may be applicable to some high-energy events* if the following assumptions are acceptable.

- Since the lifetime of a shock wave from a high-energy event is much shorter than the sampling time for airborne activity, the temporary effect of the shock wave is not considered.

- Missiles tend to travel in a straight line, and their effect on migration of the lighter airborne particulates from the room is negligible.

- The spread of airborne activity beyond the immediate area (to other rooms or corridors) is independent of the amount of force causing the initial release. On this basis, as long as the room and cabinet ventilation systems are not damaged, the migration from the room soon after the release is the same for a low-energy release and a high-energy release.

The model is a set of ratios that describe, in terms of range and magnitude, the spread of airborne activity, given that a release occurs. Each ratio represents the maximum activity that reaches a given point with time, since only the highest concentration measured at any point is used in the model.

Features

The specific features of this model are presented in Table 1 and are shown superimposed on a typical floor plan in Figure 1. Each airborne activity value is normalized to the value from the air sampler nearest to the release point, usually in the Operating Room. Normalized values from SRP incidents are averaged to provide the model values. Table 1 also shows the specific source incident and position from which each input value was taken. The design basis for the SRP facilities, on which this model is based, is shown in Table 2 along with the operating ranges for the case incidents.

---

* A high-energy event is defined as one with sufficient energy to potentially destroy both the primary containment (vessel) and the secondary containment (cabinet). A leak is an example of a low-energy event.

Table 1. Dispersion values.

Position Description	Relative Activity*	Source of Activity Value: Incident Number	Figure Number	Position Number	Model Value**
1. Operating Room (OR)	100	-	-	1	100
2. Maintenance Room (MR)	800	3	4	2	
	415	5	5	2	
	250	7	7	2	490
3. Outside Single OR Entry Door:					
A. Low Air Flow	1.4	1	2	4	
	0.58	1	2	5	
	0.7	4	-	-	
	2.7	9	9	2	1.4
B. High Air Flow	0.005	2	3	2	
	0.005	2	3	3	
	0.01	3	4	4	
	0.004	5	5	4	
	0.022	10	10	2	
	0.048	11	11	2	
	0.1	12	12	4	0.028
4. Outside Airlock	<0.005	2	3	†	
	<0.01	3	4	†	
	0.015	4	-	-	
	<0.004	5	5	†	
	0	11	11	3	
	0.02	12	12	5	
	0	12	12	6	0.008
5. Regulated Corridor					
A. from 3A	0.28	1	2	6	
	0.38	6	6	††	0.33
B. from 3B	0.008	6	6	††	
	0.016	9	9	3	0.012
6. Nearby Room					
A. from 3A	0.12	1	2	7	
	0.007	6	6	††	
	0.27	8	8	¶	
	0.17	8	8	¶	0.14
B. from 3B	0.00015	6	6	††	
	0.006	8	8	¶	
	0.004	8	8	¶	
	0.006	9	9	4	0.0040

* Normalized to: Position 1 = 100

** Average of Relative Activity Values

† Inferred Value; not shown on the figure

†† Calculated from:
(Figure 6, Position 2 or 3) x (Model Value, Position 3A or 3B)

¶ Calculated from:
(Figure 8, Position 2 or 3) x (Model Value, Position 3A or 3B)

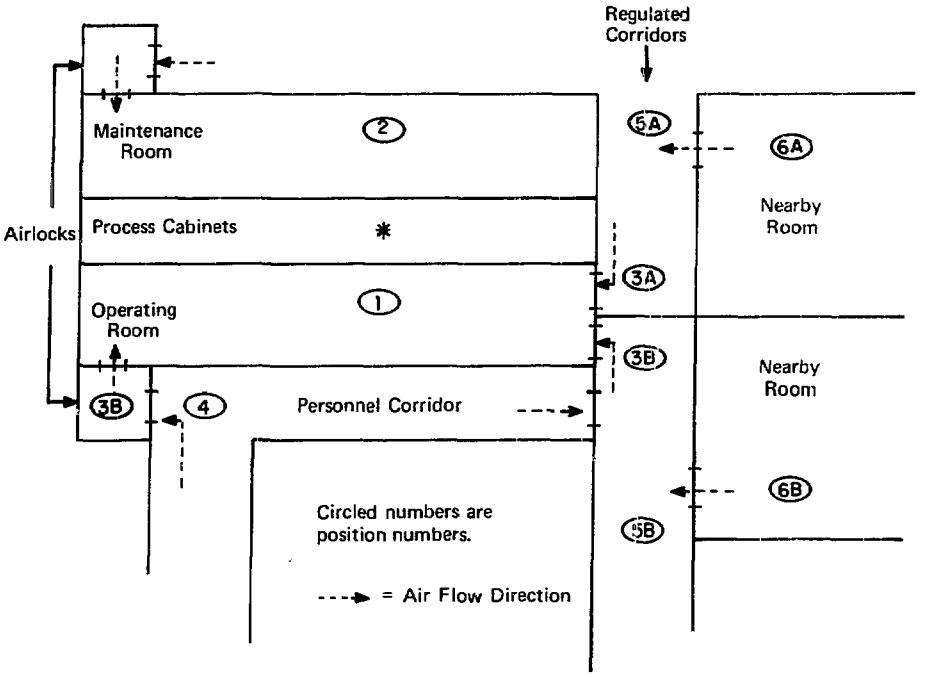

Position Number	Relative Airborne Activity
1	100
2	490
3A	1.4
3B	0.028
4	0.008
5A	0.33
5B	0.012
6A	0.14
6B	0.0040

FIGURE 1. Dispersion Model

The data indicate that undirected releases from these SRP facilities distribute unequally between the Maintenance Room (MR) and the Operating Room (OR). The ratio is almost 5 to 1. This rather high ratio indicates that, due to the design of SRP cabinets, non-directional events would be vented more to the MR (Position 2) than to the more-frequently-occupied OR (Position 1).

The entry to the OR is an important barrier to the spread of airborne activity. The model gives two different options for Position 3, depending on the efficiency of this barrier. Position 3A represents a relatively inefficient barrier, such as a single door with a low pressure differential, louvers in the door, and/or openings around the door. Position 3B represents an efficient single door or an airlock, i.e. two doors with an air supply between them. Therefore, Figure 1 shows three entries to the OR: an airlock (3B), an efficient single door (3B), and an inefficient single door (3A).

The concentration of airborne activity migrating down corridors to nearby rooms is dependent on the value at Position 3. Consequently, two values are given for Positions 5 and 6, using data from appropriate incidents (hallway migrations) and either Position 3A or 3B. (See Figure 1 and the footnotes to Table 1.)

In contrast to the data in Table 1 which involves both physical barriers and distance, Table 3 gives the effect of distance only. These values are normalized and averaged values from incidents (1, 6, 8) where several measurements were made in a room.

III. Accident Analysis

The quantity of radioactive material involved in an accidental release is not predicted by the model. Such data must come from other analyses. If the airborne activity at the monitor nearest the release (C_1) is known, the airborne activity concentration outside the operating room (C_{3B}) is:

$$C_{3B} = \frac{0.028}{100} C_1$$

The concentration at another position may be calculated from C_1 and the appropriate ratio from the model.

IV. Basis for the Model

The model is based on the data available from incidents at SRP that meet the following criteria:

- An event releasing significant airborne activity in particulate form from a containment structure, such as a glovebox. (Note that small releases become indistinguishable from background at short distances from the release point.)
- A multiple-air-zone concept for ventilation of the area.
- Adequate instrumentation for data collection.

Table 2. Pressure differentials for ventilation air.

	ΔP (in H_2O) Between		
	OR and Corridor	Cabinet and OR	MR and OR
Case Incidents:	0.01 - 0.1	0.7 - 1.0	0.01 - 0.1
Design Basis:	*	0.8	*

* Designed to maintain ventilation air flow toward areas of increasing potential contamination on a once-through basis. The ranges necessary to meet these bases at all points are taken from the Case Incidents.

OR - Operating Room

MR - Maintenance Room

Table 3. Effect of distance on the concentration of airborne activity.

Distance from Release, ft	Source of Value: Figure Number	Incident Number	Position Number	Value	Model Value*
0	-	-	-	-	100
12	12	12	2	38	40
15	2	1	2	7	
	6	6	2	27	20
21	2	1	3	3.3	
	6	6	3	0.5	
	12	12	3	5.0	3

* Average value; one significant figure.

Description of Air Samplers

Input data for the model was obtained mainly from air samplers that measure room air activity by collecting samples of particulates in the air. These samples are considered representative of air present in the room and are converted to an average concentration for the time period of the sample.

Samples are collected by filtration or by impaction. The filtration method draws air at 6 cfm through a fiberglass filter paper. The impaction method draws air through an orifice and impacts it on a planchet at 40 cfm. With the sample rate and collection efficiency known, the collected sample is counted to determine the concentration of activity present. Some filtration and impactor samples are counted while being collected; these counters are connected to a high-activity alarm system. These devices are called constant air monitors (CAM).

Case Incidents

The twelve incidents used to form this model are listed in Table 4 and are discussed individually below. In most cases, the vicinity of the release was either unoccupied or occupied by workers already wearing protective clothing and masks. Evacuation of the work area and the surrounding areas prevented exposure of other personnel. In no case was there a significant release of radioactive material to the environment.

Glovebox Fire. An overheated piece of equipment started a fire in a glovebox containing dry PuO_2 and PuF_4 powders. A plastic bag melted on a bagport near the fire, releasing airborne Pu activity to the room. Of the three entries to this room, the one nearest the fire was apparently sealed so that no air or activity moved past it, the one directly across the room was louvered for air passage but air flow through it was practically nonexistent at the time, and the door most remote from the fire was solid (non-louvered) with a small space underneath.

A simplified drawing, showing air flow directions and the relative airborne activity concentrations taken from air sampler and constant air monitor (CAM) data, is given in Figure 2. Air is supplied directly to each room from ducts shown in Figure 2. Air exhausts from the room through the glovebox, a chemical hood, and a wall-mounted exhaust fan. The pressure differential between the room and the glovebox is normally about 0.05 in. H_2O.

Cabinet Fire. A fire started from an overheated piece of equipment in a glove cabinet containing dry wastes contaminated with plutonium. A cabinet glove burned, releasing airborne Pu activity to Operating Room 1. Entry to this room is by a door from Operating Room 2 (OR2) and by an airlock to a personnel corridor. Constant Air Monitor (CAM) data, verified by impactor sampler data 500 ft^3 of air), showed no detectable airborne activity in OR2, in the airlock, or in an adjacent control room. (Pressure differentials for ventilation air at these doorways are maintained between

Table 4. Incidents used in the model.

Incident Number	Figure Number	Incident Description
1	2	Overheated equipment started fire in glovebox containing Pu, bagport breached.
2	3	Overheated equipment in cabinet started fire, glove breached.
3	4	Exhaust damper malfunctioned, cabinets pressurized.
4	-	Routine maintenance work, containment opened.
5	5	Cabinets pressurized during filter change.
6	6	Pressurized package of Pu scrap opened in a temporary hut.
7	7	Uncontrolled reaction in a scrap dissolver.
8	8	Release to regulated corridor from pressurized PuO_2 container in storage room.
9	9	Undetected leak to cabinet sump under Pu scrap dissolver.
10	10	Air reversal in Np process area.
11	11	Pu cabinet glove failure.
12	12	Release from cabinet during removal of a container.

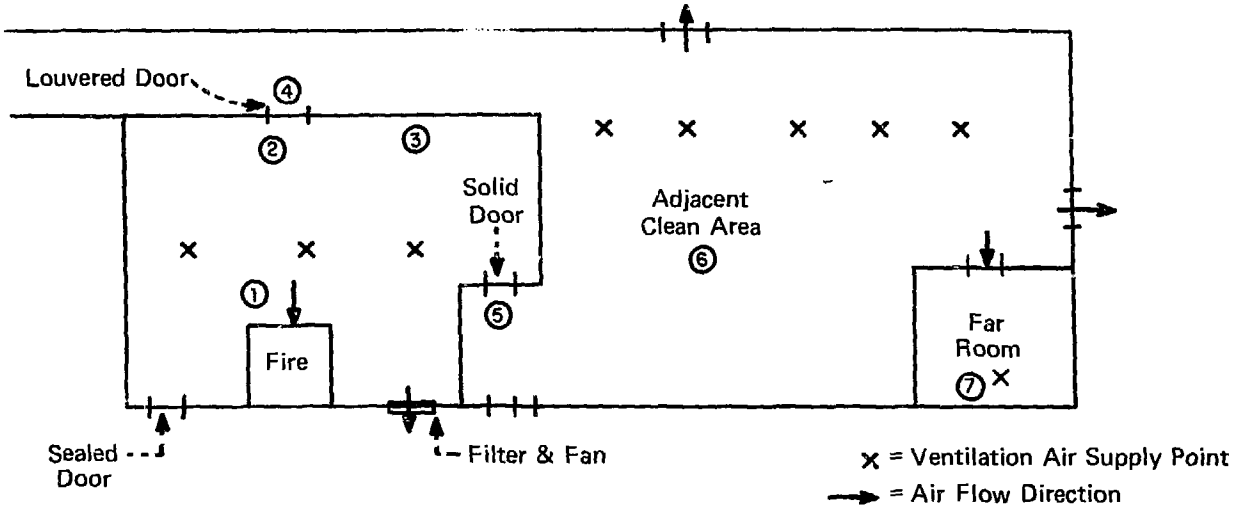

Position	Relative Airborne Activity	Description of Position and Approximate Distances	Air Flow Direction
1	100	Above glovebox	-
2	6.7	Across room from fire, 15 feet from 1	Toward fire
3	3.3	Far end of room, 15 feet from 2	Toward fire
4	1.4	Outside louvered door, 20 feet from 1	Negligible Flow
5	0.58	Outside solid door, door is 40 feet from 1	Unknown
6	0.28	Adjacent clean room, 75 feet from 4 and 30 feet from 5	Toward Fire
7	0.12	Far room, 20 feet from entry door; Door is ~45 feet from 6	From adjacent clean room

FIGURE 2. Glovebox Fire (Incident 1)

0.01 and 0.10 inches of H_2O.) Pressures inside cabinets are maintained between 0.7 and 1.0 inches of H_2O below the operating rooms. Maintenance rooms (MR) behind the cabinets are maintained at 0.01 to 0.10 inches of H_2O below the operating rooms.

A schematic drawing of this incident is shown in Figure 3. Air locks in this area are about 8 ft x 8 ft x 8 ft with ventilation air supplied from the ceiling. Doors are solid (not louvered) with narrow spaces beneath. Air flows into an air lock from the personnel corridor and then from the air lock into the operating room. Air is also supplied to operating rooms through ceiling diffusers and exits the rooms through wall-mounted grilles near the floor. A relatively small amount of room air also exits through the cabinets. OR1 is about 40 ft long and 10 ft wide.

Damper Malfunction. Glove cabinets were pressurized briefly when a mechanical malfunction occurred in a cabinet exhaust damper. Airborne activity measurements showed that the activity on the maintenance side (MR) of the line was 8.0 times that on the operating side (OR). No activity was detected in the OR or MR airlocks.* This incident is shown in Figure 4, and occurred in the same facility as Incident Number 2. Cabinet air pressure in this line is normally maintained between 0.7 and 1.0 inches of H_2O below the Operating Room air. The pressure differential between the Operating Room and the Maintenance Room is maintained between 0.01 and 0.10 inches of H_2O; the Maintenance Room is at a lower pressure so that any leakage of ventilation air goes from the Operating Room to the Maintenance Room.

Routine Maintenance. This case is composed of data from three typical maintenance jobs where containment was broken for the work, and small airborne releases were recorded in the Maintenance Room. The average airborne activity concentration in the MR airlock was 0.7% of the activity in the MR. The average outside the MR airlock entry was <0.015% of the activity in the MR. The movement of workers through the airlock may explain these relatively-high, average-concentration ratios.

These jobs were performed on the same facility described in Incidents 2 and 3, Figures 3 and 4.

Filter Change Error. Cabinet ventilation was accidentally lost for about two minutes during routine filter change operations in the cabinet exhaust treatment system. During this time the pressure inside the cabinets was higher than the pressures in the operating and maintenance room; the ventilation and room exhaust

* The OR1 airlock value is calculated by:

$$\frac{100}{800} \times (<0.1) = <.01$$

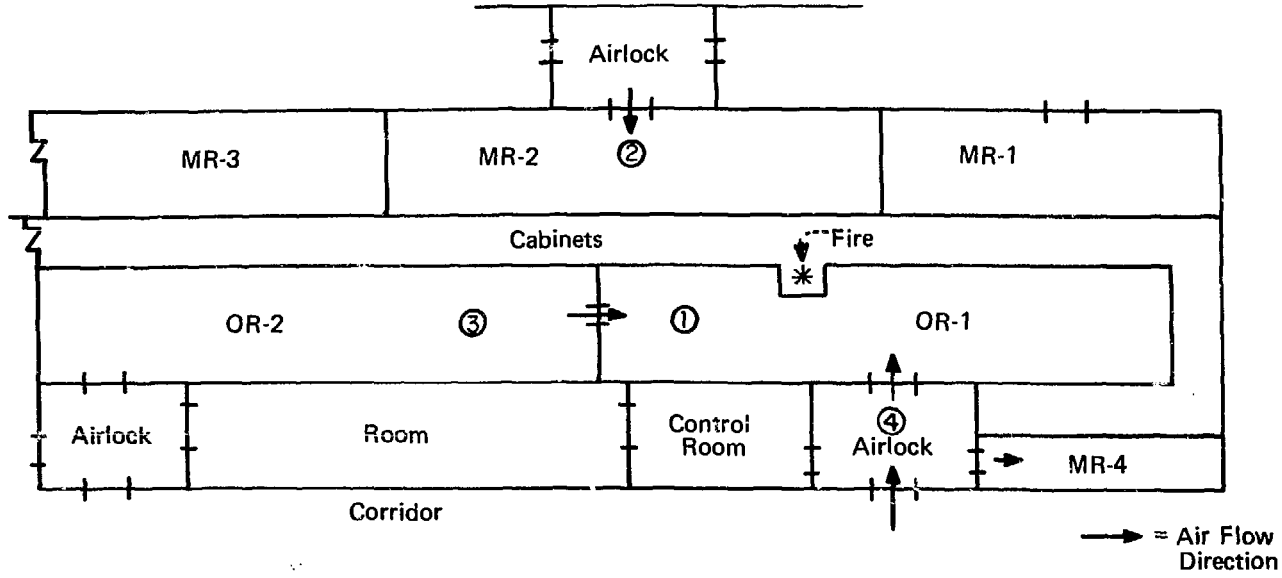

Position	Relative Airborne Activity	Description of Position and Approximate Distances
1	100	In Operating Room 1 (OR1), 10 feet from fire
2	-	Maintenance Room
3	<0.005	Adjacent Room OR2, 20 feet from 1
4	<0.005	Airlock of OR1, 12 feet from fire

FIGURE 3. Cabinet Fire (Incident 2)

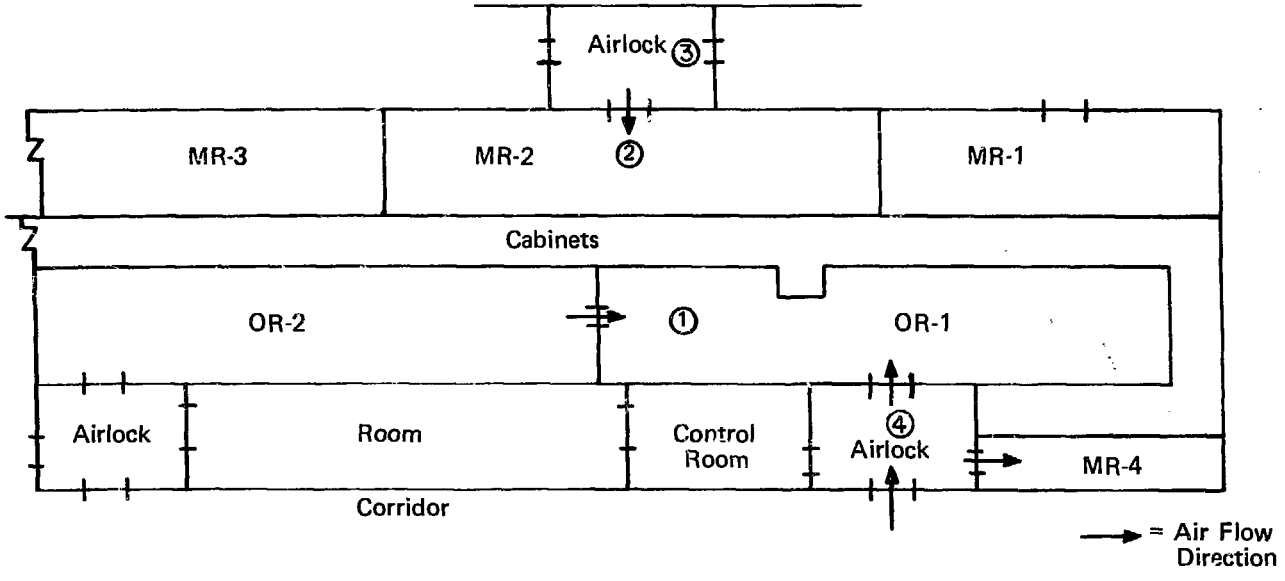

Position	Relative Airborne Activity	Description of Position and Approximate Distances
1	100	In Operating Room 1(OR1), 7 feet from cabinets
2	800	Maintenance Room 2 (MR2), 3 feet from cabinets
3	<0.1	MR2 Airlock, 12 feet from cabinets
4	<0.01	OR1 Airlock, 12 feet from cabinets

FIGURE 4. Damper Malfunction (Incident 3)

systems were not affected by the maloperation of the cabinet exhaust system. The cabinets are designed to allow some inleakage from the operating and maintenance rooms into the cabinets. Loss of the cabinet ventilation caused an air reversal at these inleakage points, releasing particulate contamination to both sides of the cabinet. The airborne activity concentration in the MR was 4.15 times that in the OR (see Figure 5). Airborne activity was not detected in the MR airlock; the concentration there was <0.017 times the OR concentration. See Incident 2 for ventilation details.

Pressurized Containment Hut. A temporary containment hut was constructed in a regulated corridor near a scrap processing facility. Air flow into this hut was 140 linear ft/min (1250 cfm) from ventilators in the corridor ceiling. The hut was being used to open shipping packages containing plutonium oxide scrap from offsite, and the packages were not expected to be pressurized. However, when one of the packages was opened, the contents (several welded cans) were suddenly expelled from the container along with a puff of aerosol (smoke). The operator felt a surge of pressure against his protective suit. Some of the airborne alpha activity detected outside the hut may have escaped through a 6-in. flap in the wall of the hut. A schematic drawing of this incident is shown in Figure 6. Dimensions of the corridor are about 5 ft wide and 25 ft long. To extract adequate data from this incident, it was necessary to use some values from portable air samplers.

Unexpected Reaction in a Scrap Dissolver. An unusual reaction occurred in a small scrap dissolver, probably because the scrap contained traces of plutonium hydride. Although no process material was observed outside the dissolver (on the cabinet floor), air samples were taken in the maintenance and operating rooms. The airborne activity concentration in the maintenance room was 2.5 times that in the operating room. The pressure inside this cabinet is maintained about 0.9 inches of H_2O below the operating room and about 0.8 inches of H_2O below the maintenance room. Pressure in the maintenance room is about 0.1 inches of H_2O below the pressure in the operating room. No airborne activity was detected in any of the airlocks (see Figure 7).

Release to Corridor. While operators in a storage room were trying to loosen a stuck cap on a $^{238}PuO_2$ container, an airborne activity release occurred. Airborne activity was detected in the regulated personnel corridor and some other process rooms, as shown in Figure 8. Some other rooms may have been contaminated, but data are not available. Typically, air flows at about 50 cfm, from this regulated corridor into the process rooms where measurements were made. This corridor is about 6 ft wide. Air is supplied to each room in this area, but not to the regulated corridor. Air exhausts from each process room through a room exhaust system.

Leak to Cabinet Sump. Corrosion caused a leak in a vessel located in a ^{238}Pu scrap recovery facility consisting of several gloved cabinets. This leak dripped into a cabinet sump under the leaking vessel. The liquid-detector in the sump failed to alarm. Airborne alpha activity spread from the cabinet to the operating

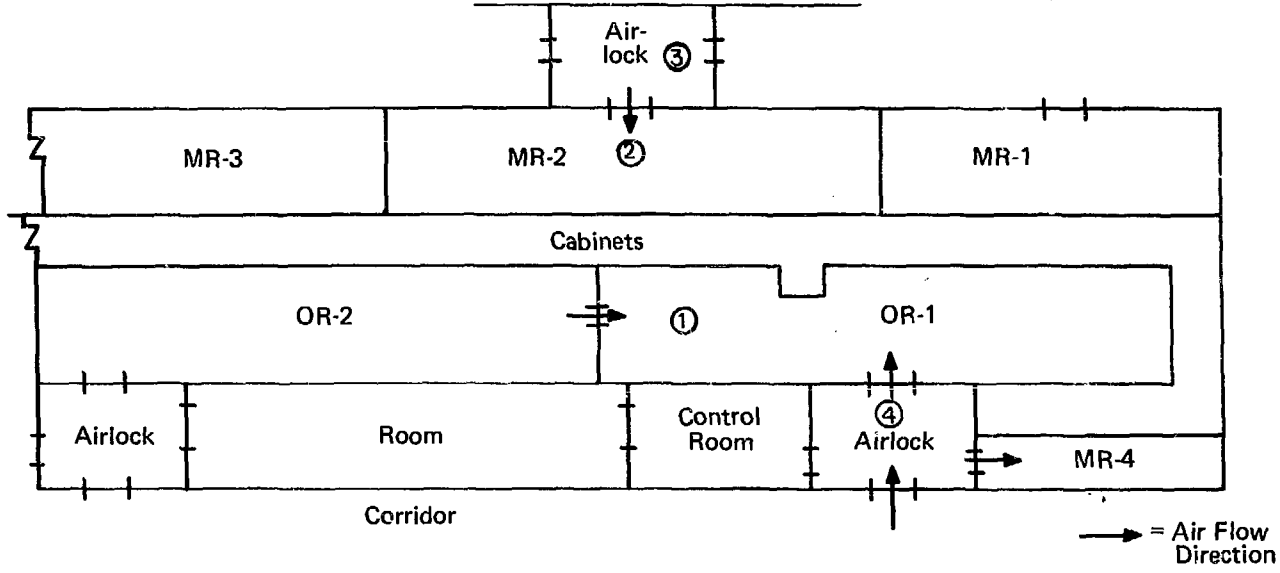

Position	Relative Airborne Activity	Description of Position and Approximate Distances
1	100	In Operating Room 1(OR1), 7 feet from cabinets
2	415	Maintenance Room 2 (MR2), 3 feet from cabinets
3	<0.017	MR2 Airlock, 12 feet from cabinets
4	<0.004	OR1 Airlock, 12 feet from cabinets

FIGURE 5. Filter Change Error (Incident 5)

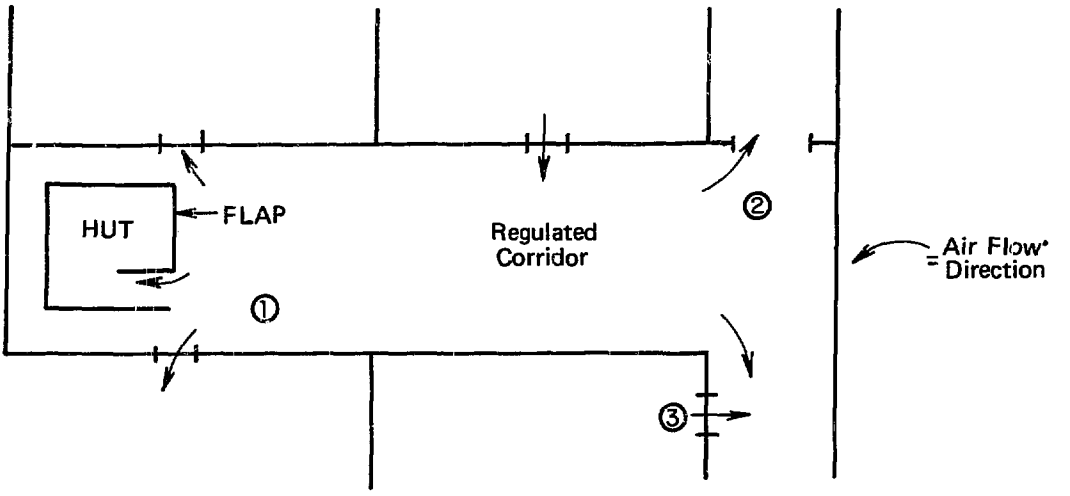

Position	Relative Airborne Activity	Description of Position and Approximate Distances
1	100	Corridor outside hut, 3 feet from hut entrance
2	27	Far end of corridor, 15 feet from hut entrance
3	0.5	Far room, 22 feet from Position 1

FIGURE 6. Pressurized Hut (Incident 6)

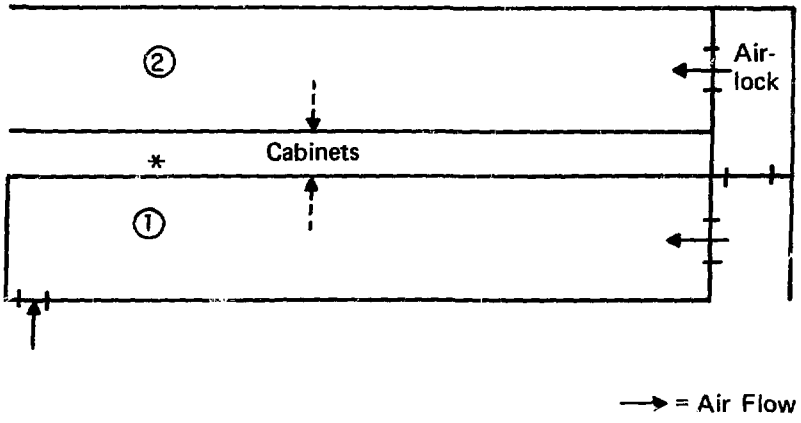

Position	Relative Airborne Activity	Description of Position
1	100	Operating Room
2	250	Maintenance Room

FIGURE 7. Unexpected Reaction in Scrap Dissolver (Incident 7)

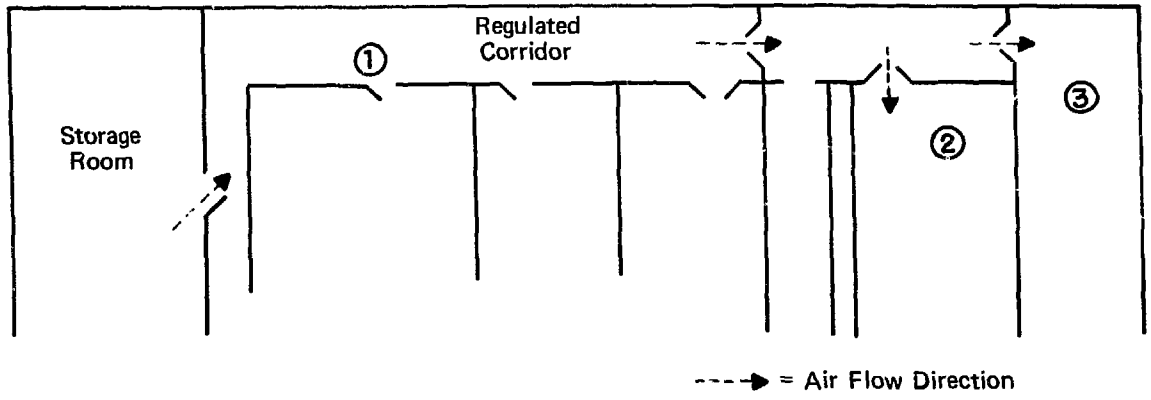

Position	Relative Airborne Activity	Description of Position and Approximate Distances*
1	100	Regulated corridor
2	19	Room down corridor; door is 28 feet from 1
3	12	Far room down corridor; door is 36 feet from 1

* Air samplers are about 10 feet from door in each room.

FIGURE 8. Release to Corridor (Incident 8)

room and to the regulated corridor outside the entry door, as shown in Figure 9. The release to the corridor was aided by low air flow from the regulated corridor into the operating room and by openings around the entry door. The widths of the operating room and the regulated corridor are each about 5 feet. Activity was undetectable in nearby rooms.

Building Air Reversal. Malfunction of the building air-supply fans caused an air reversal in a process area. Airborne activity was released from facilities in one room and migrated through the doorway into the regulated corridor as illustrated in Figure 10. This door is solid (non-louvered) with small tolerances on each side.

Glove Failure. Failure of a glove on the maintenance side of a process cabinet released airborne Pu activity to the maintenance room (MR). The activity migrated into the airlock adjoining the MR entry door. The airlock is about 5 ft wide. Other distances and air flow directions are shown on Figure 11. The entry to the MR from the airlock is a single, nonlouvered door. No activity was detected in a second airlock at the OR entry.

Release During Container Removal. As a product secondary container was moved from a cabinet to the entry hood, airborne Pu activity was released into the maintenance room (MR), apparently because of low air flow into the entry hood. This activity migrated to other regulated rooms and facilities in this building, as shown in Figure 12, partly because of a ventilation air inbalance in the building at the time. Subsequent helium leak tests revealed a migration path through some electrical conduits connecting some of the rooms. These paths were closed.

Ventilation air flows from the operating area (OR) to the maintenance area (MR) through racks at each end of the process line. The pressure differential is about 0.02 inches of H_2O. Air exhausts from the maintenance area through filters below each cabinet on the maintenance side. There are airlocks at each entry; each airlock has an air supply in the ceiling (see Figure 12).

V. Conclusions

It is concluded that the multiple-air-zone concept is an effective method of controlling released airborne particulate activity.

Since the model is based on average values from actual incidents, it may provide a method for assessing the efficiency of safety features in mitigating the consequences of incidents in other facilities. Should airborne activity migrate substantially more than predicted by the model, analysis should be made to determine why the multiple-air-zone concept, combined with physical barriers, fails to provide effective containment.

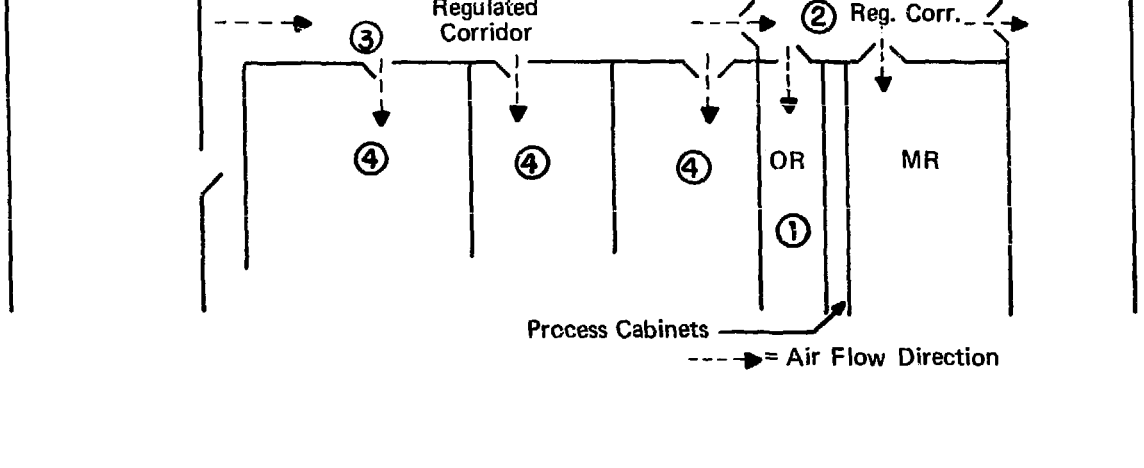

Position	Relative Airborne Activity	Description of Position and Approximate Distances
1	100	Operating Room (OR), 12 feet from entry door.
2	2.7	Regulated corridor; outside entry to OR, 3 feet from entry door
3	0.016	Regulated corridor, 22 feet from Position 2
4	<0.006	Nearby Rooms

FIGURE 9. Leak to Cabinet Sump (Incident 9)

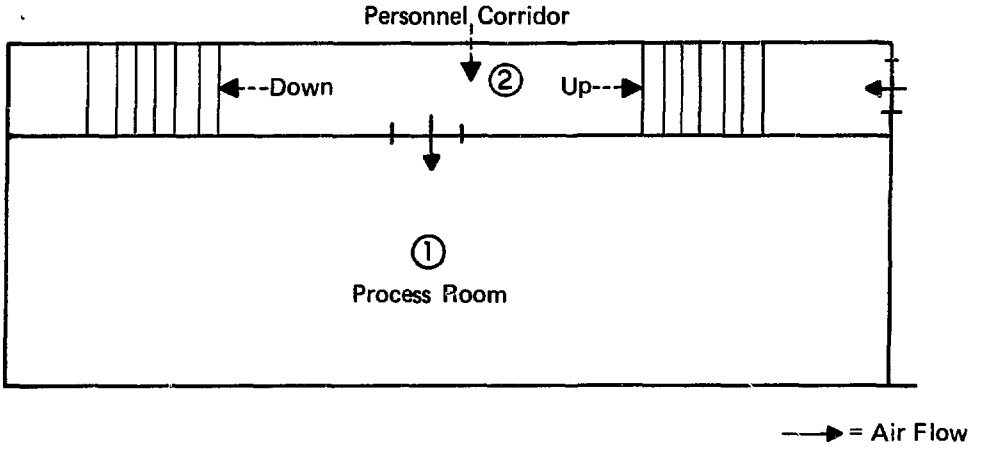

Position	Relative Airborne Activity	Description of Position
1	100	Process room
2	0.022	Regulated corridor

FIGURE 10. Building Air Reversal (Incident 10)

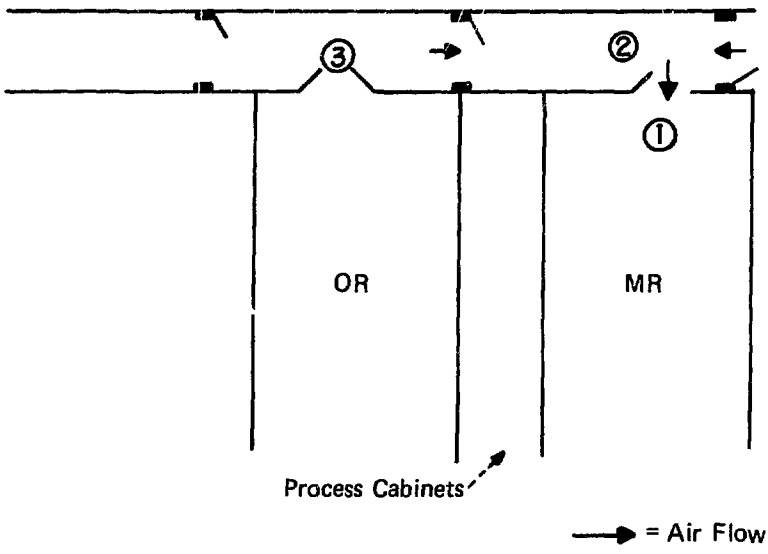

Position	Relative Airborne Activity	Description of Position and Distances
1	100	Maintenance Room, 5 feet from door
2	0.048	Regulated Airlock, 8 feet from 1
3	$<10^{-6}$	Adjacent Airlock, 20 feet from 2

FIGURE 11. Glove Failure (Incident 11)

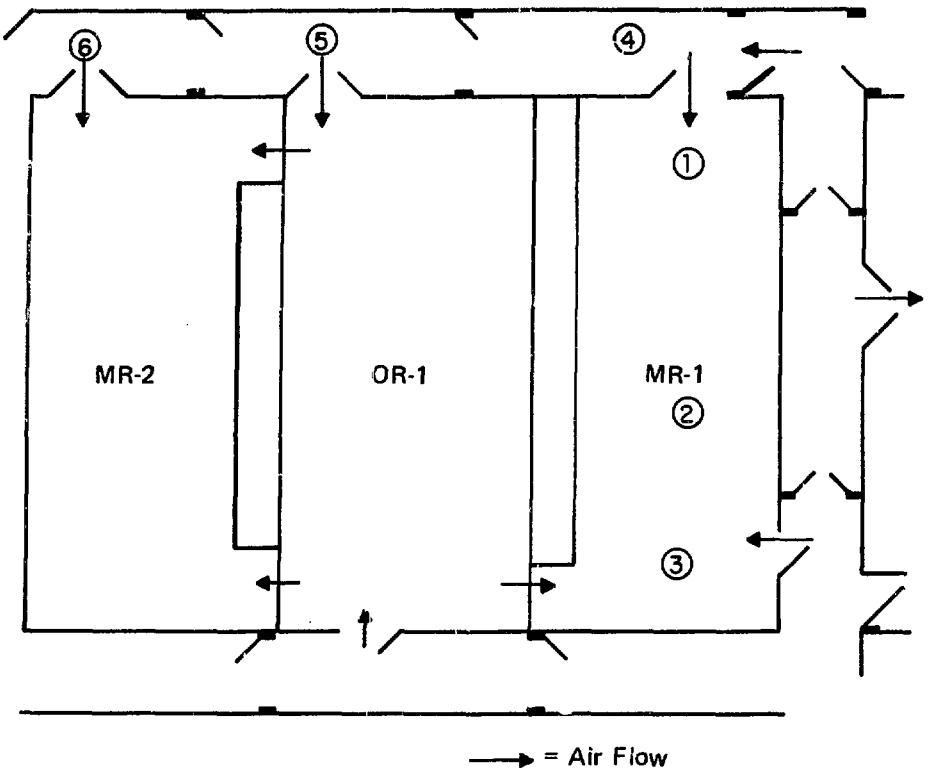

Position	Relative Airborne Activity	Description of Position and Distances
1	100	MR-1, over entry hood
2	38	MR-1 center, 12 feet from Position 1
3	5.0	MR-1 end, 21 feet from Position 1
4	0.1	MR-1 airlock, 8 feet from Position 1
5	0.02	OR-1 airlock, 12 feet from Position 4
6	$<10^{-6}$	Far airlock, 24 feet from Position 4

FIGURE 12. Release During Container Removal (Incident 12)

VI. Acknowledgment

The authors wish to acknowledge the advice and direction of W. S. Durant and W. V. Wright in the preparation of this model and also the assistance of personnel of the Separations Department, Health Protection Department, and Separations Technology Section of the Savannah River Plant in obtaining the necessary data.

VII. References

1. E. B. Sheldon, et al. Experience with Processing Irradiated Fuel at the Savannah River Plant (1954-1976). USERDA Report DP-1467, E. I. du Pont de Nemours and Co., Savannah River Laboratory, Aiken, SC (September 1977).

2. M. L. Hyder, et al. Processing of Irradiated Enriched Uranium Fuels at the Savannah River Plant. USDOE Report DP-1500, E. I. du Pont de Nemours and Co., Savannah River Laboratory, Aiken, SC (April 1979).

DISCUSSION

ETTINGER: What was the range of dilution ratios for the various release situations which provided the basis for the empirically determined values? What is the error bar for the ratios? You quoted one as 12,000 to 1. What range did you find in those 15 or so incidences which were the basis for the empirical numbers?

PERKINS: There is a Table in the paper that shows the actual numbers I averaged. The answer to the question is probably about a factor of 2. Originally, the model was intended to give us the answer within a factor of 10 for use in making a safety analysis on a conservative basis. We were quite pleased, in instances that have occurred since, that we appear to be much better than that, roughly a factor of 2. That is a nice result when you are expecting something that is to the nearest order of magnitude. If you want to do the error bars mathematically, the base numbers that were averaged were given in one of the Tables in the paper.

ORNBERG: What airflow rates did you have through the non-air-locked personnel doors when they were opened? Do you have figures for that?

PERKINS: There are some figures given in a Table in the paper. They may not be entirely satisfactory, as what they give is our average design rate. Ventilation is checked at the doorways to see if airflow is in the right direction, and that the doorways and barriers have the correct pressure drops. I do not have actual airflow measurements at those doorways, so I can't give you a complete answer. The pressure drops and the design values are given in the small Table in the paper and you may refer to that. Also in the paper, there are distances and sizes of the rooms, and distances between the doorways and the corridors, which may be of help.

DYMENT: Is it possible to use the model to predict the effects of air change rate on operator exposure, i.e., would a high or low air change rate benefit safety?

PERKINS: Certainly, it is agreed that a high air change rate usually improves safety. However, I do not see how this model can be used on this subject.

DORMAN: The Chairman said that in work with airlocks it had been found that particles migrated against the prevailing air flow. The back flow depends considerably on room and door design and the mechanisms put forward by Dr. Perkins. He agreed with the author that theoretical calculations were difficult and potentially ineffective

CLOSING REMARKS OF SESSION CHAIRMAN DORMAN:

In our first paper, Mr. Kirchner from Rockwell described a computer controlled in-situ monitoring system for in-place testing and filter efficiency. Claims of increased accuracy, lower costs, and reduced personnel exposures more than off-set the increase in equipment costs. John Ortiz, from Los Alamos, related to us his work on using a laser particle size spectrometer to measure decontamination factors as high as 10^9. This technique allows cost-effective facility testing of multiple-stage systems without interruption of production. Mr. Norman gave us the new regulations for filter testing in Sweden and presented data on both HEPA and charcoal units currently used. Bergman from Livermore commented on the interrelationships of the DOP generators and the various techniques of size and size distribution. He demonstrated that since the Laser and OWL give different average sizes and size distributions, the photometer responses might be expected to be different also. He indicated that the OWL-penetrometer relationship might be best for penetration measurements since they relate to the same physical responses. Although no new techniques or procedures were given in the papers presented, increased understanding and utilization of existing testing methods resulted.

Session 6

RECOVERY AND RETENTION OF AIRBORNE WASTES: PROTOTYPE AND OPERATIONAL SYSTEMS

TUESDAY: August 14, 1984
CHAIRMEN: A.G. Croff
W.S. Groenier
Oak Ridge National Laboratory

OPENING REMARKS OF SESSION CHAIRMAN CROFF:

Welcome to Session 6 of the 18th Airborne Waste Management and Air Cleaning Conference. The purpose of this session is to discuss the practical aspects of cleaning radioactive and chemical species from air streams in reprocessing plants. In particular, the seven papers to be presented involve the results of either operating engineering-scale equipment during development activities or, in the case of one paper, experiences in an operating reprocessing plant. The emphasis of the papers is on the performance of processes for the removal of iodine, tritium, nitrogen oxides, carbon, and krypton, with integrated systems having been used in most of the studies. The practical aspects of particulate removal from air streams are covered in other sessions of this Conference.

SELECTED OPERATING RESULTS OF THE PASSAT PROTOTYPE DISSOLVER OFFGAS CLEANING SYSTEM

J. Amend (KTB), J. Furrer, R. Kaempffer (LAF II)
Nuclear Research Center Karlsruhe
Federal Republic of Germany

Abstract

To test the HEPA filters and iodine sorption filters developed for cleaning the dissolver offgases of a reprocessing plant investigations were performed with iodine and nitrogen dioxide containing offgases at the PASSAT prototype offgas cleaning system. Corrosion caused by iodine in combination with water vapor was found on the components of the offgas cleaning system made of the materials Nos. 1.4541 and 1.4571 and the adhesive used for the HEPA filters was found to resist inadequately nitrogen dioxide.

With a view to selecting suitable materials laboratory scale tests were performed under conditions relevant to the plant. Among a number of preselected materials the material No. 1.4563 was found to be the pipe material suited for exposure to iodine containing moist offgases. A material fabricated on the basis of silicone polymer with temperature stabilizing additives proved to be a suited adhesive for HEPA filters.

I. Introduction

When nuclear fuels are reprocessed according to the PUREX process the dissolver offgas contains the volatile radionuclide iodine-129 as well as radioactive aerosols which must be retained in the facility in order to protect the environment from harmful effects and to compile with the limits fixed by the Radiation Protection Commission /1/.

To test the retention techniques developed for this purpose /2/ the PASSAT prototype test facility was built at the Karlsruhe Nuclear Research Center which permits the performance of experiments with simulated nitrogen dioxide carrying dissolver offgas and iodine as well as aerosols fed simultaneously.

The facility has been operated since July 1978; ten test campaigns of 55 weeks duration in total have been performed till now.

The layout of the facility and the results of filter development and remote handling technique were reported in detail at the 16th and 17th DOE Nuclear Air Cleaning Conferences /3,4,5/.

During the last two years work has been concentrated rather on an inspection under aspects of process engineering of the whole facility and of the filter components with simulated offgas containing iodine and nitrogen dioxide. Heavy corrosion of the pipework material Nos. 1.4541 and 1.4571 was detected in the wet part of the test facility as well as a lack of resistance of the adhesives used in the HEPA filters.

In the following chapters the results will be reported which have been obtained from special investigations into corrosion caused by iodine and into the resistance to nitrogen dioxide of adhesives used in HEPA filters.

II. Corrosion Caused by Iodine in the PASSAT Prototype Dissolver Offgas Cleaning System

1. Corrosion Damage on the CrNi Steels

As a result of test operation performed in the PASSAT facility with iodine carrying offgas, the pipework made from titanium-stabilized, molybdenum-free material No. 1.4541 and the sensors made from titanium-stabilized, molybdenum containing material No. 1.4571 underwent substantial corrosive attack. The damage occurred exclusively in the non-heated part of the pipework which had become wet by condensation, at a temperature of 30 °C upstream of the fiber pack mist eliminator (Brink filter), and at the iodine feed line.

Figure 1 shows the block diagram of the PASSAT test facility with iodine production and iodine feed systems.

In the dry part of the facility downstream of the heater W 3, no corrosion was detected with the same material, but with a substantially reduced relative humidity of < 10 % of iodine and water vapor resulting from heating the gas flow to a temperature of 80 °C.

The conclusion to be drawn was that the corrosion had been caused by iodine in combination with water saturated air.

The corrosion damage of the pipework was found after iodine loading tests had been performed. During the respective tests the facility was operated for 60 hours with moistened air at a dew point of 30°C. The offgas, volume flow rate 150 m³/h, was loaded with an average amount of 1.1 g iodine/m³ ($\varphi \approx 20$ %). At the end of loading, nitrogen dioxide was added to the gas flow for six hours up to a concentration of 5 vol.%.

The corrosion phenomena had been particularly pronounced on the welding seams and in the welded zones exposed to heat. At points where corrosion products had deposited, local corrosion attacks in the form of pitting corrosion were found by mere visual inspection after the corrosion products had been removed.

Figure 2 is a photograph of iodine induced corrosion at an unheated pipe flange.

In the corrosion products the alloy constituents of iron, chromium, nickel, titanium, manganese and molbdenum used as materials for pipework and sensors were detected by X-ray fluorescence anlyses in qualitative terms. Due to the high volatility of iodine little iodine was contained in the dry residues, but a higher amount in the wet residues.

On account of the danger of pipework fracture and failure of the sensors, it was not possible to perform further investigations involving iodine offgas in the facility. By cleaning of the damaged pipework with pickling acid (18 - 20 mass % HNO_3 + 2 - 3 mass % HF) the corrosion products were completely eliminated and the progress of pitting corrosion was stopped. The corroded sensors were replaced by new ones.

For better assessment a damaged flange was cut off 10 cm above its welding point and subject to metallographic examination. According to the results presented in /6/ no structural changes appeared up to a distance of 4.5 mm from the welding seam. At greater distance considerable amounts of carbide precipitates were detected at the grain boundary which suggests that the material had not undergone proper heat treatment in the course of welding. However, pitting corrosion was detected both in the zones with and without carbid precipitates.

Figure 3 is a photograph of pitting corrosion on the pipework material No. 1.4541.

In the flange proper the precipitation lines reaching up to the surface are determinant of corrosion attack.

Figure 4 shows the direction of corrosion attack at the pipework flange.

2. Laboratory Corrosion Investigations at CrNi Steels under the Conditions Prevailing in the Simulated Iodine Bearing Dissolver Offgas

After the materials Nos. 1.4541 and 1.4571 used in the PASSAT had been found to be non-resistant to corrosion when exposed to iodine bearing and moist offgas and only a limited number of indications of iodine induced corrosion had been found in the literature, laboratory tests were performed with a view to selecting corrosion resistant materials. The investigations had been organized in such a way that they could provide an overview of the qualitative differences in the chemical resistance of some selected steels under the operating conditions prevailing in PASSAT. The main requirement to be fulfilled was an improved resistance to pitting corrosion as compared with the materials previously used in the filter section.

2.1 Material Selection

The resistance of stainless CrNi steels to pitting corrosion depends primarily on their chromium and molybdenum contents.

To evaluate materials in terms of their resistance to pitting corrosion calculation of the active sum was introduced /7/ which is made up of the mass content of chromium and three times the mass content of molybdenum according to the formula below

$$\text{active sum} = \text{mass.\% Cr} + 3 \cdot \text{mass.\% Mo.}$$

In conformity with this criterion of evalution and the additional requirement of a high resistance to corrosion in nitric acid another four materials were selected for laboratory tests in addition to those used in PASSAT.

Table 1 shows the chemical compositions, the active sums of the materials selected for investigation and the filler metals used for welding.

The Inconel 625 material is a nickel-base alloy, the other five materials are fully austenitic steels, the materials Nos. 1.4541 and 1.4571 being stabilized with titanium.

2.2 Test Program

For the laboratory corrosion tests, specimens were taken from series produced pipes and sheet metals, respectively, 20 mm x 50 mm in size. These steels had been delivered in a cold strained, heat treated (1050 °C - 1150 °C/air) and pickled condition. To realize the technical conditions of use in PASSAT at the highest degree possible the specimens were welded in addition with filler metals made of a similar type and with higher alloy contents, respectively, and pickled subsequently. The testing vessel chosen was a multi-specimen apparatus made of quartz glass in which the steel specimens to be tested simultaneously in the liquid and in the vapor phase.

Figure 5 is a schematic representation of the testing equipment.

As iodine undergoes condensation at cold vessel walls the equipment had to be well insulated and operated on the once-through principle. The elemental iodine needed for offgas simulation was produced in the reaction vessel proper, following the reaction

$$5\ NaI + KIO_3 + 6\ HNO_3 \longrightarrow 3\ I_2\uparrow + 3\ H_2O + 5\ NaNO_3 + KNO_3.$$

However, to achieve adequate iodine stripping from the acid feed tank a temperature of at least 60 °C must be maintained.

The initial substance, potassium iodate (KIO_3), was supplied together with the nitric acid which was replaced every 24 hours in the stoichiometric amount required. The sodium iodide (NaI) was added in a quasi-continuous mode into weak nitric acid solution through a dropping funnel; the dropping liquid volume compensated for the losses occurring in distillation.

The gas stream introduced at 50 l/h flow rate into the testing vessel contained different amounts of nitrogen dioxide depending on the conditions of testing. As the iodine concentrations of 0.3 g I_2/l offgas found in the iodine feed pipe of the test facility the tests were performed at the maximum iodine concentration possible of 50 mg I_2/l offgas. Two test series were performed to take into account the different conditions in the iodine feed pipe and in the pipework of the filter section.

2.3 Conduct of Tests and Results

Besides the determination by gravimetry of the corrosion rate the specimens used were evaluated with the help of metallographic transverse microsections and scanning electron microscopy, respectively, and on the basis of deposition products formed.

2.3.1 Testing under the Conditions Prevailing in the Iodine Feed Line

The first test series was performed under the conditions prevailing in the iodine feed line; unlike the iodine concentration of approximately 0.3 g iodine/l offgas attained in the test facility, only a reduced iodine concentration of 50 mg I_2/l offgas at the maximum could be set in the laboratory scale equipment for technical reasons (iodine condensation). This corrosponds to a saturation with iodine of the offgas stream of about 20 %. The vapor phase was scavenged with an offgas stream (air) of 50 l/h to which 5 vol% nitrogen dioxide had been added. The acid feed was 3 molar nitric acid.

To determine the influence of thermal treatment on the chemical resistance of the materials used non-treated, as-delivered sheet metal specimen made from the material No. 1.4539 was placed into the testing equipment in addition to the welded specimen. Inconel 625 and material No. 1.4563 were investigated in the form of a sheet metal specimen only.

Table 2 shows the results of the test series during an exposure obtained up to 150 h in the vapor phase above boiling nitric acid.

The results show that under the prevailing conditions the materials having lower active sums of up to 23.6 mass % are attacked by pitting corrosion. Within the period of testing there had been ruptures at some points of the specimen walls. The intensity of corrosion attack is evident also from a high corrosion rate.

Despite the condensate film permanently running down the specimens corrosion products deposited at the molybdenum-free materials and became firmly attached to them.

Figure 6 is a photograph of material specimens after a duration of treatment of up to 150 h in the testing equipment under the conditions enumerated.

The steels with active sums greater than 23.6 mass % are not attacked by pitting corrosion; this applies both to the welded material specimen and to the untreated material specimens. Under both conditions of pretreatment the same numerical values were found for the corrosion rate.

2.3.2 Testing under the Conditions Prevailing in the Offgas Carrying Pipework

Another test series was performed under conditions similar to those in the offgas carrying pipework in the wet part of the filter section. On account of condensate formation at the pipe walls the material specimens were placed into the liquid as well as into the vapor phase. The iodine concentration was set at 2.5 mg I_2/l offgas (φI_2 = 20 %), the acid feed at 3.5 molar nitric acid. The nitrogen dioxide content in the offgas stream (air) was set to 0.5 vol.%.

Only welded specimens were used in the tests; Inconel 625 was not taken into account.

The results determined after a testing period of 150 h at temperatures of 60 °C, in liquid and 40 °C in the vapor phase have been entered in Table 3.

It appeared that especially the molybdenum-free material specimens suspended in the vapor phase were damaged on the whole surface by pitting corrosion whilst the material No. 1.4571 with molybdenum as an alloy constituent exhibited but a few locations affected by pitting corrosion. The materials Nos. 1.4539 and 1.4563 with active sums greater than 23.6 mass % are extremely resistant to corrosion under these conditions. The surface of the specimens is free from deposited products.

Figure 7 is a picture by scanning electron microscopy of the material specimens subject to pitting corrosion in the vapor phase.

No pitting corrosion is found on specimens immersed into the liquid. The materials show nearly identical corrosion rates with an average of 2.7 mg/m²h.

The fact that the steels immersed into the liquid was no longer attacked by pitting corrosion obviously depends on the acid feed which under these conditions has an inhibiting effect on pitting corrosion attack. Only little condensate had deposited on the specimens suspended in the vapor phase so that the said effect did not accur there.

2.3.3 Conclusion

It can be concluded from the comparison of the two test series described in 2.3.1 and 2.3.2 that active sums of the materials used of 23.6 mass % are necessary for the simulated composition of the offgas to avoid the dangerous pitting corrosion.

It was found for the specimens placed into the vapor phase that with a reduced temperature of exposure of 40 °C and an iodine concentration reduced to 2.5 mg I_2/l offgas - the relative saturation of the offgas stream containing iodine remained roughly constant - the corrosion rates of all materials diminish in some cases. However, the sensitivity to pitting corrosion of mainly the molybdenum-free materials continues to exist.

The uniform corrosion which takes place in the materials Nos. 1.4539 and 1.4563 resistant to pitting corrosion is without importance for the technical use of the materials in the PASSAT filter section. These steels with a high CrNiMo content are suitable under the tested conditions as material for the components in the PASSAT filter section.

With a view to selecting one of these two corrosion resistant materials as a material replacing the damaged PASSAT pipe section transverse microsections were prepared of the welded steel specimens which had stayed in the vapor space during the second test series (2.3.2).

Figure 8 shows the enlarged pictures of the transverse microsections. It can be seen from the pictures that compared with the basic material, the material No. 1.4563 possesses a fine crystalline boundary zone where the onset of intercrystalline corrosion can be observed at some locations. It is supposed that the structure in the boundary zone underwent changes on account of non-observance of the welding code because small specimen sizes had been chosen for the fabrication of welded specimens. Under the impact of the simulated offgas these changes led to intercrystalline corrosion. In the material No. 1.4539 welded under the same difficult conditions no damage whatsoever was detectable, neither in the basic material nor in the welding seam.

Due to the slightly better welding behaviour but also on account of the price, which was about 15 % cheaper, the material 1.4539 was selected for the refabrication of pipework for the PASSAT filter section and the iodine feed pipe. The pipework was replaced in autumn 1983; after fabrication it was treated in a pickling solution (18 - 20 % HNO_3 + 2 - 3 vol.% HF).

2.3.4 Testing under the Conditions Prevailing in the Fuel Dissolver Simulator

Another test series was intended to clarify to which extent the material No. 1.4539 selected for the pipework of the filter section was suited, besides the material No. 14306 likewise under discussion, for the fuel dissolver simulator to be erected at PASSAT. For the investigations likewise welded specimens made from the selected materials were placed into the testing equipment described and, under the same conditions as in previous experiments, tested simultaneously in the liquid phase and in the vapor phase.

The acid feed was 7 molar boiling nitric acid which was replaced every 24 hours. The offgas volume flow rate 50 l/h, was admixed 5 vol.% nitrogen dioxide. The amount of iodine feed corresponded to 2.5 mg I_2/l offgas.

The results obtained have been entered in Table 4.

Under the influence of the 7 molar boiling nitric acid and the resulting higher nitric acid vapor content in the vapor space pitting corrosion is more strongly inhibited as compared with the results obtained before; on the other hand, uniform corrosion is more pronounced in both testing media.

Pitting corrosion is still observed only on the molybdenum-free materials Nos. 1.4541 and 1.4306 suspended in the vapor space which is evident also from the elevated corrosion rates of the specimens as compared with the rates of the immersed specimens. A direct comparison of the two materials under discussion has led to preferring the material No. 1.4539 to the material No. 1.4306 currently used in nitric acid processing since there is the danger of attack by pitting corrosion under the prevailing conditions. The corrosion rate of about 52.3 mg/m²h of the material No. 1.4539 determinded is of secondary importance under the conditions of technical use at PASSAT. Also the metallographic micrographs of the material specimens tested in liquid and in the vapor phase did not reveal drawbacks associated with the recommended material No. 1.4539. The grain boundaries of the specimen surfaces had been more bearily attacked by the elevated corrosion rate. As a supplement, additional microsections were prepared of the materials Nos. 1.4306 and 1.4563.

Figures 9, 10 and 11 show enlarged pictures of the microsections.

2.5 Evaluation of the Corrosion Tests

In a conclusive evaluation of the results obtained it must be pointed out that the investigations performed were intended primarily to allow an intercomparison with respect to the susceptibility to pitting corrosion of the materials used in PASSAT and of the materials selected for the investigations. Considering the short time of exposure of 150 h at the maximum and the fact that reproducibility has not been tested, quantitative statements particularly on the corrosion rate, cannot be made. It is neither possible with the test conditions chosen to make a statement about the influence of corrosion enhancing metal ions, e.g., Cr^{6+}. However, the latter may play a role in the fuel dissolver part with a view to application of the selected materials in the offgas section of a reprocessing plant because recycled acid is used there. It is planned to investigate in long-duration studies the influence exerted by corrosion promoting metal ions on the chemical resistance of the materials selected.

III. Resistance to Nitrogen Dioxide of the Adhesive Materials Used in the HEPA Filter

1. Experience Accumulated with the PASSAT Test Facility

A major element in cleaning the dissolver offgas in a reprocessing plant consists in the retention of solid aerosols. To test the respective separators, two HEPA filters have been installed in the PASSAT filter section upstream and downstream, respectively, of the iodine filters; see Fig. 1.

In the filter cells manufactured by industry the filter material made of a glass mat and the spacers between filters made of aluminium sheat metal are attached to the filter frame with an adhesive consisting of a self-curing plastic, the requirement being that an effective sealing must be achieved between the filtered and the unfiltered air sides.

Figure 12 shows the layout of a filter cell.

The manufacturer describes the adhesive as a plastic material on the basis of polyurethane with fire inhibiting additives.

During filter testing in the PASSAT filter section with nitrogen dioxide bearing exhaust air, performed with a view to determine its suitability for the process, it appeared that the adhesive, contrary to information supplied by the manufacturer, is decomposed at an nitrogen dioxide concentration of 5 vol.% and an offgas temperature of 80 °C, both required in operation according to specification. The adhesive used was converted into a low-viscosity decay product with a fusion point of about 49 °C so that the fixation of the filter material and of the spacers as well as the leak tightness of the filter were no longer guaranteed.

Figure 13 shows the damaged HEPA filter after exposure to nitrogen dioxide carrying offgas.

As under the conditions prevailing in the offgas section the chemical resistance of the adhesive used constitutes the condition for achieving the removal efficiencies required for the filters, laboratory tests were performed on other materials recommended by the manufacturer with a view to selecting a suitable adhesive material.

2. Investigation into the Chemical Resistance to Nitrogen Dioxide of Selected Filter Adhesives

For laboratory testing the adhesives were selected with the following properties taken into account:

- pore free, pourable material,
- chemical resistance to nitrogen dioxide (NO_2) carrying offgases with an content of up to 5 vol.% NO_2,
- temperature resistance up to at least 170 °C,
- adhesive contacts with the materials used for the filter components

First, the filter manufacturer, on the basis of preliminary tests, concluded that various adhesive materials were suited to provide proper adhesive contacts between the materials used for the filter components, and six materials were selected for chemical resistance testing in the laboratory. These were four plastic products on the basis of polyurethane with various fire inhibiting additives, and two plastic products on the basis of silicone rubber with and without temperature stabilizing additives (Fe_2O_3), respectively.

Of the materials to be tested specimens were cast of 20 mm x 20 mm size and after hardening in a glass flask exposed to a mixture of air and 5 vol.% nitrogen dioxide. The sequence of testing included an initial 24 hour test at room temperature (ϑ = 22 °C) followed by a 48 hour test at an elevated temperature of 100 °C. Only nitrogen dioxide resistant specimens were taken over from the first stage into the second stage of testing.

The test results obtained have been summarized in Table 5.

It appears from the test results that under the conditions of testing both filter adhesives prepared on the basis of silicone rubber are resistant up to a temperature of 170 °C whilst all adhesives consisting of polyurethane decomposed as early as at room temperature.

To fabricate new HEPA filters silicone rubber with additives was used as adhesive on account of the better flowing properties.

In practical testing in PASSAT of HEPA filters with silicone rubber and temperature stabilizing additives as adhesive it appeared that even with a nitrogen dioxide concentration temporarily increased to 20 vol.% and a temperature raised to 170 °C at the same time the selected adhesive was resistant for a period of four weeks. This means that the HEPA filters installed upstream and downstream, respectively, of the iodine filters can be operated at 150 °C, i.e., the reaction temperature required for iodine sorption. Consequently, drying and heating of the offgas can be performed in a single step upstream of the HEPA filter. Thus, it was possible to simplify the filter section.

Literatur

/1/ Der Bundesminister des Inneren
Empfehlung der Strahlenschutzkommission zur Rückhaltung radioaktiver Stoffe bei einer Wiederaufarbeitungsanlage
BAnz. Nr. 128 (1983)

/2/ J. Furrer, J.G. Wilhelm, K. Jannakos
Aerosol and Jodine Removal System for the Dissolver Off-Gas in a Large Fuel Reprocessing Plant,
15th DOE Nuclear Air Cleaning Conference, pp. 494 (1979)

/3/ J. Furrer, R. Kaempffer, A. Linek, A. Merz
Results of Cleaning Dissolver Off-Gas in the PASSAT Prototype Dissolver Off-Gas Filter System,
CONF - 801038, Vol. 1, pp. 566 (1981)

/4/ K. Jannakos, W. Lange, G. Potgeter, J. Furrer, J.G. Wilhelm
Selected Solutions and Design Features from the Design of Remotely Handled Filters and the Technology of Remote Filter Handling,
CONF - 801038, Vol. 1, pp. 317 (1981)

/5/ J. Furrer, A. Linek
A New Method of Determining the Overall Particle Decontamination Factor for Multiple Off-Gas Cleaning Components in Reprocessing Plants,
CONF - 820833, Vol. 1, pp. 576 (1983)

/6/ R. Kraft
Zur Korrosion von metallischen Werkstoffen in simulierten jodhaltigen Abgasen von Wiederaufarbeitungsanlagen
unpublished

/7/ K. Lorenz, G. Medawar
Thyssenforschung 1 (3)
97/108 (1969)

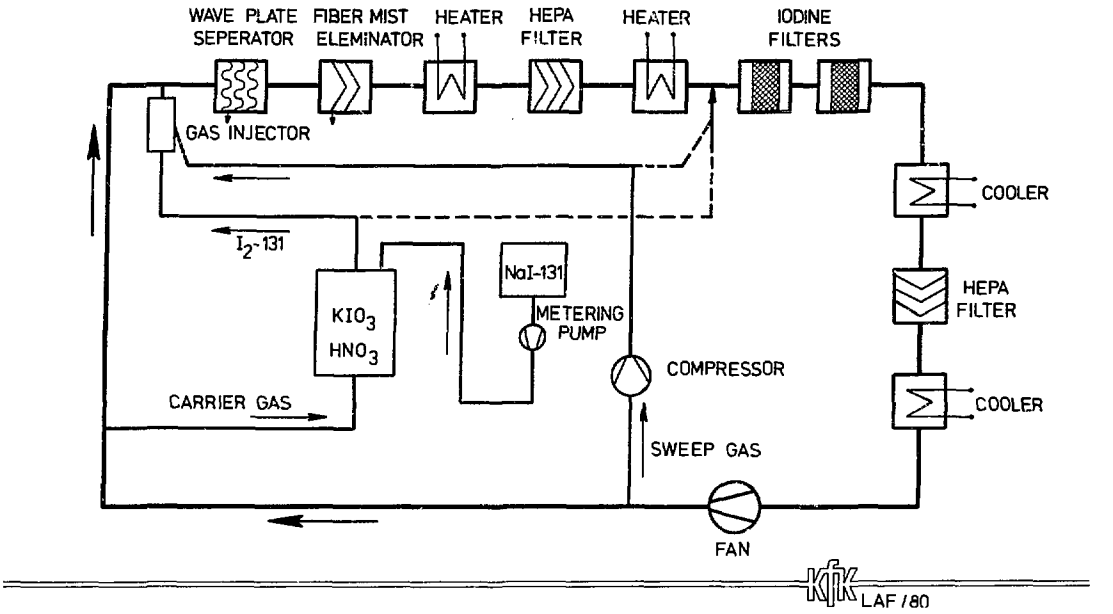

FIG. 1 BLOCK DIAGRAM OF THE PASSAT TEST FACILITY WITH IODINE PRODUCTION AND IODINE FEED SYSTEMS

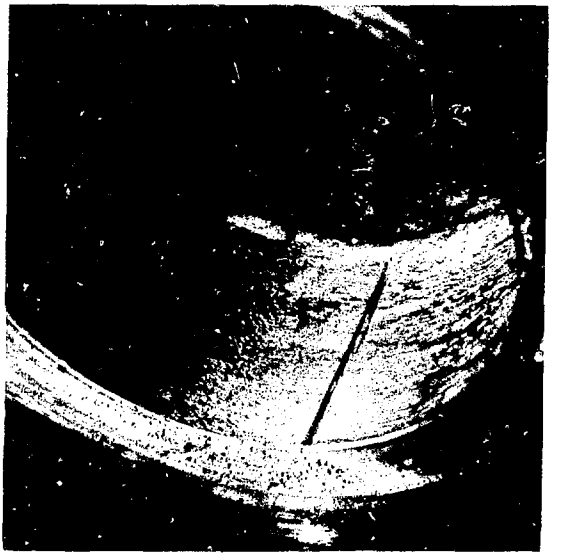

FIG. 2 CORROSION CAUSED BY IODINE AT A UNHEATED PIPE FLANGE OF THE PASSAT FACILITY

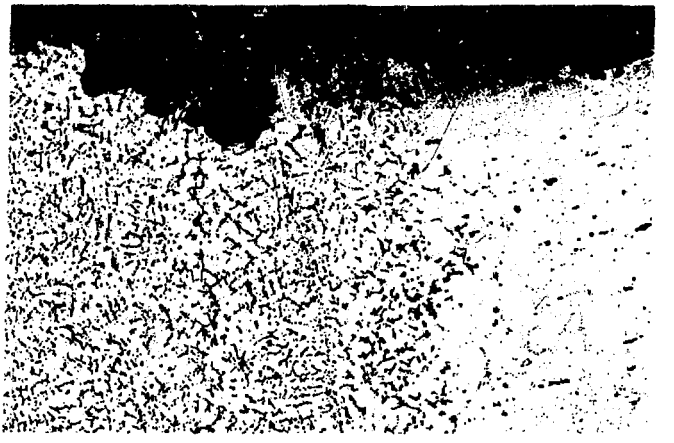

FIG. 3 PITTING CORROSION ON THE PIPE MATERIAL DIN-NO. 1.4541 FROM THE PASSAT TEST FACILITY

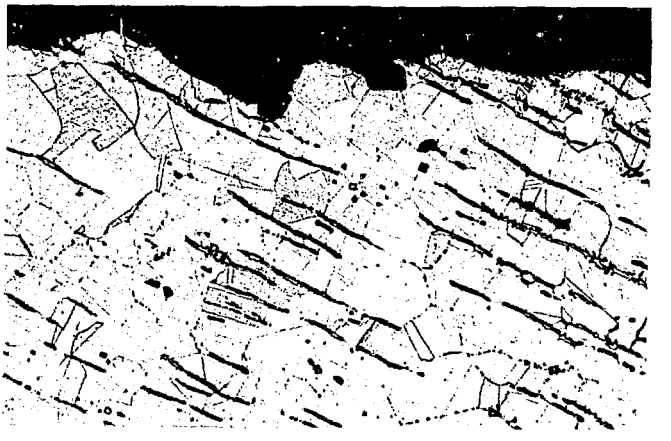

FIG. 4 DIRECTION OF CORROSION ATTACK AT THE PIPE FLANGE MADE OF MATERIAL DIN-NO. 1.4541 FROM THE PASSAT TEST FACILITY

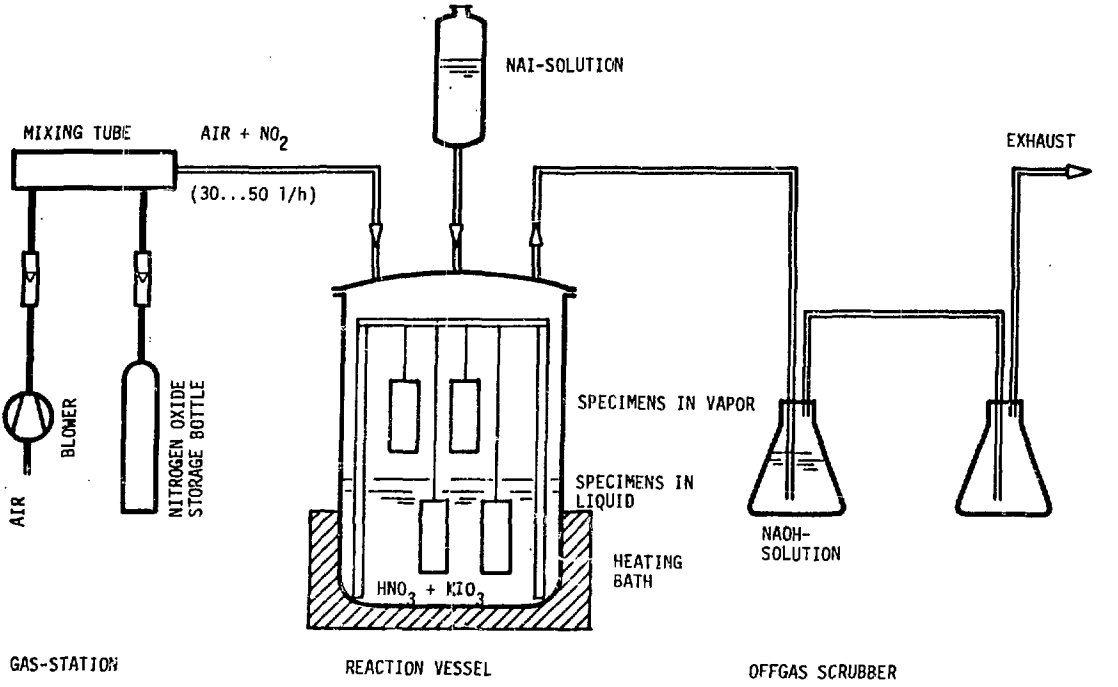

FIG. 5 SCHEMATIC REPRESENTATION OF THE LABORATORY-SCALE EQUIPMENT.

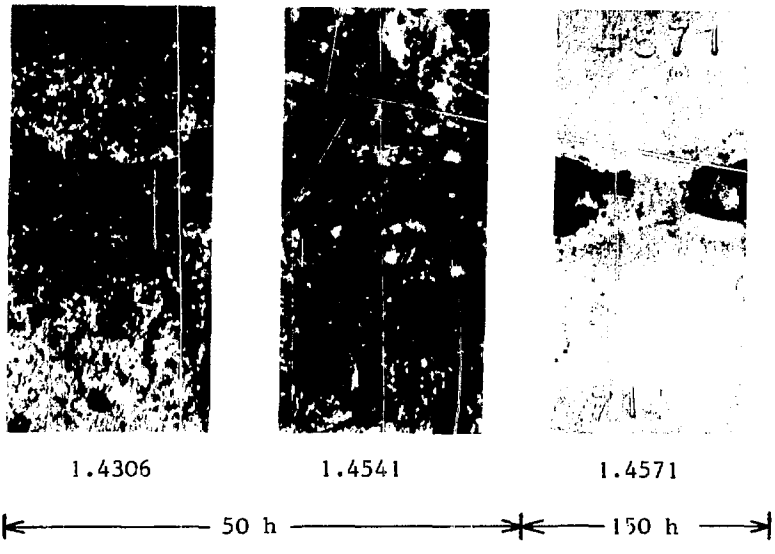

FIG. 6 PITTING CORROSION ON WELDED CrNi STEELS FOLLOWING DIFFERENT DURATIONS OF TREATMENT IN A SIMULATED DISSOLVER OFFGAS
(3 mol HNO_3, air + 5 vol.% NO_2 + 50 mg I_2/l).

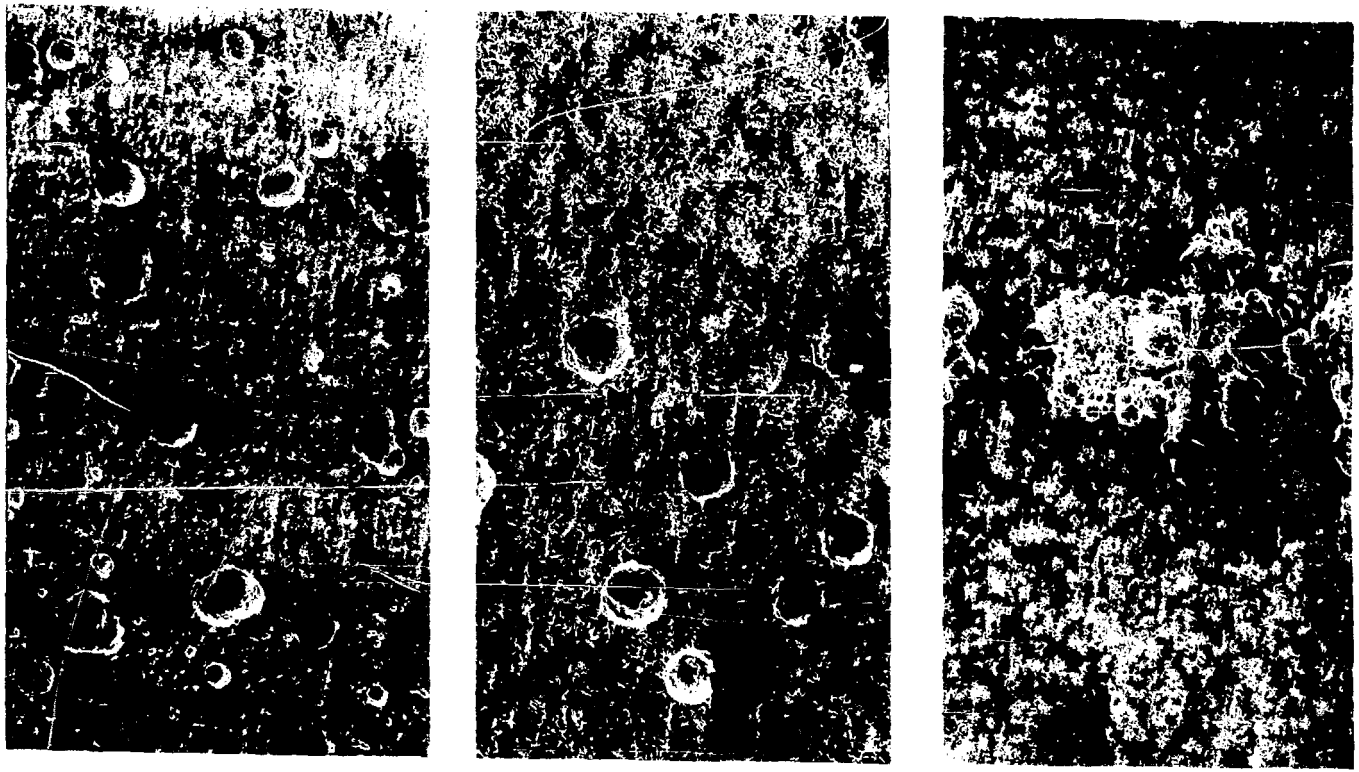

MATERIAL DIN-NO.: 1.4541 1.4306 1.4571

FIG. 7 PITTING CORROSION ON WELDED CrNi STEELS AFTER EXPOSURE IN THE SIMULATED DISSOLVER OFFGAS
(Duration of treatment 150 h, 3.5 mol HNO_3 ϑ = 60 °C, air + 0.5 vol.% NO_2 + 2.5 mg I_2/l).

100 µm

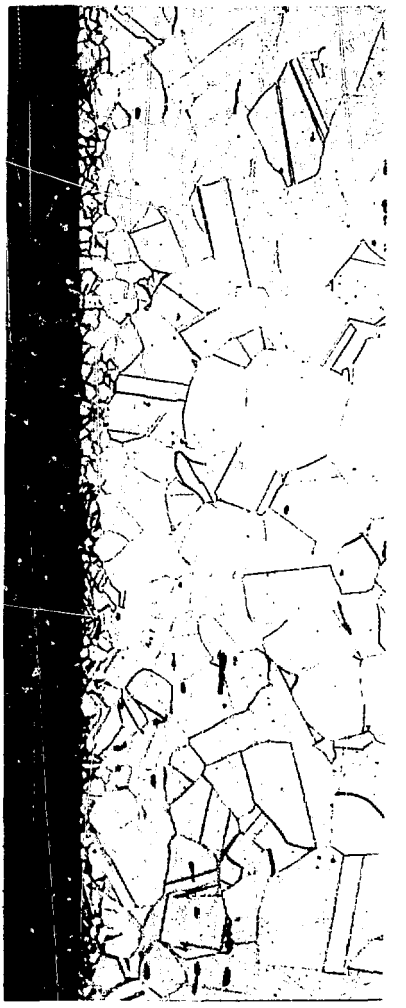

50 µm

MATERIAL DIN-NO.: 1.4539 1.4563

FIG. 8 TRANSVERSE MICROSECTION OF THE WELDED MATERIAL SPECIMENS DIN-NOS. 1.4539 AND 1.4563 FOLLOWING CORROSION IN A SIMULATED DISSOLVER OFFGAS (Duration of treatment 150 h, 3.5 mol HNO_3 ϑ = 60 °C, air + 0.5 vol.% NO_2 + 2.5 mg I_2/l).

Liquid phase

Vapor phase

FIG. 9 TRANSVERSE MICROSECTION OF THE WELDED MATERIAL SPECIMEN DIN-NO. 1.4539 FOLLOWING CORROSION IN A SIMULATED DISSOLVER OFFGAS (Duration of treatment 150 h, 7 mol boiling HNO_3, air + 5 vol.% NO_2 + 2.5 mg I_2/l).

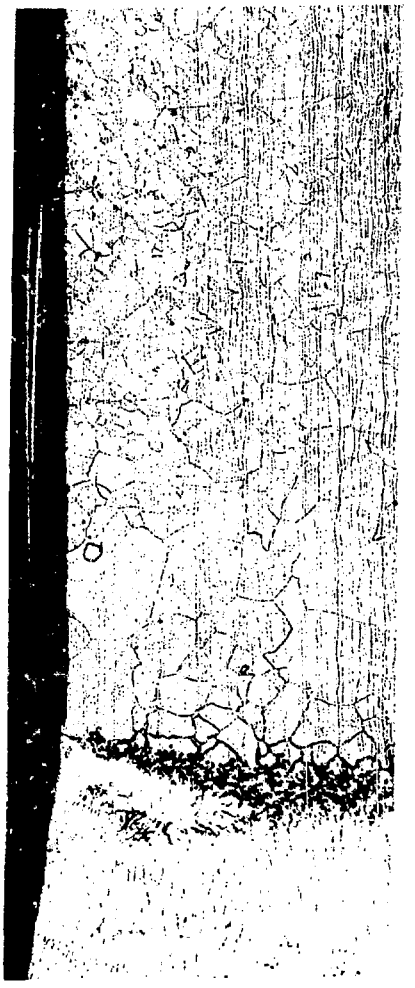

100 µm

Liquid phase

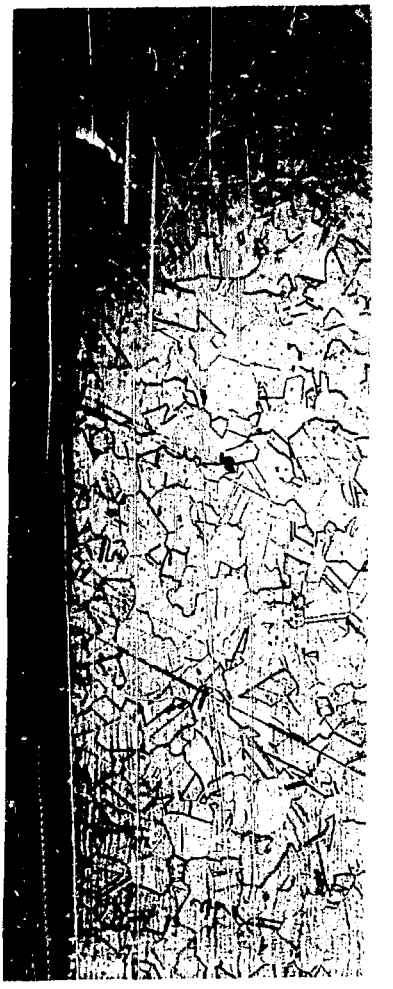

100 µm

Vapor phase

FIG. 10 TRANSVERSE MICROSECTION OF THE WELDED MATERIAL SPECIMEN DIN-NO. 1.4306 FOLLOWING CORROSION IN A SIMULATED DISSOLVER OFFGAS
(Duration of treatment 150 h, 7 mol boiling HNO_3, air + 5 vol.% NO_2 + 2.5 mg I_2/l).

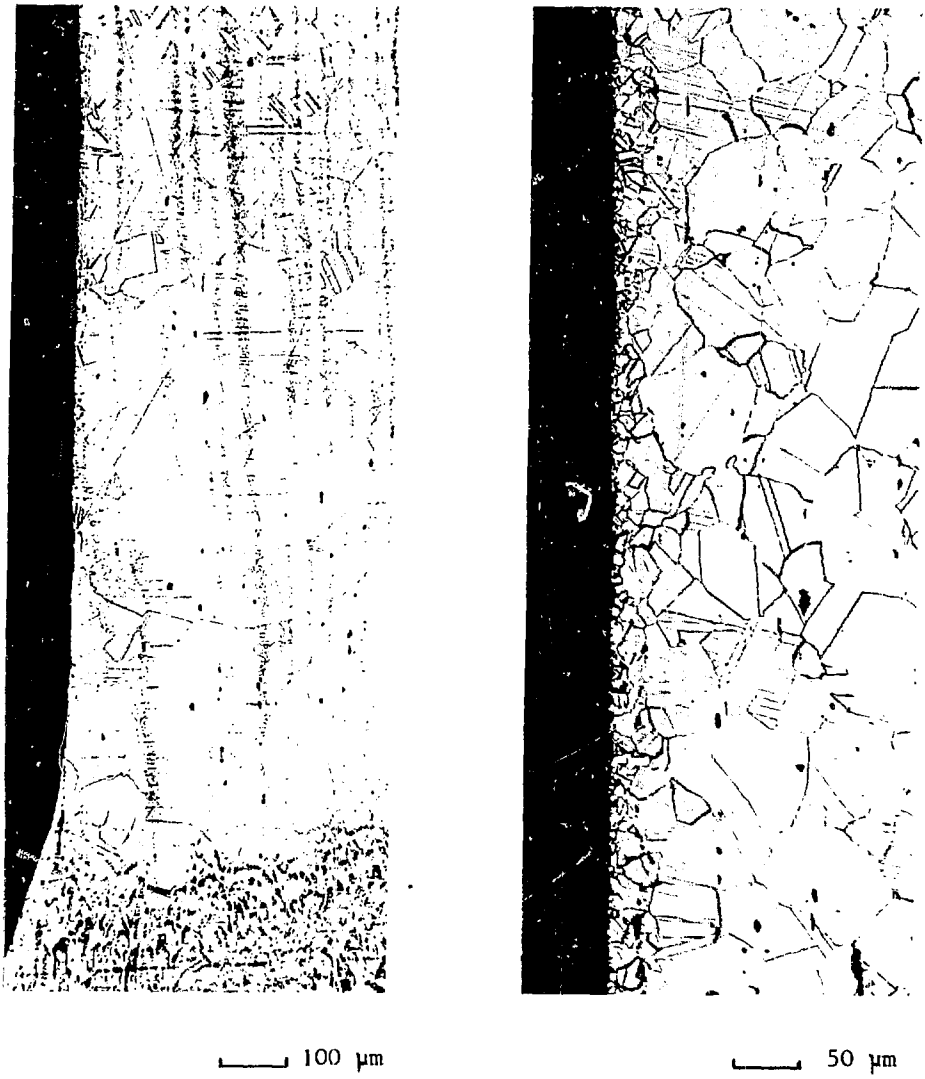

FIG. 11 TRANSVERSE MICROSECTION OF THE WELDED MATERIAL SPECIMEN DIN-NO. 1.4563 FOLLOWING CORROSION IN A SIMULATED DISSOLVER OFFGAS
(Duration of treatment 150 h, 7 mol boiling HNO_3, air + 5 vol.% NO_2 + 2.5 mg I_2/l).

FIG. 12 LAYOUT OF THE HEPA FILTER CELL

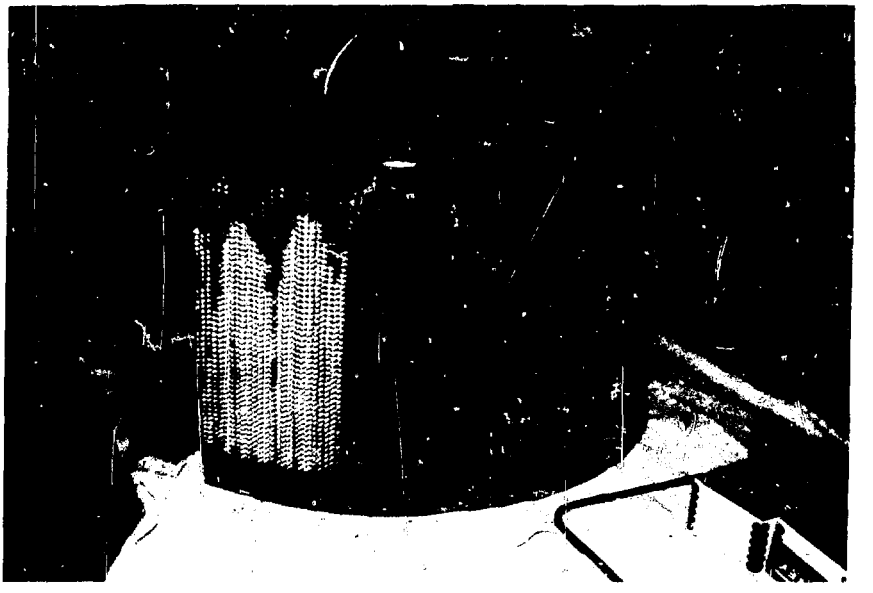

FIG. 13 DAMAGED HEPA FILTER FOLLOWING EXPOSURE TO NITROGEN OXIDE CARRYING EXHAUST AIR
(air + 5 vol.% NO_2, ϑ = 80 ^{o}C)

Material No. (DIN)	Manu-facturer	Filler Metal	Active Sum W / Mass %	Composition in Mass %										Remark
				C	Si	Mn	P	S	Cr	Ni	Co	Mo	Ti	
1.4541 (X 10 CrNiTi 18 9)	KTB	1.4316	18	0.069	0.756	1.49	0.025	0.014	17.64	9.390	0.035	0.130	0.445	
1.4306 (X 2 CrNi 18 9)	WAK	Thermanit 30/40E	19.1	0.016	0.56	1.12	0.026	0.021	18.28	10.26		0.26		
1.4571 (X 10 CrNiMoTi 18 10)	KTB	1.4530	23.6	0.035	0.402	1.76	0.038	0.007	16.65	10.40	0.182	2.22	0.414	
1.4539 (X 2 CrNiMoCu 25 20 5)	Sandvik	20.25.5L Cu	32.6	0.018	0.497	1.667	0.016	0.004	19.4	24.77		4.393		Cu = 1.4%
1.4563 (X 1 NiCrMoCu 31 27 4)	Sandvik	27.31.4L Cu	37	0.011	0.15	0.67	0.014	0.003	26.9	32.2		3.36		Cu = 1.0%
Inconel 625	Wiggin Alloys	---	49	0.006	0.30	0.05	0.005	0.006	21.8	62.3	0.027	9.05	0.2	Fe = 2.4% Ta+Nb=3.7%

TABLE 1: CHEMICAL COMPOSITION, ACTIVE SUM AND FILLER METALS OF THE MATERIALS INVESTIGATED (W = mass % Cr + 3 · mass % Mo).

Material No. (DIN)	Corrosion Rate $mg/m^2 \cdot h$	Pitting Corrosion	Corrosion Products Deposited	Remark
1.4541	∞	yes	yes	50 h treatment
1.4306	∞	yes	yes	50 h treatment
1.4571	500	yes	no	
1.4539	7	no	no	
1.4539 sheet metal	2.3	no	no	untreated
1.4563 sheet metal	1	no	no	untreated
Inconel 625 sheet metal	3	no	no	untreated

TABLE 2: CORROSION RATE AND EVALUATION OF WELDED CrNi STEELS AFTER EXPOSURE IN IODINE CARRYING OFFGAS (Duration of treatment 150 h, 3 mol boiling HNO_3, air + 5 vol.% NO_2 + 50 mg I_2/l).

Material No. (DIN)	Corrosion Rate $mg/m^2 \cdot h$		Pitting Corrosion		Remark
	Liquid	Vapor	Liquid	Vapor	
1.4541	2.3	897	no	yes	no deposits
1.4306	2.6	111	no	yes	
1.4571	2.9	2.3	no	yes	
1.4539	3.0	0.7	no	no	
1.4563	2.7	0.3	no	no	

TABLE 3: CORROSION RATE AND EVALUATION OF WELDED CrNi STEELS AFTER EXPOSURE IN SIMULATED DISSOLVER OFFGAS (Duration of treatment 150 h, 3.5 mol HNO_3 ϑ = 60 °C air + 0.5 vol.% NO_2 + 2.5 mg I_2/l).

Material No. (DIN)	Corrosion Rate $mg/m^2 \cdot h$		Pitting Corrosion	
	Liquid	Vapor	Liquid	Vapor
1.4541	30.3	119	no	yes
1.4306	27.4	59.7	no	yes
1.4571	73.2	90.4	no	no
1.4539	52.3	42.0	no	no
1.4563	22.4	13.9	no	no

TABLE 4: CORROSION RATE AND EVALUATION OF WELDED CrNi STEELS AFTER EXPOSURE IN SIMULATED DISSOLVER OFFGAS (Duration of treatment 150 h, 7 mol boiling HNO_3, air + 5 vol.% NO_2 + 2.5 mg I_2/l).

Adhesive (Trade Mark)	Manufacturer	Chemical Resistance in Air + 5 vol.% NO_2 at		Remark
		Room Temperature	100 °C	
Polyurethane	Delbag, Berlin			
- with additive 1		no	---	yellowish decay product
- with additive 2	"	no	---	
- with additive 3	"	no	---	
- with additive 4	"	no	---	
Silocone rubber				
- with additive Fe_2O_3	"	yes	yes	surface slightly sticky
- without additive	"	yes	yes	no change

TABLE 5: TEMPERATURE RESISTANCE AND CHEMICAL RESISTANCE OF THE ADHESIVES INVESTIGATED.

TREATMENT OF THE OFF-GAS STREAM FROM THE HTR REPROCESSING HEAD-END

H. Barnert-Wiemer
B. Jürgens
H. Vijgen

Kernforschungsanlage Jülich GmbH
Jülich, Fed. Rep. of Germany

Abstract

The AKUT II-facility (nominal throughput 10 m^3/h, STP) for the clean-up of the burner off-gas has been operated for 20 cold runs in parallel to the JUPITER reprocessing head-end. Two of these runs were continuous operation tests with a duration of 50 and 80 hours, respectively. The facility met or exceeded all design specifications.

In a further test series the distillation column alone was run with pure CO_2 and two- and three-component gas mixtures to determine the flooding curves and the stage height (HETP).

I. The composition of the Burner Off-Gas

The burner off-gas (Table 1) consists mainly of CO_2 with varying amounts of CO, N_2,and O_2 and impurities in the ppm-range of which I_2, Xe, Cs, part of the Kr, and T present in the form of tritiated water, are fission products.

CO_2	86	Vol%
CO	12	Vol%
N_2	1,5	Vol%
O_2	0,5	Vol%
Ar	500	ppm
H_2O	300	ppm
Xe	42	ppm
Kr	18	ppm
SO_2	2	ppm
Cl_2	2	ppm
I_2	1	ppm
Cs-Aerosols	50	mg/m^3

Table 1: Typical composition of the burner off-gas

II. Description of the AKUT II-Facility

To clean up the burner off-gas the AKUT II-facility has been built (1,2). The facility has been operated with off-gas from the JUPITER reprocessing head-end (3) and with synthetic off-gas.

The AKUT II-facility (nominal throughput 10 m^3/h, STP) is divided into a low pressure section ($p \leq 1.5$ bar) for the removal of impurities other than Kr and a high pressure section ($p \leq 100$ bar) for the enrichment and separation of the low boiling gases N_2, O_2, Ar, and Kr (Figure 1).

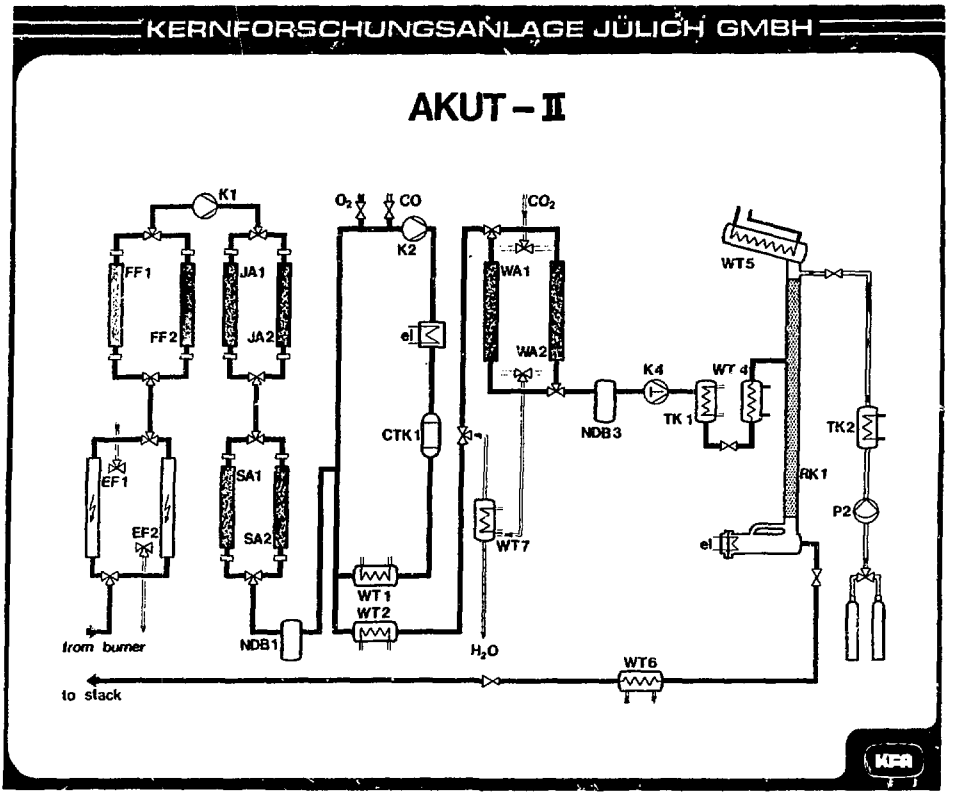

FIGURE 1
SCHEMATIC FLOWSHEET OF THE AKUT II-FACILITY

The low pressure section comprises electrostatic precipitators (EF 1+2), HEPA-filters (FF 1+2), adsorption beds for I_2 and Cl_2 (JA 1+2), SO_2 (SA 1+2), and H_2O (WA 1+2) and a recycle system with a catalytic oxidizer (CTK 1) for the conversion of CO and O_2 to CO_2 (1). The adsorption and catalyst materials and the operating conditions are listed in Table 2.

The main component of the pretreated off-gas that reaches the high pressure section is CO_2, which contains $\leq$ 0.5 % O_2, 500 ppm Ar, 18 ppm Kr, and $\leq$ 10 % N_2 which stems from air leaking into the burner. Before being able to enrich Kr by a distillation step the other low boiling gases N_2, O_2, and Ar need to be distilled off. Because of the uncertainties in designing these columns (see chapter IV) it was decided to first build only one distillation column and with the data gained during the tests design a new complete system. The distillation column (RK 1) was used to distill off N_2, O_2, and Ar during the runs with JUPITER off-gas.

AKUT II Component	Bed		Material		Operation			Regeneration		
	Volume [l]	Height [mm]	Name	Manufacturer	Pressure [bar abs.]	Temperature [°C]	Nominal Gas Velocity [m/s]	Pressure [bar abs.]	Temperature [°C]	Gas Velocity [m/s]
I_2-Adsorber (IA 1 + 2)	6.5	650	AC 6120	Süd-Chemie, München	1.4	25	0.21	–	–	–
SO_2-Adsorber (SA 1 + 2)	6.5	650	Zeolon 900 Na	Norton, Wesseling	1.3	25	0.23	1.1	250	0.24
Oxidizer (CTK 1)	12	2 x 40	1922 K (0.15 % Pd)	Kali-Chemie, Hannover	1.2	250-650	Space Velocity: 12.5 m^3 (STP)/lh	–	–	–
H_2O-Adsorber (WA 1 + 2)	6.5	650	3 A Molecular Sieve	Merck, Darmstadt	1.2	25	0.25	1.1	250	0.28

Table 2: AKUT II, adsorption and catalyst beds (1)

III. Tests with JUPITER Off-Gas

AKUT II was operated in parallel with the JUPITER head-end in 20 cold runs (1,4,5). In Table 3 the range of input and output concentrations is listed.

Tests	20	
Throughput	3.5 - 11 m^3/h (STP)	
Concentrations:		
	Input	Effluent Low Pressure Section
CO_2	40-99 %	≈ 100 %
CO	0-60 %	≤ 5 ppm
O_2	0-10 %	≤ 0.5 %
H_2O	200-15000 ppm	3 ppm
SO_2	0,05-7 ppm	0.02 ppm
		Effluent Distillation Column
N_2	0-10 %	< 5 ppm N_2+O_2 in CO_2 (Reboiler) 10-42 % N_2+O_2 in CO_2 (Distillate)

Table 3: AKUT II, test conditions for JUPITER off-gas

It can be seen that the output concentrations for most components are independent of the input concentrations, even though these varied

in a wide range.

It was found, though, that the SO_2 is adsorbed already on the silver impregnated silica gel of the I_2-adsorbers and not on the Zeolon 900 as designed. While this fact does not disturb the process, it encreases the cost for the replacement and storage of the iodine loaded silica gel.

The only slight effluent variation was found in the oxygen concentration behind the catalytic oxidizer. But since the oxidizer was equipped with a computer aided control system, where off-gas throughput, CO-, and O_2-concentrations are measured and the necessary amount of CO or O_2 for a complete reaction to CO_2 are determined, the catalytic oxidizer system has shown a very rapid response to changes in input conditions and has excellent load-following and turndown capapilities. Figure 2 shows the O_2-surplus for a stepwise change in CO input concentration (the CO output cocentration is below the detection limit of 5 ppm). The slight O_2-peak after every change in CO-concentration is due to the fact that the computer scans the analyser signals only every 10 seconds. The peaks can be reduced by more frequent scanning.

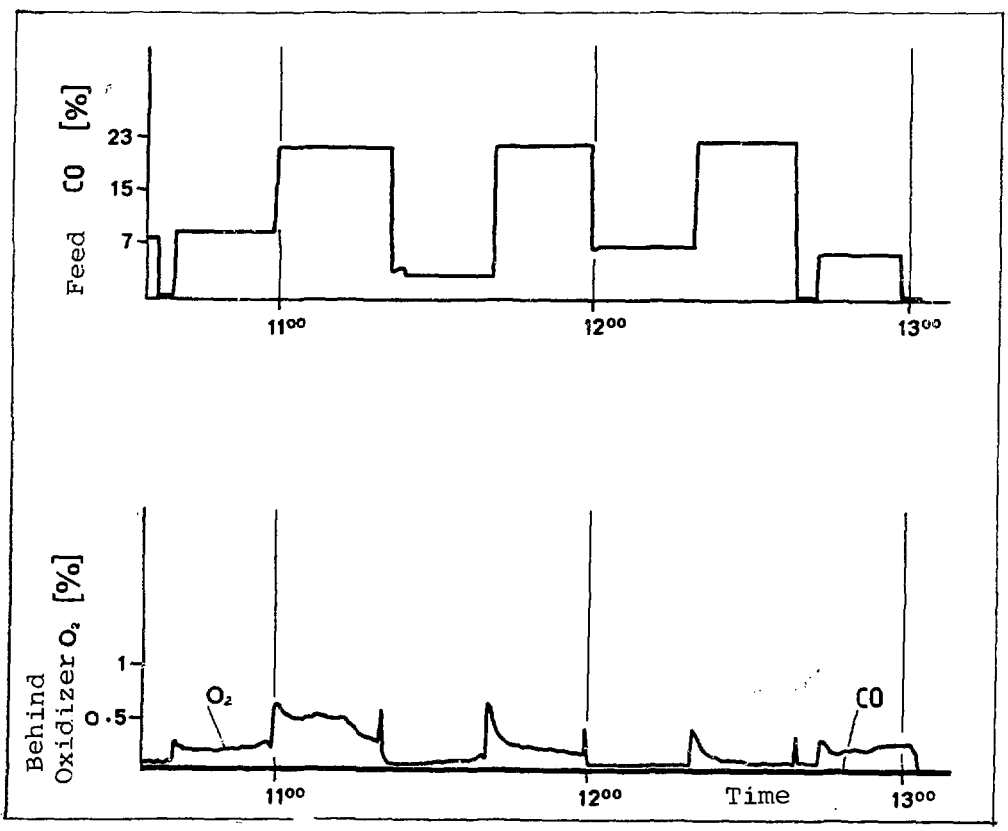

FIGURE 2
RESONSE OF THE CATALYTIC OXIDIZER CONTROL SYSTEM TO CHANGES IN INPUT CO-CONCENTRATION

The distillation column was also easy to control. The bottom product was pure CO_2 (the detection limit of the gas chromatograph

for $N_2 + O_2 + Ar$ is 5 ppm). The distillate concentration varied between 10 and 42 % $N_2 + O_2 + Ar$, depending on temperature and pressure and distillate flow, which was controlled by a hand valve, since the original automatic distillate withdrawel system was designed for the much smaller distillate flow of the CO_2-Kr-system.

It can be noted that in the tests the AKUT II-facility met or exceeded all design specifications. It was operated on automatic, except for the distillate flow of the column. The two long duration tests of 50 h and 80 h respectively confirm the reliability of the facility.

IV. Fluid Dynamic and Distillation Tests

Design of the Distillation Column

The overall length of the column is 5.8 m and the inner diameter is 40 mm. The total height of the packing (wire spirals 4 x 4 x 0.5 mm) is 4.2 m. It is divided into four parts with liquid distributors between them (2).

The diameter of the column was designed such that the vapor velocity at nominal throughput was 50 % of the flooding velocity. The flooding velocities were calculated for pure CO_2 with the empirical equation given in Perry's Handbook (6) which is based on the work of Sherwood et al. (7).

$$\frac{U_t^2 a_p}{g\varepsilon^3}\frac{\rho_g}{\rho_l}\mu_l^{0.2} = \text{function}\ \frac{L}{G}\sqrt{\frac{\rho_g}{\rho_l}} \qquad (1)$$

U_t	=	superficial gas velocity, ft./sec.
a_p	=	total area of packing, sq. ft./cu. ft. bed
ε	=	fractional voids in dry packing
g	=	gravitational constant, 32.2 ft./sec.^{2}
$\rho_{l,g}$	=	gas and liquid densities, lb./cu. ft.
L	=	liquid-mass rate, lb./(sec.)(sq. ft.)
G	=	gas-mass rate, lb./(sec.)(sq. ft.)
μ_l	=	liquid viscosity, centipoise

The decision to design the column for the rather low vapor velocity of 50 % of the flooding velocity was based on the experience at ORNL (8) where the measured flooding velocity for Goodloe packing was only 50 % of the calculated flooding velocity.

The column was designed for the CO_2-Kr-system, but it was also used for CO_2-N_2- and CO_2-N_2-Kr-tests (see following chapter). Figures 3 and 4 show the McCabe-Thiele-diagrams for the CO_2-Kr-system and for the CO_2-N_2-system for which logarithmic scales were used because of the wide range of concentrations (9).

A problem was the assessment of the stage height. In literature a HEPT value between 15 and 90 mm had been given for Goodloe packing (10), which was at that time considered the best performing packing on the market. But at ORNL a HEPT value between 150 and 300 mm was found for this packing (8). Because considerable problems also arose with the

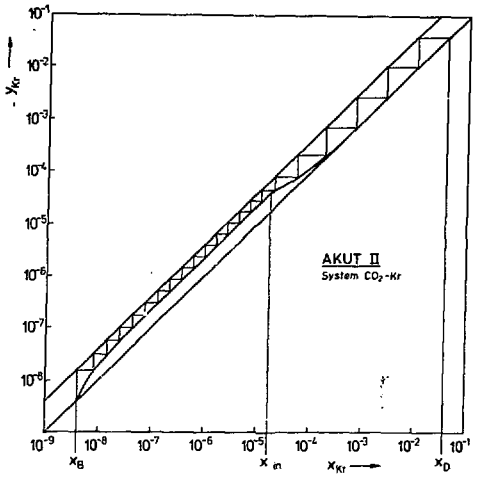

FIGURE 3
McCABE-THIELE-DIAGRAM
FOR THE SYSTEM CO_2-Kr
p = 40 bar
t = 10 °C
n_{theor} = 22

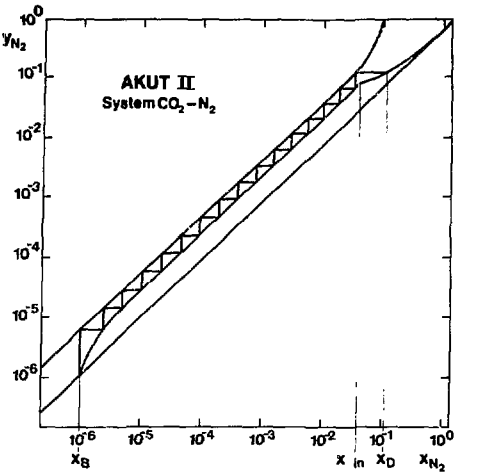

FIGURE 4
McCABE-THIELE-DIAGRAM
FOR THE SYSTEM CO_2-N_2
p = 50 bar
t = 15 °C
n_{theor} = 16

mounting of this packing, we decided to use wire spirals, even if this meant a bigger stage height. Not knowing what stage height to expect, we decided to make the column as long as possible. This resulted in 4.2 m of packing, which means a stage height of 214 mm in the case of the CO_2-Kr-system, where 22 stages are needed (Figure 3).

At five liquid distributors between the packing sections liquid and gaseous samples can be withdrawn and temperature and pressure are measured.

The column can be operated between - 30°C and + 30°C. The lower limit is given by the temperature of the refrigerant and the upper limit by the critical point of CO_2 (31°C, 74 bar).

Determination of the flooding velocities

The flooding experiments were conducted with pure CO_2. In Figure 5 the vapor velocities at the flooding points (u_F) at temperatures between - 10°C and + 20°C for $L/V \geq 1$ are shown. The calculated curves are based on the graph of Sherwood et al. (6,7) where data from numerous tests mostly in the air/water-system are correlated.

Figure 5 shows the unusually good agreement of calculated and measured values. The mean error is always below 5.5 %.

This means that the calculated flooding velocity on which the design of the column was based was right and the column operates at nominal throughput at 50 % of the flooding velocity.

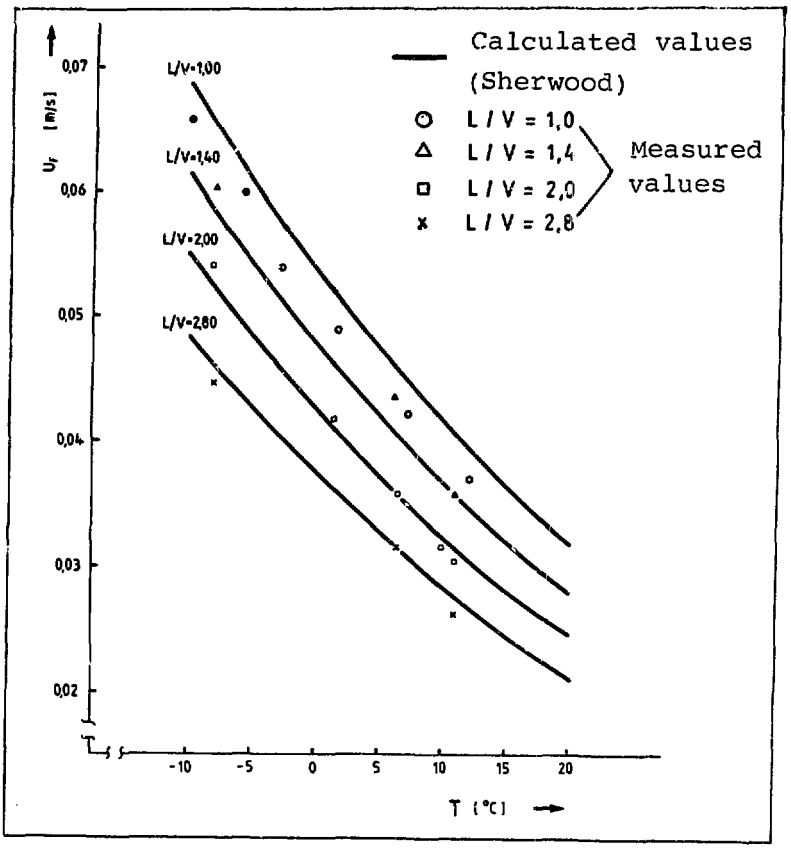

FIGURE 5
VAPOR VELOCITIES AT FLOODING POINTS (u_F) AS FUNCTION OF TEMPERATURE AND L/V-RATIO FOR CO_2

Distillation tests

The distillation tests were made with synthetic gas mixtures to guarantee a constant composition of the feed.

In Table 4 the parameters varied during the tests and their range are listed.

The measured concentration profiles in the column were compared to profiles gained with a computer model of the column (11).

Figure 6 shows the calculated and measured concentration profile of a CO_2-N_2-Kr-system distillation test, were the AKUT II column was operated as stripper column, which would be needed in the complete AKUT II-facility to remove the low boiling components N_2, O_2, and Ar prior to the final distillation step to separate CO_2 and Kr. The model fits the distillation process very well and is therefore suited to be used in designing columns for the tested systems.

Test Number	System	Pressure	Temperature	Heating Power	Feed	Distillate	L/V Ratio	Vapor Velocity	Vapor Velocity	Stage Height
		P [bar]	T [°C]	P_H [KW]	F [Nm^3/h]	D [Nm^3/h]		u_D [m/s]	u_D [% of u_F*]	HETP [cm]
1	CO_2 - N_2	55	19	0,426	9,5	2,5	2,36	0,011	52,1	7,0
2	CO_2 - N_2	55	19	0,525	9,3	2,5	2,16	0,014	61,1	6,2
3	CO_2 - N_2	55	19	0,642	11,0	1,5	2,32	0,017	77,1	6,2
4	CO_2 - N_2	55	19	0,702	10,0	1,5	2,08	0,018	80,4	6,7
5	CO_2 - N_2	50	14	0,274	11,0	0,5	4,77	0,008	46,1	7,7
6	CO_2 - N_2	50	14	0,372	11,0	0,5	3,76	0,010	53,9	8,0
7	CO_2 - N_2	40	5	0,250	11,0	0,5	5,85	0,008	41,2	6,7
8	CO_2 - Kr85	45	10	1,000	0,0	0,0	1,0	0,030	75,0	6,7
9	CO_2 - Kr85	40	5	1,000	0,0	0,0	1,0	0,032	69,6	7,6
10	CO_2 - Kr85	35	0	1,000	0,0	0,0	1,0	0,036	69,2	7,9
11	CO_2 - N_2 - Kr	50	14	0,530	15,0	1,0	3,77	0,015	57,8	8,0

Table 4: Distillation column, parametric tests
Range of concentrations: CO_2-N_2 : 1-5 % N_2
CO_2-Kr : 18 ppm Kr
CO_2-N_2-Kr : 2 % N_2, 100 ppm Kr

*u_F = Flooding velocity

It was found that in all tests the HEPT-value was 70 ± 10 mm (Table 4). In the tested ranges no dependence on gas mixture, concentration, pressure, and temperature was found. Another positive characteristic of the wire spiral packing is, that HETP at a vapor velocity between 40 and 80 % of the flooding velocity is independent of the vapor velocity. Even a total immersion of the packing in liquid CO_2 before the distillation tests were started rendered no different results, whereas for wire mesh rings a definite improvement in efficiency was determined (12).

Compared to Goodloe packing (8) the efficiency of the wire spirals tested in AKUT II is better by a factor of 2 - 4.

On the basis of the described test results the conceptual design for the complete high pressure section of a AKUT II-facility with a nominal throughput of 50 m^3/h (STP), corresponding to a reprocessing capacity of 1000 MW_e, has been completed (11).

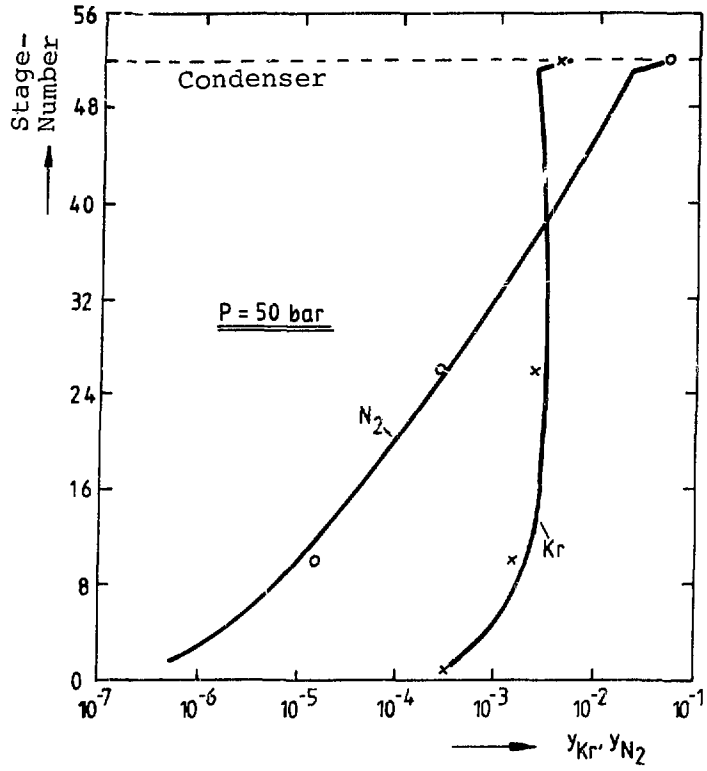

FIGURE 6
COMPARISON OF CALCULATED (SOLID LINE) AND MEASURED (x,o) CONCENTRATION PROFILES FOR A CO_2-N_2-Kr-SYSTEM DISTILLATION TEST (11)

Pressure	:	50 bar
Number of stages	:	52
Throughput	:	15 m^3/h (STP)
Distillate	:	1 m^3/h (STP)

V. References

(1) H. Barnert-Wiemer, B. Bendick, B. Jürgens, H. Nafissi, H. Vijgen, W. Krill:
"Test Results in the Treatment of HTR Reprocessing Off-Gas."
17th DOE Nuclear Air Cleaning Conference,
Denver, August 2-5, 1982

(2) H. Barnert-Wiemer, E. Merz:
"Abgasbehandlung bei der Wiederaufarbeitung von Brennelementen des Hochtemperaturreaktors (HTR)."
Jahrestreffen der Verfahrensingenieure, Straßburg
1.-3.10.1980

(3) U. Brinkmann, W. Heid, H. Huschka, G. Kaiser, W. Theymann:
"Research and Development Work in HTR Fuel Fabrication, Fuel Performance, Spent Fuel Treatment in the FRG."
Conf. on Gascooled Reactors today, Bristol, 20.-24. Sept. 1982

(4) J. Wolf, G. Kaiser:
"Ergebnisse von Komponententest- und Betriebsvorbereitungsversuchen mit dem modifizierten JUPITER-Head-End."
Jahrestagung Kerntechnik, Berlin, 14.-16. Mai 1983

(5) H. Barnert-Wiemer, B. Jürgens, H. Vijgen:
"Betriebserfahrungen mit der AKUT II-Anlage zur Reinigung des Verbrennungsabgases aus der HTR-Wiederaufarbeitung."
Jahrestagung Kerntechnik, Berlin, 14.-16. Mai 1983

(6) R.H. Perry, C.H. Chilton:
"Chemical Engineers' Handbook."
Fifth Edition
Mc Graw-Hill, 1973

(7) T.K. Sherwood, G.H. Shiplex, F.A.L. Holloway:
"Flooding Velocities in Packed Columns."
Ind. Eng. Chem. 30, 1938, Nr. 7

(8) A.D. Ryon:
"Demonstration of the KALC Process: Campain II at the ORGDP Off-Gas Pilot Plant."
ORNL/TM-5298 (July 1976)

(9) P.J. Horvath, R.F. Schuberth:
"Final Distillation Stages Graphically."
Chem. Eng. 65 (1958), 129-132

(10) L.B. Bragg:
"Goodloe Column Packing - A New Knit Packing Material for Vapor - Liquid Contacting Operations."
Ind. Eng. Chem. 49, 1957, 1062-1066

(11) B. Jürgens:
"Die destillative Abtrennung von Krypton aus dem Abgas einer Wiederaufarbeitungsanlage für graphithaltige Brennelemente des Hochtemperaturreaktors."
Als Dissertation eingereicht bei der TH Aachen, Juni 1984

(12) Untersuchungen der Herstellerfirma
Vereinigte Füllkörper-Fabriken GmbH & Co
Fuchs - Letschert - Schliebs, 5412 Baumbach/WW.

DISCUSSION

MONSON: What was the catalytic oxidizer used to reduce the oxygen? At what temperature does it operate? Do you inject hydrogen to convert O_2 to H_2O?

BARNERT-WIEMER: The catalyst is a Pd-catalyst with 0.15 wt % Pd on Al_2O_3. The lowest operating temperature is 200°C. We operate it usually at 250°C. If operated above 400°C no SO_2 poisoning occurs, or if the poisoning has occurred at lower temperatures the catalyst is reactivated at 400°C. We do not convert O_2 to H_2O but we react O_2 and CO to form CO_2.

TEST RESULTS FROM THE GA TECHNOLOGIES ENGINEERING-SCALE OFF-GAS TREATMENT SYSTEM

D. D. Jensen, L. J. Olguin,
and R. G. Wilbourn

GA Technologies Inc.
San Diego, California

Abstract

Test results are available from the GA Technologies (GA) off-gas treatment facilities using gas streams from both the graphite fuel element burner system and from the spent fuel dissolver. The off-gas system is part of a pilot plant for development of processes for treating spent fuel from high temperature gas-cooled reactors (HTGRs).

One method for reducing the volume of HTGR fuel prior to reprocessing or spent fuel storage is to crush and burn the graphite fuel elements. The burner off-gas (BOG) contains radioactive components, principally H-3, C-14, Kr-85, I-129, and Rn-220, as well as chemical forms such as CO_2, CO, O_2, and SO_2. The BOG system employs components designed to remove these constituents. Test results are reported for the iodine and SO_2 adsorbers and the CO/HT oxidizer.

Silver-based iodine adsorbents were found to catalyze the premature conversion of CO to CO_2. Subsequent tests showed that iodine removal could not be performed downstream of the CO/HT oxidizer since iodine in the BOG system rapidly deactivated the Pt-coated alumina CO catalyst. Lead-exchanged zeolite (PbX) was found to be an acceptable alternative for removing iodine from BOG without CO conversion.

Intermittent and steady-state tests of the pilot-plant SO_2 removal unit containing sodium-exchanged zeolite (NaX) demonstrated that decontamination factors $\geq$100 could be maintained for up to 50 h.

Integrated testing of major BOG system components confirmed the performance of units evaluated in individual tests. Design decontamination and conversion factors were maintained for up to 72 h.

In a reprocessing flowsheet, the solid product from the burners is dissolved in nitric or Thorex acid. The dissolver off-gas (DOG) contains radioactive components H-3, Kr-85, I-129, Rn-220 plus chemical forms such as nitrogen oxides (NO_x). In the pilot-scale system at GA, iodine is removed from the DOG by adsorption. Tests of iodine removal have been conducted using either silver-exchanged mordenite (AgZ) or $AgNO_3$-impregnated silica gel (AC-6120). Although each sorbent performed well in the presence of NO_x, the silica gel adsorbent proved more efficient in silver utilization and, thus, more cost effective.

Introduction

Engineering-Scale Off-Gas Treatment System

GA has completed the design and installation of a (radioactively) cold engineering-scale facility for the treatment of off-gases resulting from volume reduction or dissolution of spent fuel. Engineering-scale component tests have been performed to simulate the treatment of fission, activation, and decay products and nonradioactive gaseous constituents.[1,2,3] In addition, integrated testing of major off-gas components has been carried out to verify the overall arrangement and operation of the system.

The GA off-gas treatment system, shown in Fig. 1, is designed to process simulated radioactive or other noxious, volatile, and gaseous constituents in fluidized-bed BOG streams specific to HTGR spent fuel treatment. The GA off-gas treatment system also has the capability of treating DOG streams common to several nuclear fuel cycles, e.g., HTGRs, light-water reactors, and liquid-metal fast-breeder reactors. Gaseous fission products are released into the off-gas stream during spent fuel treatment activities. It is necessary to remove most, or perhaps all, of these radioactive species before releasing the gaseous effluent into the environment. In addition, other gaseous components in the off-gas stream, such as CO, SO_2, and NO_x, must be removed or converted into harmless molecular forms to prevent process or environmental contamination.

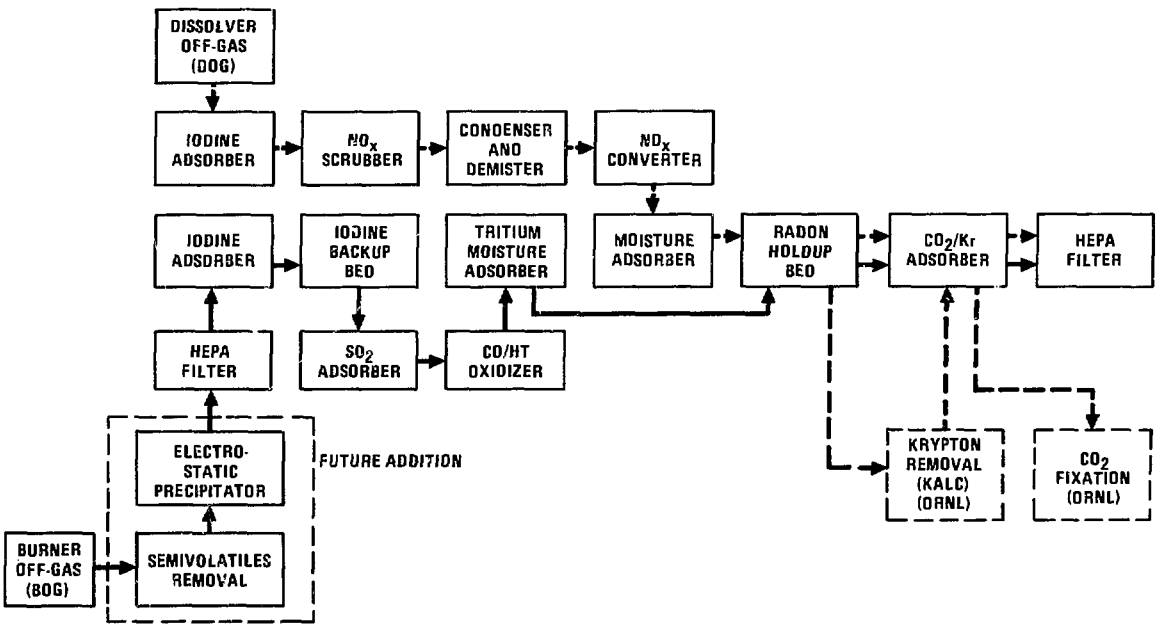

Fig. 1. Integrated GA DOG/BOG treatment system

The GA off-gas treatment system is divided into BOG and DOG subsystems. The BOG subsystem includes units for removal of iodine, SO_2, moisture (including tritiated water), radon, and CO_2, and a CO/HT oxidizer. The DOG subsystem includes units for removal of iodine, NO_x,

moisture, radon, CO_2 and krypton. Future additions to the system will include a semivolatiles (e.g., Cs, Sr, Ru) removal unit and an electrostatic precipitator. In addition, Kr-85 removal (KALC process)[4] and CO_2 fixation investigated at Oak Ridge National Laboratory (ORNL) will be incorporated.

The processes used in this engineering-scale system are based on prior laboratory-scale development that has been performed at various sites under the sponsorship of the U.S. Department of Energy (DOE) or its predecessor agencies. The GA engineering-scale off-gas treatment system is funded under the Consolidated Fuel Reprocessing Program (CFRP), which is managed by ORNL for the DOE.

Burner Off-Gas Treatment

HTGR spent fuel volume reduction is the current focus of CFRP off-gas work. The BOG stream resulting from the crush/burn process of unirradiated HTGR fuel elements typically contains CO (0 to 0.6%), O_2 (~0.2%), CO_2 (~99%), and SO_2 (≤200 ppm). During burner startup and off-balance conditions, incomplete combustion has been observed (i.e., CO = 3% to 5%, O_2 = 10% to 15%, CO_2 = 80% to 87%). Iodine and other radioactive gases and semivolatiles will be present in BOG streams from irradiated fuel.

Several iodine adsorbents for the BOG stream were tested. Initial plans called for use of either AgZ or AC-6120 in the pilot-plant tests. However, when simulated BOG streams containing iodine, CO, O_2, and CO_2 were passed through the adsorption bed at 150°C, the silver-based sorbents catalyzed the CO/O_2 reaction, resulting in rapid temperature excursions in the bed due to the exothermic nature of the reaction (ΔH_0 = -283.1 kJ/mole). In light of this finding, bench-scale tests were carried out with an iodine sorbent positioned downstream of the Pt-alumina CO/HT oxidizer catalyst. Test results (discussed below) showed that iodine rapidly poisoned the catalyst. PbX was then tested as an iodine adsorbent. PbX was found to adequately getter iodine without catalyzing the CO/O_2 reaction.

Performance of the pilot-plant SO_2 absorber was tested under both steady-state and intermittent operating modes. Acceptable performance was found for periods up to ~50 h.

Integrated testing of the iodine adsorber, SO_2 adsorber, and CO/HT oxidizer was initiated to verify overall system performance. Results demonstrated that BOG streams can be adequately treated prior to their release to the environment.

Dissolver Off-Gas Treatment

During HTGR fuel reprocessing, graphite blocks containing fuel particles are crushed and then burned in a fluidized-bed burner. Uranium carbide or oxycarbide present in the fuel is oxidized to U_3O_8 and subsequently dissolved in HNO_3. The DOG stream, containing N_2, O_2, NO_x (predominantly NO and NO_2), CO_2, iodine, and other constituents, passes through an iodine adsorption bed, NO_x scrubber, condenser/demister, and NO_x converter. The iodine adsorber is positioned upstream of the NO_x removal components since ~20% of iodine volatilized in the dissolver would otherwise be held up in the NO_x

scrubber solution. In addition, significant amounts of iodine have been observed to deposit in process piping and other system components if not removed from the process stream. Iodine losses of this magnitude prevent collection at a single process control point and reduce equipment life due to the formation of corrosive hypoiodous acid in the presence of water vapor.

The NO_x scrubber is designed to attenuate wide NO fluctuations, such as those that occur during the dissolution of U_3O_8, and to limit NO_x concentrations to 1% of total flow at the NO_x converter inlet.[5] The scrubber contains a nickel-bearing mesh that can retain NO on its surface long enough for the NO to be oxidized to NO_2. The NO_2 reacts with itself to form N_2O_4, which easily dissolves in water. As the water is recirculated, the dissolved N_2O_4 is converted to HNO_2 and HNO_3.

The NO_x converter uses NH_3 to reduce NO_x to N_2 and H_2O. Under normal operating conditions, the converter can handle a maximum NO_x inlet concentration of 1%.

Iodine adsorption tests were carried out in the pilot-plant iodine adsorption unit using either AgZ or AC-6120 as the sorbent. The objective of this work was to establish iodine decontamination factors (DFs) in the presence of NO_x and select the optimum sorbent.

Burner Off-Gas Treatment
Experimental Method

Figure 2 is a schematic of the major BOG treatment subsystem components included in current testing. The subsystem is designed to process 566 l/m (20 scfm) of simulated or actual BOG. The individual components are described in the following sections.

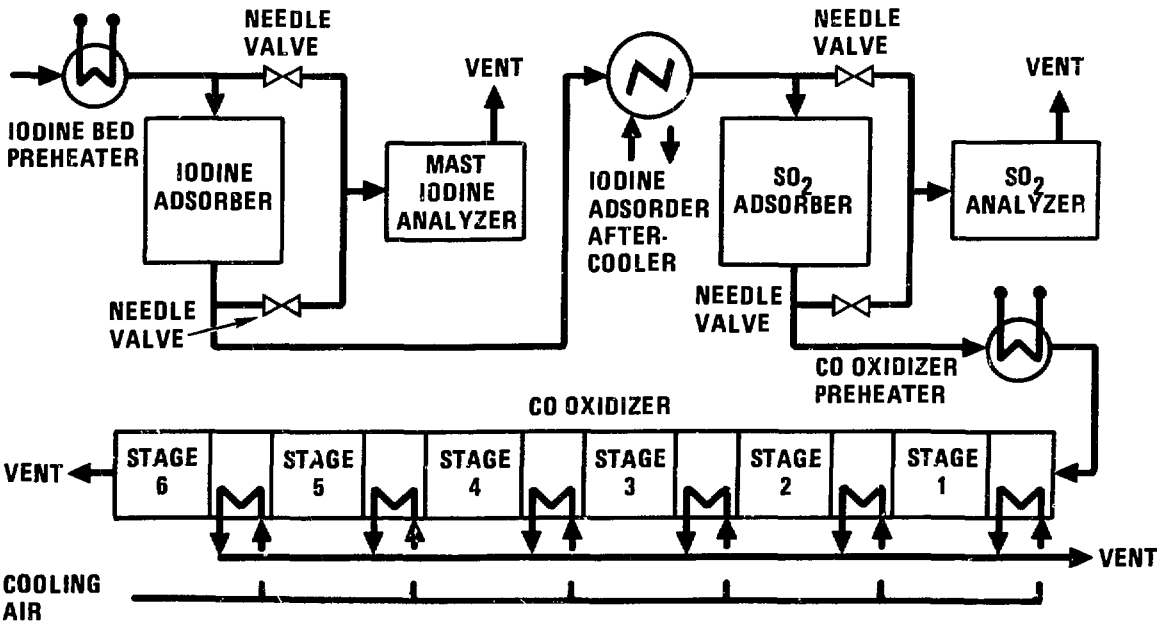

Fig. 2. BOG system components included in current tests

Iodine Adsorber

After being heated to 150°C in a preheater, the BOG stream containing iodine or CH_3I passes through an iodine adsorption bed. Depending on the material, the sorption process can be predominantly chemisorption, as with AgZ sorbent, or physisorption, as with PbX sorbent. The adsorber vessel is 211 mm (8.3 in.) in diameter by 60 mm (24 in.) deep. It is fabricated from 219 mm outside diameter (o.d.) and 3.8 mm wall thickness (8-in. Schedule 10S) 316L stainless-steel pipe with pipe end caps. Normal operating conditions are 150°C and 151 kPa (7.3 psig).

SO_2 Adsorber

Depending on the graphite and pitches used in the fuel blocks, the BOG stream will carry ≤200 ppm SO_2, which will be removed by the SO_2 adsorber. This bed is 346 mm (13.6 in.) in diameter by 457 mm (18 in.) deep, packed with 3.2 mm (1/8-in.) extrudate of Norton Zeolon 900 (sodium form) adsorbent. The vessel is fabricated from 356 mm o.d. and 4.8 mm wall thickness (14-in. Schedule 10S) 316L stainless-steel pipe with pipe end caps. The normal operating conditions are 50°C at 150 kPa (7.0 psig).

CO/HT Oxidizer

After being heated to 350°C in a preheater, the BOG stream enters the CO/HT oxidizer. Reaction occurs in a shallow bed of noble-metal-impregnated alumina catalyst. The degree of CO conversion is controlled by the catalyst loading in each segment. Each percent of CO reacted in the bed raises the exit gas stream temperature ~82°C in an adiabatic condition (in the concentration range considered in the BOG system). The exhaust stream from the bed is cooled to 350°C in an interstage air cooler, if needed, and enters the next stage catalyst bed. Reaction in any one stage is limited to ≤5% CO by the catalyst loading. The oxidizer contains six stages, permitting conversion of peak CO concentrations of 30% without any dilution of the stream. The effluent from the last catalyst bed contains ~1% of the CO concentration (DF of 100) in the oxidizer feed stream.

The oxidizer is fabricated from 152-mm (6-in. Schedule 40S) 304 stainless-steel pipe divided into six segments of catalyst bed with an interstage cooler (heat exchanger) between stages. Each catalyst bed is 152 mm (6 in.) in diameter by 178 mm (7 in.) deep, except the last segment, which is 350 mm (14 in.) deep. The oxidizer uses Pt-impregnated alumina catalyst. The bed operating temperature range is 350° to 700°C. Gas sample ports are provided on each segment.

Control and Safety Features

A Diogenes analog-digital process controller (Rosemount, Inc.) provides automatic control of all essential system operations. These include control of inlet gas flows, inlet sample gas concentration levels, cooling water and air flows, and electric heater power, among other parameters. A Hewlett-Packard 9825B desktop computer is integrated with Diogenes and Hewlett-Packard system voltmeters and scanners to allow monitoring of all necessary system flows, temperatures, pressures, and gas compositions. Continuous monitors and alarms are

provided for toxic and/or explosive gas mixtures, heater outlet temperatures, essential gas supplies, and heat exchanger outlet temperatures. Relief valves are included in both the BOG and DOG lines to ensure that the system pressure does not exceed 238 kPa (20 psig).

Gas Analyzer System

The system is designed to continuously analyze/monitor the combined off-gas at various process points for concentrations of the different component gases. Determinations are made for O_2, CO_2, CO, SO_2, iodine, and other gases. The analyzer system consists of a panel-mounted assembly of separate gas analyzer instruments. These analyzers are selectively valved into the various process points through electrically operated solenoid valves on the panel.

The Beckman 864 infrared analyzer determines the concentration of CO and CO_2 in the flowing gas mixture. The analysis is based on a differential measurement of infrared energy adsorption between the sample and a reference. Each analyzer has three selectable concentration ranges available. Meter readout is generally nonlinear, requiring a calibration curve for conversion to correct concentration values. However, for the normal operating range selected for each analyzer, an internal output-linearizer accessory has been included for direct, linear readout on the meter. The combined off-gas system utilizes six Beckman 864 analyzers for CO and CO_2 determination. A Beckman 865 infrared analyzer, functionally the same as the Beckman 864, is used to measure SO_2.

The Beckman 755 analyzer determines oxygen content of a flowing gas sample based on measurement of magnetic susceptibility. Oxygen is strongly paramagnetic, whereas essentially all other common gases are weakly diamagnetic.

Iodine is monitored with a Mast Model 724 iodine analyzer. The sensing element is a microcoulomb sensor. A chemical solution is metered into the sensor over an electrode that is also exposed to the sample gas. A bias voltage is maintained across the cathode and anode, resulting in a microampere current output that is proportional to the iodine present. Concentrations up to 10 ppm can be monitored.

Simulated Feed Gas Preparation System

Simulated off-gas mixtures are created in a gas-blending console. The individual component streams are metered in 6.35- or 12.7-mm (1/4- or 1/2-in.) diameter lines and tapped into the main 50.8-mm (2-in.) BOG line.

Individual gas supplies are available for N_2, CO_2, CO, O_2, SO_2, NO, NO_2, NH_3, I_2, H_2O, and krypton. The N_2, CO_2, and O_2 supplies are obtained from storage tanks containing the liquefied gas. The CO, SO_2, NO, NO_2, NH_3, and krypton are supplied from pressurized gas cylinders.

Brooks thermal mass flow controllers are used to regulate the flow rate of O_2, SO_2, NO, NO_2, NH_3, and krypton. The controllers maintain a preset flow to within $\pm 1.0\%$ of full-scale reading when measuring the gas at operating conditions of 21° ± 12°C and 172 ± 103 kPa

(25 ± 15 psia). The N_2 and CO_2 supplies are controlled with Masoneilan air-actuated flow-control valves in series with Brooks rotameters. The flow rates of CO, O_2, SO_2, NO, NO_2, and krypton are manually controlled with local control potentiometers. The flow rates of N_2, CO_2, NH_3 and the CO/HT oxidizer interstage O_2 are automatically controlled by an analog-digital process control system.

Test Description

CO/HT Oxidizer. Figure 3 shows the bench-scale apparatus used to determine the effects of iodine poisoning on the Pt-coated alumina catalyst present in the CO/HT oxidizer. Table 1 shows the operating conditions for the three tests performed. Simulant gases were accurately metered with calibrated mass flowmeters prior to mixing. A bypass route to vent allowed adjustment of the system pressure. The bench-scale CO/HT oxidizer was fabricated from 114 mm (4.5 in.) long, 12.7 mm (0.5 in.) inside diameter (i.d.) stainless steel pipe. The oxidizer bed was charged with ~10 g of Pt-coated alumina catalyst spheres. The oxidizer inlet and outlet gas streams were continuously monitored for iodine using the Mast iodine analyzer. Two thermocouples were provided for measuring inlet and outlet internal bed temperatures. A third thermocouple measured the outer wall temperature at mid-reactor length. A gas chromatograph was used to measure the extent of CO conversion. Decreases in CO conversion indicated iodine poisoning of the catalyst.

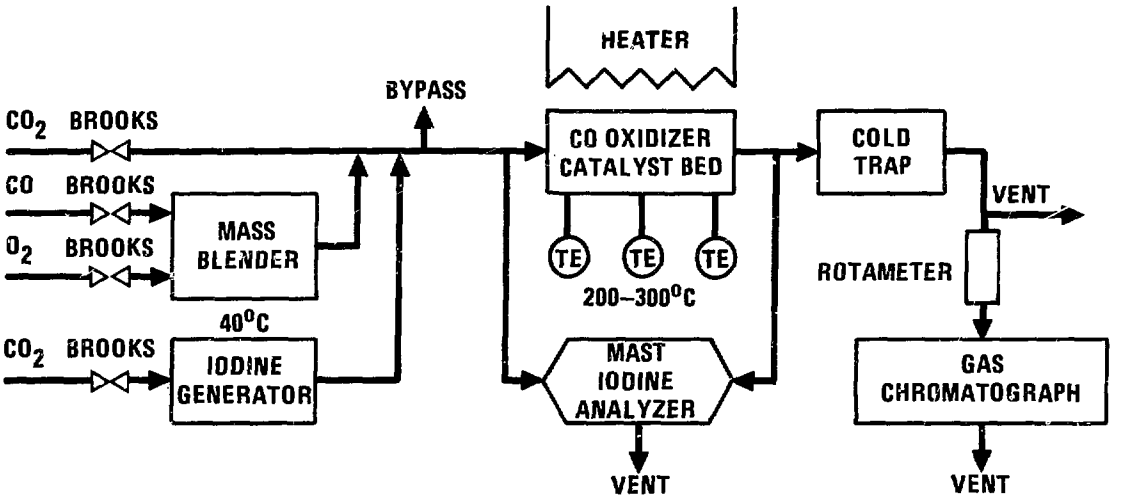

Fig. 3. Bench-scale CO oxidizer apparatus

SO_2 Sorption Bed. Tests of SO_2 sorption capacity were performed under both intermittent and steady-state conditions. A simulated BOG stream containing ~200 ppm SO_2 in CO_2 was passed through the unit at 566 l/m (20 scfm). The bed was operated in the range of 25° to 60°C. The experimental data recorded during the tests included voltage signals from thermocouples, differential pressure indicators, flow transducers, and the on-line SO_2 infrared analyzer. The Diogenes process controller unit was used to set/control operating parameters, and a computer program was used to record selected data at predetermined time intervals. Data from the intermittent tests were obtained by operating the system 8 h per day until the bed was fully saturated.

Steady-state results were derived from continuous operation tests lasting up to 100 h.

TABLE 1
BENCH-SCALE OXIDIZER TEST CONDITIONS

Test No.	Gas Flowrates (cc/min) CO_2	CO	O_2	Inlet I_2 (ppm)	Outlet Temp. (°C)
1	3990	5	5	8	220
2	3990	5	5	7	450
3	3920	40	40	3	316

Integrated Testing. The performance of a number of major components of the off-gas system was verified by integral tests with simulated BOG streams. Components included in integrated testing to date are the iodine bed preheater, iodine sorption bed, SO_2 sorption bed, CO/HT oxidizer preheater, and CO/HT oxidizer. Table 2 summarizes the simulated off-gas composition used. Note that "spikes" of CO and O_2 were intermittently introduced into the gas stream. This was used to simulate a phenomenon of CO and O_2 spikes seen during burner startup or off-normal operation. Process instrumentation and control for these tests have been described above.

TABLE 2
SIMULATED OFF-GAS COMPOSITION IN INTEGRATED BOG SYSTEM TESTS

Component	Flowrate	%
CO_2	555	98.4
CO	6(a)	1.06
O_2	3(a)	0.53
SO_2	0.11	(200 ppm)
I_2	2(b)	(9 ppm)
Mixture	566	100

(a) Including "spikes" of CO = 30 l/m and O_2 = 15 l/m for 15 min.

(b) Approximate CO_2 flow through iodine generator.

Results

CO Oxidizer. Figure 4 shows the percent of CO conversion to CO_2 on the Pt-coated alumina catalyst as a function of iodine contact time for these test conditions. Test 1 at 220°C demonstrated that low con-

centrations (8 ppm) of iodine will inhibit the catalytic conversion of CO to CO_2. The CO conversion was verified to be 100% complete prior to injection of iodine and decreased to 23% conversion following 2.5 h of iodine contact at 220°C. Apparently platinum tetraiodide (PtI_4) forms at temperatures above 200°C.(6) Platinum triiodide (PtI_3) is formed at 350° to 400°C. Platinum diiodide (PtI_2) is also formed at 350°C and remains a stable compound up to 1400°C. It is believed that a combination of these platinum iodide compounds formed on the catalyst surface, reducing the number of potential active sites. Visual examination of the poisoned catalyst revealed a dark solid on the surface that is indicative of PtI_2, PtI_3, and PtI_4.

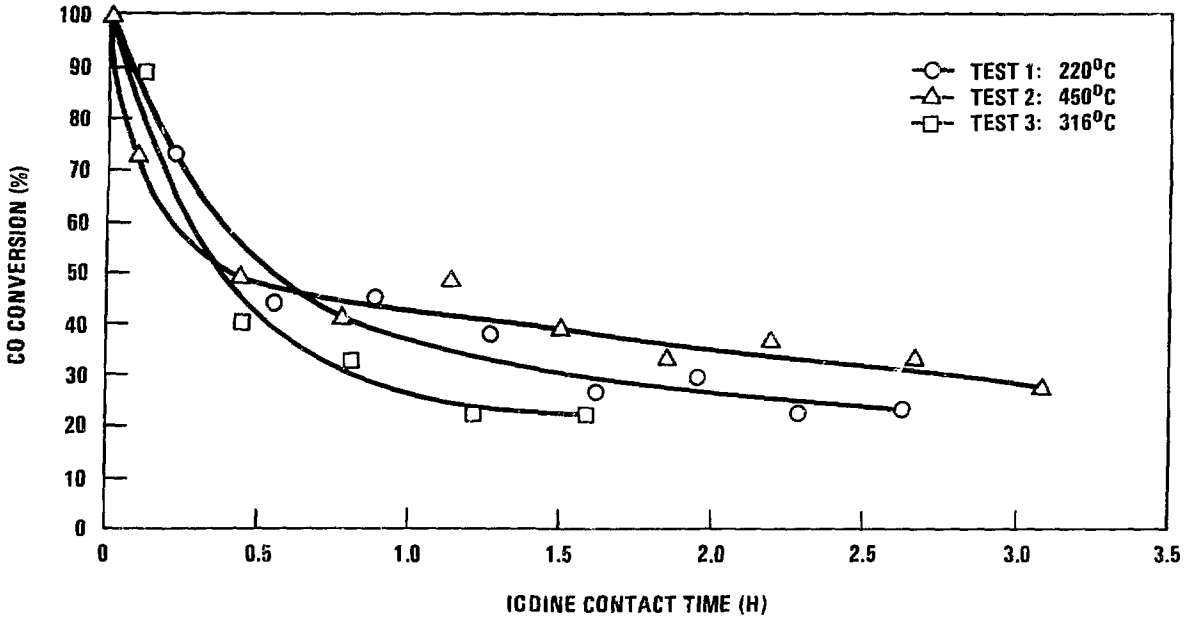

Fig. 4. CO conversion on Pt-coated alumina catalysts as a function of iodine contact time

The second experiment was conducted at 450°C to determine if higher bed temperatures affect the formation of platinum iodides. Iodine poisoning occurred at nearly the same rate as it did at 220°C. The poisoned catalyst material again had a dark black appearance.

In the final experiment, the concentrations of CO and O_2 in CO_2 were increased from 0.13% to 0.97%, and the iodine concentration was reduced from 7 to 3 ppm. The CO conversion rate decreased more rapidly than in the previous experiments. The internal bed temperature was monitored prior to iodine injection and was found to increase 96°C (220° to 316°C) due to the exothermic heat of reaction. As iodine was introduced, a sudden drop in the bed temperature was observed, indicating that less CO was reacting. The bed temperature stabilized at 232°C. As in the previous tests, the inlet and outlet concentrations of iodine varied less than 1 ppm during the course of the run.

As a consequence of this work, it was decided to retain the reference BOG treatment flowsheet incorporating iodine removal upstream of the CO oxidizer. However, PbX was substituted for catalytically

active silver-based catalyst in bench-scale tests to ascertain if it, too, catalyzed the CO/O_2 reaction. Although the ratio of chemisorbed to physisorbed iodine is much lower for PbX (0.17) than AgZ (1.59)[7] (making PbX an unsuitable medium for the long-term disposal of I-129), PbX did effectively remove iodine from the BOG stream without resulting in any apparent oxidation of CO. Thus PbX was used in the pilot plant iodine adsorber during integral testing of the system.

SO_2 Adsorber. Figure 5 shows plots of C/C_0 versus time for SO_2 sorption in the pilot-plant unit. Results for both a summed series of 8-h tests and a steady state run (100 h) are shown. Table 3 summarizes the test conditions, the calculated length of the mass transfer zone (LMTZ), and the dynamic equilibrium adsorption coefficient (DEAC).[1] With continuous operation, SO_2 broke through the bed after ~50 h. With intermittent operation, breakthrough occurred after ~30 h. Since the off-gas system will operate continuously during burner operation, the SO_2 DF of 100 can be maintained for up to ~50 h at the maximum expected SO_2 concentration of 200 ppm.

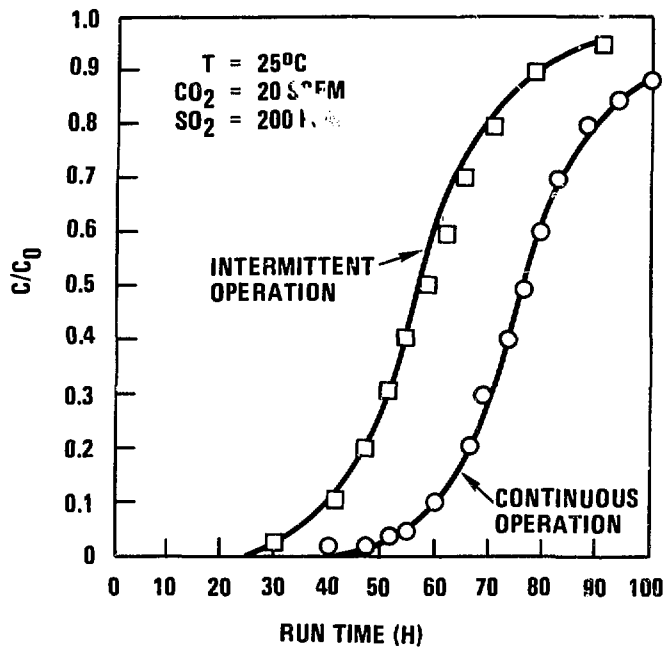

Fig. 5. Plot of C/C_0 versus time for SO_2 sorption in pilot plant unit

Integrated Testing. Intermittent and steady-state tests were performed in the integrated BOG system using simulated off-gas. A series of 8-h tests was run under uniform conditions to verify overall system performance. This was followed by a continuous 72-h test. All major components of the system performed satisfactorily. Target decontamination factors for iodine (1000) and SO_2 (100) and conversion factors for CO (100) were met. The CO oxidizer easily processed all CO/O_2 transients, with CO conversion factors of ≥1000 for all tests.

Two unexpected results were noted when monitoring system performance. The high concentration of CO_2 in the BOG stream produced a

large background signal for the SO_2 analyzer, often representing up to 80% of the total signal. It may be necessary to select an alternative region of SO_2 infrared absorption spectrum that is not as strongly affected by the concomitant CO_2 absorption. In addition, up to 25% of the CO entering the CO/HT oxidizer preheater was converted to CO_2 prior to entering the oxidizer. This makes control of process temperatures difficult under conditions of varying BOG composition. A possible remedy is the use of a silver-based catalyst in the oxidizer, which was found to effectively catalyze the CO/O_2 reaction at 150°C. A lower CO oxidizer operating temperature would require a lower preheater temperature, with an accompanying lessening of premature CO oxidation. These two problems are amenable to remedy and in no way detract from the overall performance of the BOG system.

TABLE 3
OPERATING CONDITIONS AND SUMMARY RESULTS OF SO_2 PILOT-PLANT ADSORPTION TESTS

Bed material [3.17 mm (0.125 in.) extrudate]	Zeolon 900Na
Bed length [m (ft)]	0.46 (1.5)
Carrier gas	CO_2
SO_2 concentration (ppm)	175
Bed temperature (°C)	25
Length mass transfer zone [m (ft)]	
Intermittent	0.44 (1.44)
Steady state	0.30 (1.0)
Dynamic equilibrium adsorption (mg/g - adsorbent)	
Intermittent	29.9
Steady state	42.7

Conclusions

1. Low iodine concentrations (3 ppm) severely inhibit the conversion of CO to CO_2 by Pt-based catalysts within the recommended operational temperature range of the CO/HT oxidizer.

2. Catalyst poisoning is caused by surface formation of platinum iodides, which remain stable solid compounds up to 1400°C.

3. More efficient SO_2 removal is attained under equilibrium operating conditions versus intermittent operation. This is supported by calculations of a relatively shorter LMTZ and a larger DEAC for the continuous test.

4. A DF of ~100 (i.e., the SO_2 bed design operating criterion) is achievable for at least 50 h of continuous BOG operation.

5. Integrated testing of major BOG components using simulated off-gas demonstrated that design decontamination and conversion factors can be maintained for acceptable periods of time (up to 50 h of continuous operation).

Dissolver Off-Gas Treatment Experimental Method

Figure 6 is a schematic of the dissolver/iodine removal/NO_x removal subsystem. This subsystem, like others in the off-gas system, can be isolated to allow independent testing. The dissolver/iodine removal components of the NO_x removal subsystem are described in the following sections.

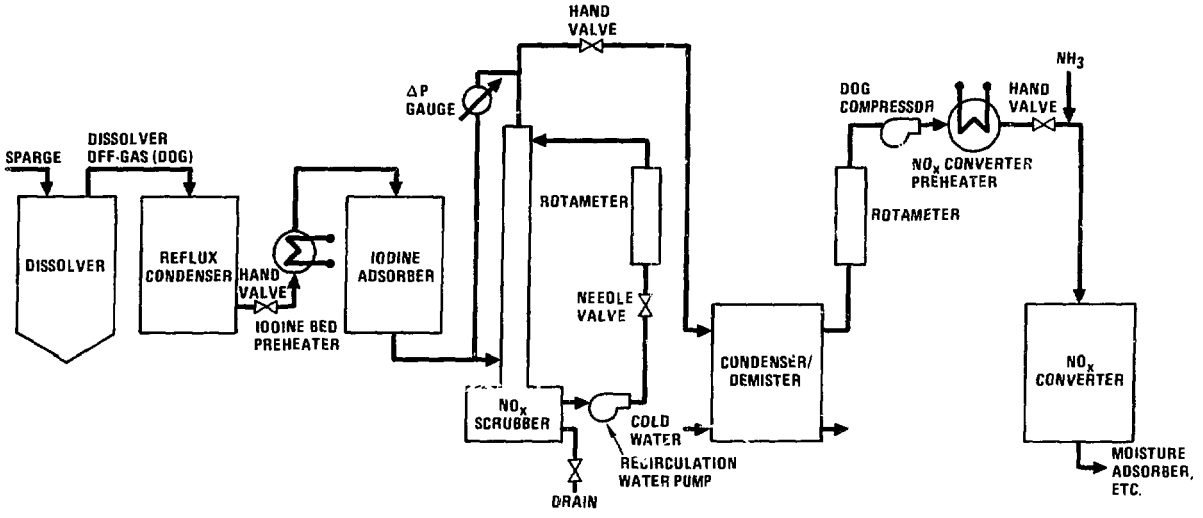

Fig. 6. DOG dissolver/iodine removal/NO_x removal subsystem

Dissolver

Tests were conducted using a 0.5 m diameter prototype-scale dissolver system. The dissolver vessel is equipped with four airlift recirculator tubes, dip legs for measuring specific gravity and weight factor, gas sparge, and heating and cooling jackets. A removable steam jet is available for slurry transport. A Sharples P-850 Super-D-Canter vertical centrifuge is used to separate the mother liquor from any solids left after dissolution. Solids are dropped from the centrifuge into a repulp tank and dryer system, while liquid product is transferred to a 1135-1 product tank. Equipment is remotely operated using the Diogenes controller.

DOG Iodine Adsorber

The DOG system iodine adsorber vessel is fabricated from 219 mm outside diameter (o.d.) (8-in. Schedule 10S), 316L stainless steel pipe. Sorbent material is loaded into the adsorber vessel through a top blind flange and discharged through the same opening using vacuum suction. A 114 mm o.d. (4-in. Schedule 10S) inspection port with a blind flange cover is located near the lower end of the vessel. An internal wire mesh screen assembly is used to support the bed material. A wire mesh basket assembly, positioned on top of the bed, allows sampling of the sorbent and also fixes the loose material in place. The adsorber has an overall length of 137 mm (54 in.) and a

bed height of 91 mm (36 in.). Five wall penetrations are provided for measurement of the vessel pressure drop and bed temperature profile.

DOG Iodine Sorbents

The two sorbent materials selected for testing in the dissolver iodine adsorber were AgZ and AC-6120. Table 4 presents a comparison of the sorbent physical characteristics, reported loading capacities, and relative costs.[8,9]

TABLE 4
DOG STREAM IODINE SORBENT PHYSICAL CHARACTERISTICS AND RELATIVE COST

Sorbent	Silver (wt %)	Particle Size (mm)	Silver Utilization (%)	$/kg[a]	Nominal Bulk Density (kg/m^3)
AgZ[b]	19	1.6 extrudate	55 - 79[c]	177	752
AC-6120[d]	12	1-2 sphere	75 - 94[e]	137	778

[a] Based on silver price of $8.80 per troy ounce.

[b] Silver-exchanged mordenite (Zeolon 900 base, manufactured by Norton Co.)

[c] Ref. 8.

[d] Silver nitrate-impregnated silica gel (manufactured by Sud-Chemie, Munich, West Germany).

[e] Ref. 9.

DOG Iodine Adsorber Sampling System

Figure 7 shows the system used to sample for iodine in the DOG stream. Sample gas streams flowing at 1.0 l/m are split from the main DOG flow upstream and downstream of the iodine adsorber, and passed through scrubbers containing 0.1 molar NaOH. Samples of the scrubber solutions are intermittently sampled for iodine. The I^- and IO^- ions formed via reaction with NaOH are oxidized using hypochlorite ion, and the resulting IO_3^- concentration is determined by ion chromatography. For iodine concentrations less than 1 ppm in the DOG stream, a concentration technique was used in which ionic iodine species were converted to elemental iodine, extracted into carbon tetrachloride, and measured spectrophotometrically.

Test Description

The dissolver vessel was charged with 200 l of 2.5 molar HNO_3 and heated to 95°C. Nitric oxide was injected into the acid solution in sufficient quantities to simulate expected NO_x generation rates. Iodine, in the form of NaI, was metered into the heated dissolver

solution. The DOG passed through a downdraft reflux condenser to remove most of the water and acid vapors. The temperature of the off-gas was increased from 30° to 150°C with a resistance-type heater before entering the adsorption bed. The iodine-free off-gas stream was scrubbed to remove NO_x before being released to the main pilot plant ventilation system. The NO_x concentration was measured with two Beckman Model 951 chemiluminescent NO_x analyzers. Iodine was measured with the iodine adsorber gas sampling system.

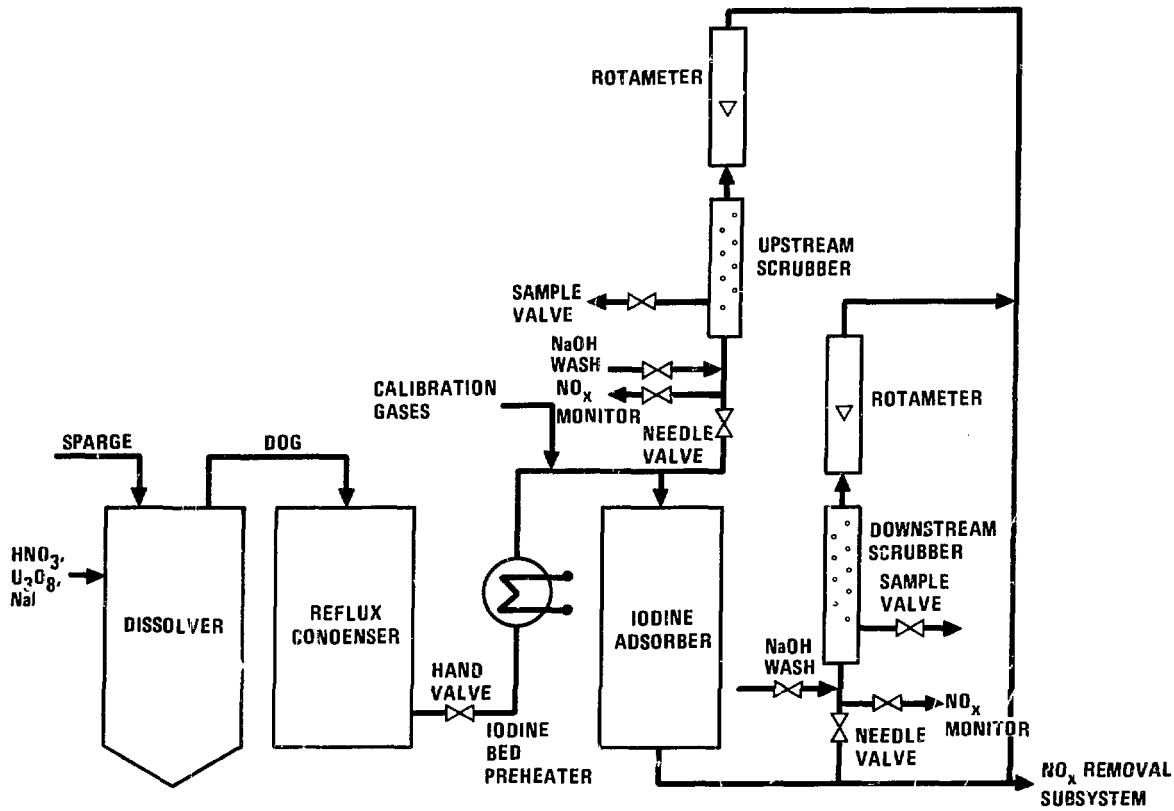

Fig. 7. DOG iodine adsorber sampling system

Results

Five tests were performed with AgZ sorbent material. Analysis of the final dissolver solution indicated complete iodine evolution into the DOG stream in each case. Outlet adsorber gas samples had less than detectable concentrations of iodine over the entire duration of each test. Iodine DFs ranged from 1400 to 3300, as shown in Table 5. These values exceed the established design criteria DF of 1000. Test 5 was conducted using NO_x generated from the dissolution of 12.3 kg of depleted U_3O_8 material. The average iodine concentration was 140 ppm with a peak concentration of 360 ppm. The average NO_x concentration was 6,100 ppm with a peak concentration of 10,500 ppm. These large-scale tests demonstrated that AgZ is effective in removing elemental iodine vapors from DOG streams containing 2,200 to 10,500 ppm NO_x. Examination of the process piping between the dissolver vessel and the iodine adsorber vessel revealed no iodine condensation.

TABLE 5
OPERATING CONDITIONS AND MEASURED DECONTAMINATION FACTORS FOR DOG STREAM IODINE ADSORBERS

Test No.	Bed Material	Inlet I_2 (ppm)	Outlet I_2 (ppm)	Inlet NO_x (ppm)	Off-Gas Flowrate l/m (scfm)	Carrier Gas	DF
1	AgZ	100	<0.06	4,400	99 (3.5)	N_2	>1,600
2	AgZ	100	<0.03	2,700	99 (3.5)	Air	>3,300
3	AgZ	100	<0.05	2,200	99 (3.5)	Air	>2,000
4	AgZ	100	<0.03	4,500	99 (3.5)	Air	>3,300
5	AgZ	140[a]	<0.10	6,100[b]	79 (2.8)	Air	>1,400
6	AC-6120	270	<0.02	220	42 (1.5)	N_2	>11,000

[a] Average (I_2) = 140 ppm; peak (I_2) = 360 ppm.
[b] Average (NO_x) = 6,100 ppm; peak (NO_x) = 10,500 ppm.

A single iodine adsorption test was performed with AC-6120 as the sorbent material. Test results showed that a DF of 11,000 was attained with an average inlet iodine concentration of 270 ppm. The outlet iodine concentration was below the detectable limit. The NO_x concentration of 2200 ppm had no effect on the sorbent's ability to remove iodine.

Conclusions

1. Iodine DFs greater than 1400 can be achieved in DOG streams with either AgZ or AC-6120 sorbent materials.

2. There were no deleterious effects from NO_x concentrations as high as 1% in the DOG.

3. AC-6120 appears to be the more attractive sorbent material in terms of silver utilization and cost effectiveness.

Acknowledgments

The authors extend their appreciation to Ken Higuchi for his contributions during the early phases of this work and to John W. McLean for his technical support in conducting the experiments and maintaining the equipment.

This work was performed under DOE Contract DE-AT03-84SF11964.

References

1. Abraham, L., and P. M. Hirsch, "Consolidated fuel reprocessing program interim development report: off-gas treatment system," DOE Report GA-A16292 (June 1981).

2. Hirsch, P. M., "Selected conversion of NO_x by catalytic reduction with ammonia," Environ. Prog. 1, 24-29 (February 1982).

3. Hirsch, P. M., K. Y. Higuchi, and L. Abraham, "Carbon dioxide-krypton separation and radar removal from nuclear fuel reprocessing off-gas streams," DOE Report GA-A16809 (July 1982).

4. Glass, R. W., et al., "Development of krypton absorption in liquid carbon dioxide (KALC) process for HTGR off-gas reprocessing," Proceedings of the 13th AEC Air Cleaning Conference, CONF-740807, 232 (1974).

5. Hostbjor, G. J., and H. Higuchi, "Evaluation of NO_x scrubber for dissolver off-gas streams," DOE Report GA-A16857 (September 1982).

6. Rolsten, R. F., Iodide metals and metal iodides, John Wiley and Sons, New York, New York, 187-188, 1961.

7. Thomas, T., et al., "Airborne elemental iodine loading capacities of metal zeolites and a method for recycling silver zeolite," ERDA Report ICP-1119 (July 1977).

8. Jubin, R. T., "A literature survey of methods to remove iodine from off-gas streams using solid sorbents," Oak Ridge National Laboratory Report ORNL/TM-6607 (March 1979).

9. Wilhelm, J. G., Furrer, J., and Schultes, E., "Head-end iodine removal from a reprocessing plant with a solid sorbent," Proceedings of the 14th ERDA Air Cleaning Conference, CONF-760822, 447 (1976).

DISCUSSION

MONSON: What was your SO_2 adsorber?

JENSEN, D.D.: Sodium zeolite operated at about 25°C.

von AMMON: We have studied iodine poisoning of noble metal catalysts used for the reduction of O_2 and NO_x with H_2 and found that Pt and Pd, in fact, are poisoned irreversibly, but Ru is regenerated at higher temperatures (450-500°C). I wonder if the same is true with CO oxidation and Ru.

JENSEN, D.D.: I do not know, we have not studied Ru, but I will try it.

EXPERIENCE OF IODINE REMOVAL IN TOKAI REPROCESSING PLANT

K. Kikuchi, Y. Komori and K. Takeda
Reprocessing Plant, Tokai Works
Power Reactor and Nuclear Fuel Development Corporation
Tokai-mura, Ibaraki-ken, Japan

Abstract

In the Tokai reprocessing plant about 170 ton of irradiated fuels have been processed since the beginning of hot operations in 1977. There was no effective equipment for iodine removal from the off-gas except for alkaline scrubbers when the plant construction was completed. In order to reduce the iodine discharge to the atmosphere, silver-exchanged zeolite(AgX) filters were installed additionally in 1979 and 1980, and they have been effective. However, those decontamination factors(DFs) were not so high as expected, and increasing the reprocessing amount of spent fuels it became necessary to lower the iodine discharge to the atmosphere. Therefore another iodine removal equipment is planed to be installed in the plant. Concerning these investigation and development of iodine removal techniques, the iodine concentration of actual off-gas has been tried to be measured and useful data were obtained.

I. Introduction

The Tokai reprocessing plant has processed the irradiated fuels of 170 ton by using the Chop & Leach and Purex Process. The average burn-up was 16,000 MWD/T and the cooling period was 1,600 days which is so long that I-131 content in fuels can be omitted due to its short life. In fact I-131 has not been detected in the off-gas stack. Therefore, with regard to the radioactive iodine, it is enough to consider only I-129. The typical I-129 content was 14 mCi/T. These data are given in Table 1.

In the design basis the iodine was expected to be effectively removed from the off-gas only with alkaline scrubbers. However, it was proved that the alkaline scrubbers were not so effective as to satisfy the criterion required for the plant. During the early operations, for a while, the neutralization and stablization were carried out experimentally for nitric acid recovered from the dissolver off-gas by using caustic soda and hydrazine. Also, the charcoal filter was installed on the ventilation duct in the waste disposal facility. These test operations on iodine removal revealed the difficulty of liquid waste treatment and the life shortness of the charcoal filter.

The new iodine removal filters made of silver exchanged or impregnated adsorbents were investigated and examined.(1) After 20 ton of spent fuels were processed, AgX filters were addopted in the plant ; one AgX filter equipment in the main plant and two in the waste disposal facility in 1979, and additional one in the latter in 1980.

Table 1. LWR fuels reprocessed in the Tokai plant

Weight of heavy metal	170 ton
Burn-up	av. 16,000 MWD/T
Initial enrichment	av. 2.3 %
Cooling time	av. 1,600 days
Iodine inventory	
I-129	av. 1.4×10^{-2} Ci/T
I-131	Trace

II. Off-gas treatment system

The off-gas treatment system in the Tokai reprocessing plant consists of Chopping off-gas(COG), Dissolver off-gas(DOG), Vessel off-gas for High-Level Liquid Waste(HLLW-VOG) and Vessel off-gas(VOG).

The COG from the chopping machine passes through dissolvers, stainless sintered filters and an absolute filter(HEPA filter) to remove the dust such as UO_2 powder. Moreover the COG is treated through an alkaline scrubber, a demister and other HEPA filters, and finally released to the atmosphere.

The DOG from two dissolvers is introduced into a condenser and an acid recovery column to remove the nitric acid fume and nitrous oxide(NOx), then passes through an alkaline scrubber, a demister and HEPA filters. The recovered nitric acid of 1 or 2 mol/l is transferred to the acid recovery process and treated together with other nitric acid from the extraction process. The recovered acid is concentrated up to about 10 mol/l and recycled into the entire main plant.

The HLLW-VOG from high-level liquid waste storage vessels is introduced into the treatment system composed of a condenser, an alkaline scrubber, a demister and HEPA filters, then discharged to the atmosphere.

The VOG from other vessels in the main plant is treated with a similar system to the HLLW-VOG, without a condenser(Fig. 1).

The liquid waste from these four alkaline scrubbers is transferred to and treated in the waste disposal facility where the vessel ventilation systems have no alkaline scrubber and the off-gas is treated only with HEPA filters.

Presently one AgX filter equipment is installed downstream of the COG, DOG, HLLW-VOG and VOG in the main plant, and three AgX filter equipments are installed in the ventilation systems in the waste disposal facility. Also AgX filters are installed for the COG and DOG in the krypton recovery facility which will start the hot operation in near future.

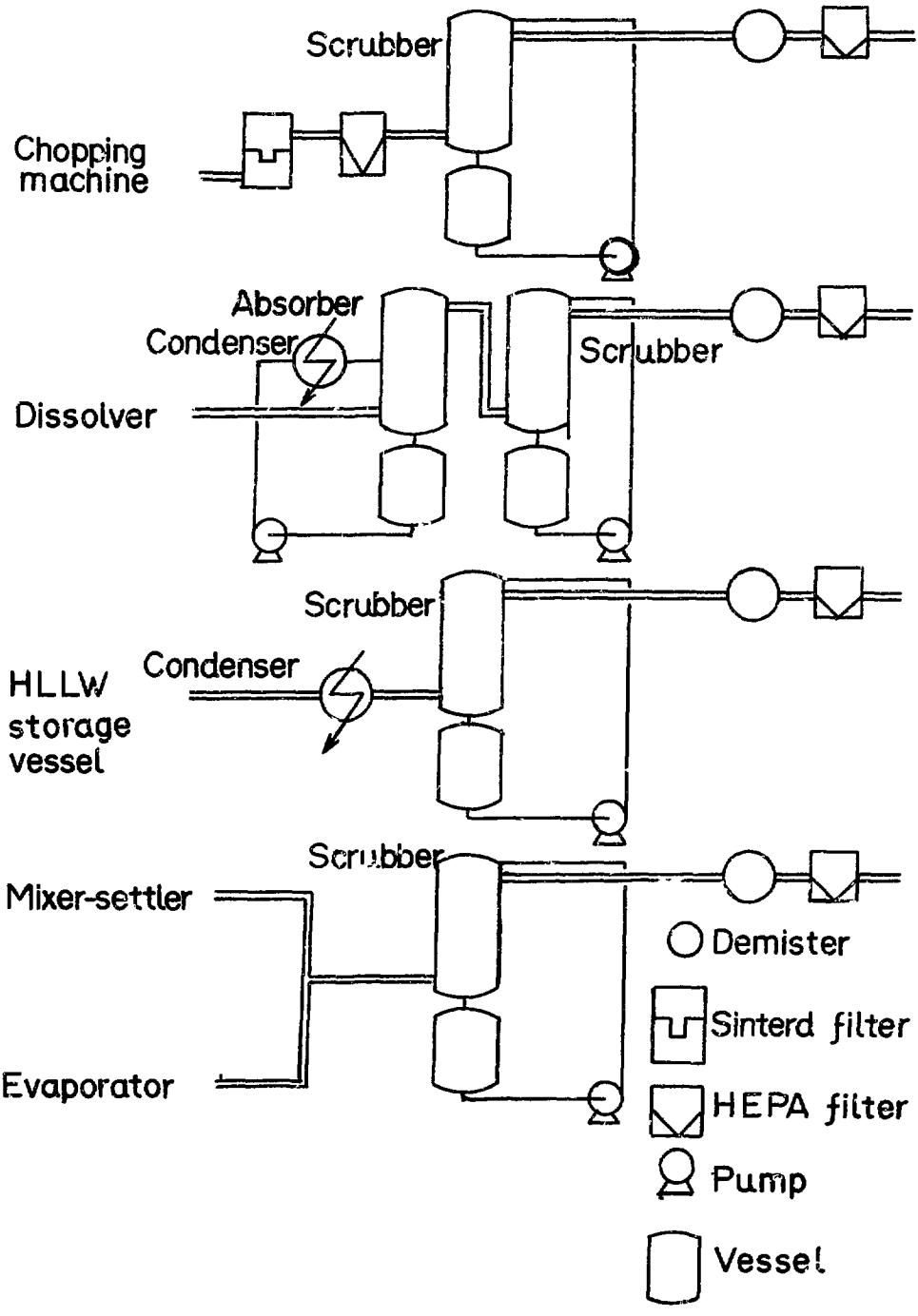

Figure 1 Off-gas treatment system in the Tokai plant

III. Iodine balance

The iodine balance has been examined using the hot operation data of the plant.

Almost all iodine involved in spent fuels is released into the DOG during the dissolution,[2] and absorbed into liquid phases in the condenser, the acid recovery column and the alkaline scrubber. There remains a small amount of iodine in the DOG after caustic scrubbing. The absorbed iodine in the recovered acid reaches to more than 50 % of the total iodine inventory, and about a half of the absorbed iodine released again to the VOG during the recovered acid concentration. The alkaline scrubber of the VOG is not so effective and it is supposed that the low DF is due to the possible presence of organic iodide.[3] About 10 % of the total iodine inventory is escaped from the alkaline scrubber.

The iodine contained in the COG and HLLW-VOG from each alkaline scrubber is negligible small in terms of the iodine balance. In the waste disposal facility, a part of absorbed iodine is released again to gas phases during treatment of the liquid waste from the main plant, however the amount of released iodine is small(Fig. 2).

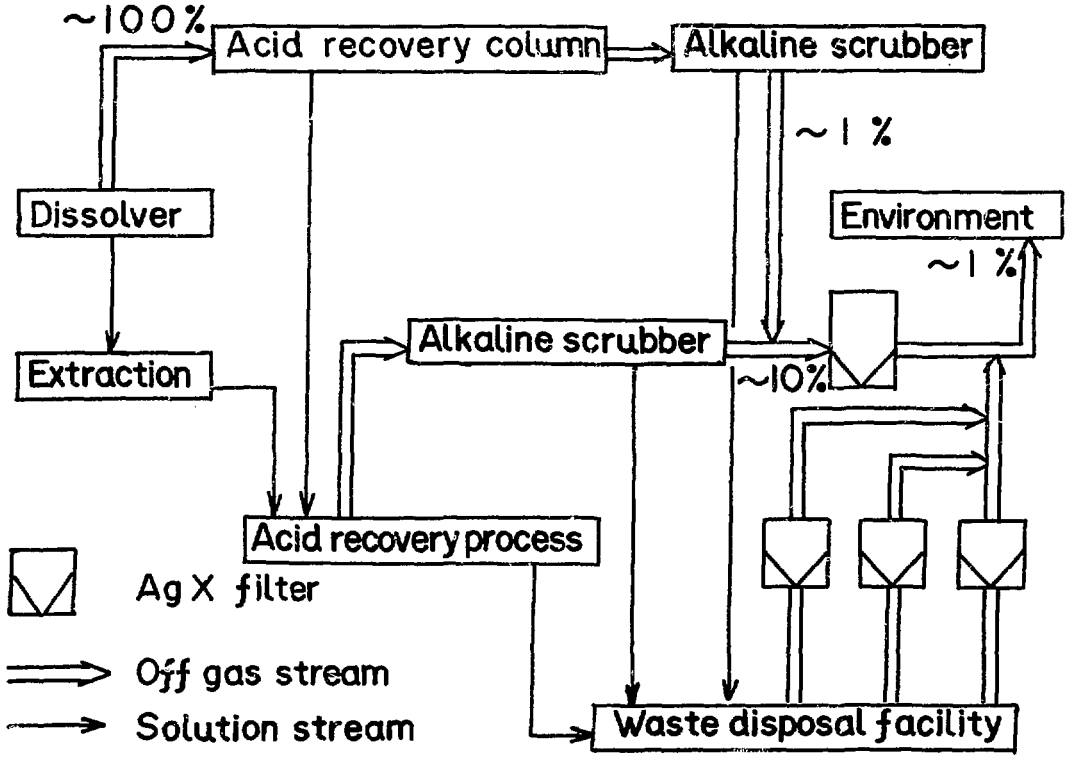

Figure 2 Iodine balance

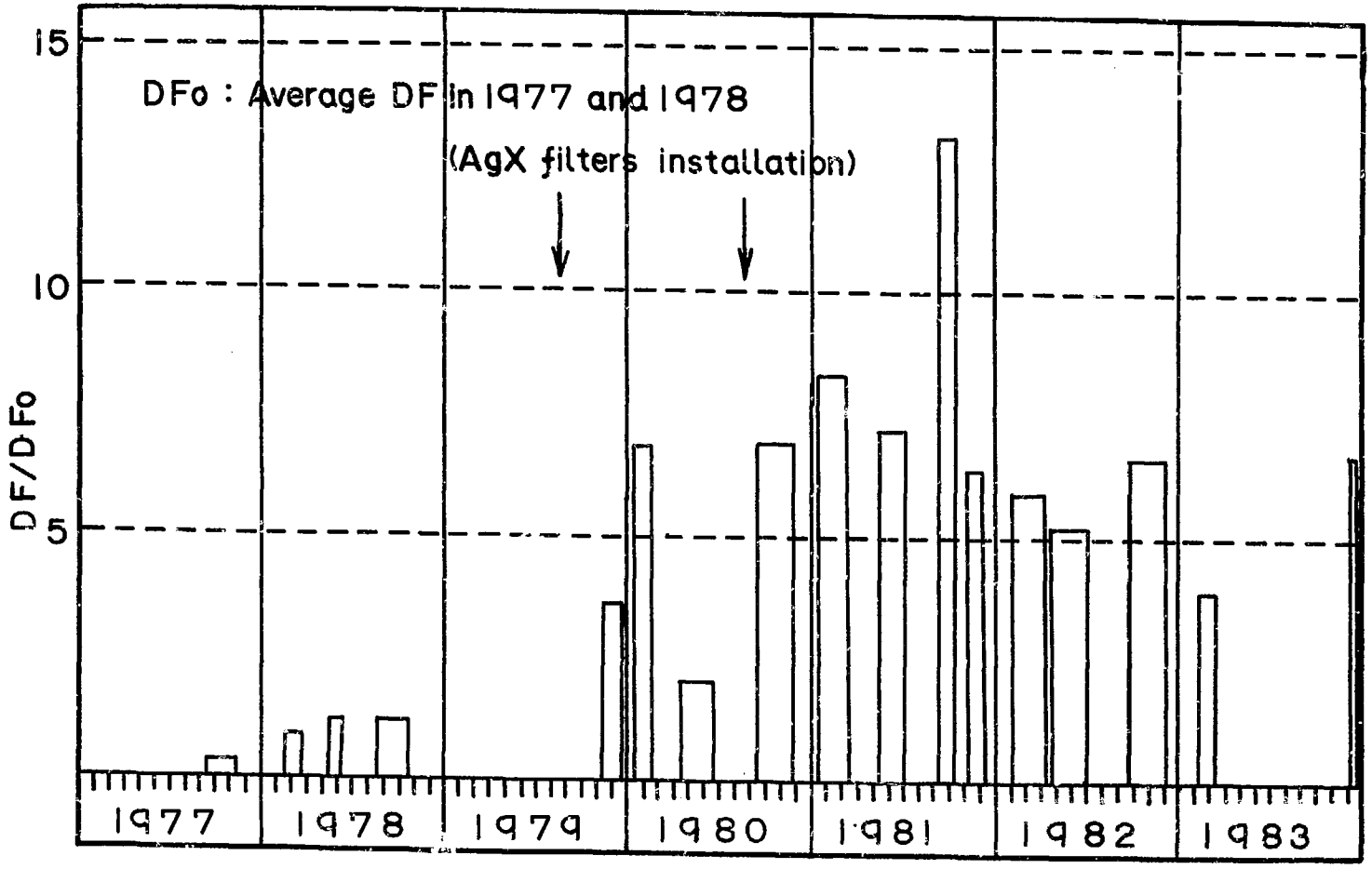

Figure 3 Total DF profile of the plant

IV. Total DF of the plant

Initially, total three AgX filters were installed ; one was at the ventilation duct where the COG, DOG, HLLW-VOG and VOG meet together in the main plant, and two were at the VOG ducts in the waste disposal facility. Based on the further investigation, one more AgX filter was installed for the off-gas from cells which contain open tanks in the waste disposal facility. Consequently the total DF of the plant was increased to be more than five times as large as before. Figure 3 shows the historical DF of the plant. The DF variation between campaigns is supposed to be caused mainly by changing the plant operation mode.

V. Operation condition of AgX filters

The iodine removal equipment consists of a heater, AgX filters and glass-fiber filters. The inlet off-gas is heated up to about 50 °C with an electric heater. Because of the low power of the heater and the hardware structure problems, the gas temperature is relatively low. The AgX bed depth is 50 mm. The glass-fiber filters are mounted downstream of AgX filters to prevent scattering AgX particles in case AgX filters are broken. The face velocity varies in 5 to 20 cm/sec since the filter size is the same for all iodine removal equipments. The iodine concentration is about 10^{-10} to 10^{-8} $\mu Ci/cm^3$ after caustic scrubbing, and the NOx concentration is about 5,000 ppm in the main plant and 10 ppm in the waste disposal facility (Table 2).

Table 2. Operation condition of present AgX filters

	I-129 conc. ($\mu Ci/cm^3$)	Temp (°C)	Humidity (%)	NOx conc. (ppm)	Face velocity (cm/sec)	DF
Main plant	max. 4×10^{-8} av. 5×10^{-9}	45	20	5000	20	10 ~20
Waste disposal facility	max. 3×10^{-8} av. 4×10^{-9}	35	60	10	5	70
	max. 4×10^{-9} av. 7×10^{-10}	40	40	10	5	10 ~30
	max. 5×10^{-9} av. 2×10^{-9}	40	50	10	17	30 ~60

VI. Problem on iodine removal

Although the iodine discharge to the atmosphere was reduced by AgX filters as described above, the DFs were not so high compared to values obtained by laboratory tests. Especially the DF in the main plant was the lowest one. It is supposed that the presence of organic iodide partly causes the low efficiency of AgX filters, because the organic iodide is less active to AgX than the elemental iodine.[4] It is probable that the organic iodide such as CH_3I is relatively rich in the main plant VOG after the treatment by caustic scrubbing. It is reported that the iodine reacts to impurities in nitric acid.[5] For the iodine in the recovered acid of the main plant, it may react to a trace of solvent which is probably retained in the liquid waste and recovered acid.

It is also supposed that the low efficiency of AgX filters is affected by the low temperature of operation condition. The gas temperature is restricted up to about 50 °C because of the electric capacity and so on, and the AgX seems to be exposed to other molecules such as NOx and H_2O. A considerable decrease of the DF was experienced in the waste disposal facility when a large amount of NOx was discharged. It is obvious that the relatively high NOx concentration in the main plant has influence on the AgX efficiency.

With regard to NOx interference, it is supposed that NO_2 reacts to H_2O on the surface of zeolite to form nitric acid[6] which may damage AgX and/or prevent iodine from reacting to silver in AgX. It was confirmed by laboratory test that heating the off-gas up to higher than 100°C expedites the reaction of CH_3I to AgX and reduces the influence of NO_2 and H_2O.

Now a new iodine removal system is prepared for the VOG in the main plant to reduce the iodine discharge to the environment. The AgX bed depth is 75 mm which is 1.5 times as thick as the present one, and the face velocity is about 20 cm/sec. The VOG will be heated up to about 150 °C. Since the demister and HEPA filters are already installed in the VOG, they are eliminated from the new equipment. The VOG will be treated by the present AgX and the new one in series. It is expected that the iodine discharge is reduced to about one half or less of the present value. The new iodine balance will be as shown in Figure 5.

VII. Iodine sampling

As a part of developing iodine removal techniques, the off-gas sampling and measurement procedures were investigated. The off-gas was drawn from the ventilation duct with a pump at a constant flow-rate and iodine was absorbed on a charcoal paper filter and charcoal cartridges. The charcoal both for filters and cartridges was impregnated with TEDA, and the bed depth of a cartridge was 20 mm. The face velocity was about 10 cm/sec and the sampling time was about one day. Iodine absorbed in charcoal was measured by gamma-ray counting for 40 keV with a NaI(Tl) scintilator or a Ge(Li) detector.

The iodine removal efficiency of more than 90 % was obtained

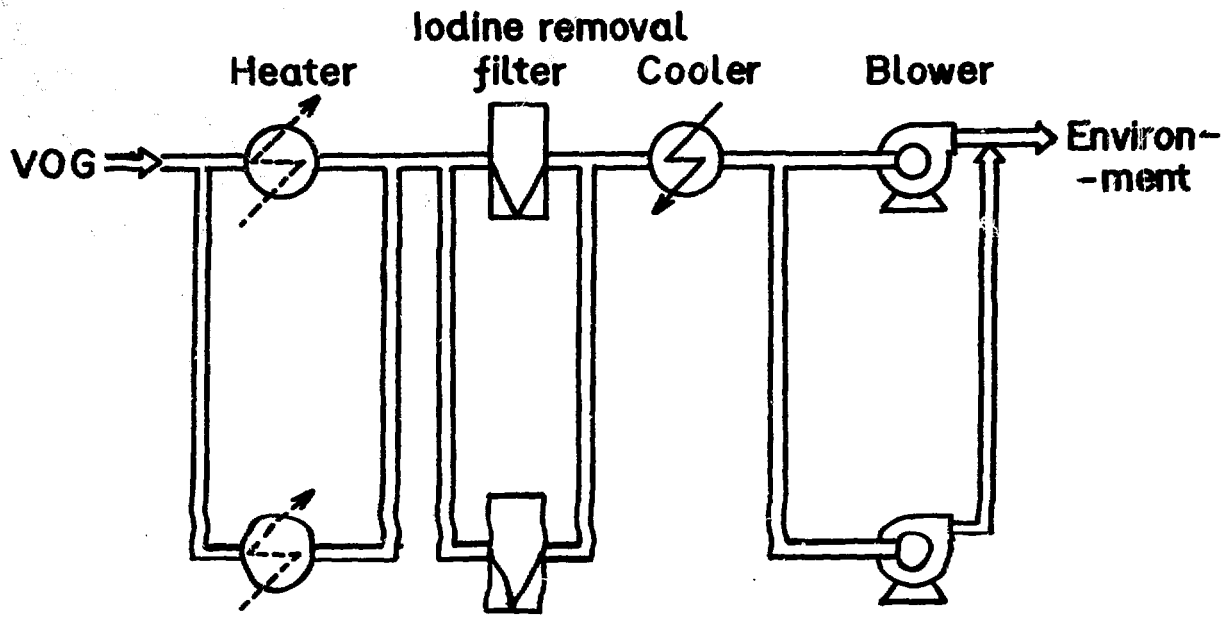

Figure 4 New iodine removal equipment for the VOG of the main plant

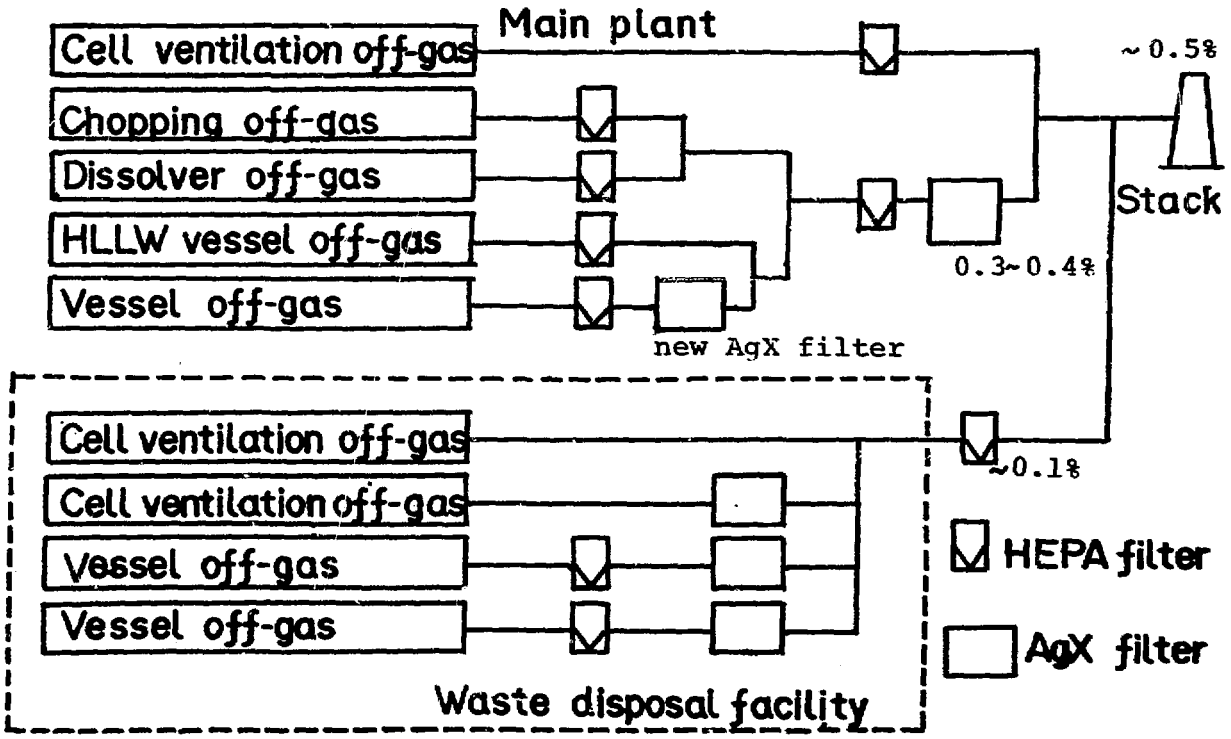

Figure 5 Estimated iodine balance after new AgX filter installation

by the combination of a filter paper and two cartridges for the off-gas from the waste disposal facility(Fig. 6). Also AgX cartridges were tested instead of the charcoal cartridge and it seems to be more effective than charcoal on iodine sampling even at room temperature. Nevertheless the gamma-ray energy is so low that the self-shielding effect is significant and the total detection efficiency is considerably low, which causes a relatively large measurement error. A possible improvement is to use thinner cartridges for suppressing the self-shielding effect and heat up the sampling off-gas to obtain the higher sampling efficiency for iodine.

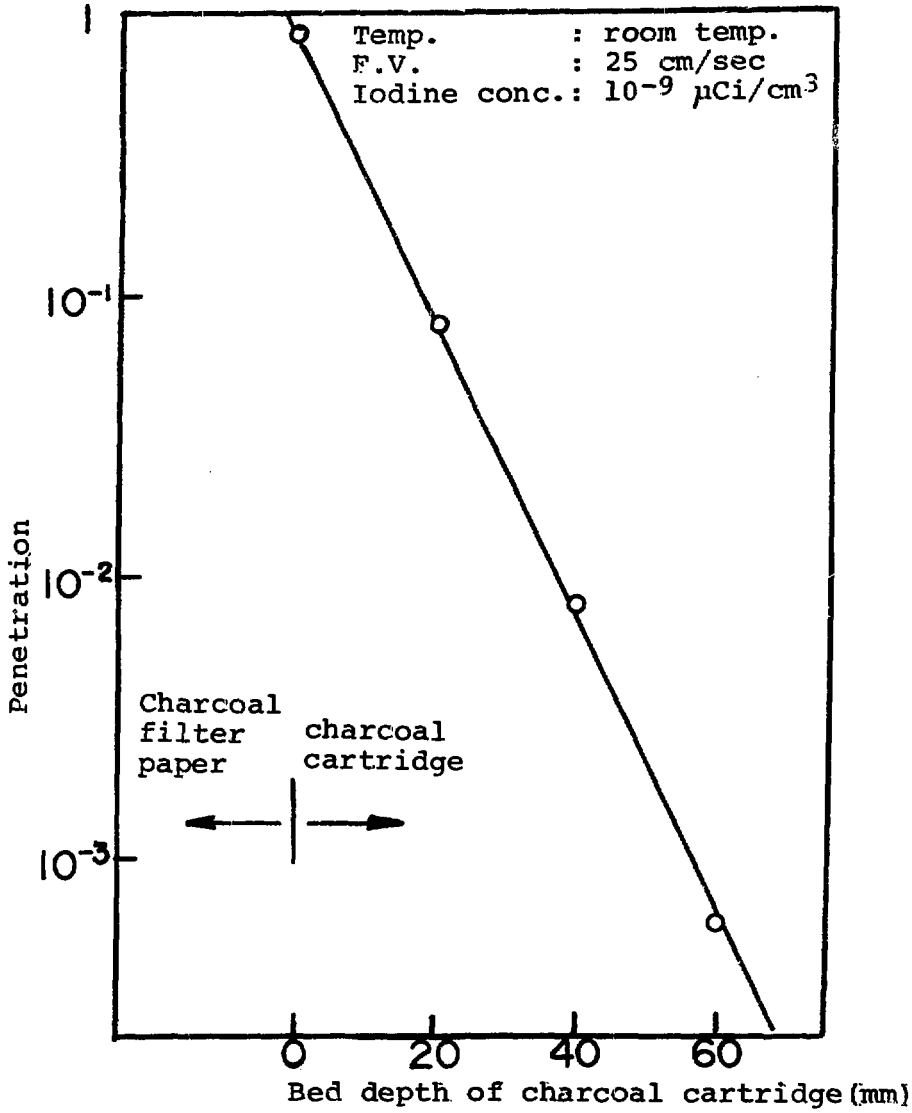

Figure 6 Penetration of iodine as a function of chrcoal bed depth

References

(1) Fukushima, M., Miyahara, K. and Matsumoto, K , "Iodine removal from the vessel off gas in Tokai reprocessing Plant", IAEA-SR-72/25(1982)

(2) Berg, R. and Schuttelkop, H., "Measurement of the distribution of ^{129}I in and its discharge from the Karlsruhe Reprocessing Plant", BNWL-TR-311(1977)

(3) Wilhelm, J.G. and Furrer, J., "Iodine separation in reprocessing plants", BNWL-TR-312(1978)

(4) Pence,D.T., "Summary report-Applications of silver zeolite for airborne iodine species removal from nuclear facility off gases", SAI-132-80-390-LJ(1980)

(5) Saeki, M., Numakura, K. and Tachikawa, E., "Carbon sources and formation mechanisms of organic iodides", Int. J. Appl. Radiat. Isot., 25, 407(1974)

(6) Kanazawa, T., et al.,"Mechanism of nitric acid generation on Ag-X zeolite", IAEA-SR-72/26(1982)

IODINE-129 PROCESS CONTROL MONITOR FOR EVAPORATOR OFF-GAS STREAMS

J. R. Burr and G. J. McManus
Westinghouse Idaho Nuclear Co.
Idaho Falls, Idaho

Abstract

The continuous monitoring of gaseous ^{129}I in evaporator off-gas at nuclear fuel reprocessing facilities is desirable from both regulatory and process control viewpoints. Although a continuous ^{129}I monitor for nuclear fuel reprocessing plant off-gas streams has already been developed, it needed to be evaluated under evaporator off-gas conditions. Characteristics of the off-gas that pose problems for ^{129}I monitoring include: 1) high concentrations of nitric acid mist, organics, and radionuclides which may interfere with ^{129}I detection, such as ^{137}Cs; 2) off-gas that is predominantly water vapor; and 3) ^{129}I in the form of liquid aerosols.

This paper reports on the development and evaluation of an ^{129}I monitor for evaporator off-gas using a laboratory-scale evaporator model. The work was performed in two phases: 1) a suitable monitor configuration was determined; and 2) a 2^4 factorial design experiment was performed to determine the monitor's response to HNO_3, organics, aerosols, and ^{137}Cs. A filter was used in the monitor configuration to vary aerosol concentrations. The concentrations of HNO_3, organics, and ^{137}Cs in the evaporator feed were also varied from low to high levels.

In the experimental monitor, a H_2O selective permeation device was used to dry the off-gas stream before it passed through a charcoal bed where the iodine was adsorbed. The bed was counted for ^{125}I with a NaI(Tℓ) detector.

Results of this study show that the monitor should be operated with a filter. Under high aerosol conditions, liquid buildup in the monitor prevented iodine from reaching the detector and thus decreased the response of the monitor. Organics increased the response of the monitor. This may be due to the formation of methyliodide which is not adsorbed on the monitor's surfaces as readily as I_2. HNO_3 and ^{137}Cs did not significantly affect the response of the monitor. The monitor had a detection limit of 6×10^{-9} μCi ^{129}I/cc for a 24 hour period.

Based on these observations, the monitor when operated with a filter, was demonstrated to be suitable for use in evaporator off-gas streams.

I. INTRODUCTION

Iodine-129 is one of the most environmentally significant radioisotopes emitted from nuclear fuel reprocessing and waste solidification facilities. The results of an ^{129}I process distribution study at the Idaho Chemical Processing Plant

(ICPP)[1] indicated that a significant fraction of the ^{129}I not volatilized during fuel dissolution eventually reached the Intermediate Level Waste (ILW) evaporator (Figure 1). The ILW evaporator is a batch operation which separates intermediate-level radioactive liquid waste into high-level and low-level liquid waste fractions. Non-volatile radionuclides are concentrated in the evaporator bottoms, while water vapor and some volatile radionuclides make up the evaporator overheads. Continuous monitoring of evaporator overheads for ^{129}I would supply the necessary information to retain ^{129}I in the evaporator bottoms, should a process control mechanism for the evaporator be developed.

Although a continuous ^{129}I monitor for nuclear fuel reprocessing plant off-gas streams has already been developed[2], it needed to be evaluated under evaporator off-gas conditions. Characteristics of the off-gas that pose potential problems for ^{129}I monitoring include:

1) High concentrations of organics, nitric acid mist, and radionuclides such as cesium-137 (a potential interference in ^{129}I detection);

2) A gas stream that is predominantly water vapor;

3) ^{129}I may be present the form of liquid aerosols.

The development and evaluation of the evaporator monitor was done in two phases. First, the proper monitor configuration was determined. For this determination, a laboratory-scale model of an evaporator was assembled to simulate evaporator off-gas.

Second, a 2^4 factorial design experiment was performed to determine the monitor's response to aerosols, organics, HNO_3, and ^{137}Cs. A 2^4 factorial design is a statistical method used to examine the response of the monitor as four factors are varied between two levels. A glass fiber filter was placed in the evaporator off-gas line to reduce aerosol concentrations to a low level. No filter in-place corresponded to high aerosol conditions. The levels used for the other three variables were 10% tri-butyl phosphate (TBP) in n-dodecane (0, 14mg TBP/L); HNO_3 (0, 0.5 mol/L); and ^{137}Cs (0, 3.3 μCi/L). These concentrations are similar to those found in actual plant feeds. The effect of each factor on both the response and reliability of the monitor was examined.

II. EXPERIMENTAL APPARATUS CONFIGURATION

The conceptual design of the evaporator monitor is shown in Figure 2. An off-gas stream is dried as it passes through a water selective permeation device. Then the off-gas flows through a charcoal bed where the iodine in the gas is adsorbed to the charcoal. The bed is counted for iodine with a thin NaI(Tℓ) detector (1 mm x 25 mm FIDLER).

Figure 3 shows the final configuration of the experimental apparatus; it consists of two main components, the ILW evaporator model and the ^{129}I monitor. The evaporator model was operated as a batch process. Carrier iodine-127 and 0.9 μCi of ^{125}I were added to 1600 mL of distilled water feed. This solution was charged to the evaporator, filling the heating vessel and storage tank. As the feed

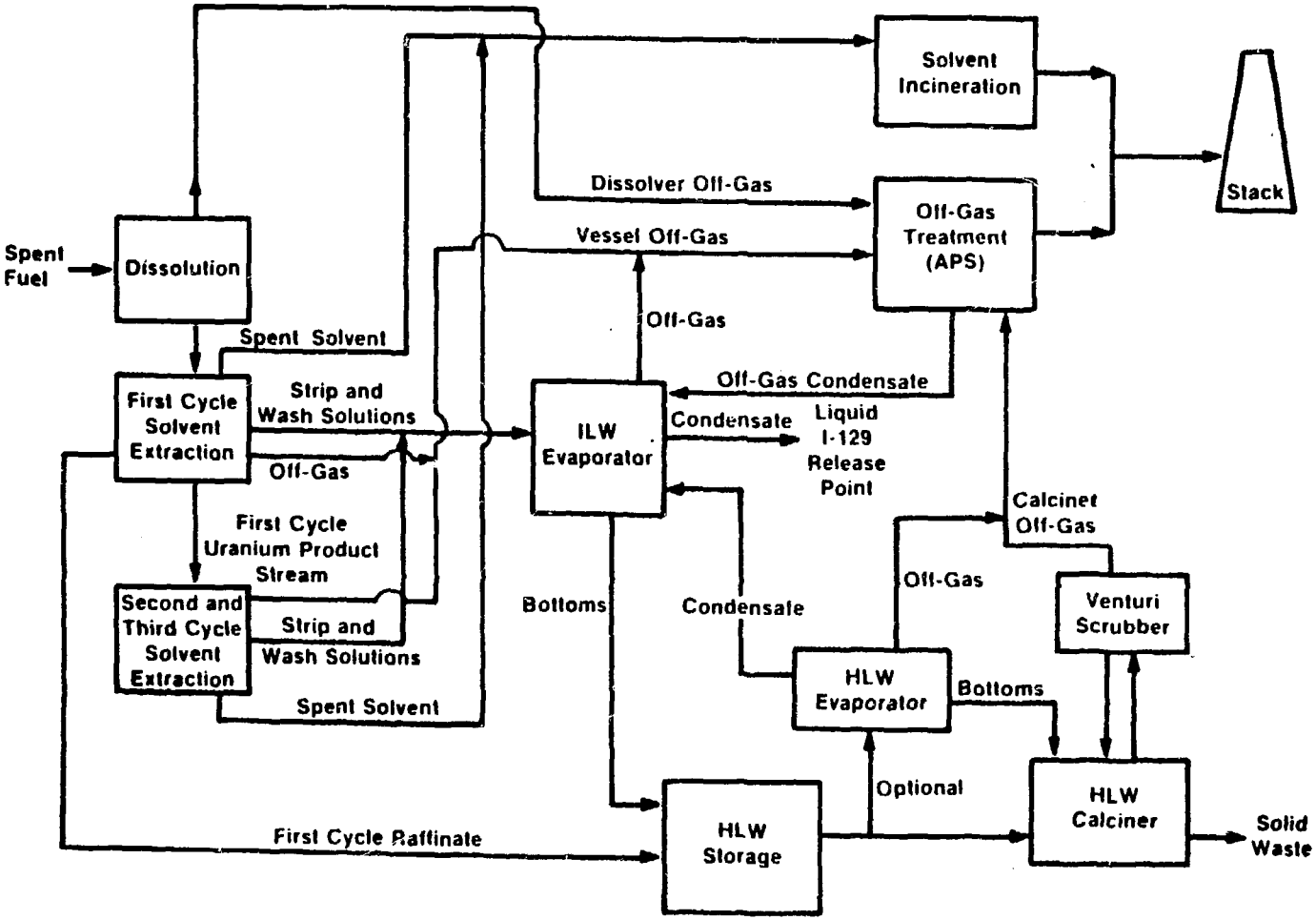

Figure 1. ICPP Pathways Block Diagram

ICPP S-7882

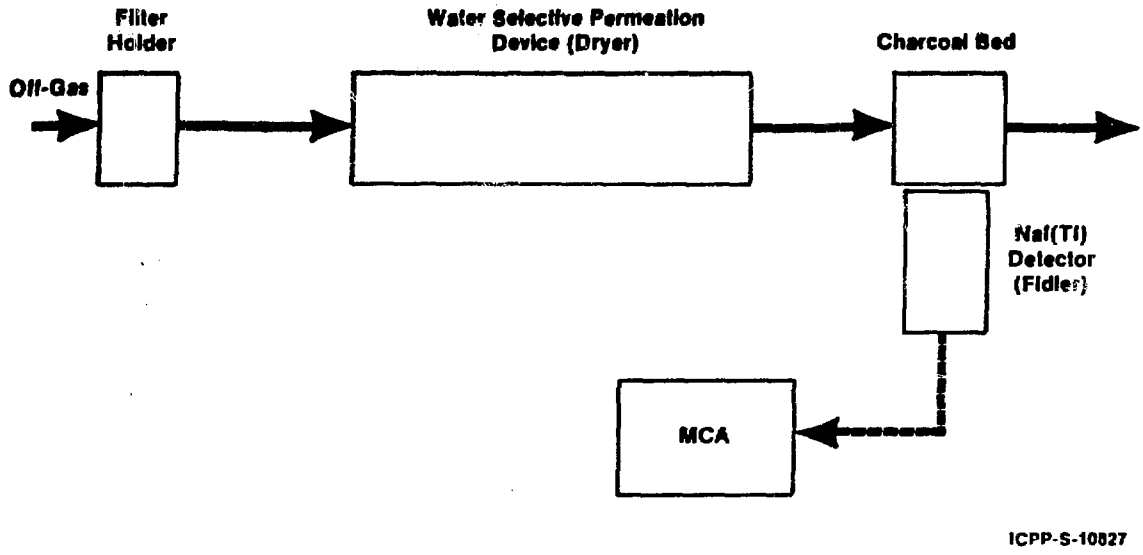

FIGURE 2. CONCEPTUAL MONITOR DESIGN

was heated under 6 in. Hg vacuum, the vapor flowed at 1.1 L/min through the mist eliminator to the off-gas condenser. Cooler liquid from the storage tank flowed to the heating vessel to replace vaporized liquid. Off-gas condensate was collected in the condensate vessel.

About 60% of the gas stream leaving the evaporator was drawn into the ^{129}I monitor upstream of the condenser. The gas stream to the ^{129}I monitor flowed through a stainless steel filter holder and into a water selective permeation device (permatube drier). As shown in Figure 4, the permatube drier contains many small tubes made of perfluorosulfonic acid polymer (Nafion®, Du Pont) membrane in a "tube and shell" configuration. A dry air stream flowed counter-currently at 6 L/min on the outside of the polymer tubing. As the off-gas passed through the permatube, water vapor permeated into the purge stream, but the majority of iodine remained in the product off-gas stream.

The ^{125}I in the product stream was collected by a 60 cm^3 triethylenediamine (TEDA) impregnated charcoal bed, and the 27 KeV X-ray was measured with a 1mm thick by 25mm diameter NaI(Tl) detector (FIDLER). The observed countrate was recorded with an ND60 programmable multichannel analyzer. An additional charcoal bed was used to collect any ^{125}I in the purge stream leaving the permatube drier.

Initial operation of the evaporator and monitor showed that the gas stream cooled sufficiently to condense water in the charcoal beds and permatube drier. Water in the charcoal beds may have caused migration of iodine through the bed,

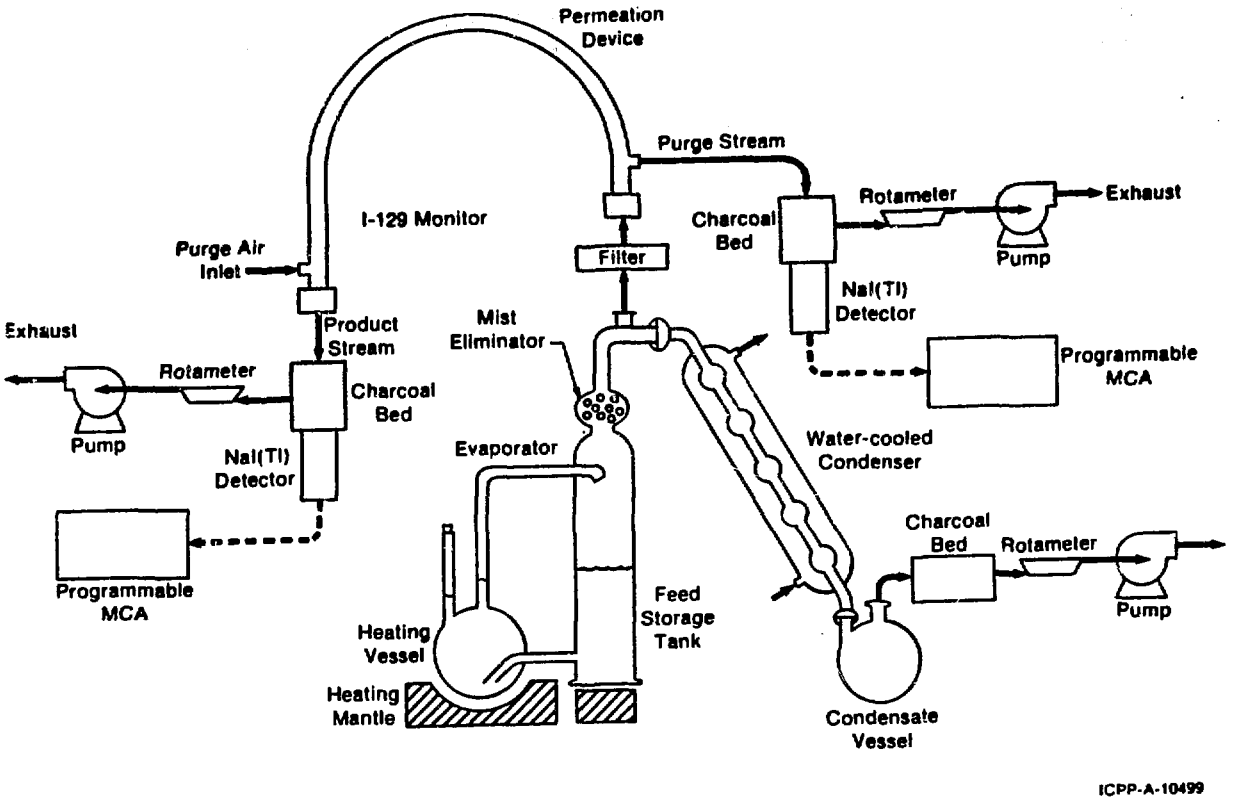

Figure 3. Experimental I-129 Monitor and Evaporator

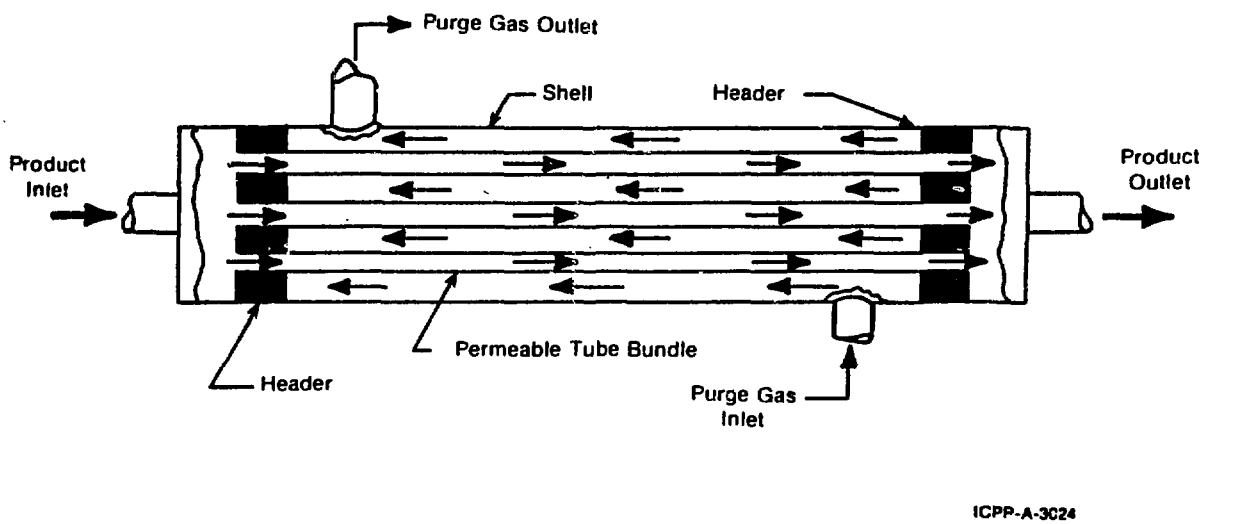

Figure 4. Schematic Diagram of a Permeation Device

and changed the counting geometry. Water in the permatube drier prevented iodine from reaching the charcoal bed and decreased the gas flow in the permatube drier. Both these conditions were unacceptable for continous iodine monitoring. These conditions were eliminated by heating the permatube and the filer holder to 75 degrees C.

III. 2^4 FACTORIAL DESIGN

Once it was determined that the experimental apparatus could be used successfully to test for ^{125}I in off-gas, a 2^4 factorial design experiment was performed. A total of 16 tests were completed, as shown in Table I. Use of a filter in the off-gas line entering the ^{129}I monitor corresponds to low aerosol conditions. No filter simulated high aerosol conditions. During each test, 4 to 9 individual counts were collected over time periods between 60 minutes and 190 minutes. Also, the amount of ^{125}I which reached the monitor during each 2^4 factorial test was determined.

To determine the amount of ^{125}I which reached the monitor, a sample of the evaporator feed remaining at the end of a run was counted for ^{125}I with a LEPS (Low Energy Photon Spectrometer) detector and the total amount of ^{125}I remaining in the feed was calculated. The amount of ^{125}I volatilized from the feed was determined by subtracting the amount of ^{125}I remaining in the feed from the amount initially added. Since the flowrates to the ^{125}I monitor and condenser were measured, multiplying the amount of volatilized ^{125}I by the fraction of the off-gas flow that entered the monitor gave the amount of ^{125}I that reached the monitor.

TABLE I

2^4 FACTORIAL EXPERIMENTAL DESIGN

		Evaporator Feed Concentration		
Test Number	Filter used	TBP (mg/L)	HNO_3 (M)	^{137}Cs (μCi/L)
1	No	0	0	0
2	Yes	0	0	0
3	No	14	0	0
4	Yes	14	0	0
5	No	0	0.5	0
6	Yes	0	0.5	0
7	No	14	0.5	0
8	Yes	14	0.5	0
9	No	0	0	3.3
10	Yes	0	0	3.3
11	No	14	0	3.3
12	Yes	14	0	3.3
13	No	0	0.5	3.3
14	Yes	0	0.5	3.3
15	No	0	0.5	3.3
16	Yes	0	0.5	3.3

To evaluate the response of the monitor for the 16 tests, the net countrate for each run was divided by the amount of ^{125}I reaching the monitor. This gave a normalized response for each run.

To evaluate the reliability (variability) of the monitor, the countrates were plotted against time (as shown in Figure 5), and the data were fit to a logarithmic curve of the form,

$$y = a + b\,(\ln x).$$

Where y equals detector response, x equals time of response, and a and b are coefficients. This form was chosen because it produced the best least squares fit of the data.

The correlation coefficient (r) is an estimate of how well the experimental data correlate to a logarithmic fit of the data. Thus, the quantity $1-r^2$, which is directly proportional to the variability of the response of the monitor, was calculated for each test. Lastly, the effects of aerosol content (filter), organics, HNO_3 and ^{137}Cs on variability and response were determined using an analysis of a 2^4 factorial design detailed in standard textbooks[3].

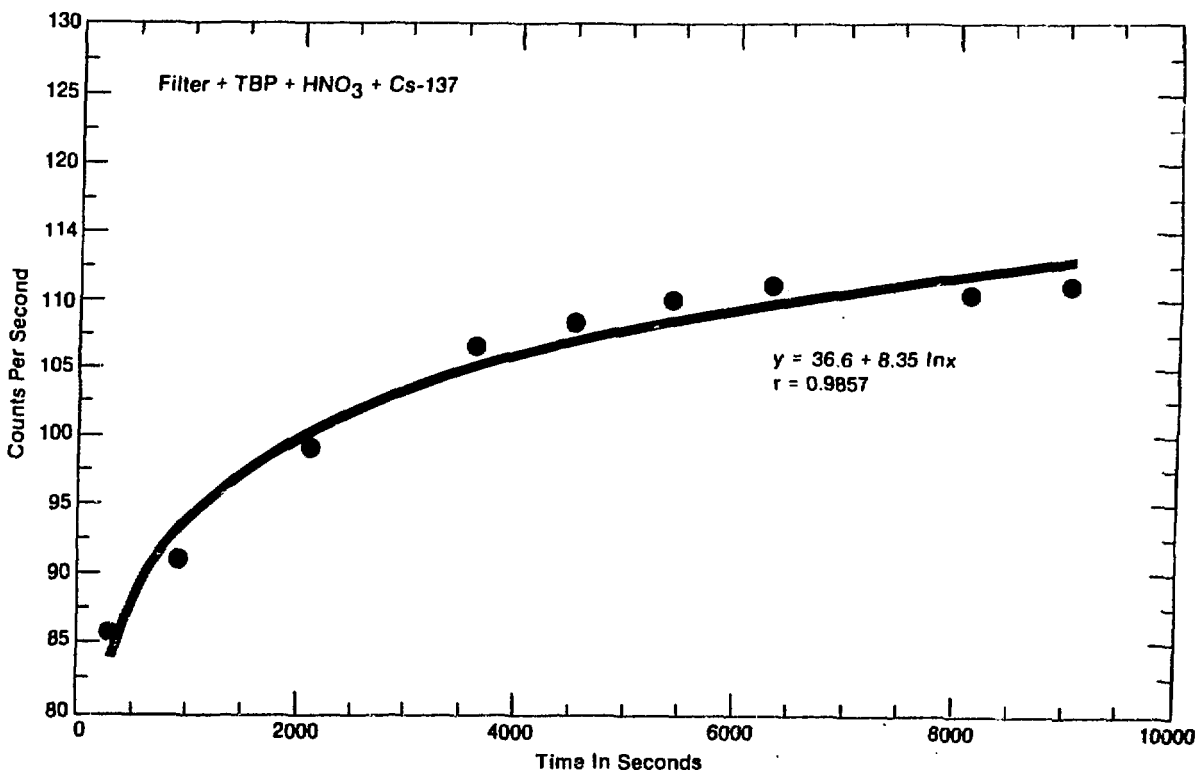

ICPP-A-10515

Figure 5. Response vs. Time - Test 16

IV. RESULTS

The results of the 2^4 factorial design experiment are summarized in Table II.

TABLE II

RESULTS OF THE 2^4 FACTORIAL EXPERIMENT

Test Number	Filter used	Organics (mg TBP/L)	HNO_3 (M)	^{137}Cs (μCi/L)	Response (cps/μCi ^{125}I)	Variability $(1-r^2)X$ 100%
1	No	0	0	0	21.8	13
2	Yes	0	0	0	9.2	36
3	No	14	0	0	6.2	33
4	Yes	14	0	0	93.9	18
5	No	0	0.5	0	5.5	1
6	Yes	0	0.5	0	11.9	12
7	No	14	0.5	0	15.1	11
8	Yes	14	0.5	0	106.5	9
9	No	0	0	3.3	11.6	37
10	Yes	0	0	3.3	23.6	25
11	No	14	0	3.3	13.5	30
12	Yes	14	0	3.3	70.4	14
13	No	0	0.5	3.3	5.1	58
14	Yes	0	0.5	3.3	75.5	34
15	No	14	0.5	3.3	5.2	24
16	Yes	14	0.5	3.3	75.1	3

Table III summarizes the effect of each factor as calculated using the Yates Technique[3] for a 2^4 factorial design.

TABLE III

INDIVIDUAL EFFECTS FOR FILTER, TBP, HNO_3 AND ^{137}Cs

Factor	Effect on Response (CPS/μCi)	Effect on Variability $(1-r^2)$ x 100%
Filter	47.8	-7
Organics	27.7	-9
HNO_3	6.1	-7
^{137}Cs	1.3	11

The results in Table III show that the filter had a very large effect on the response of the monitor. It was observed that this effect corresponded to low iodine collection in the purge stream charcoal bed. The amount of ^{125}I on each of the product and purge charcoal beds was determined at the end of each test, and the ratio of ^{125}I on the purge bed to ^{125}I on the product bed was calculated. This ratio was 0.49 + 0.30 for the tests without a filter, and 0.03 $\pm$ 0.02 for the tests with a filter. Thus, when a filter was used, iodine losses to the purge stream were less than 5% of the iodine that reached the product stream detector.

Because of high liquid aerosol conditions, liquid may have collected in the permatube drier and transported ^{125}I into the purge gas stream at a greater rate. Therfore, when the filter was used and aerosol levels were lower, less liquid collected in the permatube drier and little ^{125}I was transported to the purge stream. This may explain the increased amount of iodine in the purge stream when a filter was not used. and indicates the monitor should be operated with a filter.

Since it was determined that the monitor be operated with a filter to minimize iodine losses to the detector, only the data from runs with a filter were used to determine the effects and significance of the other three variables. This data was combined in three 2^2 factorial designs to determine the effects for organics, HNO_3, and ^{137}Cs and their interactions. The results are shown in Table IV. The mean of the response data for the filter runs is 58 cps/μCi with a standard deviation of $\pm$38 cps/μCi. The large effect of organics (+ 56 cps/μCi) is clearly significant while those for HNO_3 and ^{137}Cs are not.

The large TBP effect may be due to the formation of methyl iodides which are not adsorbed to the permatube walls as readily as I_2. Because of the increase in a response due to high organic concentrations, the monitor would need to be calibrated according to the plant operating experience with respect to organic concentrations.

Table IV

EFFECTS OF 2^2 FACTORIAL DESIGN

Factor	Effect (cps/μCi)
Organics	+56
HNO_3	+18
^{137}Cs	+6
Organic + HNO_3 Interaction	-9
Organic + ^{137}Cs Interaction	+32
HNO_3 + ^{137}Cs Interaction	+10

Although no significant effect was observed for ^{137}Cs, little ^{137}Cs was liberated from the feed. For several tests, the product and purge charcoal beds were counted using a LEPS detector. No appreciable amounts of ^{137}Cs were detected on either bed. By counting samples of the feed before and after each ^{137}Cs run, it was determined that ^{137}Cs was concentrated in the bottoms. It should be noted that while no ^{137}Cs was collected on the charcoal beds during the laboratory evaluation, it is possible that during actual plant operations ^{137}Cs may be deposited on the charcoal beds and interfere with the detection of ^{129}I.

The effect of each variable on the variability of the monitor's response is shown in Table III. Using the t distribution to calculate statistical significance at the 95% condifence level, it was determined that any effect on variability greater than 12% was statistically significant. None of the effects of the four variables or their interactions significantly affected the monitor's variability.

V. CONCLUSIONS

The major conclusions of this work were:

1) The evaporator monitor should be operated with filter, to insure maximum iodine transport to the detector;

2) The presence of organics significantly increased the response of the monitor; the monitor should be calibrated according to organic concentrations in the evaporator feed;

3) The presence of HNO_3 had no statistically significant effect on the response of the monitor;

4) Under conditions of the experiments, ^{137}Cs remained in the evaporator bottoms, and no effect of ^{137}Cs on the monitor was observed;

5) The monitor had a detection limit of $6 \times 10^{-9} \frac{\mu Ci}{cc}$ ^{129}I for a 24 hour period.

In conclusion, based on the results of the laboratory evaluation, the monitor, when used with a glass fiber filter, was demonstrated to be suitable for use in evaporator off-gas streams.

VI. REFERENCES

1. G. J. McManus, F. A. Duce, S. J. Fernandez, and L. P. Murphy, A Model of Iodine-129 Process Distributions in a Nuclear Fuel Reprocessing Plant, ENICO-1108, April 1982.

2. L. P. Murphy, F. A. Duce, and S. J. Fernandez, Continuous Tritium, Carbon-14, Iodine-129, and Kryton-85 Monitor for Nuclear Facility Off-Gas, ENICO-1092, October 1981.

3. R. E. Walpole and R. H. Meyers, Probability and Statistics for Engineers and Scientist, McMillan Co., New York 1968, p. 447.

4. J. S. Hunter, Design of Experiments Course, Factorial Designs, No. 4, Westinghouse Electric Corporation, 1968, pp. 62-82.

CONTINUOUS CHEMICAL COLD TRAPS FOR REPROCESSING OFF-GAS PURIFICATION

E. Henrich, U. Bauder, H.J. Steinhardt, W. Bumiller

Kernforschungszentrum Karlsruhe, Institut für Heisse Chemie,
Fed. Rep. Germany

ABSTRACT

Absorption of nitrogen oxides and iodine from simulated reprocessing plant off-gas streams has been studied using nitric acid and nitric acid/hydrogen peroxide mixtures at low temperatures. The experiments were carried out at the laboratory and on the engineering scale. The pilot plant scale column has 0.8 m diameter and 16 absorption plates at 0.2 m spacing. Cooling coils on the plates allow operating temperatures down to -60°C. The NO concentration in the feed gas usually has been 1% by volume and the flow rate 4-32 m^3 (STP) per hour. The iodine behaviour has been studied using I-123 tracer.

1. Results using 90 weight % HNO_3 at operating temperatures down to -55°C: Residual NO_x concentrations < 1 ppm have been obtained at -55°C even from an O_2-free off-gas. Iodine decontamination factors have been $\geq 10^4$.

2. Results using 50 weight % HNO_3 plus a slight stochiometric excess of H_2O_2 in respect to the NO in the feed gas at operating temperatures down to -18°C: Residual NO_x concentrations < 100 ppm are possible even from an O_2-free off-gas. Most of the residual NO_x is NO_2. The H_2O_2 prevents the decomposition of HNO_2 by oxidation to HNO_3. Iodine remains in the elementary form and distributes between the gas and the acid phase according to the operating conditions.

3. Results using 30 weight % HNO_3 plus a slight stoichiometric excess of H_2O_2 at operating temperatures down to -35°C: Residual NO_x concentrations of some 100 ppm have been obtained from air or an O_2-deficient gas stream. Most of the residual NO_x is NO. At the operating conditions no iodine oxidation occurs.

4. Results using 5 weight % HNO_3 plus a slight amount of H_2O_2 at operating temperatures down to 0°C: The conventional nitric acid scrub is improved with H_2O_2 and lower temperatures.

5. Results after O_3 addition: After addition of a slight O_3 excess to the feed gas, residual NO_x is oxidized to N_2O_5 and absorbed completely. Iodine is oxidized to an oxide mist.

The chemistry of the processes and the advantages and disadvantages in correlation to the various applications for an off-gas purification in a reprocessing plant are compared and discussed. The processes are compatible with the PUREX process and do not produce additional waste.

1. INTRODUCTION

In the course of the off-gas purification steps in a fuel reprocessing plant (FRP) the less volatile noxious constituents are separated stepwise from the more volatile carrier air. Continuous condensation or absorption in solvents are customary removal operations at higher concentrations; discontinuous adsorption on solids or freeze-out in cold traps are used at lower concentrations. The recovery of more reactive components can be supported by the process inherent

chemistry or additional process compatible chemicals, which aid to produce less volatile or more soluble species. An example is the NO; it is oxidized in the gas phase to NO_2 and converted to HNO_3 and HNO_2 after absorption in dilute nitric acid.

Most of the typical constituents of a FRP off-gas are simultaneously present in the dissolver off-gas (DOG) and the vapour pressures /1/ are shown in Fig.1. The off-gas components can be sub-divided into three groups according to their volatility: the very volatile carrier gases, the less volatile rare gas fission products (FP) plus CO_2 and N_2O and the least volatile aqueous phase constituents plus FP halogens and the radioactive aerosols.

At present, the DOG is released after highly efficient aerosol and efficient iodine removal; only the bulk of NO_x and water or nitric acid vapours are recovered. The usual sequence of operations is off-gas scrubbing with dilute nitric acid at about ambient temperature followed by an efficient aerosol filtration and iodine recovery /2/. Additional recovery of the rare gases and C-14 as CO_2 may be required in future plants /3/.

Prior to the usual rare gas recovery steps /4/, the aqueous phase components must be removed to the trace level. Generally solid sorbents or cold traps (defrostable feed gas coolers) are used to achieve this aim. Taking into account the DOG composition and the oxidation of NO to the less volatile NO_2, the aqueous phase constituants and the FP halogens can be adequately removed by condensation and desublimation in a cold trap at temperatures between -130 and -140°C. An additional deentrainment pad could prevent carry-over of solid particles. Low temperatures considerably improve the separation efficiency and selectivity.

Sufficient or even improved separation efficiency and selectivity can be obtained with special sorbents at temperatures above the condensation and desublimation points and sometimes even without refrigeration. The disadvantages of such processes are connected to the presence of solids: The operating mode is discontinuous, as the loaded sorbent must be regenerated periodically in a temperature or pressure swing operation or with an additional desorption gas. Two pieces of equipment are required at least and heat exchange in large sorbent beds is not simple. Small volumes of regeneration gas can be recycled into the process. At frequent regeneration cycles large volumes of regeneration gas are produced and released under supervision via the stack. Accidentally spoiled or contaminated sorbents must be replaced remotely.

The separation efficiency and selectivity of suitable liquid solvents is comparable to the solid sorbents /5/. Solvents are preferred because of the convenient continuous operating mode. Suitable solvents are compatible with the 'Purex'process and either constituents of the aqueous or the organic process streams. They can be recycled into the process without producing secondary waste streams.

Aqueous nitric acid solutions are an almost perfect solvent for water and nitric acid vapours or NO_2. Only the iodine solubility is relatively low and prior bulk iodine removal from a DOG is desirable. The distribution coefficients for the various off-gas components /6/ in Fig.2 demonstrate the separation selectivity. The more volatile components prefer the gas phase. Efficiency and selectivity increase at lower temperatures in order of the volatility.

Lower temperatures and refrigeration equipment are required anyway to achieve an efficient rare gas recovery. A stepwise temperature decrease in the upstream off-gas purification train is a natural measure. Therefore, low temperature

absorption using a more concentrated nitric acid is being investigated on the engineering scale /7/. The use of cold scrubs has advantages, if a more thorough or reliable off-gas purification downstream from the aerosol, bulk iodine and NO_x removal steps is necessary or desirable.

2. CHEMICAL BASIS OF THE LOW TEMPERATURE SCRUBS

A comparison of cold scrubs with the conventional NO_x recovery process using dilute nitric acid at atmospheric pressure and about ambient temperature /8,9,10/brings the differences into sharper focus. The simplified NO_x absorption mechanism is explained in Table 1.

1. GAS PHASE OXIDATION OF NITRIC OXIDE NO
$2\,NO + O_2 \longrightarrow 2\,NO_2$;
rate law $\dot{NO} = -k\,NO^2 \cdot O_2$; low rate at low partial pressures, negative temperature coefficient
2. GAS PHASE DIMERIZATION OF NITROGEN DIOXIDE NO_2
$2\,NO_2 \longrightarrow N_2O_4$;
fast equilibrium, increasing degree of dimerization at lower temperatures
3. LIQUID PHASE HYDROLYSIS OF DINITROGEN TETROXIDE N_2O_4
$N_2O_4 + H_2O \rightleftharpoons NO_3^- + HNO_2 + H^+$;
$\left(N_2O_4 + H_2O \rightleftharpoons NO_3^- + H_2NO_2^+;\right.$
$\left.H_2O \rightleftharpoons NO_3^- + NO^+;\right)$
equilibrium on the right side in ~12 M HNO_3, on the left side in ~16 M HNO_3
4. LIQUID PHASE DECOMPOSITION OF NITROUS ACID HNO_2
$3\,HNO_2 \longrightarrow NO_3^- + 2\,NO + H^+ + H_2O$
HNO_2 steady state concentration depends on the operating conditions
SUM: $2\,H_2O + 4\,NO + 3\,O_2 \longrightarrow 4\,HNO_3$;

KfK IHCH

Table 1 SIMPLIFIED NO-RECOMBINATION REACTIONS

Reaction 1: The volatile and scarcely soluble NO is oxidized in the gas phase to NO_2

Reaction 2: Partial dimerization of NO_2 produces some less volatile and more soluble N_2O_4

Reaction 3: The N_2O_4 is absorbed in the dilute nitric acid and quickly hydrolyzed to nitric acid HNO_3 and nitrous acid HNO_2

Reaction 4: When the HNO_2 has attained a low steady state concentration depending on the operating conditions, HNO_2 decomposition produces HNO_3 and regenerates 1/3 of the original NO, which escapes to the gas phase.

The scrub acid must be cooled to remove the reaction heat. At NO_x concentrations below about 1% by volume, direct HNO_2 (or N_2O_3) absorption from the off-gas is a competitive or predominant recovery mechanism. According to the sum reaction, the NO_x can be completely recovered as HNO_3 for process recycle, if sufficient oxygen in the off-gas and extended residence time in the scrubber are available.

The slow NO-oxidation at lower partial pressures in the gas phase is the 'bottle neck' of an efficient NO_x recovery. The usual off-gas rates and acceptable

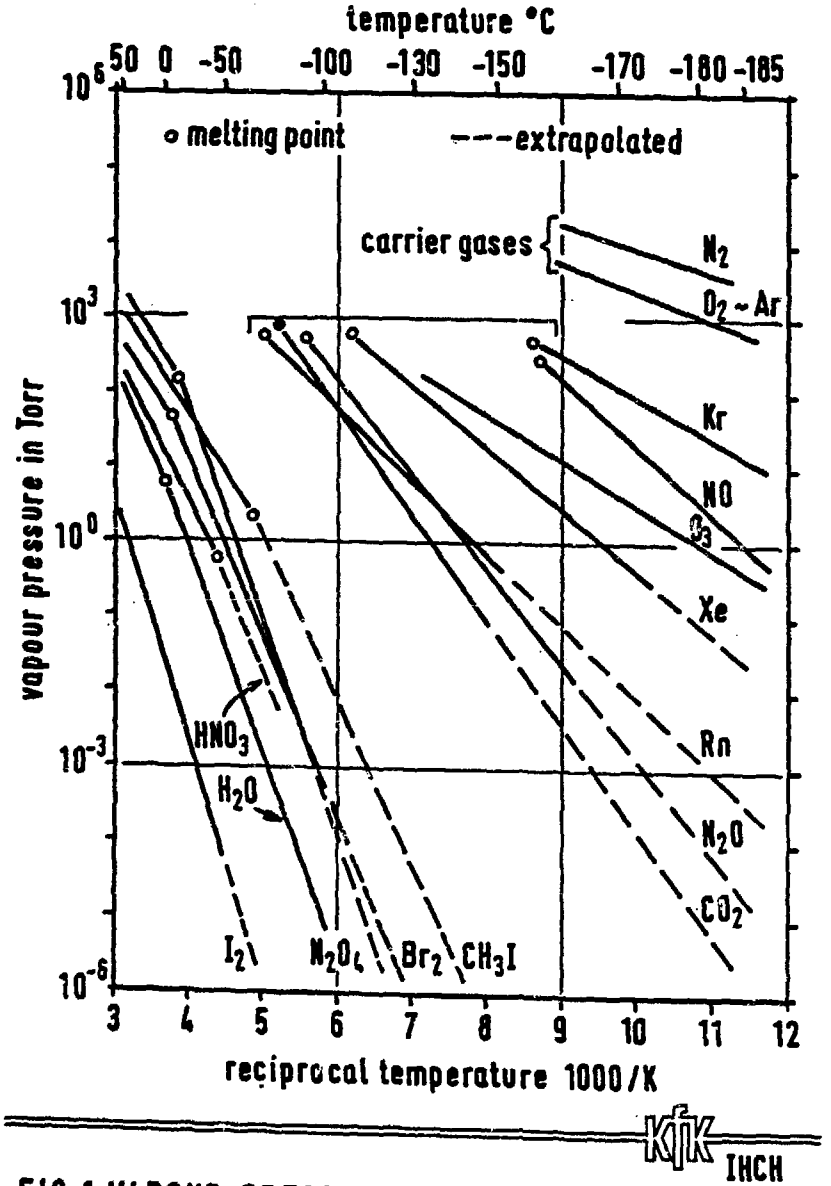

FIG.1 VAPOUR PRESSURE OF OFF-GAS COMPONENTS

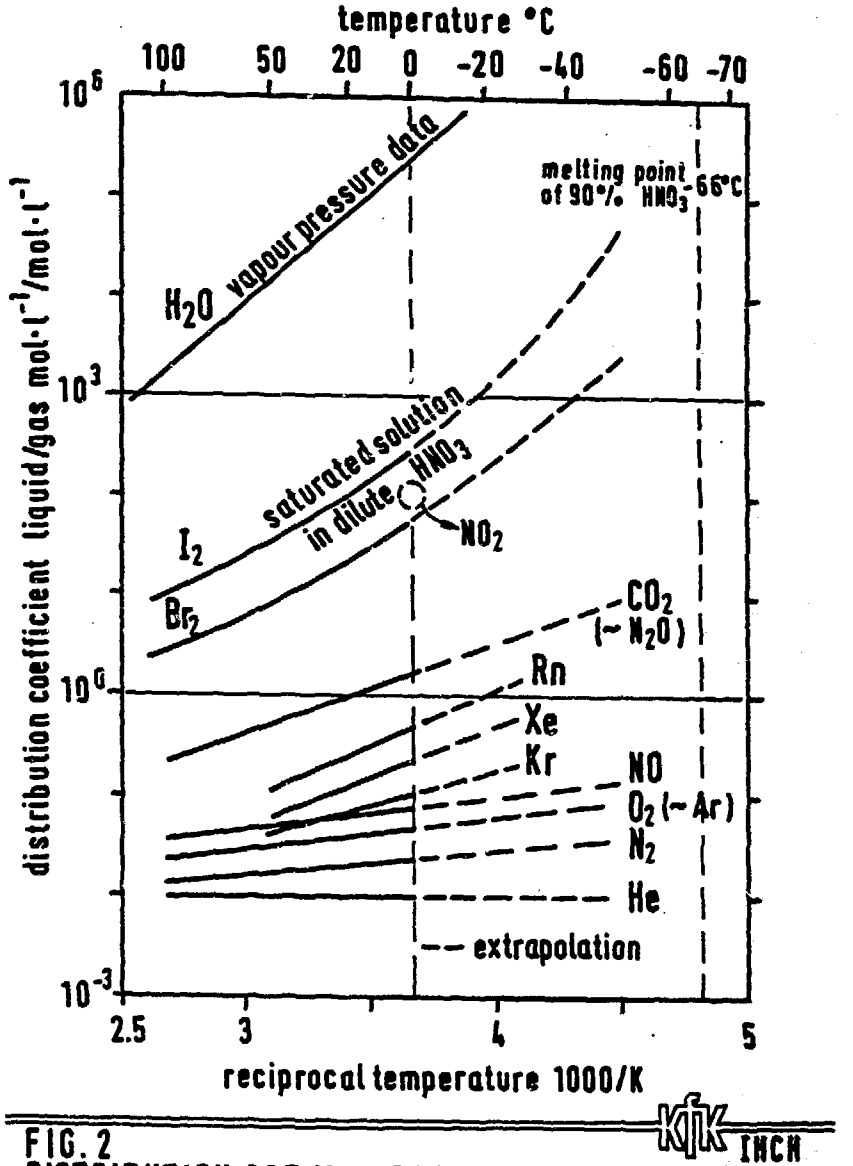

FIG. 2
DISTRIBUTION COEFFICIENTS OF OFF-GAS COMPONENTS IN WATER

dimensions of the absorption tower limit the reasonable gas residence time to few hundred seconds. In a plate column with counter-current and once-through scrub acid flow, operating at atmospheric pressure and ambient temperature, residual NO_x concentrations of about 0.3% by volume may be obtained. The NO_x removal efficiency of a single packed column with recirculating acid is lower, due to the higher steady state HNO_2 concentrations and decomposition rates in the upper part of the column; the regenerated NO recontaminates the purified off-gas.

Suitable and process compatible measures to improve the off-gas purification efficiency of a nitric acid scrubber can be derived from more detailed considerations of the equilibria and rate constants of the reactions involved:

a) Lower operating temperatures: The NO-oxidation in the gas phase is among the few reactions proceeding faster at lower temperatures /11/. Compared to room temperature, the rate constant at -50°C is about 5 times higher. The increased NO_2 dimerization and the higher distribution coefficients of N_2O_4 and iodine additionally contribute to the removal efficiency.

A more concentrated nitric acid is required at operating temperatures well below 0°C and the water and HNO_3 partial pressures in the off-gas are reduced corresponding to the off-gas dew point.

b) More concentrated nitric acid: At concentrations above about 6 M HNO_3, nitric acid is able to oxidize the NO to NO_2; the equilibrium constants /9,12/ are shown in Fig.3. The degree of oxidation increases with the HNO_3 concentration and the temperature. Contrary to a NO-oxidation in the gas phase, the oxidation with HNO_3 is more efficient at lower NO_x concentrations, e.g. after bulk NO_x removal with a conventional scrubber and does not require any O_2 in the off-gas.

In hyperazeotropic HNO_3 the N_2O_4-solubility is excellent /13/. With a counter-current flow of cold hyperazeotropic acid, residual NO_x can be oxidized and absorbed to the trace level. Absorption of elementary I_2 and subsequent oxidation to non-volatile iodic acid HIO_3 simultaneously removes traces of iodine.

c) Nitrous acid oxidation with hydrogen peroxide (H_2O_2) /14,15/: In $>$ 16 M HNO_3, lower valent N-species are present as dissolved N_2O_4 or NO_2; H_2O_2 is not stable at the higher acid concentrations and evolves nitrogen oxides after an induction period. In $<$ 12 M HNO_3 at room temperature lower valent N-species are present as undissociated HNO_2; H_2O_2 oxidizes the HNO_2 to HNO_3. The H_2O_2 is relatively stable and decomposes slowly to H_2O and O_2 in the course of hours or days. The decomposition rate increases with the H_2O_2 concentration and the temperature and in the presence of certain metal ion impurities (eg. Fe^{3+}) acting as decomposition catalyts. The oxidation of HNO_2 with H_2O_2 prevents the NO-regeneration connected with the HNO_2 decomposition. This is especially beneficial in case of acid recirculation. The acid circulation additionally helps to maintain a low surplus concentration of H_2O_2 in view of a potential decomposition. Cold 10 M HNO_3 plus H_2O_2 combines sufficient oxidative power towards residual NO and oxidizes HNO_2 prior to decomposition.

d) Ozone (O_3) addition to the off-gas: A slight stochiometric excess of few hundred ppm O_3 converts the total NO_x in the off-gas to N_2O_5 in few seconds /16,17,18/. The extremely hygroscopic N_2O_5 is very easily absorbed under formation of HNO_3. The O_3-oxidation of NO to NO_2 is very fast even at low temperatures; a sufficiently fast NO_2 oxidation at ppm levels to N_2O_5 via the unstable NO_3 intermediate requires a slight O_3 excess. Iodine traces are converted to the oxide. Downstream rare gas recovery processes should be either insensitive to O_3 or preceeded by catalytic O_3 decomposition.

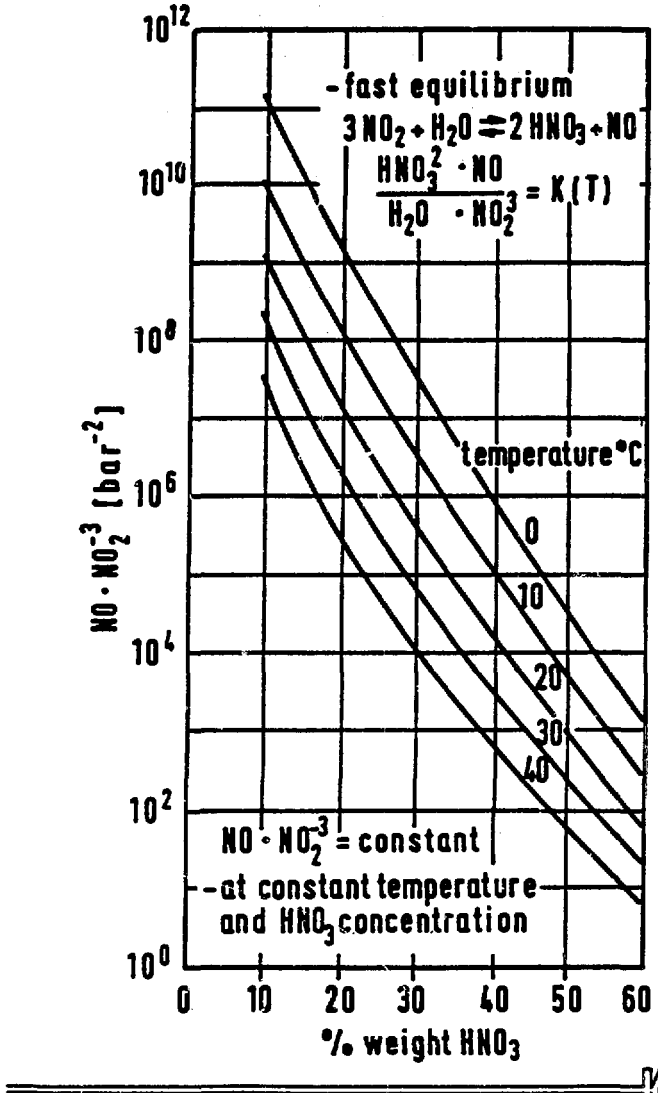

FIG.3 NO/NO_2^3 EQUILIBRIUM OVER HNO_3

In Fig.4 three HNO_3 concentration ranges are distinguished according to the process chemistry. The curve represents the crystallization temperatures of nitric acid and shows, that the liquid range extends down to -66°C at 90% by weight HNO_3.

Within the first concentration range up to about 6 M HNO_3 (30% HNO_3 by weight) the oxidation power is insufficient to oxidize substantial amounts of NO. The oxidation occurs in the gas phase as usual and can be improved at temperatures as low as about -35°C. Additional H_2O_2 aids to prevent the HNO_2 decomposition.

Within the second HNO_3-concentration range from about 7-12 M HNO_3 (35-55% by weight) the HNO_3, especially at the higher concentrations, is able to oxidize NO even without O_2 in the off-gas. The total oxygen for HNO_3 formation must then be supplied with the H_2O_2. Otherwise, up to three times as much NO_2 could be released from the sytem. Any O_2 in the off-gas reduces the H_2O_2 consumption to some extent. At the higher HNO_3 concentrations the operating temperatures are limited to about -18°C.

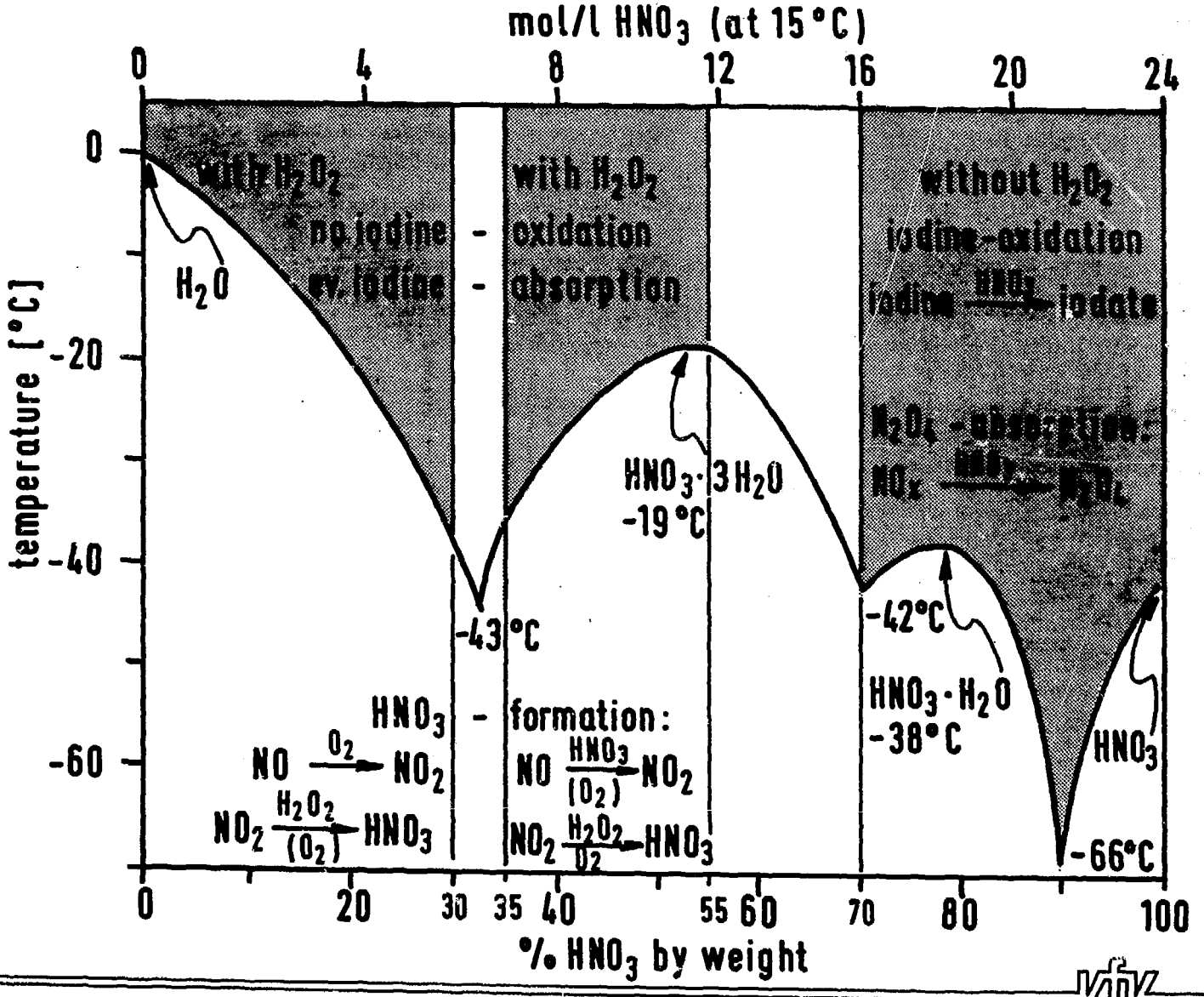

Fig.4: OPERATING CONDITIONS OF THE LOW TEMPERATURE SCRUBBERS

In up to 12 M HNO_3, with or without H_2O_2, the iodine oxidation is negligeable at low operating temperatures.

The third range represents hyperazeotropic HNO_3 ($\geqslant$ 16 M HNO_3 or $\geqslant$ 70% by weight). H_2O_2 is unstable and can not be used. The NO is oxidized completely even in an O_2-free off-gas and is efficiently absorbed as N_2O_4. Operating temperatures down to -55°C are practicable using 90 weight % HNO_3. Iodine is first absorbed physically and subsequently oxidized to non-volatile iodic acid.

3. OPERATING MODES

The removal especially of those off-gas constituents which are not transformed sufficiently fast into less volatile forms, depends on the operating modes and conditions in a cold scrubber. Essential parameters are the operating temperatures gas and acid rates, co- or counter-current gas to acid flow and once through scrub acid flow or acid recirculation with or without acid regeneration.

Below the solubility limit of the individual components, the temperature dependent distribution coefficients $D_i(T)$ in Fig.2 allow a crude estimate of the attainable decontamination factor (DF). If the solubility limit is exceeded, the scrubber acts only as a simple cold trap and the DF's can be calculated from the vapour pressure in the feed and the purified gas using the data from Fig.1.

For co-current flow or fast acid recirculation without regeneration the approximate DF's are $D_i(T) \cdot L/G+1$. L is the scrub acid volume used to purify G volumes of off-gas; flow rate variations and the concentration dependence of distribution coefficients are omitted. For counter-current flow either in the once-through mode or with acid recirculation plus regeneration, the approximate DF's are $(E^{n+1}-1) / (E-1)$ or about E^n for $E,n \gg 1$; $E = D_i(T)\ L/G$; G/L is the gas-to-liquid flow ratio on a volume basis, n is the number of theoretical absorption stages in the column /19/.

Counter-current flow at low temperatures is the more efficient mode of absorption. Low coabsorption of more volatile components e.g. Xe, Kr, N_2O or CO_2 is unimportant at gas-to-acid flow ratios of 10^2 or more, if the spent scrub acid is recycled upstream into the process. At the larger flow ratios, FP halogens or NO_2 may accumulate within the column, if the operating temperature is conveniently lowered from about ambient to suitable lower values in the course of scrubbing. The accumulation of such less volatile components is connected to the greater temperature dependence of their distribution coefficients (see Fig.2). Precooling the off-gas in co-current contact with the scrub acid prevents such disturbing effects /20/.

4. BRIEF DESCRIPTION OF THE TEST COLUMN

The simplified flowsheet of the test column is shown in Fig.5. Construction materials are stainless steel, 1.4306 (corresponding to 304 L). The column is subdivided into a lower co- and an upper counter-current part. Both parts have 0.8m diameter, a height of about 2 m and 8 absorption plates at 0.2 m spacing. The special plate design favours plug flow in the gas phase at small spacings. The total scrub acid inventory in the column is 0.4 m^3 and the gas space between the plates is about 1.4 m^3.

Acid flow via the counter- and co-current part is by gravity. The vertical distance between in- and outlet of the siphon is large enough, to compensate for

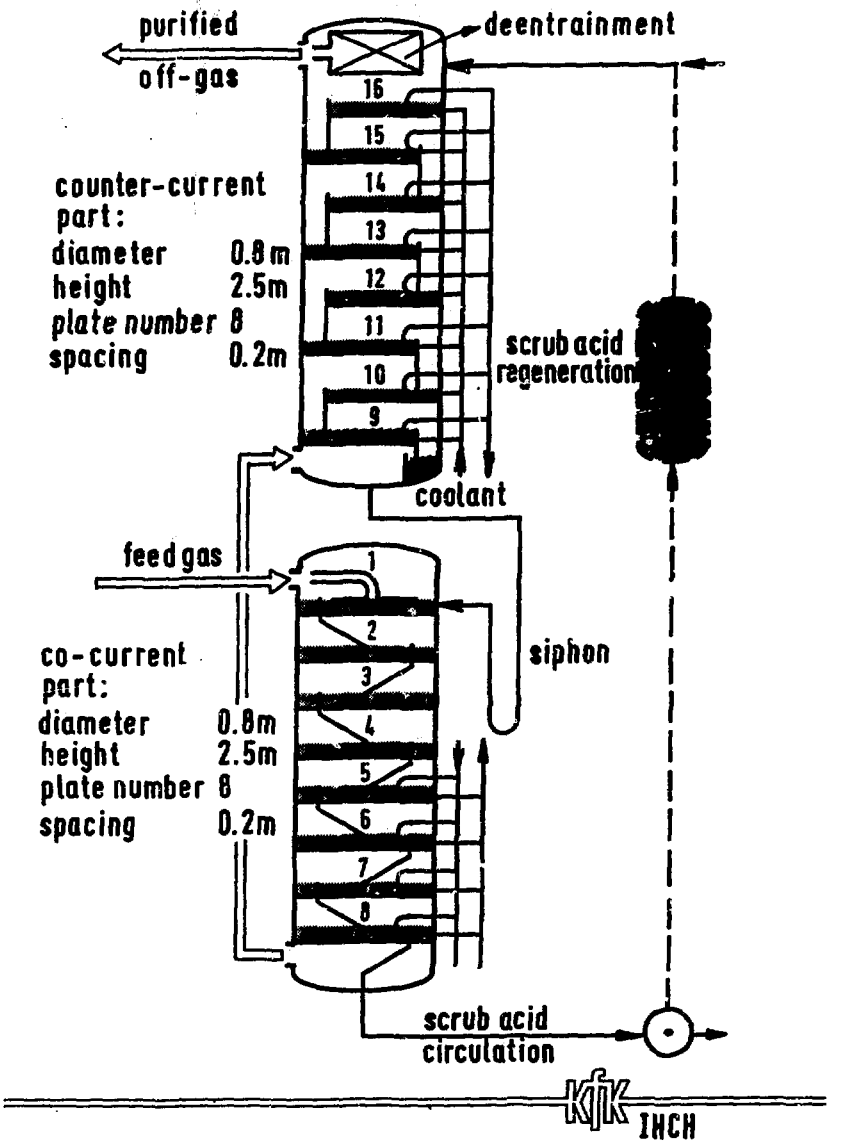

Fig.5 SIMPLIFIED FLOWSHEET OF THE LOW TEMPERATURE SCRUBBER

the pressure drop in the co-current part. Scrub acid recirculation via additional equipment for acid regeneration is important during extended test campaigns and prevents the generation of large volumes of waste acid.

Refrigeration equipment: Each absorption plate has an individual cooling coil. The heat transfer fluid is HNO_3 at about the same concentration as the scrub acid; this avoids trouble in case of accidental leaks. The acid circulates in a closed loop via a heat exchanger. Chilled refrigerant-11 (R11, CCl_3F) circulates on the cold side of the heat exchanger. R11 temperatures down to -70°C are generated with redundant 2-stage refrigeration compressors. Column temperatures down to -60°C are achieved easily. The thermal insulation of the columns and pipes consists of 10 cm thick 'Armaflex' foam (see photos of 5a and 5b of the column).

a: lower co-current part

b: upper counter-current part

Fig.5 a, b: Photos of the test column

Analytical equipment: NO and NO_2 concentrations in the purified off-gas can be monitored continually with calibrated IR and VIS photometers, chemiluminescence and paramagnetism instruments. Another set of instruments is available for NO and NO_2 determinations in the gas phase above each plate. Scrub acid samples can be taken from each plate for HNO_3 and HNO_2, N_2O_4 or H_2O_2 titration.

5. EXPERIMENTAL PROCEDURES AND OPERATING CONDITIONS

At the end of a test run, the scrub acid on each plate can be drained at will. Usually the column was not drained and the acid on the plates continually refrigerated overnight without circulation. This mode of operation allows short start up times not far distant from thermal equilibrium. The first 4 plates at the gas inlet are not cooled normally. After adjusting the desired acid circulation and carrier gas rates, thermal equilibrium was reached in less than one hour. Thereafter, the controlled addition of NO_2, 30 or 50 weight % H_2O_2 or O_3/O_2 was started. Depending on type and mode of scrubbing, steady state operating conditions were established in less than one or in few hours. Temperature and concentration profiles in the column were taken periodically to control the approach to equilibrium conditions.

The test column has been designed for flexible multi-purpose use and not to meet the requirements of a special type of process. Optimum design characteristics in regard to the number of plates, gas or acid inventories and rates, operating modes etc. will be specific for each process type and result in improved operating features and removal efficiencies.

The essential operating conditions and parameters are summarized in Table 2:

SCRUB ACID	• mol/l HNO_3 at 25°C	~0.5	~6.5	~10	~21.5
	• % HNO_3 by weight	~3	~33	~48	~90
	• addition of 30 or 50% H_2O_2	0.02-0.1mol/l excess			none
	• recirculation rate	0.15-0.25m^3/h			6-60l/h
OFF-GAS	• gas rates	4, 8, 16, 32 m^3(STP)/h			
	• carrier gas	air, O_2-deficient air, N_2			N_2
	• NO concentration	1% vol ≙ 10^5 ppmv			10^2-10^6ppmv
	• I-123 tracer	mostly lab scale experiments			
	• addition of H_2O	up to few 10^2 ppmv excess			
TEMPERATURE	• feed gas	ambient (20-25°C)			
	• counter-current part	to 0°C	to -35°C	to -10°C	to -55°C
	• co-current part	from ambient to low temperatures			
MODE	• processing mode	first co- then counter-current gas flow			
	• acid regeneration	none			either N_2 or O_3/O_2

kfk

Table 2 OPERATING CONDITIONS AND PARAMETERS

6. EXPERIMENTAL RESULTS

The essential experimental results are briefly described and summarized in the diagrams from Fig.6 to 15 and in Table 3. The operating conditions and parameters are indicated on the diagrams.

6.1 Highly concentrated 90 weight % HNO_3 without H_2O_2 at temperatures down to -55°C:

Fig.6 shows the residual NO_2 concentration in an entirely O_2-free nitrogen gas stream at low operating temperatures in the counter-current part. Even without any O_2, the hyperazeotropic nitric acid had efficiently oxidized the NO to levels far below the detection limit (< 0.5 ppmv). At -55°C the dimerized NO_2 is physically absorbed to a very low level of 1 ppmv or less, depending on the acid purity. Two different procedures were tested for continuous acid regeneration and are represented by the two lines in the diagram:

Regeneration with N_2: The NO_2 dissolved in the acid was blown out at 40-50°C in a 10 stage bubble cap column with a counter-current N_2 stream at a gas to acid volume flow ratio of about 10^2.

Regeneration with O_3/O_2: The NO_2 dissolved in the acid was oxidized at low temperatures in the same 10-stage column with a counter-current flow of ozonized O_2. The slightly stochiometric excess of 7-8% by volume O_3 in O_2 was generated in a commercial 0.1 kg/h ozonizer.

These procedures or partial vacuum distillation can be used to remove the NO_2 impurities (1-2%) from the commercial hyperazeotropic 98-99% HNO_3 prior to process application in a once-through mode. NO_2 concentration profiles at -48°C in the counter-current part of the column are shown in Fig.7. The gas to liquid volume flow ratio was 640; at 5 times higher flow ratios, the residual NO_2 concentration was about doubled. The slope of the curves and the absorption efficiency decrease at lower NO_2 concentrations, due to the lower degree of NO_2 dimerization.

The accumulation of stainless steel corrosion products (Fe, Cr, Ni) in the scrub acid was determined once a week during the test campaigns. An average corrosion rate of about 1/100 mm/y was found.

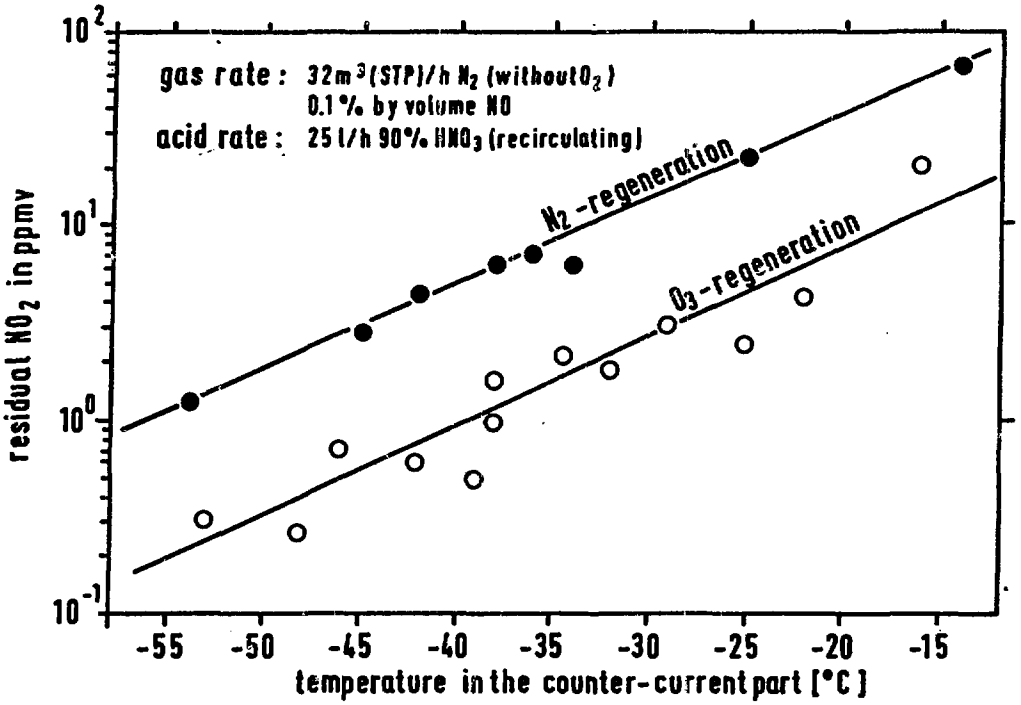

FIG.6 RESIDUAL NO_2 IN THE PURIFIED GAS
SCRUB ACID ABOUT 90% HNO_3

Previous investigations /20,23/ in a 0.1 m diameter column with 10 absorption plates at 5 cm spacing in both the co- and counter-current part, yielded similar results for NO_x decontamination. Iodine removal was investigated additionally using I-123 tracer (13h half life). Iodine DF's $\geqslant 10^4$ were obtained at about -50°C and gas to acid volume flow ratios $\leqslant 10^3$.

The iodine (I_2) vapour pressure at -55°C is about 0.1 ppmv. Even without counter-current absorption and oxidation in 90% HNO_3, the low partial pressure corresponds to an I_2 removal from the DOG of more than 99% An additional downstream cold trap at -130°C would remove residual HNO_3 and water vapours plus traces of NO_2 and iodine to negligibly low levels prior to a rare gas recovery step.

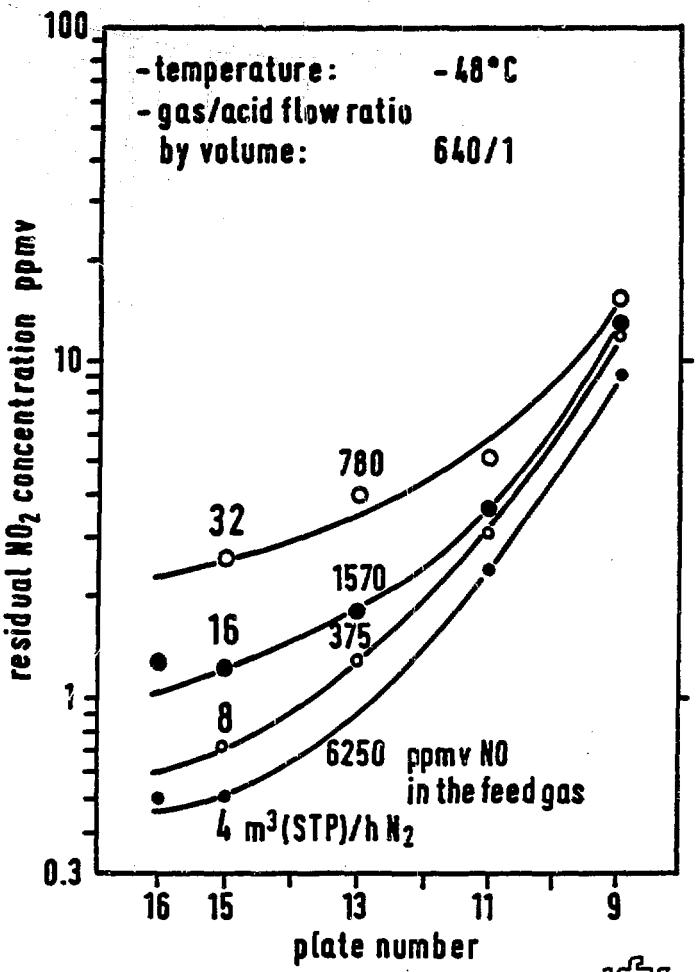

FIG. 7 NO_2-CONCENTRATION PROFILE IN THE COUNTER-CURRENT PART SCRUB ACID 90% HNO_3

6.2 10 M HNO_3 plus H_2O_2 at temperatures down to -18°C /7,22/

The oxidation power of 10 M HNO_3 at low temperatures is still sufficient to oxidize NO to NO_2 in an O_2-free off-gas. The advantage of the less concentrated acid is the possible use of H_2O_2 for the oxidation of HNO_2 The NO removed from the gas stream is thus recovered directly as HNO_3. The removal efficiency for 1 % vol. NO from N_2 carrier gas is shown in Fig.8. Low residual NO plus NO_2 concentrations between 10^2 and 10^3 ppmv have been obtained at the higher gas rates. At the less desirable lower gas rates, the residual NO_x concentrations are below 10^2 ppmv. The removal efficiency increases at lower temperatures. NO is more efficiently oxidized at ambient temperature but NO_2 is less efficiently absorbed; therefore the residual NO_2 concentration is higher than the NO concentration.

An about stochiometric H_2O_2 consumption has been found at the lower operating temperatures indicating a low H_2O_2 decomposition. Higher operating temperatures are less favourable but still satisfactory from this point of view.

Elementary iodine is not oxidized in cold 10 M HNO_3 plus H_2O_2. Iodine traces can be efficiently removed by physical absorption with a cold once-through scrub acid flow, according to the distribution coefficients (see Fig.2). With a rapidly circulating scrub acid stream without acid regeneration only partial absorption is possible. The rapid circulation helps to maintain the desired low H_2O_2 concentrations throughout the column; The higher H_2O_2 mass rate (low concentration times high circulation rate) guarantees flexibility in case of larger NO_x rate fluctuations.

The example in Fig.9 shows the NO and NO_2 concentration profiles in the column at -17°C at a relatively low gas rate.

For an O_2-free feed gas containing 1% vol. NO, total NO_x DF's at various gas rates and operating temperatures are summarized in Fig.10. At lower temperatures and gas rates the NO_x DF is $> 10^2$. Some time after a shutdown of the H_2O_2 addition, the NO_x-DF drops continually to < 2 and recovers slowly after readdition of H_2O_2. Without H_2O_2 up to 3 NO_2 could be generated from 1 NO.

6.3 6.5 M HNO_3 plus H_2O_2 at temperatures down to -35°C

At ambient temperature, low gas rates and low NO concentrations even a 6.5 M HNO_3 is able to oxidize substantial amounts of NO to NO_2; this is shown in Fig.11. But at lower temperatures and higher gas rates the oxidation power is insufficient and an efficient NO_x recovery requires the presence of O_2 in the off-gas. Residual NO and NO_2 concentrations obtained with O_2-deficient air are shown in Fig.12. Compared to room temperature. The gas phase oxidation of NO at -35°C is about 3 times faster. The low residual NO_2 concentration compared to the NO indicates two facts:

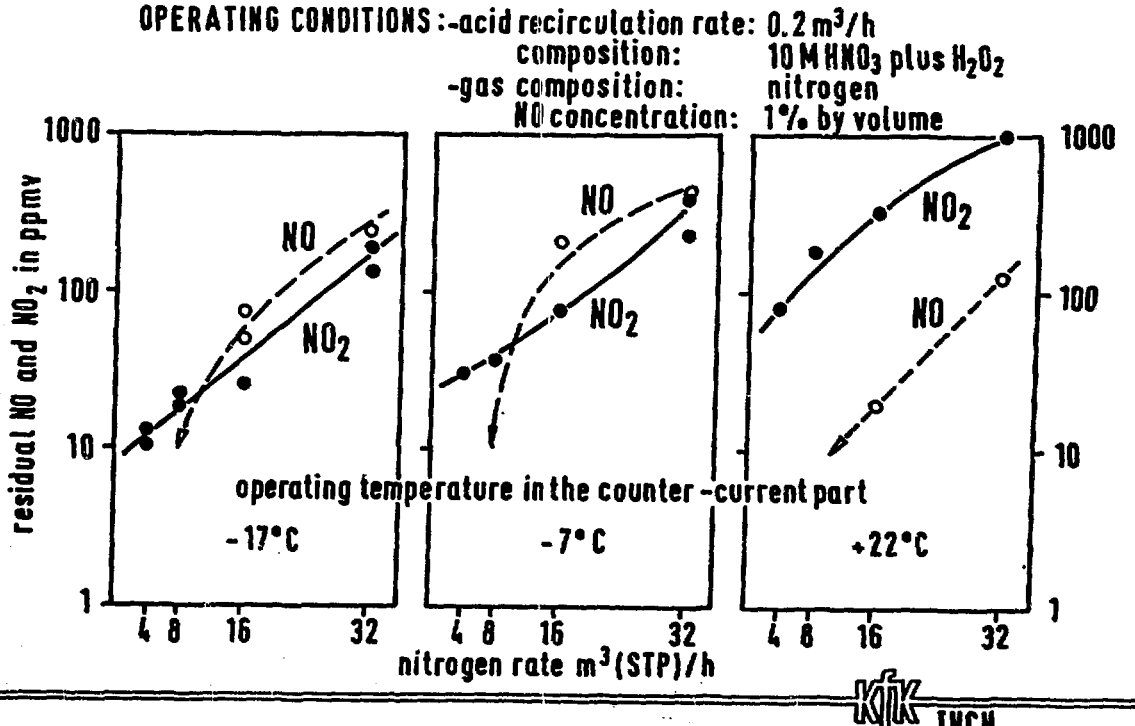

FIG.8 RESIDUAL NO AND NO_2 CONCENTRATIONS VERSUS NITROGEN RATE SCRUB ACID 10 M HNO_3 PLUS H_2O_2

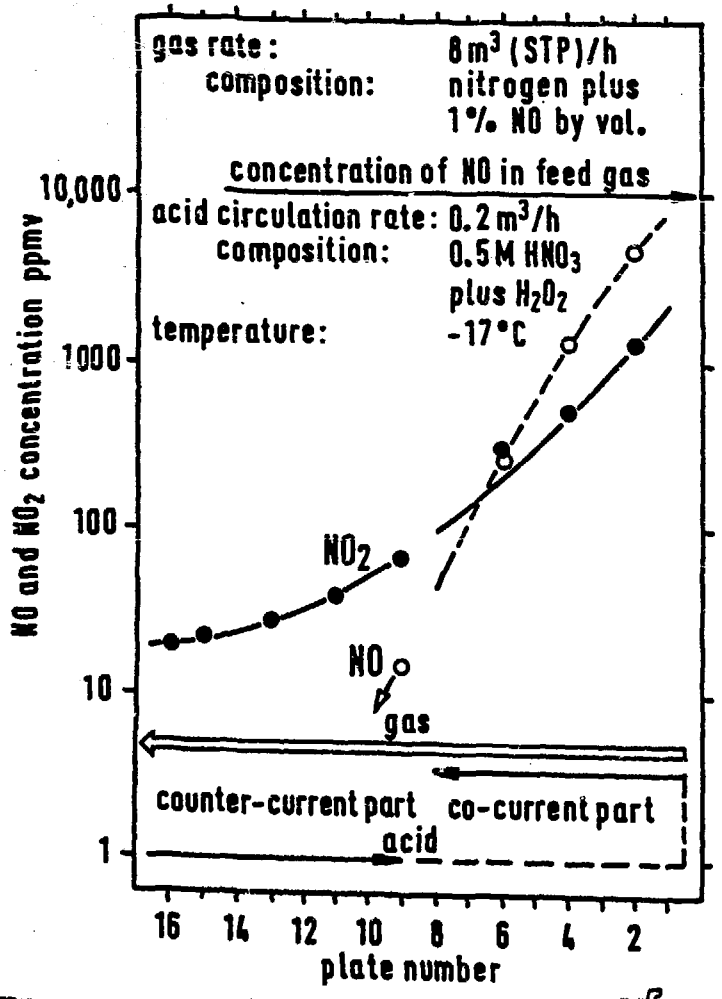

FIG.9
NO AND NO_2 CONCENTRATION PROFILE IN THE COLUMN
SCRUB ACID 10 M HNO_3 PLUS H_2O_2

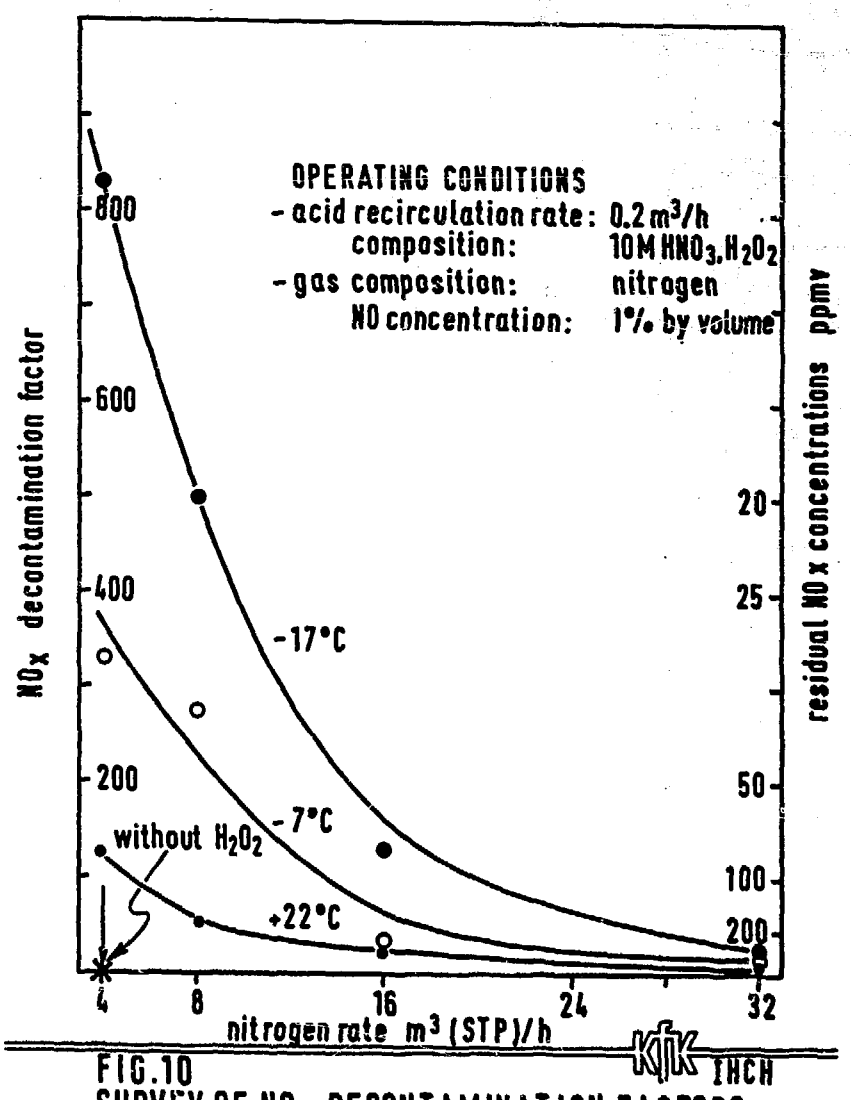

FIG.10
SURVEY OF NO_x DECONTAMINATION FACTORS
SCRUB ACID 10 M HNO_3 PLUS H_2O_2

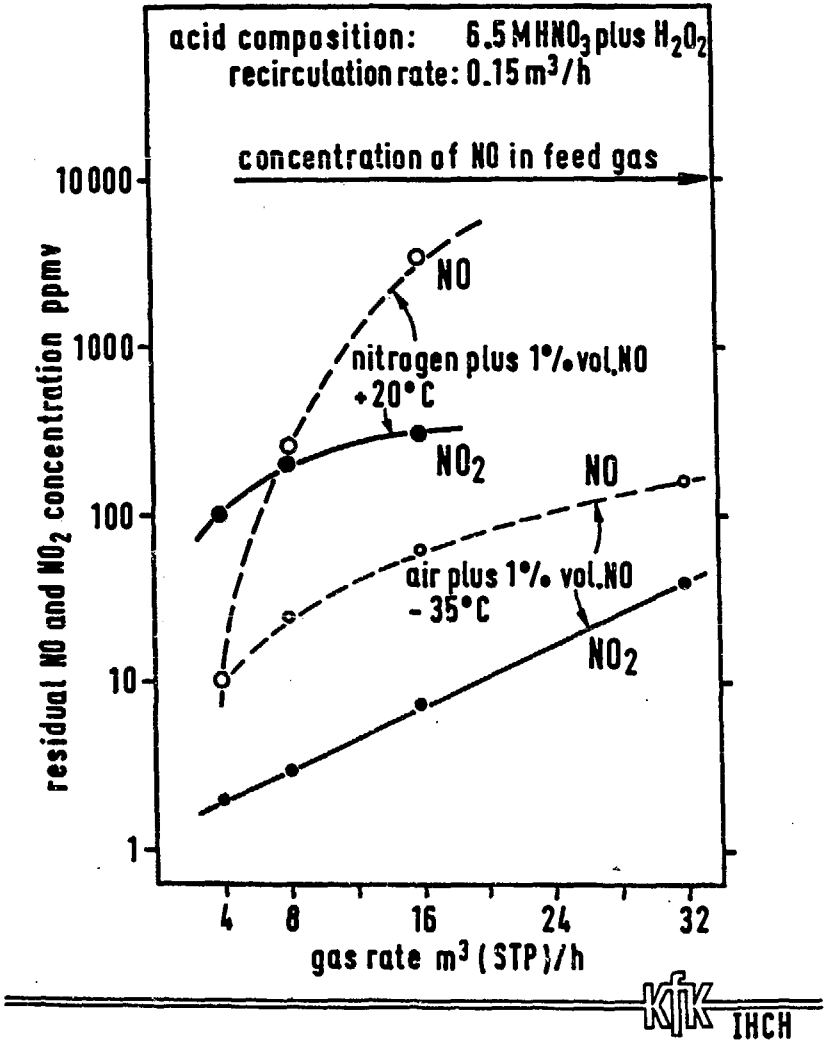

FIG.11 RESIDUAL NO AND NO_2 CONCENTRATION
SCRUB ACID 6.5MHNO_3 PLUS H_2O_2

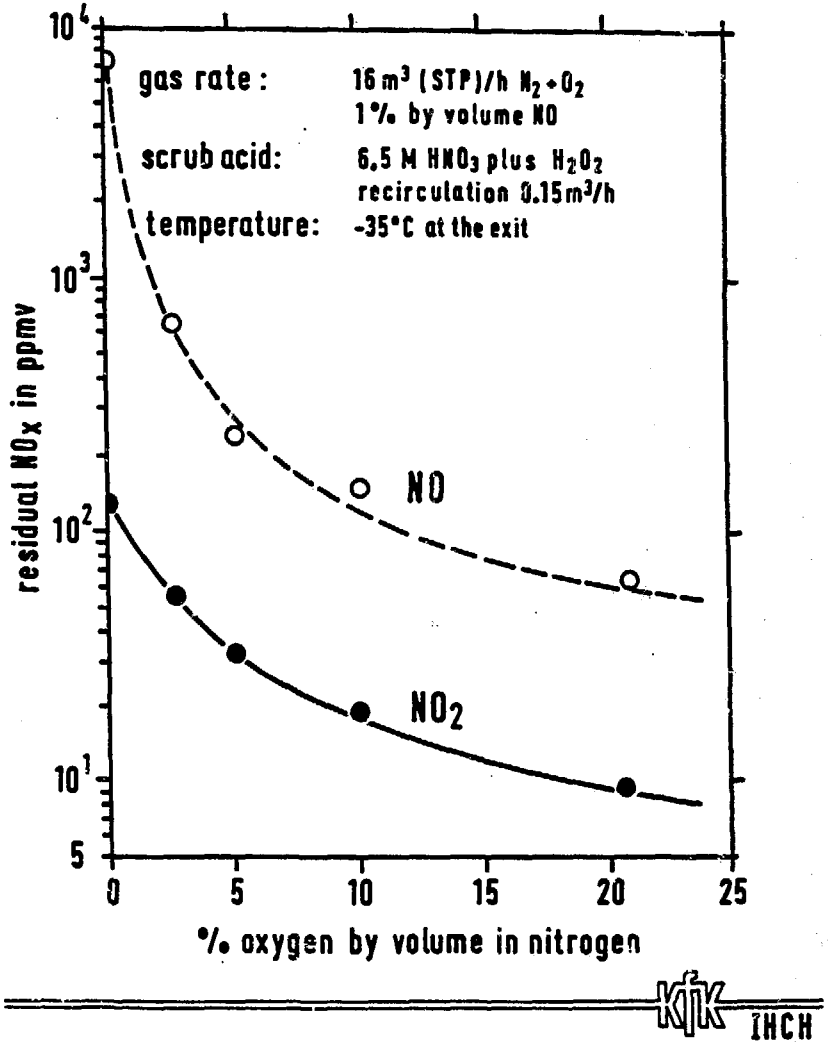

FIG.12 RESIDUAL NO_x IN THE PURIFIED GAS
SCRUB ACID ABOUT 30% HNO_3 PLUS H_2O_2

1. NO_2 is efficiently absorbed due to the higher degree of dimerization at lower temperatures.
2. The 'bottle neck' for a more efficient recovery is the slow gas phase oxidation of NO at low partial pressures.

In the presence of O_2 in the off-gas, 6.5 M HNO_3 has advantages compared to 10 M HNO_3: about 20°C lower operating temperatures are possible, the H_2O_2 consumption is up to 3 times lower and the HNO_3 concentration of the spent scrub acid is directly suited as dissolution acid for LWR spent fuel.

The example in Fig.13 shows the NO and NO_2 concentration profiles in the column at about 15 min gas residence time. The lower NO oxidation rate at the lower partial pressures towards the gas exit is indicated by the flat NO concentration profile.

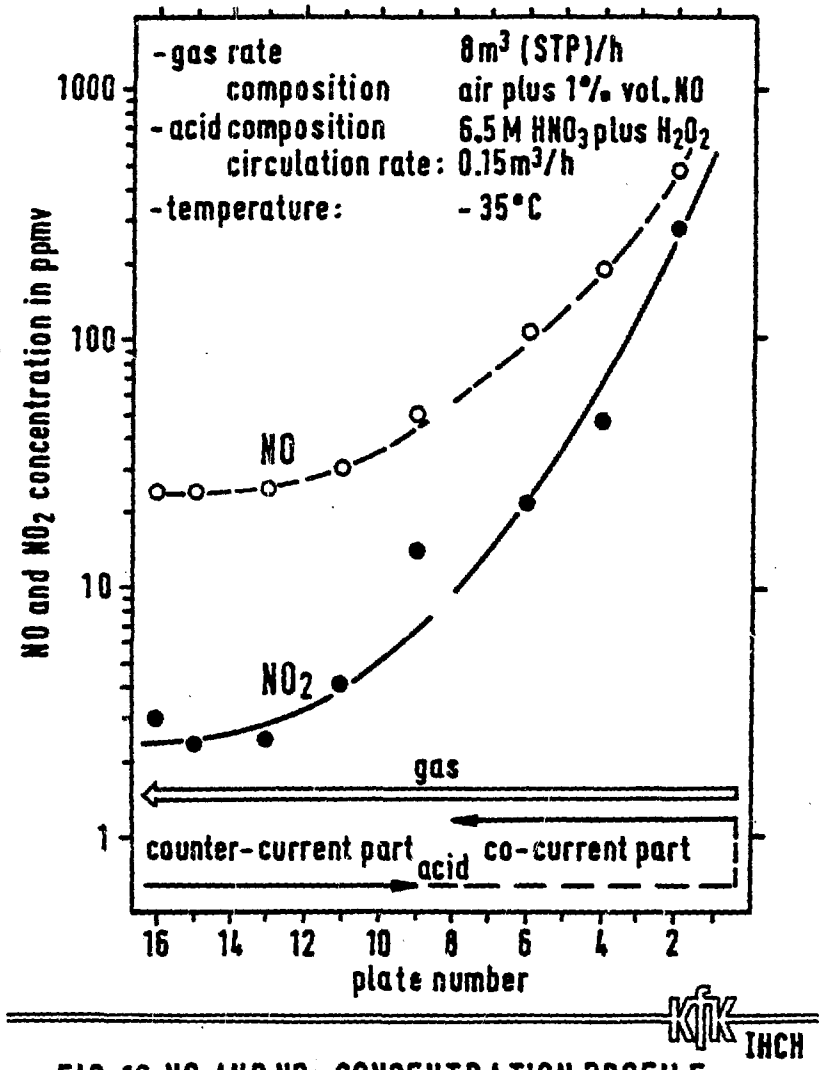

FIG.13 NO AND NO_2 CONCENTRATION PROFILE
SCRUB ACID 6.5M HNO_3 PLUS H_2O_2

6.4 0.5 M HNO_3 plus H_2O_2 at temperatures down to 0°C

The conventional NO_x scrub with dilute nitric acid at ambient temperature or somewhat below can also be improved by use of H_2O_2. An example of NO and NO_2 concentration profiles is shown in Fig.14. Without H_2O_2 addition, the NO_x-DF decreases by more than one order of magnitude due to the scrub acid recirculation. Residual NO and NO_2 concentrations at 20 and 0°C and various gas rates are summarized in Fig.15. Similar results can be obtained without H_2O_2 and a once-through scrub acid flow, since the HNO_2 decomposition rate in the counter-current part is low at low HNO_2 concentrations and temperatures.

6.5 Comparison of HNO_3-scrubs using H_2O_2

NO_x DF's at various operating conditions are compared in Table 3. At ambient temperature, the NO_x removal efficiency from air with 0.5 or 6.5 M HNO_3 plus H_2O_2 is comparable to the NO_x removal efficiency from nitrogen using a 10 M HNO_3 plus H_2O_2. At lower temperatures, with the more concentrated acids, better retention is obtained not only of NO_x but also of water and nitric acid vapours. Additional iodine retention is possible at special operating modes and conditions /20,24/.

CARRIER GAS	OPERATING TEMPERATURE counter-current part	SCRUB ACID CONCENTRATION mol/l HNO_3 plus H_2O_2	NO_x DECONTAMINATION FACTORS carrier gas rate m^3(STP)/h 4	8	16	32
nitrogen	-17 °C	10	830	500	130	25
nitrogen	- 7 °C	10	330	280	35	16
nitrogen	+22 °C	10	125	55	27	8
air	-33°C	6.5	>800	360	170	55
air	+20°C	6.5	180	100	52	-
nitrogen	+20°C	6.5	92	20	2-3	-
air	0°C	0.5	220	88	40	12
air	+20°C	0.5	115	55	20	8

NO in the feed gas 1% by volume; slight stochiometric H_2O_2 excess in the acid for NO_x oxidation

Table 3 KfK IHCH

COMPARISON OF GAS SCRUBS WITH NITRIC ACID PLUS HYDROGEN PEROXIDE

6.6 Additional observations

Some observations made during the test runs are worth mentioning even without explanation. The H_2O_2 excess in the circulating scrub acid was usually between 0.02 and 0.1 M H_2O_2. The NOx removal efficiency seems to increase somewhat towards the lower values. A slight NO break-through peak was observed frequently during start-up, indicating that a reactive intermediate species might be involved in the recovery reactions. The detailed mechanisms of the low temperature HNO_3 scrubs using H_2O_2 are not well known up to now and deserve further investigation especially for modelling the processes. At present, they are looked at as continuous chemical cold traps for off-gas purification.

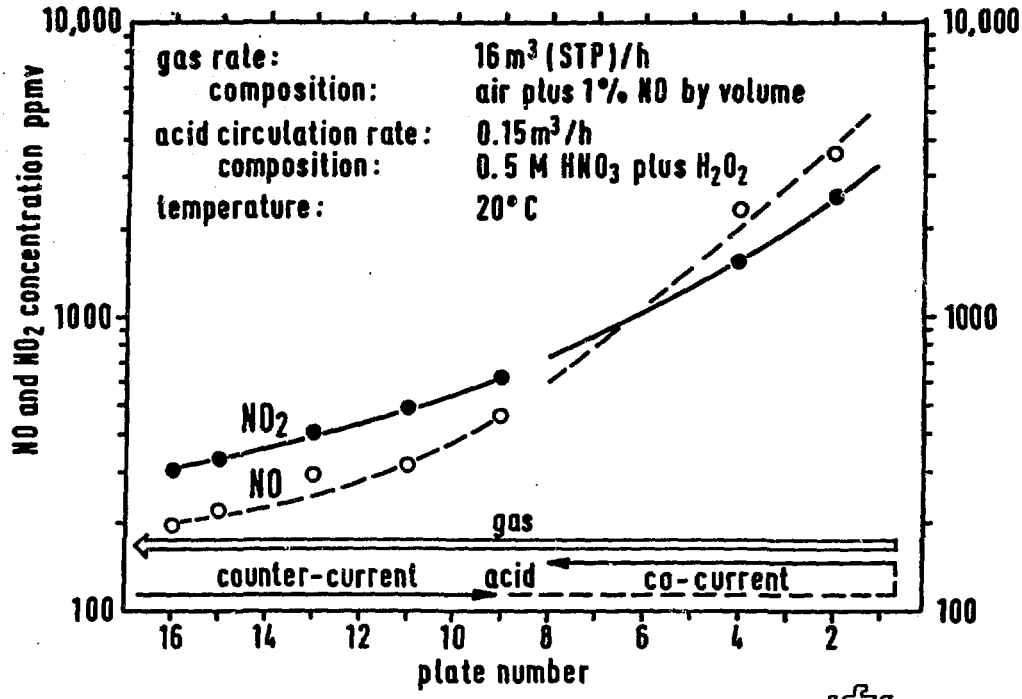

FIG. 14 NO AND NO_2 CONCENTRATION PROFILE IN THE COLUMN
SCRUB ACID 0.5 M HNO_3 PLUS H_2O_2

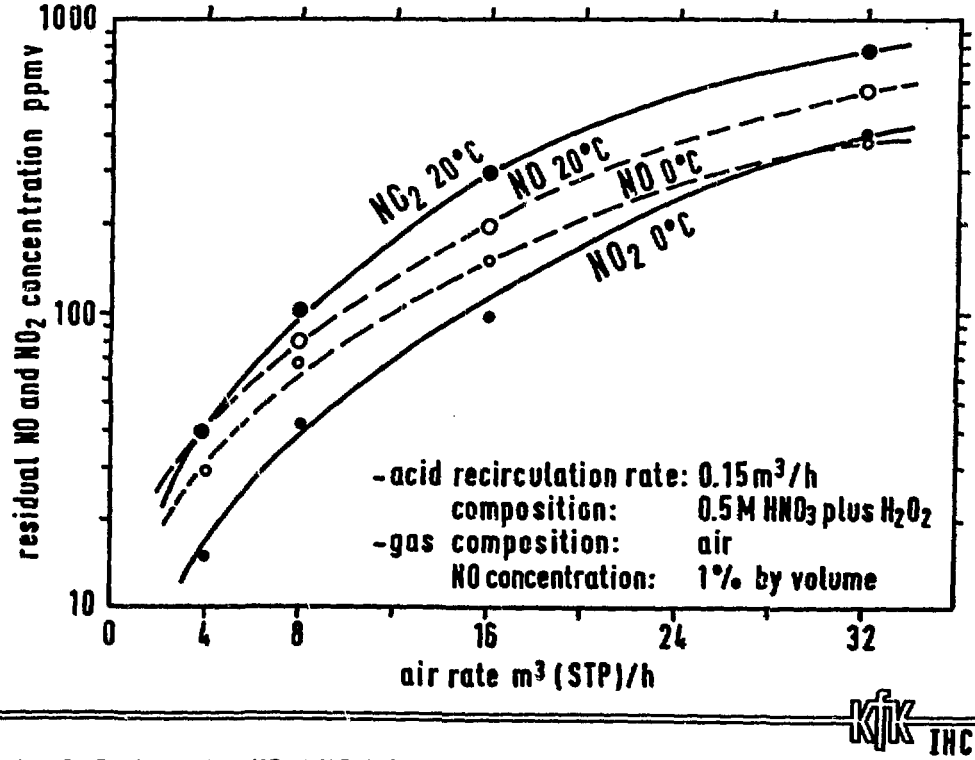

FIG. 15 RESIDUAL NO AND NO_2 CONCENTRATIONS VERSUS AIR RATE
SCRUB ACID 0.5 M HNO_3 PLUS H_2O_2

6.7 Ozone addition to the off-gas

NO_x was absorbed to below the detection limit of 0.5 ppm in dilute HNO_3 at room temperature after addition of ozonized O_2; the stochiometric O_3 excess was few 100 ppm. Lab scale experiments showed, that traces of iodine are converted to an oxide mist, which is badly scrubbed but easily removed with glass fiber filters.

7. SOME ASPECTS IN A FUEL REPROCESSING PLANT

A simple and convenient application of cold scrubs in a FRP should not create additional waste streams and should require only few operations. Regeneration or additional treatment of spent scrub acids prior to reuse or process recycle are possible but undesirable options. A suitable choice of sources and sinks for the scrub acid in the process is essential: Volume, concentration and contamination level of the acid transferred to or removed from the scrubber must be compatible with the processing mode in the plant and vice versa.

In the course of most applications the scrub acid is gradually diluted by absorption of water vapours from the off-gas, H_2O_2 addition and water produced in some absorption reactions. A minimum scrub acid exchange rate is therefore necessary to maintain the desired acid concentration.

The use of a cold scrubber in the DOG, downstream from an efficient aerosol and bulk NO_x plus iodine retention, is taken as an example. The uranyl nitrate $UO_2(NO_3)_2$ dissolved in the organic solvent removes 2 moles of nitrate per mole of U from the FRP headend. Only half the deficit is assumed to be replaced by about 300 kg 90 % weight HNO_3 per metric ton of U and first used for additional DOG purification in a once-through mode. The amount of dilution water will be about 20 kg, assuming a specific DOG volume of 500 m^3 (STP) per metric ton of U, 0.5% by volume residual NO and an off-gas dew point of 20°C. Scrub acid dilution occurs only in the co-current part of the scrubber and is acceptably low. A more smooth operation without acid recirculation via a regeneration step can be achieved with a control of the acid feed in proportion to the gas rate, e.g. using the pressure drop in the column. Residual NO_x and iodine will be removed to the trace level at -55°C especially in the counter-current part of the column. The residual HNO_3 vapours can be efficiently recovered in a defrostable feed gas cooler at < -100°C prior to a rare gas recovery step.

An equally efficient recovery at higher DOG throughputs requires regeneration and recirculation of the 90% HNO_3. Use of a (30 or) 50% HNO_3 plus H_2O_2 seems to be more favourable in this case. The small residual amounts of H_2O and HNO_3 vapours and NO_x can be recovered in a small molecular sieve bed downstream from the cold scrubber. Norton zeolon 900 H has been tested in a side stream of the cold scrubber; each of the three adsorbable constituents was removed to the sub-ppm level.

The dilution with water is less serious for 10 or 6.5 M HNO_3 plus H_2O_2 as scrub acid. Even an increase of the scrub acid concentration can be obtained using 50% H_2O_2 and higher NO_x and lower water vapour concentrations in the feed gas.

The source of a sufficiently concentrated scrub acid for the DOG may be either the highly active acid recovery system or a fresh acid. The spent scrub acid can be recycled to the dissolution acid storage tank without additional treatment.

Upstream recycle in the DOG purification system avoids the production of secondary waste streams.

Similar considerations can be made for an application of cold scrubs in the vessel off-gas systems.

The most sensitive parts of the equipment for the cold scrubbers are the refrigeration compressors. The refrigeration equipment should be redundant and located outside the process cells in an easily accessible 'cold' area. This simplifies maintenance and repair and maintains a high availability. Moreover, the contamination level of the scrubbers itself will be low, since they are used towards the end of an off-gas purification train.

The mode of refrigeration is an additional safety feature. The heat transfer fluid is HNO_3 at about the same concentration as the scrub acid and circulated in a closed loop. Small accidental leaks will not cause immediate trouble or shut-down. Contaminated coolant can be discharged into the process.

8. SUMMARY AND CONCLUSIONS

The essential operating modes, conditions and results are briefly summarized in table 4:

SUITABLE CONCENTRATION % w. HNO_3	SUITABLE OPERATING TEMPERATURE	PREFERED OPERATING MODE (1)	SLIGHT EXCESS OF ADDITIONAL CHEMICALS	OXIGEN IN THE OFF-GAS REQUIRED	RESIDUAL VAPOUR PRESSURES ppmv H_2O	ppmv HNO_3	NO_x AND IODINE REMOVAL ppmv NO_x (2)	I_2
< 30	0°C	• co- or counter-current • acid circulation without regeneration	controlled addition of 30 or 50% H_2O_2 to the scrub acid	yes	$<10^4$	$<10^1$	10^2-10^3	
30	-35°C			yes	$<10^3$	$<10^0$	$\sim 10^2$	partial removal
50	-18°C			no	$<10^3$	$\sim 10^1$	$\sim 10^2$	
90	-55°C	counter-current once-through	none	no	$\sim 10^0$	$<10^2$	≤ 1	efficient removal
various	various	various	O_3/O_2 to feed gas	no	various		<1	oxide mist

remarks: (1) other operating modes are also possible
(2) depends on column design, operating modes and conditions etc.

KfK INCH

Table 4 **BRIEF SUMMARY OF OPERATING MODES, CONDITIONS AND RESULTS**

Essential characteristics of the various low temperature scrubs for reprocessing off-gas purification are briefly summarized as follows:

- The low temperature nitric acid scrubs use a more concentrated nitric acid either with or without H_2O_2 or O_3. They are suited to achieve a more efficient or reliable off-gas purification downstream from a normal nitric acid scrub at ambient temperature.

- H_2O_2, HNO_3 and NO_x concentrations in the off-gas can be reduced by one or two orders of magnitude. NO_x and iodine can be removed to trace levels at special operating modes and conditions.

- Efficient NO_x removal can also be obtained from O2-deficient air or an O2-free nitrogen stream. This feature can be of importance for low flow ventilation

concepts, using an O_2-deficient cell atmosphere to prevent a solvent fire.

- Prior to rare gas recovery, a very efficient off-gas prepurification is required. Continuous cold scrubs upstream from the discontinuously operated sorbent beds or cold traps can considerably reduce the load to these less convenient steps. Bed size, regeneration frequency and desorption gas requirements are reduced correspondingly.

- Use of O_3 is compatible with rare gas recovery by selective absorption in R-12 /25/.

Cold scrubs provide for an in-line correction in case of defective upstream NO_x or iodine removal steps. This feature improves the reliability and availability of the total off-gas purification train.

- The convenient continuous processing mode and the simple, conventional equipment are attractive characteristics for a technical application.

- A suitable integration into the process avoids additional treatment steps of the spent scrub acids prior to process recycle.

- No secondary waste streams are produced. The nitric acid and the reaction products of H_2O_2 and O_3 are normal constituents of the process.

At present, the various low temperature scrubs are being investigated as a part of an integrated dissolver off-gas system on the engineering scale.

REFERENCES

/1/ 'Handbook of Chemistry and Physics', (Weast R.C. editor) 49th edition, 1968-1969; Cleveland, Ohio, USA (1968), (data basis)

/2/ Henrich E.; in 'Chemistry of Nuclear Fuel Reprocessing and Radioactive Waste Disposal', part III (Baumgärtner, F. editor), München 1980, p.85

/3/ Empfehlung der 'Strahlenschutzkommission' SSK vom 24.02.83 zur Rückhaltung radioaktiver Stoffe bei einer Wiederaufarbeitungsanlage.

/4/ Leudet A., Miguel P., Castellani F., Curzio G., Gentili A.; 'Methods of Kr-85 Management' , Harwood Academic Publishers (1983) in 'Radioactive Waste Management', vol.10 (Anderson D.R., Platt A.M., Girardi F., Orlowski S.; editors) (CEC editors: W. Hebel, G. Cottone)

/5/ Landolt-Börnstein; 'Zahlenwerte und Funktionen', Technik Bd. IV 4. Teil Wärmetechnik C, 'Gleichgewicht der Absorption von Gasen in Flüssigkeiten', Springer Verlag 1976

/6/ 'Chemiker Kalender', (von Vogel H.U. editor), Berlin, 1956 (data basis)

/7/ Henrich E., von Ammon R., Hutter E.; KfK-PWA status report, march 1984, to be published

/8/ Chilton T.H.; 'Strong water', The MIT Press, Cambridge, Mass., USA 1968

/9/ Hoftyzer P.J., Kwanten F.J.G.; in 'Gas Purification Processes for Air Pollution Control', (G. Nonhebel, editor), London 1972, p.164

/10/ Lefers J.B.; 'Absorption of Nitrogen Oxides into Diluted and Concentrated Nitric Acid', Delft., University Press, 1980

/11/ Bodenstein M., Lindner P.; Zeitschrift für physikalische Chemie 100, 105 (1922)

/12/ Carberry J.J.; Chem. Eng. Sci. 9, 189 (1959)

/13/ Klemenc A., Rupp S.; anorg. allg. Chemie, 194 (1930) 51

/14/ Adrian J.C., Verilhac J,; (Ugine Kuhlmann, France); Paper presented at the 2nd Int. Conf. on the Control of Gaseous Sulphur and Nitrogen Compound Emission, University of Salford, GB, (1976)

/15/ Sturm W.; Chemie Technik, 11. Jahrgang (1982) Nr.9, S.1013
/16/ Butcher S, Charlson R.J.; 'Nitrogen Compounds and Ozone', N.Y., London, Academic Press (1972), p.115
/17/ Slater S.M., Rizzone M.S.; Fuel 59 (1980) 1/12, p.879
/18/ Straubing M., Roesch W., Henrich E.; unpublished results 1982
/19/ Alders L.; 'Liquid-Liquid Extraction', Amsterdam, N.Y. 1955
/20/ Henrich E., Huefner R.; Proceedings 16th DOE Nucl. Air Cleaning Conf., San Diego, USA, 1980, p.597
/21/ KfK-IHCH; Annual report 1982; KfK-3488, February 1983
/22/ KfK-IHCH; Annual report 1983; KfK-3690, February 1984
/23/ Henrich E., Huefner R.; Int. Conf. on Radioactive Waste Management, Seattle, WA, USA, 16-20 May 1983, IAEA-CN-43/447
/24/ Henrich E.; KfK-2940, p.162, February 1980
/25/ Henrich E., Huefner R., Weirich F., Bumiller W., Wolff A.; this conference

DISCUSSION

VIKIS: With respect to your work on the effect of O_3 on I_2 and NO_x in the liquid phase, we have shown that I_2 reacts with O_3 in the gas phase to form solid iodine oxides. However, we are concerned about the economics of using O_3 in the presence of large amounts of NO_x. Have you looked at these economics in your case?

HENRICH: The oxidation of NO_x with ozonized oxygen or air does make sense only at lower NO_x concentrations of a few tenths of a percent by volume or less. It is not suited for bulk NO_x removal, e.g. from the dissolver off-gas. Therefore, a precondition is upstream bulk NO_x removal in a conventional nitric acid scrubber. The economic feasibility of this off-gas purification process is demonstrated by many applications at similar conditions in the non-nuclear industry. Large ozonizers, producing several 10 kg O_3 per hour, are commercially available today and references of applications are available from the industry.

VIKIS: If we can oxidize iodine, which is a very volatile species in the gas phase, to an iodide, and if we can deal with the NO_x problem by using high concentrations of ozone economically, then it seems to me that we can carry out the whole recovery in the gas phase and need not worry about using complex liquid scrubbers.

HENRICH: Yes, that is an alternative. What the best solution would be depends on the problem.

DEVELOPMENT OF THE ELEX PROCESS FOR TRITIUM SEPARATION AT REPROCESSING PLANTS

A. Bruggeman, L. Meynendonckx, C. Parmentier, W.R.A. Goossens, L.H. Baetslé
Studiecentrum voor Kernenergie/Centre d'Etude de l'Energie Nucléaire
Mol, Belgium

Abstract

Within the framework of the Commission of the European Communities' indirect action programmes on management and storage of radioactive waste the Belgian Nuclear Research Centre, S.C.K./C.E.N., has been developing, since 1978, the ELEX process for isotopic enrichment and separation of tritium from aqueous reprocessing effluents. The ELEX process is a combination of water ELectrolysis and tritium EXchange between hydrogen and liquid water, the exchange being promoted by a hydrophobic catalyst.

After the development of an appropriate hydrophobic catalyst and the study of the separate constituent steps of the ELEX process, an integrated bench-scale installation with a detritiation capacity of 10 mol water per hour was constructed. It comprises essentially a 1.5 kW electrolyser and two 2 cm diameter and 3 m high exchange columns. In this mini-pilot the ELEX process was successfully demonstrated by detritiating more than 1000 dm^3 water containing up to 100 mCi tritium per dm^3, which is the feed concentration expected for application of the process in a reprocessing plant. The process decontamination factor was always larger than 100 and the overall tritium balance could be kept within the experimental errors of the various measurements. Depending on the duration of the runs, the volume reduction factor was between 10 and 15, but this factor will become much higher when the present electrolyser will be replaced by the low-volume one now under construction at S.C.K./C.E.N. The technical availability of the mini-pilot amounted to 99 % or more for the last experiments. During the nearly 6000 hours of operation there were no tritium contamination problems.

At present the construction of a 280 $mol.h^{-1}$ or 0.12 m^3 H_2O (HTO) per day pilot detritiation installation nears completion. In this unit, which will have a total tritium inventory of maximum 1000 Ci, the ELEX process will be demonstrated with a volume reduction factor of 100 and a process decontamination factor of 100. Again the feed concentration will be 100 Ci tritium per m^3. In the future this installation will be supplemented with a pre-treatment unit for the removal of fission products, organics and nitric acid.

I. Introduction

Within the framework of the European Community's programmes "Management and Storage of Radioactive Waste" the Belgian Nuclear Research Centre, S.C.K./C.E.N., has been developing, since 1978, the ELEX process for isotopic enrichment and separation of tritium from aqueous reprocessing effluents [1, 2]. The ELEX process is a combination of water ELectrolysis and tritium EXchange between hydrogen and liquid water, the exchange being promoted by a hydrophobic catalyst. The development stage of this process will be described in this paper.

II. The tritium management for an inland reprocessing plant

Inside the fuel elements of present light water reactors about 0.75 PBq (20 kCi) tritium are formed per GW(e).a, mostly by ternary fission. Depending on the time-temperature history in the reactor, a smaller or a larger part of this tritium diffuses out of the fuel and is fixed by the Zircaloy cladding. When the spent fuel is reprocessed this latter fraction is retained in solid wastes. But the remainder of the tritium, and this represents 50 % or more, is not immobilized and if no special treatment is used it ends up nearly quantitatively as HTO in the aqueous effluents of the reprocessing plant.

With the increase in nuclear power and in the corresponding reprocessing capacity, release of these tritium-bearing effluents by discharge into local rivers or evaporation to the atmosphere will have to be restricted. For some suitable reprocessing plant sitings alternative low cost management schemes for tritiated aqueous wastes may be possible, such as direct disposal into the ocean or on-site deep well injection. At most inland plants, however, decay storage on site or transport to a repository will be required and in both cases the tritium must be immobilized, probably in a solid form, from which it does not leak or leach [3]. To minimize the cost of immobilization and long-term storage, previous concentration of tritium in a small volume will be necessary.

Technically, a normal chop and leach process is still preferred for present and future reprocessing plants. Starting with the dissolution, the tritium in the fuel is repeatedly diluted isotopically as aqueous reagents are introduced. To confine the tritium into a relatively small volume, several schemes for segregation and recycling of the tritiated plant streams and decontamination of the process reagents have been studied and proposed [4, 5, 6]. At future reprocessing plants the volume of tritiated aqueous effluents might thus be reduced to about 5-1 m^3 per ton of light water reactor fuel processed, with a tritium level of the order of 3.7 TBq (100 Ci) m^{-3} or a HTO : H_2O ratio of about 10^{-7} [7, 8, 9]. In many cases a further reduction of the waste volume will, however, be required and an isotopic enrichment and separation of tritium will be needed. Such method will then produce a product stream that is sufficiently enriched in tritium (volume reduction factor, VRF) to be economical for storage or disposal and a waste stream that is sufficiently depleted in tritium (decontamination factor, DF) to be discharged to the biosphere.

III. The ELEX process for separation of tritium from aqueous effluents

S.C.K./C.E.N. proposed earlier an ELectrolysis-EXchange process for isotopic enrichment and separation of tritium from the aqueous effluents of a reprocessing plant [10]. This ELEX process is a combination of water electrolysis and tritium exchange between hydrogen and liquid water, the exchange being promoted by a hydrophobic catalyst. The process is thus based on two large isotope effects : the equilibrium isotope effect in the tritium exchange reaction between hydrogen gas and liquid water and the kinetic isotope effect in the electrolytic hydrogen evolution reaction. Both isotope effects favour concentration of tritium in the liquid water relative to the hydrogen gas. Analogous processes are being studied in Canada, U.S.A., Japan and Germany [11, 12, 13, 14].

Figure 1 shows a schematic illustration of the ELEX process. It comprises essentially an electrolyser for production of hydrogen and a countercurrent packed-bed reactor for tritium exchange between hydrogen gas and liquid water. As the liquid water trickles down the column, it becomes more and more enriched in tritium. The hydrogen gas, which is already depleted in tritium relative to the electrolyte

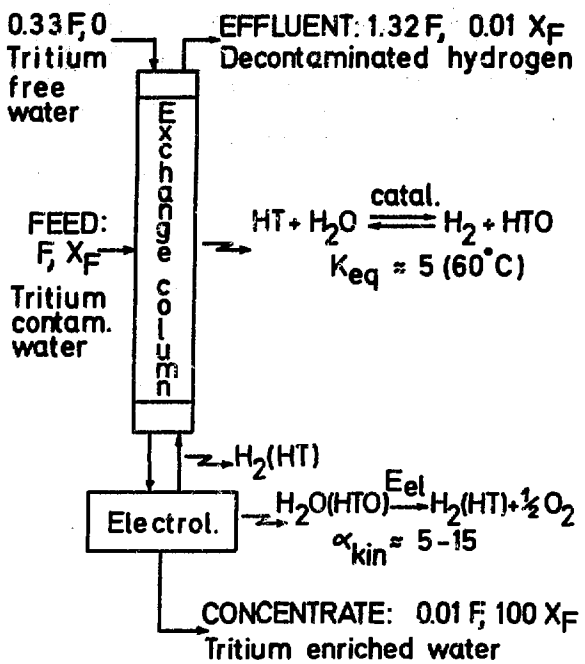

Fig. 1. ELEX process for detritiation of water.

from which it evolved, becomes more and more depleted in tritium when it flows from bottom to top. The tritium contaminated water is fed into the exchange column at the point where its tritium content corresponds to the local tritium content of the originally tritium free water that has been added at the top of the column. The tritium poor hydrogen stream at the top of the column can be vented and a small tritium enriched water fraction is removed as condensate from the electrolyser for immobilization and storage. Alternatives are possible : If reliable fuel cells become available, the decontaminated hydrogen can be oxidized in stead of vented and the electricity can be delivered to the electrolyser.

Assuming an elementary tritium-protium separation factor of 10 for the water electrolysis and an exchange temperature of 50 °C, the ELEX process needs only 5 overall exchange transfer units to concentrate 90 % of the original tritium in 1 % of the original volume. On these assumptions a technico-economical comparison of the ELEX process with two other possible methods for isotopic enrichment and separation of tritium from aqueous reprocessing effluents, namely water distillation and water electrolysis, shows that the total operating costs per year for the ELEX method can be expected to be about two to four times lower than for these other methods [10].

IV. The experimental investigation of the two steps separately

Initially the R & D work at S.C.K./C.E.N. concentrated on the separate constituent steps of the ELEX process. Electrolytic separation factors were experimentally determined and after the development of an own appropriate hydrophobic catalyst, studies in countercurrent packed-bed reactors allowed to optimize the overall tritium exchange rate.

For the study of electrolytic detritiation a test installation was constructed in a walk-in processing hood. This installation, which is shown schematically in Fig. 2, consists essentially of a transformer rectifier which allowed to work in constant current mode, a small (1.4 kW) but still industrial type of electrolyser with peripheric equipment for the conditioning of electrolyte and gases, and a sampling train for (tritiated) hydrogen. The electrolyser is of the bipolar and atmospheric pressure type and is composed of 12 cells in series. As the cathodes are made of mild steel, rather high tritium separation factors could be expected, especially at lower temperatures [15].

From a comparison of the tritium content of the water electrolysed and the tritium content of the hydrogen produced, the tritium-protium separation factor for the electrolysis installation described and for a 25 % potassium hydroxide solution was determined at current densities from 370 to 2600 $A.m^{-2}$ and at temperatures from 20 to 60 °C. The cell voltage that had to be applied was also measured and it increased from 1.85 to 2.23 V with increasing current density and with decreasing temperature. All experiments carried out yielded high separation factors, i.e. larger than 10. For "normal" working conditions, i.e. current densities from 1500 to 2600 $A.m^{-2}$ and temperatures from 40 to 60 °C (cell tension 2.06 to 2.21 V), a mean separation factor of 11.6, with a standard deviation of 6 %, was obtained. At lower current densities and at lower temperatures less reproducible but higher separation factors were obtained. Economically the latter working conditions are however less attractive.

The elementary separation factor for the exchange of tritium between hydrogen and liquid water is given by the equilibrium constant of the exchange reaction. This equilibrium constant equals about 7.2 at 20 °C and it decreases with increasing temperature. The isotope exchange is thus carried out at rather low temperatures and a catalyst is needed to obtain a sufficiently high exchange rate. Before starting the investigation in a trickle-bed installation, a catalyst development programme was thus executed. The aim of this programme was to find a suitable hydrophobic catalyst which promotes effectively the isotopic hydrogen exchange between hydrogen gas and water vapor while being in contact with liquid water. About 30 different types of hydrophobic catalysts were prepared and tested at S.C.K./C.E.N. The details of this selection procedure have been presented elsewhere [16, 17]. Finally, a home-made platina-on-carbon-plus-teflon catalyst appeared to show the best characteristics for application in the ELEX process [18].

For the trickle-bed experiments several test installations were constructed, one of which is shown schematically in Fig. 3. The exchange column, a thermostatically controlled plexiglass cylinder with an inner diameter of 20 or 30 mm and a length of about 2 m, comprised a catalytic section with the proprietary catalyst, surrounded at each end by a layer of inert glass spheres. To improve the liquid flow distribution within the exchange column and to increase the gas-liquid interface area, the hydrophobic catalyst particles were mixed with water wettable inerts in a volumetric ratio of about 1 : 2. The H_2-HT mixture was prepared in batches by evacuating a research-grade hydrogen tank (volume 50 dm^3), adding H_2-HT gas by means of a tritium gas dispenser and pressurizing with hydrogen. The liquid flow rate was controlled by a metering pump and to control the gas flow rate a mass flow regulator was used. Both feeds were heated before entering the reactor and gas flowing out of the bed was consecutively sent through a cooler condensor and a liquid nitrogen cooled trap to remove water vapor. The liquid level at the bottom of the column was kept constant with the aid of a double-level controller acting on a magnetic valve between the reactor and the water collecting tank. In a revised version a level controlling pump was used and the water leaving the exchange column pre-saturated the hydrogen feed. Furthermore the gas flowing out of the exchange column was sent

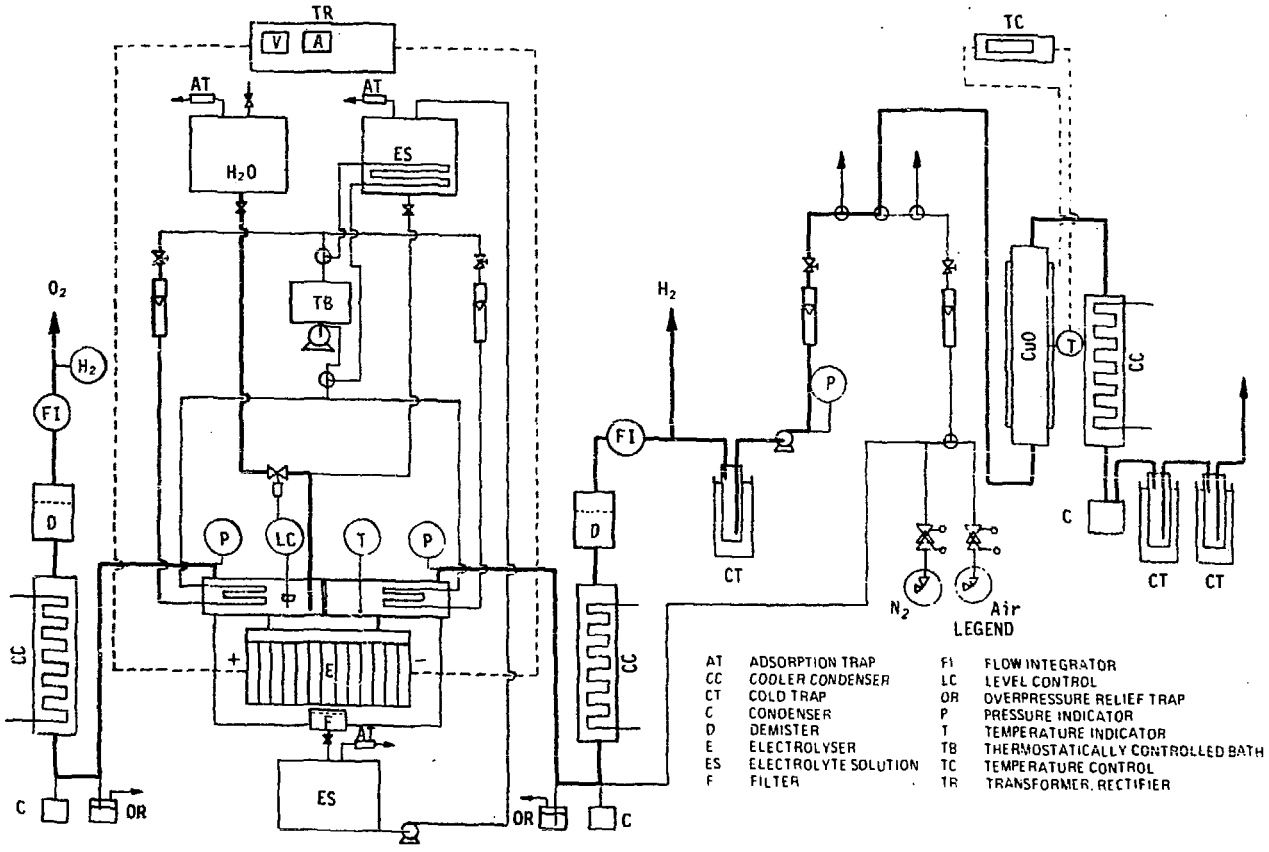

Fig. 2. Installation for the study of electrolytic detritiation

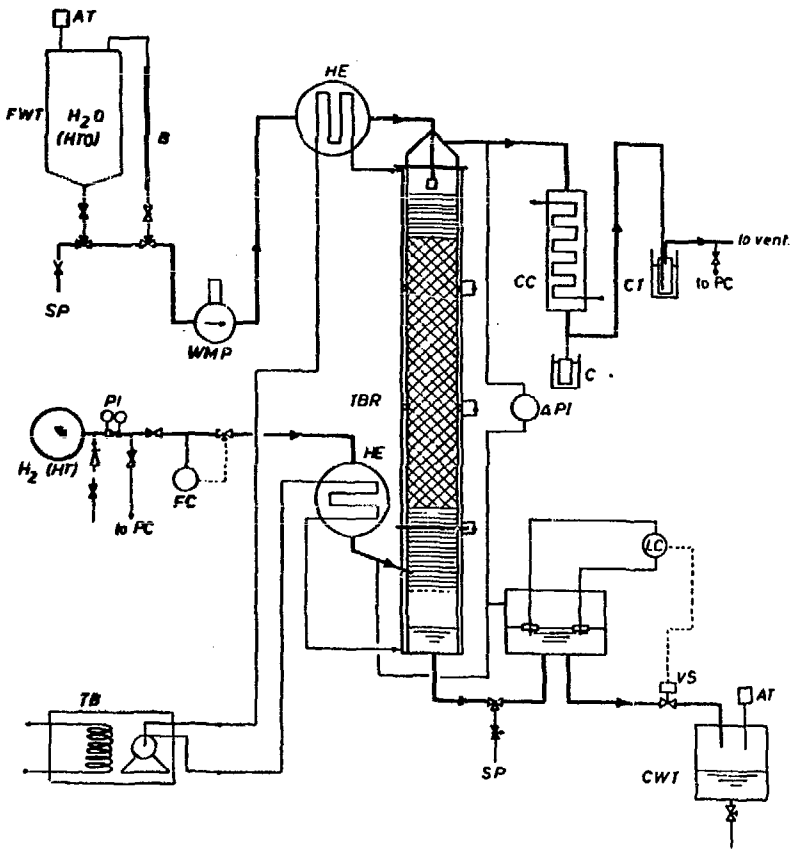

LEGEND

ΔPI	DIFFERENTIAL PRESSURE INDICATOR
WMP	WATER METERING PUMP
VS	SOLENOID VALVE
TBR	TRICKLE-BED REACTOR
TB	THERMOSTATICALLY CONTROLLED BATH
SP	SAMPLE POINT
PI	PRESSURE INDICATOR
PC	PROPORTIONAL COUNTER
LC	LEVEL CONTROL
HE	HEAT EXCHANGER
FWT	FEED WATER TANK
FC	FLOW CONTROL
CWT	COLLECTED WATER TANK
CT	COLD TRAP
C	CONDENSER
CC	COOLER CONDENSER
B	BURETTE
AT	ADSORPTION TRAP

Fig. 3. Installation for the study of tritium exchange in a countercurrent trickle-bed reactor.

through a stainless steel condensor cooled at 2 °C and placed on top of the column. Water samples for tritium determination by liquid scintillation counting were withdrawn before and after the reactor. The dry hydrogen before the reactor or after the liquid nitrogen cooled trap was continuously sampled and measured by proportional counting.

In the trickle-bed installations several experimental runs were performed with different batches of home-made hydrophobic catalyst particles in combination with various packing materials. Furthermore other parametric experiments were carried out during which the composition of the catalytic bed was kept constant. Most of these experiments were carried out at relatively low operating temperature, and to evaluate the performance of a particular combination of hydrophobic catalyst particles and water wettable inerts the presence of water vapor could thus be neglected [19]. Considering a small height of catalyst packing dZ(m) where the mol fraction of HT in the gaseous hydrogen is y and the mol fraction of HTO in the liquid water is x, the tritium exchange rate per unit column area can then be written as :

$$G'dy = k\,(y - y_e)\,dZ$$

where : G' : gas (hydrogen) flow rate per unit column area in $mol.s^{-1}.m^{-2}$

k : overall exchange rate constant in $mol.s^{-1}.m^{-3}$

Y_e : $\frac{x}{K}$, with K the equilibrium constant of the overall tritium exchange reaction

By definition, $H_{OG} \equiv \frac{G'}{k} \equiv$ height of an overall exchange transfer unit.

Using tritium free water and tritium containing hydrogen as feeds the steady-state tritium exchange rate was measured for bed depths of 0.5 to 2 m, at atmospheric pressure, at temperatures between 20 and 80 °C and at liquid and gas flow rates between 2 and 20 $mol.s^{-1}.m^{-2}$. In the experimental range the overall exchange rate constant k was independent of column height. The influence of column diameter was not systematically studied but the results in a 3 cm diameter column were comparable to those in a 2 cm diameter one. k was nearly independent of the gas and liquid flow rates, except for some decrease at the lowest liquid flow rates. Up to 60 °C k increased with increasing temperature but at higher temperatures this increase became marginal or nonexisting. For some column fillings, experiments at high temperature and at high gas and liquid flow rates were impossible because of flooding problems. By ameliorating the hydrophobic catalyst without increasing its platinum content (1 wt %) and by combining it with more suitable, etched packing materials, overall exchange rate constants of 100 to 140 $mol.s^{-1}.m^{-3}$ at 40 °C could finally be obtained in a reproducible way. These values are about 10 times higher than those reported earlier [16, 17].

V. The experimental study in an integrated bench-scale installation

The promising results obtained in the separate steps have incited us to the further development of the ELEX process. Therefore an integrated bench-scale detritiation unit with a nominal through-put of 10 $mol.h^{-1}$ has been built. Fig. 4 gives a partial view of this ELEX mini-pilot, which consists essentially of the above described electrolyser of 1.5 kW, two 2 cm diameter stainless steel exchange columns, partially filled with a mixture of hydrophobic catalyst particles and water wettable

Fig. 4. Partial view of the bench-scale ELEX installation.

packing material, and an available oxidation-adsorption installation which was modified to recombine the vented hydrogen. A detailed description of this installation, its components and its related safety aspects has been given elsewhere [2].

According to the regular working procedure, a fixed flow rate of 60 $cm^3.h^{-1}$ tritium free water is added at the top of the stripping column, and the water to be detritiated is added between the two exchange columns. By using a capacitive level sensor within the electrolyser, the latter flow rate is controlled as a function of the amount of water electrolysed. The electrolysis current is normally fixed at 60 A (2220 $A.m^{-2}$) over the 12 cells in series. No tritium enriched fraction is taken off. Electrolyte (droplets) and water (vapor) removed from the electrolytically produced hydrogen and oxygen gases, are recycled into the electrolyser. During each long-duration experiment the tritium concentration or the tritium to protium ratio of the feed water is kept constant, but with consecutive runs it has been gradually increased until a value of 100 $mCi.dm^{-3}$ because this concentration is expected for real reprocessing effluents. Before starting an experiment, the electrolyser is filled with a 25 wt % aqueous solution of potassium hydroxide which has about the same tritium to protium ratio as the water to be treated. The columns are preflooded with tritium free demineralized water, and their operating temperature is fixed at 40 °C.

For each experiment the overall tritium balance is rigorously checked. Statistical errors are minimized by multiple sampling and measuring. The most important uncertainty in preparing the overall tritium balance is the total amount of tritium enriched electrolyte at the end of the experiment, since after emptying the electrolyser and weighing the electrolyte a certain amount of electrolyte still remains in the electrolyser. This amount is determined on the basis of the measured dilution factor for KOH and for tritium when the electrolyser has been refilled by adding a known amount of water.

The integrated mini-pilot is provided with an extensive measuring and sampling system. Real-time measurements by proportional counting of tritium in the gaseous hydrogen stream are possible before, after and between the two exchange columns. Low-volume counters are used for the more active gas streams. Methane is added as a counting gas. For tritium determination by liquid scintillation counting, samples can be taken from the feed water, from the lye, from the water removed from the hydrogen and oxygen gas, from the aqueous streams leaving and entering the exchange columns, and from the water formed by oxidation of the effluent hydrogen. Before measurement appropriate dilution is carried out.

In the 10 $mol.h^{-1}$ bench-scale installation several integrated, long-duration detritiation experiments were carried out. As an example, the most interesting results of a continuous run of 941 h during which 174 dm^3 or 185 $cm^3.h^{-1}$ water with a tritium concentration of 20 mCi per dm^3 were detritiated are given in Fig. 5. The central catalytic part of the enrichment column, 74 cm, was filled with a mixture of 67 vol. % non-etched Dixon packings and 33 vol. % hydrophobic Pt-C-PTFE catalyst particles. In the stripping column the height of the catalytic bed, which was composed of 67 vol. % etched Dixon packings and 33 vol. % hydrophobic Pt-C-PTFE catalyst particles, was 208 cm. The total amount of water electrolysed was 232 dm^3 or 246 $cm^3.h^{-1}$, including 58 dm^3 or 61 $cm^3\ h^{-1}$ tritium free water for reflux. At 60 A the theoretical value is 242 $cm^3.h^{-1}$ plus 1.5 $cm^3.h^{-1}$ for the residual water in the effluent oxygen and hydrogen. The final volume reduction factor (enrichment factor) was 11.6 and the mean process decontamination factor was 372. The overall tritium balance fell within the experimental error limits.

In another experiment, which lasted 1371 h, 232.5 dm^3 water with a concentration of about 100 mCi tritium per dm^3 water were detritiated, or 169.5 $cm^3\ h^{-1}$.

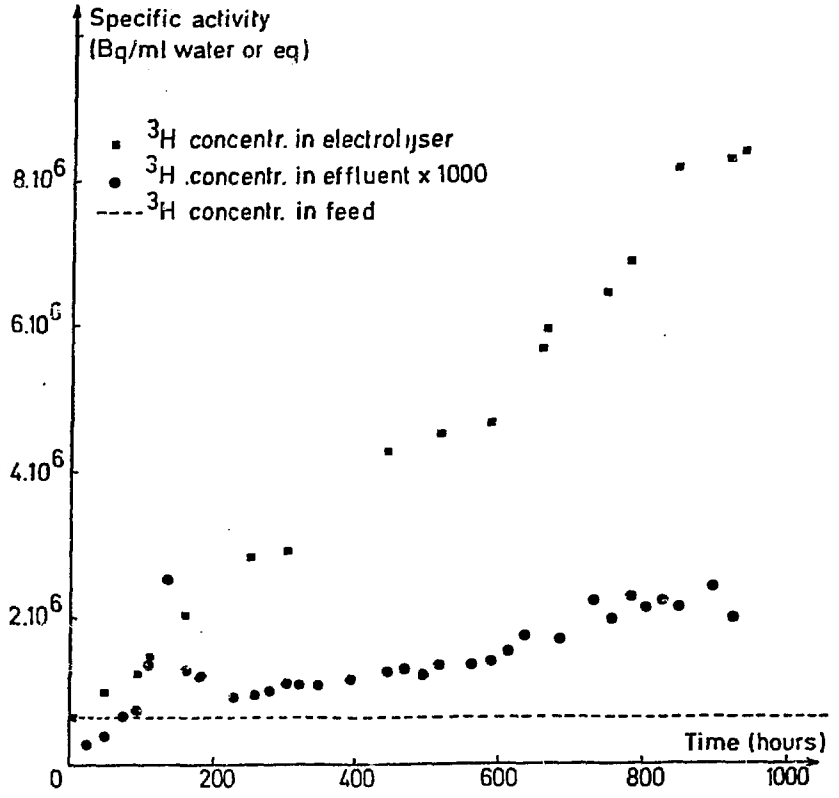

Fig. 5. Results of a bench-scale detritiation experiment

This is somewhat less than in the previous experiment because the minipilot did not always function at full capacity (60 A). 82.9 dm^3 or 60.5 cm^3 h^{-1} tritium free water were added. The final volume reduction factor was 14.1. The mean process decontamination factor was 295 although there was again a peak in the breakthrough of tritium, resulting from an accidental interruption in the addition of tritium free water at the top of the stripping column. Within the experimental errors, the overall tritium balance was in equilibrium.

The integrated and long-duration bench-scale experiments with an active feed demonstrated succesfully the feasibility of the ELEX process for isotopic enrichment and separation of tritium from water. They confirmed the results obtained earlier during the study of the separate constituent steps of the process. The electrolytic tritium-protium separation factor, about 15, and the overall tritium exchange rate constants, about 35 $mol.s^{-1}.m^{-3}$ when the hydrophobic catalyst particles were mixed with non-etched Dixon packings and about 50 $mol.s^{-1}.m^{-3}$ when they were mixed with etched Dixon packings, were approximately in accordance with previous experiments in the separate units. More exactly they were respectively somewhat higher and somewhat lower than expected. In a working period of more than 5000 hours the hydrophobic catalyst had not to be replaced. The water wettable Dixon packings were once re-etched.

More than 1 m^3 water containing up to 100 mCi tritium per dm^3 were detritiated, representing nearly 6000 working hours. The mean process decontamination factor was always higher than 100 and a continuous on-line monitoring of the tritium in the effluent hydrogen, with alarm and shut-down action, can further increase this factor. It could be useful to adapt the installation in such a way that the amount of water added at the top of the stripping column would be controlled as a function of the continuously measured breakthrough of tritium. The volume reduction factor increased linearly with time and for the 1000 to 1500 hours experiments it lay between 10 and 15. Higher volume reduction factors will become possible as soon as the present modified CJB electrolyser will be replaced by a new, low-volume electrolyser which will be constructed at S.C.K./C.E.N. The overall tritium balance could be kept within the experimental errors of the various measurements, indicating small overall tritium losses.

The technical availability of the installation amounted to 99 % or more for the last experiments. Remaining technical problems were caused by an insufficient gas-liquid separation within the present electrolyser and by false alarms, especially during thunderstorms. There were no contamination problems. The tritium concentration of the air in the processing hoods was continuously measured, but it never attained the maximum allowable HTO concentration for the laboratory, namely 2.10^{-5} $Ci.m^{-3}$. It was concluded that, although the bench-scale ELEX installation could be further improved, the technique had matured sufficiently to justify, in complete agreement with the successful results, the promotion of the ELEX study to a pilot-scale demonstration.

VI. The pilot detritiation installation

Based on these experiences a pilot detritiation installation has been designed and constructed as the ultimate step before industrial application. The principal components of the ELEX pilot are an electrolyser with a hydrogen production capacity of maximum 12 $m^3.h^{-1}$ (20 °C, 10^5 Pa) and a countercurrent packed-bed reactor with an internal diameter of 10 cm and a total height of 8 m. The construction material is mainly stainless steel. The 80 kW electrolyser is provided with a water recovery system and the thermostatically controlled exchange column, which contains the proprietary hydrophobic catalyst, has a saturator-evaporator at the bottom and a cooler-condensor at the top. Other main parts of the installation are the feed water system, the gas and liquid sampling system and the liquid waste system. Control instrumentation and health and safety equipment are amply provided. All tritium (and hydrogen) containing parts of the pilot are surrounded by a ventilated secondary enclosure which is at a lower pressure than the rest of the building and which is connected to an extant 60 m high stack. In this installation, which will have a tritium inventory of maximum 1000 Ci HTO, demonstration of the ELEX process will be performed, according to the following design specifications :

* through-put : 0.12 m^3 H_2O (HTO) per day or 280 mol h^{-1}
* feed concentration : 100 Ci tritium per m^3
* volume reduction factor : 100
* process decontamination factor : 100.

Fig. 6 shows the 80 kW electrolyser made by Teledyne C° while it was tested in advance. It appeared that some modifications are necessary to guarantee an uninterrupted and stable hydrogen production rate such as required for a good operation of the trickle-bed exchange part of the ELEX installation. Furthermore, from a process point of view, the tritium losses from the Teledyne electrolyser, as delivered, are too high and therefore several additional equipment pieces are necessary : The

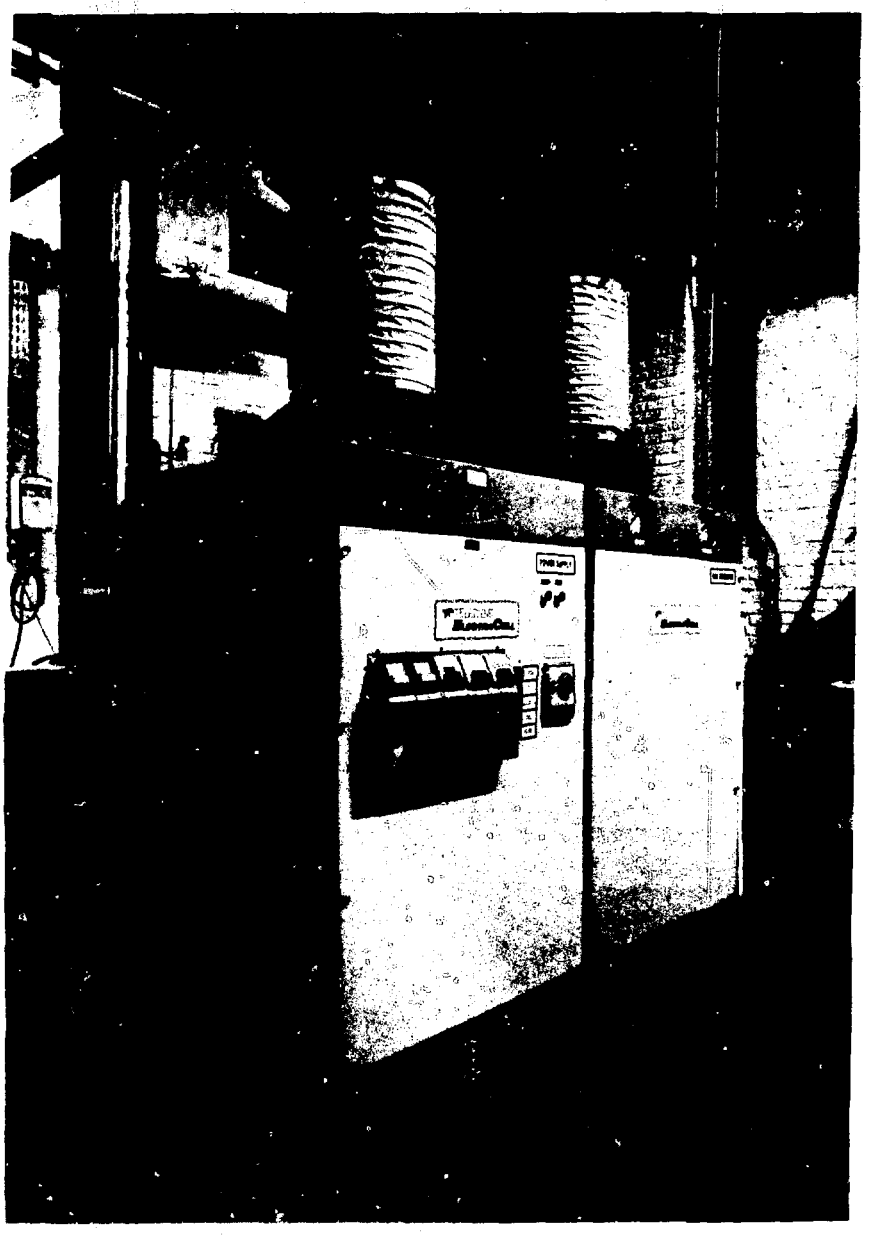

Fig. 6. The 80 kVA electrolyser fabricated by Teledyne C°, before its adaptation and installation in the ELEX pilot.

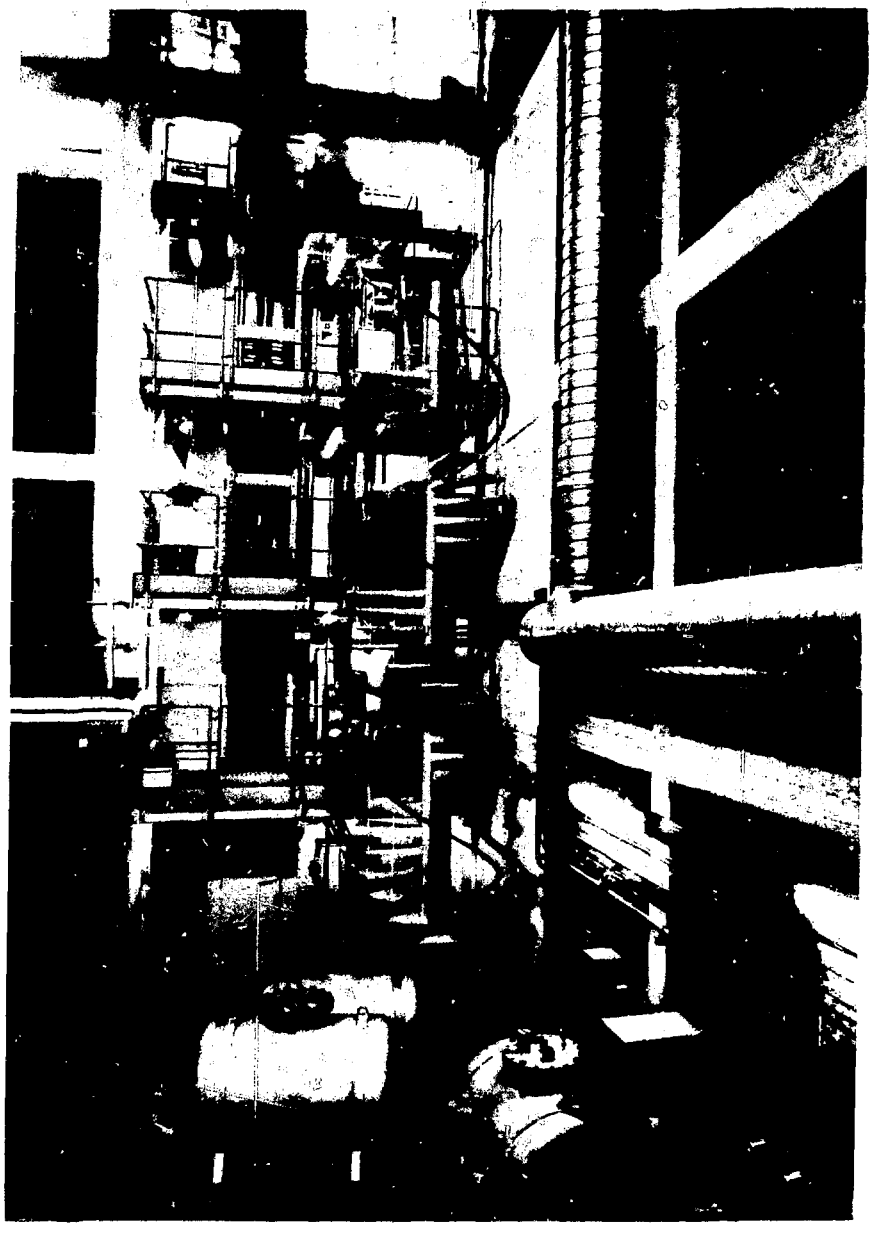

Fig. 7. The exchange part of the ELEX pilot installation during mounting.

tritiated water has to be removed from the vented gas streams and recycled into the electrolyser or stored as the tritium enriched fraction, while the tritiated hydrogen has to be added to the main hydrogen stream which is vented after decontamination in the exchange column. These adaptations are now assembled. Fig. 7 shows the exchange part of the ELEX pilot during mounting. After leak testing, precommissioning of the mechanical equipment and instrument testing, hydrodynamical commissioning of the exchange column is now under way. The startup with tritiated water is foreseen for early 1985. In a farther future the pilot installation will be supplemented with a pre-treatment unit because real reprocessing effluents will probably contain organic impurities, fission products and nitric acid, which would be detrimental to the ELEX system by adsorption on the catalyst or accumulation in the electrolyser. The removal conditions are already investigated on a laboratory scale.

VII. Conclusion

Experimental evidence has been obtained on the technical feasibility of the ELEX process for isotopic enrichment and separation of tritium from aqueous reprocessing effluents. Final experimental experience will be gained in the pilot installation that will soon be put into operation.

Design considerations have started to apply this knowledge for the treatment of tritiated streams in nuclear fusion reactors.

Acknowledgments

This work has been sponsored by the European Communities under contracts number 090-78-7 WAS B, WAS-159-B(D) and WAS-405-83-8-B (RS). The authors would also like to thank their colleagues from the Chemistry Department for stimulating discussions and valuable help. Thanks are also due to several members of the S.C.K./C.E.N. Electrochemistry Section and last but not least to the S.C.K./C.E.N. Technical Services, the collaboration of which was essential for the realization of the ELEX pilot installation.

References

[1] BRUGGEMAN, A., et al., "Separation of tritium from aqueous effluents", European Appl. Res. Rept. - Nucl. Sci. Technol., 4, 1 (1982) 63.

[2] BRUGGEMAN, A., et al., "Separation of tritium from aqueous effluents", EUR 9107 EN (1984).

[3] McKAY, H.A.C., "Tritium immobilization", European Appl. Res. Rept. - Nucl. Sci. Technol., 1, 3 (1979) 599.

[4] BURGER, L.L., TREVORROW, L.E., "Release of tritium from fuel and collection for storage", Controlling Air-borne Effluents from Fuel Cycle Plants (Proc. ANS-AIChE Topical Meeting Sun Valley, 1976), ANS, Hinsdale (1976).

[5] MIQUEL, P., GOUMONDY, J.P., SCHNEIDER, E., "Maîtrise du tritium dans les usines de retraitement", Radioactive Effluents from Nuclear Fuel Reprocessing Plants (Proc. CEC Seminar Karlsruhe, 1977), CEC, Luxemburg (1978) 497.

[6] HENRICH, H., SCHMIEDER, H., NEEB, K.H., "The concentration of tritium in the aqueous and solid waste of LWR fuel reprocessing plants", IAEA-SM-245/15 (1980).

[7] BAETSLE, L.H., BROOTHAERTS, J., "Reprocessing off-gas treatment research in Belgium", Radioactive Effluents from Nuclear Fuel Reprocessing Plants (Proc. CEC Seminar Karlsruhe, 1977), CEC, Luxemburg (1978) 421.

[8] GRIMES, W.R., et al., "An evaluation of retention and disposal options for tritium in fuel reprocessing", ORNL/TM-8261 (1982).

[9] INTERNATIONAL ATOMIC ENERGY AGENCY, "Management of tritium at nuclear facilities", Technical Reports Series No. 234, IAEA, Vienna (1984).

[10] BRUGGEMAN, A., et al., "Assessment of some methods for the separation of tritium from the aqueous effluents of a reprocessing plant", Reprocessing of Spent Nuclear Fuel (Proc. Tripartite Symposium Mol, 1978), Internal report R.2604, SCK/CEN, Mol (1978) 110.

[11] HAMMERLI, M., STEVENS, W.H., BUTLER, J.P., "Combined electrolysis catalytic exchange (CECE) process for hydrogen isotope separation", Separation of Hydrogen Isotopes (RAE, H.K., Ed.), Am. Chem. Soc. Symp. Ser. 68 (1978) 110.

[12] ELLIS, R.E., et al., "Final report : Development of combined electrolysis catalytic exchange", MLM-2952 (1982).

[13] MORISHITA, T., et al., "Tritium removal by hydrogen isotopic exchange between hydrogen gas and water on hydrophobic catalyst", Tritium Technology in Fission, Fusion and Isotopic Applications (Proc. ANS Topical Meeting, Dayton, Ohio, 1980), CONF-800427 (1980) 415.

[14] FIEK, H.J., ROMAKER, J., SCHINDEWOLF, U., "Tritium-Anreicherung durch Isotopen-Austausch zwischen Wasserstoff und Wasser mittels hydrophoben Katalysators für die Kernbrennstoff-Wiederaufbereitung", Chem.-Ing.-Tech., 52, 11 (1980) 892.

[15] VILLANI, S., "Isotope Separation", ANS (1976).

[16] BRUGGEMAN, A., et al., "Separation of tritium from reprocessing effluents", IAEA-SM-245/52 (1980).

[17] BRUGGEMAN, A., et al., "The ELEX process for tritium separation from aqueous effluents", Proceedings Tritium Technology in Fission, Fusion and Isotopic Applications (Proc. ANS Topical Meeting, Dayton, Ohio, 1980), CONF-800427 (1980) 411.

[18] BRUGGEMAN, A., et al., United States Patent No. 4,376,066, Mar.8, 1983.

[19] SHIMIZU, M., KITAMOTO, A., TAKASHIMA, Y., "New proposition on performance evaluation of hydrophobic Pt catalyst packed in trickle-bed", J. Nucl. Sci. Technol., 20, 1 (1983) 36.

CLOSING REMARKS OF SESSION CHAIRMAN GROENIER:

Three of the seven papers of this session have addressed a prime concern of mine relative to airborne waste retention and recovery. That concern is the integrated performance of tandem treatment steps. One paper reported on the inadequacies of materials of construction, not discovered when developing individual steps. Two others reported unsatisfactory performance of one or more components arising from the presence of several airborne waste constituents in a single process stream (SO_2 trapped in unit intended for I_2, CO oxidation in iodine sorber, and I_2 contamination of CO oxidizer catalyst). These papers confirm the need for additional work using an integrated systems approach and realistic feed streams.

Three of the remaining four papers have been excellent reports of basic R & D on process monitors, a low-temperature version of the U.S. Iodox process which also cleverly handles the problem of NO_x recovery, and the ELEX process for concentrating and recovering tritium from reprocessing waste streams. These are valuable additions to the off-gas treatment literature.

Finally, a paper on the operating performance of an actual treatment system in a production plant has generally confirmed previous data, much of it reported through this conference's proceedings, with regard to iodine retention systems.

I thank you all for coming to this session and for your participation. Especially, we thank the speakers for an interesting morning and encourage each of them to continue their work in this field.

Session 7

WORKING LUNCHEON

TUESDAY: August 14, 1984
CHAIRMAN: D.W. Moeller
Harvard School of Public Health

INVITED SPEAKER:

TITLE: THE SEARCH FOR GREATER STABILITY IN NUCLEAR REGULATION

SPEAKER: COMMISSIONER JAMES K. ASSELSTINE
U.S. Nuclear Regulatory Commission

INTRODUCTION BY CHAIRMAN MOELLER:

We are honored to have as our speaker today Commissioner James K. Asselstine of the U. S. Nuclear Regulatory Commission.

Mr. Asselstine was nominated for appointment to the Commission by President Reagan, his appointment was confirmed by the U. S. Senate, and he was formally sworn in in May, 1982. Prior to his appointment, Mr. Asselstine served as Associate Counsel for the Committee on Environment and Public Works, U. S. Senate. Previous to this assignment, he was Minority Counsel for the Committee's Subcommittee on Nuclear Regulation. During this assignment, Mr. Asselstine played a major role in the formulation of the Nuclear Waste Policy Act of 1982 which has proven to be one of the most beneficial and far reaching pieces of recent nuclear energy legislation. Mr. Asselstine also served as Co-Director of the Senate's investigation into the accident at Three Mile Island, Unit 2.

From 1975 - 1977, Mr. Asselstine served as Assistant Counsel for the former Congressional Joint Committee on Atomic Energy. From 1977 - 1978, he was a staff attorney in the Regulations Division of the NRC's Office of the Executive Legal Director, and from 1973-1975 he was a legal intern and staff attorney for the NRC's Atomic Safety and Licensing Board.

With that background, it is easy to understand the rapid pace with wnich Mr. Asselstine has assumed a position of leadership within the Nuclear Regulatory Commission. Coupled with his detailed knowledge of the legal and legislative aspects of the field of nuclear energy, Mr. Asselstine has endeared himself to the technical community through his insistence on becoming familiar with the real world aspects of nuclear power production. It was my

privilege to join him on a tour of the St. Lucie Nuclear Power Plant in March, 1982, and also to accompany him during the Federal Field Emergency Exercise conducted in Florida at that time. These are but two examples of his direct involvement in nuclear activities at the working level. If further proof is needed, I might also mention that during the two years he has served on the Commission, Mr. Asselstine has visited over 30 nuclear power plants within the U. S.

It is a pleasure to present Mr. Asselstine to you. His topic today will be "The Search for Greater Stability in Nuclear Regulation." Mr. Asselstine.

The Search for Greater Stability in Nuclear Regulation

remarks by
Commissioner James K. Asselstine
U.S. Nuclear Regulatory Commission

before the
18th DOE Nuclear Airborne Waste
Management and Air Cleaning Conference
August 14, 1984

Good afternoon, ladies and gentlemen. It is a real pleasure to be with you today to participate in the 18th Department of Energy Nuclear Airborne Waste Management and Air Cleaning Conference. I have chosen as the topic for my remarks the search for greater stability in nuclear regulation. At the outset, I should say that I support the objective of providing greater stability to our regulatory process. Today, I want to discuss two possible approaches for dealing with the problems of new and rapidly changing regulatory requirements. The first approach relies heavily on the more traditional licensing reform initiatives that have been considered off and on for the past decade. The second approach would consider a new regulatory philosophy aimed at the root causes of the proliferation of new safety requirements that have been imposed in recent years.

For the past few years, the concepts of deregulation and regulatory reform have been in fashion in Washington, and the commercial nuclear power program has not remained unaffected. Many look to these concepts

to provide greater stability in our regulatory program. The NRC, the nuclear industry and the Administration have all been avidly pursuing regulatory reform initiatives, which take the form of both legislative and administrative proposals. Many of these proposals really look to the future, and, if adopted, would have little impact on currently operating nuclear power plants or plants now under construction. However, a few would apply to the present generation of plants.

In their less controversial aspects, these proposals seek to establish a framework for future plant applications that would encourage the expanded use of more complete standardized plant designs in this country. Typically, these proposals would provide for the issuance of standardized plant design approvals, early site permits that can be issued separate from a specific plant design, and combined construction permits and operating licenses that would resolve most, if not all, design questions prior to the start of plant construction. Although many of these provisions are useful and I have supported them , I have to say that given the absence of interest in new plant orders, they are less relevant today and probably for some years to come than are matters affecting the plants now in operation and under construction.

In their more controversial aspects, the various licensing reform proposals would have a direct and significant impact on the Commission's ability to impose new safety requirements and the extent of public involvement in our licensing process. Certainly the nuclear industry's first priority has been backfitting -- the process for imposing new

safety requirements on existing plants. Backfitting proposals sponsored by the nuclear industry and the Administration seek to set a high safety threshold, to impose requirements for detailed written analyses, to establish requirements that imply the need for a quantifiable comparison of economic costs and safety benefits, and to set internal NRC review procedures that would apply to the Agency's consideration of any new generic or plant-specific requirement. In my judgment, these proposals would severely restrict the Commission's discretion to require new safety measures for existing plants, particularly in those cases in which the safety benefit of the measure is more judgmental in nature and cannot be precisely quantified.

A second category of more controversial licensing reform proposals involves changes to the NRC's hearing process for licensing nuclear power plants. These proposals attempt to eliminate altogether some opportunities for obtaining a hearing on significant safety and environmental issues. This would be the case, for example, for plant construction quality assurance issues, for emergency planning, and for issues regarding the qualifications of the plant operating staff under some of the proposals for the use of combined construction permits and operating licenses. The hearing proposals also attempt to change the type of hearing required from the present trial-type hearing to a more informal approach involving a combination of legislative-style and trial-type hearing procedures. In addition, some of the hearing proposals attempt to curtail the rights of public participants in the hearing by restricting their access to information, by imposing a higher

threshold for the admission of contentions, by requiring the early filing of contentions before all relevant information is available and by restricting opportunities for cross-examination.

Still a third category of these licensing reform proposals involves changes to the internal management of the NRC licensing process. These include changes to the role of the NRC staff in licensing hearings, changes to the ex parte restrictions that prevent Agency decisionmakers from communicating privately with NRC staff members on issues that are in controversy in the hearings, changes to the internal appeal process for reviewing initial licensing board decisions, and changes to the process by which the Commissioners personally review and approve the issuance of each full-power operating license for a nuclear power plant.

Taken together, these more controversial "reform" proposals would result in a significant measure of deregulation. The Commission would be hampered to a considerable degree in its ability to impose new safety requirements for existing plants, and opportunities for public participation in the NRC licensing process would be much more limited. In those areas in which members of the public could still participate, their hearing rights would be much more narrowly defined. All of this would bring some measure of short-term stability to nuclear regulation by decreasing both the number of new NRC safety requirements and the uncertainty associated with licensing hearings. But those gains are likely to be transitory at best given the failure of these reform measures to address the root causes that have led to the proliferation

of new and changing regulatory requirements in recent years. Moreover, any short-term gains in regulatory stability will likely be accompanied by a substantial loss in public confidence in the Commission's ability to assure safety, in the basic fairness of our regulatory program, and ultimately, in the safety of the plants that we regulate. For these reasons, I conclude that the more radical regulatory reform proposals do not provide a prudent or effective solution to the problem of new and changing requirements.

This does not mean that all efforts to improve the licensing process should be abandoned. Some regulatory reform measures can and should be adopted. These include a more modest legislative proposal that focuses on the less controversial elements of a licensing framework for future standardized designs. In addition, some measures to address backfitting are appropriate. These measures could establish a more formal and disciplined review process for new requirements that does not turn our staff into cost-benefit analysis writers and that avoids establishing artificial barriers to the adoption of justified safety improvements. Some improvements in the internal NRC management of the licensing process and in our hearing procedures could also be made. The focus of all of these changes should be on improving the quality of our safety and licensing decisions. However, by assuring sound decisions as early as possible in the licensing process, these measures will provide at least some additional measure of regulatory stability. But these gains are likely to be gradual, and most evident in the case of any future plants.

If sweeping changes to our licensing process are not the answer, I nevertheless see an alternative path to greater regulatory stability. That path would more directly address the problems that have led to the proliferation of new safety requirements and the manner in which those requirements have been imposed. But to better understand this approach, it is perhaps useful to spend a few minutes on the origins of the nuclear regulatory philosophy in this country and the positive and negative sides of the current nuclear safety ledger.

The first regulatory philosophy was formulated, in concert with congressional direction, in the mid-1950's. According to that philosophy, the AES should impose the minimum amount of regulation while fulfilling its obligations to protect the public health and safety. To nurture further development of the technology in the private sector, the Federal Government offered free R&D in government laboratories and waived certain loan charges to those utilities willing to undertake a demonstration project. These incentives and the regulatory philosophy behind them were justified on the ground that the private industry had assumed the economic risk of the proposed project. The initial regulatory philosophy of the 1950's and early 1960's was also premised on the AEC's excellent reactor safety record which, in turn, was based on careful, conscientious, and skillful operations; and adequate maintenance. In short the minimum regulatory philosophy was based on the assumption that each project would be done correctly, and would be done correctly the first time. As we began to learn more about the plants in the 1970's, it became apparent that some of the assumptions underlying the minimum regulation

philosophy were incorrect. This led to an ever-increasing number of new and progressively more prescriptive requirements, regulations and reinterpretations. By far the greatest number of these occurred after the Three Mile Island Accident.

In terms of the present safety ledger, I see several elements on the positive side. First, there has been a significant change in safety attitudes among our licensees since the TMI accident. Most, if not all, fully understand the enormity and complexity of the challenge they face in assuring the safe operation of the plants. Second, many of the post-TMI safety improvements are now in effect. More personnel are involved in plant operations, and they are better trained and qualified to deal with emergency situations. Emergency procedures, which are oriented toward understanding and responding to the symptoms of accident situations, have been developed. Better accident diagnostic tools and instrumentation are now available. Emergency planning has been substantially improved. And some hardware changes have been developed to address specific accident problems. The success of many of these post-TMI efforts has been evident in utility responses to serious operating events such as those at Crystal River and Ginna.

Third, the nuclear industry has initiated a coordinated effort to improve operational performance. The centerpiece of this effort is INPO, the Institute for Nuclear Power Operations. Finally, there has been generally good start-up experience for the new plants licensed since the Three Mile Island Accident. For operating reactors, plant operations

have been generally successful, with some notable improvements in plants that had been consistently weak performers.

However, I also see several elements on the negative side of the safety ledger. Just as there have been some notable successes in the past-TMI period, there have been some notable failures. Examples are the Salem ATWS event, the Grand Gulf start-up program and the Zimmer construction quality assurance breakdown. Second, a number of post-TMI changes are taking much longer than anticipated. These include the Safety Parameter Display Systems, the Technical Support Centers, the Post Accident Sampling Systems and the Reactor Coolant Inventory instrumentation. The last item, in particular, probably will not be installed and operational in some plants until 10 years after the TMI accident.

Third, we are having great difficulty in resolving some lingering problems. Two examples are fire protection and the environmental qualification of electrical equipment. With regard to fire protection, we are now approaching four years after the adoption of the Commission's rule. Yet a substantial number of plants still do not comply and some utilities are still arguing over the requirements. Similarly, for environmental qualification, it is now nearly two years after the Commission issued its rule, and the majority of the equipment in operating plants has not been demonstrated to have the ability to withstand the effects of an accident environment and still perform its intended function.

Fourth, we are continuing to experience problems with plant equipment and components that significantly affect reliability and that are of potential safety significance. Two examples are pipe cracks for boiling water reactors and steam generator tube ruptures for pressurized water reactors. Fifth, the role of plant personnel continues to be a key factor in safety significant operating events. Personnel errors in maintenance and surveillance testing have become the principal contributor in about one-half of all abnormal occurrences reported to Congress by the NRC in the past few years.

A sixth problem area relates to acquiring and retaining qualified plant personnel, particularly licensed reactor operators. A number of utilities, including some with substantial nuclear operating experience, are having difficulty in putting together qualified operating crews for the new plants. These utilities are experiencing particular difficulty in obtaining operators with previous licensed operating experience at a similar type of plant. As a result, some plants will begin operating without having any member of the licensed operating crew with any previous experience as a licensed reactor operator. In such cases, the industry has proposed, and the Commission has accepted, an approach that would rely on either the experience gained at a six-month visit to an operating plant or the use of non-licensed shift advisors with previous operating experience.

Finally, the Commission and the industry have not yet faced up to the severe accident question. The Three Mile Island accident demonstrated

that a severe accident leading to large-scale degradation of the reactor core can occur. Despite this fact, NRC's principal severe accident efforts thus far have focused on future plant designs rather than on the roughly 120 plants now in operation or under construction. In addition, there is a disturbing tendency to emphasize procedural changes -- changes that would inevitably place a greater burden on plant operating personnel -- rather than to consider possible hardware modifications to prevent or mitigate the consequences of severe accidents.

What this all means to me is that we are not yet to the point that would justify a return to the minimum regulation approach of the 1950's and 1960's. We have much to do in addressing the safety problems we are now aware of, and I expect that we will continue to identify new ones. If we continue with our current regulatory approach, we will be involved in a continual exercise to address the latest safety problem. This reactive approach to safety is likely to lead to further new requirements, prescriptive regulations and reinterpretations. The more extreme regulatory reform measures that I have described would only serve to postpone this result, perhaps with disastrous consequences.

Given this state of affairs, it seems prudent to consider alternative regulatory approaches that would put the Commission in a more active regulatory mode. Such a new regulatory philosophy might well include one or more of the following elements: a shift in regulatory focus to industry management; the establishment of reliability standards or performance objectives, particularly in areas of general weakness

throughout the industry; increased emphasis on inherent safety, and the use of more creative NRC-industry relationships.

A key element in the success or failure of a nuclear plant operation is the licensee's staff, management and organization. We ought to recognize this fact and target our regulatory efforts toward assuring effective, capable plant management with a strong commitment to safety as the first priority. We should give particular attention to the weak performers and we should reward the strong ones. Such an approach could effectively reduce the number of operating problems that have led to the development of new, prescriptive requirements in the past.

The development of more detailed reliability standards and performance objectives could help assure overall improvement in areas of weakness, while minimizing the potential for changing prescriptive requirements.

Greater attention to inherent safety could both improve our overall assurance of the ability to prevent or mitigate severe accidents and minimize the need for subsequent prescriptive responses to individual plant operating events. It is clear that many other countries have given much greater weight to the benefits of inherent safety measures than we have. Finally, new relationships between the NRC and the industry, including the recognition of industry efforts such as INPO that are having demonstrated success and the use of designated Federal representatives within the industry, could help improve industry performance.

Taken together, these elements of a new regulatory philosophy could perhaps more effectively address the types of problems that have led us to the present reactive and prescriptive approach to regulation. It seems to me that now is the time to think about constructive new approaches -- approaches that will not merely postpone problems but rather will solve them. Thank you.

Session 8

FIRE, EXPLOSION, EARTHQUAKE, TORNADO

TUESDAY: August 14, 1984
CHAIRMEN: H.J. Ettinger
S.C. Soderholm
Los Alamos National Laboratory

SEISMIC SIMULATION AND FUNCTIONAL PERFORMANCE EVALUATION OF A SAFETY RELATED, SEISMIC CATEGORY I CONTROL ROOM EMERGENCY AIR CLEANING SYSTEM
D.K. Manley, R.D. Porco, S.H. Choi

COMPARISON AND VERIFICATION OF TWO COMPUTER PROGRAMS USED TO ANALYZE VENTILATION SYSTEMS UNDER ACCIDENT CONDITIONS
S.H. Hartig, D.E. Wurz, Th. Arnitz, V. Ruedinger

RESPONSE OF AIR CLEANING SYSTEM DAMPERS AND BLOWERS TO SIMULATED TORNADO TRANSIENTS
W. Gregory, E. Idar, P. Smith, E. Hensel, E. Smith

FIRE SIMULATION IN NUCLEAR FACILITIES -- THE FIRAC CODE AND SUPPORTING EXPERIMENTS
M.W. Burkett, R.A. Martin, D.L. Fenton, M.V. Gunaji

THE MATHEMATICAL MODELLING OF FIRE IN FORCED VENTILATION ENCLOSURES
G. Cox, S. Kumar

OPENING REMARKS OF SESSION CHAIRMAN ETTINGER:

This session is entitled "Fire, Explosion, Earthquake, Tornado". I am very pleased to have the Nuclear Air Cleaning Conference focused on different aspects of atypical situations of concern from an air cleaning and waste management point of view

SEISMIC SIMULATION AND FUNCTIONAL PERFORMANCE EVALUATION OF A SAFETY RELATED, SEISMIC CATEGORY I CONTROL ROOM EMERGENCY AIR CLEANING SYSTEM

D. K. Manley and R. D. Porco
Filter Products Division
Mine Safety Appliances Company
Evans City, Pennsylvania 16033

S. H. Choi, P.E.
Plant Engineering Department
Yankee Atomic Electric Company
Framingham, Massachusetts 01701

Abstract

Under a nuclear contract MSA was required to design, manufacture, seismically test and functionally test a complete Safety Related, Seismic Category I, Control Room Emergency Air Cleaning System before shipment to the Yankee Atomic Electric Company, Yankee Nuclear Station in Rowe, Massachusetts. The installation of this system was required to satisfy the NRC requirements of NUREG-0737, Section III, D.3.4, "Control Room Habitability".(1)

The filter system tested was approximately 3 ft. (1 meter) wide by 8 ft. (2.5 meters) high by 13 ft. (5.5 meters) long and weighed an estimated 8,300 pounds (3,265 kilograms). It had a design flow rate of 3,000 SCFM (1,416 liters/sec.) and contained four (4) stages of filtration - prefilters, upstream and downstream HEPA filters and Type II sideload charcoal adsorber cells.

The filter train design followed the guidelines set forth by ANSI/ASME N509-1980. Seismic Category I Qualification Testing consisted of resonance search testing and triaxial random multifrequency testing. Seismic qualification testing was performed in accordance with IEEE Standard 344-1975 and Yankee Atomic Electric Company's RRS (Required Response Spectra). Seismic testing consisted of three (3) single-axis sine sweeps, one (1) in each of the three (3) orthogonal axes; five (5) triaxial OBE (Operating Basis Earthquake) test responses; and one (1) triaxial SSE (Safe Shutdown Earthquake) test response. Functional tests, in accordance with ANSI/ASME N510-1980, were conducted both before and after seismic qualification testing to demonstrate system integrity.(2,3,4,5)

In addition to ANSI/ASME N510-1980 testing, triaxial response accelerometers were placed at specific locations on designated prefilters, HEPA filters, charcoal adsorbers and test canisters along with accelerometers at the corresponding filter seal face locations. The purpose of this test was to demonstrate the integrity of the filters, filter seals, and monitor seismic response levels which is directly related to the system's ability to function during a seismic occurrence.

The Control Room Emergency Air Cleaning System demonstrated the ability to withstand the maximum postulated earthquake for the plant site by remaining structurally sound and functional.

I. Introduction

In commercial nuclear power plants, filtration systems are used for various air cleaning purposes. The applications vary from release prevention of fission products, to in-house environmental cleanup. The most critical air filtration systems are classified Safety Related, Seismic Category I.

The Control Room Emergency Air Cleaning System, designed by MSA for Yankee Atomic Electric Company, is one such system. Its purpose is to provide clean, contamination free air to the control room operators during an incident to enable the operators to bring the reactor to a safe shutdown. The ultimate means of demonstrating a system's ability to withstand an earthquake is to functionally test the system under the most severe earthquake postulation for the plant site. The system was tested in accordance with the requirements of IEEE Standard 344-1975 and ANSI/ASME N510-1980. By doing so, Criterion III of Appendix B to 10CFR50, Section 3.10 of the "Standard Review Plan" NUREG-0800 and Regulatory Guide 1.52 are satisfied.[6,7,8]

The purpose of this paper is twofold. The first is to demonstrate that the Control Room Emergency Air Cleaning System maintained it's structural integrity when tested under simulated seismic conditions. The second is to prove the system's ability to function before, during and after a seismic occurrence.

II. Test Specimen

A schematic of the Control Room Emergency Air Cleaning System, hereinafter called the system, is shown in Figure 1. The air enters the system through a 20 inch (51 cm) diameter primary inlet and backdraft damper located on the left side as you face the system doors. An auxiliary inlet is located perpendicular to the primary inlet on the back side of the system. The air then travels through a mixing transition and continues through the prefilter and first stage HEPA filters. The air then enters the Type II sideload charcoal adsorber section and proceeds through the final HEPA section and exits through a flanged outlet transition.

The filter system was fully instrumented. Differential pressure gages were installed across the prefilter, upstream HEPA, charcoal adsorber stage and downstream HEPA banks. A high temperature fire detection system was installed on the charcoal adsorber stage.

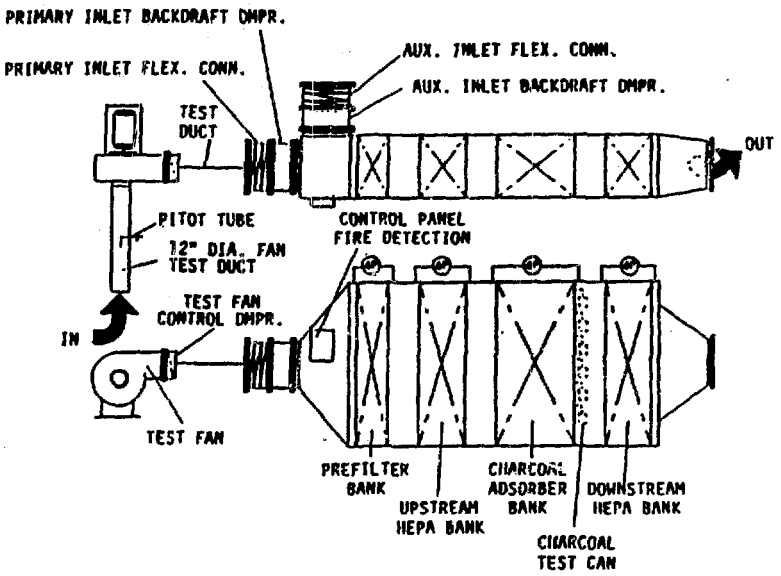

Figure 1. Control Room Emergency Air Cleaning System Schematic.

Qualification testing of the instrumentation, with the exception of the prequalified high temperature fire detection system was not required, however, MSA tested the unit with all equipment installed to simulate site installation. The system fan was prequalified and not retested with the unit due to space limitations of the test table. Figure 2 depicts the unit as it was mounted on the test table.

The installed prefilters, HEPA filters, Type II, sideload, charcoal adsorber cells and charcoal test canisters are as shown in Figures 3, 4, 5 and 6, respectively. Each filter shown is representative of a design that MSA has previously seismically qualified.

III. Pre-Seismic ANSI/ASME N510-1980 Testing

Procedures

All inspections, tests and calculations were performed in accordance with procedures outlined in the ANSI/ASME N510-1980 Standard. Inspections, tests and calculations consisted of the following:

- Visual Inspection
- Air Flow Capacity Testing
- Air Distribution Testing
- Adsorber Residence Time Calculation (not required by ANSI/ASME N510-1980)
- Air-Aerosol Mixing Uniformity Testing
- HEPA Filter Bank, In-Place Leak Testing
- Adsorber Stage, In-Place Leak Testing

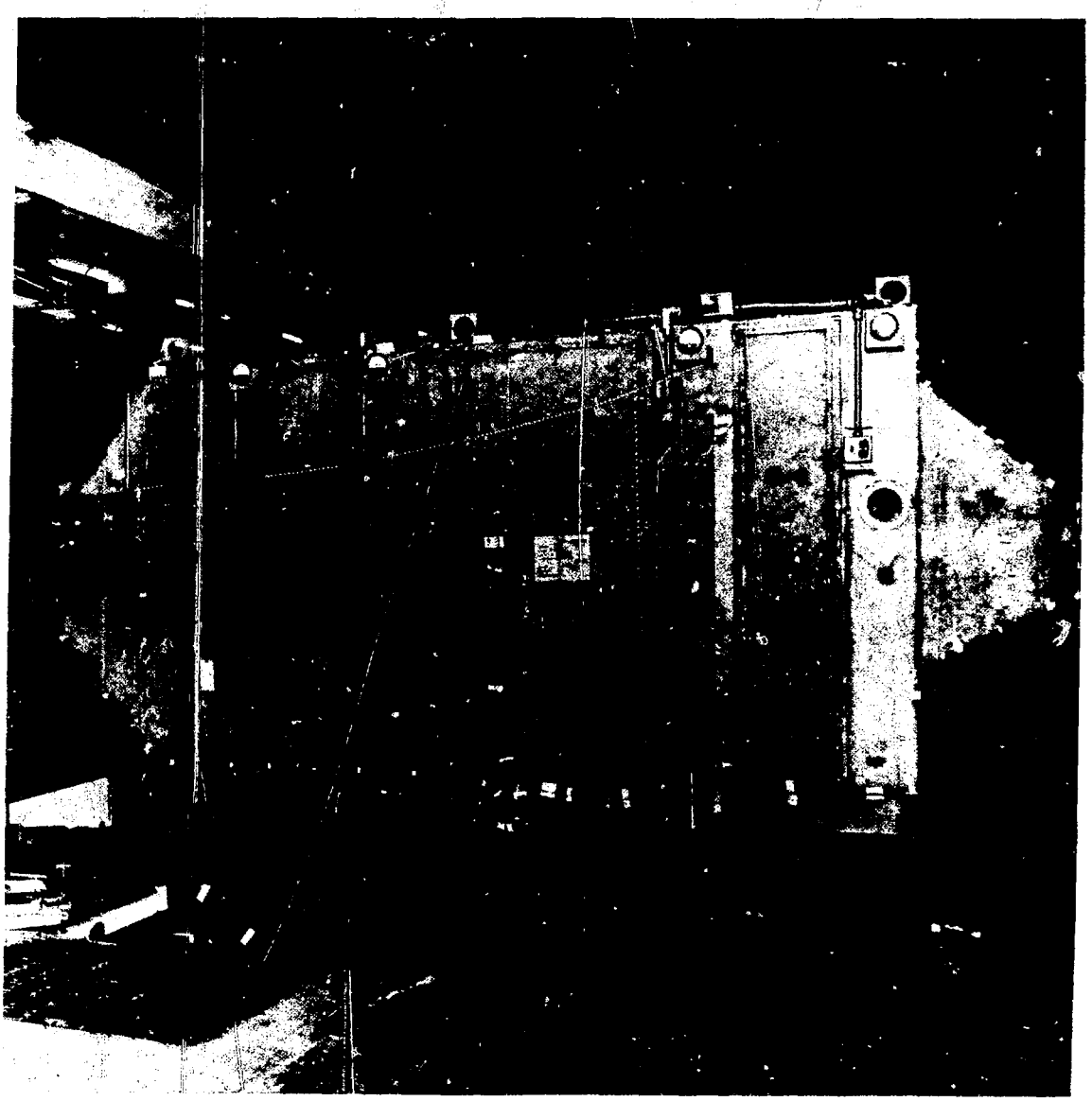

Figure 2. Unit and Test Table.

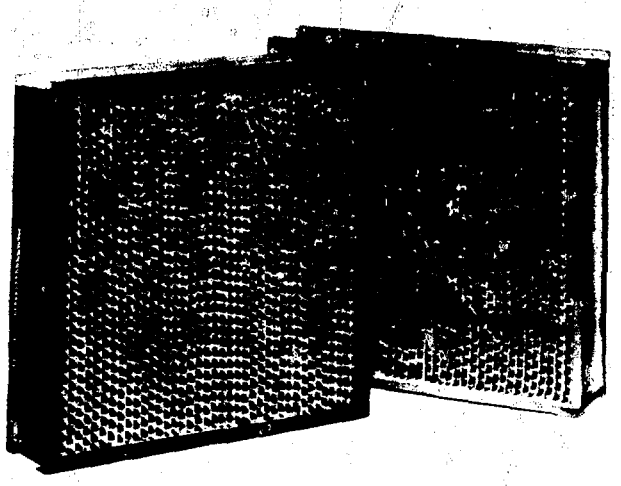

Figure 3. MSA Dustfoe Series Prefilter.

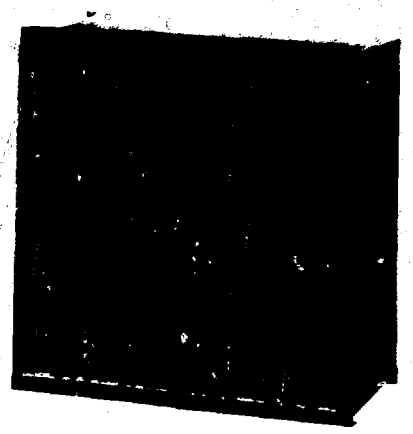

Figure 4. MSA HEPA Filter.

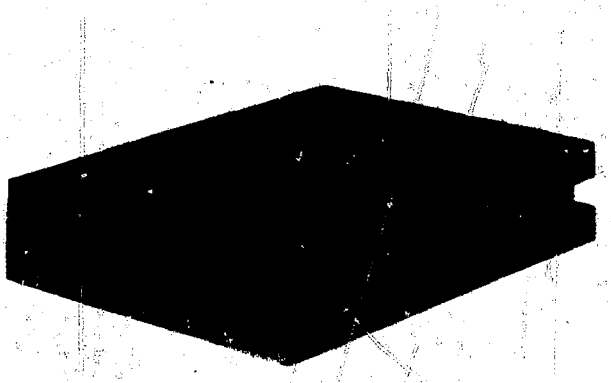

Figure 5. MSA Type II, Sideload, Charcoal Adsorber Cell.

Figure 6. MSA Charcoal Test Canister.

Since the procedures for the above are standard throughout the industry, they are not detailed herein.

Visual Inspection

Visual inspection of the system was performed in accordance with Paragraph 5.1 of ANSI/ASME N510-1980 to reveal deficiencies, if any, that might result in failure of the system to pass testing or invalid test results. Visual inspection found no deficiencies.

Air Flow Capacity Test

An air flow capacity test was performed in accordance with Paragraph 8.3.1 of ANSI/ASME N510-1980. The pitot tube traverse method was employed with a total of twenty (20) sample point readings being taken in a twelve (12) inch (30.5 cm) diameter duct, located on the inlet of the test system fan. Readings were taken in both the horizontal and vertical directions.

To set the air flow for testing, MSA monitored the differential pressure gauges located across the HEPA filter banks. The fan manual control damper was adjusted until a pressure drop reading of approximately one (1) inch W.G. (1.9 mm Hg) was achieved. At this point flow measurements were taken. The flow measurement readings are as listed in Table 1.

Table 1. Air Flow Capacity.

	Velocity, FPM									
Horiz. Readings	2900	3300	3550	3550	4250	4600	4400	3750	3800	3400
Vert. Readings	3300	3550	3700	4000	4100	4100	4100	3900	3675	3175

The system volumetric flow rate was calculated as follows: first, the average sample duct velocity was calculated from the following equation:

$$\bar{V} = \frac{\Sigma_i^n V_i}{n}$$

ANSI/ASME N510-1980, Para. 8.3.1 4. (1)

$\bar{V}$ = 3,755 FPM (1908 cms/sec.)

where: $\bar{V}$ = average velocity through the housing
V_i = individual velocity readings
n = number of velocity readings

second, the volumetric flowrate, Q, was calculated from the equation shown below:

$$Q = A\,\bar{V}$$

ANSI/ASME N510-1980, Para. 8.3.1 4. (2)

Q = 2,948 SCFM (1391 liters/sec.)

where: A = cross-sectional area where velocity traverse was made 0.785 $ft.^2$.

The volumetric flowrate per ANSI/ASME N510-1980, Paragraph 8.3.1.8 has an acceptance criteria of ±10% of design flow or 2,700 to 3,300 SCFM based on the system's 3,000 SCFM design. The actual volumetric flowrate is therefore within -1.7% of the allowable.

Air Distribution Testing

The air distribution test was performed, by taking readings downstream of the first HEPA filter bank, in accordance with ANSI /ASME 510-1980, Paragraph 8.3.2. The data collected during this test is shown in Table 2.

Table 2. Air Distribution Velocity Readings.

Velocity, FPM					
280	240	230	260	300	250
260	260	260	230	260	260

The average velocity was calculated by using the same velocity equation as that of the air flow capacity test. The average velocity calculated is 257.5 FPM (131 cms/sec.). Per ANSI/ASME N510-1980, Paragraph 8.3.2.4, "All readings shall be within ±20% of the average velocities measured." Therefore, based on the aforementioned average velocity calculated, the high reading is 16.5% above the calculated average and the low reading is 10.6% below.

Adsorber Residence Time Calculation

The Type II Charcoal Adsorber Cell residence time was calculated from the equation:

$$T = \frac{nNt\ (A-b)}{28.8\ Qs}$$

ANSI/ASME N510-1975, Para. 8.3.3[9] (3)

where:

- T = residence time, sec.
- n = number of cells in system
- N = number of adsorbent beds per cell
- t = thickness of adsorbent-bed, inches
- A = gross area of all adsorbent-bed screens of one cell, inches^2
- b = area of baffle, margin, and blank area of all adsorbent-bed screens of one cell, inches^2
- Q = volumetric flow rate of system, CFM
- s = number of screens of one cell

$$T = \frac{(9)(2)(2)(2,880-296)}{(28.8)(2,948)(4)}$$

$$T = 0.27 \text{ seconds}$$

The above result indicates that the residence time for the adsorber cells exceeds the system requirement of 0.25 second, minimum.

Air-Aerosol Mixing Uniformity

The air-aerosol mixing uniformity test was performed in accordance with Section 9 of ANSI/ASME N510-1980. DOP (dioctyl phthalate) aerosol was introduced into the air stream by injecting at the test fan inlet. Aerosol concentration readings were taken a short distance upstream and across a plane parallel to the first HEPA filter bank. Penetrometer meter readings are given in Table 3.

Table 3. Air-Aerosol Mixing Uniformity.

Penetrometer Meter Reading					
.60	.60	.60	.60	.63	.58
.60	.60	.65	.60	.67	.60

The average concentration for the penetrometer readings was calculated using the following formula:

$$\bar{C} = \frac{\Sigma_i^n C_i}{n} \qquad \text{ANSI/ASME N510-1980, Para. 9.4 5.} \qquad (4)$$

$$\bar{C} = 0.60$$

where:

$\bar{C}$ = average concentration readings
C_i = individual concentration readings
n = number of readings taken

The average concentration is 0.60 or 60%. Per ANSI/ASME N510-1980 the maximum and minimum readings must be within ±20% of the average air-aerosol uniformity reading. For this particular test the maximum reading is 8.3% high and the minimum reading is 3.3% low. Both readings are well within the allowable, therefore the uniformity of these readings establishes the acceptability of the injection location.

HEPA Filter Bank, In-Place Leak Test

In-place HEPA filter bank leak tests were performed on both the upstream and downstream HEPA filter banks. The tests were performed in accordance with Section 10 of ANSI/ASME N510-1980.

The upstream DOP (dioctyl phthalate) aerosol concentration, in both test instances, was set at 100%. The percent penetration for each filter bank was calculated from the equation:

$$P = 100 \frac{C_d}{C_u} \qquad \text{ANSI/ASME N510-1980, Para. 10.5 9.} \qquad (5)$$

where:

P = percentage penetration
C_d = downstream concentration, from photometer readings
C_u = upstream concentration, from photometer readings

The results of the in-place DOP tests are shown in Table 4.

Table 4.

	1st Filter Bank	2nd Filter Bank
U.S. DOP Conc. %	100	100
D.S. DOP Pen. %	.002	.001
Filter Bank Eff. %	99.998	99.999

Adsorber Stage, In-Place Leak Test

The Type II, charcoal adsorber cell stage was leak tested in accordance with Section 12 of ANSI/ASME N510-1980. R-11 refrigerant tracer gas was used at a concentration of 20 PPM. The efficiency was determined by the following equation:

$$\text{Eff.} = 1 - \frac{R_{ds}}{500\ R_{us}} \qquad \text{Savannah River Report DP-1082 (10)} \qquad (6)$$

where:

R_{ds} = recorder units downstream
R_{us} = recorder units upstream

The data from the adsorber leak test is shown in Table 5.

Table 5.

	Time	Reading
R_{ds}	60 sec.	4.5
R_{us}	150 sec.	31.5

$$\text{Eff.} = 1 - \frac{4.5}{500 \times 31.5} = 0.9997 \text{ or } 99.97\%$$

The Type II, charcoal adsorber cell stage meets the leak test requirement of ANSI/ASME N510-1980.

Pre-Seismic ANSI/ASME N510-1980 Testing Conclusions

The system demonstrated its functional integrity by successfully completing the prescribed ANSI/ASME N510-1980 pre-seismic inspections, tests and calculations.

IV. Seismic Simulation Testing

A seismic simulation test was performed in accordance with IEEE Standard 344-1975 as outlined in Wyle Laboratories' Seismic Test Procedure 541/8499/WB. The test program consisted of resonance search testing and triaxial random multifrequency testing. During all phases of seismic testing, air flow was maintained through the system at the design flow rate of 3,000 SCFM. The results of the test are contained in Wyle Laboratories' Test Report No. 46563-1.[3,11,12]

Due to the combined length of Wyle Laboratories' Seismic Test Procedure and Test Report, only a condensed summary is contained herein.

V. Procedures and Results

System Mounting and Orientation Procedures

The system was mounted on a test fixture which simulated the in-service mounting configuration of the unit. Ten (10) 3/4 inch diameter bolts were utilized and torqued to 200 foot-pounds.

The system was installed on Wyle Laboratories' triaxial seismic simulator, such that, the horizontal axes of the unit were colinear with the horizontal excitations of the test table, as shown in Figure 2.

System Response Procedures

A total of eighteen (18) triaxial accelerometers consisting of fifty-four (54) uniaxial piezoelectric accelerometers (reference Figure 7) were utilized. Three (3) of the uniaxial accelerometers were control accelerometers located on the bottom of the base. The remaining fifty-one (51) were response accelerometers positioned in various locations. The system accelerometer locations are listed in Table 6, and shown in Figures 8 through 20. A magnetic tape recorder was used to record each accelerometer response.

Resonance Search Procedures

A low-level single-axis sine sweep was performed in each of the three (3) orthogonal axes to determine resonant frequencies at each of the fifty-four (54) accelerometer locations. The approximate input acceleration (g) levels were 0.4g horizontally and 0.2g vertically. The frequency range of each sine sweep was from 1 to 40 Hz at a sweep rate of one octave per minute. Run Numbers 1, 2 and 3, Table 7, contain descriptions of the resonance search.

Table 6. Accelerometer Locations.

Location Number	Location Description	Quantity Per Location (Uniaxial)	Accelerometer
1	Bottom of Base	3	Control
2	Top of Base	3	Response
3	Middle of Housing Door-side Exterior Skin	3	Response
4	Top, Inlet, Door-side Corner of Housing	3	Response
5	Top, Center, Door-side Corner of Housing	3	Response
6	Top, Outlet, Rear-side Corner of Housing	3	Response
7	End Inlet Flange	3	Response
8	Outlet Flange	3	
9	Top Mounting of Fire Detection Control Panel	3	Response
10	Mounting of Upstream HEPA ΔP Gage	3	Response
11	Top of Prefilter Rack Seal Face for Upper Filter	3	Response
12	Top of Upstream HEPA Rack Seal Face for Upper Filter	3	Response
13	Top of Upstream HEPA Rack Seal Face for Center Filter	3	Response
14	Top of Adsorber Rack Seal Face for Uppermost Cell	3	Response
15	Top of Adsorber Rack Seal Face for Fifth Cell from Unit Bottom	3	Response
16	Prefilter Elements near Top Seal Face	3	Response
17	HEPA Filter Elements near Top Seal Face	3	Response
18	Adsorber Cells near Top Seal Face	3	Response

Figure 7. Triaxial Accelerometer Consisting of Three (3) Uniaxial Piezoelectric Accelerometers.

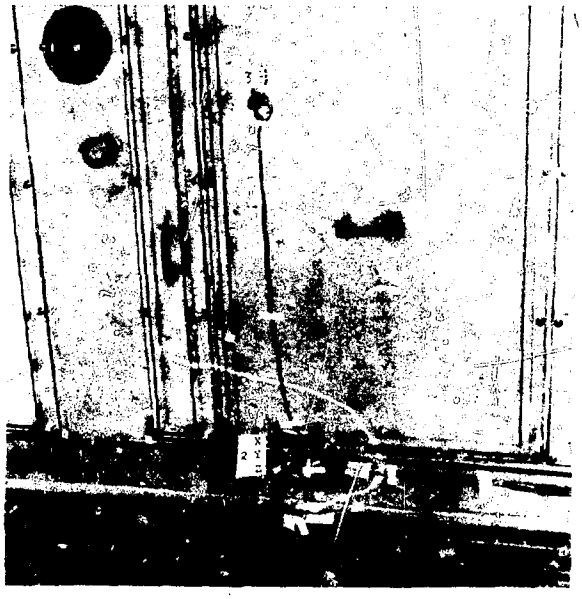

Figure 8.
ACCELEROMETER LOCATIONS
1 X, Y and Z
2 X, Y and Z
3 X, Y and Z

Figure 9.
ACCELEROMETER LOCATIONS
4 X, Y and Z
9 X, Y and Z
16 X, Y and Z

Figure 10.
ACCELEROMETER LOCATIONS
5 X, Y and Z
10 X, Y and Z

Figure 11.
ACCELEROMETER LOCATIONS
6 X, Y and Z

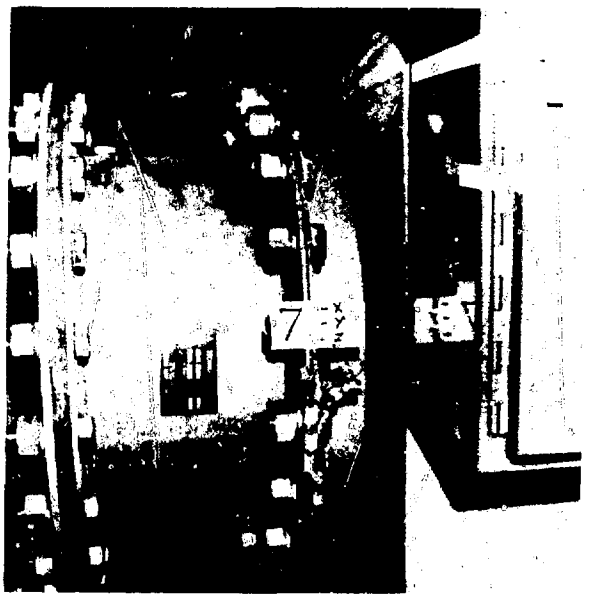

Figure 12.
ACCELEROMETER LOCATION
7 X, Y and Z

Figure 13.
ACCELEROMETER LOCATION
8 X, Y and Z

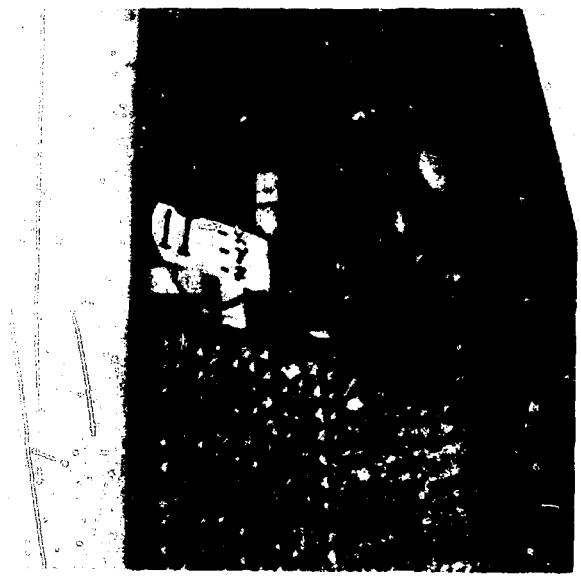

Figure 14.
ACCELEROMETER LOCATION
11 X, Y and Z

Figure 15.
ACCELEROMETER LOCATION
12 X, Y and Z

Figure 16.
ACCELEROMETER LOCATION
13 X, Y and Z

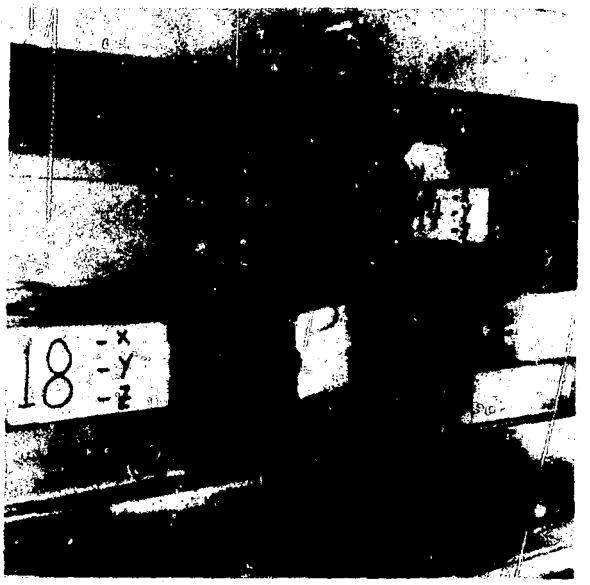

Figure 17.
ACCELEROMETER LOCATIONS
14 X, Y and Z
16 X, Y and Z

Figure 18.
ACCELEROMETER LOCATION
15 X, Y and Z

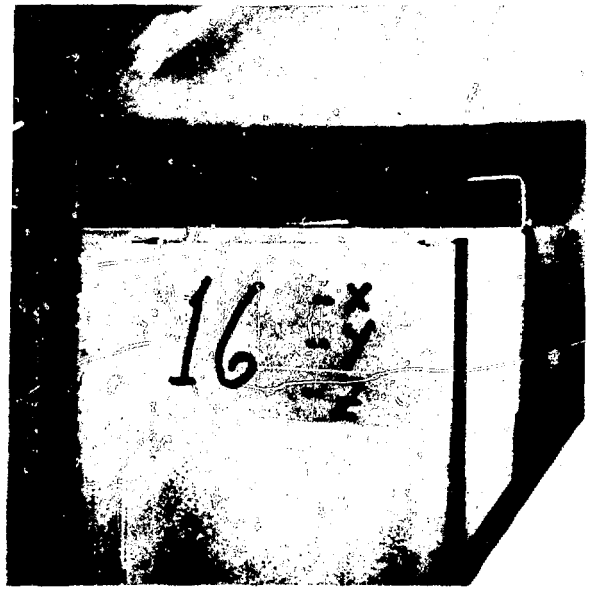

Figure 19.
ACCELEROMETER LOCATION
16 X, Y and Z

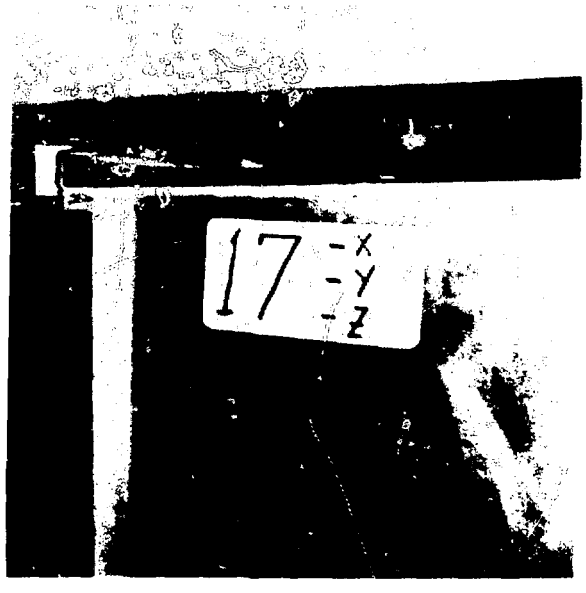

Figure 20.
ACCELEROMETER LOCATION
17 X, Y and Z

Table 7. Test Run Descriptions.

Run No.	Type Test	Axes	Level	Acceleration (g)		
				FBZPA	SSZPA	VZPA
1	Sine Sweep	SS	---	---	0.4	---
2	Sine Sweep	FB	---	0.4	---	---
3	Sine Sweep	V	---	---	---	0.2
4	RMF	TRI	OBE	0.95	1.0	0.70
5	RMF	TRI	OBE	0.75	0.75	0.40
6	RMF	TRI	OBE	0.70	0.70	0.50
7	RMF	TRI	OBE	0.70	0.75	0.40
8	RMF	TRI	OBE	0.65	0.70	0.40
9	RMF	TRI	SSE	1.2	1.3	0.80

Legend:
RMF = Random Multifrequency
SS = Side-to-Side
FB = Front-to-Back
V = Vertical
ZPA = Zero Period Acceleration
TRI = Triaxial
OBE = Operating Basis Earthquake
SSE = Safe Shutdown Earthquake

Resonance Search Results

Three typical transmissibility plots for each axis for the in-line system response accelerometers from the resonance search tests are shown in Figures 21, 22 and 23. The peaks indicate the frequency at maximum amplification of the input acceleration and the degree of amplification for the given accelerometer location.

This information, although not highly important in relation to the tested system, provides useful information for similar future systems designed analytically. The proof of a tested system's capability to remain operative is in its ability to pass random multifrequency testing, regardless of acceleration amplification levels.

Random Multifrequency Test Procedures

The unit was subjected to triaxial multifrequency random motion in 30-second intervals consisting of five (5) OBE (Operating Basis Earthquake) tests, followed by one (1) SSE (Safe Shutdown Earthquake) test. The frequency was amplitude-controlled in one-third octave bandwidths spaced one-third octave apart over a frequency range of 1 to 40 Hz. To produce phase-incoherent motions in the vertical and two (2) horizontal axes, three (3) simultaneous, but independent, random signals were produced. The amplitude of each bandwidth was independently adjusted in each axis until the TRS (Test Response Spectrum) enveloped the RRS (Required Response Spectrum). The Zero Period Acceleration (ZPA), as well as other areas of the RRS, were exceeded, as required, to

FULL SCALE TRANSMISSIBILITY

Figure 21

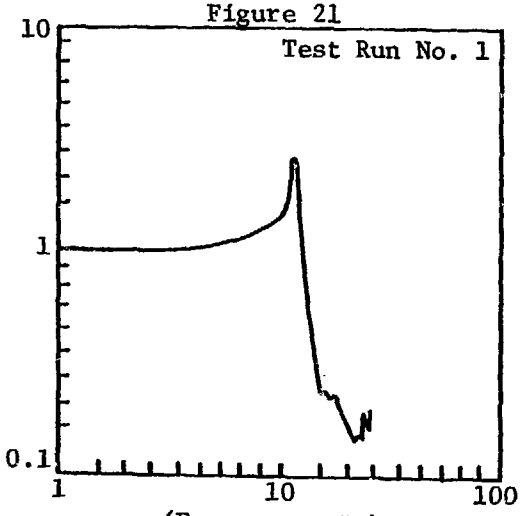

Figure 22

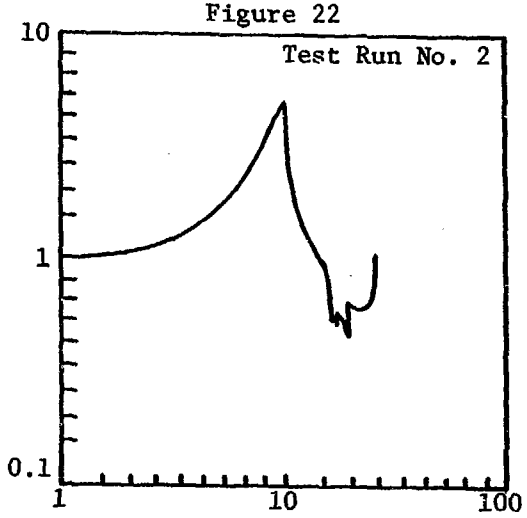

Figure 23

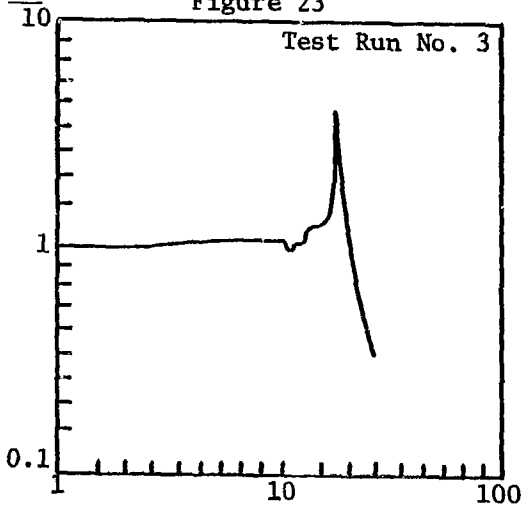

meet the peaks of the curves. The resulting table motion was analyzed by a response spectrum analyzer at the percent damping required (2% for the OBE tests and 3% for the SSE tests), and plotted at one-sixth octave intervals over a frequency range of 1 to 200 Hz. Reference Figures 24 through 29.

Run Numbers 4 through 9 in Table 7 show the ZPA Accelerations for each axis for the five (5) OBE level and one (1) SSE level RMF (Random Multifrequency) tests.

Figure 30 depicts a simulation view of the system during random multifrequency testing.

Random Multifrequency Test Results

It was demonstrated, upon successful completion of the random multifrequency tests, that the system, as a whole, possessed sufficient structural integrity to withstand the prescribed simulated seismic environment.

Seismic Simulation Testing Conclusions

As previously stated, the system demonstrated it's ability to maintain structural integrity by successfully completing the prescribed seismic simulation tests. However, in order to verify the system's ability to operate and function during and after a seismic occurrence, MSA conducted the same ANSI/ASME N510-1980 tests performed for the pre-seismic testing segment.

VI. Post-Seismic ANSI/ASME N510-1980 Testing

Procedures

The post-seismic ANSI/ASME N510-1980 testing performed was identical to the pre-seismic testing reported in Section III. All methods, calculations and formulas are as stated in the aforementioned section, therefore, only test results are given below.

Visual Inspection

The visual inspection found no deficiencies.

Air Flow Capacity Test

The sample point readings, for the post-seismic air flow capacity test, are as indicated in Table 8.

Table 8. Air Flow Capacity.

	Velocity, FPM									
Horiz. Readings	3200	3250	3400	3625	4100	4100	3975	3850	3225	3500
Vert. Readings	3250	3200	3350	3650	4100	4100	3850	3650	3525	3400

FULL SCALE SPECTRUM (g PEAK)

Figure 24

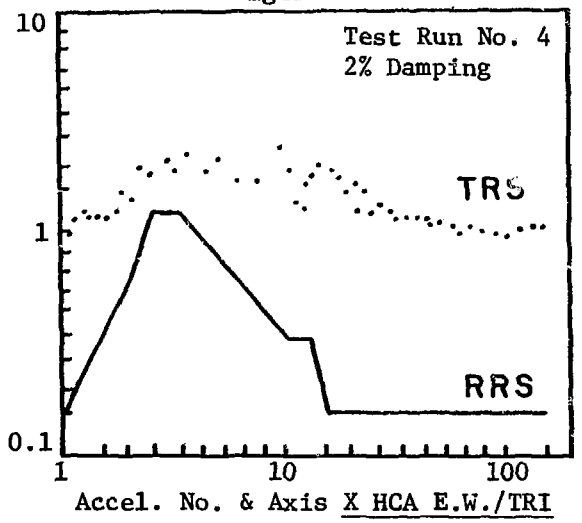

Figure 25

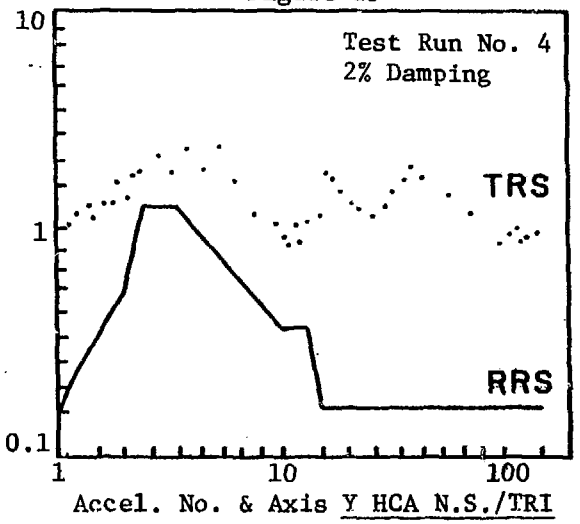

Figure 26

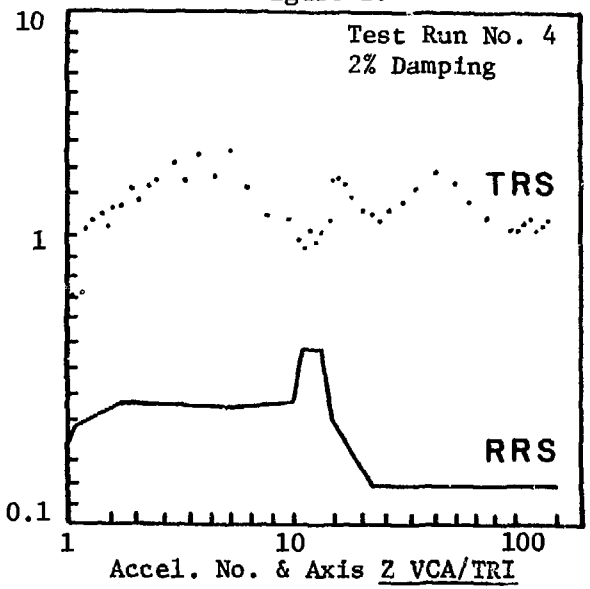

SCALE

Vertical: g Peak

Horizontal: Frequency, Hz

FULL SCALE SHOCK SPECTRUM (g PEAK)

Figure 27

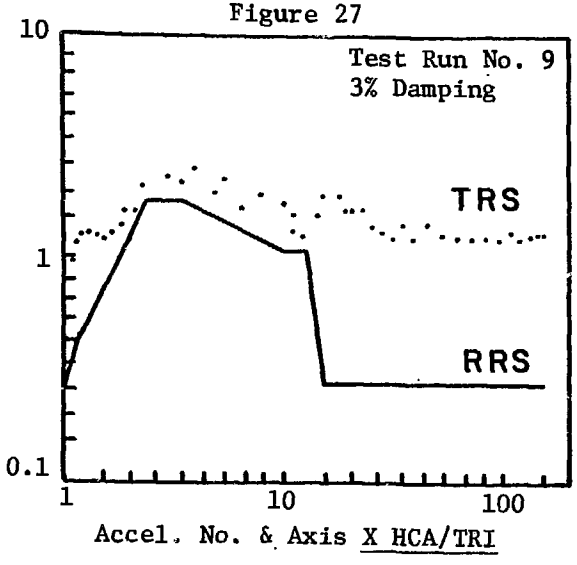

Accel. No. & Axis X HCA/TRI

Figure 28

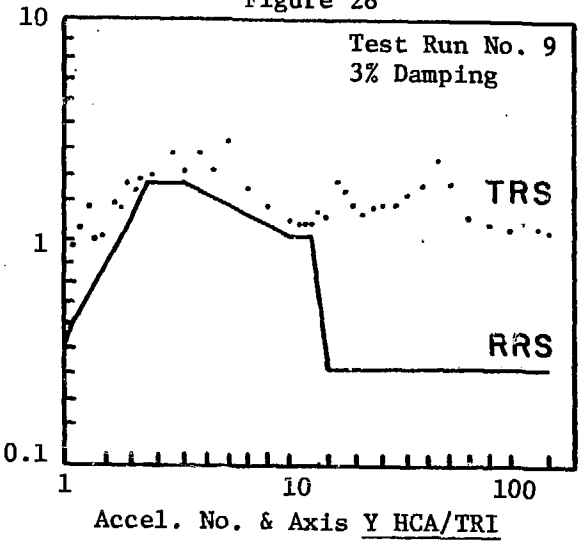

Accel. No. & Axis Y HCA/TRI

Figure 29

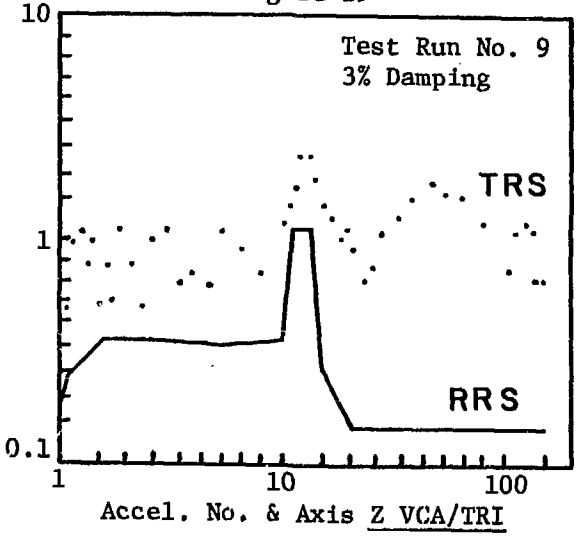

Accel. No. & Axis Z VCA/TRI

SCALE

Vertical: g Peak

Horizontal: Frequency, Hz

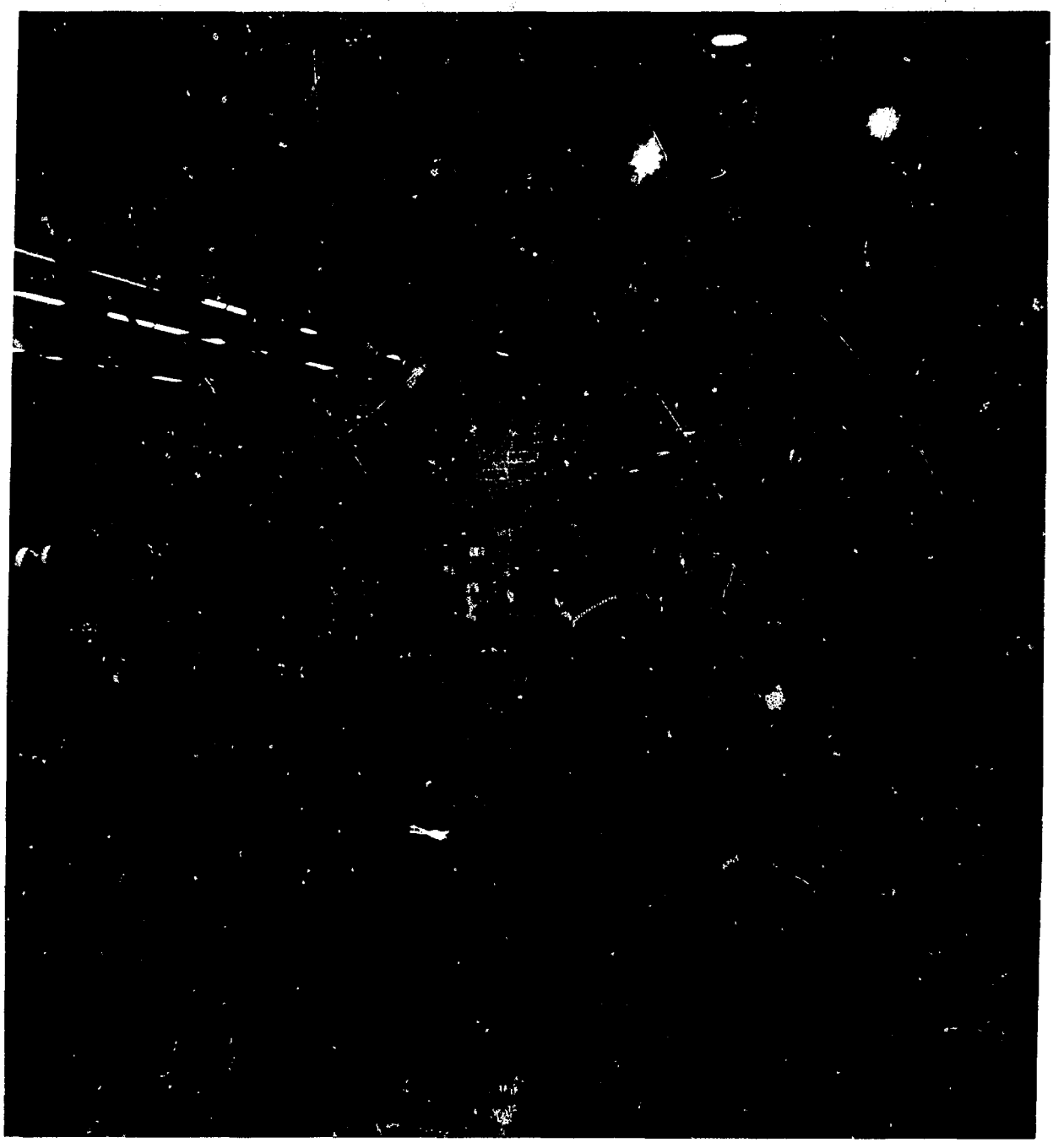

Figure 30. Simulation View of System During Random Multifrequency Testing.

The average sample duct velocity was recalculated from the following equation:

$$\bar{V} = \frac{\Sigma_1^n V_i}{n}$$

ANSI/ASME N510-1980, Para. 8.3.1 4. (7)

$\bar{V}$ = 3,615 FPM (1836 cms/sec.)

The volumetric flowrate, Q, was recalculated from the equation shown below:

$$Q = A\,\bar{V}$$

ANSI/ASME N510-1980, Para. 8.3.1 4. (8)

Q = 2,838 CFM (1340 liters/sec.)

The volumetric flowrate is within -5.4% of the allowable.

Air Distribution Testing

The data collected during post-seismic air distribution testing is shown in Table 9.

Table 9. Air Distribution Velocity Readings.

Velocity, FPM					
250	230	220	210	240	250
270	250	210	250	240	260

The average velocity calculated is 240 FPM (122 cms/sec.). The high reading is 12.5% above the calculated average velocity, and the low reading is 12.5% below.

Adsorber Residence Time Calculation

The Type II, sideload, charcoal adsorber cell residence time was recalculated from the following equation:

$$T = \frac{nNt\ (A-b)}{28.8\ Qs}$$

ANSI/ASME N510-1975, Para. 8.3.3 (9)

T = 0.28 seconds

The result indicates that the residence time for the adsorber cells is above the system requirement of 0.25 second, minimum.

Air-Aerosol Mixing Uniformity

The post-seismic air-aerosol mixing uniformity penetrometer meter readings are shown in Table 10.

Table 10. Air-Aerosol Mixing Uniformity.

Penetrometer Meter Reading					
.60	.60	.60	.60	.58	.58
.60	.62	.58	.60	.60	.58

The average concentration for the penetrometer readings was recalculated using the following formula:

$$\overline{C} = \frac{\Sigma_i^n C_i}{n}$$

ANSI/ASME N510-1980, Para. 9.4 5. (10)

$\overline{C} = 0.595$

The average concentration is 0.595 or 59.5%. For this test the maximum reading is 4.2% high and the minimum reading is 2.5% low. Both readings are well within the allowable, therefore, the uniformity of these readings re-establishes the acceptablity of the injection location.

HEPA Filter Bank, In-Place Leak Test

An in-place HEPA filter bank leak test was reperformed on both the upstream and downstream HEPA filter banks.

The percent penetration for each filter bank was calculated from the equation:

$$P = 100 \frac{C_d}{C_u}$$

ANSI/ASME N510-1980, Para. 10.5 9. (11)

The results of the post-seismic in-place DOP tests are shown in Table 11.

Table 11.

	1st Filter Bank	2nd Filter Bank
U.S. DOP Conc. %	100	100
D.S. DOP Conc. %	.002	.0015
Filter Bank Eff.	99.998	99.998

Adsorber Stage, In-Place Leak Test

The post-seismic efficiency of the adsorber stage was determined by the following equation:

$$\text{Eff.} = 1 - \frac{R_{ds}}{500\ R_{us}}$$

Savannah River Report DP-1082 (12)

The data from the post-seismic adsorber leak test is shown in Table 12.

Table 12.

	Time	Reading
R_{ds}	60 sec.	2
R_{us}	150 sec.	15.5

$$\text{Eff.} = 1 - \frac{2}{500 \times 15.5} = 0.9997 \text{ or } 99.97\%$$

The Type II, charcoal adsorber cell stage meets the leak test requirement of ANSI/ASME N510-1980.

Post-Seismic ANSI/ASME N510-1980 Testing Conclusions

Upon successfully completing the prescribed ANSI/ASME N510-1980 post seismic inspections, tests and calculations, the system was proven to possess sufficient functional integrity.

VII. Conclusions

The system's ability to function during a seismic occurrence was demonstrated in two (2) ways - first, by successfully completing ANSI/ASME N510-1980 testing, second, by visual inspection and observation. Air flow was maintained during testing, filters and carbon cells sustained no damage, filter seals remained intact, and no loss of instrument performance or structural damage was evident. Therefore, the Control Room Emergency Air Cleaning System demonstrated the ability to withstand the maximum postulated earthquake for the plant site by remaining structurally sound and functional.

VIII. References

1. U.S. Nuclear Regulatory Commission, NUREG-0737, "Clarification of TMI Action Plan Requirements", (1980).

2. American National Standards Institute/American Society of Mechanical Engineers (ANSI/ASME) N509-1980, "Nuclear Air Cleaning Units and Components," (1980).

3. IEEE Standard 344-1975, "IEEE Recommended Practices for Seismic Qualification of Class 1E Equipment for Nuclear Power Generating Stations," (1975).

4. Yankee Atomic Electric Company Required Response Spectra (RRS).

5. Ameri an National Standards Institute/American Society of Mechanical Engineers (ANSI/ASME) N510-1980, "Testing of Nuclear Air-Cleaning Systems," (1980).

6. United States Nuclear Regulatory Commission, "Rules and Regulations," Title 10 - Chapter 1, Code of Federal Regulations, (1976).

7. U.S. Nuclear Regulatory Commission, NUREG-0800, "Seismic and Dynamic Qualification of Mechanical and Electrical Equipment," (1981).

8. U.S. Nuclear Regulatory Commission, Regulatory Guide 1.52, "Design, Testing and Maintenance Criteria for Post Accident Engineered-Safety Feature Atmospheric Cleanup System Air Filtration and Adsorption Units of Light-Water-Cooled Nuclear Power Plants," (1978).

9. American National Standards Institute/American Society of Mechanical Engineers (ANSI/ASME) N510-1975, "Testing of Nuclear Air-Cleaning Systems," (1975).

10. Muhlbaier, D.R., Savannah River Laboratory Report DP-1082, "Standardized Nondestructive Test of Carbon Beds for Reactor Confinement Applications," (1967).

11. Wyle Laboratories Test Procedure No. 541/8499/WB, Revision A, "Seismic Test Procedure for a Control Room Emergency Air Filtration System," (1982).

12. Wyle Laboratories Test Report No. 46563-1, Revision A, "Seismic Simulation Test Program on a Control Room Emergency Air Cleaning System," (1983).

DISCUSSION

PAPAVRAMIDIS: During the in-place leak test of adsorbers, do you measure the background of R-11 refrigerant? How long do you have to wait between a failed test and the retest?

MANLEY: Yes, we measure the background in accordance with ANSI/ASME N 510. The test results are given in the text of the paper. We did not fail any ANSI/ASME N 510 tests. Each test was performed immediately after the completion of the preceding test, as detailed in the body of the paper.

BELLAMY: Please define what you mean by a vapor-proof light fixture inside the housing, and explain its function.

MANLEY: The light is gas tight to prevent any air leakage in or out of the housing. The electrical components are located on the outside, or clean side, to prevent possible contamination and for ease of replacement of the bulb.

WHITE: What is the design (normal) air flow rate of the control room filter system and what air flow rate was maintained during the vibration test? What acceleration was applied at the base of the unit?

MANLEY: Design air flow rate is 3,000 cfm. This flow rate was maintained during the test. The applied acceleration was 0.4 g horizontally; 0.2 g vertically, for sine sweeps. Please refer to Table 7 of the paper for multifrequency values.

COMPARISON AND VERIFICATION OF TWO COMPUTER PROGRAMS USED TO ANALYZE VENTILATION SYSTEMS UNDER ACCIDENT CONDITIONS

S. H. Hartig and D. E. Wurz
Institut für Technische Thermodynamik, Universität Karlsruhe

Th. Arnitz and V. Ruedinger
Laboratorium für Aerosolphysik und Filtertechnik
Kernforschungszentrum Karlsruhe GmbH
Federal Republic of Germany

Abstract

Two computer codes, TVENT and EVENT, which were developed at the Los Alamos National Laboratory (LANL) for the analysis of ventilation systems, have been modified to model air-cleaning systems that include active components with time-dependent flow-resistance characteristics.

With both modified programs, fluid-dynamic transients were calculated for a test facility used to simulate accident conditions in air-cleaning systems. Experiments were performed in the test facility whereby flow and pressure transients were generated with the help of two quick-actuating air-stream control valves. The numerical calculations are compared with the test results. Although EVENT makes use of a more complex theoretical flow model than TVENT, the numerical simulations of both codes were found to be very similar for the flow conditions studied and to closely follow the experimental results.

I. Introduction

In nuclear facilities during normal operation, the air-cleaning systems function to protect human health from ionizing radiation. To ensure that the containment of fission products is also maintained during an accident situation, the response of an air-cleaning system to the conditions imposed upon it by the accident, should be known. For the analysis of ventilation-system response to pressure transients induced by respectively, tornados and explosions, the computer codes TVENT /1/ and EVENT /2/, were developed at LANL.

For the case of a Loss-Of-Coolant-Accident (LOCA), elevated temperatures and high relative humidities are to be expected as well as possible high air-flow rates and differential pressures. To evaluate the performance of an air-cleaning system exposed to these combined challenges, the behavior of individual components under such challenges as well as the resultant fluid-dynamic and thermodynamic conditions within the air-cleaning system must be known.

To this end, the test facility BORA /3/, which is capable of generating transient air flow at high velocities, temperatures, and relative humidities, was recently put into operation. With this facility, components of air-cleaning systems can be tested with a variety of simulated accident conditions. Furthermore, the test facility can be used to help develop and to verify computer codes for analysis of ventilation systems exposed to the fluid-dynamic transients and the thermodynamic conditions expected during a LOCA.

As a first step in the development of such a code, the fluid-dynamic behavior of BORA during transient flows at constant ambient temperature and humidity was numerically simulated with both of the two LANL computer programs. Each code was designed to model a particular type of transient within ventilation systems and the underlying equations as well as the input and computational complexities are correspondingly different. By modelling the identical test facility with both codes , under fluid-dynamic conditions which could be expected during a LOCA, a comparision of the respective numerical calculations from both codes, with each other as well as with the test results, allow the required complexity of the to-be-developed LOCA code to be evaluated.

II. The Verification Test Facility

The test facility BORA is located at the Kernforschungszentrum Karlsruhe in the rotunde of a decommisioned nuclear reactor. Fig. 1 shows a scaled plan of the installation. The elements relevant for the fluid-dynamic modeling are schematically illustrated in Fig. 3.

The facility is designed as a recirculating-flow system with a vent to the ambient environment. The two identical speed-controlled radial blowers, of 420 kW electrical input each, can be operated in individual, series, or parallel modes, dependent on the desired static pressure and volumetric flow rate. In a following finned heat exchanger with a 2 m^2 cross section, the test air is conditioned to the desired temperature. After the air cooler a bypass duct (d=0.6 m) branches off, which can be closed by a pneumatic butterfly-type valve, K2. In the main duct (d=0.75 m) follows the structural test section with a transition section for the air-cleaning component to be tested. For the verification experiments reported here, a clean 610x610x292 mm HEPA filter was installed.

This section is followed by a rectangular observation chamber which permits photo and video observation of the downstream side of the test component. A duct 0.8 m in diameter exits this chamber, joins the bypass section and returns the test air to the blowers' inlet via a filter bank and a second air cooler. As is also the case in the bypass with valve K2, flow in the test section can be controlled with a quick actuating valve, K1.

Fig. 2 is a photograph of the test section with the valve K1 and drive mechanism. The filter bank consists of 10 parallel-flow, 610x610x292 mm HEPA filters with a total facial area of 3.4 m^2. The second cooler (1.0x0.6 m) is used to limit the blower inlet air-temperature during operation at high temperatures. A short vent duct connects the ductwork with the ambient atmosphere via a muffler.

During an experimental run, steady and unsteady, flows and differential pressures are generated within the facility by the use of valves K1 and K2. During the initial flow-conditioning period, valve K1 is completely closed to direct the recirculating air flow via the bypass only. Required flow rate and static pressure are adjusted by setting blower speed and then positioning valve K2, as a partially open differential-pressure control valve. Leakage in valve K1 causes a negligible flow rate through the test section, this effect however is intended and guarantees identical thermodynamic conditions there. To produce an unsteady flow through the structural test section, valve K1 is opened as valve K2 is closed. During the resultant diversion of air flow from bypass to test section, a differential pressure pulse is generated at the test component.

Flow-resistance characteristics, actuating speed, and coordination of the control valves K1 and K2 are parameters which govern the shape and slope of this pressure pulse. Therefore, reaction time and coordination can be varied over a wide range by means of regulator valves installed in the air-supply line of the pneumatic drive mechanisms.

III. Instrumentation and Data Acquisition

Each of the experiments reported here involved a sequence of 3 distinct conditions of air flow within the facility; an initial steady flow through the bypass only, an intermediate transient flow during which the air stream was diverted from bypass to structural test section, and a final steady flow through the test section only.

Since both steady and unsteady flows were of interest, the data acquisition systems and procedures used to measure and record the relevant test parameters varied accordingly.

Steady flow

Measured and recorded during initial and final steady flow were ambient temperature and barometric pressure, as well as the temperatures and the static and velocity pressures within the air stream at the pertinent locations in the facility. Ambient temperatures and barometric pressure were manually recorded from a mercury-filled thermometer and barometer, respectively. Air-stream temperatures were measured with sheathed 4-wire platinum - resistance thermometer probes and manually recorded from digital displays mounted in the control panel.

Air-stream pressures were measured with probes and transducers, and digitally recorded, all as described below for unsteady flow.

Unsteady flow

For these experiments during conditions of unsteady flow, the only parameters to vary significantly from steady-flow values were air-stream pressures and flow rates. Consequently, only static, differential, and velocity pressures of the air streams in the facility were recorded digitally during unsteady-flow conditions.

Static and differential pressures were measured with variable-capacitance transducers mounted directly to T-shaped probes of 6 mm ID and 0.5-0.7 m length. The velocity pressures were measured with variable-capacitance transducers mounted directly to pitot tubes for which the total-pressure tubes were of 2.5 mm ID and 0.6-0.9 m length. The nominal natural frequencies for the transducers were given by the manufacturer to be 2 kHz and those for the internal-volume geometries of probes and transducers, analyzed as pressure-transmitting systems, were calculated to be in the 1-3 kHz range. The output signals of the pressure transducers were low-pass filtered to remove undesirable frequencies above 10 Hz, to improve recording of the transient pressures for which only frequencies of < 1 Hz were of primary interest. Registration of the transient pressures was performed by an A/D data recorder which wrote the output voltages of the pressure transducers onto magnetic disk at a rate of 80 Hz for each of 8 channels.

IV. Numerical Simulation

TVENT and EVENT computer codes

The TVENT and EVENT computer codes were developed as analytical tools to predict the fluid dynamics within ventilation networks, subjected to induced pressure and flow transients. Both codes assume single-phase ideal-gas behavior for a flow medium of air and employ a lumped parameter formulation that neglects spacial distribution. Complex ventilation systems which include blowers, filters, dampers, rooms, and ducts are modeled as networks of branches joined together at nodes. Rooms and components of larger capacity are represented by storage nodes with corresponding assigned volumes. Blowers are represented as branches which perform dynamically according to the measured blower characteristic curves. Passive elements such as filters, dampers, valves, and ducts are also modeled as branches and are described by specified flow-resistance relationships (Table I).

Computation of unsteady flow is undertaken as a sequence of quasi-stationary calculations. Therefore, the problem run time is subdivided into n equal time intervals, Δt. With consideration for the imposed boundary conditions, such as pressure, temperature, mass-injection, and energy-injection rate as well as the capacitance in the storage nodes, a system of non-linear equations is set up and solved by an iterative procedure for each point in time, t_i $(1 \leq i \leq n)$. The succession of all these quasi-stationary solutions then simulates the transient flow.

The opening or closing of a control valve is a time- dependent action, during which the flow-resistance characteristics of the valve are altered. By setting up the equation of motion and by use of the resistance coefficients as a function of the valve position, a resistance-time function, $R=f(t)$, can be determined for any control valve. Therefore, for every point in time, t_i, the actual flow-resistance relation, $\Delta p(t_i)=R(t)\cdot Q^2$, is known and may be put into the equation system for the quasi - steady - state calculation. By this method and a sufficiently fine time subdivision, continuous valve action can be modeled satisfactorily. Fig. 5 shows a simplified flow chart of the modified codes. The codes were altered so that up to 20 control valves can be modeled in one network. Associated with every control valve is a resistance-time function, which is approximated by a series of straight line segments and prompted point-by-point. This universal input formulation allows a variety of components with time-dependent flow-resistance characteristics to be modeled. If for example, the change in resistance due to progressive structural damage of a system component can be described by a resistance-time relationship, the consequences of this failure for the performance of the ventilation system may be evaluated with either of the two modified codes.

Computer model of BORA

The numerical simulation requires a modeling of all components relevant to the fluid-dynamic behavior of the facility. This model is shown in Fig. 4. Node 1 represents the environment with the imposed ambient conditions, P_a=100 kPa and T_a=293 K. The connection between the system and the environment is established by branch 1, the vent duct. The blowers operate in parallel mode and are described by identical characteristic curves. The correspondence between the other facility components and the respective branches can be seen by comparison of Fig. 3 to Fig. 4. The rooms which represent mass-storage nodes, are dimensioned according to the volumes of the adjacent components.

The flow-resistance characteristics of the facility were determined during steady-flow conditions with the instrumentation described above. Blower characteristic curves were determined at constant blower speed, while static pressure and volumetric flow rate were varied by means of control valve K2. To determine resistance coefficients for the test filter, filter bank, and air coolers, pressure drops across the respective components were measured at different volumetric flow rates of 10 - 20 m^3/s.

The resultant air velocities cause turbulent flow in the entire facility loop. Therefore the pressure-flow relationship of coolers and filters obey a parabolic law and can be described by the equations $\Delta p = R \cdot Q^2$ and $\Delta p = R \cdot \frac{\rho}{2} v^2$, respectively. Filter characteristic curves obtained from the measurements coincide well with earlier experiments of Ruedinger /8/.

The resistance-time function required to model the control valves were determined as follows. With a position-angle indicator attached to the pivot shaft of the valve, the equations of motion were obtained in the form of angle-time relationships for several actuation speeds. In a second step, the resistance coefficients for valve K2 were determined as dependent variables of the valve-angle positions, by measuring pressure drops across the valve at 3 different volumetric flow rates for a number of positions. With this data, a characteristic curve of the resistance coefficient as a function of angle position was obtained for valve K2, and after geometric scaling, also for valve K1. Combination of the motion equations and the curves of flow-resistance as a function of valve angle resulted finally in the resistance-time function, R=R(t), for control valves K1 and K2.

Because TVENT requires an incompressible flow-resistance relationship, $\Delta p = R \cdot Q^2$, the experimentally determined volumetric flow rates were converted to conditions at P=100 kPa and the resistance coefficients were corrected for TVENT input.

V. Verification Experiments

Several verification experiments with unsteady flows were performed with the test facility BORA. The values of some relevant operating parameters are listed in Table II.

Table II: Values of some relevant operating parameters for the verification experiments with BORA.

Exp. No.	Valve actuation time K1	K2	Static pressure	Rated flow	Test filter diff. press.	Test filter differential pressure slope	Flow temp.
I	3.0 s	6.1 s	23 kPa	14 m^3/s	19 kPa	12 kPa/s	307 K
II	3.0 s	3.3 s	23 kPa	14 m^3/s	19 kPa	14 kPa/s	307 K
III	3.0 s	3.3 s	33 kPa	17.5m^3/s	27 kPa	19 kPa/s	310 K

Table I: Pressure-flow relationships for several ventilation system components employed in TVENT and EVENT.

Component	TVENT	EVENT
Blower	$\Delta p = f(Q)$	$\Delta p = f(Q)$
Damper	$\Delta p = R \cdot Q^2$	$\Delta p = R \cdot \frac{\rho}{2} \cdot \frac{Q^2}{A^2}$
Duct	$\Delta p = R \cdot Q^2$	$\Delta p = R \cdot \frac{\rho}{2} \cdot \frac{Q^2}{A^2}$
Filter	$\Delta p = R \cdot Q$ resp. $\Delta p = R \cdot Q^2$	$\Delta p = K_L \cdot \mu \frac{Q}{A^{1.5}} + K_T \cdot \frac{\rho}{2} \cdot \frac{Q^2}{A^2}$
Valve	$\Delta p = R \cdot Q^2$	$\Delta p = R \cdot \frac{\rho}{2} \cdot \frac{Q^2}{A^2}$

TVENT is based on the assumptions of:
one-dimensional,
isothermal, and
incompressible
flow, but allows for fluid storage or capacitance in storage nodes. The effects of shock and inertia are neglected.

The theoretical flow model employed in EVENT is more detailed /4/ and considers the effects of:
compressibility,
inertia,
choking, and also
mass and energy exchange.

For both codes, verification experiments with simple model networks subjected to transient pressure conditions have been reported. Experimental results and numerical simulation were found to be in good agreement /5-7/.

Code modification

Preconditional to numerical simulations of the test facility BORA was a modification of both codes to enable the quick actuating control valves K1 and K2 to be modeled. The method of solution was the same for both TVENT and EVENT.

For a verification experiment, blower speeds are increased to obtain the required flow rate, during which time valve K1 is closed and the flow is directed through the bypass section. Control valve K2 is then positioned so, that the pressure drop across the bypass corresponds with the desired maximum pressure drop to be generated across the test section. By this procedure, changes in the operating point of the blowers during subsequent flow diversion from bypass to test section can be avoided. After registration of the steady-flow data, the drive mechanisms of both K1 and K2 are actuated together with the start of unsteady-flow data recording. As valve K1 opens and valve K2 closes, the static pressure downstream of the test filter decreases to nearly an ambient value and, since the static pressure upstream the filter remains almost constant, differential pressure across the filter simultaneously increases. At the end of the diversion process, steady flow has been established through the test section.

VI. Results and Discussion

Figures 6-11 show the results of the tests and of the numerical simulations with both modified codes. The continuous curves represent the recorded data, while the dashed lines for EVENT and the dotted lines for TVENT indicate the calculated results.

For Exp. 1, some results of which are shown in Figs. 6 and 7, the opening time for valve K1 was set to 3 s and K2 closed in 6.3 s. The delayed action of K2 resulted in a temporary reduction of the collective resistance of bypass and test section. Accordingly the total mass flow rate (branch 3) increased during the flow-diversion process, while the static pressure decreased. This pressure decrease upstream of the test section (node 4) also influenced the differential pressure increase across the filter (branch 4). After an initial steep ascent of 12 kPa/s the pressurization rate decreased to zero slope indicated by the part of the trace parallel to the trace of static pressure upstream of the test section.

With the same opening time for K1, valve K2 was closed in 3.1 s for Exp. II, of which some results are shown in Figs. 8 and 9. Pressure and flow perturbations were of shorter duration and smaller amplitude, and differential pressure across the filter rose at 14 kPa/s. While calculated and recorded pressures coincide very accurately for Exp. I (Fig. 6), the actual differential- pressure ramp across the filter proceeds smoother than that calculated for Exp. II (Fig. 8). This difference is possibly caused by inertial effects delaying the release of air from the observation chamber and is also indicated by the record of the flow rate through branch 4. Although EVENT, in contrast to TVENT, considers the effects of compressibility and inertia, calculated flows and differential pressures are here almost identical for both codes.

The same valve-control parameters of Exp. II were employed in Exp. III, but the blower speeds and accordingly the static pressure and flow rate were increased. Fig. 10 shows the again distinctly delayed differential pressure ascent, where a slope of 23 kPa/s was calculated with both TVENT and EVENT, but 19 kPa/s were recorded.

For all experiments performed, the recorded and the calculated unsteady pressures and flows coincided rather well. The observed deviations are possibly caused by physical effects which are not sufficiently taken into account by the underlying theory of either of the two codes. However, it is also conceivable that inadequately accurate models of the individual components of the experimental facility produced the differences between test results and numerical simulations. It did appear that both modified codes reacted quite sensitively to variations in the control-valve time functions.

In summary, the close agreement between TVENT calculations and EVENT calculations for all verification experiments performed with BORA were somewhat unexpected. Although the theoretical bases for the two codes raise expectations of different prediction accuracy for the examined air-velocities and overpressures, the calculated transient flows and pressures were found to be almost identical with each other.

VII. Conclusions

The close agreements, between the numerical calculations and the experimental results for fluid-dynamic transients in BORA, show that the modified codes TVENT and EVENT can be used to model a relatively simple ventilation system that includes active components which have time-dependent flow-resistance characteristics.

From the close agreements between the calculations and the measurements, it can be concluded that the less complex code, TVENT, is capable of successfully modeling flow and pressure transients for the test conditions investigated. These conditions include overpressures up to 35 kPa, pressurization rates up to 20 kPa/s, air velocities up to 30 m/s, and ambient temperatures. Based upon the results reported here as well as the verification experiments performed by LANL /5-7/, it is expected that the more complex nuclear-facility air-cleaning systems, which contain similar types of active components, can also be successfully modeled with the modified versions of TVENT and EVENT.

The one-dimensional flow model, originally selected for use in both codes to permit a simplified lumped-parameter formulation of the modeled network, is judged to be an effective and practical approach to minimize input and computational complexities without a sacrifice in accuracy.

The code EVENT that uses a more complex fluid-dynamic model did not in all cases result in more accurate calculations, so that for the fluid-dynamic transients studied, the less complex code TVENT would be recommended. However, since EVENT is not much more time consuming in application, its use would be advantageous in such cases, where higher temperatures and differential pressures are also to be taken into account. The verification experiments will be extended to such conditions and subsequently the accuracy of both codes will again be compared.

Given the effectiveness of TVENT and EVENT in prediction of fluid-dynamic transients, neither was originally developed to take into account the process of water condensation and the transport of liquid-water aerosols that may develop during a LOCA in a nuclear-power facility. In order to model the response of air-cleaning systems to such challenges, additional code development work is necessary.

References

/1/ Duerre, K.H., Andrea, R.W., Gregory, W.S.;
"TVENT - A Computer Program for Analysis of Tornado-Induced Transients in Ventilation Systems,"
LA-7397-M (1978).

/2/ Tang, P.K., Andrea, R.W., Bolstad, I.W., Gregory, W.S.;
"EVENT User's Manual - A Computer Code for Analysing Explosion -Induced Gas-Dynymic Transients in Flow Networks,"
LA-9624-M (1983).

/3/ Rüdinger, V., Arnitz, Th., Ricketts, C.I., Wilhelm, J.G.;
"BORA - A Facility for Experimental Investigation of Air Cleaning During Accident Situations,"
Proc. 18th DOE Nuclear Airborne Waste Management and Air Cleaning Conference (1984)
To be published.

/4/ Tang,P.K. et al.;
"Analysis of ventilation Systems Subjected to Explosive Transients - Far Field Analysis,"
LA-9094-MS (1981).

/5/ Andrea, R.W. et al.;
"Investigation of Air Cleaning System Response to Accident Conditions,"
CONF-801038 (1980), pp. 1142-62.

/6/ Tang, P.K., Gregory, W.S., Ricketts, C.I.;
"A Numerical and Experimental Investigation of Simulated Explosions Inside a Flow Network,"
LA-9340-MS (1982).

/7/ Martin, R.A. et al.;
"Analytical and Experimental Studies of Ventilation Systems Subjected to Simulated Tornado Conditions: Verification of the TVENT Computer Code,"
To be published in 1984.

/8/ Rüdinger, V., Ensinger, U.;
"Studium des Verhaltens von Schwebstoffiltern unter Störfallbedingungen,"
KfK 3350, p. 4400-20 (1983).

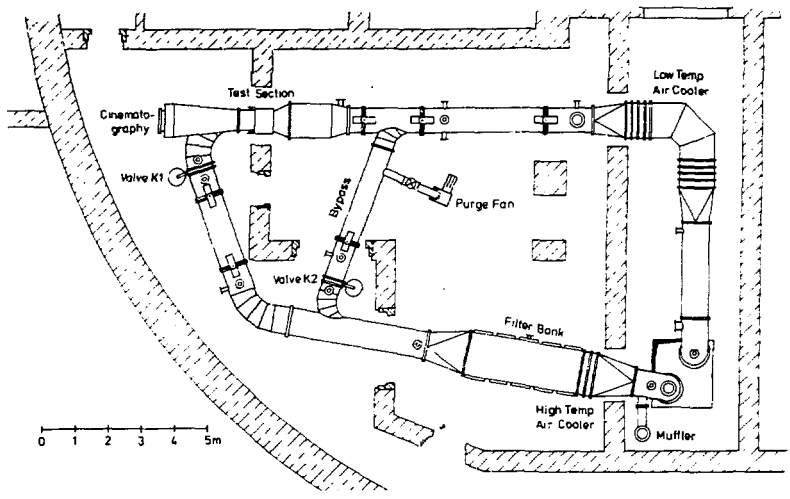

Fig. 1: Plan view of the layout of the facility BORA (second floor level); blowers and control room are installed on the first level.

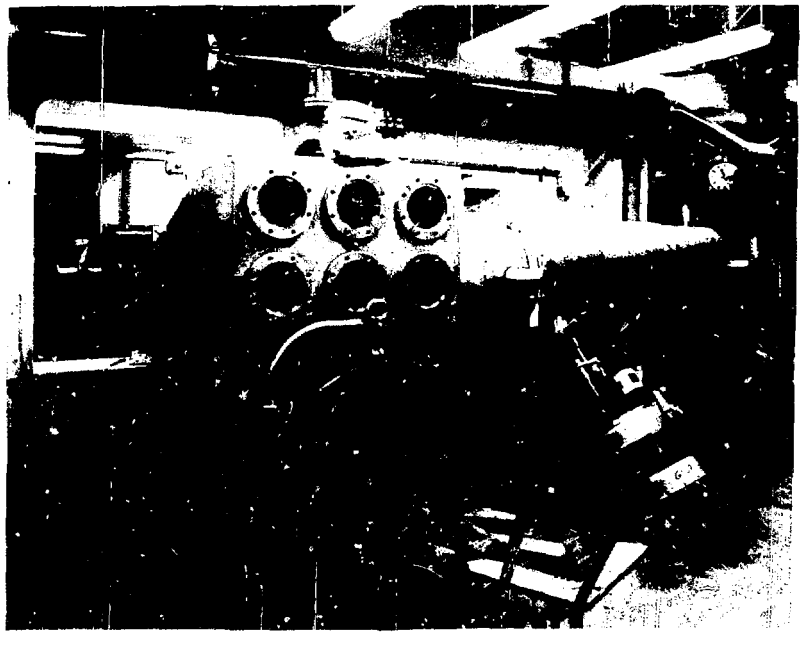

Fig. 2: Photograph of the end wall of the observation chamber. On the right, the dismantled butterfly valve K1 with the associated drive mechanism.

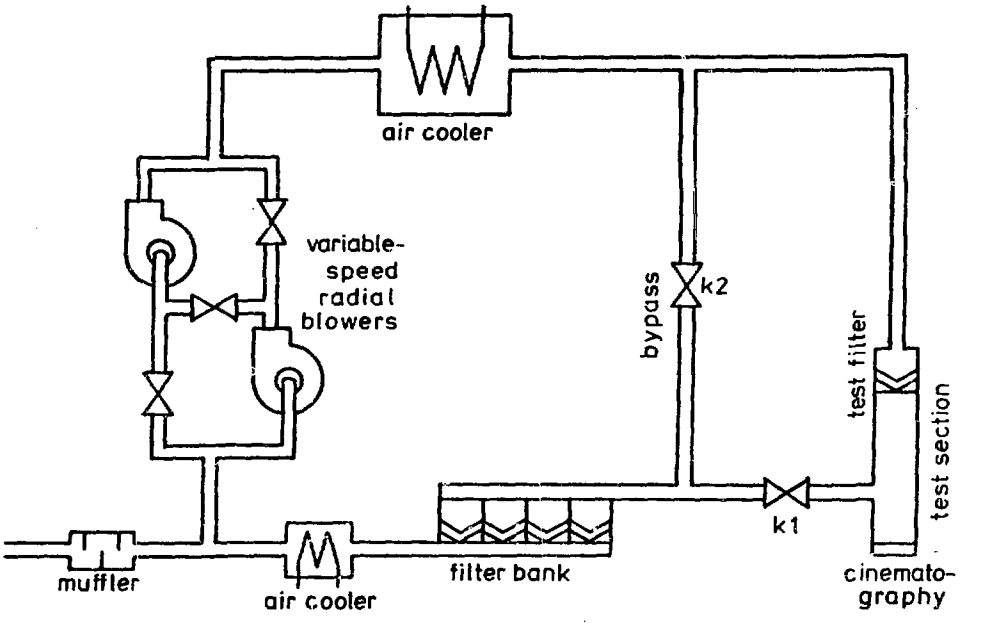

Fig. 3: Schematic of the facility BORA with components relevant for the fluid-dynamic behavior.

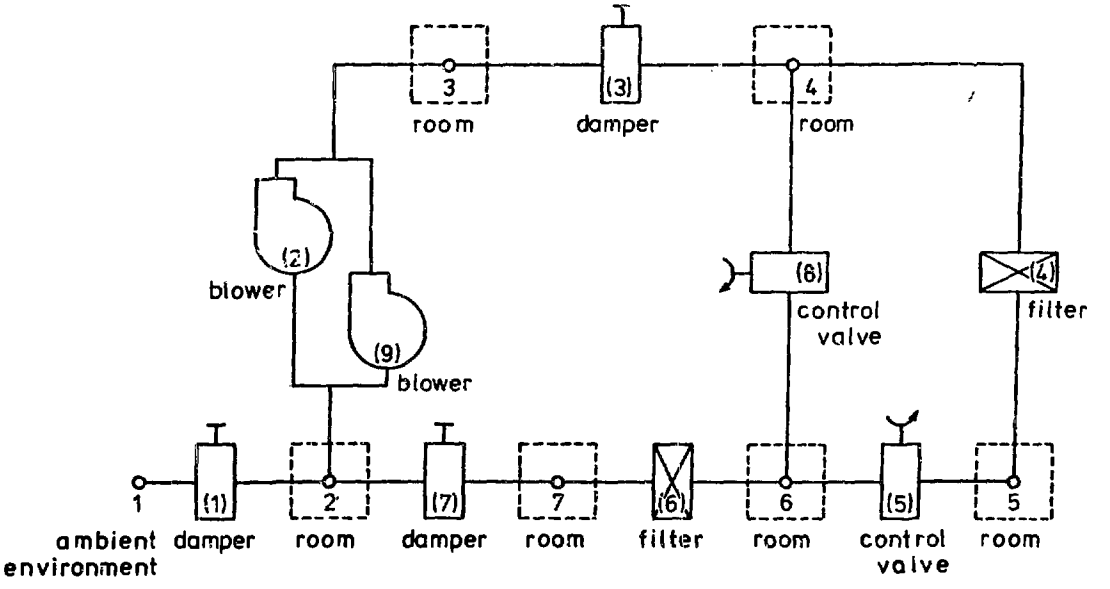

Fig. 4: Computer model of the facility BORA for the numerical simulation.

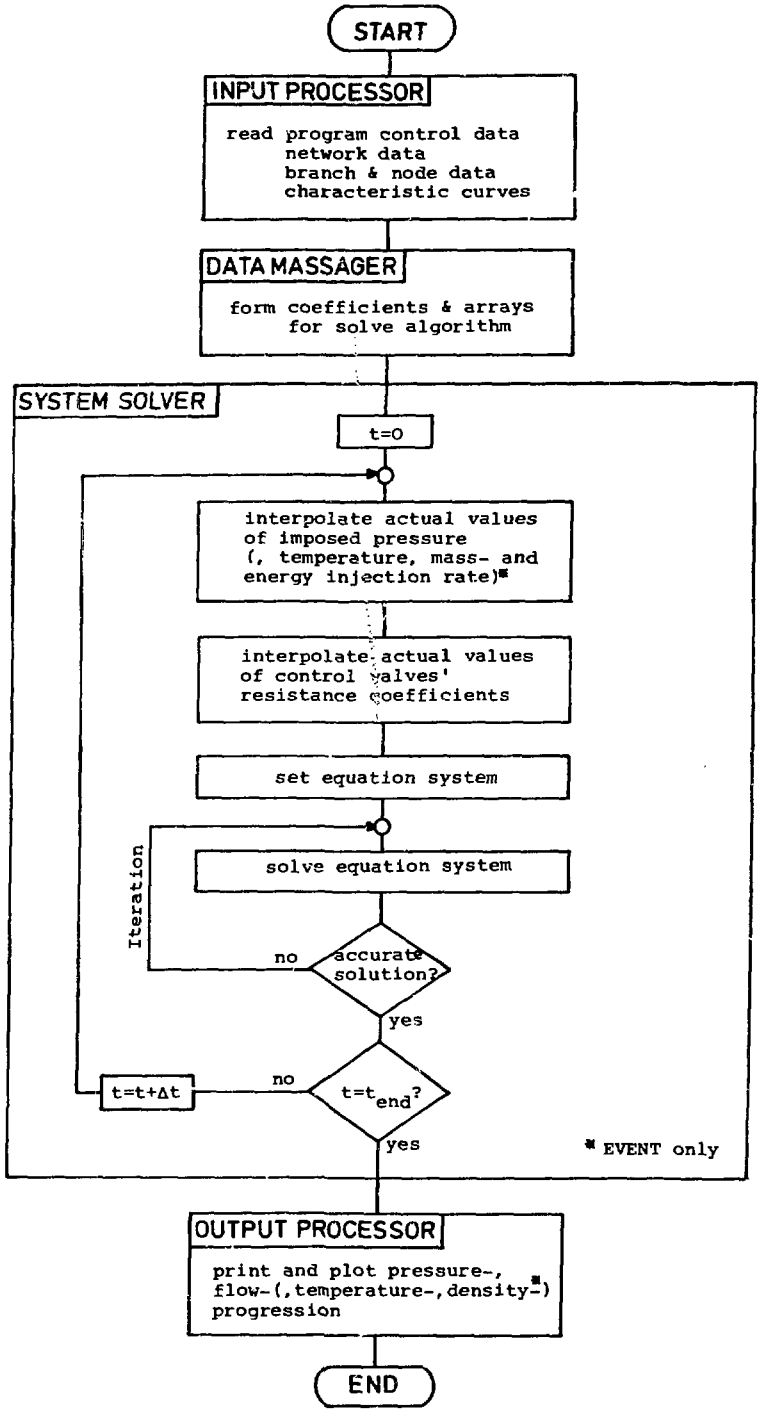

Fig. 5: Simplified flow chart of the modified TVENT and EVENT computer codes.

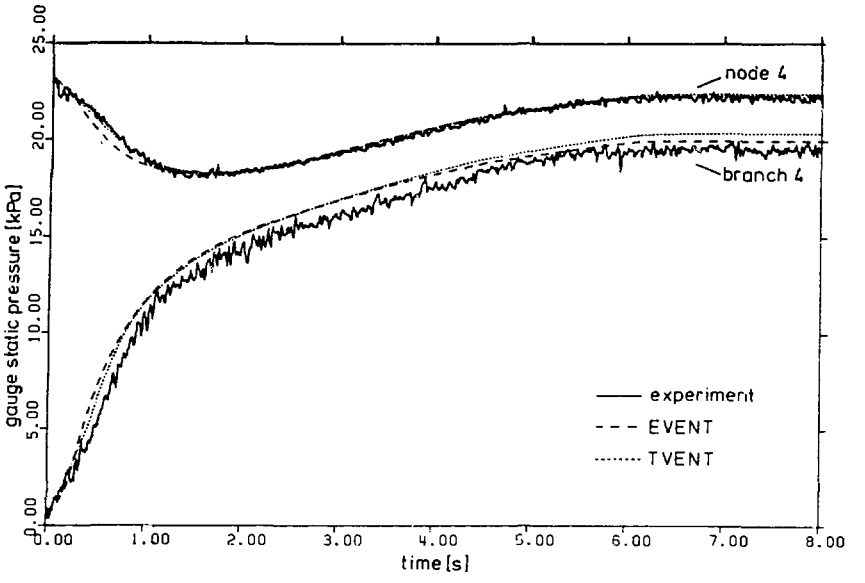

Fig. 6: Comparison of calculated and experimental results for Exp. I. Static pressure upstream of filter (≙ node 4) and differential pressure across filter (≙ branch 4).

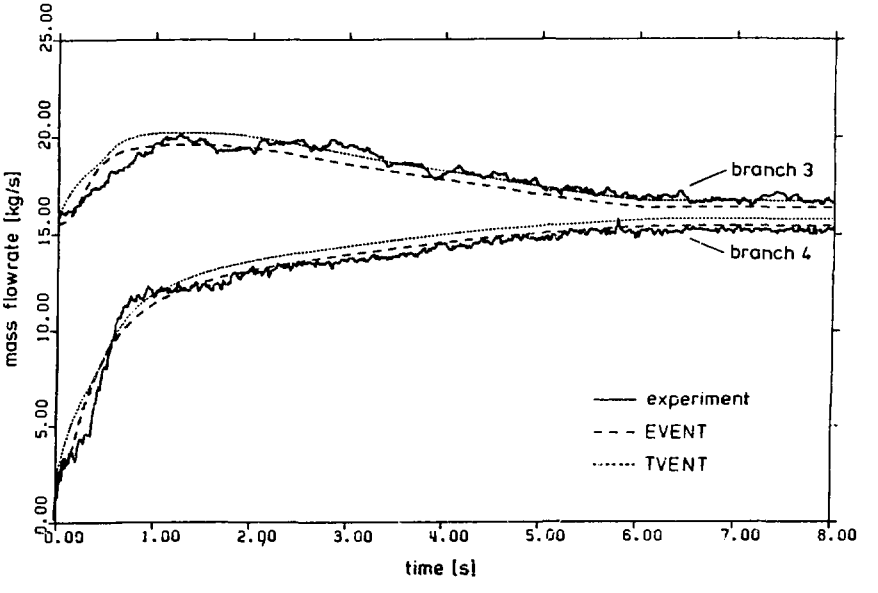

Fig. 7: Comparison of calculated and experimental results for Exp. I. Mass flow rate through air cooler (≙ branch 3) and test section (≙ branch 4).

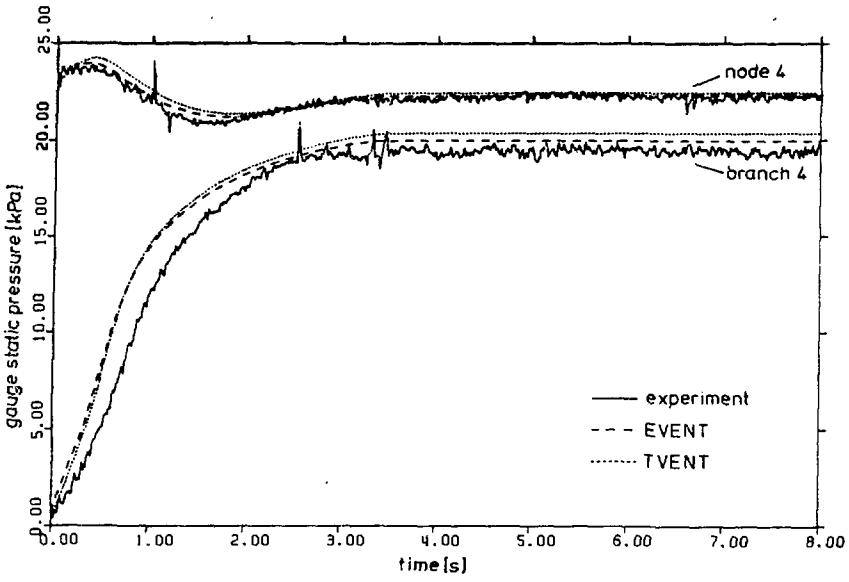

Fig. 8: Comparison of calculated and experimental results for Exp. II. Static pressure upstream of filter (≙ node 4) and differential pressure across filter (≙ branch 4).

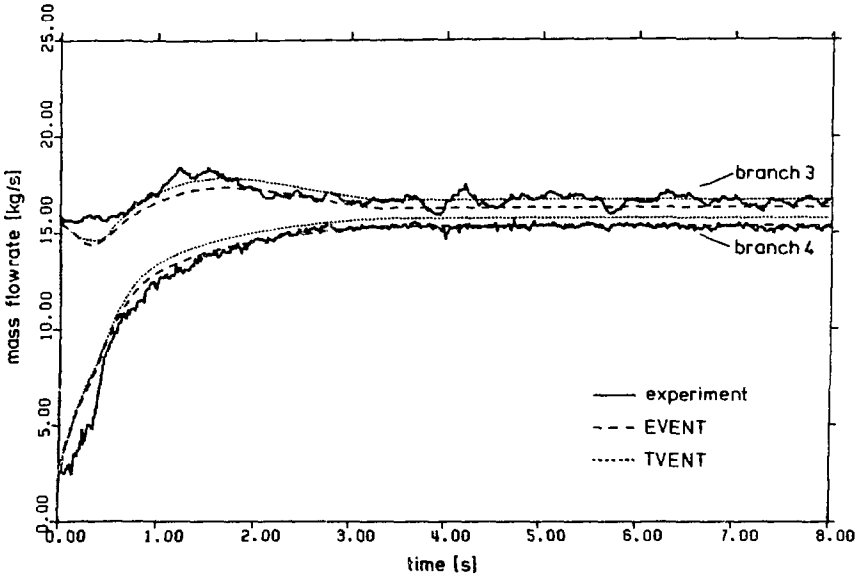

Fig. 9: Comparison of calculated and experimental results for Exp.II. Mass flow rate through air cooler (≙ branch 3) and test section (≙ branch 4).

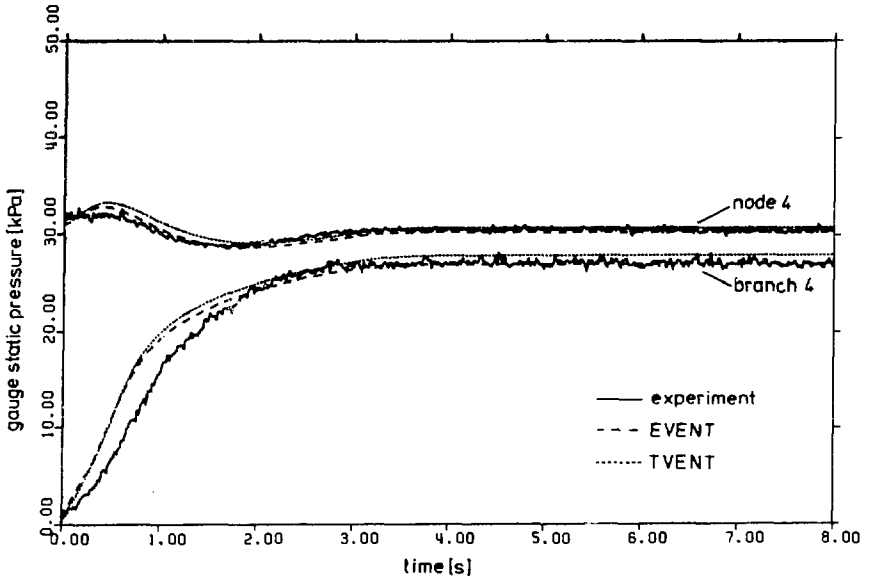

Fig. 10: Comparison of calculated and experimental results for Exp. III. Static pressure upstream of filter (≙ node 4) and differential pressure across filter (≙ branch 4).

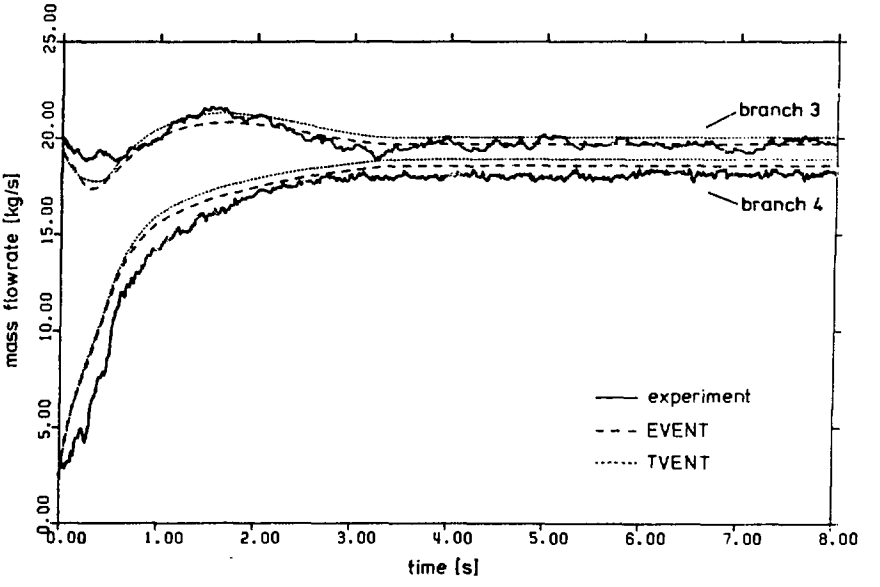

Fig. 11: Comparison of calculated and experimental results for Exp. III. Mass flow rate through air cooler (≙ branch 3) and test section (≙ branch 4).

RESPONSE OF AIR CLEANING SYSTEM DAMPERS AND BLOWERS TO SIMULATED TORNADO TRANSIENTS

W. Gregory, and E. Idar
Los Alamos National Laboratory
Los Alamos, New Mexico
P. Smith, E. Hensel, and E. Smith
New Mexico State University
Las Cruces, New Mexico

Abstract

The effects of tornado-like pressure transients upon dampers and blowers in nuclear air cleaning systems were studied. For the dampers pressure drop as a function of flow rate was obtained and an empirical relationship developed. Transient response was examined for several types of dampers, as was structural integrity. Both centrifugal and axi-vane blowers were tested and transient characteristic curves were generated in outrunning and backflow situations. The transient characteristic curves do not necessarily match the quasi-steady characteristic curves.

1. Introduction

Safety analysis reviews in the nuclear industry require the analyst to evaluate the effect of natural phenomena on facility design. The potential effect of tornado depressurization on facility air cleaning systems can be evaluated using computer codes such as TVENT[1]. This code calculates the transient pressures and flows throughout the facility and its ventilation system. However, a code such as TVENT has its limitations and is dependent on empirical response relationships determined from experimental data. Ventilation components such as filters, blowers, and dampers can cause significant effects on the flow dynamics of the system.

The response of ventilation system dampers and blowers to simulated tornado-generated transients is the subject of this paper. Light- and medium-duty ventilation dampers, a backdraft damper, one tornado protective damper, centrifugal blowers, and one axi-vane blower were evaluated. The data needed for integration into flow dynamics computer codes were obtained, and these include damper response time vs. flow rate, pressure drop vs. blade angle, and pressure drop vs. flow rate. These data then were transformed into empirical response relationships. The structural response of the dampers also was studied for several flow transients. Quasi-steady and transient characteristic curves were generated for the centrifugal and axi-vane blowers for both outrunning and backflow conditions.

II. Description of Dampers

Dampers are used as valves to obtain desired directions, flows, and pressures within a ventilation system. In conventional air conditioning and ventilating applications, little consideration is

given to rigid specifications for the dampers; however, many specifications are considered for nuclear applications. Depending on its function, a damper may be constructed in several configurations. Opposed- and parallel-blade configurations are discussed in detail below.

In this investigation we had to select representative dampers used in the nuclear industry. We chose to use the type of dampers used in the Los Alamos National Laboratory's plutonium research building as a basis. Although the size of the dampers can vary over a wide range, most of the dampers used in the plutonium research building for pressure balancing and flow control are 0.61-m by 0.61-m (2 ft by 2 ft) in cross section. However, tornado and backdraft dampers can be as large as 3.66 m (12 ft) in diameter. Isolation dampers of this size recently were installed at the Department of Energy's Rocky Flats plant at Denver, Colorado. For our tests, the dampers were approximately 0.61-m by 0.61-m (2 ft by 2 ft) in cross section. Our survey indicated that this size commonly is used, and in addition, our blowdown system is limited to this size.

Five devices were tested:

- an opposed-blade, medium-duty damper,
- an opposed-blade, light-duty damper,
- a parallel-blade, light-duty damper,
- a backdraft damper, and
- a tornado damper.

Figures 1 and 2 show the configurations of these dampers. Each has a 57.15 cm by 57.15 cm (22.5 in. by 22.5 in.) inside cross section.

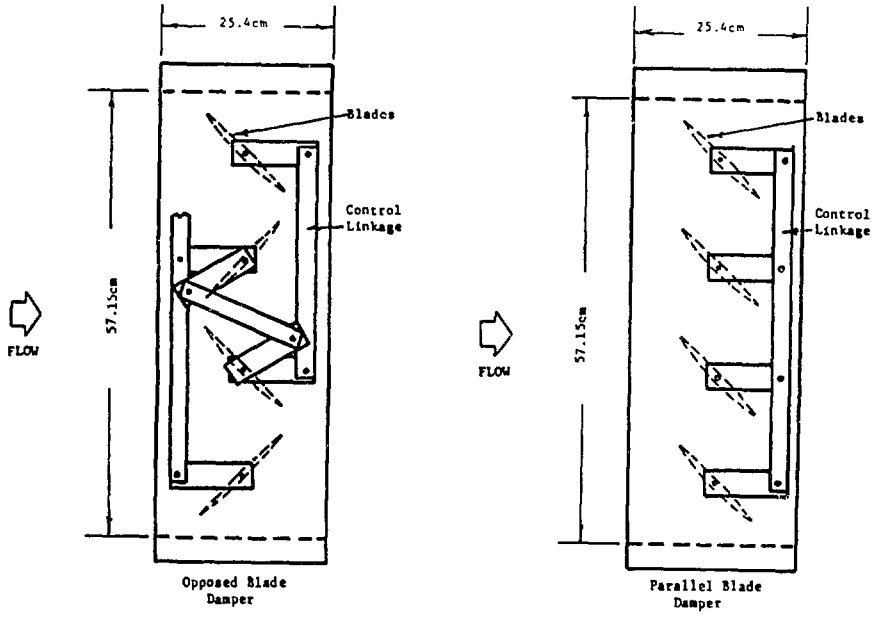

Figure 1 Side Views of the Opposed-Blade and the Parallel-Blade Dampers

Alternate blades of the opposed-blade dampers opened in opposite directions, whereas all the blades of the parallel-blade dampers opened in the same direction (Figure 1). The blades of the backdraft damper also opened in the same direction (Figure 2).

The opposed-blade and parallel-blade dampers all were built to allow actuation by pneumatic controllers. However, during the quasi-steady testing of these dampers, their blades were all fixed at the desired angles by clamping the blade actuating mechanism. In this way, quasi-steady resistance profiles could be obtained for the dampers at fixed blade angles. The backdraft damper was controlled by a weight on a variable-length lever arm. A high-speed motion picture camera was trained on a blade angle dial indicator during transient testing to measure blade angle as a function of time.

The tornado damper has a 50.8-m by 71.12-cm (20 in. by 28 in.) inside cross section, as shown in the schematic diagram in Figure 3. The damper's two valve plates face opposite from the direction in which a tornado pulse is expected. The extension springs hold the

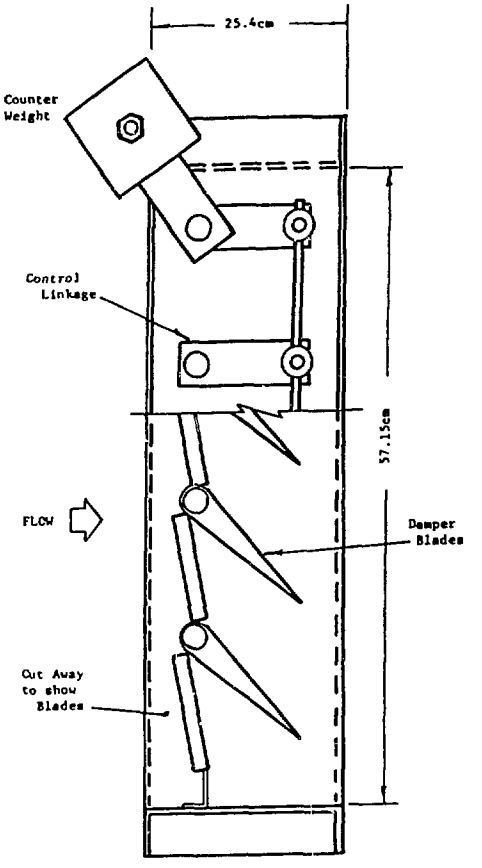

Figure 2 Side View of Backdraft Damper

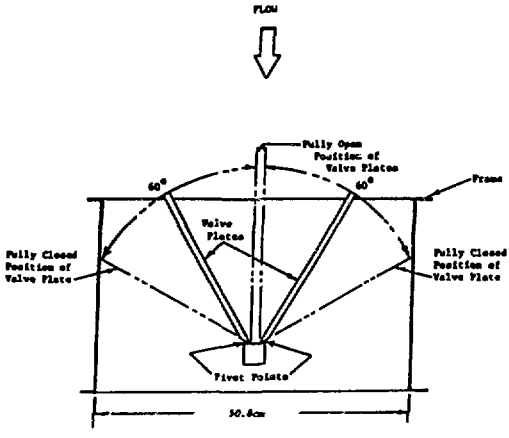

Figure 3 Top View Cut-Away of the Tornado Damper

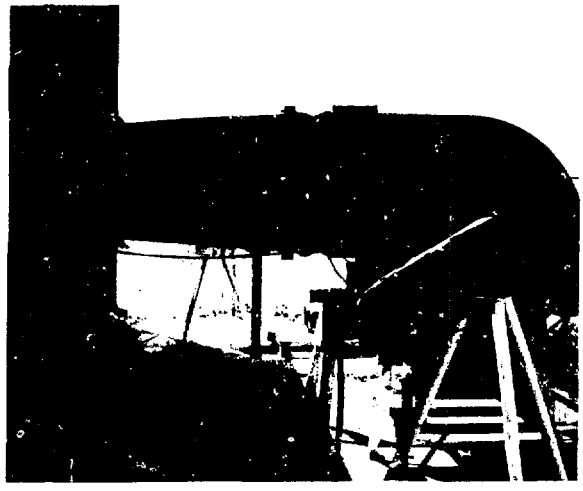

Figure 4 61 cm Centrifugal Blower in place for an Exhaust Pulse

valve plates in the open position against normal exhaust flow forces. An increase in flow, such as might be expected from the presence of a tornado inducing a negative pressure downstream of the damper, will cause the plates to close against the spring forces. Return to normal atmospheric conditions allows the springs to reopen the valve plates.

III. Description of Blowers

Three blowers were tested: a 61cm (24 in.) centrifugal blower, a 30.5 cm (12 in.) centrifugal blower, and a 83.8 cm (33 in.) axi-vane blower. Each blower was subjected to pressure pulses at their exhaust and at their inlet, which caused backflow and out-running flow, respectively. The pressure pulses used simulated tornado pressurization rates, but peak pressures were kept below magnitudes which might destroy the blowers.

Figures 4, 5, and 6 are photographs showing the 61 cm (24 in.), 30.5 cm (12 in.) and 83.8 cm (33 in.) blowers connected to the blowdown wind tunnel.

IV. Test Apparatus and Procedures

Blowdown System

Figure 7 is a schematic diagram of the blowdown wind tunnel used to simulate a tornado pressure pulse. Air from two large storage tanks is supplied at pressures up to 2760 KPa (400 psig) to 12 sonically limited solenoid valves connected to a 3.05-m by 3.05-m by 3.05m (10-ft by 10-ft by 10-ft) prefilter chamber. The valves are opened sequentially by an electric timer in a pattern can produce a pressure pulse equivalent to the Nuclear Regulatory Aommission (NRC) Region I standard tornado (Figure 8). The tunnel also can be operated in a quasi-steady mode by opening all or some of the valves simultaneously and allowing the storage tank to empty slowly. Various pressure drops across the dampers can be obtained by controlling the initial pressure in the tanks and by the number of valves opened.

The duct of the blowdown wind tunnel is 57.15 cm by 57.15 cm (22.5 in. by 22.5 in.) in inside cross section. Transition sections 1.22 m (4 ft) long connect the various dampers and blowers to this duct. The flow straighteners and the placement of pressure and temperature probes within the duct conform to Air Movement and Control Association (AMCA) standards[2,3]

Instrumentation

The locations of the primary instrumentation for the damper tests are shown in Figure 7. Velocity pressure (P_{v3}) is measured by a centerline pitot tube located 4.84 m (15.875 ft) upstream of the test device. A T-probe (P_{s3}) to measure static pressure and a copper-constantant thermocouple to measure air temperature (t_{d3}) are also at this location (PL-3). A second T-probe was placed on the centerline of the duct 57.15 cm (22.5 in.) upstream of the test device to

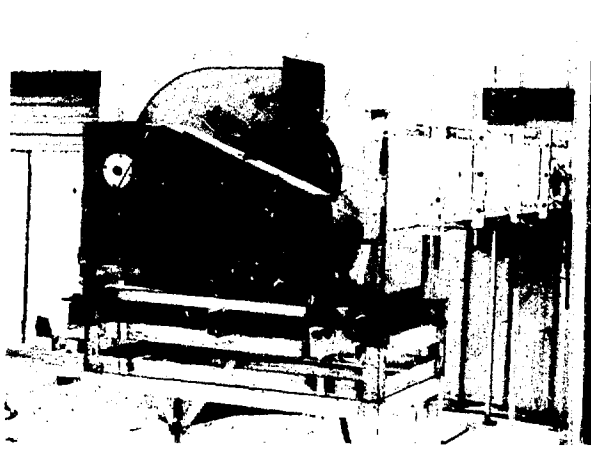

Figure 5 30.5 cm Centrifugal Blower in Place for an Exhaust Pulse

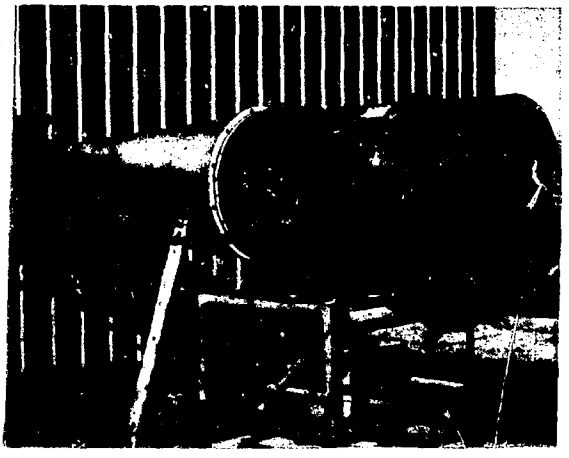

Figure 6 83.8 cm Axi-Vane Fan in Place for an Exhaust Pulse

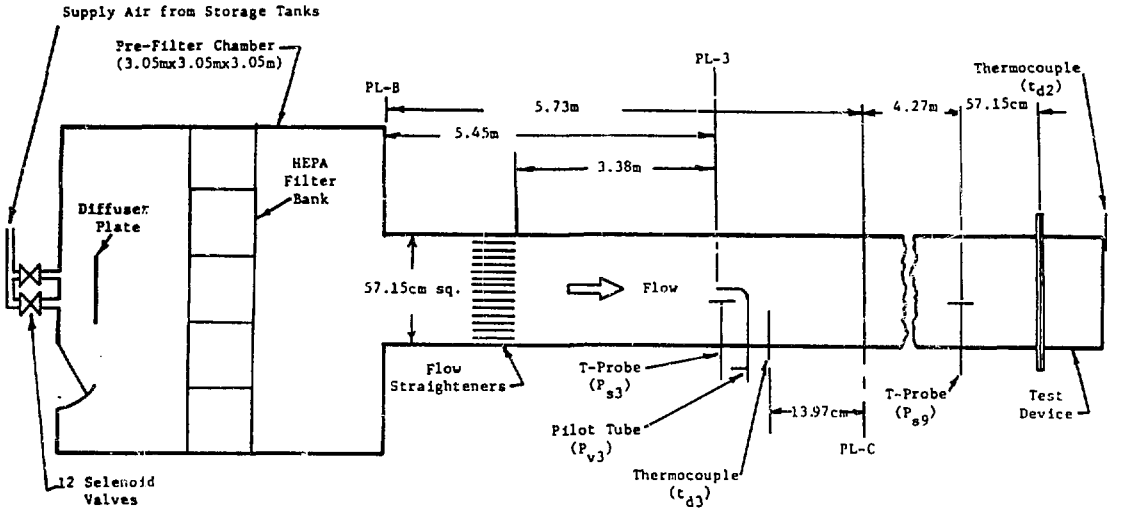

Figure 7 Blowdown Wind Tunnel Used to Simulate Tornado Pressure Pulses

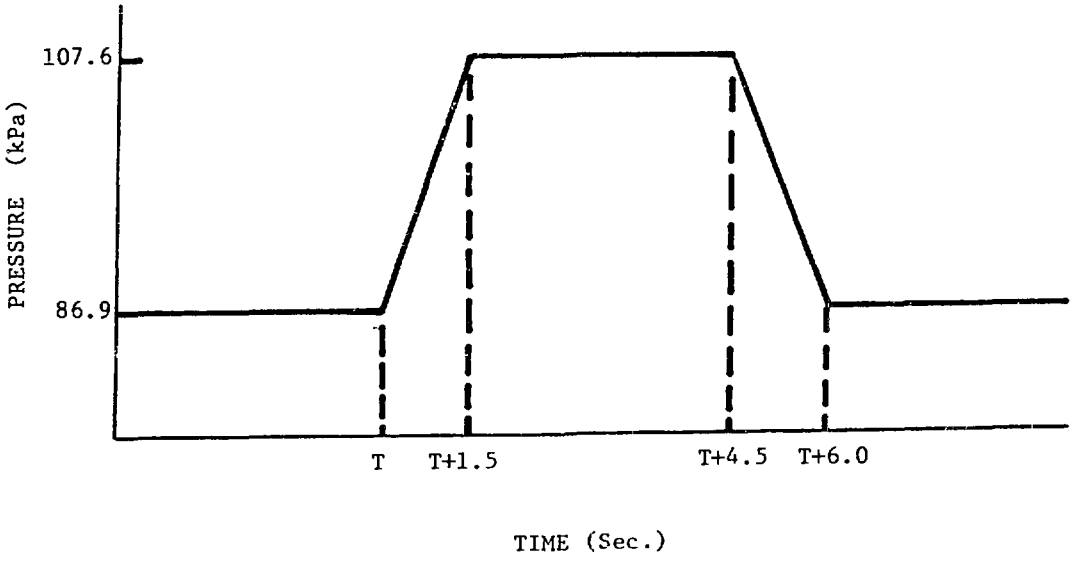

Figure 8 Simulated Region I Tornado Pressure Pulse

measure the static pressure (P_{s9}), which is equivalent to the pressure drop across the device. The pressure sensing elements used for all three duct pressure measurements were Validyne model DP7 differential pressure transducers with an output voltage range of 0 to 10 V; thermocouple output voltage was in the millivolt range. For both quasi-steady and transient testing, data from these transducers were recorded by a Digital Equipment Corp. (DEC) PDP11/05 digital computer. Other instrumentation included dry and wet bulb thermo-

meters, a mercury barometer, a Visual Instrumentation Corp. Locam high-speed motion picture camera, and a Himmelstein (SHC) torque meter and rotary speed pick-up.

Procedures

Each damper or blower test began with the calibration of the pressure transducers and by recording the ambient conditions.

Quasi-steady Tests. The quasi-steady tests were run after first charging the storage tanks to approximately 2070 KPa (300 psig). Only the opposed-blade and parallel-blade dampers and blowers were subjected to these tests. The inlet valves of the prefilter chamber were limited sonically in flow rate, and the flow rate remained relatively constant for several seconds. Low flow rates were obtained by opening only one or two valves. After recording the pressure drop, static pressures, velocity pressure, and temperatures, one or two more valves were opened to increase the flow rate. This procedure was continued until all 12 valves were open.

Transient Tests. The sonically limited inlet valves were programmed to open sequentially to produce a pressure pulse across the test device that closely approximated a tornado pressure pulse (Figure 8). Pressure and temperature data were recorded continuously by the digital computer and analog recorder during the test. Figure 9 is a typical analog plot of the pressure during a transient test of the tornado damper. The timing circuit that opened the valves of the blowdown wind tunnel also started a high-speed motion picture camera

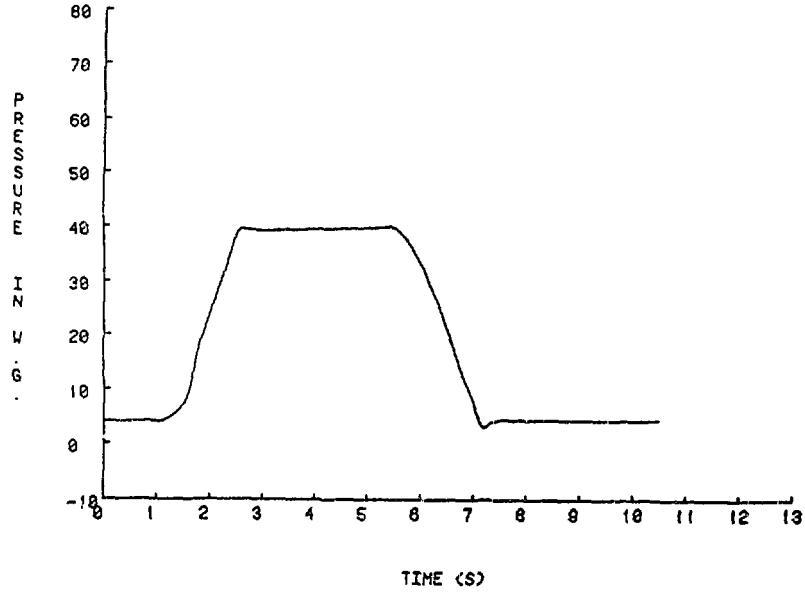

Figure 9 Typical Tornado Pulse Generated on Test Facility

that recorded the angle of the valve plates as a function of time. Timing marks on the film were synchronized with timing marks sent to the digital computer and to the analog recorder.

V. RESULTS

Quasi-steady Tests of Dampers

Figures 10 through 12 show the pressure drop through the opposed-blade dampers as a function of the flow rate of five fixed blade angles. The opposed-blade, medium-duty damper results are shown in Figure 10; the opposed-blade, light-duty damper results are shown in Figure 11; and the parallel-blade, light-duty damper results are shown in Figure 12. Each data point on these curves represents one quasi-steady test condition.

At the wide open position (that is, a blade angle of 90°), there is very little pressure drop through the dampers for all three types even at high flow rates. Also, the curve of pressure drop as a function of flow rate at 90° blade angle is virtually identical for all three types of dampers. For the fully closed position (that is, a blade angle of 0°), the curve of pressure drop as a function of flow rate also is virtually identical for all three types of dampers. In the closed position, the dampers offer maximum resistance to flow, and pressure drop increases very rapidly with flow rate.

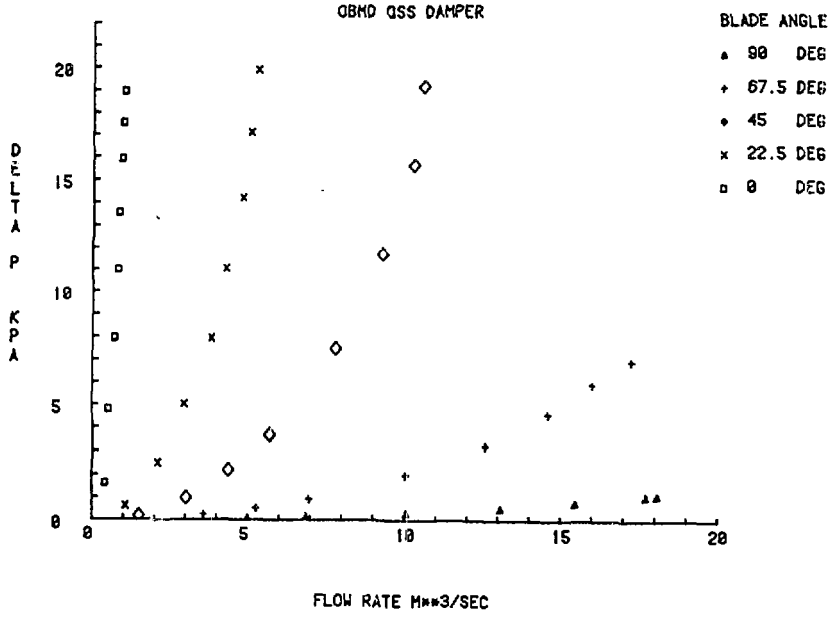

Figure 10 Opposed-Blade, Medium-Duty Damper, Quasi-Steady State

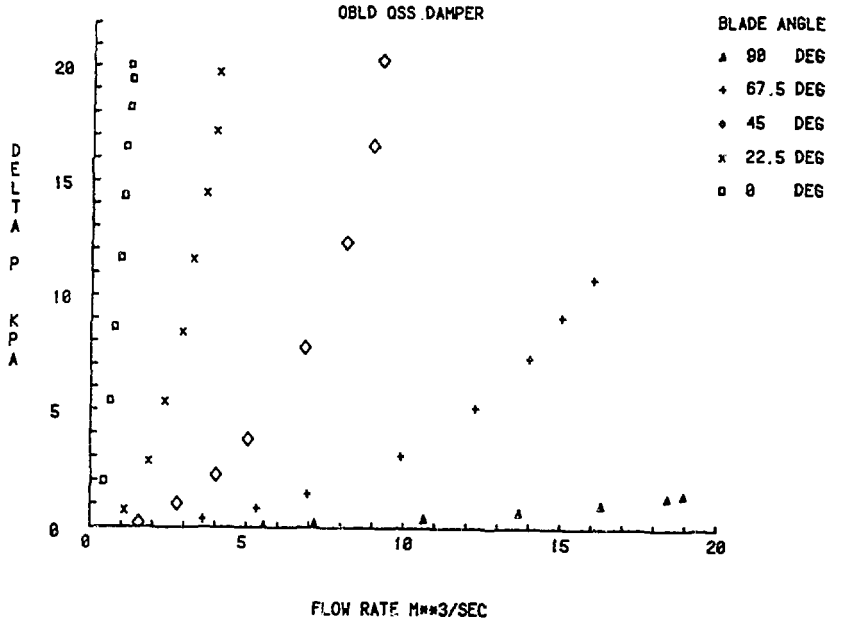

Figure 11 Opposed-Blade, Light-Duty Damper, Quasi-Steady State

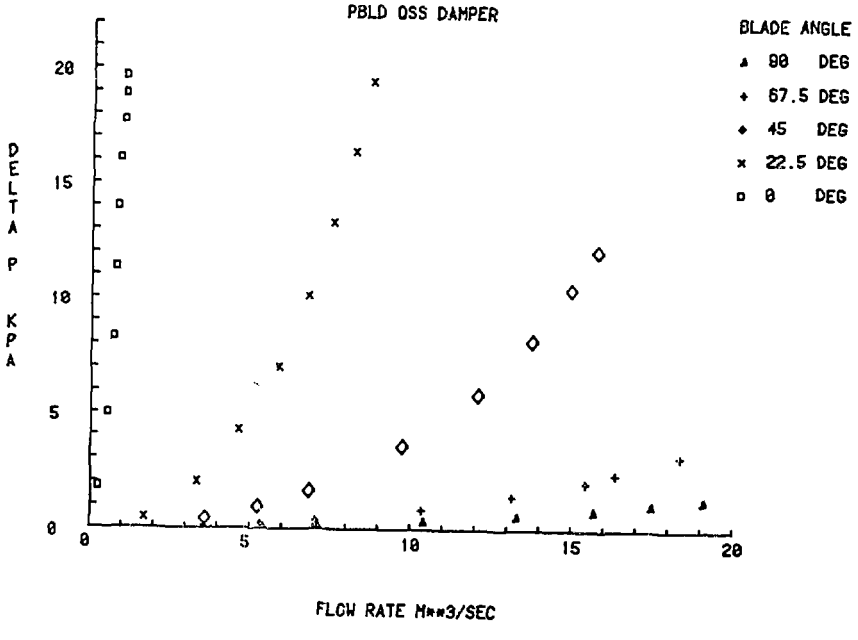

Figure 12 Parallel-Blade, Light-Duty Damper, Quasi-Steady State

The opposed-blade, medium-duty dampers and the opposed-blade, light-duty dampers were nearly identical in configuration except for the guage of the metal used in their construction. However, the light duty version offered more resistance to the flow than did the medium-duty version at the same flow rate for blade angles of 22.5°, 45°, and 67.5°. One apparent reason for this is the tendency for the blades of the light-duty version to twist toward closure when subjected to high airflow rates. Hence, their effective angle of attack was higher than the blades of the medium-duty damper for the same indicated blade angle. Another reason may be the presence of ribs on the blades of the light-duty damper, which apparently are needed to give the blades rigidity but add to their drag.

At all blade angles other than fully open or fully closed, the parallel-blade, light-duty damper created less pressure drop then did the opposed-blade dampers (medium or light duty) at the same flow rate.

The data in Figures 10 through 12 can be presented in the following form for ease of use in ventilation system simulation code such as EVENT or TVENT.

$$Q = P_i(\Delta P)^{.5} , \qquad (1)$$

where P_i is a resistance coefficient, Q is the flow rate, and ΔP is the pressure drop across the dampers. P_i, tabulated in Table 1, was determined by a least squares fit to the data in Figures 10 through 12.

The data in Table 1 were analyzed further and incorporated into Equation (1) to yield a relationship for P_i as a function of blade angle, θ. A least squares polynomial fit was made to these data. The resulting equations are quartics of the following general form:

$$P_i = a + b\theta + c\theta^2 + d\theta^3 + e\theta^4 . \qquad (2)$$

The coefficients in Equation (2) are listed in Table 2.

Transient Tests of Dampers

Figures 13 and 14 show the flow rate and pressure drop as a function of time for a typical transient test (BD 100) of the backdraft damper. The solenoid valves supplying the high-pressure air to the prefilter chamber began opening at time t = 0 s. They opened sequentially in such a way that all 12 were open at 1.0 s and remained open for 3.0 s thereafter. The valves began closing at time t = 4.0 s; by time t = 6 s, all 12 were closed and the flow stopped. Because of the compressibility of the flow and the capacitance of the prefilter chamber, the flow rate did not begin to increase at location PL-3 until about time t = 0.28 s. As the velocity continued

Table 1

Resistance Coefficients for Opposed-Blade, Medium-Duty (OBMD), Opposed-Blade, Light-Duty (OBLD) and Parallel-Blade, Light-duty (PBLD) Dampers

Damper	Blade Angle	P_i
OBMD	0.0°	0.237
	22.5°	1.254
	45.0°	2.632
	67.5°	6.739
	90.0°	17.359
OBLD	0.0°	0.273
	22.5°	0.967
	45.0°	2.267
	67.5°	5.168
	90.0°	16.166
PBLD	0.0°	0.226
	22.5°	2.074
	45.0°	4.758
	67.5°	10.584
	90.0°	16.698

Table 2

Coefficients for Eqs. (2)

Damper	a	b	c	d	e
OBMD[a]	2.371×10^{-1}	5.642×10^{-2}	-6.941×10^{-4}	3.460×10^{-6}	2.308×10^{-7}
OBLD[b]	2.732×10^{-1}	-2.943×10^{-2}	4.622×10^{-3}	-1.066×10^{-4}	8.969×10^{-7}
PBLD[c]	2.237×10^{-1}	1.556×10^{-1}	-6.154×10^{-3}	1.475×10^{-4}	-8.419×10^{-7}

[a]Opposed-blade, medium-duty damper

[b]Opposed-blade, light-duty damper

[c]Parallel-blade, light-duty damper

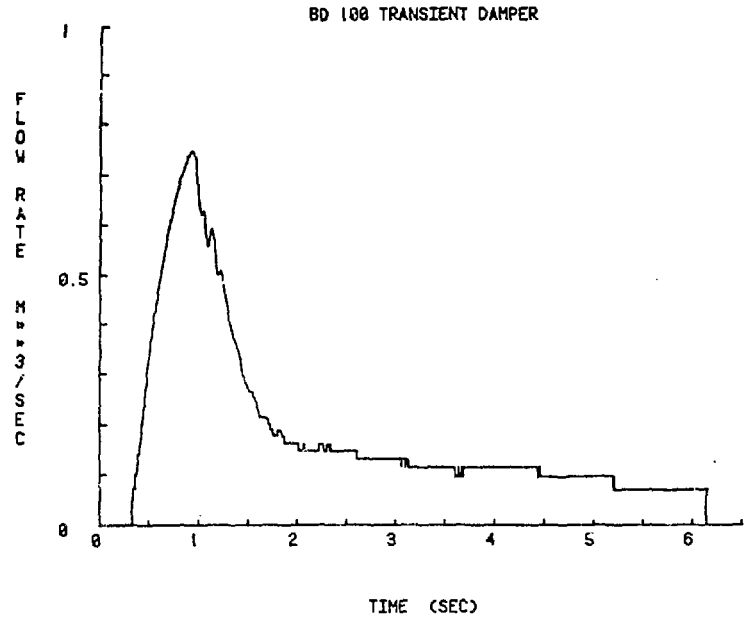

Figure 13 Backdraft Damper, Transient Test, Flow Rate vs. Time

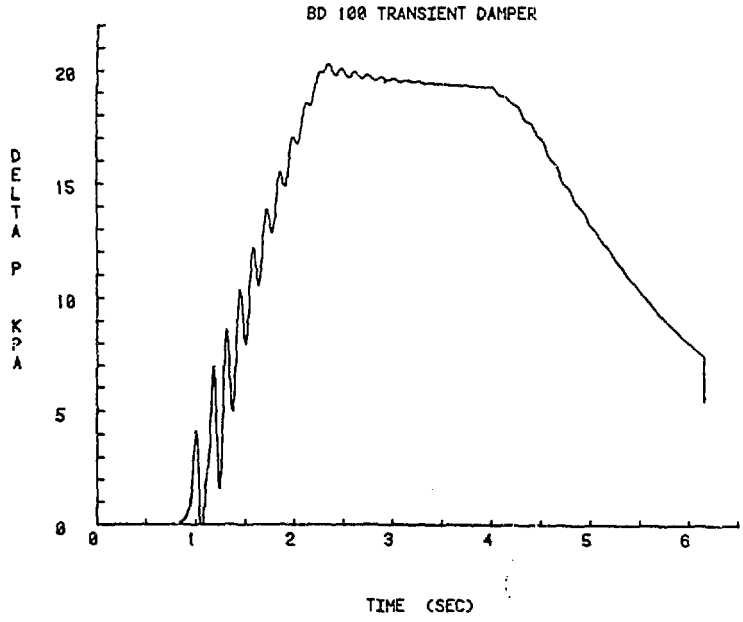

Figure 14 Backdraft Damper, Transient Test, ΔP vs. Time

to increase, the damper began to close at time t = 0.31 s (as shown in Table 3) and was closed completely at about time = 0.91 s, at

which time the flow rate dropped dramatically. The pressure drop across the damper climbed to a maximum value of 20 KPa (3 psi) at time t = 2.2 s, where it remained essentially constant until time t = 4.0 s. The leakage flow rate for the fully closed damper at a pressure drop of 20 kPa (3 psi) appeared to average about 0.10 m^3/s.

Table 3, which presents the blade angles as a function of time for three backdraft transient tests (BD 98, BD 99, and BD 100), shows that, once this damper is set in motion, closure time ranges from 0.8 s to 1.8 s. Because this is a fairly short time, the event could be modeled by assuming that the damper immediately closes when the local flow rate exceeds the design flow rate at the damper by a specified amount, such as 5. The leakage flow rate for the fully closed damper would be assumed to be related to pressure drop according to Equation (1). Then,

$$0.1 = P_i(20)^{.5} ,$$

or

$$P_i = 0.1/(20)^{.5} = 0.0224 .$$

Thus, for use in a ventilation system simulation code like EVENT or TVENT, the relation between flow rate and pressure drop for a closed backdraft damper could be assumed to be

$$Q = 0.0224(\Delta P)^{.5} . \qquad (3)$$

Table 3

Blade Angle as a Function of Time for Three Backdraft Damper Tests

Blade Angle, Deg.	Time, Secs.		
	BD 98	BD 99	BD 100
84	0.88	0.4	.31
63	1.40	0.71	.63
42	1.59	0.83	.71
21	1.69	0.91	.76
0 (closed)	1.79	0.98	.80

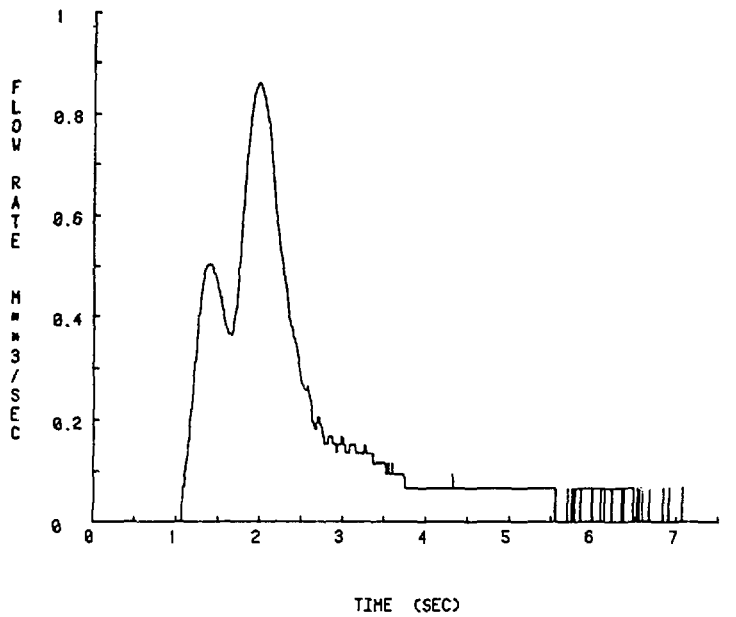

Figure 15 Tornado Damper, Transient Test, Flow Rate vs. Time

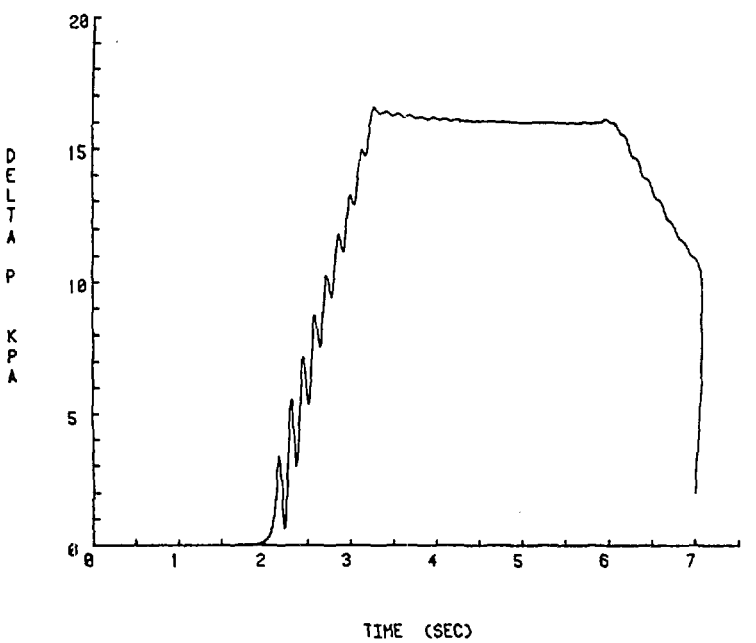

Figure 16 Tornado Damper, Transient Test, ΔP vs. Time

Figures 15 and 16 present the flow rate and the static pressure rise through the damper as functions of time and for one test of the tornado damper. These figures were plotted from the digital computer data taken during a typical transient test. The valves supplying the prefilter chamber began opening at time t= 0 s, and all 12 valves were fully open at time t = 1.5 s and remained so until time t = 4.5 s, when they began closing. All 12 were closed by the time t = 6 s. Because of the compressibility of the air and the capacitance of the prefilter chamber, the flow rate does not begin to increase at locations PL-3 until time t = 1 s. As the velocity increases, the valve begins to close at about 1.42 s, which causes the pressure to begin rising across the damper. Table 4 shows the blade angle as a function of time for this test. At a time of 1.74 s, the blades were fully closed but then began to bounce about 1° at a frequency of 100 Hz. After about three cycles, the blades bounced open to about 5° at a time of 1.8 s. The flow rate reaches its maximum value at about this time because all 12 supply valves are still fully open. At a time of 1.84 s the blades again are closed and the flow rate drops off rapidly, but the pressure drop across the valve remains constant at about 16 KPa (2.3 psi). The leakage flow rate at full closure and 16 KPa is approximately 0.08 m^3/s.

Special Problems Encountered with Dampers

Two noteworthy structural problems arose during the testing of the dampers. The first was the flexibility of the control linkage of the opposed-blade and parallel-blade dampers, especially the light-duty versions. Although clamped in a set position to keep the blades at a fixed angle, the linkages would flex and cause the effective blade angle to change. When this problem was recognized, the linkages were strengthened by adding more clamps. In this way, most of the blade movement during quasi-steady testing was eliminated and

Table 4

Blade Angle as Function of Time
For Tornado Damper
Test No. 13

Time, Sec.	Valve Position, Deg.
1.42	55
1.56	44
1.63	33
1.68	22
1.71	11
1.74	0
1.75	1
1.76	0
1.77	1
1.78	0
1.80	5
1.84	0

probably was not important except for the light-duty versions of the dampers.

The second structural problem occurred for the backdraft damper. The blades of the damper are made of sheet metal folded around a shaft about which they pivot. The sheet metal is spot welded to the shafts in about four places. Transient testing of the backdraft damper caused these spot welds to fail randomly and allowed the blades to twist relative to the shafts. This would occur differently for each test, causing a great variance in the test results. The problem was solved by adding more welds to the blades. The data obtained for transient testing of the backdraft damper after the blade/shaft connection was strengthened proved to be repeatable and consistent; they are the data presented in this report.

Quasi-steady Tests of 61 cm (24 Inch) Centrifugal Fan

Fan static pressure produced for both exhaust pulsing and inlet pulsing of the 61 cm (24 inch) centrifugal blower are plotted as a function of volumetric flow in Figures 17 and 18. Figure 17 represents the first and fourth quadrants of the fan characteristic curve

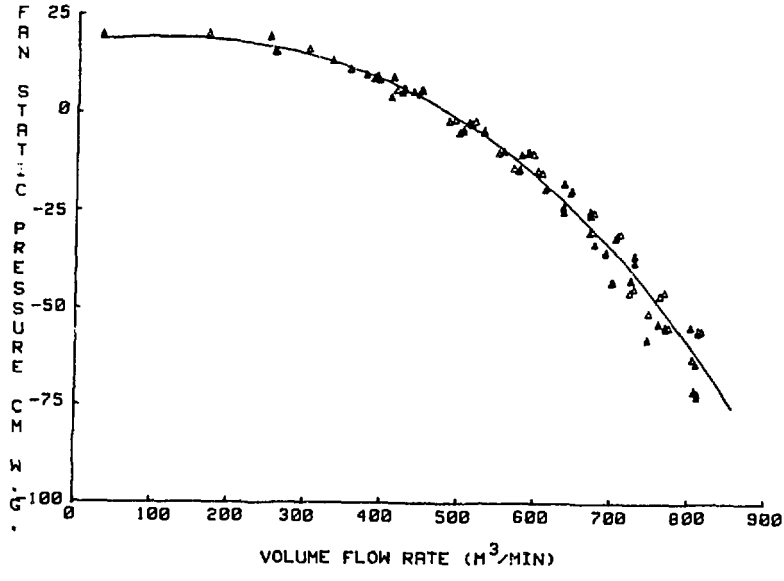

Figure 17 Quasi-Steady Characteristic Curve of 61 cm Centrifugal Blower Quadrant 1 and 4

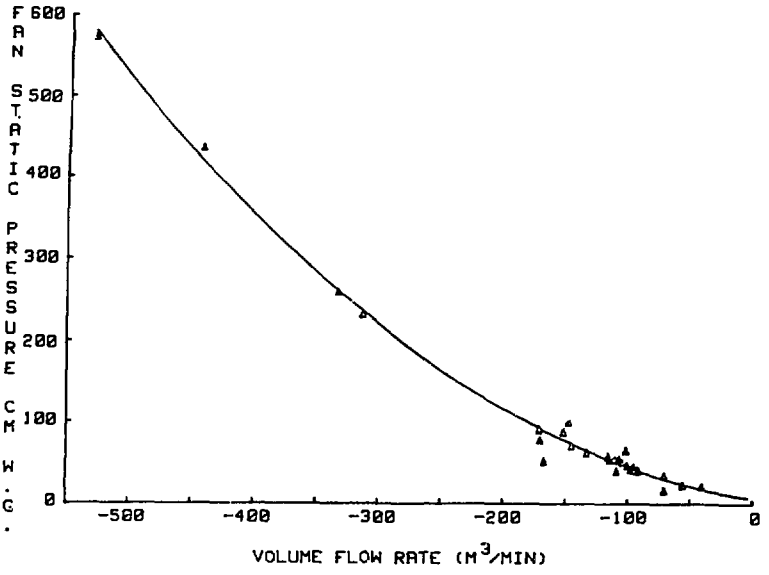

Figure 18 Quasi-Steady Characteristic Curve for 61 cm Centrifugal Blower - Quadrant 2

and Figure 18 the second quadrant. The curves were fit through the experimental data points shown using a cubic spline.

Transient Tests of 61 cm (24 Inch) Centrifugal Fan

A total of 15 transient tests were run, 8 with inlet pulses, and 7 with exhaust pulses. For the inlet pulses, three nominal pressurization rates were used [4.14 KPa/sec (0.6 psi/sec), 8.28 KPa/sec (1.2 psi/sec), and 14.49 KPa/sec (2.1 psi/sec)] while peak pressure was held constant at 3.45 KPa (0.5 psig). One replication was made of each test. Further, at a nominal pressurization rate of 4.14 KPa/sec (0.6 psi/sec) two tests were run having a nominal peak pressure of 6.9 KPa (1.0 psig).

Similarly, for the exhaust pulses, three nominal pressurization rates were used [4.14 KPa/sec (0.6 psi/sec), 8.28 KPa/sec (1.2 psi/sec), and 13.8 KPa/sec (2.0 psi/sec)] at nominal peak pressures of 10.35 KPa (1.5 psig) and 18.63 KPa (2.7 pisg).

A typical inlet pulse and exhaust pulse are presented in this section for discussion. Figures 19 and 20 are "movie frame" representations of tests CBIN29 and CBEX61. That is, as the static pressure P_{s3} and the calculated fan static pressure change with time, their values are presented for all times up to the test time represented in the duct static pressure (P_{s3}) figure. For the calculated

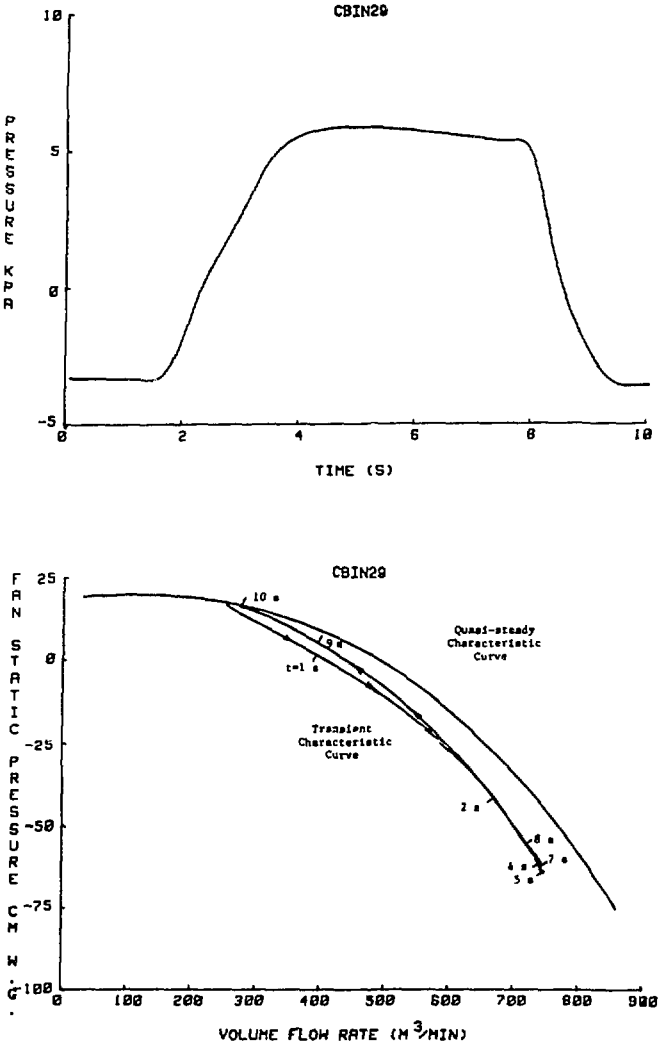

Figure 19 "Movie Frame" Sequence of Transient Test of 61 cm Centrifugal Blower (Frame 10)

fan static pressure the quasi-steady characteristic curves are also plotted for comparison.

Notice the "movie frame" sequence for the inlet pulse for test CBIN29, Figure 19. As the static pressure in the duct inceases the fan static pressure begins to decrease and the volume flow rate increases. When the duct static pressure has reached its minimum value of about -58.42 cm (-23) in. of water. The flow rate in the mean time has increased from about 226.5 m^3/min. (8000 CFM) to over

679.6 m^3/min. (24000 CFM). With the duct static pressure essentially constant at about 676 KPa (0.98 psig) for a period of 2 seconds, the fan static pressure and the flow remain essentially constant at -58.42 cm (-23 in.) of water and 679.6 m^3/min. (24000 CFM). Then, as the duct static pressure begins to drop, the fan static pressure begins to increase and the flow rate to decrease. Finally, when the duct static pressure has dropped back to the steady state operating point, the fan static pressure and the flow rate have also returned to their steady state conditions.

Notice two important things about the transient characteristic of the blower. First, the transient characteristic exhibits hysterisis, that is the curve does not follow the same path when the duct static pressure is decreased as it did when the duct static pressure was increased. Second, the transient characteristic curve of the fan falls below the quasi-steady characteristic curve. Therefore, one cannot use the quasi-steady characteristic curve to approximate the transient operation of this centrifugal blower.

The other seven inlet pulse tests essentially duplicate the results of test CBIN29 and lend confidence to the results.

The response of the blower to pressurization rate can be determined for inlet pulses by examination of the results of tests CBIN 44, CBIN 48, and CBIN 51. Maximum static duct pressure attained was the same [3.45 KPa (.5 psig)] for all three of these tests, but pressurization rates were 4.17 KPa/sec (0.605 psi/sec), 8.14 KPa/sec (1.18 psi/sec), and 14.14 KPa/sec (2.05 psi/sec), respectively. Comparison shows the transient characteristic curve to be essentially identical for all three of these tests. The only effect that pressurization rate appears to have is the speed at which the characteristic curve is traversed at the on-set of pressurization. For example, at 2 seconds into the pulse the fan static pressures for CBIN 44, CBIN 48, and CBIN 51 are -2.54 cm (-1 in.) of H_2O, -20.32 cm (-8 in.) of H_2O and -38.1 cm (-15 in.) of H_2O, respectively.

Now, turn to the "movie frame" results of exhaust test CBEX 61 shown in Figure 20. As the static pressure is increased in the duct the fan static pressure increases and the volume flow rate decreases. At the maximum static duct pressure of 10.9 KPa (1.58 psig) the fan static pressure is about 134.6 cm_3 (53 in.) of water and the volume flow rate is a negative 198.2 m^3/min. (7000 CFM). As the duct static pressure is decreased the fan static pressure also decreases and the flow rate increases until the steady state operating point is again reached.

Notice that once again the transient characteristic curve exhibits hysterisis and does not follow the quasi-steady characteristic. Also notice that the fan speed is decreased substantially for this type of test. For other tests the blower rotation was actually reversed causing stall of air flow around the fan blades and the fan characteristic, therefore, exhibited a very erratic behavior for the remainder of the test.

The response of the blower to pressurization rate can be determined for exhaust pulses by examination of the results of tests CBEX 59, CBEX 60, and CBEX 62. Maximum static duct pressure attained

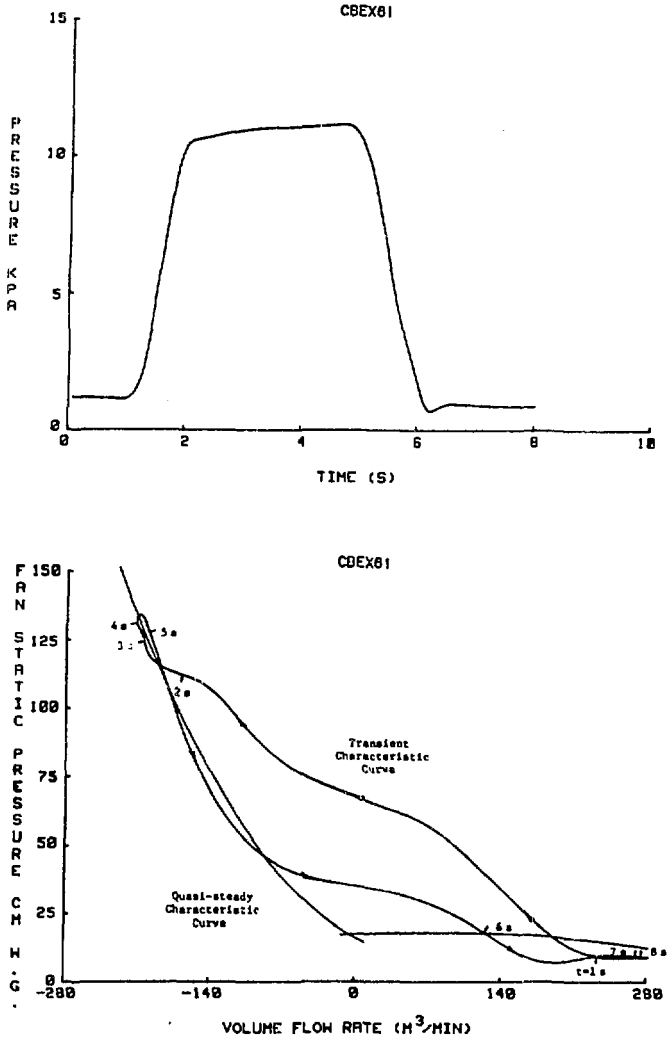

Figure 20 "Movie Frame" Sequence of Transient Test of 61 cm Centrifugal Blower (Frame 8)

was essentially the same for all three of these tests, but pressurization rates were 4.07 KPa/sec. (0.59 psi/sec), 8.28 KPa/sec (1.2 psi/sec) and 13.3 KPa/sec. (1.93 psi/sec), respectively. Comparison shows the transient characteristic curves to be similar, but not identical, for these three tests. With the on-set of the pressure transient the higher pressurization rate causes the fan static pressure to be higher than it is for the lower pressurization rates. However, during the drop in duct static pressure all three transient characteristic curves are essentially the same. Further-

more, the pressurization rate affects the speed at which the transient characteristic curve is traversed during the on-set of the pressurization, just as it did in the case of inlet pulsing.

Tests of 30.5 cm (12 inch) Centrifugal Fan

Quasi-steady and transient testing of the 30.5 cm (12 inch) centrifugal blower was similar to that of the 61 cm (24 inch) centrifugal blower. Results were also similar and the blowers appear to scale in accordance with fan scaling laws.

Quasi-steady Tests Of 83.8 cm (33 Inch) Axi-vane Blower

Figure 21 presents the results of the quasi-steady testing of the 83.8 cm (33 inch) axi-vane blower. Cubic splines were used to fit the curve to the experimental data.

Transient Tests of 83.8 cm (33 Inch) Axi-vane Blower

Two transient tests were run on the axi-vane blower. AVFIN37 was an inlet pulse test with a pressurization rate of 8.16 KPa (1.83 psi/sec) and a peak duct static pressure of 1.52 KPa (0.22 psig), while AVFEX73 was an exhaust pulse test with a pressurization rate of 9.87 KPa/sec (1.43 psi/sec) and a peak duct static pressure of 9.66 KPa (1.4 psig).

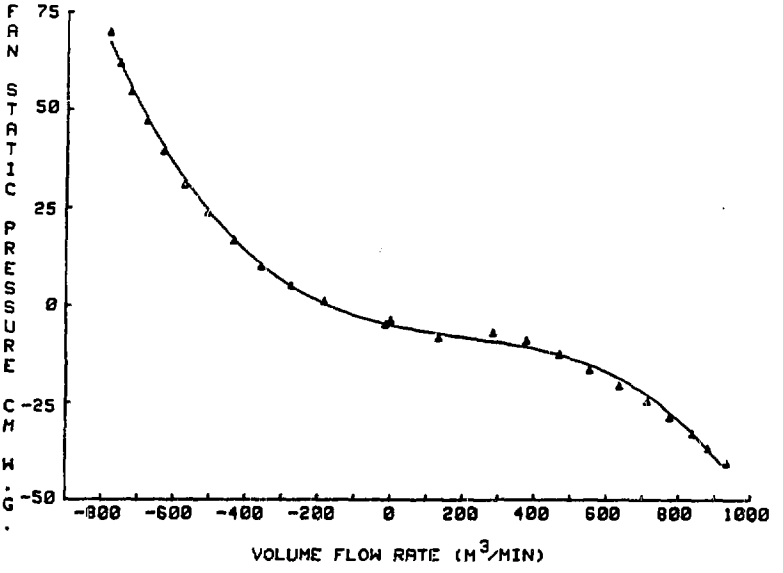

Figure 21 Quasi-Steady Characteristic Curve for the Axi-Vane Fan

The "movie frame" sequence for inlet pulse test AVFIN37 is presented in Figure 22. As the duct static pressure is increased the fan static pressure decreases and the volume flow rate increases. At the maximum duct static pressure of 1.52 KPa (0.22 psig) the fan static pressure is approximately -27.9 cm (-11 in.) of water and the volume flow rate is about 991.1 m^3/min. (35,000 CFM).

As the duct static pressure decreased the fan static pressure began to increase and the flow rate to decrease. Unfortunately, data was not obtained for the full return of the fan operation to steady state conditions. Notice that the transient characteristic curve of

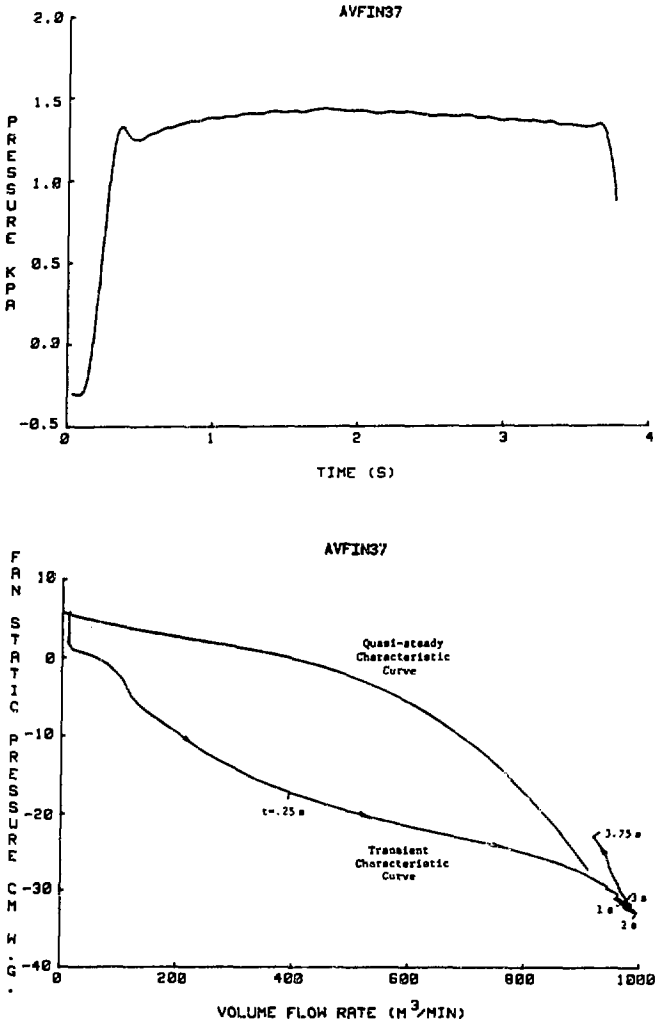

Figure 22 "Movie Frame" Sequence of Transient Test of 83.8 cm Axi-Vane Fan (Frame 5)

the blower fell well below the quasi-steady characteristic curve as the duct pressure was increased and on the return toward steady state the transient characteristic curve is not following the same path, i.e. it exhibits hysterisis. Apparently the transient characteristic curve brackets the quasi-steady characteristic curve, as can be seen in Figure 22.

Figure 23 presents the "movie frame" sequence for the exhaust pulse test, AVFEX73. As the duct static pressure is increased the fan static pressure increases and the volume flow rate decreases very rapidly. At the maximum duct static pressure of 9.66 KPa (1.4 psig) the fan static pressure is approximtely 86.36 cm (34 in.) of water and the flow rate is negative 821.19 m^3 (29,000 CFM). Unfortunately, no data was obtained for the return to steady state operation.

Notice that the transient characteristic curve lies above the quasi-steady characteristic curve (Figure 23).

V. Summary and Conclusions

Dampers

The quasi-steady testing of the opposed-blade and parallel-blade dampers provided information about the relationship between the pressure drop through the dampers and the flow rate for fixed blade angles. This relationship was approximated by a formula that can be used in a computer simulation of flow and pressure drop through a nuclear facility ventilation system. Further, this relationship was extended to relate the damper resistance coefficient as a function of blade angle. If this relationship is coupled with the control system that maintains pressure or flow control for the ventilation system, the dynamic response of the control system can be included in the analysis. For example, if a pressure point is controlled within the system, the damper blade angle can be adjusted as the pressure varies to respond to the pressure change. This would require a control system module to be added to computer simulation codes such as TVENT.

Transient testing of a backdraft damper proved that it closed within a range of 0.8 s to 1.8 s. The assumption that the leakage flow rate for the fully closed backdraft damper can be related to the pressure drop through the damper by a formula similar to that developed for the opposed-blade and parallel-blade dampers appears valid. The backdraft damper has a serious structural problem for pressure pulses equivalent to the NRC Region I tornado pulse. The welds that hold the sheet metal blades to the shaft on which they pivot break, rendering the damper ineffective. When subjected to a tornado-like pressure pulse, the tornado damper closes in about 1.84 s after bouncing several times. Closure time for this damper could be reduced to 1.74 s if the bounce could be eliminated.

61 cm (24 Inch) Centrifugal Blower

The transient characteristic curve of the 61 cm (24 inch) centrifugal blower exhibits hysterisis in both the outrunning (quadrants 1 and 4) and the backflow (quadrants 1 and 2) cases. The transient characteristic curve did not coincide with the quasi-steady

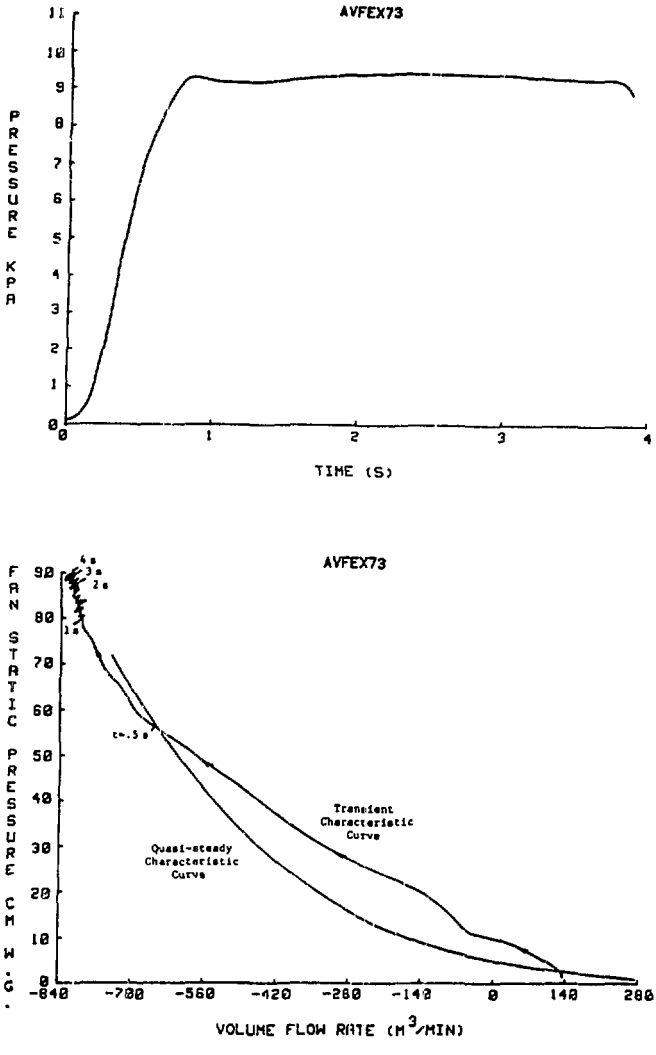

Figure 23 "Movie Frame" Sequence of Transient Test of 83.8 cm Axi-Vane Fan (Frame 5)

characteristic curve of the blower, hence the latter should not be used to approximate transient operation of the blower.

Pressurization rate did not appear to have a significant affect upon transient blower operation for the range of pressurization rate 4.14 KPa/sec to 13.8 KPa/sec (0.6 psi/sec to 2.0 psi/sec) used in this study for inlet pulses (quadrants 1 and 4). Larger pressurization rates caused the fan static pressure to be larger during the on-set of the pressure rise for an exhaust pulse.

83.8 cm (33 Inch) Axi-Vane Blower

The transient characteristic curve of the 83.8 cm (33 inch) axi-vane fan exhibited hysterisis in the outrunning (quadrants 1 and 4) case. The transient characteristic curve of the fan did not coincide with the quasi-steady characteristic curve for either the outrunning (quadrants 1 and 4) or the backflow (quadrants 1 and 2) cases.

References

1. Duerre, K. H., Andrae, R. W., and Gregory, W. S., "TVENT-a computer program for analysis of tornado-induced transients in ventilation systems," Los Alamos Scientific Laboratory report LA-7397-M, (1978).

2. "Test methods for louvers, dampers and shutters," AMCA Standard 500-75, Air Movement and Control Association, Inc., (1973).

3. "Laboratory methods of testing fans for rating," AMCA Standard 210-74, Air Movement and Control Association, Inc., 6th ed. (1967).

DISCUSSION

SODERHOLM: Is there a potential lack of reality in this paper and in the previous one, especially in the blowdown system, because you have pressure on one side, whereas in a tornado situation you have a lack of pressure on the other side. I am thinking specifically of a problem due to flexibility in ducting. Does this ever occur?

SMITH, P.: You can always envision a situation when it would be important but if the ducts are rigid enough, it is not going to cause too much of a problem. When we first started these studies, about 7 or 8 years ago, we investigated, on a small scale, the difference between having a blowdown system and a vacuum system. It turns out that the situation was the same for both types of flow, so there didn't seem to be any difference between them. When we went to larger flow systems, to investigate flows through bigger components, we went to the blowdown system because it is much more convenient. Yes, if you do have a very flexible system, you could have some problems. So you want to make sure the ducting system, and so forth, are rigid enough to take the vacuum.

FIRE SIMULATION IN NUCLEAR FACILITIES-- THE FIRAC CODE AND SUPPORTING EXPERIMENTS

Dup

M. W. Burkett and R. A. Martin
Los Alamos National Laboratory
Los Alamos, New Mexico

D. L. Fenton and M. V. Gunaji
New Mexico State University
Las Cruces, New Mexico

Abstract

The fire accident analysis computer code FIRAC was designed to estimate radioactive and nonradioactive source terms and predict fire-induced flows and thermal and material transport within the ventilation systems of nuclear fuel cycle facilities. FIRAC maintains its basic structure and features and has been expanded and modified to include the capabilities of the zone-type compartment fire model computer code FIRIN developed by Battelle Pacific Northwest Laboratory. The two codes have been coupled to provide an improved simulation of a fire-induced transient within a facility. The basic material transport capability of FIRAC has been retained and includes estimates of entrainment, convection, deposition, and filtration of material. The interrelated effects of filter plugging, heat transfer, gas dynamics, material transport, and fire and radioactive source terms also can be simulated. Also, a sample calculation has been performed to illustrate some of the capabilities of the code and how a typical facility is modeled with FIRAC.

In addition to the analytical work being performed at Los Alamos, experiments are being conducted at the New Mexico State University to support the FIRAC computer code development and verification. This paper summarizes two areas of the experimental work that support the material transport capabilities of the code: the plugging of high-efficiency particulate air (HEPA) filters by combustion aerosols and the transport and deposition of smoke in ventilation system ductwork.

I. Introduction

The development of the FIRAC computer code and the supporting experimental work are being sponsored by the Nuclear Regulatory Commission (NRC). The NRC is responsible for ensuring that nuclear fuel cycle facilities are designed and operated in a safe manner so that the release of radioactive material under both normal and accident conditions will not result in unacceptable radiological effects on the surrounding population and the environment.(1)

The NRC requested the original FIRAC computer code be modified and expanded to include the capabilities of the zone-type compartment fire model FIRIN, which was developed by Battelle Pacific Northwest Laboratories (PNL). The two codes have been coupled to allow an improved simulation of a fire-induced transient within a facility.

The expanded version of FIRAC is designed to predict the radioactive and nonradioactive source terms that lead to gas dynamics, material transport, and heat transfer transients in a nuclear facility when it is subjected to a fire. The code is directed toward nuclear fuel cycle facilities and the primary release pathway--the ventilation system. However, the code is applicable to other facilities and can be used to model other airflow pathways within a structure.

The physical models used in the code may be divided into four principal categories.

- Gas dynamics model
- Material transport models
- Heat transfer models
- FIRIN fire and radioactive source term models

A brief summary of the gas dynamics, convective material transport capabilities, heat transfer capabilities, and FIRIN source term models is presented. Details of the gas dynamics, material transport, and heat transfer capabilities can be found in Reference 2. More information on the FIRIN source terms is provided in Reference 3.

In addition to the FIRIN fire compartment option, the code allows the user to employ any fire compartment model provided that the output of the compartment model is in one of two forms:

- pressure and temperature time histories or
- energy and mass time histories.

An application of the code using the FIRIN source term models to a typical nuclear facility is presented, as is a summary of experiments in two areas that support the development and verification of FIRAC. The two areas of experimental support are: high-efficiency particulate air (HEPA) filter plugging by combustion aerosols and smoke transport and deposition in ventilation system ductwork.

Physical Models

The lumped-parameter method is the basic formulation that describes the airflow system. No spatial distribution of parameters is considered in this approach, but an effect of spatial distribution can be approximated by noding. Network theory, using the lumped-parameter method, includes a number of system elements called branches joined at certain points called nodes. Ventilation system components that exhibit flow resistance and inertia (such as dampers, ducts, valves, and filters) and that exhibit flow potential (such as blowers) are located within the branches of the system.

Nodes are the connection points of branches for components that have finite volumes, such as rooms, gloveboxes, and plenums, and for boundaries where the volume is practically infinite. When the FIRIN source-term models are selected to simulate a fire accident, internal boundary nodes are used to represent the fire compartment within the ventilation network. Even though they are zero-volume nodes within the numerical scheme, the fact that they are coupled to a fire compartment model that accounts for mass and energy balances keeps the computational formulation consistent.

Material Transport Models

The object of the material transport portion of the code is to estimate the movement of material (aerosol or gas) in an interconnected network of ventilation system components representing a given fuel cycle facility. Using this capability, the code can calculate material concentrations and material mass flow rates at any location in the network. Furthermore, the code will perform these transport calculations for various gas-dynamic transients. The code solves the entire network for transient flow and in so doing takes into account system interactions.

A generalized treatment of material transport under fire-induced accident conditions could become very complex. Several different types of materials could be transported. Also, more than one phase could be involved, including solids, liquids, and gases with phase transitions. Chemical reactions could occur during transport, leading to the formation of new species. Further, for each type of material there will be a size distribution that varies with time and position depending on the relative importance of effects such as homogeneous nucleation, coagulation (material interaction), diffusion (both by Brownian motion and by turbulence), and gravitational sedimentation. We know of no codes that can handle transient flow induced material transport in a network system subject to the possibility of all of these complications. The transport portion of the code also does not include this level of generality. However, this version of the code does provide a simple material transport capability.

The material transport components of this code consist of the following.

1. Material characteristics
2. Transport initiation
3. Convective transport
4. Aerosol depletion
5. Filtration

Material characteristics and transport initiation are areas that must be considered by the user as he begins to set up the code to solve a given problem. Calculations of convective transport, aerosol depletion, and filtration are performed automatically by the code. Items 2--5 are actually separate subroutines or modules within the code. Item 3, convective transport, is a key subroutine that calls on items 2, 4, and 5 as needed during the course of the calculation. We also will specify the required user specifications and provide appropriate references for the theory in each case.

Duct Heat Transfer

The purpose of the duct heat transfer model is to predict how the combustion gas in the system heats up or cools down as it flows throughout the ducts in the ventilating system. The model predicts the temperature of the gas leaving any section of the duct if the inlet temperature and gas properties are known. An ancillary result

of the calculations yields the duct wall temperature. A duct component is the only one for which a heat transfer calculation is performed. Furthermore, the calculation is performed in a given duct only if that branch has been flagged in the user specifications. Experience in using the code has shown that duct heat transfer calculations can increase the computer running time by a factor of 2. Therefore, we advise that duct heat transfer calculations be performed only where needed. The main region of interest and concern is generally those ducts downstream from the fire compartment and especially between the fire compartment and any filters downstream from the fire compartment.

The overall model is composed of five distinct sub-models of heat transfer processes along with a numerical solution procedure to evaluate them. The heat transfer processes modeled are the following.

- Forced convection heat transfer between the combustion gas and the inside duct walls.
- Radiation heat transfer between the combustion gas and inside duct walls
- Heat conduction through the duct wall
- Natural convection heat transfer from the outside duct walls to the surroundings
- Radiation heat transfer from the outside duct walls to the atmosphere

FIRIN Fire and Radioactive Source Term Simulation

Accidental fire-generated radioactive and nonradioactive source terms for nuclear facilities are estimated in the FIRIN module of the FIRAC code. FIRIN uses a zone-type compartment fire model. A zone-type fire compartment assumes that the gas in the room is divided into two homogeneous regions, or layers, during a fire. One layer (the hot layer) develops near the ceiling and contains the hot combustion products released from the burning material. The cold layer, which is located between the hot layer and the floor, contains fresh air. FIRIN predicts the fire source mass loss rate, energy generation rate, and fire room conditions (temperatures of the two layers and room pressure) as a function of time. It also calculates the mass generation rate and particle size distributions for radioactive and nonradioactive particles that can become airborne for a given fire accident scenario. The radioactive release factors incorporated within the FIRIN module are primarily those developed in experimental work at PNL, and the combustion product data were developed from a literature search of combustibles that commonly are found in nuclear facilities. More information on the fire and radioactive source term models and FIRIN code assumptions is available in Reference 3.

Fire Accident Analysis Example

Description and Computer Model of the Facility. This example calculation will illustrate how the improved fire code can be applied to a complex facility as shown in Figure 1. This facility is representative of most nuclear fuel cycle ventilation systems in that it contains multiple fans, compartments, dampers, filter systems, and parallel/series flow configurations. The facility model features 39 branches, 24 nodes [19 capacitance (room) nodes, 2 standard boundary nodes, and 3 internal boundary nodes], 2 blowers, and 9 filters. For this calculation, the FIRIN fire compartment model is used to characterize the nonradioactive and radioactive source terms resulting from the fire. Within the facility ventilation network, internal boundary nodes 9, 21, and 22 represent the fire compartment. (A closeup of the fire compartment noding is shown in Figure 2.) The inlet and outlet branches (connections) to the fire compartment have been positioned so that the ventilation flow direction is downward in the room. That is, the inlet is located near the ceiling, and the outlet is near the floor.

The fire compartment is assumed to be 39 ft (12 m) long, 39 ft (12 m) wide, and 20 ft (6 m) high. The centerline elevation (measured from the floor) of the two inlet vents is 18.74 ft (5.71 m), and the elevation of the outlet vent is 3.0 ft (0.9 m). Also, the fire compartment is assumed to have a concrete floor, ceiling, and walls. The ceiling and floor are assumed to be 1.0 ft (0.3 m) thick; the walls are assumed to be 0.5 ft (0.2 m) thick.

When the system is operating under steady-state conditions, the fire compartment has a pressure of -0.30 in. w.g. (-0.76 cm w.g.) at a temperature of 70°F (21°C). The two inlet vents (branches 16 and 17) supply 3250 ft^3/min (1.534 m^3/s) and 300 ft^3/min (0.141 m^3/s) of air to the compartment. The outlet ventilator exhausts 3550 ft^3/min (1.675 m^3/s) under steady-state conditions. The fire compartment exhaust filter (branch 14) is assumed to be 50% efficient and have a plugging factor of 10.0 1/kg. A low fire compartment exhaust filter efficiency was selected to illustrate the transport of particulate material to the facility exhaust filter and the potential for deposition of material in the two ducts (branches 38 and 39) located downstream of the fire compartment (Figure 2).

Fire Accident Scenario

In defining an accident scenario, the combustible materials susceptible to ignition and the radioactive materials at risk must be identified. For a compartment fire, typical combustible materials are elastomers (neoprene gloves), cellulosic materials (rags, paper, wood), flammable and combustible liquids (solvents and hydraulic oil), and plastic (polymethylmethacrylate and polyvinyl chloride). The materials at risk could include contaminated noncombustible surfaces, contaminated combustible liquids and solids, and open containers of divided powders or liquids. After the amount and type of

REPRESENTATIVE FACILITY

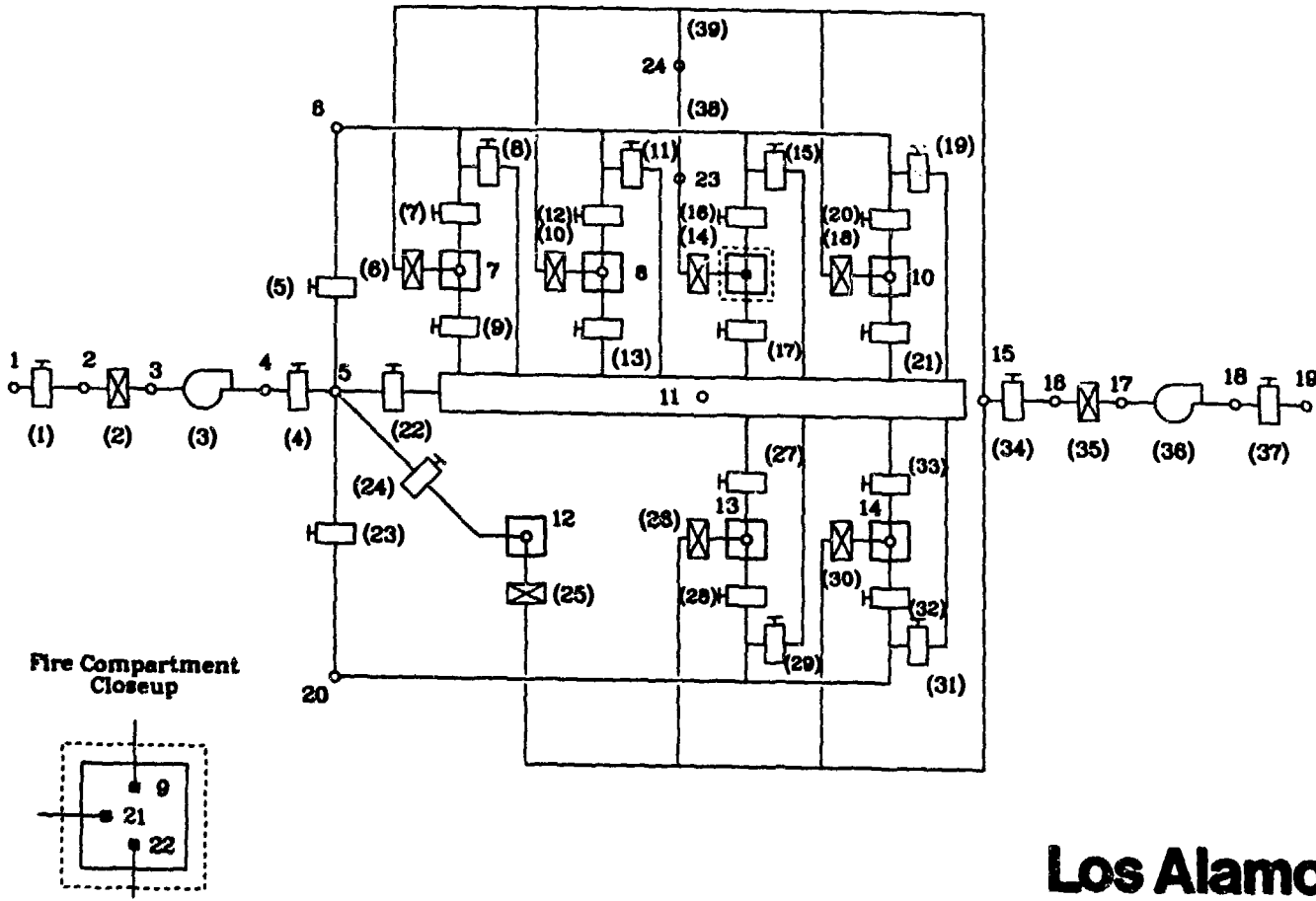

Figure 1. Representative facility ventilation system schematic.

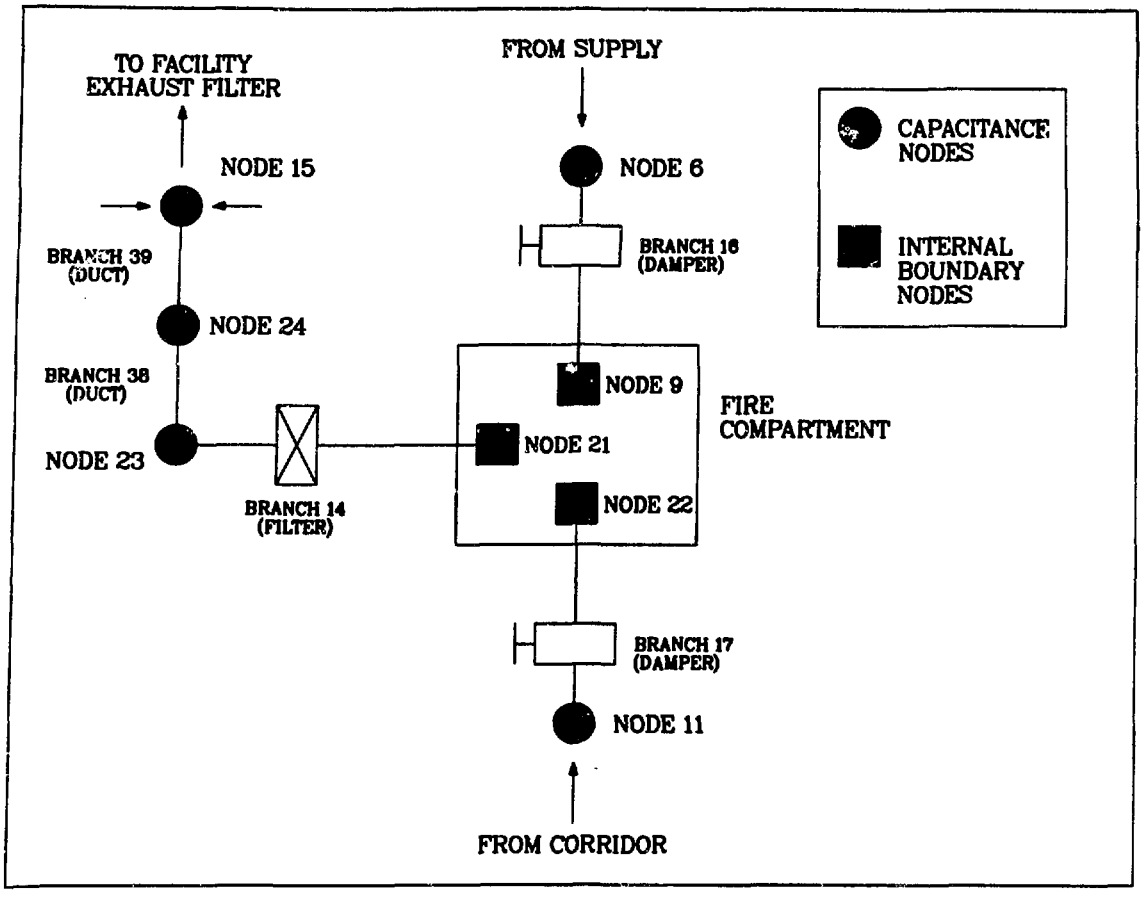

Figure 2. Closeup system schematic near the fire compartment.

combustibles and at-risk radioactive materials have been identified, the fire growth sequence (the order in which the combustible materials are assumed to burn) can be formulated. It is recognized that fire accidents most probably occur under abnormal operating conditions (spilled combustibles or improper use of solvents) or from unanticipated events (failed electrical equipment or faulty processing equipment).

For the sample calculation two combustibles are assumed to be at risk within the fire compartment: a container of flammable solvent (kerosene) and several pairs of rubber (polychloroprene) gloves. The fire begins after the solvent container overturns and is accidentally ignited. The rubber gloves are assumed to be located near the overturned solvent. As the solvent burns, the gloves are gradually heated and ignite as the solvent stops burning. The spilled solvent is assumed to have an exposed surface (burn) area of 5.0 ft^2 (0.5 m^2) and an initial mass of 3.0 lbm (1.4 kg). The rubber gloves are assumed to have an exposed surface area of 4.0 ft^2 (1.8 m^2) and an initial mass of 8.1 lbm (3.6 kg). The FIRIN sequential burning option was used to achieve the fire growth sequence described above.

Two mechanisms for the release of radioactive material located within the fire compartment are used in the example calculation: the release of material associated with the heating of contaminated surfaces and of material associated with the burning of a contaminated combustible solid. The fire compartment floor and walls are assumed to be contaminated with 0.165 lbm (0.075 kg) of mixed oxide powder. In addition to the fixed surface contamination, the combustible polychloroprene gloves are contaminated with 0.033 lbm (0.015 kg) of mixed oxide powder. The radioactive particulate release rates for the single nonradioactive (smoke generation rate) and the two radioactive release mechanisms are calculated within the FIRIN module.

Calculative Results

The sequence of events for the example calculation is presented in Table 1. The kerosene ignition initiates the accident sequence 2 s into the simulation. The fire compartment (represented by nodes 9, 21, and 22 in the system model) rapidly pressurizes from its steady-state operating value of -0.30 in. w.g. (-0.76 cm w.g.) to approximately 0.55 in. w.g. (1.40 cm w.g.) because of the rapid volumetric expansion of the compartment gases caused by the fire. Figure 3 shows the fire compartment pressure response for the entire transient. As a result of the pressure increase in the compartment, a reduction in flow at the intakes (branches 16 and 17) and an increase in flow at the compartment exhaust (branch 14) is calculated by FIRAC. Volumetric flow rate results for the fire compartment are presented in Figure 4.

Between 2 s and 175 s, the hot layer gradually expands and descends toward the outflow ventilator (Figure 5). As the outflow ventilator begins to exhaust the hot combustion products/gases composing the hot layer, the fire compartment begins to depressurize

Table 1. Transient event sequence for example calculation.

Event	Time (s)
Kerosene ignites	2
Maximum system temperature (150°F) attained	5
Hot layer descends to centerline elevation of inflow boundaries	15
Hot layer descends to centerline elevation of outflow boundary	205
Contaminated polychloroprene ignites	275
Radioactive material appears in system	275
Polychloroprene stops burning	350
End of calculation	500

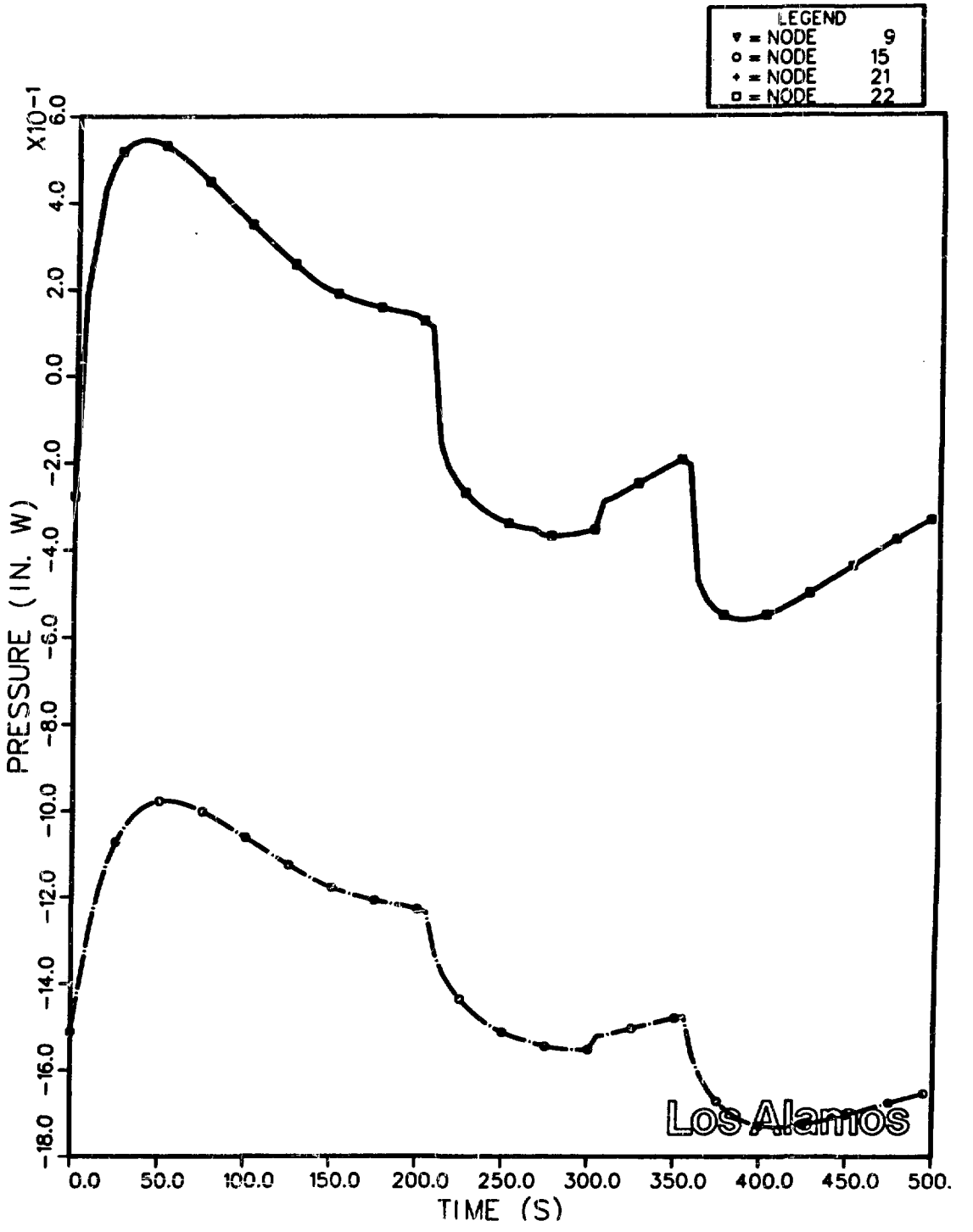

Figure 3. Calculated pressure response for nodes 9, 15, 21, and 22.

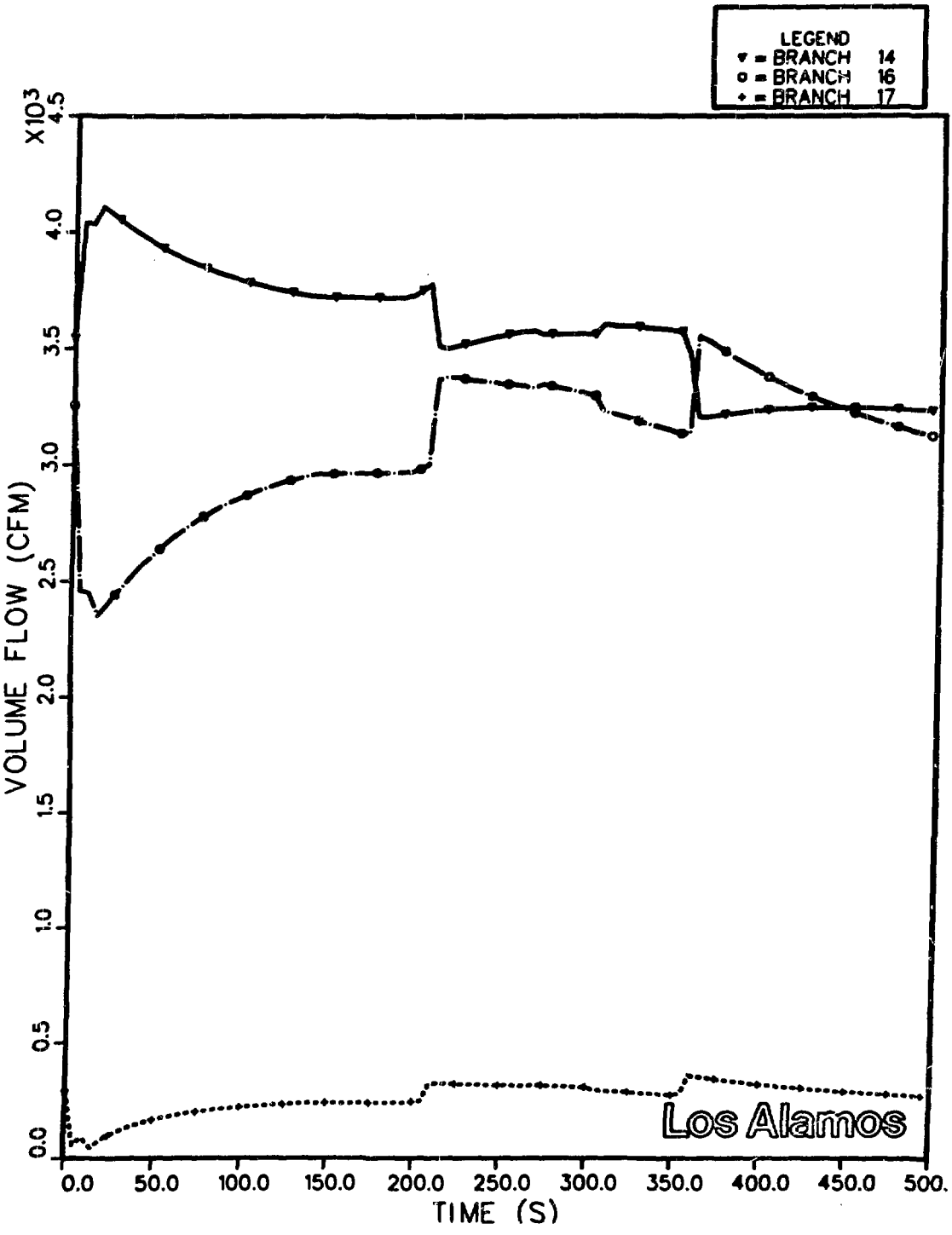

Figure 4. Calculated for compartment volumetric flow rates (branches 14, 16, and 17).

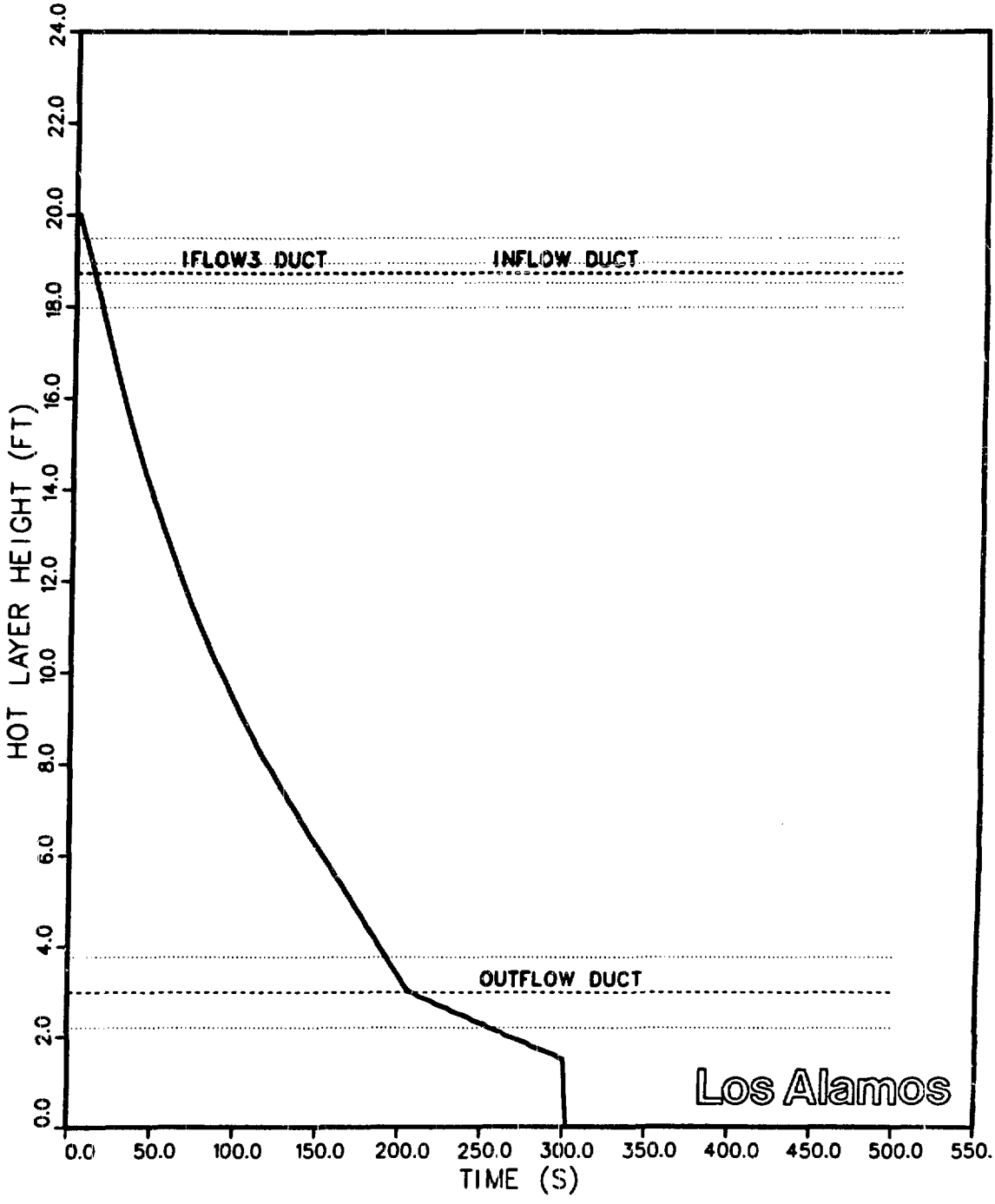

Figure 5. Calculated hot layer height versus time.

slightly. The volumetric and mass flows at the intakes to the compartment are enhanced by the depressurization. The compartment exhaust flow rate decreased because of the depressurization and the presence of the hot (less dense) combustion gases at the outflow ventilator. The temperature history for the fire compartment is shown in Figure 6.

The system is perturbed again as the kerosene fire terminates and the contaminated polychloroprene ignites via the sequential burning option. The ignition of the polychloroprene repressurizes the fire compartment to -0.2 in. w.g. (-0.5 cm w.g.) by 350 s. The flow rates to the compartment are affected by the repressurization: the exhaust flow (branch 14) is enhanced and flow at the intakes (branches 16 and 17) is reduced. As the polychloroprene burns, the compartment becomes more filled with smoke particulates because burning polystyrene releases a larger amount of smoke particulate than does burning kerosene.

The production of smoke at a faster rate within the compartment begins to deplete the amount of oxygen available to the fire. The fire compartment oxygen concentration never dropped below 20% because the polychloroprene burned for only a short time (90 s). By 355 s, all the combustible materials within the compartment have been consumed and the system begins to recover from the fire-induced transient.

Even though the filter plugging option was used in the calculation, the fire compartment exhaust filter does not plug and therefore does not influence the system response to the fire. The low fire compartment filter efficiency (50%) prevents the filter from collecting enough mass to plug. However, the low efficiency value does allow smoke and radioactive material to be transported to the facility exhaust filter (branch 35). Figures 7 and 8 show the mass accumulations for the smoke and total radioactive particulates on the fire compartment exhaust filter (branch 14), the two ducts located between the compartment exhaust filter, the facility exhaust filter (branches 38 and 39), and the facility exhaust filter (branch 35).

The primary release mechanism for radioactive material is the burning of a contaminated combustible solid (polychloroprene). The releases associated with the heating of a contaminated surface are simulated in this calculation but are not evident in the mass accumulation results (Figure 8). Once the hot layer has descended to the outflow elevation, material released as a result of the contaminated surface being heated is convected through the system. The release rates for the contaminated surface mechanism are several orders of magnitude less than the release rates for the burning contaminated combustible. Significant quantities of radioactive material are not transported until the polychloroprene ignites at 275 s. The polychloroprene is assumed to ignite after the kerosene pool fire has ended.

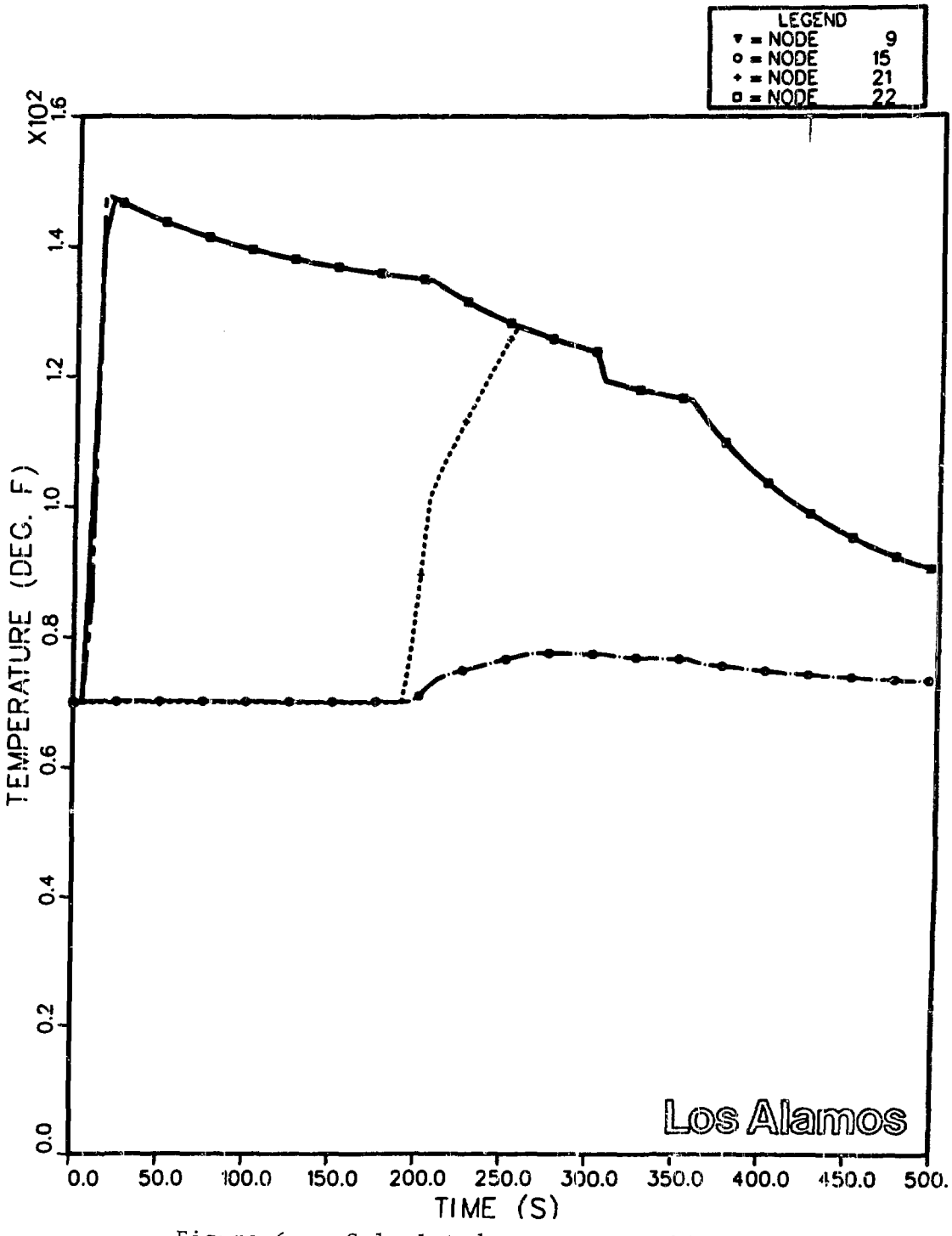

Figure 6. Calculated temperature history for nodes 9, 15, 21, and 22.

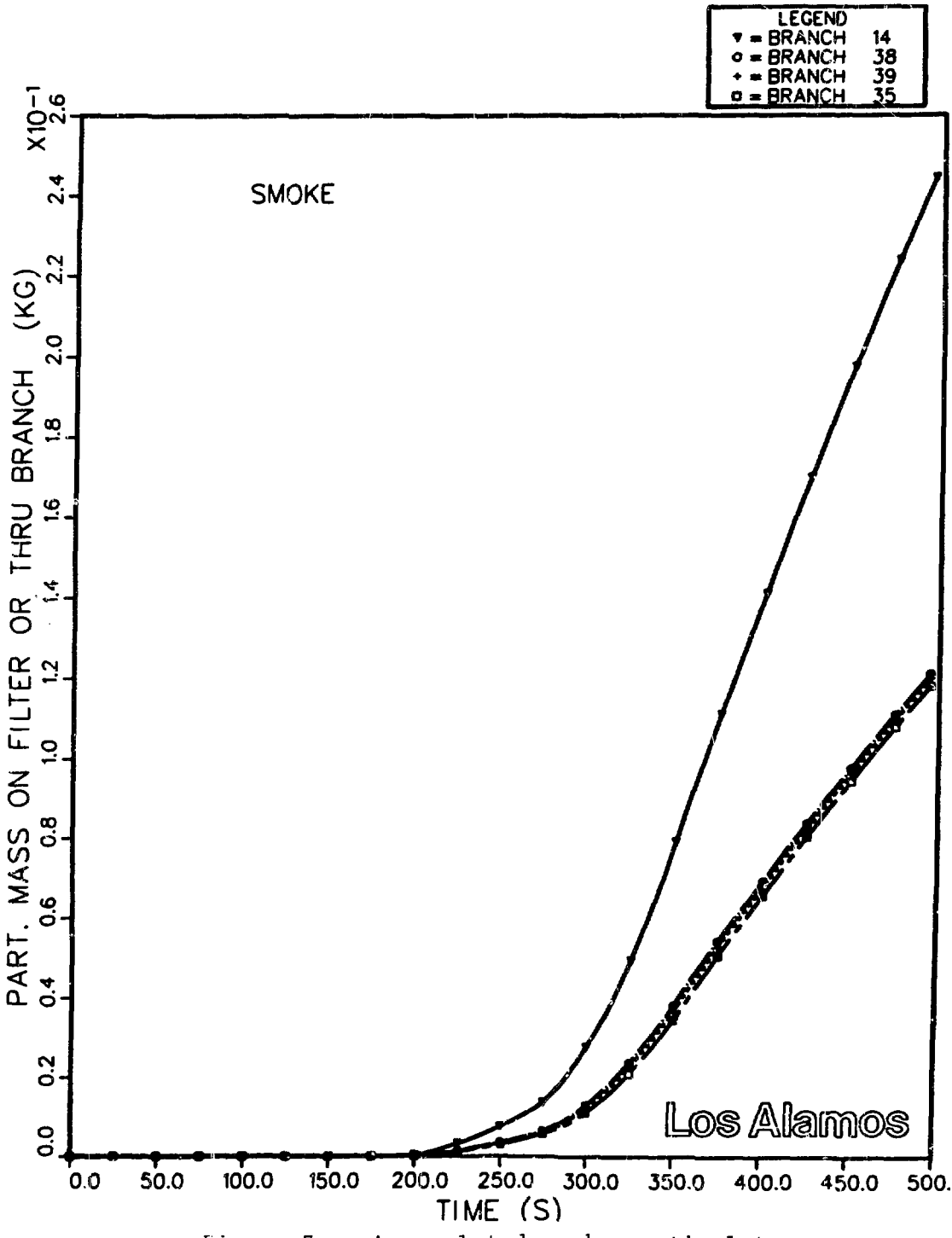

Figure 7. Accumulated smoke particulate mass for branches 14, 38, 39, and 35.

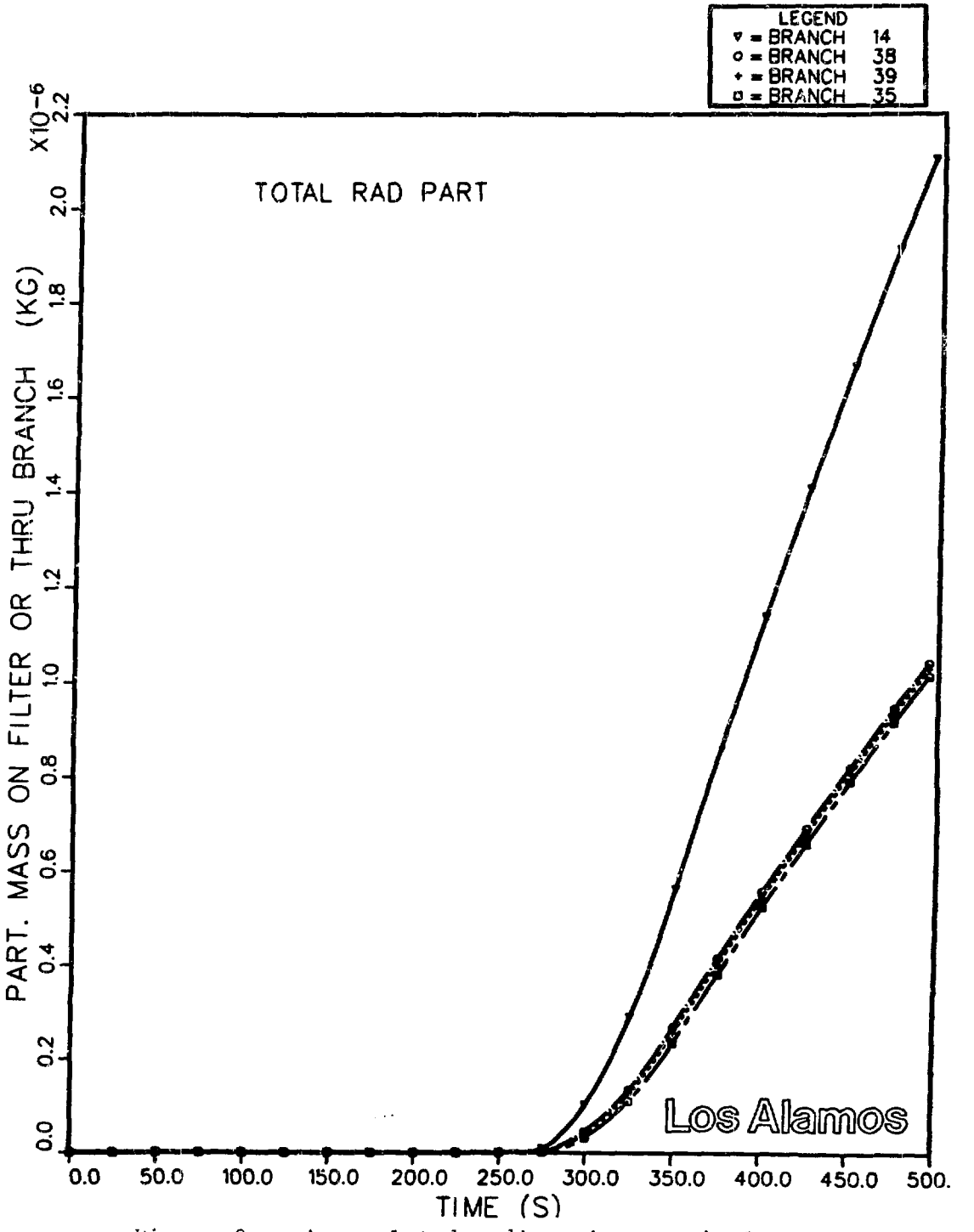

Figure 8. Accumulated radioactive particulate mass for branches 14, 38, 39, and 35.

Following the termination of the fire (350 s), the smoke and radioactive particulate flow rates begin to decrease as the particulate concentrations in the hot layer decrease and as the compartment exhaust flow rate decreases. The system gradually will reestablish the steady-state operating conditions.

An important result of any fire-induced transient is the calculated gas temperatures at various locations in the system. The temperature values are useful in assessing the damage to system components, especially HEPA filters. The temperature variation from the fire compartment to the facility exhaust is shown in Figure 9. As the warm gases are convected to the facility exhaust, convection and radiation heat losses occur in the duct components (branches 38 and 39). As a result of the heat losses, a decrease in gas temperature with increasing distance from the fire compartment is calculated.

Summary

The example calculation illustrated how the improved FIRAC code can be used to simulate a fire within a facility. Also, implementation of the FIRIN complex sequential burning option, the release of radioactive material by burning a contaminated combustible solid and the heating of a contaminated surface, the transport of smoke and radioactive particulates, and the internal boundary nodes representing the fire compartment were demonstrated. The example calculation also indicates how complicated the interpretation of the calculated results can become when several user options are enabled.

II. Full-scale Measurements of HEPA Filter Plugging and Particulate Deposition by Combustion Products

This section of the paper summarizes the results of experiments in two areas that were conducted by Los Alamos and New Mexico State University. The areas are (1) HEPA filter plugging by combustion aerosols[4] and (2) smoke transport and deposition in ventilation system ductwork.[5] In both cases, the work was part of Los Alamos' efforts to obtain experimental data to support FIRAC computer code development and verification.[1],[2],[6-8] A specialized facility was constructed to supply the needed experimental data.

Test Facility and Fuels

The test facility[9,10] was designed to supply experimental data for 0.61- by 0.61-m HEPA filters under conditions simulating those postulated as credible for fires in nuclear facilities. Industrial fires such as these are expected to differ from other kinds of fires in the types of materials involved and the ventilation conditions (availability of oxygen). A typical fuel mixture may be composed of the materials listed in Table 2.[7] These materials are likely to burn under both oxygen-rich and oxygen-starved conditions (over- and under-ventilated conditions) to produce particulate material, water vapor, and gaseous combustion products.

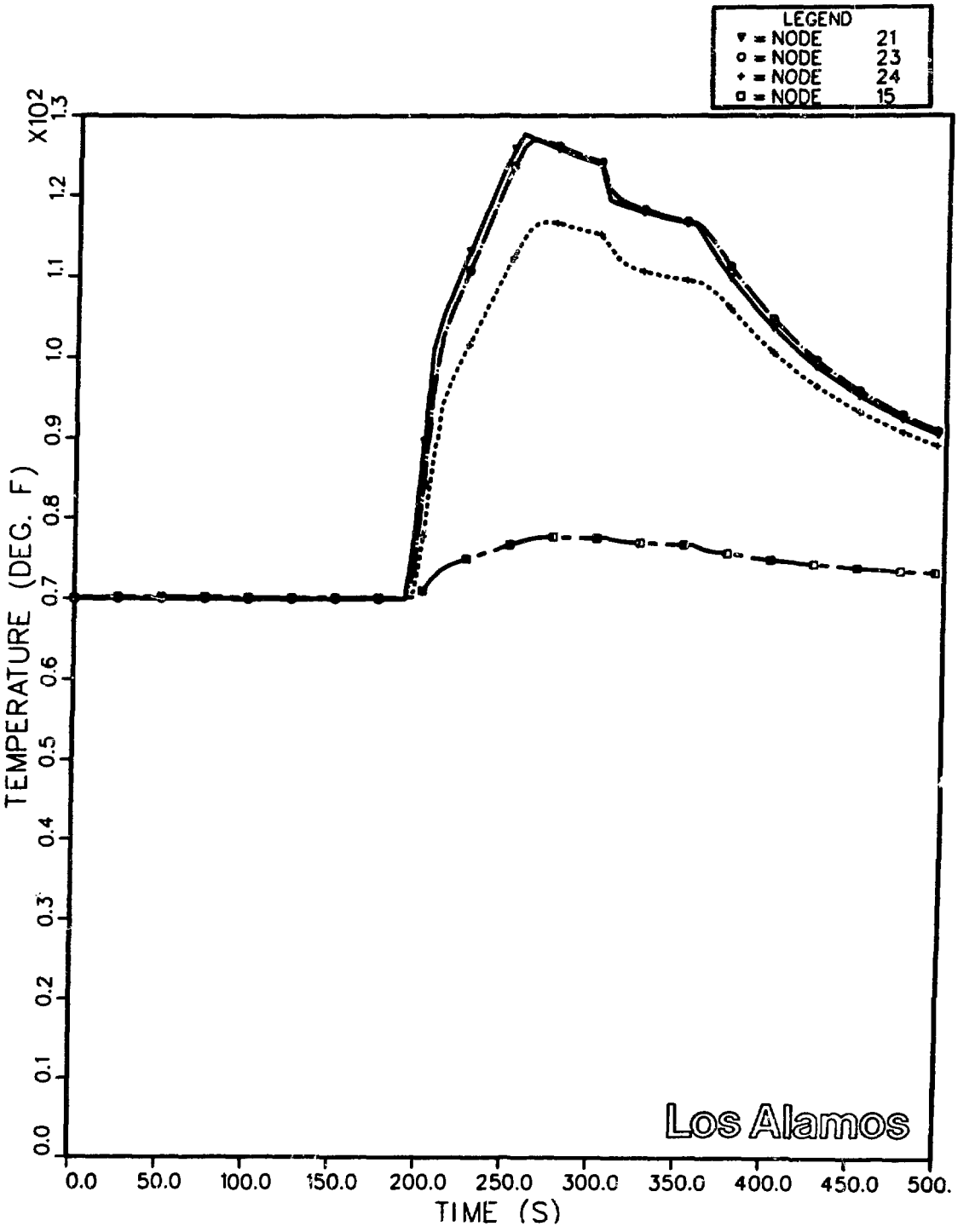

Figure 9. Calculated temperature history for nodes 21, 23, 24, and 15.

Table 2. Typical fuel mixture composition.

	Component	Composition (%)
1.	Polymethylmethacrylate	45
2.	Cellulosic	26
3.	Elastomer	18
4.	Polyvinyl Chloride	8
5.	Hydraulic Fluids	2
6.	Polystyrene	1

Some unique capabilities were required of the test facility. First, we needed the capability to burn fuels or mixtures of fuels listed in Table 2. Two pure materials were selected from Table 2, polystyrene (PS) and polymethylmethacrylate (PMMA). Although PS is not found in large proportions in nuclear fuel cycle facilities (PMMA is), it is the most severe smoke producer in Table 2. On the other hand, PMMA is known to produce relatively low quantities of smoke in comparison with the amount of mass burned. Hence, by selecting these two fuels we attempted to bracket the extremes of smoke generation--the mass fraction of solid or liquid fuel that converts to smoke--expected in plants. For liquid PS and PMMA burned at over-ventilated conditions, Tewarson[11] experimentally measured smoke mass fractions ($Y_S = m_s/m_b$) and got 0.33 and 0.021, respectively, where both the soot and low vapor pressure liquids are included in the aerosolized combustion products or "smoke." The quantities m_s and m_b are mass of smoke produced and mass of fuel burned, respectively.

To burn the fuels and control the burning efficiency, a special combustor was designed and manufactured for use in these studies by PNL.[12] The two mass burning rates were achieved by controlling the inlet air supply rate. Each burning rate was repeated two times. The repetitions were used to assess the reproducibility of the test results.

To obtain the filter plugging data,[4] we needed the capability to determine the accumulated mass gain of a clean 14-kg HEPA filter because of smoke and moisture clogging. Previous tests using polystryrene latex spheres led us to expect plugging (arbitrarily defined to be a 50% reduction in flow rate from the design value) to occur from an accumulation of under 500 g of dry solid material. We designed and constructed a special null-balance filter-weighing apparatus to resolve 2- to 3-g smoke accumulations out of 14 kg for a clean filter.

To obtain the deposition data,[5] the burn products had to be introduced into as long a duct as practical to enhance deposition and aerosol concentration changes for better resolution. We also needed to simulate rapid diffusion (mixing) of the smoke plume to make an upstream, centerline smoke concentration measurement. Finally, we needed special experimental apparatus suitable for making surface measurements of total aerosol mass deposition.

The facility described in References 9 and 10 was modified to facilitate the current experiments. The major modifications included

1. coupling to the combustion chamber,
2. the design and installation of a biplanar grid of round tubes to promote turbulent mixing,
3. the construction of a metal hot duct,
4. adding extra ductwork to bring the test section length for deposition up to about 45.6 ft (13.9 m), and
5. installation of specially designed nuclepore filter holders to collect deposition samples.

Instrumentation

Appropriate instrumentation was set up and calibrated to obtain measurements of the following.(4),(5)

1. Ambient pressure and temperature
2. Average or bulk volumetric airflow rate in the duct
3. Air temperature at four locations
4 Relative humidity
5. Fuel mass burning rate
6. Filter pressure drop
7. Filter incremental weight gain
8. Smoke mass concentration using two cascade impactors at two locations on the duct centerline [downstream of the mixing grid and 45.6 ft (13.9 m) further downstream]
9. Smoke size distribution using the same eight-stage cascade impactors to obtain the mass median aerodynamic diameter and geometric standard deviation (for a log-normally distributed aerosol)
10. Total mass deposition at one downstream location but on three surfaces (ceiling, one side wall, and floor) at the 45.6-ft (13.9-m) downstream mass concentration measurement location (See Item 6.)

Combustion Product Characterization

The characterization of the combustion products included only particulate constituents.(4),(5) The particulate combustion products were not monitored continuously, but rather intermittent samples were taken and analyzed.

Particulate mass concentrations (milligrams per cubic meter) were determined with Anderson Mark III stainless-steel in-stack inertial impactors incorporating straight nozzles. These impactors also measure aerodynamic particle diameter (based on unit density spheres) through seven stages of particle collection and a back-up filter. Pre-impactors for use in conjunction with the impactors were determined to be unnecessary for this application. Real-time particle sizing equipment also was used. The units used were a Royco Model 225 optical aerosol particle counter and a Thermal Systems Model 3030 electrical mobility analyzer. The real-time equipment was less suitable in this experiment because the particle size characteristics and mass concentration varied with the burn time.

Because about 1 min to 3 min of cycling time was required by each particle counter, respectively, the actual aerosol characteristics could not be resolved. In contrast, the inertial impactors were operated in such a manner (nozzle diameter and sampling time) to sample over the entire fuel burn. For this reason, the impactor size data are considered pertinent.

PS and PMMA combustion aerosol particulate size distributions were measured using the cascade impactors. The PS data are shown in Figure 10; this figure indicates that, for the high and low mass burning rates, the particle size distribution is nearly the same for particles less than 2.0μm. However, for particles greater than 2.0μm in diameter, there is a significantly greater relative number of particles at the higher burning rate compared with the lower burning rate. Also, the aerodynamic mean particle diameter varies from about 1.5 to 2.5 μm.

The change in particle size with transport along the 45.6-ft (13.9-m) length can be observed in Figure 10. With the exception of the larger (greater than 2.0μm) particles, no clear shift in size distribution occurs. However, with these PS particles, the upstream size distribution by aerodynamic diameter relative to the corresponding downstream data of the same test suggests an average particle size reduction of about 1 μm.

The volumes of soot particles generated by the burner for the two fuels were measured using the Royco counter. The main features observed were large variations of soot particle output rates and variations from burn to burn under the same conditions. Peak volumetric output rates for the PS and PMMA fuels varied by more than an order of magnitude. Similar particle size data for PMMA are presented in Reference 5. These data show that the mass median aerodynamic diameter of PMMA was significantly smaller than that of PS--about 0.7 to 1.0 μm.

HEPA Filter Plugging by Combustion Aerosols

The experimental results reported here represent a continuation of work reported at the 17th DOE Nuclear Air Cleaning Conference.(1),(8)

Exposing a HEPA filter to heat and smoke significantly alters its operating characteristics.(2),(6),(8),(13),(14) This investigation focused on the characteristics that relate to filter plugging or to the increase in pressure drop across a filter as a result of the collection of particulate material on the filtration media. Such information is required to better understand how filters are plugged with combustion-generated aerosols, and it will improve our FIRAC-based estimates of ventilation system response to compartment fires.

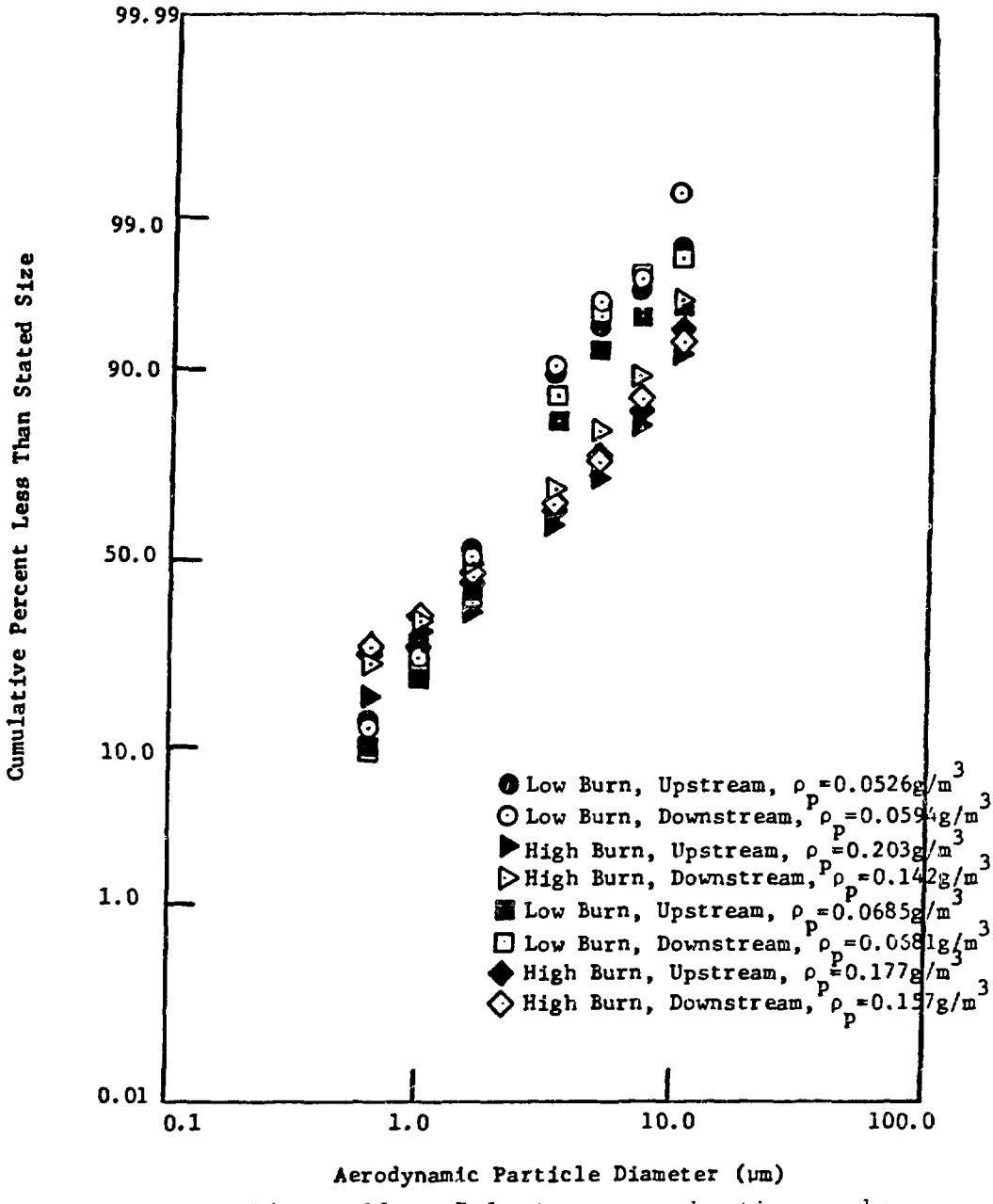

Figure 10. Polystryene combustion smoke particle size distribution.

Specific questions about the problem we investigated included the following.

1. What is the correlation between accumulated combustion particulate mass on the HEPA filter and flow resistance across the filter?
2. What is the effect of the soot fraction (as manifested by fuel type) on HEPA filter plugging?
3. What is the effect of fuel mass burning rate on HEPA filter plugging?
4. What is the penetration of the aerosols within the filtration medium?
5. Does the HEPA filter upstream faceguard influence HEPA filter plugging?
6. Does the mechanism causing plugging vary from fuel to fuel?

Table 3 summarizes conditions associated with combustion of the filter plugging test fuels. Results for both fuels are given in Table 4. These data are the result of burning many cups of fuel in each case, and thus the mass burning rates are average values. The HEPA filters tested with PS had protective metal face screens (1-cm by 1-cm mesh size) with the exception of filters numbered 6 and 7. The HEPA filters tested with PMMA all had the metal screens removed.

The details of the plugging process for each filter are shown in Figure 11. The actual resistance, R or W, is normalized by the initial clean filter resistance. The data shown the influence of the PS mass burning rate on the quantity of the particulate material collected that is necessary for plugging. From Figure 11, the importance of the protective screen on HEPA filter plugging can be seen to be negligible. Similar data for PMMA are presented in Reference 4.

Rather than trying to construct any realistic physical mechanism for the cause of plugging, we propose a phenomenological approach as follows.[2],[4],[6]

$$\frac{W}{W_o} = F\,(M_p) \quad ,$$

where $W = \Delta p/Q$ is the resistance coefficient. W_o is the value of W for a clean filter, Δp is pressure differential, and Q is volumetric flow rate. F is a monotonically increasing functon of M_p, which is the total mass of particulate accumulated on the filter and is the relative resistance. To satisfy the clean filter requirement, we must have

$$F\,(M_p = 0) = 1.$$

Table 3. Test fuel combustion conditions.

Fuel	Chemical Formula	Combustion Efficiency	Stoichiometric Airflow Rate (m^3/h)	Ratio of Actual to Stoichiometric Airflow Rates	Comments
PS (granular)	CH	0.6	7.4	0.23	Low Burn Rate, Underventilated
				0.93	High Burn Rate, Underventilated
PMMA	$CH_{1.60_{0.4}}$	0.9	4.0	0.85	Low Burn Rate, Underventilated
				2.1	High Burn Rate, Overventilated

Table 4. Summary of combustion products plugging of HEPA filters.

Fuel	Test No.	Clean Static Pressure Drop (cm w.g.)	Apparent Mass Burning Rate (g/min)	Total Particulate Mass Collected at Plugging* (g)
PS	1	2.1	19.4 (high)	527
PS	2	2.1	21.3 (high)	432
PS	3	2.1	15.4 (low)	1256
PS	4	2.0	21.7 (high)	405
PS	5	2.1	17.5 (low)	1207
PS	6	2.1	22.9 (high)	432
PS	7	2.1	21.3 (high)	391
PMMA	8	2.2	11.6 (high)	233
PMMA	9	2.2	12.4 (low)	257
PMMA	10	2.2	15.6 (high)	186
PMMA	11	2.2	13.4 (low)	309

*The HEPA filter resistance ratio has a value of 12.0 for each filter.

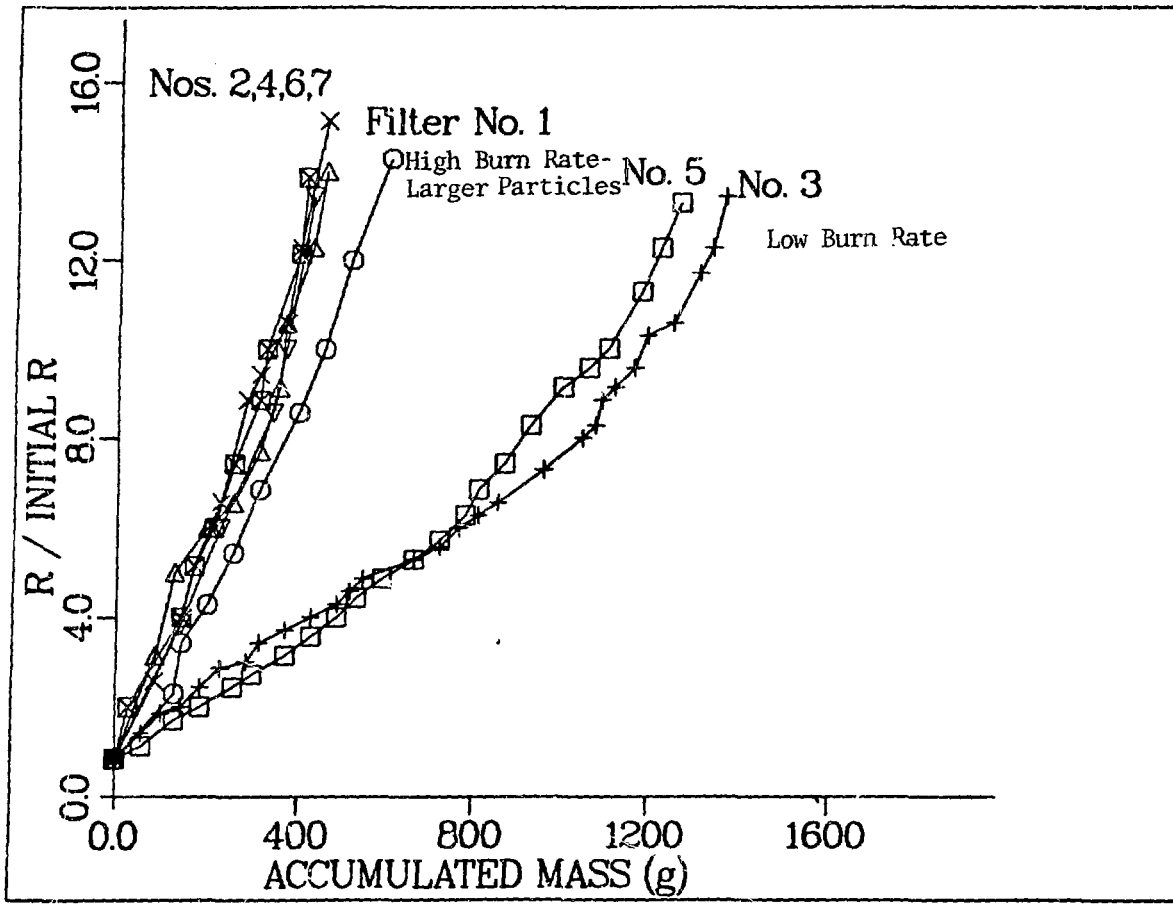

Figure 11. Variation of resistance ratio with accumulated mass for polystyrene combustion.

We believe the following expression should be adequate for all practical purposes.

$$F = 1 + \alpha M_p + \beta M_p^2 \quad ,$$

where α and β are two coefficients determined by experimentation. Their evaluation from data such as that shown in Figure 11 forms the basis of the filter plugging test program.

Table 5 shows the values for α and β obtained by curve-fitting techniques for the combustion conditions tested. The resistance ratio is observed to be a strong function of the linear term in M_p--the β values are relatively small. The filter plugging coefficients given in Table 5 can be used in the input data deck of the Los Alamos fire accident analysis computer code FIRAC. An equation for F(Mp) in the code allows the user to simulate an infinite range of plugging conditions depending on the values of α and β input.

Table 5. Compilation of HEPA filter resistance ratio.

Fuel	Combustion Condition	FUNCTION* COEFFICIENTS α	β
PS	High O_2 (Underventilated)	0.022248	0.64249×10^{-6}
PS	Low O_2 (Underventilated)	0.0057105	0.17108×10^{-5}
PMMA	Underventilated	0.0476796	-0.30826×10^{-4}
PMMA	Overventilated	0.0641064	-0.57276×10^{-4}

*The HEPA filter resistance ratio has a value of 12.0 for each filter.

Particle size data were used in Reference 4 to explain the variation in PS combustion particulate mass necessary to plug the HEPA filters. In Reference 4, we showed that the particles greater than 2.0 μm in diameter dominate the plugging of the filter. Particles less than 2.0 μm apparently penetrate the filter medium and contribute to the mass of collected particulate material but contribute little to increase the static pressure drop across the filter. Removal of the HEPA filters from the test apparatus supports this speculation because the upstream face had a thick "mat" of fragile particulate material that tended to fall off the filter even when disturbed by the most careful handling.

Tentative qualitative conclusions can be made regarding the plugging characteristics involving particulate mass concentration and accumulated particulate mass on the filter.

- Normalized HEPA filter flow resistance can be correlated with the accumulated mass gain on the filter for a given combustion aerosol (PS and PMMA). When the combustion conditions change (fuel and/or oxygen availability), the HEPA filter plugging characteristics change and are explained with the particulate mass concentration for particles greater than 2.0 μm.
- For these PS and PMMA tests, the lower the fuel soot fraction, the smaller the accumulated mass gain on the HEPA filter required for plugging. This results from the physical characteristics of the particulate material--mass concentration and particle size. Evidently, for PS and PMMA, a different physical mechanism was responsible for the plugging.

Smoke Transport and Deposition in Ventilation System Ductwork

Although intuition might suggest that aerosol losses because of deposition are insignificant, a previous study has indicated that such losses can be appreciable in mass percentage. Qualitative cascade impactor measurements in the duct downstream of the full-sized compartment fire test facility at Lawrence Livermore National Laboratory (LLNL) have indicated that as much as 60% of combustion product aerosol mass can be removed by deposition in a relatively short (about 32-ft-long) duct.[13] In case of a fire in a nuclear facility, the presence of combustion products poses a threat to the

HEPA filters.(1),(2),(6),(7),(8),(13),(14) A reduction in smoke concentration because of deposition can delay filter plugging. Because deposition is size dependent,[6] it also can modify the size distribution function of the smoke challenging the filters.

Further, for fuel cycle facilities under fire accident conditions, the smoke (solid and liquid aerosol) could be contaminated with radioactive material. In this case it becomes important to know where hazardous material is deposited within the plant ventilation system. A reduction in airborne material concentrations will reduce the quantity of radioactive material accumulating on the HEPA filters and passing through them. We are particularly interestesd in the location and concentration of radioactive material in the respirable size range, namely, about 0 to 15 μm. This time- and location-dependent concentration will be continually changing because of deposition and material interaction (coagulation).

For these reasons there is a need to check (under realistic conditions) the accuracy of deposition equations available in the literature. Some of these idealized deposition equations currently are being used to compute unsteady material depletion in FIRAC and other Los Alamos accident analysis computer codes.[2,6] However, at this stage of computer code development, we have relatively little confidence in the predictions of deposition losses for combustion aerosols.

In this study we performed smoke transport and deposition tests under realistic conditions using real combustion products (particulate and gaseous, including water vapor) in full-sized ducts at typical airflow rates. We are unaware of adequate data of this kind in the available literature.[5] With such depletion/modification data we can help answer three questions for realistic fire conditions.

1. How important is deposition; that is, how much material accumulates on the walls?
2. How much change in smoke characteristics (concentration and size distribution) can occur over reasonable duct lengths?
3. Are our idealized equations from the literature giving us reasonable, and preferably conservative, quantitative estimates of deposition?

Table 6 summarizes the numerical data obtained during the duct wall deposition tests. In these tests, the accumulated particulate mass on the HEPA filters and actual particulate mass deposits at the duct wall were measured in addition to the physical characteristics of the airborne particles as already described. The values reported for the duct volumetric flow rate are arithmetic averages of the flow at the initiation and conclusion of each test.

The particulate mass concentration data, in conjunction with the mass burning rate given in Table 6, imply an important feature associated with PS combustion. This feature is that the total particulate mass concentration measured near the HEPA filter is proportional

to the mass burning rate. This is established by ratioing the average high burning rate to the average low burning rate and obtaining the value of 2.0. Calculating the corresponding ratio for average total particulate mass concentrations gives 2.3. The correspondence (deviation from mean less than 7%) implies a constant soot fraction for underventilated conditions.

The effect of the 45.6-ft (13.9-m) transport length on duct centerline particulate mass concentration is summarized in Table 7. The

Table 6. Duct wall deposition experimental data.

Fuel Type	Burn Condition	Fuel Mass Burned (g)	Total Time Time (min)	Fuel Mass Burn Rate, $\dot{m}_b$ (g/min)	Volumetric Duct Air Flow Rate, Q(m^3/h)
PS	1.7 m^3/hr Combustion Air Low Burn Rate, Underventilated	200.7	21.9	9.16	1642
PS	1.7 m^3/hr Combustion Air Low Burn Rate, Underventilated	250.0	29.7	8.96	1470
PS	6.8 m^3/hr Combustion Air High Burn Rate, Underventilated	250.0	14.35	17.42	1589
PS	6.8 m^3/hr Combustion Air High Burn Rate, Underventilated	250.3	13.60	18.40	1439
PMMA	3.4 m^3/hr Combustion Air Low Burn Rate, Underventilated	600.5	50.1	12.0	1607
PMMA	3.4 m^3/hr Combustion Air Low Burn Rate, Underventilated	600.0	52.4	11.48	1448
PMMA	8.5 m^3/hr Combustion Air High Burn Rate, Overventilated	1000.3	81.9	12.26	1700
PMMA	8.5 m^3/hr Combustion Air High Burn Rate, Overventilated	1000.0	85.6	11.70	1530

Table 6. (Cont.)

Fuel Type	Burn Condition	Upstream Impactor Conc. (g/m^3)	Downsteam Impactor Conc. (g/m^3)	Accumulated HEPA Mass Gain (g)	Wall Nuclepore Filter Mass Deposit (mg) Top	Side	Botton
PS	1.7 m^3/h Combustion Air Low Burn Rate, Underventilated	0.0526	0.0594	14.76	0.2	0.2	1.1
PS	1.7 m^3/h Combustion Air Low Burn Rate, Underventilated	0.0685	0.0681	32.3	0.1	0.1	0.8
PS	6.8 m^3/h Combustion Air High Burn Rate, Underventilated	0.2027	0.1415	71.02	0.02	0.3	1.5
PS	6.8 m^3/h Combustion Air High Burn Rate, Underventilated	0.1765	0.1566	65.0	0.2	0.4	1.4
PMMA	3.4 m^3/h Combustion Air Low Burn Rate, Underventilated	0.0154	0.0150	22.9	0.1	0.1	0.4
PMMA	3.4 m^3/h Combustion Air Low Burn Rate, Underventilated	0.0202	0.0157	13.0	0.0	0.1	0.4
PMMA	8.5 m^3//h Combustion Air High Burn Rate, Overventilated	0.0045	0.0038	5.43	0.1	0.1	0.4
PMMA	8.5 m^3/h Combustion Air High Burn Rate, Overventilated	0.0051	0.0048	5.64	0.0	0.1	0.3

Table 7. Variation of particulate mass concentration by transport*.

Fuel	Combustion Condition	$\left(\frac{\rho_p}{\rho_{po}}\right)_{exp.}$	$\left(\frac{\rho_p}{\rho_{po}}\right)_{theo.}$
PS	high	0.70	0.81
PS	high	0.89	0.89
PS	low	1.13	0.83
PS	low	0.99	0.84
PMMA	overventilated	0.84	0.89
PMMA	overventilated	0.94	0.75
PMMA	underventilated	0.97	0.75
PMMA	underventilated	0.78	0.86

* Duct length (from impactor to impactor) was 13.9 m.

last two columns give calculations of ρ_p/ρ_{po}, the particulate mass concentration ratio at the two impactors, for the experiments and the theory based only on gravitational settling. Note that the averages of each of the four conditions are predicted by the theory with an error of less than 10% (based on averages) with the exception of the PS low burning rate condition where the experimental result should be rejected.

Experimental deposition results have been compared with predictions with gravitational settling theory (currently being used in FIRAC) in Table 8. The important operational conditions are given to identify each test. Under the columns labeled "Experimental Data," the experimental results alone are presented where the final result is a particulate mass ratio, m_d/m_b. This ratio is the mass deposited on duct walls divided by the initial mass of unburned fuel. The mass deposited on the walls, m_d, is given by

$$m_d = Y_s m_b - m_f,$$

where m_f is the accumulated particulate mass on the HEPA filter for the fuel burned. The ratio m_d/m_b identifies that portion of the fuel mass that was deposited on the walls. The m_d calculations assume a constant value for Y_s (0.33 for PS and 0.021 for PMMA) regardless of the burning condition. This mass-balance calculation for m_d using data from Reference 11 for Y_s did not resolve wall mass deposition for the underventilated PMMA burn rate.

Table 8. Experimental deposition results compared to gravitational settling theory predictions.

Fuel Type	Burn Condition	Fuel Mass Burned, m_b(g)	$m_p J_p$ $\left(\frac{gm}{m^2\ h}\right)$	U_{ps} $\left(\frac{m}{h}\right)$	ρ_{poc} $\left(\frac{g}{m^3}\right)$	Accumulated HEPA Mass Gain, m_f(g)
PS	Low	200.7	2.66	44.8	1.10×10^{-1}	14.8
PS	Low	250.0	1.43	21.0	1.21×10^{-1}	32.3
PS	High	250.0	5.53	39.1	2.17×10^{-1}	71.0
PS	High	250.3	5.44	34.7	2.53×10^{-1}	65.0
PMMA	Low	600.5	0.422	28.1	9.42×10^{-3}	22.9
PMMA	Low	600.0	0.808	51.5	9.96×10^{-3}	13.0
PMMA	High	1000.3	0.258	67.9	9.06×10^{-3}	5.43
PMMA	High	1000.0	0.185	38.5	9.66×10^{-3}	5.66

Table 8. (Cont).

		Gravitational Settling Theory				Experimental Data		
Fuel Type	Burn Condition	m_{dg}	$\frac{m_{dg}}{m_b}$	Total Mass Accounted (g)	Apparent Soot Fraction Y_{sa}	$m_b Y_s$	$m_d = Y_a m_b - m_f$	$\frac{m_d}{m_b}$
PS	Low	17.8	0.0887	32.6	0.16	66.2	51.4	0.256
PS	Low	13.4	0.0536	45.7	0.18	82.5	50.2	0.201
PS	High	20.4	0.0816	91.4	0.37	82.5	11.5	0.046
PS	High	20.0	0.0799	85.0	0.34	82.6	17.6	0.070
PMMA	Low	2.31	0.0385	25.2	0.042	12.6	-10.3	----
PMMA	Low	4.24	0.0707	17.2	0.029	12.6	-0.4	----
PMMA	High	7.76	0.0776	13.2	0.013	21.0	15.6	0.0156
PMMA	High	5.31	0.00531	11.0	0.011	21.0	15.4	0.0154

Comparing the predicted and experimental PS combustion aerosol deposition quantities in Table 7 suggests that, within a factor of 2 or 3, the values of m_{dg}/m_b agree. This level of agreement weakly supports the gravitational settling theory. In addition, the calculated or apparent PS soot fraction, Y_{sa}, is within 12% of the 0.33 value at the high burn rate. This confirms Y_s for the PS fuel at these conditions. For the low burn rate conditions, the Y_{sa} values are significantly lower than the assumed Y_s value of 0.33. With the PMMA tests, comparisons can be made only for the overventilated combustion condition (m_d is negative for the underventilated condition). Again, the mass ratios and soot fractions agree to a factor of 3 or less. However, the consistency of Y_{sa} data suggests that Y_s is indeed different for the two conditions--by a factor of at least 2 for these experiments.

Gravitational settling is accompanied by other deposition mechanisms in a horizontal duct and includes turbulent and Brownian diffusion, inertial impaction, and electrostatic effects. For the horizontal straight duct used in these experiments, inertial and electrostatic effects were not significant. Considerations of other deposition mechanisms, including calculations and comparisons with the data obtained in the current study, have been made elsewhere.[2,5-7]

The deposition rates predicted by theory are not fully supported by the experimental data. Two reasons for this are the preliminary, and thus relatively crude, nature of the particle deposition experiments and the simplistic theoretical model used in FIRAC at present. Further, because the mean particle diameters determined by the impactors are much too small, the gravitational settling theory currently used by FIRAC is not conservative, but rather significantly underpredicts the actual particulate mass deposition rates of the combustion aerosols tested. Successful particle deposition studies where theory and experimental results are mutually supportive will require improved theoretical developments incorporating additional deposition mechanisms and improved experimental techniques and procedures.

The conclusions developed from this experimental work involving deposition of combustion products of PS and PMMA fuel are as follows.

1. Particulate mass deposition is an important feature associated with the flow of combustion products and, even for short duct lengths (31 hydraulic diameters), may reach 25% of the unburned fuel as with PS.

2. Physical changes associated with the transport of the particulate combustion products include a 10 to 30% reduction in mass concentration and a small (~1μm) reduction in particle size only observable for the PS combustion particles with an aerodynamic diameter greater than 2.0 μm.

3. Comparisons of the experimental results with the theory incorporating gravitational settling provide some preliminary checks.

4. The experimental techniques used in this effort are not sufficiently sensitive to verify the deposition models described.

Because HEPA filter plugging rates and efficiencies are dependent on the airborne particulate mass and size distributions arriving at the filter, deposition is an important consideration. The experimental work performed here establishes some support for the theory developed and used by FIRAC. However, improved experiments directed at the deposition problem alone are required to establish the important deposition mechanisms that should be included in the FIRAC code.

REFERENCES

1. R. W. Andrae, J. W. Bolstad, W. S. Gregory, F. R. Krause, R. A. Martin, P. K. Tang, M. Y. Ballinger, M. K. W. Chang, J. A. Glissmeyer, P. C. Owczarski, J. Mishima, S. L. Sutter, E. L. Compere, H. W. Godbee, and S. Bernstein, "Methods for Nuclear Air Cleaning System Accident Consequence Assessment," Proc. 17th DOE, Nuclear Air Cleaning Conference, Denver, Colorado, August 2--5, 1982.

2. R. W. Andrae, J. W. Bolstad, M. Burkett, W. S. Gregory, R. A. Martin, and P. K. Tang, "FIRAC Users Manual - A Computer Code for Analysis of Fire-induced Flow and Material Transport in Nuclear Facilities," Los Alamos National Laboratory report in preparation.

3. M. K.Chan, M. Y. Ballinger, P. C. Owczarski, and S. L. Sutter, "User's Manual for FIRIN1: A Computer Code to Characterize Accidental Fire and Radioactive Source Terms in Nuclear Fuel Cycle Facilities," Battelle Pacific Northwest Laboratory report PNL-4532 NUREG/CR-3037, (December 1982).

4. D. L. Fenton, M. V. Gunaji, W. S. Gregory, and R. A. Martin, "Investigation of High-efficiency Particulate Air Filter Plugging by Combustion Aerosols," Los Alamos National Laboratory report in preparation.

5. R. A. Martin and D. L. Fenton, "Full-scale Measurements of Smoke Transport and Deposition in Ventilation System Ductwork," Los Alamos National Laboratory report in preparation.

6. R. A. Martin, P. K. Tang, A. P. Harper, J. D. Novat, and W. S. Gregory, "Material Transport Analysis for Accident-induced Flow in Nuclear Facilities," Los Alamos National Laboratory report LA-9913-MS, NUREG/CR-3527 (October 1983).

7. "Fuel Cycle Facility Accident Analysis Handbook," Los Alamos National Laboratory report LA-9180M, NUREG/CR-2508, PNL-4149 in preparation.

8. W. S. Gregory, R. A. Martin, P. R. Smith, and D. L. Fenton, "Response of HEPA Filters to Simulated Accident Conditions," Proc. of the 17th DOE Nuclear Air Cleaning Conference, Denver, Colorado, August 2--5, 1982.

9. D. L. Fenton, J. J. Dallman, P. R. Smith, R. A. Martin, and W. S. Gregory, "The Los Alamos National Laboratory/New Mexico State University Filter Plugging Test Facility--Description and Preliminary Test Results," Los Alamos National Laboratory report LA-9929-MS, NUREG/CR-3242 (October 1983).

10. J. J. Dallman, "HEPA Filter Loading by Simulated Combustion Products," Masters Thesis submitted to Mechanical Engineering Department, New Mexcio State University (Las Cruces, New Mexico, 1982).

11. A. Tewarson, "Physico-Chemical and Combustion Pyrolysis Properties of Polymeric Materials," Factory Mutual Research Corp. Technical Report FMRC J. I. OEON6.RC/RC80-T-79 (November 1980).

12. M. K. W. Chan, "Testing and Calibration Results of the Filex Smoke Generators," Pacific Northwest Laboratory draft report (March 30, 1982).

13. N. Alvares, D. Beason, W. Bergman, J. Creighton, H. Ford, and A. Lipska, "Fire Protection Countermeasures for Containment Ventilation," Lawrence Livermore National Laboratory progress report UCID-18781 (September 1980).

14. W. Bergman, H. Hebard, R. Taylor, and B. Lum, "Electrostatic Filters Generated by Electric Fields," Lawrence Livermore National Laboratory paper UCRL-81926 (July 1979), submitted to Second World Filtration Congress (London, September 18--20, 1979).

DISCUSSION

BERGMAN: I think I have one agreement with your presentation, where there is smoke there is fire. But I think that is about the limit of it. I would like to point out that some of the assumptions of the code, namely, the mass generation rates, the size distribution of the aerosol, are critical to any prediction and this is something that no one, either in this country or in Russia, has yet developed a capability to predict. This is one of the difficult scientific technical problems. That is for a general comment. Now for a specific comment on HEPA filter plugging, you say the larger particles, normalized for mass, plug at a faster rate than the smaller particles. It is well known that it is the opposite way, and I just want to point out there are some discrepancies. There is a theory, that I developed about 7 years ago, that is consistent with the other plugging rate theories as a function of particle size. Not to bring all bad comments, this problem of HEPA filter plugging with smoke aerosols is just astonishingly difficult. I don't say it as a negative comment on your paper, but artifacts are extremely easy to create in fire, especially a dense smoke aerosol fire. So I am not discounting your measurements, but what I am saying is, you are not dealing with 2-3 μm diameter aerosols; they are 0.1 μm. I think what you are seeing is a highly dense aerosol, rapidly agglomerating, under-ventilated. You can, for example, have a net ratio of excess oxygen, but the critical parameters are those where the aerosol is forming, and this may be extremely fuel rich. I am just bringing this up as a possible suggestion, but I do want to express caution that in this field we are far from being able to predict safety features in nuclear plants. I wish it weren't so, but that's the situation.

SMITH, P.P.: One thing I would like to mention is that our compartment fire model is predicting the size distribution of both the smoke particles and the radioactive materials. In the case of the smoke particles, the data are based on Factory Mutual studies. I know that Pacific Northwest Laboratory is doing extensive studies right now to look at burning in under-ventilated conditions. I refer you to their data. I agree with much of what was said. I think the data that are in the code are the best available. I am not sure that you can find anything better in terms of the distribution of radioactive material as a source term. Otherwise, I appreciate your comments and the difficulty of the overall problem.

THE MATHEMATICAL MODELLING OF FIRE IN FORCED VENTILATED ENCLOSURES

G Cox and S Kumar
Fire Research Station
Borehamwood, Hertfordshire, England

Abstract

The paper describes the application of a computer fire simulation model to the prediction of conditions in a forced ventilated experimental fire test cell at the Lawrence Livermore National Laboratory. Comparisons between theoretical and experimental determinations are shown to be in reasonable agreement and areas requiring further research indicated.

I. Introduction

Fire and explosion pose a threat in nuclear plant because of the conflicting requirements of venting the combustion products, the accepted practice in conventional installations, and the need to contain the hazards from ionizing radiation. There is a need to develop a predictive capacity for dealing with these problems in both industrial and nuclear containment buildings. This is perhaps particularly necessary in the confined ventilation systems used in nuclear plant where industrial fire protection experience is used in an area where some of the principles may not be applicable. Such a capacity would not only allow alternative fire protection design strategies to be examined but also may be used in the training of plant operators and fire fighters and perhaps even eventually be used for decision making during the course of a fire.

Mathematical models of fire can be classified as either deterministic or stochastic and within the deterministic grouping divided into two types of model known as the zone and field formulations. Zone models rely on empiricism and experience to assemble and solve a set of equations linking readily identifiable zones of behaviour. Field models attempt to go back to first principles as much as possible and solve the governing equations of motion describing the heat and mass transfer processes within the compartment. Stochastic models, in general, do not specifically address the problem of predicting local fields of the physical variables such as temperature, velocity, pressure etc but concentrate on the probability of occurrence of a particular event or series of events, such as spread of fire from one article to another.

The distinctions between these different model types have been discussed in the nuclear containment context by Cox[1] and Galant[2] and in more general terms by Kumar[3]. Suffice it to say here that the so-called deterministic field models, which are firmly based in the rapidly expanding subject of computational fluid dynamics, a subject much broader than just fire dynamics, are very general in their formulation. They can, in principle, be applied to any configuration with little extra concern as to the validity of this transfer. However, because of the empirical nature of the deterministic zone models this generality cannot be claimed for them.

As an illustration of the different types of enclosure currently being studied with field models, the Fire Research Station is using them to examine fire in domestic rooms, hospital wards, road tunnels and airport terminal buildings, whilst other groups have applied them to fires in aircraft[4] and to the urban mass fire problem (cities)[5].

This paper describes the application of the Fire Research Station's field model known as JASMINE[6,7] to the experimental conditions of the forced ventilated experimental fire test cell at the Lawrence Livermore National Laboratory (LLNL). Experiments in this thoroughly instrumented test cell have been specifically designed to assess the capabilities of mathematical models of fire and so provide an ideal vehicle for model validation.

II. Theoretical model

The physical problem concerns the movement of combustion products in three-dimensional enclosures of arbitrary geometrical complexity. In this problem the flow is dominated by buoyancy and the turbulence serves to promote the rate of diffusion of heat, mass and momentum. Simple combustion and radiation models are included in the calculation procedure and non-uniform buoyancy forces are allowed to affect both the mean flow and the fluctuating motions.

The fluid dynamics

The independent variables of the problem are the three components (x,y,z) of a Cartesian co-ordinate system, and time (t). The main dependent variables characterising the flow are the three velocity components (u,v,w), the pressure p, enthalpy h, the kinetic energy of turbulence k, and the energy dissipation rate ϵ.

All these dependent variables, with the exception of pressure, appear as the subjects of differential equations of the general form

$$\frac{\partial}{\partial t}(\varrho\phi) + \mathrm{div}(\varrho \mathbf{u}\phi + \mathbf{J}_\phi) = S_\phi \qquad (1)$$

where ϕ stands for a generic fluid property and ϱ, $\mathbf{u}$, $\mathbf{J}_\phi$ S_ϕ are density, velocity vector, diffusive-flux vector and source rate per unit volume, respectively.

The diffusive-flux $\mathbf{J}_\phi$ is given by

$$\mathbf{J}_\phi = -\Gamma_\phi \mathrm{grad}\phi \qquad (2)$$

where Γ_ϕ denotes the effective exchange coefficient of ϕ determined from the set of turbulence parameters (k,ϵ), which are themselves dependent variables of differential equations of the form of equation (1). The sources and exchange coefficients for velocities and turbulence quantities have been discussed elsewhere[7] together with the effects of buoyancy[8] and are not repeated here. Pressure is calculated from the pressure correction equation[8] deduced from the mass continuity equation $\phi = 1$.

Combustion

Fires are examples of buoyant turbulent diffusion flames with very low source momentum. The buoyant process gives rise to a large scale irregular motion which governs the rate of mixing of fuel volatiles and air. The rate of reaction of fuel and air is thus controlled by this relatively slow turbulent mixing process and not by the fast reaction kinetics.

In JASMINE a simple one step reactive is used to describe the combustion. Unit mass of fuel combines with the stoichiometric mass requirement, s, of air to give (1+s) mass units of product. Nitrogen is assumed to act only as a diluent and does not take part in the reaction.

The reaction rate, R_{fu}, is taken to be the slowest of the turbulence dissipation rates of either fuel, oxygen or hot product:

$$R_{fu} = -\varrho \frac{\epsilon}{k} \min\left[C_R m_{fu}, C_R \frac{m_{ox}}{s}, C_R' \frac{m_{pr}}{(1+s)}\right] \qquad (3)$$

where m_{fu}, m_{ox}, m_{pr} are the local mass fractions of fuel, oxygen and product and C_R and C_R' are constants given the value 4 and 2 respectively. This is Magnussen and Hjertager's[9] version of Spalding's[10] eddy-break-up model.

Two further transport equations of the form of equation (1) are solved simultaneously with those describing the fluid dynamics. The first is for the fuel mixture fraction, f, where

$$f = \frac{\psi - \psi_\infty}{\psi_o - \psi_\infty} \tag{4}$$

and $\psi = m_{fu} - m_{ox}/s$, m_{ox} is the mass fraction of oxygen and the subscripts o, ∞ denote fuel and ambient air conditions for ψ. No source term is needed in the transport equation for f since it is a conserved scalar. The final transport equation is for the fuel mass fraction m_{fu} where the source term is a linearised version of R_{fu}[7].

After solution of these equations for f and m_{fu}, the mass fractions of oxygen, CO_2, H_2O and unburnt fuel may be readily deduced throughout the compartment as a function of time. In the predictions which follow, any oxidation of the fuel is assumed to go to completion ie no carbon monoxide appears in the product. For the experiments considered (Section III) the fuel was isopropyl alcohol and so the reaction assumed to be simply

$$2C_3H_7OH + 9O_2 \rightarrow 6CO_2 + 8H_2O$$

Boundary conditions

To complete the mathematical analysis, it is necessary to provide boundary conditions. For the LLNL test cell there are two types of boundary: solid or free. On a solid boundary the non-slip condition on the velocity components is employed. The momentum fluxes to the walls obey the wall-function relations of Launder and Spalding[11] and the heat fluxes to the walls are calculated from a fixed heat transfer coefficient. This latter treatment has been found to be a simple way of accounting for both convective and radiative heat losses to boundaries. A more general treatment is currently being developed which uses the wall law treatment but for rough surfaces for the convective component and a radiative contribution is added from a flux model[7]. Heat losses through the compartment walls are calculated from a one dimensional conduction equation given wall conductivity and thickness.

On the free boundary, at the compartment inlet, a fixed pressure boundary condition in imposed. At the outlet, the forced extract duct, a fixed volume flux is prescribed.

Method of solution

The task is now to solve the nine simultaneous non-linear partial differential equations of the form of equation (1) for the variables u, v, w, h, k, ϵ, m_{fu}, f and p subject to the above boundary conditions. Details of the formulation of the finite difference equations from equation (1) and the features of the numerical algorithm are given elsewhere and are not repeated here[6,8,12].

III. Experiment considered

A complete description of the LLNL experimental test cell, measurement equipment and fire tests conducted is given by Alvarez et al[13]. A schematic diagram of the cell is shown in Figure 1. The compartment is 4 m × 6 m in plan and 4.5 high. A rectangular duct 0.65 m square, centres 3.6 m above the floor of the compartment provides forced ventilation by control of an axial fan. High efficiency particulate air (HEPA) filters may be installed in the extract duct to examine clogging by soot deposition. Air inlet is at low level through slots in a cylindrical duct close to one face of the compartment. This has been approximated in the model by one slit 0.12 m high, 2 m long, 0.1 m above the floor.

Fires of different fuels and types have been conducted in this cell with a variety of extraction rates. The case considered here concerns only one of these configurations designated Mod 8 by Alvarez et al. A spray of isopropyl alcohol is formed from an opposed jet nozzel located in the centre of a steel pan of diameter 0.91 m. The ambient fuel is quickly evaporated and burnt before it contacts the pan surface. The resulting fire is very similar to a natural pool fire. The fuel injection rate in Mod 8 was 13.1 grams/sec adjusted to give a heat release rate of 400 kW, assuming efficient combustion. The ventilation extraction rate was adjusted to 500 litres/second of air prior to ignition. The duration of the fire was around 20 minutes.

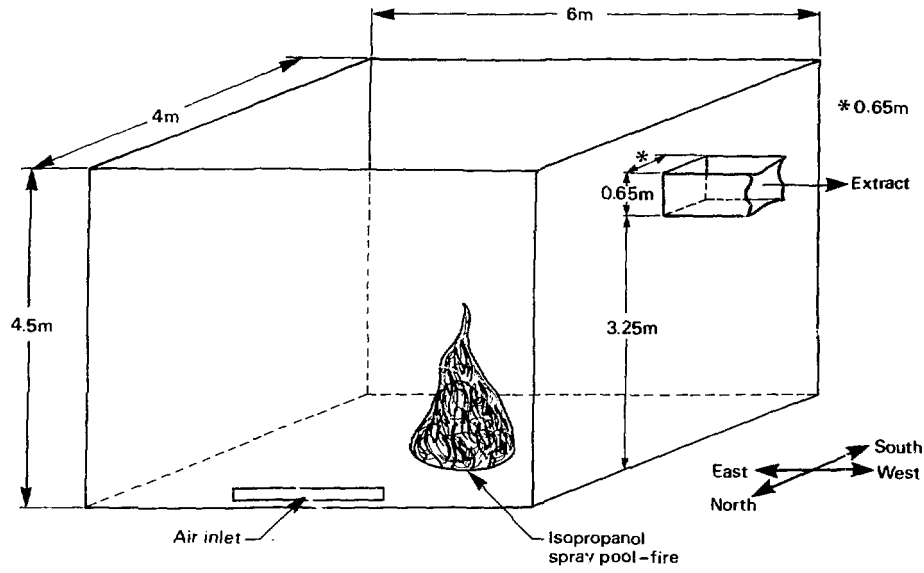

FIGURE 1
SCHEMATIC DIAGRAM OF LAWRENCE LIVERMORE TEST CELL

The walls, floor and ceiling of the compartment consisted of 0.1 m thick Al_2O_3/SiO_2 refractory with estimated thermal properties, thermal conductivity, density and specific heat for the walls of 0.39 W/m°K, 1440 kg/m^3 and 1 kJ/kg°K and for the ceilings and floor 0.63, 1920 and 1 respectively. Alvarez et al suggest a thermal wave penetration of 3 cm into the compartment boundaries during the course of these experiments.

For simplicity the predictions have been made for the steady state and comparisons made with experimental conditions, just before test completion (20 minutes from ignition). This saves computational time. Transient analysis is, of course, quite possible[6]. The air extraction rate had dropped to 400 litres/second at this time and was used in the simulation to prescribe the extract boundary conditions.

IV. Results

One of the difficulties of validating this type of model is the considerable quantity of detailed information predicted and the very difficult task of obtaining enough experimental data to examine the details. Even in such a thoroughly instrumented experimental rig as the LLNL test cell it is only possible to compare predictions and experiments at comparitively few points.

Predictions of velocity vectors are shown on two orthoganol planes in a perspective view of the cell viewed from the east in Figure 2. The two planes are the horizontal, one through the air inlet slot and the vertical one through the centre of the fire tray and extract duct (hereinafter known as the central plane).

The processes of air entrainment into the fire, buoyant vertical acceleration of the plume, formation of a ceiling jet and the establishment of recirculation in the cell are clearly evident. Examination of vectors on vertical planes parallel to that shown here clearly demonstrate a leaning of the fire towards the south wall. A sample streamline is illustrated in Figure 3, starting at the inlet slot and rising three times before finally leaving at the extract duct.

The predictions of temperature, pressure and mass fractions of fuel, oxygen and product on the vertical plane through the centre of fire tray and exit duct are shown in Figures 4 to 8. Inspection of these shows ambient pressure to occur around 0.5 m above the floor with oxygen mass fraction above this height being uniform at between 10% and 11% and product ($3CO_2 + 4H_2O$) concentration at between 16% and 17%. The unburnt fuel mass fraction is everywhere very low except at the source.

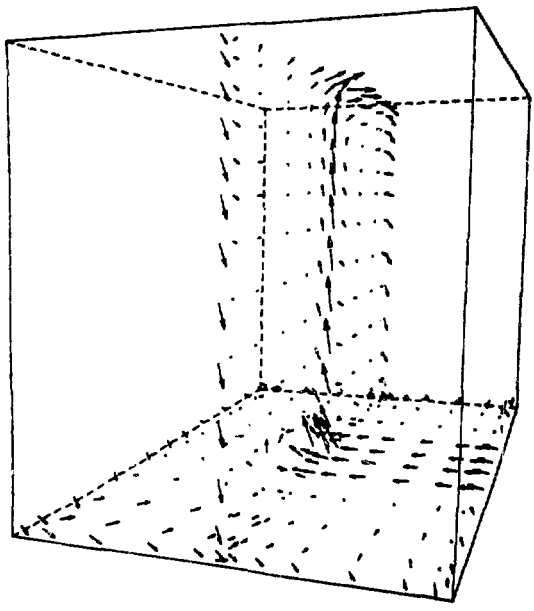

FIGURE 2
VELOCITY VECTORS ON TWO ORTHOGANOL PLANES VIEWED FROM THE EAST

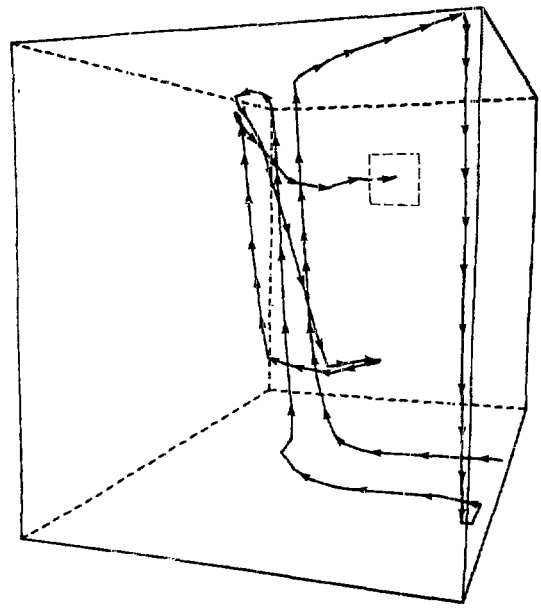

FIGURE 3
SAMPLE STREAMLINE STARTING AT INLET SLOT, VIEWED FROM THE EAST

Gas temperatures in the compartment show a steady increase from floor to ceiling in good agreement with the experiment. Over and within the fire source itself temperatures decay in the expected way but peak values are low compared with experimental determinations (around 1250°K). This results from using a coarse grid. To obtain a more accurate representation of the source itself a much finer grid would be necessary in that part of the calculation domain. Temperatures measured at two vertical thermocouple rakes situated 1.5 m either side of the fire tray on the central plane, and each comprising 15 thermocouples are compared with predictions in Figure 9. Wall surface temperature predictions are compared with measurements on the vertical centreline of the south wall and on the continuation of this line onto the ceiling to its centre (over the fire tray) are compared in Figure 10.

Overall agreement can be seen to be reasonably good, although gas temperatures close to the floor and ceiling are predicted somewhat high. This is almost certainly due to the treatment of heat losses to the boundaries assumed to be prescribed by a fixed heat transfer coefficient of 20 W/m^2°K. The modifications suggested in Section II should improve this aspect of the predictions.

Overall properties and some point determinations are compared in Table 1. In general agreement is seen to be excellent. The difference between computed inlet and outlet mass flow rates corresponds to the 13 grams/sec injection rate of fuel. The gas composition predictions are somewhat disappointing compared with the success of the thermal predictions.

This is not surprising given the simplicity of the combustion model. It is well known that fires exhibit strong combustion intermittency[14] and current research is directed towards more realistic modelling of the turbulence-chemistry interactions[15,16].

The predicted pressure at the level of the extract duct differs markedly from the measurement. The reason for this is not clear but is likely to be caused by the contribution of dynamic pressure to the measurement.

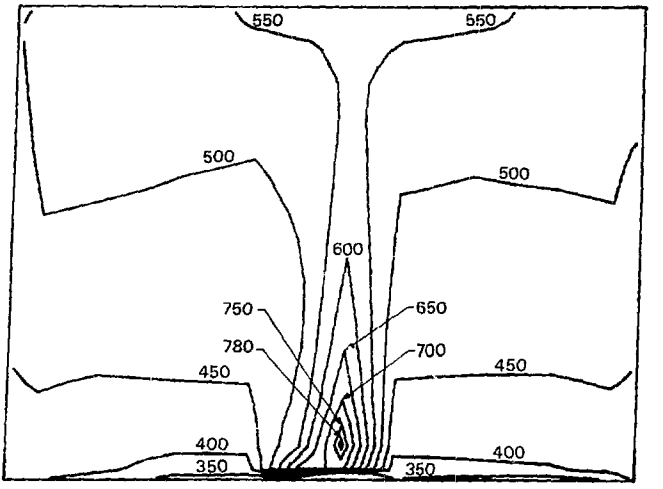

FIGURE 4
ABSOLUTE TEMPERATURE CONTOUR (°K)
ON CENTRAL PLANE

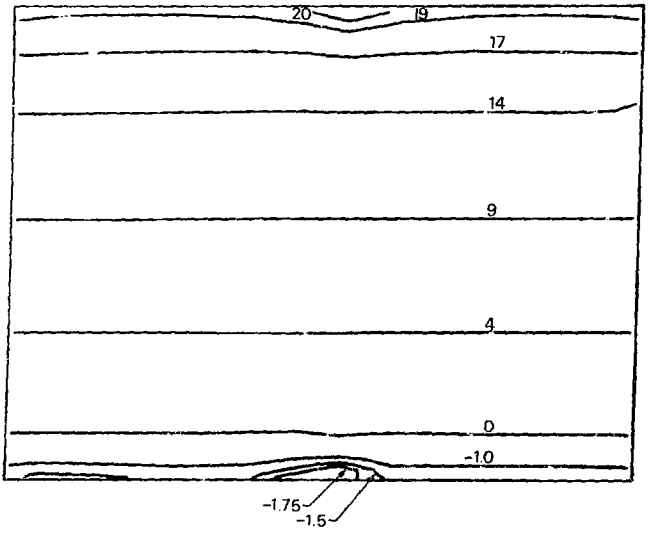

FIGURE 5
PRESSURE CONTOURS (PASCALS) ON
CENTRAL PLANE

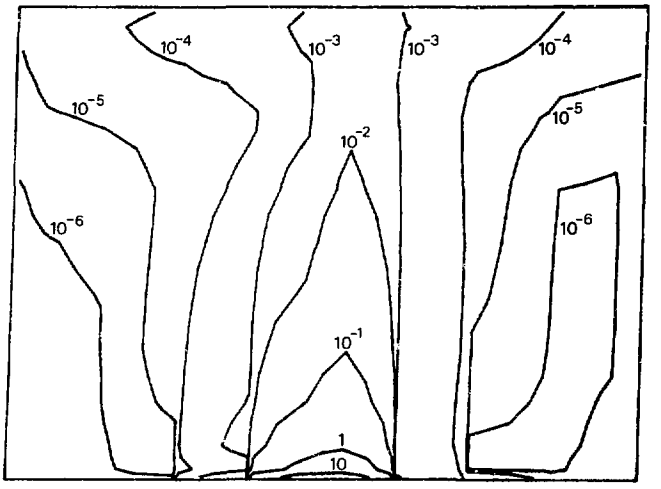

FIGURE 6
PERCENTAGE MASS FRACTION OF FUEL
ON CENTRAL PLANE

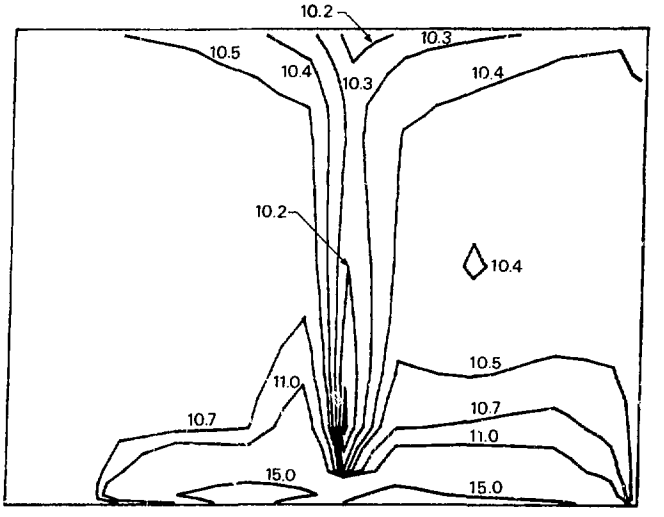

FIGURE 7
PERCENTAGE MASS FRACTION OF OXYGEN
ON CENTRAL PLANE

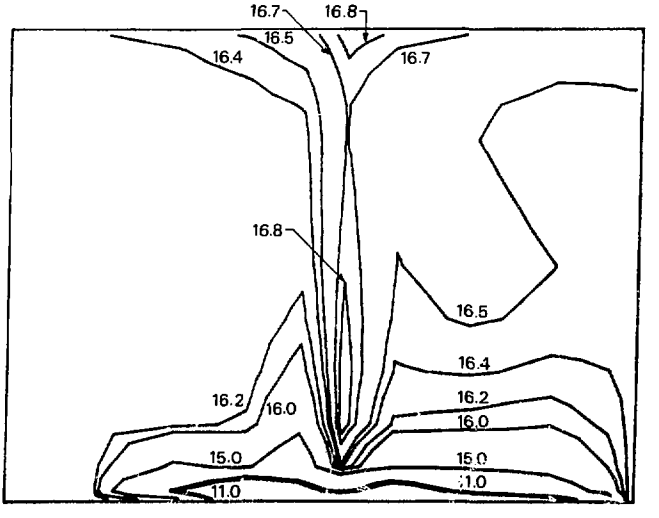

FIGURE 8
PERCENTAGE MASS FRACTION OF
PRODUCT ON CENTRAL PLANE

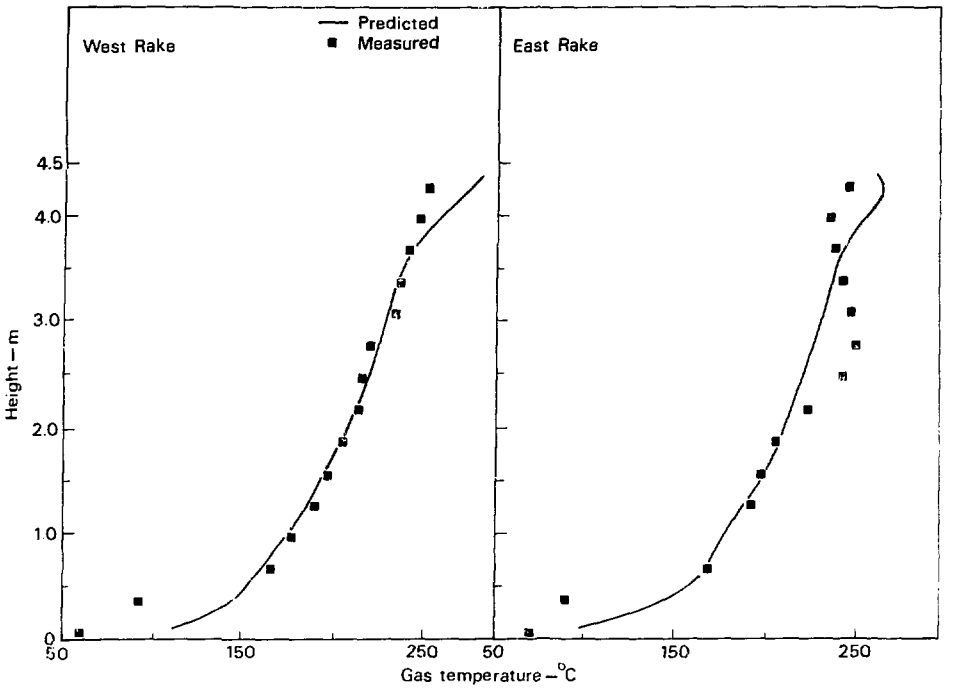

FIGURE 9
GAS TEMPERATURE WITH HEIGHT AT TWO THERMOCOUPLE RAKES

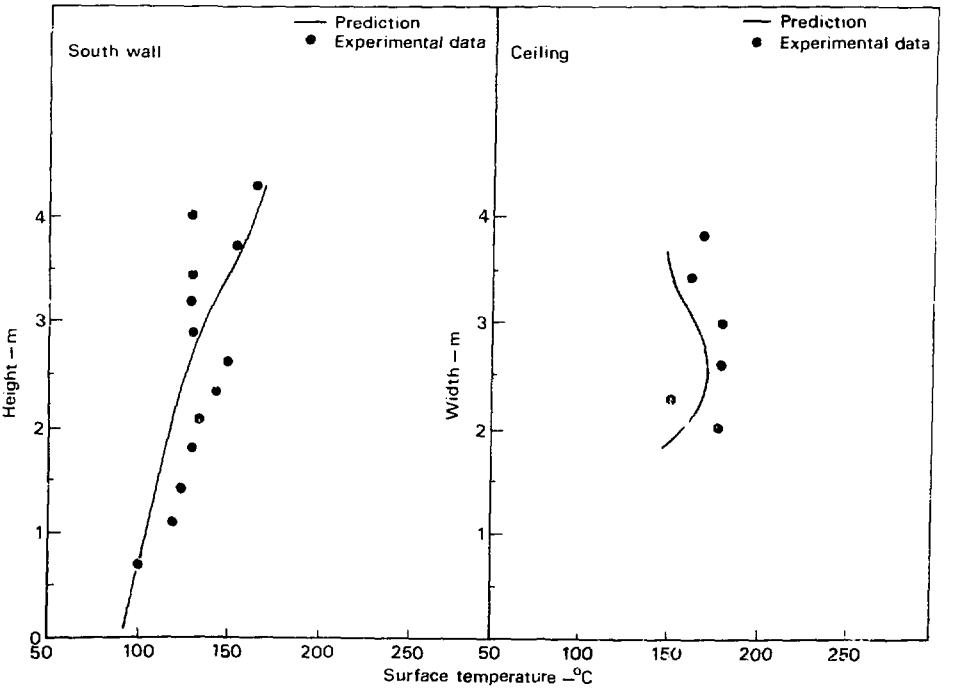

FIGURE 10
SURFACE TEMPERATURE WITH HEIGHT ON SOUTH WALL AND CEILING

Table 1. Comparison of predictions and measurements of integral properties and some point determinations

Property	Predicted	Measured
Mass inflow rate (kg/s)	0.269	0.30
Mass outflow rate (kg/s)	0.257	0.24
Exit gas temperature (°C)	249	275
Exit heat flow (kW)	66	68
Exit pressure above ambient (Pa)	14.3	−5
Exit O_2 concentration (%) (dried gas)	10.4	14
Exit CO_2 concentration (%)(dried gas)	7.5	5.5
Heat loss to boundaries (kW)		
Ceiling	87	—
Floor	62	—
North Wall	55	—
South Wall	57	—
East Wall	37	—
West Wall	36	—
Total	334	332

V. Computational details

The grid used was relatively coarse ($12 \times 14 \times 13$) and some grid refinement checks were made to ($18 \times 20 \times 20$) to ensure insensivity of solutions to the grid. These showed insignificant changes in the results. Execution times on the VAX11/780 amounted to around 450 mins for one thousand sweeps of the calculation domain using the coarse grid, this being typical of the requirement for convergence for a change in conditions from an already converged flow field. More sweeps of the domain are needed to establish the first converged solution from an initial guess.

It should be observed here that grid refinement checks are not sufficient alone to give confidence in the numerical technique. However, experience has shown that this along with reasonable agreement with experimental data does give cause for optimisum. Further studies[17] of various numerical schemes are currently under way to clarify some of these difficulties.

VI. Conclusions

Alvarez et al requested predictions of a fire model of the time evolution of the following physical quantities:

1. Inlet mass flow rate
2. Gas temperatures at exit duct

3. Gas temperatures throughout the room
4. Room surface temperatures
5. Gas concentrations at exit duct
6. Gas concentrations throughout room
7. Radiative and convective heat fluxes to room surfaces
8. Room pressure
9. Mass pyrolysis rate of pool fires
10. Heat release rate of fire

The model described here has given predictions of items 1-8 for the steady state, given the properties 9 and 10 for one particular situation Mod 8. The agreement between predicted and measured values give considerable cause for optimism. It is a straightforward matter to extend this prediction to the transient conditions as has already been demonstrated for naturally ventilated enclosures[6,7].

There are problems which remain, for example, the current treatment has not specifically distinguished between convective and radiative heat transfer to the compartment surfaces. This is because of difficulties in specifying convective losses to real building materials and in modelling radiation transfer. The detailed treatment of the combustion process must be improved to include effects such as intermittency for accurate predictions close to the fire source if, for example, fire spread from one item to another is to be predicted. There may, however, be many applications where this detail is not required and some improvement in the combustion model to allow for partially oxidised products (eg CO) may be adequate.

Finally the numerical techniques employed are subject to error and work is necessary to identify the most suitable for the current purpose. All these areas of research are currently being pursued to improve the capability of these general purpose computational fire dynamics models.

Acknowledgement

The authors are grateful to Norman Alvarez of the Lawrence Livermore National Laboratory for supplying the considerable volume of experimental data used in this validation study.

This paper forms part of the work of the Fire Research Station, Building Research Establishment Department of the Environment, UK. It is contributed by permission of the Director, Building Research Establishment.

References

1 Cox G, Proc CSNI Specialist Meeting of Interaction of Fire and Explosion with Ventilation Systems in Nuclear Facilities, CSNI Report No 83, Los Almos Report LA-9911-C, p 199, 1983.
2 Galant S, ibid, p 119, 1983.
3 Kumar S, *Fire and Materials*, 7, 1 (1983).
4 Satoh K, *Report of Fire Research Institute of Japan*, 53, 48, (1982).
5 Hasemi Y, 'Numerical Computation of Plume Behaviour in Large-Scale Fires', Private Communication (1981).
6 Cox G and Markatos N C, *Physicochemical Hydrodynamics*, 5, 53 (1984).
7 Markatos N C and Pericleous K A, 'An Investigation of Three Dimensional Fire in Enclosures', 21st National Heat Transfer Conference, Seattle, 1983.
8 Markatos N C, Malin M R and Cox G, *Int J Heat Mass Transfer*, 25, 63, (1982).
9 Magnussen B F and Hjertager B H, Sixteenth Symposium (International) on Combustion, p 719, The Combustion Institute, 1976.
10 Spalding D B, Thirteenth Symposium (International) on Combustion, p 649, The Combustion Institute, 1971.
11 Launder B E and Spalding D B, Mathematical Models of Turbulence, Academic Press, London, 1972.
12 Spalding D B, 'Mathematical Modelling of Fluid Mechanics, Heat Transfer and Mass Transfer Processes', Computational Fluid Dynamics Unit Report HTS/80/1, Imperial College (1980).
13 Alvarez N J, Foote K L and Pagni P J, 'Characteristics of Fire in a Forced Ventilated Enclosure' to be published in *Comb Sci and Technology* (1984).

14 Cox G and Chitty R, *Fire and Materials,* 6, 127, (1982).
15 Liew S K, Bray K N C and Moss J B, 'The Predicted Structure of Stretched and Unstretched Methane-Air Diffusion Flames', 9th ICODERS Meeting, Poiters, 1983.
16 Patel M, Markatos N C and Cross M, 'A critical evaluation of seven discretization schemes for convection-diffusion equations'm *Int J Num Meths in Fluids,* to be published (1984).
17 Spalding D B, *Physiochemical Hydrodynamics,* 4, 323 (1983).

CLOSING REMARKS OF SESSION CHAIRMAN SODERHOLM:

We have seen some high-technology approaches to some complex problems. These problems occur due to natural phenomena, which have been plaguing man since the lowest technology days of crawling in and out of caves, when we talk about earthquakes, tornado, and fire. In the first presentation, we had a video tape of seismic testing which I found quite interesting. And in the second paper we were talking about having active components to increase the complexity and applicability of computer codes which are being applied in the BORAC facility to deal with some of these accident situations. Third, we looked at some experiments with dampers and blowers in simulated tornado experiments, an area of great interest. Then we viewed some computer movies showing capabilities of the Fire Act Code. Now, there are some very difficult questions in that work, and in the last paper, as we try to get into the aerosol problem. I would certainly agree with that, but I think these are our approaches and they will help us learn, if nothing else, how much we don't know. The filter plugging results in the fourth paper certainly have high interest, and it was very interesting in the last paper to see the first-principles approach to the fire situation, mainly applied in the steady state. It shows a surprising amount of promise. I didn't realize that first principles could still be so popular and match experimental results so well.

Panel 9

SOURCE TERM IN RELATION TO AIR CLEANING

TUESDAY August 14, 1984
MODERATOR: J.L. Kovach
Nuclear Consulting Services

PANEL MEMBERS:
A.P. Malinauskas
Oak Ridge National Laboratory
J.A. Gieseke
Battelle Columbus Laboratory
P.S. Littlefield
Yankee Atomic Electric Company
R.M. Bernero
U.S. Nuclear Regulatory Commission

FISSION PRODUCT SOURCE TERMS AND ENGINEERED SAFETY FEATURES
A.P. Malinauskas

AEROSOL CHALLENGES TO AIR CLEANING SYSTEMS DURING SEVERE ACCIDENTS IN NUCLEAR PLANTS
J.A. Gieseke

UTILITY VIEW OF THE SOURCE TERM AND AIR CLEANING
P.S. Littlefield

SOURCE TERMS IN RELATION TO AIR CLEANING
R. M. Bernero

OPENING REMARKS OF PANEL MODERATOR:

We have had some changes in the composition of the panel so I am going to make brief introductions starting with Robert Bernero who is Director, Division of Systems Integration, U.S. Nuclear Regulatory Commission and I wish to acknowledge his excellent key note address on source terms. Next is Pete Littlefield from Yankee Atomic Electric Company who represents the minority, a nuclear power utility. Next, Dr. James Gieseke from Battelle Columbus Laboratory, who is our expert on aerosols. And, finally, Anthony Malinauskas, Director of NRC programs at ORNL. I have to say just one word about him, when everyone was looking for the iodine at TMI, he was the one who said, "Where is the beef?"

I want to make sure that none of you think that Kovach suddenly became an expert on source terms. I am just a moderator here and wish to make a little introduction that really has very little to do with the technology of the source term. In the fall of 1944, my home country, Hungary, was overrun by the German armies and the Russians were already within the borders of the country. The German newspaper headlines said, the situation is bad but not hopeless. The Hungarian newspaper stated, the situation is hopeless but not bad. Somewhere between the sentiments of these two statements lies todays source term definition.

As we started to build nuclear power plants based on the experience of our military nuclear technology, instead of building on common sense, we generated a plethora of myths to guide us into todays dead end, and along the way codified our misinformation. To impress ourselves with the seriousness of the problems we thought we were solving, we imagined auguries to be slaughtered. But to do so in an orderly fashion, we wrote regulatory guides for Sir Callahad's behavior and hired hordes of QA personnel capable of breathing, but not necessarily thinking, to audit our fears that the accident we prevent may not be big enough. We imagined perfect, incredible accidents, and we wanted to design for them and convince the general public that we, in fact, succeeded, while we ignored the little accidents that were likely to happen. In the process of doing so, we nearly killed the safest means of electric power generation in the U.S. We talked of massive amounts of iodine belching into reactor containments and, failing that containment, draining onto the countryside. At the same time, we expressed frustration over not being able to run iodine adsorption gas rates because the iodine plated out or reacted with almost everything on its way to the sample disaster, without realizing the conflict between fact and theory. It became a classic story of the king's invisible clothes, and instead of somebody yelling that the king is naked, we wrote standards and procedures to define the precise tailoring of the king, and carefully specified the yarns that should be used. We developed and evaluated laboratory experiments which proved only the individuality of that particular laboratory experiment, and we ignored the studies of the consequences of accidents that happened in the past. And somewhere along the way, we passed into the dark ages with a certain semblance of heretic burning procedures. I stress procedures because the procedures became more important than the fact. Even today, we are finally seriously dis-

cussing the realities of iodine quantities and form on a far more realistic basis than heretofore, while, on a legal licensing basis, we are still designing, and have been for years, after even TMI, and after the realization of the validity of prior accident consequences, on the basis of iodine volumes, which we know, are incorrect. Yes, the earth is round. However, on the temporary worst case assumption that it is flat, we wrote regulatory guides and standards on how to circumnavigate it, in spite of the logical assumption that such a process is impossible. I told you, I am not going to say anything about technology - I leave that to the panel.

Thank you very much for your time.

Dup

FISSION PRODUCT SOURCE TERMS AND ENGINEERED SAFETY FEATURES*

A. P. Malinauskas
Oak Ridge National Laboratory
Oak Ridge, Tennessee

Let me begin by considering the situation just over six years ago, in January 1978. Interest in source term research was clearly waning. The Reactor Safety Study, WASH-1400, had been published more than two years previously, and although some of the conclusions and the methodology had been criticized, the areas of contention largely concerned the probabilistic approach that was employed and thermalhydraulics features. As best I can ascertain, however, not a single criticism was made regarding the manner in which fission product release and transport was handled.

There was, in fact, a slight flurry of activity in the source term area shortly after the release of WASH-1400, but this was motivated by the very large uncertainties that were cited in the Reactor Safety Study for the fission product release values. Curiously, the main concern was not with so-called "risk dominant" or "degraded core" accidents; the low probabilities of occurrence predicated for such accidents were apparently accepted by the nuclear community as tolerable.

Instead, the main thrust of the research was directed toward a realistic evaluation of the consequences of design basis accidents, and foremost among these was the loss of coolant accident in which the engineered safety features functioned as designed, the so-called "controlled loss-of-coolant accident." From the standpoint of the safety of the general public, controlled loss-of-coolant accidents proved to be relatively benign, regardless of the probability of occurance or of the details of the thermalhydraulics. For example, the most recent studies at that time indicated that only about 1% of the noble gas inventory of the entire core, 0.03% of the cesium inventory, and 0.05% of the iodine inventory would be released from failed fuel rods in the course of a controlled loss-of-coolant accident in a light water reactor.(1) For radioiodine, then, only a few thousand curies would be released from the fuel rods, and ample opportunities existed for significant attenuation of this release regardless of its chemical form. Moreover, the newer release values were themselves some two orders of magnitude less than corresponding results derived from the Reactor Safety Study.(1)

As is well recognized, the accident at Three Mile Island (TMI) in March, 1979 had a significant impact on the course of reactor safety research in general, and of studies of fission product source terms in particular. The accident, which could be described as an "eventually controlled" loss-of-coolant accident, also served to turn the attention of the nuclear community away from more probable, relatively benign, accidents in which the engineered safety features operate as designed, and toward considerations of much less likely, but more consequential, severe core damage accidents.

---

*Research sponsored by the Office of Nuclear Regulatory Research, U.S. Nuclear Regulatory Commission under Interagency Agreement No. DOE 41-551-75 with the U.S. Department of Energy under contract DE-AC05-840R21400 with Martin Marietta Energy Systems, Inc.

Early interest in fission product release and transport during the accident at Three Mile Island did not focus on what did happen, but rather on what did not occur. In particular in this regard, a major problem involved the relative releases of radioiodine and the noble gases. During the accident, about 8 million curies of ^{133}Xe were released into the atmosphere, but only about 15 curies of ^{131}I similarly escaped. In contrast, the accident at the Windscale reactor in 1957 resulted in the release into the atmosphere of only some 300,000 curies of ^{133}Xe but about 20,000 curies of ^{131}I.

The answer to the problem of almost negligible iodine release at TMI lay, of course, in a careful consideration of the chemistry involved. Radioiodine released from failed fuel rods was traditionally considered to be in elemental form. As a consequence, it had been assumed that the fission product similarly exists primarily in elemental form in the containment building, although small fractions were additionally assumed to convert to organic iodides and to become associated with particulates. In view of the chemically reducing conditions which are an inherent characteristic of severe core damage accidents in light water reactors, and the likely formation of cesium iodide within the fuel rod or within the core region, the release and transport of fission product iodine in elemental form is most improbable.(2) Moreover, with the exception of silver iodide, other likely iodides involved are extremely soluble in water; this factor can result in a significant reduction of the source terms for radioiodine for those accidents in which the escape pathway is intercepted by water, such as occurred at Three Mile Island. As a consequence, except for accidents involving the introduction of aerosols in high concentration in the reactor containment atmosphere, the dominant volatile form of radioiodine is probably organic in nature. Moreover, this form is dominant, not because of its presence in high concentration, but because the remaining chemical forms are nonvolatile. (Interestingly, the precise mechanisms for the formation of organic iodides in reactor accidents are not clearly established.)

Since the Three Mile Island Accident in March, 1979, considerable research has been performed on severe core damage accident source terms. This research will culminate shortly in the development of new methodologies for establishing source terms, as embodied both in the Industry Degraded Core Rulemaking (IDCOR) Program and in the Nuclear Regulatory Commission's Severe Accident Program. These approaches will unquestionably lead to more sophisticated and more realistic evaluations of the consequences of severe nuclear reactor accidents.

Unfortunately, these evaluations will largely be directed only toward giving people (mostly pro-nuclear) a warm feeling about the consequences of highly improbable events. Thus far, however, little use has been made of the knowledge gained of the behavior of fission products to modify and improve existing strategies for mitigating the consequences of accidents of high or of low probability. Nor has the adequacy of these existing strategies yet to be re-examined in light of current research findings.

For example, caustic is added to pressurized water reactor containment building spray systems, presumably to capture radioiodine (in the wrongly assumed elemental form) in order to prevent its escape into the environment in the event of an accident. Spurious trips of this spray system under normal operating conditions of course result in the dispersal of caustic solutions into the containment building. Subsequent cleanup can be quite expensive.

The use of caustic sprays appears to be totally unwarranted to mitigate the consequences of traditional design basis accidents. The need for caustic is likewise questionable at the other extreme as well, for in severe core damage accidents the dominant carrier of airborne radioiodine is believed to be aerosol particles. In addition, the containment building spray systems are normally activated by indications of high pressure, not of high radiation level, and these two parameters are not necessarily related. At Three Mile Island, for example, the spray system was activated (because of a hydrogen burn) long after fission products had been introduced into the containment building. There is thus adequate reason to re-examine the use of caustic in such spray systems.

In a similar vein, although the situation is more complex, the strategy for the use of standby off-gas treatment systems, as well as their design, should be re-examined in light of current research results.

I seriously doubt whether any of the engineered safety features that are installed in currently operating reactors would aggravate the consequences of a serious reactor accident, but this aspect certainly merits examination. However, there is reason to believe that some of these systems will never perform their intended function, or that their efficacy will be severely compromised, primarily because the assumptions underlying their design and operation, though conservative, are wrong.

In summary, we shall have in hand shortly new, technically defensible, methodologies to establish realistic source term values for nuclear reactor accidents. Although these methodologies will undoubtedly find widespread use in the development of emergency response procedures, that is, procedures to be implemented external to the plant, such as sheltering or evacuation of the surrounding population, it is less clear that the industry is preparing to employ the newer results to develop a more rational approach to the implementation of engineered safety features for the mitigation of fission product releases in the event of a nuclear reactor accident.

References

1. R. A. Lorenz, J. L. Collins, and A. P. Malinauskas, Nucl. Technol. 46, 404 (1979).
2. D. O. Campbell, A. P. Malinauskas, and W. R. Stratton, Nucl. Technol. 53, 111 (1981).

AEROSOL CHALLENGES TO AIR CLEANING SYSTEMS DURING SEVERE ACCIDENTS IN NUCLEAR PLANTS

J. A. Gieseke
BATTELLE
Columbus Laboratories
Columbus, Ohio 43201

A variety of air cleaning systems may be operating in nuclear power plants and under severe accident conditions, these systems may be treating airborne concentrations of aerosols which are very high. It is instructive to review predictions of airborne aerosol concentrations in nuclear power plant containments under severe accident conditions to provide a basis for evaluating the potential effects on the air cleaning systems. The air cleaning systems include filters, absorber beds, sprays, water pools, ice beds, and condensers. Not all of these were intended to operate as air cleaners but will in fact be good aerosol collectors. Knowledge of expected airborne concentrations will allow better evaluation of system performances.

The information presented here is obtained from work being performed as part of the Nuclear Regulatory Commission's source term reassessment efforts. Calculations of the release of radionuclides from overheated fuel and their transport through the reactor coolant system and containment structures were made using a series of computer codes describing the evolution of thermal hydraulic conditions and vapor and aerosol transport[1]. Within the containment and auxiliary (safeguards) buildings where air cleaning systems are located, the important fission product species are expected to be aerosols formed from CsI, CsOH, Te, and other materials (less volatile fission products, fuel, and structural materials from the reactor core region). The airborne concentrations and aerosol size distributions are of interest here.

In Figures 1 through 4 predicted aerosol concentrations are presented as a function of time for the Surry and Peach Bottom power plants and for several assumed accident sequences. The sequence designations are taken from the WASH-1400 report[2]. The general shapes of the airborne concentration curves are similar showing an early-time release of mass from the reactor coolant system followed by a decrease in concentration as the melting core moves from the pressure vessel to the cavity floor during which time there is no source of aerosols to the containment. The high concentrations at later times arise because of aerosol input from interaction between the molten core and the concrete floor of the reactor cavity. The mass leaked from the compartment of consideration in each figure is also shown. The rapid increases in leaked mass, when they occur, are the result of a failure of the compartment or building.

The important information to be derived from these figures is the predicted high and variable levels of aerosol concentration. Because of the predicted high mass input rates, agglomeration and hence sedimentation is rapid. However, the airborne mass concentrations appear to be excessively high to permit extended operation of filter or adsorber systems without excessive buildup or blinding

occurring. The predicted particle sizes as shown for one case in Figure 5 are not out of line with effective operation of most air cleaning systems and as collection continues, some air cleaning systems will suffer diminished effectiveness.

Table 1 summarizes results from calculations for a number of power plants and a number of accident sequences. The previous observations of high mass loadings are again valid for the entire set of sequences shown in this table. It appears that the effective lifetime for air cleaning systems that are susceptible to becoming overloaded with aerosol deposits may be extremely limited under severe accident conditions.

References

1. Gieseke, J. A., et al, "Radionuclide Release Under Specific LWR Accident Conditions, Volumes I-VI", BMI-2104.

2. "Reactor Safety Study -- An Assessment of Accident Risks in U.S. Commercial Nuclear Power Plants", WASH-1400, NUREG-75/014 (October, 1975).

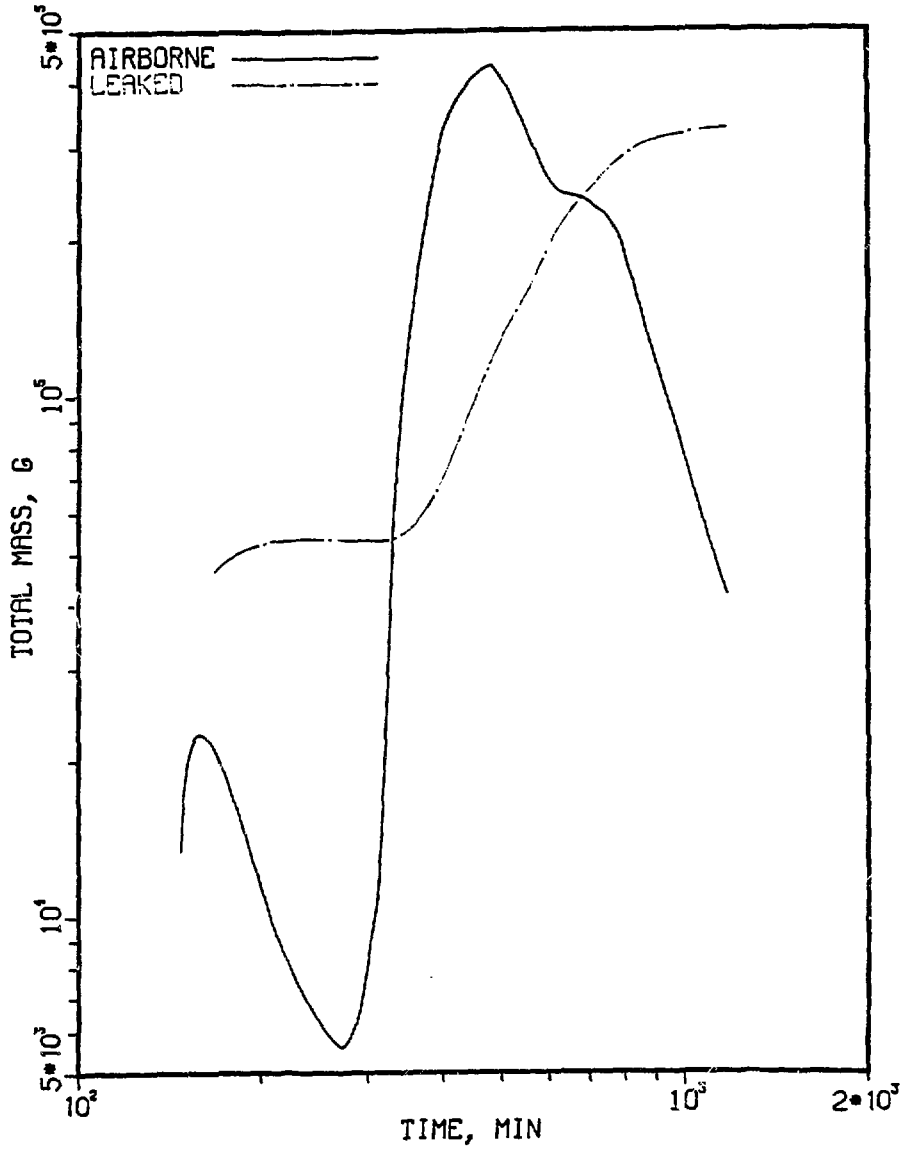

Figure 1 Airborne and leaked masses, Surry plant, Sequence TMLB'-δ (Containment volume = 51,000 m^3)

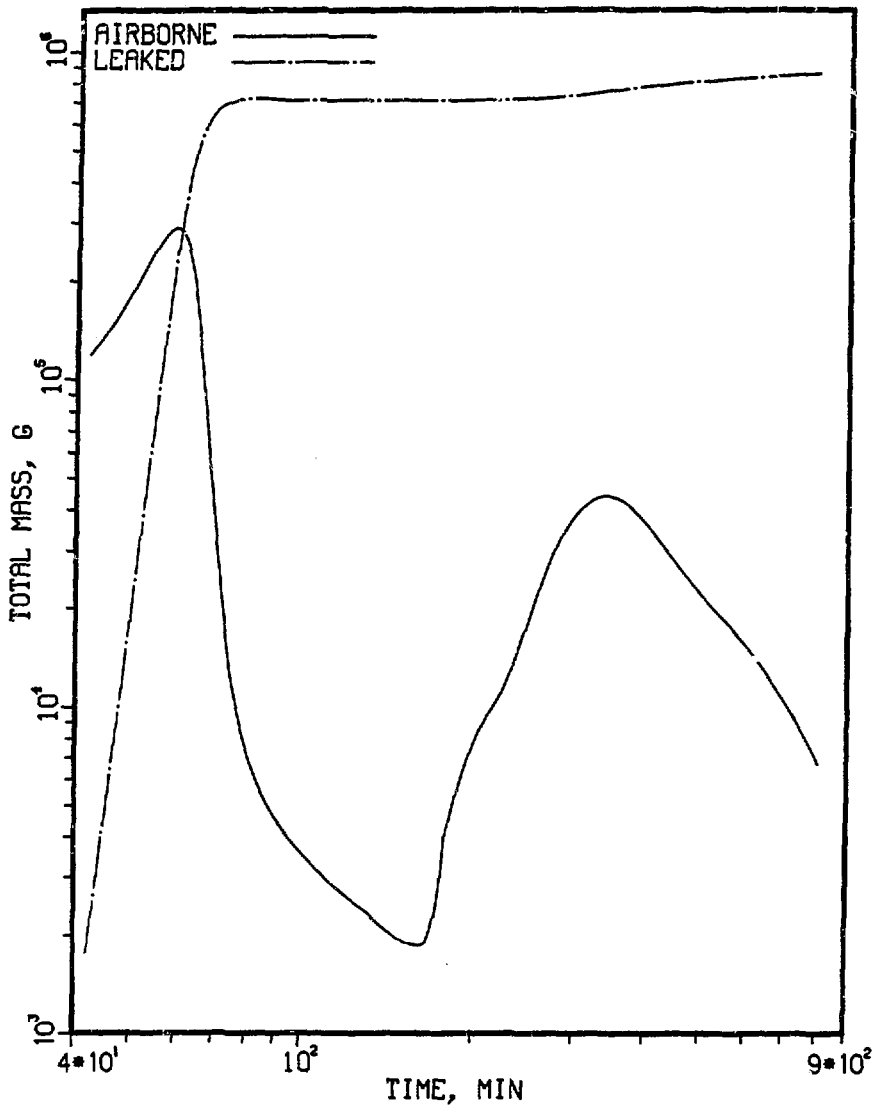

Figure 2 Airborne and leaked masses, Surry plant, Sequence V (Auxiliary building volume = 4,250 m^3)

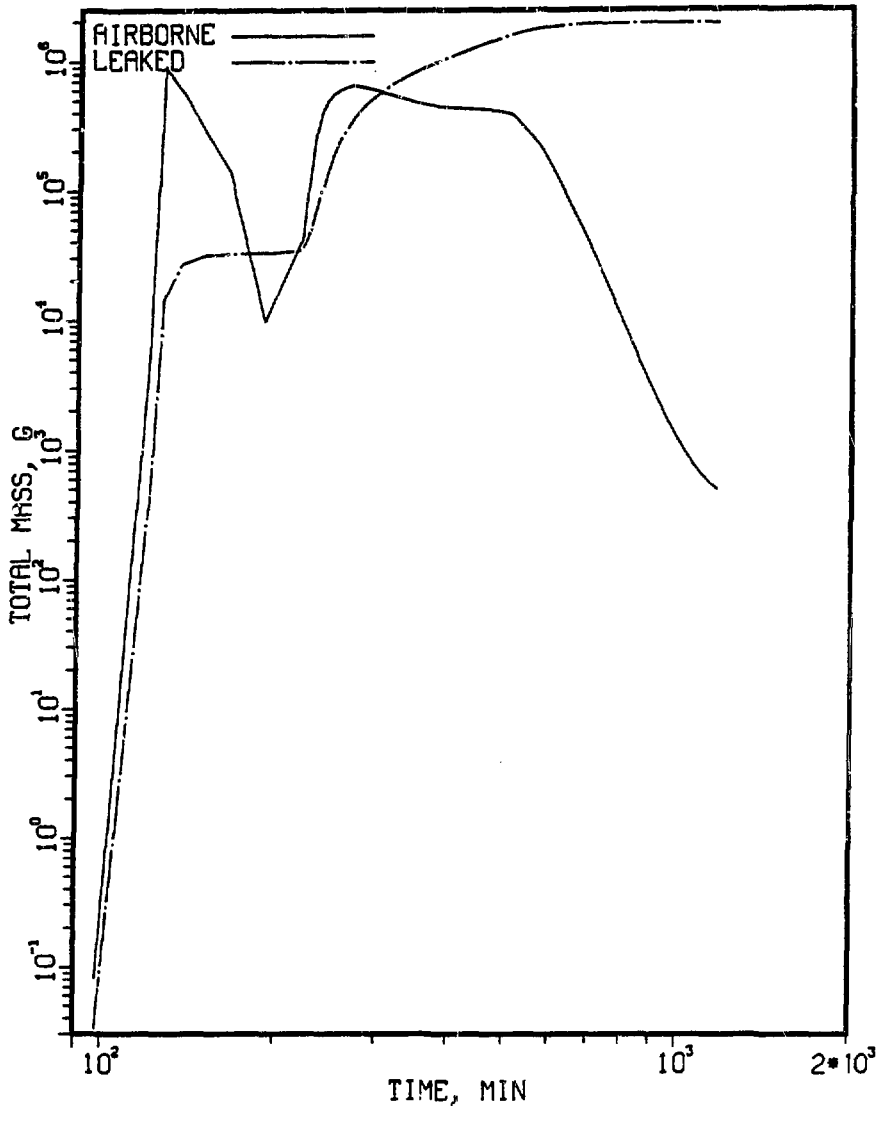

Figure 3 Airborne mass for the secondary containment as a function of time, Peach Bottom plant, Sequence TC-γ (Reactor building volume = 68,000 m^3)

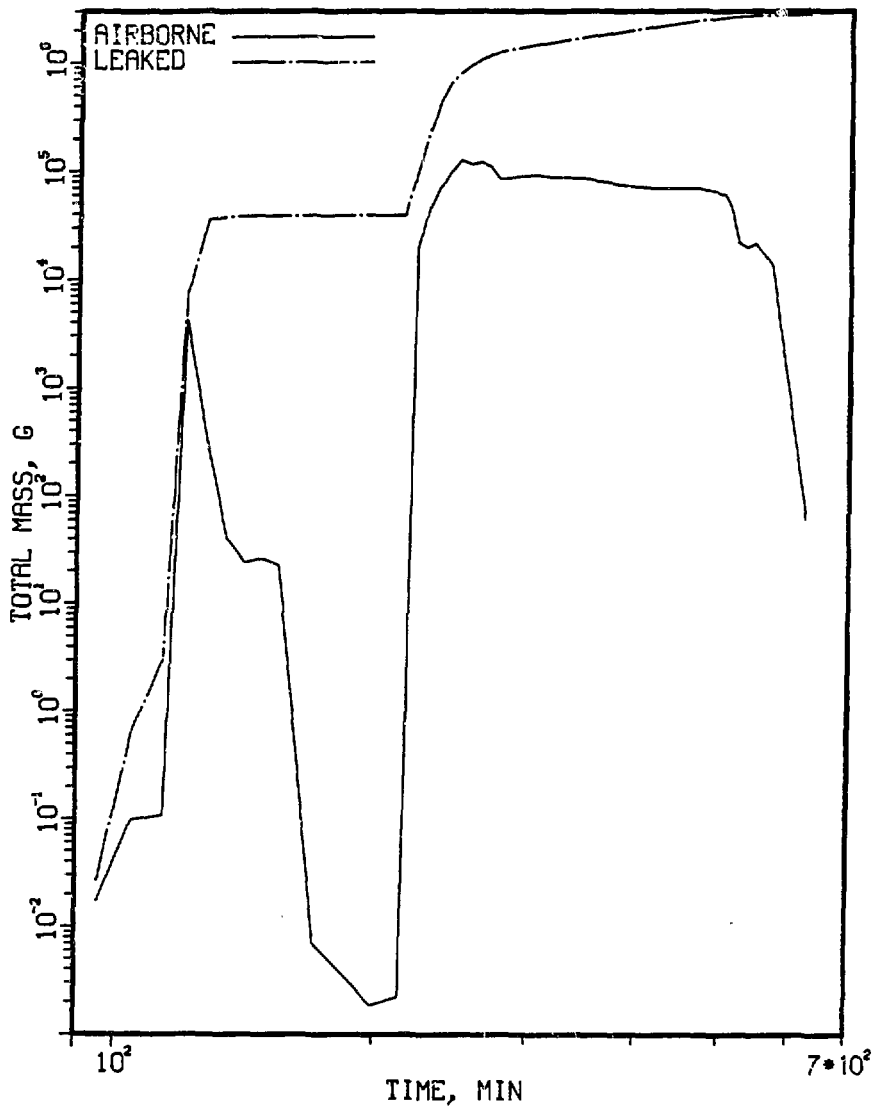

Figure 4 Airborne and leaked aerosol mass for the drywell as a function of time, Peach Bottom plant, Sequence TC-γ' (Drywell volume = 4500 m^3)

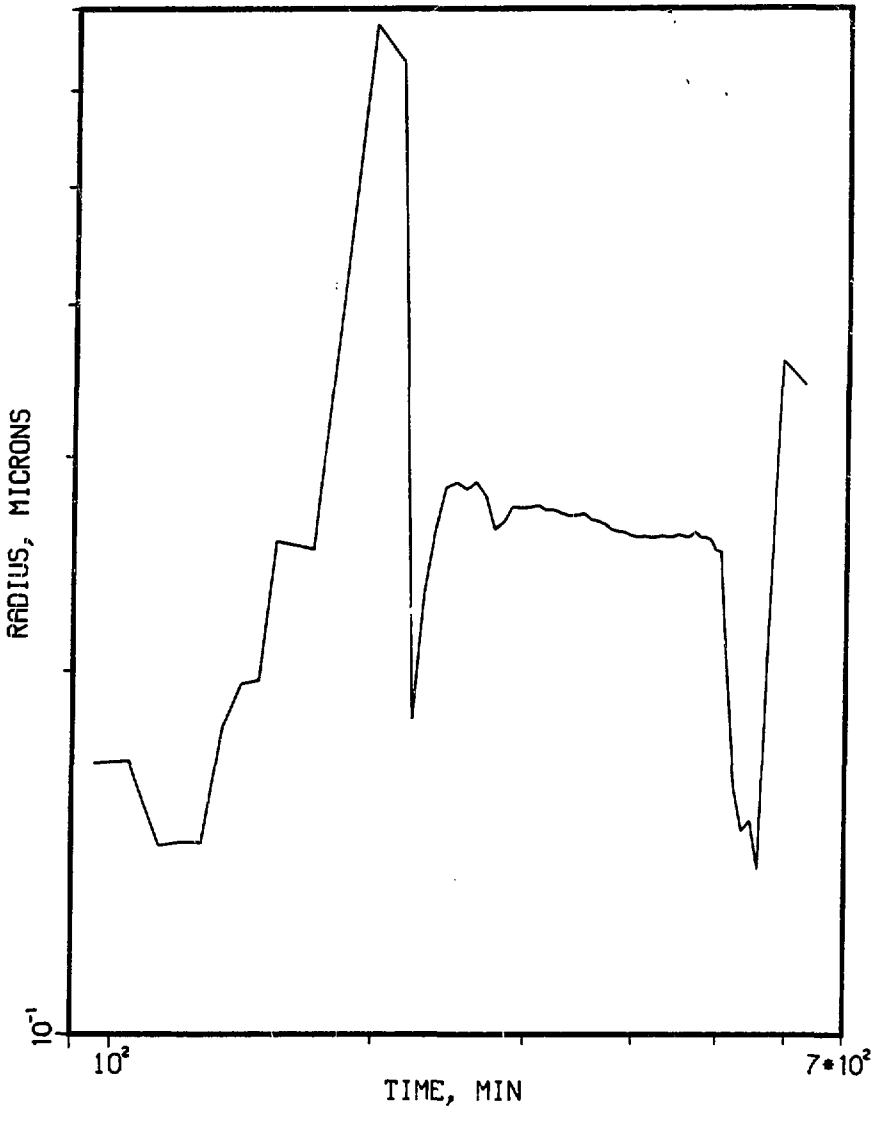

Figure 5 Geometric mean particle radius in drywell, Peach Bottom plant, Sequence TC-γ'

Table 1. Aerosols in containment during accidents.

Plant	Sequence	Max. Aerosol Conc. g/m^3	Mass Median Particle Diam. μm
Surry	AB-β	90.	2 - 10 (Aux Bldg)
	-γ	60.	2 - 4
	-ξ	50.	1 - 3
	TMLB'-δ	9.	--
	-ξ	550.	--
	S_2D -γ	6	--
	-ξ	0.05	--
	V	40.	2 - 4 (Aux Bldg)
Peach Bottom	AE -γ'	20.	1.5 - 2
	TC -γ'	20.	0.15 - 0.7
	TW -γ	40.	--
Grand Gulf	TC	0.1	--
	TPI	0.1	--
	TQUV	0.5	0.4 - 2
	S_2E	0.7	2 - 4
Sequoyah	TMLB' -γ	0.8	0.4 - 2
	-δ	60.	0.4 - 5
	TML -γ	2.2	0.5 - 2
	-δ	0.04	0.1 - 0.2
	S_2HF -γ	60.	1.5 - 10
Zion	TMLB' -ξ	11.	1.5 - 4
	S_2D -ξ	105.	0.2 - 0.4

UTILITY VIEW OF THE SOURCE TERM AND AIR CLEANING

P.S. Littlefield
Yankee Atomic Electric Company
Framingham, Massachusetts

The utility view of the source term and air cleaning is something I had to think about a little because, while I have been working with air cleaning systems for a number of years and with the source term issue in the more recent past, I wasn't sure I had a good grasp on how the two went together. The source term is made up of: 1. noble gases, which we have all tended to ignore in the past because we assume there was nothing we could do with them anyway, 2. the halogens, which we have dealt with in these Air Cleaning Conferences a great deal in the past in terms of charcoal and other systems for removing them and, 3. the solid components of the source term which particulate filters are designed to handle. Air cleaning systems consist of filters, adsorbers, containment sprays, suppression pools in boiling water reactors and ice beds in ice condenser-equippped plants.

Being an engineer, I first investigated the cost of air cleaning systems to see if it was worth the trouble. Looking at rough costs, we see that, for a typical plant, we are looking at a purchase cost of one million dollars for filter systems and between two and three million dollars by the time we add overhead and installation costs to the systems. A containment spray system is in the order of six million dollars installed. These numbers came from our Seabrook plant which is in construction. So the message from this is, yes, there will be significant dollar impact for air cleaning systems if it should be decided that backfits are necessary.

Now I would like to look at the source term in more simplistic terms than it has been presented previously. The design basis source term that most of our air cleaning systems have been designed to cope with, consists of 100% of the noble gases, 50% of the halogens, and 1% of the solids released from the fuel. Now, we are dealing with another concept in source term, that I have labeled Calss 9 for lack of anything better, that says, 100% of the noble gases, close to 100% of the halogens, and somewhere between 0 and 100% of the solids, depending on what elements we are talking about, will be released. The biggest difference here, as far as an impact on air cleaning systems is concerned, will be in what I call the solids component of the source term.

The total mass in the core that is available to form aerosols in the containment is very large, as was brought out by the previous speakers, whereas just a few kilograms of aerosol particles will plug-up a typical HEPA filter. There is no question that there will be adequate aerosol mass to plug up a filtration system.

From the utility perspective, the source term is related to risk assessments, so popular today for calculating offsite consequences from low probability events. The relationship of the source term to some of the other issues that we deal with is not quite so clear, for example, the siting issue. Utilities are not yet sure what impact a new source term is going to have on siting, but it probably doesn't matter because, unfortunately, we are not doing very much siting work these days. Emergency planning is an area we hope a new source term will help by decreasing the size of the emergency zones. The design area is going to be impacted in terms of qualification doses to safety equipment after an accident, and in terms of designing plant shielding for the protection of workers after an accident.

Finally, the subject of our panel discussion today is the source term impact on the design of air cleaning systems. Air cleaning systems in the nuclear stations are primarily designed to do two things, one, is to protect the control room operators from an accident, and the other is to protect the public. Control room filtration systems operate in a mild environment. For most accidents, no matter how severe the source term , it is not going to have any great impact on control room filtration systems.

One of the systems that will work to protect the public is the suppression pool in boiling water reactors. The suppression pool, Figure 1, is primarily a passive device and we do not expect the performance of the suppression pool to be compromised by a high source term. Another system is the standby gas treatment filter trains that take air and gases from the reactor building, outside the primary containment where the large mass of aerosols will be generated. For most accident sequences, standby gas treatment filter systems will also be operating on a relatively mild environment and their performance will not be compromised. If we should have a massive failure of the primary containment boundary, the reactor building would also rupture and the standby gas treatment systems would not perform a useful function. Similar statements can be made about auxiliary building filter systems for pressurized water reactors. For most accident sequences, they will be operating as they were at TMI, on a relatively mild environment in terms of high concentrations of aerosols.

A few pressurized water reactors have recirculating air cleaning systems inside containment, Figure 2, and, as I noted earlier, generation of high concentrations of aerosols could compromise the performance of the filters. We expect that containment spray systems would not be compromised by a high source term of aerosols or iodine in the containment. There are some questions that have to be addressed such as blocking of the containment sump where the containment spray systems take their suction.

The final message that I would like to leave is that the greatest air cleaning system that we have in these plants is the containment vessel itself. The message that has come out of risk assessment studies is that if we can maintain containment integrity, the natural processes of deposition, diffusion, and plateout will remove the source term regardless of the performance of any of the other air cleaning systems.

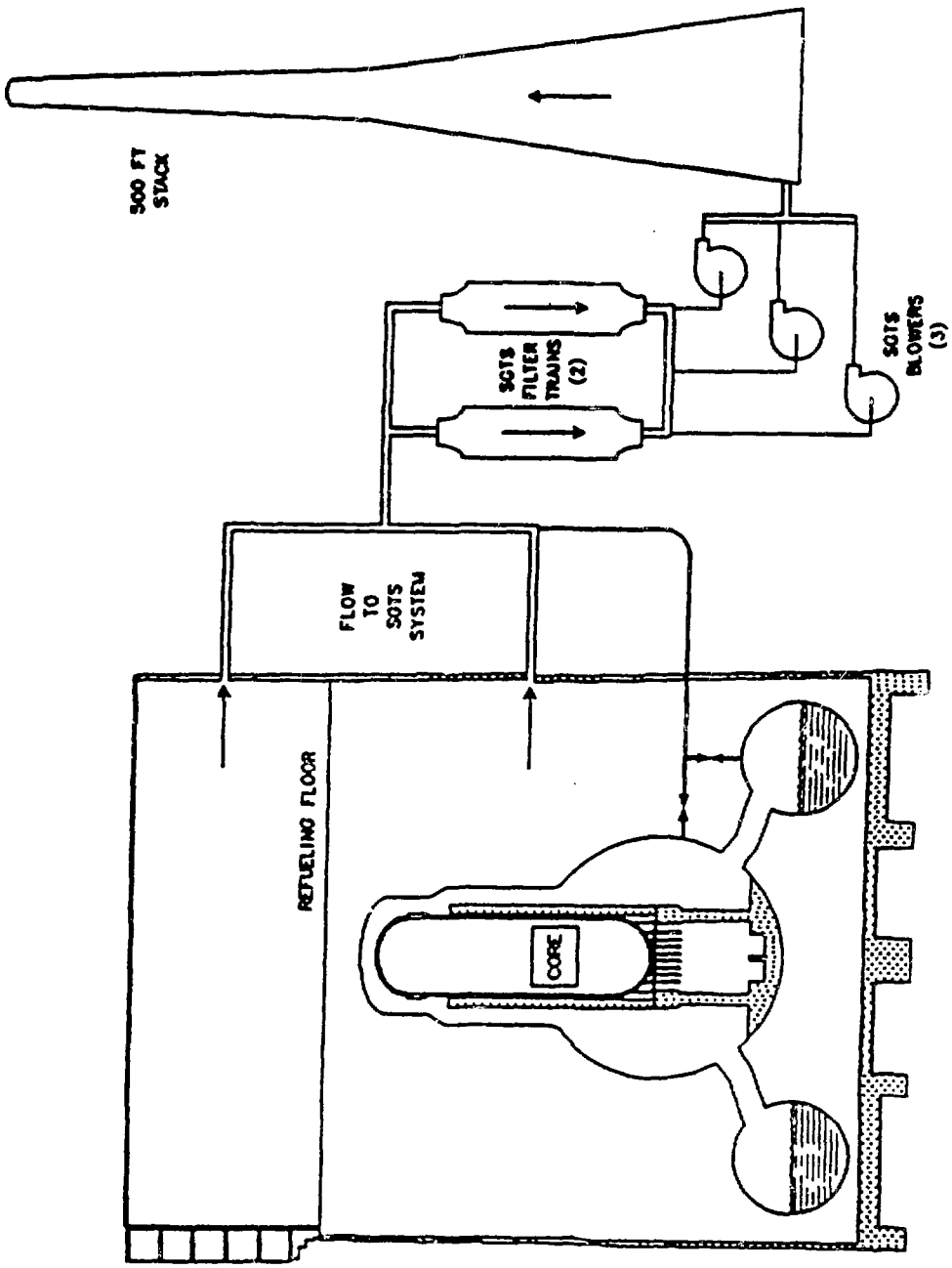
500 FT
STACK
SGTS
FILTER
TRAINS
(2)
SGTS
BLOWERS
(3)
FLOW
TO
SGTS
SYSTEM
REFUELING FLOOR
CORE

Figure 1

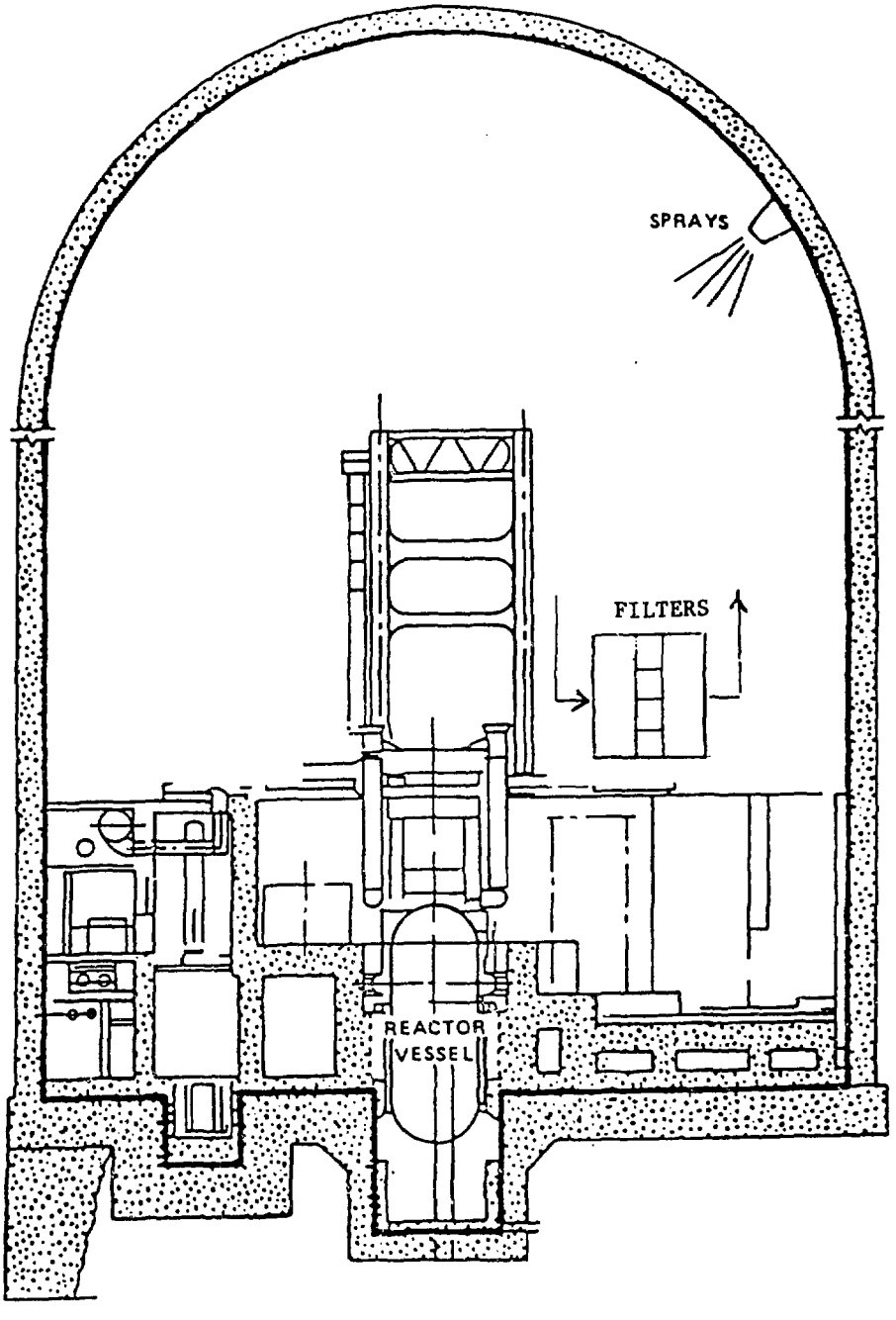

LARGE, HIGH PRESSURE CONTAINMENT
Figure 2

SOURCE TERMS IN RELATION TO AIR CLEANING

Robert M. Bernero
Director, Division of Systems Integration
U.S. Nuclear Regulatory Commission

There are two sets of source terms for consideration in air cleaning, those for routine releases and those for accident releases. Now, with about one thousand reactor years of commercial operating experience in the U.S. done, we have an excellent data base for routine and expected transient releases. Specifications for air cleaning can be based on this body of experience with confidence.

Specifications for air cleaning in accident situations is another matter. Fortunately, there is very little accident experience to work with. We must work with models of accident behavior which are tested by experiment in order to establish reliable estimates of accident conditions, and thereby a basis for air cleaning requirements. For many years we have used simple, relatively non-mechanistic models for accident behavior. As a result we have set air cleaning requirements that are very strongly biased toward capture of volatile radioiodine. We have required many carbon filters and added chemical agents such as caustic and even sodium thiosulfate to containment spray water.

Recent investigations of severe accident behavior are offering a new basis for source terms and air cleaning specifications. Reports by many experts in the field describe an accident environment notably different from our previous models. It is an atmosphere heavy with aerosols, both radioactive and inert. Temperatures are sometimes very high; radioiodine is typically in the form of cesium iodide aerosol particles; other nuclides, such as tellurium, are also important aerosols.

Some of our present air cleaning requirements may be very important in light of these new accident behavior models. Others may be wasteful or even counterproductive. We must use the new data to reevaluate our requirements promptly.

One consolation of being a spokesman for the NRC is you usually get the last word. The subject of this meeting and the comments that have been made are all of very strong interest. I would like to say a few things in self defense about the preceding speaker's remarks and then make some independent statements of my own. When Dr. Kovach spoke at the beginning of the session about the severe conservatism, or unreality, of the source term, I agreed with him. Our regulatory characterization of source terms has been, as I said yesterday, non-mechanistic, unrealistic, and perhaps, even counterproductive. But I would caution you that I remember with a somewhat distinct degree of bitterness that, prior to the TMI accident, I had discussions with many people about the likelihood of a severe core damage accident because I happened to believe that WASH-1400 was fairly accurate in its risk assessment. At the time, many in the nuclear community looked upon WASH-1400 as an exaggeration of the likelihood of such an accident. After than, in essence validating the prediction that core damage accidents are likely, we have to be careful of our impact on the public if we now say, "Well, they don't hurt anybody, anyway, and nothing gets out." I think we have to give real attention to the source term and get realistic estimates, but be careful that we do not pooh-pooh severe accidents. If nothing else, such an accident can bankrupt the owner of the plant. Now, I find it interesting that Tony Malinauskas said that, at the time WASH-1400 was published, there was relatively little controversy about the consequence model for the source term. And it is rather interesting that that report, the Reactor Safety Study, even said, right in one of the appendices, "iodine is most likely in the form of cessium iodide, but there is not really a large enough body of data to demonstrate that." So, the analysts said they would assume that it is all elemental iodine, and treat it that way, and they got into partition coefficients, vapor-liquid equilibria for elemental iodine, which, of course, is relatively soluble in water. And I remember that the regulators, at the time, said, "the partition coefficients are too optimistic and involve too much dissolution in water." We now have an opportunity to look over new data and do something much more intelligent. I am pleased that Dr. Gieseke had a chance to give you an overview of some of his results. When I spoke yesterday, I had to speak from the perspective of the NRC. We sponsored this work, we believe very strongly in the quality of it, but we have not completed our peer review, so I am not going to give you numbers. I encourage you to get the report. Dr. Gieseke is the principal author of the reports I referred to yesterday, and that set of reports is called BMI 2104. If any of you want a set, write to the Document Control Division of NRC, Washington, DC 20555. That is all you have to do, and you are entitled to one copy.

It is interesting to look at the results Jim Gieseke and Pete Littlefield presented, what you might call, the before and after source term. What we see now, from the mechanistic analysis, is a lot of aerosol, relatively little, if any, volatile halogens, and of course, noble gases. In current procedures for the boiling water reactors, at least, the operators are urged to vent the wet well of the containment. In other words, rather than let the containment reach some bursting pressure, it is recommended that they vent the wet well so that whatever comes out to relieve the pressure in containment passes through the suppression pool and is scrubbed. What we are

dealing with now in the area of air cleaning, are, noble gases, that you can hold up a bit but are not really practical to remove, and solids, a lot of solids. I hope you notice in Gieseke's results the different outcomes, sequence to sequence, and plant to plant. There is not one source term, there are many souce terms. There are many scenarios leading to different source terms even in the same plant. And so the message we have, and the need we have, is to look at our design requirements and to re-evaluate them. I share the feeling previously spoken that it is not likely that we have a counter-productive engineered safety feature. The only one I ever worry about is when a plant has happened to put, in a series train, the reactor building coolers with their fan filters. If you plug the filters you could block the coolers. But aside from that sort of configuration, it is pretty hard for me to see something that is truly counterproductive, other than some of the things that we have mentioned. Thank goodness, today, we don't have sodium thiosulfate in the spray any more; we used to, in some of the plants. Once again, that is a feature that is really not a good idea, but was intended to go after that will-of-the-wisp, volatile radioiodine. We have to look at the air cleaning features, at all the engineered safety features, and take a hard look at what's worth doing, what is no longer worth doing. The costs to design and install, just shown by Pete Littlefield, are not trivial. They do not reflect the costs that are associated with plant delay or plant shutdown. By a twist of irony, just yesterday and today, I am involved in a case with one plant that is suffering a very costly delay, and it is associated with very refined subtleties about engineered safety features. I can say with confidence that the issue is not serious-risks versus non-serious risks, but one of trivia.

I can corroborate something Pete Littlefield said, the most important engineered safety feature is the containment itself. Anything that enhances its ability to hold, even for a little while, for just a few hours, is the greatest single thing you can do to protect the public health and safety. Anything that threatens containment, directly threatens public health and safety.

DISCUSSION

EDWARDS: My question is to Mr. Bernero. With the discovery that volatile iodine is not nearly the problem that it was conjectured to be some years ago, will the NRC be considering petitions by utilities to reduce iodine-readiness requirements? I have in mind a particular utility that had to re-evaluate their auxillary building exhaust because of the additional iodine load that was conjectured on a 10 CFR 100 review.

BERNERO: Let me answer the question with a weasel word, possibly. One of the knotty things that we are working on right now is appraisal of the risk and the regulatory significance of the information. Pete Littlefield pointed out the areas of interest; siting, emergency planning, design, and so forth. There are many areas in the regulatory process where the TID source term, in particular, has crept into the fabric, and it shows up in so many ways, it is mind boggling. We are trying to sort them out right now to identify the ones where we clearly need to re-evaluate, or rebase, the regulations. With respect to siting, I don't know how many of you know we had a siting rule-making effort in progress using the old source terms. Basically, the rule making conclusion was that the existing siting standard, Regulatory Guide 4.7, is good enough; don't bother to change it. With the new source terms, you can easily support that conclusion. In fact, you might even entertain the idea of less restricted siting criteria. But the tough ones, and the really costly ones, are going to be things just like that (carbon filters, readiness of particular plant features, satisfaction of technical specifications, containment leakage requirements). Everything you can trace back to the TID source term has got to be under question. Everything related to NUREG-0956, which I mentioned yesterday, is subject to challenge. What we are trying to do in the first document, NUREG-0956, is to identify for public comment those areas that are appropriate for that kind of reconsideration.

SGALAMBRO: Mr. Bernero and Mr. Littlefield concluded their presentation with confidence in the primary containment. From this point of view, the primary containment integrity is not in doubt. My question is, in the new study that Mr. Bernero reported there is an accident sequence in which the containment integrity is not available. Because we know that the standby gas treatment system is not useful in this case, what will be the action with some kind of containment venting? In the past, Sandia Laboratories has initiated some sort of standard on this subject.

BERNERO: The calculations done by Dr. Gieseke and his colleagues are calculations made under specific conditions where the containment fails in a certain way, and their attention is on how fission products move, given that scenario. In our evaluation, NUREG 0956 I referred to, we are drawing on other work being covered in separate reports. It is re-examining how containments are challenged, that is, what we call containment loadings, pressure, temperature, hydrogen, that sort of thing. And examining the mechanical response of the containment, i.e., does it leak before it breaks or does it go

up to a burst pressure? In NUREG-0956, we are describing the risk of the plant, taking into account whether or not the containment fails, and how often it would fail one way or the other way. I would point out that in U.S. reactors, we have many designs. It is clear that some have containments that are much better than others, much less likely to fail.

WILHELM: In calculations of the environmental burden caused by serious accidents of the Three Mile Island type, we see a steep decrease in the magnitude of the assumptions made about the environmental burden when handling a system made up of iodine, water, steam, iodide particles, other fission products, and taking into account three different forms of iodine: particulate iodine, elementary iodine, and organic iodine. All the measurements are done with methyl iodide and give a result for organic iodine alone We have heard, here, the results of calculations of what will be airborne and what will be released. I, personally, think we may be able to reduce the source terms, maybe by an order of magnitude, maybe more. However, all the experiments that are done, are mostly done in a very simplistic way. Experiments are performed with elementary iodine and experiments are performed with methyl iodide, but when you look at what really happens in a reactor, when you look at the decontamination factors you get in practice, and when you look in the literature, you find very few figures for the decontamination factors of reactor-borne iodine. We know there are tens of thousands of figures for tests with clean and synthetic iodine compounds, but are we sure that they cover the real problem? Do we know what the compounds will be when, for example, in a severe reactor accident, the core melts through the pressure container and reacts with the concrete? Or when we have organics which will burn? Or when we have high radiation levels that generate radicals that will react with iodine? Do we really know what compounds will then be in the air? Do we not, now, use overly simple calculations and models? Are we really not aware of the different forms we could have? Do we know what happens when we have a fire in a reactor and there is iodine in the air, or when plastics burn, and things like that? I mean, are we really able to give an exact answer? That is only one question. The second question is, when you have an accident, you can calculate the sedimentation of particles, but what happens if you have a crack in your containment, even a very small one? Or, if you loose all your coolant and there is no more water to condense? That means that the source term of the first thousand minutes or, maybe, two thousand minutes, won't be the source term after three or five days. I am quite sure that we are able to come up with a source term, but I think we should do it very seriously. My question is, do we really have the knowledge at the moment? I doubt this, especially after the last experience we had.

KOVACH, J.L.: An accident, by definition, is an unforeseen event. Therefore, I don't think we will ever known exactly how an accident happens. If we did, we wouldn't have to experience the accident.

GIESEKE: For the first part of your question, we have made aerosol calculations, but we also looked at some of the measurements made at Three Mile Isalnd and the results of some experiments done at Oak Ridge. After someone went through all the material for us, we came to the conclusion as a sort of bottom line on reductions, that is is likely that some volatile iodides will come into the containment in time; perhaps, out of water. We thought it likely that it would be of the order of a 5×10^{-4} fraction of the fuel inventory. That is a little lower than some people talk about for methyl iodide. We tried to put footnotes in all our tables where we show lower numbers, to indicate that it does not include this material, and we give some backup for this assumption in the text.

Re-evolution is a question that I think is coming to the front again. Re-evolution from decay heating in the containment is certainly an issue for the reactor coolent system design. I expect it will be carried over to the containment over some period of time, and there will probably be calculations made of that effect.

LITTLEFIELD: You mentioned the source term in the containment two to three days after the accident. From a utility's point of view, the plant is already destroyed, and from a public safety point of view, it ought to be possible to evacuate the sites surrounding the plant by then. I am not quite sure why we care what the source term will be in the containment two to three days after this kind of event.

KOVACH, J.L.: I have one question. I recollect that Gordano Burno was burned for saying, "the earth is round". Since then, we know that he was really right. How many people feel the technical arguments will be hanged, while we know that the statute will be revoked anyway? When can we start to see more refined values for designing the various processes that we use and the new criteria we must satisfy? Are we talking about a year or two basis? I remember some very optimistic remarks shortly after Three Mile Island, that, within a few months, we would have revised regulatory guides. I am now asking what is a realistic date when we can expect changes, not only in the NUREGs but also in the regulatory guides that are now full of the old TID numbers.

BERNERO: As I said, we expect to publish the report, NUREG-0956, which identifies the risks and the regulatory significance of this new information at the beginning of next year, 1985. I hope that we are well on our way, by then, toward taking appropriate action on the key things; in particular, emergency preparedness and engineered safety featured design. I think due to the complexity of the engineered safety feature requirements that it would be false to promise complete revision in a year or so. I think it will take at least several years to bring complete order because the source term is so deeply threaded through all of the regulatory requirements. Let me make one precautionary statement, I have spent a good deal of my career in probablistic risk and analysis, and I think we can learn a great deal from probablistic risk analysis about nuclear safety, but no one

should be so foolish as to think that you can regulate nuclear safety with probablistic risk analysis. If you try, you will have my arm waver and your arm waver arguing about probablities, neither one of you talking about safety, and neither one of you getting anything done. I think we are going to have to live with this insight and live with the discomfort of erroneous regulation, i.e., poorly founded regulation, for a little while. I think it will take several years to sort that out. In some cases, you won't have to change regulations. The emergency planning radius is just that, 10 miles. There is nothing wrong with planning for ten miles. It is this insane idea that people have, that you automatically have to evacuate the ten miles. You don't even need a new source term to know that is silly. The real attention for public protection by evacuation, or sheltering, or something like that, is at two miles, or one mile. There, you don't even have to change your regulation, you have to change your preception. We have a preception that is alive in the land today that ten miles is not enough, that for some plants we should have a planning radius of twenty miles, or thirty miles. And this is what we have to change, the preception. But in the engineered safety features, where you people have such a significant role, it just isn't easy to all. It pervades the whole regulatory fabric and it is a very serious problem. It will take years.

MALINAUSKAS: I would like to add a little bit to what Bob Bernero said. A mind set is a term that has been used quite extensively. A mind set developed on the chemistry of iodine, correctly or incorrectly, and on the source terms in general. To remove a mind set will take a fair amount of time, it is not going to happen overnight. We have mind sets on the other side as well, and Bob Bernero pointed to one of those when the probability of core melt was covered in the WASH-1400 report. People refused to believe that core melt accidents could occur with even that very low probability. At Three Mile Island, we saw the very same kind of mind set. We knew that between 40 and 60% of the noble gases had been released, and that cesium had been released, but until quick look No. 1 occurred, we were still talking about removing intact fuel assemblies as part of the defueling operation. So, this whole business is going to take time. We have to present sound technical arguments to the regulators in order to have changes made.

KOVACH, J.L.: I want to thank all of the panel members for their contributions. We now know what our guide lines are going to be, what direction they are going in, and we will keep our fingers crossed that changes will happen as soon as technically feasible.

Session 10

RECOVERY AND RETENTION OF AIRBORNE WASTES: PREPARATION FOR DISPOSAL

TUESDAY: August 14, 1984
CHAIRMEN: C.B. Bastin
R. Philippone
U.S. Department of Energy

OPENING REMARKS OF SESSION CHAIRMAN BASTIN:

Our session this afternoon is on Recovery and Retention of Airborne Wastes: Preparation for Disposal. As in other nuclear activities, airborne radionuclii present interesting and important challenges in their preparation for disposal. Some of these challenges may not have been fully considered by those planning to dispose of high level and transuranic wastes. The work being done for preparing airborne wastes for disposal is important. The four papers in this session cover difference aspects of this work and I am looking forward to hearing about them.

CHOICE OF MATERIALS FOR THE IMMOBILIZATION OF 85-KRYPTON IN A METALLIC MATRIX BY COMBINED ION IMPLANTATION AND SPUTTERING*

D.S. Whitmell
United Kingdom Atomic Energy Authority
AERE Harwell, Didcot, Oxfordshire, U.K.

Abstract

Immobilization in a metal matrix by combined ion implantation and sputtering promises to offer an ideal method for the containment of krypton-85 arising from the reprocessing of nuclear fuel.

A 50 kW inactive pilot plant has been built and operated to prepare a copper deposit 22 mm thick weighing 23 kg and containing over 300 litres of inactive gas. The gas incorporation rate exceeded the design figure of 0.3 litres/hour and the vessel was operated at powers up to 30 kW, which corresponds to that envisaged for the industrial vessel. The power consumption was less than 100 kWh/litre. A full-scale vessel (1 m long, 0.26 m diameter) has also been tested at low power.

Samples of alternative candidate materials: stainless steel, incaloy, nickel and nickel-lanthanum have been prepared and tested. Nickel appears to be the most promising since it incorporates gas with an efficiency 70% greater than copper and also retains the gas to a temperature at least 100°C higher than copper.

An extensive range of measurements has been carried out on the gas filled matrices in order to determine the retention of the gas and the resistance to temperature, corrosion and irradiation effects. The release of gas from thick deposits as a function of temperature has been measured over periods of more than 1 year and leads to a prediction that the amount released over 100 years at a storage temperature of 150°C would be less than 0.05% from copper and nickel. No gas was released when the matrix was irradiated with 1 Mev beta or by gamma irradiation to doses up to those expected during storage for 100 years. The corrosion rates in both distilled water and brine are very low. Other properties of the matrix are also described.

Tests are being carried out with 100 Curies of radioactive krypton in order to demonstrate that the process will operate satisfactorily at the high internal beta irradiation levels that will exist in an active plant and to prepare samples containing krypton-85 for long term leakage measurements and for assessment of any effects caused by the build-up of the decay product rubidium.

Introduction

Immobilization in a metallic matrix promises to offer an ideal method for the containment of krypton-85 arising from the reprocessing of nuclear fuel. The principles of the process

*Work performed in the Indirect Action Research Programme on the Management and Storage of Radioactive Waste of the European Atomic Energy Community.

developed at Harwell[1,2] are shown in Figure 1. A glow discharge is generated between the cylindrical electrodes by applying a negative

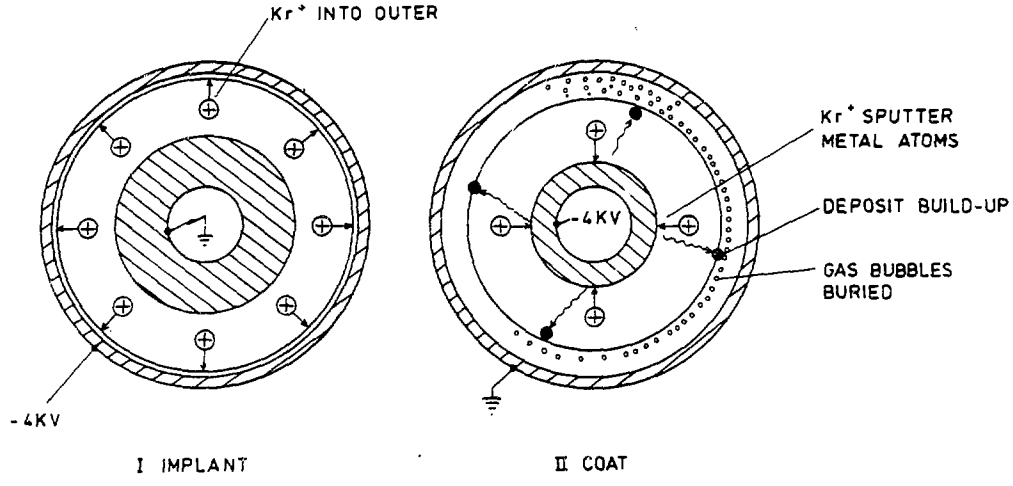

Figure 1 Principles of the process.

potential of 3-5 kV in the presence of krypton gas at a pressure of about 10 Pa. Ions produced in the discharge bombard the negative electrode causing both ion implantation and sputtering of the electrode. Gas is implanted into the outer electrode when the negative potential is applied to this electrode. The implanted gas layer is then coated with a layer of metal sputtered from the central electrode by switching the voltage to the central electrode. A thick layer of matrix containing gas at a concentration of 170 l(at STP) per litre of metal is built up by repeating the process typically a few times per second. The process is controlled by adjusting the voltages and the relative electrical charges used for each stage. When used on a plant for immobilizing radioactive krypton, the krypton will be separated from other gaseous products and the matrix laid down in a cylindrical, water cooled containment vessel. When the matrix has a suitable thickness, typically 20 mm, a layer containing inactive gas will be laid down, a sealing cap welded on, and the vessel removed without dismantling to provide a secondary container, as shown in Figure 2.

Tests have shown that the process operates without external pumps and that impurities in the gas are also incorporated, thus producing no effluent[3].

The method offers an ideal form of containment, since a wide range of metals can be used, the gas is in the form of minute gas bubbles which are stable to high temperatures, and corrosion resistance can be provided by choosing a metal which is resistant to the environmental conditions. The vessel itself provides additional protection for the required storage period of 100 years. If the matrix were to be mechanically damaged, only an insignificant fraction of the gas would be released.

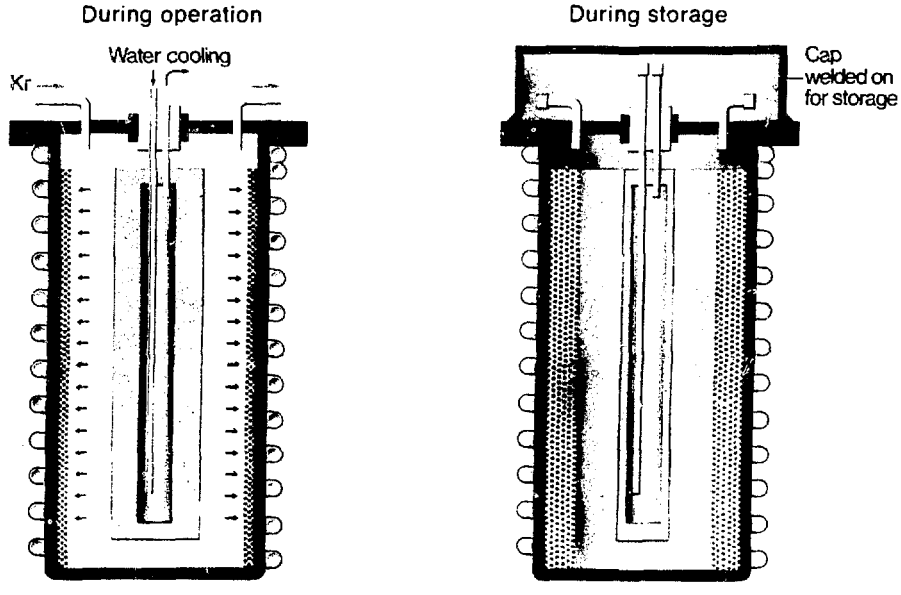

Figure 2 Envisaged industrial vessel.

The size of the vessel is not critical. Initially a vessel 0.25 m diameter, 1 m long was considered. This would incorporate gas at 1l/hour with a power input of 100 kW and have a useful lifetime of 3 months and a storage capacity of 2400 litres of activity 2.4 10^5 Curies. Larger vessels would provide correspondingly larger capacities and throughput.

Pilot Plant Demonstration

The process has been demonstrated using a half-scale, 50 kW inactive pilot plant to prepare a copper matrix 22 mm thick, weighing 23 kg and containing over 300 litres of krypton in a vessel 0.3 m long and 0.26 m diameter[4,5]. The gas incorporation rate exceeded the design figure of 0.3 litres/hour, the vessel was operated at powers up to 30 kW and the power consumption was less than 100 kWh/litre. The efficiency remained unchanged at full power even when the matrix reached the maximum thickness. The process was tested using a gas mixture containing 15% of argon and nitrogen which were incorporated at the same rate. These measurements confirmed the predicted behaviour of the envisaged plant design.

An automatic control system suitable for forming the basis for the control system for an industrial plant has been developed and proved over long periods of satisfactory operation without supervision. The plant controller is monitored by a PDP-II computer which is used for data collection, analysis and for the adjustment of running parameters to give optimum plant efficiency. The electrical characteristics of a vessel 1 m long (shown in Figure 3) have been measured.

Selection of the Optimum Matrix Material

The choice of matrix material depends upon a combination of environmental resistance, thermal stability, process efficiency and other costs. Samples of copper, nickel, iron, aluminium, stainless steel, incaloy, monel, and the glassy alloy, nickel-10% lanthanum have been prepared and tested to determine the long term retention of the krypton by the matrix and its leach, corrosion and temperature resistance. Most were prepared in vessels 0.2 m long, 0.2 m diameter (shown in Figure 3).

Figure 3 Photograph of two experimental vessels. Small vessel for materials tests and 50 litre vessel.

The process worked well with all these metals except the glassy alloy Ni-La, where the presence of the rare earth appeared to modify the surface electrical characteristics severely and made the discharge unstable. The measured gas incorporation efficiencies are

shown in Figure 4 as a function of the gas implant voltage (and with the cost/implant charge ratio set to give the maximum efficiency for each metal). Nickel showed the highest efficiency (1.75 10^{-2} litres/kWh) which is significantly greater than that of copper. The improvement is even more marked when a comparison is made at the conditions to give gas concentrations of 5 atomic%, since for copper the efficiency drops from the maximum value of 1,3 to about 1.0 10^{-2} litre/kWh whereas the nickel remains at 1.75 10^{-2} litres/kWh. The improvement in efficiency of nickel over copper represents a significant improvement in the requirements for an industrial plant, not only in terms of the savings in electrical consumption but also in the number of vessels required on line. For a plant reprocessing

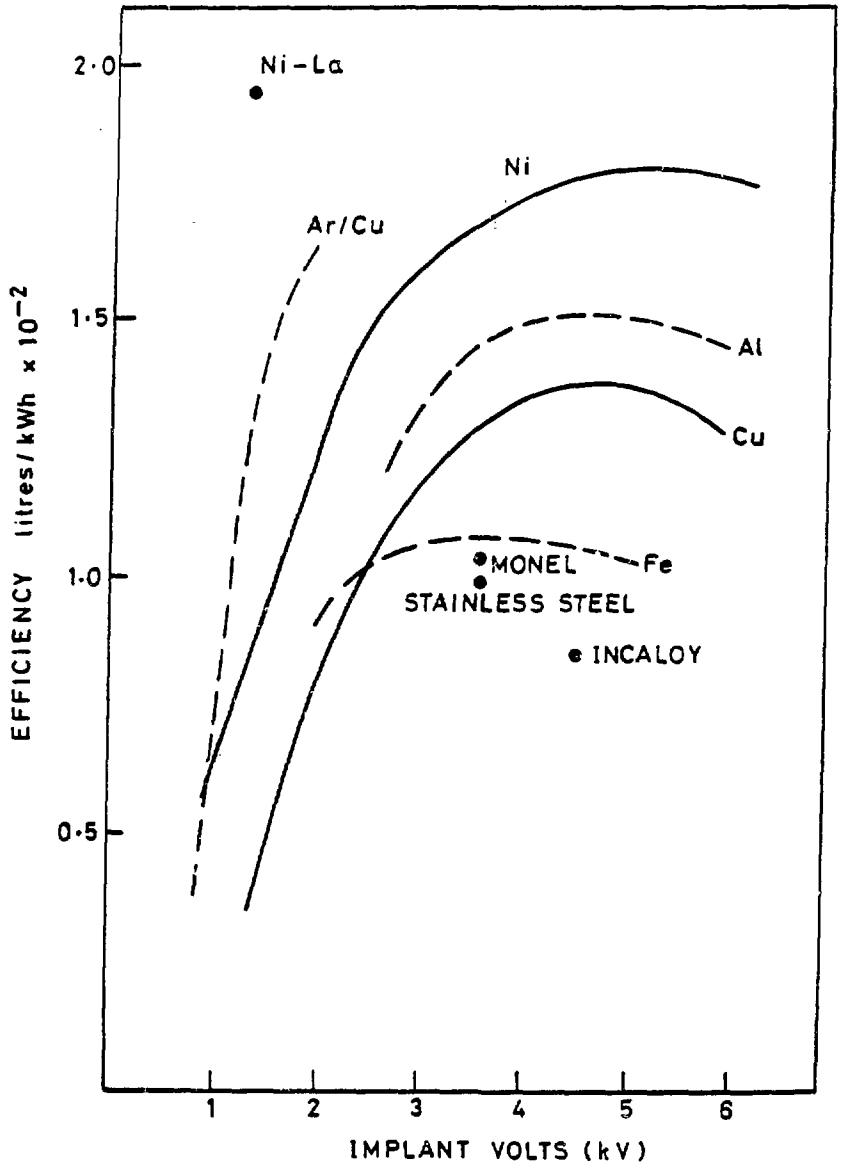

Figure 4 Gas incorporation efficiency for various metals as a function of voltage.

1000 tonne/year, the use of nickel rather than copper would result in a reduction of power consumption from 0.8 MW to 0.5 MW and the number of 50 litre vessels from 8 to 5.

Assessment of the Matrix and its Physical Properties

An extensive range of measurements have been carried out on the gas-filled matrices in order to determine the retention of the gas and the resistance to temperature, corrosion and irradiation effects. The physical properties have also been measured since the material is unique.

Corrosion tests were carried out on copper and nickel in water and brine. The weight losses of the copper and nickel in distilled water at 100°C were found to be only 0.003% and 0.03% per year respectively. The corrosion rates in brine at 90°C in the presence of oxygen were 1% and 0.1% per year respectively.

The release of gas as a function of temperature has been measured from the thick copper matrix for 1 year and the nickel measurements are still continuing. The gas release follows a diffusion controlled dependence after an initial incubation period, with the total amount increasing with the square root of time (Figure 5). Extrapolation of the results has led to a prediction that the amount released from copper during storage for 100 years at a temperature of 150°C would be less than 0.05%. Even at 300°C the amount released will be less than 1%. The early results of gas release from nickel indicate that the thermal stability will be greater and that the equivalent temperature for a given amount of release will be at least 100°C higher.

Metallurgical examination showed that the matrix contains a very high density of minute bubles (1 to 2 nm diameter) in grains of typical size 0.5 μm. When the matrix is heated above 400°C the gas bubbles in the grain boundary grow, agglomerate and form long pipes of gas which finally intersect the surface (Figures 6 and 7). Gas release measurements on copper over short periods (i.e. ~ 410 hours) show that at low temperatures (less than 400°C) the amount of release is very small and falls with time, following a 1/t dependence, which is associated with a single jump release from surface sites. At higher temperatures the release rate initially falls with the square root of time with a diffusive mechanism and an activation energy of about 2 eV. When the grain boundary bubbles interlink, the release rate increases markedly with bursts of gas and then, as shown in Figure 8, again start to fall. If the matrix is prepared on a hot substrate the grain and bubble sizes are increased and the gas is not released until the temperatures are about 100°C higher.

Figure 9 shows that the amount of gas released from the copper matrix by gamma irradiation was negligible for doses up to 1000 Mrad. No effects were observed when electron microscope samples were bombarded with electrons of energy and dose comparable with the total beta dose for 100 years containment. The matrix is therefore resistant to the effects of radiation emitted by Kr-85.

The production of thick gas-filled sputter deposited metal has provided a unique opportunity for those studies of the properties of

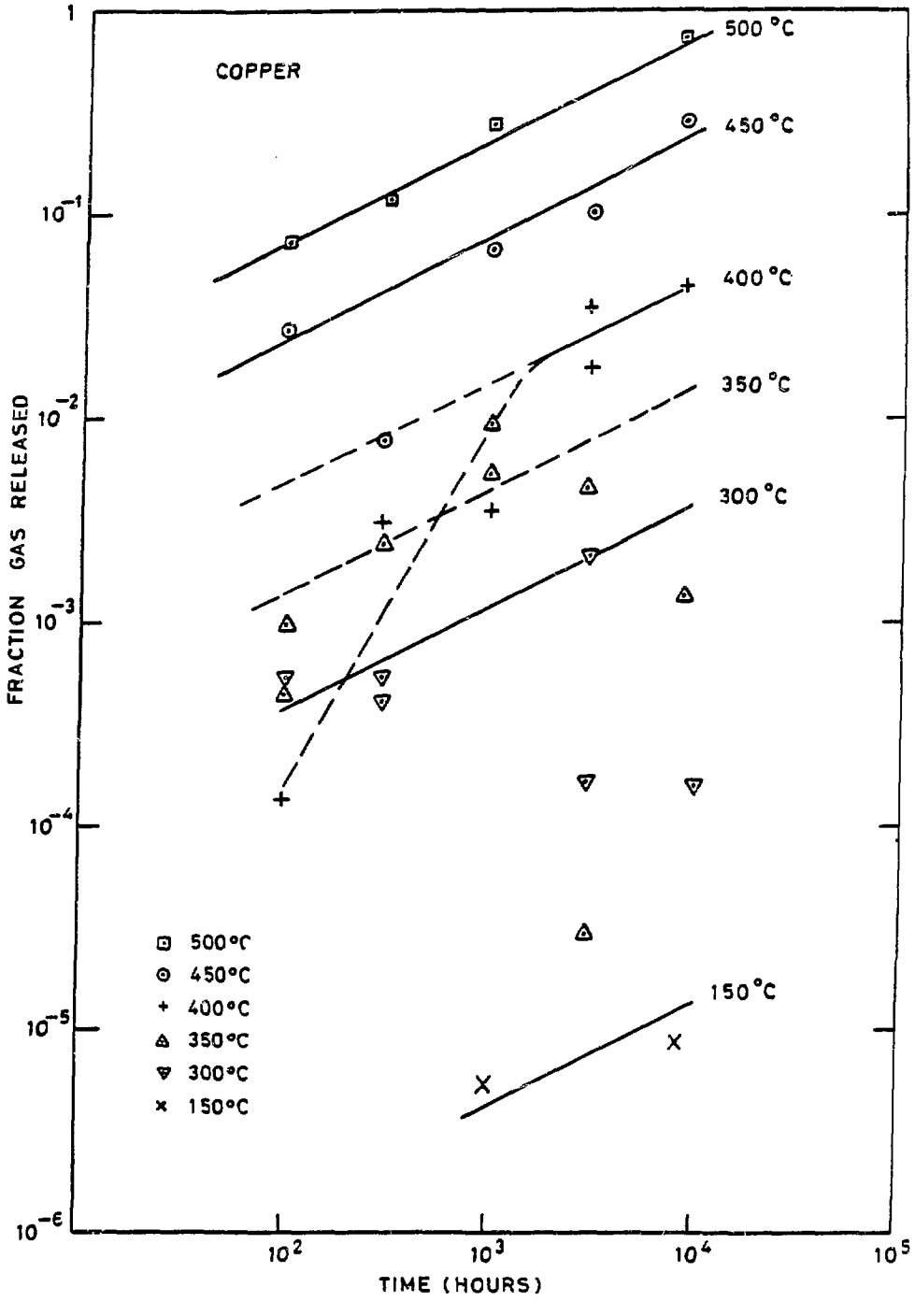

Figure 5 Fraction of gas released from copper matrix as a function of time (both scales logarithmic).

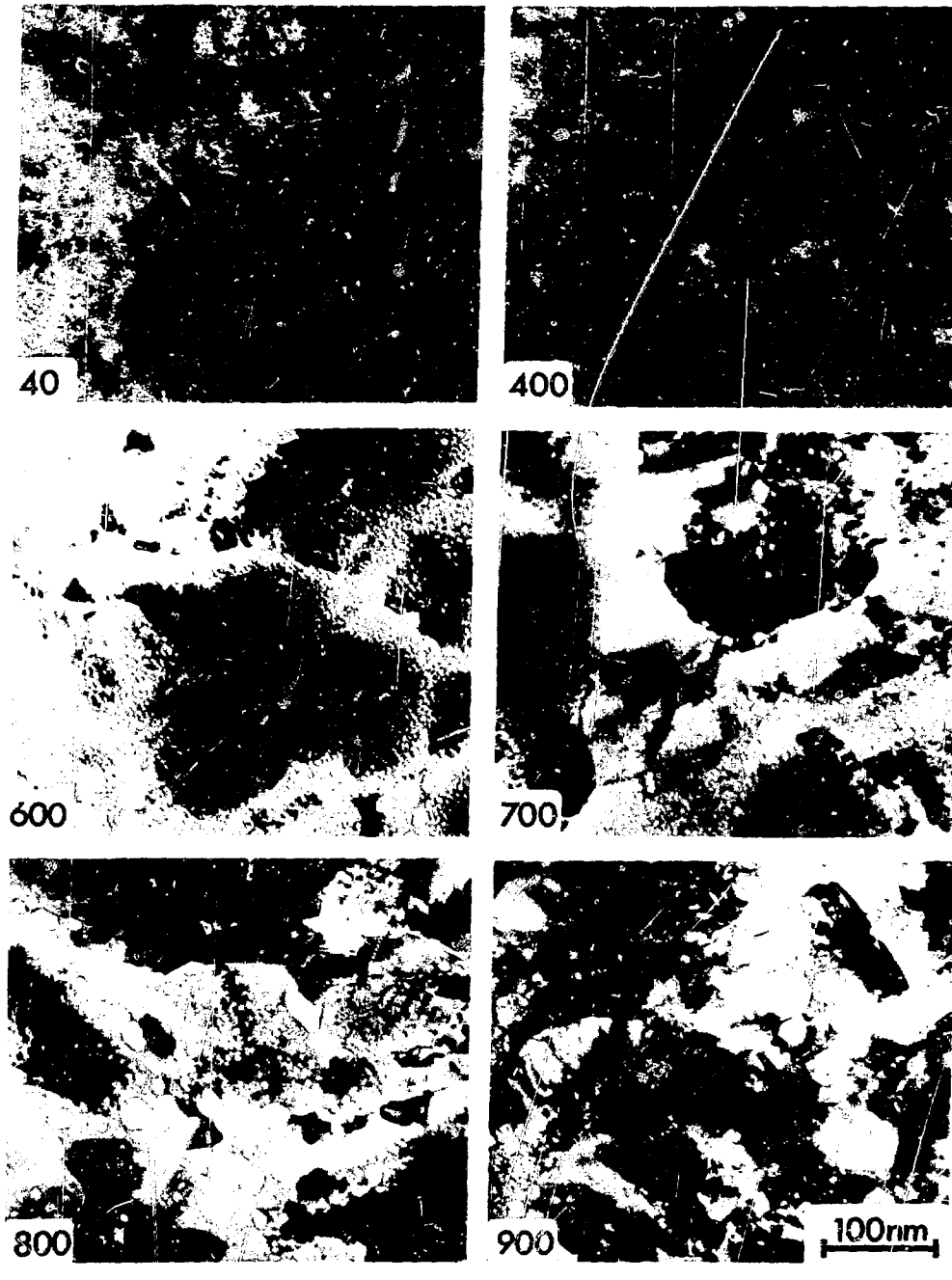

Figure 6 Transmission electron micrographs show the annealing behaviour of krypton bubbles in a nickel matrix. (Annealing carried out in the microscope.)

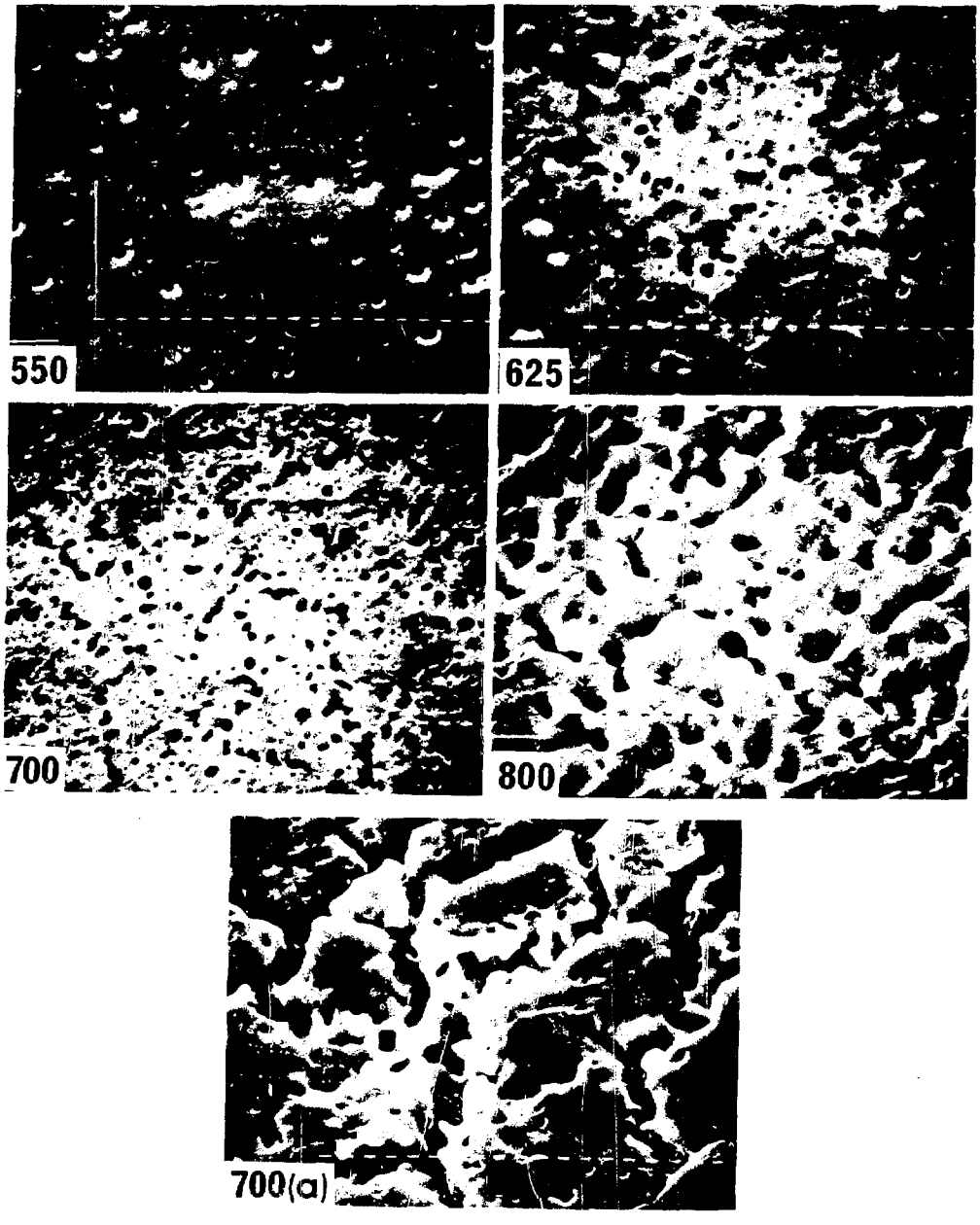

Figure 7. Scanning electron micrographs of surface of copper matrix after annealing for 1 hour at 550°C-800°C showing the development of pin holes and sponge-like structures. Markers are 1 μm. 700(a) shows enhanced effects at internal grain boundary.

gas-implanted materials which require thick samples, for example, neutron diffraction and positron annihilation.

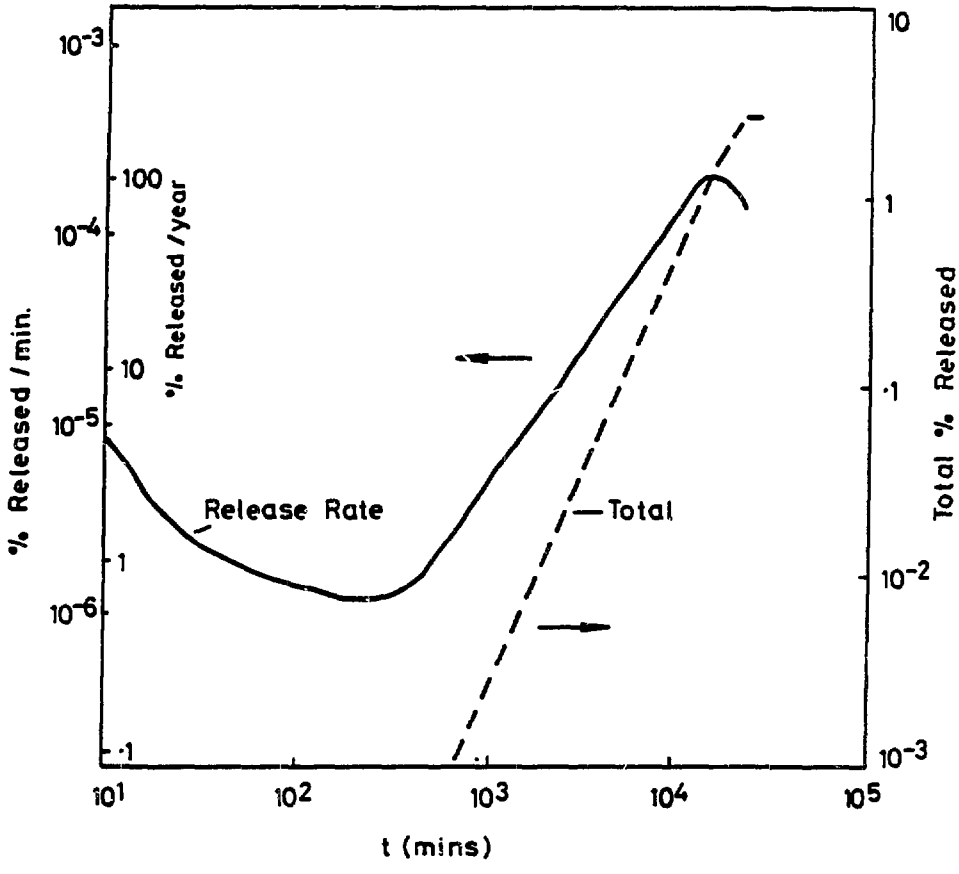

Figure 8 The initial release of gas from copper held at 400°C, showing the incubation of interlinkage of bubbles in the grain boundaries.

Details of the physical measurements may be found in Refs. (5,6). The densities of gas-filled matrices are typically 95% of the bulk parent material. X-ray diffraction gave broadened peaks and lattice parameters about 0.5% greater than the bulk material. When copper was annealed above 250°C the lattice parameter began to fall and reached the normal value at 500°C. The matrices were initially very hard (copper 330 VHN and nickel 700 VHN) but the hardness decreased on annealing. When gas was not implanted the hardness of the nickel was only 140 VHN. The thermal conductivity of the copper was about 20% of that for pure copper, and nickel about 30%, which are similar to the thermal conductivities found in conventional alloys. The thermal expansion coefficient was measured as a function of annealing temperature since it is possible that changes in bubble size and internal pressure might alter the coefficient significantly. Some variations were seen but there were also random fluctuations in the measurements. Differential scanning calometric measurements of the variation of specific heat with

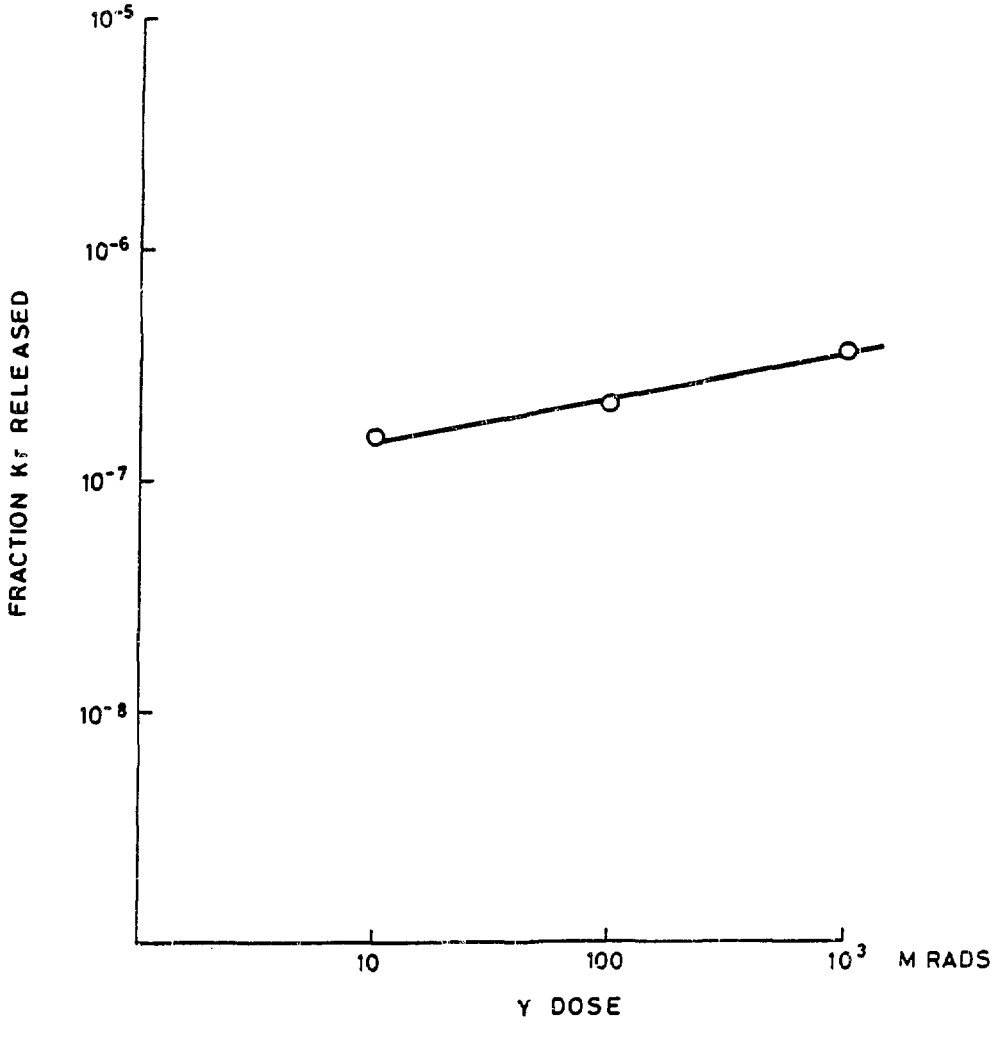

Figure 9 Logarithmic plot of gas released as a function of gamma dose, showing that the amount of gas released is negligible.

temperature showed small exothermic energy releases at 450 K, and 620 K in copper and at 490 K, 720 K and 870 K in nickel as shown in Figure 10. The low temperature peaks can be associated with stress relief, and the higher temperature peaks with the initiation of gas release. Neutron small angle scattering and positron annihilation experiments[7] have tended to confirm the electron microscope observations that most of the gas is distributed in the form of small bubbles.

Tests with Active Gas

Tests are being carried out to demonstrate that the process works equally well in the radiation levels which will develop in a fully active plant. Calculations showed that the beta radiation level inside the vessel rises rapidly as the krypton-85 is incorporated in the matrix but saturates at 80,000 R/hour when the layer is about 0.1 mm thick. The gamma dose continues to increase to give a maximum of about 4000 R/hour internally when the matrix is 20 mm thick. The external radiation level will be about 6 R/hour at 1 metre, requiring about 150 mm of lead shielding.

Preliminary experiments with active gas have already been made for a short period of time. Since the supply of Kr-85 is limited, tests are being carried out with 100 curies of Kr-85 which is sufficient to enable the internal beta levels to reach about 95% fo the saturation level. The rig, shown in Figure 11, consists of a small vessel, (0.2 m long, 0.2 m diameter), within a 50 mm lead shield and mounted upon a trolley. A layer of nickel containing inactive gas will be deposited and then the gas changed to the fully active gas and the active layer deposited. The gas will then be changed back to another inactive gas to form a surface closure layer. The vessel will then be sealed, a cap placed over the insulators to provide additional protection during transit to the store and the vessel stored for up to 5 years at 150°C using a heater wound around the vessel. Samples of the gas will be taken from the vessel to provide a sensitive method of measuring gas leakage from the matrix. Subsequently, samples of the nickel containing the active gas and its decay product, rubidium, can be examined to determine the effects of the irradiation and the formation of rubidium.

Tests into the effects of gamma will be carried out by placing gamma sources around the vessel but it is not expected that the gamma radiation will have any effect on the matrix or process.

The Design of a Full-scale Plant

Previous conceptual designs for a plant have considered process vessels 1 m long, 0.26 m diameter with a nominal volume of 50 litres so that comparisons can be made wth alternative storage methods. A vessel of this size has been tested at powers up to 50 kW in order to determine its electrical characteristics. The performance was satisfactory ad the discharge current densities were slightly greater than in the shorter vessel due to the longer electrical paths. The current density follows a relationship of the form

$$j^{\frac{1}{2}}/p = a + b.V.$$

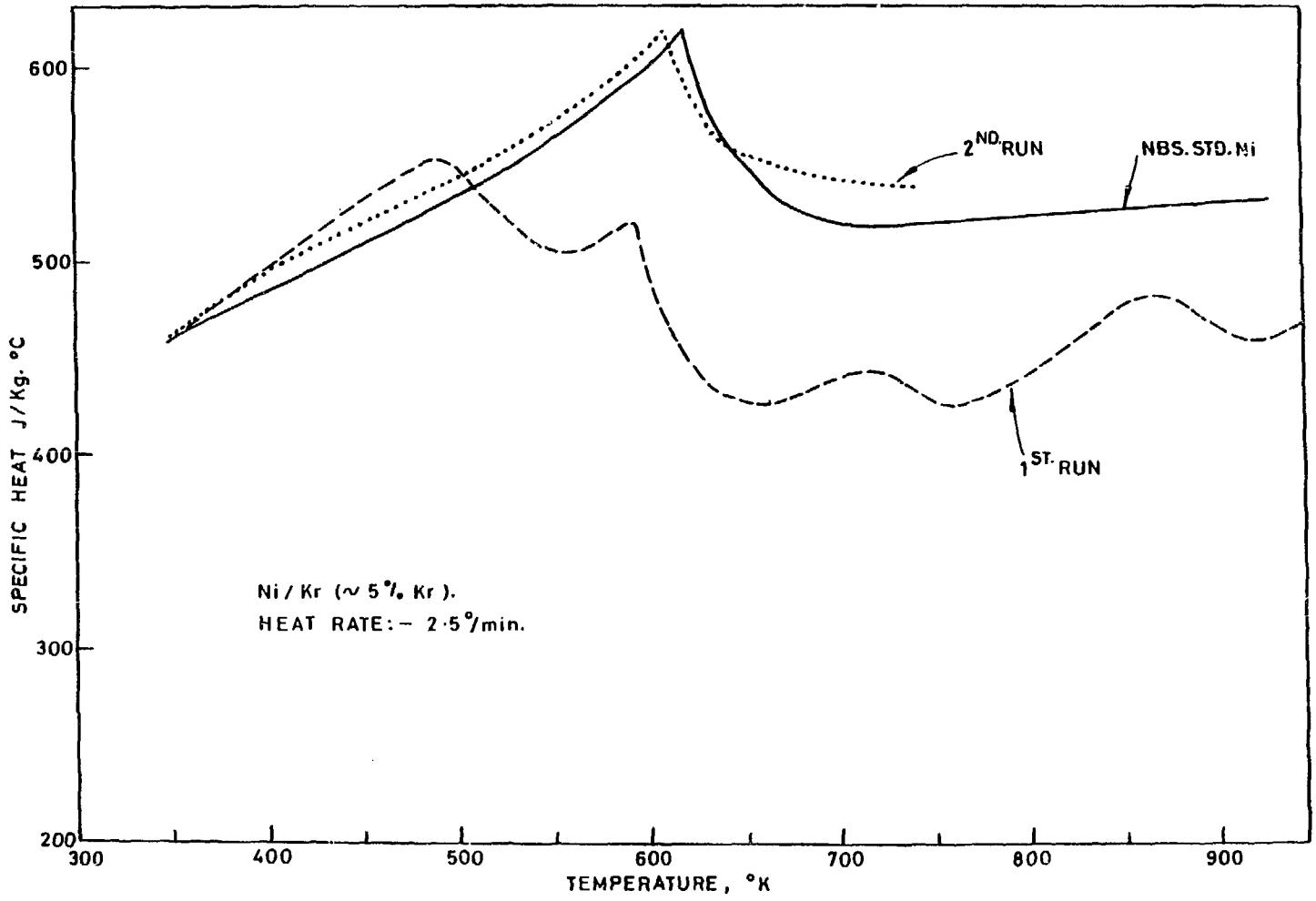

Figure 10 Differential scanning calometric measurements on nickel matrix. Heating rate 2.5°C/min. Second run obtained after heating to 730°C for 10 minutes.

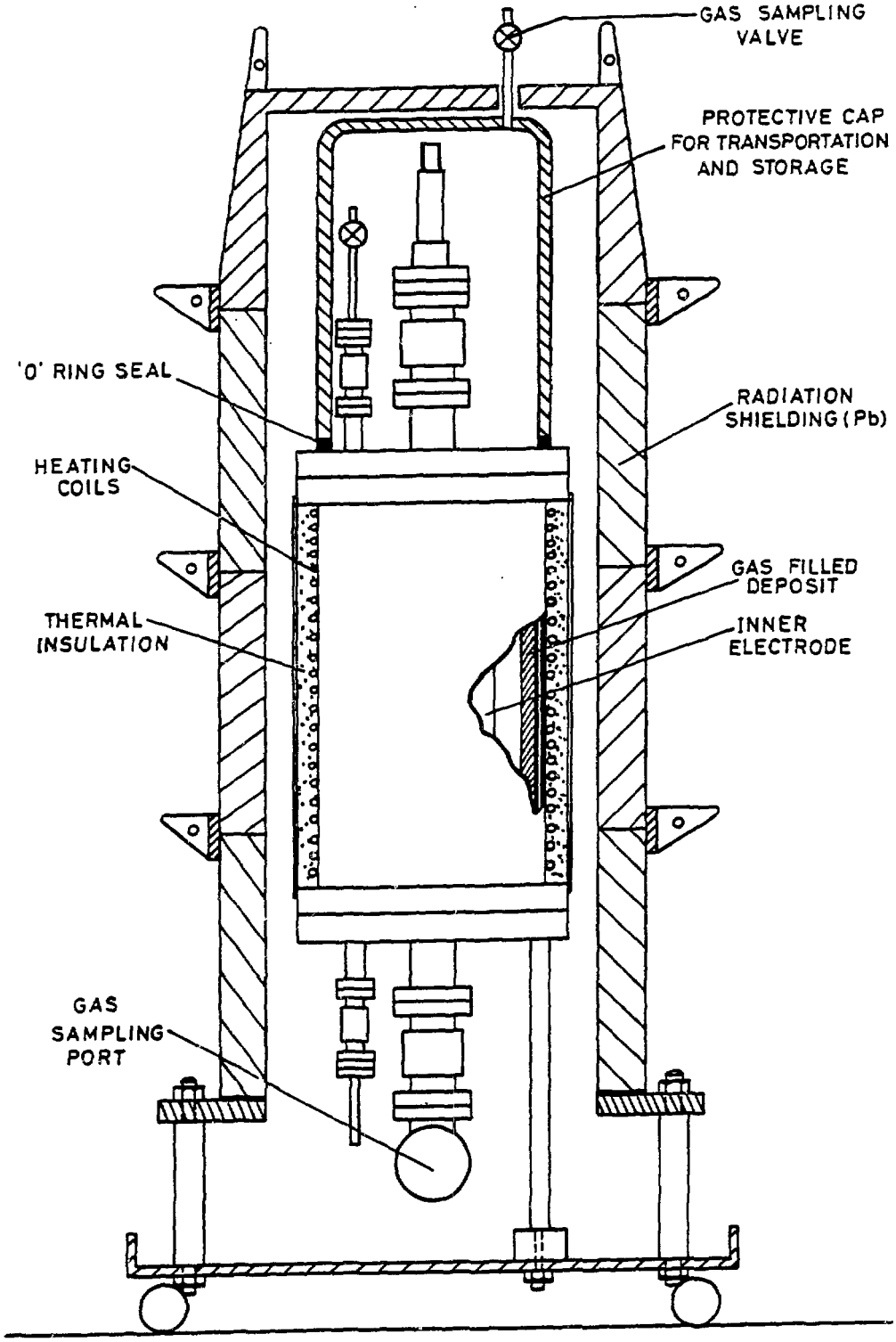

Figure 11 Schematic diagram of vessel for tests with fully active gas.

where the square root of the current density j depends upon the pressure p and the voltage V. The results indicate that even larger vessels are likely to be feasible which would reduce the number of vessels required to be on line at a large reprocessing plant. A vessel 0.4 m diameter, 1.6 m long would have a throughput 2.5 times larger. A 1000 tonne/year plant would need only 2-3 vessels on line, which would be changed every 60 days. The main operating costs are the energy costs; labour costs are low since the process can be controlled automatically and handling requirements are minimal.

Two plant concepts are being considered. The vessels could be operated in shielded cells and then transferred to a welding bay for the insulator sealing caps to be fitted. Since there will be no residual activity in the cells, the vessels could be installed manually, but remote handling will be necessary to break the electrical, coolant and gas connections at the end. In the second arrangement, vessels are placed within transportable shielding (similar to that used for the active test), with all connections brought outside the shielding. At the end of use, the shielded vessel is taken to the welding bay and removed from the trolley for welding and then moved to the storage area. This concept reduces the amount of remote handling required.

Discussion and Conclusions

The metal matrix process offers an ideal method for the immobilization of krypton arising from the reprocessing of nuclear fuel. Operation of the inactive pilot plant has demonstrated that the process is suitable and that thick matrices can be prepared. Tests indicate that vessels larger than those initially envisaged are feasible and that they would substantially reduce plant costs. The costs of the process, typically US $0.5/kg uranium, are small compared with other reprocessing and waste management costs.

The process can be used with a wide range of materials, but nickel appears to be the best of those tested, giving a high process efficiency and also good gas retention properties. The corrosion rate of nickel in brine is a factor of 10 lower than that of copper. At 90°C, the corrosion rate corresponds to a gas release rate of 0.1%/year, but it is most unlikely that this rate will be reached since the matrix will only be exposed if the outer container, which can be made from suitable materials, is so badly fractured or breached by corrosion that the whole surface of the matrix is exposed.

Nickel also offers excellent resistance to the effects of heat. Extensive tests on copper have shown that if it is held at 150°C throughout a storage time of 100 years, the total amount released from the matrix would only be 0.05%. The release from nickel is expected to be similar, since these small quantities are released from the surface regions by a single-jump mechanism rather than by bulk diffusion and can be suppressed by a surface sealing layer. Since the vessel is operated and sealed at sub atmospheric pressure, these small quantities of gas released from the matrix will be retained within the vessel and will not even raise the internal pressure to atmospheric. The behaviour of the gas at higher temperatures depends upon the previous heat treatment history. The

amount released from copper at 400°C for 380 hours, is only 2%, which is just sufficient to raise the vessel pressure to 1 bar. The corresponding equivalent temperature for nickel is about 500°C. Therefore the nickel matrix will be resistant to the effects of a fire. The gas retention can be enhanced still further by increasing slightly the temperature at which the matrix is formed, since the gas bubbles are then larger and less mobile.

Acknowledgements

Many colleagues have contributed to the programme and their help is gratefully acknowledged: M.J.S. Smith, R.W. Williamson, J. Shailes, S.J. Lane, J.H. Evans, J. Muncie, D.J. Mazey, K.A. Boult, F. Cullen, M.D. Poole, R. Hawes, K.E. Gilchrist, R. Sinclair and S. Third.

References

1. Nelson, R.S., et al., British Patent No. 1485266 (1974).
2. Whitmell, D.S., Williamson, R. and Nelson, R.S., Proceedings 'IPAT 77', CEP Consultants, 202, Edinburgh 1977.
3. Whitmell, D.S., Nelson, R.S., Williamson, R. and Smith, M.J.S., Nuclear Energy, 13, 349 (1979).
4. Whitmell, D.S., Nuclear Energy, 21, 181 (1982).
5. Whitmell, D.S., Nelson, R.S., Williamson, R., Smith, M.J.S. and Bauer, G.J., European Applied Research Reports, 5, 513 (1983).
6. Williamson, R. and Whitmell, D.S., To be published.
7. Eldrup, M. and Evans, J.H., J. Phys. F: Met. Phys., 12, 265 (1982).

OFF-GAS TREATMENT AND CHARACTERIZATION FOR A RADIOACTIVE IN SITU VITRIFICATION TEST*

K. H. Oma and C. L. Timmerman
Pacific Northwest Laboratory**
Richland, Washington 99352

Dup

Abstract

Effluents released to the off gas during the in situ vitrification (ISV) of a test site have been characterized by Pacific Northwest Laboratory. The site consisted of a 19 L waste package of soil containing 600 nCi/g transuranic and 30,000 nCi/g mixed fission products surrounded by uncontaminated soil. Radioactive isotopes present in the package were ^{241}Am, $^{238/239}Pu$, ^{137}Cs, ^{106}Ru, ^{90}Sr, and ^{60}Co. The ISV process melted the waste package and surrounding soil and immobilized the radionuclides in place, producing a durable, 8.6 metric ton glass and crystalline monolith. The test successfully demonstrated that the process provides containment of radioactive material. No release to the environment was detected during processing or cooldown.

Due to the high temperatures during processing, some gases were released into the off-gas hood that was placed over the test site. The hood was maintained at a slight negative pressure to contain any volatile or entrained material during processing. Gases passed from the hood to an off-gas treatment system where they were treated using a venturi-ejector scrubber, a tandem nozzle gas cleaner scrubber followed by a condenser, heater, and two stages of HEPA filters. The off-gas treatment system is located in the semi-trailer to allow transport of the process to other potential test sites.

Retention of all radionuclides by the vitrified zone was greater than 99%. Soil-to-off-gas decontamination factors (DFs) for transuranic elements averaged greater than 4000 and for fission products, DFs ranged from 130 for ^{137}Cs to 3100 for ^{90}Sr.

I. Introduction

The Department of Energy has contracted Pacific Northwest Laboratory (PNL) to develop the in situ vitrification (ISV) process as a potential in-place stabilization technique for immobilizing selected zones in radioactively contaminated soil sites. The process melts the soil to produce a durable glass and crystalline waste form.[1-3] In the process, an electric current is established between electrodes inserted in the soil. A hood is placed over the vitrification zone to contain any gas or particulates that may be released. The ISV processing sequence is illustrated in Figure 1.

* Work supported by the U.S. Department of Energy under Contract DE-AC06-76RLO 1830.
** Operated for the U.S. Department of Energy by Battelle Memorial Institute.

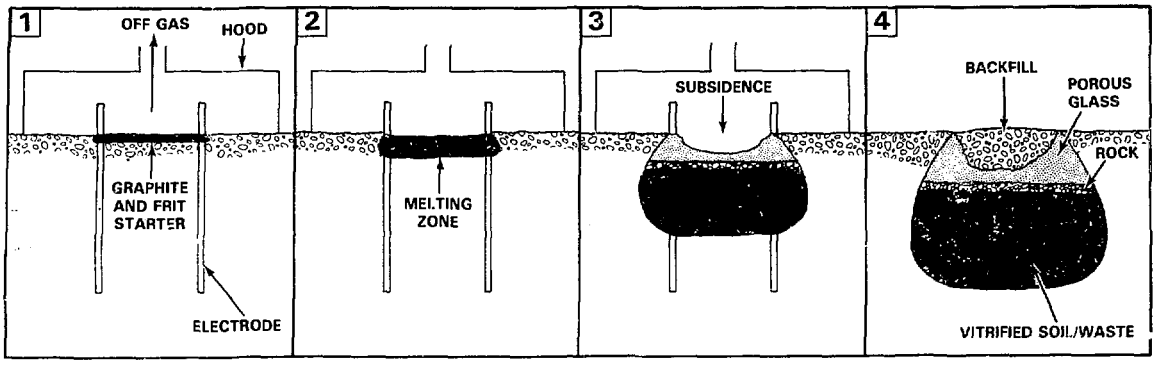

Figure 1. Process sequence of in situ vitrification.

A pilot-scale radioactive test was conducted in which a make-up site containing known quantities of ^{241}Am, $^{238/239}Pu$, ^{137}Cs, ^{106}Ru, ^{90}Sr, and ^{60}Co was successfully vitrified. The test demonstrated the viability of ISV as a concept for immobilizing radioactively contaminated soil sites. An off-gas system mounted in a semi-trailer was used to treat the off gases released during the test. The off-gas system is a second generation design, building upon experience and a data base established during four previous pilot-scale tests[4,5] and a series of engineering-scale tests.[6] This paper describes the pilot-scale ISV system and presents an analysis of the off-gas characterization data collected during the radioactive test.

II. Pilot-Scale ISV System Description

The pilot-scale radioactive test system, pictured in Figure 2, consists of an off-gas containment hood over the waste site and a process trailer. The off-gas hood, which is maintained at a slight negative pressure, also provides support for the four electrodes. The electrodes are inserted into the soil in a square pattern measuring 1.2 m (4 ft) on a side. The process trailer houses the off-gas treatment system, a closed loop air/glycol cooling system, a 500 kW electrode power supply and associated instrumentation for process monitoring, control and data acquisition.

The off-gas treatment system is shown schematically in Figure 3. The gases pass through a venturi-ejector scrubber and separator, a Hydro-Sonic® scrubber, separator, condenser, another separator, heater, two stages of HEPA filtration, and a blower. Liquid to the two wet scrubbers is supplied from two independent scrub recirculation tanks, each equipped with a pump and heat exchanger. Equipment layout within the process trailer is illustrated in Figure 4. All off-gas treatment components except the second stage HEPA filter and blower are housed within a containment module pictured in Figure 5. The module has gloved access and is maintained under a slight vacuum.

® Hydro-Sonics, Dallas, Texas.

Figure 2. Pilot-scale ISV hood and process trailer.

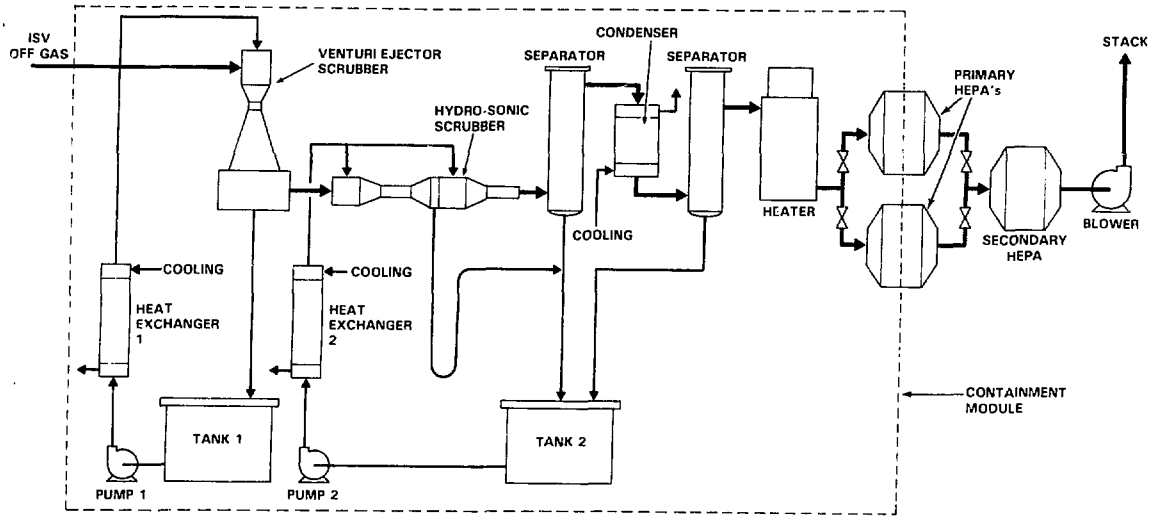

Figure 3. Off-gas system schematic for the pilot-scale ISV process.

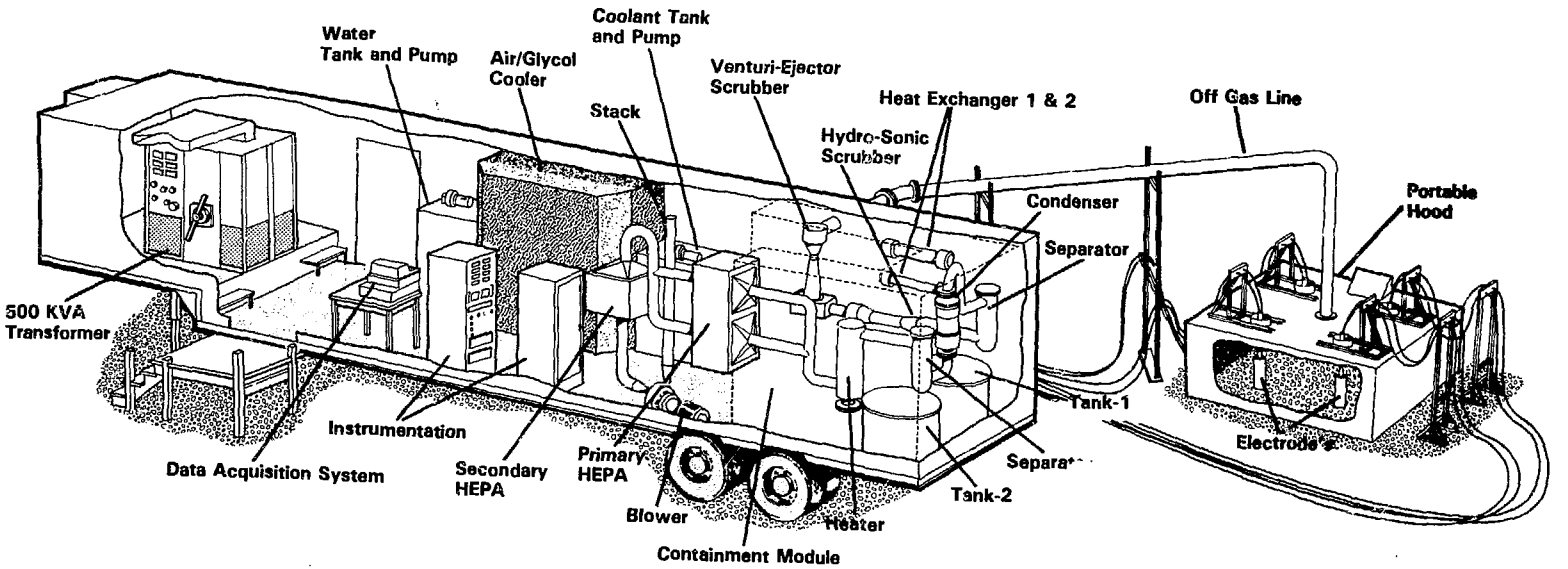

Figure 4. Cutaway view of pilot-scale ISV process trailer and hood.

Figure 5. Containment module for the off-gas treatment system

The off gas from the hood enters the venturi-ejector scrubber which serves both as a quencher and high energy scrubber for removal of particles larger than 2 μm. The gas is then passed through a two stage Hydro-Sonic® scrubber (tandem nozzle fan drive) as illustrated in Figure 6. The first stage condenses vapors, removes larger particles and initiates growth of the finer particles so they can be more easily captured in the second stage. High velocity gas exiting the subsonic nozzle acts to atomize the water as it is sprayed from an injection ring at the nozzle exit. This atomized water captures the particles as the off gas and water continue down the length of the mixing tube. The droplets containing the captured particles are then removed by a vane separator and drained back into the scrub tank. The unit is designed to remove 90% or more of all particles larger than 0.5 μm dia when operated at a differential pressure of 127 cm (50 in.) water. The particle removal efficiency increases with an increase in pressure differential.

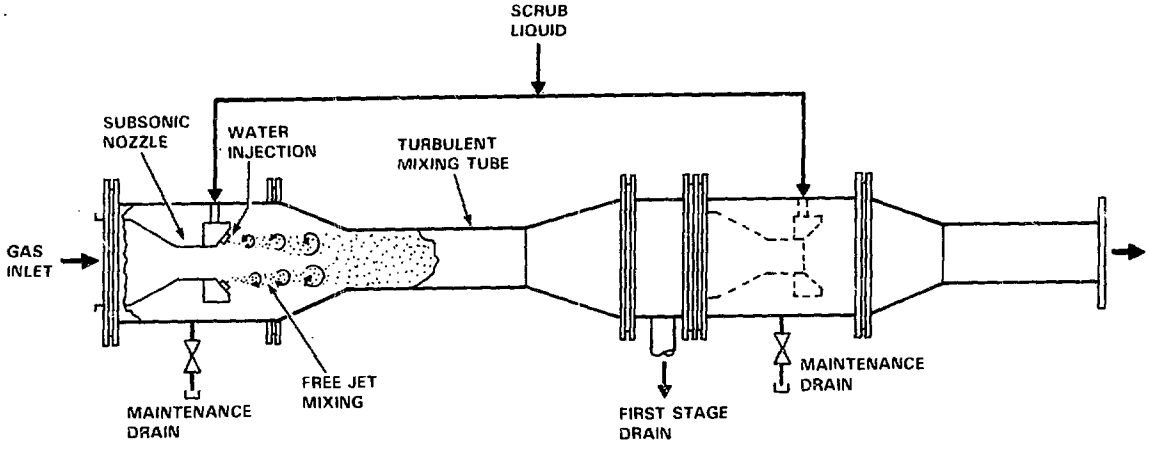

Figure 6. Tandem nozzle Hydro-Sonic (Hydro-Sonics, Dallas, Texas) scrubber.

Additional water is removed from the gas stream by a condenser and separator. The gases are then reheated approximately 25°C in a 39 kW heater to prevent condensate carryover to the filters.

The primary stage of filtration consists of two 0.61 x 0.61 x 0.29 m (24 x 24, 11.5 in.) HEPA filters in parallel. During operation, one filter is used and the other remains as a backup in case the active filter becomes loaded. A primary filter can be changed out during operation without interrupting the process. The secondary HEPA filter acts as a backup in case a primary filter fails.

Heat is removed from the off gas by a closed loop cooling system, which consists of an air/liquid heat exchanger, a coolant storage tank, and a pump. A 50% water/ethylene glycol mix is pumped from the storage tank through the shell side of the condenser and the two scrub solution heat exchangers, then through the air/liquid exchanger, where heat is removed from the coolant.

III. Test Description

A make-up site was selected for the radioactive test in which known quantities of radionuclides were introduced. The radioactive material, listed in Table 1, was placed in a 19 L (5 gal) container and was centrally positioned within the soil zone to be vitrified (Figure 7). One objective was to demonstrate that ISV would contain

Table 1. Waste container radionuclide inventory.

Radionuclide	Total Curies	Original Concentration nCi/g
^{241}Am	0.0095	370
^{239}Pu	0.0053	210
^{238}Pu	0.0013	70
^{137}Cs	0.020	780
^{106}Ru	0.021	820
^{90}Sr	0.680	26600
^{60}Co	0.010	390

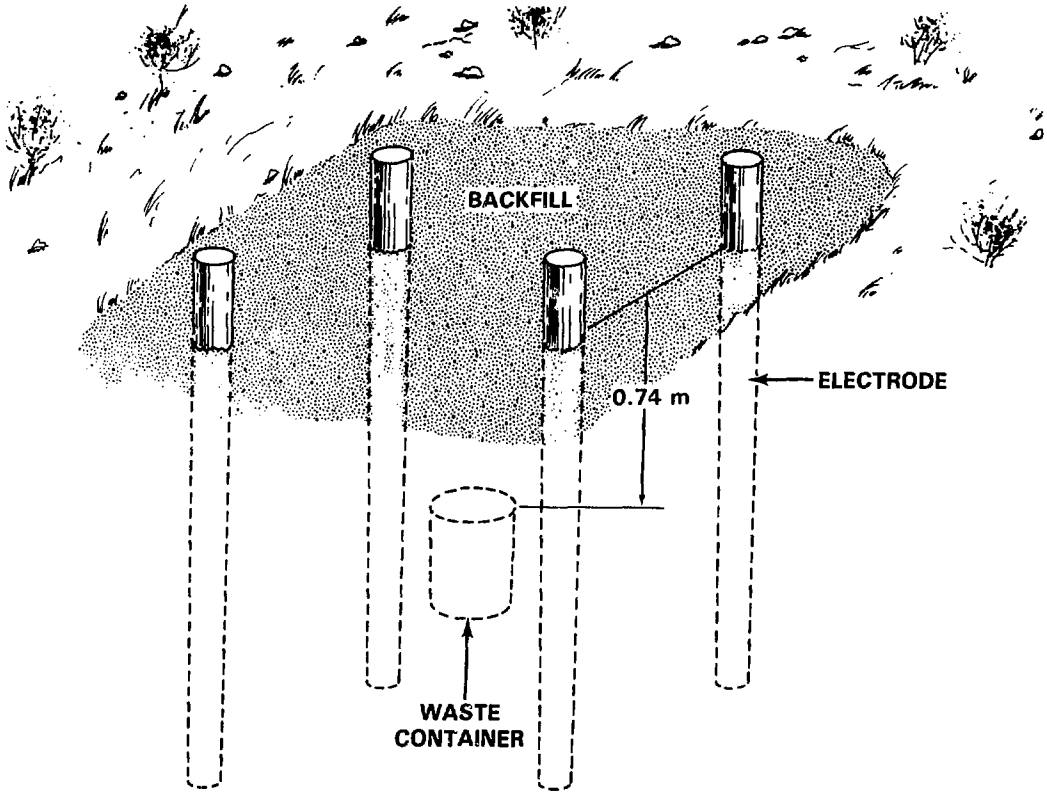

Figure 7. Waste container placement before vitrification.

and immobilize the radionuclides within the vitrified zone without release to the environment. A second objective was to determine the fractional release of radionuclides to the off gas and to determine the off-gas treatment system performance characteristics.

The radionuclide content chosen for the test was based on 100 times the detection limits of the radiochemical analytical equipment for each radionuclide excluding ^{241}Am. Predicted radionuclide releases to the off-gas system and predicted distribution within the vitrified block were used in conjunction with the hundred fold increase over the detection limits to establish the minimum amount of each radionuclide added. Americium-241 was present since it occurs as a decay product of ^{241}Pu. Post test radiochemical analysis included ^{241}Am even though the quantity present in the test did not meet the 100-fold increase criteria to determine the minimum quantity.

IV. Off-gas Analysis

Radionuclide analysis, particle mass analysis and gas composition analysis were performed to characterize off-gas effluents from the test. Figure 8 illustrates the off-gas system and associated sampling locations for radionuclides, particulates, and gaseous constituents. Numbers 1 through 8 indicate positions of the radionuclide samples.

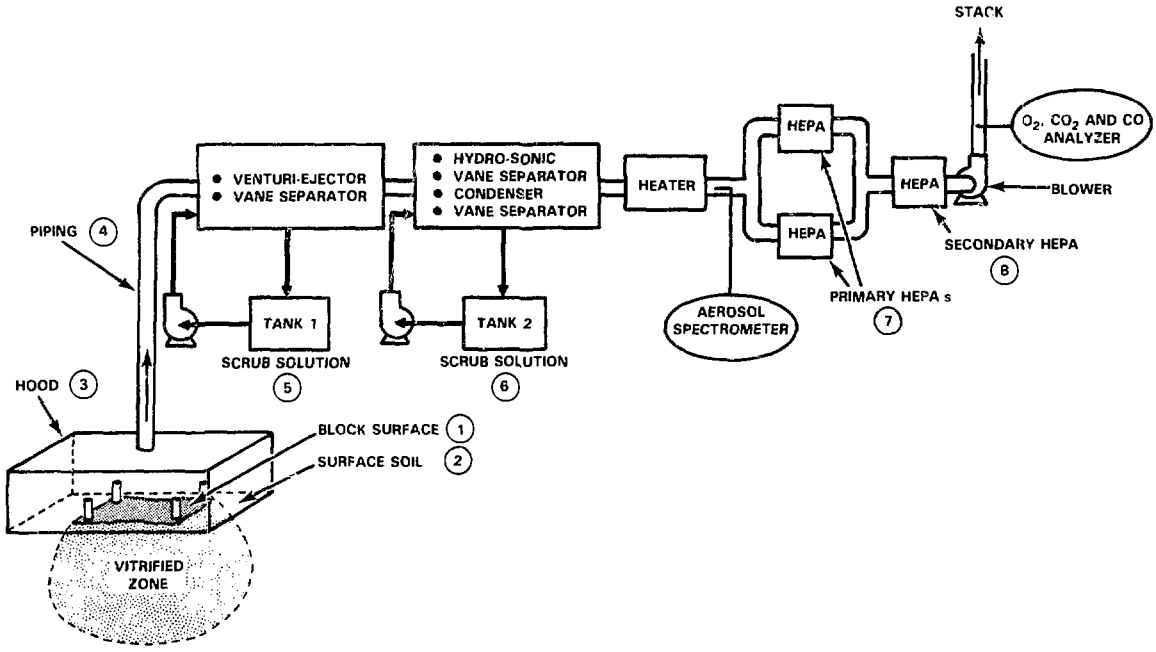

Figure 8. Off-gas system with the associated sampling positions.

Decontamination Factors

Soil-to-off-gas decontamination factors (DFs)* were calculated from alpha, beta, and gamma analysis of samples taken from points shown in Figure 8. The scrub solution was sampled periodically during the test. Samples of the block surface (smearable), surface soil, hood, piping, and HEPA filters were taken during the post-run analysis period. The analytical results calculated from the sampling data are presented in Table 2.

Table 2. Off-gas system radionuclide distribution.

Sample Location	Radionuclide Activity, Ci					
	^{241}Am	^{tot}Pu	^{137}Cs	^{106}Ru	^{90}Sr	^{60}Co
Original	9.5 E-3	7.1 E-3	2.0 E-2	2.1 E-2	6.8 E-1	1.0 E-2
1. Block surface	2.6 E-8	5.8 E-10	2.5 E-7	9.7 E-8	9.5 E-8	2.5 E-8
2. Surface soil	6.3 E-10	4.3 E-10	1.3 E-8	5.5 E-9	7.0 E-9	9.1 E-10
3. Hood	1.8 E-7	7.1 E-8	2.6 E-6	3.2 E-6	9.5 E-6	1.7 E-7
4. Piping	7.0 E-8	4.0 E-8	7.1 E-6	4.3 E-7	7.4 E-6	7.8 E-7
5. Tk 1 soln	5.2 E-7	1.4 E-6	2.7 E-5	9.3 E-6	1.9 E-4	1.3 E-6
6. Tk 2 soln	4.4 E-9	4.4 E-8	1.1 E-4	2.4 E-5	9.3 E-6	3.0 E-6
7. Primary HEPA	(a)	1.5 E-8	5.0 E-6	1.1 E-6	2.3 E-7	1.8 E-7
8. Secondary HEPA	(b)	(b)	<1.0 E-9[a]	<2.2 E-8[a]	(b)	<3.6 E-9[a]

(a) Not detected. Values shown are based on analytical detection limits.
(b) Analysis of these nonvolatile species was not performed.

For each sample analyzed, the entire sample (liquid and solid residue) was counted to determine the quantity of the gamma emitting radionuclides-^{241}Am, ^{137}Cs, ^{106}Ru, and ^{60}Co. Then an acid leach and chemical separation were performed on both the liquid and solid residue to extract Pu for alpha counting and ^{90}Sr for beta counting. The gamma scanning technique utilized an intrinsic germanium detector for counting, while a gold surface barrier silicon detector and a proportional gas flow beta counter were used for alpha and beta counting, respectively.

Table 3 shows the retention, percent release and soil-to-off-gas DF for the radionuclides in the test. Retention of all radionuclides by the vitrified zone was greater than 99%. Decontamination factors for transuranic elements averaged greater than 4×10^3. Fission product DFs ranged from 1.3×10^2 for the more volatile ^{137}Cs to 3.1×10^3 for ^{90}Sr.

Off-gas releases of the more volatile fission products (^{137}Cs, ^{106}Ru, and ^{60}Co) are a function of gas releases as the melt passes through the contaminated soil and of the relative volatility of each radionuclide. Data also show that once the waste associated with these radionuclides has been vitrified, radionuclide releases to the off-gas system are relatively minor. The releases of ^{137}Cs, ^{106}Ru,

* DF = reciprocal of the fraction of material released.

Table 3. Radionuclide retention and releases.

Radionuclide	Retention by Vitrified soil, %	Release to Off Gas, %	Soil-to-Off-Gas DF
(transuranics)			
^{241}Am	99.992	0.008	1.2×10^4
total Pu	99.978	0.022	4.5×10^3
(fission products)			
^{137}Cs	99.23	0.77	1.3×10^2
^{106}Ru	99.82	0.18	5.5×10^2
^{90}Sr	99.968	0.032	3.1×10^3
^{60}Co	99.945	0.055	1.8×10^3

and ^{60}Co from the molten soil to the hood area, piping, scrubbers, and HEPA filter are presented as a function of run time in Figure 9. Low quantities of each radionuclide began to appear in the first scrub samples at 2.1 hours into the run when the molten zone first contacted the waste container. The melt zone reached the bottom of the container at approximately nine hours into the test. Once the radionuclides were incorporated into the molten soil, the element releases began to slow down as depicted by the reduced slope of the Figure 9 curves. The curves indicate that the release rate is highest when the waste material is being actively melted. The higher release rate to the off gas during melting of the waste container can be attributed to

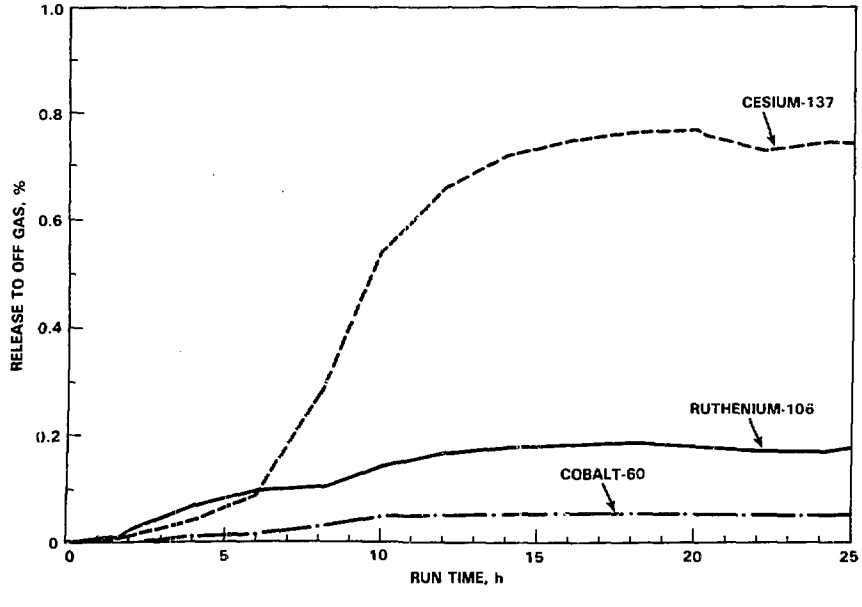

Figure 9. Cesium, ruthenium and cobalt released to the off-gas system.

combustion of the container and the reaction of the radionuclides from a nitrate to an oxide. It is expected that gases released during these reactions increase entrainment of particles and create a more direct pathway to the surface for release of the more volatile elements. This effect was seen to a greater extent during previous pilot-scale tests with combustibles and chemical nitrates.[4] The relative volatility of each radionuclide is also represented in Figure 9 by the range of the releases, Cs being the most volatile and Co exhibiting the lower release potential.

Releases of off-gas particulates (Pu and ^{90}Sr) occur only during the initial melt contact of the contaminated zone and the gas release associated with vitrifying gas generating wastes such as combustibles or nitrates. Similar cumulative percent release data for ^{241}Am, total Pu, and ^{90}Sr are presented in Figure 10. Plutonium and Sr releases both peaked 4 hours into the run and appeared to decrease to a steady value later in the test. This apparent decrease (approximately a factor of 2) is not real and in fact the total radionuclides collected in the off gas system increases slightly. The decrease indicated in Figures 10 and 11 is apparently caused by a decrease in the leaching efficiency of the extractive chemistry technique applied to the solid phase residue used to separate and analyze these radionuclides. A similar leaching extraction is used for both the Pu and Sr. This technique was not adequate to remove these elements from the solid phase prior to the alpha and beta counting. When leachates from the same samples were analyzed for gamma emitting radionuclides, a

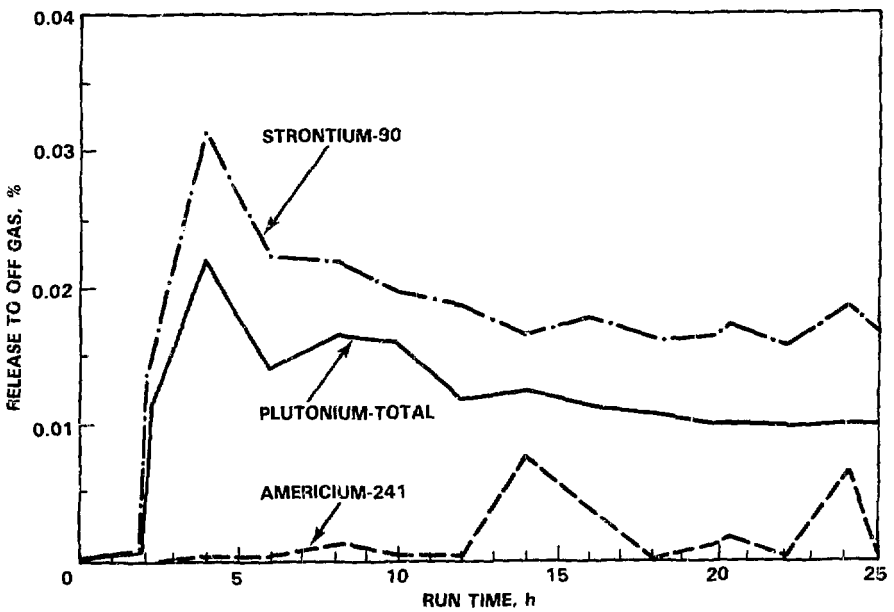

Figure 10. Americium, plutonium and strontium released to the off-gas system.

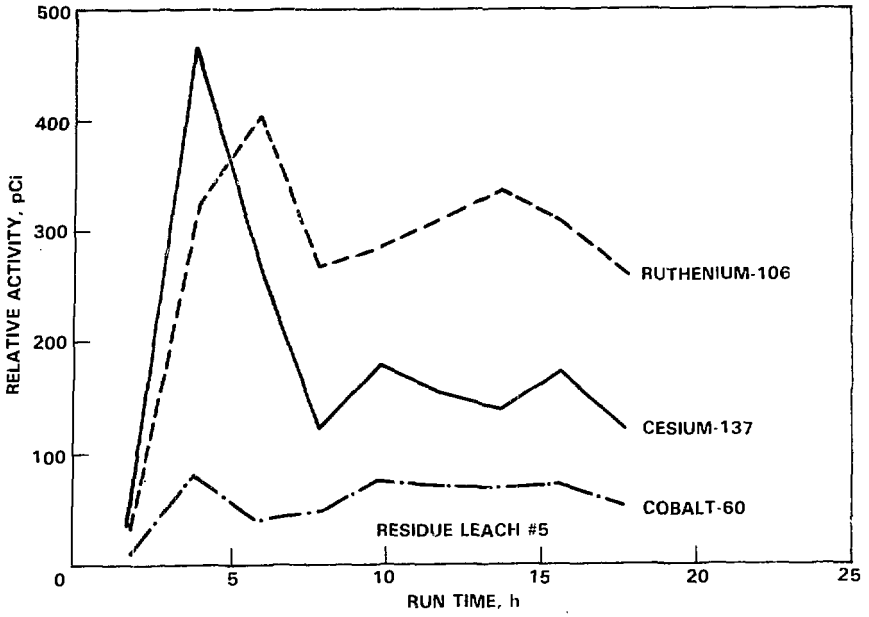

Figure 11. Relative activity in extractive leach solutions of gamma isotopes.

similar decline in the relative activity occurred later in the test as illustrated in Figure 11. This leachate activity decline is also due to the decrease in ability to effectively leach the radionuclides from the scrub solution solid phase residue. Cesium, ruthenium, and cobalt activity decline is inconsistent with previous total sample counts of these radionuclides shown in Figure 9, which illustrates that the gamma emitting radionuclides were released to some constant value later in the run. Apparently an insoluble matrix was being formed which inhibits the leaching efficiency. The apparent decline later in the test is only observed for isotopes in the solid phase. The liquid phase of all the radionuclides showed a slight increase as a function of time which is the normal pattern. An example of the solid/liquid phase variation as a function of run time using Pu data is presented in Figure 12. Past experience in similar test conditions[4,6] has indicated that off-gas particulates, which the Pu and Sr represent, are released during the initial melt contact with the contaminated zone and are not measurably released later in the test. This initial release corresponded to the gas release[4] produced by the vitrification zone contacting the container of radioactively contaminated soil. Therefore, the peak values for these and all radionuclides were used as the total release losses to the off-gas system for this test.

Higher analytical errors were associated with ^{241}Am, a softer gamma emitter, due to the extremely low activity relative to other radionuclides. The errors and associated lower detectability and higher background energy levels in the scrub solutions resulted in the more random off-gas loss curve as seen in Figure 10. However, the indicated detectable losses are relatively low as depicted.

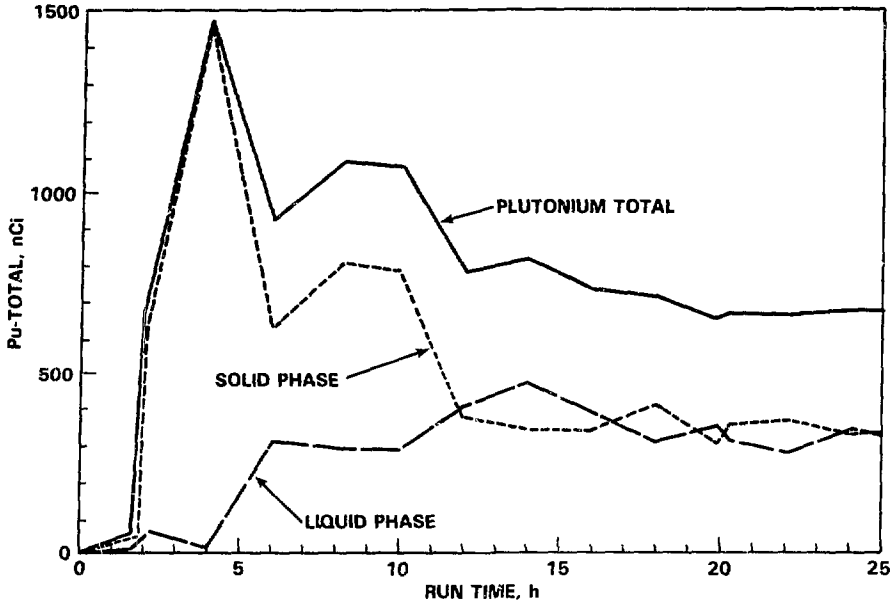

Figure 12. Plutonium distribution between solid and liquid phase of scrubber solution.

The relative efficiencies of each off-gas equipment component can be determined from the distribution of the radionuclides throughout the off-gas system. Table 4 presents this data. As seen, only a small percentage of the elements remain on the soil and glass surface inside the hood. The scrubbers accounted for removal of from 65 to 92% of the radionuclides released as indicated by the distribution in scrub tanks 1 and 2. Based on the data, 97% or more of these radionuclides were removed from the off-gas stream prior to HEPA filtration

Table 4. Distribution of radionuclides released from the melt zone.

	Radionuclide Distribution (% of Total Released)						
Radionuclide	Ground Surface[a]	Hood	Piping	Tank 1	Tank 2	Primary HEPA	Secondary HEPA
(transuranic)							
^{241}Am	3.3	22	8.7	65	0.5	(b)	(c)
total Pu	0.06	4.5	2.5	89	2.8	1.0	(c)
(fission products)							
^{137}Cs	0.17	1.7	4.7	18	72	3.3	<0.0007[b]
^{106}Ru	0.27	8.4	1.1	24	63	2.9	<0.06[b]
^{90}Sr	0.05	4.4	3.4	88	4.3	0.11	(c)
^{60}Co	0.47	3.1	14	24	55	3.3	<0.07[b]

(a) Includes block surface and surface soil.
(b) Not detected. Numbers shown are based on analytical detection limits.
(c) Analysis of these nonvolatile species was not performed.

and the balance was removed by the first stage HEPA. No gamma emitting radionuclides were detected on the second stage HEPA filter or on stack sample filters, thus demonstrating containment of radionuclides by the off-gas system.

Entrained particulates in the off gas exiting the ISV hood were measured during previous nonradioactive pilot-scale tests to have an average mass-mean diameter of 0.7 μm. The scrubbing efficiency of a venturi-ejector typically drops off for particles smaller than about 2 μm diameter. The hydro-sonic scrubber is more efficient since the lower limit of high efficiency is typically 0.5 μm diameter. The distribution data between tanks 1 and 2 (Table 4) indicate that the more volatile components, ^{137}Cs and ^{106}Ru, are being released as smaller particles since the removal by the venturi-ejector is low. Both Cs and Ru have been shown to vaporize from molten waste glasses.[7] The vapors recondense as extremely fine particles. The radionuclide distribution indicates that Co is very small also; however, the reason is not apparent from the data. Americium, Pu and Sr, on the other hand, were collected primarily by the venturi-ejector (tank 1). This indicates that the majority of these elements were released from the melt as particles larger than 2 μm with other nonvolatile soil species. It also confirms Am, Pu, and Sr releases as particulates and assists in corroborating earlier statements relating their releases with the initial contact of the melt with the waste package.

Particle Characterization

During the radioactive test, particle mass loading and size distribution measurements were made at a point in the off-gas line between the heater and HEPA filters. The purpose of the measurements was to characterize the entrained solids which were not removed by the venturi-ejector and hydro-sonic scrubbers. Data was obtained using an Active Scattering Aerosol Spectrometer Probe mounted adjacent to the off-gas line in the containment module (see Figure 8). A gas sample stream was drawn isokinetically from the off-gas line, then through a sheath airflow heater to prevent condensate from forming, and was injected into the measuring chamber with an aerodynamically focused jet. The particle count and size is determined by measuring the light scattering from a He-Ne laser beam passing through the focused sample stream. The probe counts the particles in four overlapping size ranges and has a useful range of 0.12 μm to 7.5 μm. The smaller size ranges have increased resolution over the larger ones, giving the probe extremely good resolution in the submicron region. Particle data is transferred from the probe to a computer controller for printing.

The entrained particle mass loading down stream of the scrubbers was extremely low during the test, averaging 0.8 mg/m^3. As seen in Figure 13, the highest loading of 2.18 mg/m^3 occurred when the graphite starter material was actively burning. Although the off-gas particle loading at the hood exit was not measured during the test, it was typically greater than 1000 mg/m^3 during the start-up period of previous pilot scale tests.[4] As shown in Figure 13, the mass mean particle diameter averaged less than 0.5 μm (the approximate lower limit of the hydro-sonic scrubber).

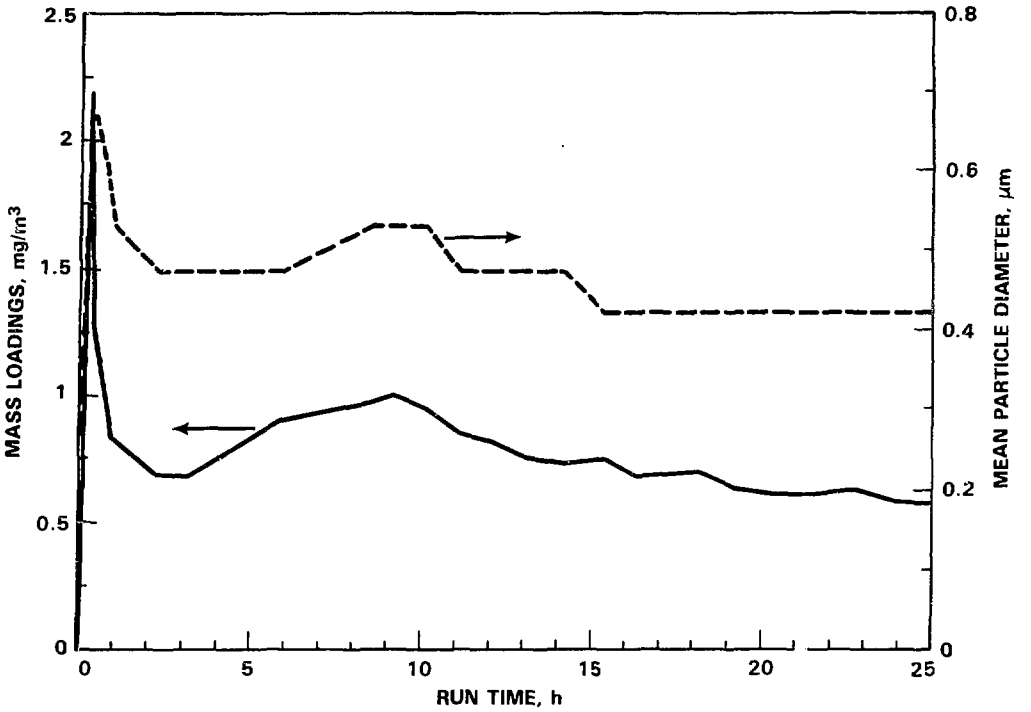

Figure 13. Off-gas particle characteristics down stream of the scrubbers.

Histograms of the particle mass distribution before the run (control data), during startup, and later in the run are presented in Figure 14. The mass loading was extremely low (0.01 mg/m^3) prior to the ISV test with a distribution from less than 0.12 µm to ~2.0 µm. During startup, the mass was primarily between 0.3 and 1.0 µm. The mass distribution shifted downward later in the run but still remained above 0.2 µm. This particle size range is well within the removal capability of the HEPA filters.

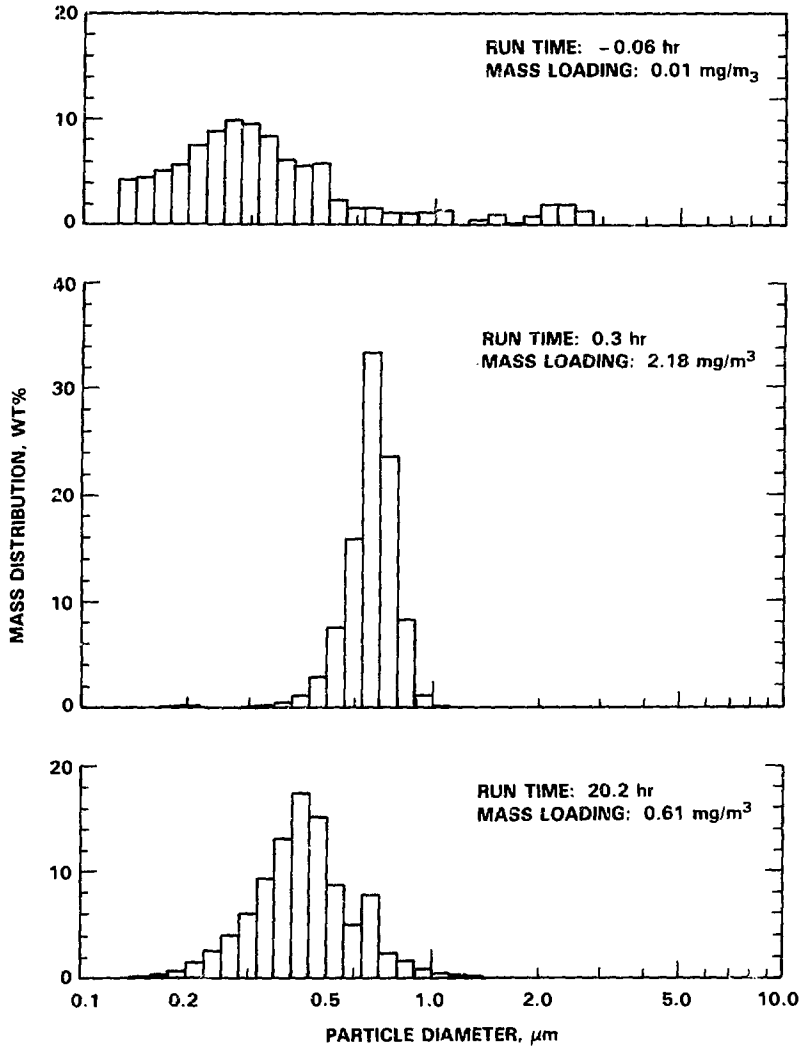

Figure 14. Histograms of particle mass distribution down stream of the scrubbers.

Off-Gas Characterization

Gases were analyzed for O_2, CO, and CO_2 at a point down stream from the off-gas blower (see Figure 8). The O_2 analysis was performed by a coulometric process whereby the gas sample is passed through an electrochemical cell. Both the CO and CO_2 analysis was performed using a non-dispersive infrared monitoring technique.

Figure 15 presents the CO and CO_2 concentrations as a function of run time. The CO_2 level in the off-gas peaked at 2.25%, approximately 1.2 hours into the test. This corresponds to the period of most active combustion of the graphite/frit startup path. This also corresponds to a period of higher power input.

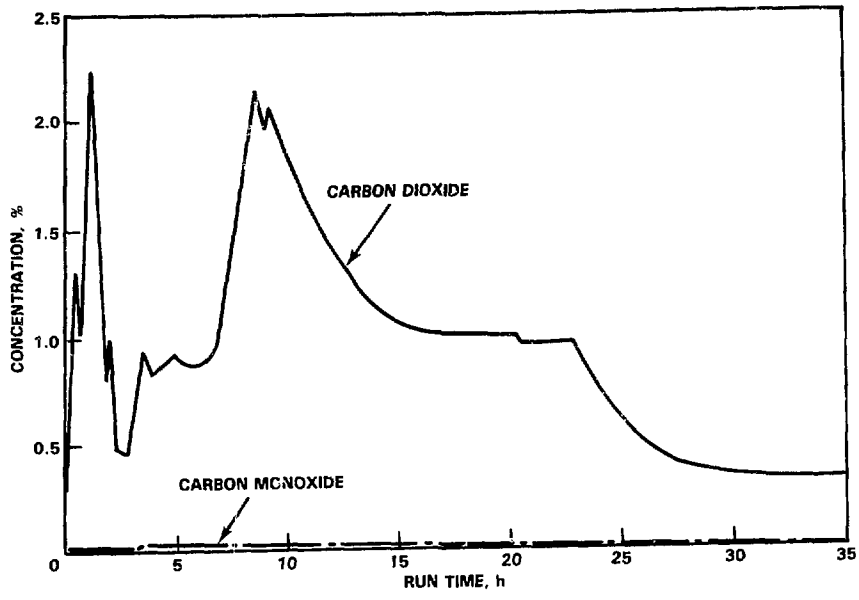

Figure 15. Carbon dioxide and carbon monoxide concentrations.

The CO_2 level after the initial startup period can be explained by graphite electrode oxidation due to heating from the molten zone. Maximum power on the 650 V tap was achieved at 3.1 hours and maximum power on the 430 V tap was realized at 8.3 hours. Just prior to these maxima, the CO_2 levels begin climbing as the electrode oxidation rate increased. During these power maxima, the melt zone temperature increased causing the electrode to reach higher temperatures and oxidize faster. It is hypothesized that the electrode temperature at the 3.1 hour power maxima was lower than during the 8.3 hour maxima because the thermal mass of the melt zone was much smaller early in the test. The CO_2 concentration supports this, since the level was highest (excluding startup) at 2.15% during the second power maxima at 8.3 hours. As the melt continued to grow downward and the power declined, the CO_2 concentration in the off gas also decreased to approximately 1% where it remained until the power was turned off. Carbon monoxide was detected during the test, however, the concentration remained low, never exceeding 0.04% at the stack.

The O_2 concentration supports this graphite oxidation mechanism since it basically mirrors the CO_2 concentration. Significant combustion of the graphite only occurred early in the test, with O_2 levels approaching those of atmospheric conditions in the remainder of the run.

Conclusions

The in situ vitrification pilot-scale radioactive test has taken this technology one step further toward the feasibility of selective, in-place stabilization of TRU contaminated soils. The test provided the following conclusions regarding off-gas ISV characteristics and system performance.

- The off-gas treatment system effectively contained all radionuclides released during the test and during the cooldown period.
- Greater than 99% of all radionuclides are retained within the vitrified block.
- Radionuclide losses to the off-gas system varied from 0.02% for Pu to 0.8% for the more volatile Cs. Corresponding DF's varied from over 4000 to 130.
- The venturi-ejector scrubber removed the majority of the Am, Pu, and Sr, which indicates they are associated with particles larger than 2 μm that were released during the test.
- Particles down to 0.5 μm were effectively removed by the scrubber system. The first stage HEPA filter effectively removed the remaining particles without showing any sign of increased flow resistance during the test.
- The maximum particle loading exiting the scrubbers and entering the HEPA filters occurs during burnoff of the graphite starter material before any radioactive material was contacted. The mass loading reached 2.2 mg/m^3 during startup and averaged 0.8 mg/m^3 for the remainder of the test.
- Both CO_2 and CO appear in the stack off gas as a result of graphite starter burnoff and graphite electrode oxidation. The CO level remained very low and did not pose an environmental problem.

Acknowledgments

Use of trademarks and tradenames does not imply endorsement by the Battelle Memorial Institute or the U.S. Department of Energy.

References

1. Brouns, R. A., J. L. Buelt, and W. F. Bonner. "In Situ Vitrification of Soil." U.S. Patent 4,376,498, March 1983.

2. Brouns, R. A. and C. L. Timmerman. "In-Situ Thermoelectric Stabilization of Radioactive Wastes." In Proceedings of the Symposium on Waste Management, 1982, University of Arizona, College of Engineering, Tucson, Arizona, pp. 449-463. 1982.

3. Timmerman, C. L. and R. O. Lokken. "Characterization of Vitrified Soil Produced by In Situ Vitrification." Nuclear Waste Management, Advances in Ceramics, The American Ceramic Society, Columbus, Ohio, Vol. 8, pp. 619-626, 1984.

4. Oma, K. H., R. K. Farnsworth, and C. L. Timmerman. "Characterization and Treatment of Gaseous Effluents from In Situ Vitrification." Radioactive Waste Management and the Nuclear Fuel Cycle. Harwood Academic Publishers, New York, Vol. 4, No. 4, pp. 319-341, 1984.

5. Timmerman, C. L., R. A. Brouns, J. L. Buelt, and K. H. Oma. "In Situ Vitrification: Pilot-Scale Development" Nuclear and Chemical Waste Management, Pergamon Press Inc., Elmsford, New York, Vol. 4, No. 3, 1984.

6. Oma, K. H., D. R. Brown, J. L. Buelt, V. F. FitzPatrick, K. A. Hawley, G. B. Mellinger, B. A. Napier, D. J. Silviera, S. L. Stein, and C. L. Timmerman. In Situ Vitrification of Transuranic Wastes: Systems Evaluation and Applications Assessment. PNL-4800, National Technical Information Services, Springfield, Virginia, 1983.

7. Gray, W. J. "Volatility of Some Potential High-Level Radioactive Waste Forms," Radioactive Waste Management, Harwood Academic Publishers, New York, Vol. 1, No. 2, pp. 147-169, 1980.

DISCUSSION

BASTIN: In the mid 50s, I participated in studies which indicated radionuclides from leaking tanks would be stabilized in soil at Hanford, and would not harm the environment. Does this work suggest a change in the earlier conclusions?

OMA: The Hanford Environmental Impact Statement under preparation will address this question. The results will determine how in situ vitrification will fit into the overall waste stabilization program at Hanford. Initial application of this process would likely be for stabilization of selected zones within liquid drain sites. However, this is yet to be determined.

18th D O E NUCLEAR AIR CLEANING CONFERENCE

THE BEHAVIOUR OF RUTHENIUM, CESIUM AND ANTIMONY DURING SIMULATED HLLW VITRIFICATION

M. Klein, C. Weyers, W.R.A. Goossens
C.E.N./S.C.K., MOL, Belgium

Abstract

Work performed within a contract with DWK in Germany in the framework of the HAW technological programme for the vitrification of HLLW.

The behaviour of ruthenium, cesium and antimony during the vitrification of simulated HLLW in a liquid fed melter has been studied on a laboratory scale and on a semi-pilot scale. In the laboratory melter of a 2.5 kg capacity, a series of tests with the simulate traced with ^{103}Ru, ^{134}Cs and ^{124}Sb, has shown that the Ru and Cs losses to the melter effluent are generally higher than 10 % whereas the antimony losses remain lower than 0.4 %. A wet purification system comprising in series, a dust scrubber, a condensor, an ejector venturi and an NOx washing column retains most of the activity present in the off-gas so that the release fractions for Ru at the absolute filter inlet ranges between 5.10^{-3} to 5.10^{-5} % of the Ru fed, for Cs the corresponding release fraction ranges between 3.10^{-3} to 10^{-4} % and for Sb the release fraction ranges between $1.7\ 10^{-4}$ to $1.7\ 10^{-5}$ %.

The same experiments have been performed at a throughput of 1 to 2 l h^{-1} of simulated solution in the semi-pilot scale unit RUFUS. The RUFUS unit comprises a glass melter with a 50 kg molten glass capacity and the wet purification train comprises in series a dust scrubber, a condensor, an ejector venturi and an NOx washing column. The tracer tests were restricted to ^{103}Ru and ^{134}Cs since the laboratory tests had shown that the antimony losses were very low. The melter effluent losses occuring during LEWC feed and during the succeeding calcinate layer digestion ranges for ruthenium from 13 to 26 % and for cesium, from 8 to 48 %. The mean DF of the wet purification system amounts to $2\ 10^3$ for ruthenium whereas a mean value of 400 is obtained for the cesium. In combination with the total melter losses, that means that the ruthenium release fraction at the HEPA filter inlet amounts to $1.3\ 10^{-2}$ % of the ruthenium fed and the corresponding cesium release amounts to 8.10^{-2} of the cesium fed.

I. Introduction

High Level radioactive liquid waste (HLLW) generated from LWR spent fuel reprocessing is considered to be treated by vitrification techniques in order to incorporate the fission products and the actinides into a glass matrix prior to disposal. In the framework of a contract between DWK in Germany and the CEN/SCK in Mol, a study has started in 1979 on the behaviour of so-called semi-volatile products which could be released during the vitrification process in the PAMELA plant.

The PAMELA plant, in construction on the Eurochemic site in Belgium, will treat 59 m^3 of lewc (Low Enriched Waste Concentrate) solution. LEWC refers to the liquid waste solution from the first cycle extraction of low enriched (< 5 % U - 235) uranium fuel. LEWC is a waste solution evaporated to a concentration of about 0.5 m^3 LEWC per ton of U reprocessed.

The experiments were performed on laboratory scale and on semi pilot scale using simulated LEWC solutions tagged with radio isotopes of the suspected volatile fission products. The composition of the simulated LEWC solution is given in table I.

The choice of the three elements Ruthenium, Cesium and Antimony is based on the assumption that those elements in a high temperature oxydative medium can form volatile compounds. The aim of this study is to determine on one hand the melter losses to the off-gas (i.e. the fraction of these elements not incorporated into the molten glass) and on the other hand the behaviour of these elements in the off gas purification system.

Due to its strong tendency to form volatile compounds, the behaviour of Ruthenium has first been studied. The main observations drawn from these studies are reported here after. In order to simulate the Pamela concept, laboratory units called VITRILAB I, II, III are then used to study the behaviour of Ru, Cs and Sb. Finally, the Pamela concept has been tested on a semi-pilot scale (1/10 of the real scale) in a unit called RUFUS.

Table I : Composition of the LEWC feed

Element	Element g/l	Nitrate salt	Oxide formed g/l	
Na	46.5	$NaNO_3$	Na_2O	62.7
Fe	15.7	$Fe(NO_3)_3$	Fe_2O_3	22.5
Cr	1.7	$Cr(NO_3)_3$	Cr_2O_3	2.5
Al	8	$Al(NO_3)_3$	Al_2O_3	15.0
Mn	4	$Mn(NO_3)_2$	MnO_2	6.3
Cs	1.5	$CsNO_3$	Cs_2O	1.6
Sr	0.5	$Sr(NO_3)_2$	SrO	0.6
Ba	0.1	$Ba(NO_3)_2$	BaO	0.11
Ce	1.8	$Ce(NO_3)_3$	Ce_2O_3	2.1
Zr	0.2	$Zr(NO_3)_4$	ZrO_2	0.27
Mo	1.3	Na_2MoO_4	MoO_3	1.95
Rb	0.25	$RbNO_3$	Rb_2O	0.27
Y	0.3	$Y(NO_3)_3$	Y_2O_3	0.38
La	1.6	$La(NO_3)_3$	La_2O_3	0.25
Ru	1	$RuNO(NO_3)_x$	RuO_2	1.32

II. Behaviour of Ruthenium in high temperature processes

A detailed description of these studies is given in (1), (2), (3). The main observations drawn from these studies are :

1. Gaseous Ruthenium tetraoxide

- RuO_4 is a strong oxidant which can rapidly be reduced to solid oxides of valencies 4 or 3 by reaction at room temperature with organic compounds.

- RuO_4 is unstable at temperatures higher than 100°C and decomposes into oxides of lower valencies. The rate of reaction is enhanced by the presence of metallic surfaces on which the ruthenium oxide deposit is strongly bounded.

- RuO_4 is physically adsorbed on Silica-gel at temperatures lower than 80°C; above this temperature the adsorption capacity is negligible.

- RuO_4 is catalytically reduced to solid oxides on Fe/Cr catalyst operating at 300°C and the ruthenium oxide deposit enhances the reaction rate.

2. Volatile Ruthenium nitrosyl species

- Volatile RuNO species are formed either by reactions of RuO_4 with NO_x, either by calcination of Ru nitrosyl nitrate solutions in nitric acid.

- RuNO is more stable than RuO_4, more easily adsorbable on Silica gel (tenfold increase of the capacity) and is adsorbed at temperatures as high as 120°C.

- RuNO is also catalytically reduced on Fe/Cr catalyst at 300°C but with a lower reaction rate and the RuO_2 deposit also enhances the reaction rate.

- The RuNO species has a lower vapor pressure than the RuO_4 species; at 20°C the partial pressure of RuNO is lower than $2\ 10^{-3}$ atm so that almost the Ru is condensed whereas the corresponding RuO_4 partial pressure amounts to 10^{-2} atm.

- During calcination of Ru nitrosyl compounds dissolved in nitric acid, a fraction of Ru is plated out on the calciner walls, another fraction is volatile (RuNO species) and a last fraction is present in the off gases as submicronic aerosols. The distribution of Ru between these different states depends largely on the calcination temperature. At 600°C, the Ru release is mainly under the RuNO gaseous form (less than 0.2 % aerosol form), whereas at 1100°C, 8 % of the Ru release is in aerosol form.

Experiments were performed with the aim of comparing the volatilities of different Ru species fed simultaneously with a simulated high level liquid waste solution on a glass pool of an Inconel melter operated at 1100°C. The Ruthenium release in the melter off-gas depends on the nature of the Ru species fed.

- For a solution of $RuNO(NO_3)_x\ (OH)_{3-x}$ dissolved in the waste simulate (LEWC), the melter losses to the off gas amounts to 7 % of the quantity fed. A fraction deposits on the crucible walls but the major part is incorporated into the glass.

- For a suspension of solid RuO_2 in LEWC, the melter losses amounts to only 2.5 %.

- When gaseous RuO_4 is simultaneously fed with liquid LEWC on the glass pool, the gaseous RuO_4 is partly decomposed on the hot

walls of the crucible and only 12 to 30 % of the Ru fed is lost to the melter off-gas; only a minor fraction is incorporated into the molten glass.

III. Laboratory vitrilab unit

3.1. Description of the laboratory units VITRILAB I, II and III

In the three vitrilab units, the liquid fed melter concept is used, but three sligthly different purification schemes are tested.

The glass melter is an Incoloy 825 crucible with a 2.5 kg capacity molten glass externally heated by a resistance furnace. The simulated liquid waste solution (LEWC) traced with Ruthenium-103, Cesium 134 and Antimony 124 is directly fed by a menbrane pump on the molten glass surface. The liquid through put on the melting surface area of 57 cm^2 varied between 20 and 40 $l/h\ m^2$. The off gas purification line of the three vitrilab units is different (Fig. 1).

In Vitrilab I, it comprises in series a packed bed dust scrubber, a specific Ru filter, an ejector venturi, a condensor and finally a washing bottle and an absolute filter.

In Vitrilab II, the specific ruthenium filter is removed and the condensor is installed between the dust scrubber and the ejector venturi.

In Vitrilab III, the specific ruthenium filter is removed and the positions of the condensor and of the ejector venturi can be interchanged by a by-pass valve system.

Liquid and gas samplings performed at various locations in these units allow to follow the evolution of the melter losses to the off-gas and to determine the efficiency of the off-gas cleaning system.

The particle size distribution of the aerosol present in the off-gas is determined by sampling with a cascade impactor followed by a condensor, a wash bottle and a final filter. The distribution between aerosol form and volatile form is determined with the same system where the impactor is replaced by a sampling filter.

3.2. Melter releases to the off-gas

3.2.1. Ruthenium. The melter DF for Ru lies between 3.3 and 67 with a mean value of 10.8 corresponding to a 9.3 %

entrainment. Generally, the entrainment by the off-gas in maximum at the start of a run and decreases as soon as a molten salt layer covers the molten glass surface. The particle size distributions, determined with a cascade impactor, appear all to be bimodal in nature. The large diameter component is deposited mainly on the first stage of the cascade impactor with a cut-off diameter of 14μm. The small diameter component is deposited on the last stages of the cascade impactor with cut offs of 2, 1 and 0.6 μm. The rest is retained on the back-up absolute filter. The fraction of Ru found after the impactor represents the gaseous ruhenium release of the melter. The major part of this volatile component is found in the condensate. A low melter DF is always observed when volatile Ru species are formed. For two runs, with melter DF's of only 4.4 and 3.3 the volatile fraction of the ruthenium in the off-gas reached respectively 18 and 50 % of the total Ru loss to the off-gas.

Ru losses during melter idling. If the melter, containing the glass-waste oxides mixture kept at high temperatures (1000°C), is sparged with air volatilization of certain glass components may occur during that period and so lower the global melter DF. (This situation is called 'idling melter"). For Ru, after glass refining during some hours, air sparging leads to a loss of $5\ 10^{-3}$ % to $2\ 10^{-2}$ % pro hour of the Ru activity present in the molten mixture. The particle size distribution of the aerosol during melter idling is shifted towards small values; all the activity is found on the last stage (cut-off of 0.3 μm) and on the back-up filter of the cascade impactor.

3.2.2. Cesium. The entrainment of Cesium in the off-gas varies widely between runs. The minimum and maximum entrainment observed are 0.3 % and 20 % respectively and the mean values for all the tests is 4 % corresponding to a DF of 25. The Cesium behaviour is quite different from the ruthenium behaviour. The fraction of Cesium in the entrained dust trapped on the first stage of the cascade impactor is also high (30 to 70 %), but the fraction of Cesium present on the last stage is always higher than the ruthenium or antimony fraction. That means that the melter release in the micron and submicron range is enriched in Cesium vs ruthenium and antimony. The fraction of Cesium still present after the cascade impactor is very low (from 0.1 to max 2 %) which means that cooling down of the gases to 120°C induces nearly total condensation of the volatile Cesium oxides to submicronic aerosols.

The Cesium release to the off-gas by air sparging during idling of the melter at 1000°C is one order of magnitude higher than the ruthenium loss. Off gas entrainments of 0.1 to 0.7 % pro hour of the cesium activity are measured during air sparging and this phenomenon can significantly lower the melter DF; for example after 15 hours of air sparging, the melter DF decreases from 24 to 9 for a mean hourly entrainment of 0.27 %.

3.2.3. Antimony. The melter DF for antimony lies between 58 and 2300 with a mean value of 260 corresponding to a 0.4.% volatility which shows that antimony releases to the melter off gas are very low. The antimony entrainment during an "Idling test" is also very low; values from 4 to 6 10^{-4} % of antimony entrainment pro hour from the glass melt were measured during 15 hours long sparging tests.

3.3. Packed bed dust scrubber

The characteristics of the dust scrubber and the values of the DF's are given in table I. In order to avoid an increase of the volume of the circulating solution of the dust scrubber, the scrubber operates at a temperature regulated in such a way that the water vapour content of the off gases does not condense out in this scrubber. The liquid flow is chosen to work below flooding conditions for the highest operating temperature.

3.3.1. Ruthenium. The Ruthenium trapped in the circulating solution is only partially soluble in this weak acidic medium and ruthenium dioxide deposits rapidly in the solution and also on the Raschig rings of the packing. The mean DF of the Vitrilab III scrubber is one order of magnitude higher than the corresponding DF of I and II vitrilab unit. The dust scrubber III is 30 % higher and has a free section 18 % greater which means that the residence time of the gas is higher, which allows to work with higher liquid to gas ratio. When the volatile fraction at the melter outlet is high (Low melter DF), than the dust scrubber DF is very high (DF ~ 10^3). In these cases, the colour of the washing solution is orange-yellow characteristic of the presence in the weak nitric acid of several Ru nitrosyl nitrates complexes. On the contrary, when the melter DF is high and when the volatile fraction is low than the dust scrubber DF is lowered to values around 25. The aerosol leaving the dust scrubber has a narrow size distribution and volatile species are not any more present in the off gas. The activity mass median aerodynamic diameter of the aerosol leaving the dust scrubber lies between 0.6 and 0.9 μm and the standard deviations varies between 1.25 and 1.4. This means, that when volatile ruthenium is present in the melter off gases, this species is completely washed out by the dust scrubber and the only species still present at the scrubber outlet is a sub-micronic aerosol.

Table I. Packed bed dust scrubber

GEOMETRIC CHARACTERISTICS			
	VITRILAB I	VITRILAB II	VITRILAB III
Diameter (cm)	5	5.8	6.4
Heigth (cm)	25	25	35
Packing	Raschig Rings D = H = 7 mm d = 4 mm		
	OPERATING CHARACTERISTICS		
Liquid flow (l/h)	100	80 - 100	120
Temperature (°C)	90 - 95	90 - 95	90 - 95
	DF FOR RUTHENIUM		
MIN	10	7	24
MEAN	20	22	305
MAX	50	230	2100
	DF FOR CESIUM		
MIN	*	1.7	4.5
MEAN	*	2.3	19
MAX	*	3.3	160
	DF FOR ANTIMONY		
MIN	*	*	20
MEAN	*	*	58
MAX	*	*	280

* The corresponding tracer is not used.

During an idling test, the DF of the dust scrubber decreases towards values of 3 to 5. This decrese is clearly bound to the aerosol particle size decrease which lies in the sub-micronic range (lower than 0.3 μm).

3.3.2. Cesium. As shown in the table, the efficiency for Cesium is lower than for Ruthenium due to the fact that the melter release in the micron and sub-micron range are enriched in Cesium v.s. Ruthenium and to the fact that there is no volatile Cesium species still present in this temperature range. The dust scrubber DF during idling test is not strongly reduced v.s. the LEWC feed period which shows that the release mechanisms are probably not significantly different.

3.3.3. Antimony. Due to the high value of the melter DF and to the low concentration of Sb in the feed, the concentration of antimony in the off gas is 1000 times lower than Cesium. Nevertheless, the dust scrubber DF for antimony is higher than the Cesium DF, probably due to the fact that antimony is evenly distributed on the aerosols leaving the melter.

3.4. Specific volatile ruthenium trapping bed

As described with more details in 3, the second barrier for Ru in the off gas line as initially foreseen in the Pamela project, was a Silica-gel bed operating at 120°C. Such a filter, which had given favourable resuts when placed at the exit of a calciner appeared useless in the Vitrilab off gas purification line after the dust scrubber. A ferric-oxide chromium oxide catalyst operating at 300°C gave also very low DF's. This can easily be explained by the fact that these filters were developed to trap gaseous ruthenium species whereas it has been shown that after the packed dust scrubber the only species still present is a stable, non reactive submicronic aerosol. Therefore, it was decided to remove this unit from the off-gas line for the further experiments (Vitrilab II and Vitrilab III) and also to discard it in the design of the active Pamela plant.

3.5. Condensor

Although, the condensors in vitrilab II and III have not the same dimensions, no significant differences are observed between their performances. The condensors, placed after the dust scrubber, have roughly the same DF of 5 for the three elements. This suggest a similar trapping mechanism for the aerosols leaving the dust scrubber. The still entrained solid submicronic aerosols work as condensation nuclei and are retainable in the condensor thanks to their size increase.

During Idling test, the condensor DF decreases to 1. This is expectable, since there is no water condensation and moreover the aerosol particle size is decreased to values down to 0.3 μm or less.

3.6. Ejector venturi

The ejector venturi operates at a nozzle pressure of 3 bars and a liquid flow rate of 300 l/h. The circulating solution is maintained at 30 to 48°C.

The ejector DF mean values (64 and 80) of vitrilab II and III do not differ significantly for ruthenium. (Table II) The DF variation is large since values ranging from 10 to 10^3 were measured. Generally, the DF of the ejector increases when the DF of the system melter-dust scrubber-condensor decreases and the DF decreases in the opposite case. The DF for antimony is similar to the Ru DF.

The DF's for Cesium are systematically higher than the Ru and the Sb DF's, this is perhaps due to the fact that Cesium species are soluble in the washing solution whereas ruthenium and antimony species are insoluble.

Table II. Ejector Venturi

	Ruthenium DF		
Unit	Vitrilab I	Vitrilab II	Vitrilab III
MIN	10	16	10
MEAN	25	64	80
MAX	50	1000	290
	Cesium DF		
Unit	Vitrilab I	Vitrilab II	Vitrilab III
MIN	*	1670	80
MEAN	*	4800	256
MAX	*	14000	5800
	Antimony DF		
Unit	Vitrilab I	Vitrilab II	Vitrilab III
MIN	*	*	18
MEAN	*	*	60
MAX	*	*	226

* Tracer not used in this unit

3.7. Global DF of the system

The global DF of the system is the product of the melter DF and of the wet gas purification system DF.

The wet gas purification system is different in vitrilab I, II and II as shown hereafter.

- Vitrilab I : Melter - dust scrubber I - ejector venturi - consensor - washing bottle
- Vitrilab II : Melter - dust scrubber II - condensor - ejector venturi - washing bottle
- Vitrilab III : Melter - dust scrubber III - ejector venturi - condensor - washing bottle.

The minimum, maximum and mean global DF values are given in table III.

Table III. Global DF's for the different Vitrilab Units

MIN GLOBAL DF

	Ru	Cs	Sb
VITRILAB I	10^4	-	-
VITRILAB II	$1.1\ 10^4$	$2.2\ 10^5$	-
VITRILAB III	$2\ 10^5$	$3.5\ 10^4$	$6.8\ 10^5$

MEAN GLOBAL DF

	Ru	Cs	Sb
VITRILAB I	$3.2.10^4$	-	-
VITRILAB II	$1.1\ 10^5$	$4.7.10^5$	-
VITRILAB III	$3.8\ 10^5$	$1.7.10^5$	$2.5.10^6$

MAX GLOBAL DF

	Ru	Cs	Sb
VITRILAB I	10^5	-	-
VITRILAB II	$8.6\ 10^5$	10^6	-
VITRILAB III	$2\ 10^6$	$1.2\ 10^6$	$6\ 10^6$

3.8. Conclusion of the vitrilab tests

The series of tests performed in the various Vitrilab units has shown that the Ru and Cs losses to the melter effluent are generally higher than 10 % whereas the Sb losses remain lower than 0.2 %. For the vitrilab III unit, the release fractions for Ru at the absolute filter inlet ranges between $5\ 10^{-3}$ % to $5\ 10^{-5}$ % of the Ru fed, for Cs the corresponding release fraction ranges between $3\ 10^{-3}$ to 10^{-4} % and for Sb the release fraction ranges between $1.7\ 10^{-4}$ to $1.7\ 10^{-5}$ %.

Antimony, due to its low volatility, will not be used in the RUFUS unit.

IV. Semi pilot scale unit RUFUS

4.1. Description of the RUFUS unit

The spatial projection of the Rufus installation (Retention Unit for the Filtration of Unidentified Species) is given in fig. 2.

The main characteristics of the RUFUS installation are given hereafter.

4.1.1. Vitrification unit

The vitrification unit comprises four elements.

- Vitrification oven : The crucible in Incoloy 825 has a molten glass capacity of 50 kg and the molten glass surface reaches 1328 cm^2. The total available power delivered by external resistance heating elements can be varied between 8 and 9.6 kw.

- Molten glass feed : The glass frit from the dosing vessel is molten in an Incoloy crucible heated by a furnace of 2.2 kw and flows by gravity into the vitrification oven.

- LEWC liquid feed : The simulated LEWC solution is directly fed on the molten glass surface with a diaphragm dosing pump. The throughput during the tests was varied between 0.9 and 1.9 l/h corresponding to 6.3 to 14 l/h m^2 molten surface.

- Crucible emptying : The emptying of the crucible is performed via a freeze valve and the receiver is installed in a heated box to minimize the thermal stresses during glass cooling.

4.1.2. Dust Scrubber

The dust scrubber is a packed bed countercurrent dust scrubber with a glass spiral ring packing. The column has a diameter of 100 mm and a packing height of 880 mm.

4.1.3. Condensor
The condensor is a spiral type industrial glassware condensor with an exchange surface of 1.5 m^2.

4.1.4. Ejector Venruri. The ejector Venturi is a SAPS stainless steel ejector operating at a nozzle pressure of 6 bars and a liquid flow of 500 l/h.

4.1.5. NOx washing columns. The NOx washing tower is a packed bed counter current column in industrial glassware with a packing of ceramic Raschig rings. The column has a diameter of 100 mm and two beds of 700 mm height.

4.1.6. Air Ejector. The installation is maintained in slight under pressure by a compressed air driven ejector placed at the end of the off gas purification after the final absolute filter. An under pressure of 10^3 to 1.5 10^3 Pa is maintained in the melter phenum by a guard siphon placed on the air inlet.

Two configuration can be chosen by a system of valves and by-pass :

- Configuration I
  Dust-scrubber/Condensor/Ejector Venturi/NO_x Tower
- Configuration II
  Dust-scrubber/Ejector Venturi/ Condensor/NO_x Tower

The dust scrubber operates always in a temperature range of 75-85°C so that the water vapour content of the off-gas remains nearly constant. The ejector venturi in configuration I operates always at low temperature (about 30°C) whereas in configuration II the ejector venturi can also be operated at 75-85°C so that the water vapour content of the off-gas remain nearly constant and so does also the ejector liquid volume.

4.2. Melter releases to the off-gas

The release of Ru and Cesium is determined by liquid sampling of the various scrub solutions and by gas sampling on absolute glass fiber filter. The activities of ^{103}Ru and ^{134}Cs are determined with a Ge (Li) detector

4.2.1. Description of the melter behaviour. During operation of the melter, three succeeding steps can be distinguished namely the LEWC feed period, the calcinate layer digestion period and the melter idling period.

- LEWC feed period
  At the start of a run, the molten glass surface is at about 1050°C. The liquid feed on the molten glass surface induces a drop of temperature of the glass surface and a colder cap of dry solids is formed on the surface. If the liquid flow is sufficiently high, a liquid covered area will finally appear on the glass surface. The extend of the three zones (uncovered melt, dry solid layer, liquid covered area) depends mainly of the liquid flow rate, the heating power and the working time.

- Calcinate layer digestion period
  When the liquid feed is stopped, after vaporization of the remaining liquid phase, the calcinate layer is progressively decomposed into oxides which are incorporated into the mass of the glass to finally form an homogeneous waste oxides-glass mixture.

- Idling period
  When the calcinate layer digestion period is finished, the molten glass surface has reached again a temperature of about 1050°C and the uncovered glass mixture-waste oxides is exposed to the sparging air.

In fig. 3, the temperature evolution of the glass surface is given in function of working time for two liquid flowrates.

4.2.2. Presentation of the results. The Ruthenium and Cesium release to the off-gas are different for each period. The main observations drawn from the 7 runs are the following :

- LEWC feed period
  The Ruthenium and Cesium losses to the off-gas decrease when the mean temperature of the calcinate layer formed during LEWC feed decreases. This is illustrated in fig. 4 and 5, which gives the Ru and Cs fraction volatilized in function of the mean glass surface temperature. However, for Cesium, it seems that the volatility depends not only of the quantity of Cesium in the liquid feed but it depends also of the quantity of Cesium already present in the molten glass. When this fact is taken into account, the relationship between cesium volatility and mean surface temperature appears, indeed, more clearly.

- Calcinate layer digestion
  The Ru and Cs losses to the off-gas are generally high during the first four hours after the feed stop and level off to a very low value whereas for Cesium the release tends to a roughly constant value. This is illustrated in fig. 6 for the run 6/10.

- Melter idling
  Air sparging of the melter leads to low Ru losses of about $3\ 10^{-3}$ %/hour of the Ru activity in the molten glass whereas for Cesium 0.33 %/hour is released to the off-gas.

4.2.3. Release mechanisms of Ruthenium and Cesium. The particle size distribution of the dust leaving the melter has not been determined, because the use of a cascade impactor in a gas with a high dust loading appeared practically not feasible. The results obtained in the vitrilab where some impactor data were collected had lead to the following observations.

- The Ruthenium loss of the melter is partly under the form of a volatile species, partly under the form of entrained dust and the rest is a submicronic aerosol. The distribution between these forms vary widely and mainly depends on the temperature at the molten glass surface.

- The Cesium release is partly under the form of entrained dust and partly under the form of submicronic condensation aerosols. At the low outlet temperature of the melter, no volatile species are still present. In general the aerosol size distribution is bimodal in nature.
  This suggests that the overall size distribution is composed of two independent components, each heaving its own characteristic size distribution. The large component is certainly associated with a gross entrainment mechanism whereas the small diameter component of the overall distribution is probably a volatilization/condensation process that occurs within the melter plenum.

The different behaviour of ruthenium and Cesium during the LEWC feed and during the idling test can be explained by differences in the probable release mechanism.

The gross entrainment mechanism result in a dust emitted which has the same composition as the LEWC feed. For the small diameter component, generally, the submicronic loss fraction is enriched in Cesium vs ruthenium indicating a different mechanism.

Ruthenium loss mechanism

The formation of volatile species RuO_3 and RuO_4 by RuO_2 oxidation is very limited below 1200°C (Equilibrium constant $K = 10^{-3}$ at 1200°C). Even formed, these volatile species are highly unstable at the outlet melter temperature and are again decomposed into RUO_2. This mechanism is probably responsible for the Ru release during idling test.

During LEWC feed, volatile RuO_4 can be formed by reaction between RuO_2 and NO_2 from 900°C ($K = 10^{-1}$ at 900°C). Again the gaseous RuO_4 is highly reactive and can at lower temperatures react with NO to give Ru nitrosylcomplexes or be decomposed again to solid RuO_2.

Another way of volatile Ru formation and the most probable is the formation of a volatile Ru nitrosyl complexe by partial decomposition of the nitrosyl nitrate.

Cesium loss mechanism

Solid Cs_2O, formed by $CsNO_3$ decomposition from 500°C onwards, can be transformed into volatile species in a temperature range of 750°C to 1200°C. Cooling of the gas induces condensation of these gaseous species to solid submicronic aerosols.

During LEWC feed, i.e. in the presence of great amounts of water vapour (till 50 %), volatile cesium hydroxides such as CsOH and $(CsOH)_2$ can be formed. In the absence of water vapour, i.e. during calcinate layer digestion and idling melter, volatile species such as CsO and CsO_2 can be formed.

4.3. Dust scrubber

4.3.1. Operation of the dust scrubber.

- The liquid flow in the dust scrubber itself is fixed at 800 l/h corresponding to a liquid rate of 102 $m^3/h.m^2$.
  The nominal gas flow amounts to 7.2 m^3/h when the dust scrubber operates at 82°C corresponding to a water vapour content of 50 %, the normalised gas rate equals to 904 m^3/m^2 h.

- During idling test, the gas flow amounts to 3.3 m^3/h when the dust scrubber is operating at 40°C corresponding to a water vapour content of 5 %.

- The by-pass liquid flow is kept at 300 l/h. The function of this flow is to clean the connecting tube between the melter and the dust scrubber.

- In practice, the temperature of the circulating liquid is kept between 75 and 92°C depending on the LEWC flow rate. The aim is to maintain the volume of the circulating liquid constant. In all the tests, the dust scrubber was operating at a higher temperature than the dew point of the gas so that a reduction of the circulating liquid volume was always observed - Generally the final volume was 70 to 80 % of the initial volume -

- In all the tests, an insoluble component appeared after some hours of operation. This insoluble component, essentially ruthenium dioxide, deposits in the circulating tank and on the packing.

4.3.2. Presentation of the results.

- Particle size distribution of the aerosol at the dust scrubber outlet

The particle size distribution of the aerosol leaving the dust scrubber has been determined by sampling with a low flow rate (1 m^3/h) 4 stages cascade impactor.

During LEWC feed and calcinate layer digestion, the major part of the aerosol leaving the dust scrubber is in the 0.3 to 0.5 µm range. When the calcinate layer is nearly completely digested, the distribution is shifted towards smaller values concentrated of around 0.4 µm. During idling test, the major part of the activity is found back on the back-up filter which means that the distribution is again shifted towards values smaller than 0.4 µm.

- Distribution between soluble and insoluble form

As shown in the table hereafter, the Cesium trapped in the dust scrubber is nearly completely soluble whereas for Ru about 14 % of the total Ru trapped is not soluble and forms black ruthenium dioxide which deposits in the tank, on the spiral rings of the packing and in the pipes. It is obvious that the insoluble fraction will increase with the Ru trapped concentration. Indeed in the vitrilab laboratory installation, insoluble fraction of about 50 % were found for Ru concentrations of 200 mg/l.

	^{103}Ru	^{134}Cs
insoluble %	14	0.4
concentration mg/l	90	150

- Dust scrubber DF

During normal operation i.e. during LEWC feed and calcinate layer incorporation, the mean DF for Ru reaches 5.5 and is always higher than the mean DF for Cs which only reaches 2.5. During idling test, the DF's for Ru and Cs decrease to respectively 1.9 and 2.1.

	^{103}Ru		^{134}Cs	
DF	Normal operation	Idling test	Normal operation	Idling test
MEAN MIN MAX	5.5 2.8 9.5	1.9	2.5 2 4	2.1

The lower efficiency of the dust scrubber observed for Cesium is probably bound to a difference in particle size distribution at the dust scrubber inlet.

Conclusion

The dust scrubber DF of the RUFUS unit is one order of magnitude lower than the dust scrubber of the vitrilab unit. Reasons for these differencies can be :

- a lower dust concentration at the melter outlet due to a higher ratio inert air/l LEWC for the Rufus (1.8 m^3 air/l LEWC for Rufus v.s. 0.6 m^3 air/l LEWC for the vitrilab unit)
- a different particle size distribution at the Rufus melter outlet
- a higher L/G ratio for the vitrilab (370 l/m^3) than for the Rufus (111 l/m^3)
- a lower superficial gas velocity for the vitrilab (3 cm/s) than for the Rufus (25 cm/s).

4.4. Condensor and ejector venturi

4.4.1. Operation of the condensor and the ejector venturi

- 50 l of drinking water is used as washing solution in the ejector-venturi. The liquid flow of 0.5 m^3/h obtained for a nozzle pressure of 6 bars induces a draft of 300 Pa on the gas flow.

- If the venturi solution is not directly removed, a deposit of ruthenium oxide can appear in the tank.

- Three different purification schemes have been tested :
  I Condensor followed by ejector venturi operating at 30°C
  II Ejector operating at 30°C followed by condensor
  III Ejector at 70-85°C followed by condensor.

In the cases I and III, the ejector washing solution volume remains nearly constant whereas in the case II the volume in the ejector steadily increases because it in fact, acts as condensor.

4.4.2. Decontamination factor of the ejector venturi and the condensor

Ejector venturi

The mean DF's obtained during the various runs are given in table IV. The main observations drawn from these results are :

- The over-all DF is always lower than the DF obtained during the feeding period of a run, this is probably bound to a shift of

the particle size distribution towards the smaller values and to a decrease of concentration in the gas effluent.

- The DF for Cesium is always lower than the Ru DF when no significant difference in the particle size distribution were observed.

- In spite of the small number of experimental runs for each configuration, it seems that the ejector shows the highest efficiency when it is used at a low temperature and after the condensor.

Condensor

The values of the operating temperature and the DF's are given in table V. The main observation drawn from these tests are :

- the condensor DF is generally lower for Cs than for Ru;

Table IV : Ejector Venturi DF in function of the chosen purification shemes

Mean DF values	DF during feed		Global DF	
	Ru	Cs	Ru	Cs
DS-C-V (32°C)	670	109	240	122
DS-V (32°C)-C	99	65	66	43
DS-V (75°C)-C	30	22	30	29

* The operating temperature is given between brackets.

Table V : Condensor Df in function of the chosen purification scheme

MEAN GLOBAL DF	Ru	Cs
A) Condensor at 30°C Followed by E.V.	1.4	1.2
B) Condensor at 30°C After E.V. at 35°C	1.2	1.1
C) Condensor at 30°C After E.V. at 70-85°C	4.6	2.4

- It seems that the best Df's are obtained when the condensor is installed after the ejector operating at high temperature. The activity ratio condensate/feed is given here after for the three purification shemes.

$\frac{\text{activity in condensate}}{\text{activity in feed}}$	Ru	Cs
Scheme I C-V^{32}	3.10^{-5}	$1.5.10^{-4}$
Scheme II V^{32}-C	2.10^{-5}	8.10^{-5}
Scheme III V^{75}-C	6.10^{-6}	8.10^{-6}

This table shows that the lowest activity level in condensate is found for the scheme III.

Comparison of the performance of the three purification schemes

The three purification schemes give total DF's which are of the same order of magnitude. Due to the small number of tests a choice can not be made on the basis of the total Df for condensor and Venturi-ejector together.

All the three schemes have their advantages and disadvantages which are summarized here after.

	ADVANTAGES	DISADVANTAGES
I C-V^{30}	- Venturi operates at low temperature - Constant washing solution volume	- Highest activity level of the condensate - water cooling of the venturi
II V^{30}-C	Venturi operates at low temperature and can act as a condensor (which can be suppressed	Increase of the washing solution volume
III V^{75}-C	Lowest activity level of the condensate/constant volume of the washing solution	Venturi works at high temperature

The choice between the different possibilities can then be governed by the recycling philosophy adopted in the process.

For the schemes I and III, the constancy of the washing solution volume, in the ejector, allows to recycle a small fraction of the solution to the melter feed without the need of an evaporator.

For the condensate recycling, which needs always an evaporator, the scheme III is the most advantageous since the activity levels handled are one order of magnitude lower than for scheme I.

For the scheme II, a volume equivalent to the waste volume fed must be removed and sent to an evaporator prior to go to the melter.

4.5. NO_x washing tower

4.5.1. Operation of the NO_x washing tower

20 l of drinking water solution are used as washing solution in the NO_x tower. The liquid flow varied during the tests between 300 and 500 l/h with a corresponding pressure drop op 800 to 2000 Pa.

4.5.2. Efficiency for the removal of Cs and Ru

The main operating parameters as well as the DF's values for Ru and Cs are given in table VI.
The DF and the gas pressure drop increase with the liquid flow rate. A reasonable DF is obtained when the NO_x scrubber operates near the flooding point of the column (Flooding point L = 600 l/h, G = 3 m^3/hl).

Table VI NO_x washing tower

Date	Gas flow rate at 40°C	Liquid flow rate	Pressure drop	Global DF	
	m^3/h	l/h	Pa	Ru	Cs
02/08	3.1	300	800	1	1.3
10/08	3.1	300	800	1.6	1.2
11/08	3.1	350	1000	2	1.4
27/09	3.1	400	1200-1500	1.4	1.4
29/09	1.7	450	1600-1700	2	1.8
06/10	3.1	500	1800-2000	3	3.4

V. Comparaison with the Pamela design DF's

Table VII and table VIII give a comparaison of the results obtained in RUFUS with the PAMELA design values. The DF obtained in the gas purification train RUFUS are lower than the PAMELA design values.

For Ru, it appears that the weak points in the purification systems are the dust scrubber and the condensor. The venturi ejector shows a better efficiency than expected. The NO_x dust scrubber has a DF which is of the same order of magnitude as the design value.

For Cs, it appears that the melter loss is greater than the design value (16 to 25 % instead of the expected 4 %). The weak points in the purification system are also the dust scrubber and the condensor whereas the ejector and the NO_x tower satisfy the requirements.
Several actions can be undertaken in order to improve the system DF for Ru and for Cs.

5.1. Reduction of the melter losses

- Long duration tests with a constant covering of the molten glass with a calcinate layer give generally lower losses for Ru and Cs due to the lower temperature at the top level of the melt. Ru release of 15 % and Cs release of 10 % can be achieved for a top level temperature of 700°C for example.

- Lower the surface temperature of the melt during idling in order to minimize the Cesium release mainly. This can be obtained by applying a water feed such as is foreseen in the Pamela design.

Table VII : Mean DF's values of the purification units in RUFUS compared to the PAMELA design values

	Ru			Aerosols	Cs	
	Pamela design	During LEWC feed	Global DF	Pamela design	During LEWC feed	Global DF
Melter	6.7	12.7	6.1	25	6	3.9
Dust scrubber	10	8.8	6.5	10	2.4	2.5
Condensor	10	2	2	5	1.5	1.5
Venturi	20	95	78	20	52	52
NO_x	2.5	1.9	1.8	2.5	2.1	1.6

Table VIII : Mean DF's values of the purification system RUFUS compared to the VITRILAB results and to the PAMELA design values

	Mean DF of the wet purification system		
System DF	Pamela design	Vitrilab	Rufus
Ru	$5\ 10^3$	$3.5\ 10^4$	$2\ 10^3$
Cs	$2.5\ 10^3$	$6.8\ 10^3$	400

5.2. Increase of the dust scrubber efficiency

The dust scrubber used was a low pressure drop counter-current bed dust scrubber. Test are foreseen to design a new type of more efficient dust scrubber. The idea is to use a co-current dust scrubber with impingement plate followed by a counter-current impingement plate dust scrubber. The two columns would be installed on the same circulating tank.

5.3. Increase of the condensor efficiency

A classical stainless steel tube and shell condensor will be tested in the future with the hope op a better efficiency due to more efficient contact between the condensate flow and the gas.

VI. Conclusion

The RUFUS experiments have shown that the vitrilab laboratory results could not directly be extrapolated to semi-pilot size units. The off-gas line consisting of a dust scrubber, a condensor, an ejector venturi and an NO_x tower is quite effective for trapping of semi-volatile species of ruthenium and Cesium whereas some improvements mainly in the dust scrubber should increase the overall system DF. For the two isotopes tested and in the context of the LEWC composition, Cesium, with accounts for about 73 % of the gamma radiation appears to be the reference isotope for the volatile elements released from the melter. Ru is not a problem on the point of view of gas purification but can cause local radiation problem due to its trend to deposit on metal and to form insoluble components.

References

1. Filtration and capture of semi-volatile nuclides
M. Klein, M. De Smet, W.R.A. Goossens, L.H. Baetslé
IAEA-SM-245/51 (1980)

2. Volatilization and trapping of Ruthenium during calcination of nitric acid solutions
M. Klein, C. Weyers, W.R.A. Goossens
IAEA-SR-72/03 (1982)

3. Volatilization and trapping of Ruthenium in high temperature processes
M. Klein, C. Weyers, W.R.A. Goossens
17th DOE Nuclear Air Cleaning Conference (1982)

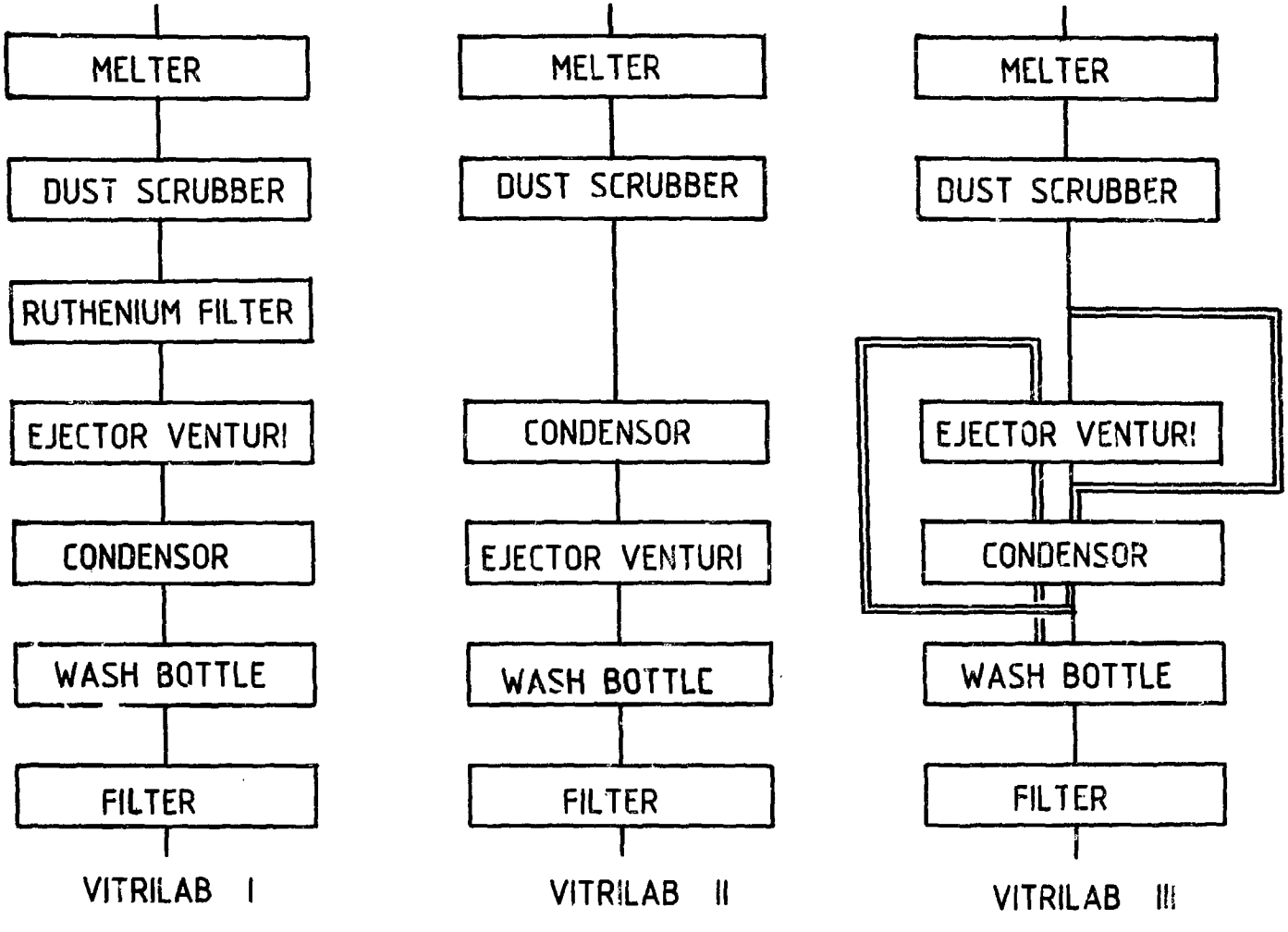

FIG. 1 BLOCK DIAGRAMM ON THE VITRILAB UNITS

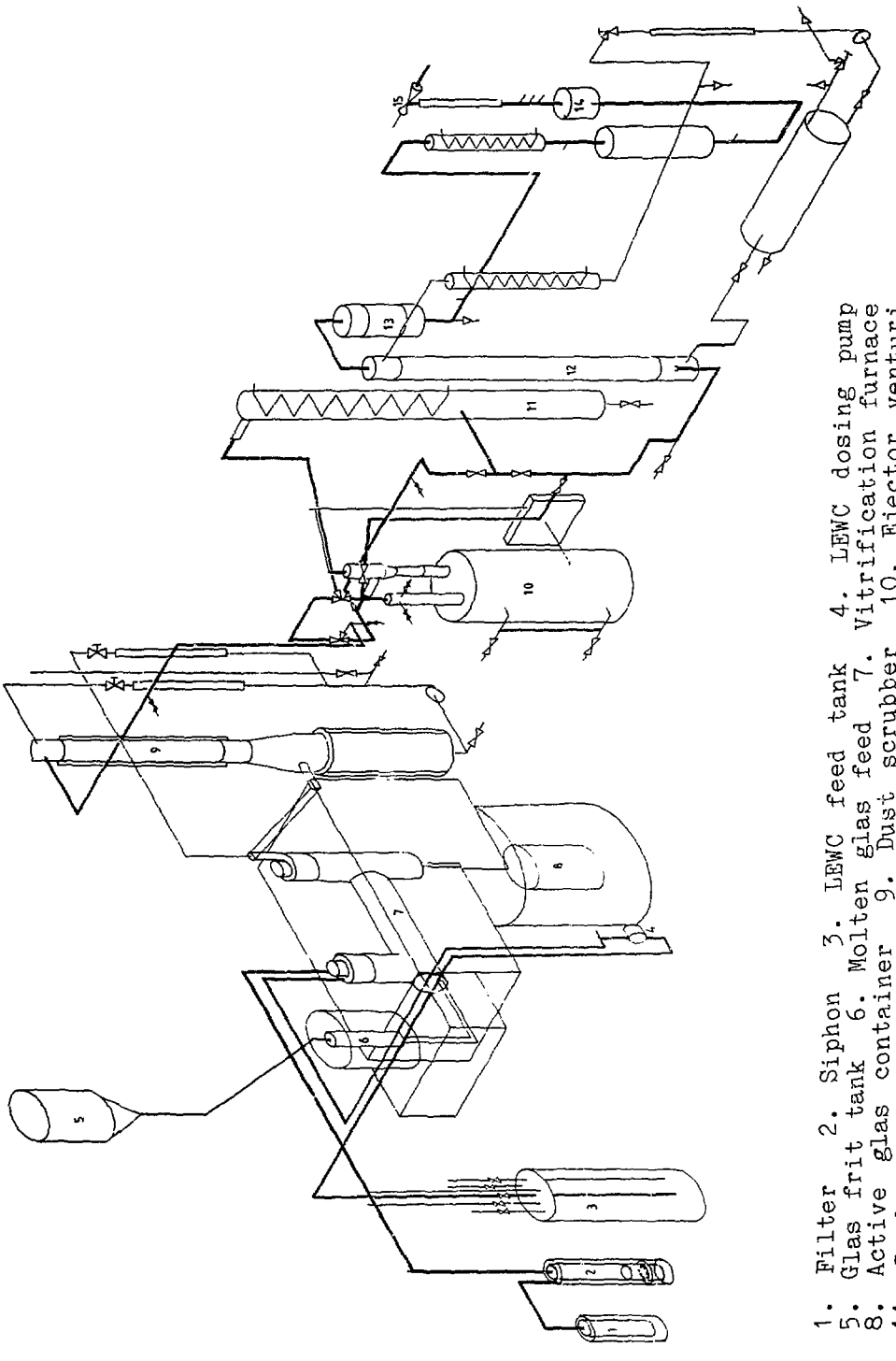

1. Filter 2. Siphon 3. LEWC feed tank 4. LEWC dosing pump
5. Glas frit tank 6. Molten glas feed 7. Vitrification furnace
8. Active glas container 9. Dust scrubber 10. Ejector venturi
11. Condensor 12. NOx washing tower 13. Demister
14. HEPA filter 15. Air ejector.

Fig. 2. : Vitrification unit "RUFUS" ---- treatment of LEWC type liquid waste.

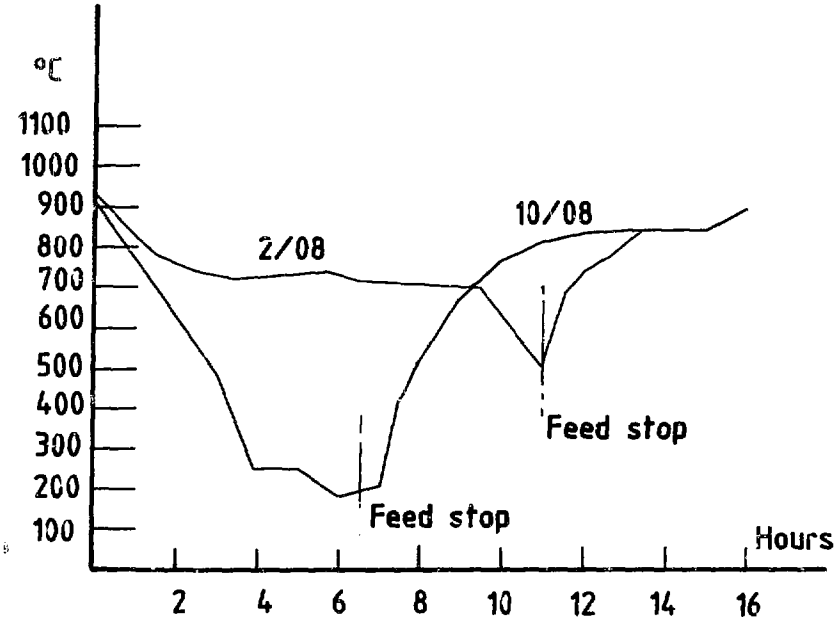

FIG. 3 GLASS SURFACE TEMPERATURE PROFILE

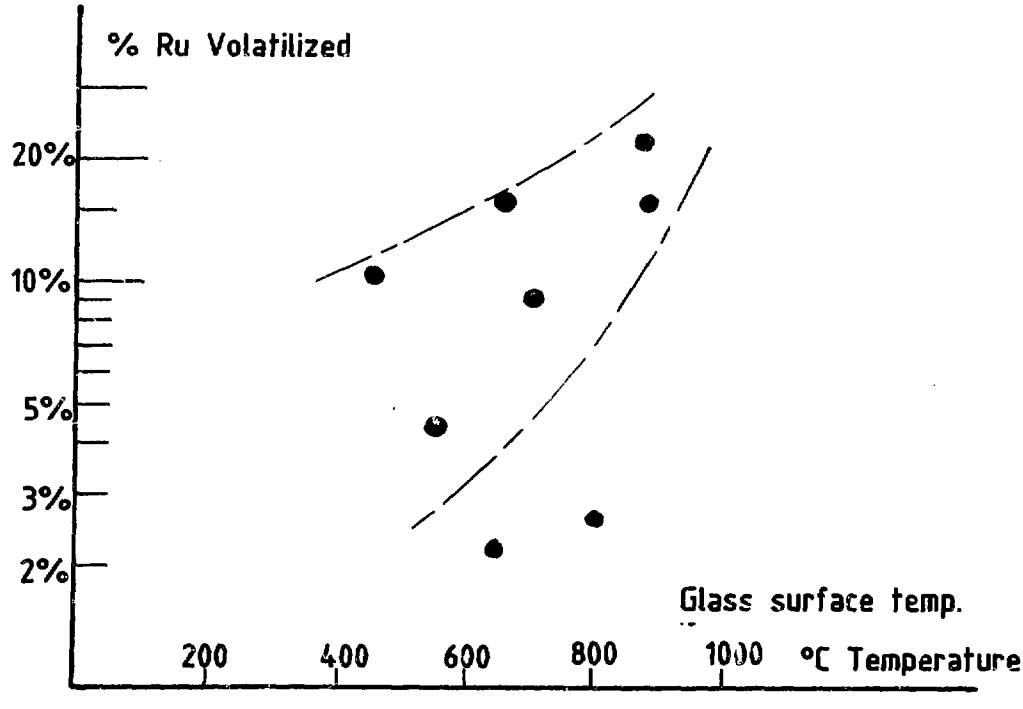

FIG. 4 VOLATILIZATION OF Ru DURING L.E.W.C. FEED

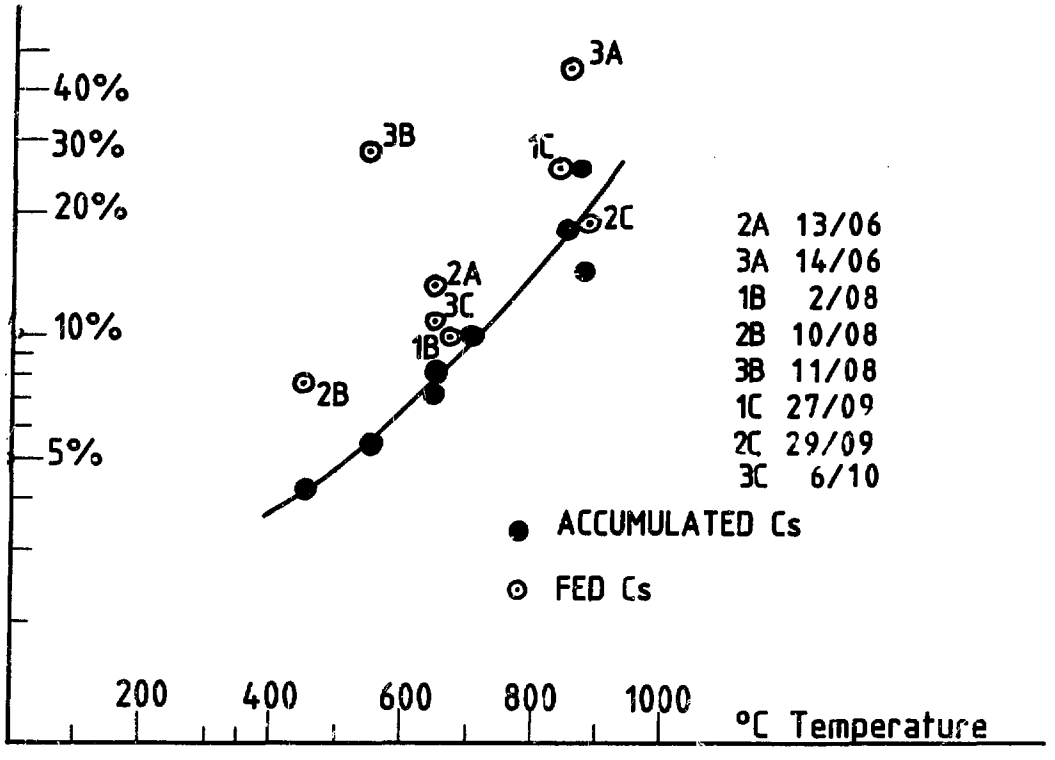

FIG. 5 CESIUM RELEASE IN FUNCTION OF THE GLASS SURFACE TEMP.

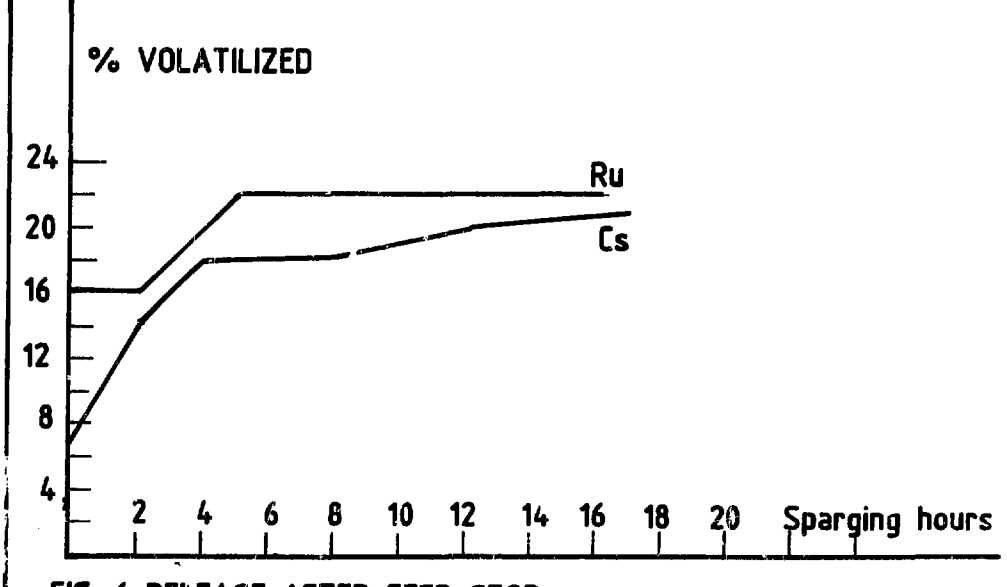

FIG. 6 RELEASE AFTER FEED STOP

PREDICTIONS OF LOCAL, REGIONAL AND GLOBAL RADIATION DOSES FROM IODINE-129 FOR FOUR DIFFERENT DISPOSAL METHODS AND AN ALL-NUCLEAR FUTURE

D.M. Wuschke, J.W. Barnard, P.A. O'Connor and J.R. Johnson*

Atomic Energy of Canada Limited
Environmental and Safety Assessment Branch
Whiteshell Nuclear Research Establishment
Pinawa, Manitoba R0E 1L0 Canada

*Health Sciences Division, Chalk River Nuclear Laboratories
Chalk River, Ontario K0J 1J0 Canada

Abstract

The radioactive isotope ^{129}I produced by nuclear fission becomes globally distributed if released to the environment In this report the consequences of several options for management of ^{129}I are discussed. In the first part of the report, estimates are presented of radiation doses from the ^{129}I produced in generating 1000 GW(e).a of nuclear electricity, the total production expected in Canada up to about 2040. Individual thyroid dose rates from ^{129}I, and accumulated collective effective dose equivalents to three groups are compared for four ^{129}I management strategies. These groups are: local persons living in the immediate vicinity of a discharge zone from a fuel reprocessing facility or waste disposal vault in the Canadian Shield, regional persons living in the lower Great Lakes basin, and average global persons. The four management strategies studied were: atmospheric discharge from a reprocessing facility, ocean dumping, subseabed disposal, and isolation in a deep vault in plutonic rock in the Canadian Shield. Doses associated with each of these options are compared with each other and with proposed Canadian regulatory limits.

In the second part of the report estimates are presented of doses to the same groups from fission-product ^{129}I, if fission supplied all future world energy needs. The two management options considered were geological disposal in vaults that would each eventually discharge ^{129}I at the rate estimated for a disposal vault in the Canadian Shield, and ocean dumping. Again, doses arising from these options are compared with each other and with proposed regulatory limits. The second comparison allows estimates to be made of the time at which such intensive use of fission could produce unacceptable levels of ^{129}I in the environment.

I. Introduction

Scope

The radioactive isotope ^{129}I is produced by fission in nuclear reactors. It has a high fission yield (about 0.0083 Mg ^{129}I per Mg material fissioned), and, because of its long half-life (16 million years) and high mobility in the environment, it becomes globally distributed if released to the environment.

Three general strategies are potentially available for management of fission product ^{129}I: direct discharge to the environment in

liquid or gaseous effluents from a nuclear fuel reprocessing plant; geologic disposal in a solid waste form; or elimination from earth by transmutation or space disposal. In this report the consequences of several management options in the first two categories are discussed.

In the first part of the report estimates are presented of radiation doses from the ^{129}I produced in generating 1000 GW(e).a of nuclear electricity, the total production expected in Canada up to about 2040. Individual thyroid dose rates from ^{129}I, and accumulated collective effective dose equivalents to three groups are compared for several ^{129}I management strategies. These groups are: local persons living in the immediate vicinity of a discharge zone from a reprocessing facility or waste disposal vault in the Canadian Shield, regional persons living in the lower Great Lakes basin, and average global persons. The four management strategies studied were: atmospheric discharge from a reprocessing facility, ocean dumping, subseabed disposal, and isolation in a deep vault in plutonic rock in the Canadian Shield. Doses arising from each of these options are compared with each other and with proposed Canadian regulatory limits for nuclear facilities.

In the second part of the report estimates are presented of doses to the same groups from fission-product ^{129}I, if fission supplied all future world energy needs. The two management options considered were geological disposal in vaults that would each eventually discharge ^{129}I at the rate estimated for a disposal vault in the Canadian Shield, and ocean dumping. Again, doses arising from these options are compared with each other and with proposed regulatory limits. The second comparison allows estimates to be made of the time at which such intensive use of fission-based energy could produce unacceptable levels of ^{129}I in the environment.

Background

Several studies have been made to assess doses to regional and global populations that might result from direct releases of ^{129}I to the environment as a gaseous or liquid effluent[1][2][3][4]. In addition, ^{129}I has been identified as a major contributor to dose to man in studies to assess potential long-term effects of geological disposal of high-level nuclear waste[5][6][7][8]. One of these[5] was a study of the Canadian concept of nuclear waste disposal in a deep vault in plutonic rock in the Canadian Shield[9].

Several models[2][10][11][12][13] have been developed to describe the global transport of iodine. One of these is a compartment model developed by Kocher[2]. Kocher estimated the amounts of stable ^{129}I in nine environmental compartments comprising the global atmosphere, hydrosphere, lithosphere and terrestrial biosphere. Global transport of ^{129}I was described by time-invariant transfer rates between compartments.

Kocher's global model was reviewed and revised by Smith and White[13]. Both Kocher, and Smith and White noted that the specific activities of ^{129}I in the region of a discharge might take thousands of years to decline to global average values, and that a more detailed model of iodine transport on local and regional scales was needed if estimates were required of maximum individual dose rates, or of col-

lective dose commitments to sub-populations that receive doses above the global average.

Johnson et al.[14] extended Kocher's revised model[13] to include fourteen compartments describing local and regional iodine transport (Figure 1). Since this model was intended primarily for assessment of the Canadian concept of disposal in a deep vault in plutonic rock in the Canadian Shield, they used transport and inventory data for the Canadian Shield/Great Lakes[15].

White and Smith[16] interfaced several initial dispersion models with Kocher's revised model for global circulation, and used these models to estimate local, regional and global doses for several management modes for ^{129}I.

Johnson's model[14] is capable of accepting time-varying discharges of ^{129}I into any of its local, regional or global compartments. In the current study we exploit this capability to study and compare several management modes for ^{129}I.

II. Description of Model

Introduction

The model used for this analysis is the compartment model developed and described by Johnson et al.[14] (Figure 1), except for some minor revisions in the assumed sources and amounts of stable iodine in the diet.

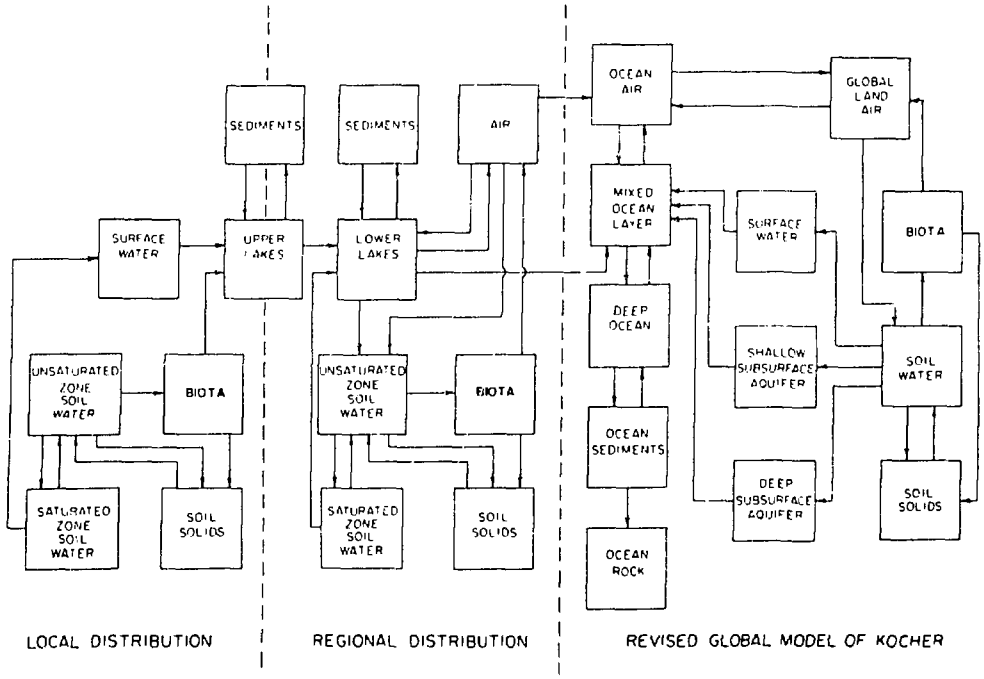

FIGURE 1
THE COMPARTMENT MODEL USED TO DESCRIBE ^{129}I TRANSPORT IN THE ENVIRONMENT

The Local System

A conceptual drawing of the local system appears in Figure 2. The critical group in the local system, that is those persons who would receive the highest dose because of their proximity to the discharge, were considered to be residents of a 1000-ha farm adjacent to a disposal or reprocessing facility. These people would eat food grown on the farm and drink water from a well drilled into the local saturated soil zone. However, they would supplement their local diet with freshwater fish from regional surface water, and with ocean fish.

If the facility is a disposal vault in plutonic rock, as depicted in Figure 2, vault discharge could enter the saturated zone soil water, the unsaturated zone soil water or surface water. It is assumed that iodine discharged to surface water would flow directly to the upper Great Lakes without entering the local biosphere. Iodine entering the soil compartments would be exchanged between these compartments as a result of percolation, capillary action and seasonal changes in the water table. Transfer to local biota would be via soil water in the unsaturated soil zone. The model takes into account transfer of iodine from biota to the atmosphere via decay of organic material and forest fires. This vapourized iodine is assumed to be transported directly to upper Great Lakes water, since the airborne transport and precipitation are so rapid that the iodine is returned to the upper Lakes watershed before it can contribute significantly to iodine concentrations in the local environment. Reversible sedimentation in the upper Lakes has been included.

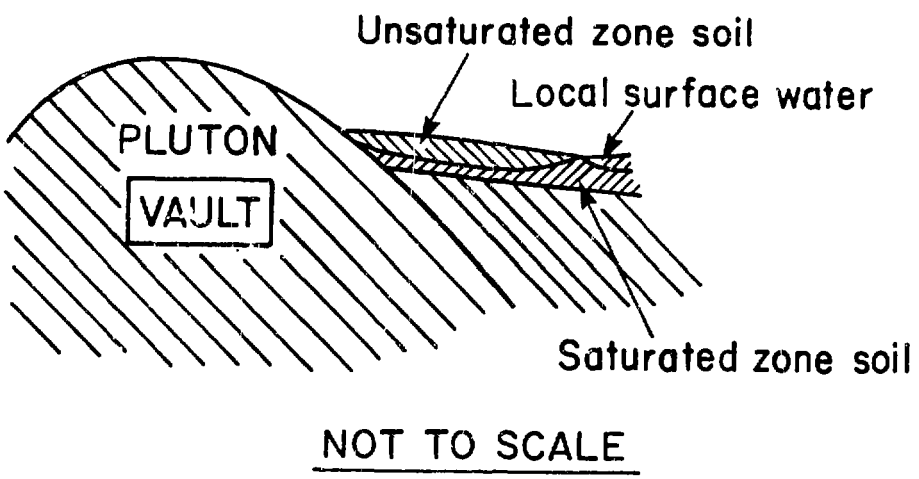

FIGURE 2
SCHEMATIC OF ENVIRONMENT OF LOCAL REFERENCE INDIVIDUAL

The Regional System

The regional system is the lower Great Lakes basin, downstream of the local system and encompassing the major commercial and industrial centres of southwestern Ontario and portions of upstate New York and Ohio. It was assumed that residents of the region would eat mainly food gathered from this region, but would supplement their diet

with ocean fish. Drinking water would be supplied from the lower Great Lakes.

The compartments in the regional model are similar to those in the local model. However, a regional air compartment that exchanges iodine with the lower Lakes, unsaturated zone soil water, biota and ocean air has been added.

The Global System

The compartment network used for modelling global iodine transport is essentially Kocher's scheme[2], as modified by Smith and White[13]. The only change has been the explicit addition of a surface water compartment.

Fractional Transfer Rate Constants

The model assumes that the efflux from each compartment is proportional to its inventory, and that influxes are proportional to inventories in neighbouring donor compartments. This results in a set of linear first-order differential equations relating inventories to their time rate of change[2]. Any program for solving systems of linear differential equations may be used to solve for compartment inventories as a function of time. We have used the AECL program FORSIM[17].

The fractional transfer coefficients for the local and regional systems are given in Tables 1 and 2, respectively, and are based on data for ecosystems of the upper Great Lakes and Hudson's Bay watershed[15].

TABLE 1. FRACTIONAL TRANSFER COEFFICIENTS (a^{-1}) FOR TRANSFER OF IODINE FROM THE COMPARTMENTS DESCRIBING THE LOCAL SYSTEM

Pathway	Value
Sediments to Upper Lake	6.8(-6)
Upper Lake to Sediments	7.3(-5)
Atmosphere to Unsaturated Zone	0.0
Biota to Atmosphere	1.0(-1)
Surface Water to Upper Lake	3.7(2)
Upper Lake to Regional	5.5(-3)
Unsaturated Zone to Biota	2.5(1)
Soil Solids to Unsaturated Zone	1.0(-3)
Unsaturated Zone to Soil Solids	3.0(1)
Biota to Soil Solids	9.2(-1)
Saturated Zone to Surface Water	1.2(-1)
Saturated Zone to Unsaturated Zone	3.1(-2)
Unsaturated Zone to Saturated Zone	5.5(-1)

TABLE 2. FRACTIONAL TRANSFER COEFFICIENTS (a^{-1}) FOR TRANSFER OF IODINE FROM THE COMPARTMENTS DESCRIBING THE REGIONAL SYSTEM

Pathway	Value
Regional Air to Global Air	1.2(2)
Atmosphere to Unsaturated Zone	1.5(1)
Biota to Atmosphere	1.0(-1)
Surface Water to Atmosphere	2.0(-3)
Atmosphere to Surface Water	2.1(1)
Surface Water to Mixed Ocean	8.1(-2)
Surface Water to Unsaturated Zone	3.5(-3)
Unsaturated Zone to Biota	8.2(0)
Soil Solids to Unsaturated Zone	1.0(-3)
Unsaturated Zone to Soil Solids	1.0(1)
Biota to Soil Solids	9.2(-1)
Saturated Zone to Surface Water	2.0(0)
Saturated Zone to Unsaturated Zone	2.5(-1)
Unsaturated Zone to Saturated Zone	4.0(1)
Sediments to Surface Water	2.5(-5)
Surface Water to Sediments	2.7(-4)

TABLE 3. FRACTIONAL TRANSFER COEFFICIENTS (a^{-1}) FOR TRANSFER OF IODINE FROM THE COMPARTMENTS DESCRIBING THE GLOBAL SYSTEM

Pathway	Value
Land Air to Ocean Air	3.5(0)
Land Air to Soil Water	1.8(1)
Biota to Land Air	5.2(-3)
Surface Water to Mixed Ocean	1.0(5)
Soil Water to Surface Water	2.1(0)
Soil Water to Biota	1.4(-1)
Soil Solids to Soil Water	1.0(-3)
Soil Water to Soil Solids	1.6(1)
Biota to Soil Solids	4.7(-2)
Ocean Sediments to Ocean Rock	2.0(-8)
Ocean Air to Land Air	1.4(0)
Ocean Air to Mixed Ocean	2.3(1)
Mixed Ocean to Ocean Air	1.5(-3)
Shallow Aquifer to Mixed Ocean	1.0(-3)
Deep Aquifer to Mixed Ocean	7.0(-5)
Mixed Ocean to Deep Ocean	5.3(-2)
Deep Ocean to Mixed Ocean	8.9(-4)
Ocean Sediments to Deep Ocean	2.0(-6)
Deep Ocean to Ocean Sediments	2.2(-5)
Soil Water to Shallow Aquifer	4.2(-1)
Soil Water to Deep Aquifer	8.2(-3)

The values for the transfer coefficients for the global system are given in Table 3. Except for the following minor adjustments the values have been taken from Smith and White's modified model[13]. Since the surface water compartment flushes soil-water iodine rapidly to the mixed ocean this transfer coefficient was given a relatively high value of $10^{3} a^{-1}$. Also, the transfer rate to ocean rock was recalculated using the ocean surface area rather than the land area to estimate ocean rock inventories.

Dose Calculation

In order to calculate dose with this model, intake rates of stable iodine were estimated for components of man's diet, Kocher[2] estimated intake rates based on the diet of reference man[18] and globally averaged stable iodine concentrations. Rowsell and McKee's[15] data on concentrations of stable iodine in the Canadian Shield were used to estimate iodine intake rates for man in the local and regional systems. The intake and sources of dietary iodine are listed in Table 4.

TABLE 4. SOURCES AND INTAKE RATES OF DIETARY IODINE FOR REFERENCE MAN[18] AND THEIR RELATIONSHIP TO THE COMPARTMENTS OF THE MODEL

Dietary Source	Annual Intake+ (g)	Compartment		
		Local	Regional	Global
Inhalation and Foliar Deposition	8.0×10^{-4}	Global Air	Regional Air	Global Air
Freshwater Fish	9.2×10^{-4}	Lower Great Lakes	Lower Great Lakes	Global Surface Water
*Ocean Fish	6.1×10^{-3}	Ocean Mixed Layer	Ocean Mixed Layer	Ocean Mixed Layer
Vegetables, Cow's Milk and Beef	4.3×10^{-2}	Local Biota	Regional Biota	Global Biota
Fluid, except milk	5.6×10^{-4}	Local Saturated Zone Soil Water	Regional Surface Water	Global Surface Water

+ Calculated from data supplied by Rowsell and McKee[15], except for *, from Kocher[2].

To estimate dose to the thyroid the average specific activity of the intake was calculated. It was assumed that the specific activity of ^{129}I in the thyroid would be the same as the average specific

activity of ingested ^{129}I. The thyroid dose would then be proportional to the specific activity of dietary iodine. The proportionality constant is given by[14]:

$$\text{Dose rate } (Sv.a^{-1}) = 2.1 \times 10^{2} S_A,$$

where S_A is the average specific activity of ^{129}I in the diet in GBq per gram of total iodine.

Thyroid dose as a function of time was calculated to 10^8 a. To assess total radiological detriment to global and regional populations, the effective dose equivalent was calculated by multiplying the thyroid dose by the weighting factor 0.03[20]. This was multiplied by the population and integrated over time to obtain the accumulated collective effective doses to the global and regional populations.

III. Comparison of Doses from ^{129}I for Four Management Options

Introduction

Analyses were carried out to estimate individual thyroid dose rates from ^{129}I, and accumulated collective effective dose equivalents for each of four management strategies for ^{129}I: atmospheric discharge from a reprocessing facility, ocean dumping, subseabed disposal, and isolation in a deep vault in plutonic rock in the Canadian Shield. Only the last of these management options is being considered by Canada.

For each option, the analysis was based on 7.81 Mg (5.04×10^4 GBq) of ^{129}I, corresponding approximately to the production of 1000 GW(e).a of nuclear electricity. This is about 150 times the amount of nuclear electricity produced in Canada in 1983. It was assumed that this amount of ^{129}I would be either released as an effluent at a constant rate over 20 years (i.e. 0.39 Mg. a^{-1} ^{129}I), or emplaced all at once in a single disposal facility in subseabed sediments or in plutonic rock in the Canadian Shield.

Rates of Discharge of ^{129}I to the Environment

For the first option, atmospheric discharge from a reprocessing facility, a constant release into the local atmosphere from a 100-m stack was assumed. A Gaussian plume model[19] and data from a site in the Canadian Shield were used to estimate local doses at the boundary of a 1-km exclusion zone during this release, since the compartment model is not sufficiently detailed for this calculation. The compartment model was used to estimate local doses after the release was over, and regional and global doses.

For ocean dumping, discharge of ^{129}I at a constant rate over 20 years into the mixed ocean compartment was assumed.

For the two geological disposal options, subseabed disposal and isolation in a vault in plutonic rock, releases to the environment were calculated by the computer code SYVAC[5][8], developed to assess the Canadian concept of nuclear waste disposal. The release function for subseabed disposal is for separated ^{129}I immobilized in a waste

form with release characteristics similar to borosilicate glass, and buried 30 m deep in subseabed sediments. It was assumed that the mean time for container failure would be 500 years, and that the waste form would dissolve over 1000 years, releasing its ^{129}I, which would be transported through the sediments to the deep ocean compartment. The release rate to the deep ocean calculated by SYVAC is shown in Figure 3.

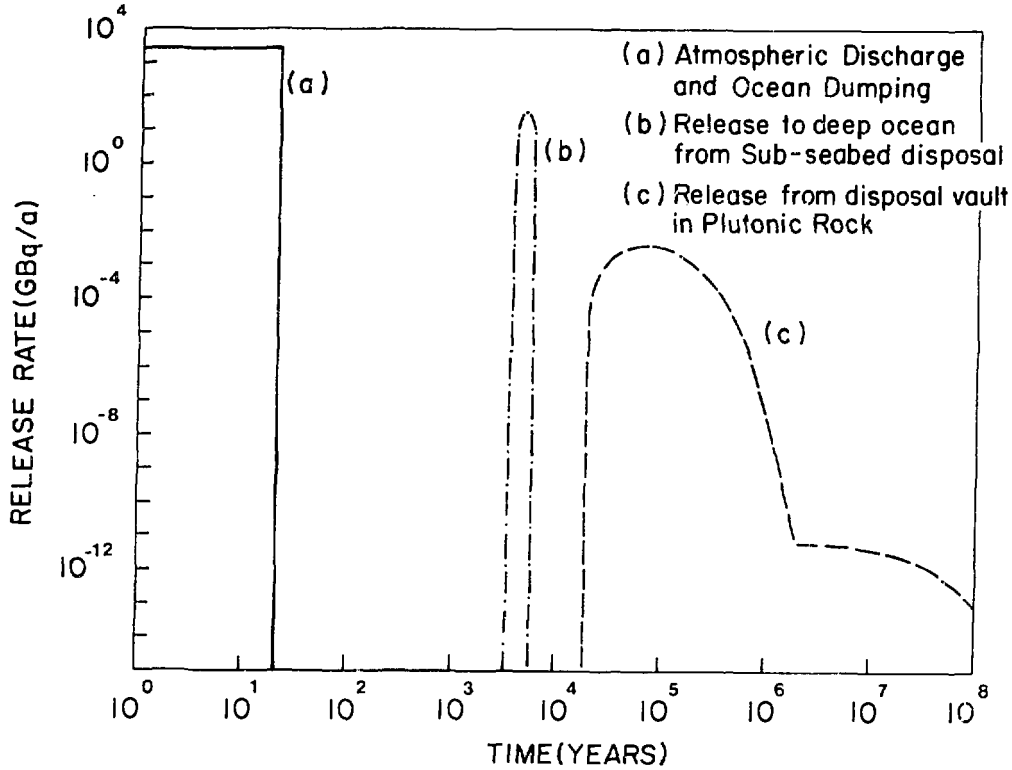

FIGURE 3
RATES OF DISCHARGE OF ^{129}I TO THE ENVIRONMENT

Release of ^{129}I from a deep disposal vault in plutonic rock would result from the action of groundwater which would corrode the containers of used fuel, leach the waste and transport it to the surface, where it could be released to surface water, or to saturated or unsaturated zone soil. The highest doses are predicted if release is to the unsaturated zone soil water compartment[14], and release to this compartment was assumed for this analysis. The rate of discharge to this compartment was calculated by SYVAC for used CANDU* fuel buried 1000 m deep in plutonic rock in the Canadian Shield. It was assumed that the mean time for container failure would be 2.0×10^4 years, and that only ^{129}I that migrated to the fuel-sheath gaps while the fuel was in the reactor (about 1% of the total vault inventory)

* Canada's natural-uranium-fuelled, heavy-water-moderated and cooled reactor. (CANada Deuterium Uranium)

would be released immediately following container failure. The remainder of the ^{129}I is assumed to be released by congruent dissolution of the uranium dioxide fuel matrix. This release rate is predicted to be extremely slow, about 10^{-17} a^{-1}, so that most of this ^{129}I would decay before release.

Consequently, for used fuel in plutonic rock only about 1% of the total ^{129}I inventory, the fraction initially in the fuel-sheath gaps, would discharge to man's environment whereas, for subseabed disposal of ^{129}I in an immobilized waste form, the entire inventory would discharge to the deep ocean. The predicted discharge rates to the local biosphere are shown in Figure 3.

Results

Calculated individual dose rates to the adult human thyroid for each of these options are compared in Figure 4. For the two land-based options, atmospheric discharge from a reprocessing facility, and disposal in plutonic rock in the Canadian Shield, "local" doses would be much higher than "regional" or "global" doses during the discharge, but, later, when most of the ^{129}I would have entered global circulation, these doses would become similar. For the ocean dumping and subseabed disposal options, members of local and regional groups

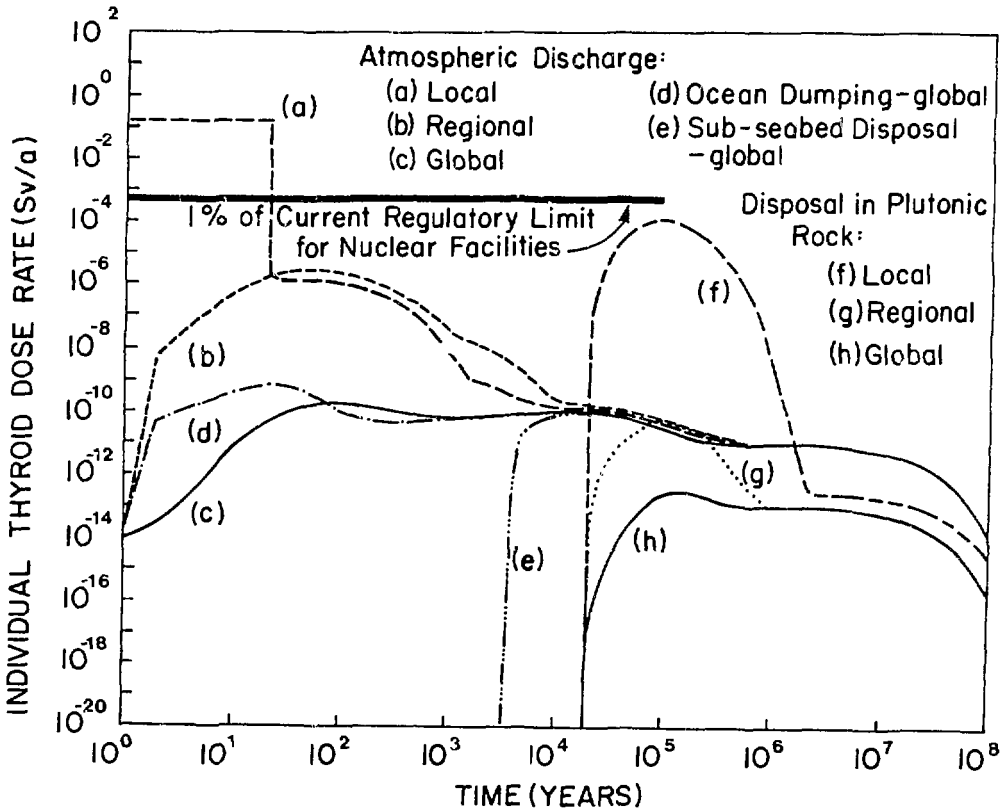

FIGURE 4
CALCULATED INDIVIDUAL DOSE RATES TO THE ADULT HUMAN THYROID FOR FOUR DISPOSAL OPTIONS

living in the Canadian Shield would receive doses only from ^{129}I in global circulation. Hence, doses to members of these groups would be the same as those to average "global" persons, and the "global" doses illustrated for these options in Figure 4 apply also to members of the local and regional groups in the Canadian Shield.

In Figure 4, a line at 0.5 mSv represents 1% of the proposed Canadian regulatory limit for thyroid dose rates to members of the public from present-day nuclear facilities. This limit is based on recommendations of the International Commission on Radiological Protection[20]. The only dose predicted to exceed 1% of this limit is the local dose due to atmospheric discharge from a reprocessing facility. This dose is three orders of magnitude higher than the estimated "local" dose from discharge from a disposal vault in plutonic rock, and many orders of magnitude higher than estimated doses from either ocean dumping or disposal in subseabed sediments.

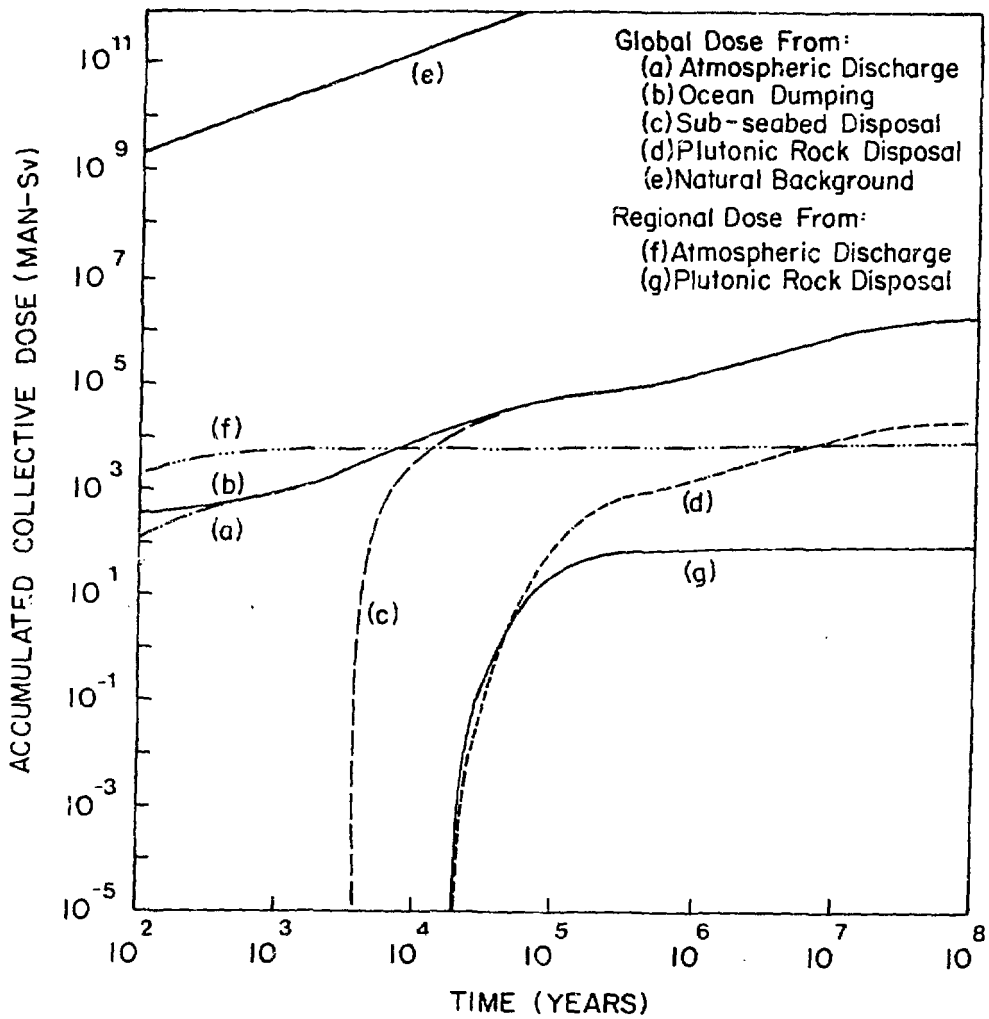

FIGURE 5
ACCUMULATED COLLECTIVE EFFECTIVE DOSE EQUIVALENT
FOR FOUR DISPOSAL OPTIONS AND FROM NATURAL BACKGROUND

Calculated accumulated collective effective doses to an assumed constant global population of ten billion are illustrated in Figure 5 for each of the four options. For atmospheric discharge from a reprocessing facility and disposal in plutonic rock in the Canadian Shield, collective doses are also shown for the regional population, assumed to be constant at ten million. Until about 5 000 and 38 000 years, for atmospheric discharge and disposal in plutonic rock, respectively, most of the collective dose would be to the regional population.

Calculated accumulated collective doses to the global population from atmospheric discharge and ocean dumping are almost identical at all times. For subseabed disposal the accumulated collective effective dose would be zero for about 4 000 years, until release of ^{129}I from the ocean sediments begins, but would then approach the values for the other two options. The collective dose for disposal in plutonic rock would be zero until about 20 000 years, when its discharge begins. Since, for this option, it is estimated that nearly 99% of the ^{129}I would decay before reaching man's environment, the accumulated collective effective dose at 10^8 years is about two orders of magnitude lower than for the other options.

The accumulated collective effective dose from natural background to a constant population of ten billion is also illustrated in Figure 5, assuming a constant average individual dose rate of 2 $mSv.a^{-1}$. For all management options, the accumulated collective dose equivalent from ^{129}I is at least six orders of magnitude lower.

Discussion

There are many uncertainties in this analysis. The validity of all the calculations depends on how well the mathematical models represent the real system. Also there is wide variability in the values of system parameters for both the natural environment and engineered systems, and the results of the analysis are highly dependent on the values selected for some of those parameters. In interpreting or applying these results, both the applicability of the mathematical models and the parameter values used should be reviewed, and their suitability assessed. Some factors that could have a major influence on the results are discussed in the following paragraphs.

Doses from atmospheric discharge of ^{129}I from a reprocessing facility depend on the annual throughput of the facility; local weather, topology and agricultural practices; and the stack height and site of the exclusion zone of the facility. They also depend on the degree of control of plant effluents; for this analysis it was assumed that there was no control of effluents.

Doses from ocean dumping and subseabed disposal depend on the diet of the individuals receiving the dose, and on the degree of dispersion of the ^{129}I before incorporation in man's food chains. For these analyses it was assumed that the ^{129}I would be globally dispersed throughout the mixed ocean or deep ocean compartments, for dumping and subseabed disposal, respectively, before entering man's food chains. These may not be valid assumptions, especially for ocean dumping.

For subseabed disposal, an additional uncertainty is in the rate of release of ^{129}I from the sediments into the deep ocean. This depends on many factors, including depth of burial, container failure rate, leach rate of the waste, and properties of the sediments. However, provided all the ^{129}I is released from the sediments to the deep ocean compartment before significant irreversible removal of ^{129}I by radioactive decay or incorporation in ocean rock, the shape of the release function has little influence on the magnitude of the maximum dose, although it does affect the time at which this dose would be received.

For a disposal vault in plutonic rock, there is even more uncertainty in the release rate of ^{129}I. Furthermore, for this option, the predicted dose is highly dependent on the shape of the release function; maximum dose depends on the maximum value of the release function, as well as the total amount of ^{129}I released from the vault before decaying. Because the assumed waste form is intact, used CANDU fuel, it is predicted that only about 1% of its ^{129}I inventory would be released before decaying, but that this fraction would all be released immediately upon container failure. Doses could be about 100 times higher if the entire inventory of ^{129}I were released over a short time; they could be many orders of magnitude lower if the ^{129}I inventory were incorporated in a waste form from which release of ^{129}I was entirely by very slow congruent dissolution.

Conclusions

In spite of the uncertainties discussed in the preceding section, the following conclusions are drawn:

1. Uncontrolled atmospheric discharge of ^{129}I from a reprocessing facility with the throughput assumed in this analysis is unlikely to be acceptable. However, a considerable reduction from the individual dose levels estimated here could be achieved by facility design and careful site selection.

2. Doses resulting from ocean dumping of ^{129}I would be low if global dispersion throughout the mixed ocean before incorporation in man's food chains could be assured. However, it is unlikely that such assurance would be established; furthermore, the London and Barcelona conventions presently prohibit dumping of nuclear fuel waste in the oceans. Therefore, this might not be an allowed option.

3. Subseabed disposal is likely to produce the lowest individual doses of any of the management options studied. However the technical and engineering feasibility of this option have not yet been demonstrated. Until an international regulatory mechanism is in effect, the subseabed disposal option will likely be unacceptable.

4. In spite of large differences in maximum individual doses for the above three options, accumulated collective effective dose equivalents to the world population are likely to be similar.

5. Disposal in a deep underground vault in plutonic rock will probably reduce individual doses from ^{129}I to acceptable levels, and may also provide a substantially lower accumulated collective dose than

the other options. This option is considered technically feasible, and is not prohibited by Canadian legislation or international agreement. This is the option being studied by Canada, as well as by several other countries, for disposal of nuclear fuel waste. This ongoing research should substantially reduce the uncertainties presently associated with the dose calculations for this option.

IV. Potential Dose from ^{129}I if Fission Supplied All Future Energy Needs

Introduction

Further calculations were carried out to estimate potential doses to members of local, regional and global groups (as defined in Section I) from ^{129}I produced by nuclear fission, if fission supplied all future world energy needs.

Rate of Production of ^{129}I

In order to estimate the maximum rate at which ^{129}I might be produced, and the resulting maximum dose rates to future populations, the following assumptions were made:

(1) Predicted future energy needs will be met entirely by fission in Canada and globally. Currently, the world uses about 0.2 Q of energy per year ($Q=1.06 \times 10^{18}$ kJ), and it has been estimated that world energy production must rise to between 3 and 10 Q per year to provide a North American standard of living for a predicted stable world population of ten billion[21].

The maximum predicted rate of 10 Q per year for global energy use was assumed for this analysis, with one-twentieth of this (0.5 $Q \cdot a^{-1}$) assumed to be used in Canada. It has been estimated that there is enough uranium and thorium in the earth's crust to sustain this rate for about 10^8 years[22]. These energy consumption rates correspond to annual global and Canadian productions of about 830 and 42 Mg ^{129}I, respectively. Note that the production rate of ^{129}I is essentially independent of nuclear fuel cycles, since fission yields for ^{129}I from all important fissile nuclides are similar[22]. The production rate of ^{129}I therefore depends only on the rate of energy use.

(2) Radioactive decay will be the only process removing ^{129}I from the planet; there will be no removal by other processes such as transmutation or space disposal.

Rate of Entry of ^{129}I into Local, Regional and Global Environments

To predict the rate of entry of ^{129}I produced by fission into the local, regional and global environments defined in Section II, it was assumed that disposal of ^{129}I will be carried out at a rate corresponding to its rate of production.

Two disposal options were considered: geological disposal and ocean dumping of high-level waste. For geological disposal, the form of the waste was assumed to be either intact used fuel bundles or a

waste form resulting from reprocessing, with release characteristics similar to that for CANDU fuel bundles of current design.

For geological disposal, it was assumed that one-half of the ^{129}I produced in Canada, 21 Mg.a^{-1} ^{129}I, would be isolated in vaults in the Canadian Shield, and that each of these vaults would eventually discharge ^{129}I to the local biosphere at the rate shown in Figure 3, curve (c), but delayed by a time corresponding to the time of production and disposal of the waste. Discharges from these vaults would enter the Great Lakes Basin via a local discharge zone in the Canadian Shield, and would be carried to global oceans and the atmosphere. It was assumed that the remaining one-half of the ^{129}I produced in Canada, and all that produced in the rest of the world would enter the global environment at the same rate as the portion discharged from the vaults in the Canadian Shield, but without passing through the Canadian Shield or Great Lakes Basin.

It was assumed that only one vault, containing 7.8 Mg of ^{129}I, equivalent to about 0.09 Q of energy production, would contribute directly to "local" doses, and that only vaults in the Canadian Shield would contribute directly to "regional" doses. However, all the ^{129}I released globally would eventually enter global circulation, and contribute to both local and regional doses.

For the ocean dumping option, it was assumed that all ^{129}I produced globally (830 Mg.a^{-1} ^{129}I) would be dumped into the mixed ocean compartment, in a soluble form, as soon as it was produced.

Results

Calculated individual dose rates to the human thyroid vs. time are illustrated in Figure 6 for the scenarios described above. Curve (a) shows individual thyroid dose rates from ocean dumping of all the ^{129}I produced globally. As discussed in Section III, calculated "local", "regional" and "global" doses from this option would be identical.

Curves (b), (c) and (d) show "local", "regional" and "global" dose rates for geological disposal in plutonic rock. The local dose transient illustrated in curve (b) applies to the first vault discharging in the Canadian Shield; local doses from other disposal vaults would be similar, but delayed. For this disposal scenario, the "local" dose rate would initially be identical to that shown in Figure 4, curve (f), since it is based on the same amount of ^{129}I, and the only contributor to dose at first would be a single "local" vault. However, discharges of ^{129}I from other regional and global vaults would produce steadily increasing amounts of ^{129}I in global circulation, and after about 10^5 years, this globally circulating ^{129}I would be the major contributor to local dose. Similarly, "global" ^{129}I would eventually become the major contributor to regional dose. Local, regional and global doses would then approach the same value.

After about 10^5 years the rate of increase of all doses begins to fall off, due to removal to ocean sediments and irreversible incorporation in ocean rock. And after 10^8 years, the total ^{129}I inventory will have been reduced significantly by radioactive decay.

Nevertheless, at 10^8 years the amount of ^{129}I in global circulation, and the resulting doses, would still be increasing. As discussed in Section III, only about 1% of the initial inventory of ^{129}I would be released before decaying, so doses from this option remain about two orders of magnitude lower than for ocean dumping.

In Figure 6, a line at 0.5 mSv represents 1% of the proposed Canadian regulatory limit for thyroid dose from existing nuclear facilities. In spite of the tremendous rate of production of fission energy assumed, and the correspondingly high rate of production of ^{129}I, the predicted local, regional and global doses from disposal in plutonic rock are still below this level at 10^8 years, and doses from ocean dumping of ^{129}I do not exceed it until 10^5 years.

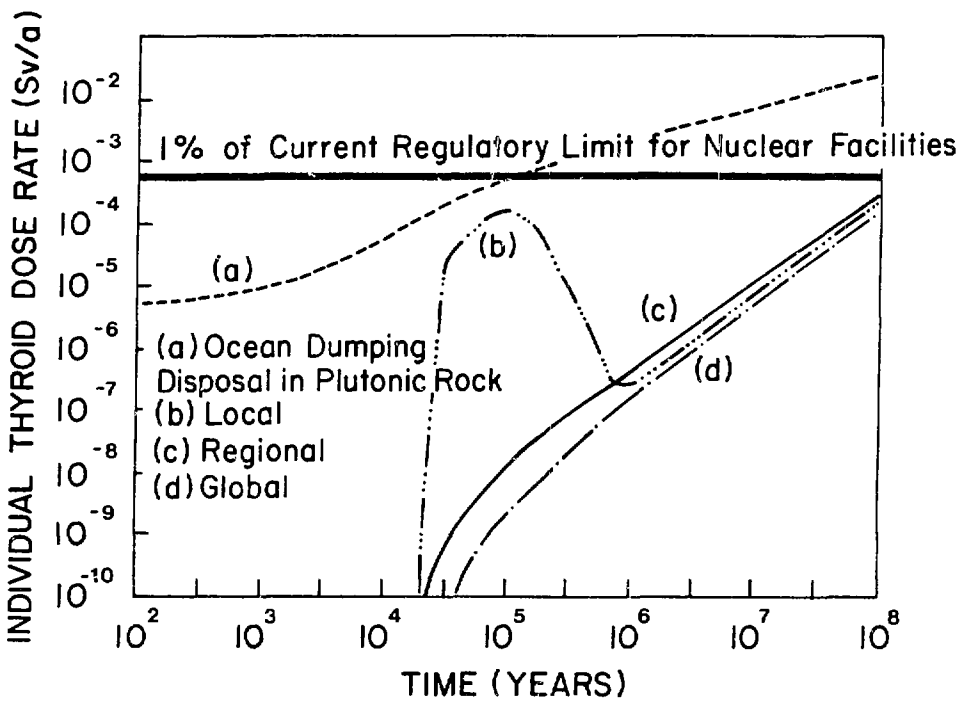

FIGURE 6
INDIVIDUAL THYROID DOSE RATES FROM OCEAN DUMPING OR DISPOSAL IN PLUTONIC ROCK OF ^{129}I FROM GLOBAL ANNUAL ENERGY PRODUCTION OF 10 Q

Figure 7 shows calculated accumulated collective effective doses that would result from ocean dumping or disposal in plutonic rock of ^{129}I equivalent to energy production of 10 $Q.a^{-1}$. Stable future populations are assumed, comprising ten billion and ten million, respectively, for global and regional populations. As for individual dose rates, and for the same reason, the collective dose commitment from disposal in plutonic rock is about two orders of magnitude lower than that from ocean dumping.

The accumulated collective effective dose from natural background is also illustrated in Figure 7. This was calculated assuming

that the present average individual background dose rate of 2 $mSv.a^{-1}$ is maintained. The global collective dose remains below this level for 10^6 years for disposal in plutonic rock, and does not exceed it until about three million years for ocean dumping.

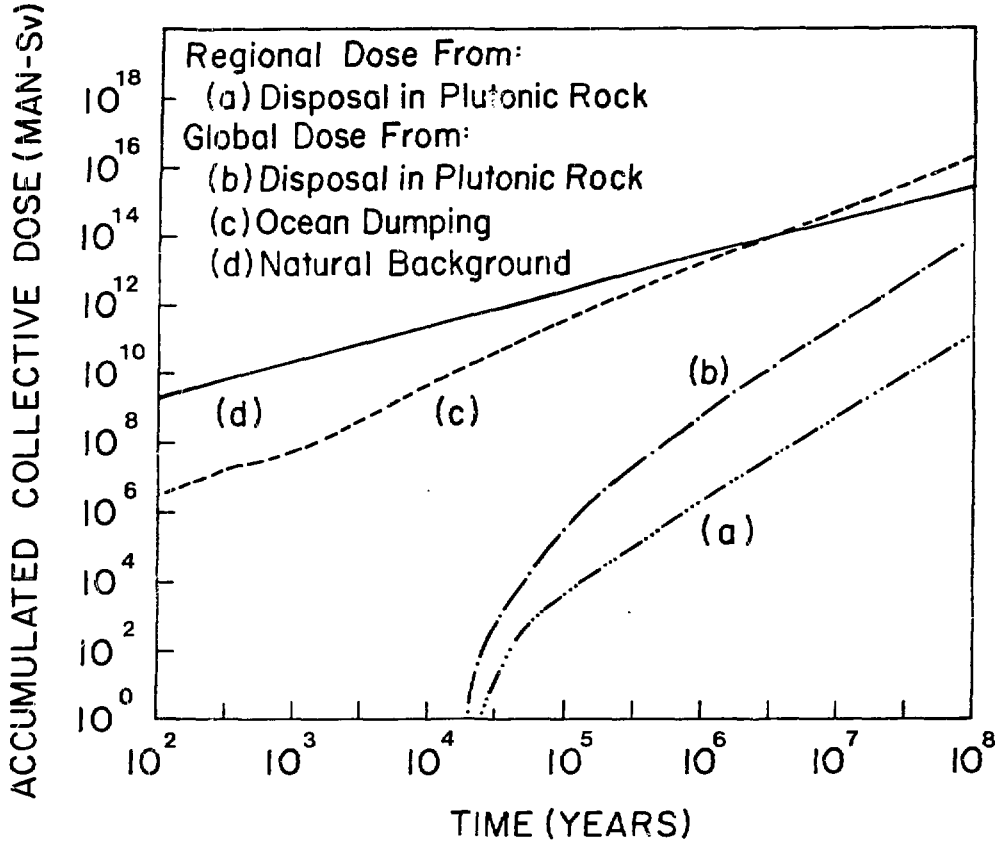

FIGURE 7
ACCUMULATED COLLECTIVE EFFECTIVE DOSES FROM OCEAN DUMPING OR DISPOSAL IN PLUTONIC ROCK OF ^{129}I FROM GLOBAL ANNUAL ENERGY PRODUCTION OF 10 Q

Discussion

The uncertainties discussed in Section III also apply to this analysis, and there is the additional uncertainty of predicting future production of energy from fission. The assumption made that all future energy will be supplied by fission is obviously completely unrealistic, but should represent an upper limit for future production of ^{129}I.

Conclusions

In spite of the uncertainties in this analysis, the following conclusions are drawn:

1. Even with global use of 10 Q of fission energy annually, the highest dose rates would likely be to local individuals in the vicinity of a discharge from either a reprocessing facility or disposal vault. Adequate control of these local doses should ensure that regional and global doses would also be acceptably low.

2. If fission were the only source of future energy and, if disposal were by ocean dumping or in vaults in plutonic rock, world energy requirements could be met for hundreds of thousands of years before thyroid doses from ^{129}I would exceed 1% of current Canadian regulatory limits for nuclear facilities. The performance of other geologic disposal options is likely to be similar.

V. References

(1) Nuclear Energy Agency, "Radiological significance of and management of tritium, carbon-14, kryton-85, iodine-129 arising from the nuclear fuel cycle," Nuclear Energy Agency, Organization of Economic Co-operation and Development, report by an NEA Group of Experts, OECD, Paris, France (1980).

(2) Kocher, D.C., "A dynamic model of the global iodine cycle for the estimation of dose to the world population from releases of iodine-129 to the environment," Oak Ridge National Laboratory Report, NUREG/CR-0717 (ORNL/NUREG-59) (1979).

(3) McKay, H.A.C. (ed.), Miguel, P. and White, I.F. "Management modes for iodine-129," in: Hebel, W. and Cottone, G. (ed), Management Modes for Iodine-129. Harwood Academic Publishers, Chur (CH). EUR 7953 (1982).

(4) Brown, R.A., Christian, J.D. and Thomas, T.R., "Airborne radioactive waste management," Department of Energy Report, ENICO-1132 (1983).

(5) Wuschke, D.M., Mehta, K.K., Dormuth, K.W., Andres, T., Sherman, G.R., Rosinger, E.L.J., Goodwin, B.W., Reid, J.A.K., Lyon, R.B., "Environmental and safety assessment studies for nuclear fuel waste management. Volume 3: Post-closure assessment," Atomic Energy of Canada Limited Technical Record, TR-127-3* (1981).

(6) Nilsson, L.B., and Papp. T., "' concept for safe final disposal of spent nuclear fuel," in: Radioactive Waste Management, Volume 3, International Atomic Energy Agency, Vienna, IAEA-CN-43/70, 93-106 (1984).

(7) Hill, M.D. and Grimwood, P.D., "Preliminary assessment of the radiological protection aspects of disposal of high-level waste in geologic formations" National Radiological Protection Board Report, NRPB-R69 (1978).

(8) Wuschke, D.M., Rice, A.M., and Gillespie, P.A., "Environmental assessment of subseabed disposal of nuclear waste: a demonstration probabilistic systems analysis," in: Eighth Interna-

tional NEA/OECD Seabed Working Group Meeting, 1983 May 30-June 3. Sandia National Laboratories Report, D.R. Anderson, ed., SAND83-2122, 280-331 (1984).

(9) Rummery, T.E. and Rosinger, E.L.J., "The Canadian nuclear fuel waste management program," in: International conference on radioactive waste management. Proceedings of a conference held in Winnipeg, 1982 September 12-15. Canadian Nuclear Society, Toronto, Canada, 6-15 (1982).

(10) Kelly, G.N., Jones, J.A., Bryant, P.M., and Morley, F., "The predicted radiation exposure of the population of the European community resulting from discharges of kryton-85, carbon-14 and iodine-129 from the nuclear power industry to the year 2 000," Doc. V/2676/75, Commission of the European Communities, Luxembourg (1975).

(11) Bergmar, R., Bergstrom, V. and Evans, S., "Environmental transport and long term dose. A preliminary study of iodine-129," Aktiebolaget Atomenergi Report, 5-575, Sweden (1977).

(12) Kocher, D.C. and Killough, G.C., "A review of global environmental transport models for ^{3}H, ^{14}C, ^{85}Kr and ^{129}I," International Atomic Energy Agency International Conference on Radioactive Waste Management, Seattle, Wash., 1983 16-20 May. IAEA-CN-43/419 (1983).

(13) Smith, G.M. and White, I.F., "A revised global model for iodine-129." National Radiological Protection Board Report, NRPB-M81 (1983)

(14) Johnson, J.R., Van Heteren, J.G. and Wuschke, D.M. "A model to calculate dose from iodine-129 on a local, regional and global scale from the proposed Canadian high level waste vault," in: International conference on radioactive waste management. Proceedings of a conference held in Winnipeg, 1982 September 12-15. Canadian Nuclear Society, Toronto, Canada, 567-73 (1982).

(15) Rowsell, J.A. and McKee, P.M., "A model of the iodine cycle in local ecosystems of the Ontario portion of the Canadian Shield, and in the great lakes and Hudson Bay regions," Atomic Energy of Canada Limited Technical Record, TR-247* (1984).

(16) White, I.F. and Smith, G.M., "Management modes for iodine-129." Research contract 161-81-8-WAS-UK. Work performed under European Community's research program on radioactive waste management, project 8 (1983).

(17) Carver, M.B., Stewart, D.G., Blair, J.M., and Selander, W.N. "The FORSIM VI simulation package for the automated solution of arbitrarily defined partial and/or ordinary differential equation systems." Atomic Energy of Canada Limited Report, AECL-5821 (1978).

(18) International Commission on Radiological Protection. "Report of

the task group on reference man," ICRP Publication 23, Pergamon Press, Oxford, 1974.

(19) Dormuth, K.W. and Lyon, R.B., "EFFAIR: A computer program for estimating the dispersion of atmospheric emissions from a nuclear site," Atomic Energy of Canada Limited Report, AECL-6309 (1978).

(20) International Commission on Radiological Protection, "Recommendations of the international commission on radiation protection," ICRP Publication 26, Pergamon Press, Oxford, 1977.

(21) Hart, R.G., "Sources, availability and costs of future energy," Atomic Energy of Canada Limited Report, AECL-5816 (1977).

(22) Wuschke, D.M., and Gillespie, P.A., "Potential dose to human thyroid from ^{129}I produced by fission of uranium and thorium," Atomic Energy of Canada Limited Technical Record, TR-203* (1982).

---

*Technical Records are unrestricted, unpublished reports available from SDDO, Atomic Energy of Canada Limited Research Company, Chalk River, Ontario K0J 1J0

CLOSING REMARKS OF SESSION CHAIRMAN PHILIPPONE:

I guess it is my job to summarize Session 10. The first paper given was "Immobilization of ^{85}Krypton in a Metallic Matrix by Combined Ion Implantation and Sputtering". In this paper we heard some of the very good work that is being carried out in the United Kingdom on this particular technique. Actually, they have conducted a very thorough program of comprehensively testing this particular method of capturing, retaining and storing krypton. This includes running corrosion as well as radiation tests on this particular material.

The second paper was on "Off-Gas Treatment and Characterization for a Radioactive in situ Vitrification Test". This was describing some of the work that was being done at the Pacific Northwest Laboratory concerning the in situ treatment of some of the soils there. The method may be of use in the Richland Washington Area to take care of some of the liquid drain sites in that particular location. The method would be one of the methods considered in the Environmental Impact Statements presently being written.

A paper entitled "The Behavior of Ruthenium, Cesium and Antimony During Simulated HLLW Vitrification" described the work done at Mol, Belgium. This particular paper talks about some of the work in trying to recover cesium, antimony and ruthenium. This particular paper brought out the fact that the process did not scale up well. The results were much closer on the laboratory scale than they were in a pilot scale demonstration. It was a very frank paper describing the actual work that was carried out at Mol.

The last paper "Predicitions of Local, Regional, and Global Radiation Doses from Iodine-129 for Four Different Disposal Methods and and All-Nuclear Future" looked at this from what would happen locally, as well as regionally and globally. The conclusion was that even if we went to an all nuclear future we were well protected and, actually, that old statement that we should only fear fear itself was really reflected in this paper because there was nothing presented which stated that there was a problem as far as iodine-129 retention was concerned.

Panel 11

BEST AVAILABLE AND MOST READILY AVAILABLE TECHNOLOGY FOR OFF-GAS TREATMENT AND GASEOUS WASTE RETENTION

TUESDAY: August 14, 1984

ARRANGED BY: R.T. Jubin
Oak Ridge National Laboratory

MODERATOR: A. G. Croff
Oak Ridge National Laboratory

PANEL MEMBERS: W.S. Groenier
Oak Ridge National Laboratory
K. Naruki
Tokai Works
W. Hebel
Commission of the European Communities
E. Henrich
Kernforschungszentrum Karlsruhe

OPENING REMARKS OF PANEL MODERATOR:

Allen Croff, Oak Ridge National Laboratory, Chairman, replacing Robert Jubin. This panel session is entitled "Best Available and Most Readily Available Technology for Off-Gas Treatment and Gaseous Waste Retention".

The panel members are: Mr. Groenier from Oak Ridge National Laboratory, Mr. Naruki from the Tokai Works in Japan, Mr. Hebel from the Commission of European Communities, and Mr. Henrich from Karlsruhe. The purpose of this panel is to discuss two things. First, the available technology for offgas treatment in its most general sense, that is, what processes are available for the retention and recovery of radionuclides and their relative merits and demerits. Second, how the individual processes may be put together to constitute a complete offgas treatment system for a reprocessing plant. The approach we will follow is for each panel member to give a brief presentation of his views and then to open the session for general discussion.

Consolidated Fuel Reprocessing Program

SUMMARY OF UNITED STATES ACTIVITIES IN COMMERCIAL NUCLEAR AIRBORNE WASTE MANAGEMENT*

W. S. Groenier, Fuel Recycle Division
Oak Ridge National Laboratory
Oak Ridge, Tennessee 37831

Dup

ABSTRACT

Most of the U.S. nuclear air cleaning technology development in recent years has addressed advanced retention concepts in response to environmental concerns. In particular, efforts have centered in the fuel reprocessing portion of the nuclear fuel cycle. Although generally well developed on a cold engineering scale, the individual retention steps for hydrogen-3 (^{3}H), carbon-14 (^{14}C), krypton-85 (^{85}Kr), and iodine-129 (^{129}I) must yet be demonstrated in an active integrated facility. Fixation and disposal technologies for retained airborne constituents are generally less well developed.

I. Basis for United States (U.S.) Activities Conducted in the Past Five to Ten Years

New technology development has proceeded in response to environmental concerns which have (1) led to new or revised governmental policies and regulations for certain gaseous releases from commercial nuclear facilities, or (2) brought about increased pressures to attain "as low as reasonably achievable" releases. The principal airborne wastes of concern are tritium, ^{14}C, ^{85}Kr, ^{129}I, radon-222 (^{222}Rn), and radioactive particulates. Recovery of ^{85}Kr, ^{129}I, and particulates, as well as nitrogen oxides, is mandated by current regulations.

Recognizing that licensed facilities exist for airborne waste retention in the front end of the nuclear fuel cycle, recent efforts have addressed retention for fuel reprocessing plants, although much of the technology can also be applied to other portions of the fuel cycle where future regulatory changes may dictate increased retention.

New retention technology development has been directed toward meeting both existing and anticipated regulations, but deployment is necessarily dependent upon the needs of the fuel cycle and cost effectiveness.

*Research sponsored by the Office of Spent Fuel Management and Reprocessing Systems, U.S. Department of Energy, under Contract No. DE-AC05-84OR21400 with Martin Marietta Energy Systems, Inc.

Fixation and disposal of retained airborne radionuclides are necessary waste management steps and new technology development has also occurred in these areas, but to a lesser extent, since general agreement on disposal concepts and criteria is presently lacking.

II. General Status of Technology

First-generation retention steps are generally well developed since processes for the retention of iodine and particulates have been used for decades in the Department of Energy nuclear materials production plants. Advanced retention steps for iodine, noble gases, tritium, and ^{14}C have been extensively developed separately through the cold pilot-plant stage. The design and demonstration of a hot integrated flowsheet that treats typical airborne waste streams to the extent necessary to meet applicable retention regulations remains to be done.

Fixation processes for retained airborne species are generally less well developed, but concepts exist for most cases that have been verified by limited cold laboratory-scale operations.

Interim storage and transportation of solidified airborne wastes will probably not require new development since these wastes would be similar to low-level wastes currently produced at reactors; however, safety and accident analyses would be required for new waste forms.

Waste disposal concepts are the least well developed aspect of airborne waste management technology. The lack of repository criteria and of agreement as to which wastes will require a geologic repository and which can be emplaced in shallow-land burial grounds can have serious repercussions on future retention and fixation process deployment.

III. Justification for Centering Airborne Waste Retention Efforts in the Fuel Reprocessing Portion of the Nuclear Fuel Cycle

Tritium

It is estimated that 94% of the tritium release from a commercial nuclear fuel cycle would originate from fuel reprocessing plants [for light water reactors (LWRs)]. Releases by this pathway from breeder fuel reprocessing plants would be somewhat less, though still significant.

Carbon-14

In the LWR fuel cycle, although 33% of ^{14}C releases would occur at the reactors, a 90% control of ^{14}C at the reprocessing plants would provide ~60% control for the total fuel cycle.

Krypton-85

Fully 99.9% of krypton releases would occur from reprocessing plants in the LWR fuel cycle and this figure would not change appreciably for the breeder fuel cycle.

Iodine-129

Virtually all of the iodine release would occur from reprocessing plants for either LWR or breeder fuel cycles.

For high temperature gas-cooled reactors (HTGRs), the reprocessing portion of the fuel cycle is also the major source of radioactive gaseous releases in the absence of control systems. In addition, radon control is of greater importance for this case, which involves the thorium fuel cycle.

IV. Status and Availability of Newly Developed Technology

Tritium

The voloxidation process has been developed through the cold engineering scale for application to metal oxide breeder fuels. It recovers tritium as HTO vapor from a rotary kiln oxidative heat treatment that converts UO_2 to U_3O_8. The off-gas is dried on molecular sieves which are regenerated to yield tritiated water. Fixation as cement is the preferred concept. In the case of sodium-cooled, stainless-steel-clad (breeder) fuels, only ~10% of the tritium would be present at the time of reprocessing, the rest having diffused through the cladding within the reactor. For Zircaloy-clad (LWR) fuels, much of the tritium may be chemically bound to the cladding. Voloxidation is believed to be effective only for tritium within the fuel matrix. No further development of the process is planned at this time.

In conventional aqueous processing of spent fuels, ~93% of the tritium goes into the liquid dissolver product stream and reports to the high-level liquid waste from the first cycle of solvent extraction. One concept for recovery is to couple an isotopic enrichment process to this liquid waste stream. Other than preliminary feasibility studies, no effort has been expended to develop this concept.

Carbon-14

Caustic scrubbing has been proposed for recovery of ^{14}C as sodium carbonate as this is a common industrial process. Fixation would entail reaction with calcium hydroxide to form the insoluble calcium carbonate for incorporation in cement. No nuclear applications have been demonstrated and no efforts are currently active.

Molecular sieve adsorption of CO_2 from an off-gas stream, from which NO_x and water vapor have been removed, has been proposed as a means for concentrating ^{14}C prior to treatment in a caustic scrubber

(as described above). This extra step has the advantage of allowing smaller scrubber units to be used, although the volumes of solidified waste are unchanged. No efforts are currently active.

Fluorocarbon absorption (described below) will quantitatively remove CO_2 along with the noble gases. The process has been demonstrated on a cold engineering scale. Recovery of CO_2 on molecular sieves (as indicated above) has been proposed followed by caustic scrubbing or direct solid-gas reaction with barium hydroxide octahydrate (as described below). The fixation steps have not been demonstrated in conjunction with fluorocarbon absorption, and no current efforts exist.

Direct recovery and immobilization of CO_2 on barium hydroxide octahydrate has been demonstrated in cold engineering-scale equipment. The process has the advantages of directly providing a solid waste form that is thermally and chemically stable and of eliminating any liquid-solid separation steps. It must yet be demonstrated with a typical dissolver off-gas composition.

Krypton-85

Cryogenic distillation in liquid nitrogen or oxygen has been used commercially for many years to recover rare gases and has been also used in nuclear facilities to a limited extent. Cold engineering-scale operations have been studied in most nuclear-active free world countries, and a small active system has operated for several years at the Idaho Chemical Processing Plant. Pretreatment of a dissolver off-gas is necessary to remove water vapor, NO_x, and CO_2. More importantly, the removal of oxygen is apparently necessary (when using liquid nitrogen) to prevent the formation of ozone by radiolysis. Catalytic reaction with hydrogen has been proposed. When using liquid oxygen, other steps must be taken to minimize the accumulation of ozone. Other impurities in the feed gas can be concentrated to an undesirable extent; for example, methane has been noted to accumulate to levels which could lead to safety problems. Operational problems also exist. Systems operated to maximize krypton retention have been sometimes plagued with xenon freezeout problems. These have been solved with a variety of methods including temperature cycling, operation at a higher pressure, altering the feed point location, and removal of xenon in advance on silica gel. In spite of the various concerns with regard to operability and safety, the technology exists to design full-scale facilities. Hot operation at a significant scale remains to be demonstrated. Separation of xenon and krypton in the product stream and fixation of krypton are addressed below. These steps have not been demonstrated to date on a significant scale.

The fluorocarbon absorption process has been developed through the cold engineering scale using the solvent CCl_2F_2 to selectively absorb the noble gases and CO_2 which are recovered by stripping. The process will also remove traces of I_2, CH_3I, NO_x, and water, although these are not stripped from the solvent but must be removed by distillation or with solid sorbents. The product is a concentrated stream containing the noble gases, CO_2, and CCl_2F_2 which is further

processed using molecular sieves for CCl_2F_2 and CO_2 removal, and a selective desublimation step for xenon-krypton separation. The krypton can be stored in pressurized cylinders or fixed as a solid using ion implantation or zeolite encapsulation techniques. These fixation steps have not yet been demonstrated at full scale. Development of the ion implantation technique has continued at the Battelle-Pacific Northwest Laboratory.

Iodine-129

The mercurex process uses a mixture of $Hg(NO_3)_2$ and HNO_3 in aqueous solution to scrub iodine species from the off-gas and convert them to iodates and mercury complexes. Development has been completed through the cold engineering scale and units were designed and tested for the Barnwell Nuclear Fuel Processing Plant. A mercurex system is also installed at Dounreay. Suitable methods for removing the iodate as a solid and recycling the mercury remain to be developed. An appropriate form for disposal has not been identified, but conversion to barium iodate appears feasible.

The Iodox process uses hyperazeotropic nitric acid to scrub iodine species from the off-gas and form iodates. A separate source of hyperazeotropic acid is recommended as in-plant systems for production from dilute acid [via an extractive distillation process using $Mg(NO_3)_2$] are complicated by operational and maintenance problems owing to high corrosion rates and MgO plugging. The Iodox process itself must use tantalum or titanium equipment because of the corrosive nature of the iodine-containing hyperazeotropic nitric acid. The process has been developed through the engineering scale including experience with an actual dissolver off-gas at Oak Ridge, but full-scale demonstration is required. Decontamination factors are higher than those realized in the mercurex process, particularly for organic iodides. Conversion to barium iodate has been proposed for disposal, but this step has not been demonstrated.

Silver reactors, in which unglazed Berl saddles are impregnated with silver nitrate, have been used for iodine absorption in Hanford and Savannah River production facilities. Reported decontamination factors vary widely, and methods for regeneration or disposal are not well developed. There is some evidence that iodine may be displaced in time by other halogen off-gas impurities such as chlorine. The degree of silver utilization (bed capacity) is not well characterized.

Silver-loaded adsorbents, such as silver-exchanged or silver-impregnated zeolites, silica, and alumina substrates, have been extensively tested in cold and hot facilities and have been installed in many nuclear facilities. Generally, these are used downstream of a scrubber for final removal of trace quantities of iodine, but can be used as a primary filter. Recent U.S. development has completed extensive testing of silver mordenite with an emphasis on increasing silver utilization. Techniques for regenerating the beds have generally proved unsuccessful. The German adsorbent AC-6120 has been the subject of much testing, including prototype-scale operations. This technology is well-developed for iodine retention but subsequent treatment or packaging for final fixation remains undemonstrated. Concepts include incorporation of the adsorbent in cement.

HTGR-Specific Off-Gas Treatment Technology

For ^{14}C and krypton, the KALC process was developed through cold engineering scale for treatment of the CO_2-rich exhaust gases from fuel block burning. In this process, liquid CO_2 is used to scrub the burner off-gas and concentrate krypton for storage or as feed for final fixation steps.

For the thorium HTGR fuel cycle, solid sorbent beds have been tested in small scale for radon holdup that is sufficient for extensive isotopic decay.

Engineering-scale units have been tested for the catalytic oxidation of CO and HT in HTGR burner off-gas.

Solid sorbents have been evaluated for SO_2 removal from HTGR burner off-gases.

V. Primary Development Requirements

Integrated operation of the various treatment and fixation steps for nuclear plant off-gases in prototypic equipment and with realistic feed streams is the greatest need yet remaining. The development of any single step cannot be considered as complete until its operation within an integrated facility is proven. Currently, efforts are under way at GA Technologies, Inc., to operate an integrated test system for off-gas treatment in the HTGR fuel cycle. This work has already provided valuable insight into the difficulties that can be encountered when operating tandem treatment units, problems that were not evident in single-unit tests.

Suitable conversion steps that lead to final waste forms for the various off-gas constituents need to be developed in many cases. The final waste forms must be defined.

Differences between U.S. and foreign off-gas treatment programs must be identified and understood.

RESEARCH AND DEVELOPMENT ON AIR CLEANING SYSTEM OF REPROCESSING PLANT IN JAPAN

K. Naruki
Tokai Reprocessing Plant
Tokai Works
Power Reactor and Nuclear Fuel Development Corporation
Tokai-mura, Ibaraki-ken, Japan

Abstract

Present status in Japan of R & D on air cleaning system, especially of the fuel reprocessing plant is summarized. Description is centered on the R & D and experience of Tokai-reprocessing plant, which cover the plant air cleaning system, effort carried out for decreasing I_2 effluence in the actual vented off-gas, and R & D for recovery of Kr and ^3H. And some experimental results for the evaluation of HEPA filter are also described.

I. Introduction

Reduction of radio-activity of the airborne radionuclides from fuel reprocessing plant is one of major concern in Japan, since the construction of a commercial reprocessing plant for LWR fuel is planned and also designing work for pilot plant of FBR fuel reprocessing is being done. ALAP is a fundamental philosophy in conducting R & D for reducing the airborne radionuclides. This report presents the summary of R & D effort being done for that purpose especially in Tokai reprocessing plant.

II. Off-gas Treatment System of Tokai Reprocessing Plant (TRP)

Off-gas treatment system flowsheet of TRP is shown in Fig. 1. The gaseous radioactive wastes are composed of exhaust from the shearing machine, the dissolvers and other vessels. These exhausts are treated by the radioactive gaseous treatment process, and after these exhausts flow through iodine filter and HEPA filter, they are discharged into the atmosphere from main stack.

(a) Shearing off-gas (SOG)

The off-gas of the fuel shearing machine, initially flows into the dissolver and sintered-filter installed at the dissolver loading cell. After running into HEPA filter at maintenance cell and scrubber and HEPA filter at vessel ventilation system, it is sent to cell ventilation. It is possible to send the off-gas after cleaning at vessle ventilation to the Kr recovery pilot plant.

(b) Dissolver off-gas (DOG)

The off-gas of the dissolvers, which contains a major portion of gaseous wastes, flows into HEPA filter at vessel ventilation system after treatment at the acid absorber and the alkaline scrubber. It is

possible to send the off-gas after cleaning into Kr recovery pilot plant.

(c) Other vessel off-gas (VOG)

Other vessel off-gas consists of the off-gas of Pu storage, purification and concentration process, HLLW concentration process and storage, etc. These off-gas systems have the scrubber or the acid absorber.

III. R/D of Gaseous Waste Treatment

III.1 Kr Recovery

For the recovery of radioactive krypton in the off-gas from fuel reprocessing plant, several processes have been investigated in many institutions. They are cryogenic distillation process, solvent absorption process, charcoal adsorption process, and membrane separation process. PNC initiated the study on the Kr recovery in 1966 and surveyed these process conducting basic experiments for comparison. In 1973, cryogenic distillation process was selected as the most practical method being based on both the results of the experiments and the information of development status on other countries. Therefor a cryogenic distillation system for the recovery of Kr-85 has been installed in Tokai reprocessing plant and will become active in 1986. The system, illustrated by a simplified flow sheet in Fig 2, is designed as an experimental hot-pilot plant. The system capacity is rated at 110 Nm^3/h and 8000 Ci/d of Kr-85. The combined SOG and DOG is pretreated to remove I-129 by caustic scrubbing and by AgX adsorbent. O_2, NOx and hydrocarbon are removed by a hydrogen recombiner, and H_2O and CO_2 are removed by adsorbent beds. The Xe is adsorbed on silica-gel at -160°C and 3×10^5 Pa to avoid possible problems due to Xe crystallization in the cryogenic distillation column. Not shown in Fig 2 are duplicate parallel adsorbent beds for H_2O, CO_2 and Xe; one as adsorbent bed is in the regeneration mode while the other is removing a contaminant gas. The H_2O collected is sent to LLLW treatment process, the CO_2 is vented to the stack, and the Xe stored in high pressure cylinder storage. After pretreatment, the gas stream containing N_2 and Kr is passed through liquid N_2 in the Kr distillation column to absorb Kr; the liquid N_2 enriched in Kr is transferred to a second column where Kr is separated by fractional distillation to produce a product containing more than 90% Kr. The Xe desorbed from the adsorbent bed (heated to 180°C) is passed through a third distillation column which produces high purity Xe (more than 95%). Although recovered Kr is stored in pressurized cylinder, other methods are being studied. These are encapsulation in zeolite and ion-implantation in metal.

III.2 IODINE-129

III.2.1 Development of iodine removal in PNC

(1) Experience of iodine removal in TRP

In Tokai plant there was no effective equipment except for

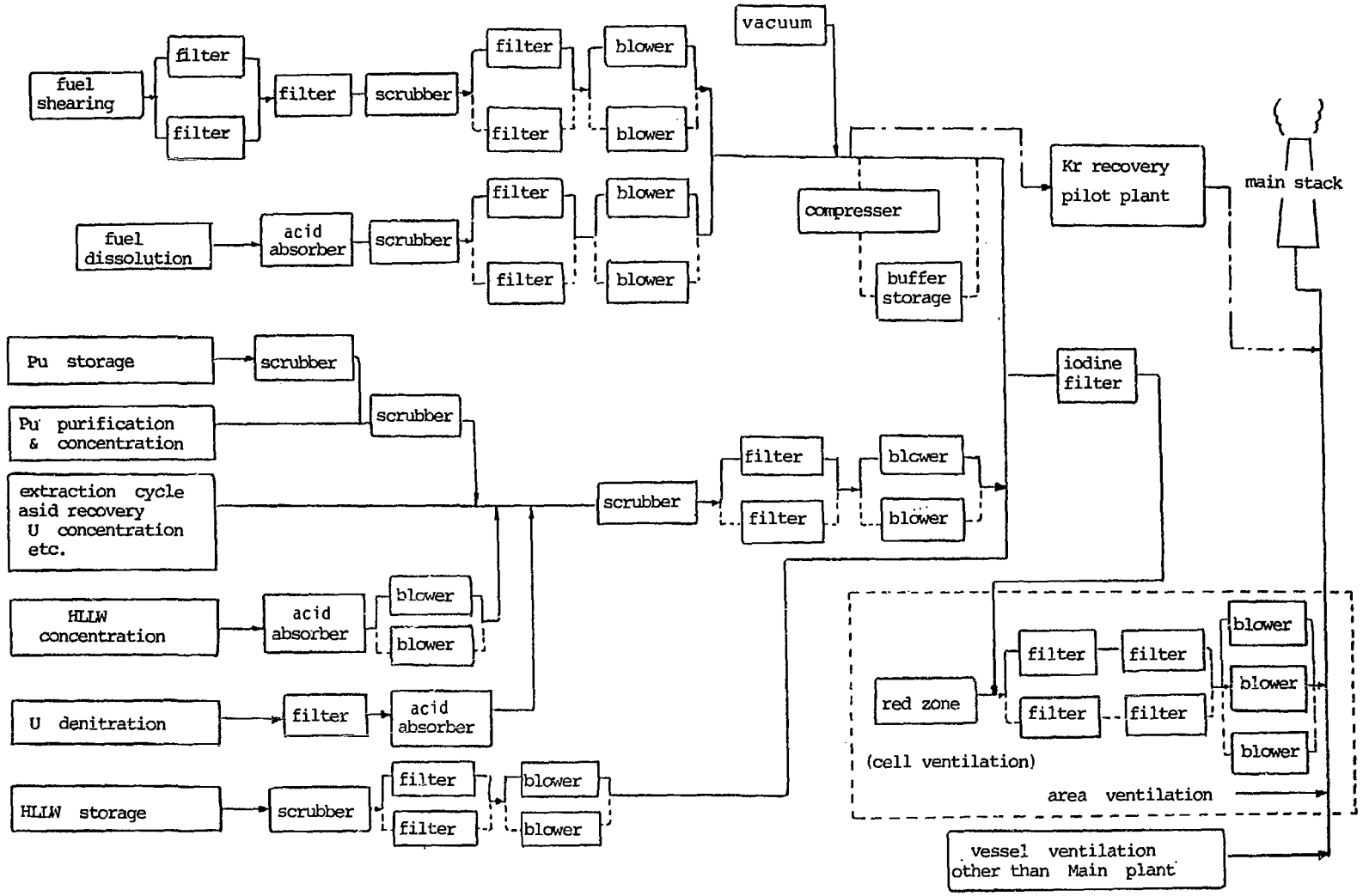

Fig. 1 Off-gas treatment system flow sheet (Main part)

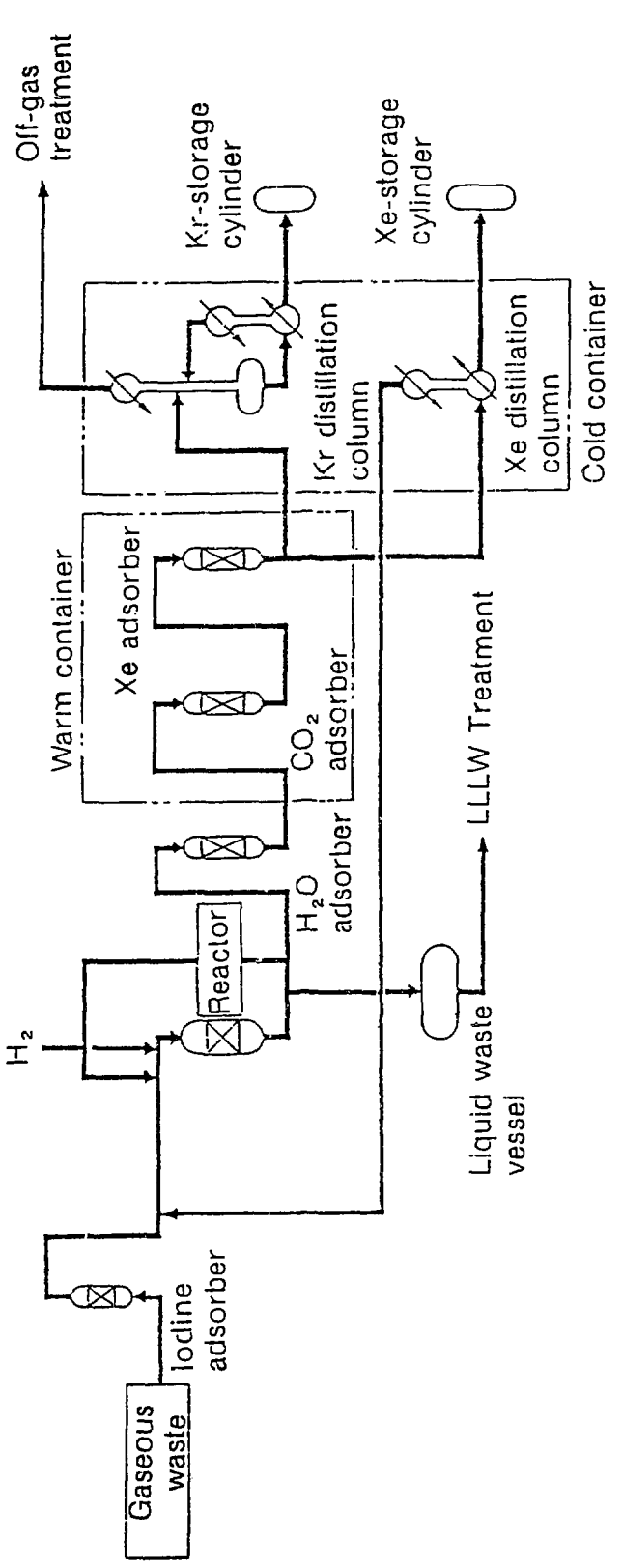

Fig. 2 Krypton recovery process flow diagram

alkaline scrubbers when the plant construction was completed. In a short time after hot operation began, it became very important problem how to reduce gaseous iodine discharge to the atmosphere.

At first, to solve this problem, we tried to keep iodine absorbed in liquid waste from releasing again to the off-gas. Therefore, a vessel was prepared for liquid waste of the off-gas treatment system. Recovered acid from the DOG, which contains more than 50% of iodine inventory, was transferred to the tank. Caustic soda and hydrazine were added in it for neutralization and stabilization. Liquid waste of the SOG, VOG and HLLW VOG treatment could be also transferred to the vessel. This method was relatively effective but not applied in Tokai plant since it proved that the liquid waste from that vessel contained too much amount of salt to treat in the waste disposal facility.

To establish efficient airborne iodine removal system, we researched the characteristic of several solid iodine adsorbents. Our demands for the adsorbent are as follows.

-High decontamination factor (in order to reduce the iodine discharge to the environment)

-High adsorption capacity (in order to reduce the maintenance work)

-Resistance to NOx and/or humidity, etc....

At first, charcoal adsorbent was tested, and then silver-exchanged adsorbents test was carried out.

Activated charcoal impregnated with SnI_2 was tested with vessel off-gas of the waste disposal facility. The charcoal adsorbent filter was filled up with 2 filter units (Dimension: 610mm×610mm×290 mm, for an unit) with a bed depth of 25 mm. The face velocity was 3.6 cm/sec., so that total residence time was 1.4 sec. The test was carried out at the room temperature. Also measurement of I-129 concentration at the upstream and downstream was carried out by means of charcoal adsorbent.

In Fig. 3 it is shown that breakthrough occurred after 1000 hr. loading with vessel off-gas of waste disposal facility. Because of this characteristic of charcoal adsorbent, we concluded that charcoal adsorbent didn't meet our demand.

To find out another suitable solid adsorbent for our plant, several tests were performed with Ag-X, Ag-13X, Ag-$A\ell_2O_3$. The gas condition was almost same as in the charcoal test case except adsorbent bed dimension. Bed depth was 20 mm or 40 mm.

Relative humidity, NO and NO_2 concentration were also measured as well as iodine concentration. They were in the range of 84 to 93%, and 2 to 5 ppm, respectively, at room temperature. Two kinds of tests were performed. One test was made at room temperature and the other was at 50°C heating the test bed electrically. The residence time was 0.5 or 0.2 sec. Fig 4 shows the decontamination factor as a function of loading time at room temperature. The initial

decontamination factor was about 200 and that was saturated rapidly in first 200 hr loading. When the test bed was heated up at 50°C, there was remarkable improvement in the adsorption characteristic of Ag-X and Ag-13X i.e. (See Fig. 5). The decontamination factor was elevated and initial DF value was held by loading time 1000 hr. On the other hand, the DF of Ag-$A\ell_2O_3$ was not improved. As a result of these tests we chose the Ag-X as iodine removal adsorbent in our off-gas system instead of charcoal.

According to this conclusion we installed Ag-X filters at the vessel ventilation duct in the main plant where SOG, DOG, HLLW VOG and other VOG flow together and at the VOG ducts of the waste disposal facility. Also, according to further investigation, we added another Ag-X filter for the off-gas from cells which contain open tanks in the waste disposal facility. (See Fig. 6)

Iodine removal system in Tokai plant is composed of a heater, Ag-X filters and glass fiber filters. Ag-X bed depth is 50 mm and face velocity varies from 5 to 20 cm/sec. Iodine concentration is ranging in 10^{-10} to $10^{-8}\mu Ci/cm^3$. NOx concentration is about 5000 ppm in the main plant and about 10 ppm in the waste disposal facility when the plant is running. (See Table 1.) Total DF of the plant is

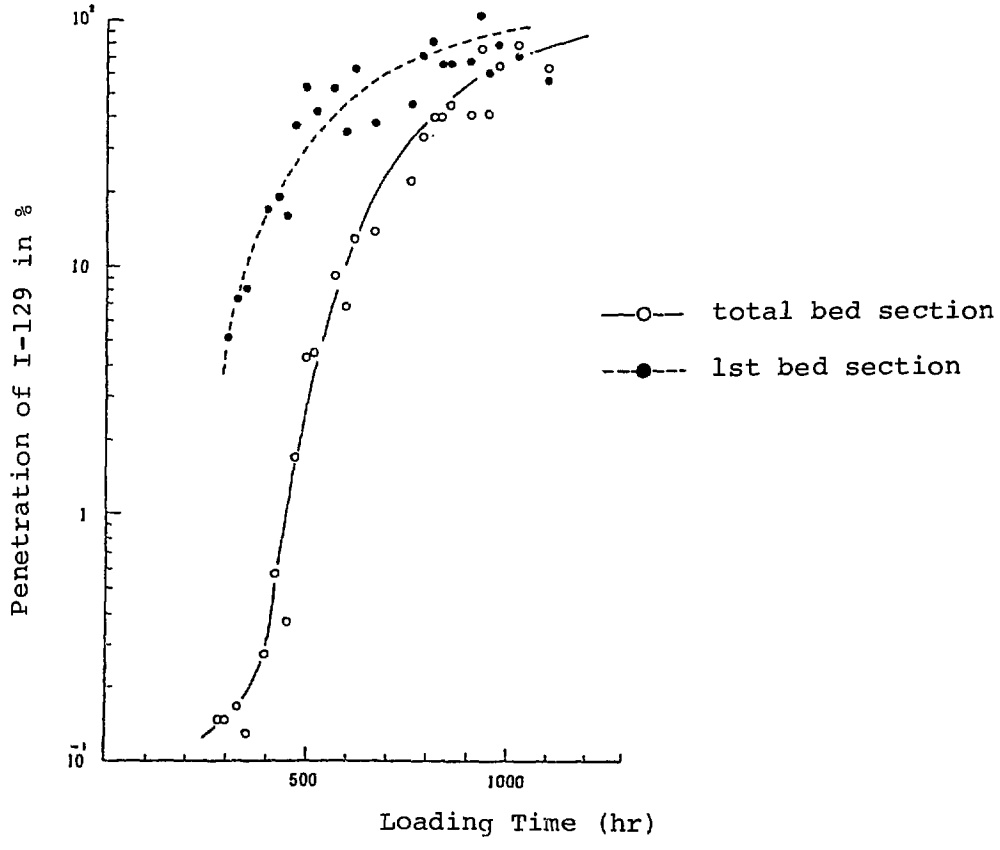

Fig. 3 Penetration of the charcoal filter by ^{129}I as a function of loading time

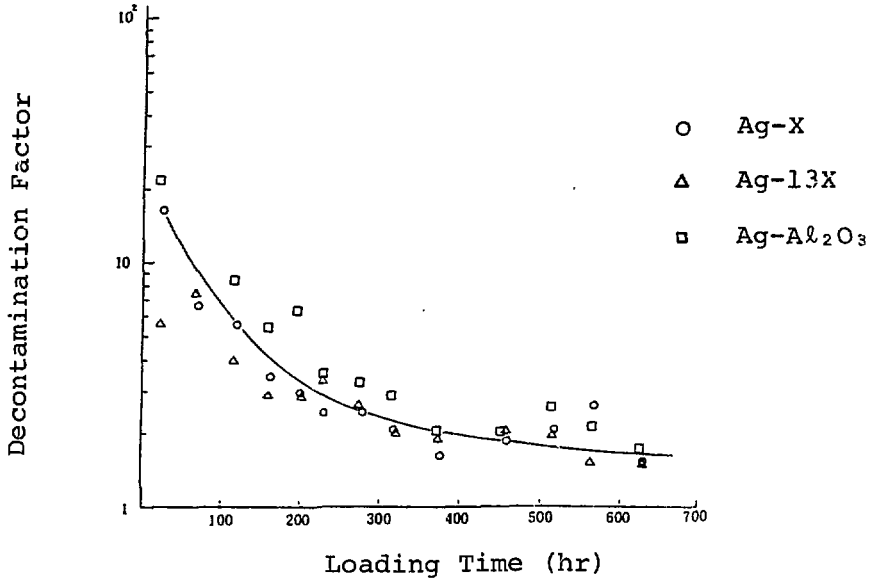

Fig. 4 Decontamination factor for test beds of silver-exchanged adsorbents as a function of loading time (room temperature)

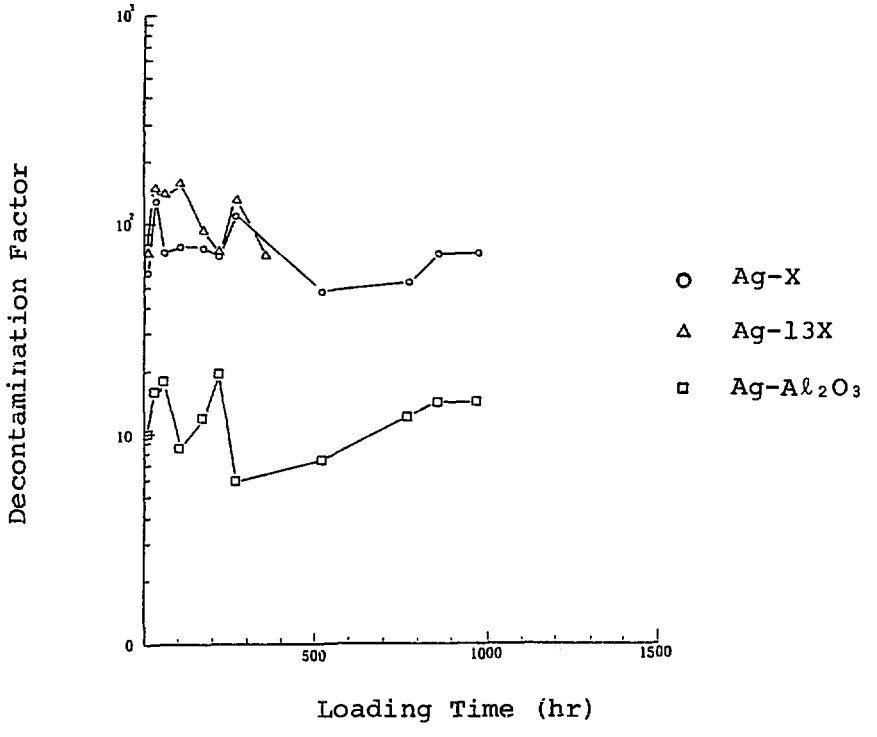

Fig.. 5 Decontamination factor for test beds silver-exchanged adsorbents as a function of loading time (heated to 50°C)

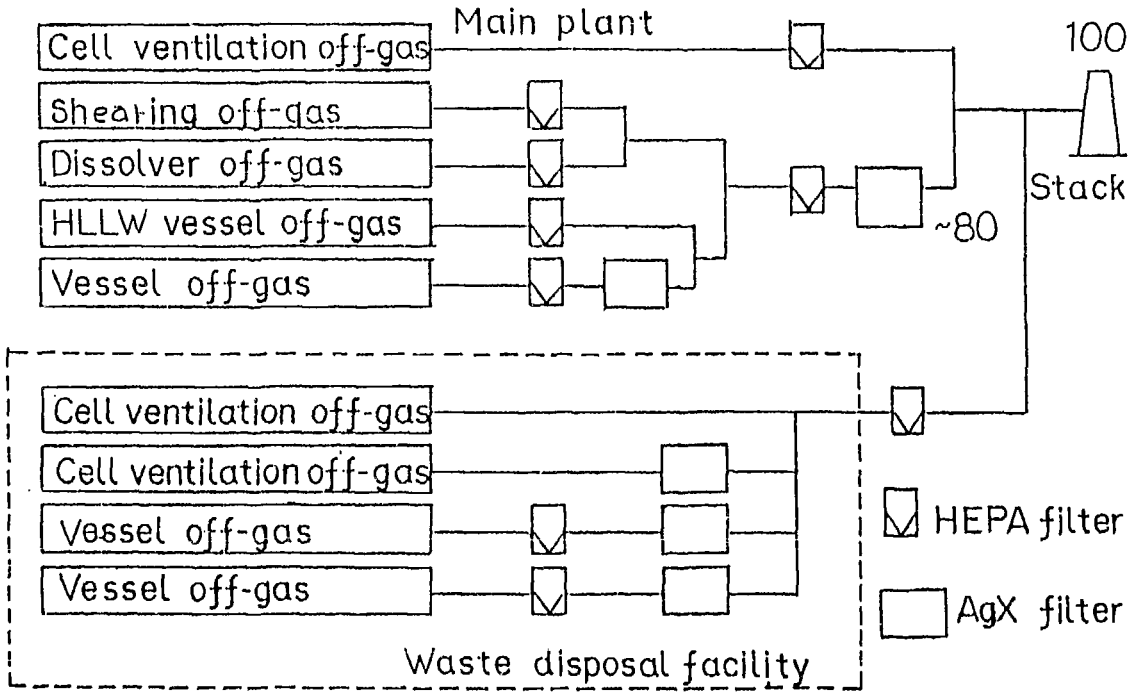

Fig. 6 Iodine mass balance

approximately 5 times as high as before installation of Ag-X filters. But the DFs of those Ag-X filters are not so high as we expected. So, we are going to execute further iodine removal for the VOG of the mainplant which has the largest contribution of the iodine discharge to the environment, by adding another iodine removal system for the VOG. In this system, the Ag-X filter will be 1.5 times as thick as the present ones and face velocity is 20 cm/sec. According to the fact that high NOx concentration causes the low decontamination factor, in this new equipment the VOG will be heated up at higher temperature in order to reduce the NOx influence. We hope that iodine discharge to the atmosphere will be less than half by means of the new system.

(2) Evaluation of IODOX process[1]

In the irradiated FBR fuel reprocessing, there are many problems peculiar to FBR fuel to be solved and the iodine removal in the off-gas is very important among them.

The quantity of radioactive iodine in the irradiated FBR fuel is estimated to be 120 Ci per metric ton of heavy metal which correspond to 800 gram of iodine element, on the conditions of 120 days cooling and burn-up of 95,000 MWD/T. This value is several times as much as for LWR irradiated fuel.

As one of the iodine removal methods without distributing it into the process in the plant, we examined the IODOX process to evaluate the possibility to applying for the FBR fuel reprocessing plant. IODOX process utilizes the highly concentrated nitric acid to convert iodine to non-volatile chemical forms and is superior in removing the organic iodine which cannot be removed by the activated charcoal and, consequently, the nitric solution of high iodine content can be obtained.

Table 1. Operation conditions of AgX filters

	I-129 conc. ($\mu Ci/cm^3$)	Temp. (°C)	Humidity (%)	NOx conc. (ppm)	Face velocity (cm/sec)	DF
Main plant	max. 4×10^{-8} av. 5×10^{-9}	45	20	5000	20	10 ~20
Waste disposal facility	max. 3×10^{-8} av. 4×10^{-9}	35	60	10	5	70
	max. 4×10^{-9} av. 7×10^{-10}	40	40	10	5	10 ~30
	max. 5×10^{-9} av. 2×10^{-9}	40	50	10	17	30 ~60

The IODOX process consists of (1) oxidation and absorption, (2) iodine concentration and nitric acid recovery and (3) iodine product storage.

Aiming at the evaluation of IODOX process, we construct a packed column made of Pyrex glass (29 mm dia. and 200 mm high) and examined the oxidation and the absorption process of iodine by the concentrated nitric acid.

A fundamental experiment of oxidation and absorption was carried out to determine the DF of a methyliodide in the off-gas.

As a result, under the condition of sufficient nitric acid flow rate, the most sensitive parameter for DF was nitric acid concentration and a high DF was attained at the concentration more than 19N, while logarithm of DF is inverse proportion to feed gas flow rate and the effect of methyliodide concentration is small.

And then, we examined the effect of NO_2 on oxidation and absorption. As shown in Fig. 7, nitric acid with NO_2 removed gives higher DF. And DF is reduced exponentially with NO_2 concentration in the gas phase as shown in Fig. 8.

Based on the results of these fundamental experiments, an engineering scale packed column was designed and manufactured. This apparatus was designed with the specification of 4 m^3/hr. as the maximum gas flow rate and 10 ℓ/hr. as the maximum HNO_3 flow rate. The inside diameter and packed height are 76 mm and 2500 mm, respectively.

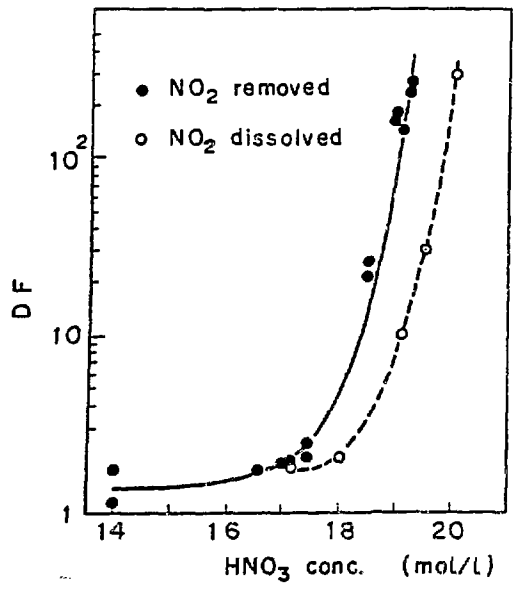

Fig. 7 Effect of HNO_3 concentration on DF.

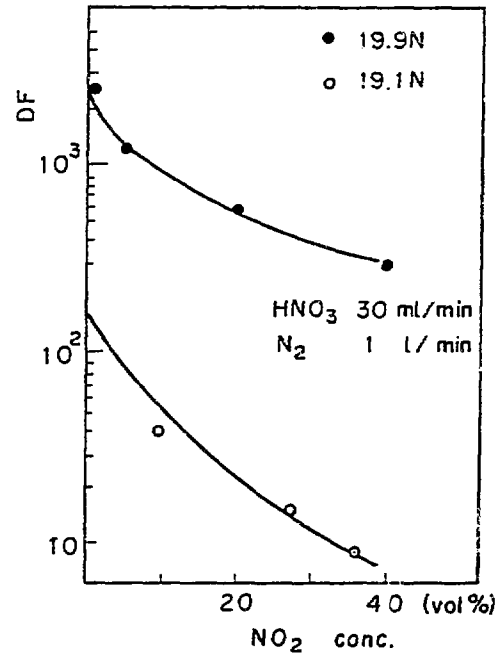

Fig. 8 Effect of NO_2 concentration in gas phase on DF.

DFs are approximately constant under the various flow rate of 18.5 N nitric acid, while logarithm of DF is inversely proportional to feed gas flow rate. These facts are in agreement with the result of the fundamental experiments.

Through the fundamental and engineering studies, it was confirmed that IODOX process is useful for removing iodine in dissolver off-gas.

However in order to apply this process to the actual reprocessing plant, there are still problems to be solved such as the corrosion of material due to the high concentration of nitric acid and the conversion of removed iodine into a suitable form for storage and future disposal.

(3) R/D program in TRP

As mentioned before, the development to remove the radioactive iodine in both the dissolver and the vessel off gas have been proceeded since 1978. Through these activities, we have investigated the iodine pathway in TRP, and developed the adsorbent to remove the radioactive iodine in the off gas.

However, since these development had to be performed only using the active ventilation circuit, they were not necessarily carried on systematically.

Based on these experiences, we are planning a long range R & D program to develop the effective iodine removal system for the reprocessing plant.

This program consists of an engineering demonstration experiment of iodine removal at the technical scale test facility (EDF), an adsorbing test of various adsorbents using the actual ventilation circuit, and the investigation on method to stabilize or solidify the used adsorbents. The study in EDF will cover the remote handling for each equipments, an adsorbing test using inactive iodine, a development of method to remove water vapor and NOx in the off-gas and an investigation of poisoning effects by humidity and NOx.

III.2.2 Other R/D in Japan

Other R/D about the removal of radioactive iodine in Japan are as mentioned below, which have been done at other institutions than TRP.

(1) Comparative study of adsorbents

The effects of relative humidity, NO_2, SO_2, pore size, etc. on the removal efficiency and the change of the adsorption ability after regeneration are reported about some adsorbents such as AgX, AgA, AgS, and so on.[2]

The research for the possibility of using only zeolite for the removal of radioactive iodine is also reported.[3]

(2) Adsorption characteristic under various conditions

The effect of contaminant gases are dominant especially of relative humidity and NOx concentration. Kanazawa et al. reported the reactions of the water vapor and NO_2 on the surface of adsorbents and their influence on the adsorption ability.[4]

Shimoi et al. evaluated quantitatively the removal efficiency of an AgX filter and an activated charcoal filter related to various conditions such as relative humidity, temperature, face velocity, etc.[5]

(3) Chemical reaction kinetics study between gas and liquid phases

This is the theoretical and experimental investigation about the absorption of radioactive iodine into a dilute alkaline solution and its partition coefficient between the two phases.[6]

(4) Others

Kobayashi et al. calculated the iodine distribution in an activated charcoal filter and its breakthrough curve and found an agreement of tendency with experimental results.[7] Matsuoka et al. reported that there were three kinds of iodine adsorption types on an AgX adsorbent.[8]

III.3 Tritium

III.3.1 Behavior of tritium at reprocessing plant[9]

The tritium is generated in LWR by the ternary fission, of which more than 99% is bound in the fuel matrix and the zircaloy cladding, and the very minor amount in the gas plenum of the fuel rods.

According to the experience of Tokai reprocessing plant, during dissolution, about 18% of tritium generated in the fuel which is estimated by ORIGEN-79 was released into the off gas stream and about 70% of it was found in the fuel solution.

However, most of tritium contained in the off gas is scrubbed into the solution of the acid recovery column, and consequently less than 1% of tritium is released into the atmosphere through the main stack.

On the other hand, the tritium in the fuel solution is appeared in the first cycle aqueous waste and then is carried into the HLLW concentration process.

The tritium in the off gas scrubbing solution and the condensate of HLLW evaporator is transferred into the low active liquid waste treatment process after the acid recovery. And then it is discharged into the sea after the monitoring.

This amount corresponds to 30∿60% of tritium contained in the LWR fuel estimated by ORIGEN-79. Through the active operation with irradiated PWR fuels, about 30% of tritium estimated by ORIGEN-79

could not be found. It is supposed that this difference between the detected amount and the estimation of the ORIGEN code is due to the tritium in the zircaloy cladding whose amount is to be correlated with the linear power rating in the LWRs.(10)

III.3.2 R/D of tritium recovery process

As the tritium removal techniques, there are several methods such as water-distillation, electrolysis, water-hydrogen exchange and laser method, which have been investigated in Japan.

On this paper, we present the status of R & D of the Water-Hydrogen Exchange process which is the technique to remove a tritium by the water-hydrogen exchange catalyst.

A development program was started in 1981. At first we carried out the study to develop the catalyzer and then investigated the problems applying this technique to the large reprocessing plant, which were the influence of impurities on catalysis, the method to remove impurities, the evaluation of the internal structure for the gas-liquid contactor, and the estimation of efficiency of the catalytic reaction.

As a result of the experiment, it became clear that iodine and nitric acid lowered the activity of the exchange catalyzer and TBP and n-dodecane slightly deactivated the catalyzer at the high concentration respectively. Therefore, it is necessary to remove these impulities when this technique is applied to the plant. But the problem of iodine and nitric acid can be solved by the alkaline distillation and the TBP can be removed by the activated charcoal column which have been already demonstrated at TRP.

As the internal structure of the gas-liquid contactor, two kinds of sieve trays (hole/pitch: 1/2.5, 1.2/4.8) and packings such as Sulzer BX and Sulzer Kerapak showed a good result.

On the basis of the result of this experiment, the dimension of the column for the actual plant was estimated as 0.56 m in diameter and 22 m in height under the conditions described below.

Catalystic reaction efficiency	0.9
Gas-liquid contactor efficiency	0.8
Capacity	5 m^3/day
Initial concentration of tritium	10^3 Ci/m^3
Tritium concentration in waste water	10 Ci/m^3
Tritium concentration in waste recovered water	10^5 Ci/m^3

This column dimension are smaller than the water distillation column.

It was confirmed, through the engineering experiment, that this process will be useful for removing a tritium at a reprocessing plant.

In order to study the effect of impurities and radiations for

the catalyzer, the next program of experiment using the actual solution will be started in this autumn at TRP.

IV. Conclusion

Through the operation of Tokai reprocessing plant, the practical approach has been applied to the reduction of airborne radionuclides especially radioactive iodine, installation of Aq-X filter was very effective for it. Iodox process is being studied for the application to FBR fuel reprocessing.

Regarding Kr recovery, a pilot plant by cryogenic distillation has been constructed and will become active in 1986.

Behavior of tritium in the Tokai-reprocessing plant has been grasped, and water-hydrogen exchange method is being studied, as a promising one for the recovery of tritium.

V. References

(1) H. Kaneko, H. Muramoto, H. Takeda, et al., Iodine Removal in the PUREX Reprocessing Process, Symposium of the Society of Chemical Industry (May 1979)
(2) M. Kikuchi, et al. 17th DOE Nuclear Air Cleaning Conference
(3) T. Sakurai, et al. Journal of Nuclear Science and Technology, 20 [3], 264 (1983)
(4) T. Kanazawa, et al. IAEA seminar on the testing and operation of off-gas cleaning system at nuclear facility (1982)
(5) H. Shiomi, et al. 17th DOE Nuclear Air Cleaning Conference
(6) W. Eguchi, et al. Journal of Nuclear Science and Technology, 12 [9], 467 (1975)
(7) S. Kobayashi, et al. Nihon Genshiryoku Gakkaishi, 19 [10], 702 (1977)
(8) S. Matsuoka, et al. Nihon Genshiryoku Gakkai Yokoshu (1984)
(9) M. Fukushima, S. Araya, T. Yamanouchi, et al. Behavior of tritium at Tokai Reprocessing Plant, PNC SN-81-37 (March 1981)
(10) B.J. Kullen, L.E. Trevorrow, M.J. Steindler, Tritium and Noble Gas Fission Products in the Nuclear Fuel Cycle, II. Fuel Reprocessing Plants, ANL-8135 (March 1975)

STATUS OF R&D IN THE FIELD OF NUCLEAR AIRBORNE WASTE SPONSORED BY THE EUROPEAN COMMUNITY

W. Hebel
Commission of the European Communities
Brussels, Belgium

Abstract

An overall review is given on the research activities that have been supported by the European Community for the last 8 years in the field of management of radioactive gaseous waste. The major subjects of concern are management possibilities for Krypton-85, Iodine-129, Carbon-14 and tritium. After a short introduction to the kind and contents of this specific research activity, summary statements are given successively for each of the four radionuclides concerning the state of development now achieved within the scope of the joint programme.

Introduction

The management of airborne wastes from the reprocessing of nuclear fuel is part of the European Community's research programme on radioactive waste management and storage. Since its first multi-annual R&D programme in that field on terms of shared cost, started in 1975, numerous research works were and are being supported by the Commission through contracts concluded with various organizations and companies in the Member States. The actual 2nd R&D programme, 1980-1984, runs out at the end of this year.

The share of financing supported by the Community usually amounts to 40% of the total expenses incurred by the contractors. During the last 8 years, about 11 million ECU (i.e., about 9 million US dollars) were spent in total for airborne waste research. Almost half of it was spent on Krypton-85, followed by tritium (27%), aerosols (11%) and the characterization of fuel dissolution off-gases (10%). About 6% of the Community expenses were determined to review studies on Iodine-129 and Carbon-14.

As to Krypton-85, the methods studied concern trapping by cryogenic distillation (cf. paper 14-1 of this conference), incorporation into metal matrices by ion-sputtering (cf. paper 10-1), enclosure into zeolites and filling into pressure bottles. For the latter, temporary storage in engineered structures on land and sea disposal have been evaluated, along with liquid metal embrittlement of structural and container materials that may be caused by rubidium, the decay product of krypton. A review study on the methods of Krypton-85 management was made available in 1982. (1)

Concerning tritium, the fixation to calcium phosphates and metal hydrides has been studied as well as its removal from aqueous effluents by electrolysis combined with catalytic exchange.

For Iodine-129, a comprehensive study has been drawn up in 1980 and 1982, respectively, giving a status of the relevant management technologies and of the radiological aspects (2) (3).

Finally, regarding Carbon-14, a similar assessment study has recently been completed (4).

The major issues of these activities may be summarized as follows.

Krypton-85

Most of the Community sponsored work concerns the immobilization techniques for krypton by developing the methods mentioned above. A specific report on the ion sputtering technique, developed at Harwell (U.K.) is presented at this conference and supplementary information can be found elsewhere (5). However, as to the situation of krypton management on the whole, reference can be made here to a specialists' meeting organized by the Commission of the European Communities in 1982 (1). The material presented at this meeting was reviewed by a following panel discussion and some of its major conclusions might be useful to recall here for discussion :

1. The existing international recommendations and national regulations with regard to possible release of radio krypton into the atmosphere, are not fully consistent and may be subject to change.
   As to those applicable in the Federal Republic of Germany and in the U.S.A., any large scale industrial reprocessing of nuclear fuel will require most of the emerging krypton to be retained.

2. Similarly, the existing recommendations or regulations on public transportation of radioactive materials would not allow the shipment of radio-krypton in gaseous form by industrial quantities under high pressure.

3. Mainly two techniques of trapping Krypton-85 from the fuel dissolution off-gas are being developed : the cryogenic rectification process and the fluorocarbon absorption process. The former has reached the stage of inactive pilot plant testing in several countries (e.g., U.S.A., Japan, Germany, Belgium, France).
   Apart from an older plant at the Idaho National Laboratory (U.S.A.), operation under radioactive or industrial conditions has not been performed and needs testing and demonstration.
   Problems of operational safety remain to be solved for the cryogenic rectification process. They are due mainly to the specific composition and the relatively high air flow-rate of the dissolver off-gas (e.g., treatment of oxygen and NOx gases, radiation induced formation of ozone).
   The fluorocarbon absorption process, being considered as an alternate or back-up technique, has been developed to the inactive pilot plant scale in the U.S.A. but is less advanced towards industrial application.

4. Techniques for the immobilization of trapped krypton are being developed. They concern the confinement in pressure bottles, the incorporation in metal matrices and the enclosure into the porous structure of zeolites.
   The embedment of krypton in a metallic matrix by ion sputtering is a preferred process which has reached the state of half scale technical testing under non-radioactive conditions. Hot demonstration with representative quantities of radio-krypton would need to be done.

Iodine-129

A specialists' meeting similar to the one for krypton, was likewise organized by the Commission on Iodine-129 management, a year earlier, 1981 (2). Also here final conclusions could be formulated after panel discussion of the review

papers presented at the meeting. Some highlights of these conclusions may again be cited hereafter and put forward for consideration :

1. Iodine-129 should be trapped, to a high extent, from gaseous effluents of a reprocessing plant in order to prevent its release into the local environment. Methods and techniques are presently available for trapping more than 99% of the Iodine-129 from the dissolver off-gas which usually contains by far the most of this radionuclide. If considered necessary, the cleaning of the vessel off-gas would need more development work.
   By cleaning the dissolver off-gas alone, a plant decontamination factor of about 100 can be achieved.

2. Concerning the immobilization of the retained radio-iodine, no industrial experience is available at present. Further research is needed on this subject.

3. The possible disposal options, radiologically assessed on a generic basis, concern the disposal on the deep ocean bed and into certain geological formations as well as the discharge to coastal waters.
   No single strategy, of those discussed has been identified as an optimum and general solution for iodine management.

4. An important objective of future investigations should be the formulation of accepted criteria for possible Iodine-129 release into the biosphere. These guidelines need to be carefully evaluated and they seem to be a function of the chosen disposal strategy.
   In the meantime, it seems indicated to solidify and immobilize trapped Iodine-129 to an acceptable standard for safe interim storage and transport, until a disposal method has been identified.

In a follow-up study (3) conducted under contract by the National Radiological Protection Board (U.K.) in 1982-1983, the radiological assessment of Iodine-129 management modes has further been refined and was complemented by the addition of a cost benefit analysis. The earlier findings as summariezed above, were confirmed in general and the latter analysis showed that the costs of abatement of atmospheric discharges of Iodine-129 would be outweighed by the radiological benefits.

Carbon-14

The situation with regard to the waste management of Carbon-14 was reviewed, in 1982, by a contractual study conducted jointly by UKAEA and NRPB (4) at Harwell (U.K.). The following findings may be briefly noted.

A reliable picture of the production and release of carbon-14 from various reactor systems has been built up for the purpose of this study. It is based on a critical analysis of reported calculations and measurements and some new calculations in the case of AGRs and Magnox reactors. Generally, a good agreement exists between various sources of data.

The key problem in carbon-14 management is its retention in off-gas streams, particularly in the dissolver off-gas stream at reprocessing plants. In this stream, the nuclide is present as carbon dioxide, and is extensively isotopically diluted by the carbon dioxide content of the air. The size of plant required for

retention, and the quantities of solid waste produced, are therefore determined by the air flow-rate through the dissolver.

Three alternative trapping processes that convert carbon dioxide into insoluble carbonates have been suggested. Any of them could be used as a preliminary to krypton removal, or as part of the product purification system of a fluorocarbon separation process for krytpon, or to treat gas regenerated from a molecular sieve bed or cold trap. They are :

* The double alkali process. Carbon dioxide is absorbed by sodium hydroxide solution. The resulting liquor is treated with calcium hydroxide to form calcium carbonate and to regenerate sodium hydroxide for re-cycle.

* The direct process. Carbon dioxide reacts with an aqueous slurry of calcium hydroxide to give calcium carbonate directly.

* The barium hydroxide octahydrate process. Carbon dioxide reacts with a fixed bed of solid barium hydroxide octahydrate to give barium carbonate.

Any of these processes is capable of giving a high decontamination factor for carbon-14.

It is probable that calcium or barium carbonates, produced in the above processes, could be incorporated into cement or bitumen matrices to provide satisfactory immobilized waste forms. However, the stability of such waste forms to prolonged irradiation and to leaching needs to be investigated.

A number of disposal options for solid carbon-14 wastes have been identified. The acceptability of the various options will be determined by the ALARA principle, i.e., that all exposures should be as low as reasonably achievable, economic and social factors being taken into account.

The maximum individual doses arising from the atmospheric discharge of Carbon-14 from a reference PWR reprocessing plant (1200 t/a spent uranium) are estimated at around 0,5 mrem/a.

Conversion to a solid waste followed by disposal to a geologic repository could, in some circumstances, substantially reduce the collective dose commitment, relative to that arising from discharge.

Tritium

Unlike the foregoing subjects, the management of tritium containing wastes has not been assessed by a recent study in the scope of the Community programme.

For several years, however, the development of a process is being supported which aims at the removal of tritium from the aqueous effluents of a reprocessing plant (6). The work is conducted at the nuclear research centre in Mol (Belgium). It concerns a process (called ELEX) which uses water electrolysis combined with catalytic exchange between gas and liquid phase, in order to concentrate the tritium in a small liquid volume while the bulk of the aqueous effluent may be released with a strongly reduced tritium content. The effect of both volume concentration and tritium decontamination is estimated at a factor of about 100. After having tested the process on a laboratory scale, a technical pilot plant is presently being assembled for demonstration purposes.

References

1. W. HEBEL, G. COTTONE (ed.) :
"Methods of Krypton-85 Management. Proceedings of a meeting held in Brussels on June 29, 1982"
EUR 8464 (1983) Harwood Academic Publishers, Radioactive Waste Management, Volume 10.

2. W. HEBEL, G. COTTONE (ed.) :
"Management modes for Iodine-129. Proceedings of a meeting held in Brussels on September 25, 1981"
EUR 7953 (1982) Harwood Academic Publishers, Radioactive Waste Management, Volume 7.

3. I.F. WHITE, G.M. SMITH :
"Management modes for iodine-129"
EUR 9267 (in print) Nuclear Science and Technology.

4. R.P. BUSH, I.F. WHITE, G.M. SMITH :
"Carbon-14 Waste Management"
EUR 8749 (in print) Nuclear Science and Technology.

5. W. HEBEL, G. COTTONE :
"CEC Research activities into the immobilization of volatile radionuclides from reprocessing"
IAEA-SM-261/47 (1983) Vienna.

6. A. BRUGGEMAN, R. LEYSEN, L. MEYENENDONCKX, C. PARMENTIER :
"Separation of tritium from aqueous effluents"
EUR 9107 (1984) Nuclear Science and Technology.

7. D.S. WHITMELL, R.S. NELSON, R. WILLIAMSON, M.J.S. SMITH, G.J. BAUER :
"Immobilization of krypton by incorporation into a metallic matrix by combined ion implantation and sputtering"
EUR 8711 (1983) European Applied Research Reports.

8. R.D. PENZHORN, H.E. NOPPEL, A. DOREA, K. GUNTHER, H. LEITZIG, P. SCHUSTER :
"Long-term storage of Kr-85 in amorphous Zeolite 5A"
EUR 9106 (in print) Nuclear Science and Technology.

9. M.G. NICHOLAS, P. TREVENA :
"Screening of materials for embrittlement by rubidium"
EUR 8184 (1983) European Applied Research Reports.

DEVELOPMENT OF TECHNOLOGIES FOR THE WASTE MANAGEMENT OF I-129, Kr-85, C-14 AND TRITIUM IN THE FED. REP. OF GERMANY

E. Henrich, K. Ebert

Kernforschungszentrum Karlsruhe, Institut für Heisse Chemie
Fed. Rep. of Germany

ABSTRACT

The main source of I-129, Kr-85, C-14 and tritium in germany will be a 10-15 GWe LWR fuel reprocessing plant (FRP), expected to be in operation in the mid nineties. The recommendations of the Reaktorsicherheits- und Strahlenschutz-komission RSK, SSK (German "Reactor Safety and Radiation Protection Commissions") are the guidelines for release regulations and development efforts. It has been recommended to limit the annual I-129 release to less than 0.2 curies. The uncontrolled release of Kr-85, C-14 or tritium via the stack resulting from the 15 GWe power will not exceed the limits derived from the German "radiation protection ordinary". The development and hot demonstration of a Kr-85 control technology is recommended in view of the anticipated increasing use of nuclear power in the future. Commercial use of Xe and Kr may also contribute to the incentive for recovery. It would be simple to recover 14-CO_2 once separated in the course of the I-129 or Kr-85 removal operations. Tritiated waste water once it has been separated in the course of processing, should not be deliberately released. Therefore tritium control technology is being developed.

General concepts and the present status of reference and back-up technologies as well as additional research in view of advanced processes are summarized briefly. The following steps will be covered:

(1) Consequences of headend operations on subsequent steps:
Suitable processing especially in the plant headend is an important first step of waste management and may have consequences for all the subsequent steps. The aim of desirable process modifications is (a) confinement of the volatile nuclides to a small volume to prevent dispersion throughout the plant and (b) routing the nuclides to a small, single waste stream to avoid secondary waste streams.

(2) Removal of I-129, Kr-85 and C-14 from the dissolver off-gas and of tritiated waste water from the highly active raffinate (HAW) stream.

(3) Treatment and conditioning options for the recovered radionuclides to produce suitable waste packages for storage or disposal.

(4) Initial storage on site or at a central facility and final disposal options: sea dumping generally is not approved by the federal government. In a close cooperation with the nuclear industry the Physikalisch-Technische Bundesanstalt, PTB ("Federal Institute of Physics and Technology") has the responsibility for construction and operation of appropriate final disposal facilities and is developing criteria for the disposal of waste packages.

International agreements for the control of airborne radionuclides are desirable in the future.

1. INTRODUCTION

Iodine-129, krypton-85, carbon-14 and tritium are produced by fission and neutron activation reactions in the fuel and various core zone components of nuclear power plants. The decay characteristics and amounts of these nuclides generated in LWRs per GWe·year are shown in table 1. Contributions to the air-borne waste in a fuel reprocessing plant (FRP) originate only from the radionuclide fraction which is produced in the oxide fuel matrix and does not escape from the hot fuel pellets and the gas plenum during irradiation. The amount, activity and isotopic dilution of volatile radionuclides liberated into the gaseous, liquid or solid FRP waste streams are shown in table 2. About half the tritium and C-14 are discharged as solid waste together with the leached zircaloy hulls.

Gaseous waste management at nuclear power plants concerns especially the short-lived isotopes of iodine and the rare gases and is not addressed in this paper. A release of I-129 or Kr-85 from the LWR is negligeable compared to the FRP. The release of tritium is less than 10% and of C-14 less than 50% of the amount produced in the LWR.

The major source of the long-lived airborne radionuclides in the Fed. Rep. Germany will be an about 12 GWe LWR-FRP, expected to be in operation in the mid nineties. Experience and research and development efforts in airborne waste management for a FRP in Germany are briefly summarized.

2. RECOMMENDATIONS FOR CONTROL OF AIRBORNE RADIONUCLIDES

A German state government will be the licensing authority for a FRP. Licensing conditions are especially based on the recommendations of experts in the "Reaktorsicherheitskommission" (RSK: "reactor safety commission") and the "Strahlenschutzkommission" (SSK: "radiation protection commission"). The SSK-recommendations /1/ and the RSK-comments /2/ are in accordance with the "Strahlenschutzverordnung" (StrlSchV: "radiation protection ordinary") and pay attention to specific aspects of an inland LWR-FRP in a densely populated region. They are the guidelines for future release regulations and present R + D efforts and are briefly summarized in table 3.

(a) Iodine-129: The annual release of I-129 with the gaseous FRP waste streams should be less than 0.2 Ci. An uncontrolled iodine release exceeds the dose limit for a hypothetical maximum exposed individual, according to § 45 StrSchV.

An uncontrolled release of Kr-85, C-14 and H-3 via the stack does not exceed the release limits, even for a 30 GWe LWR-FRP according to § 45 StrlSchV. The following recommendations have been made in view of the "ALARA" principle in § 28 StrlSchV.

(b) Krypton-85: The development and hot demonstration of a Kr-85 control technology is to be recommended, on account of the probable future increase of the nuclear power economy. An additional incentive for recovery might be a commercial use of Kr-85 and Xe. Xe is a valuable material, the most abundant fission product and inactive after 1 y cooling time.

(c) Carbon-14: Control technology development for C-14 has a low priority. On the other hand, it would be simple to recover 14-CO_2 once separated in the course of I-129 or Kr-85 removal operations.

radionuclide	iodine-129	krypton-85	carbon-14	tritium
		DECAY CHARACTERISTICS		
half life	$1.6 \cdot 10^7$ y	10.8 y	$5.7 \cdot 10^3$ y	12.3 y
decay mode (energies in keV)	β^- 100% (150) γ 100% (40)	β^- 99.6% (687) γ 0.4% (514)	β^- 100% (155) no γ	β^- 100% (19) no γ
specific activity	$1.8 \cdot 10^{-4}$ Ci/g	$3.9 \cdot 10^2$ Ci/g	4.5 Ci/g	$9.7 \cdot 10^3$ Ci/g
		PRODUCTION PER GWe·YEAR in LWRs		
• reactions	fission	fission	n-activation	ternary fission
in oxide fuel • activity	1.2 Ci	$3.2 \cdot 10^5$ Ci	N14 (n,p); O17(n,α) $\leq$20 Ci	Li6 (n,α); Li7 (n,n,α) 2[-3]$\cdot 10^4$ Ci
matrix • volume	129-I_2 0.58m^3(STP)	Kr-85 0.22m^3(STP)	14-CO_2 $\leq$8.3 l (STP)	HTO 15 [-23] l (STP)
• weight	6.7 kg	0.8 kg	C $\leq$4.4 g	T 2[-3] g
neutron activation in core materials (cladding, structure control rods moderator, coolant etc.)	-	-	n-activation reactions in core materials N14 (n,p), O17 (n,α) B10 (n,2α) etc. do not contribute to FRP airborne waste	
production of non-radioactive airborne fission products, LWR spent fuel $>$1 y cooling time:				
	Br_2: 0.1·I_2 volume	Xe: 10·Kr volume	—	—

Table 1: DECAY CHARACTERISTICS AND PRODUCTION OF AIRBORNE NUCLIDES IN THE LWR (1GWe·year corresponds to 30 MTHM at 34 GWd/MTHM burn-up)

radionuclide	iodine 129	krypton-85	carbon-14	tritium
FRP airborne waste percent escaped from LWR spent fuel and plenum	negligeable	negligeable	negligeable	about 50% (remainder in Zry cladding)
isotopic dilution factor major diluant in FRP	~1.2 inactive FP I-127	~15 inactive FP Kr	$\sim 10^3$ (1) C-impurities in fuel CO_2 in DOG air	$\sim 10^7$ (2) water input to FRP headend
airborne - activity waste - volume in FRP - weight waste stream in FRP	1.2 Ci I_2 0.7 m^3 (STP) 8 kg DOG	$3.2 \cdot 10^5$ Ci Kr 3.2 m^3 (STP) 12 kg DOG	~20 Ci CO_2 ~8 m^3 (STP) C ~4 kg DOG	$\sim 10^4$ Ci water ~120 m^3 H_2O ~120 MT HAW
short - lived nuclides produced by spontaneous fission of Cm-244, 242	8 d-I-131 21 h-I-133 7 h-I-135	2.8 h-Kr-88 5.3 d-Xe-133 9.2 h-Xe-135		

Abreviations: DOG dissolver off-gas. HAW Purex 1. extraction cycle raffinate, Zry zircaloy

Remarks: (1) 500 m^3 (STP) DOG assumed per MTHM
(2) no water recycle from HAW assumed

Table 2: AIRBORNE RADIONUCLIDES PER GWe·year IN THE LWR FUEL REPROCESSING PLANT

(d) Tritium: Tritiated waste water, once it has been separated in the plant, should not be deliberately released as water vapour via the stack. More rigorous release restrictions are applied to the aqueous effluents from an inland FRP at a dry site. Therefore, a control technology for tritium is being developed.

IODINE-129 : ANNUAL RELEASE LIMIT FOR EFFLUENTS < 0.2 Ci

UNCONTROLLED RELEASE OF KRYPTON-85, CARBON-14 AND TRITIUM VIA THE STACK DOES NOT EXCEED RELEASE LIMITS

RECOMMENDATIONS REFER TO THE "ALARA" PRINCIPLE

KRYPTON-85: TECHNOLOGY DEVELOPMENT AND HOT DEMONSTRATION PRECAUTIONS FOR THE FUTURE

CARBON-14 : TECHNOLOGY DEVELOPMENT HAS A LOW PRIORITY

TRITIUM :
- TRITIATED WASTE WATER ONCE SEPARATED IN THE COURSE OF PROCESSING, SHOULD NOT BE DELIBERATELY RELEASED AS WATER VAPOUR VIA THE STACK.
- IN AN INLAND PLANT MORE RIGOROUS RELEASE RESTRICTIONS ARE APPLIED TO AQUEOUS DISCHARGES

TABLE 3: KfK IHCH

RECOMMENDATIONS FOR CONTROL OF AIRBORNE NUCLIDES IN A LWR FUEL REPROCESSING PLANT

3. SUCCESSIVE AIRBORNE WASTE MANAGEMENT STEPS

Airborne waste management is a complex set of interdependent operations, integrated into a complex processing system. The successive waste management steps have been divided into four successive sub-groups shown in table 4.

(a) Processing concepts: A suitable processing concept in the FRP is the first and essential step of waste management and precondition for a simple, safe and economic control.

- The airborne radionuclides should be confined to a small plant volume in the headend. This prevents a dispersion throughout the plant and obviates additional and expensive control measures in large plant volumes.

- The airborne radionuclides should be routed into a single, small waste stream. This avoids secondary waste streams and simplifies recovery and waste treatment.

Exactly the same processing philosophy is observed for the non-volatile waste nuclides: They are confined to the aqueous headend streams and routed to the highly active raffinate HAW to more than 99%. Iodine and tritium confinement and concentration in a single waste stream requires minor process modifications in the FRP headend.

1 PROCESSING CONCEPTS IN THE FRP HEADEND

PRECONDITION FOR A SIMPLE SAFE AND ECONOMIC CONTROL ARE MINOR PROCESS MODIFICATIONS IN THE HEADEND

- CONFINEMENT TO A SMALL PLANT VOLUME
- ROUTING INTO A SINGLE AND SMALL WASTE STREAM

2. RECOVERY STEPS FROM WASTE STREAMS

- I-129,Kr-85 AND C-14 FROM THE DISSOLVER OFF-GAS
- TRITIUM FROM THE HIGHLY ACTIVE RAFFINATE

3 TREATMENT AND CONDITIONING OF RECOVERED PRODUCTS

- WASTE PACKAGES COMPATIBLE WITH STORAGE OR DISPOSAL OPTIONS

4 TRANSPORT,STORAGE OR DISPOSAL

- UNDERGROUND DISPOSAL OF GASEOUS WASTE FORMS OR SEA DUMPING ARE NOT APPROVED

TABLE 4: IHCH

SUCCESSIVE AIRBORNE WASTE MANAGEMENT STEPS

(b) Recovery steps: Recovery is simple, if iodine, rare gases and C-14 as CO_2 are routed exclusively into the dissolver off-gas (DOG) stream. The DOG stream is relatively small and contributes only few percent to the total process off-gas flow. Removal from a small gas volume improves the efficiency and cost-effectiveness of the recovery steps.

Tritiated waste water can be routed to the HAW stream and is removed and purified from nonvolatile radionuclides by distillation from the acid recovery system.

(c) Treatment and conditioning: Treatment and conditioning procedures for the recovered products must be compatible with the individual recovery steps and vice versa. On the other hand, the waste form and the waste packages must be compatible with the subsequent transport, storage or disposal requirements.

(d) Transport, storage and disposal: Storage and decay over about a century in an on-site storage building is one of several options for the relatively short-lived 11y-Kr-85 and 12y-tritium. Disposal in deep geological formations is suited to the very long-lived 5730 y C-14 and $1.6 \cdot 10^7$y I-129. Sea dumping is not approved by the federal government /3/, if a safe on-land disposal option is available.

4. PROCESSING CONCEPT FOR I-129, KR-85 AND C-14

The confinement volume for I-129, Kr-85 and C-14 is the FRP headend equipment vented to the DOG purification system. Individual pieces of the equipment are the shears, dissolvers and some surrounding vessels. It is desirable to route essentially all the volatile radionuclides to the DOG. Special care has to be paid to the iodine, due to the higher confinement factor required.

(a) Rare gases: Rare gases contained in the gas plenum of spent fuel pins are liberated during chopping. The liberated fraction amounts to less than 10% for LWR and up to 90% for FBR spent fuel. The fraction contained within the spent fuel pellets is liberated in the course of dissolution. In a chop and leach headend, the off-gas from the shear (SOG) is routed to the dissolvers and is the major DOG diluent. Thus, a complete liberation of the rare gases Kr and Xe into the DOG is straightforward.

(b) Carbon-14: The bulk of about 10-100 ppm carbon impurities in the fuel matrix and the C-14 originating from the activation of N-impurities is oxidized to volatile CO_2 during fuel dissolution; 1-2% forms CO /4/. The probability for the formation of organic materials in the hot nitric acid dissolver solution is low.

(c) Iodine-129

1. Iodine confinement:

In a conventional FRP the iodine contaminates a large number of aqueous, organic and gaseous streams. A reliable retention necessitates a complex variety of expensive removal steps and control measures at very low iodine concentrations in the presence of difficult-to-remove organic iodine. Iodine confinement to the headend equipment is not straightforward, but requires some minor process modifications. An efficient iodine removal from the dissolver solution into the DOG is the most important step to prevent an iodine dispersion throughout the plant. This can be achieved by fractional distillation, or more conveniently by boiling under reflux. The removal process can be improved by additional chemical treatment, e.g. addition of carrier iodate and NO_x sparging. Transformation and stabilization of iodine,especially at lower concentrations,in the volatile elementary form is precondition for an effective and clear performance of most operations. A convenient reagent for this purpose is the nitrous acid HNO_2, normally present in most aqueous phases.

2. Consequences of organic impurities:

Provided that the confinement volume is not contaminated with organic impurities, the behaviour of inorganic iodine is clear and sufficiently well defined. A formation of non-volatile organic iodine may retain some iodine in the dissolver solution. Formation of volatile organic iodine may complicate the iodine recovery from the off-gas. Routine iodine removal from the large vessel off-gas volumes has to deal with this inconvenient situation and should be avoided. A possible source of organic impurities is the nitric acid recycled from the highly active recovery system into the dissolvers and DOG scrubbers. Acceptable concentration levels for the various organic species, which are compatible with a reliable iodine treatment, are not well specified. Production of a sufficiently pure acid should be possible, especially, if attention is paid to the details of the acid recovery operations from the HAW.

3. Spontaneous fission produces short-lived iodine isotopes:

Large storage tanks for the highly active waste contain some Cm. The 0.4 y-Cm-242 and the 18y-Cm-244 have a spontaneous fission half life of about 10^7y and generate continuously small amounts of 8d-I-131, 21h-I-133 7h-I-135 and additional short lived isotopes e.g. of rare gases. The operating mode of the tank may allow sufficient time for decay in solution. Another option for the highly active waste tank ventilation and the vitrification off-gas, is the delay of release in an off-gas purification system, if iodine retention should be required. Cm-244 production increases considerably with the fuel burn-up /5/. The Cm amounts produced in LWR

fuel are shown in Fig.1; they are about one order of magnitude higher for Pu recycle fuel in thermal reactors and about one order of magnitude lower for fast reactor fuel. Compared to the Cm, the spontaneous fission of even Pu-isotopes is much lower.

4. Release from the confinement volume:
An accidental release of I-129 from the confinement area must be prevented by reliable processing and should be a rare event. Such an event will be less serious if the iodine process inventory is low. The following procedure has been proposed to be prepared for emergencies: The acid in the vessel off-gas scrubbers can be replaced by a 'mercurex' solution (about 10 M HNO_3 plus 0.2 M Hg^{2+}) from a standby-tank for some days or weeks /6/ until the iodine is sufficiently flushed out.

A brief summary of the processing concepts is given in table 5.

- I-129,Kr-85 AND C-14 ARE ROUTED INTO THE DISSOLVER OFF-GAS
- THE CONFINEMENT VOLUME IS THE HEADEND EQUIPMENT VENTED TO THE DOG PURIFICATION SYSTEM

Kr-85	COMPLETE LIBERATION INTO THE DOG IS STRAIGHTFORWARD
C - 14	BULK OF C FORMS VOLATILE CO_2 DURING DISSOLUTION
I-129	REQUIRES SLIGHT PROCESSING MODIFICATIONS IN THE HEADEND:
	— EFFICIENT IODINE REMOVAL FROM THE DISSOLVER SOLUTION BY BOILING UNDER REFLUX, IMPROVED BY ADDITIONAL CHEMICAL TREATMENT : E.G. CARRIER IODATE PLUS NO_x - SPARGING
	— NITROUS ACID AND A LOW ORGANICS CONTAMINATION AID TO MAINTAIN THE IODINE IN THE VOLATILE ELEMENTARY FORM
	— SPENT SCRUB ACIDS FROM THE DOG SYSTEM MAY CONTAIN SOME IODINE AND ARE RECYCLED TO THE DISSOLVERS
I-131 I-133 I-135	AND OTHER SHORT-LIVED ISOTOPES ARE PRODUCED BY SPONTANEOUS FISSION OF Cm-244 AND Cm-242 CONTROL BY DELAY OF RELEASE IS AN OPERATIONAL PROBLEM

TABLE 5: KfK HCH

PROCESSING CONCEPT FOR I-129, Kr-85 AND C-14

5. PROCESSING CONCEPT FOR TRITIUM

(a) Voloxidation: A small confinement volume in the FRP and an extremely small volume of tritiated waste water can be achieved by voloxidation of chopped fuel prior to aqueous processing /7/. The additional high temperature step is complex and expensive and is not approved as a desirable processing concept. Moreover, most of the tritium has escaped from FBR spent fuel pins, only few percent are still contained.

(b) Tritium behaviour in the LWR and FBR FRP: Tritium contained in the fuel matrix forms HTO and less than 1% HT during dissolution. In a LWR-FRP about half of the tritium is discharged as solid waste together with the leached zircaloy hulls; the remainder accompanies the aqueous phases as water. Less than 10% of the tritium will arrive in a FBR-FRP, since most of it has escaped from the hot fuel during irradiation through the stainless steel cladding into the reactor sodium coolant. In the FBR fuel cycle the problems of tritium confinement and control are shifted to the reactor site.

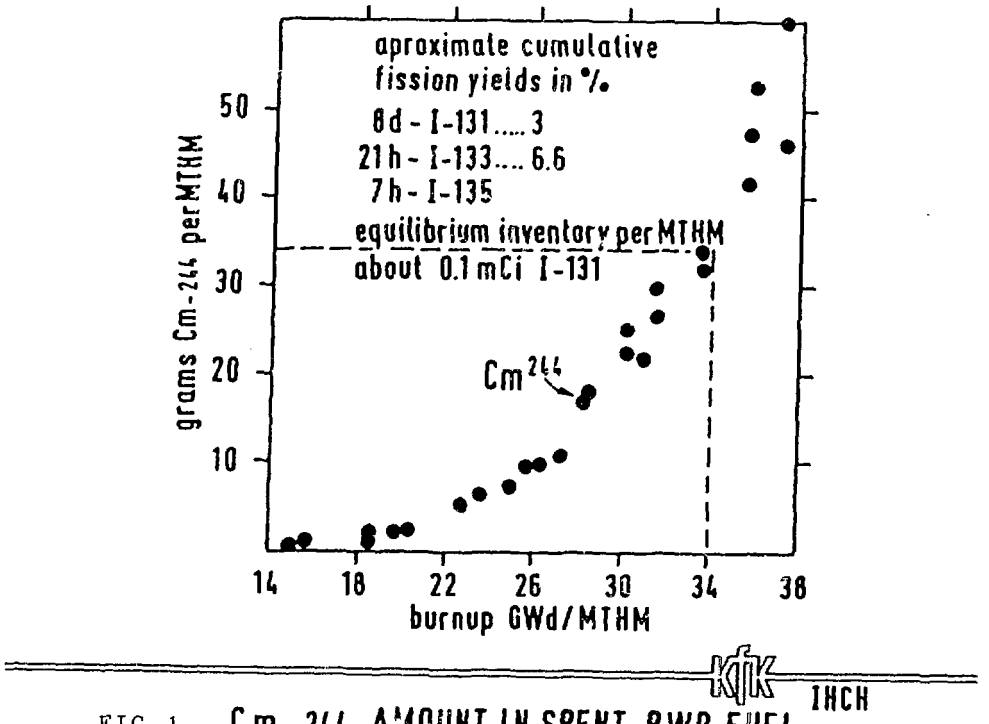

FIG. 1 Cm-244 AMOUNT IN SPENT PWR FUEL

(c) Confinement and recycle of tritium in the FRP: The simplified flowsheet in fig.2 shows the processing concept, which is preferred for tritium control /8/. The standard flowsheet is slightly modified, to confine the tritium to the aqueous headend streams and to route it to the highly active raffinate HAW. The processing concept for the non-volatile fission products (FP) is similar and the tritium accompanies the FPs into the HAW. A non-tritiated scrub acid is used in the final scrub extractor HS2 prior to reextraction, to replace the dissolved and entrained aqueous phase in the organic solvent. This prevents the carry-over of tritium to the subsequent extraction cycles. Radiolytic tritiation of the organic solvent in the highly active extractor HA was found to be negligeable. The aqueous phases recovered from the HAW stream are recycled exclusively to the tritiated aqueous headend streams. The disadvantage of this concept is an increased tritium concentration level.

A small fraction of tritiated waste water is removed and discharged from the acid recovery system. As a consequence, the input of non-tritiated aqueous phase to the confinement volume is limited to a correspondingly low value. The disadvantage is a decreased process flexibility, e.g. the recycle of non-tritiated concentrates from the subsequent extraction cycles is limited.

(d) Practicability of the processing concept: Individual process steps e.g. scrubbing the tritiated aqueous phase from the loaded solvent have been investigated, but the practical limits of this concept are not known. Existing FRPs are not well suited for a reliable demonstration of the flexibility or availability limits of the over-all concept. Experience can be accumulated in suitably designed and operated future plants. A moderate tritium confinement factor and a moderate

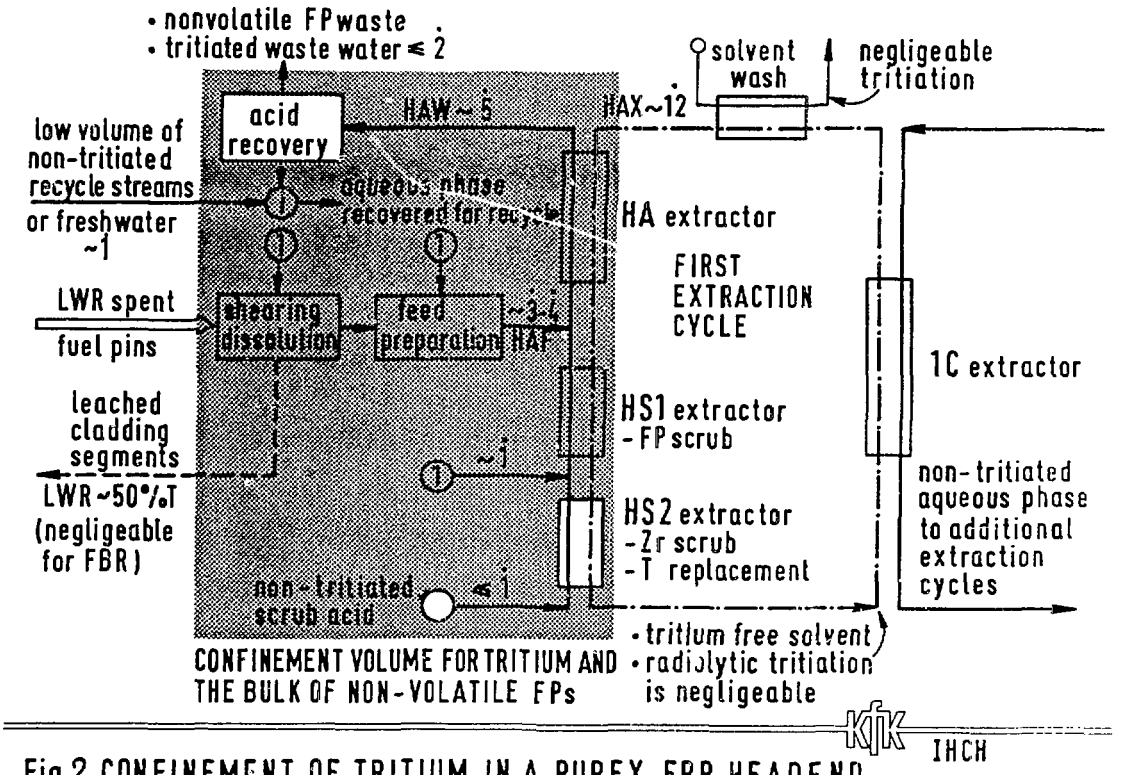

Fig.2 CONFINEMENT OF TRITIUM IN A PUREX FRP HEADEND

—— aqueous —·—·— organic - - - - waste streams x volume flow rate x m^3 per MTHM

reduction of the tritiated waste water volume is expected to be a reasonably cost-effective and practicable compromise. Discharge of some tritiated waste water with the off-gas via the stack and a moderate recycle factor for the aqueous headend streams of about 3, will result in about 2 m^3 tritiated waste water per MTHM containing about 400 Ci tritium (PWR fuel).

(e) Consequences of waste treatment options: If the relatively cheap on-site injection of large volumes of tritiated waste water is a licensable disposal option, an extreme tritium concentration by recycling of aqueous phases within the FRP headend does not make very much sense. Additionally, higher confinement factors can be obtained without too much effort at the expense of larger tritiated waste water volumes. On the contrary, if extremely expensive conditioning and storage or disposal procedures are required, concentration by water recycling within the plant and even additional tritium enrichment processes to reduce the tritiated waste water volumes must be taken into account.

(f) HT-dilution option in the atmosphere: In view of the high global inventory of tritium, which has been produced and dispersed in thermonuclear weapons tests, the tritium concentration in the biosphere will decrease for many decades in spite of an additional tritium release from the nuclear fuel cycle. Dilution and dispersion of HT via the stack generated from the HTO at the FRP, does not meet the approval of experts /9/.

The processing concept for tritium is summarized in table 6.

MINOR MODIFICATIONS OF THE PUREX FLOWSHEET ARE REQUIRED FOR CONFINEMENT AND HTO VOLUME REDUCTION

- CONFINEMENT TO THE AQUEOUS HEADEND STREAMS
  - "Tritium scrub" of the loaded solvent prior to reextraction
  - Separate acid recovery system within the confinement volume
- REDUCTION OF THE TRITIATED WASTE WATER VOLUME
  - Reduced input of non-tritiated aqueous phases
  - Recycle of recovered aqueous phases
- MODERATE CONFINEMENT AND HTO WASTE VOLUME REDUCTION IS A PRACTICABLE COMPROMISE AND MAINTAINS PROCESS FLEXIBILITY

VOLOXIDATION PRIOR TO AQUEOUS PROCESSING IS NOT APPROVED

TABLE 6: KfK IHCH

PROCESSING CONCEPT FOR TRITIUM IN THE FRP

6. INDIVIDUAL RECOVERY STEPS FOR IODINE, RARE GASES AND 14-CO_2

From the various alternative recovery processes for volatile radionuclides from the DOG, only a few are listed in table 7: (1) present reference processes, (2) processes developed to the engineering or pilot plant scale and (3) additional R+D expected to be of interest for improved or advanced processes in the future.

(a) Iodine recovery

Iodine filters: A reliable iodine recovery from the DOG has been demonstrated in the Karlsruhe reprocessing plant since 1976. The iodine filters contain the commercially available AC 6120 material (silicagel impregnated with $AgNO_3$, price about 250 DM per kg, ~ 12% Ag). At an operating temperature of about 150° C, an iodine decontamination factor of 10^4 and a high loading have been obtained. Further improvements, including the remote replacement of spent filters, detailed component design and operating conditions for the planned FRP, are tested in a cold prototype facility /10/.

Caustic scrubbers: A caustic scrub is a well-known, simple, cheap and convenient process and removes the bulk of inorganic iodine plus 14-CO_2 simultaneously; organic iodine is badly removed. Plant experience is scarcely reported in the open literature. Improved efficiency and renewed attractivity is expected for the large FRP's in the future and the required preconditions are as follows:

- An improved upstream NO_x removal and a reasonably low DOG flow prevents an excessive formation of nitrate, nitrite and carbonate salt waste and results in a reasonably small volume of spent scrub solution per MTHM.
- The organic contamination level in the aqueous headend streams must be low in order to obtain an efficient iodine removal from the dissolver solution. This improves also the iodine removal efficiency of a caustic scrub.

- Iodine removal from the DOG to the extreme trace level occurs automatically in the course of downstream rare gas recovery steps. Upstream recycle of the recovered iodine traces avoids a secondary iodine waste stream. The additional in-line iodine recovery step improves the safety in case of upstream upsets.

Nitric acid scrubbers: In an integrated DOG purification system, the iodine behaviour in the nitric acid scrubbers is of interest and has been investigated under different modes of operation /24/. Simultaneous and efficient absorption of nitrous gases NO_x plus iodine is possible from a concentrated DOG; such conditions correspond to a processing mode usually termed as "fumeless dissolution". Absorbed iodine must be desorbed from the spent scrub acid prior to dissolver recycling, to prevent an iodine accumulation in the DOG-system.

Residual NO_x plus iodine can be removed to the trace level in a low temperature scrubber with 90% weight nitric acid. Low temperatures in general are extremely effective for off-gas purification and are found automaticly in the course of the rare gas recovery steps /13/.

(b) Recovery of rare gases:
Two alternative rare gas recovery processes are being developed in the FRG /11/:

A cryogenic distillation process without oxygen has been investigated in the 50 m³ (STP)/h cold engineering scale "KRETA" facility since 1976. In the first distillation column the N_2 is separated from the FP rare gases at 5 bar pressure; the second column separates the Xe from the Kr at about 3 bar. Prepurification steps required prior to cryodistillation are also investigated on the 50 m³ (STP)/h cold engineering scale. In the "REDUCTION" facility oxygen and residual NO_x in the DOG are burned with hydrogen at about 500°C on a Ru-catalyst. Further purification is accomplished by adsorption on silicagel and molecular sieves in the "ADAMO" facility.

A selective absorption process using freon-12 solvent at low temperatures and atmospheric pressure is being investigated in an 25 m³ (STP)/h cold engineering scale test column ("TED"-facility) since the end of 1983 /12/. Xe and Kr are separated from each other in two absorption columns. The first column recovers the Xe plus 14-CO_2, N_2O and traces of Rn from the DOG; the second column recovers the Kr. Prepurification steps required prior to selective absorption have been investigated on the 25 m³ (STP)/h cold engineering scale /13/. The freezing DOG impurities can be removed for recycle in a low temperature nitric acid scrubber and a defrostable feed gas cooler.

Technical as well as safety advantages are expected for the selective absorption process. A comparison of both alternatives will be made, if the state of development is considered to be comparable.

Recovery of rare gases by adsorption on molecular sieves is being investigated at the laboratory scale /14/.

(c) Recovery of 14-CO_2: CO_2 absorption in caustic scrubbers or adsorption on molecular sieves are well-known processes and are described in many textbooks. Caustic scrubbing regains attractivity in the case of a simultaneous removal of bulk iodine plus 14-CO_2 from the main DOG flow. It is almost impossible to avoid the removal of CO_2 in the course of any rare gas recovery steps either by adsorption on molecular sieves or by absorption in a solvent. For these processes, caustic scrubbing is also well suited to recover CO_2 from the product or desorption gas streams.

		status
I-129	● IODINE FILTERS ($AgNO_3$-silicagel) commercially available AC 6120 material	demonstration at WAK 100m^3/h since 1976
	○ IMPROVED CAUSTIC SCRUBBING	laboratory scale
	◎ absorption and/or oxidation in nitric acid scrubbers	engineering scale 25m^3/h since 1979
	○ low temperature absorption in R12 and/or cold traps (see Kr)	preliminary investigations
Kr-85	○ CRYOGENIC DISTILLATION WITHOUT O_2 plus prepurification steps	engineering scale 50m^3/h since 1976
	◎ SELECTIVE ABSORPTION IN R12 plus prepurification steps	engineering scale 25m^3/h since 1984
	○ ADSORPTION AT MOLECULAR SIEVES	laboratory scale
C-14 as CO_2	◎ CAUSTIC SCRUBBING (see I-129)	available technology
	○ ADSORPTION AT MOLECULAR SIEVES	} see Kr recovery
	○ ABSORPTION IN R12	

KfK HCH

TABLE 7:
INDIVIDUAL RECOVERY STEPS FROM THE DISSOLVER OFF-GAS
(cold or tracered engineering ○ or laboratory ○ scale , ● hot plant conditions)

7. INTEGRATED DOG PURIFICATION SYSTEMS

A reliable evaluation of individual recovery steps can be made only as a part of an integrated DOG purification system. Many different tasks must be performed in an integrated DOG system: FP iodine and bromine, rare gases Xe and Kr and 14-CO_2 are recovered for conditioning and storage or disposal on the one hand. On the other hand, radioactive particulates, large volumes of NO_x, water and nitric acid vapours and traces of RuO_4 must be removed for recycle into the process. The treatment of so many different components creates a comparatively complex total purification train. A reliable operation of the complex total system is essential, since the large gaseous waste volumes cannot be stored in case of malfunctions.

A single version of a DOG purification system is not suited to deal with different demands in different FRPs /15/. Important aspects for system design are: release regulations, processing modes in the plant headend, compatibility with subsequent waste treatment steps etc. An example of such differences is the DOG dilution range from about 10^2-10^4 m^3 (STP) per MTHM found in existing plants.

Two examples of DOG-systems under investigation at Karlsruhe on the cold engineering scale are shown in the simplified flowsheets of fig.3 and fig.4. The names of the individual experimental facilities are indicated below /11/.

The first part of the flowsheet in fig.3 comprises a nitric acid scrubber plus aerosol and iodine filters and corresponds in principle to the DOG-system demonstrated in the Karlsruhe FRP (WAK) at a throughput of about 100 m^3 (STP)/h. The following part shows the cryogenic reference process and the required precleaning steps. Integrated operation of these facilities is not planned.

The first part of the simplified flowsheet in fig.4 shows a conventional DOG system comprising a nitric acid scrubber and a caustic scrubber plus aerosol filters /16/. The second part is located in a cold box and contains a low temperature nitric acid scrubber and the absorption columns for rare gas recovery. The total system is a conventional sequence of scrubbers and filters, operating at atmospheric pressure and stepwise temperature decrease. Integrated operation is scheduled for 1985.

8. CONDITIONING OF RECOVERED MATERIALS, STORAGE OR DISPOSAL OPTIONS

Treatment and conditioning steps are the link between recovery and storage or disposal steps. A suitable choice of processes should provide for simplicity and compatibility of the successive operations. Suitable waste forms and waste packages depend on the selected storage, transport or disposal processes.

According to a German Law (§23 "Atomgesetz") the "Physikalisch-Technische Bundesanstalt", Braunschweig (PTB: "federal institute of physics and technology") is responsible for the construction and operation of federal repositories. The PTB is the applicant for repositories in a licencing procedure and has to demonstrate the safety of the disposal mine. Acceptable specifications for waste forms and packages will be established in an iterative process between the nuclear industry and the PTB /17,18/. There are limitations in view of a release of volatile radionuclides in those mines, which are accessible during disposal operations. A release of volatile radionuclides from waste packages in a disposal mine may contaminate the weathering and contribute to the dose rate of the operating personnel. Preliminary upper release rate limits for waste packages have been proposed.

Some more important treatment, conditioning and storage or disposal options are briefly summarized in table 8:

Iodine-129 and carbon-14: The design capacity for the iodine filters is about 1.5 GWe·year. Spent units are not regenerated but replaced remotely and transferred into 400 l drums. Incorporation of the filter material into a cement matrix improves the leach resistance.

Simultaneous precipitation of barium iodate and carbonate has been proposed for spent caustic scrub solutions, preceded by oxidation and addition of a barium hydroxide slurry /15/. The precipitates may be incorporated into a cement matrix plus additives, to produce a suitable waste form.

Krypton-85: Separation of Xe and Kr from each other is desirable for two reasons: (1) to recover the inactive Xe for commercial use and (2) to reduce the Kr storage volume. The thermal decay power of FP krypton cooled for 1 year is about 1kW per 7 m^3 (STP) and the concentrated waste forms produce heat and require cooling during storage.

Gas storage in cylindrical pressure vessels is a familiar technology. Rb induced corrosion has been investigated and resistant construction materials have been specified. Heat removal by natural air convection is sufficient and concepts for storage in an engineered building have been developed. The building may also serve as a second containment barrier.

Solid storage forms can be produced by continuous fixation in a metal matrix using ion sputter pumps or, alternatively, by encapsulation into zeolite 5A. In this situation the first containment is the stable solid waste form and the second containment is the sputter pump cylinder or the vessel containing the zeolite. The

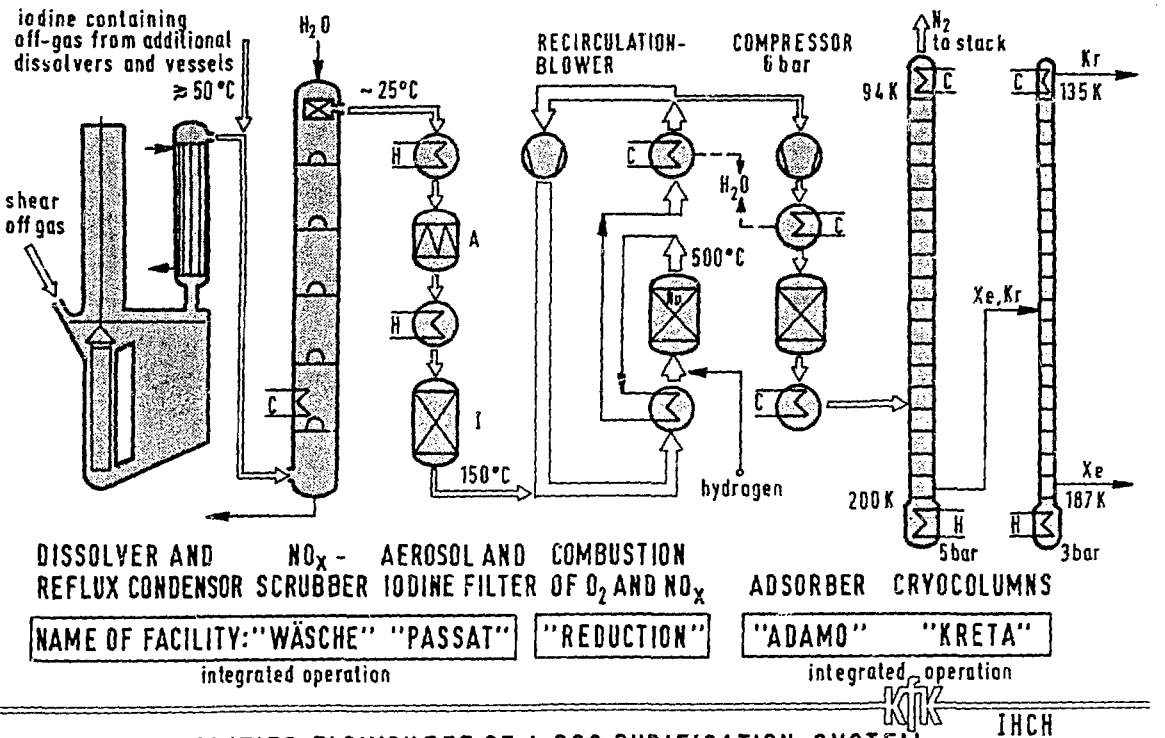

Fig.3 SIMPLIFIED FLOWSHEET OF A DOG PURIFICATION SYSTEM WITH RARE GAS RECOVERY BY THE CRYOGENIC REFERENCE PROCESS

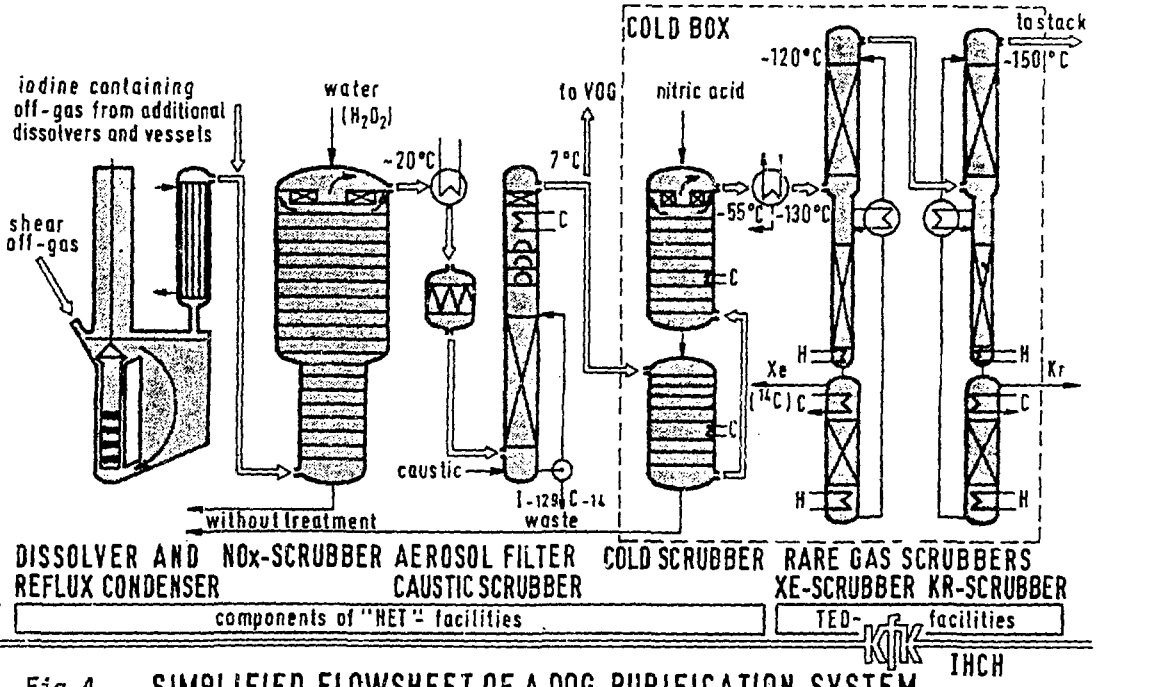

Fig.4 SIMPLIFIED FLOWSHEET OF A DOG PURIFICATION SYSTEM WITH RARE GAS RECOVERY BY SELECTIVE ABSORPTION

improved waste form is expected to reduce the cost for storage or disposal. Both alternatives are being investigated /19,20/.

Tritium: The reference process for the elimination of tritiated waste water is an injection deep underground, into isolated porous geological formations. On-site injection is preferable and avoids additional costs connected with transport. The back-up process is HTO fixation in a cement matrix, packed into tight 400 l drums and storage in an on-site facility. Tritium enrichment by catalytic H_2O/H_2 exchange /21/ and fixation of the tritiated concentrates in a zeolite matrix or as Zr-hydride is an additional area of research /19,22/.

A general disposal option for low and medium active waste which is expected to reduce the dose rate to the plant personnel is the 'in-situ' process /23/. Cold tests are made at the "ASSE" salt mine. LAW and MAW fixed in aged cement granules is mixed with about the same volume of fresh cement and pumped into a large engineered on-site underground cavern. Admixing of tritiated waste water, iodine filter material or Kr, encapsulated into zeolite, has been proposed. The "in-situ" process or HTO injection are attractive in case of colocation of reprocessing and disposal facilities.

16,000,000y I-129	⊙ SPENT IODINE FILTERS —remote replacement without regeneration —incorporation in cement matrix in 400 l drums	
plus 5730y C-14	○ SPENT CAUSTIC SCRUB SOLUTION —pretreatment and precipitation of $Ba(IO_3)_2$ and $BaCO_3$ —precipitate incorporation in inorganic matrix	
DISPOSAL	of long-lived nuclides in solid form in geological formations	
10.8y Kr-85	⊙ PRESSURE VESSELS —batchwise cryopumping in cylindrical pressure vessels • ION SPUTTER PUMPS —continuous fixation in a metal matrix • ZEOLITE ENCAPSULATION —batchwise encapsulation into zeolite 5A	} storage of solid forms is less expensive
ON-SITE STORAGE	in engineered building, air cooling by natural convection	
12.3y H-3	⊙ HTO INJECTION into deep geological formations ○ HTO FIXATION IN CEMENT in tight 400 l drums • HTO IN FRESH CEMENT injection into engineered underground cavern	
ON-SITE STORAGE OR DISPOSAL	transport off-site is more expensive	
	• TRITIUM ENRICHMENT, waste form Zr-hydride etc.	

TABLE 8:
TREATMENT, CONDITIONING AND STORAGE OR DISPOSAL OPTIONS

⊙ present reference process ○ back-up • R+D ○ proposal for future R+D

9. SUMMARY AND CONCLUSIONS

- The airborne waste management steps are part of a complex integrated system. The total interacting system must be optimized, not only the individual steps.
- The important first step of waste treatment is a suitable processing mode in the FRP headend. The general strategy is to confine the volatile nuclides to a small plant volume and to route them completely into a single, small waste stream. This is straightforward for the rare gases and 14-CO_2. Confinement of iodine and tritium requires minor process modifications.
- Tritium is concentrated by recycling the aqueous phases in the FRP headend. Tritiated waste water is removed from the highly active acid recovery system.
- Iodine, rare gases and 14-CO_2 are recovered from the DOG stream. Few recovery processes are demonstrated, many recovery alternatives are being developed using advanced technologies to improve safety, reliability and economy of the entire DOG purification system. An additional incentive for the recovery of rare gases could be a commercial use; this should not be neglected in a cost-benefit analysis.
- A pointless dilution of the DOG does not contribute to safety and cost-effectiveness. The recovery processes will be more simple, safe and economic, if the DOG flow is reduced to a reasonably low value. This is valid for all off-gas treatment.
- Conditioning, storage and disposal procedures are the least well developed steps and various alternatives are being investigated.
- Recovery and concentration of the airborne radionuclides in the course of the treatment steps may create an additional hazard for the operating personnel. An evaluation of alternatives should pay special attention to this safety aspect.
- International agreements for release limits would be desirable. In view of the large inventories of iodine, hydrogen and CO_2 in the sea water, sea dumping or , sea disposal might be a suitable choice. The 'London Convention' governing sea disposal, should be reviewed on an international basis.

REFERENCES

Many surveys and reviews on methods for gaseous waste management in FRP's are available in the literature. Some up-dated recent monographs and reviews represent the state of development up to about 1980-1981.

- Iodine-129: W. Hebel, G. Cottone (CEC, editors)
  "Management Modes for Iodine-129", Vol.7 (1982),
  "Radioactive Waste Management", series vol.7
  editors: D.R. Anderson, A.M. Platt, F. Girardi, S. Orlowski

- Krypton-85: W. Hebel, G. Cottone (CEC, editors)
  "Methods of Krypton-85 Management", Vol.10 (1983), 309 p.
  "Radioactive Waste Management", series vol.10
  editors: D.R. Anderson, A.M. Platt, F. Girardi, S. Orlowski

- Carbon-14: R.P. Bush; IAEA-CN-43/26, Seattle, WA, USA, 16-20 May 1983
  "Carbon-14 Waste Management - A Review"

Only references not covered in these reviews are cited in the following.

1. Empfehlung der "Strahlenschutzkommission" SSK vom 24.02.83 zur Rückhaltung radioaktiver Stoffe bei einer Wiederaufarbeitungsanlage

2. Stellungnahme der "Reaktorsicherheitskommission" RSK vom 22.06.84 zu konzeptrelevanten sicherheitstechnischen Fragestellungen der geplanten Wiederaufarbeitungsanlage.
3. BGBL.II S.156 vom 16.02.1977 und Bericht der Bundesregierung zur Entsorgung der Kernkraftwerke und anderer kerntechnischer Einrichtungen, 30.08.1983
4. A. Leudet, P. Miquel, J.P. Goumondy, G. Charrier; Proc.17th DOE Nucl. Air Cleaning Conference, Denver, USA (1982)40
5. U. Fischer, H.W. Wiese; KfK 3014, January 1983
6. F. Baumgärtner, K. Ebert, E. Gelfort, K.H. Lieser (editors) "Nuclear Fuel Cycle", vol.2, Proceed. Seminar on Reprocessing of FBR spent fuel, march 1981, Obertraun, Austria, p.115; Verlag Chemie, Weinheim 1982
7. J.H. Goode; ORNL-TM 3723 (1973)
8. E. Henrich, H. Schmieder, K.H. Neeb; IAEA-SM-245/15 (1980)
9. H. Brücher, K. Hartmann; Jül.-1838 (1983)
10. K. Jannakos, W. Lange, G. Potgeter, J. Furrer, J.G. Wilhelm; Proc. 16th DOE Nucl. Air Cleaning Conf., San Diego, USA (1980)317
11. E. Henrich, R. von Ammon, E. Hutter; KfK-PWA status report, march 1984, to be published
12. E. Henrich, R. Hüfner, F. Weirich, W. Bumiller, A. Wolff; this conference
13. E. Henrich, U. Bauder, H.J. Steinhardt, W. Bumiller; this conference
14. H. Ringel; Proc.17th DOE Nucl. Air Cleaning Conf., Denver, USA (1982)664
15. E. Henrich, R. Hüfner; IAEA-CN-43/447; Seattle, USA, 16-20 May (1983) IAEA, "Radioactive Waste Management", Vol.2, Vienna 1984
16. G. Koch, H. Goldacker, H. Haug, E. Henrich, W. Ochsenfeld, H. Schmieder, G. Böhme, W. Köhler, L. Grimm; KfK-Nachrichten 15 (1983)158
17. E. Warnecke, H. Illi; in J.G. Moore (editor), "Scientific Basis for Nuclear Waste Management", vol.3, p.19, NY/London (1981)
18. E. Warnecke, H. Illi, D. Ehrlich; in R. Odoj, E. Merz (editors), Jül.-Conf-42, *vol.2, p.792, Jülich (1982)*
19. R. Penzhorn; KfK-PWA status report, march 1984, to be published
20. E. Henrich, H.J. Schmidt, T. Fritsch, A. Wolff; KfK-Nachrichten 14,2 (1982)109
21. U. Schindewolf, Universität Karlsruhe, private communication 1984
22. Knöchel, Universität Hamburg, private communication 1984
23. R. Krämer, R. Kröbel; 5. Int. Symp. on Scientific Basis for Radioactive Waste Management, Berlin FRG, June 1982
24. E. Henrich; KfK-report 2940, (1980), p.162

DISCUSSION

CROFF: Thank you for the excellent papers. From the descriptions of the activities of the various countries and organizations, we have gotten a good overview of the various retention and recovery technologies that exist and some of the approaches being used to put them together.

BELLAMY: I would like to address my question to each panel member, but I think I am addressing it principally to the last speaker. I get, as a common thread, a sense of pessimism that an actual fuel reprocessing plant with an acceptable offgas treatment system may ever really be achieved. Am I misinterpreting your comments? Do you have optimism, or pessimism, that we will ever see an operating fuel reprocessing plant with a very efficient offgas treatment system?

HENRICH: I am very optimistic because I think efficiency, safety, and cost effectiveness do not necessarily exclude each other. I am not pessimistic, by any means.

BELLAMY: I am curious whether other panel members agree or disagree.

GROENIER: I think if you detected pessimism in my presentation, it was not whether or not we could achieve adequate offgas retention in a reprocessing system, it was just whether we will ever have a reprocessing system.

THOMAS, R.T.: My first question is to Mr. Henrich regarding the proposed 350 ton per year fuel reprocessing plant. I followed the activities in West Germany for a number of years. Orginally, a 1400 ton per year plant with krypton recovery was proposed and now I realize a 350 ton per year plant, without krypton recovery, is being proposed. I am also aware of the recent ruling by the Radiation Protection Board that the dose impact does not justify krypton recovery. Nevertheless, it occurs to me that it would be an excellent opportunity to demonstrate krypton recovery, as the Japanese are trying to do. I wonder why West Germany is not taking the opportunity, also, to demonstrate at least a partial recovery since you have a fairly small hot pilot plant. Would you know the reasoning behind it?

HENRICH: The licensing authorities for a reprocessing plant in Germany will be the state governments. On one side, is Lower Saxony, on the other, is Bavaria. Therefore, there could be different decisions. Statements by the Reactor Safety and Radiation Protection Commissions are only recommendations. Regulations are made by the governments. Although what really will happen has not yet been decided; a demonstration of krypton removal technology has been recommended. However, a "hot" demonstration of krypton recovery will wait for a future reprocessing plant.

THOMAS, R.T.: So the possibility exists that you might still demonstrate krypton recovery on a small scale?

HENRICH: Yes, of course.

THOMAS, R.T.: I have a second question for Mr. Henrich. I am aware that you have been developing cryogenic distillation since 1976 and that now you are working on carbon adsorption and recovery. Is the purpose for investigating both technologies to decide in the near future which is better? I think you are in a unique position to do this, inasmuch as both technologies are being looked at in the same laboratory. This is not the situation in the U.S. I am wondering by what method, or by whom in your company, the decision will be made. If you were to go to a "hot" demonstration, would the decision be made at your company level, or would it be made by your Government, or by a private industry?

HENRICH: When the development of both alternatives is at a comparably level, a comparison will be made. Not by K-of-K people but by others. It is not desirable that we do this. It will happen in a year or two.

THOMAS, R.T.: Will it be done by private industry, by an expert group, by a panel, or by some other mechanism?

HENRICH: By an expert group, not by K-of-K members.

THOMAS, R.T.: This is addressed to Mr. Groenier. It is academic, but suppose we had to make the same decision in the U.S. Do you have any idea what process we would use? I certainly don't. If we had to decide on a technology for krypton recovery, say for 1990, what kind of a procedure do you suppose we would use? Would we have hearings, perform some more environmental impact studies, make cost effectiveness analyses, or what? What do you think would happen?

GROENIER: It is very difficult to answer because of the large number of sources from which we receive directions. I can only answer from my own viewpoint, which also reflects the viewpoint within the program that I belong to at Oak Ridge. We would select the Freon selective absorption process. Primarily, because we bypass the ongoing safety concerns about the cryogenic process. We also recognize that the pretreatment steps required for cryogenic distillation make it a complicated process in comparison with the Freon process.

THOMAS, R.T.: Having thought about it for a number of years, I am wondering if it would be a good idea to combine the two technologies. I understand that fluorocarbon is a very robust technique, insensitive to contaminents, whereas cryogenic distillation requires very precise control of temperature, pressure, and reduction of contaminents to trace levels. I have always seen that to be a problem. The fluorocarbon process reduces the effluent flow by a factor of 1,000, roughly; that is, you take in a very large flow and then the product stream will be 1/1000th the input stream. Wouldn't it be a good idea, perhaps, to put the cryogenic technology on the tailend of the Freon process?

GROENIER: That is quite true. In a sense, we already do it because our overall flow sheet takes the product stream from the selective absorption process, which is picked off in the single column concept at the concentration peak for both xenon and krypton, and then they are further separated by what we call a selective desublimation technique. It is cold trapping, a cryogenic cold trapping, if you will. So, in a sense, we do what you suggest in a way, although it is not done in the conventional cryogenic distillation sense. It could be, and it probably is, worth considering.

THOMAS, R.T.: I would think from the standpoint of temperature control and mass transfer it would be easier than sublimation and cold trapping. I would think the liquid phase trapping would be a little easier to control. It seems to me, a marriage of those two processes might give us the best technology of all.

HENRICH: I would like to add something. Our selective absorption process is a little bit different from the U.S. process. The experience we have up to now with our test column is that we are separating xenon and krypton with two columns. The purity of the krypton product will be 99% or more, and the same will be true for xenon products. I do not see what an additional cryogenic process would do. We use very much lower temperatures and you can say that this is a cryogenic absorption process. With lower temperature, the separation selectivity and efficiency increases. You can say this is a combination of both, that it is crogenic absorption that we are doing with our process. We have very low temperatures: in the first absorber we have -120°C and we have tested the second with -140°, and we intend to go to -150°C. So you can see, it is a combination of both. We get about the same product purity as with the cryogenic process.

von AMMON: I think the discussion about the best process of Kr retention is academic as long as there is no chance of a hot demonstration. There is no such chance in the near future in this country (U.S.) or in Germany, where Kr retention won't go into operation before the mid-nineties, and this only if regulatory authorities will demand it for the planned 350 t/a plant. I see only one place in the world where it will be possible soon, in Tokai Works. I heard, however, that the Japanese hesitate to put their cryogenic Kr system into hot operation because they are afraid of handling the hot Kr cylinders. Could Mr. Naruki comment on this?

NARUKI: Thank you for your encouragement. We are hesitant to go into active operation. Demonstration is all right, but we have a great need for shielded storage for the recovered krypton. When we once store the recovered krypton, we must keep it many long years, but we have not yet made any decisions what to do about storage of the recovered krypton. Maybe a small storage facility will be accepted, but to plan a large storage facility will require a big decision. Maybe we will go to hot operations in the near future.

HENRICH: I have a comment regarding an active demonstration of a krypton recovery process. Active means that radiokrypton is in the process. Looking at the krypton inventories of a cryogenic process and of a selective absorption process, there

could be a large difference, about a factor of 100. It would be very simple to have a hot demonstration with the selective absorption process on an engineering scale, but with the cryogenic process, where you have about 100,000 curies, this would be difficult. Though a hot demonstration of an individual process can be done, you need no plans for this if the inventory is sufficiently low. You do not need a plan for a hot demonstration for a proce with a low inventory.

Session 20

CODES, STANDARDS, REGULATIONS

THURSDAY: August 16, 1984
CHAIRMAN: M.W. First
Harvard School of Public Health